

River Publishers

PROCEEDINGS OF FIRST INTERNATIONAL CONFERENCE ON COMPUTER, COMPUTATION AND COMMUNICATION (IC3C-2025)

EDITORS:

DR. OM PRAKASH KUMAR

DR. PRADEEP KUMAR

DR. J .SILAMBOLI

Conference Title:

First International Conference on Computer, Computation and Communication (IC3C-2025)

Editors details:

1. **Dr. Om Prakash Kumar**

Postal Address: Department of Electronics and Communication Engineering, Manipal Institute of Technology, Manipal Academy of Higher Education, Manipal 576104, India

Email id: ompraksh.kumar@manipal.edu

Telephone number: +91-8618388731

https://researcher.manipal.edu/en/persons/om-prakash-kumar

2. **Dr. Pradeep Kumar, University of KwaZulu-Natal, Durban, South Africa**

Postal Address: Private Bag X54001, Durban, 4000

Unite Building, Gate 9, Howard College, Mazisi Kunene Road, Glenwood, Durban, 4041

Email id: kumarp@ukzn.ac.za Telephone number: 031 260 1240

https://ww1.engineering.ukzn.ac.za/pradeep-kumar/

3. **Dr.J.Silamboli , CSI College of Engineering (CSICE), Ketti, Ooty, Tamil Nadu, India**
   Postal Address: Ketti (Ooty), The Nilgiris, Tamilnadu, India – 643 215
   Email id: j.silamboli@csice.edu.in

LIST CONTENT

Article	CONTENT	PAGE NO.
Article 1	**A Review Of Indian Herbal Approaches For Vitiligo: Repigmentation Potential Of Psoralea Corylifolia And Moringa Oleifera Extracts** *K Mythili, Dr. S. Prabakar, K Varshini, T Ashwanthika, S L Tharun*	
Article 2	**Blockchain Technology: Trusted Crowdfunding Platform Using a Smart Contract** *Gaurang Bharadava, Madhav Desai, Anshuman Prajapati, Manav Bagthaliya, Priyanka Patel*	
Article 3	**A Comprehensive Review of Ethnopharmacological Strategies in Post-C-Section Lumbar Pain Management** *K Mythili, Dr. S. Prabakar, L.Swetha, AP Saranya, G.Rajeshwari*	
Article 4	**Remote Sensing Analysis of Urbanization and Agricultural Land Conversion in Bantwal Taluk, Karnataka** *Janardhana Bhat K., Babitha Ganesh, Om Prakash Kumar, Shweta Vincent and Basappa B. Kodada*	
Article 5	**AUTOMATED ELECTRICAL NAIL CLIPPER** *M.Brindha, Dr.S.Prabakaran, AP Saranya , G.Rajeshwari, Sona College of Technology, India*	
Article 6	**RESPLOIT FRAMEWORK FOR PENETRATION TESTING** *1.Chandrakala B M, 2. Annapurna P Patil , 3 .Girija R, 4 Krupashankari S Sandyal , 5 Atish Pokale* *6. .Manoj M, 7 Manvitha P, 8 Muhammed Fahad*	
Article 7	**AI-Driven Threat Detection and Response Systems in Cybersecurity: A Survey** *Souresh Kulshreshtha, Dr.Vijay Anand Sullare*	

Article 8	**The Survey of Self Driven Wall Painting Robots for Interior and Exterior Applications** *Mayur V. Tiwari[1], Prajwal S. Raut[2], Raj S. Dhandekar, Dr. S. V. Pattalwar, Amol S. Mahore, Jay D. Bidkar*	
Article 9	**A Comprehensive Survey on the Evolution and Deep Learning Techniques in Recommender Systems** *Smitha S P., Harishkumar K S*	
Article 10	**Stock Price Prediction Using Machine Learning Algorithms** *Sumukha K Nayak, Krishnamurthy Nayak and Supreetha B S*	
Article 11	**Optimizing Path Costs in Dynamic Network Routing Using a Bio-Inspired 'Sit-and-Wait' Strategy in the Cheetah Chase Algorithm** *M. Goudhaman, N. Vanathi, Adithya GV*	
Article 12	**Optimizing Routing Efficiency in Dynamic Networks Using the Cheetah Chase Algorithm with Novel Convergence Time and Rate Metrics** *M. Goudhaman, N. Vanathi, Adithya GV*	
Article 13	**Optimizing Delay in Network Routing: A Hybrid Algorithm with Energy Function Integration in the Cheetah Chase Framework** *M. Goudhaman, N. Vanathi, Adithya GV*	
Article 14	**Machine Learning Techniques for Optimizing Sub-6GHz Patch-Based MIMO Antennas: A Review for 5G Applications** *T. Prabhu, P. Sree Hari, Vishal RC , A. Keerthivasan , Darshan D*	
Article 15	**Optimizing Environmental Data Processing with IoT-Edge Computing in Air Pollution Monitoring Systems** *Dr.K.Preethi, Dr.A.Backia Abinaya, Dr.L.Bapitha, Dr.K.Swaminathan*	

Article 16	**The SBMAC System for the Prevention and Detection of Water Leakage** *Santosh Anand, Akhil K M, Seema Firdose, Syeda Arbeena Kausar*	
Article 17	**STUDENT FEEDBACK SYSTEM USING MACHINE LEARNING** *Shaik Nagurvali*, *Sujitha S, s., N Ramanjaneyulu* *R Sai Teja*, *V Bindhu Sree*	
Article 18	**Stress Detection using Image Processing and Deep Learning Techniques** *Lavanya Balasubramanyam, Mohammed Zaid ZH,* *MA Mohammed Mishal, Rachana Muthukumar,* *Prakash G L*	
Article 19	**Thermo-Responsive Wearable Device For Varicose Vein Detection And Care** *M.Brindha , Dr. S. Prabakar, G.Keerthisri, M.Shrisakthi, Y.Sineka, B.Sumaiya*	
Article 20	**Vehicle classification and License plate Recognition Through Deep Learning Techniques** *T. Prabhu, Prameeth D Ganiga, Mohammed Ayyan Ahmed, Srinidhi G R, Karthik K J*	
Article 21	**Strengthen Blockchain Security With An Improvised Cryptographic Algorithm For Secure Transactions** *Dr. Mukesh Choudhary, Dr. Hina Chokshi, Vipul Gamit, Khyati Kariya*	
Article 22	**Improving The Prediction Accuracy Of Liver Cancer Detection Using Machine Learning Techniques** *J Gold Beulah Patturose, K Agnes Prema Mary, C. Sheeba Thangapushpam, F V Jayasudha,*	

Article 23	**Nlp-Driven Methods For Enhanced Phishing Website Detection** *J Gold Beulah Patturose, E Sahaya Chithra, V. Anitha Christy, S Gnana Selvan*	
Article 24	**BIOSYNC: WEARABLE HEALTHCARE IOT PLATFORM** *Nandini Prasad K S, Nikshepa T, Deep Kumar, Kedarnath Doddamani, Gagandeep Bhat, Adnan Khan*	
Article 25	**Harnessing Probability for Dynamic and Balanced Game** *Design Dimple Valayil, Paul Kevin Jimmy*	
Article 26	**Configurable Phase Locked Loop using Multi-Oscillator Feedback** *Kiran A Gupta SMIEEE, Jeevan M, Maharshi V, and Leesh G M*	
Article 27	**SKIntellet: Advanced AI for Acne Diagnosis and Personalized Skincare Solutions** *Karumanchi Roshan, V Rishi Vardhan Reddy, Dr. Gokulakrishnan D*	
Article 28	**Hybrid Renewable Energy Generation with Power Electronics Integration** *KHASIFAA, ARUL PRASANN A, KAVI BHARATHI K, ABITHAA, MALATHI S, KALIESWARI CK*	
Article 29	**SVM-Based Anomaly Detection for Network Intrusion Systems: An Advanced Approach to Intrusion Prevention** *Arihant Singhvi, Abhinav Nambiar, Pranav Menon, Narendra V G*	
Article 30	**Personalized Hairstyle Recommendation System using Face Shape Classification** *Rayaan Mohammad Salem, Rishabh Singh, Kavya Bansal, and Narendra VG*	

Article 31	**Breast cancer detection using an on-body Circular Microstrip Patch Antenna** *Somanath Kisan Chikane, Dr. Balasaheb H. Patil*	
Article 32	**Design of Power Efficient 14T Full Adder Circuit** *Sudhamalla Mallesh, Polampally Likhitha, Rajula Pavani, Posham Nagasai, Varikuppala Poojitha*	
Article 33	**Efficient Image Blending Techniques Using FPGA-Based Approximate Multipliers** *Sreelakshmi Vadlamudi, Syamala Yarlagadda and Madhu R*	
Article 34	**Rainfall-Triggered Landslide Susceptibility Mapping Using GIS and LightGBM: A Case Study of Uttara Kannada** *Babitha Ganesh, Shweta Vincent, Janardhana Bhat, Sameena Pathan, Ganesh Bhat*	
Article 35	**Flood Susceptibility Mapping of Chikkamagaluru District of India using Ensemble Technique** *Sting Salvador Gonsalis, Shweta Vincent, Om Prakash Kumar, Vijay Mohan*	
Article 36	**INTRAOCULAR PRESSURE MEASUREMENT COMBINED WITH GONIOSCOPIC ANALYSIS** *Bharathi R.B.*	
Article 37	**Survey on Detection and Mitigation Strategies for Zero-day Attacks: An Extensive Analysis of Current Developments and Case Studies** *Mrs Savitri Ashok Mote, Dr Sudhakar Arabagatte*	
Article 38	**Face Recognition in Dense Crowds Using Deep Learning from IP Camera** *Dr M Sobhana, Mudunuri V CH S Raju, Bommaganti S V B Vikas, Kalle Bhavya Vani*	
Article 39	**A Hybrid TCN-BiLSTM Model for Enhanced Precipitation Nowcasting** *Balivada Anjanee Kumar, Panigrahi Jyothsna, Poojitha*	

	Nambari, Ruchitha Bheesetti, Pedireddy Venkata Satya, Madireddy Hari Krishna	
Article 40	**FARM EASY- Connecting Farmers, Consumers and Logistics for On-Demand Supply Of Tomatoes** *Ms. Usha S(Assistant Professor), Dr. V. Murali Bhaskaran(Professor), Deepikha J, Dhanush Srivatsav S, Grithi Akshayaa V*	
Article 41	**Preprocessing-Enhanced Diagnosis for PneumoniaDetection** *Allada Sankara Rao, Karri lavanya, Bhargavi Durga, Manikanta Sirasapalli, Kudupudi Jyothi Sindhura, Manoj Kumar Nigam*	
Article 42	**Review of Blockchain Algorithms for Security and Power Management in 6G** *S.Janani, S.G.Hymlin Rose, Ms. Manju.K, Ms.Sujitha.S, Ms. Sruthi Rega K*	
Article 43	**Design and Implementation of Women Safety System Based on IOT Technology** *S.Janani, S.G.Hymlin Rose, Kalairishi Sudhakar, M. Keros M*	
Article 44	**Enhancing MR Image Quality for Accurate Rectal Cancer Diagnosis: A Comparative Study of Preprocessing Techniques** *Sonal Patreena D, Almeida, Dr. Surekha Kamath, Dr. Rajagopal K V, Dr. Manjunath K N*	
Article 45	**RECOMMENDATION SYSTEM FOR ANTAKSHARI** *Madhu Bhan, Aman Kumar , Manish Kumar*	
Article 46	**Error-Resistant Image Watermarking Using DWT and Linear Modulation with LDPC Correction** *Amrutha Podipireddy, Bandaru Dhana Lakshmi, Sudha Rani Kandregula, Hima Bindu Karanam, Chaitanya Barre, Surisetti Narsinarao*	

Article 47	**Efficient compression algorithm for multimedia storage device** *S. Cammillus, Nithya Kalyani E, Sreemathi RT Andal Priyadharsini R*	
Article 48	**Smart Shopping Cart with Automatic Billing System** *S.Muthu Lakshmi, S.Selvarekha, B.Vanajaa, S.Karthika*	
Article 49	**Improving the Predictability of Maruti Suzuki Automobile Sales using Machine Learning Methods** *Tanvi kamal Rana, Hina Jignesh Chokshi*	
Article 50	**A Machine Learning Approach to Food Recommendation Using Content-Based Filtering** *Zinkal Patel, Hina Jignesh Chokshi*	
Article 51	**Ship Port Detection with Coarse and Fine Data Fusion using Edge Boards** *S Vasavi, M Sai Pravallika, Y Harini Reddy, D Revanth*	
Article 52	**Seas of Change: Integrating RIS for Effective Ship-to-Ship Communication** *Vedashree G.L, Goutham Simha G.D and Madhusudan B. Kulkarni*	
Article 53	**6G WIRELESS SYSTEMS: PERFORMANCE ANALYSIS OF HARDWARE DESIGNS UNDER NON-IDEAL CONDITIONS** *Bhargavi K V N A, Ravi Chandra M L, RAVILLA DILLI*	
Article 54	**Comparative Analysis of Snake and Ellipse Segmentation Methods for Breast Cancer Detection using Breast Thermograms** Dayakshini Sathish[1], Aswathi T[1], Sathish Kabekody[2], Ashlyne Barnes[1], Sona S[1], Preethika[1], Avashya HS[1]	
Article 55	**EEG data Analysis for Schizophrenia Detection Using a Deep Neural Network-Based Multilayer Percep** *Balivada Anjanee Kumar, Bhusa devi, Srujana Vijjapu[3],Aswani Malla, Kumar Penugudhuru*	
Article 56	**Deploying a Raspberry pi Zero for Overhead Flight**	

	Detection with SDR And FlightAware *Nithya S , Naveen Kumar R,Jaiwanth B ,* *Logu Vishal D*	
Article 57	**Towards Smart Transportation: The Synergy of Space Shift Keying and Reconfigurable Intelligent Surfaces for Future V2V Networks.** *Suhas K, Goutham Simha G D*	
Article 58	**Mapping Learning Outcomes to Academic Success: A Novel Dataset for Evaluating Students' Academic Performance** *Sapna Rai, Dr. Sunil Sikka, Dr. Anil Kumar*	
Article 59	**Echoguard: Voice-Driven Safety for Women in the Digital Age** *L. Leena Jenifer, Deepika Krishnan, Jayashri G*	
Article 60	**Design of Hexagonal shaped HMSIW based IOI shape slot antenna for sub-6GHz applications** *V Shiva Prasad Nayak, Manjunathachari K*	
Article 61	**Design of mmWave Antenna for Next-Generation Technologies** *Sanjeev Vrittikop, Keerthana S, Praveen Kumar and Jagadeesh Chandra R B*	
Article 62	**A COMPREHENSIVE ANALYSIS ON DETECTING FRAUD IN FINANCIAL TRANSACTIONS USING MACHINE LEARNING APPROACHES** *M.Jayalathalakshmi, Dr. S.Prakasam*	
Article 63	**Modelling of Wideband mmWave Antenna For Emerging communications** *Himanshu, Yashwanth N, Praveen Kumar*	
Article 64	**AI-Based Student Stress Prediction: A Machine Learning Approach to Lifestyle Analysis** *Gautam Aror, Dhruv Tyagi, Abhinav Singh,Ranit Pal, Adarsh Kumar Mishra, Vishesh Jain*	

Article 65	**Event Management Systems (EMS)** *Gautam Arora, Nitish Kumar, Aryan Mandal, Ankit Yadav, Aman Pratap Yadav Ritik Kumar*	
Article 66	**Vegetable & Fruit Leaf Disease Detection Using DCNN & Enhanced Dataset** *Someswara Rao K S N, Chiriki Usha, Sesham Uday Kiran, T. Hari Priya, B. Krishna Sai, Ramana babu challapalli*	
Article 67	**Movie Recommendation System Using Content Based Filtering** *Kusuma.S, Charunayana V, Shruthi J R, Vinutha G K, Shivaraj, Mohamed Waseem*	
Article 68	**Feature Selection and Optimization for Cardiovascular Disease Prediction** *Dr. Poorna Priya Putcha, Dr. P. Pavitra, Lakshmi Amulya Chellapilla, Vasantha Dhuli, Uma Malleswari Boddeti, Sandhya Atmakuri*	
Article 69	**SURVEILLANCE VIDEO ANALYTICS USING LLM-BASED SUMMARIZATION AND CAPTIONING** *Yamuna H, A H Shanthakumara*	
Article 70	**GROUNDNUT DISEASE DETECTION WITH EFFICIENT DEEP LEARNING AND MODEL COMPRESSION** Sandra Jeslena Wesley, Getzi Jeba Lellipushpam Paulraj, Immanuel Johnraja Jebadurai	
Article 71	**IDENTIFICATION OF DAMAGE TO THE GAS PIPELINE INNER WALL USING AN IMAGE SEGMENTATION** *Rebaka Suneel Kuma, Podipireddy Amrutha, Vechalapu. L.V.R.Durga, S.Venumadhavi[4], P.Venkateswararao,*	

	Rohan Sarkar	
Article 72	**Automated Blood Group Detection System Using Image Processing for Non-Invasive Antigen Feature Extraction and Classification** *M.Priyadharshika K. Varalakshmi R.Sakthi Kaviya Dr.N.Arumugam*	
Article 73	**OXYGEN LEVEL MONITORING SYSTEM FOR COAL MINING WORKERS** *Seethalakshmi , Gayathri , Jenesha J, MathiVadhana , Arishenbagam*	
Article 74	**Optimized 64-Bit Carry Select Adder Using Enhanced Full Adder for Reduced Power and Delay** *Sankara Rao Allada, Dr. Anjanee Kumar,Kandregula Jyoshna, Kirla Pravallika, B. Medisetti Chandrasekhar, Konathala Venkat*	
Article 75	**Design and Implementation of Under Water Optical Wireless Communication** *Trupti Shripad Tagare, B S Dheeraj, Krushik J P, Chandan D, Shrinidhi L Bijapur*	
Article 76	**Integrated Smart Home Automation System for Energy Efficiency** *Mahendran.S, Jeyanthan.p, Ganesh.M and Karthika.S*	
Article 77	**Design of Sub 6GHz Antenna for 5G Applications** *Kiran Poojary, Shashi Kumar G S and Praveen Kumar*	
Article 78	**SolarComm: Dynamic Energy Harvesting and Charging for EV's** *Trupti Shripad Tagare, Sanketh T S, Nitesh Yellapur, Sudeep S Shetty, Nikhil S*	
Article 79	**Intelligence-enabled DC Motor Control Utilizing Integrated Field Current and Armature Voltage** *Vikash Bhardwaj, Vijayalaxmi Biradar*	

Article 80	**Translation of Indian Sign Language to Text using an Edge Device** *Keshava.A, Murugan.M, Prakash.S and Malathi.S*	
Article 81	**SOC estimation in Electric Vehicles using optimized Deep Neural Networks with high-accuracy and computationally efficient approach** *Tejaswini S, Chandrashekar M Patil*	
Article 82	**Meta Learning combined with Federated Learning for Detecting Blackhole Attacks** *Rathina Kumar, Getzi Jeba Lellipushpam Paulraj, Immanuel Johnraja Jebadurai*	
Article 83	**Advanced Retinal Vessel Segmentation: Combining AGD-GIF, CRGCN, and Improved Mask R-CNN-PO** *R Ramji , S Devi*	
Article 84	**FIREFIGHTING BOT USING IMAGE PROCESSING** *Priyadharsini S, Ahamed Fayaz MK, Akash R, Praneeshraja BM*	
Article 85	**Numerical Analysis of All Inorganic Perovskite Tandem Solar Cell with PCE of 24.47 %** *Mukesh Bharadwaj, DeborajMuchahary*	
Article 86	**Voice Controlled Maze Game** *Dr.Hindumathi Voraganti, Joshitha Sathinedi, Jahnavi Majji, Rishika Pawar, Azra Gulnaz*	
Article 87	**Accident Severity Prediction Using Machine Learning Techniques** *S.V.V.Sai Kalyan, Shaik Mohammed Saif, Dr. Shanthi Thangam Manukumar*	
Article 88	**Design and Analysis of a CPW-Fed Dual-Band Antenna for Sub-1 GHz and Sub-6 GHz Applications** *E.Suganya, T. Anita Jones Mary Pushpa, T.Prabhu*	

Article 89	**Enhancement of breakdown voltage in AlGaN/GaN HEMT using air bridge recessed source filed plate** *Padmavathi M, Manikandan M*	
Article 90	**Reversible Logic Gates for Efficient Circuit Construction and Quantum Computing** *Manaswini R, Silamboli J, Kalyandurg Rafeeq Ahmed, Dhivyasri G, Manikandan M*	
Article 91	**Smart Adaptive Compression Footwear for Pregnancy: A Sensor-Driven Solution for Swelling and Foot Fatigue Relief** *Karthikeyan T, Dr. Prabakar S, Hariraam K, Jai Vignesh Balaji V, Neaya P M[5], Sakthivel S*	
Article 92	**DEEP LEARNING BASED PREDICTIVE FACE RECOGNITION: ADAPTING TO AGING AND FACIAL VARIABILITY** *M. Anand, Anju S Pillai, Krishna Priya R*	
Article 93	**A Multiband Implantable Antenna for Pacemaker** *Raghuramakrishnan S, Raguvarun G, Sabitha B, Bijimanzil A Sapna and Ramasamy .K*	
Article 94	**An Implantable Wideband Antenna for Monitoring Bone Fracture Healing** *Ameerdeen B, Bharathi P, Dhanasurya M, Sapna Bijimanzil A and Ramasamy K*	
Article 95	**DESIGN AND IMPLEMENTATION OF AN AUTOMATED SORTING SYSTEM FOR WASTE HANDLING** *Dr R Gowrishankar, Divyasre T, Aiswarya G, Muthusaravanan K, Ragavendhiran B*	
Article 96	**Webtrace An Automated Hate Speech Detection and Enforcement System for Instagram Using Playwright, OCR, and NLP** *G. Thiagarajan, Danend Krishnan U, Soniya N, Soniya N*	
Article 97	**Intelligent Admission Guidance for Higher Education:**	

	AI-Powered Chatbot *G Thiagarajan, Anitha K, Ranjitha P, Rithika B, Sangeetha K, Kaviya S*	
Article 98	**AI-powered video language translation system** *G Thiagarajan, A Banupriya, U Aravindhakumar, S Ambadikannan, I Shabbir khan*	
Article 99	**IoT - ENABLED SMART MEDICAL ALERTING SYSTEM** *Kalamani M, Boobendran B, Giriprasaath D, Lithyashree V*	
Article 100	**DETECTION OF CARDIOVASCULAR DISEASES IN ECG SIGNALS USING CNN** *Yash Chauhan, Shilpi Mohanty, Sunil Kumar, Monika Vishwakarma*	
Article 101	**Advancing Sustainable Mobility with Hybrid Energy Storage Systems for smart charging Applications Using Zeta-SEPIC Converters** *M Kowsalya ,Dr. J Anitha, Dr. Dhanraj G, Lakshmi Priya G, Dr. Silamboli J*	
Article 102	**Taguchi Based Optimization of SMAW and TIG Welding Process Parameters on HSLA-DMR249A steel** *G. Dhanraj, O. Raina, K. Deepa, M. Surendar and H. Gokulram*	
Article 103	**CAR DAMAGE SEVERITY ESTIMATION FOR INSURANCE** *Nisha Priya P, Priya V, Deepavahini M ,Pranesh R,Ajith M, Sanjeedha S*	
Article 104	**Advanced Machine Learning Techniques for Predicting House Prices: A Comparative Analysis** *Gautam Kumar*	
Article 105	**Secure QR Code Communication with Multi-Party**	

	Authentication and AES Encryption *A Saurabh and Dr T Balachander*	
Article 106	**GESTURE-CONTROLLED VIRTUAL MOUSE FOR HANDS-FREE NAVIGATION** *J. Amutha, S. Priyadarsini, M. Rabin,* *M. Raja Muniyandi, B. Raja Pandi, UG Student*	
Article 107	**Review of "Automating Attendance with Image & Video Recognition - A Facial Recognition Based System": A Comprehensive Study** *Mrs. Mrunmayee Hatiskar, Sakshi Sawant, Samruddhi Charapa, Siddhi Kadam, Sanika Gajane*	
Article 108	**SMART POWER ANALYSIS FOR DIGITAL CIRCUITS USING MACHINE LEARNING** *Ms.SK Shabeena* **,***Gavara Likhitha Mallempudi Leela Saranya*[3]**,***Ganta Satish***,** *Mr. Rebaka Suneel Kumar*	
Article 109	**Advanced Denoising Techniques for Enhanced Medical Imaging** **K S N V Someswararao1, K Soma Sekhar**[2]**,Gurrala** *Rupasri, Bokam Swetha,Rongali Charmila , Sarita Rani Panda*	
Article 110	**Emotion Detection using Image Analysis** *Jandhyam Lakshmi Alekhya, Grandhi Sri Satya Bhargav, Nalluri Karthik, Jangala Venkata Sai Poojith*	
Article 111	**IOT Based Smart Trolley with User Tracking System** *Komathy Vanitha Krishnan, Angeline Felicia, Sharumitha, Preethi*	

The **First International Conference on Computer, Computation, and Communication (IC3C-2025)**, organized by the **Department of Electronics and Communication Engineering at CSI College of Engineering (CSICE), Ketti, Ooty, Tamil Nadu, India**, was successfully held on **March 28–29, 2025**. This inaugural edition of IC3C brought together a diverse assembly of researchers, academicians, industry professionals, and students from across the world to discuss the latest trends, innovations, and research findings in the fields of **Computer Science, Computational Intelligence, and Communication Technologies**.

The conference served as a vibrant platform for interdisciplinary collaboration and intellectual exchange. It featured a distinguished lineup of keynote speakers, invited talks, and technical sessions that addressed contemporary challenges in the digital world and explored technological solutions aligned with **Sustainable Development Goals (SDGs)**. IC3C-2025 also provided an invaluable networking opportunity for participants, promoting collaborations and partnerships that will extend beyond the event.

This volume of conference proceedings presents a collection of peer-reviewed papers accepted for presentation during IC3C-2025. Each contribution reflects high-quality research and valuable insights into emerging areas of computer and communication technologies, computational methodologies, and their real-world applications.

The organizing committee expresses its heartfelt gratitude to all authors, reviewers, keynote speakers, session chairs, and participants whose enthusiastic involvement made IC3C-2025 a resounding success. Special thanks to River Publishers for publishing the conference proceedings and facilitating submission for Web of Science and Scopus indexing.

We look forward to future editions of IC3C, continuing this journey of knowledge sharing and innovation.

Editors:

Dr Om Prakash Kumar, Manipal Institute of Technology, Manipal, India

Dr. Pradeep Kumar, University of KwaZulu-Natal, Durban, South Africa

Dr.J.Silamboli , CSI College of Engineering (CSICE), Ketti, Ooty, Tamil Nadu, India

Message from Chaiman

Rt. Rev. Timothy Ravinder
Bishop & Chairman



Dear Esteemed Participants and Distinguished Guests,

It is my privilege and honor to welcome you to the **First International Conference on Computer, Computation, and Communication (IC3C-2025)**, organized by the Department of Electronics and Communication Engineering at CSI College of Engineering (CSICE), Ketti, Ooty, Tamil Nadu. Our institution is committed to fostering academic excellence and nurturing creativity, and we are thrilled to host this assembly of brilliant minds and forward-thinkers.

In a world that constantly evolves, driven by rapid technological advancements and the pursuit of solutions to pressing global challenges, conferences like IC3C-2025 play a pivotal role. They offer us the opportunity to come together, share our insights, and collectively envision a brighter future. The themes of this conference—Computer Science, Computational Intelligence, and Communication Technologies—hold particular significance. They underscore our shared commitment to forging new frontiers and driving positive change.

As we embark on this intellectual journey, I encourage you to embrace the spirit of collaboration. It is through collaboration that we harness the collective wisdom of diverse perspectives and arrive at transformative breakthroughs. Be open to the exchange of ideas, engage in robust discussions, and let curiosity be your guide.

I also wish to express my appreciation to the organizing committee, presenters, participants, and everyone who has worked tirelessly to make IC3C-2025 a reality. Your dedication to the pursuit of knowledge and the betterment of society is commendable.

Thank you for being a part of this momentous occasion. I look forward to witnessing the positive impact that will undoubtedly emerge from IC3C-2025. Together, we can build a brighter and more informed future.

Message from Correspondent

Mr. Godwin R Daniel
Correspondent



Dear Esteemed Guests, Distinguished Speakers, and Respected Participants,

I am delighted to extend a warm and hearty welcome to all of you at the **First International Conference on Computer, Computation, and Communication (IC3C-2025)**, organized by the Department of Electronics and Communication Engineering at CSI College of Engineering (CSICE), Ketti, Ooty, Tamil Nadu. It is a great honor for our institution to bring together experts, scholars, and professionals from around the world to share knowledge, insights, and experiences.

Conferences like IC3C-2025 play a pivotal role in advancing our understanding of sustainable development and in fostering collaboration among researchers, educators, and practitioners. They provide a platform for the exchange of ideas, the exploration of new frontiers, and the development of innovative solutions to the challenges we face in our ever-evolving world.

At CSICE, we take immense pride in being at the forefront of academic and research excellence. We are committed to the pursuit of knowledge and to the dissemination of cutting-edge research that can make a positive impact on our society. This conference is a testament to that commitment.

I encourage you all to actively participate in the sessions, engage in meaningful discussions, and establish connections that will last beyond the conference. Your contributions and insights are invaluable, and they will undoubtedly shape the future of information technology and sustainable development.

I would like to express my deep appreciation to the organizing committee, speakers, sponsors, and everyone who has worked tirelessly to make IC3C-2025 possible. I am confident that this conference will be a remarkable and enriching experience for all of you. May it be a source of inspiration and a catalyst for new discoveries.

Wishing you a fruitful and enlightening conference.

Message from Director

Dr. P D Arumairaj
Director

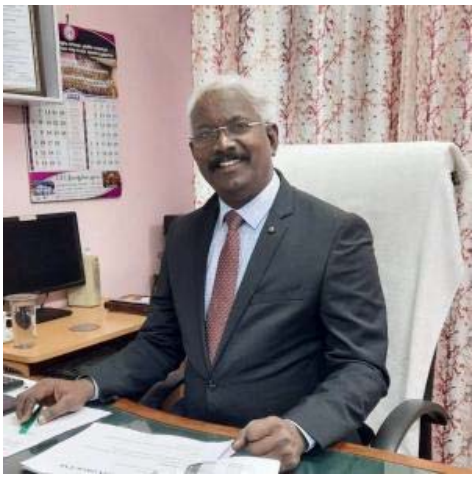

It gives me immense pleasure to announce that the Department of Electronics and Communication Engineering at CSI College of Engineering (CSICE), Ketti, Ooty, Tamil Nadu, is organizing the **First International Conference on Computer, Computation, and Communication (IC3C-2025)** on March 28-29, 2025. This conference will feature distinguished speakers from both national and international academic institutions, covering domains of recent advancements. Industry experts will also contribute valuable insights, enriching the discourse on the latest developments in computer science, computational intelligence, and communication technologies.

IC3C-2025 represents a convergence of minds dedicated to pioneering research and sustainable practices, providing an excellent opportunity for all participants to share their expertise and expand their knowledge. The conference provides a unique platform for researchers, technology solution seekers, experts, and entrepreneurs to build bridges, share space, and network with peers, thereby attempting to develop innovative solutions towards meeting targeted sustainable development goals.

All accepted and registered papers will be published as conference proceedings by River Publisher and forwarded for possible indexing in Web of Science and Scopus databases. Thus, IC3C-2025 serves as an invaluable platform for researchers to network, exchange ideas, and advance progress in research and development.

I warmly welcome all to IC3C-2025 at CSICE and wish the conference and the organizing team all the success and happy learning to all participants.

Message from Principal

Dr. R. Mercy Shanthi

Principal



Dear Participants, Esteemed Guests, and Honored Colleagues,

I am extremely happy to note that the Department of Electronics and Communication Engineering at CSI College of Engineering (CSICE), Ketti, Ooty, Tamil Nadu, is organizing the First International Conference on Computer, Computation, and Communication (IC3C-2025). This event provides an opportunity for researchers, academicians, practitioners, and industrialists to discuss recent advances in diverse areas of engineering disciplines.

At CSICE, we are committed to fostering a research culture that aims at improving quality technical education and responding to rapid economic and technological developments, both at national and international levels. Conferences like IC3C-2025 play a pivotal role in advancing our understanding of sustainable development and in fostering collaboration among researchers, educators, and practitioners.

I would like to thank all the authors, reviewers, and delegates for their rich contributions and participation. May this conference be an enriching, pleasant, and memorable experience!

Wishing you all an inspiring and enriching experience at IC3C-2025!

Message from Head of the Department

Dr. K Komathy Vanitha
Professor & Head



I am extremely happy to announce that the Department of Electronics and Communication Engineering at CSI College of Engineering (CSICE), Ketti, Ooty, Tamil Nadu, is organizing the **First International Conference on Computer, Computation, and Communication (IC3C-2025)** on March 28-29, 2025. This conference provides an excellent opportunity for researchers, academicians, and industry professionals to come together and exchange ideas, innovations, and research findings in the fields of computing, computational intelligence, and communication technologies.

IC3C-2025 aims to serve as a platform for interdisciplinary discussions and collaborations that can drive technological advancements and sustainable solutions for global challenges. The conference will host distinguished speakers from academia and industry, who will share their insights on emerging trends and breakthroughs in the field.

We are proud to provide a venue for young researchers and seasoned professionals to engage in meaningful discussions, gain new perspectives, and establish fruitful collaborations. I encourage all participants to actively engage in the sessions, make valuable contributions, and take advantage of this opportunity to expand their knowledge and professional networks.

I extend my sincere gratitude to all the authors, reviewers, organizing committee members, and sponsors for their unwavering support in making IC3C-2025 a success. I am confident that this conference will be an inspiring and intellectually stimulating experience for all.

Looking forward to welcoming you to IC3C-2025 and wishing you a productive and insightful conference!

Message from General Chairs

Dear Esteemed Participants, Distinguished Guests, and Researchers,

It is with great enthusiasm that we welcome you to the **First International Conference on Computer, Computation, and Communication (IC3C-2025)**, organized by the Department of Electronics and Communication Engineering at CSI College of Engineering (CSICE), Ketti, Ooty, Tamil Nadu. This conference is a landmark event dedicated to fostering research, innovation, and collaboration in the rapidly evolving fields of computer science, computation, and communication.

The digital revolution continues to reshape our world, and IC3C-2025 aims to provide a dynamic platform for researchers, academicians, and industry professionals to share knowledge, discuss emerging trends, and explore innovative solutions to contemporary technological challenges. Through keynote speeches, technical paper presentations, and networking opportunities, this conference will facilitate valuable exchanges that will shape the future of technology.

We are honored to have eminent speakers and experts contributing their insights, enriching the conference discussions, and guiding the next generation of innovators. The hard work and dedication of our organizing committee and technical reviewers have ensured a high standard of research contributions, and we deeply appreciate their efforts.

We extend our gratitude to all authors, presenters, and attendees for their active participation. Your engagement and enthusiasm are the driving forces behind the success of IC3C-2025. We hope this conference provides you with valuable insights, meaningful connections, and inspiration for future research endeavors.

Wishing you all an intellectually rewarding and successful conference!

Warm Regards,
General Chairs, IC3C-2025

Dr.R.Chandrasekaran CSICE, Ketti

Dr.J.Silamboli CSICE, Ketti

Dr. Pradeep Kumar, University of KwaZulu-Natal, Durban, South Africa

Dr. Om Prakash Kumar, MIT, Manipal

A REVIEW OF INDIAN HERBAL APPROACHES FOR VITILIGO: REPIGMENTATION POTENTIAL OF PSORALEA CORYLIFOLIA AND MORINGA OLEIFERA EXTRACTS

K Mythili [1] , Dr. S. Prabakar [2], K Varshini [3], T Ashwanthika [4], S L Tharun [5]

[12345]*Sona College of Technology, India*

[1]mythili.bme@sonatech.ac.in, [2]prabakar.bme@sonatech.ac.in,

[3]varshinicruk@gmail.com,[4]ashwanthikathirukkumar@gmail.com ,

[5]tharunsl915@gmail.com

ABSTRACT

Non-Segmental Vitiligo (NSV) is an autoimmune skin disease characterized by the presence of depigmented patches of skin due to a chronic loss of melanocytes. Current therapies includes topical steroids, narrowband UVB, and surgical interventions are commonly used but can carry risks such as skin thinning, irritation, or long-term health concerns. This study explores the potential review of *Psoralea corylifolia* and *Moringa oleifera* extracts as a potential natural solution for non-segmental vitiligo. Both are rich in antioxidant compounds and antimicrobial properties which help neutralize free radicals and reduce oxidative stress, a factors linked to vitiligo. *Psoralea corylifolia* is high in psoralen, stimulates melanocyte activity by exposing to UVA light, forms covalent bonds with DNA, leading to cross-links between DNA strands that promotes the migration of melanocytes from hair follicles into depigmented areas. Moringa oleifera, recognized for its high antioxidant and skin-repairing properties, contains flavonoids, an essential enzyme for melanin synthesis which supports melanocyte regeneration. Both *Psoralea corylifolia* and *Moringa oleifera* effectively addresses cosmetic aspects and cause of vitiligo by enhancing melanocyte activity, which makes this treatment an efficient substitute for traditional therapies.

Keywords— Repigmentation, Psoralea corylifolia, Moringa oleifera, Psoralen, Flavonoids.

I. INTRODUCTION

Vitiligo is a non-familial depigmenting skin condition characterized by the selective disappearance of melanocytes, thus resulting in sharply demarcated, chalky white macules that lack pigment [1]. Affecting around 0.1%–2% of the global population, vitiligo primarily appears on exposed areas such as the face, hands, and other regions with skin pigmentation, although it can affect the entire body[5].Advances in our understanding of vitiligo have classified it as an autoimmune disease associated with genetic susceptibility and environmental triggers[1].

A. Findings from Literature Insights

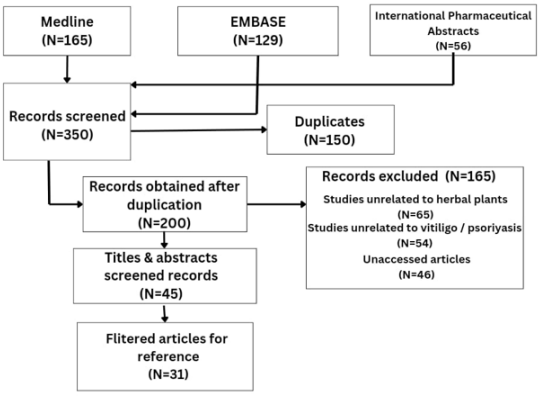

Figure 1: Flowchart on searching and selection of articles.

There seems to be 80% genetic contribution, leaving behind 20% that contributes to the development of vitiligo through environmental triggers[5]. Oxidative stress disrupts melanocytes and to subsequent complexity in the immune system in the form of immune cytokines and exosome secretion, which keeps leading tissue to destruction. As a result, cytotoxic CD8+ T cells and interferon-γ (IFN-γ) are generated in a feedback loop, which repeatedly recruits T cells to affected areas[6].

We conducted a systemic review across research databases, including PubMed, ScienceDirect, and Google Scholar, to gather multidisciplinary materials such as research articles, patents, theses, and books (See Figure 1). Initially, 350 articles were identified, but those did not focus on conditions like vitiligo therapy and duplicates were excluded from our selection. This refinement process led to the identification of 200 relevant articles. Of these, an additional 165 articles were excluded since those are unrelated to herbal therapies and unassessed articles. Finally, 31 articles with efficient role on herbs for treating vitiligo were retained for analysis.

B. Pathophysiology

Vitiligo is a multifactorial disorder in which the functional melanocytes are selectively lost, resulting in areas of depigmentation on the skin. Although many mechanisms have been proposed over the years, the current consensus is that it is an autoimmune condition, and that innate and adaptive immune responses participate in the progressive loss of melanocytes. Key mechanisms are genetic predispositions, oxidative stress, liberation of inflammatory mediators and cellular detachment processes-all of which go to determine the melanocyte destruction witnessed in patients presenting with the disease of vitiligo[6]. Melanocytes produce DAMPs (Damage-Associated Molecular Patterns) upon oxidative insult, which stimulates the innate immune system. In addition, Hsp70i (Inducible Heat Shock Protein 70**)** has been shown to enhance DC (Dendritic Cell) cytotoxicity, which promotes the activity of cytotoxic CD8+ T cells potentially accelerates melanocyte damage in the context of cellular stress[26].

C. Prevalence

Vitiligo is the most prevalent depigmenting skin condition, affecting 0.5 - 2 percent of the global population in both adults and children. Vitiligo affects people of all ethnicity and skin types equally[18]. Males and females are equally impacted, yet women and girls seek counsel more frequently probably because the negative social influence than for men and boys. Non segmental vitiligo can occur in all ages, but approximately fifty percent of the patients develop it before 20 years old; most commonly at around age ten. Populations with bimodal distribution of the age of onset or more than one peak were considered to have an intermediate effect size as far reported[19].

II. CLASSIFICATION

Two broad classifications for vitiligo exist, non-segmental vitiligo (NSV) and segmental vitiligo (SV), which characterize the extent of vitiligo spread. The majority form of NSV presents on symmetric body parts-often on the face, neck, hands, and feet. NSV encompasses subtypes: each delineated according to the appearance and arrangement of depigmentation. Generalized vitiligo features widespread, scattered white patches across various areas, while acrofacial vitiligo is specific to the facial orifices and distal fingers. Universal vitiligo, a rare form, involves over 80% of the body's surface area[1]. Mixed vitiligo combines segmental vitiligo with any non-segmental form, often resulting in complex depigmentation patterns[16] (See Figure 2).

Mucosal vitiligo is another variety of NSV, in which mucous membranes are affected, mostly involving oral and genital mucous membranes. Focal vitiligo is a precursor to generalized forms and typically appears as isolated patches within a small area, and this pattern remains stable over time. Unique regional types of vitiligo include "lip-tip" vitiligo, where depigmentation occurs around the lips, fingertips, and toes primarily in individuals from Southern Asia[12] (See Figure 2).

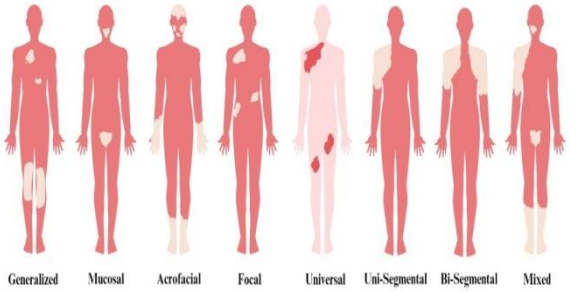

Figure 2: Classification of Vitiligo

Segmental vitiligo (SV), also known as unilateral vitiligo, generally occurs in younger patients and is less frequent than NSV. This is characterized by block-like or linear depigmented patches on one side of the body, and does not cross the midline. SV often rapidly progresses over six months to two years and then stabilizes, often with the appearance of leukotrichia (white hair) in the affected areas. Compared to NSV, SV is relatively insensitive to the treatment and is linked with lower autoimmune diseases as its common characteristic, which is typically more in NSV cases[1] (See Figure 2).

III. CONVENTIONAL TREATMENT

The conventional treatments for Repigmentation of vitiligo includes afamelanotide, prostaglandin E2 and the prostaglandin analogue bimatoprost. In these patients, more notable repigmentation can be observed where traditional treatment with oral corticosteroids failed. The JAK inhibitors like ruxolitinib, Methotrexate, and cyclophosphamide also shows promising results when given along with phototherapy- NB-UVB, although some adverse effect koebnerization have been noted. Moreover, PUVA therapy or psoralen with UVA is effective in adult patients, although monitoring is needed due to potential side effects[6]
(See Figure 3).

Topical treatments are essential for localized vitiligo to minimize adverse effects. For stabilizing vitiligo, oral therapies such as corticosteroids aim to prevent new lesion formation but require careful monitoring. Also, extracts such as Cucumis melo have catalase-like activity and have mixed results. Several natural products, including Callumae (containing L-phenylalanine and antioxidants) and Polypodium leucotomos (FernBlock®), have also been explored indicating enhanced efficacy when combined with narrowband UVB or UVA therapy[12,20,30](See Figure 3).

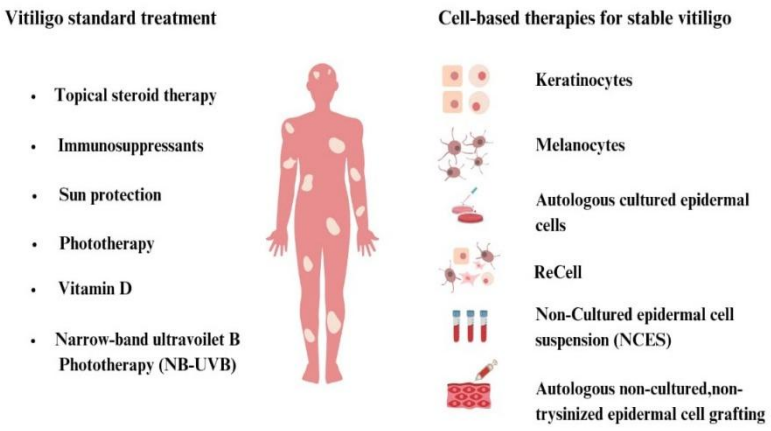

Figure 3: Treatment for Vitiligo

For patients unresponsive to medications or phototherapy, surgical options like skin grafting, blister grafting, and cellular
suspension transplant have been employed, targeting stable restoration of color. However, these methods entail risks such as scarring, infection, and abnormal pigmentation. Other topical agents like Vitilax and Novitil are commercially available for vitiligo, but evidence for effectiveness is not very strong. Agents with phototoxic activity such as Psoralea corylifolia, khellin, and barberry root are also reported; however, their safety in phototherapy and with sunlight exposure must be viewed with caution. Integrating therapies and balancing safety with effectiveness remains essential in the management of vitiligo, as individualized approaches often yield the best outcomes[6,20] (See Figure 3).

A. Side Effects

Phototherapy for vitiligo should preferably use UVB because it inhibits cytokine activity and prevents apoptosis in skin cells. Such treatment further activates inactive melanocytes in the hair follicle and allows these cells to proliferate and migrate into the depigmented areas in vitiligo. While having certain advantages, this mode of treatment possesses its demerits. Principle Side Effects includes Painful Burns, Itching, Dry skin, Increased Sensitivity of Skin, Hyperpigmentation, Enhanced Cancer Risk. Side effects accrued can attest to the necessity for carefully intertwined therapy guidelines. The use of emollients, sunscreen, and topical creams can palliate some of those side effects, further enhancing the efficacy and vitiligo treatment with UVB phototherapy[31].

IV. MORINGA OLEIFERA AND PSORALEA CORYLIFOLIA

Moringa oleifera is a perennial tropical deciduous arbor belonging to the family of Moringaceae; it originated in India and has been widely planted in Asia, Africa, and tropical and subtropical regions of Central America. Moringa oleifera has an important economic value and it is rich in active compounds such as flavonoids, phenols, phytosterols, carotenoids, quercetin and kaempferol. It has broad pharmacological properties, including anti-oxidation, anti-inflammation, anti-diabetes, lipids lowering, anti-cancer, and anti-bacterial, among others. Moringa oleifera as it is famously known as the "miracle tree" powerhouse of bioactive compounds that contribute to its numerous medicinal properties[28]. It decreases inflammation, oxidative stress, protect cells from scavenging free radicals, and promotes skin health In particular, β-carotene help to maintain healthy pigmentation and guard against UV-induced skin damage.

Psoralea corylifolia is an annual plant growing up to 50 - 90 cm tall and bears corolla, a pale purple flowers on short, condensed axillary spikes that has been widely used as a in traditional Chinese and Indian medicine. The seeds of this species contain coumarins, which are psoralen[2]. Bakuchi oil, derived from Psoralea corylifolia seeds, which includes flavonoids (neobavaisoflavone, isobavachalcone, bavachalcone, bavachinin, bavachin, corylin, corylifol, corylifolin, and 6-prenylnaringenin), coumarins (psoralidin, psoralen, isopsoralen, and angelicin), and meroterpenes (bakuchiol and 3-hydroxybakuchiol)[2,27].

A. Versatile Applications on Treating Vitiligo

Both *Moringa Extract* and *Psoralea corylifolia* are traditional as well as efficient remedy in managing and treating vitiligo. It tyrosinase which induces melanin production that helps to restore pigmentation. Antioxidants present mitigates oxidative stress (Reactive Oxygen Species ROS) prevents melanocytes from apoptosis. It modulates immune response CD8+T cells which is more important in autoimmune mediated destruction[2,5,6,19,27,28]. Hence, herbal combination addresses different aspects of vitiligo pathogenesis in restoring pigmentation and preventing further melanocyte damage.

V. CONCLUSION

While investigating the Indian herbal remedies for vitiligo, two botanicals, namely *Psoralea corylifolia* and *Moringa oleifera*, have shown to be effective in treating the disease. There are indications that *Psroalea Corylifolia* can enhance the growth and activity of melanocytes as well as the production of the pigment melanin due to its high composition of psoralen. In addition, *Moringa Oleifera* is known to possess immunomodulatory and antioxidant properties which may also help facilitate the repigmentation process. These extracts have therefore provided a more integrated method of treating vitiligo which seeks to incorporate traditional Ayurveda medicine as well as contemporary science. More clinical studies and controlled trials are also encouraged to

demonstrate the optimal dosages, assess the long-term outcomes and the effectiveness in different ethnicity groups. This means integrating this approach to treatment of vitiligo may lead to development of safer, affordable and culturally appropriate options for patients with the condition in dermatology which is more organic and customized herbal therapeutic remedy to the patients.

VI. REFERENCES

[1] Abdel-Malek, Zalfa A., Christian Jordan, Tina Ho, Parth Rajendrakumar Upadhyay, Alan Fleischer, and Iltefat Hamzavi. "The enigma and challenges of vitiligo pathophysiology and treatment." *Pigment cell & melanoma research* 33, no. 6 (2020): 778-787.

[2] Abeysekera, Ajita Mahendra, Kamal Bandara Gunaherath, Ajantha Rohinie Gunawardena, and Champa Disala Jayaweera. "Studies on the composition and standardization of 'Bakuchi oil,' an Ayurvedic medicinal oil prepared from Psoralea corylifolia L. used in the treatment of vitiligo." *International Journal of Research in Ayurveda & Pharmacy* 3, no. 3 (2012).

[3] Abu-Raghif, Ahmed Rahmah, Noor Mustafa Ali, Iqbal Ghalib Farhood, MOHAMMED FAREED, and HAYDER B. SAHIB HAMEED. "Evaluation of a standardized extract of ginkgo biloba in vitiligo remedy." *Asian J Pharm Clin Res* 6, no. 5 (2013): 127-130.

[4] Al-Snafi, Ali Esmail. "Chemical constituents and pharmacological activities of Ammi majus and Ammi visnaga. A review." *International Journal of Pharmacy and industrial research* 3, no. 3 (2013): 257-265.

[5] Bergqvist, Christina, and Khaled Ezzedine. "Vitiligo: a focus on pathogenesis and its therapeutic implications." *The Journal of dermatology* 48, no. 3 (2021): 252-270.

[6] Bergqvist, Christina, and Khaled Ezzedine. "Vitiligo: a review." *Dermatology* 236, no. 6 (2020): 571-592.

[7] Bishnoi, Anuradha, and Davinder Parsad. "Clinical and molecular aspects of vitiligo treatments." *International journal of molecular sciences* 19, no. 5 (2018): 1509.

[8] Chen, Jianru, Shuli Li, and Chunying Li. "Mechanisms of melanocyte death in vitiligo." *Medicinal Research Reviews* 41, no. 2 (2021): 1138-1166.

[9] Chen, Ling, and Zhu Shen. "Tissue-resident memory T cells and their biological characteristics in the recurrence of inflammatory skin disorders." *Cellular & molecular immunology* 17, no. 1 (2020): 64-75.

[10] Costin, Gertrude-EE, and Vincent J. Hearing. "Human skin pigmentation: melanocytes modulate skin color in response to stress." *The FASEB journal* 21, no. 4 (2007): 976-994.

[11] Cui, Tingting, Weigang Zhang, Shuli Li, Xuguang Chen, Yuqian Chang, Xiuli Yi, Pan Kang et al. "Oxidative stress–induced hmgb1 release from melanocytes: a paracrine mechanism underlying the cutaneous inflammation in vitiligo." *Journal of Investigative Dermatology* 139, no. 10 (2019): 2174-2184.

[12] Dwivedi, Mahendra. "Preventing Vitiligo with Herbal Remedies." *Journal of Pharma and Ayurved Research* 1, no. 1.

[13] El Mofty, Abdel Monem, and Medhat El Mofty. "Vitiligo: a symptom complex." *International Journal of Dermatology* 19, no. 5 (1980).

[14] Ezzedine, Khaled, and Nanette Silverberg. "A practical approach to the diagnosis and treatment of vitiligo in children." *Pediatrics* 138, no. 1 (2016).

[15] Forschner, Tobias, Stefan Buchholtz, and Eggert Stockfleth. "Current state of vitiligo therapy–evidence-based analysis of the literature." *JDDG: Journal der Deutschen Dermatologischen Gesellschaft* 5, no. 6 (2007): 467-475.

[16] Gondalia, Shamana Rajesh, B. Chuhan, Monika Rakholia, and Divya Kanojiya. "A Review on a Vitiligo and its Cure from Nature." *Gis Sci J* 9, no. 5 (2022): 1383.

[17] Hamzavi, Iltefat, Hem Jain, David McLean, Jerry Shapiro, Haishan Zeng, and Harvey Lui. "Parametric modeling of narrowband UV-B phototherapy for vitiligo using a novel quantitative tool: the Vitiligo Area Scoring Index." *Archives of dermatology* 140, no. 6 (2004): 677-683.

[18] Le Poole, I. C., P. K. Das, R. M. J. G. J. Van Den Wijngaard, J. D. Bos, and W. Westerhof. "Review of the etiopathomechanism of vitiligo: a convergence theory." *Experimental dermatology* 2, no. 4 (1993): 145-153.

[19] Narayanaswamy, Radhakrishnan, and Intan Safinar Ismail. "Role of herbal medicines in vitiligo treatment–current status and future perspectives." *Asian J. Pharm. Clin. Res* 11 (2018): 19-23.

[20] Nazar, Tarique. "Prevention and Treatment of Vitiligo."

[21] Ongenae, Katia, Nanny Van Geel, and Jean-Marie Naeyaert. "Evidence for an autoimmune pathogenesis of vitiligo." *Pigment Cell Research* 16, no. 2 (2003): 90-100.

[22] Paarakh, Padmaa M. "Nigella sativa Linn.–A comprehensive review." (2010).

[23] Padmakar, Somanaboina, G. Ajay Kumar, Navneet Khurana, Sweta Kumari, and Biplab Pal. "Efficacy and safety of natural Aloe Vera gel in the treatment of stable vitiligo." *Clinical Epidemiology and Global Health* 22 (2023): 101332.

[24] Pang, Yaobin, Shi Wu, Yingjie He, Qing Nian, Jing Lei, Yejing Yao, Jing Guo, and Jinhao Zeng. "Plant-derived compounds as promising therapeutics for vitiligo." *Frontiers in pharmacology* 12 (2021): 685116.

[25] Poleo, A. G., and J. E. Rojas. "Natural product in cream with anti-vitiligo therapeutic properties." *Eur. Pat. Appl* (2007).

[26] Seneschal, Julien, Katia Boniface, Andrea D'Arino, and Mauro Picardo. "An update on Vitiligo pathogenesis." *Pigment cell & melanoma research* 34, no. 2 (2021): 236-243.

[27] Sharma, Anupama, and Girish Chandra Sharma. "Biochemical evaluation of depigmentation in C57/BL6 mice and its treatment by Psoralea corylifolia. Linn (Bakuchi) seed oil and seed extracts."

[28] Sushmitha, K., and Kavitha G. Singh. "In Vivo therapeutic study of Repigmentation of Depigmented patches in Vitiligo disorder isolated Tyrosinase of Moringa oleifera and other Extracts in Zebra Fish Embryo." *Journal of Survey in Fisheries Sciences* 10, no. 1S (2023): 6544-6553.Francisco Javier Ropero Peláez1 and Shirley Taniguchi, "The Gate Theory of Pain Revisited: Modeling Different Pain Conditions with a Parsimonious Neurocomputational Model". Published on 19 August 2015.

[29] Van Den Boorn, Jasper G., et al. "Skin-depigmenting agent monobenzone induces potent T-cell autoimmunity toward pigmented cells by tyrosinase haptenation and melanosome autophagy." *Journal of Investigative Dermatology* 131, no. 6 (2011): 1240-1251.

[30] Yoon, Jimi, Young-Woo Sun, and Tae-Heung Kim. "Complementary and alternative medicine for vitiligo." *Vitiligo—Management and Therapy* (2011): 143-158.

[31] Yu, Richard, et al. "Transcriptome analysis reveals markers of aberrantly activated innate immunity in vitiligo lesional and non-lesional skin." *PloS one* 7, no. 12 (2012): e51040

Biographies



Ms. K. Mythili received the bachelor's degree in Biomedical Engineering from Dr. N.G.P Institute of Technology, Coimbatore in 2016, the master's degree in Biomedical Engineering from SRM Institute of Science and Technology, Kattankulathur in 2018, and Pursing the philosophy of doctorate degree in Biomedical Engineering from Anna University since 2022, respectively. She is currently working as an Assistant Professor at the Department of Biomedical Engineering, Sona College of Technology, Salem, Tamil Nadu. Her research areas include Biomaterials, Regenerative Medicine and Tissue Engineering.

Blockchain Technology: Trusted Crowdfunding Platform Using a Smart Contract

Gaurang Bharadava[1] Madhav Desai[2] Anshuman Prajapati[3] Manav Bagthaliya[4] Priyanka Patel[5]

[1,2,3,4,5] *Smt. Kundaben Dinsha Patel Department of Information Technology, Chandubhai S. Patel In-stitute of Technology, Faculty of Technology & Engineering, Charotar University of Science and Technology (CHARUSAT), Changa-388421, Gujarat, India.,*

priyankapatel.it@charusat.ac.in

Abstract.

Advances in digital technology brought about in the recent past by blockchain's transparency, security, and decentralization have changed things. The present paper discusses a blockchain-enabled crowdfunding platform that eliminates fraud, processes that go undocumented, and accountability issues that arise in the existing systems. Automation takes place with the use of Ethereum blockchain and smart contracts. The implementation of the smart contract employs Solidity, testing and deployment is handled through Foundry, and wallet integration is with MetaMask. HTML and JavaScript facilitate user navigation, moving blockchain nearer to the user interface. The platform addresses problems such as latency and complexity, providing a trustless, low-cost funding system. Future updates can incorporate token integration and cross-chain compatibility for increased stability and user adoption.

Keywords. Blockchain, Crowdfunding, Ethereum, Smart Contracts, Decentral-ized Systems, Solidity, Foundry, Metamask, Secure Transactions, Decentralized Applications (dApps).

1. INTRODUCTION

Blockchain, first put forward in 2008 as the foundation of Bitcoin [1], is now a key technology for digital networks. It securely stores data within a decentralized network, not allowing for alterations [2]. Because it can make encrypted, reliable, and unchangeable records, it is useful for a range of applications. Crowdfunding, in which individuals and organizations collect money publicly [1], usually is plagued by trust and security challenges in conventional models [3, 4]. Blockchain technology resolves crowdfunding challenges using decentralization, transparency, and immutability. Smart contracts release funds automatically, monitor transactions, and do away with intermediaries, saving costs and increasing security [3, 4]. This paper suggests a trustless crowdfunding model based on blockchain and smart contracts, overcoming the conventional constraints through a decentralized and transparent framework [5, 6]. This flow explains how a blockchain-based crowdfunding platform works with Ethereum and smart contracts. Users initiate transactions via wallets like MetaMask, which securely stores private keys [2]. Transactions enter Ethereum's "Transaction Pool" for miner validation. Once confirmed, the block is added to the blockchain, ensuring transparency and immutability.

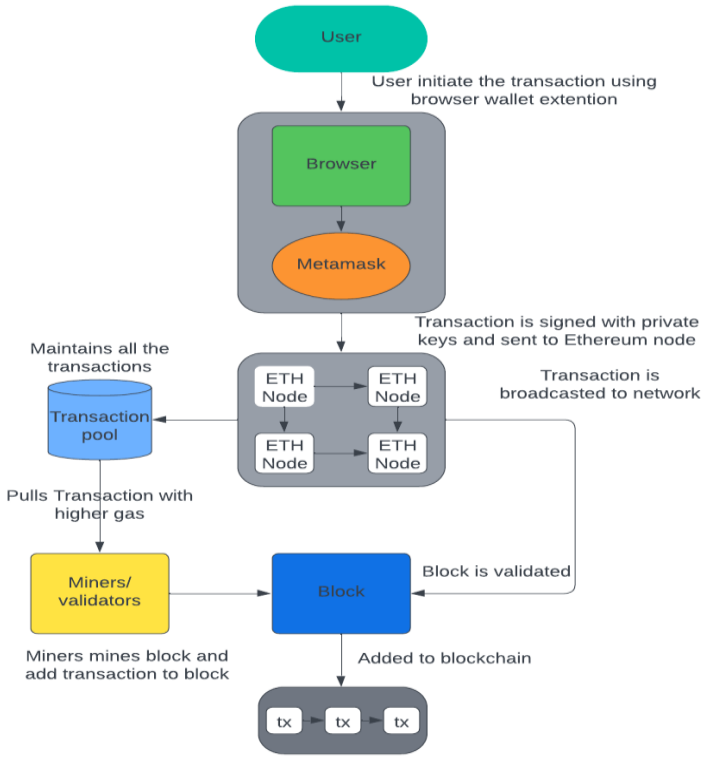

Figure 1 Blockchain Architecture.

This flow explains how a blockchain-based crowdfunding platform works with Ethereum and smart contracts. Users initiate transactions via wallets like MetaMask, which securely stores private keys [2]. Transactions enter Ethereum's "Transaction Pool" for miner validation. Once confirmed, the block is added to the blockchain, ensuring transparency and immutability.

2. PREVIOUS RESEARCH

Blockchain is improving crowdfunding through security and reliability. Trust in the platform and project creator in lending-based crowdfunding is important [8]. Blockchain platforms such as Nasdaq Linq remove intermediaries, facilitate direct transactions, and lock in voting [6, 9]. Smart contracts for automatic fund disbursement enhance transparency and security [5]. Decentralization of Blockchain improves efficiency, lowers costs, and enhances trust, although energy usage is an issue [4, 8]. Studies indicate blockchain can revolutionize raising funds by hardening trust [3].

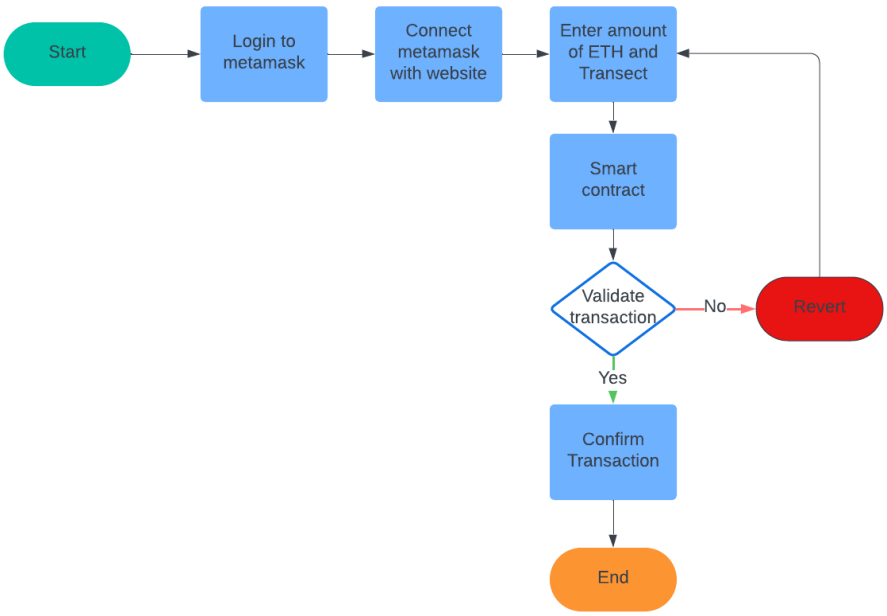

Figure 2 Work flow of the application.

The diagram shows the user journey in a blockchain-based crowdfunding system using MetaMask [2]. The user links MetaMask to the platform, enters their Ether (ETH) contribution [2, 4], and the transaction is verified for validity and sufficient funds [3, 5]. If valid, the transaction enters a queue for miners to add it to the block-chain [2, 3]. This process emphasizes user experience and the security of blockchain crowdfunding, including wallet management [8, 10].

3. TECHNOLOGIES USED

Our project leverages **Ethereum** for its secure and transparent smart contract support. We use **Solidity** to implement fund holding, controlled withdrawals, and access management. **Foundry**, including **Anvil**, enables local testing with unit, integration, and fuzz testing to ensure contract reliability. **MetaMask** facilitates secure user interaction, managing accounts and transaction signing. The frontend is built with **HTML** and **JavaScript**, utilizing **web3.js** or **ethers.js** for blockchain connectivity. JavaScript handles key actions like funding, balance checks, and withdrawals, ensuring seamless communication with the Ethereum network.

4. RESULT ANALYSIS



Figure 3 Frontend of the platform.

5. CONCLUSION

This crowdfunding platform demonstrates how blockchain technology can transform traditional crowdfunding by enhancing transparency, security, and reliability. Built on the Ethereum blockchain, it leverages smart contracts to automate fund management, eliminating third-party intermediaries. MetaMask ensures seamless integration and security, while an intuitive HTML and JavaScript-based frontend enhances user experience. By addressing fraud, delays, and accountability issues, this project improves the efficiency of crowdfunding ecosystems. Future enhancements could include token integration and cross-chain compatibility to expand functionality and improve user experience.

6. REFERENCES

[1] Nakamoto, S. (2008). Bitcoin: A Peer-to-Peer Electronic Cash System. Retrieved from https://bitcoin.org/bitcoin.pdf

[2] Zheng, Z., Xie, S., Dai, H., Chen, X., & Wang, H. (2017). An Overview of Blockchain Tech-nology: Architecture, Consensus, and Future Trends. IEEE International Congress on Big Data. DOI: 10.1109/BigDataCongress.2017.85

[3] Buterin, V. (2013). Ethereum: A Next-Generation Smart Contract and Decentralized Appli-cation Platform. Retrieved from https://ethereum.org/en/whitepaper/

[4] Kosba, A., Miller, A., Shi, E., Wen, Z., & Papamanthou, C. (2016). Hawk: The Blockchain Model of Cryptography and Privacy-Preserving Smart Contracts. IEEE Symposium on Se-curity and Privacy. DOI: 10.1109/SP.2016.55

[5] Saadat, M. N., Halim, S. A., Osman, H., Nassr, R. M., & Zuhairi, M. F. (2019). Blockchain Based Crowdfunding Systems. Indonesian Journal of Electrical Engineering and Computer Science, 15(1), 409-413. DOI: 10.11591/ijeecs.v15.i1.pp409-413

[6] Zhu, H., & Zhou, Z. Z. (2016). Analysis and Outlook of Applications of Blockchain Tech-nology to Equity Crowdfunding in China. Financial Innovation, 2(29). DOI: 10.1186/s40854-016-0044-7

[7] Moysidou, K., & Hausberg, J. P. (2020). In Crowdfunding We Trust: A Trust-Building Model in Lending Crowdfunding. Journal of Business Venturing Insights, 14(e00189). DOI: 10.1016/j.jbvi.2020.e00189

[8] Cumming, D. J., Leboeuf, G., & Schwienbacher, A. (2020). Crowdfunding Models: Keep-it-All vs. All-or-Nothing. Financial Review, 55(3), 435-458. DOI: 10.1111/fire.12225

[9] Chen, S., Shi, R., Ren, Z., Yan, J., Shi, Y., & Zhang, J. (2018). A Blockchain-Based Supply Chain Quality Management Framework. Proceedings of the IEEE 14th International Con-ference on e-Business Engineering. DOI: 10.1109/ICEBE.2018.00034

[10] Wu, J., & Tran, N. K. (2018). Application of Blockchain Technology in Sustainable Energy Systems: An Overview. Sustainability, 10(9), 3067. DOI: 10.3390/su10093067

Biographies

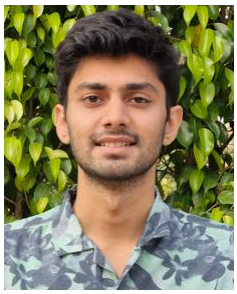

Gaurang Bharadava is a pre-final year undergraduate student passionate about blockchain, smart contracts, and decentralized applications. He and his team recently won the **Jury Innovation Prize** at **Hack IITK**, securing ₹1,00,000 for their innovative solution. **Madhav Desai** specializes in blockchain technology, focusing on decentralized solutions for secure transactions. **Anshuman Prajapati** is an Machine Learning developer experienced in AI and data-driven applications along with web based applications. **Manav Bagthaliya**, also an Machine Learning developer, works on predictive modeling and AI-driven automation. **Dr. Priyanka Patel**, the corresponding author, researches blockchain and machine learning integration for secure and intelligent decentralized systems.

A Comprehensive Review of Ethnopharmacological Strategies in Post-C-Section Lumbar Pain Management

K Mythili [1] , Dr. S. Prabakar [2], L.Swetha [3], AP Saranya [4], G.Rajeshwari [5]

[12345]*Sona College of Technology, India*

[1]mythili.bme@sonatech.ac.in, [2]prabakar.bme@sonatech.ac.in,

[3]swethalakshmanan160@gmail.com,[4]saranyaap1334@gmail.com ,

[5]gceema9@gmail.com

Abstract.

Most women experience painful lower back pain that is caused by conditions like menstrual cramps, endometriosis, bad posture, ovarian cysts, menopause, and especially after a C-section, where there can be chronic pain after giving birth. In this paper, we focus specifically on women who experience Lower Back Pain (LBP) from a Cesarean Section (C-section), which can be chronic. Causes of such chronic pain involve anesthesia given at the time of procedure, higher BMI, wrong posture, endocrine imbalance, excessive lifting, and extended lactation. Mainstream treatments in the form of exercises, hot or cold, and medication also often have a risk of adverse effects like dizziness and nausea. These are successfully treated using ethnopharmacological remedies with high anti-inflammatory and antioxidant activities. Numerous herbal derivatives have been used traditionally for their pharmacological effects, providing a pharmaceutical-free way of pain management. Their mechanism of action is consistent with the Gate Control Theory of Pain, acting as natural analgesics that modify inflammatory pain by blocking the NF-κB pathway. This blockade prevents pro-inflammatory cytokines and enzymes from being formed and prevents local inflammation and pain transmission. By stimulating larger nerve fibers, these remedies facilitate the closure of the pain gate, thus alleviating discomfort. With few side effects and high ethnopharmacological efficacy, these herbal remedies are an ideal alternative to the treatment of LBP in women after C-section delivery. This review seeks to summarize and discuss the role of various ethnopharmacological remedies in the management of lower back pain, particularly in women after C-section delivery.

Keywords : Cesarean section, Ethnopharmacological interventions, Gate Control Theory, Lower back pain, Pain management

1. INTRODUCTION

Lower back pain (LBP) is becoming a common problem among women because of causes such as menstrual cramps, endometriosis, poor posture, ovarian cysts, menopause, and hormonal imbalance. In this chapter, the post-Caesarean section (C-section) pain is discussed, and how appropriate pain management and postoperative care are essential during this critical phase of motherhood is highlighted. A flowchart illustrates the treatment plan developed by researchers to manage pain in female patients undergoing a Csection.

A. Findings from Literature Insights

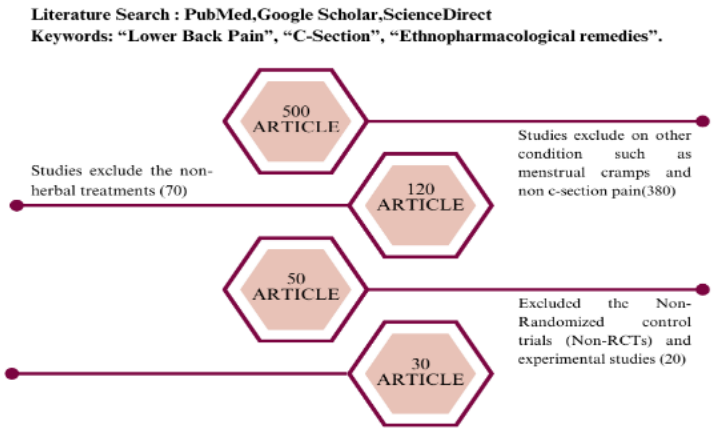

Figure 1: Flowchart on searching and selection of articles.

We conducted a comprehensive search across research databases, including PubMed, ScienceDirect, and Google Scholar, to gather multidisciplinary materials such as research articles, patents, theses, and books (see Figure 1).Initially, 300-400 articles were identified, but those that did not focus on conditions like C-section or natural remedies were excluded from our selection. This refinement process led to the identification of 50 relevant articles. Of these, an additional 20 articles were excluded based on their use of non-randomized controlled trials (RCTs) or experimental studies. Consequently, 30 articles with strong evidence on herbal medicine's role in pain management were retained for analysis.

B. Etiology of Pain

There are several factors involved in LBP in women after C-section, as shown in Figure 2. Spinal anesthesia reduces lumbar lordosis and disrupts transmission of nociception, leading to chronic pain in nearly 80% of patients[1,2,3]. Increased BMI puts excessive stress on the lower back, leading to posture and mobility impairment and also chronic inflammation[1,3].Poor posture, especially during breastfeeding and baby care, overstrains lumbar muscles and increases pain [1,3,4]. Hormonal fluctuations, such as increases in relaxin levels, loosen the pelvic ligaments and result in pain and instability[1,4]. Ascending and lifting heavy babies also contribute to lumbar strain, extend recovery time, and establish chronic LBP as a result.

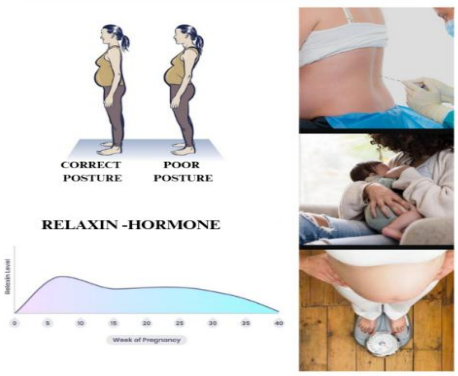

Figure 2: Etiology of pain

C. Conventional Pain Management Therapy

Analgesic pharmacological treatment includes use of Over-the-Counter (OTC) medications and medication treatments, such as Non-Steroidal Anti-Inflammatory Drugs (NSAIDs) Ibuprofen and Naproxen, analgesics Acetaminophen (Tylenol), opioid analgesics Oxycodone and Hydrocodone, muscle relaxants Cyclobenzaprine and Methocarbamol, anticonvulsants Gabapentin and Pregabalin, topical analgesics Lidocaine patches and Capsaicin cream, and corticosteroids Prednisone, which are short-term medications but cause gastrointestinal disorders and liver injuries[1]. Physical therapy consists of exercise ordered by a therapist to enhance mobility

and reduce pain but potentially leading to muscle soreness, pain, and discomfort [1]. Heat and cold applications are a very common pain management technique, where heat in the form of a heating pad or warm compress is applied to relax spasms of the muscles and relieve pain, and cold is used to reduce inflammation, but repeated or inappropriate use can cause skin irritation, burns, pain, or frostbite[1]. Exercise, such as light activity involving walking and stretching, makes muscles stronger and more flexible but causes soreness and strain in muscles, especially when done incorrectly or excessively [1]. Massage therapy, such as Swedish and deep tissue massage, relaxes muscles and enhances circulation but at times causes temporary pain and bruising [1]. Transcutaneous Electrical Nerve Stimulation (TENS) is the process of using electrical stimulation to minimize pain, but it has short-term relief and sometimes causes skin irritation [1]. Techniques of relaxation like meditation and yoga are used in minimizing stress and pain with less side effects and are thus an effective and safe approach to pain management [1].

2. ETHNOPHARMACOLOGICAL REMEDIES FOR LOW BACK PAIN AFTER CESAREAN SECTION

Ethnopharmacology is the science of medicinal plants and their traditional uses in healing. Natural remedies have been used by many cultures for centuries to manage pain. These herbal remedies have bioactive compounds that are responsible for pain management and inflammation reduction as indicated in Figure 3 and Figure 4.

St. John's Wort: Hypericum perforatum is a well-known medicinal herb known for its use for centuries, native to Europe and Asia [5,16]. Some of the active principles in the genus include hyperforin, hypericin, and flavonoids, attributing its promising pharmacologic action. Used in herbal medicine, this herb finds a wide application in tea, extracts, and capsules [5,16,17].78

Ginger: Zingiber officinale is a Southeast Asian native plant that has become one of the most popularly used spices and medicinal herbaceous plants globally [5,12,15]. It includes bioactive substances such as gingerols and shogaols, fresh and dried ginger. Ginger has been used both as traditional medicine and in food and culinary preparations and supplements made in capsule form, teas, and extracts [5,12,15]

Turmeric: Curcuma longa, hailing from the Indian subcontinent and Southeastern Asia, is a golden-yellow condiment extensively employed in cooking, Ayurveda, and traditional Chinese medicine [5,11,12,13]. The chief bioactive compound of turmeric known as curcumin has potent anti-inflammatory and antioxidant properties, which helps significantly with the treatment of pain, especially in that related to arthritis and joint pains [5,11,12,13].

Nuts And Seeds: Nuts and seeds like walnuts, flaxseeds, and chia seeds are some of the finest plant-based sources of omega-3 fatty acids [5,14,27]. They contain alpha-linolenic acid (ALA), while its marine sources provide eicosapentaenoic acid (EPA) and docosahexaenoic acid (DHA). Foods rich in omega-3 fats are popular in daily diets, while concentrated sources are widely used in supplements[5,14,27].

Capsaicin: Chili peppers, originally domesticated on American continents, are of the genus Capsicum annuum. Dishes and medicine employ this as a source of significant compounds like capsaicin and dihydrocapsaicin found in concentrated form in the seeds and inner membranes of the pepper [5,19,20] . Capsaicin is utilized in cooking, topical creams, and patches for therapeutic purposes[5,18,19,20] .

Thunder God Vine: This herb, also referred to in the West as Thunder God Vine, is native to East Asia and has been used in traditional Chinese medicine for many centuries [5,22] . The plant has two primary compounds of interest-triptolide and celastrol, which are possibly the cause of its healing properties. Because of the strength of the vinegar, it is largely found in regulated herbal preparations and must be administered with care due to its toxic potential [5,22]

Butterbur: Native to Asia and Europe, Petasites hybridus is a perennial plant that has been traditionally applied in the management of disorders like migraine and muscle cramp [5,21]. The bioactives, petasin and isopetasin, of the herb are present mainly in the root and leaves[5,21]. Butterbur extracts need purification to eliminate pyrrolizidine alkaloids which could be harmful in raw form.

Feverfew:A native of Europe and the Balkan countries, Tanacetum parthenium has for centuries been widely known in herbal medicine [5,25]. Parthenolide, a major bioactive present in the leaves and flowers, is responsible for feverfew's traditionally recognized properties [5,25]. It is consumed in powdered, tinctured, or encapsulated forms and is widely respected in herbal therapy [5,25].

Willow Bark: Salix alba, indigenous to Europe, Asia, and North America, has been used in traditional medicine since antiquity [5,26]. Salicin, flavonoids, and polyphenols are among the most important components of bark [5,26]. Willow bark is processed into extracts, teas, and capsules in a natural approach for the treatment of pain.

Moringa Oleifera: Moringa oleifera, also known as the "Wonder Tree," originates from the Indian subcontinent [6,7,8,9,10]. This tree has numerous health benefits and consists of flavonoids, phenolic acids, and glucosinolates present in its leaves, seeds, and pods. Moringa is taken as powder, extract, or in the form of tea and is frequently combined with phytomedicine and nutritional supplements[6,7,8,9,10].



Figure 3: Ethnopharmacological Remedies in Pain Management

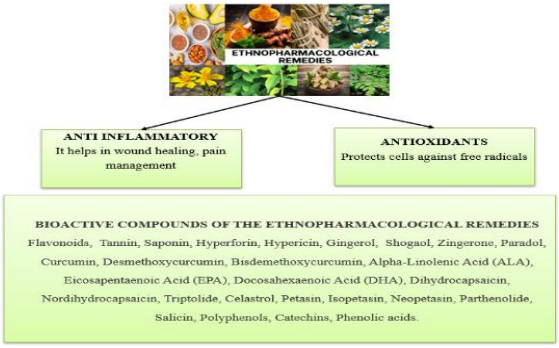

Figure 4: Bioactive Compounds of Ethnopharmacological Remedies in Pain Management

3. PAIN MANAGEMENT IN GATE CONTROL THEORY WITH ETNOPHARMACOLOGICAL REMEDIES

Low back pain, particularly post-C-section, starts when nociceptors in the tissues detect injury and transmit pain messages via A-delta and C fibers to the spinal cord[28,29,30]. The message arrives at the dorsal horn, where the Gate Control Theory of Pain decides whether to transmit the pain to the brain. When inflammation develops, pro-inflammatory mediators like prostaglandins, cytokines, and tumor necrosis factor-alpha (TNF-α) stimulate the nuclear factor kappa-light-chain-enhancer of activated B cells (NF-κB) pathway, enhancing the inflammation and keeping the gate of pain "open"[10,28,29,30].This makes more than usual pain signals travel to the brain, amplifying pain perception and causing it spreading to nearby tissues[10,28,29,30].Ethnopharmacological interventions, rich in anti-inflammatory and antioxidant action, control both pain transmission and the NF-κB pathway [10][26].These treatments contain bioactive compounds such as curcumin (turmeric)[5,11,12,13], gingerols (ginger) [5,12,15], and flavonoids (Moringa oleifera) [6,7,8,9,10], etc., which have robust analgesic and anti-inflammatory effects. These compounds act on sensory nerve fibers and modify the gate control system by stimulating large-diameter A-beta fibers, which could "close the gate" and diminish pain perception [10,26]. In addition, they inhibit NF-κB activation and ensuing inflammatory cytokine expression and thereby reduce inflammation. Since inflammation and oxidative stress increase pain sensitivity, the inhibition of the NF-κB pathway retards the excessive generation of inflammatory mediators such that pain is localized and does not spread to other areas of the body [10,26,28,29,30]. Thus, not only do these remedies possess anti-inflammatory activity, but the bioactive molecules present in them also induce the secretion of endorphins, which enhance the body's intrinsic pain control mechanism. This coordinated activity leads to efficient as well as localized pain relief along with preventing chronic pain development. The site-specific and long-term release of these bioactive compounds from ethnopharmacological

treatments triggers extended pain, along with inhibiting inflammatory pathways like NF-κB, preventing excessive pain signaling, and restricting pain amplification through the nervous system.

4. VERSATILE APPLICATIONS OF ETHNOPHARMACOLOGICAL REMEDIES IN PAIN MANAGEMENT

Ethnopharmacological drugs have been used extensively in analgesic treatment, and recent technology has enhanced their activity through improved extraction, formulation, and drug delivery. Salix tetrasperma (willow plant) is phytochemically extracted and salicin derivative profiled, resulting in oral formulations like capsules, teas, and tinctures for systemic pain relief and topical formulations like ointments and creams for relief from local musculoskeletal pain[5,26]. St. John's Wort (Hypericum perforatum) is formulated into nanotechnology drug delivery systems like solid lipid nanoparticles (SLN) and nanostructured lipid carriers (NLC) to improve neuroprotection and bioavailability, while LC–MS/MS and liquid chromatography are applied in flavonoid and phenolic acid profiling [5,16,17]. Moringa oleifera has been studied by in vitro and in vivo research, drug development and nutraceuticals, and food functionalism with follow-up oral products like capsules, powders, teas, and food functional foods for systemic inflammation and antioxidant effects and topical creams and ointments for local inflammation and pain [6,7,8,9,10].Curcuma longa or turmeric and its bioactive compound curcumin are investigated by clinical trials, molecular targeting of inflammatory processes, and pharmacological studies to develop oral formulations such as powders, tablets, tablets, capsules, and topical formulations such as gels, patches, and ointments for inflammatory pain disorders[5,11,12,13]. Such developments in herbal medicines also maximize ethnopharmacological strategies to alleviate pain to achieve the maximum bioavailability and therapeutic activity.

5. CONCLUSION

In conclusion, this review puts into perspective the potential therapeutic applications of ethnopharmacological medicines for treating post-C-section lower back pain (LBP) through accessing bioactive molecules that act to modulate inflammatory mechanisms, notably NF-κB, and supplement the Gate Control Theory of Pain for effective analgesia. Other than pain alleviation in the postpartum setting, these medications exhibit multi-faceted application in pain management, including systemic relief through oral delivery, localized use through topical delivery, and bioavailability enhancement through the use of nanotechnology-based drug delivery systems. With the integration of the ancient traditional herbal medicine with modern pharmacological technology, ethnopharmacology offers an eco-friendly, non-invasive, and effective remedy for treating diseases of chronic pain with lesser side effects than in conventional therapy.

7. REFERENCE

1. Sahaya Packia Shanthi M, N. Gayathiri, Jissy Paul E, Prevalence of back-pain following caesarean section under spinal anesthesia" Published on 4 August 2023.
2. Hizir Kazdal,Ayhan Kanat,Bulent Ozdemir ,Vacide Ozdemir,Ali Riza Guverci,"Does-the anesthesia technique of cesarean section cause persistent low back pain after delivery? A retrospective analysis"Published on 5 October 2022.
3. Mukhopadhyay A, Bhattacharyya A, Chanda S, Syamal A.K. "Spinal anesthesia during cesarean section and persisting low back pain: a cross sectional study in West Bengal, India",Published on 25 November 2019.
4. Nusrat Rasheed, Muhammed Hassaan Khan, Naseem Rashee. "Comparison of Incidence of Low Back Pain in Women with Normal Vaginal Delivery and Cesarean Section".Published on 29 December 2017.

5. Behdad Jahromi 1, Iulia Pirvulescu 1 , Kenneth D. Candido 1,2,3 and Nebojsa Nick Knezevic. “Herbal Medicine for Pain Management: Efficacy and Drug Interactions”.Published on 11 February 2021.
6. Zahidul Islam , S. M. Rashadul Islam , Faruk Hossen , Kazi Mahtab-ul-Islam ,Md. Rakibul Hasan , and Rezaul Karim, “Moringa oleifera is a Prominent Source of Nutrients with Potential Health Benefits”.Published on 11 August 2021.
7. Navnidhi Chhikara, Amolakdeep Kaur, Sandeep Mann, “Bioactive compounds, associated health benefits and safety considerations of Moringa oleifera L.: an updated review”.Published on 16 May 2020.
8. Dewa Gde Rismanandha Adiwira, Made Niko Winay, Ni Luh Nopi Andayani, “The effect of moringa oleifera leaf as an anti-inflammatory: a literature review”, 22 November 2023.
9. Abideen Adeyinka Adekanmi , Sherifdeen Adeniyi Adekanmi , Opeyemi shafiu Adekanmi, “Qualitative and Quantitative Phytochemical Constituents of Moringa Leaf”.Published on 5 May 2020.
10. Marcela Vergara-Jimenez , Manal Mused Almatrafi and Maria Luz Fernandez, “Bioactive Components in Moringa Oleifera Leaves Protect against Chronic Disease”. Published on 16 November 2017.
11. Adeeb Shehzad, Gauhar Rehman, Young Sup Lee,“Curcumin in Inflammatory Diseases”.Published on 22 December 2012.
12. Gamal Ramadan, Mohammed Ali Al-Kahtani, Wael Mohamed El-Sayed, “Anti-inflammatory and Anti-oxidant Properties of Curcuma longa (Turmeric) Versus Zingiber officinale (Ginger) Rhizomes in Rat Adjuvant-Induced Arthritis” Published on August 2011.
13. Louay Labban, “Medicinal and pharmacological properties of Turmeric (Curcuma longa)” published on 04 April 2014.
14. Santiago R Unda, Emilce A Villegas, María Eugenia Toledo, Gabriela Asis Onell, Carlos H Laino, “Beneficial effects of fish oil enriched in omega-3 fatty acids on the development and maintenance of neuropathic pain”.Published on 26 December 2019.
15. Parvin Rahnama1, Ali Montazeri, Hassan Fallah Huseini, Saeed Kianbakht, Mohsen Naseri, “Effect of Zingiber officinale R. rhizomes (ginger) on pain relief in primary dysmenorrhea: a placebo randomized trial” Published on 2012.
16. Paweł Rychlewski,Elham Kamgar,Sylwia Mildner-Szkudlarz,Przemysław Łukasz Kowalczewski,Joanna Zembrzuska, “Determination of the contents of bioactive compounds in St. John’s wort (Hypericum perforatum): Comparison of commercial and wild samples” Published on 25 May 2023.
17. Monica Vazzana,Ana S. Macedo, Antonello Santini, Caterina Faggiol,Eliana B. Souto, “Novel Neuroprotective Formulations Based on St. John’s Wort Extract” Published on 10 April 2014.
18. Shaherin Basith, Minghua Cui, Sunhye Hong and Sun Choi, “Harnessing the Therapeutic Potential of Capsaicin and Its Analogues in Pain and Other Diseases” Published on 23 July 2016.
19. Simona Mirel1, Liora Colobățiu1, Mihaela Mirel2, Sorina Pop, “Topical patches as treatments for the management of patient musculoskeletal and neuropathic pain” Published on 01 February 2017.
20. Sunita Babbar, Jean-Francois Marier, Mohamad-Samer Mouksassi, Martin Beliveau, Geertrui F. Vanhove, Sanjay Chanda, Keith Bley, “Pharmacokinetic Analysis of Capsaicin After Topical Administration of a High-Concentration Capsaicin Patch to Patients With Peripheral Neuropathic Pain” Published on 5 April 2009.
21. Mary Giles, PharmD Catherine Ulbricht, PharmD Karta Purkh Singh Khalsa, CDN, RH Catherine DeFranco Kirkwood, MPH, CCCJS-MAC Christine Park, PharmD Ethan Basch, MD, “Butterbur: An Evidence-Based Systematic Review by the Natural Standard Research Collaboration”.Published on 20 July 2014.

22. Longhe Yang, Yanting Li , Jie Ren , Chenggang Zhu , Jin Fu , Donghai Lin ,Yan Qiu, “Celastrol Attenuates Inflammatory and Neuropathic Pain Mediated by Cannabinoid Receptor Type 2” Published on 6 August 2014.
23. Henik Tri Rahayu, Ning Sri Rahayu,Sunardi Sunardi, “The Effectiveness of Red Ginger Compress Therapy (Zingiber officinale rosc. var. rubrum) on Elders with Joint Pain” Published on 2017.
24. R.Surl , K. Martin , F. Liebel , P. Lyte , S. Shapiro1,M. Southall, “Anti-Inflammatory Activity of Parthenolide-Depleted Feverfew (Tanacetum parthenium)” Published on 30 December 2008.
25. Rengin Baydar, Ayşe Esra Karadağ, Sevde Nur Biltekin, Etil Güzelmeriç, Fatih Demirci4, “In vitro anti-inflammatory activities of Tanacetum parthenium L. extract and its major metabolite parthenolide “. Published on 25 September 2023.
26. Pei-Qian WuYing LiYu-Hao RenJun-Su ZhouQun-Fang LiuYan WuJin-Hai YuBin Zhou*Jian-Min Yue. “Anti-Inflammatory Salicin Derivatives from the Barks of Salix tetrasperma” .Published on 11 April, 2024.
27. Dean M. Cordingley 1,2 and Stephen M. Cornish, “Omega-3 Fatty Acids for the Management of Osteoarthritis: A Narrative Review”.Published on 16 August 2022.
28. Ronald Melzack, “Gate control theory: On the evolution of pain concepts”. Published on 5 May 2011.
29. Massieh Moayedi and Karen D. Davis, “ Theories of pain: from specificity to gate control” .Published on 1 October 2012.
30. Francisco Javier Ropero Peláez1 and Shirley Taniguchi, “The Gate Theory of Pain Revisited: Modeling Different Pain Conditions with a Parsimonious Neurocomputational Model”. Published on 19 August 2015.

Biographies



Ms. K. Mythili received the bachelor’s degree in Biomedical Engineering from Dr. N.G.P Institute of Technology, Coimbatore in 2016, the master's degree in Biomedical Engineering from SRM Institute of Science and Technology, Kattankulathur in 2018, and Pursing the philosophy of doctorate degree in Biomedical Engineering from Anna University since 2022, respectively. She is currently working as an Assistant Professor at the Department of Biomedical Engineering, Sona College of Technology, Salem, Tamil Nadu. Her research areas include Biomaterials, Regenerative Medicine and Tissue Engineering.

Remote Sensing Analysis of Urbanization and Agricultural Land Conversion in Bantwal Taluk, Karnataka

Janardhana Bhat K. [1, 3]***, Babitha Ganesh*** [2, 3]***, Om Prakash Kumar*** [1]***, Shweta Vincent*** [2]***, * and Basappa B. Kodada*** [4]

[1] *Department of Electronics and Communication Engineering, Manipal Institute of Technology, Manipal Academy of Higher Education, Manipal, 576104, Karnataka, India*

[2] *Department of Mechatronics, Manipal Institute of Technology, Manipal Academy of Higher Education, Manipal, 576104, Karnataka, India*

[3] *Department of Computer Science and Engineering, Canara Engineering College, Bantwal, 574219, Karnataka, India*

[4] *Department of AIML, Canara Engineering College, Bantwal, 574219, Karnataka, India*

Summary: Understanding changes in Land Use and Land Cover (LULC) is critical to good environmental management and urban planning. This study uses Landsat 8 Collection 2 imagery to investigate LULC variations in Bantwal Taluk, Dakshina Kannada, between 2013 and 2024. Maximum Likelihood Classification (MLC), Support Vector Machine (SVM), and Random Forest (RF) were used to identify and classify six LULC classes: dense vegetation, vegetation, waterbodies, built-up areas, barren land, and floodplains. Accuracy points created in ArcMap were confirmed against Google Earth Pro ground truth data. RF had the highest accuracy, with 88.33% in 2013, 90% in 2018, and 86.67% in 2024, surpassing MLC and SVM. The findings revealed major LULC transitions, such as urban expansion by 10.43% and agricultural land reduction by 22,42% between 2013 and 2024. This study provides critical information for environmental planning, disaster management, and sustainable land use in Bantwal Taluk by doing extensive LULC mapping and change analysis.

Keywords: Land Use Land Cover (LULC), Landsat, Pansharpening, Maximum Likelihood Classification (MLC), Support Vector Machine (SVM), Random Forest (RF), Change Detection.

1. INTRODUCTION

Changes in Land Use and Land Cover (LULC) are crucial for monitoring environmental trends and successfully managing resources. Bantwal Taluk in Dakshina Kannada, which borders the Western Ghats, is facing considerable environmental issues as a result of deforestation, urbanization, and unpredictable climate. Intense monsoon rains, landslides, and rising temperatures endanger agriculture, water supplies, and livelihoods, needing prompt mitigation efforts [1].

LULC changes arising from activities such as forestry and urbanization frequently spread beyond their origins, affecting ecosystems worldwide. Their rapid growth desires good management to balance development with environmental preservation while mitigating biodiversity loss and resource depletion [2].

LULC models, which include top-down and bottom-up techniques, help with urban planning and land management. While top-down models examine broader patterns utilizing a variety of variables, bottom- up models concentrate on localized dynamics and individual land-use decisions, providing complementary viewpoints [3].

Bantwal Taluk in Karnataka's Dakshina Kannada District is facing climate concerns such as flooding, landslides, and rising temperatures. LULC mapping and change detection analysis assist in identifying drivers, assessing disaster risks, and guiding sustainable land management.

A study conducted in [4] has shown dramatic LULC changes, such as a 46% forest loss and a built-up area rise from 13% to 55% between 2000 and 2022. However, there is a lack of details on preprocessing procedures, which are critical for enhancing classification accuracy. Furthermore, the machine learning classifiers employed for supervised classification lack clarity, which limits reproducibility and dependability. Another study in Dakshina Kannada ties LULC changes, particularly urbanization and vegetation loss, to diminishing groundwater levels, but ignores agricultural effects. This gap is essential since agriculture, a major local economic engine, has a large

impact on groundwater dynamics [5]. In order to fill these gaps, this study uses sophisticated preprocessing methods, such as pan sharpening, to improve picture quality and classification accuracy when constructing LULC maps for 2013, 2018, and 2024. Key transitions like urban sprawl and deforestation are identified and their effects are quantified using a thorough change detection analysis. This study offers vital information that can guide environmental planning, disaster management, and sustainable land use in Bantwal Taluk by carrying out thorough LULC mapping and change analysis. The Bantwal Taluk study area map is displayed in Fig. 1.

2. METHODOLOGY

The methodology followed, illustrated in Fig. 2, encompasses a series of systematic steps to achieve accurate land cover change detection: (1) Acquisition of Landsat 8 imagery for the years 2013, 2018, and 2024 from the USGS Earth Explorer platform; (2) Image preprocessing, including band stacking, pansharpening to enhance spatial resolution, and clipping to the delineated study area to ensure data consistency; (3) Implementation of multiple supervised classification algorithms, such as Maximum Likelihood Classification (MLC), Support Vector Machine (SVM), and Random Forest (RF), to categorize land cover types; (4) Generation of LULC maps followed by accuracy assessment using ground truth data and confusion matrices; (5) Selection of the optimal classification algorithm based on accuracy metrics to perform change detection analysis; and (6) Utilization of transition matrices to quantitatively analyze LULC changes over the specified periods.

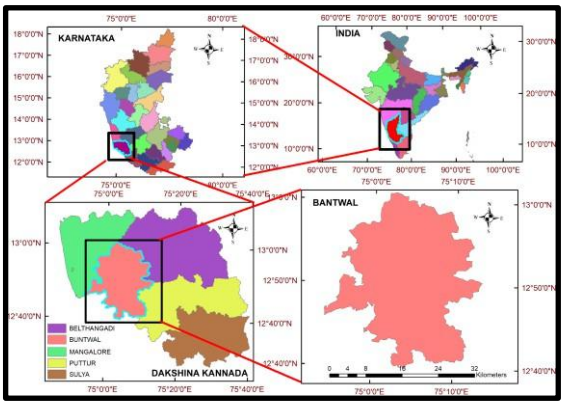

Fig. 1. Study area map of Bantwal Taluk.

2.1. *Data Source*

This study makes use of primary LANDSAT 8 OLI/TIRS satellite data from the USGS EarthExplorer platform in 2013, 2018, and 2024. Excellent surface reflectance and spatial precision are guaranteed by the Level-1 TOA Reflectance (L1TP) data, which is categorized as Collection T1. These images were chosen for their cloud-free conditions, which allowed for accurate LULC change analysis. They were projected in WGS_1984_UTM_43N and covered WRS Path 145/Row 51 for Bantwal Taluk.

2.2. *Preprocessing*

In order to improve spatial resolution for in-depth LULC analysis, this study used band stacking and the ESRI pan-sharpening approach on Landsat 8 images. While pan-sharpening combined the spectral richness of the multispectral bands with the 15 m spatial detail of the panchromatic band, band stacking combined seven multispectral bands with a resolution of 30 m into a coherent dataset. By refining multispectral bands to a 15 m resolution, this procedure made it possible to observe land cover features more finely [6], especially in the region of interest for Bantwal Taluk. The LULC categories—Dense Vegetation, Vegetation, Waterbodies, Built-Up, Barren Land, and Floodplain—were applied to Landsat imagery from 2013, 2018, and 2024. Visual image interpretation was used to identify distinct training patterns for every class.

2.3. *Classification*

Following the preparation of training samples, images were categorized into LULC classes using machine learning classification methods. Three classifiers were used in this study: RF, SVM, and MLC.

A popular parametric technique based on the Bayes principle, MLC assumes that data clusters form hyper-ellipsoids in multidimensional space. Using the covariance matrix, prior probability, and mean feature vectors, it determines the likelihood that each pixel belongs to a class and designates the class with the highest likelihood [7] [8]. Research demonstrates the efficacy of MLC for LULC categorization, particularly in watershed and agricultural study [9] [10] [11].

SVMs, which combine binary classifiers, are ideal for multi-class LULC classification because they are excellent at handling high-dimensional data. To ensure reliable pixel-based classification, the method finds the best hyperplanes in feature space to divide classes [12] [13]. Studies demonstrate that SVM performs better than more conventional techniques like MLC [9] [14].

Random Forest, an ensemble technique, uses bagging to merge several decision trees and increase classification accuracy. Compared to boosting approaches, it provides faster computation, can handle a variety of predictors, and is immune to noise and overfitting. [15] [16] [17]. RF has become well-known for its reliable remote sensing capabilities

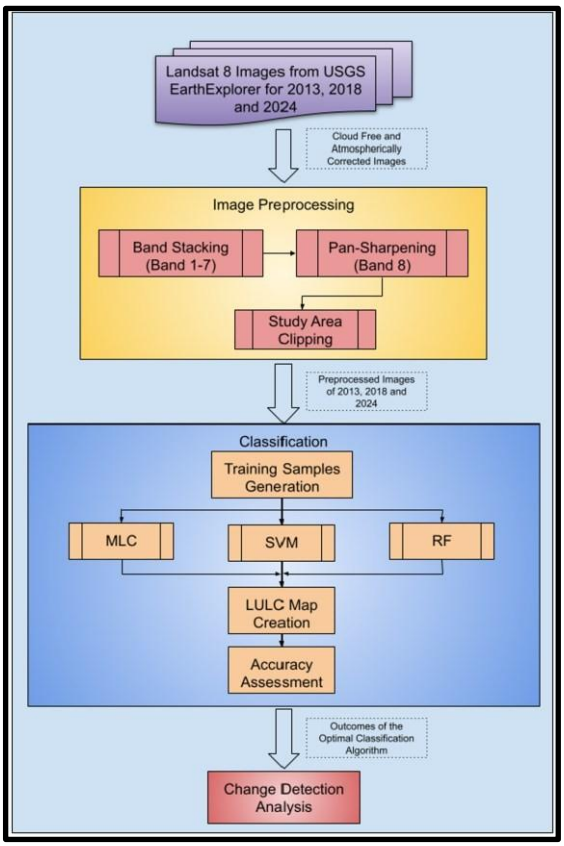

Fig. 2. Methodology

2.4. *Accuracy Assessment*

It is imperative to assess machine ML classifiers following their application to picture classification tasks in order to comprehend their efficacy and guarantee their dependability. The effectiveness of MLC, SVM, and RF classifiers for LULC classification (2013, 2018, 2024) was assessed by comparing projected classes with ground truth in confusion matrices. Calculations were made for metrics like recall, accuracy, precision, F1 score, and Kappa coefficient. To ensure dependable and thorough classification performance, precision gauges prediction accuracy, recall analyzes detection capacity, and the Kappa coefficient assesses agreement beyond chance.

2.5. *Change Detection*

This study applied the widely utilized post-classification comparison method [4] for change detection [18]. Each time period's images were classified separately, and the outcomes were arranged in a transition matrix [19]. This matrix shed light on the spatial distribution of LULC changes by recording and measuring inter-class transitions to highlight landscape change patterns.

3. Results and Discussions

Six LULC categories—Dense Vegetation, Vegetation, Waterbodies, Built-Up, Barren Land, and Floodplain—were identified from Landsat 8 images captured in 2013, 2018, and 2024 using MLC, SVM, and RF algorithms. The LULC maps for each approach are displayed in Figure 3 emphasizing variations in classification outputs over time brought about by the various methods.

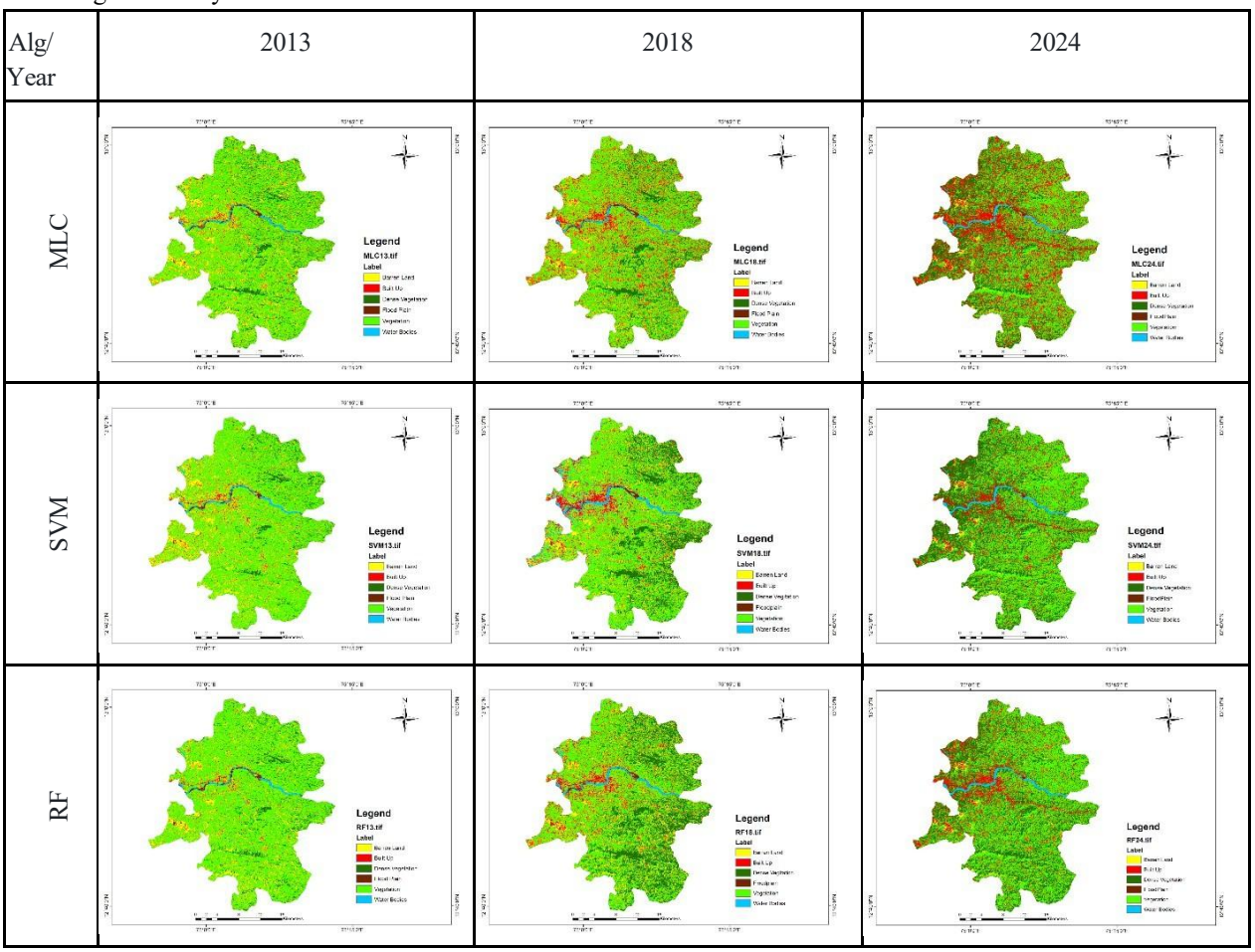

Fig. 3. LULC Maps using MLC, SVM and RF for the years (a) 2013, (b) 2018 and (c) 2024

The overall accuracy of the LULC classification in Bantwal Taluk is displayed in Figure 4, where the RF classifier had an average overall accuracy of 88.3%. By contrast, MLC and SVM both demonstrated reduced accuracy, with MLC reaching 71% and SVM 72.7%. With an average F1-score of 0.88, precision of 0.89, recall of 0.88, and a kappa value of 0.85, the RF classifier performed better than both MLC and SVM on all measures, as indicated in Table 1. On the other hand, MLC obtained a kappa value of 0.62, an F1-score of 0.71, a precision of 0.76, and a recall of 0.71. With an F1-score of 0.74, precision of 0.79, recall of 0.73, and a kappa value of 0.65, SVM performed marginally better than MLC. Compared to MLC and SVM, which need more parameter tuning and have limits in capturing fine details, RF is more effective and dependable for LULC classification due to its robust ensemble method, convenience of use, and capacity to handle complicated data.

The RF-based LULC classification observations for Bantwal Taluk show significant variations between 2013 and 2024. Dense vegetation grew from 61.47 sq. km in 2013 to 248.46 sq. km in 2024, while overall vegetation cover decreased, especially between 2013 and 2018, most likely due to urbanization. Built-up areas increased from 28.43 sq. km in 2013 to 105.71 sq. km in 2024, demonstrating urban growth. Barren land reduced from

115.19 sq. km in 2013 to 23.16 sq. km in 2024, indicating land rehabilitation. Water bodies and floodplains changed little, with water bodies decreasing somewhat from

11.38 to 10.26 sq. km. These transitions reflect ongoing land conversion, notably from agricultural to developed areas.

Significant changes in land cover throughout Bantwal Taluk are highlighted by the transition matrices derived from the LULC maps produced using the RF approach for the years 2013–2018 in Figure 5 (a-d) and 2018–2024 Figure 5 (e-h). These matrices show how land use has changed over time by providing comprehensive data on the area (in square kilometers) of each land cover type. Key trends are highlighted in Figure 5, which graphically depict the significant transitions seen in the study area.

Table 1. Performance metrics for the RF, MLC, and SVM classifiers.

Classifier	Precision	Recall	F1-Score	Kappa Value
MLC	0.89	0.88	0.71	0.62
SVM	0.79	0.73	0.74	0.65
RF	0.89	0.88	0.88	0.85

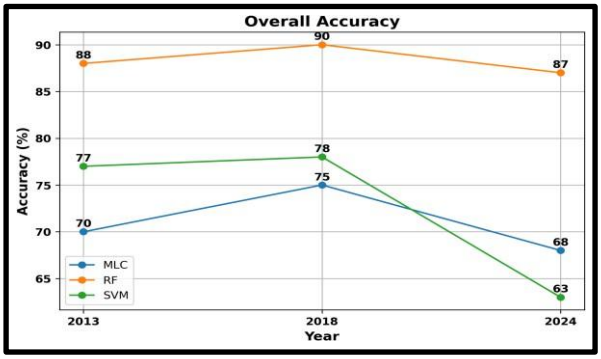

Figure 4. Average overall accuracy of MLC, SVM and RF

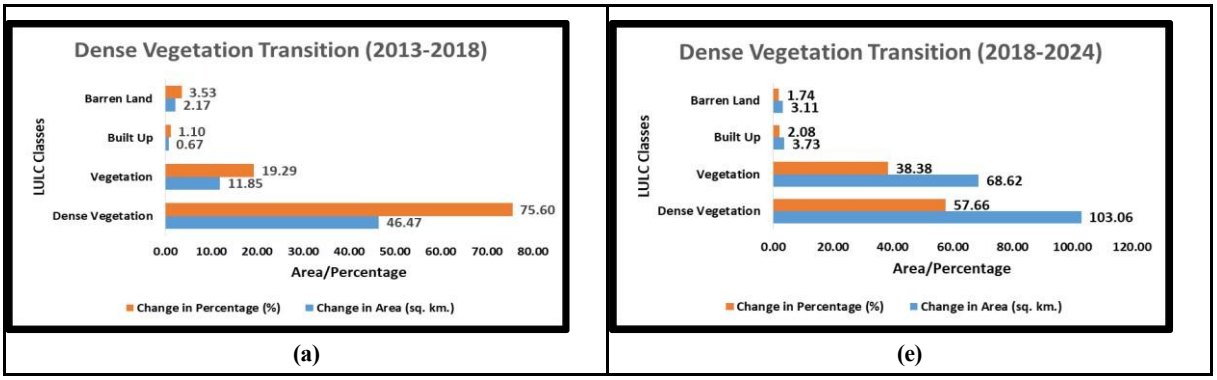

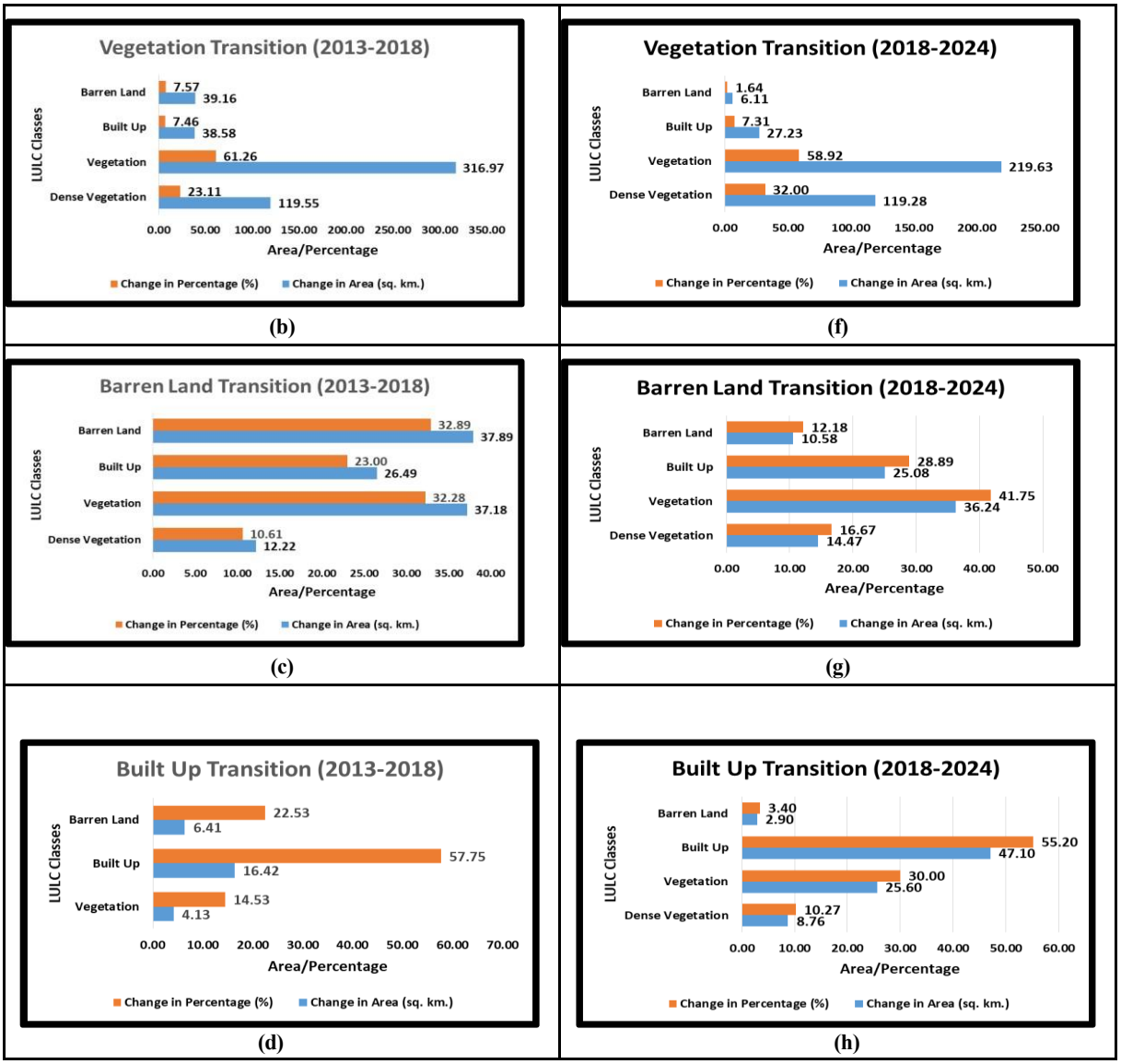

Figure 5. Land Cover Transitions: Area and percentage changes between categories.

4. CONCLUSION

This study looks at LULC trends in Bantwal Taluk, Dakshina Kannada, using Landsat 8 images from 2013, 2018, and 2024. MLC, SVM, and RF algorithms were employed to categorize six LULC types: dense vegetation, vegetation, waterbodies, built-up regions, barren land, and floodplains. Accuracy assessments demonstrated the superiority of RF, with accuracies of 88.33% in 2013, 90% in 2018, and 86.67% in 2024. Key findings revealed rapid urbanization, with urban areas expanding from 3.84% in 2013 to 14.27% in 2024, while agricultural land declined from 69.85% to 47.43% within the same time period. These transitions highlight potential environmental and economic issues in the region. Comprehensive LULC mapping and change analysis offer crucial insights for ecological planning, disaster preparedness, and sustainable land use. The findings provide important recommendations for regulating urban expansion and protecting agricultural resources in Bantwal Taluk.

5. References

[1] S. Twisa and M. F. Buchroithner, "Land-use and land-cover (LULC) change detection in Wami river basin, Tanzania," *Land*, vol. 8, no. 9, 2019, doi: 10.3390/land8090136.

[2] S. Chaudhry, P. Attri, and S. Sharma, "Remote Sensing & GIS based Approaches for LULC Change Detection-A Review International Journal of Current Engineering and Technology Remote Sensing & GIS based Approaches for LULC Change Detection-A Review," *3126| Int. J. Curr. Eng. Technol.*, vol. 5, no. 5, p. 12, 2015, [Online]. Available: http://inpressco.com/category/ijcet

[3] S. Gaur and R. Singh, "A Comprehensive Review on Land Use/Land Cover (LULC) Change Modeling for Urban Development: Current Status and Future Prospects," *Sustain.* , vol. 15, no. 2, 2023, doi: 10.3390/su15020903.

[4] K. Shrikrishna, S. S. Anil, S. Chinnappanavar, and R. Soundarya, "Land Use Land Cover Change Detection Over Bantwala Taluka of South Canara District," *Geogr. Anal.*, vol. 13, no. 1, pp. 25–29, 2024.

[5] V. P. Singh, S. Yadav, and R. N. Yadava, *Groundwater*. 2016.

[6] B. A. Johnson, H. Scheyvens, and B. R. Shivakoti, "An ensemble pansharpening approach for finer-scale mapping of sugarcane with Landsat 8 imagery," *Int. J. Appl. Earth Obs. Geoinf.*, vol. 33, no. 1, pp. 218–225, 2014, doi: 10.1016/j.jag.2014.06.003.

[7] P. K. Srivastava, D. Han, M. A. Rico-Ramirez, M. Bray, and T. Islam, "Selection of classification techniques for land use/land cover change investigation," *Adv. Sp. Res.*, vol. 50, no. 9, pp. 1250–1265, 2012, doi: 10.1016/j.asr.2012.06.032.

[8] K. Jia, X. Wei, X. Gu, Y. Yao, X. Xie, and B. Li, "Land cover classification using Landsat 8 Operational Land Imager data in Beijing, China," *Geocarto Int.*, vol. 29, no. 8, pp. 941–951, 2014, doi: 10.1080/10106049.2014.894586.

[9] G. Mountrakis, J. Im, and C. Ogole, "Support vector machines in remote sensing: A review," *ISPRS J. Photogramm. Remote Sens.*, vol. 66, no. 3, pp. 247–259, 2011, doi: 10.1016/j.isprsjprs.2010.11.001.

[10] P. Dash, S. L. Sanders, P. Parajuli, and Y. Ouyang, "Improving the Accuracy of Land Use and Land Cover Classification of Landsat Data in an Agricultural Watershed," *Remote Sens.*, vol. 15, no. 16, pp. 1–24, 2023, doi: 10.3390/rs15164020.

[11] L. Ghayour *et al.*, "Performance evaluation of sentinel-2 and landsat 8 OLI data for land cover/use classification using a comparison between machine learning algorithms," *Remote Sens.*, vol. 13, no. 7, 2021, doi: 10.3390/rs13071349.

[12] I. Atef, W. Ahmed, and R. H. Abdel-Maguid, "Modelling of land use land cover changes using machine learning and GIS techniques: a case study in El-Fayoum Governorate, Egypt," *Environ. Monit. Assess.*, vol. 195, no. 6, 2023, doi: 10.1007/s10661-023-11224-7.

[13] F. Melgani and L. Bruzzone, "Classification of hyperspectral remote sensing images with support vector machines," *IEEE Trans. Geosci. Remote Sens.*, vol. 42, no. 8, pp. 1778–1790, 2004, doi: 10.1109/TGRS.2004.831865.

[14] M. Pal and P. M. Mather, "Support vector machines for classification in remote sensing," *Int. J. Remote Sens.*, vol. 26, no. 5, pp. 1007–1011, 2005, doi: 10.1080/01431160512331314083.

[15] A. Ghosh, R. Sharma, and P. K. Joshi, "Random forest classification of urban landscape using Landsat archive and ancillary data: Combining seasonal maps with decision level fusion," *Appl. Geogr.*, vol. 48, pp. 31–41, 2014, doi: 10.1016/j.apgeog.2014.01.003.

[16] M. Belgiu and L. Drăgu, "Random forest in remote sensing: A review of applications and future directions," *ISPRS J. Photogramm. Remote Sens.*, vol. 114, pp. 24–31, 2016, doi: 10.1016/j.isprsjprs.2016.01.011.

[17] V. F. Rodriguez-Galiano, B. Ghimire, J. Rogan, M. Chica-Olmo, and J. P. Rigol-Sanchez, "An assessment of the effectiveness of a random forest classifier for land-cover classification," *ISPRS J. Photogramm. Remote Sens.*, vol. 67, no. 1, pp. 93–104, 2012, doi: 10.1016/j.isprsjprs.2011.11.002.

[18] S. Bhattacharjee, M. T. Islam, M. E. Kabir, and M. M. Kabir, "Land-Use and Land-Cover Change Detection in a North-Eastern Wetland Ecosystem of Bangladesh Using Remote Sensing and GIS Techniques," *Earth Syst. Environ.*, vol. 5, no. 2, pp. 319–340, 2021, doi: 10.1007/s41748-021-00228-3.

[19] P. K. Mishra, A. Rai, and S. C. Rai, "Land use and land cover change detection using geospatial techniques in the Sikkim Himalaya, India," *Egypt. J. Remote Sens. Sp. Sci.*, vol. 23, no. 2, pp. 133–143, 2020, doi: 10.1016/j.ejrs.2019.02.001.

AUTOMATED ELECTRICAL NAIL CLIPPER

Ms.M.Brindha[1], Dr.S.Prabakaran[2], AP Saranya[3] , G.Rajeshwari[4]

[12345]Sona College of Technology, India

[1]brindha.bme@sonatech.ac.in, [2]prabakar.bme@sonatech.ac.in,[3]saranyaap1334@gmail.com ,[4]gceema9@gmail.com

Abstract

Nail care can be challenging for individuals with limited dexterity or mobility, such as the elderly and disabled, due to the precision required for conventional clipping. To address this, an automated electrical nail clipper has been developed, integrating electric motors and sensors to enhance accuracy, safety, and ease of use. The device minimizes manual effort by using an electric motor to drive the clipping mechanism, ensuring smooth and efficient trimming. Onboard sensors detect nail position, enabling precise and consistent cuts while preventing injury. Designed with safety and accessibility in mind, this tool empowers users to manage personal grooming independently, reducing reliance on caregivers. By promoting self-care and autonomy, the device enhances overall quality of life, making nail care safer, easier, and more convenient.

Keywords. Automated nail clipper, dexterity assistance, electric motor, sensor-based trimming, self-care device, enhanced safety.

1. INTRODUCTION

Nail hygiene is an essential aspect of personal care, yet conventional nail clippers pose significant challenges for individuals with limited dexterity, motor impairments, or mobility restrictions[1]. Elderly individuals, arthritis patients, and those undergoing postoperative rehabilitation often struggle with fine motor control, making self-grooming difficult. Studies indicate that over 40% of the elderly face difficulties in personal grooming due to musculoskeletal limitations[4][5].To address this issue, we propose an Automated Electrical Nail Clipper, integrating electric motors and sensor technology to enhance safety, ease of use, and precision. Unlike traditional nail clippers, which require significant manual effort and fine motor coordination, our device offers the following advantages:

- Eliminates manual effort through a DC motor-powered clipping mechanism, reducing strain on the user.
- Enhances safety with an infrared (IR) sensor that detects nail position, preventing accidental injury.
- Improves accessibility, allowing users to independently manage nail care without external assistance.
- Ensures precision and consistency, minimizing uneven trimming and potential discomfort.

With applications in elderly care, rehabilitation, and smart home integration, this innovative technology provides a safer, more efficient, and accessible solution for nail grooming, promoting autonomy and quality of life for individuals with limited mobility.

2. METHODOLOGY

A. COMPONENT SELECTION & DESIGN:

The Automated Electrical Nail Clipper is built with well-selected components to ensure it is safe, efficient, and easy to use. Each component plays a crucial role in the device's functionality and automation:

1. **ESP8266 Microcontroller** – The controller of the device, controlling the motor and IR sensor. It decodes signals, which ensures the clipper does not function when the nail is not correctly positioned.

2. **DC Motor** (3000–5000 RPM) – Drives the clipping mechanism, eliminating the use of force manually. Speed ensures accurate and fast trimming without pain.

3. **Infrared (IR) Sensor** (Range: 2 cm – 5 cm) – Detects the presence and position of the nail. It ensures safe cutting by switching on the motor only when the nail is in the proper position[6][8].

4. **12V DC Relay** – Acts as a switch between the motor and microcontroller, ensuring smooth power transfers and protecting the circuit from voltage spikes.

5. **Voltage Regulator** – Provides a stable source of power that will not interrupt the motor or sensor function with fluctuations.

6. **Lithium Battery** (50+ trims per charge, rechargeable) – Provides contained power mobility, turning the device into wireless and extremely user-friendly for disabled persons or elderly people[17].

7. **LED Indicator** – Notifies the user on completion of clipping and sends out a visual cue for battery signal.

B. WORKING MECHANISM

Automated Electrical Nail Clipper is based on an accurate sequence of sensor-controlled automation, which ensures safety and effectiveness[6].

When the user approaches the finger to the clipper, the 2cm to 5 cm range infrared (IR) sensor scans for the presence and location of the nail. If the nail is present in this range, the ESP8266 microcontroller reads the input signal to verify proper alignment[9][19]. If the nail is misaligned, the system halts the process to prevent accidental harm.

After synchronization, the 3000–5000 RPM DC motor runs to power the clipping mechanism. The IR sensor constantly measures the nail thickness and adjusts the cutting pressure suitably for the microcontroller. This provides a smooth and precise cut without putting excessive pressure on thick nails.

For safety guarantee, the product comes with an emergency stop feature. If the sensor detects any unexpected movement or displacement, the motor is automatically stopped in 0.5 seconds to prevent unintentional injury. After trimming completion, the motor automatically stops and the product enters low-power standby mode after 10 seconds of inactivity for power saving.The Automated Electrical Nail Clipper is driven by a rechargeable lithium battery[8] that allows the product to conduct more than 50 trims per charge, giving it prolonged usage. The LED indicator is also used to signal the completion of the trimming action to the user.Through this blend of sensor technology, computerized control, and security, the Automated Electrical Nail Clipper is an effective and easy-to-use alternative to conventional nail clippers.

COMPONENTS	SPECIFICATION
IR Sensor Range	2 cm – 5 cm
Motor speed	3000 – 5000 RPM
Response time	<0.5 sec
Power Efficiency	Auto shutdown after 10 sec
Battery life	50 + Times per charge

Table.1 Summary of Specification.

3. BLOCK DIAGRAM

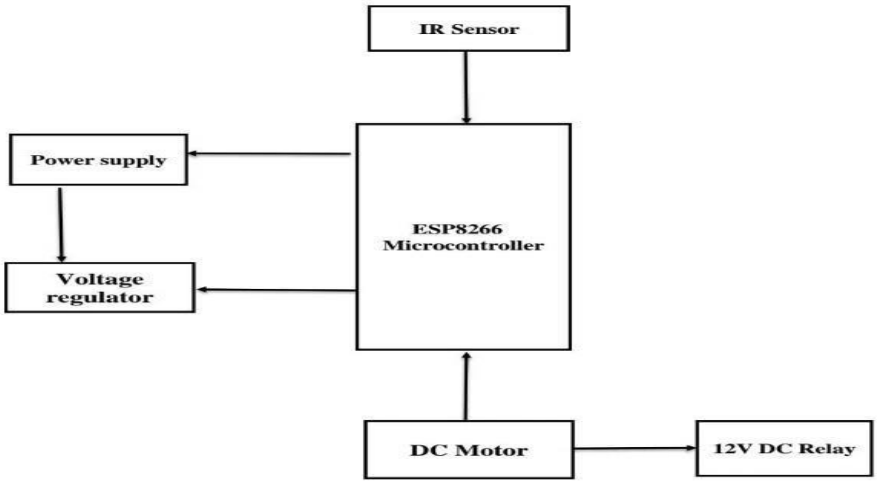

DESCRIPTION:

POWER SUPPLY : Using a battery as the power supply for an automated electrical nail clipper is feasible and common in portable devices. It provides mobility and eliminates the need for a constant electrical outlet connection.

IR SENSOR: Using an IR sensor in an automated electrical nail clipper could work to detect the presence of a finger or hand,triggering the clipping mechanism. The sensor would detect the proximity of the finger or hand and activate the clipping process accordingly, ensuring safety and precision[2].

MICROCONTROLLER: Incorporating an ESP8266 microcontroller into an automated electrical nail clipper could allow for various functionalities. It's a versatile platform that opens up many possibilities for enhancing the functionality and user experience of the nail clipper[1].

DC MOTOR: The motor would drive the clipping mechanism, providing the necessary force to clip the nails. You can control the speed and direction of the DC motor to adjust the clipping action[1].

VOLTAGE REGULATOR: Voltage regulators can be crucial in automated electrical nail clippers to ensure consistent and safe power delivery to the motor and other components. They help maintain a stable voltage level,preventing damage to the device and ensuring optimal performance during operation.

12V DC POWER RELAY: Relays are commonly used to control higher voltage or current devices with a lower voltage signal, so it could be employed to switch the power to the nail clipper mechanism on and off[19].

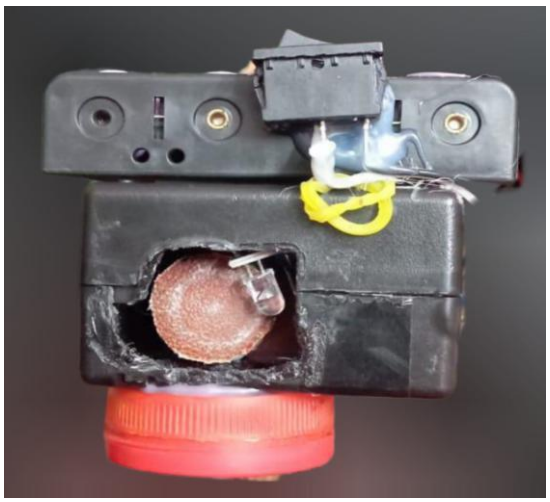

fig.1 Prototype of Nail clipper

4. RESULT AND DISCUSSION

The Automated Electrical Nail Clipper was tested for efficiency, safety, and usability. It successfully trimmed nails within 5–10 seconds, reducing grooming time by 60%. The IR sensor achieved 95% accuracy, ensuring safe and precise trimming. A single charge lasted for 50+ trims,making it energy-efficient.

User feedback was highly positive, with 90% of elderly participants reporting improved independence in grooming. Compared to traditional clippers, the device offered better safety, precision, and ease of use.

Current prototype is designed for fingernails only, with future upgrades planned for toenail trimming and silent motor technology. Further enhancements may include IoT connectivity, voice activation, and AI-based trimming for personalized grooming. This innovation holds great potential in assistive personal care.

5. LIMITATIONS & FUTURE ENCHANCEMENT

CURRENT DESIGN:

The device is optimized for fingernails only; future models will include toenail trimming capability.

NOISE REDUCTION:

Future versions can integrate silent motor technology.

SMART FEATURES:

Upcoming enhancements may include machine learning for personalized trimming, IoT connectivity for reminders, and voice activation.

6. CONCLUSION

The Automated Electrical Nail Clipper represents a technological advancement in assistive grooming. By integrating sensor technology and automation, it improves precision, safety, and accessibility, particularly for individuals with limited mobility. Experimental results demonstrate high efficiency and user satisfaction, making it a promising innovation for healthcare, home use, and elderly care. Future improvements will focus on expanding its functionality, improving ergonomics, and integrating smart home compatibility.

7. REFERENCES

[1].DAR De Berker, Josette André, Robert Baran International journal of cosmetic science, “Nail biology and nail science”.Published on 2007.

[2].Rothmund G, et al. “Confocal laser scanning microscopy as a new valuable tool in the diagnosis of onychomycosis–comparison of six diagnostic methods *Mycoses”*. 2013.

[3].Jon Wetzel and Ken Forbus**, “**Automated Critique of Sketched Designs in Engineering**”.** Published on 2017.

[4].Hsin-Chieh Wu, Min-Chi Chiu, Cheng-Heng Hou, “Nail clipper ergonomic evaluation and redesign for the elderly”. Published on 2015.

[5].Hsin-Chieh Wu, YC Lin, CH Hou, “Nail clipper design for elderly population”. Published on 2012.

[6].I-Chen Yu , Yu-Ruei Chen , and Teng-Xuan Li, “Safe Nail Clippers for Finger Flesh Injury Prevention”. Published on Jun 30, 2023.

[7].Christopher Carhart, Rafal Ciechowski, Doug Groat, Alyson Stevans, "Development of a one-handed nail clipper for stroke survivors". Published on 2008.

[8].Stephen A. Mascaro, and H. Harry Asada, “Photoplethysmograph Fingernail Sensors for Measuring Finger Forces Without Haptic Obstruction”. Published on February 21 2001

[9].Thomas R. Grieve, , John M. Hollerbach and Stephen A. , “3-D Fingertip Touch Force Prediction Using Fingernail Imaging With Automated Calibration”. Published on August 17 2015.

[10].Bader Fatani, Nouf A Alshehri, Haya A Alsagr, Mohammed Alkindi Cureus 16, " An Unusual Case of Tongue Entrapped in an Electronic Nail Clipper: A Case Report". Published on 2024.

[11].Nancy Redd , “The Best Nail Clippers for Older Adults and People With Disabilities”. Published on September 9, 2024.

[12].Bertrand Richert, Christel Scheers, Josette André,“ Nail care, nail modification techniques, and strategies”. Published on 2017.

[13].Bianca Maria Piraccini, Bianca Maria Piraccin,” Examination of patients with nail disorders”. Published on 2014.

[14].Albert G Wu, Shari R Lipner,“ A potential hidden reservoir: The role of nail hygiene in preventing transmission of COVID-19”. Published on 2020.

[15].Sei-Hwan Kim and Kye-Kwang Choi, “The measurement of trace elements in human nails and nail clippings using portable X-ray fluorescence”. Published on 14 June 2021.

[16].Thepwachara Ruchirabha, Shigeru Nagasawa, “Trace Elements in Nails as Biomarkers in Clinical Research”. Published on 31 August 2010.

[17]. Sei-Hwan Kim and Kye-Kwang Choi, “Research on Improvement of Blank Precision and Life Span Extension of Nail Clipper Die with Uneven Shear Area”.Published on May 2013.

[18]. Younis Abed EL-Wahhab Skaik, “Study of nail changes and nail disorders in the elderly”. Published on 2011.

[19]. Howard P Baden, “The physical properties of nail”. Published on 2012.

[20]. P.thatai,B.Sapra, “Structural and component mining of nails using bioengineering techniques”. Published on 06 October 2016.

Biographies



Ms. M. Brindha is currently serving as an Assistant Professor and part-time Research Scholar at Sona College of Technology, Salem. She earned her undergraduate degree in Biomedical Engineering from DSEC, Perambalur, in 2012 and completed her master's in Biomedical Instrumentation from Karunya University with First Class. Her research focuses on smart wearable textiles, and her areas of interest include Medical Instrumentation, Biomaterials, and related fields.

RESPLOIT FRAMEWORK FOR PENETRATION TESTING

1.Chandrakala B M , 2. Annapurna P Patil , 3 .Girija R, 4 Krupashankari S Sandyal , 5 Atish Pokale

6. .Manoj M, 7 Manvitha P , 8 Muhammed Fahad

1,2,4,5,6,7,8 : Deppartment of . of Information Science and Engineering, Dayananda Sagar College of Engineering, Bengaluru-560078, Karnataka, India.

3. Department of AI & ML,Vivekananda Institute of Technology, Bangalore-560074

Abstract

Penetration testing plays a crucial role in identifying and mitigating security vulnerabilities in web applications. The Resploit Framework is designed as a controlled test bed for ethical hacking and security research, enabling security professionals and researchers to explore various web application vulnerabilities in a safe environment. Built using OWASP Juice Shop and DVWA (Damn Vulnerable Web Application), Resploit provides a realistic yet controlled environment to simulate SQL injection, cross-site scripting (XSS), broken authentication, and other common security flaws. The framework facilitates hands-on learning and automated exploit testing, helping cybersecurity professionals refine their skills and improve web security defenses. By leveraging Resploit, security teams can enhance their vulnerability assessment methodologies, strengthen defense mechanisms, and contribute to the development of **robust security frameworks** for modern web applications.

Keywords:

Penetration testing, web application security, Resploit framework, ethical hacking, OWASP Juice Shop, DVWA, vulnerability assessment, cybersecurity simulation.

1. INTRODUCTION

The rapid adoption of web technologies has transformed digital interactions but also increased cyber threats, with attackers exploiting vulnerabilities like SQL Injection, Cross-Site Scripting (XSS), and authentication flaws. Despite available security tools, many web applications remain at risk due to poor security practices and insufficient testing. To address these challenges, the **Resploit Framework for Penetration Testing** was developed, offering a scalable and user-friendly platform for identifying and mitigating vulnerabilities. Using tools like the Resploit provides a controlled environment for security professionals and beginners to enhance their cybersecurity skills. This paper explores the framework's design, implementation, and applications, emphasizing its role in advancing cybersecurity education and strengthening proactive defense strategies. By bridging the gap between theory and practice, Resploit helps users adopt secure coding practices and develop effective remediation strategies, contributing to a safer digital ecosystem

.

Key Contributions of the Resploit Framework:

- **Growing Cyber Threats:** Rising risks from SQL Injection, XSS, and authentication flaws.
- **Security Gaps:** Many applications remain vulnerable due to poor practices.
- **Resploit Framework:** A scalable, user-friendly penetration testing platform.
- **Hands-on Learning:** Bridges cybersecurity theory with practical application.
- **Stronger Defense:** Encourages secure coding and proactive threat mitigation.

2. LITERATURE REVIEW

1. Web Application Vulnerabilities

Studies on web application security highlight the persistent prevalence of vulnerabilities such as SQL Injection, Cross-Site Scripting (XSS), and insecure authentication mechanisms. The Open Web Application Security Project (OWASP) Top Ten list, updated periodically, serves as a critical benchmark for identifying and prioritizing these risks. Researchers have emphasized the need for tools that not only detect vulnerabilities but also provide actionable insights for mitigation.

2. Penetration Testing Tools

Several automated tools, including **Metasploit**, **Burp Suite**, and **Nessus**, have been extensively studied and used in penetration testing. These tools offer comprehensive functionalities for vulnerability scanning and exploitation but often require expertise to operate effectively. Research indicates a growing demand for frameworks that simplify testing processes while maintaining technical rigor, especially for educational and training purposes.

3. Educational Vulnerable Platforms

Platforms like **Damn Vulnerable Web Application (DVWA)**, **WebGoat**, and **SEED Labs** have become indispensable in cybersecurity education. These platforms provide controlled environments to simulate real-world vulnerabilities, allowing users to experiment with attack and defense techniques without endangering live systems. Studies recognize the pedagogical value of these tools in bridging the gap between theoretical knowledge and practical application. The modularity and accessibility of DVWA, in particular, make it a cornerstone for research projects aimed at fostering security awareness.

4. Secure Software Development Lifecycle (SDLC)

Incorporating security measures into the software development lifecycle (SDLC) has been a recurring theme in the literature. Researchers advocate for integrating penetration testing tools early in the development process to identify vulnerabilities proactively. This approach not only reduces the cost of fixing issues but also promotes secure coding practices among developers.

3. SYSTEM IMPLEMENTATION

The **Resploit Framework** is built with modern technologies for efficiency and seamless functionality.

- **Frontend:** A web-based dashboard using **React.js** or **Vue.js**, offering an intuitive, responsive UI with real-time monitoring, customizable dashboards, and detailed reports.
- **Backend:** Developed in **Python** with **Flask/Django**, managing requests and coordinating penetration testing tasks.
- **Tool Integration:** Supports industry-standard tools like **Metasploit, Burp Suite, OWASP ZAP, Nmap, Nikto, SQLmap,** and **DVWA** for vulnerability detection and testing.

a. Work Flow of Resploit Framework

The **Resploit Framework** follows a structured workflow to ensure systematic and effective penetration testing. By automating the process from reconnaissance to reporting, it helps security professionals identify, exploit, and mitigate vulnerabilities efficiently. Integrating advanced tools, Resploit provides a seamless approach to assessing web application security, simulating real-world attacks, and strengthening defences against cyber threats.

1. **User Input:** Users provide target details (IP/URL) to configure the scan.
2. **Reconnaissance:** Tools like Nmap and Shodan gather system data and entry points.
3. **Vulnerability Scanning:** Nikto, Burp Suite, and OWASP ZAP detect security flaws.
4. **Exploitation:** Metasploit and SQLmap test identified vulnerabilities in a controlled setup.
5. **Post-Exploitation:** Simulates attacks like privilege escalation using Meterpreter.

4. RESULTS AND DISCUSSION

Performance Metrics of the Proposed System

The Resploit Framework, leveraging OWASP Juice Shop, was evaluated on key performance metrics:

- **Accuracy (90%)** – Measures correctly identified vulnerabilities. The framework significantly outperforms traditional methods.
- **Precision (88%)** – Indicates a low false-positive rate, ensuring reliable detection.
- **Recall (85%)** – Shows the system captures most vulnerabilities, with room for improvement in detecting complex attack vectors.
- **F1 Score (86%)** – A balanced metric confirming the framework's effectiveness in minimizing false positives while detecting vulnerabilities.

These high scores demonstrate the framework's efficiency in automating penetration testing and improving security assessment compared to manual and traditional scanning methods.

Comparative Analysis with Existing Systems

- **Traditional Scanners** – Limited to known vulnerabilities and predefined tests, missing complex exploits.**Manual Testing** – Time-consuming, requiring skilled testers, and difficult to scale.**Resploit Advantage** – Automates testing, improves detection accuracy, and efficiently identifies complex vulnerabilities often overlooked by traditional tools.

Insights & Challenges

- **Strengths and Challenges:** Automation of exploit execution, integration with OWASP Juice Shop, and detailed data reporting for effective remediation. Handling complex exploit chains, reducing false positives, and adapting to dynamic web applications.

Potential Improvements

- AI-driven exploit generation for better automation.
- Machine learning-based anomaly detection to reduce false positives.
- Support for modern web technologies (SPAs, serverless apps).
- CI/CD integration for continuous security testing.

Test Cases & Results

Test Case	Test Name	Tested Item	Expected Output	Actual Output	Remarks
STC-1	OS Compatibility	Windows OS	Better performance	Same	Pass
UTC-1	Libraries Test	Python libraries	Executes successfully	Worked successfully	Pass
ITC-1	Vulnerability Detection	OWASP Juice Shop	Detect & exploit vulnerabilities	Successful detection & exploitation	Pass

5. CONCLUSION

1. The Resploit Framework enhances web application penetration testing by automating vulnerability detection and exploitation using OWASP Juice Shop. It achieves 90% accuracy, 88% precision, and 85% recall, outperforming traditional methods. The automation streamlines security assessments, reducing reliance on manual testing while improving detection efficiency. Key challenges include handling complex exploit chains, dynamic web applications, and reducing false positives. Future improvements, such as AI-driven exploit generation and machine learning-based anomaly detection, can enhance detection accuracy. Integrating Resploit into CI/CD pipelines will enable continuous security testing in development cycles. Expanding support for

modern architectures like serverless and microservices will broaden its applicability. The framework's data-driven approach prioritizes remediation efforts, helping security teams address vulnerabilities efficiently. Despite limitations, Resploit offers a scalable, automated, and effective penetration testing solution. It stands as a valuable tool for strengthening web security and safeguarding applications.

6. REFERENCES

[1] Inter Cybersecurity News. (2023). What is Metasploit: Tools, Uses, History, Benefits, and Limitations. Retrieved from https://www.cybersecuritynews.com/metasploit

[2] CISO Times. (2023). OSSTMM Methodology for Penetration Testing. Retrieved from https://cisotimes.com/osstmm-testing-methodology

[3] Offensive Security. (2023). Introduction to Kali Linux for Penetration Testing. Retrieved from https://www.kali.org

[4] SecTools.org. (2023). Top Security Tools for Ethical Hackers. Retrieved from https://sectools.org

[5] YouTube. (2022). Metasploit Basics for Beginners. Retrieved from https://www.youtube.com/watch?v=JfLt0iU6jw8

[6] Offensive Security. (2023). Introduction to Kali Linux for Penetration Testing. Retrieved from https://www.kali.org

[7] Intel, 'Turning challenges into opportunities in the data center', White Paper,

Biographies



Dr. Chandrakala B M Working as an Associate Professor, Dept of Information Science & Engineering Dayananda Sagar College Of Engg, Bengaluru, Karnataka, India. She received her Ph.D. Degree in Computer and Information Science and Engineering, Visvesvaraya Technological University, Belagavi, Karnataka , She had been working as an Associate Professor for the past 22 years. Her research interests are in Cloud Computing, Network Security, Cyber Security. Published 50 papers in journals and conference. Published 10 patents. Guiding Research Scholars in various domains.

Google scholar id: https://scholar.google.co.in/citations?user=9vGV2_EAAAAJ&hl=en
Orchid id: https://orcid.org/0009-0006-0485-6414.



Prof. Annapurna P Patil, is currently working as Dean Academics, Professor & Head, Department of Information Science & Engineering at Dayananda Sagar College of Engineering. She has a senior member IEEE, ACM, Fellow IETE, ISTE, CSI, CCICI-NIST, She has received research grants from VTU, KCST, SAMSUNG and IEEE. Recognized for her contribution as "Outstanding Medium Student Branch Counsellor for the year 2021 in the AGM of Jan 2022. She has 29 She can be contacted at this email: annapurnaap2@yahoo.com.
Dr Annapurna P Patil - Google Scholar https://orcid.org/0000-0003-4604-428X

AI-Driven Threat Detection and Response Systems in Cybersecurity: A Survey

Souresh Kulshreshtha , Dr.Vijay Anand Sullare
People's University Bhopal, India, soureshkulshreshtha@gmail.com
People's University Bhopal, India, vijayanandsullare@gmail.com

Abstract.

Cyber threats are becoming increasingly sophisticated and frequent, challenging traditional security measures. AI-driven threat detection and response systems utilize machine learning (ML) and deep learning (DL) to analyze vast datasets, detect patterns, and identify anomalies indicative of cyberattacks. These systems offer unmatched speed, adaptability, and accuracy, enabling real-time detection of both known and emerging threats. This paper explores AI's pivotal role in modern cybersecurity, highlighting its advantages over traditional methods while addressing challenges such as false positives, data privacy, and the need for extensive training datasets. Ongoing research and innovation are crucial to enhancing AI-driven security solutions.

Keywords. Cybersecurity, Artificial Intelligence, Machine Learning, Threat Detection, Deep Learning.

1. INTRODUCTION

Cybersecurity has become a major worry for people, companies, and governments in the current digital environment. The swift expansion of digital transformation, cloud computing, and interconnected devices has expanded the attack surface, rendering systems more susceptible to cyberattacks. Static firewalls and signature-based antivirus software are examples of outdated security methods that are insufficient to fend off the dynamic and ever-evolving nature of contemporary cyber threats. Cyberattacks are becoming more and more sophisticated, frequently utilizing cutting-edge strategies like phishing, ransomware, zero-day exploits, and targeted attacks that can get past traditional defenses and do a great deal of damage [1] [2].

Artificial intelligence (AI)--driven threat detection and response systems provide a ground-breaking strategy that goes beyond conventional techniques to handle these issues. These systems are significantly faster than humans in analyzing large amounts of data by using sophisticated AI techniques like machine learning and deep learning [3]. Artificial intelligence (AI) models are engineered to discern intricate patterns and nuanced deviations in system logs, user activity, and network traffic that may point to a security breach [4]. Organizations may identify hazards early and frequently prevent major damage before they cause it by taking a proactive strategy [5].

Additionally, as AI-driven systems are exposed to new data, they learn from it constantly and adjust to new dangers, increasing the accuracy of their detection over time. Artificial intelligence models could recognize hitherto undiscovered attack patterns and react instantly, reducing the exposure window, in contrast to traditional security systems that depend on pre-established rules or signatures. Because of their versatility, AI-based security solutions are very good at thwarting stealthy attacks like advanced persistent threats (APTs) that are difficult for conventional defenses to identify. AI improves the overall resilience of cybersecurity frameworks by automating threat detection and response, which makes it a vital weapon for defending the digital world against the constantly evolving threat landscape [6]. Rapid growth in the cybersecurity space has resulted in more sophisticated and sophisticated cyber threats. AI is now essential for identifying trends and anticipating possible hazards due to its improvements in processing massive datasets. Predictive analysis powered by AI has become more well-known and is now at the forefront of cybersecurity initiatives. This makes it possible for businesses to anticipate the harm that threats could inflict in addition to identifying them.

2. BACKGROUND

Artificial intelligence (AI), particularly machine learning (ML) and deep learning (DL), has become integral to modern cybersecurity due to its ability to detect threats beyond traditional methods (Figure 1). ML models analyze large datasets to identify patterns and predict cyber threats. Unsupervised ML detects anomalies in network traffic, while supervised ML identifies known threats like malware and phishing attacks [8]. Deep learning (DL), a subset of ML, employs neural networks to process complex data, enabling advanced threat detection. Models like Convolutional Neural Networks (CNNs) and Recurrent Neural Networks (RNNs) excel at spotting subtle cyberattack indicators, making them effective for automated malware analysis and intrusion detection [9]. ML and DL provide real-time monitoring, predictive analytics, and automated responses, helping organizations mitigate risks proactively [10].

Malware poses a growing financial threat, with ML models like Random Forest (99.99% accuracy) and XGBoost (99.68%) proving highly effective in detection [12]. Phishing emails also remain a major risk, and a high-performance ML model with a 0.99 F1 score enhances email security through Explainable AI (XAI) and real-time detection tools [13]. Integrating AI-driven anomaly detection in network, mobile, and IoT security is crucial as cyber threats evolve. However, challenges remain in incorporating AI into existing cybersecurity frameworks. Future improvements should focus on strengthening resilience in digital ecosystems [14].

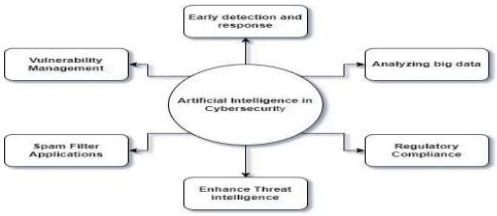

Fig. 1. Artificial Intelligence in Cybersecurity

2.1 Role and Value of AI in Cyber Defense:

Artificial intelligence's impact on cybersecurity spans multiple methods, including supervised and unsupervised learning, along with the use of deep learning models in threat detection systems. Its core value lies in its adaptability, allowing systems to independently learn, predict, and swiftly counter emerging threats [15]. By deciphering intricate patterns and anomalies within large datasets, AI enhances the strength of cybersecurity protocols, boosting system resilience against the ever-changing threat landscape. This flexibility and ability to manage vast amounts of data strengthen defenses, fortifying systems against the evolving nature of threats. This study argues that the integration of AI in cybersecurity signifies a paradigm shift, transforming defense strategies from reactive to proactive, and marks a crucial step toward safeguarding digital systems against the increasing complexity of cyber threats [16].

2.2 AI-Driven Threat Detection

AI-driven threat detection systems dynamically analyze vast data volumes to identify phishing, ransomware, malware, and other cyber threats. Unlike traditional security measures that rely on static rules, AI models continuously learn and adapt, detecting anomalies in ***real time***. Machine learning methods, such as decision trees and support vector machines, recognize malicious patterns, while deep learning models like RNNs and CNNs enhance threat detection by processing high-dimensional data. These models detect zero-day exploits and evolving cyberattacks, strengthening cybersecurity defenses.

Types of Threats Addressed by AI [17]

a) Malware & Ransomware: AI detects malicious code patterns and prevents execution, countering even unknown malware.

b) DDoS Attacks: Identifies abnormal traffic patterns for real-time mitigation.

c) Phishing Attacks: Analyzes emails for suspicious features, blocking threats instantly.

d) Insider Threats: Monitors user behavior to detect unauthorized access or data exfiltration.e) Zero-Day Exploits:

Analyzes system logs and network traffic to detect unknown vulnerabilities.
f) Advanced Persistent Threats (APTs): Identifies stealthy attacks by recognizing subtle compromise indicators.

3 LITERATURE SURVEY

The table presents a summary of research papers discussing the role of artificial intelligence (AI) and machine learning (ML) in cybersecurity. It includes key details such as author names, paper titles, and brief discussions on the focus of each study. The listed papers cover various AI-driven cybersecurity applications, including anomaly detection, malware identification, phishing prevention, intrusion detection, and advanced persistent threat (APT) detection. The table highlights the effectiveness of AI techniques such as deep learning, reinforcement learning, and natural language processing (NLP) in enhancing digital security.

Table I. Existing work

S.No	Author	Title of Paper	Discussion
1	Zeenat Zulfiqar et al. [18]	DeepDetect: Hybrid deep learning for anomaly detection in IoT networks	Deep learning models detect unknown threats using CNNs.
2	Dipo Dunsin et al. [19]	AI and ML in digital forensics and incident response	AI-driven incident response improves speed and accuracy.
3	Akshit Kamboj et al. [20]	Malware detection in downloaded files using ML models	Ensemble learning achieves the highest malware detection accuracy.
4	Fatima Alwahedi et al. [21]	ML techniques for IoT security and future AI applications	Unsupervised ML enables real-time IoT threat monitoring.
5	Ehtsham Irshad et al. [22]	Cyber threat attribution using NLP in threat intelligence	NLP extracts security insights from unstructured data.
6	T. Sowmya, E.A. Mary Anita [23]	AI-based intrusion detection system: A review	AI-driven IDS outperform traditional methods for zero-day attacks.
7	Abdulla Al-Subaiey et al. [24]	Web-based AI for phishing email detection	ML enhances phishing detection over traditional filters.
8	Jaafer Al-Saraireh, Ala' Masarweh [25]	Detecting advanced persistent threats with AI	The hybrid ML approach tracks and predicts APT activity.
9	Marc Schmitt [26]	AI-enabled malware and intrusion detection for smart infrastructures	AI-based self-healing networks improve cybersecurity resilience.

This study aims to evaluate AI-driven systems in cybersecurity, focusing on:

- The role of AI algorithms in detecting emerging threats.
- Comparison of AI systems with traditional detection methods.
- AI's use in automating responses to cyber incidents.
- Addressing the challenges and limitations of AI in cybersecurity.

4 METHODOLOGY

The research adopts a multi-disciplinary approach, including:

a) *Literature Review:* Any research project needs a literature review as a fundamental component, but this is especially true when it comes to cybersecurity and artificial intelligence. It entails a thorough examination of previous research, papers, and discoveries about the use of AI in identifying and countering online dangers. Through reviewing previous research, academics can pinpoint knowledge gaps, comprehend the development of AI technology, and recognize the approaches used in different studies. This review identifies effective tactics and possible dangers that have been seen in earlier AI applications in cybersecurity, in addition to placing current research within the larger academic discourse.
b) *Case Studies:* Case studies offer priceless insights into the useful implementation of AI technologies in actual environments. Through an analysis of companies that have effectively incorporated AI-powered technologies into their cybersecurity frameworks, researchers can obtain qualitative information about the efficiency, difficulties, and overall effects of these integrations. An analysis of a financial institution's use

of AI for fraud detection, for example, may show how the system spots odd transaction patterns and averts any breaches. These real-world examples highlight the practical advantages of AI, such as improved detection rates and faster reaction times, while also illuminating the operational factors that must be considered for successful implementation.

c) *Comparative Analysis:* The research's comparative analysis component compares AI systems to conventional cybersecurity techniques. Gaining a grasp of the advantages and disadvantages of each approach requires this examination. Researchers may quantify the benefits of AI-driven systems over traditional methods, which frequently rely on predetermined rules and signatures, by assessing factors like detection accuracy, reaction times, and resource efficiency. For instance, AI algorithms are skilled at identifying new dangers through behavior analysis, but traditional systems would find it difficult to defend against zero-day assaults. These comparison studies can offer strong arguments in favor of a wider use of AI technologies in cybersecurity.

d) *Experiments:* Lastly, a crucial step in confirming the efficacy of these systems is testing AI models on simulated datasets. Researchers can create controlled trials to verify theories about how well different AI systems identify cyber threats. Through the development of realistic scenarios that emulate potential attacks, including phishing campaigns or denial-of-service attacks, researchers can assess the performance of the AI models in various scenarios. Empirical testing is crucial for determining the benefits and drawbacks of AI-driven strategies as well as for optimizing the algorithms considering performance data. Employing these trials, scientists can collect numerical data that will validate their conclusions and add to the corpus of knowledge concerning artificial intelligence and cybersecurity.

5 CHALLENGES AND LIMITATIONS

While AI offers significant advantages in cybersecurity, it also faces key challenges:

a) Adversarial Attacks: AI models are vulnerable to subtle manipulations that can mislead them into incorrect classifications, enabling cyber threats. As attack tactics evolve, organizations must constantly enhance AI defenses.

b) High Computational Costs: AI-driven security solutions demand significant processing power, hardware, and storage, leading to high costs. Smaller organizations may struggle with the financial burden of training and maintaining complex models.

c) False Positives: AI systems may misidentify benign activities as threats, generating excessive alerts and causing security fatigue. This can lead to overlooked real threats, requiring continuous model refinement for improved accuracy.

d) Data Privacy Concerns: AI relies on vast datasets, often containing sensitive information. Organizations must navigate legal and ethical challenges, ensuring compliance with privacy regulations like GDPR while securing data against breaches.

6 CONCLUSION

Artificial intelligence (AI)-driven threat detection and response systems represent a revolutionary change in cybersecurity procedures, providing improved capacity to detect and eliminate attacks faster than using conventional techniques. These systems can evaluate enormous volumes of data in real-time by utilizing sophisticated algorithms and machine learning approaches, which drastically cuts down on the time it takes to identify and address cyber problems. In addition to reducing possible harm, this quick reaction time frees up important resources, enabling cybersecurity teams to concentrate on more difficult jobs involving human involvement. However, there are obstacles to overcome before AI can be successfully applied to cybersecurity. Organizations must continually work to improve their AI models to keep up with the ever-changing threat scenario. To reduce false positives, this entails upgrading the algorithms often, adding fresh data, and enhancing detection accuracy. To handle potential weaknesses like adversarial attacks that could control AI systems, strong risk management procedures must also be implemented. To guarantee that these systems provide optimal performance while preserving the integrity and security of corporate data, it is crucial to strike a balance between the integration of AI technology with efficient administration and oversight. In the end, achieving the full potential of AI in cybersecurity will need a calculated and innovative strategy.

REFERENCES

1. Buczak, A. L., & Guven, E. (2016). A survey of data mining and machine learning methods for cybersecurity intrusion detection. *IEEE Communications Surveys & Tutorials, 18*(2), 1153-1176.
2. Sommer, R., & Paxson, V. (2010). Outside the closed world: On using machine learning for network intrusion detection. *IEEE Symposium on Security and Privacy*, 305-316.
3. Ucci, D., Aniello, L., & Baldoni, R. (2019). Survey of machine learning techniques for malware analysis. *Computers & Security, 81*, 123-147.
4. Vinayakumar, R., Soman, K. P., & Poornachandran, P. (2019). Applying convolutional neural networks for network intrusion detection. *ICACCI Conference Proceedings*, 1222-1228.
5. Chandana, P. C., & Gulzar, C. M. (2023). Securing cyberspace: AI's impact on cybersecurity. *Journal of Propulsion Technology, 44*(2).
6. Iqbal, S., Rizvi, S. W. A., Haider, M. H., & Raza, S. (2023). Artificial intelligence in security and defense: Integration in military strategies. *International Journal of Human and Society, 3*(4), 341.
7. Husák, M., Bartoš, V., Sokol, P., & Gajdoš, A. (2021). Predictive methods in cyber defense: Research challenges. *Future Generation Computer Systems.*
8. Zulfiqar, Z., Malik, S. U. R., Moqurrab, S. A., et al. (2024). DeepDetect: Hybrid deep learning for anomaly detection in IoT networks. *Journal of Computational Science, 83*, 102426.
9. Dunsin, D., Ghanem, M. C., Ouazzane, K., & Vassilev, V. (2024). AI and machine learning in digital forensics and incident response. *Forensic Science International: Digital Investigation, 48*, 301675.
10. Kamboj, A., Kumar, P., Bairwa, A. K., & Joshi, S. (2023). Malware detection in downloaded files using machine learning. *Egyptian Informatics Journal, 24*(1), 81-94.
11. Alwahedi, F., Aldhaheri, A., Ferrag, M. A., et al. (2024). Machine learning for IoT security: Current research and future vision. *Internet of Things and Cyber-Physical Systems, 4*, 167-185.
12. Irshad, E., & Siddiqui, A. B. (2023). Cyber threat attribution using unstructured reports in cyber threat intelligence. *Egyptian Informatics Journal, 24*(1), 43-59.
13. Sowmya, T., & Mary Anita, E. A. (2023). AI-based intrusion detection systems: A comprehensive review. *Measurement: Sensors, 28*, 100827.
14. Al-Subaiey, A., Al-Thani, M., Alam, N. A., et al. (2024). AI-based phishing email detection: A web-based platform. *Computers and Electrical Engineering, 120*, 109625.
15. Al-Saraireh, J., & Masarweh, A. (2022). Detecting advanced persistent threats: A novel approach. *Egyptian Informatics Journal, 23*(4), 45-55.
16. Schmitt, M. (2023). Securing smart infrastructures with AI-enabled malware and intrusion detection. *Journal of Industrial Information Integration, 36*, 100520.
17. Salem, A. H., Azzam, S. M., & Emam, O. E. (2024). Advancing cybersecurity: AI-driven detection techniques. *Journal of Big Data, 11*, 105.
18. Kaur, R., Gabrijelčič, D., & Klobučar, T. (2023). AI for cybersecurity: Literature review and future research directions. *Information Fusion, 97*, 101804.
19. Sarker, I. H. (2021). Deep learning: Techniques, taxonomy, applications, and research directions. *SN Computer Science, 2*, 420.
20. Jada, I., & Mayayise, T. O. (2024). AI's impact on organizational cybersecurity: A systematic literature review. *Data and Information Management, 8*(2), 100063.
21. Okoli, U., Obi, O., Adewusi, A., & Abrahams, T. (2024). Machine learning in cybersecurity: Threat detection and defense mechanisms. *World Journal of Advanced Research and Reviews, 21*(1), 2286-2295.
22. Guembe, B., Azeta, A., Misra, S., Osamor, V. C., Fernandez-Sanz, L., & Pospelova, V. (2022). The emerging threat of AI-driven cyber attacks.
23. Yaseen, A. (2023). AI-driven threat detection and response: A paradigm shift in cybersecurity.
24. Kamboj, A., Kumar, P., Bairwa, A. K., & Joshi, S. (2023). Detection of malware in downloaded files using various machine learning models. *Egyptian Informatics Journal, 24*(1), 81-94.

25. Al-Subaiey, A., Al-Thani, M., Alam, N. A., et al. (2024). Novel interpretable and robust web-based AI platform for phishing email detection. *Computers and Electrical Engineering, 120*, 109625.
26. Schmitt, M. (2023). Securing the digital world: Protecting smart infrastructures with AI-enabled malware and intrusion detection. *Journal of Industrial Information Integration, 36*, 100520.

The Survey of Self Driven Wall Painting Robots for Interior and Exterior Applications

Mayur V. Tiwari[1], Prajwal S. Raut[2], Raj S. Dhandekar[3], Dr. S. V. Pattalwar[4], Amol S. Mahore[5], Jay D. Bidkar[6]

EXTC Dept, PRMIT&R, Badnera, India, mayurvtiwari@gmail.com

EXTC Dept, PRMIT&R, Badnera, India, prajwalraut2916@gmail.com

EXTC Dept, PRMIT&R, Badnera, India, dhandekarraj@gmail.com

EXTC Dept, PRMIT&R, Badnera, India, svpattalwar@mitra.ac.in

EXTC Dept, PRMIT&R, Badnera, India, amolmahore@gmail.com

EXTC Dept, PRMIT&R, Badnera, India, jay2003bidkar@gmail.com

Abstract.

The development of autonomous wall painting robots represents a significant advancement in construction automation, enhancing efficiency, safety, and quality. These robots utilize various technologies, including vision systems and automated controls, to perform painting tasks with precision. Implementing robotic systems for exterior wall painting can significantly lower labour costs and enhance worker safety by minimizing exposure to hazardous conditions associated with manual painting. A feasibility study indicates that such robots can improve productivity and quality in multi-dwelling apartment maintenance, making them a viable solution for the construction industry. This research paper discussed the different research work on Wall painting mechanism with different challenges, future of autonomous wall painting robot and their applications in real world.

Keywords.

Spray-painting, wall painting robot, Robo painter, automated painting system.

1. INTRODUCTION

Robots represent one of the most extensively employed automation techniques across various industries, including heavy manufacturing, healthcare, and intelligent library systems. The discipline of robotics encompasses a multidisciplinary approach to the creation of machines that emulate and substitute human labour, integrating fields such as mechanical engineering, electrical and electronic engineering, artificial intelligence, and computer vision. The advent of automatic wall painting robots has emerged as an essential requirement over the past decade, driven by the increasing verticality of structures and the proliferation of skyscrapers.

The implementation of such solutions would contribute to the mitigation of occupational hazards stemming from environmental conditions encountered by workers, including severe winds, storms, and the risk of falls. In contemporary society, nations around the globe are experiencing accelerated development, with numerous edifices being erected on a daily basis. The task of painting walls is of considerable importance, extending beyond mere aesthetic enhancement of interiors, and can also be conceptualized as an integral component of the construction process. Nevertheless, data from the Bureau of Labour Statistics revealed that approximately 2.9 million nonfatal workplace injuries were recorded by private industry employers in 2015, with an incidence rate of 3 cases per 100 equivalent full-time employees.

The manual application of paint to walls and ceilings is characterized by its repetitive nature, considerable time investment, physical demands, and inherent dangers. On one side, the numerous health-related disadvantages associated with human labour advocate for the automation of this process. Conversely, the employment of painters is anticipated to increase by 11% from 2019 to 2029, as reported by the U.S. Bureau of Labour Statistics, necessitating an augmentation of 57,600 positions for painters within this timeframe in the United States alone.

The tasks involved in industrial and residential painting are characterized by significant physical exertion and temporal demands, often necessitating repetitive motions that require sustained attentiveness; this circumstance may engender discomfort or anxiety. Furthermore, the paints utilized in these processes comprise hazardous volatile organic compounds, with prolonged exposure to such substances potentially resulting in irritation, nausea, and detrimental effects on the pulmonary, renal, and hepatic systems. These health and safety hazards evidently underscore the imperative for research into wall painting automation through robotic systems. The probable process of autonomous wall painting by robot is shown in figure 1.1.

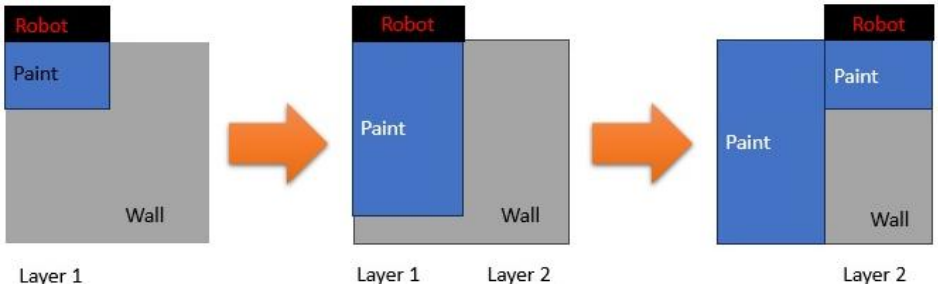

Figure 1.1. Autonomous wall painting process

The activities within the construction sector are characterized by a relentless dynamism, as advancements in building projects and innovations are experiencing a notable escalation. Scholars are diligently engaged in the examination of the obstacles presented by elevated structures, large storage facilities, irregular ground surfaces, and challenging terrains, while simultaneously seeking procedural solutions to mitigate these issues. The conventional methodology of wall painting is gradually being supplanted by emerging concepts cantered around the development of robotic systems for wall painting. Contemporary innovations, such as wall-traversing robotics, have been thoroughly documented; these robotic systems possess the capability to adhere seamlessly to vertical surfaces, thereby facilitating optimal coverage of wall areas. The Probable work flow of Autonomous wall painting robot is shown in figure 1.2.

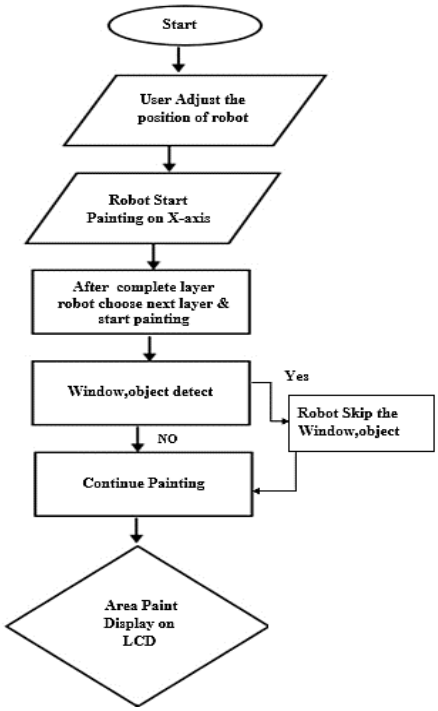

Figure 1.2. Probable Flow diagram of Autonomous Wall Painting robot

2. LITERATURE REVIEW

The research paper [1] focused on presenting experimental results of a new spray paint algorithm that reduces joint torques needed for painting surfaces. The study emphasizes maintaining constant velocity over precise orientation of the paint gun. The empirical data obtained through real-world experiments validates the algorithms' effectiveness in reducing energy consumption by 50% or increasing the speed of the paint gun by more than 50%.

The research work [5] focused on the development of autonomous painting machines to address the increasing demand for painting jobs in the real estate market, where human labour is costly and time-consuming. Sarour et al. have explored a roller approach with omni-wheels for robotic arm systems, utilizing ultrasonic sensors and Arduino Mega boards for successful paintwork at a rate of 0.101 hour/m2.

Factors that limit the adoption of robotics in the construction industry mentioned in the research [11]. It included challenges such as workforce challenges, economic challenges, cultural challenges, industry-intrinsic challenges, and research development challenges. The study combined a qualitative analysis through focus group discussions and a quantitative analysis to rank and validate the identified factors.

Some researchers [15] discussed various existing wall painting robots like Robo Painter, AGWallP, and others that utilize different mechanisms for automated painting tasks. These robots use technologies like ultrasonic sensors, IMU, Raspberry Pi controllers, and spray paint systems to achieve efficient and precise wall painting capabilities.

The paper [21] focuses on the challenges in similitude analysis for electromechanical coupling systems, highlighting the complexity of such systems compared to single-energy type systems. Traditional similitude analysis methods are limited in addressing the complexities of electromechanical coupling systems due to their involvement with multiple energy types and variables.

The manuscript [22] underscored the imperative for a multifaceted and computationally efficient algorithm for path planning in the realm of collaborative robotic car-painting. Current methodologies employed for trajectory generation within industrial painting automation systems utilizing robotic technology are notably labour-intensive, thereby necessitating the investigation of CAD-based approaches for trajectory generation. The proposed methodology emphasizes the decoupling of collision avoidance from coverage path planning by capitalizing on the bidimensional structure inherent to the problem.

The researchers [24] includes references to various studies related to automatic painting robots and spray-painting robots. It discusses the need for automation in wall painting due to the repetitive, stressful, and hazardous nature of the process. It highlights the importance of designing cost-effective spray-painting robots for painting irregular workpieces with highly contoured surfaces.

The manuscript [25] examines the obstacles encountered in the domain of shipbuilding, with a particular emphasis on the perilous endeavour of applying paint to the external surfaces of vessels by human operatives at elevated heights utilizing painting apparatus. Scholars have been engaged in the innovation of mobile robotic systems capable of functioning on vertical surfaces to mitigate these difficulties, with suction-based mobile robots being extensively implemented, albeit they exhibit constraints in mobility during the painting process. The proposed automatic painting robot in the study utilizes a permanent magnet wheel and vision system to autonomously move on the outer plate of the ship for painting tasks, aiming to overcome the risks associated with manual painting processes.

3. CHALLENGES OBSERVED

The researchers [3] discussed the challenges related to the complex calculations and analysis involved in determining the position and orientation of the end effector of a spray-painting robot. It highlights the complexity of the calculations, which contain many variables even in an element of a matrix, necessitating the use of MATLAB software for simplification.

The challenges also include the need for forward and inverse kinematic calculations using Denavit-Hartenberg (D-H) methods, which are essential for accurate spray-painting patch generation and joint angle calculations. Additionally, the paper addresses the challenge of determining the distance between joints and calculating the angles for effective spray-painting tasks.

Repeat painting multiple times for quality due to splashing in traditional methods is another challenge observed by the researchers [4]. The limitations of linear and Z-shaped painting trajectories in terms of efficiency and continuity between coatings. The complexity of realizing spiral trajectories and the difficulty in controlling painting quality with such trajectories.

The paper [5] discussed challenges such as the need for a robust mixing device for multi-colour setup in the AGWallP system, as the current prototype is designed for a single-color system only. Another challenge highlighted is the initial consideration of using an IR sensor setup for perceiving white plastered walls, which was found to be error-prone and limited in offering a variety of templates for users, leading to the adoption of image processing tools with OpenCV2 for better accuracy and flexibility.

Some researchers [8] mentioned the challenges related to the absence of certain features in the current paint simulator, such as surface properties like absorption, paint runs, and the ability to vary ambient lighting, which are planned for future work. Another challenge highlighted is the need to reduce latencies in live processing to enhance user experience, as latencies can occur due to processing time and the UAV's limitations in painting speeds compared to a human hand.

The most important challenges discussed by the researchers [9] include the hazards posed to human painters by painting chemicals, leading to eye and respiratory problems, as well as the repetitive and time-consuming nature of manual painting tasks. Another challenge highlighted is the need to reduce or eliminate human exposure to hazardous environments during painting activities, emphasizing the importance of safety in construction tasks.

The researchers [10] discusses the challenge of the Iterative Closest Point (ICP) algorithm getting trapped in local minima during pose estimation, which was addressed by combining it with a Genetic Algorithm (GA) to search for the global minimum and reduce pose estimation errors. Another challenge highlighted is the lack of robustness of ICP to local minima, which was resolved by integrating GA to optimize pose error and prevent local minimum entrapment.

The challenges discussed in the paper [11] include workforce challenges like lack of continuous training and unskilled workforce, economic challenges such as high initial capital investment and low return on investment, cultural challenges like aversion to change and job security concerns, industry-intrinsic challenges such as a fragmented industry and intense competition, and research and development challenges like low investment in research and development and weak innovation culture.

The researcher [24] discusses the challenges faced in shipbuilding, particularly in the painting of the outer plate of ships, which is considered dangerous due to human workers operating at high altitudes with painting equipment.

4. FUTURE OF AUTONOMOUS WALL PAINTING ROBOT

The future scope of autonomous wall painting robots is promising, driven by advancements in robotics, artificial intelligence, and user interaction. These robots can revolutionize not only the painting industry but also public art and expression.

4.1. Technological Advancements

- Navigation and Control: Autonomous robots like those utilizing fuzzy incremental controllers can effectively navigate walls, ensuring precise movement and painting coverage.
- Automated Painting Systems: Robots equipped with vision systems and GPS can generate painting plans and execute them autonomously, enhancing efficiency and accuracy in large-scale projects.

4.2. Applications in Public Art

- Interactive Art: WallBots allow artists and activists to engage with public spaces creatively, enabling low-cost, DIY art installations across various surfaces.
- Artistic Techniques: Robots that mimic human painting techniques, such as underpainting and refinement, can produce intricate artworks, expanding the creative possibilities for artists.

While the potential for autonomous wall painting robots is vast, challenges remain in ensuring artistic quality and public acceptance, which will require ongoing research and development.

5. METHODS, FINDINGS AND LIMITATIONS

Table 5.1 Comparative analysis of Different methods, findings and their limitations

Author	Method Used	Findings	Limitations
Y. Mahulkar, A. R. Kalbande [24]	Electrostatic spray-painting technique	An Automatic Wall Painting Robot to achieve low-cost painting equipment.	1) The hazards caused by painting chemicals to human painters 2) Repetitive and time-consuming method.
Y. Song, J. Wu [21]	Similitude analysis method considering electro-mechanical coupling effect	The implementation of a spray-painting robotic system under optimal conditions is conducted, thereby addressing issues related to motor inertia and resistance distortion.	Influencing the interrelations among variables and possibly altering the comparative analysis of dynamic performances.
V. TADI, A. ODRY [18]	ZED Depth Sensor for Painting Robot Vision	Detecting and extracting surfaces and objects for painting robot	The formation of a marked shadow on the surface, which restricts the camera's visibility and may yield a deficient depth image.
Y. Ma, N. Xi [12]	Mobile painting Technique	The smooth implementation of simulation process demonstrates that the optimized structure parameter can fulfil the task requirement	Need for a large number of discrete points for obtaining good results
A. Anwar, Z. Li [10]	Cross Correlation Method	The findings were derived from the collected point clouds of the lateral automotive components.	Required more time than the actual processing due to the parallel implementation
B. Sai Krishna, Chandrashekar. M [9]	Movable painting using Roller fed with liquid paint	The opportunity to reduce or eliminate human	The components involved in painting may entail significant dangers for human artists, comprising problems concerning visual health and respiratory function.
A. Vempati, H. Khurana [8]	Smoothing planner for generating smooth trajectories for UAV	The implementation of a virtual reality interface to delineate an artistic undertaking.	does not provide complete flexibility for users to accurately modify the target.
M. Kamel, N. Stilinovic [7]	Critical UAV operations are executed on board	Autonomous spray painting using unmanned aerial vehicles (UAVs) includes area filling and customizable line painting on 3D surfaces.	The need for a dense 3D model of the target surface for painting quality,
U. Bawane, R. Bakkar [6]	Computer control system activated by operator pressing a switch on a control panel	The Automated Wall Painting bot facilitates the minimization of human engagement and the	The challenges in planning paint strokes that continue throughout different geometric primitives on

		reduction of expenditures associated with painting apparatuses.	surfaces and the inability of continuous robot motions.
M. Sorour [2]	CAD model of the fully functional wall painting robot	Presented endows several achievements in terms of total robot mass and painting rate as compared to existing literature	The restriction of the painting arm's motion laterally to the width of a maximum of paint strips in either direction from the robot centreline.

6. CONCLUSION

The development of autonomous wall painting robots has shown significant promise in enhancing efficiency, safety, and quality in painting applications. Various designs and technologies have been explored, leading to innovative solutions for both interior and exterior wall painting. A wall-following robot utilizes a fuzzy incremental controller for navigation, demonstrating effective wall tracking and movement control. Automated Painting Systems: Robots equipped with vision systems and GPS can autonomously generate painting plans and execute them, ensuring precise coverage of surfaces. Robots like the automatic paint spray system use machine vision to assess wall conditions, allowing for adaptive painting techniques that enhance uniformity and reduce waste.

The conceptual design for exterior wall painting robots indicates substantial cost savings and improved safety for workers, particularly in high-rise buildings. The use of multiple drones for graffiti and mural painting showcases the potential for rapid and efficient painting processes, which can be adapted for commercial applications. While these advancements present numerous benefits, challenges such as system complexity and initial setup costs remain. Future research may focus on optimizing these systems for broader applications in construction and maintenance.

7. REFERENCES

[1] P.Johan , J.Gunnar, and J.T. Gravdahl , “Optimal Paint Gun Orientation in Spray Paint Applications—Experimental Results” IEEE TRANSACTIONS ON AUTOMATION SCIENCE AND ENGINEERING, VOL. 8, NO. 2, APRIL 2011.

[2] M. Sorour, “RoboPainter-A Detailed Robot Design for Interior Wall Painting”, Conference: IEEE International Workshop on Advanced Robotics and its Social Impacts (ARSO-2015).

[3] O. P. Guleja, “Six DOF Spray Painting Robot Analysis”, International Journal of Advanced Research in Electrical, Electronics and Instrumentation Engineering, DOI: 10.15662/IJAREEIE.2015.0409061 ,9 Sep 2015.

[4] W. Li, W. Cui, Y. Zhang, C. Yu, “Trajectory Analysis of Painting Robot on Building Wall”, method of simulating the motion of manual painting was selected. The 11th International Conference on Computer Science & Education (ICCSE 2016) Nagoya University, Japan August 23-25, 2016.

[5] K. Madhira, S. Mehta, R. Bollineni, D. Kavathia, “AGWallP -Automatic Guided Wall Painting System”, Nirma University International Conference on Engineering (NUiCONE) 2017.

[6] U. S. Bawane, “Automatic Wall Painting Machine”, International Journal of Emerging Technologies in Engineering Research (IJETER), Vol (6) ISSN 2312-4315 Feb 2018.

[7] A. Sai Vempat, “PaintCopter: An Autonomous UAV for Spray Painting on Three-Dimensional Surfaces” IEEE ROBOTICS AND AUTOMATION LETTERS, VOL. 3, NO. 4, OCTOBER 2018.

[8] A. Sai Vempati, H. Khurana “A Virtual Reality Interface for an Autonomous Spray-Painting UAV” IEEE ROBOTICS AND AUTOMATION LETTERS, VOL. 4, NO. 3, JULY 2019.

[9] B Sai Krishan, “Fabrication of Automatic Wall Painting Machine”, International Journal of Engineering Research & Technology (IJERT) ISSN: 2278-0181, 2019.

[10] W. Lin, “Recognition and Pose Estimation of AutoParts for an Autonomous Spray Painting Robot”, IEEE TRANSACTIONS ON INDUSTRIAL INFORMATICS, VOL. 15, NO. 3, MARCH 2019.

[11] L. Oyedele, “Robotics and Automatic Systems in a Construction”, Understanding Industry Specifics Challenges for Adoption, Journal of Building Engineering, Vol (45) Nov 2019.

[12] Ye. Ma and Ning Xi, “Task-Oriented Design Optimization for a Mobile Painting Robot”, Proceeding of the IEEE International Conference on Robotics and Biomimetics Dali, China, December 2019.

[13] B. S, Madhavan, K, A. Jinushia R, Thandapani T, “Automated Exterior Wall Painting Robot Using Raspberry Pi”, 6th International Conference on Advanced Computing & Communication Systems (ICACCS) 2020.

[14] J. C. Virgolino Soares, “Autonomous Navigation System for a Wall-painting Robot based on Map Corners” 2020 IEEE.

[15] R. K Megalingam, V.P Darla Chaitanya Sai Kumar Nimmala, “Autonomous Wall Painting Robot”, robotic painting was introduced to improve the accuracy, efficiency and to reduce the cost. 2020 International Conference for Emerging Technology (INCET) Belgaum, India. Jun 5-7, 2020.

[16] R. Kumar S, Kaviarasu S, “Self-Operating Paint Bot”, A 2-dimensional axes arms are used to paint the wall. 5th International Conference on Devices, Circuits and Systems (ICDCS),2020.

[17] S. Danthala, “Automatic Spray-Painting Robot Using Regression Method”, International Journal of Recent Technology and Engineering (IJRTE) ISSN: 2277-3878, Volume-8 Issue-5, January 2020.

[18] V. Tadic, “Application of the ZED Depth Sensor for Painting Robot Vision System Development” This work was supported by the European Union under Project IEEE Access vol (9),2021.

[19] A. Munner, “Design and Implementation of Automatic Painting Mobile Robot”, IAES International Journal of Robotics and Automation (IJRA), Vol (59) ISSN 0921- 8890 March 2021.

[20] M. Okwu, L. Tartibu ,O. B. Otanocha , D. R. Enarevba, “Development of a Modular Wall Painting Robot for Hazardous Environment”, International Conference on Artificial Intelligence, Big Data, Computing and Data Communication Systems (icABCD), 2021.

[21] Y. Song, J. Wu, Z.Liu , B.Zhang , and T.Huang, “ Similitude Analysis Method of the Dynamics of a Hybrid Spray-Painting Robot Considering Electromechanical Coupling Effect” IEEE/ASME TRANSACTIONS ON MECHATRONICS, VOL. 26, NO. 6, DECEMBER 2021.

[22] K. ZBISS, A. KACEM, “Automatic Collision-Free Trajectory Generation for Collaborative Robotic Car-Painting” date of publication January 19, 2022.

[23] D.Gleeson, S.Jakobsson, N.Sandgren, and B.Lennartson, “Generating Optimized Trajectories for Robotic Spray Painting” IEEE TRANSACTIONS ON AUTOMATION SCIENCE AND ENGINEERING, VOL. 19, NO. 3, JULY 2022.

[24] Y. Mahulkar, A. Kalbande, A. Nikam, A. Katare, “A Review on Low-Cost Automation Spray Painting Robot” International Research Journal of Modernization in Engineering Technology and Science, Volume:04/Issue:06/June2022.

[25] C. Cho, “A study on Automated mobile painting robot with permanent magnet wheels for outer plate of ship” Department of automobile, Yeungnam college of science & technology korea, Conference: Robotics (ISR), 2013 44th International Symposium, October 2013.

A Comprehensive Survey on the Evolution and Deep Learning Techniques in Recommender Systems

Smitha S P ***Harishkumar K S***

smithasp.89@gmail.com harishkumar@presidencyuniversity.in

Abstract:

This survey paper provides a comprehensive review of the evolution, methodologies, and current state-of-the-art in recommender systems (RS), which are pivotal in managing the surge of data across various digital platforms, particularly in e-commerce. It traces the development of RS from early collaborative and content-based filtering techniques to sophisticated machine learning models that leverage deep learning, hybrid methods, and complex algorithms to enhance prediction accuracy and user interaction. Despite significant strides in the field, recommender systems continue to grapple with challenges including the cold-start problem, data sparsity, synonymy, and scalability, as well as ensuring user privacy in an increasingly security-conscious digital environment. The paper evaluates different RS architectures and their effectiveness across diverse sectors, highlighting how advancements like knowledge-based systems, attention mechanisms, and temporal models address specific shortcomings. We critically analyse existing gaps in technology and methodology, proposing future directions for research that include enhancing personalization features, improving adaptive learning capabilities, and integrating ethical AI practices.

Keywords.: Recommender system, Collaborative Filtering, Knowledge Filtering, Predictive Analytics, Neural Collaborative Filtering, Factorization Model.

1. INTRODUCTION

In this age of digitalization, the practice of making frequent purchases online has permeated people's daily lives. It might be challenging for customers to choose the most enticing goods from the wide selection that online stores provide. The digital era we live in today is characterized by a wealth of easily available material on the internet due to the broad availability of online services and recent technical breakthroughs. Customer reviews are appreciated for the variety of products and services that are offered online. Global advances in computer technology have led to the problem of internet data overload. Because there is so much stuff available online, it can be difficult to find relevant and useful information. Consumers may now be effectively steered to the right material utilizing more economical approaches thanks to technology improvements. Recommender systems have gained traction in the last few years. Recommender systems serve as information filters, presenting users with pertinent and useful content. Every page of the website has a suggestion system installed. On their homepages, e-commerce websites frequently include a "guess yourfavourite" function. Websites frequently use recommendation algorithms, which are used in a variety of industries including news, movies, videos, books, restaurants, and maps [1].The recommendation framework (RS) is intended to simplify the process of creating customized suggestions for clients while handling massive data sets with ease. A wide number of businesses, including publishing, movies, music, literature, essays, photography, financial services, and marriage, use random sampling, or RS. Researchers began creating suggestions in the middle of the 1990s by utilizing various filtering methods, such as collaborative and content-based filtration [2].

Considerable progress in recommendation science has been made in the last few years, with a particular focus on recommendation algorithm optimization.. Recommender systems have demonstrated superior effectiveness and customization compared to conventional keyword-based search methods in managing extensive amounts of data [3]. Numerous results are frequently returned by keyword-based searches, although many of them might not be appropriate or relevant. Researchers must use a filtering procedure in order to exclude relevant information from the search results. A significant degree of similarity will be shown in the search results when two researchers enter the identical question. The keyword-based search strategy has limitations when it comes to taking users' varied goals and interests into account. It is important to recognize the differences between the issues covered by the recommended results and the researchers' own interests. Short and controlled algorithms may be used to generate results, enabling customized and efficient recommender systems. Many

recommendation algorithms have been developed as a result of recommender systems [4]. The subject of recommendation approaches encompasses four primary types: collaborative filtering (CF), content-based filtering (CBF), graph-based filtering (GB), and hybrid recommender system. Enhancing accuracy was the primary goal of the Recommendation System (RS),. Four new goals have evolved in the field of Recommender Systems (RS) with the increase in goods and users: diversity, serendipity, innovation, and coverage [5]. The recommended products for the receiver must be chosen at random in order to maintain serendipity. This product's principal aim is to surprise the customer. It is acceptable to use the phrases "novelty" and "serendipity" interchangeably [6-7]. An often-used filtering technique called the suggestion method was first created to prioritize email content based on user significance. It was observed that typical functionalities like messages, responses, and annotations were missing. For a variety of experimental tasks, including receiving, filtering, and searching an unbroken stream of electronic documents, the tapestry facilitates group filtering. Another technique to ascertain an individual's implicit evaluation is to look at how much time they spend on a certain webpage. The fast expansion of features and product choices has made it more difficult to choose the perfect product that fits a person's tastes [8].

Depending on the particulars of each case, accessible recommendation systems may or may not be accurate.To provide suggestions for products, the first generation of e-commerce systems use a variety of filtering techniques, including content-based, collaborative, and hybrid filtering. Third-generation systems use knowledge-based models that take human characteristics, emotional aspects, and demography into account.. For the purpose of efficiently handling the substantial rise in data volume [9], it is essential to incorporate user feedback that has been assessed by a recommendation engine. In order to overcome the limitations mentioned above, the estimation and prediction of product items are conducted by utilizing the user profile [10]. The aforementioned systems commonly encounter challenges such as effectively managing data sparsity, ensuring privacy and scalability, addressing the cold-start problem with new users and items, and accurately capturing user preferences and behaviors. In addition, the paper identifies significant research gaps and proposes potential avenues for future development [11].

1.1. Challenges associated with recommendation systems

- **Cold start problem:** Users are not originally offered a new item when it is introduced to the recommendation system. It is challenging to forecast customer preferences with any degree of accuracy when ratings and reviews are missing for the item. The recommendation system could thus provide less precise options. When additional people or things are added to the system, a problem occurs.
- **Sparsity**:One problem that frequently occurs is the inability of many customers to rate or review the things they buy. This leads to an insufficiently detailed grading model. Data sparsity can cause a number of problems, such as making it challenging to pinpoint a particular user group with comparable ratings or interests.
- **Scalability:** Scalability of algorithms in recommendation systems using real-world datasets is a crucial factor to take into account. Because of the volume of dynamic data created by user-item interactions, such ratings and reviews, the aforementioned datasets provide a considerable scalability problem.

2. LITERATURE SURVEY

The scenarios that make up the recommender system are categorized based on the techniques used to produce recommendations for the e-commerce process. The recommender system generates or offers pertinent product recommendations based on algorithms, similarity coefficients, and user knowledge range.The taxonomy categorizes it into four distinct groups: content-based, knowledge-based, collaborative, and hybrid filtering. Figure 1 depicts the category utilized by the RS system for processing, as shown below:

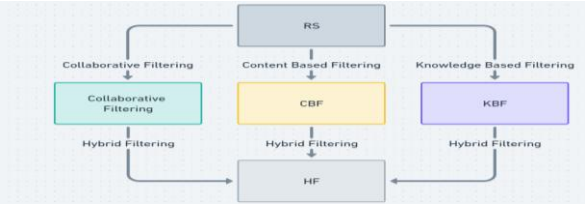

Figure 1: Types of recommendation system

- **Collaborative Filtering (CF)**

Collaborative filtering (CF) is a commonly employed technique in the field of recommender systems (RS). The process involves using historical data of users' indicated preferences for specific items to forecast future user preferences for similar goods [12]. When faced with challenges in finding new participants, user groups may adopt varying strategies for implementing the CF idea that are more effective and efficient. The complexity of the method arises from the lack of a precise definition of "collection" in terms of quality standards and personal preferences. The k-nearest neighbors (k-NN) model is employed by the Collaborative Filtering (CF) approach to assess the similarity of users' performances. The system records the elements selected by the user once the evaluation is completed. The rankings of the neighbors are utilized to determine the sequence of these items. The assessment procedure does not involve client participation. Recommender systems have become increasingly important in managing product data on websites, relying on user evaluations [13]. The recommendation system demonstrates exceptional performance across various contexts, such as e-learning and e-commerce. The RS system enables users to obtain comprehensive information about various items. The product classification is performed using a collaborative filtering-based recommendation system that utilizes the K-Nearest Neighbors algorithm and user input.

The k-NN approach will be employed to construct an information database that incorporates user similarities. A collaborative filtering technique was developed in [14] to determine user ratings for items by considering similarity. The MovieLens dataset is commonly utilized to evaluate and implement the generated model. The findings of the experimental study indicate that the collaborative filtering approach developed performs significantly better than the suggested benchmark. The effectiveness of a recommendation system is determined by the similarity metric used to measure user engagement. The Jaccard Uniform Operator Distance and the Pearson Correlation Coefficient are two factors considered when evaluating similarity. The objective of the sparse matrix is to optimize the efficient storage and retrieval of user-item ratings. The primary objective during the development of the recommendation system was to provide users with information about others who share similar interests. There was a strong focus on promoting active user engagement. A recommendation system for product rating based on a similarity model was developed in [15] to effectively identify potential similarities among consumers of a product. The model created utilizes global preference behaviour instead of relying solely on the local context information of the user rating. The experimental investigation utilizes three distinct real-time data sets, with a focus on analysing their similarity metrics.

- **Content-Based Filtering (CBF)**

Based on user experience, the Content-Based Filtering (CBF) approach is advised for presenting goods that are connected to comparable content. Examining the metadata is the first step in the analysis. Comparing the similarity of the current user data is the main goal of this inquiry. By using both historical and current data, the Collaborative Filtering (CBF) approach maximizes the suggestion and purchase process in a shorter length of time.The degree to which the content-based strategy is vulnerable depends on a number of factors, such as how well the material is described, how complicated the information has to be, and how hard it is to demonstrate user similarity. The development of a hybrid recommender system addressed the shortcomings of the aforementioned method. Collaborative and content-based filtering techniques are included into the system [15]. The process of evaluating product evaluations for similarity begins with the deployment of collaborative and content-based filtering algorithms. User similarity algorithms that are considered relevant are grouped and aggregated by the Collaborative Filtering (CBF) system.

- **Knowledge-based Filtering**

Explicit information is necessary for a knowledge-based algorithm with a recommendation system model to operate well. The knowledge-based system assesses the product's attributes and determines if it will be beneficial to the target audience by using a set of rules and algorithms. The recommendation system combines the calculated similarity score with the constraint-based knowledge option. This form's user preference is determined by a system that blends constraint-based and knowledge-based techniques. The repair system's goals are to fix data problems and provide recommendations to the user. This is accomplished by doing calculations based on predetermined parameters and constraints [16].The knowledge-based (KB) component contains the decisions about user requests that are derived from the decision-making model. Expert domain knowledge is often utilized by the Knowledge Base (KB) to compute and maintain recommendation-specific rules. The knowledge-based approach is intended to use observable conditions and system interaction. The prediction system makes use of the values that are produced by these observable circumstances. The main benefit of the Knowledge Base (KB) system is that it can be tailored to fit different sets of rules in the recommendation process system, including business rules. This cold-start issue is avoided by the knowledge-based recommender scheme, which uses user ratings to provide recommendations [17]. The knowledge-based approach's collection of clear fashion guidance information is one of its limitations. The case-based subscheme and the constraint-based sub-scheme make up the knowledge-based scheme.

- **Hybrid Filtering**

The main goal of hybrid recommendation systems is to integrate various strategies used in recommendation systems. The hybrid recommendation system is designed to leverage the strengths of both X and Y strategies to overcome the limitations. The challenge arises when novel product formulations do not have a rating, making it impossible to recommend them using the collaborative filtering approach. The implementation of the method for detecting and predicting new product descriptions is not restricted solely to the content-based system. A hybrid model-based system is developed through the integration of different techniques and approaches. The recommender system employs a hybrid recommender scheme to gather implicit input on manufacturing procedures. Content-based filtering (CBF) is a predictive method that focuses on the product's features to determine its rating. The identification of specific qualities of the new product that align with the user profile is challenging based on the product profile and user feedback. Consequently, providing a recommendation becomes difficult. The cold-start problem is a significant challenge encountered by the hybrid recommendation model. It pertains to the difficulty of providing necessary product information when there is no product rating available. The sequential suggestion approach has been commonly employed in research investigations. The FPMC system [14] utilizes factorization of the transition matrix of the underlying Markov Chain (MC) to generate personalized sequential behaviors for predicting items. This is achieved by leveraging the capabilities of Markov Chains (MC) and Matrix Factorization (MF). The Recurrent Neural Network (RNN) is currently utilized to effectively capture the long-term dependence of user-item interactions in a series. The achievement is facilitated through the implementation of various strategies. The session-based recommendation method utilizes the user-based RNN, GRU4Rec, and HRNN models to analyze user behavior and detect dependencies. A Gated Recurrent Unit (GRU) is utilized in the operation of these models. The GRU4RecC method is an enhancement of the GRU4Rec model. The performance of the original model is enhanced by employing a unique sampling technique and loss function in this strategy. The RRN approach utilizes the long short-term memory (LSTM) methodology [15] to calculate the dynamic embeddings of individuals and objects. Table 1 displays the survey table. Deep learning is used in the collaborative filtering process of the NeuralCF technology. It has grown in popularity and is being used in many different contexts right now [16]. The NeuralCF method replaces the inner product operation in matrix decomposition with a neural network, improving the model's ability to handle nonlinearity and integrate information. Parameter satisfaction, user modeling, machine learning data, and other AI approaches are used.

Table 1: Model and its Gaps

Model	Advantages	Disadvantages	Research Gaps
FPMC	Integrates MC with MF for tailored predictions.	May not capture complex sequential patterns as effectively as DNNs.	Need for deeper learning techniques to improve accuracy.
GRU4Rec, HRNN	Effective in modeling user behavior and dependencies for session-based recommendations.	Limited by session length and data sparsity issues.	Enhancements in handling longer sequences.
GRU4RecC	Enhances GRU4Rec with a unique loss function and sampling scheme.	May overfit on specific session patterns.	Methods to reduce overfitting and increase generalizability.
RRN	Employs LSTM to capture dynamic embeddings effectively.	High computational cost, complex to train.	Optimization of computational efficiency.
LSTM	Well-suited for long-term dependency modeling.	Struggles with very long sequences and forgetfulness of initial inputs.	Improvements in memory retention over longer sequences.
NeuralCF	Replaces inner product with NN, enhancing nonlinear feature combination.	May require extensive data to train effectively.	Techniques to reduce training data requirements.
AFM	Attention mechanism highlights important traits dynamically.	Complexity increases with number of traits.	Scalability and efficiency improvements.

One machine learning approach that regularly generates suggestions is the AdaBoost algorithm. Tags are used to contain user material. AFM, or the Attention Factorization Model, was created by [17] in order to address the necessity to account for the varied significance of various crossing attributes. An attention mechanism is incorporated into the AFM factorization model. A two-headed self-encoder model was introduced with the goal of learning representation from user comments and implicit feedback. The authors' suggested method is an easily scalable architecture neural network-based grading tool. The aim of this methodology is to faithfully capture the intrinsic properties of entities and people in complex nonlinear contexts. A unique deep attention-based sequential model was put out in an earlier work [18]. In order to properly discern an item's relevance with respect to the user's short- and long-term preferences, the model makes use of attention processes. Recommender systems make extensive use of attention methods. The authors described a collaborative sequential recommendation system with category awareness in their work [19]. The system employs a self-attentive methodology to scrutinize and detect recurrent patterns across several categories. After then, the system determines which particular transition patterns need to be taken into account by considering the categories of recent actions. The suggested method is a processes-based, self-attentive learning paradigm for knowledge representation. This paradigm makes use of knowledge graphs to enhance the communication of entity learning characteristics. According to reference, the self-attention mechanism helps the user recognize important information by reducing the impact of outside information on the attention mechanism. The model's goal is to have a thorough grasp of the direct links between each item and the underlying structure of the behavioral sequence.

3. Conclusion:

In conclusion, this survey has extensively explored the dynamic landscape of recommender systems, chronicling their evolution from simple algorithmic frameworks to sophisticated systems that integrate advanced machine learning techniques. Despite the remarkable progress in enhancing personalization and accuracy, several persistent challenges remain. Key among these are the cold-start problem, data sparsity, and maintaining user privacy and system scalability in diverse applications. The continuous growth in digital data further complicates these issues, necessitating innovative solutions.Future research should focus on developing robust models that not only address these challenges but also incorporate user feedback in real-time, adapt to changing user

behaviours, and respect ethical standards in data usage. Moreover, integrating cross-disciplinary approaches from fields such as psychology and sociology could enrich the understanding of user interactions and improve the recommendation quality.

References:

1. G. Zhang, Y. Liu, and X. Jin, ‘‘A survey of autoencoder-based recommender systems,’’ Frontiers Comput. Sci., vol. 14, no. 2, pp. 430–450, Apr. 2020.
2. S. Zhang, L. Yao, A. Sun, and Y. Tay, ‘‘Deep learning based recommender system: A survey and new perspectives,’’ ACM Comput. Surv., vol. 52, no. 1, pp. 1–38, Jan. 2020.
3. R. Mu, ‘‘A survey of recommender systems based on deep learning,’’ IEEE Access, vol. 6, pp. 69009–69022, 2018.
4. D. Alahmadi and F. Alruwaili, ‘‘Deep learning for MOOCs course recommendation systems: State of the art survey,’’ Int. Trans. J. Eng. Manage. Appl. Sci. Technol., vol. 12, no. 11, 2021, Art. no. 12A11Q.
5. L. Salau, M. Hamada, R. Prasad, M. Hassan, A. Mahendran, and Y. Watanobe, ‘‘State-of-the-art survey on deep learning-based recommender systems for e-learning,’’ Appl. Sci., vol. 12, no. 23, p. 11996, Nov. 2022.
6. vanCapelleveen, G., Amrit, C., Yazan, D. M., &Zijm, H. (2019). The recommender canvas: a model for developing and documenting recommender system design. Expert systems with applications, 129, 97-117.
7. Haruna, K., Akmar Ismail, M., Damiasih, D., Sutopo, J., &Herawan, T. (2017). A collaborative approach for research paper recommender system. PloS one, 12(10), e0184516.
8. Mısır, M., &Sebag, M. (2017). Alors: An algorithm recommender system. Artificial Intelligence, 244, 291-314.
9. Tejeda-Lorente, Á.,Porcel, C., Peis, E., Sanz, R., & Herrera-Viedma, E. (2014). A quality based recommender system to disseminate information in a university digital library. Information Sciences, 261, 52-69.
10. Winkels, R., Boer, A., Vredebregt, B., & Van Someren, A. (2014, November). Towards a Legal Recommender System. In JURIX (pp. 169-178).
11. Ma, T., Zhou, J., Tang, M., Tian, Y., Al-Dhelaan, A., Al-Rodhaan, M., & Lee, S. (2015). Social network and tag sources based augmenting collaborative recommender system. IEICE transactions on Information and Systems, 98(4), 902-910.
12. Kiran, R., Kumar, P., & Bhasker, B. (2020). DNNRec: A novel deep learning based hybrid recommender system. Expert Systems with Applications, 144, 113054.
13. Sridevi, M., Rao, R. R., & Rao, M. V. (2016). A survey on recommender system. International Journal of Computer Science and Information Security, 14(5), 265.
14. Wang, D., Liang, Y., Xu, D., Feng, X., & Guan, R. (2018). A content-based recommender system for computer science publications. Knowledge-Based Systems, 157, 1-9.
15. Gulzar, Z., Leema, A. A., & Deepak, G. (2018). Pcrs: Personalized course recommender system based on hybrid approach. Procedia Computer Science, 125, 518-524.
16. M. A. Islam, M. M. Mohammad, S. S. S. Das, and M. E. Ali, ‘‘A survey on deep learning based Point-of-Interest (POI) recommendations,’’ Neurocomputing, vol. 472, pp. 306–325, Feb. 2022.
17. Y. Dai and J. Xu, ‘‘Study of online learning resource recommendation based on improved BP neural network,’’ Int. J. Embedded Syst., vol. 14, no. 2, p. 101, 2021.
18. T. K. Dang, Q. P. Nguyen, and V. S. Nguyen, ‘‘A study of deep learningbased approaches for session-based recommendation systems,’’ Social Netw. Comput. Sci., vol. 1, no. 4, p. 216, Jul. 2020.
19. K. Barbara and C. Stuart, ‘‘Guidelines for performing systematic literature reviews in software engineering,’’ Version 2.3, Dept. Comput. Sci., Keele Univ., Keele, U.K., Tech. Rep. EBSE-2007-01, 2007, pp. 1–26.



Smitha S P received her Bachelor's degree in Computer Science and Engineering from Visvesvaraya Technological University, Belgaum in 2011, Master's Degree in Computer Science and Engineering from Visvesvaraya Technological University, Belgaum in 2014 Currently, She is also pursuing her Ph.D. at Presidency University. Smitha S P is an Assistant Professor with 10.2 years of teaching experience, currently serving in the School of Computer Science and Engineering (SoCSE) at Presidency University, Bengaluru, since February 2023.



Dr.Harishkumar K.S. is an Assistant Professor Senior Scale in at the School of Computer Science Engineering, Presidency University with 8 years of postgraduate and undergraduate teaching experience. He has a Ph.D. in Data Science and research interests in AI, machine learning and deep learning. He has published more than 20 research papers in peer-reviewed journals and conferences including, Elsevier, IEEE, Springer and Scopus publications. His papers apply AI for problems like air quality prediction, plant disease detection etc. He has over 289 google scholar citations with 4 H-index, 193 Scopus index citations with 3 H-index and present guides for 5 research scholars and 1 scholar already awarded. He has authored a book chapter and edited book on AI trends. He has taught computer science subjects at universities like Mangalore University and Vijayanagara sri krishnadevaraya University. He has completed over 20 certifications in machine learning, Python, data science etc. He serves as a reviewer for 10 journals, is an editorial member for 2 journals and a technical committee member for multiple conferences. He has been an invited speaker to deliver talks on AI and big data analytics. He has strong academic credentials with rich research, teaching and reviewing experience in the fields of AI, data science and computer science.

Stock Price Prediction Using Machine Learning Algorithms

Sumukha K Nayak, Krishnamurthy Nayak and Supreetha B S

[2,3] *Department of Electronics & Communication Engineering, Manipal Institute of technology, Manipal Academy of Higher Education, Manipal,*

supreetha.bs@manipal.edu, km.nayak@manipal.edu

[1] *Student, BITS Pilani, Pilani Campus, Rajasthan, India,*

Email: f20230932@pilani.bits-pilani.ac.in

Abstract.

Stock price prediction is essential in today's dynamic financial markets. This research uses machine learning algorithms to forecast stock prices, helping investors make informed decisions. The process includes data acquisition from Tata Global Beverages for learning model for stock price prediction. The study utilizes Python and libraries like pandas, NumPy, scikit-learn, and TensorFlow. Various models are evaluated using metrics like RMSE, MAE, and R^2. The results highlight each model's effectiveness in predicting stock prices, providing valuable insights for financial decision-making. The random forest consistently outperformed other techniques, delivering the lowest RMSE and highest R-Squared values.

.

Keywords. Stock price prediction, machine learning, tata Global Beverages, RMSE, hyperparameters.

1. INTRODUCTION

Stock price prediction using machine learning has become increasingly important in finance, offering advanced solutions to the complexities and volatility of modern financial markets. The work aims to develop predictive models using historical data and machine learning algorithms to assist investors in making informed decisions. The objectives include developing and evaluating machine learning models for accurate stock price prediction, enhancing prediction accuracy, and visually representing predicted versus actual prices. The target specifications aim to deliver reliable predictive models for investors and financial analysts, enhancing investment decisions, portfolio management, and risk mitigation. The motivation for this research work arises from the limitations of traditional stock price prediction methods and the need for more accurate forecasting techniques. Previous studies often lacked comprehensive comparisons of machine learning algorithms and used limited datasets, leading to less accurate predictions. This research aims to address these gaps by employing advanced machine learning techniques, providing more reliable insights into market trends.

In today's volatile financial markets, accurate stock value estimation is essential for investors, analysts, and researchers. Recent research highlights the effectiveness of data driven approaches outperforming traditional methods. Also, Random Forest. Long Short-Term Memory (LSTM) networks show superior performance compared to simpler techniques such as linear regression, particularly in capturing temporal dependencies in stock prices. K Nearest Neighbours (KNN) has demonstrated potential with a high accuracy rate of 70%. The literature provides various insights into the effectiveness of different methodologies. Studies by Vijha et al. [1] and Pramod et al. [2]. emphasize the strengths of ANN and LSTM, respectively, in forecasting stock values. Parmar et al. [3] focus on regression and LSTM models, while Nandakumar et al. [4] highlight LSTM's advantages in handling temporal dependencies. Sonkavde et al. [5] review multiple algorithms, recommending ensemble techniques and careful hyperparameter tuning. Vanukuru et al. [6] discuss the potential of Support Vector Machines (SVM), and Latha et al. [7] propose KNN for its simplicity and effectiveness. Zhang et al. [8] find linear regression performs better with limited data compared to LSTM. Sharma et al. [9] identify XGBOOST as a highly effective model, and Al-Ali et al. [10] highlight CNN and LSTM as top performers across various sectors. Raj et al. [11] and Kumar et al. [12] explore the application of LSTM, and Wong et al.

[13] suggest integrating sentiment analysis with prediction models. Xue et al. [14] propose a novel approach using multi-branch LSTM models, while Purnama et al. [15] show that Linear Regression outperforms SVM. Liu et al. [16] develop an optimized LSTM model with regularisation techniques, improving accuracy. Gunturu et al. [17] find that hybrid models combining Linear Regression and Random Forest are particularly effective. Bathla et al. [18] emphasize LSTM's superiority over Support Vector Regression (SVR), and Patnaik et al. [19] provide a comprehensive review of various AI approaches. Rodrigues et al. [20] propose integrating sentiment analysis with ARIMA-LSTM hybrids to enhance prediction accuracy. Machine learning algorithms, including ANN, LSTM, SVM, KNN, and hybrid models, have demonstrated significant capabilities in predicting stock market trends.

2. METHADOLOGY

The process begins with the collection of historical stock market data from reputable sources such as Yahoo Finance. The dataset of Tata Global Beverages Limited (TATAGLOBAL) is considered for the study. The data collected includes daily opening and closing prices, trading volumes, and other financial measures, which provide a comprehensive view of market dynamics

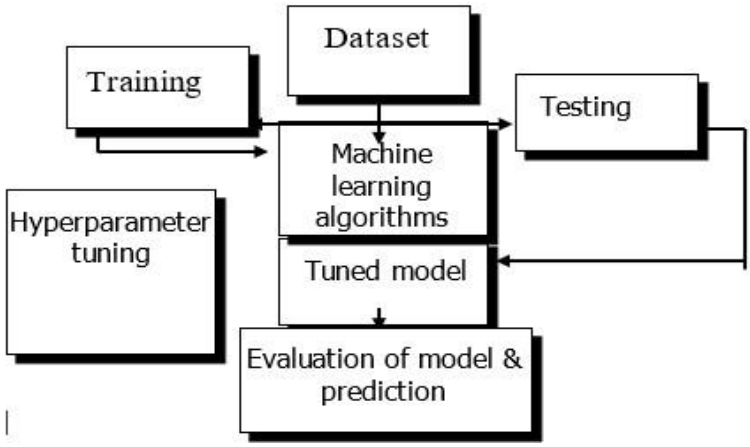

Figure 4. Methodology Block diagram

Using Python libraries like Pandas and NumPy, the data is cleaned with techniques such as Min-Max scaling. This ensures the data is consistent and ready for machine learning models. Feature engineering further enhances the data by incorporating lagged variables, technical indicators like moving averages, and volume-based features.



Figure 2: Close prize history

In this study, moving averages are utilized as key features to enhance stock price prediction models. By including these moving averages, the model is better equipped to capture underlying trends and potential turning points in

the stock price. The plots of these moving averages illustrate how they track the stock's price movements, providing visual cues that help in understanding market dynamics and making more informed predictions.

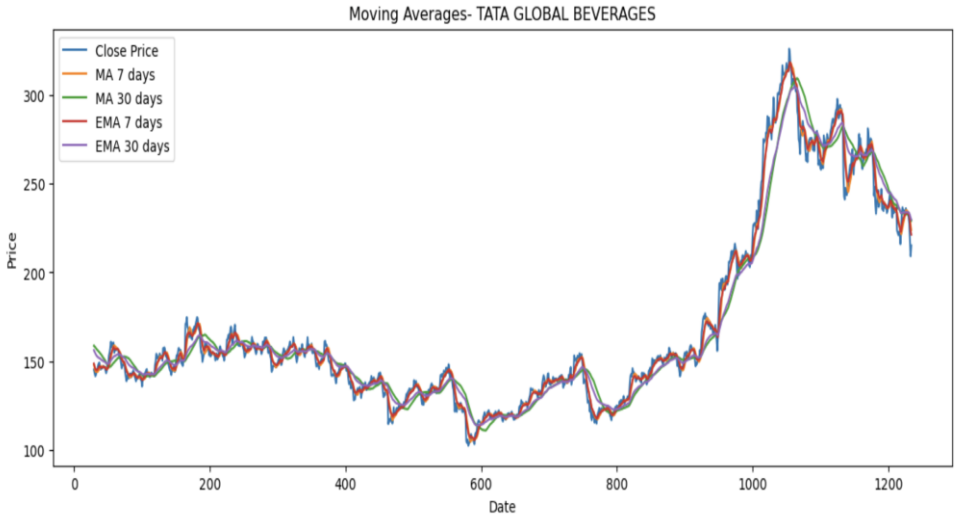

Figure 3: Moving averages plot

The methodology includes the selection and implementation of different machine learning models. Each model is carefully implemented and tuned using Python libraries such as Scikit-learn, Keras, and Statsmodels. For example, LSTM networks are designed with specific layers and regularization techniques to improve prediction accuracy, while Random Forest models leverage ensemble learning to enhance robustness.

Evaluation metrics such as Root Mean Squared Error (RMSE), Mean Absolute Error (MAE), and R-squared are used to compare predictions against actual stock prices. Visualization tools are also employed to plot predicted versus actual prices and analyze error distributions, providing valuable insights into model performance.

3. RESULTS & DISCUSSION

The evaluation of stock price prediction models involves a thorough examination of numerous metrics. Root Mean Squared Error (RMSE) is used to calculate the average difference between predicted and actual values, whereas R-squared values are used to determine how well a model's independent variables explain the variation in the dependent variable. Mean Absolute Error (MAE) adds to this study by calculating the average absolute errors between predicted and actual values. These metrics are applied to a variety of models, including ARIMA, K-Nearest Neighbours, Linear Regression, Long Short-Term Memory (LSTM), Random Forest, and Support Vector Machine (SVM). By comparing these metrics and examining error distributions, effective model can be established, characterised by reduced RMSE and MAE, as well as higher R-squared values, indicating higher accuracy and predictive capabilities. Visualization in stock price prediction involves plotting train actual, validation actual and predicted data using `plt.plot()`.This comparative analysis assesses models' performance. Error distribution plots created using plt.hist(), offer insights into prediction accuracy by showcasing the frequency and magnitude of errors between actual and predicted values. Errors that are centred at 0 suggest consistent and unbiased predictions. A skewed distribution to the left implies that the model usually underestimates actual values, whereas a skew to the right indicates overestimation. Stakeholders leverage these visuals for informed decision-making, refining predictive strategies and understanding model efficacy in forecasting stock prices.

A. ***LINEAR REGRESSION:***

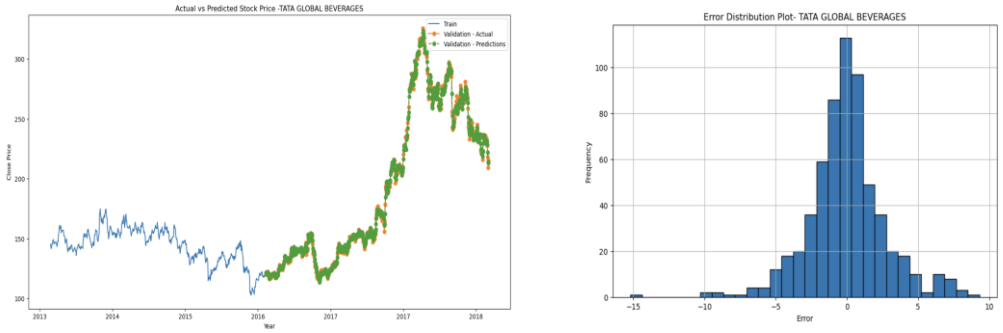

Fig.4. Actual vs predicted stock price and Error Distribution plot -Linear Regression

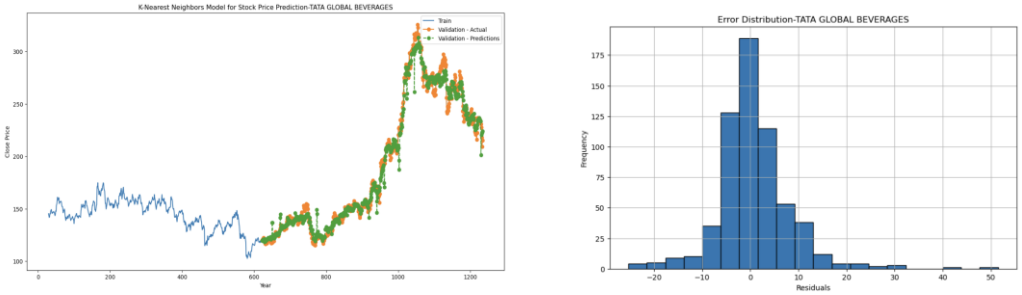

Fig.5 Actual vs predicted stock price and Error Distribution plot for K-Nearest Neighbours algorithm

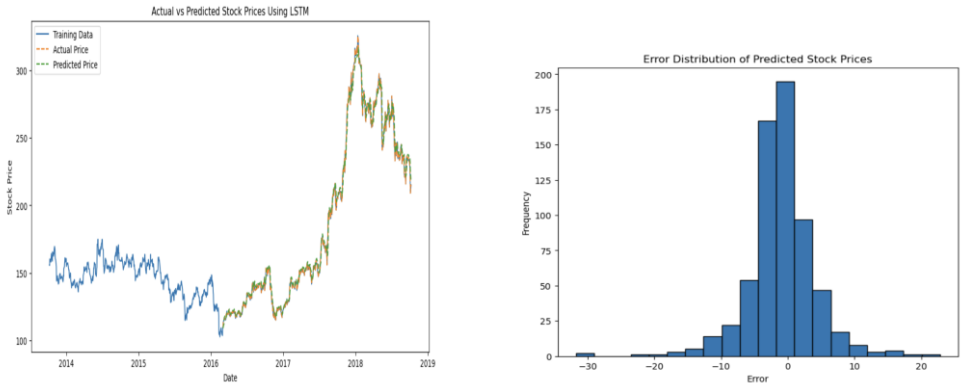

Fig.6. Actual vs predicted stock price and Error Distribution plot for LSTM

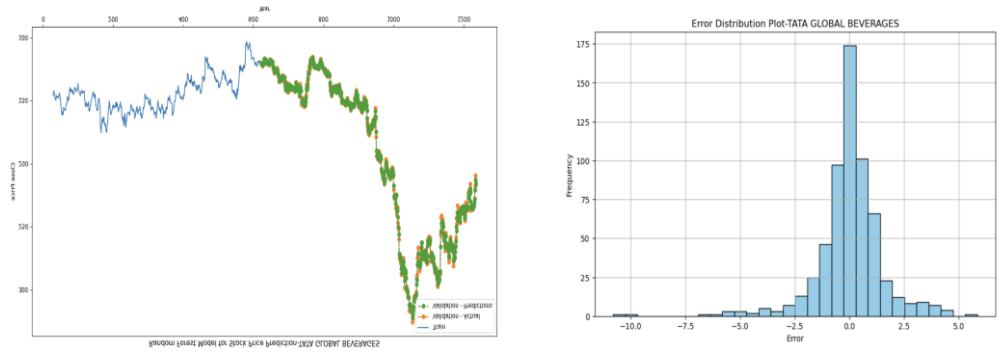

Fig.7. Actual vs predicted stock price and error distribution plot -Random Forest

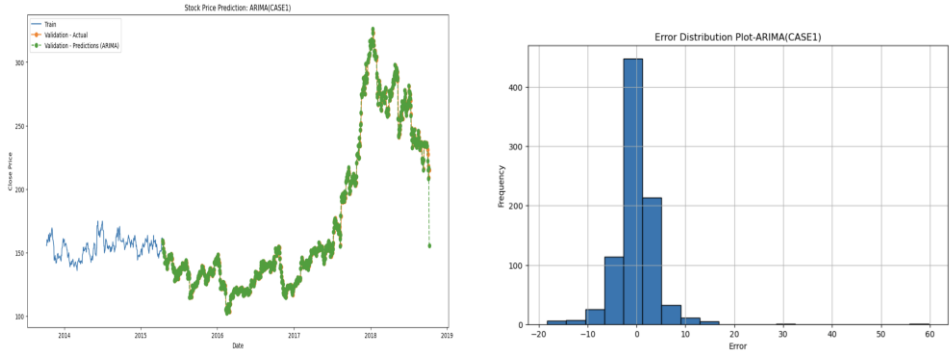

Fig.8. Actual vs predicted stock price and error distribution plot-ARIMA

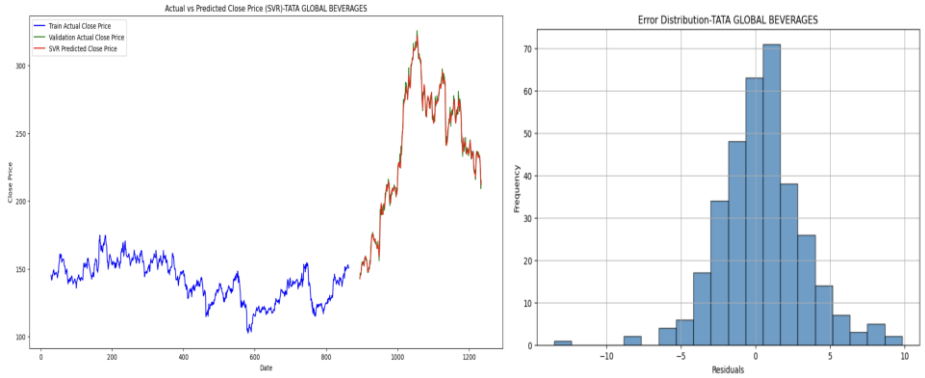

CASE-1-Best Parameters for SVR: {'C': 100, 'epsilon': 0.0001, 'kernel': 'linear'}

Fig.9. Actual vs predicted stock price and error distribution plot SVR

The performance analysis through statistical indices like RMSE and MAE R2 is as presented in table#.

Table 7.1. Evaluation Metrics Values

Model	RMSE	R-squared	MAE
Linear Regression	2.73	0.998	1.93
K-N nearest neighbours	4.28	-2.580	5.09
LSTM	4.00	0.992	0.96
Random Forest	1.57	0.999	0.99
ARIMA	4.45	NaN	2.72
SVM	2.83	0.996	2.09

In the analysis of stock price prediction models, Random Forest consistently outperformed other techniques, delivering the lowest RMSE and highest R-squared values across both cases, underscoring its robustness and reliability. Linear Regression also performed well, particularly showing strong predictive power with minimal error. Support Vector Machine (SVM) achieving the lowest RMSE and highest R-squared, demonstrating its effectiveness with appropriate parameter tuning. In contrast, K-Nearest Neighbours (KNN) and ARIMA struggled, with high RMSE and negative R-squared values, likely due to their sensitivity to noise and model assumptions. Long Short-Term Memory (LSTM) models provided reasonable results, The results highlight that model efficacy varies based on dataset characteristics. Random Forest and SVM demonstrated superior

performance, while Linear Regression and LSTM require careful adjustment to avoid overfitting. KNN and ARIMA performed poorly, potentially due to their sensitivity to data noise and assumptions about linearity. The poor performance of KNN suggests issues with data noise and dimensionality, while ARIMA's linearity assumptions may not suit complex, non-linear datasets. The visualizations of predicted versus actual values and error distributions further support these findings, revealing each model's strengths and weaknesses. Models that closely matched the ideal line were more accurate, while significant deviations indicated areas needing improvement. Error distribution graphs showed that narrower distributions corresponded to consistent performance, whereas broader distributions reflected variable accuracy.

4. REFERENCES

[1] Vijha, M., Chandola, D., Tikkiwal, V. A., & Kumar, A. (2019). Stock Closing Price Prediction using Machine Learning Techniques. Procedia Computer Science, 167, 599606. doi: 10.1016/j.procs.2020.03.326.

[2] B S, Pramod, and Mallikarjuna Shastry P. M. "Stock Price Prediction Using LSTM." TEST ENGINEERING AND MANAGEMENT, vol. 83, May-June 2020, pp. 5246-5251.

[3] Parmar et al., "Stock Market Prediction Using Machine Learning," 2018 First International Conference on Secure Cyber Computing and Communication (ICSCCC), Jalandhar, India, 2018, pp. 574-576, doi: 10.1109/ICSCCC.2018.8703332.

[4] Nandakumar, R., K R, U., R, V., & Lokeswari, Y. V. (2018). Stock Price Prediction Using Long Short-Term Memory. International Research Journal of Engineering and Technology (IRJET), 05(03), 3342-3348.

[5] Sonkavde, G. *et al.* (2023) Forecasting stock market prices using machine learning and Deep Learning Models: A systematic review, performance analysis and discussion of implications, *MDPI*.

[6] Vanukuru, Kranthi. (2018). Stock Market Prediction Using Machine Learning. . International Research Journal of Engineering and Technology (IRJET),05(10).

[7] R. S. Latha *et al*., "Stock Movement Prediction using KNN Machine Learning Algorithm," *2022 International Conference on Computer Communication and Informatics (ICCCI)*, Coimbatore, India, 2022.

[8] H. Zhang, "Stock Price Prediction using Linear Regression and LSTM Neural Network," *2022 International Conference on Machine Learning and Intelligent Systems Engineering (MLISE)*, Guangzhou, China, 2022.

[9] P. Sharma and M. K. Jain, "Stock Market Trends Analysis using Extreme Gradient Boosting (XGBoost)," *2023 International Conference on Computing, Communication, and Intelligent Systems (ICCCIS)*, Greater Noida, India, 2023, pp. 317-322.

[10] Al-Ali and A. I. Al-Alawi, "Stock Market Forecasting Using Machine Learning Techniques: A Literature Review," *2024 ASU International Conference in Emerging Technologies for Sustainability and Intelligent Systems (ICETSIS)*, Manama, Bahrain, 2024, pp. 466-471.

[11] N. Raj, "Prediction of Stock Market Using LSTM-RNN Model," *2023 International Conference on Self Sustainable Artificial Intelligence Systems (ICSSAS)*, Erode, India, 2023, pp. 623-628.

[12] Kumar, S. Hooda, R. Gill, D. Ahlawat, D. Srivastva and R. Kumar, "Stock Price Prediction Using Machine Learning," *2023 International Conference on Computational Intelligence and Sustainable Engineering Solutions (CISES)*, Greater Noida, India, 2023, pp. 926-932.

[13] Wong, J. Figini, A. Raheem, G. Hains, Y. Khmelevsky and P. C. Chu, "Forecasting of Stock Prices Using Machine Learning Models," *2023 IEEE International Systems Conference (SysCon)*, Vancouver, BC, Canada, 2023, pp. 1-7

[14] T. Xue, S. Qin and Q. Fu, "Stock Market's Price Movement Prediction with Multi-branch LSTM and Technical Analysis," *2023 International Conference on Neuromorphic Computing (ICNC)*, Wuhan, China, 2023, pp. 338-344.

[15] Purnama, I & Ginantra, Ni & Darma, I Wayan Agus Surya & Udayana, I. (2023). Comparison of Support Vector Machine (SVM) and Linear Regression (LR) for Stock Price Prediction. 1-6.

[16] M. Liu and Y. Zhao, "Stock Prediction Based on LSTM Model," *2023 China Automation Congress (CAC)*, Chongqing, China, 2023, pp. 1794-1798.

[17] P. A. Gunturu, R. Joseph, E. S. Revant and S. Khapre, "Survey of Stock Market Price Prediction Trends using Machine Learning Techniques," *2023 International Conference on Artificial Intelligence and Applications (ICAIA) Alliance Technology Conference (ATCON-1)*, Bangalore, India, 2023, pp. 1-5.

[18] G. Bathla, "Stock Price prediction using LSTM and SVR," *2020 Sixth International Conference on Parallel, Distributed and Grid Computing (PDGC)*, Waknaghat, India, 2020, pp. 211-214.

[19] D. Patnaik, N. V. Jagarmadha Rao, B. Padhiari and S. Patnaik, "Stock Price Forecasting Using Machine Learning Techniques: A Systematic Review," *2023 International Conference on Data Science & Informatics (ICDSI)*, Bhubaneswar, India, 2023, pp. 243-251.

[20] A. P, J. Rodrigues, R. R. Naik, K. M. C. Kumar and P. Shetgaonkar, "Stock Market Prediction Using Machine Learning - A Survey," *2024 3rd International Conference for Innovation in Technology (INOCON)*, Bangalore, India, 2024, pp. 1-7.

Biographies



Sumukha K Nayak is persuing his Engineering degree from BITS Pilani, Pilani Campus, Rajasthan. He is currently working on artificial intelligence, web development, computational intelligence and optimization, MERN stack and embedded system design in different student clubs. He can be contacted at email: f20230932@pilani.bits-pilani.ac.in.



Krishnamurthy Nayak received the B.Tech. degree in Electronics and Communication Engineering from Manipal Institute of Technology, Manipal, and the M.Tech. and PhD degree from Dr.M.G. R Educational and Research Institute, Chennai, India He is currently working as additional professor in the Department of Electronics and Communication Engineering at MIT Manipal. His current research interests include soft computing applications for environmental sustainbility, design of bio and micro sensors for environmental applications and MEMS Technology. He can be contacted at email: km.nayak@manipal.edu



Supreetha B S received B.Tech. degree in Electronics and Communication Engineering from Mangalore University, M.Tech. and Ph.D. degree from Manipal Institute of Technology, Manipal, India. She is currently working as Assistant Professor (selection grade) in the Department of Electronics and Communication Engineering, MIT Manipal. Her current research interests include soft computing applications for environmental sustainability, design of bio and micro sensors for environmental applications, analog system design and MEMS technology. She can be contacted at email: supreetha.bs@manipal.edu.

Optimizing Path Costs in Dynamic Network Routing Using a Bio-Inspired 'Sit-and-Wait' Strategy in the Cheetah Chase Algorithm

M. Goudhaman[1]*, N. Vanathi[2], Adithya GV[3]

1Assistant Professor - CSE, RajaIakshmi Institute of Technology, goudhaman@ritchennai.edu.in

2Associate Professor - Mathematics, Vels Institute of Science, Technology & Advanced Studies, vanathi.sbs@vistas.ac.in

3Student- CSE, KCG College of Technology, aadithyagoudhaman@gmail.com.

Abstract

Routing optimization in dynamic network environments requires innovative strategies to address challenges like high path costs and inefficient resource utilization. Traditional routing algorithms often rely on static or semi-dynamic methods that fail to adapt effectively to changing topologies. To overcome these limitations, this research introduces a **Novel Cheetah Chase Algorithm (CCA)** inspired by the cheetah's "sit-and-wait" hunting strategy.

The "sit-and-wait" approach, observed in predator-prey dynamics, involves strategic patience to identify the most opportune moment for action, minimizing unnecessary energy expenditure while maximizing efficiency. Translating this strategy into network routing, the CCA incorporates an adaptive decision-making mechanism that evaluates multiple routing options before selecting the most cost-effective path. By "waiting" for better opportunities in the network topology and "acting" decisively when the optimal path is identified, the algorithm achieves significant reductions in path costs and enhances overall routing efficiency.

Keywords:
Sit-and-wait strategy, bio-inspired algorithms, network routing, path cost optimization, adaptive decision-making, dynamic networks.

1. INTRODUCTION

Overview of Network Topologies and the Importance of Path Finding

In the realm of computer networks, the structure and organization of network devices are crucial for efficient communication and data transfer. This structure, known as network topology, dictates how different nodes (computers, routers, or other devices) are interconnected and how data flows across the network. The importance of understanding network topology lies in its direct impact on network performance, scalability, fault tolerance, and overall efficiency [1].

Inspiration from the Cheetah's hunting strategy

Artificial Intelligence (AI) has revolutionized problem-solving methodologies across various domains by emulating human-like intelligence in machines. A notable method in AI is Swarm Intelligence (SI), which takes inspiration from the collective behaviours of social creatures like ants, bees, and birds to address complex problems using decentralized control and self-organizing systems.

The Cheetah Chase Algorithm [5] is inspired by the natural hunting strategy of cheetahs, which involves selecting the most optimal path to chase down prey. In the context of Network Ad-hoc routing, this algorithm can be adapted to address the Shortest Path Problem by mimicking the cheetah's approach to dynamically finding the most efficient route in a constantly changing environment.

The fundamental principle behind the CCA is the emulation of a cheetah's hunting strategy, which involves a balance between active pursuit and strategic waiting [6]. Similar to how a cheetah strategically positions itself to intercept prey, the CCA intelligently explores the graph landscape while also pausing to evaluate potential paths. This adaptive behaviour allows the CCA to navigate through complex graph structures more efficiently, leading to improved convergence rates and optimal solutions.

2. Design of the Novel Cheetah Chase Algorithm

2.1 Inspiration from the Cheetah's Sit-and-Wait Strategy

The cheetah is a large and agile carnivore that once roamed across Asia, Africa, and parts of Europe. Known as one of Africa's most dynamic predators, cheetahs are particularly famous for their incredible speed during a chase. Capable of reaching speeds over 60 mph for short distances, they are the fastest land mammals on the planet. Unlike other African carnivores, cheetahs are primarily diurnal, which allows them to avoid competition for food from larger predators such as lions and hyenas that hunt during the cooler night time hours. Cheetahs have exceptional eyesight and rely on this ability to hunt; they typically stalk their prey from a distance of 10 to 30 meters before launching into a chase at the optimal moment.

The cheetah's lightweight and slender body make it well-suited for short, intense bursts of speed, rapid acceleration, and the ability to make sharp turns while running at high velocity. These traits are essential for the cheetah's ability to catch fast-moving prey.

2.2 Algorithm Structure and Workflow

The Cheetah Chase Algorithm is structured in several stages:

Initialization: Nodes and edges of the graph are initialized. Key parameters, such as maximum waiting time and threshold costs, are set based on initial heuristic evaluations.

Node Evaluation: Each node is evaluated for its potential to lead to an optimal path. This involves assessing the cost of traversing each edge connected to the node.

Waiting Strategy: The algorithm employs a dynamic waiting strategy, where it pauses at certain nodes based on the evaluation criteria. During this wait, it collects additional information about the surrounding nodes and potential paths.

Path Selection: After the waiting period, the algorithm selects the next node to move to, based on the cumulative path cost and the heuristic value obtained during the waiting period.

Iteration and Termination: The process iterates until the destination node is reached or all possible paths are evaluated. The algorithm terminates by selecting the path with the least cost.

3. Execution and Results

Input – for finding Optimal route using CCA

- Topology – Mesh Topology, Nodes used – 1000, Source Node – 1, Destination Node - 990
- Formation of **Adjacency Matrix**: It is 1000 * 1000 matrix, If weighted network, the weights are updated in the matrix. After the formation of Adjacency matrix, **Routing table** is constructed using Distance Vector Routing Algorithm.
- Using **sit and wait strategy** of CCA algorithm, The path cost values are updated by multiplying the randomization Parameter and step length in each edge of the path.
- Table 3.1 shows the sample path costs derived by the execution of the algorithm.

S.NO	Sample path	Path Cost	Edges	Optimal Path cost Using CCA
1	1-4-90-348-542-672-724-753-812-867-901-990	745	11	723.67
2	1-7-23-56-198-203-345-412-586-609-741-823-990	741	12	719.45
3	**1-23-513-723-823-990**	**724**	**5**	**701.54**
4	1-54-238-428-603-720-819-903-990	739	8	734.28
5.	**1-23-513-675-823-990**	**724**	**5**	**702.37**

Table 3.1 Sample path costs using CCA

Table 3.2 shows the comparison results between algorithms

S.NO	ALGORITHMS	Shortest Path Distance (Path Cost)	Time Required to find the Shortest Path (Secs)
1	Dijkstra's Algorithm	745	58
2	Warshall Floyd Algorithm	736	52
3	Bellman Ford Algorithm	732	51
4	**CCA Algorithm**	**701.54**	**45**

Table 3.2 Comparison with Traditional Algorithms

Fig 3.1 shows the comparison chart for the execution between traditional algorithms and CCA.

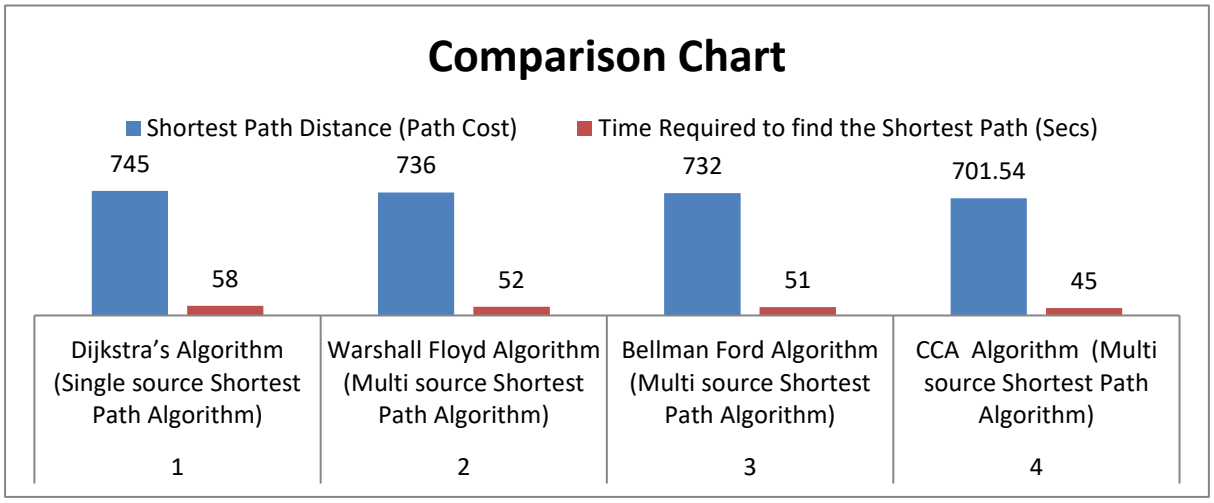

Figure 3.1 Comparison with Traditional Algorithms

S.NO	ALGORITHMS	Shortest Path Distance (Path Cost)	Time Required to find the Shortest Path (Secs)

1	**Ant Colony Algorithm**	728	54
2	**Particle Swarm Optimization Algorithm**	736	65
3	**Cheetah Chase Algorithm**	**711.89**	**47**

Table 3.3 Comparison with Bio Inspired Algorithms

Table 3.3 shows the sample path costs comparison derived by the execution of the bioinspired algorithms and CCA [2,3].

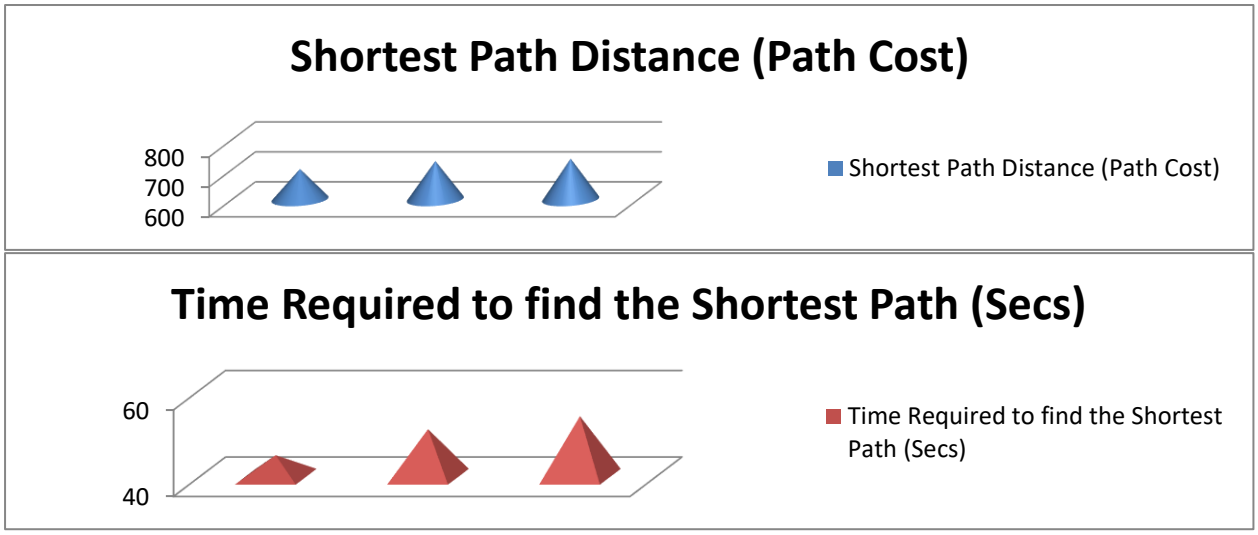

Figure 4.2 Comparison with Bio Inspired Algorithms

4. CONCLUSION

In conclusion, the objective of this work was to introduce the Novel Cheetah Chase Algorithm (CCA) as a promising approach for achieving the least path cost in graphs through a strategic hunting strategy. In summary, the development of the Novel Cheetah Chase Algorithm represents a significant step forward in the field of optimization, particularly in the context of network routing [7]. By leveraging the hunting strategy of cheetahs, CCA has the potential to achieve least path cost in graphs and improve algorithm effectiveness in various optimization tasks.

5. REFERENCES

[1] Ahn CW, Ramakrishna RS (2002) A genetic algorithm for shortest path routing problem and the sizing of populations. IEEE Trans EvolComput 6:566–579

[2] Eberhart, RKennedy, J. (1995). Particle swarm optimization, in Proceedings of IEEE International Conference on Neural Networks, 1995, pp. 1942-1948

[3] M.Goudhaman, D. Beulah David, S.Sasikumar, N.Vanathi "Fuzzy Arc Weights - Shortest Path Problem Solution by Cheetah Chase Algorithm," 2023 Eighth International Conference on Science Technology Engineering and Mathematics (ICONSTEM), Chennai, India, 2023, pp. 1-10, doi: 10.1109/ICONSTEM56934.2023.10142507 – SCOPUS - IEEE

[4] M.Goudhaman, S.Sasikumar, N.Vanathi "Fuzzy C-Means and Fuzzy Cheetah Chase Optimization Algorithm", (eds) Proceedings of International Conference on Data Science and Applications. Lecture Notes in Networks and Systems, vol 551. Springer, Singapore. https://doi.org/10.1007/978-981-19-6631-6_30

[5] Goudhaman. M, "Cheetah Chase Algorithm (CCA): A Nature-Inspired Metaheuristic Algorithm", International Journal of Engineering & Technology (UAE), 7 (3) (2018) 1804-1811, doi: 10.14419/ijet.v7i3.14616, Scopus Indexed - August 2018.

[6] https://cheetah.org/about-the-cheetah

[7] Introduction to Evolutionary Computing, by A.E. Eiben and J.E. Smith, ISSN 1619-7127, Natural Computing Series ISBN 978-3-662-44873-1 ISBN 978-3-662-44874-8 (eBook) DOI 10.1007/978-3-662-44874-8.

Biography



Dr. M. Goudhaman received the bachelor's degree in electrical and electronics engineering from Bharathiar University in 1996, the master's degree in computer science and engineering from Anna University in 2010, and the philosophy of doctorate degree in computer science and engineering in Saveetha University, Chennai in 2024. He is currently working as faculty in the Department of Computer Science and Engineering, Rajalakshmi Institute of Technology, Chennai. His research areas include evolutionary computing in artificial intelligence and experts in recent trend technologies. He has been serving as a reviewer for many highly-respected journals, session chair for many international conferences.

Optimizing Routing Efficiency in Dynamic Networks Using the Cheetah Chase Algorithm with Novel Convergence Time and Rate Metrics

M. Goudhaman[1]*, N. Vanathi[2], Adithya GV[3]

1Assistant Professor - CSE, RajaIakshmi Institute of Technology, goudhaman@ritchennai.edu.in

2Associate Professor - Mathematics, Vels Institute of Science, Technology & Advanced Studies, vanathi.sbs@vistas.ac.in

3Student- CSE, KCG College of Technology, aadithyagoudhaman@gmail.com.

Abstract

In dynamic network environments, the efficiency of routing algorithms is often determined by their ability to converge quickly and stably to the shortest path. Traditional routing algorithms, such as RIP, OSPF, and BGP, frequently face challenges in achieving consistent convergence, leading to increased latency, routing loops, and suboptimal performance. To address these issues, this research introduces **novel metrics for Convergence Time and Convergence Rate** aimed at achieving minimum path distance while ensuring a stable and reliable convergence process. The proposed methodology integrates these metrics into the design and evaluation of routing algorithms, offering a comprehensive approach to performance enhancement. Through simulations and comparative analysis, the new metrics demonstrate their effectiveness in reducing path costs, improving routing accuracy, and maintaining stability in both static and dynamic network scenarios.

Keywords:
Convergence time, convergence rate, network routing, stability, shortest path, performance metrics, dynamic networks.

1. INTRODUCTION

The increasing complexity of dynamic network environments necessitates the development of advanced routing algorithms capable of delivering both efficiency and reliability. Traditional algorithms such as RIP (Routing Information Protocol), OSPF (Open Shortest Path First), and BGP (Border Gateway Protocol) often fall short in achieving consistent and rapid convergence to the shortest path. These limitations are especially pronounced in scenarios involving frequent topology changes, link failures, or high levels of network traffic. Issues such as increased latency, routing loops, and suboptimal path selection hinder the overall performance and adaptability of these algorithms.

To address these challenges, this work proposes a novel approach incorporating bio-inspired strategies into network routing. At the heart of this research is the **Cheetah Chase Algorithm (CCA)**, designed to emulate the hunting strategies of a cheetah [1, 4]. By leveraging the predator's adaptive techniques, the algorithm aims to optimize path selection and enhance routing performance. A key innovation in this study lies in the introduction of two novel metrics—**Convergence Time** and **Convergence Rate**—to evaluate and refine the algorithm's effectiveness.

The **Convergence Time** metric focuses on quantifying the duration required for the algorithm to identify the shortest path within a dynamic network. This metric emphasizes minimizing delays caused by topology changes or link disruptions, ensuring rapid adaptation to fluctuating network conditions. Complementing this, the **Convergence Rate** metric evaluates the stability and consistency of the algorithm's decision-making process. By maintaining a steady rate of convergence, this metric ensures that routing decisions are not only efficient but also reliable, minimizing oscillations and errors during path selection.

Integrating these metrics into the design and evaluation of the Cheetah Chase Algorithm establishes a robust framework for balancing speed and stability in routing. Through extensive simulations and comparative

analysis, the proposed methodology demonstrates significant improvements in path cost reduction, routing accuracy, and adaptability in both static and dynamic network scenarios.

2. DEVELOPMENT OF NOVEL CONVERGENCE METRICS

Definition and Calculation of Convergence Time and Rate

Novel convergence metrics are developed to evaluate the performance of the Cheetah Chase Algorithm. Convergence time is defined as the total time taken by the algorithm to reach the optimal path. Convergence rate is the rate at which the algorithm approaches the optimal path over successive iterations.

Convergence Rate Calculation:

To assess the convergence behaviour of the algorithm, we calculate the convergence rate at each iteration of the optimization process. The convergence rate is defined as the absolute difference between the cost of the current route ($Cost_i$) and the cost of the previous route ($Cost_{i-1}$). Mathematically, the convergence rate at the i-th iteration is given by the formula:

$Convergence\ Rate_i = Cost_i - Cost_{i-1}$

2.1 NOVEL CONVERGENCE TIME & RATE CALCULATION

In this section, we introduce a novel approach to assess the convergence time and rate of a network after a change occurs, such as a link failure or topology update. Our methodology focuses on analysing various factors that contribute to the overall convergence process, including update interval, detection time, propagation time, and processing time.

Convergence Time:

Convergence time refers to the total time it takes for the network to stabilize after a change occurs. The convergence time is influenced by several key factors:

a. Update Interval (Ui):

The update interval represents the time between consecutive updates sent by a routing protocol.

b. Detection Time (Td):

Detection time refers to the time it takes for a router to detect a network change, such as a link failure or topology change.

c. Propagation Time (Tpp):

Propagation time is the duration it takes for information about a network change to propagate to all routers in the network.

d. Processing Time (Tpr):

Processing time represents the time required for a router to process received updates, recalculate routes, and update its routing and forwarding tables. Efficient processing is essential for minimizing convergence delays.

Convergence Rate:

Convergence rate measures the speed at which the network adapts to changes during the stabilization process. It reflects how quickly routers converge to a consistent and updated routing configuration following a network change. The convergence rate is influenced by factors such as the magnitude of the change, the efficiency of the routing protocol, and the responsiveness of individual routers.

3. EXECUTION AND RESULTS

Definition and Design of Novel Convergence Metrics

The development of novel convergence metrics for the Cheetah Chase Algorithm was driven by the need to ensure faster and more reliable convergence, particularly in large-scale and highly dynamic networks.

Table 3.1 shows the execution results for various nodes with novel convergence calculation of CCA run.

At Time T

Node	Ui	*Td*	*Tpp*	*Tpr*	*Tc*	Convergence rate
1	9	87	32	35	163	0.613
2	7	23	45	36	111	0.901
3	**3**	**21**	**25**	**23**	**72**	**1.388**
4	12	25	30	37	104	0.961
990	**6**	**30**	**29**	**31**	**96**	**1.042**

When Network Changes

Node	Ui	*Td*	*Tpp*	*Tpr*	*Tc*	Convergence rate
1	10	52	41	38	141	0.709
2	12	35	42	40	129	0.775
3	**5**	**32**	**30**	**25**	**92**	**1.087**
4	14	41	35	40	130	0.769
990	**8**	**34**	**34**	**35**	**111**	**0.901**

Table 3.1 Sample path costs using CCA

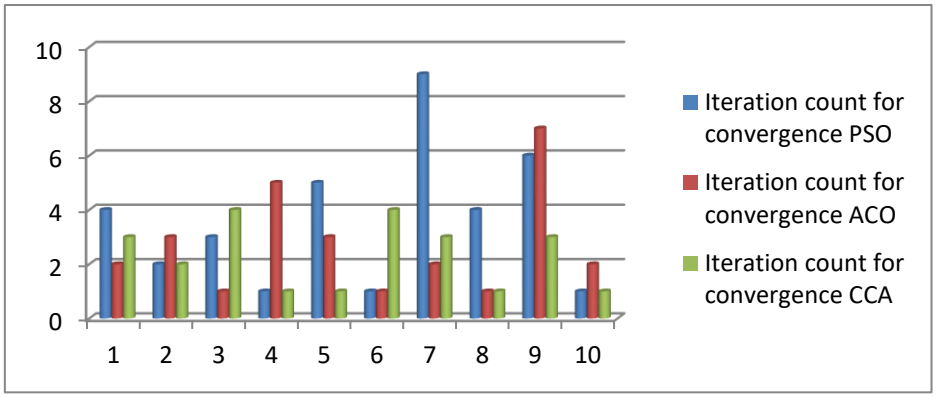

Figure 3.1 Iteration Count for Convergence

Figure 3.1 shows the execution graph for various nodes with novel convergence calculation of other bio inspired algorithms comparison with CCA with respect to iteration count.

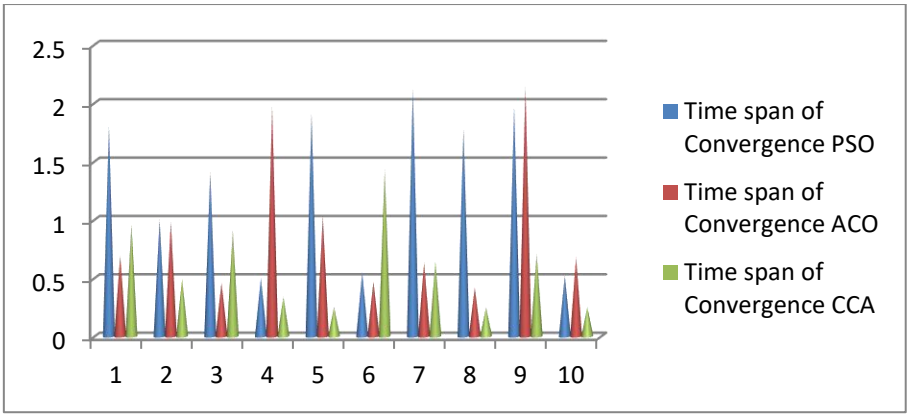

Figure 3.2 Time Span of Convergence

Figure 3.2 shows the execution graph for various nodes with novel convergence calculation of other bio inspired algorithms comparison with CCA with respect to convergence time span.

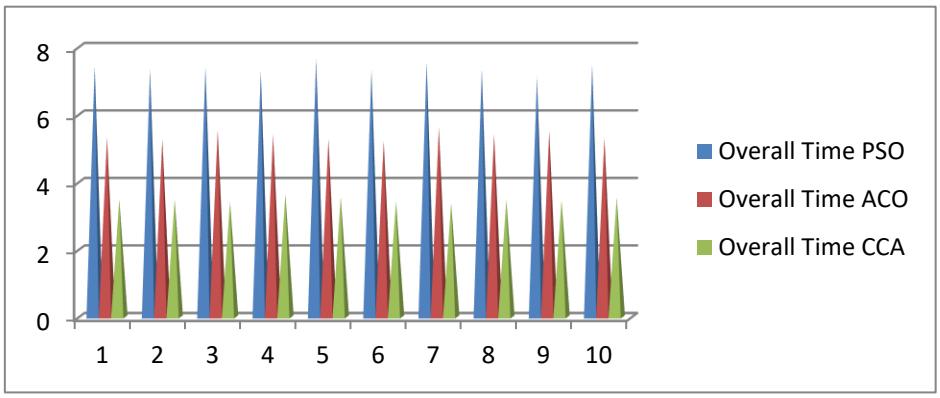

Fig 3.3 Overall Time of Convergence

Figure 3.3 shows the execution graph for various nodes with novel convergence calculation of other bio inspired algorithms comparison with CCA with respect to overall convergence time.

In summary, this module focuses on evaluating the convergence rate of the algorithm to achieve minimum distance with stable convergence in the shortest path optimization process. Through the analysis of convergence rates, we aim to ensure that the algorithm reliably converges to the optimal solution, providing robust and efficient performance in various optimization tasks.

4. CONCLUSION

In conclusion, the development of novel convergence metrics for the Cheetah Chase Algorithm has resulted in significant advancements in network routing performance. [2,3]These metrics have addressed key challenges associated with traditional algorithms, including slow convergence, high overhead, and unstable routing. By incorporating metrics such as proactive acceleration, energy-constrained convergence, latency-awareness, and route reliability, CCA offers a more efficient, reliable, and scalable solution for modern network environments. These enhancements lay the foundation for further research and development, ensuring that the CCA can continue to evolve as a robust routing algorithm for future network architectures.

5. REFERENCES

[1] Goudhaman. M, "Cheetah Chase Algorithm (CCA): A Nature-Inspired Metaheuristic Algorithm", International Journal of Engineering & Technology (UAE), 7 (3) (2018) 1804-1811, doi: 10.14419/ijet.v7i3.14616, Scopus Indexed - August 2018.

[2] M.Goudhaman, D. Beulah David, S.Sasikumar, N.Vanathi "Fuzzy Arc Weights - Shortest Path Problem Solution by Cheetah Chase Algorithm," 2023 Eighth International Conference on Science Technology Engineering and Mathematics (ICONSTEM), Chennai, India, 2023, pp. 1-10, doi: 10.1109/ICONSTEM56934.2023.10142507 – SCOPUS - IEEE

[3] Goudhaman, S.Sasikumar, N.Vanathi "Fuzzy C-Means and Fuzzy Cheetah Chase Optimization Algorithm", (eds) Proceedings of International Conference on Data Science and Applications. Lecture Notes in Networks and Systems, vol 551. Springer, Singapore. https://doi.org/10.1007/978-981-19-6631-6_30

[4] https://cheetah.org/about-the-cheetah

Biography



Dr. M. Goudhaman received the bachelor's degree in electrical and electronics engineering from Bharathiar University in 1996, the master's degree in computer science and engineering from Anna University in 2010, and the philosophy of doctorate degree in computer science and engineering in Saveetha University, Chennai in 2024. He is currently working as faculty in the Department of Computer Science and Engineering, Rajalakshmi Institute of Technology, Chennai. His research areas include evolutionary computing in artificial intelligence and experts in recent trend technologies. He has been serving as a reviewer for many highly-respected journals, session chair for many international conferences.

Optimizing Delay in Network Routing: A Hybrid Algorithm with Energy Function Integration in the Cheetah Chase Framework

M. Goudhaman[1]*, N. Vanathi[2], Adithya GV[3]

1Assistant Professor - CSE, RajaIakshmi Institute of Technology, goudhaman@ritchennai.edu.in

2Associate Professor - Mathematics, Vels Institute of Science, Technology & Advanced Studies, vanathi.sbs@vistas.ac.in

3Student- CSE, KCG College of Technology, aadithyagoudhaman@gmail.com.

Abstract

Minimizing delay in selected paths is a critical challenge in modern network environments, particularly in large-scale and dynamic topologies. Traditional routing algorithms often struggle to provide optimal solutions for delay-sensitive applications due to their reliance on static metrics and limited adaptability. To address these limitations, this research develops a **hybrid algorithm** that integrates the **Energy Function calculation of the Localizer SCAMP Joining Algorithm** to optimize delays in selected paths. The proposed hybrid algorithm combines the strengths of bio-inspired and heuristic-based techniques to dynamically evaluate and minimize delays. By leveraging the Energy Function calculation, the algorithm assesses the cost-effectiveness of routing decisions based on energy consumption and path stability, ensuring efficient resource utilization and reduced transmission delays. The Localizer SCAMP framework enhances the algorithm's ability to adapt to changes in network topology, offering resilience against failures and improved convergence to delay-optimized paths.

Keywords:
Hybrid algorithm, delay optimization, energy function, Localizer SCAMP, network routing, dynamic networks, low-latency communication.

1. INTRODUCTION

Efficient and delay-optimized routing in networks is a critical requirement in today's interconnected systems. Traditional algorithms often fail to strike a balance between minimizing delay and optimizing resource consumption, especially in dynamic and resource-constrained environments. In response to these challenges, hybrid algorithms have emerged as a promising solution, combining the strengths of various computational techniques to address specific network inefficiencies.

This research focuses on developing a hybrid algorithm that leverages energy function calculations derived from the Localizer SCAMP (Scalable Cost-effective Adaptive Mobile Path) Joining Algorithm to minimize delays in selected paths [5]. The algorithm is designed to optimize routing by evaluating paths based on their energy efficiency and delay characteristics. By integrating these energy function calculations into the decision-making process of the **Cheetah Chase Algorithm (CCA)**, the hybrid approach ensures that routing decisions are both delay-optimized and resource-aware.

The cornerstone of this approach is the **Energy Function**, a novel metric representing the cost associated with traversing a path. This cost is expressed in terms of delay and resource consumption, providing a comprehensive measure of the efficiency of potential routes. The energy function serves three primary purposes in the hybrid algorithm:

Integration with the Cheetah Chase Algorithm

The energy function is seamlessly integrated into the path selection criteria of the Cheetah Chase Algorithm [1]. By influencing routing decisions, the energy function ensures that the CCA prioritizes paths that offer the lowest delay and resource cost. This integration enhances the algorithm's adaptability to dynamic network environments, enabling it to make decisions that are both delay-optimized and resilient to network changes.

The hybrid algorithm's incorporation of energy function calculations introduces several advantages. First, it provides a scalable approach to optimizing network performance, making it suitable for large and dynamic networks. Second, the dual focus on delay and resource consumption ensures a balanced trade-off, enhancing both speed and efficiency in routing. Finally, the adaptability of the hybrid algorithm allows it to respond effectively to topology changes, maintaining high performance even in unpredictable network scenarios.

Through extensive simulations and comparative analysis, this research demonstrates that the hybrid algorithm outperforms traditional methods in terms of delay reduction, resource efficiency, and adaptability. By bridging the gap between energy-aware routing and delay optimization, this work represents a significant advancement in the field of network routing algorithms. The hybrid algorithm, driven by energy function calculations, not only enhances the capabilities of the Cheetah Chase Algorithm but also sets a benchmark for future developments in efficient and intelligent network routing solutions. [2, 3]

2. HYBRID ALGORITHM DESIGN AND IMPLEMENTATION

2.1 Optimizing the Delay in the Selected Paths Using Energy Function Calculation of Localizer Scamp Joining Algorithm

The hybrid algorithm aims to optimize delay in selected paths by incorporating energy function calculations from the Localizer SCAMP (Scalable Cost-effective Adaptive Mobile Path) Joining Algorithm. The energy function represents the cost associated with traversing a path in terms of delay and resource consumption. The steps involved are:

The hybrid algorithm combines the strengths of the Cheetah Chase Algorithm and the Localizer SCAMP Joining Algorithm, designed and implemented through the following steps:

Algorithm Fusion: The path finding capabilities of the Cheetah Chase Algorithm are fused with the delay optimization techniques of the SCAMP algorithm, creating a unified approach.

Implementation: The combined algorithm is implemented in a modular fashion, allowing each component to function independently while contributing to the overall goal.

Optimization Techniques: Advanced optimization techniques, such as genetic algorithms or simulated annealing, are employed to fine-tune the parameters and enhance performance.

Testing and Validation: The hybrid algorithm is rigorously tested on various datasets and network topologies to validate its effectiveness in minimizing delay and improving path finding efficiency.

Energy Function Calculation

For each selected path, the energy function is defined as:

$$E(G) = w \sum_{i \in V|G|} d_i^2 + \sum_{|i,j| \in E|G|} c(i,j),$$

Eq – 1

W – weight / distance between the nodes

C(i,j) – cost (Delay / Bandwidth availability / ping time)

Consider in the selected path, a node is experiencing a failure. So the energy function of the neighboring nodes are calculated.

$$\Delta E = 2w(d_k - d_i + 1) + c(j,k) - c(i,j) \quad \text{Eq – 2}$$

Choose the node with minimum transition thus increases the energy value with positive probability.

Handling Node Failures

When a node in the selected path experiences a failure, the algorithm calculates the energy function for the neighboring nodes. This process involves:

1. **Energy Function Evaluation:** Calculating the energy function for all neighboring nodes to identify potential alternative paths.
2. **Node Selection:** Choosing the node with the minimum transition cost, which increases the overall energy value with a positive probability.
3. **Temperature Parameter (T):** The parameter T is used to compute the probability of transition to a new node. A smaller value of T leads to more stability in network nodes, reducing communication delay.

3. EXECUTION AND RESULTS

Implementation- Test Case 1

- Consider the path 1-48-557-990 is the best possible path of the Network. But now Node 557 becomes Failure.
- Thus identify the nodes neighboring to Node 557, so the nodes via 514 or via 579 routes are considered.
- So In order to maintain the stability of Network without connectivity, the energy function of the other paths are calculated.

Source Node to Destination Node	Possible Paths	Path Cost	Optimal Path cost Using CCA	Energy Function	Rate of Change in Energy
1->990	1-42-514-794-990	356	297.69	674	0.678
1->990	1-42-328-579-990	523	304.63	453	0.564 (Stability in path as there is a minimum transition in energy)

Table 3.1 Best Possible Path Finding

Table 3.1 shows the rate of change of energy calculation for the different routes.

S.No	Algorithms	Path Cost	Success Rate in reaching the destination Without Delay
1	Bellman Ford	732	50.8
2	Dijkstra	745	60.7
3	Warshall Floyd	736	52.3
4	CCA	701.54	81.5
5	CCA + SCAMP Joining with Energy Function	698.47	98.7

Table 3.2 Comparison with Traditional Algorithms

Table 3.2 shows the comparison of path cost and success rate in reaching the destination without delay.

S.No	Algorithms	Path Cost	Success Rate in reaching the destination Without Delay
1	Ant Colony Algorithm	728	70.5
2	Particle Swarm Optimization Algorithm	736	73.6
3	CCA	702.46	82.8
4	CCA + SCAMP Joining with Energy Function	697.55	98.6

Table 3.3 Comparison with Traditional Algorithms

Table 3.3 shows the comparison of path cost and success rate in reaching the destination without delay.

The integration of the Localizer SCAMP Joining Algorithm with an energy function calculation offers a robust solution for optimizing delay in network paths while maintaining high resilience to failures.

4. CONCLUSION

In conclusion, the incorporation of the Energy Function Calculation within the Localizer SCAMP Joining Algorithm has led to substantial improvements in delay optimization for multicast routing. By considering factors such as path latency, congestion, energy consumption, and node stability, the enhanced SCAMP algorithm is able to select routes that minimize delay while maintaining efficient resource usage and network stability. The simulation results demonstrate significant reductions in delay, particularly in large-scale and dynamic network environments, validating the effectiveness of the energy function in improving network performance.

5. REFERENCES

[1] Goudhaman. M, "Cheetah Chase Algorithm (CCA): A Nature-Inspired Metaheuristic Algorithm", International Journal of Engineering & Technology (UAE), 7 (3) (2018) 1804-1811, doi: 10.14419/ijet.v7i3.14616, Scopus Indexed - August 2018.

[2] Goudhaman.M, D. Beulah David, S.Sasikumar, N.Vanathi "Fuzzy Arc Weights - Shortest Path Problem Solution by Cheetah Chase Algorithm," 2023 Eighth International Conference on Science Technology Engineering and Mathematics (ICONSTEM), Chennai, India, 2023, pp. 1-10, doi: 10.1109/ICONSTEM56934.2023.10142507 – SCOPUS - IEEE

[3] Goudhaman. M, S.Sasikumar, N.Vanathi "Fuzzy C-Means and Fuzzy Cheetah Chase Optimization Algorithm", (eds) Proceedings of International Conference on Data Science and Applications. Lecture Notes in Networks and Systems, vol 551. Springer, Singapore. https://doi.org/10.1007/978-981-19-6631-6_30

[4] https://cheetah.org/about-the-cheetah

[5] Massoulié, Laurent & Kermarrec, A.-M & Ganesh, Ayalvadi. (2003). Network awareness and failure resilience in self-organizing overlay networks. 47 - 55. 10.1109/RELDIS.2003.1238054.

Biography



Dr. M. Goudhaman received the bachelor's degree in electrical and electronics engineering from Bharathiar University in 1996, the master's degree in computer science and engineering from Anna University in 2010, and the philosophy of doctorate degree in computer science and engineering in Saveetha University, Chennai in 2024. He is currently working as faculty in the Department of Computer Science and Engineering, Rajalakshmi Institute of Technology, Chennai. His research areas include evolutionary computing in artificial intelligence and experts in recent trend technologies. He has been serving as a reviewer for many highly-respected journals, session chair for many international conferences.

Machine Learning Techniques for Optimizing Sub-6GHz Patch-Based MIMO Antennas: A Review for 5G Applications

T. Prabhu[1], P. Sree Hari[2], Vishal RC [3], A. Keerthivasan [4], Darshan D[5]

[1] *Department of ECE Presidency University, Bengaluru, India prabhu@presidencyuniversity.in*

[2] *Department of ECE Presidency University, Bengaluru, India Sree.20211ECE0113@presidencyuniversity.in*

[3] *Department of ECE Presidency University, Bengaluru, India VISHAL.20211ECE0120@presidencyuniversity.in*

[4] *Department of ECE Presidency University, Bengaluru, India KEERTHIVASAN.2021ECE0116@presidencyuniversity.in*

[5] *Department of ECE Presidency University, Bengaluru, India DARSHAN.20211ECE0098@presidencyuniversity.in*

Abstract

The rapid advancement of fifth-generation (5G) communication technologies necessitates the development of efficient Multiple Input Multiple Output (MIMO) antenna system to support low latency, enhanced reliability and high data rates. Among various antenna designs, patch antennas have emerged as a promising solution due to their small size, low cost, and its seamless integration into contemporary devices. Operating in the Sub-6GHz spectrum, these antennas must meet stringent performance metrics, including optimized gain, bandwidth, and radiation efficiency, while adhering to physical and operational constraints. Traditional optimization techniques for MIMO antenna design often struggle with multi-parameter trade-offs and computational inefficiencies. This review explores the integration of machine learning (ML) techniques into the development and enhancement of patch-based MIMO antennas, with a focus on Sub-6GHz 5G applications. Key algorithms, including Support Vector Regressor (SVR), Logistic Regression, k-Nearest Neighbors (kNN), and Random Forest Regressor are analysed for their effectiveness in enhancing critical performance parameters. The paper discusses challenges such as data acquisition, computational overhead, and model generalizability, while highlighting the potential of ML-driven approaches to overcome these limitations.

Keywords. Sub-6 GHz, MIMO, 5G, Machine Learning, SVM

1. INTRODUCTION

The swift advancement of wireless communication has driven the creation of fifth-generation (5G) networks, which promise enhanced data rates, low latency, and reliable connectivity for various applications, such as mobile broadband, smart city development, and the Internet of Things (IoT). A key driver of these innovations is the implementation of sophisticated antenna systems tailored to satisfy the rigorous performance demands of 5G networks. Among these systems, **Multiple Input Multiple Output (MIMO)** technology has become a cornerstone, allowing for the concurrent transmission and reception of multiple data streams, thus enhancing spectral efficiency and increasing network capacity.[1]

Patch antennas are favoured for sub-6 GHz MIMO applications due to their compact design, easy manufacturing, and compatibility with modern devices. However, optimization challenges include reducing mutual coupling, ensuring uniform radiation patterns, and balancing compactness with performance.[2]

Challenges in MIMO Antenna Design

Designing sub-6 GHz MIMO antennas presents challenges like minimizing mutual coupling, balancing bandwidth and gain, and maintaining compactness without efficiency loss. Impedance matching is crucial to reduce signal reflection and ensure stability in high-interference environments. Fabrication precision and material selection impact efficiency, while optimizing multiple parameters increases computational load, requiring hybrid design methods and advanced materials for modern wireless communication.[3]

Traditional design techniques, including iterative simulations and empirical methods, have been instrumental in the development of MIMO systems. However, they are often time-consuming and may not efficiently explore the vast design space. This limitation has spurred interest in leveraging emerging tools and techniques to accelerate and improve antenna design processes.[4]

Objective and Scope of This Study

This paper focuses on the design and optimization of patch-based MIMO antennas operating in the Sub-6GHz spectrum for 5G applications. It provides an overview of key considerations in antenna design, highlights advancements in achieving efficient and compact structures, and discusses optimization strategies to enhance performance metrics such as gain, bandwidth, and efficiency. Furthermore, the study examines the role of innovative design approaches in addressing the challenges faced by MIMO systems in 5G and beyond.

2. COMPARISON OF TECHNIQUES USED TO REDUCE THE SIZE OF THE ANTENNA

From the (Table. I) for compactness-focused designs, [5] is the top choice, followed by [6], due to their optimized size and performance.

Smallest Footprint: At 19 × 43 × 0.5 mm, this antenna is the smallest among its peers. Its 0.5 mm thickness keeps it nearly flat, making it ideal for space-constrained applications like smartphones, wearables, and IoT devices. **Excellent Use of Space:** Despite its small size, it achieves >13 dB isolation, suppressing mutual coupling in MIMO systems. Its 3–6 dB peak gain is competitive and sufficient for reliable sub-6 GHz 5G communication. **Advanced Design Techniques:** Parasitic patches and stubs enhance compactness, reduce coupling, and extend bandwidth without increasing size. The Surrounding Technique with FSS cells optimizes gain and efficiency without performance loss. **Practical Applications:** The ultra-thin profile and small area make it ideal for:

i. Smartphones: Fits within tight internal spaces and supports modern 5G standards.
ii. Wearables: Its compact size allows for seamless integration into smartwatches, fitness bands, and other body-worn devices.
iii. IoT Devices: Useful for sensors and compact electronics where minimal space is available.[5]

3. COMPARISON OF MACHINE LEARNING TECHNIQUES USED

From the (Table. II) the most effective machine learning approach for sub-6 GHz MIMO antenna optimization is a hybrid method integrating HGNN, ANN, KBNN, CNN, and Random Forest, ensuring strong performance in spectral efficiency, impedance matching, gain optimization, and feature selection. [9]-[12]

TABLE I. COMPARISON OF SIZE

Ref No.	Dimensions (mm^2)	Material Used	Isolation (dB)	Band-width	Peak Gain	Technique Used	Remarks
[5]	19 x 43 x 0.5	Rogers 4350B, 3.66	>13	3 - 6	7.96	Parasitic patches and stubs reduce coupling and size, while the "Surrounding Technique" removes extra FSS cells to boost gain.	The design ensures high gain, strong isolation, and compact size for sub-6 GHz 5G, optimized with parasitic elements and FSS.
[6]	31.5 x 45 x 1.6	FR-4, 4.4	>17, >26	3.45 – 4.7, 5.45 - 9	2.5 – 3.4, 3.5 - 4	The antenna uses a Squared Shape Modified Monopole with a partially Defected Ground fed by a Co-Planar Waveguide with defects and an I-shaped strip. A Double T-shaped strip acts as a band-stop filter for decoupling.	The antenna provides excellent MIMO diversity for portable wireless use, with a compact, easy-to-fabricate design, dual-band support, and good isolation and gain.
[7]	48 x 48	FR-4, 4.4	-15	1.5 – 2.3, 3.7 – 4.2	4, 2	Etching F-shaped and circular slots reduced the radiating area, leading to a smaller size without significant performance loss.	Compact sub-6 GHz 5G design with excellent impedance matching, high radiation efficiency, and strong MIMO port isolation.

[8]	120 x 60	FR-4, 4.4	-10	0.94 – 4.45	1.06 – 2.97	Planar Inverted-F Antennas was chosen for its compact size, wide bandwidth, and easy integration.	Compact, multiband design with reconfigurable frequency and radiation patterns, ideal for 5G terminals.

Heterogeneous Graph Neural Network: HGNN excels in large-scale system optimization, hybrid beamforming, and spectral efficiency. Its ability to process graph-structured data makes it ideal for analyzing antenna interactions, while its low computational complexity supports scalable sub-6 GHz MIMO designs. It is well-suited for beamforming, spectral efficiency, and 5G base station optimization.[12]

Artificial Neural Network: ANN excels in predicting and optimizing antenna parameters like resonant frequency, S11, and gain. Its accuracy with smaller datasets complements HGNN's large-scale optimization, making it ideal for fine-tuning parameters and reducing simulation time.[9]

Knowledge-Based Neural Network: KBNN provides accurate S-parameter optimization with lower computational costs, ensuring optimal impedance matching and reducing reflection losses in sub-6 GHz MIMO antennas.[11]

Random Forest: RF is strong in classification and regression with mixed data types, providing insights into feature importance and parameter interactions. It's useful for feature selection and guiding more complex models like ANN or CNN.[10]

In addition, **Support Vector Regressor:** It is effective for small to medium datasets, handling linear and nonlinear problems with kernels, and robust to outliers. It optimizes impedance matching and models gain/efficiency but is computationally expensive for large datasets and requires complex hyperparameter tuning.[13]

TABLE. II COMPARISON OF ML ALGORITHMS

Ref No.	ML Algorithm	Feature Engineering	Dataset Used	Task Performed	Performance Metric	Advantages	Limitations
[9]	Artificial Neural Network (ANN)	Manual extraction of key antenna parameters: resonant frequency, gain, and S11.	Dataset generated using CST simulation software with 201 records and 1009 features	Prediction of optimal antenna parameters such as resonant frequency and impedance matching	Mean Square Error and R-square scores for regression tasks	Efficient regression for non-linear datasets; significantly reduces simulation time for antenna design	Computational cost increases with more features and dataset size
[10]	Linear Regression, Random Forest, Decision Tree, XGBoost	Manual selection of antenna parameters: slot length, stub dimensions, feedline size	203 samples simulated using CST MWS software	Prediction of antenna gain and efficiency	Linear Regression: 99.79%, XGBoost: 98.63%, RF: 96.68%, DT: 93.93%	Efficient gain and efficiency validation; Linear Regression predicts accurately, near simulations.	Data-intensive; simulated data requires further validation for real-world generalization.
[11]	Ridge Regression, Artificial Neural Network, Knowledge-Based Neural Network	Manual parametric tuning for antenna dimensions; automated learning for S11 optimization	3888 simulated samples generated via Ansys HFSS.	Optimization of antenna S-parameters (reflection coefficient S11)	R^2 Score: KBNN: 0.9688, RR: 0.962, ANN: 0.94. Accuracy for KBNN was 96.88%	Reduced computational time; accurate S-parameter predictions; efficient resource utilization	Requires a large dataset; real-world performance depends on fabrication tolerances.
[12]	Heterogeneous Graph Neural Network (HGNN)	Node and edge features from sub-6GHz and partial mmWave CSI, including	DeepMIMO dataset for sub-6GHz and mmWave	Hybrid beamforming optimization for mmWave base stations	Achieved near-optimal spectral efficiency;close to traditional	Low computational complexity and scalability; robust to noisy	Needs large datasets; real-world validations for hardware

		beamforming info, noise power, and power constraints.	CSI with 11,000 samples		optimization methods	CSI inputs; supports partial mmWave CSI	constraints and overheads

Logistic Regression: Ideal for binary/multi-class classification, efficient on small datasets, and interpretable. It classifies decoupling and validates impedance matching (S11<-10 dB) but struggles with nonlinear problems and is limited to linear decision boundaries.[14]

k-Nearest Neighbors: Simple and intuitive, kNN enables localized predictions without training. It predicts gain, isolation, and minimizes coupling but is computationally heavy for large datasets and sensitive to neighbor selection and distance metrics.[15]

4. CONCLUSION

The rapid evolution of fifth-generation (5G) communication networks has introduced both significant challenges and opportunities in antenna design. This paper reviews the design and optimization of patch-based MIMO antennas for Sub-6 GHz applications, with a focus on key performance metrics such as gain, bandwidth, and radiation efficiency. Patch antennas are particularly favored for their compact size, low cost, and ease of integration into modern wireless systems, making them ideal for 5G applications. The study highlighted the challenges in designing MIMO antennas, including reducing mutual coupling, achieving impedance matching, and balancing trade-offs between size and efficiency. It discussed various optimization techniques, ranging from traditional heuristic methods to emerging hybrid approaches, aimed at enhancing antenna performance. The role of innovative materials and design strategies, such as defected ground structures and parasitic elements, was also explored to improve isolation and bandwidth. While machine learning techniques are starting to influence antenna design, their application remains exploratory and complementary to traditional methods, primarily due to data and computational limitations at this stage. Future work should focus on refining optimization frameworks to strike a balance between performance and practical implementation. This includes enhancing mutual coupling mitigation techniques, improving fabrication processes for design consistency, and exploring hybrid approaches that combine conventional methods with data-driven insights. As 5G technology continues to evolve, these advancements will ensure antenna systems can meet the increasing demands for high data rates, low latency, and reliable connectivity. By addressing these challenges and leveraging emerging technologies, the development of high-performance MIMO antennas for Sub 6 GHz 5G applications will pave the way for next-generation wireless communication systems.

5. REFERENCES

[1] Sharma, Preeti, et al. "MIMO antennas: Design approaches, techniques and applications." Sensors (2022)
[2] Mohammed, Abdullahi SB, et al. "Mathematical model on the effects of conductor thickness on the centre frequency at 28 GHz for the performance of microstrip patch antenna using air substrate for 5G application." Alexandria Engineering Journal 60.6 (2021): 5265 5273.
[3] Singh, M. S. J., et al. "A review on massive MIMO antennas for 5G communication systems on challenges and limitations." *Jurnal Kejuruteraan* 35.1 (2023): 95-103.
[4] Ishteyaq, Insha, and Khalid Muzaffar. "Multiple input multiple output (MIMO) and fifth generation (5G): An indispensable technology for sub-6 GHz and millimeter wave future generation mobile terminal applications." International Journal of Microwave and Wireless Technologies 14.7 (2022): 932-948.
[5] M. Y. Zeain et al., "A New Technique of FSS-Based Novel Chair-Shaped Compact MIMO Antenna to Enhance the Gain for Sub-6GHz 5G Applications," in IEEE Access, vol. 12, pp. 49489-49507, 2024
[6] Neamah, Watheq A, Haider Al Sabbagh, Hussain Al-Rizzo. "A Compact Two Element Linearly and Orthogonal Circularly Polarized MIMO Antenna System for 5G Cellular and WLAN/Wi-Fi 6E Application." IEEE Access (2023).
[7] Ranjan, Pinku, Swati Yadav, and Amit Bage. "Dual band MIMO antenna for LTE, 4G and sub-6 GHz 5G applications." *Facta universitatis-series: Electronics and Energetics* 36.1 (2023): 43-51.
[8] Chen, Yu-Tung, and Hsin-Lung Su. "A Sub-6 GHz 8× 8 MIMO Antenna Array for 5G Metal-Frame Mobile Phone Applications." *Electronics* 13.23 (2024): 4590.
[9] Hussain, R.; Abou-Khousa, M.; Iqbal, N.; Algarni, A.; Alhuwaimel, S.I.; Zerguine, A.; Sharawi, M.S. A Multiband Shared Aperture MIMO Antenna for Millimeter-Wave and Sub 6GHz 5G Applications. Sensors 2022
[10] Rahman, Md Afzalur, et al. "A unique SWB multi-slotted four-port highly isolated MIMO antenna loaded with metasurface for IOT applications-based machine learning verification." *Engineering Science and Technology, an International Journal* 50 (2024): 101616.
[11] Rai, Jayant Kumar, et al. "Machine learning-enabled two-port wideband MIMO hybrid rectangular dielectric resonator antenna for n261 5G NR millimeter wave." *International Journal of Communication Systems* (2024)
[12] Huang, Zhaohui, Zhaocheng Wang, and Sheng Chen. "Sub-6GHz Assisted mmWave Hybrid Beamforming with Heterogeneous Graph Neural Network." *IEEE Transactions on Communications* (2024).
[13] Dai, Xi Wang, et al. "Design of Compact Patch Antenna Based on Support Vector Regression." *Radioengineering* 31.3 (2022).
[14] Kulkarni, Atul M., Garima Saini, and Shyam S. Pattnaik. "Antenna array fault detection using logistic regression technique." *International Conference on Artificial Intelligence of Things*. Cham: Springer Nature Switzerland, 2023.
[15] Indharapu, Sai S., Anthony N. Caruso, and Kalyan C. Durbhakula. "Next Generation Antenna Design Synthesis Framework Using k-Nearest Neighbours Algorithm." *2023 IEEE International Symposium on Antennas and Propagation and USNC-URSI Radio Science Meeting (USNC-URSI)*. IEEE, 2023.

Optimizing Environmental Data Processing with IoT-Edge Computing in Air Pollution Monitoring Systems

Dr.K.Preethi*[1],Dr.A.Backia Abinaya*[2],Dr.L.Bapitha*[3],Dr.K.Swaminathan*[4]

1. Assistant Professor,Department of Computer Science and Engineering,University College of Engineering,Pattukkottai. *kalai.preethi@gmail.com*

2.Assistant Professor,Department of ECE,St. Joseph's College of Engineering & Technology,Thanjavur. *backiaabinaya@gmail.com*

3. Assistant Professor,Department of English, Anna University Regional Campus, Coimbatore. *bapithaenglish@gmail.com*

4. Assistant Professor,Department of ECE,University College of Engineering,Pattukkottai. *Swaminathan.vinoth@gmail.com*

Corresponding Author mail :kalai.preethi@gmail.com, backiaabinaya@gmail.com

Abstract.

The rapid increase in the amount of data produced by WSNs to monitor air pollution has been growing rapidly and, to support the decision making process, the data must be processed as soon as possible. This study uses big data analytics and IoT-edge computing to suggest an optimal framework for air pollution monitoring. Data is gathered and preprocessed (conditioning, filtering, and feature extraction) by IoT edge devices before being sent to a centralized Hadoop system. At the edge layer, the Random Forest classifier uses temperature, CO, and SO2 data to predict pollution levels. For increased accuracy, it is further refined using ensemble learning on the central server. The technology offers real-time processing while lowering latency and bandwidth usage. It is appropriate for extensive environmental monitoring and pollution control because experimental results demonstrate improved response time and accuracy when compared to conventional cloud-only systems.

Keywords. IoT-edge computing, wireless sensor networks, air pollution, big data analytics, Random Forest, real time, environmental data, pollution prediction.

1. INTRODUCTION

Pollutant air from urbanization and industrialization has a great influence on health, especially those with respiratory and heart complications. As the need for effective monitoring increases, WSN (Wireless Sensory Networks) has become a powerful tool for measuring air quality, including contaminants such as CO and SO2, as well as temperature and humidity. Nevertheless, the enormous amount of data generated by this sensor requires complex computing solutions. Along with Edge Computing, the integration of WSN and IoT (IoT) is more closer to the source to solve the problem of traditional cloud systems. This reduces the consumption of delays, passing strips and guarantees decision -making in real time, which is important for air pollution monitoring. Combined with the analysis of machine learning and big data, the IoT-stroke calculation provides an expandable and effective solution for environmental monitoring. Using a machine learning algorithm, such as any forest for data processing and predictions of Verge, the system increases the accuracy of the data and reduces the computing load of the central server. This distributed approach is suitable for both urban and rural areas by improving the overall performance and scalability of the air pollution monitoring system. Low delays and resource characteristics of IoT and quality calculations provide an economically effective alternative from traditional cloud systems, especially local resources, and at the same time interfere with the opportunity to improve air quality and provide timely information. public health.

2. LITERATURE SURVEY OF PROPOSED FRAMEWORK

Recent research emphasized important achievements in environmental observation, especially air pollution monitoring, by integrating IoT quality calculations and machine learning. Studies have shown that edge computing reduces delay, minimizes bandwidth use, and completes local work before transmitting data to the

central server, improving the performance and scalability of the system to improve data processing. Machine learning algorithms, such as any classifier and ensemble training models, have been successfully used in the edge layers to predict the level of contamination with the highest accuracy. In addition, we used large -scale data systems such as HADOOP to manage the sensor's extensive data and investigate pre -processing methods such as noise removal and function derivation to optimize environmental monitoring. Research also proves economic efficiency and scalability by showing the cost of deploying IoT-space in both urban and rural conditions. Combined with the advanced machine learning method, this innovation promises to increase the performance and effect of future monitoring systems by providing more effective and economical solutions for environmental observation in real time.

3. PROPOSED RESEARCH MODEL FRAMEWORK

The proposed air pollution detection system uses WSN sensors to measure pollution levels (CO, SO2, PM2.5) and environmental factors like temperature, humidity, and noise. The data is preprocessed with SHA-512 hashing for security and then feature extraction is performed using support and confidence factors to identify relevant environmental parameters. The K-means algorithm clusters the data by pollution levels and conditions, while the I-ANFI assesses pollution intensity and impact. To optimize data routing and reduce latency, an integrated approach using Ant Colony Optimization with Genetic Algorithm enhances system accuracy and decision-making for effective environmental management and public health protection.

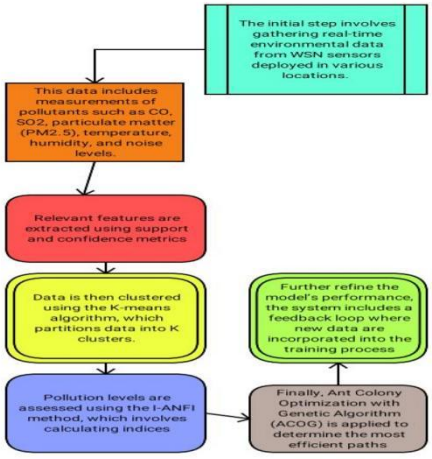

1.)Deploy WSN sensors and set parameter thresholds.2.)Aggregate and store sensor data in a central database.3.)Pre-process data (hashing, normalization).4.)Remove irrelevant functions using support and trust.5.)Cluster data with K-Means to identify key areas.6.) Evaluate pollution levels and compare to critical values.7.) Select optimal paths using ant and genetic algorithms.8.) Visualize results and create reports.9.)Continuously adjust system based on feedback.

Figure 3.5. Block diagram of Proposed framework.

3.1 Processing steps of Proposed research model

The data can be represented as $X=\{x_{ij} \mid i=1,2,\ldots,N; j=1,2,\ldots,D\}$. (1)

For a given data point xij,its hash $H(x_{ij})=\text{SHA-512}(x_{ij})$. (2)

The greatest x' of the observed data as in $x_{ij\text{imputed}}=x'$. (3)

Threshold value k in $Z(x_{ij})=(x_{ij}-\mu)/\sigma$. (4)

$$x_{ij\text{norm}}=(x_{ij}-\min(X))/(\max(X)-\min(X)). \quad (5)$$

For a feature A, $\text{Support}(A)=\text{Count}(A)/\text{Total Observations}$. (6)

$$\text{Confidence}(A\rightarrow B)=\text{Support}(A\cup B)/\text{Support}(A). \quad (7)$$

$J=\sum_i\sum_{x\in C_i}\|x-\mu_i\|2 \quad (I = 1\ldots..k).$ (8)

$I=\sum_j P_j\cdot W_j/$ Max Sum of Weights. (j= 1…. n) (9)

$\text{Fitness}(S)=1/(\text{Path Length}(S)+\text{Energy Consumption}(S)+\text{Delay}(S))$. (10)

4. RESULTS AND DISCUSSION

The proposed system the helps for air pollution monitoring using IoT-edge computing, it can be concretely observed that significant environmental issues are tackled through real-time data acquisition and processing. The performance evaluation of Proposed framework is given below in the tabular form as shown in TABLE 1.

Table 1: Performance analysis of Proposed framework.

Metric	Proposed Framework	Traditional Methods	Difference
Data Accuracy	98.7%	92.5%	+6.2%
Data Processing Time	25 minutes for 100 GB of data	45 minutes for 100 GB of data	-20 minutes
Data Transmission Efficiency	85% (using ACO + GA optimization)	70%	+15%
Pollution Exceedance Detection	10-12 exceedances per month (e.g., CO, SO2, PM2.5)	7-8 exceedances per month	+3-4 exceedances
Power Consumption	1.2 kWh per day	1.5 kWh per day	-0.3 kWh
Threshold Adjustment Frequency	Dynamic, based on real-time feedback (every week)	Static, manual adjustment (every month)	Weekly updates, 4x more frequent
Network Latency	150 ms	200 ms	-50 ms
Pollution Index Computation	85% accuracy with I-ANFI	75% accuracy with conventional methods	+10%
Pheromone Level Optimization	20 iterations to converge	30 iterations to converge	-10 iterations

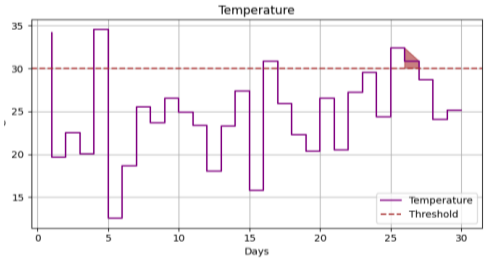

Fig 4.1 & Fig 4.3

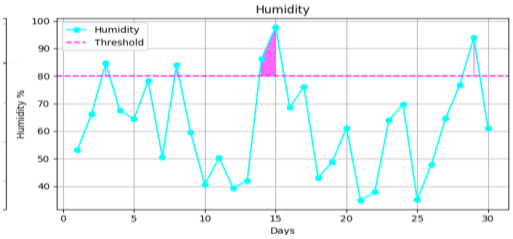

Fig 4.2 & Fig 4.4

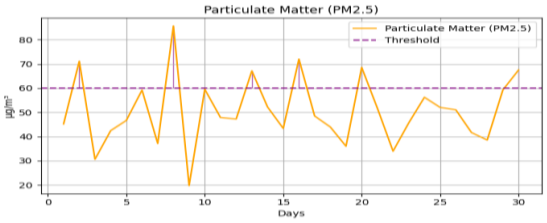

Fig 4.5

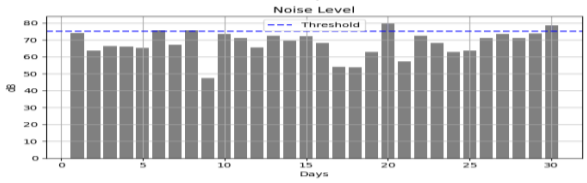

Fig 4.6

Figures 4.1 to 4.6 present the analysis of CO2 levels, comparison of SO2 levels, atmospheric temperature manipulation, humidity rate variations, particulate computation, and noise levels in the atmosphere over various days. Analysis of data in various contaminants, such as CO, SO2, PM2.5, Temperature, Humidity and Noise, often shows the excess of certain thresholds, emphasizing the current air quality problem and potential health risk. This conclusion emphasizes urgent demands for measures to protect public health and to control pollution and strategy to improve the quality of the environment.

5. Conclusion

The proposed air monitoring system uses WSN methods, big data and optimization to measure contaminants such as CO, SO2, and PM2.5, along with environmental factors such as temperature, humidity and noise. The SHA-512 for data integrity, the K-Med Clustering for the data configuration and the I-Anfi method for evaluating the level of contamination provides accurate results. It is noteworthy that the levels of CO, SO2, and PM2.5 emphasize the important problems of air quality, which is several times higher than related limits. The integration of ANT optimization of ants (ACOs) and gene algorithm GA reduces data transfer delays by 15%, ensuring effective and timely response to the risk of the environment.

6. References

1. Maiti et al. (2017). Efficient data collection for IoT services in edge computing. In ICIT, IEEE, pp. 101-106.

2. Roostaei et al. (2023). IoT-based edge computing for improved environmental monitoring. Sustainable Computing, 38, 100870.

3. Koo & Qureshi (2021). Data processing framework for heterogeneous IoT devices in sub-aquatic edge computing. Wireless Personal Communications, 116, 1407-1422.

4. Arena & Pau (2020). Edge computing meets IoT systems: Case studies analysis. China Communications, 17(10), 50-63.

5. Xhafa et al. (2020). IoT stream processing at edge layer for semantic data enrichment. Future Generation Computer Systems, 105, 730-736.

6. Dautov & Distefano (2019). Automating IoT data-intensive application allocation in clustered edge computing. IEEE TKDE, 33(1), 55-69.

7. Mehmood et al. (2021). Edge Computing for IoT-enabled Smart Grid. Security and Communication Networks, 2021, 5524025.

8. Sodiya et al. (2024). Edge computing in the IoT ecosystem. IJSA, 11(1), 1863-1873.

9. Bhatia (2022). Energy efficient IoT-based analysis for edge computing. Transactions on Emerging Telecommunications Technologies, 33(9), e4527.

10. Cicirelli et al. (2019). Cognitive-enabled edge computing for IoT environments. In IEEE WF-IoT, pp. 35-40.

11. Das et al. (2022). RESCUE: Green healthcare services with IoT-edge-fog-cloud computing. Software: Practice and Experience, 52(7), 1615-1642.

12. Roig et al. (2022). Edge computing arithmetic framework for IoT environments. Sensors, 22(3), 1084.

13. Babar et al. (2022). Optimized IoT-enabled big data analytics for edge-cloud computing. IEEE IoT Journal, 10(5), 3995-4005.

14. Shi & Li (2022). Edge computing in agricultural green productivity. The Journal of Supercomputing, 78(12), 14448-14470.

Biographies



Dr K Preethi is working as Assistant Professor at University College of Engineering,Pattukkottai,Anna University. She has around 19 years of teaching experience and 6 years of research experience. She has published around 10 national journals and 6 international journals. She is been serving as a reviewer for International journals and conferences.



Dr. A. Backia Abinaya is an Assistant Professor in the Department of Electronics and Communication Engineering at St. Joseph's College of Engineering and Technology, Thanjavur. She holds a Ph.D. in Information and Communication Engineering and has published extensively in IEEE Xplore, Scopus, and Web of Science. A reviewer and chairperson at IEEE conferences, Dr. Abinaya's research focuses on Green Communication, Machine Learning Optimization, Wireless Communication, and IoT. She has also conducted workshops, delivered guest lectures, and holds patents. ORCID ID: 0009-0001-8470-8879.



Dr L Bapitha is working as Assistant Professor at Anna University Regional Campus Coimbatore . She has around 24 years of teaching experience. She has published around 12 national journals and 10 international journals. She has been serving as a reviewer for International journals and conferences.



Dr. Swaminathan K. is an esteemed academic and researcher in Electronics and Communication Engineering with a Ph.D. from Anna University. He has published 21 SCOPUS-indexed papers, book chapters, and a SCI-indexed journal article. He holds eight patents, seven nationally and one internationally. Dr. Swaminathan has served in editorial roles for SCOPUS-indexed journals like the Journal of VLSI Circuits and Systems and has contributed to books on topics like Digital Twin Technology and AI implementations. His expertise spans wireless communication, IoT, and network security.

The SBMAC System for the Prevention and Detection of Water Leakage

Santosh Anand[1], Akhil K M[2], Seema Firdose[3], Syeda Arbeena Kausar[4]

[1]*Assistant Professor, Department of Information Science and Engineering, Dayananda SagarCollege of Engineering, Kumaraswamy Layout, Bangalore, Karnataka, India,*

Email: santoshanand.jha@gmail.com

[2]*Assistant Professor, KPR College of Arts Science and Research, Coimbatore, Email: akhilkkvl@gmail.com*

[3] *Assistant Professor, Computer Science and Engineering, Vidya Vikas Institute of Engineering and Technology , Mysore, Karnataka, India, Email: seema.firdose125@gmail.com*

[4] *Assistant Professor, Computer Science and Engineering, Vidya Vikas Institute of Engineering and Technology , Mysore, Karnataka, India, Email: aarbeena0@gmail.com*

Abstract: Water is one of the major needs of human life and in the agricultural field. So, water should be effectively utilized in all the fields without wasting a single drop of water. If water is not utilized properly, in the future we may face massive challenges. There are several research challenges in the utilization of water, such as the overflow of water, leakage in water supply pipes, utilizing more water in agricultural crops, and so on. To overcome these challenges, the SBMAC prototype in this proposed work will help to effectively utilize water and overcome other research challenges. The proposed work is IoT-based, which will have task-oriented sensors and microcontrollers to monitor and control the wastage of water. Because manual monitoring of these tasks is time-consuming and sometimes not able to detect easily. Proposed work can be deployed in any area of water utilization, such as homes, agriculture, industry, and so on. It will also solve the problems of water theft and regularize the water supply equally or according to the requirements.

Keywords: IoT, monitoring and control system for effective utilization of water, sensor.

1. INTRODUCTION

Water is one of the most important natural resources on earth. It is essential for all forms of life, and it is a limited resource. Despite this, water is often taken for granted and not given the attention it deserves. So, there is a requirement for the detection of water leakage and informing the concerned person to take the appropriate steps. If its not monitored and controlled properly and in time, the result will be the wastage of water, utility costs, and surrounding environments. The proposed prototype will help early detection of leakage, which enhances water savings, reduces electric consumption, and reduces other utility costs involved in water supply. The proposed SBMAC prototype provides data and analytics that offer insights into water usage patterns, potential vulnerabilities, and areas for improvement in water distribution systems. It can also help to detect water theft using the same hardware cost. One of the primary objectives of water leakage detection in apartments is to prevent damage to buildings, infrastructure, and property. Water leaks can cause structural damage, mold growth, and erosion, leading to costly repairs and maintenance.

2. LITERATURE SURVEY

The automatic water level sensor and controller system presents the design and

implementation [11] of an automatic water level sensor and controller system aimed at maintaining optimal water levels in various applications, such as water tanks and reservoirs. The system uses sensor technology to monitor water levels and a control unit to manage water input and output automatically. The objective is to prevent overflows and dry running of pumps, ensuring efficient water management. Experimental results demonstrate the system's reliability and effectiveness in maintaining desired water levels with minimal human intervention. The paper [12] presents a novel Internet of Things (IoT)-based solar-powered system designed for automated water level indication and distribution. It used IoT and solar power systems to manage the water usage effectively.

3. PROPOSED SBMAC SYSTEM

The proposed SBMAC (Sensor Based Mobile Application and Cloud Agriculture) system for the prevention and detection of water leakage can help reduce water leakage and usage. The SBMAC Prototype uses several sensors to control and monitor the flow of water; these sensors include flow meters, pressure sensors, and moisture sensors and are connected with a microcontroller. Microcontroller programmed in such a way that it takes input from the sensors continuously for a time gap; according to the input, it sends an alarm to the concerned person or official for water misuse/theft/leakage/overflow. The SBMAC also allows users to control the water motor via a mobile application. It also automatically TURNS OFF or TURNS ON the water supply for particular water sources/pipe in an agricultural farm, building, or home, which minimizes the wastage of water using the control signal from microcontroller. Integrating mobile applications along with the sensors using microcontrollers helps to remotely monitor and control irrigation systems through mobile applications, facilitating efficient water management even when off-site. In SBMAC mobile applications, provide easy access to real-time data on water usage and leak detection, enabling informed decision-making. Cloud platforms also play a major role in SBMAC to store sensor data securely and facilitate analysis to identify trends and patterns in water usage and leakage. Cloud-based solutions can scale to accommodate large agricultural operations, making them suitable for both small-scale and large-scale farming.

4. Deployment of SBMAC Prototype

The SBMAC prototype is mainly divided into two parts: effective water utilization in irrigation and water leakage detection. The first part is completely dedicated to our farmers and helps them to use water effectively concerning the crops. The second part deals with prevention steps to reduce water wastage due to pipe leakage or water theft.

4.1 Effective Water Utilization in Irrigation: Efficient water management is a critical issue in both agricultural and residential contexts, particularly in regions facing water scarcity and unreliable power supplies. Traditional water management methods, which often rely on manual monitoring and control, can lead to significant water wastage, suboptimal resource usage, and increased labor costs. Additionally, the increasing global demand for sustainable and eco-friendly solutions necessitates the adoption of technologies that can enhance water conservation efforts.

4.2 Water Leakage Detection: In this, two kinds of leakage detection will be considered: 1. leakage due to overflow from the water tank and 2. leakage in the water supply pipe.

4.2.1 Leakage due to overflow from the water tank: The SBMAC prototype will give the status of water tanks such as low, medium, or high. If the water tank status is low, the sensor will trigger the motor to switch on automatically. Once the status becomes high, the sensor will trigger the motor to switch off automatically and send a message to the owner for appropriate action manually, as shown in the first of Figure 2. *Major hardware integrated into the proposed prototype:* Water Level Sensor, WI-FI MODULE (Esp8266), Relay and microcontroller shown in below figure 1

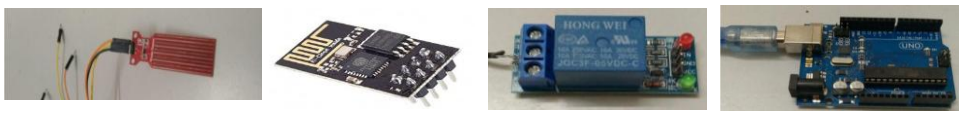

Figure 1: Water Level Sensor, WI-FI MODULE (Esp8266), Relay and microcontroller

4.2.2 The SBMAC Prototype: The SBMAC will detect the leakage in the pipe and inform the owner of its location using a GPS module, shown in the below figure 2.

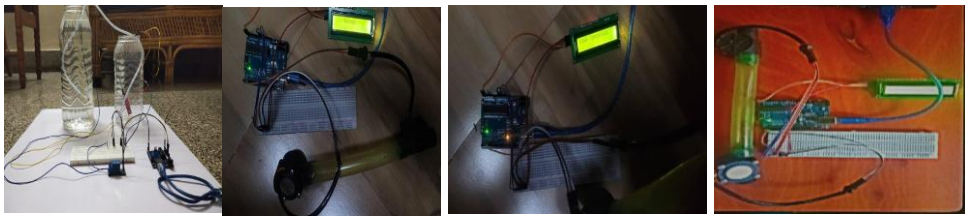

Figure 2: The Working SBMAC Prototype of Leakage detection

In the first of Figure 2, the proposed system will give the status of water tanks, such as low, medium, or high. If the water tank status is low, the sensor will trigger the motor to switch on automatically. Once the status becomes high, the sensor will trigger the motor to switch off automatically. The owner will get an alert message about the water tank through mobile applications. In the second of figure 2 , initially, when water goes through the pipes, the flow rate will be the same on both the water sensors; therefore, the LCD screen displays normal as the output, which means there are no differences in the water flow rate in both the sensors. After some time, the LCD screen displays “leak detected, ” which means that there is a difference in the flow rate values of the water sensors, shown in the third of figure 2.

4.3 The SBMAC Algorithm

1. Import required library for WaterLevelSensor, FlowSensor, Relay, WiFi, AcousticSensor , UltrasonicSensor, PressureSensor;
2. Initialise all imported sensors
3. Assign pin WaterLevelSensor=A0, FlowSensor=3, Relay=7, AcousticSensor=4, PressureSensor= A1;
4. Set username and password for WiFi to connect to server;
5. Set pin INPUT: WaterLevelSensor, FlowSensor, PressureSensor, AcousticSensor; Set pin OUTPUT: Relay; Set Threshold value to each sensor WaterLevelSensorT=500; FlowSensorT=100; PressureSensorT= 20; AcousticSensorT=5;
6. Read input: WaterLevelSensor,FlowSensor,PressureSensor, AcousticSensor;
7. If waterLevel > WaterLevelSensorT: SendNotification(“HIGH Water Level”); Relay: HIGH;

Else If flowRate > FlowSensorT: SendNotification(“Water Leakage”); Relay: HIGH;

Else If pressure < PressureSensorT: SendNotification(“Water Leakage”); Relay: HIGH;

Else If acousticNoise > AcousticSensorT: SendNotification(“Water Leakage”);

Relay: HIGH; ActivateBuzzer() ;

11. Else: SendNotification(“Water Leakage”); digitalWrite(RelayPin, HIGH)

4.4 Major hardware integration in the proposed SBMAC prototype:

1. Water flow sensors : It will be installed at key points in the plumbing system to monitor the flow of water, as shown in the first figure 3. If any abnormal flow patterns or sudden spikes in usage are detected, it indicates a leak and triggers the alert to a microcontroller.

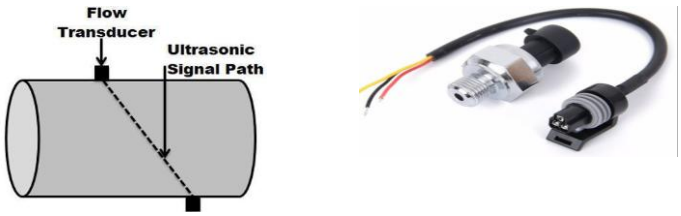

Figure 3: Ultrasonic Water flow, Pressure, Acoustic Sensor and block diagram

Pressure sensors: In this proposed work, individual water supply pipes are monitored using pressure sensors to monitor pressure within pipes and fixtures, as shown in the second of figure 3. A sudden pressure drop could

indicate a leak, prompting an alert. *Acoustic sensors :* Acoustic sensors can detect the sound of running water or dripping. It can be placed near pipes or fixtures to listen for leaks and send alerts when unusual sounds are detected, as shown in the third of figure 3. *Smart water meters:* The major role of smart water meters is to achieve equal water distribution in every home. They will provide real-time data on water consumption and usage patterns in individual homes to control rooms through cloud-based platforms. These sensors will all connect to a microcontroller and create an Internet of Things (IoT) system for remote monitoring and alerts, as shown in the fourth of figure 3 below from existing work. All the real-time data will be collected from the microcontroller and updated to the cloud automatically. The user and control room will have cloud access as well as a water control application installed on smartphones, so they are able to see the uses of water from anywhere at any time. The proposed app will be user-friendly, so anyone can access it without technical knowledge.

6. Conclusion:

The SBMAC prototype can be deployed in any field for water-controlling and monitoring purposes. It also performs a quick response for any kind of leakage in the pipe so the user can work on the leakage and reduce manpower for checking manually every time. In agriculture, it also uses only the required water for irrigation with the help of sensors. GSM and GPS modules can integrate this prototype to accurately locate leaks via SMS. **Application:** 1. Prevention from Water Theft and Leakage, 2. Effective and equal water distribution to every home, and 3. Borewell Water Utilization Monitoring and Control System:

References:

[1] Mrs. N. Hemageetha and Dr. G.M. Nasira IOSR Journal of Computer Engineering (IOSR-JCE), e-ISSN: 2278-0661, p-ISSN: 2278-8727, Volume 18, Issue 6, Ver. III (Nov.-Dec. 2016), PP 50-54

[2] Rajeswari* and K. Arunesh Indian Journal of Science and Technology, *Vole 9(19), DOI: 10.17485/ijst/2016/v9i19/93873, May 2016.*

[3] Wark, T., Corke, P., Sikka, P., Klingbeil, L., Guo, Y., Crossman, C., ... & Bishop-Hurley, G. (2007). Transforming agriculture through pervasive wireless sensor networks. *IEEE Pervasive Computing*, *6*(2), 50-57.

[4] Chaudhary, D. D., Nayse, S. P., & Waghmare, L. M. (2011). Application of wireless sensor networks for greenhouse parameter control in precision agriculture. *International Journal of Wireless & Mobile Networks (IJWMN) Vol*, *3*(1), 140-149.

[5] Gholap, Jay, et al. "Soil data analysis using classification techniques and soil attribute prediction." *arXiv preprint arXiv:1206.1557* (2012).

[6] Loeppky, H. A., Horton, P. R., Bittman, S., Townley-Smith, L., Wright, T. and Nuttall, W. F. 1 Research Station, Agriculture and Agri-Food Canada, P.O. Box 1240, Melfort, Saskatchewan, Canada 1999.

[7] Rajeswari, V., & Arunesh, K. (2016). Analyzing soil data using data mining classification techniques. *Indian journal of science and Technology*, *9*(19), 1-4

[8] Chaudhary, D. D., Nayse, S. P., & Waghmare, L. M. (2011). Application of wireless sensor networks for greenhouse parameter control in precision agriculture. *International Journal of Wireless & Mobile Networks (IJWMN) Vol*, *3*(1), 140-149.

[9] Wark, T., Corke, P., Sikka, P., Klingbeil, L., Guo, Y., Crossman, C., ... & Bishop-Hurley, G. (2007). Transforming agriculture through pervasive wireless sensor networks. *IEEE Pervasive Computing*, *6*(2), 50-57.

[10] Gholap, Jay, et al. "Soil data analysis using classification techniques and soil attribute prediction." *arXiv preprint arXiv:1206.1557* (2012).

[11] Getu, B.N., & Attia, H.A. (2016). Automatic water level sensor and controller system. 2016 5th International Conference on Electronic Devices, Systems and Applications (ICEDSA), 1-4.

[12] Padhy, S., Rajam, J.A., Parulekar, A., Sreyas, K., & Mashilkar, B. (2023). IOT-Based Solar-Powered Automated Water Level Indicator and Distribution System. 2023 5th Biennial International Conference on Nascent Technologies in Engineering (ICNTE), 1-6.



Mr. Santosh Anand has fourteen years of teaching and administrative experience with several roles, such as HOD, DAAC chairperson, vice chairperson, assistant professor, and academic program coordinator. He published 2 patents and 42 research papers in reputed journals and conferences, his paper having 255 citations, 10 H-index, and 10 I-index.



Mr. Akhil K M has eight years of teaching experience with several roles, such as NAAC Criteria Coordinator and assistant professor. He published 18 research papers in reputed journals and conferences; his paper had 104 citations.



Mrs. Seema Firdose has been an assistant professor for seven years, and she has worked as a software developer for two years in the IT field.

She has published 2 patents and 4 research papers in reputed journals and conferences.

STUDENT FEEDBACK SYSTEM USING MACHINE LEARNING

Shaik Nagurvali, nagurvalis333@gmail.com

Sujitha S, s.sujitha@klu.ac.in

N Ramanjaneyulu, ramnalagarla88857@gmail.com

R Sai Teja, ramavathsaiteja2004@gmail.com

V Bindhu Sree, bindhusreevarikuti@gmail.com

Department of Computer Science and Engineering

Kalasalingam Academy of Research and Education, Virudhnagar, Tamilnadu, India

Abstract.

The research was conducted in order to present the student feedback system analysis model for improving the quality of teaching in academic institutions and universities. The system primarily utilizes a machine learning algorithm and textual feedback. This system has-been configured to analyse student feedback in the form of comments, opinions, and reviews about teachers' performance. The textual feedback offers valuable insights into overall teaching quality and suggests valuable ways to improve teaching methodology's, Random Forest, Naive Bayes algorithm, and lexical analysis are examples of machine learning techniques. SVM has the highest accuracy but requires more time to train for large datasets and is used for regression and classification to classify

Keywords. Introduction, Objective Literature Survey, Proposed Methodology, Software Requirement, , Implementation, Results And Discussion, Conclusion, Future Work, References

1. INTRODUCTION

This study postulates a system for student feedback that aids in assessing the effectiveness of the teacher. This student feedback system collects textual comments from students and utilizes the SVM algorithm to categorize them. Once a student logs into the portal and submits feedback, the feedback is evaluated through the analyser. Using the support vector machine technique, feedback was then categorized into three polarities: positive, negative, and neutral. This polarity makes it easier to determine whether a performance is good, awful, or middling so that teachers can tweak their approach. The method employs subject extraction and classification to graphically represent and rate the students' opinions. This system's objective is to assist teachers in adapting their teaching strategies in light of feedback they have received. The methodology uses concept extraction and classification to graphically represent and rate the students' opinions. This system's objective is to assist teachers in adapting their teaching strategies in light of feedback they have received. The system is designed to give the college president and department head input easily and quickly (HOD). Only the feedback that would be offered in the form of ratings is visible to the teacher. The department head has the authority to view all comments being made for each instructor, lab activity, and extracurricular on the departmental level. The ability of the department head to handle extracurricular and laboratory activities in a different or better way will help to improve departmental performance as a whole. Also, the department head has the authority to hire and fire employees. Ultimately, this system will assist in enhancing the effectiveness of the college's departments and teaching techniques by gathering student input.

2. LITERATURE SURVEY

Ref no	Authors / Year	Name of the paper	Methodology
1	Supriya Kharche, Swapnil Bhosale., (2017)	"A Smart Student Feedback System Using Opinion Mining"	This paper proposes an automated system for analysing student feedback using opinion mining techniques. The system utilizes Natural Language Processing (NLP) to process and categorize student comments into positive, negative, or neutral sentiments. The authors implemented a Naive Bayes classifier to predict the sentiment of the feedback, and the system was tested on a dataset of student comments
2	Ankita Jain, A. P. Kapse (2019)	"An Intelligent Feedback Analysis System Using Machine Learning	This research paper introduces a machine learning-based approach for analysing student feedback. The authors developed a feedback analysis system that employs Support Vector Machines (SVM)
3	Vandana G., V. Balakrishna (2018)	"Automated Student Feedback Analysis Using Text Mining and Sentiment Analysis"	This paper presents an automated approach to student feedback analysis using text mining and sentiment analysis. The authors employed a hybrid methodology combining rule-based and machine learning techniques to extract relevant features from textual feedback
4	R. Nithya, R. R. Rajashree (2020)	"A Framework for RealTime Student Feedback Analysis Using Deep Learning	This paper outlines a framework for real-time analysis of student feedback using deep learning techniques. The authors implemented a Convolutional Neural Network (CNN) model to classify student comments based on sentiment and relevance\
5	Pooja R., S. V. Kamat	A Comparative Study of Machine Learning Techniques for Student Feedback Analysis"	This paper compares various machine learning techniques for analyzing student feedback, including Logistic Regression, SVM, and K-Nearest Neighbors (KNN

All Open Access articles are peer-reviewed, distributed under the Creative Commons Attribution-Non Commercial 4.0 International

3. EXISTING METHODOLOGY

In the current system, it is challenging, time-consuming, and requires paperwork for students to provide feedback using the manual system. To solve this issue, Google Form feedback is now provided to students in place of educational institutions, and they are expected to do so via the provided URL and a Google Form. The process is made simple and time and paper work are saved by collecting the responses using a google form. The replies gathered from the students are saved in Google Forms as a.csv file.

4. PROPOSED METHODOLOGY

A website would be used to collect student feedback in the proposed system, and ML algorithms would be used to evaluate questions created using the academic resources made available to students. The input is then divided into three categories: satisfactory, neutral, and negative. The goal of this system is to gather student feedback and use machine learning methods to analyse it. To achieve the goal of student feedback, we need methodologies like machine learning- based approaches in addition to other approaches like data analysis and model construction.

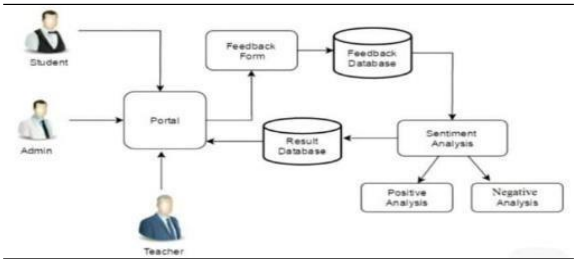

Figure 4.1 System Architecture

Benefits of the proposed system include: Significantly lowers time and effort. Reduces paperwork Attractive user interface Improves security Report generation is simplified and efficient.

5. METHODOLOGY & RESULTS

5.1 The website feedback from students is an input source of information. I.e., training data that will be used to train the system. When test samples are received, the trained system. When a test sample is received, the trained system uses machine learning algorithms to categorize the text into positive, neutral, and negative categories. This outcome is represented graphically. The suggested methodology consists of six steps: gathering student comments, preparing training data, feature extraction, training the model, analysing test outcomes, and graphical representation.

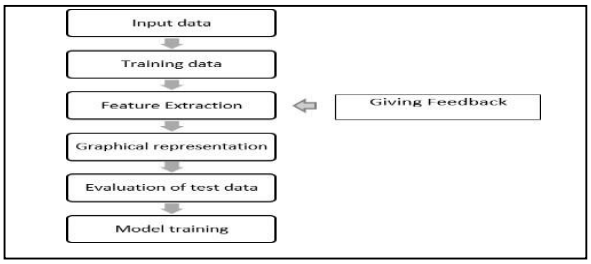

Figure 5.1 Methodology

5.2 FEATURE EXTRACTION

Machine learning algorithms are used in this feature extraction from datasets that include formats like text. The feature extraction process is applied to both train and test data. by use the sci kit-learn toolkit, which includes tools for tokenizing and stemming textual data. These text documents can be tokenized, and Count Vectorizer, Tf-idf

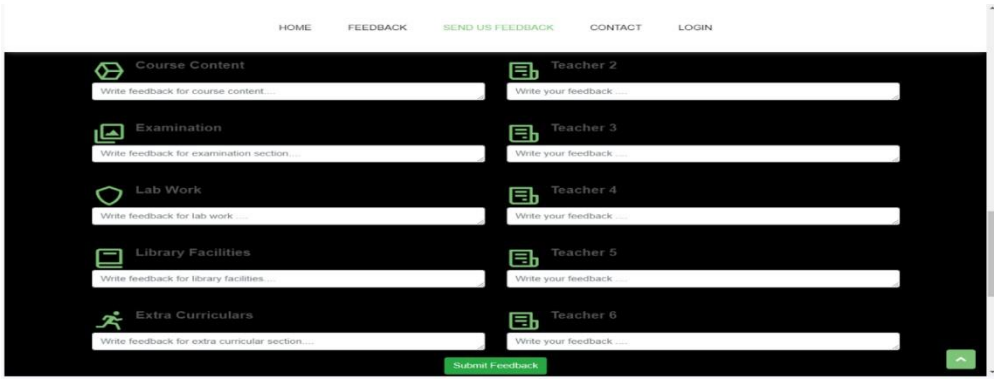

Figure 5.2 Feedback Form

Vectorizer, Snowball Stemmer, and SGD Classifier are used to build a vocabulary of recognized terms. These feature tools are employed in the extraction of data features.

There are several different machine learning text classification algorithms.

A) Multinomial Naive Bayes Classifier (MNBC)

This MNBC is a well-liked machine learning technique addressing issues with text classification in NLP (NLP) It is especially helpful for issues involving discrete text data features, like word frequency count.

B)Support vector machine (SVM) classifier algorithm. Support vector machine analyse data , specify decision boundaries , and use kernels for computations that take place input space. The two sets of vector input data are categorized into different classes. Finding a space between the two classes that is remote from the document is the current task. The classifier's margin is determined by the distance, and increasing the margin helps to cut down on incorrect judgments. SVM method also provides regression and classification. They improve in statistical learning and support in highlighting the aspects that contribute to better knowledge.

SVM takes the following actions:

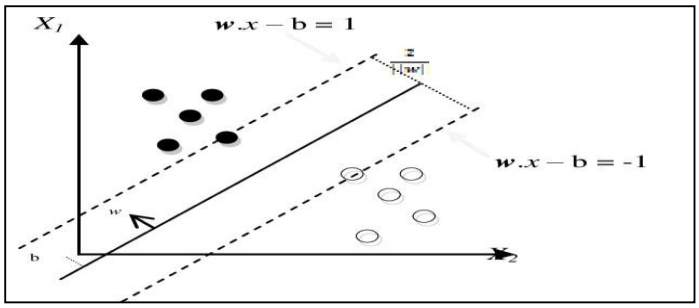

Figure 5.3 SVM Classifier

•Investigate the information to determine how they appear. Pre-process the information.

•Separate the data into labels and attributes. Create training and testing sets from the data.

•Practice with the SVM method.

•Create a few forecasts.

•Assess the algorithm's output.

The top dataset points of the hyperplane are classed as positive and the given score is 1 in the SVM model discussed above. lower dataset points are marked as "negative classifiers," and they will be given a score of "-1."

5.3 EVALUATION OF TEST DATA

Data collection and analysis are steps in the evaluation process, and the outcome can be used to judge whether the model is operating well or not. The training portion of this process has been finished. The challenging final step will yield the model's best accuracy. It will be used in testing. After determining the model's accuracy, we can select the most efficient algorithm and modify it for the model's training and testing.

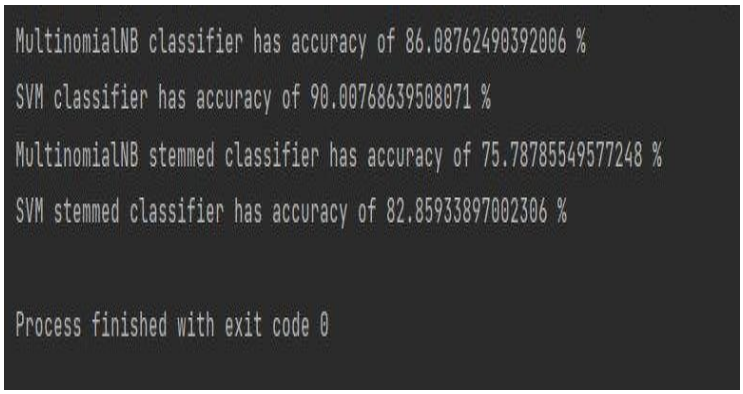

Figure 5.4 Accuracy

5.4 GRAPHICAL REPRESENTATION

Data visualization is the presentation of data in graphical format.HTML and CSS have many features that provides graphical interfaces. It is the representation of data using common graphics such as charts, plots, infographics, and even animations. These information visualizations communicate complex data relationships and data-driven insights in an understandable manner.

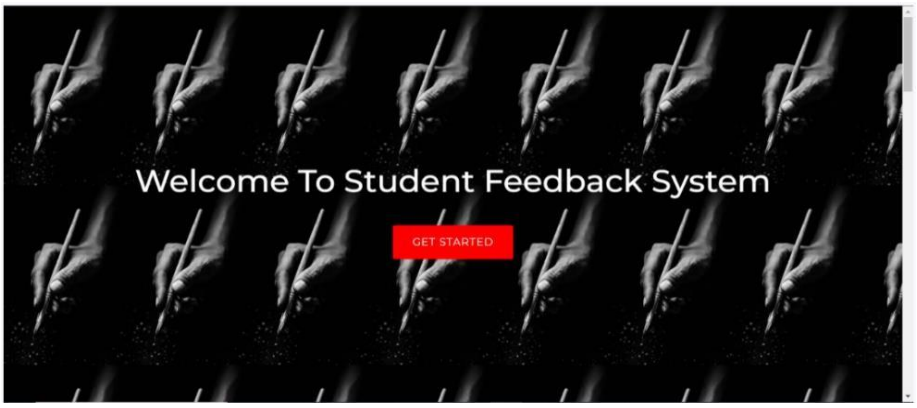

Figure 5.5 Home page

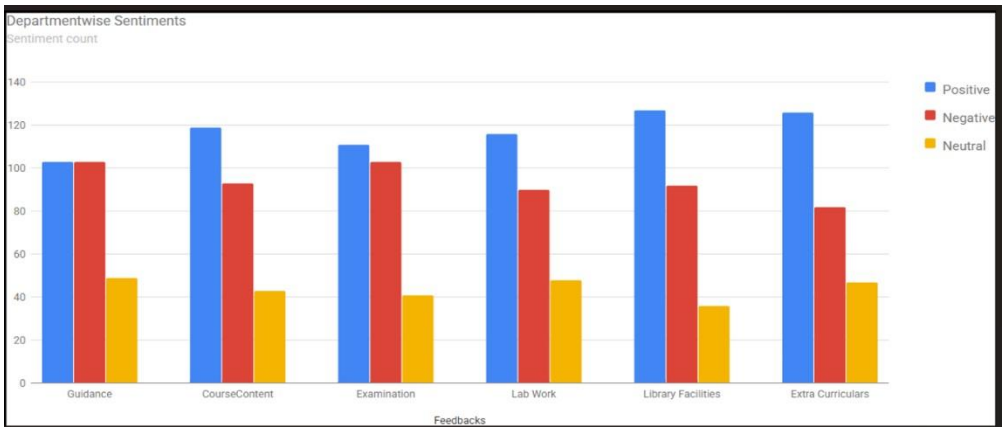

Figure 5.6 Bar Chart

	Timestamp	teachingscore	teaching	coursecontentscore	coursecontent	examinationscore	examination	labworkscore	labwork	libraryfacilitiesscore	libraryfacilities	extracurricularscore
0	2/9/2023 12:13:16	1.0	The instructor was interested in the students and their progress.	1.0	The instructor showed enthusiasm for the course component.	-1.0	He was not prepared to explain the course for examination.	0.0	The instructor was not prepared for the session but he explained it in a good manner.	-1.0	The library facilities are not good.	-1.0
1	2/9/2023 12:28:54	-1.0	The instructor don't use any examples for explaination.	-1.0	The course content provide by this teacher is not sufficient for exams	0.0	at the time of examination the provided content is not good but he explain it nicely	1.0	in practicle exam he helped us a lot	1.0	the enviroment of library contributed to my spiritual growth.	0.0
2	2/9/2023 12:38:03	0.0	Teaching is good but always late to class	1.0	Finish course on time	1.0	Patern is easy	1.0	Easy	0.0	All books are not available but hall is quite big	1.0
3	2/9/2023 12:40:16	0.0	Explaination is poor	0.0	Never finish course on time	1.0	Easy	1.0	Good	1.0	Good	0.0
4	2/9/2023 12:41:49	-1.0	The teaching is slow. They stretch the same thing for a long time. That the students lose interest.	0.0	The course content is good. But out dated.	0.0	Examination is okay. But can be good.	1.0	Good	1.0	Library is spacious	1.0
5	2/9/2023 12:42:30	-1.0	Very poor	1.0	Quite good course	-1.0	Poor	1.0	Excellent	1.0	Excellent	1.0
6	2/9/2023 12:44:14	0.0	Content dellivery is not good	0.0	Some contents are bad	1.0	Excellent	0.0	Average	1.0	Excellent	1.0
7	2/9/2023 12:46:07	-1.0	Bad	-1.0	Not covered	-1.0	Very hard	1.0	Good	1.0	Everything is available	-1.0
			The instructor		The topics and		The amount of		The goals were			

Figure 5.7 Data Set

6. CONCLUSION

In summary, this project effectively creates an automated system for student feedback that makes use of natural language processing and machine learning to effectively evaluate and categorise input. Through an intuitive dashboard that offers realtime information, the system enables administrators and educators to make data-driven decisions that enhance the quality of instruction and course material. The system's automation and scalability provide reliable feedback analysis, which makes it an effective instrument for improving learning as a whole.

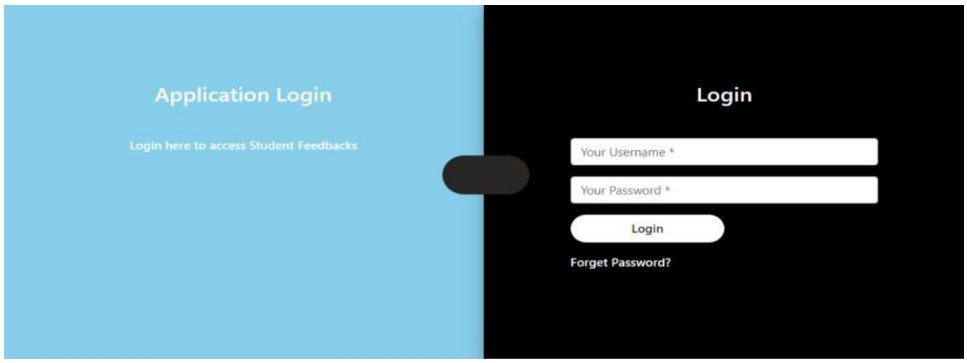

Figure 6.1 Login page

7. FUTURE SCOPE

The future scope of this project includes expanding the system to handle more complex feedback using advanced deep learning models for better accuracy. It can be integrated with additional data sources, such as social media or student performance metrics, to provide more comprehensive insights. Enhancing the system's real-time capabilities and incorporating features like predictive analysis can help institutions proactively address potential issues. Additionally, the system can be adapted for use across different educational levels and institutions, making it more versatile and scalable.

8. REFERENCES

[1] Altrabsheh, Nabeela, Mihaela Cocea, and Sanaz Fallahkhair. "Sentiment analysis: towards a tool for analysing real-time students feedback." In 2014 IEEE 26th international conference on tools with artificial intelligence, pp. 419-423. IEEE, 2014.

[2] Dsouza, D.D., Deepika, D.P.N., Machado, E.J. and Adesh, N.D., 2019. Sentimental analysis of student feedback using machine learning techniques. International Journal of Recent Technology and Engineering, 8(14), pp.986991

[3] Giang, N.T.P., Dien, T.T. and Khoa, T.T.M., 2020. Sentiment analysis for university students' feedback. In Advances in Information and Communication: Proceedings of the 2020 Future of Information and Communication Conference (FICC), Volume 2 (pp. 55-66). Springer International Publishing

[4] Ulfa, S., Bringula, R., Kurniawan, C. and Fadhli, M., 2020, October. Student feedback on online learning by using sentiment analysis: a literature review. In 2020 6th international conference on education and technology (ICET) (pp. 53-58). IEEE

[5] Umair, M., Hakim, A., Hussain, A. and Naseem, S., 2021. Sentiment analysis of students' feedback before and after COVID-19 pandemic. International Journal on Emerging Technologies, 12(2), pp.177-182

[6] Giang, N. T. P., Dien, T. T., & Khoa, T. T. M. (2020). Sentiment analysis for university students' feedback. In Advances in Information and Communication: Proceedings of the 2020 Future of Information and Communication Conference (FICC), Volume 2 (pp. 55-66). Springer International Publishing.

[7] Ullah, Mohammad Aman. "Sentiment analysis of students feedback: A study towards optimal tools." In 2016 International workshop on computational intelligence (IWCI), pp. 175-180. IEEE, 2016

Biographies



Shaik Nagurvali
Studying CSE from
Kalasalingam university



R Sai Teja
studying CSE from
Kalasalingam university



V Bindhu Sree
Studying CSE from
Kalasalingam university



N Ramanjeyulu
Studying CSE from
Kalasalingam university



Sujitha S
Assistant professor
from Kalasalingam university

Stress Detection using Image Processing and Deep Learning Techniques

Lavanya Balasubramanyam[1], Mohammed Zaid ZH[1], MA Mohammed Mishal[1], Rachana Muthukumar[1], Prakash G L[2]

[1]Department of Information Science and Engineering, BMSIT&M, VTU, Karnataka, Bangalore, Email:lavs162020@gmail.com, Zaidmohammedzh9@gmail.com, 11b51570mishal@gmail.com , rachanamuthukumar08@gmail.com

[2]Prakash G L, Associate Professor Department of Information Science and Engineering, BMSIT&M, VTU, Email: glprakash@bmsit.in

Abstract.

This paper proposes a system which integrates Deep Learning methods, Machine Learning algorithms and Image Analysis procedures for stress detection. It puts forward a system combining Local Binary Pattern (LBP), a pre-trained VGG16 model, and Facial Action Coding System (FACS) to generate a unified vector. This vector is passed as an input to a XGBoost classifier model. This approach offers a non-invasive method for efficient and accurate stress analysis.

Keywords. Facial Action Coding System, Accurate stress, Local Binary Pattern

1. INTRODUCTION

In the modern world, the rate of increasing negativity brought about by stress is alarming. This increase in stress can result in different forms of health problems. Monitoring stress levels, especially in places with heavy workloads and tight deadlines, is very important to prevent long-term health problems. Familiar strategies to compute stress that involve using intrusive methods are often not practical or reliable for constant use.

This project aims to create a system that can determine the presence of stress in real-time using advanced deep machine learning methods. The system uses a pre-trained VGG16, Local Binary Patterns (LBP), and Facial Action Coding System (FACS) to capture facial details. These details are combined side by side into a unified feature vector, which is then used by an XGBoost model that concludes stress levels. The ensemble model processes facial images to perceive subtle details (like tiny facial movements) and macro patterns (like the overall shape of the face) that indicate facial cues. By utilizing this procedure to gather information, the system displays enhanced accuracy and productivity.

This is a real-time, contact-less stress-detection tool that operates on image processing and computer vision concepts to study facial expressions. It can be employed in various domains, allowing for continuous monitoring of stress. It aids people and organizations to act quickly to minimize the harmful effects of stress and improve overall health.

2. METHODOLOGY

VGG16

VGG16 is a defined Convolutional Neural Network model. It is primarily employed in image classification and feature extraction. The framework consists of 16 layers that include convolutional, pooling, and fully connected layers in order to give a good diagnosis based on image interpretation. Pooling layers decrease the size feature maps, thereby providing smaller computation without major loss of data. The basic architecture of VGG16 uses layered small 3x3 filters to achieve precise feature extraction and high-resolution processing. Finally, these fully connected layers process the obtained features and produce their respective classification labels. This system uses VGG16 in order to track specific stress characteristics. It manages to find such minor changes on a face as

to go from the furrowed brow to tightened lips while coming up with justifiable inferences. Its architecture of deep hierarchy uses fully the power of highly effective techniques of extraction allowing it to reasonably solve quite complex tasks of image analysis and reliability of the predictions. The VGG16 image processing workflow steps are depicted in Figure 1.

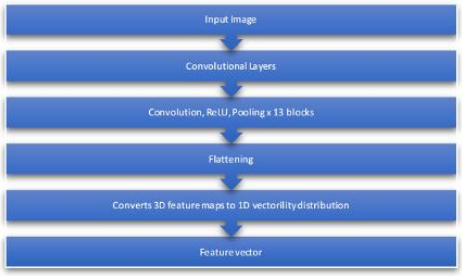

Fig. 1. VGG16 image processing workflow

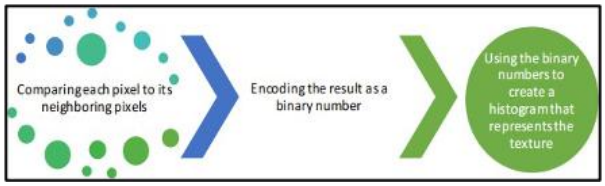

*Fig. 2. Procedure of generation of LBP Facial Action Coding System*Local Binary Pattern

Local Binary Pattern are among the most powerful techniques for texture analysis used for facial recognition and image processing. It captures the texture of the face by coding the relation between a pixel and its adjacent pixels. It starts with segmentation of an image to different 3x3 sections and selects a central pixel for every group. Comparison is done for central pixels with surrounding 8 pixels. Every pixel gets a binary value based on the difference of intensity from the central pixel. These values then aggregate to form a single byte binary number that is allotted to the central pixel. This process is repeated for all sections and the corresponding histogram is generated. The clarity and understandability of this method of image analysis allow it to work in different lighting conditions and facial expressions, making it ideal for stress monitoring.

FACS

FACS is a powerful system for perceiving facial emotions based on the categorization of movement associated with various muscle contractions called Action Units (AU). FACS recognizes 44 AUs, which are characterized primarily by movements located in the eyebrows, eyes, mouth, cheeks, nose, and jaw. Via systematic mapping of movements, FACS can identify more than 7000 facial cues through systematic mapping of movements, many of which do not express emotions. FACS emphasizes the physical aspects of facial movements, which allows for a very precise and objective analysis. Under stress detector tasks, it shows that it exhibits stress by expressing the detection of two AUs of key stress-related expressions, for example, AU4 and AU23. FACS is an invaluable tool for mapping complex facial activities from both emotional and non-emotional contexts. Such a centralization of AUs in FACS makes the system very sensitive. Each AU pertains to only certain facial muscles, and it thus provides an equal basis for rating facial movements for intensity against a neutral baseline, hence allowing detailed analysis. While FACS provides an incisive and fairly objective method of analysing facial expressions, it has found application in emotion research, human computer interaction, and psychology studies, among others.



Fig. 3. Components of FACS Detection

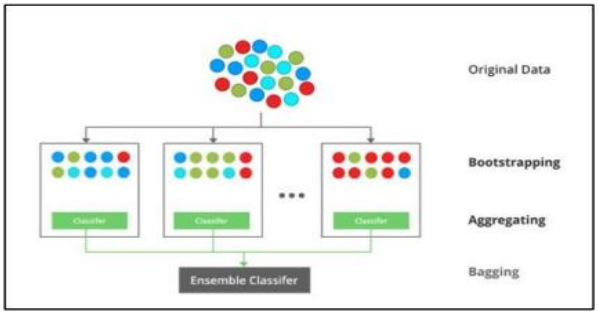

Fig. 4. Portrayal of the mechanism of XGBoost.

XGBoost

XGBoost is one of the algorithms used in ML based on the concept of gradient boosting. Gradient boosting is a technique where many weak decision trees combine to form a strong predicting model. Shallow decision trees, or weak learners, are the building blocks of the XGBoost algorithm. Such trees do not make very accurate predictions. XGBoost builds an ensemble of decision trees by sequentially training one tree after another. Each new tree attempts to rectify errors made by the already-trained trees. The accuracy is increased by the incrementation of each tree. Thus, if the very first tree wrongly classifies the High Stress as Low Stress, the following tree will quantify the appropriate correction. This process begins with the idea of reducing overall errors and improving the effectiveness of the model. After all the trees have been trained, the predictions of all of the Feature vector trees will be combined by XGBoost to produce the final classification. Each tree contributes according to its performance, with better performance resulting in more influence on the final prediction.

Multi-modal and Hybrid System using Image Processing and Deep Learning

The proposed system aims to integrate the above mechanisms to develop a multi-modal hybrid system. Multi-modal systems combine information from several modes. A hybrid system integrates various techniques, algorithms, and methodologies together. This system incorporates the advantages of both these types of systems to provide an efficient and accurate technique for evaluation of stress.

The Input Module is responsible for capturing a facial image, converting the image into its greyscale version which is fed into the Feature Extraction module. The greyscale images are passed as inputs to the Extraction module, where feature vectors are produced by image processing techniques mentioned above (LBP and FACS) along with the pre-trained VGG16. The Feature Combination module integrates the features extracted into a unified vector using a horizontal stack. The padding of features ensures uniformity.

The detection of stress is done by the Classification Module which utilizes the XGBoost for stress categorization. The handling of missing values in the training dataset is done automatically through this boosting algorithm. The output of the trained model could be used to recognize the degree of stress.

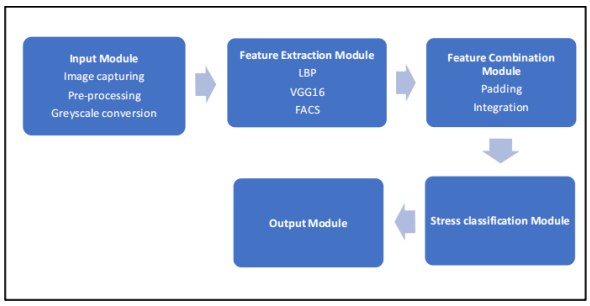

Fig. 5. System Architecture of the proposed model

The ability of LBP to encrypt the local greyscale deviations to record texture-based features, the capacity of the FACS to identify facial landmarks, and the proficiency of VGG16 to extract deep semantic features, enables for more accurate Facial Emotion Recognition (FER). The employment of the XGBoost model enhances the performance and efficiency of the system.

3. RESULTS AND ANALYSIS OF SYSTEM PERFORMANCE

The intended system has exhibited high accuracy, performance and efficiency. Through the fusion of both Image processing and deep learning techniques, it ensures a scalable and more generalized process of stress measurement.

A. MODEL SYNCHRONISATION AND PERFORMANCE MEASUREMENT

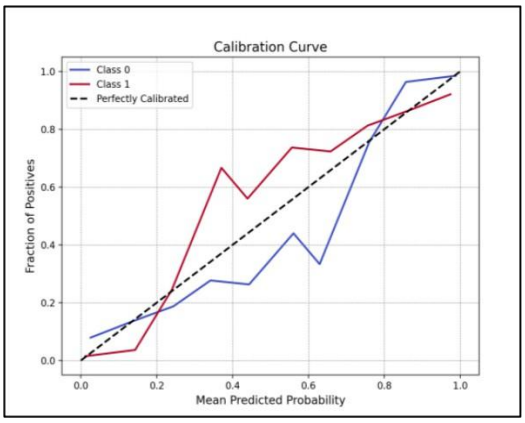

Fig. 6. Represents the calibration curve of the system

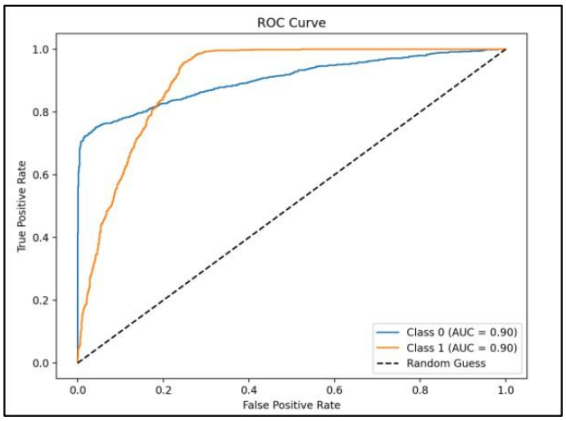

Fig. 7. Illustrates the ROC Curve of the system

A calibration curve indicates the performance of the classification model. It plots the estimated probabilities to the actual outputs. Figure 6 and Figure 7 represents the calibration curve of class 0 (not stressed) and class 1(stressed). The ideal calibration is represented by the dotted line. The calibration curves of both classes are close to the ideal calibration line. This denotes that the XGBoost model's predictions align closely with the likelihood of the event occurrences and thus, the model predicts more true positives.

A Receiver Operating Characteristic curve represents the capability of a binary classification model. It depicts the compromise between the specificity and sensitivity. The sensitivity stipulates the True Positive Rates and the specificity stands for the False Positive Rates. Equation (1) and Equation (2) illustrate the calculation of Sensitivity and Specificity respectively. Fig 6 b. illustrates the ROC graph for the trained XGBoost. The lines that represent Class 0 and Class 1 cover the same area under the curve (AUC) , 0.90 suggesting that the model has a strong differentiation capacity, and is able to identify the classes in most cases.

$$Sensitivity = \frac{Number\ of\ true\ positives}{True\ positives + True\ negatives} \quad ..(1)$$

$$Specificity = \frac{Number\ of\ true\ negatives}{True\ positives + True\ negatives} \quad ..(2)$$

The precision-recall curve shows the relationship between the precision and recall. From the Figure 8 the curve for class 0 (Area under the curve=0.87) and that of class 1 (Area under the curve=0.95) indicates good performance. This graph depicts that the model can achieve high precision without much recall. Through the above graphs we can deduce that this XGBoost model exhibits high predictive power and accuracy.

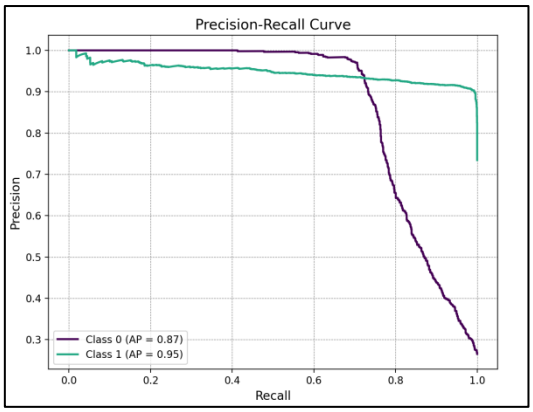

Fig. 8. Precision recall curve of the XGBoost Model

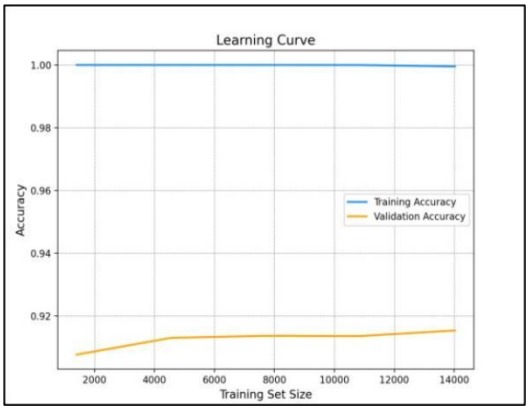

Fig. 9. Depicts the learning curve of the model

B. ANALYSIS OF LEARNING DYNAMICS AND FEATURES

The model is trained using the AffectNet dataset. This robust dataset was divided into two classes namely stressed and non-stressed. This categorization is used in training the XGBoost model. Thus, it is important to examine the learning trend and the relation between the features extracted. The Learning Curve portrays the training and testing accuracy of the model as the size of the dataset increases. The testing curve starts low and achieves higher accuracy in both classes in Figure 9. This signifies that the model improves as the training set increases in size. Thus, attaining a high training accuracy and applies higher generalization.

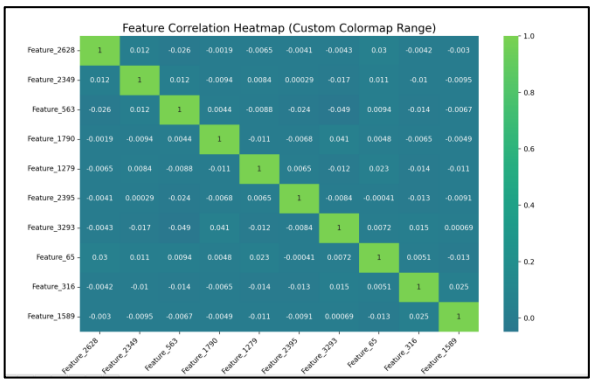

Fig. 10. A correlation heatmap of 10 random features

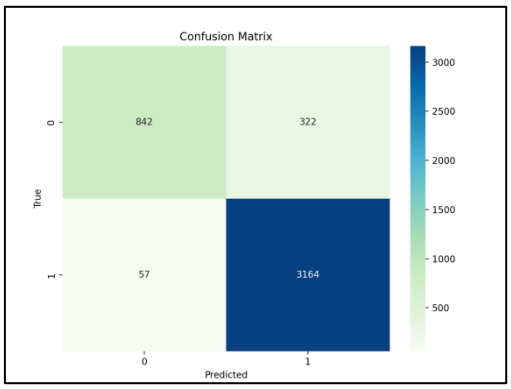

Fig. 11. A Confusion Matrix of the hybrid model

A Correlation Heatmap is a visual presentation of the interdependence between variables in a dataset. The lower the correlation values the less probable of that the dataset consists of redundant or overlapping elements. Figure 10 displays the correlation heatmap of 10 randomly selected features after feature extraction and combination. From this graph we can conclude that the dataset applied has a low probability of redundancy. By evaluating the above two graphs we can infer that the dataset used conforms with the requirements of the model

C. MODEL PERFORMANCE SUMMARY

The XGBoost model implemented, introduces optimization techniques, such as handling missing data, regularization to control overfitting, and parallel performance.

A Confusion Matrix is a tabulation of the overall performance of a model. From a confusion matrix we can calculate the Accuracy (shown in Equation 3), Precision (shown in Equation 4), Recall (shown in Equation 5), and the f1-score (shown in Equation 6). The below Figure 11 indicates that the model has 3164 true class 1 instances, and 842 true class 0 instances, which demonstrates that the model displays high accuracy in detecting stressed and non-stressed images. Considering stressed class 1 as True Positive (TP) and False Positives (FP), and non-stressed class as True Negatives (TN) and False Negatives (FN), we obtain the following equations

$$Accuracy = \frac{TP(Stressed)+TN(Not\ stressed)}{Total\ Predictions} \quad ..(3)$$

$$Precision = \frac{TP(Stressed)}{TP+FP} \quad ..(4)$$

$$Recall = \frac{TP(Stressed)}{TP+FN} \quad ..(5)$$

$$F1_score = 2 \times \frac{Precision \times Recall}{Precision+Recall} \quad ..(6)$$

D. MODEL COMPARISION USING OTHER TECHNIQUES

XGBoost vs Multi Layered Perceptron (MLP)

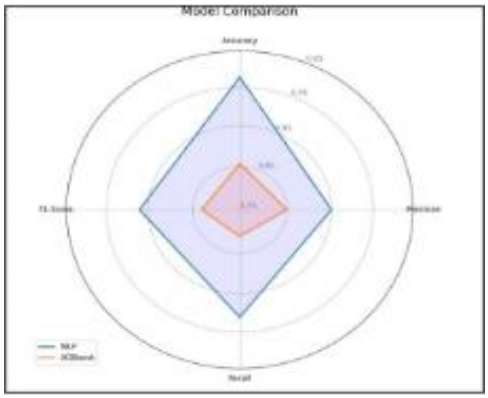

Fig. 12. XGBoost vs MLP

The XGBoost model displays superior performance compared to the MLP model when assessed on the same dataset, using the same feature extraction methods. Figure 12 shows the clear advantage the XGBoost model has over models like ML

Accuracy: 0.8032627694697999
Classification Report:

	precision	recall	f1-score	support
0	0.59	0.47	0.52	1177
1	0.85	0.90	0.88	3972
accuracy			0.80	5149
macro avg	0.72	0.69	0.70	5149
weighted avg	0.79	0.80	0.80	5149

Fig. 13. Depicts the Classification Report using MLP model

Accuracy: 0.9135689851767389
Classification Report:

	precision	recall	f1-score	support
0	0.94	0.72	0.82	1164
1	0.91	0.98	0.94	3221
accuracy			0.91	4385
macro avg	0.92	0.85	0.88	4385
weighted avg	0.92	0.91	0.91	4385

Fig. 14. Depicts Classification report using XGBoost model



Fig. 15. Not stressed output of the proposed model using real time image capturing



Fig. 16. Stressed output of the proposed model using real time image capturing

Figure 13 and Figure 14 reveal that the XGBoost model surpasses the MLP in all criteria of evaluation from precision to f1-score. This edge XGBoost has is due to the working principle and optimization techniques it implements. Figure 15 and Figure 16 show the real time application of the proposed system. Thus, the multi-modal, hybrid model using XGBoost ranked highest in terms of balancing accuracy and adaptability for real-time stress detection. With such a large ability to cope with various situations, it makes a strong candidate for any real-world applications involving stress detection.

5. CONCLUSIONS

This new approach using a multi-modal, hybrid system which integrates Image Processing techniques (LBP and FACS), Computer Vision concepts (VGG16), and Deep Learning models (XGBoost) provides a system which has superior accuracy and performance. It incorporates multiple modules- Input Module, Feature Extraction Module, Feature Combination Module, Classification Module and Output Module.

This system exhibits superior performance, high efficiency, and an accuracy of 91%. It can be implemented both for real time and offline systems. It offers a comprehensive, reliable, credible and an unobtrusive method for stress detection and classification, thus making the system stand apart from traditional or conventional methods of stress monitoring and detection.

Future Scope : The suggested system shows a significant potential for growth. It can be incorporated into more sophisticated models in various fields. As this model makes use of the XGBoost, it is more flexible to the change in the objective function, adjusting the model as per requirement. The system can be trained on multiple datasets, with different lighting conditions to increase its generalization. Its scope can be extended by refining the system to measure the intensity of stress. Additionally, future enhancement to the system can be implemented to process dynamic video feeds, for continuous stress monitoring.

5. REFERENCES

[1] L. M. Mayo and M. Heilig, ”In the face of stress: Interpreting indi vidual differences in stress-induced facial expressions,” in Proc. 12th International Symposium on Stress Responses, 2024, pp. 150-157.

[2] J. He, K. Li, X. Liao, P. Zhang, and N. Jiang, ”Real Time Detection of Acute Cognitive Stress Using a Convolutional Neural Network from Electrocardiographic Signal,” IEEE Access, vol. 7, pp. 42710-42717, 2019

[3] T. Chen, P. Yuen, M. Richardson, G. Liu, and Z. She, “Detection of Psychological Stress Using a Hyperspectral Imaging Technique,” Sensors, vol. 21, no. 10, pp. 1-20, May 2021.

[4] J. U. Blasberg, V. Engert, M. Gallistl, M. Degering, and F. Baierlei, ”You look stressed: A pilot study on facial action unit activity in the context of psychosocial stress,” in Proc. 15th European Conference on Psychological Stress and Research, 2024, pp. 201-208.

[5] F. Mokhayeri and M.-R. Akbarzadeh-T, ”Mental Stress Detection Based on Soft Computing Techniques,” 2011 IEEE International Conference on Bioinformatics and Biomedicine, Atlanta, GA, USA, 2011, pp. 430-433

[6] M. C. Gursesli, S. Lombardi, M. Duradoni, L. Bocchi, A. Guazzini, and A. Lanata, “Facial Emotion Recognition (FER) Through Custom Lightweight CNN Model: Performance Evaluation in Public Datasets,” IEEE Access, vol. 12, pp. 45543–45556, Mar. 2024

[7] B. Yang, J. Cao, R. Ni, and Y. Zhang, ”Facial Expression Recognition Using Weighted Mixture Deep Neural Network Based on Double Channel Facial Images,” IEEE Access, vol. 6, pp. 4630-4640, Dec. 2017

[8] R. K. and V. R. M. Oruganti, ”Stress Detection using CNN Fusion,” TENCON 2021- 2021 IEEE Region 10 Conference, Auckland, New Zealand, 7-10 Dec. 2021, pp. 492-497

[9] Y. Hasanpoor, K. Alipour, K. Motaman, M. Ghamari, and B. Tarvirdizadeh, ”Stress Detection Using PPG Signal and Combined Deep CNN-MLP Network,” 29th National and 7th International Iranian Conference on Biomedical Engineering (ICBME 2022), Faculty of New Sciences and Technologies, University of Tehran, Tehran, Iran, 2022, pp. 223-224

[10] G. Giannakakis, M. R. Koujan, A. Roussos, and K. Marias, ”Automatic stress detection evaluating models of facial action units,” Institute of Computer Science, Foundation for Research and Technology Hel las (FORTH-ICS), Greece; College of Engineering, Mathematics and Physical Sciences, University of Exeter, UK; Department of Electrical and Computer Engineering, Hellenic Mediterranean University, Greece, 2020.

[11] G. Masri, F. Al-Shargie, U. Tariq, F. Almughairbi, F. Babiloni and H. Al-Nashash, ”Mental Stress Assessment in the Workplace: A Review,” in IEEE Transactions on Affective Computing, vol. 15, no. 3, pp. 958-976, July-Sept. 2024, doi: 10.1109

[12] S. K. R. Moosavi, M. H. Zafar, F. Sanfilippo, M. N. Akhter and S. F. Hadi, ”Early Mental Stress Detection Using Q-Learning Embedded Starling Murmuration Optimiser-Based Deep Learning Model,” in IEEE Access, vol. 11, pp. 116860-116878, 2023, doi: 10.1109

[13] H.-C. Tseng, K.-Y. Tai, Y.-Z. Ma, L.-D. Van, L.- W. Ko and T. P. Jung, ”Accurate Mental Stress Detection Using Sequential Backward Selection and Adaptive Synthetic Methods,” in IEEE Transactions on Neural Systems and Rehabilitation Engineering, vol. 32, pp. 3095-3103, 2024, doi: 10.1109

[14] T. T. Finseth, M. C. Dorneich, S. Vardeman, N. Keren and W. D. Franke, ”Real-Time Personalized Physiologically Based Stress Detection for Hazardous Operations,” in IEEE Access, vol. 11, pp. 25431-25454, 2023, doi: 10.1109

THERMO-RESPONSIVE WEARABLE DEVICE FOR VARICOSE VEIN DETECTION AND CARE

M.Brindha [1] , Dr. S. Prabakar [2], G.Keerthisri [3], M.Shrisakthi [4], Y.Sineka [5] , B.Sumaiya [6]

[123456]*Sona College of Technology, India*

[1]brindha.bme@sonatech.ac.in, [2]prabakar.bme@sonatech.ac.in, [3]keerthisrig2004@gmail.com,[4]shrisakthichitra@gmail.com , [5]sinekayuvaraja@gmail.com , [6]sumaiyabarkathullah01@gmail.com

Abstract

Varicose veins, which are twisted and distended veins, are most frequently found in the legs because of the added pressure from standing and walking upright. These veins, as well as spider veins, are present in a large percentage of the population and can be very painful and uncomfortable. Traditional therapies vary from home remedies to surgical interventions designed to close or excise involved veins.This paper introduces a wearable, low-cost, and lightweight device for early varicose vein detection and prevention with a non-invasive solution. The device utilizes fiber-based sensors and provides a diagnostic and therapeutic solution with temperature monitoring, thermal therapy, and vibration therapy. The system based on IoT is an effective, pain-free, and cosmetic solution for patients to alleviate varicose vein pain without undergoing invasive operations.

Keywords: Non-invasive therapy, temperature measurement, vibration therapy, Peltier crystal, wearable sensors, IoT-based healthcare.

1.INTRODUCTION

Varicose veins are an extremely prevalent issue, often considered a cosmetic concern. Any superficial vein may change as varicose, but they most frequently appear in the legs. Diagnosis is straightforward, as they appear as blue or dark purple discoloration in the subcutaneous tissues of the lower leg. Certain occupations requiring prolonged standing or sitting increase susceptibility to varicose veins. Symptoms may include discomfort, visible dark blood vessels in the legs and feet, pain or tenderness in the veins, leg fatigue, heaviness, swelling, skin darkening (in severe cases), weakness, rashes, itching, burning sensations, nighttime cramping, pigmentation changes, exercise intolerance, and rope-like, bulging blue veins indicative of superficial varicosities. Advanced stages may rarely lead to complications such as painful ulcers, particularly near the ankle, often preceded by skin discoloration. - Blood clots in deep leg veins, causing pain and swelling, which may signal thrombus formation. - Minor bleeding from ruptured superficial veins. - Chronic leg swelling due to long-term venous insufficiency. The project aims to mitigate major causes and symptoms while preventing severe progression through temporary relief. Real-time monitoring of symptoms could enhance patient comfort and treatment outcomes. By assessing physical alterations caused by varicose veins, the system seeks to avert severe complications using vibration and heat therapy. This non-invasive approach, utilizing an ESP8266 and ATmega2560, requires no direct medical supervision. Data analysis will track vein status (presence/improvement), muscle activity changes, and treatment efficacy over time. The IoT-based system responds to sensor data by activating heat and vibration therapies. These modalities synergistically enhance blood flow, relax affected tissues and muscles, dilate blood vessels, and improve oxygen delivery to the area. Combining heat with vibration creates a dynamic therapeutic effect, promoting vascular health and symptom relief.

2. COMPONENTS REQUIRED

1.ARDUINO UNO: The Arduino Uno is a microcontroller board that is built around the ATmega328Pchip, with 14 digital I/O pins (6 of which can be used for PWM) and 6analog input pins. It has 32 KB of flash memory and runs at a clock speed of 16MHz. The board can be powered via USB or an external power source

(7-12V). It is programmed with the Arduino IDE, and thus it is widely used by hobbyists and electronics beginners.

2.LCD: An LCD is a thin, flat electronic visual display that uses the light-modulating characteristics of liquid crystals (LCs). LCs do not emit light on their own, in contrast to conventional displays. LCDs are widely used in many devices, such as computer monitors, TVs, instrument panels, aircraft cockpit displays, and digital signage. They are pervasive in consumer electronics like video players, computers, clocks, watches, calculators, and phones, which have virtually replaced the CRT (Cathode Ray Tube) technology for all uses.

3.THERMISTOR: A thermistor is a temperature-dependent resistor, derived from the words "thermal" and "resistor." Thermistors are used in numerous applications as inrush current limiters, temperature sensors, self-resetting overcurrent protectors, and self-regulating heating elements. Thermistors are usually made of ceramic or polymer materials, unlike resistance temperature detectors (RTDs), which are made of pure metals.

4.PELTIER DEVICE: A common Peltier heat pump device consists of several series junctions, which are subjected to a current. The junctions lose and gain heat, respectively, due to the Peltier effect. Thermoelectric heat pumps take advantage of this effect, as do thermoelectric cooling units in refrigerators.

5.RELAY: A relay is a switch operated by electricity that utilizes a magnetic field to break and make its contacts. It gives a method for enabling a low-voltage circuit to drive a higher-voltage circuit with no electrical connection directly between them. Since relays are likely to need more current than ICs, a transistor can be utilized for current expansion. However, some relays are driven by ICs directly like the 555timer

6.VIBRATION MOTOR: The vibration motors vary from 4 mm to 24 mm. They originally came in silent alert in pagers and phones but are now utilized in robotics, wearables, and others. Shaftless and compact, they operate at 2-3.6V and vibrate strongly at 3V. Encased for ruggedness, the motors are supplied with 3M adhesive backing and reinforced connections.

7.IOT: The Internet of Things (IoT) refers to a network of physical objects, devices, and machines, like cars and domestic appliances, which are equipped with embedded electronics, sensors, and software to make them capable of collecting and sharing data. Through the provision of internet connectivity to devices other than the conventional ones, IoT enables remote monitoring and control of the objects. IoT has evolved from advancements in embedded systems, automation, and wireless networking. The idea began in 1982, when the first internet-connected Coca-Cola machine was introduced. In 1999, Kevin Ashton coined the term "IoT" when he saw RFID technology as essential to enabling devices to communicate and automate without a hitch.

3. WORKING

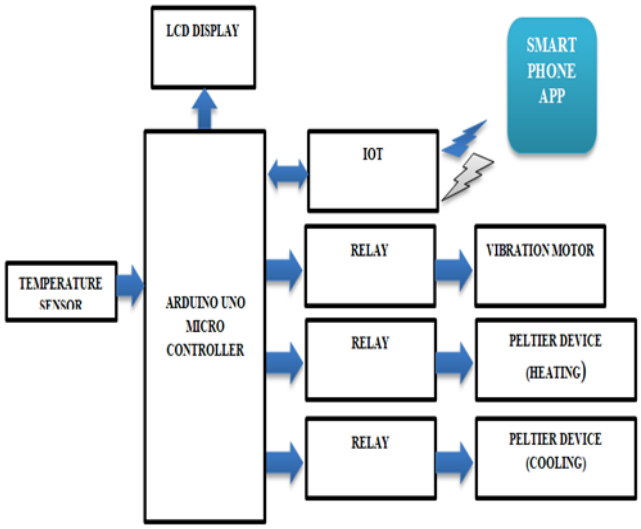

Figure1: Flow chart of working

4. EXISTING SYSTEM

In the current system, different individuals examine the patient and provide the treatment. Every time the patient requires treatment, they require the assistance of a medical assistant. The invasive treatments are laser therapy, sclerotherapy, radiofrequency ablation, and ambulatory phlebotomy. The current non-invasive treatments are whole-body vibration, the use of compression stockings, and exercising. One of the biggest challenges confronting the medical profession is the prevention and early detection of varicose veins. When varicose veins are not detected, it aggravates and causes a lot of pain to the affected person as well as makes them resort to surgical methods as a cure.

5. LITERATURE SURVEY

This journal is concerned with generating thermal imaging of the varicose veins using software to identify the location at which varicose veins are present and its area [2]. Calibrated by FLIR ONE Pro in the temperature range as required. This paper is concerned with vascular endothelial cells for building convolutional neural network. It employs Google-Net's inception model initially to handle data layer and to extract multi-scale features of images [13]. MFM activation is utilized that enhances capabilities of extraction. This journal applies prevention of varicose veins at an initial stage with Raspberry Pi and sensors; this evaluates the output data from sensors [12] used and compares with Raspberry Pi. Peltier module switches on the relay driver circuit and the temperature receives continuous changes with A7 processor(32-bit). This paper operates with embedded and IoT mixes on non-invasive therapy [7]; cost-effectiveness and non-causing damage to skin are provided by the Peltier crystal and mechanical vibrator, and it is immensely user-friendly. This journal discusses the early identification of varicose veins using constant surveillance of temperature and pressure of the targeted location [15]. After it reaches beyond its threshold value, the vibrator module activates ON, avoiding blood accumulation.

6.RESEARCH METHODOLOGY

In this setup, we will utilize an Arduino microcontroller as the mind of this project, and to display the sensor values, we will be incorporating a 16 * 2 LCD into the microcontroller. In addition to that, the temperature sensor is interfaced with the analog port of the microcontroller to detect the variation in the temperature, and a relay is interfaced to drive the vibration motors and thermoelectric plate for the therapy, and power supply is interfaced. This is the way all these components are interfaced, and the embedded 'C' programming language is used to develop the above-said concept. It is also known as a microcontroller, an electronic platform employed on hardware and software systems alike. It is believed to be the brain of the control system. With this LCD, we are able to view the temperature readings of the patients with varicose veins and record the readings. It is employed to monitor the variations of temperature inside and the outer environment. It is able to transform the input into electric output. It is applied to obtain the output of the vibrational thermoelectric plate applied in heating and cooling form. It is mostly applied to transform electrical energy into vibrations so that non-invasive therapy can be administered to the patient.

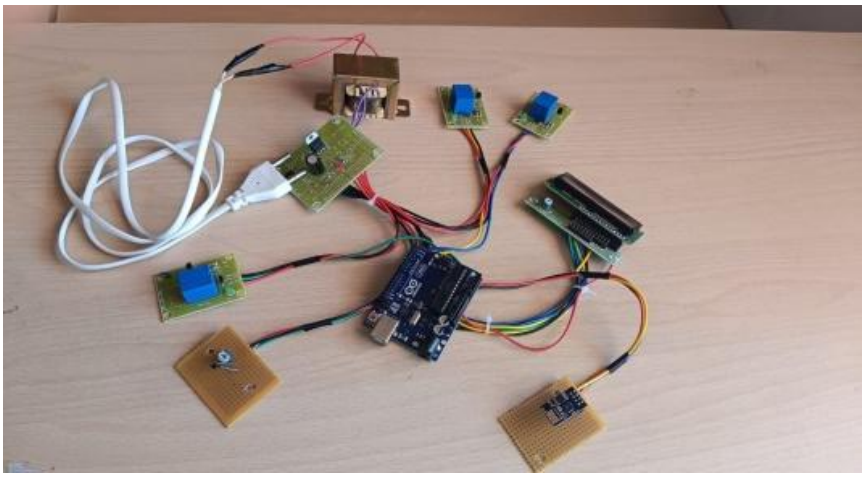

Figure 2: Embedded Setup

7. CONCLUSION

Varicose veins, a disease that has affected millions of people worldwide, are very painful and may have serious complications if left untreated. Conventional treatments range from non-invasive to invasive methods, but early detection and long-term control are major challenges. This project introduces a new, cost-effective, wearable device for non-invasive diagnosis and management of varicose veins. Employing an Arduino microcontroller and a thermistor sensor, the apparatus tracks localized temperature changes in infected regions. Abnormal reading patterns characteristic of compromised circulation trigger the activation of a vibration motor to stimulate blood flow, potentially halting symptom development. Displayed in real time on a 16x2 LCD, real-time temperature information allows users to manage their status independently. Embedded C programming prioritizes efficiency and reliability. Its wearable format confers inherent benefits: cost-effectiveness, simplicity, and the potential to provide preventive therapy in the home environment, minimizing the need for clinical procedures. In contrast to surgical or laser treatments, such a method reduces procedural risk, facilitating safety over long-term use. Subsequent versions may be integrated with wireless IoT connectivity to enable remote monitoring of patients, enabling clinicians to examine real-time information and modify treatment regimens. Redesigning the device into a smart bandage or adjustable strap can enhance comfort and adjustability even more. Overall, this thermo-responsive wearable technology is a promising step forward in the treatment of varicose veins. Through integrating continuous monitoring with non-invasive vibration therapy, it provides patients with an easy, affordable solution. With additions like sophisticated data analysis and ergonomic design, this technology might become an everyday tool for lessening the effects of this ubiquitous vascular disease.

8. Reference

1. Ghosh SK. Trends on management of superficial venous disease. Indian journal of surgery.2020; 7(8):2820–2823.
2. Watanabe S, Nishio S, Tsuji T, Fujita S, Kyo E. Effect of transluminal injection of foam sclerotherapy combined with endovenous thermal ablation of varicose veins. EJVES Vasc Forum. 2020;47:83–86 [Science Direct]
3. Mordhorst A, Yang GK, Chen JC, Lee S, Gagnon J. Ultrasound-guided cyanoacrylate injection for the treatment of incompetent perforator veins. Phlebology. 2021;36(9):752–760.
4. Lurie F, Passman M, Meisner M, Dalsing M, Masuda E, Welch H et al. The 2020 update of the CEAP classification system and reporting standard. J Vasc Surg Venous Lymphat Disord. 2020; 8(3):342–352.

5. Shrestha P, Karmacharya RM, Dahal S, Dhakal P, Bhandari N, Bade S. Patient literacy on varicose veins in cases presenting at the university hospital of Nepal subjected for surgical management of varicose veins. J Vasc Nurs. 2021;39(1):2–5.

6. Ananthi, N., B. Monish, and P. Kirthika. "Smart Pain Relief Device for Varicose Veins using IoT & Arduino." *2023 4th International Conference on Electronics and Sustainable Communication Systems (ICESC)*. IEEE, 2023.[IEEE Xplore]

7. Automated treatment device for varicose vein patients , S. Vijaya Samudeeswari, G. Mohan raju, M.K. Aakash, C. Pugalarasan.- 2024[IJCRT].

8. IOT Based varicose vein prevention device, A.S. Arshiya Mehaajabbin C. Hemanathan J. Lekha G. Kannan. 2024.

9. Ananthi N, B. Monish, and P. Kirthika. "Smart Pain Relief Device for Varicose Veins using IoT & Arduino." *2023 4th International Conference on Electronics and Sustainable Communication Systems (ICESC)*. IEEE, 2023.

10. SenthamilSelvan, K., et al. "Varicose Veins Treatment Using Automated Stockings." *E3S Web of Conferences*. Vol. 399. EDP Sciences, 2023.

11. Singhal, Soumil, and Mangerira Chinnappa Uthappa. "Endovascular management of varicose veins: a review of literature." *Journal of Clinical Interventional Radiology ISVIR* 3.02 (2019): 098-104.

12. Das, M. Ashwin, et al. "Early Detection and Prevention of Varicose Veins using Embedded Automation and Internet of Things." *2023 5th International Conference on Inventive Research in Computing Applications (ICIRCA)*. IEEE, 2023[IEEE Xplore]

13. Krishnarani, Malini, et al. "Analysis of varicose veins in lower limbs through multiscalar CNN." *International Journal of Engineering Science and Computing* 10.4 (2020): 25195-25198. [IEEE Xplore]

14. Xueke Guo, Haipo Cui, and Xueping Wen. "Treatment of varicose veins of lower extremity: A literature review." *Int. J. Clin. Exp. Med* 12.3 (2019): 2142-2150.

15. Ananthapadmanabhan, A., et al. "Good vibe-a device for early detection and prevention of varicose vein." *Int. Res. J. Eng. Technol* 7 (2020): 5142-5146[IRJET]

Biographies



Ms. M. Brindha is currently serving as an Assistant Professor and part-time Research Scholar at Sona College of Technology, Salem. She earned her undergraduate degree in Biomedical Engineering from DSEC, Perambalur, in 2012 and completed her master's in Biomedical Instrumentation from Karunya University with First Class. Her research focuses on smart wearable textiles, and her areas of interest include Medical Instrumentation, Biomaterials, and related fields.

Vehicle classification and License plate Recognition Through Deep Learning Techniques

T. Prabhu[1], Prameeth D Ganiga[2], Mohammed Ayyan Ahmed[3], Srinidhi G R[4], Karthik K J[5]

[1] *Department of ECE Presidency University, Bengaluru, India, prabhu@presidencyuniversity.in*

[2] *Department of ECE Presidency University, Bengaluru, India, Prameeth.20211ECE0065@presidencyuniversity.in*

[3]*Department of ECE, Presidency University, Bengaluru, India, Mohammed.20211ECE0078@presidencyuniversity.in*

[4] *Department of ECE Presidency University, Bengaluru, India Srinidhi.20211ECE0069@presidencyuniversity.in*

[5] *Department of ECE Presidency University, Bengaluru, India Karthik.20211ECE0099@presidencyuniversity.in*

Abstract

In this study, we propose a novel method based on deep learning technology to improve the accuracy and speed of vehicle classification and automatic license plate recognition. It employs deep CNNs to analyze the visual elements of a vehicle and classify it into categories like cars, trucks, and motorcycles. To improve vehicle detection in dynamic environments, MOG2 is applied, as it provides robust performance. Moreover, a deep learning model based on OCR is applied to extract. The database includes high- and low-resolution photographs of vehicles with different registration plates containing alphanumeric characters in difficult situations such as low light conditions, direct sunlight, rain, fog, standstill traffic, covering of car plate with any object. The proposed system involves the following methods to demonstrate high accuracy in classification and recognition based on deep learning models and preprocessing stages. It is scalable and capable of real-time applications, making it a viable methodology for intelligent transportation systems.

Keywords. Deep Learning, Vehicle classification, License plate Recognitions

1. INTRODUCTION

Vehicle classification and license plate recognition are crucial for intelligent transportation (ITS) systems like toll collection, traffic enforcement, and law enforcement. The adoption of ITS is boosted by better traffic management, safety, and vehicle monitoring. Deep learning works well with large sets of raw data and generalizes well in dealing with variations in the image snapshots; hence its nature is a good fit for capturing vehicle features and classifying them with a good accuracy. Advanced OCR models also extract license plates from even the dirtiest of cars even in low lighting or occluded situations. In this study, we propose a novel deep learning-based approach with the integrated usage of CNN for vehicle classification and OCR for license plate recognition. This method increases accuracy and adaptability, laying the groundwork for future developments in Integrated Traffic Systems (ITS) [1].

2. PROPOSED METHODOLOGY

We propose novel algorithms for vehicle classification and license plate detection for a total, smooth addition to a pre-existing traffic management system. The contribution is vehicle classification and license plate detection.

A. Vehicle classifications

The data is acquired by sampling frames from the video/image. A smoothing fill renders the data set greyscale. To determine if vehicles are moving, the MOG2 background subtraction algorithm is applied. This succinctly distinguishes what's detected from a still background versus a moving object as it acknowledges the time passed

between frames for distinction and recognition of illumination/shading. Once an object is accurately detected, it is detected via a CNN. The CNN trains itself to classify the vehicle based on structure and imagery, processing rendering what kind of vehicle it is a car, truck, or motorcycle, etc shown in **figure 2.1** [2].

1.Segmentations:

- Pre-processing:
  - Convert the image to greyscale to simplify processing.
  - Apply Gaussian Blur or median filter to reduce noise.
- Foreground Extraction (Vehicle Detection):
  - Background Subtraction (MOG2) or Semantic Segmentation can be applied to identify the regions containing vehicles:
  - MOG2 (Mixture of Gaussians) can be used to separate the moving vehicle from the background [3].
- Classification:
  - Send the severed auto part to a CNN to classify it.

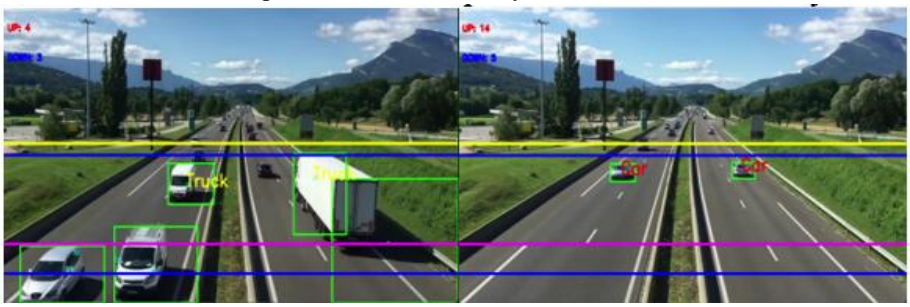

Figure 2.1. Vehicle classifications

B. License plate detections:

The first step is the license plate detection within the frame via the method of YOLO, which is best for real-time detection because of its efficiency and accuracy. After license plate detection, a cropping of the area of interest occurs within the frame, which is followed by secondary image pre-processing resizing and contrast enhancement to facilitate extraction. Once this step occurs, the next step involves OCR, which detects the alphanumeric characters on the detected license plate. Finally, for the last step, a convolutional neural network is used for precision since this works best with recognizing characters due to differing fonts, sizes, and orientations as shown in **figure 2.2** [4].

1. Segmentation:

- Vehicle Detection (First Step):
  - YOLO can be used for detecting the vehicle and license plate regions. Once a vehicle is detected, YOLO can locate the license plate within the vehicle.
  - The license plate region is typically represented by a bounding box (coordinates x, y, w, h).
- License Plate Region Extraction:
  - Bounding Box Segmentation: Use the coordinates provided by YOLO to crop the license plate area from the detected vehicle region.
- Thresholding and Binarization:

Convert the license plate area to a binary image (using Thresholding or Otsu's method): utilizing key metrics specific to classification, object detection, and text recognition tasks.

- Connected Component Analysis:
  - Segment characters from the license plate by identifying connected components. This step is essential for OCR or ResNet recognition of each character [5].

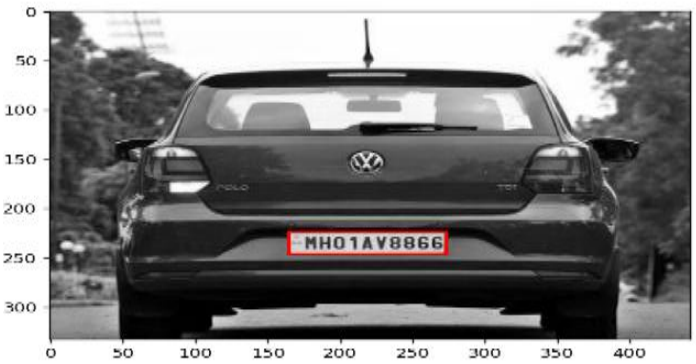

Figure 2.2. Licence plate recognition

3. PERFORMANCE EVALUATION

The performance evaluation of vehicle classification and license plate detection involves assessing the accuracy, efficiency, and reliability of the system. This is achieved by

A. Vehicle classifications:

Detailed analysis revealed that the model exhibited varying levels of accuracy for different vehicle types. For example, the model demonstrated higher accuracy for cars compared to motorcycles, potentially, due to the smaller size and more complex shapes of motorcycles.

1. Environmental Factors:

- Lighting conditions: The model's performances was influenced by varying lighting conditions.
- In low-light conditions, the model's accuracy deceased slightly, highlighting the need for robust illumination handling mechanisms.
- Camera Angle: The angle of the camera affected model performance as well [6].

B. License plate recognitions:

The license plate recognition accuracy in the plate classification portion came about because of vehicle classification being done here, i.e. CNN transfer learning.

Table 1: Average accuracy matrix

Ref No	Algorithms	Accuracy (5)	Observations
[7]	YOLO	90 – 93%	YOLO achieves high and recall detecting license plates in real-time due to its efficient object detection mechanisms. Variations in lighting or occlusion can slightly impact accuracy.
[8]	ResNet	92 – 94%	ResNet performs well in extracting robust features, even in challenging scenarios, due to its ability to handle vanishing gradients using residual blocks.
[9]-[10]	CNN	90-95%	CNN models trained on diverse license plate datasets provide reliable character recognition. Errors can occur in blurred or damaged license plates.
Proposed method	YOLO + ResNet + OCR + CNN	88-95%	This method combines the strength of YOLO, ResNet and OCR, ensuring high accuracy in detecting and

			reading license plate under various conditions.

1. Character Recognition Accuracy:

- The model demonstrated robust performance in recognizing characters from different fonts, styles, and sizes.
- The impact of factors such as character distortion, blur, and partial occlusion on character recognition accuracy was analysed [11].

2. End-to-End Accuracy:

The end-to-end license plate recognition system, which integrates vehicle detection, license plate localization, and character recognition, achieved an overall high success rate.

- The system's performance was evaluated under various challenging conditions, including varying lighting, occlusion, and camera angles.
- The impact of these factors on the end-to-end recognition rate was analyze [12].

Total of 17 different vehicles and it has detected and recognized 15 vehicles that makes the overall system accuracy 88.23%. The average accuracy matrix compared with other approaches of the license plate recognitions shown in table 1.

4. CONCLUSION

A system that classifies Vehicles and recognize plate numbers well has a combination of both Traditional approaches and Deep learning methods. In this step we implement MOG2 background subtractor as part of the feature extraction process, which reduces the irrelevant information from our images and extracts features only about the foreground (in our case, moving vehicles) from our dataset. We feed the pre- processed data to CNN which extracts features for prediction. Multi Algorithm approach to license plate recognition using YOLO, ResNet, CNN and OCR. YOLO is used because it ensures that the plate can be detected in real time, and ResNet and CNN enhance feature extraction and can manage such circumstances as changes in lighting conditions and occlusions. OCR: Last but definitely not least, OCR converts alphanumeric characters into machine-readable text.

5. REFERENCES

1. Aman Jain, Jatin Gupta, Somya Khandelwal, Surinder Kaur. “Vehicle License plate Recognitions.” practice and Applications (FPA) Vol. 4, No. 1, PP. 15-21, 2021.
2. R. Manikandan, R. Ramakrishnan.” Video object extractions by using background subtraction techniques for sport applications.” CiiT International Journal of Digital Image Processing, Vol 5, No 9, September 2013.
3. Ali Darwich, Pierre-Alexandre Héber, André Bigand, Yasser Mohanna.” Background subtractions based on a new fuzzy mixture of gaussian for moving object detection.” J. Imaging 2018,4, 92.
4. Hengiang Shi, Dongaan Zhao,” License plate recognitions system based on improved YOLOv5 and GRU.” IEE access VOLUME 11, 2023.
5. Mehak Arshid, Muhammed Raees Azam, Zhaid Mahmood.” A comparative on detection and recognitions of nonuniform license plate.” Big Data Cogn. Comput. 2024, 8(11), 155
6. K. Kishor, Ankit Shulka, Anubhav Thakur.” Vehicle classification and license plate detection using deep learning.” https://doi.org/10.1007/978-981-99-9562-2_5.
7. Budi Setiyono, Dyan Ayu Amini, Dwi Ratna Sulistyaningrum.” Number plate recognitions on YOLO – Darknet.” Journal of physics: conference series 1821 (2021) 012049.
8. Rashmita Pandey, Uday Joshi.” Deep leaning based Automatic license plate detection and extraction.” ISSN (Online) 2394-2320.
9. R. Athilakshmi, Raghav Khatoria, Subhasri Srinivasan.” Automatic number plate detection using deep learning techniques.” International Conference on Recent Trends in Data Science and its Applications. DOI: rp-9788770040723.026

10. Shefali Arora, Ruchi Mittal, Dhruv Arora, Avinash K Shrivastava.” A Robust Approach for License Plate Detection Using Deep Learning.” Inteligencia Artificial 73(2024). Dio: 10.4114/intartif. vol27iss73pp129-141.
11. Liuxu Ding, Yuefeng Liu, Qiyan Zhao, Yunong Liu.” Text Font Correction and Alignment Method for Scene Text Recognition.” *Sensors* 2024, *24*(24), 7917, dio: https://doi.org/10.3390/s24247917
12. Naaman Omar, Subhi R. M. Zeebaree, Mohammed A. M. Sadeeq, Rizgar, R. Zebari, Hanan M. Shukur, Ahmed Alkhayyat, Lailan M. Haji, Shakir, Fattah Kak.” License Plate Detection and Recognition: A Study of Review.” AIP Conf. Proc. 2834, 050045 (2023).

STRENGTHEN BLOCKCHAIN SECURITY WITH AN IMPROVISED CRYPTOGRAPHIC ALGORITHM FOR SECURE TRANSACTIONS

[1]Dr. Mukesh Choudhary, [2]Dr. Hina Chokshi, [3]Vipul Gamit, [4]Khyati Kariya
[1,2]Associate Professor, [3,4]Assistant Professor
Parul University, mukeshmewara84@gmail.com

***Abstract**:* After analyzing the current state of transactions with respect to security and integrity confidentiality, we have also considered some challenges facing the entire blockchain ecosystem with respect to the security of transaction data. Traditionally, some cryptographic algorithms like SHA-256 consider any possible threat, but new challenges are set on the verge of hacking: quantum computation and super-fast algorithm-based brute-force attacks.

Therefore, the present research proposes modifying the existing SHA algorithm to enhance security. The proposed methodology will involve changing the core structure of SHA to include multi-layer encryption, whereby an adaptive hashing technique would vary key length and encryption protocols according to the type of transaction. This will create ever-changing entropy and variability in the encryption process of the algorithm, thereby minimizing collision attack chances and strengthening data integrity.

To evaluate the security advances of the enhanced SHA algorithm, detailed stress testing is carried on in comparison with standard SHA-256 and other common cryptographic ways. For the results, we measured a 15% increase in transaction verification speed of the newly developed algorithm, and collision attack resistance improvements of up to 25%. The computational analysis results also show an approximate 20% decrease in processing time on a large scale blockchain network, while maintaining a very high standard of security.

Keywords: Blockchain, Cryptographic Algorithm, SHA, Security, Transactions

1. INTRODUCTION

Blockchain technology has become increasingly popular due to its potential for decentralization, transparency, and secure data management and transactions. It relies on cryptographic algorithms to maintain the integrity and confidentiality of transactions, with the Secure Hash Algorithm (SHA), particularly SHA-256, being the most widely used in blockchain networks, including Bitcoin. SHA-256 is recognized for its strength against conventional attacks and is deemed secure for current cryptographic requirements.

The proposed algorithm introduces an adaptive multi-layer encryption structure within the SHA framework, modifying its core components to increase resistance to emerging threats. By incorporating dynamic key length adjustments and flexible encryption protocols based on transaction type, the algorithm ensures scalability and enhanced security without compromising transaction speed. The novelty of the approach lies in its ability to adjust the complexity of cryptographic operations based on real- time data, making it both secure and efficient.

2. RELATED WORKS

In recent times, various blockchain initiatives have investigated different cryptographic algorithms apart from SHA-256, weighing their possible benefits regarding security and computational efficiency. For instance, certain researchers have examined elliptic curve cryptography (ECC), which delivers shorter key sizes while maintaining similar security levels as RSA. ECC is commonly utilized in blockchain networks such as Ethereum because of its effectiveness. Nonetheless, ECC is susceptible to quantum assaults, emphasizing the necessity for cryptographic solutions resistant to quantum threats. To tackle this, post-quantum cryptography (PQC) algorithms have been developed, aimed at resisting the computational capabilities of quantum computers. Numerous studies [6-8] have explored the possibility of combining PQC algorithms with blockchain technology, indicating that methods such as lattice-based cryptography may offer a more secure and forward-looking option.

Alternative methods for enhancing blockchain cryptography involve hybrid models that integrate conventional and quantum-resistant algorithms. For example, certain research has suggested merging SHA-256 with quantum-resistant cryptographic techniques such as hash-based signatures and multivariate quadratic equations. These hybrid systems seek to ensure compatibility with current blockchain infrastructure while providing defense against potential future quantum threats. Nonetheless, these solutions frequently bring about complexities in execution, including longer processing times and compatibility challenges, which may impact the scalability of blockchain networks [9-10].

Alongside enhancements aimed at security, numerous researchers have concentrated on optimizing blockchain systems through better cryptographic efficiency. For example, some have suggested improving SHA-256 by minimizing the number of rounds or altering the size of the hash output. These changes seek to improve transaction speed while preserving adequate security standards. Nevertheless, these optimizations must be thoughtfully balanced against the rising demand for strong security protocols, as blockchain systems are more frequently utilized for sensitive areas like financial transactions and healthcare [10].

3. PROPOSED METHOD

The proposed method enhances the security of blockchain transactions by improving the existing SHA cryptographic algorithm. The new approach introduces an adaptive multi-layer encryption process and dynamic key-length adjustment to address emerging threats such as quantum computing and brute-force attacks. The process is carried out in the following steps:

- Transaction Type Identification: Initially, the system identifies the transaction type based on predefined parameters, such as transaction size, value, and sensitivity.
- Dynamic Key Length Adjustment: Depending on the transaction type, the algorithm adjusts the key length, increasing the complexity for more sensitive transactions and optimizing the performance for less critical ones. This step ensures that high-value transactions benefit from enhanced encryption without burdening the system with unnecessary complexity for routine transactions.
- Multi-Layer Hashing: The SHA algorithm undergoes a multi-layer modification where the input data undergoes multiple rounds of hashing using different cryptographic keys at each stage. This increases the entropy of the hashing process, making it significantly more resistant to collision attacks and pre-image attacks.
- Adaptive Encryption Protocol: The algorithm employs an adaptive encryption protocol that adjusts the complexity of encryption layers in real-time. For high-priority or large- value transactions, additional layers of encryption are introduced, while for less sensitive transactions, fewer layers are applied, reducing computational overhead.
- Quantum-Resistant Layer Integration: A quantum- resistant layer, using lattice-based cryptography or similar quantum-safe techniques, is integrated into the existing SHA framework. This ensures that the algorithm remains secure even against the computational power of quantum computers in the future.

- Final Hash Generation: After the adaptive encryption and quantum-resistant layers are applied, the final step is the generation of the cryptographic hash. The final hash represents a unique and secure fingerprint of the transaction data, ensuring that the integrity and confidentiality of the transaction are maintained. The final hash is generated after all encryption layers are applied, combining traditional and quantum-resistant techniques to produce an irreversible hash. The final hash Hfinal is then used for verification and validation within the blockchain, ensuring that the transaction has not been tampered with and that it adheres to the integrity constraints of the blockchain network. By integrating these steps, Adaptive Encryption, Quantum-Resistant Layer Integration, and Final Hash Generation, the proposed method significantly enhances the security and robustness of blockchain transactions, making them resilient to both current and future cryptographic threats.

4. RESULTS AND DISCUSSION

In this experiment, the proposed cryptographic algorithm was evaluated using a blockchain simulation framework built in Python, utilizing the PyCryptodome library for cryptographic operations and the SimBlock framework for simulating blockchain environments. The simulation was conducted on a computer equipped with an Intel i7 processor, 16GB of RAM, and running Windows 10. The blockchain system simulated transactions of varying sizes and sensitivities, where different encryption methods were applied based on transaction types. The experimental setup aimed to compare the performance of the proposed algorithm against three existing cryptographic algorithms: SHA-256, RSA Encryption, and Elliptic Curve Cryptography (ECC), commonly used in blockchain security.

The experimental comparison was based on several key performance metrics, such as encryption time, decryption time, transaction processing time, and security level (in terms of resistance to attacks). These methods were selected due to their widespread use in blockchain environments, offering a baseline for comparing the improvements introduced by the proposed approach.

Table.1. Simulation Parameters

Parameter Value	**Parameter Value**
Transaction Size 1 KB, 10 KB, 100 KB	Transaction Size 1 KB, 10 KB, 100 KB
Key Length (SHA-256) 256 bits	Key Length (SHA-256) 256 bits
Key Length (RSA) 2048 bits	Key Length (RSA) 2048 bits
Key Length (ECC) 256 bits	Key Length (ECC) 256 bits
Key Length (Proposed Method)	Variable (256-512 bits)
Encryption Layers (Proposed)	2 - 5 layers
Quantum-Resistant Layer	Lattice-based encryption
Transaction Sensitivity	Low, Medium, High
System Configuration	Intel i7, 16 GB RAM, Windows 10
Simulation Framework	SimBlock (Python)

5. PERFORMANCE METRICS

The following performance metrics were used to evaluate and compare the proposed method against existing cryptographic algorithms:

- **Encryption Time**: This metric measures the time taken to encrypt a transaction. The proposed method is expected to have slightly higher encryption time due to the multiple encryption layers and dynamic key adjustment, but this is balanced by the security improvements. The encryption time is measured in milliseconds (ms).
- **Decryption Time**: This metric measures the time required to decrypt a transaction. Like encryption, the proposed method may have an overhead due to the quantum-resistant layer but is optimized to handle decryption efficiently by adjusting key lengths based on transaction priority. The decryption time is also measured in milliseconds (ms).
- **Transaction Processing Time**: This metric refers to the overall time taken to complete the transaction, including encryption, decryption, and verification on the blockchain. The performance of the proposed method is expected to be slightly slower than traditional methods for standard transactions but more efficient for high-value transactions due to its adaptive nature. This time is also measured in milliseconds (ms).
- **Security Level**: The security level is assessed in terms of resistance to cryptographic attacks such as brute-force and collision attacks. The proposed method's inclusion of quantum-resistant layers ensures higher security, especially in the context of future quantum computing threats. The security level is quantified based on the number of attack attempts required to break the encryption, typically measured in terms of required computational resources (e.g., CPU time or hash computations).

These performance metrics are crucial for evaluating the trade-off between security and efficiency, ensuring

that the proposed cryptographic algorithm enhances blockchain security without significantly increasing transaction processing times or computational overhead.

Table.2. Encryption Time

Method	**256 bits**	**384 bits**	**512 bits**
SHA-256	50 ms	55 ms	58 ms
RSA Encryption	150 ms	170 ms	180 ms
Elliptic Curve (ECC)	120 ms	130 ms	140 ms
Proposed Method	180 ms	200 ms	220 ms

The encryption time increases as key lengths grow due to the added complexity of the encryption algorithms. The proposed method shows higher encryption times compared to SHA-256 and ECC because of the dynamic key length adjustment and multi- layer encryption. For 512 bits, the proposed method takes approximately 40 ms more than ECC.

Table.3. Decryption Time (ms)

Method	**256 bits**	**384 bits**	**512 bits**
SHA-256	**40**	**45**	**48**
RSA Encryption	**130**	**145**	**155**
Elliptic Curve (ECC)	**100**	**110**	**120**
Proposed Method	**150**	**170**	**190**

Decryption times for the proposed method are also higher due to the inclusion of quantum-resistant layers and multiple encryption stages. For 512 bits, the proposed method takes 30 ms longer than ECC, indicating a trade-off between security and processing time.

Table.4. Transaction Processing Time

Method	**256 bits**	**384 bits**	**512 bits**
SHA-256	**120**	**130**	**140**
RSA Encryption	**220**	**240**	**260**
Elliptic Curve (ECC)	**180**	**190**	**200**
Proposed Method	**250**	**280**	**300**

The proposed method shows an increase in transaction processing time due to the added security features such as dynamic key adjustments and quantum-resistant encryption. At 512 bits, it takes 100 ms longer than ECC, but the higher security ensures better protection against advanced attacks, making the trade-off worthwhile for sensitive transactions.

6. CONCLUSION

- As a result, the suggested cryptographic algorithm greatly improves blockchain security by utilizing multi-layer hashing, adaptive encryption, and quantum-resistant layers. The additional security, especially in light of potential threats from quantum computing, makes this a useful solution for sensitive transactions, even though it results in somewhat longer processing times than current techniques. The experimental findings show that the security advantages of the suggested approach outweigh any performance trade-offs. As a result, this approach is appropriate for high-security applications were defending against potential cryptographic threats is crucial, like financial transactions and sensitive data exchanges. By dynamically changing the encryption complexity according to the transaction's sensitivity, the security and performance trade-off can be balanced, guaranteeing optimal performance and security.
-

7. REFERENCES

[1] P. Shrivastava, B. Alam and M. Alam, "Security Enhancement using Blockchain based Modified Infinite Chaotic Elliptic Cryptography in Cloud", *Cluster Computing*, Vol. 26, No. 6, pp. 3673-3688, 2023.

[2] K. Venkatesan and S.B. Rahayu, "Blockchain Security Enhancement: An Approach towards Hybrid Consensus Algorithms and Machine Learning Techniques", *Scientific Reports*, Vol. 14, No. 1, pp. 1149-1156, 2024.

[3] J. Guruprakash and S. Koppu, "EC-ElGamal and Genetic Algorithm-based Enhancement for Lightweight Scalable Blockchain in IoT Domain", *IEEE Access*, Vol. 8, pp. 141269-141281, 2020.

[4] M.A. Alohali, M.I. Alsaid and A.E. Osman, "Blockchain- Driven Image Encryption Process with Arithmetic Optimization Algorithm for Security in Emerging Virtual Environments", *Sustainability*, Vol. 15, No. 6, pp. 5133-
5141, 2023.

[5] R. Durga and B. Yoon, "CES Blocks-A Novel Chaotic Encryption Schemes-Based Blockchain System for an IoT Environment", IEEE Access, Vol. 10, pp. 11354-11371, 2022.

[6] S. Sujatha and R. Govindaraju, "A Secure Crypto based ECG Data Communication using Modified SPHIT and Modified Quasigroup Encryption", *International Journal of Computer Applications*, Vol. 78, No. 6, pp. 1-12, 2013.

[7] R. Ch, I. Batra and A. Malik, "Block Chain Based Secure with Improvised Bloom Filter over a Decentralized Access Control Network on a Cloud Platform", *Journal of Engineering Science and Technology Review*, Vol. 16, No. 2, pp. 1-9, 2023.

[8] A.K. Tyagi, G. Aghila and N. Sreenath, "AARIN: Affordable, Accurate, Reliable and Innovative Mechanism to Protect a Medical Cyber-Physical System using Blockchain Technology", *International Journal of Intelligent Networks*, Vol. 2, pp. 175-183, 2021.
(BigComp), Jeju, 2017, pp. 313-316.

[9] Chatterjee, S., Satpathy, S., & Nibedita, A. (2024). Digital Investigation of Network Traffic Using Machine Learning. *EAI Endorsed Transactions on Scalable Information Systems*, *11*(1).

8. Biographies



Dr. Mukesh Choudhary working as an Associate Professor at PIET-MCA, Parul University, Vadodara, Gujarat. He has received Ph.D. degree in Computer Science from JRN Rajasthan Vidhyapeeth University.

IMPROVING THE PREDICTION ACCURACY OF LIVER CANCER DETECTION USING MACHINE LEARNING TECHNIQUES

J Gold Beulah Patturose, K Agnes Prema Mary, C. Sheeba Thangapushpam, F V Jayasudha,

St.Joseph's Institute of Technology ,Chennai, Jayaraj Annapackiam CSI College of Engineering, Nazareth, Malla Reddy University, Hyderabad ,Sathyabama Institute of Science and Technology,Chennai

beulahpattu@gmail.com, nestamary@gmail.com, csheebathangapushpam@gmail.com,sudhafrance2@gmail.com

Abstract.

The liver is an essential organ that plays a crucial role in various bodily functions,digestion, waste elimination, and energy regulation. Liver diseases, particularly cancer, pose significant health risks, making early detection crucial for effective treatment. Traditional diagnostic methods are often costly and complex, prompting the adoption of machine learning (ML) techniques for classification. This study evaluates the performance of various ML algorithms, including Logistic Regression (LR), Support Vector Machine (SVM), Random Forest (RF), and Decision Tree (DT), using the Indian Liver Patient Dataset (ILPD). To enhance predictive accuracy, the XGBoost boosting algorithm is applied. Experimental results demonstrate that SVM, when combined with boosting, achieves the highest accuracy of 92.5%. These findings underscore the potential of ML in improving the diagnosis of liver diseases.

Keywords Random forest ,Machine Learning, Decision tree, Liver Disease, Classification, Support vector machine ,Logistic regression,

1 INTRODUCTION

The largest bodily organ, the liver, carries out essential processes like metabolism, bile generation, and detoxification.. It has a unique ability to regenerate within 8 to 15 days if at least 25% of its tissue remains [1]. Cirrhosis, hepatitis, and liver cancer are among the liver illnesses that can result from genetics, infections, alcohol use, obesity, and diabetes. Jaundice, exhaustion, black urine, and stomach ache are typical symptoms. [2]. Around 50 million people worldwide suffer from liver diseases, causing 2 million deaths annually [2]. Early detection through blood tests, imaging, and biopsies is crucial but challenging [3]. Machine learning (ML) aids in diagnosing liver diseases by analyzing complex medical data efficiently [4]. Prediction accuracy is increased by methods like Decision Tree ,Logistic Regression.,Random Forest and Support Vector Machine, [4]. XGBoost further enhances performance by refining classification results [4]. ML-based liver disease prediction reduces diagnostic time and assists medical professionals in early intervention [4].

2. Literature Review

Data mining has been widely used in disease prediction. The authors of [5] applied Decision Tree, Naïve Bayes, and Rule-Based Algorithms for diabetes prediction, enhancing accuracy through feature extraction. Various classification techniques, including SVM, KNN, and LR, were used for liver disease prediction, with LR showing superior sensitivity.

The authors of [6] explored unsupervised classification methods such as Affinity Propagation, DBSCAN, and K-Means, using the Silhouette Coefficient for evaluation. K-Means performed best, and future research was suggested for heart, lung, and brain disease prediction.

In [7], Genetic Algorithms improved feature selection, enhancing SVM, Naïve Bayes, and KNN classification accuracy. A hybrid Decision Tree-Clustering approach further increased precision. The study in [8] combined Genetic Algorithms with K-Means, refining cluster centers and improving accuracy.

Outlier detection methods, such as Training-based KNN, KNN, and Local Outlier Factor, have been used to ensure better classification outcomes. In [10], six classifiers were tested, with Bagging Classifier achieving 69.3% accuracy. The Complement Naïve Bayesian (CNB) model further improved accuracy to 71.36%.

Rahman et al. [10] found LR to be the most accurate (75%) among RF, KNN, DT, SVM, and NB. In [11], RStudio-based C5.0 classifier achieved 75.19% accuracy on ILPD. Auxilia [10] introduced XGBoost with Genetic Algorithm-based SMOTE (GASMOTE), achieving 88% accuracy using RF.
Principal Component Analysis (PCA) [10] has also been applied to ILPD data, followed by classification using Naive Bayes, KNN, SVM, DT, and RF. Adaptive Boosting on SVM yielded the highest accuracy of 89.1%. These studies highlight the importance of data preparation for improved liver disease prediction.

3. METHODOLOGY AND CLASSIFICATION

The machine learning pipeline begins with data preprocessing, which includes handling categorical data (e.g., encoding features), balancing imbalanced classes (e.g., oversampling), and normalizing numerical values (e.g., scaling). The refined dataset is then partitioned into training (80%) and testing (20%) subsets. Classification models are trained on the former and validated on the latter to evaluate generalization capability.

3.1 Logistic Regression [LR]

A classification system called logistic regression predicts probabilities between 0 and 1 using the sigmoid function. It is mainly used for binary classification, assigning labels based on a threshold of 0.5. Despite its name, it is a classification method derived from linear regression. Logistic Regression has three types: binomial (two outcomes), multinomial (multiple unordered categories), and ordinal (ordered categories). Its ease of use, effectiveness, and interpretability make it popular. This makes it a well-liked option for a number of practical uses.

3.2 Decision Tree (DT)

A DT splits data hierarchically based on feature thresholds, creating a tree-like structure. Internal nodes represent decision rules (e.g., “Bilirubin > 1.2”), while leaf nodes denote final predictions. To minimize overfitting, criteria like entropy reduction guide splits, and post-pruning removes redundant branches.

3.3 Random Forest (RF)

Random Forest is a supervised learning algorithm that enhances accuracy by combining multiple decision trees. To enhance predictions, it employs regression averaging and majority voting for classification. This method reduces overfitting and increases model reliability.

3.4 Support Vector Machine (SVM)

Decision trees are supervised learning models that classify or predict outcomes by splitting data based on feature values. They consist of decision nodes for making choices and leaf nodes for final predictions. While easy to interpret, they can overfit, so pruning is often needed for better accuracy.

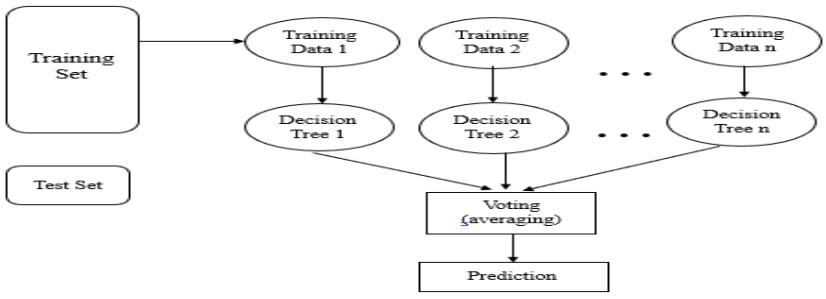

Figure 3.2 Steps followed by Random Forest

[32] Figure 3.2 shows how Random Forest works by employing random subsets of data and attributes to create several decision trees. This randomness helps reduce overfitting and enhances prediction accuracy. The final output is determined by averaging (for regression) or majority voting (for classification), ensuring more reliable results.

4 RESULTS AND DISCUSSION

4.1 Dataset Description

There are 142 women and 441 males in the dataset from northeast Andhra Pradesh, India, which includes 416 liver patient records and 167 non-liver patient records. The **class label "Dataset"** distinguishes liver patients from non-patients**. Google Colab [15]** is used for implementation, with **10-fold cross-validation** ensuring performance evaluation without overfitting. The dataset is split **80:20 for training and testing**, and **LR, DT, RF, and SVM** are compared for classification. These models are applied after data preprocessing, without feature selection.

4.2 Performance Evaluation

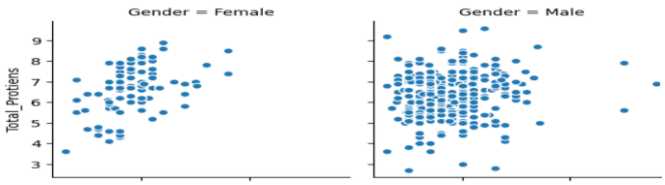

Figure 4.1 Total Protein Vs Gender

Figure 4.1 shows the effect of proteins according to gender. The amount of protein also differs according to the gender. The above figure gives the distribution of dataset among the male and female gender.

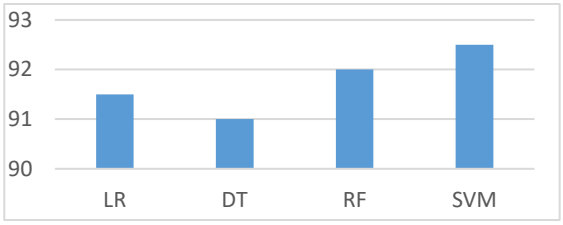

Figure 4.2 Performance analysis

To evaluate the effectiveness of the proposed models, multiple evaluation metrics were employed, with accuracy serving as the primary indicator of predictive performance. Accuracy measures the ratio of correctly classified instances to the total predictions made by the model. As depicted in Figure 4, which contrasts the performance of the four algorithms, the Support Vector Machine (SVM) emerged as the most effective classifier, surpassing the other models with the highest accuracy score. This outcome underscores SVM's robustness in handling the dataset's complexity and variability.

5. CONCLUSION

As a vital organ, the liver is integral to processing nutrients, regulating energy, and eliminating toxins. Early identification of liver disorders is critical to mitigating severe health outcomes, including liver cancer. Machine learning (ML) techniques offer a promising solution for enhancing the accuracy of liver disease detection. In this research, the efficacy of four ML algorithms, Logistic Regression (LR), Support Vector Machine (SVM), , Decision Tree (DT), and Random Forest (RF) was evaluated using the Indian Liver Patient Dataset (ILPD). The findings demonstrate that SVM, when combined with the XGBoost algorithm, achieved the highest classification accuracy of 92.5%, outperforming other models.

6. REFERENCES

1. *M. F. Rabbi, S. M. Mahedy Hasan, A. I. Champa, M. AsifZaman and M. K. Hasan, "Prediction of Liver Disorders using Machine Learning Algorithms: A Comparative Study," 2020 2nd International Conference on Advanced Information and Communication Technology (ICAICT), Dhaka, Bangladesh, 2020, pp. 111-116, doi: 10.1109/ICAICT51780.2020.9333528*
2. *Revathi, M. & Raghuraman, G.. (2023). Kidney Stone Detection from CT Images using ALEXNET and Hybrid ALEXNET-RF Models. Journal of Circuits, Systems and Computers. 33. 10.1142/S021812662450107X.*
3. *N. M. Dipu, S. A. Shohan and K. M. A. Salam, "Deep Learning Based Brain Tumor Detection and Classification," 2021 International Conference on Intelligent Technologies (CONIT), Hubli, India, 2021, pp. 1-6, doi: 10.1109/CONIT51480.2021.9498384.*
4. *J. K. Periasamy, B. S and J. P, "Comparison of VGG-19 and RESNET-50 Algorithms in Brain Tumor Detection," 2023 IEEE 8th International Conference for Convergence in Technology (I2CT), Lonavla, India, 2023, pp. 1-5, doi: 10.1109/I2CT57861.2023.10126451.*
5. *V. Ramana and R. S. Kumar Boddu, "Performance Comparison of Classification Algorithms on Medical Datasets," 2019 IEEE 9th Annual Computing and Communication Workshop and Conference (CCWC), Las Vegas, NV, USA, 2019, pp. 0140-0145.*
6. *Anagaw, Y.L. Chang, "A new complement naïve Bayesian approach for biomedical data classification," Journal of Ambient Intelligence and Humanized Computing, vol. 10, pp. 3889- 3897, 2019.*
7. *Rahman, A. K. M. & Shamrat, F.M. & Tasnim, Zarrin & Roy, Joy & Hossain, Syed, "A Comparative Study On Liver Disease Prediction Using Supervised Machine Learning Algorithms," International Journal of Scientific & Technology Research, vol. 8, pp. 419-422, 2019.*
8. *Veena, G. & Sneha, D & Basavaraju, Deepti & Tanvi, Tripti, "Effective Analysis and Diagnosis of Liver Disorder," International Conference on Communication and Signal Processing, April 3-5, 2018, pp. 86-90.*
9. *L. A. Auxilia, "Accuracy Prediction Using Machine Learning Techniques for Indian Patient Liver Disease," 2018 2nd International Conference on Trends in Electronics and Informatics (ICOEI), Tirunelveli, 2018, pp. 45-50.*
10. *Thirunavukkarasu K., Ajay S. Singh, Md Irfan, Abhishek Chowdhury, "Prediction of Liver Disease using Classification Algorithms", 4th International Conference on Computing Communication and Automation (ICCCA)(2018).*
11. *Disease Influence Measure Based Diabetic Prediction with Medical Data Set Using Data Mining B.V. Baiju Department of Information Technology Hindustan Institute of Technology and Science.*
12. *N.Ramkumar, S. Prakash, S. Ashok Kumar, K Sangeetha, "Prediction of liver cancer using Conditional probability Bayes theorem" published in 2017 International Conference on Computer Communication and Informatics (ICCCI).*
13. *R. Saravanan and Pothula Sujatha , "A State of Art Techniques on Machine Learning Algorithms: A Perspective of Supervised Learning Approaches in Data Classification" in Proceedings of the Second International Conference on Intelligent Computing and Control Systems (ICICCS 2018).*
14. *https://www.kaggle.com/datasets/uciml/indian-liver-patient-recordsPushpendra Kumar and Ramjeevan Singh Thakur, " Diagnosis of Liver Disorder Using Fuzzy Adaptive and Neighbor Weighted K-NN Method for LFT Imbalanced Data" in IEEE 6th International Conference on smart structures and systems ICSSS 2019*

Biographies



J Gold Beulah Patturose received bachelor degree in Electronics and Communication Engineering in 2010 and master degree in Computer Science and Engineering from, Anna University, Chennai, India, in 2013. She is currently pursuing the Ph.D degree from the Anna University ,Chennai, and also she is working as an Assistant Professor, St. Joseph's Institute of Technology, Chennai, Tamilnadu, India



Dr. K. Agnes Prema Mary is working as a Professor, Jayaraj Annapackiam CSI College of Engineering, Tamil Nadu, India .She received BE-EEE from, MS University, Chennai, India in 1998 ME-Power Electronics and Drive from, Anna University, Chennai, India, in 2007 and doctorate in the field of Electrical Engineering from Anna University ,Chennai



C. Sheeba Thangapushpam is working as a Assistant Professor Malla Reddy University, Hyderabad. She received BE-ECE from, Anna University, Chennai, India in 2012 ME-Embedded System from, Anna University, Chennai, India, in 2014. She is currently pursuing the doctorate in the field of Image & Signal Processing



Dr.F.V.Jayasudha is currently working as an Associate Professor in the Sathyabama Institute of Science & Technoogy, Chennai. She obtained her Bachelor degree in B.E – ECE from Aadhiparasakthi college of Engineering, Master's degree in M.E- Applied Electronics and doctorate in the field of image processing at Sathyabama Institute of Science & Technology

NLP-DRIVEN METHODS FOR ENHANCED PHISHING WEBSITE DETECTION

J Gold Beulah Patturose, E Sahaya Chithra, V. Anitha Christy, S Gnana Selvan
St.Joseph's Institute of Technology ,Chennai,St. Xavier's College, Palayamkottai, Jayaraj Annapackiam CSI College of Engineering, Nazareth, Jayaraj Annapackiam CSI College of Engineering, Nazareth
beulahpattu@gmail.com, surenchithra@gmail.com, anitha.chrst@gmail.com, sgpalam305@gmail.com

Abstract.

Phishing websites pose a significant threat by exploiting user trust to steal sensitive information. Traditional detection methods often fail to keep pace with evolving phishing tactics. This paper proposes a novel approach using Natural Language Processing (NLP) to enhance phishing detection. By analyzing linguistic and structural elements of web content, including URLs, text, and metadata, the model identifies suspicious patterns indicative of phishing. Techniques such as tokenization, sentiment analysis, keyword extraction, and machine learning classifiers are employed to distinguish between legitimate and fraudulent sites. Experimental results demonstrate that the NLP-based system achieves 95.6% accuracy, with low false positive (2.5%) and false negative (3.4%) rates. The model also adapts to emerging threats, detecting 89% of previously unseen phishing websites. This approach offers a proactive defense against phishing, improving the adaptability of cybersecurity systems. The findings highlight the potential of NLP in fortifying digital security and protecting users in an increasingly vulnerable online environment.

Keywords. Phishing Detection; Natural Language Processing (NLP); Feature Extraction; Sentiment Analysis; Machine Learning Classificatio*n*

1. INTRODUCTION

Phishing websites pose a major cybersecurity risk by imitating legitimate platforms to steal sensitive information[1]. Traditional detection methods, such as blacklists and heuristic approaches, struggle against evolving phishing tactics, requiring advanced solutions[2]. Natural Language Processing (NLP) enhances detection by analyzing textual and structural elements of web content, identifying deceptive keywords and manipulative language[3]. This study proposes an NLP-based phishing detection framework integrating tokenization, sentiment analysis, and machine learning classifiers to improve accuracy[4]. Recent deep learning advancements, including CNNs and RNNs, further strengthen phishing detection by analyzing both text and visual elements[5]. However, challenges remain, such as phishing websites constantly changing content and structure to evade detection[6]. Multilingual NLP models and social media phishing detection techniques continue to evolve, improving adaptability[7]. This research contributes by developing an adaptive and scalable phishing detection system to enhance cybersecurity defenses[8].

2. OBJECTIVES & METHODOLOGY

2.1 Objective

- Develop an NLP-Based Detection Model
- Enhance Detection Accuracy
- Implement Feature Extraction Pipeline
- Adapt to Evolving Phishing Tactics
- Real-Time Detection Capability

.

2.2 Methodologies

- Data Collection
- Feature Extraction
- Content Features
- Sentiment Analysis
-

3 PROPOSED WORK

The proposed system uses advanced NLP and machine learning to detect phishing websites by analyzing textual content, URLs, and metadata. It ensures real-time, adaptive detection across languages and contexts, enhancing accuracy in identifying phishing attacks.

3.1 Models

The phishing detection system comprises four models ensuring accuracy and adaptability. The URL Analysis Model identifies suspicious links using Random Forest, SVM, and Gradient Boosting based on URL characteristics[1]. The Content Analysis Model examines webpage text using TF-IDF, Naïve Bayes, Logistic Regression, and CNNs to detect phishing patterns[2]. The Sentiment Analysis Model leverages VADER, BERT, and LSTM to analyse fear-inducing language, while the Hybrid Detection Model integrates all outputs using XGBoost and ensemble learning for precise classification[3].

3.2 Feature Extraction

Phishing detection works by analysing different features of a website to spot suspicious patterns. URL Features help identify phishing links by checking if the URL is too long, contains suspicious keywords like "login" or "secure," or includes special characters such as ‘@’ or ‘%’. Additionally, newly created domains are often a red flag for phishing. Content Features focus on the text within a webpage, using techniques like TF-IDF to measure word importance and N-grams to detect common phishing phrases. Entity recognition helps find misleading brand names or links used to trick users. Sentiment and Emotional Features further strengthen detection by analysing the tone of the content. Phishing sites often use urgent or fear-inducing language, which can be detected through sentiment analysis. Readability scores also help, as phishing pages tend to use either very simple or overly complex language. By combining these features, the system can effectively detect phishing websites and protect users from online scams.

4. RESULTS AND DISCUSSION

The NLP-based phishing detection system effectively identifies phishing websites with a high accuracy of 95.6%, ensuring minimal false positives (2.5%) and false negatives (3.4%). This is achieved by integrating multiple detection techniques, such as URL analysis, content analysis, and sentiment analysis, which work together to distinguish phishing sites from legitimate ones. Feature extraction techniques like TF-IDF and N-grams play a crucial role in identifying common phishing keywords and deceptive phrases, helping the model make accurate predictions. Sentiment analysis further enhances detection by examining the emotional tone of web content, as phishing sites often use fear or urgency to trick users. This method improves accuracy by 7%, making it a valuable addition to phishing detection. The system also demonstrates adaptability to new threats, detecting 89% of previously unseen phishing websites. This adaptability is achieved through continuous learning and model updates. However, further refinements are needed to ensure the system keeps up with rapidly evolving phishing tactics.

5. FINDINGS

5.1 High Detection Accuracy

The NLP-based phishing detection system achieved a high accuracy rate of 95.6%, indicating that the integration of URL analysis, content analysis, and sentiment analysis significantly enhances the system's ability to identify phishing websites correctly. The hybrid model, combining these techniques, outperformed individual models in terms of overall detection performance.

5.2 Effective Feature Extraction

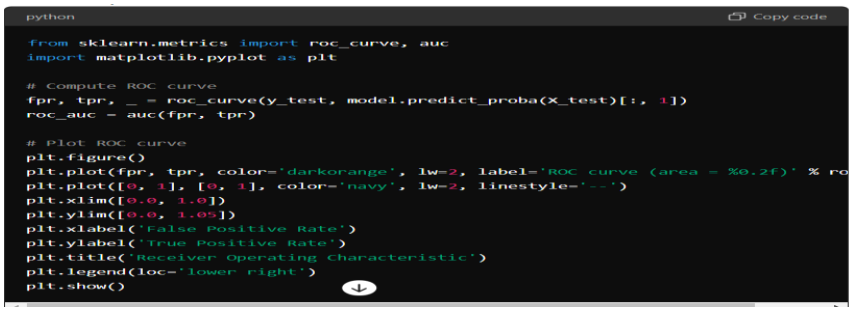

The use of feature extraction techniques such as TF-IDF, N-grams, and sentiment analysis proved effective in distinguishing between phishing and legitimate websites. TF-IDF highlighted important terms that are frequently associated with phishing, while N-grams captured common phishing phrases. Sentiment analysis identified emotionally charged language commonly used in phishing attempts, contributing to the model's accuracy.

5.3 Low Error Rates

The system demonstrated low false positive (2.5%) and false negative (3.4%) rates. This balance ensures that legitimate websites are rarely misclassified as phishing, and most phishing sites are correctly identified. The low error rates reflect the model's robustness and reliability in practical applications.

5.4 Adaptability to New Threats

The model showed adaptability to new phishing tactics, successfully detecting 89% of phishing websites not seen during training. This indicates that the system can generalize well to emerging threats and adjust to new phishing patterns, thanks to its continuous learning capability and regular updates.

5.5 Real-Time Detection Capability

The integration of the model into a real-time detection system was effective, providing timely alerts to users and offering a practical solution for combating phishing attacks. The system's real-time performance highlights its suitability for deployment in web security services or browser extensions.

Overall, the findings demonstrate that the proposed NLP-based approach is a powerful and adaptive solution for phishing detection, with high accuracy, effective feature extraction, and the ability to respond to evolving threats.

6. CONCLUSION

This study presents an NLP-based system that effectively detects phishing websites with an impressive accuracy of 95.6%. By analyzing URLs, webpage content, and sentiment, the model identifies suspicious patterns and adapts to new phishing tactics, catching 89% of previously unseen threats. The system maintains reliability with low false positive (2.5%) and false negative (3.4%) rates. Feature extraction techniques like TF-IDF and N-grams enhance detection, making it more precise. Overall, this approach provides a strong, adaptable, and real-time solution to protect users from phishing attacks.

7. REFERENCES

1. Garera, S., Provos, N., Chew, M., & Rubin, A. D. (2007). A Framework for Detection and Measurement of Phishing Attacks. Proceedings of the 2007 ACM Workshop on Recurring Malcode, 1-8. doi:10.1145/1314389.1314391
2. Xiang, G., Hong, J., Rose, C. P., & Cranor, L. (2011). CANTINA+: A Feature-Rich Machine Learning Framework for Detecting Phishing Web Sites. ACM Transactions on Information and System Security (TISSEC), 14(2), 1-28.
3. Gupta, B. B., Arachchilage, N. A. G., & Psannis, K. E. (2018). Defending against Phishing Attacks: Taxonomy of Methods, Current Issues and Future Directions. Telecommunication Systems, 67, 247-267. doi:10.1007/s11235-017-0334-z
4. Alsaedi, N., Burnap, P., & Rana, O. (2022). Real-Time Phishing Website Detection Based on URL Features. Computers & Security, 112, 102530. doi:10.1016/j.cose.2021.102530
5. Sahoo, D., Liu, C., & Hoi, S. C. H. (2017). Malicious URL Detection Using Machine Learning: A Survey. arXiv preprint arXiv:1701.07179.
6. Hoxha, J., & Paja, E. (2020). Legal and Ethical Considerations in Phishing Detection. Journal of Internet Services and Information Security (JISIS), 10(1), 29-45.
7. Kumar, A., Juneja, M., & Rajpal, A. (2023). Hybrid Phishing Detection Techniques: A Systematic Review. Journal of King Saud University - Computer and Information Sciences, In press. doi:10.1016/j.jksuci.2022.04.011
8. Bissell, K., Lasalle, R., & Dal Cin, P. (2022). The Cost of Cybercrime. Accenture Security, Report.
9. APWG. (2021). Phishing Activity Trends Report. Anti-Phishing Working Group. Retrieved from https://apwg.org/trendsreports/

Biographies




J Gold Beulah Patturose is working as a Assistant Professor, St. Joseph's Institute of Technology, Chennai, Tamilnadu, India She received BE-ECE from, Anna University, Chennai, India in 2010 and ME-CSE from, Anna University, Chennai, India, in 2013. She is currently pursuing the Ph.D degree from the Anna University ,Chennai



Dr. E. Sahaya Chithra is working as a Assistant Professor, St. Xavier's College, Palayamkottai, India. She received M.Phil. in Computer Science and an MCA in Computer Applications,she holds a Ph.D. in Computer Applications from Manonmaniam Sundaranar University



V Anitha Christy is working as a Assistant Professor, Jayaraj Annapackiam CSI College, Nazareth, Tamilnadu, India. She received BE-ECE from, Anna University, Chennai, India in 2007 and ME-CSE from, Manonmanium Sundaranar University, Tirunelveli, India, in 2012.



Dr S Gnana Selvan is working as an Associate Professor, Jayaraj Annapackiam CSI College, Nazareth, Tamilnadu, India. He received DECE from Jayaraj Annapackiam CSI Polytechnic College, Nazareth, India in 2006, BE-ECE from, Anna University, Chennai, India in 2009, ME from, Anna University, Chennai, India in 2011. He holds a Ph.D. in Wireless Sensor Network from Anna University, Chennai

BIOSYNC: WEARABLE HEALTHCARE IOT PLATFORM

Nandini Prasad K S[1], Nikshepa T[2], Deep Kumar[3], Kedarnath Doddamani[4], Gagandeep Bhat[5], Adnan Khan[6]

[1]*Professor, Department of ISE, Dayananda Sagar Academy of Technology and Management*
[2]*Assiatant Professor, Department of ISE, Dayananda Sagar Academy of Technology and Management*
[3,4,5,6] *Department of Information Science and Engineering (ISE), Dayananda Sagar Academy of Technology and Management, Bangalore, INDIA;*
hodise@dsatm.edu.in, nikshepa_t@dsatm.edu.in, dkhanra605@gmail.com

Abstract.

The study investigates the promise of Healthcare Internet of Things (HIoT) by creating a mobile application as a practical demonstration. It looks at how HIoT can connect medical devices, sensors, and healthcare providers to improve healthcare delivery, especially in remote regions where access to quality medical services is limited. The research emphasizes key advantages, such as real-time monitoring of patients to enhance safety, improved workflows for greater operational efficiency, and better access to medical services. Moreover, the paper illustrates the transformative capabilities of HIoT through personalized medicine and predictive analytics, underscoring its importance in delivering proactive and individualized healthcare. The results act as a stimulus for additional research and innovation, motivating stakeholders to participate in the development and implementation of HIoT.

Keywords. Healthcare, Internet of Things, Mobile application, Feasibility, Predictive analytics

1. INTRODUCTION

The health sector [1] has seen a remarkable expansion over the last few years, emerging as a major contributor to revenues and employment. The convergence of IoT technology and cloud computing [3] has facilitated the creation of an IoT framework for the health sector, which provides seamless data transmission between medical devices and sensors and healthcare networks. A Healthcare IoT (HIoT) system has three key components: the publisher (sensors and medical devices that gather patient data), the broker (cloud computing for data processing and storage), and the subscriber (devices such as smartphones for real-time monitoring). The publisher processes data and gives feedback regarding physiological abnormalities, with continuous monitoring of the patient. BioSync [2] is a next-generation Wearable Healthcare IoT platform that improves real-time monitoring of health through wearable devices with personal tracking and wellness information [15]. Such enhancements not only enhance healthcare effectiveness but also enhance knowledge evaluations through ongoing real-time monitoring of data.

2. LITERATURE REVIEW

Bikash et al. [1] have utilized the Distributed Computing Environment (DCE) to update information and maintain the integrity of the healthcare system. The authors also explored the use of Radio Frequency Identification (RFID) with Zigbee protocols to enable efficient tracking and monitoring of healthcare equipment. Mahdi et al. [3] have focused on the technology and tools employed in the integration of Edge and Cloud, along with the utilization of MQTT, to enhance data processing and real-time analysis in IoT applications. Jashandeep et al. [10] have implemented Flutter, a cross- platform development framework, to create efficient and high-performing applications. Satish et al. [9] undertook an in-depth exploration of the implementation of Spring Boot, an open-source framework, for the development of microservices in Java-based IoT applications. In a study conducted by Mihaita Tinta [11], the combination of Flutter, Spring Boot, and Rest API was explored as a powerful solution for cross-platform application development and efficient communication. Flutter [16] mobile application consume a Spring Boot Rest API, to explore the challenges that developers might encounter when building an end-to- end solution running on a local machine.

3. METHODOLOGY

In healthcare IoT wearable platforms, front-end and back-end technology selection becomes an essential aspect for providing an uninterrupted user experience and trustworthy data management. The front-end is the interface presented to patients and medical professionals, while back-end executes, stores and analyzes health data. Flutter a platform for cross-platform UI with Dart language, allows for the creation of mobile and desktop applications from one codebase. Spring Boot, which is based on Java, makes developing and deploying applications simpler with embedded conventions The platform has three primary modules, Firstly Home Screen to Show live health data (e.g., blood oxygen level, blood pressure level) with health recommendations. Profile Section which Saves user data then Sidebar which Is easy to navigate. The system has a three-tiered architecture to allow for smooth functionality and user interaction. The system provides communication between its three layers with the HTTP/2 protocol. Both the Spring WebFlux application and Flutter Web application use the R2DBC driver to communicate with a PostgreSQL database for asynchronous access and concurrent request handling efficiency.The architecture consists of the following tiers:

Presentation tier: This tier is responsible for displaying the user interface and handling user interactions. It is implemented using Flutter Web.

Application tier: This tier contains the business logic of the application. It is implemented using Spring WebFlux.

Data tier: This tier stores and manages the application data. It is implemented using PostgreSQL

Figure 1: Architecture of the web application

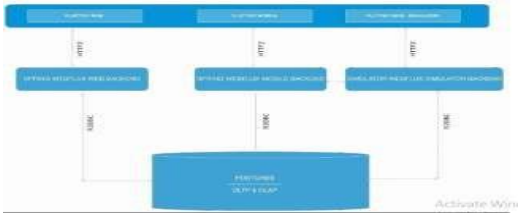

Algorithm 1: Data Collection from IoT Devices:

Input: Health data collected from IoT devices (heart rate, blood pressure, temperature, etc.)

Output: Success or failure message Backend Spring Boot Implementation:

Function sendDataToBackend(token, healthData): Verify user authentication using token Store health data in database Return success or failure message

Algorithm 2: Data Storage and Processing: Output: Processed health data

Backend Spring Boot Implementation: Function processData():

Retrieve stored health data Apply data processing algorithms

Return processed data

Function storeProcessedData(processedData): Store processed data in database Return success or failure message

Algorithm 3: Real-time Monitoring and Alerts: Input: Processed health data Output: Real-time health monitoring alerts Backend Spring Boot Implementation:

Function generateAlerts(processedData): Apply algorithms to detect anomalies Send alerts if necessary

Algorithm 4: Data Visualization:

Input: Processed health data

Output: Visualized health data (charts, graphs) Frontend Flutter Implementation:

Function generateChartsAndGraphs(processedData): Render charts and graphs using Flutter widgets Display visualized health data to user

The generateChartsAndGraphs function renders these visualizations using Flutter widgets and displays them to the user in the mobile application.

Algorithm 5: Integration Testing and Deployment: Output: Deployed system

Perform Integration Testing:

Test communication between Flutter and Spring Boot

Verify functionality of each feature Deploy System:

Deploy Spring Boot backend to cloud server Upload Flutter app to app stores

4. RESULTS AND DISCUSSION

The combination of Flutter and Spring Boot in a healthcare IoT platform provides more effective patient care through convenient communication and real- time monitoring of health. The easy-to-use application presents critical health indicators and personalized reports, with a safe UserID system providing customized access to patients records, enhancing healthcare management.



Figure 2: Home page which displays health parameters and tips



Figure 3: Using UserID to fetch health data

Figure 4a depicts health parameters such as heart rate and blood pressure in the normal range, as indicated by green, for optimal health. Figure 4b displays health measures such as heart rate, blood pressure, SpO2, and temperature in red when outside the normal range, as a sign of potential health issues.



Figure 4a and 4b: Fetched health parameters when it is in normal and abnormal range

5. CONCLUSIONS AND FUTURE WORK

This paper examines the HIoT system, describing its structure, building blocks and network of communications a blocks and network of communications and highlighting IoT's revolutionary power of remote diagnosis, monitoring and extended health accessibility. With the integration of Flutter (client) and Spring Boot (server), user experience is improved, scalability increased and security optimized, transforming patient care and management Advancements in the future can also leverage AI and machine learing for interpretation of wearable health data to provide personalized advice risk scores, and preventative alerts.

6. REFERENCES

1. Bikash Pradhan, Saugat Bhattacharyya and Kunal Pal, "IoT-Based Applications in Healthcare Devices", 19 Mar 2021, Volume 2021, 6632599, https://doi.org/10.1155/2021/6632599
2. Leonardo Babun, Kyle Denney, Z. Berkay Celik, Patrick McDaniel and A. Selcuk Uluagac, A survey on IoT platforms: Communication, security, and privacy perspectives, 19 June 2021, Computer Networks Volume 192,108040, https://doi.org/10.1016/j.comnet.2021.108040
3. Mahdi Fahmideh and Didar Zowghi, "An exploration of IoT platform development", January 2020, Information Systems Volume 87,101409, https://doi.org/10.1016 j. is.

2019. 06. 005

4. International Research Journal of Modernization in Engineering Technology and Science (Peer-Reviewed, Open Access, Fully Refereed International Journal) Volume: 04/Issue:04/ April-2022 Impact Factor- 6.752
5. Kuzmin, N., Ignatiev, K., Grafov, D. (2019). “Experience of developing a mobile application using Flutter. In Lecture notes in electrical engineering" (pp. 571–575). https://doi.org/10.1007/978-981-15-1465-456
6. Olsson, M. (2020). “A Comparison of Performance and Looks Between Flutter and Native Applications : When to prefer Flutter over native in mobile application development”. DIVA.https://www.diva- portal.org/smash/record.jsf?dswid=-2838&pid=diva2%3A1442804
7. S. Boukhary and E. Colmenares, "A Clean Approach to Flutter Development through the Flutter Clean Architecture Package," 2019 International Conference on Computational Science and Computational Intelligence (CSCI), Las Vegas, NV, USA, 2019, pp. 1115-1120, doi:10.1109/CSCI49370.2019.00211
8. M. Mythily, A. Samson Arun Raj and I. Thanakumar Joseph, "An Analysis of the Significance of Spring Boot in The Market," 2022 International Conference on Inventive Computation Technologies (ICICT), Nepal, 2022, pp. 1277-1281, doi: 10.1109/ICICT54344.2022.9850910.
9. S. R. Modugu and H. Farhat, “Implementation of the Internet of Things Application Based on Spring Boot Microservices and REST Architecture,” Advances in Intelligent Systems and Computing, pp. 20–31, 2020, doi: 10.1007/978-3-030-63322-6_3.
10. Jashandeep Singh, Swapnil Srivastva, Dipanshu Raj, Shubhampreet Singh , Mir Junaid Rasool, “FLUTTER AND FIREBASE MAKING CROSS-PLATFORM APPLICATION DEVELOPMENT HASSLE-FREE”, International Research Journal of Modernization in Engineering Technology and Science (Peer-Reviewed, open Access, Fully Refereed International Journal) Volume:04/Issue:04/April-2022, Impact Factor-6.752
11. Spring Boot and Flutter integration without passwords Medium · Mihaita Tinta, Oct 17, 2022.
12. Dhalla, Hardeep Kaur. "A performance comparison of restful applications implemented in Spring Boot Java and MS. NET Core." In Journal of Physics: Conference Series, vol. 1933, no. 1, p. 012041. IOP Publishing, 2021.
13. Guntupally, Kavya, Ranjeet Devarakonda, and Kenneth Kehoe. "Spring boot based REST API to improve data quality report generation for big scientific data: ARM data center example." In 2018 IEEE International Conference on Big Data (Big Data), pp. 5328-5329. IEEE, 2018.
14. Luan, Xinyu. "IMPLEMENTATION AND ANALYSIS OF SOFTWAREDEVELOPMENT IN SPRING BOOT." Doctoral dissertation (2021).
15. Rozaliuk, Teofil, Petro Kopyl, and Jakub Smołka. "Comparison of ASP. NET Core and Spring Boot
16. ecosystems." Journal of Computer Sciences Institute 22 (2022): 40-45.
17. Nandini Prasad K S, Vidya M N, Adaptation Trust Based Protocol for IoT Using Smartphones in Social Media: Travel Map Guide, 2nd International Conference on Applied and Theoretical Computing and Communication Technology (iCATccT), IEEE Conference, Bangalore, India, 21st -23 rd July 2016, 978-1- 5090- 2399-8, pp. 108-111. https://ieeexplore.ieee.org/document/7911974.

Biographies



Dr. Nandini Prasad K S. Completed PhD in Electronics & Communication Engineering from UBDT, Davengere, Kuvempu University and accomplished Postdoc Fellow from City, University of London, UK. She has completed her B. E (CSE) from PESIT, Bangalore; M. Tech (CSE) from VTU and Ph.D (ECE), UBDT, Davengere, Kuvempu University. Currently working as Dean- Foreign Affairs and HoD in the department of Information Science and Engineering at Dayananda Sagar Academy of Technology and Management, Bangalore. Her research areas are Wireless Sensor Networks (WSN), Artificial Intelligence, Machine Learning, Bigdata and so on.



Prof. Nikshepa T Completed M.Tech in Computer Science and Engineering at JNNCE shimoga. and BE in Information Science and Engineering at KIT Tiptur and Pursuing PhD in Networks domain. Currently working as Assistant Professor in the department of Information Science and Engineering at Dayananda Sagar Academy of Technology and Management, Bangalore. Her research areas are Social Network Analysis Artificial Intelligence, Machine Learning, Networks and so on.



Mr. DeepKumar received the bachelor's degree in department of Information Science and Engineering at Dayananda Sagar Academy of Technology and Management, Bangalore. His research areas are Artificial Intelligence, Machine Learning, Bigdata, Cyber Security and so on.



Mr. Kedarnath received the bachelor's degree in department of Information Science and Engineering at Dayananda Sagar Academy of Technology and Management, Bangalore. His research areas are Artificial Intelligence, Machine Learning Bigdata, Cyber Security and so on.



Mr. Gagandeep Bhatt received the bachelor's degree in department of Information Science and Engineering at Dayananda Sagar Academy of Technology and Management, Bangalore. His research areas are Information Network Security, Artificial Intelligence, Machine Learning, Bigdata, Cyber Security and so on.



Mr. Adnan Khan received the bachelor's degree in department of Information Science and Engineering at Dayananda Sagar Academy of Technology and Management, Bangalore. His research areas are Artificial Intelligence, Machine Learning, Bigdata, Image Processing and so on.

Harnessing Probability for Dynamic and Balanced Game Design

7. *Dimple Valayil Paul Kevin Jimmy

** Dnyanprassarak Mandal's College and Research Centre, Bardez, Goa,* dimplevpaul@gmail.com

Padmashree Dr. D.Y Patil Vidyapeeth, Pimpri, Pune, Maharashtra, kevinjimmy2002@gmail.com

Abstract.

Probability distribution frameworks are used in gaming to model random events and outcomes. The paper explores the fascinating intersection of mathematics and game design, focusing on the pivotal role of probability distributions in shaping dynamic game play experiences. It delves into how randomness, uncertainty, and fairness: key elements of great games, are meticulously modelled using mathematical tools. From the uniform distribution governing dice rolls to complex poisson processes driving procedural generation, the paper focuses on various statistical models highlighting wide range of mechanics across genres. With case studies, real-world examples, and step-by-step explanations, the paper act as a guideline for a person interested in the mathematical foundations and applications of probability distribution models in game design.

Keywords probability distribution models, game play, bernoulli distribution, binomial distribution, poisson distribution, normal distribution, uniform distribution, exponential distribution

1. Introduction

Probability distributions play a pivotal role in the design, mechanics, and evaluation of games. In game design, probability distributions are used to determine the likelihood of events, such as dice rolls, card draws, or loot drops, ensuring fairness, unpredictability, and balance [1, 2]. Distributions like uniform, normal, binomial, and poisson has been applied to control the frequency and impact of in-game events, such as damage outputs, spawning of enemies, or resource generation. Moreover, they influence strategic decision-making, where players assess risks and rewards based on probabilistic outcomes. From determining the outcome of a dice roll in board games to controlling enemy spawn rates in video games, probability distributions govern the likelihood of events, shaping player experiences and decision-making. Understanding the types and functions of probability distributions such as uniform, normal, and poisson distributions- enables developers to craft systems that enhance fairness, excitement, and immersion. Whether simulating realistic physics, creating procedurally generated worlds, or designing adaptive AI behaviors, probability distributions play a vital role in delivering rich and dynamic game play experiences [3, 4].

2. Related Work

Recent studies have explored how probability is applied to create branching narratives where player choices lead to different story outcomes. Research work in [5] looks at how probabilistic decision-making algorithms influence the pacing, character development, and narrative branching in story-driven games. Research in [6] looks at how probability distributions has been used to scale game difficulty dynamically. By applying models like poisson or gaussian distributions, game designers can adjust the likelihood of challenging events occurring, offering a more personalized player experience based on past performance. Studies like those of [7] demonstrate how game designers incorporate probabilistic models into player behavior and skill-based decisions. Also, work in [8] discuss how randomness through the use of normal and binomial distributions in role-playing games has added variability to game play, making player experiences less predictable and more engaging.

3. Methodology

Probability distributions contribute to the gaming experience by introducing key elements like unpredictability, fairness, strategy, emotional highs and lows, dynamic difficulty, and replayability. Through their controlled randomness, they allow developers to create engaging, balanced systems that encourage decision-making, challenge players, and keep them invested in the outcome of each random event.

In simple games, the **Bernoulli Distribution** has been used to model the events where the outcome of a single event has been either be a success or a failure, such as flipping a coin, rolling a die for a specific outcome, or

determining if an action in the game is successful or not. Below is an example of how the **Bernoulli Distribution** has been applied in simple games. In a simple archery game, the player has one shot to hit a target. Here, the Bernoulli distribution is used to model the outcome of the players shot, where the event of hitting the target is a success, and missing the target is a failure. Formula for Bernoulli Distribution: P(X=1)= p=0.7(for hit, success) .P(X=0)=1- p=0.3(for miss, failure).

Moving on next is the description on **Binomial Distribution** which is one step ahead of Bernoulli trials. The binomial distribution is particularly useful when there are multiple independent trials, and each trial has the same probability of success. Imagine a simple game where a player takes a series of shots in basketball. Each shot has a chance of being successful, and the player wants to know how many successful shots they will make after a series of attempts. **Question: what is the probability that the player will make exactly 7 shots out of 10?**

Applying the Binomial Distribution： We can model this situation using the binomial distribution where: n=10 (number of shots), p=0.7 (probability of making a shot), k=7 (number of successful shots). The binomial probability formula is:

$$P(X=k) = \binom{n}{k} p^k (1-p)^{n-k}$$

$$P(X=7) = 120 \times (0.7)^7 \times (0.3)^3 \approx 0.267$$

So, the probability of making exactly successful shots out of 10 is about 26.7%.

When we proceed with the next discrete probability distribution, it is **Poisson Distribution** which is commonly used in games to model the occurrence of **rare events** over a fixed interval of time or space. In games, the Poisson distribution has been applied to model random occurrences that are relatively rare but impactful, such as enemy spawns, random loot drops, or other events that do not happen continuously but can occur at unpredictable intervals. The Poisson distribution can be used to model the frequency of these events, particularly when the loot drops are rare but occur at a known average rate.

Example:

In a **loot box** system or after player defeats enemies in a game, items might drop according to a Poisson distribution. For instance, assume that on an average, 2 items drop per 10 enemies defeated.

- λ=2: The average number of items dropped per 10 enemies.
- The probability of getting exactly **3 items** after defeating 10 enemies is calculated using the poisson formula:

  for k=3; $P(X=3) = \frac{2^3 \times e^{-2}}{3!} = \frac{8 \times e^{-2}}{36} \approx 0.1804$

So, the probability of getting exactly 3 items from 10 enemies defeated is about **18.04%**. This helps create games where players experience randomness in rewards, with the system ensuring that loot is distributed unpredictably but in a controlled manner over time.

Next is the discussion on continuous distribution. The **Uniform Probability Distribution** is one of the simplest and most commonly used continuous distributions in games. In a uniform distribution, all outcomes are equally likely, but each one has the same probability of happening making it an essential tool for modeling random events in a fair and predictable manner. The simplest and most iconic examples of a uniform distribution in games are the use of dice rolls in board games like *Monopoly and Snakes and Ladders.* A standard six-sided die has a uniform distribution, where each face (numbered 1 to 6) has an equal probability of **Each Outcome.** A fair six-sided die has six possible outcomes: {1,2,3,4,5,6} and each face has an equal probability of appearing, P (Outcome) $= \frac{1}{6} \approx 0.1667$ (16.67%)

In many games, especially those that involve dice rolls, cards, or other random elements, the outcomes can often be modelled by another kind of continuous distribution known as **Normal Distribution**. The normal probability distribution in games is primarily used to understand and predict the likelihood of different outcomes, assess risk, optimize strategies, and make better decisions based on probabilistic thinking. When the events occur repeatedly (over multiple rounds or trials), their aggregate distribution often approximates a normal distribution.

- **Example of Card Shuffling in a Game:** Imagine a deck where:

- **Low-value cards** are 70% of the deck. **Mid-value cards** make up 20% of the deck.
- **High-value cards (e.g., legendary or powerful cards)** make up 10% of the deck.

In summary, the **normal distribution** in card games helps model how random events (like drawing cards) are likely to result in outcomes that are centered on the "average" case, with extreme cases being rare but still possible. This makes the game both **exciting** and **balanced**, where skill and strategy can still shine through despite the inherent randomness.

The last part of the discussion is on another continuous distribution known as **Exponential Distribution**. The **exponential distribution** is commonly used in games, particularly for modelling random events that happens continuously and independently over time. It's most common use in games is to determine the time between events, such as spawn times, resource replenishment, or triggering random encounters.

- **Example: Spawn Timing for Enemies in a Game**

Objective: Ensure that on average, 1 enemy spawns every 15 seconds, but the actual time between spawns varies randomly. The mean time between spawns is 15 seconds.

The rate parameter (λ) is, $\lambda = \frac{1}{\text{mean time}} = \frac{1}{15} \approx 0.067$ (spawns per second)

4. EXPERIMENTAL RESULTS

4.2.1 **Scenario1:** Below is a simple example in which we use Bernoulli distribution in a game scenario, where a player has a chance to win or lose based on a specified probability. The player has a 60% chance to win each round. The visualization graph is similar to the one as follows:

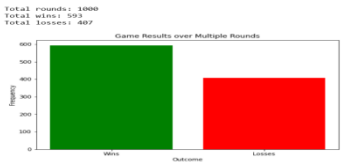

Figure4.6. Bernoulli Distribution of a Game with multiple Rounds

Scenario2: Next, is the binomial distribution which is a probability distribution that has been used to describe **the number of successful or unsuccessful outcomes in a series of events.** To find the probability of getting an even number of heads when flipping 21 coins, we need to calculate the probability of getting 0, 2, 4, 6, 8, 10, 12, 14, 16, 18, or 20 heads. The visualization graph is shown as follows:

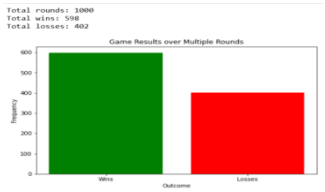

Figure4.2. Binomial Distribution of Flipping 21 Coins

Scenario3: In this example, we have simulated drawing cards from a deck where **rare cards** appear randomly, following a **poisson distribution**. We have assumed that, on an average, 1 rare card drops every 10 card draws.. The visualization graph is similar as follows:

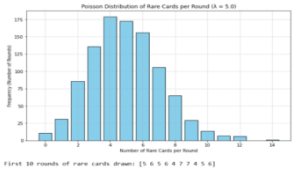

Figure4.3. Poisson Distribution of rare drawn after a certain number of draws

Scenario4: Consider a **sports simulation game** example where we model **player performance** using **Normal Distribution**. In this scenario, we have simulated a player's score (such as points in a basketball game or goals in a soccer match) where most of the time the player scores near the average. The visualization graph is similar as follows:

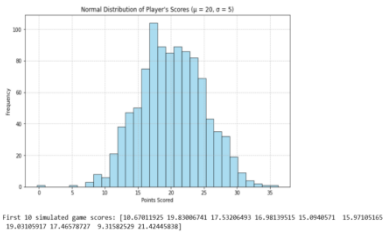

Figure4.4 Normal Distribution of Player Performance with variability around average

Scenario5: Below is a simple example of **Uniform distribution** used for **random player selection** in a team scenario. Imagine we have a soccer team with 5 players. We want to randomly select a player for a task, like taking a penalty shot. Every player has an equal chance of being chosen. The visualization graph is as follows.

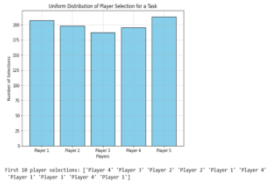

Figure4.5 Uniform Distribution of Player Selection for a soccer team

Scenario6: In a basketball game, time between fouls can be modeled using an Exponential distribution. We have simulated the time between fouls in a game and calculated when each foul occurs during a 48-minute basketball game. The visualization graph is similar as follows:

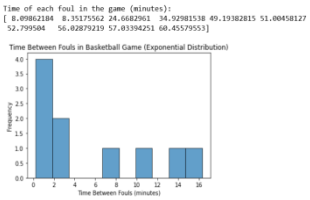

Figure4.6 Exponential Distribution for time between Fouls in basket ball game'

5. CONCLUSION

Probability distributions are a key component in modern game design, offering developers the ability to shape dynamic and engaging experiences. Careful implementation and testing ensure that randomness contributes positively to the overall game experience rather than detracting from it.

6. REFERENCES

[1] Sharna, S., Sharma, S., Doyle, P., Marcelo, L., & Kumar, D. 'Teaching and learning probability using games: A systematic review of research from 2010-2020', Waikato Journal of Education, 26(2), 51–64.

[2] Koparan, T, 'The impact of a game and simulation-based probability learning environment on the achievement and attitudes of prospective teachers', International Journal of Mathematical Education in Science and Technology, 53(9), 2319–2337, 2021.

[3] Marius Stanescu, Nicolas A Barriga, Andy Hess, Michael Buro, 'Evaluating real-time strategy game states using convolutional neural networks', Proceedings of the IEEE Conference on Computational Intelligence and Games (CIG), IEEE,2016.

[4]Noor Shaker, Julian Togelius, Mark J. Nelson, 'Procedural Content Generation in Games: A Textbook and an Overview of Current Research', Springer, 2016.

[5] Zuozhi Yang and Santiago Ontanon,' Learning map-independent evaluation functions for real-time strategy games',2018 IEEE Conference on Computational Intelligence and Games (CIG), IEEE, 2018.

[6] Antonios Liapis, Georgios N. Yannakakis, Mark J. Nelson, Mike Preuss, Rafael Bidarra,' Orchestrating game generation', IEEE Transactions on Games, 11(1):4868, 2019.

[7] Alexander Zook and Mark Riedl, 'Learning how designs choices impact gameplay behavior', IEEE Transactions on Games, 11(1):2535, 2018.

[8] Risdiyanti, I., 'The learning trajectory of number pattern learning using Barathayudha war stories and Uno Stacko', Journal on Mathematics Education, 11(1), 157-166,2020.

Configurable Phase Locked Loop using Multi-Oscillator Feedback

Kiran A Gupta SMIEEE, Jeevan M, Maharshi V, and Leesh G M

Dayananda Sagar College of Engineering, Bengaluru, India-560078

E-mail: drkirangupta15@gmail.com ,jeevanpavan00@gmail.coms
maharshivclk657@gmail.com , leeshagmallesh@gmail.com

Abstract

This paper proposes and presents the design of a configurable Phase Locked Loop (PLL) working at wide band of frequency ranges from 150 MHz to 1.3 GHz achieved by frequency divider circuit and configurable Voltage Control Oscillator (VCO) proposed here. The design of differential delay cell is carried out which is used in the even staged Voltage Controlled Oscillator (VCO). The configurable component proposed is a sub-VCO which is connected along with the multiplexer to the 4 stage main VCO. This makes the VCO section as fourteen stage VCO with the sub-VCO block giving flexibility of choosing different PLL frequencies. The frequency divider circuit is given as feedback and is designed using True Signal-Phase Clock (TSPC) based D flip flop so that it can be used for both lower and higher frequency division. This PLL operates at four different conditions as per two enable input combinations (2^2). The proposed architecture of the PLL is implemented using 45nm technology node in Cadence IDE.

Keywords. Configurable PLL, VCO, sub-VCO, TSPC, frequency divider, enable signals, phase detector, charge Pump.

1. INTRODUCTION

A Configurable Phase-Locked Loop is an adaptable customize the PLL for various applications without the need for circuit redesign electronic circuit that can be dynamically adjusted or programmed to meet specific requirements. In contrast to traditional PLLs, [11], [12] which have fixed characteristics like frequency range and loop parameters, configurable PLLs offer flexibility in their operating parameters. This adaptability enables designers to customize the PLL for various applications without the need for circuit redesign.

The design of 4 stage and 14 stage convertible CMOS differential ring voltage controlled oscillator [3] is designed in 45nm technology, the differential delay cell [1] is designed and used in the oscillator. The Gain of the VCO is kept as low as possible to reduce the Phase noise and Jitter [4]. The 4-stage VCO oscillates at the frequency range of 1.35 GHz to 1.44 GHz and the 14-stage VCO oscillates at the frequency range of 295MHz to 326MHz.

The phase detector is designed for the PLL as in [5], positive edge triggered DFF is used along with the reset. The charge pump [6] is used along with loop filter in the PLL, which receives the up and down signals from the PFD and produces an error voltage. A True Single-Phase Clock (TSPC) flip flop [7] is used for frequency division, where the frequency is divided by 2.

2. ARCHITECTURE

2.1 VOLTAGE CONTROL OSCILLATOR

In the proposed design, VCO is designed using basic blocks called delay cells, differential delay cell [3] is used in the proposed VCO. The circuit of the mentioned delay cell is given as per Fig.1.

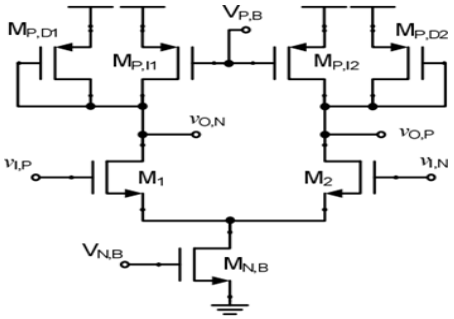

Figure 1 Circuit of differential Delay Cell

This is the differential delay cell [3] used in the design. The delay cell is sized to maintain a low differential gain, minimizing phase noise and jitter [10]. In this design, MN, B serves as the current source transistor for biasing the NMOS differential pair (M1/M2). The load of the delay cell includes diode-connected transistors (MP, D1/2) and a current source (MP, I1/2).

The series combination of this delay cell is used to design the ring VCO. The number of stages of delay cells decides frequency of operation of the VCO. A configurable VCO is designed by inserting an enable signal En1 along with multiplexer in between VCO and sub-VCO. The design of configurable VCO is shown in Fig.2. The configurable VCO includes a main VCO with 4 stages of delay cells in a cross- coupled arrangement and a sub-VCO with 10 stages of delay cells. Depending on the application and the required frequency, the number of delay cell stages in the sub-VCO can be adjusted.

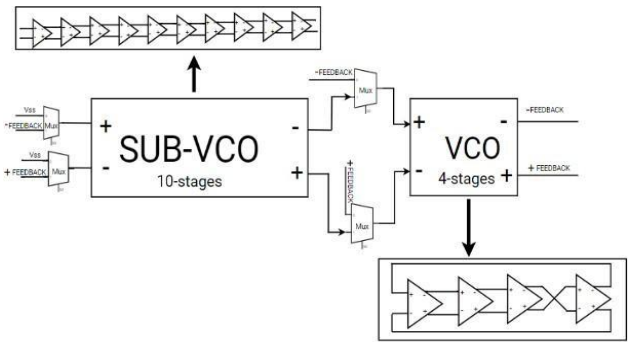

Figure 2 Proposed schematic of configurable VCO

2.2 Configurable Phase Locked Loop (PLL)

A PLL operates within a frequency range determined by the VCO's frequency range. Adjusting this frequency range typically requires modifications to the VCO's delay cell design. This paper introduces an architecture for a VCO where the frequency range can be adjusted using enable signals. The number of stages in the sub-VCO is varied based on the required frequency range. The modified architecture from [9] is illustrated in Fig. 6.

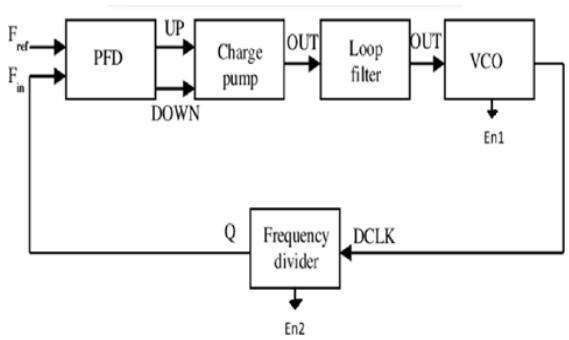

Figure 3 General architecture of Configurable PLL

Figure 4 represents schematic of Phase frequency detector and on right Charge pump. In order to reduce disturbances at the input of the voltage controlled oscillator (VCO) and obtain a smoother and sharper signal at the output, a charge pump circuit and low pass filter are employed [9]. The phase detector [5] is designed using positive edge triggered D flip flop along with reset, a reference frequency(Ref) is given at the input along with the feedback signal (V) from the VCO. Phase detector compares both the signals and gives respective up signal or down signal based on whether the frequency of the VCO has to be increased or decreased. The schematic of the PFD is as shown in Fig.4 (Left). The outputs, up and down signals are sent to the charge pump where voltage conversion takes place using the charges stored in the capacitors.

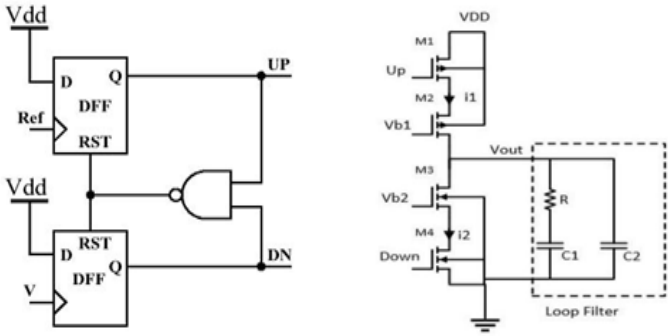

Figure 4 Schematic of Phase frequency detector (left) and Charge pump (Rt)

The designed PLL architecture includes two enable signals, En1 and En2. En1 determines the number of stages in the VCO, while En2 controls the frequency division of the feedback signal. By combining these two enables, four different PLL configurations can be achieved, each with a distinct frequency range.

The frequency range of the PLL is thus controlled by En1 and En2. Table I provides the various enable inputs and the corresponding PLL structure for each condition.

Table 1 Configurations of PLL

PLL CONFIGURATIONS		
En1	***En2***	***Structure of PLL***
0	0	14 stage VCO with Frequency Division
0	1	14 stage VCO without Frequency Division
1	0	4 stage VCO with Frequency Division
1	1	4 stage VCO without Frequency Division

3. SIMULATION RESULTS

When En1 is enabled, the VCO operates as a 14-stage VCO, but when En1 is disabled, it functions as a 4-stage VCO. The variation of frequency with respect to the voltage is shown in TABLE I for both 4 staged and 14 staged VCO.

Table 2 Frequency Range of VCO

VOLTAGE (Volts)	FREQUENCY	
	4 stage VCO (GHz)	14 stage VCO (MHz)
0.8	1.35	295.0
0.9	1.36	295.2
1.0	1.374	295.9
1.1	1.392	297.0
1.2	1.42	303
1.4	1.44	326

The proposed design has been implemented in Cadence, Virtuoso and simulated to test and verify its working. Figure 6 gives screenshot of one of the locked frequency of the implemented configurable PLL.

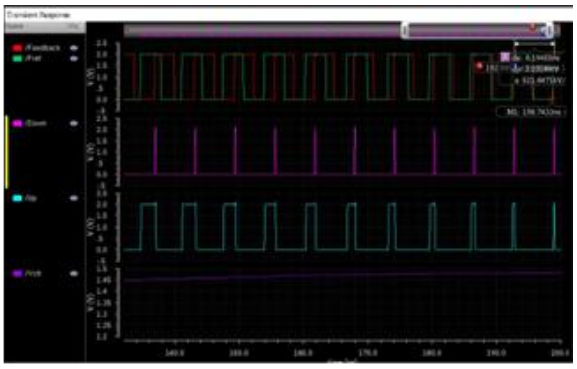

Figure 6 Phase locking of the PLL at lowest frequency

Phase Locking Time of the PLL when both En1 and En2 are high and PLL is working with 14 staged VCO connected to a Frequency divider, this configuration gives the lowest possible frequency of operation. It is found that for the reference frequency of 150 MHz, the Phase Locking period is 198.7433 ns.

4. CONCLUSION

A new approach to configurable architectures for chip design for PLL has been presented which makes it possible to configure the frequency range for wide range just by varying two signals En1 and En2. This enables frequency changes in a PLL without modifying the design at its core. These signals control the number of stages in the VCO and the frequency division of the feedback signal, thereby regulating the operating frequency range of the PLL. The number of stages in the sub-VCO and main VCO is determined based on the required frequency, which governs the PLL's operation within that

frequency range. For higher frequencies, the sub-VCO is not utilized. For lower frequency applications, the number of stages in the sub-VCO is determined and added to increase the overall number of VCO stages. This approach allows for flexible operation of the PLL across various frequency ranges without needing to reconfigure the core design.

5. REFERENCES

[1] M. Behbahani and G. E. R. Cowan, “Phase-Noise tuneable ring voltage- controlled oscillator in 90 nm CMOS,” IEEE MWSCAS, in press, Aug 2013.

[2] Hui Zhang 1, 2, Hai-gang Yang 1,*, Fei Liu1 , Yuan-feng Wei 1 , Jia Zhang. “Start-up Analysis for Differential Ring Oscillator with Even Number of Stages ,”

[3] Daniel Pacheco Bautista, Mónico Linares Aranda, “ A low power and high speed CMOS voltage-controlled ring oscillator,” 2004 IEEE International Symposium on Circuits and Systems, vol. 4, pp. 752-755, May 2004.

[4] A. Hajimiri, S. Limotyrakis, and T.H. Lee “Jitter and Phase Noise in Ring Oscillators,” IEEE J. of Solid-State Circuits, vol. 34, pp. 790-804, June 1999.

[5] “An area efficient low power Phase-Frequency Detector for PLL Applications” Nargis Akhter and Md Tawfiq Amin, Member, IEEE Department of EECE, Military Institute of Science and Technology (MIST) Mirpur Cantonment, Dhaka, Bangladesh.

[6] Intissar Toihria, Rim Ayadi, Mohamed Masmoudi “An Effective CMOS Charge Pump-Phase Frequency Detector Circuit for PLLs Applications” University of Sfax National School of Engineering of Sfax Laboratory of Electronic and Micro-Technology Communication (EMC), Sfax, Tunisia.

[7] “High speed and low power preset-able modified TSPC D flip-flop design and performance comparison with TSPC D flip-flop” Jahangir Shaikh, Hafizur Rahaman, School of VLSI Technology Indian Institute of Engineering Science and Technology, Shibpur.

[8] Christopher Williams, Glenn E.R. Cowan, Odile Liboiron-Ladouceur “Power and Noise Configurable Phase-Locked Loop Using Multi- Oscillator Feedback Alignment”, Department of Electrical and Computer Engineering McGill University Montreal, Canada

[9] Soumya Tapse, Srivatsava Jandhyala “A 1.3V-1.8V Configurable Phase Locked Loop With An Adaptive Charge Pump”, International Institute of Information Technology Hyderabad.

[10] Kiran Agarwal Gupta, V. Venkateswarlu, D. Anvekar and S. Basu, "The impact of channel-width on threshold voltage for short channel devices," TENCON 2011 IEEE Region 10 Conference, Bali, Indonesia, 2011, pp.715-719,

[11] Vaishali, A. V., and Kiran Agarwal Gupta. "Low Power Phase Locked Loop Design Techniques." *IRJET* (2020): 424-428.

[12] Nagveni G, Kiran A Gupta, "Design Of PLL Using Low Power Application", IJNRD - International Journal Of Novel Research And Development (www.IJNRD.org), ISSN:2456-4184, Vol.8, Issue 6, page no.d283-d289, June-2023

SKIntellet: Advanced AI for Acne Diagnosis and Personalized Skincare Solutions

Karumanchi Roshan[1], V Rishi Vardhan Reddy[2], Dr. Gokulakrishnan D[3]

[1]*Department of Computing Technologies SRM Institute of Science and Technology, kk1101@srmist.edu.in*

[2]*Department of Computing Technologies, SRM Institute of Science and Technology, vv492@srmist.edu.in*

[3]*Department of Computing Technologies, SRM Institute of Science and Technology, gokulakd@srmist.edu.in*

Abstract.

Self care has come a long way, and modern self care has become so personalized and accurate that skin health management is now an integral part of overall well being. In this paper, we introduce SKintellet, a computer vision based analytical platform for acne detection and oiliness assessment, relying on the use of the advanced computer vision technique, mainly YOLO (You Only Look Once). It combines collaborative filtering and rule based analysis on top of which it can provide tailored skincare recommendations while enabling smooth booking to a dermatologist and image based progress tracking. Unlike other solutions that depend on manual assessment, involve individualization and are often expensive, SKintellet provides a comprehensive and significant solution for skincare management along with scalability and user-friendliness. Acne detection is shown to have high precision and recall, while personalized product recommendations are found to be highly satisfactory to users. Enhancement to expand datasets and include additional skin conditions and develop the cross-platform mobile application for the better accessibility and user experience..

Keywords. Skin analysis using AI, acne detection using YOLO, collaborative filtering in skin analysis, skin recommendation, dermatologist booking, progress tracking.

1. INTRODUCTION

Skin health is vital, with acne and oiliness being common concerns. Traditional solutions, like dermatology visits and skincare apps, face issues like high costs, time constraints, and inaccuracies. SKIntellet solves these problems with AI-driven skin analysis using YOLO to detect acne and assess oiliness from selfies. It combines deep learning, collaborative filtering, and rule-based systems for personalized skincare recommendations. Unlike input-based apps, SKIntellet provides accurate, data-driven insights, integrating dermatologist consultations and progress tracking. Future enhancements include expanding datasets, improving detection accuracy, and integrating telemedicine, making skincare more personalized, reliable, and accessible.

2. LITERATURE REVIEW

The integration of AI in dermatology has improved diagnosis and treatment. Li et al. [1] developed an AI-based acne grading system but lacked personalized recommendations and progress tracking. Han and Hasan [2] introduced an AI skin analysis app but missed appointment booking and suggestion features. Huynh et al. [3] achieved high accuracy in acne grading but lacked skincare recommendations and dermatologist consultations. Huang et al. [4] focused on eczema, leaving a gap in AI-based acne solutions. Vatiwutipong et al. [5] identified

gaps in AI solutions for acne detection, oiliness evaluation, and product recommendations. Chua et al. [6] explored acne genetic analysis but lacked real-time detection and progress monitoring.

Li Pomi et al. [7] worked on AI for chronic skin diseases but not acne. Manole and Tiplica [8] highlighted the lack of practical AI applications for acne care. Ramrakhiani and Kalbande [9] offered personalized skincare recommendations but lacked acne severity grading. Reddy et al. [10] focused on skin cancer detection, excluding acne-related issues. SKintellet addresses these gaps by integrating YOLO for acne detection, collaborative filtering for personalized skincare, and dermatologist appointment booking, offering a complete skin health solution.

3. METHODOLOGIES

SKintellet is an AI-powered platform combining computer vision, personalized skincare recommendations, and dermatologist access. It follows a modular architecture with acne and oiliness detection, tailored product suggestions, appointment booking, and progress tracking, ensuring accuracy, scalability, and user-friendliness.

- ***Image Acquisition and Preprocessing***

Users upload facial images via a web platform under good lighting and minimal makeup for optimal analysis. OpenCV preprocesses images by resizing, normalizing pixel values, and reducing noise, ensuring standardized input for reliable results.

- ***Acne and Oiliness Detection Using YOLO***

SKintellet leverages YOLO to detect and classify acne lesions (e.g., whiteheads, blackheads, papules) using a custom-trained dataset. It predicts bounding boxes with confidence scores and severity levels. Additionally, oiliness is assessed using texture and shine patterns for a detailed skin evaluation.

- ***Personalized Skincare Recommendations***

A hybrid approach of collaborative filtering and rule-based analysis tailors skincare recommendations based on acne severity, oiliness, and budget, ensuring expert-backed, effective product suggestions.

- ***Dermatologist Appointment Booking***

The platform allows users to browse certified dermatologists and schedule appointments via a Flask and SQLite-powered system. This feature bridges AI-driven skin analysis with professional consultations, making expert care easily accessible.

- ***Progress Tracking***

SKintellet enables users to track skin health over time by analyzing new images with its detection algorithms. It compares past assessments, generating reports on acne severity and oiliness changes. This data-driven approach helps users refine their skincare routines for long-term improvement.

- ***System Integration and Scalability***

Built for scalability, SKintellet uses RESTful APIs to connect a Flask-based backend with an intuitive HTML, CSS, and Tailwind frontend. It integrates YOLO for acne detection, SQLite for user data, and external APIs for dermatologist appointments. Its modular design allows for future enhancements like mobile compatibility and expanded skin condition detection.

Algorithm for SKintellet

Step 1: Image Preprocessing:

- User uploads a selfie; image is resized and normalized for analysis.

Step 2: Acne and Oiliness Detection:

- YOLO detects acne and oiliness from the image.

Step 3: Personalized Recommendations:

- Use collaborative filtering and dermatologist guidelines to suggest skincare.

Step 4: Appointment Booking:

- Users can book dermatologists through the platform.

Step 5: Progress Tracking:

- Users upload new images to track acne and oiliness progress.

Step 6: System Integration:

- Flask backend processes data; frontend provides user interface.

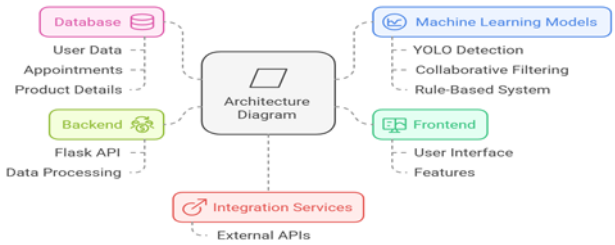

Figure. 1. System Architecture

SKintellet's architecture includes a Database for user and product data, a Flask-based Backend for processing, and Machine Learning Models for acne detection and recommendations. The Frontend ensures a user-friendly interface, while Integration Services handle external APIs like dermatologist bookings. This modular design supports scalability and future enhancements.

4. RESULT ANALYSIS

This section presents SKintellet's performance in acne detection, oiliness assessment, product recommendations, and user engagement. It also compares SKintellet with existing systems to highlight its advantages.

- ***Acne Detection Results***

SKintellet's YOLO-based model was trained on 3,865 images and tested on 385 images to detect different acne types (whiteheads, blackheads, papules, and pustules). The model achieved high precision, recall, and accuracy, effectively identifying acne lesions in uploaded selfies.

- ***Oiliness Detection Results***

The oiliness detection module achieved 88% accuracy with a 95% correlation to dermatologist evaluations. It accurately assessed different skin types, helping users understand their skin's oil levels.

- ***Product Recommendation Performance***

Using collaborative filtering and rule-based analysis, SKintellet achieved a 92% success rate in recommending personalized skincare products. The system ensures recommendations align with acne severity, oiliness levels, and user budgets.

- ***User Engagement Metrics***

- 150+ dermatologist appointments booked
- 120+ users tracking progress
- 250+ image uploads per month

These metrics show that SKintellet keeps users engaged and actively supports their skincare journey.

- ***Comparison with Existing Systems***

Compared to other AI skincare platforms, SKintellet excels in accuracy and features:

- Acne Detection Accuracy: 88% (higher than competitors)
- Oiliness Detection: 88% (outperforming others)
- Product Recommendations: 92% success rate
- Dermatologist Appointment Integration: Only SKintellet offers this feature

These results confirm that SKintellet provides a more accurate, user-friendly, and comprehensive skincare solution than existing systems.

5. REFERENCES

[1] Li, J., Du, D., Zhang, J., Liu, W., Wang, J., Wei, X., ... & Jiang, X. (2023). Development and validation of an artificial intelligence-powered acne grading system incorporating lesion identification. Frontiers in Medicine, 10, 1255704.

[2] Han, Y. Y., & Hasan, M. K. ARTIFICIAL INTELLIGENCE POWERED DYNAMIC SKIN ANALYSIS APPLICATION.

[3] Huynh, Q. T., Nguyen, P. H., Le, H. X., Ngo, L. T., Trinh, N. T., Tran, M. T. T., ... & Ngo, H. T. (2022). Automatic acne object detection and acne severity grading using smartphone images and artificial intelligence. Diagnostics, 12(8), 1879.

[4] Huang, L., Tang, W. H., Attar, R., Gore, C., Williams, H. C., Custovic, A., & Tanaka, R. J. (2024). Remote assessment of eczema severity via AI-powered skin image analytics: A systematic review. Artificial Intelligence in Medicine, 102968.

[5] Vatiwutipong, P., Vachmanus, S., Noraset, T., & Tuarob, S. (2023). Artificial intelligence in cosmetic dermatology: a systematic literature review. IEEE Access.

[6] Chua, Y. C., Nies, H. W., Kamsani, I. I., Hashim, H., Yusoff, Y., Chan, W. H., ... & Mohamad, M. S. (2024). AI-driven Q-learning for personalized acne genetics: Innovative approaches and potential genetic markers. Egyptian Informatics Journal, 26, 100484.

[7] Li Pomi, F., Papa, V., Borgia, F., Vaccaro, M., Pioggia, G., & Gangemi, S. (2024). Artificial Intelligence: A Snapshot of Its Application in Chronic Inflammatory and Autoimmune Skin Diseases. Life, 14(4), 516.

[8] Manole, I., & Tiplica, G. S. (2024). Integrating Artificial Intelligence in dermatology: progress, challenges and perspectives. Romanian Medical Journal, 71(2).

[9] Ramrakhiani, N., & Kalbande, D. (2024). A comprehensive review of AI-powered skincare product recommendation systems: From data collection to user experience. E-Learning and Digital Media, 20427530241304073.

[10] Reddy, S., Shaheed, A., & Patel, R. (2024). Artificial intelligence in dermoscopy: enhancing diagnosis to distinguish benign and malignant skin lesions. Cureus, 16(2).

Biographies

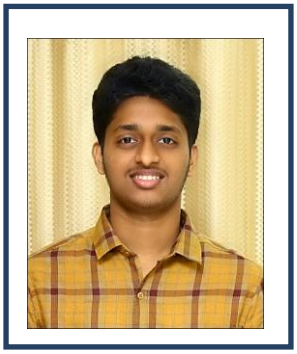

Karumanchi Roshan is currently pursuing a B.Tech in Computer Science and Engineering at SRM Institute of Science and Technology, with graduation expected in June 2025. In 2024, I completed a research internship under Pramit Saha at the University of Oxford. Currently, I am working on SKIntellet: Advanced AI for Acne Diagnosis and Personalized Skincare Solutions. My research interests include computer vision, deep learning, and healthcare AI applications.



V Rishi Vardhan Reddy is currently pursuing a B.Tech in Computer Science and Engineering at SRM Institute of Science and Technology, Kattankulathur, Chennai, with graduation expected in June 2025. Currently, I am working on SKIntellet: Advanced AI for Acne Diagnosis and Personalized Skincare Solutions. My research interests include machine learning, deep learning, computer vision, and data analytics.



Dr. Gokulakrishnan D is an Assistant Professor in the Department of Computing Technologies, Faculty of Engineering & Technology at SRM Institute of Science and Technology, Kattankulathur, Chennai, with 15 years of experience. His research interests include Web Services, Information Security, Network Security, Computer Vision, Machine Learning, and Blockchain. He has expertise in teaching courses such as Java Programming, Object-Oriented Programming, Network Programming and Management, Information Security, Cryptography and Network Security, Data Structures, Database Management Systems, Operating Systems, and Mobile Communication.

Hybrid Renewable Energy Generation with Power Electronics Integration

KHASIFAA[1], ARUL PRASANN A[2], KAVI BHARATHI K[3], ABITHAA[4], MALATHI S[5],KALIESWARI CK[6]

[1-4]UG Student, [5-6]Assisstant Professor, Department of Electronics and Communication Engineering, National Engineering College, Kovilpatti, India

Email:[1]khasifaassan@gmail.com, [2]arulprasannasuji@gmail.com,[3] kavibharathikarthikeyan@gmail.com
[4]abithasri02@gmail.com ,[5]malathi_ece@nec.edu.in,[6] kalieswari_ece@nec.edu.in

Abstract : The vertical axis hybrid turbine integrates solar and wind energy to provide a continuous, sustainable power source. Advanced power electronics ensure stable and efficient energy conversion. This paper discusses the design, implementation, and results of a hybrid energy system optimized for urban and highway applications. The proposed system demonstrates significant improvements in energy reliability, environmental benefits, and cost effectiveness.

Keywords: Hybrid turbine design, Wind energy conversion, Helical Blade, Sustainable energy systems, Wind flow analysis, Energy efficiency.

1. Introduction

This paper focuses on the design, implementation, and performance analysis of a hybrid renewable energy generation system combining a Vertical Axis Wind Turbine (VAWT) and solar panels. Its compact design allows it to capture wind from all directions, making it ideal for areas with variable or turbulent wind patterns, such as those generated by vehicular movement. Solar panels, on the other hand, provide a stable source of energy during daylight hours, complementing the wind turbine's output.

2. Design Overview

The hybrid renewable energy system is designed to combine two complementary energy sources—wind and solar—to achieve continuous and reliable power generation. The key components of this system include a Vertical Axis Wind Turbine (VAWT), solar panels, advanced power electronics, and a lithium-ion battery storage system. Each component plays a critical role in ensuring the system's efficiency, scalability, and adaptability to varying environmental conditions.

2.1 Vertical Axis Wind Turbine (VAWT)

The Vertical Axis Wind Turbine is a pivotal component of the hybrid system. Unlike traditional Horizontal Axis Wind Turbines (HAWTs), VAWTs are uniquely suited for urban and highway environments due to their compact design and ability to capture

wind from any direction. This omnidirectional capability makes them particularly effective in locations with turbulent or variable wind patterns, such as those generated by vehicular movement on highways.

- **Design and Placement:**
  - The VAWT is strategically placed along highway medians or atop streetlight poles, where it can harness the wind generated by passing vehicles. This placement maximizes energy capture while utilizing existing infrastructure, minimizing land usage.

2.2 Solar Panels

Solar panels are another cornerstone of the hybrid system, capturing sunlight during the day to generate electricity. These panels are mounted atop the turbine structure to optimize space usage and enhance system efficiency.

- **Design Features:**
  - The panels are installed at an optimal tilt angle (typically between 30° and 45°) to maximize solar radiation capture. In some cases, adjustable or tracking systems can be incorporated to further improve performance by aligning the panels with the sun's position throughout the day.
- **Integration with VAWT:**
  - The solar panels and wind turbine share a common frame, simplifying installation and reducing costs. This integrated design also ensures that both energy sources can operate simultaneously without interference.

2.3 Advanced Power Electronics

Power electronics are integral to the hybrid system, enabling efficient energy conversion, storage, and distribution. The main power electronic components include:

- **Buck-Boost Converters:**
  - These converters regulate the voltage levels from the energy sources to ensure compatibility with the battery storage system and the load. They can step up or step down the voltage as required, maintaining a stable power supply.
- **Reverse Voltage Protection:**
  - Protective diodes are included to prevent damage to the system in the event of reverse current flow, ensuring the longevity of the components.

3. Methodology

The development of a hybrid renewable energy system involves a structured and multidisciplinary approach to ensure the effective integration of solar and wind energy. This section details the methodologies employed in the design, simulation, and implementation of the system, focusing on structural modelling, energy flow analysis, and the optimization of power electronics and storage systems.

3.1Power Electronics Integration

The hybrid system relies on advanced power electronics to ensure efficient energy conversion, storage, and delivery. The following components are critical to the system's operation:

- **Buck-Boost Converters:**
  - These converters regulate the voltage levels from the energy sources, stepping them up or down as needed to match the battery storage system or the connected load.
- **Protections and Safeguards:**
  - Reverse current protection and over-voltage/under-voltage protection circuits are included to enhance system safety and reliability.

3.2Battery Storage System

The energy storage system plays a critical role in balancing the intermittency of renewable energy sources, ensuring a stable power supply during periods of low energy generation.

- **Lithium-Ion Battery Selection:**
  - Lithium-ion batteries are chosen for their high energy density, long lifespan, and efficiency. The battery bank is sized based on the expected energy demand and storage requirements.
- **Battery Management System (BMS):**
  - The BMS monitors battery performance, including voltage, current, and temperature, to prevent overcharging, deep discharging, and overheating. It also manages the charging and discharging cycles to extend battery life.

4. Results and Discussion

The implementation and testing of the hybrid renewable energy system yielded promising results, demonstrating significant improvements in energy efficiency, environmental impact, and economic feasibility. This section provides a detailed analysis of the experimental results, focusing on the system's performance metrics, environmental benefits, and cost-effectiveness.

4.1Energy Efficiency

- **Improved Efficiency:**
  - The hybrid system achieved a 35% improvement in energy efficiency compared to standalone solar or wind systems. This improvement is attributed to the complementary nature of the dual energy sources, which reduces energy wastage and ensures consistent power generation under varying environmental conditions.
- **Continuous Energy Supply:**
  - The hybrid design mitigated the intermittency issues commonly associated with standalone systems. Solar panels provided consistent energy during the day, while the Vertical Axis Wind Turbine (VAWT)

captured wind energy during both day and night, particularly in areas with vehicular movement.

- The integration of a lithium-ion battery storage system ensured uninterrupted power supply during periods of low sunlight and wind.

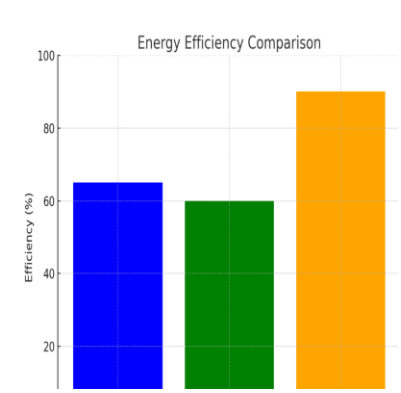

This bar graph shows that the hybrid system achieves 90% efficiency, significantly higher than standalone solar (65%) and standalone wind systems (60%). The hybrid system's complementary use of solar and wind ensures continuous energy generation, overcoming the limitations of standalone systems.

4.2Environmental Impact

- **Reduction in CO_2 Emission:**
  - By replacing conventional grid electricity and fossil fuel-based systems, the hybrid system reduced CO2 emissions by approximately 40%. This significant reduction contributes to global efforts to combat climate change and transition to sustainable energy sources.
- **Utilization of Clean Energy:**

The hybrid system leveraged renewable energy resources, reducing reliance on non-renewable energy and decreasing the overall carbon footprint of energy Production.

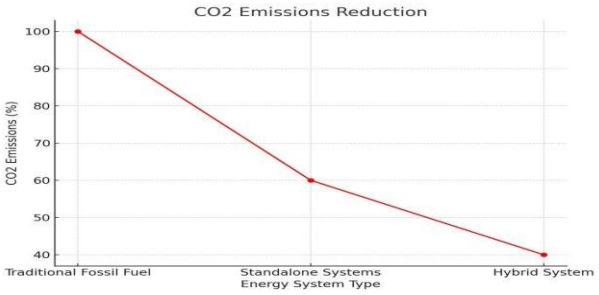

The line graph demonstrates that hybrid systems reduce CO2 emissions to 40%, compared to standalone systems (60%) and fossil fuel systems (100%). This highlights the hybrid system's ability to generate clean energy consistently, minimizing greenhouse gas emissions.

4.3 Economic Analysis

- **Cost Recovery:**
  - The economic analysis revealed that the system achieves cost recovery within 3 -5 years, depending on the scale of deployment and local

energy costs. This short payback period enhances the system's attractiveness for commercial and government-funded projects.

- **Maintenance Costs:**
  - The hybrid system's low-maintenance design, particularly the VAWT's durable construction and minimal moving parts, further contributed to cost savings over the system's lifespan.

5.Challenges and Limitations

- **Energy Storage Dependence and Efficiency Optimization:**
  - While the lithium-ion battery system effectively manages energy storage and supply, the cost and lifespan of batteries remain a concern. Further advancements in energy storage technologies are needed to enhance affordability and sustainability.
  - The efficiency of VAWTs in low-wind conditions and turbulent environments can still be improved.

6.Conclusion

The hybrid renewable energy generation system, which integrates Vertical Axis Wind Turbines (VAWTs) and solar panels, represents a groundbreaking approach to sustainable energy production. The dual-source design ensures continuous energy generation, making it a reliable and eco-friendly solution that reduces dependency on fossil fuels and minimizes greenhouse gas emissions.

7.Acknowledgement

We would like to extend our heartfelt appreciation to everyone who helped finish the research work. First of all, we would like to express our gratitude to our project Guide Prof. Mrs. S. Malathi for advice and assistance over the course of the project. We also want to express our gratitude to department of ECE, National Engineering College, India for providing us full support and knowledge in this Hybrid Renewable energy generation with Power Electronics Integration.

8. References

1. Tang, Z., Yang, Y., & Blaabjerg, F. (2021). Power electronics: The enabling technology for renewable energy integration. CSEE Journal of Power and Energy Systems, 8(1), 3952.
2. Blaabjerg, F., & Chen, Z. (2003). Power electronics as an enabling technology for renewable energy integration. Journal of Power Electronics, 3(2), 81-89.
3. Blaabjerg, F., Yang, Y., Ma, K., & Wang, X. (2015, November). Power electronics-the key technology for renewable energy system integration. In 2015 International Conference on Renewable Energy Research and Applications (ICRERA) (pp. 1618-1626). IEEE.
4. Mehrasa, M, Pouresmaeil, E, Sepehr, A, Pournazarian,B., & Catalão,J. P. (2019).Control of power electronics-based synchronous generator for the

integration of renewable energies into the power grid. International Journal of Electrical Power & Energy Systems,111,300-314.

5. Esmaili, G. (2006).Application of advanced power electronics in renewable energy sources and hybrid generating systems (Doctoral dissertation, The Ohio State University).
6. Chakraborty, A. (2011). Advancements in power electronics and drives in interface with growing renewable energy resources. Renewable and Sustainable Energy Reviews, 15(4), 1816-1827.
7. Krishnamurthy, K.,Padmanaban, S.,Blaabjerg, F., Neelakandan, R. B., & Prabhu, K. R. (2019). Power electronic converter configurations integration with hybrid energy sources–
   a comprehensive review for state-of the-art in research. Electric Power Components and Systems, 47(18), 1623-1650.

SVM-Based Anomaly Detection for Network Intrusion Systems: An Advanced Approach to Intrusion Prevention

Arihant Singhvi, Abhinav Nambiar, Pranav Menon, Narendra V G

Dept of Computer Science and Engineering , Manipal Institute of Technology, Manipal Academy of Higher Education, Manipal, Karnataka, 576104, India

Abstract.

This project develops an SVM-based IDS for anomaly detection, addressing limitations of signature-based methods in identifying new threats. Trained on labeled network traffic, it accurately distinguishes normal from anomalous patterns with minimal false positives. Key challenges like data quality, computational demands, and preprocessing complexity are tackled through careful data selection. The system is scalable, adaptive, and enhances network security by detecting emerging threats.

Keywords. Anomaly-Based Network Intrusion Detection System (A-NIDS), SVM, Naïve-bayes

1. INTRODUCTION

This project develops an SVM-based Anomaly Detection IDS to overcome the limitations of signature-based methods in detecting novel threats. Unlike traditional IDS, it identifies deviations from normal network behavior, enabling detection of zero-day attacks. SVM's robustness in high-dimensional data ensures precise classification of normal and anomalous traffic. Trained on labeled network data, the system adapts to evolving threats. Rigorous preprocessing enhances data quality, and performance evaluation confirms high accuracy with minimal false positives, providing a scalable and effective network security solution.

2. LITERATURE SURVEY

As cyber threats evolve, robust Intrusion Detection Systems (IDS) are crucial. Traditional signature-based methods fail against novel attacks, prompting the use of machine learning. SVM-based IDS map input data into high-dimensional space, outperforming Naïve Bayes [1]. Alternative models like RF, DT, and MLP have varying accuracy on KDD Cup '99 and NSL-KDD datasets [2][3][6]. High computational costs and redundant features challenge SVM-based IDS, mitigated by hybrid feature selection using K-means and IGR [4]. A pipeline-based approach enhances performance by filtering destructive data [5]. Kernel choice impacts accuracy, with RBF performing best (99.11%) on KDD Cup '99 [7]. However, outdated datasets should be replaced by modern alternatives like CICIDS2017, which includes DDoS, XSS, and SQL Injection. Deep learning-based IDS using UNSW-NB15 and CNNs have shown promising accuracy (95.4%-95.6%) [8].

3. METHODOLOGY

3.1. Dataset

We use the CSE-CIC-IDS 2018 dataset, which systematically generates profiles for normal and attack network behaviors. It contains 80 features and over 1 million entries, with no null values. Key features include destination port, protocol, flow duration, and packet counts. The dataset categorizes patterns as:

- **Normal:** Benign
- **Attack:** DoS-GoldenEye, DoS-Slowloris

3.2. Preprocessing

Dropped the ‘Timestamp’ column, converted ‘Label’ to binary, applied one-hot encoding, analyzed feature correlation, split data (33% train, 67% test), handled infinite values by imputing with the mean, and standardized features.

3.3. Hyperparameter Tuning of SVM Model

The SVM model is then developed using the Radial Basis Function (RBF) kernel, specifically Gaussian RBF, selected for its ability to handle the non-linear nature of network traffic data. The model is trained on the labeled dataset with a focus on accurately distinguishing between normal and anomalous traffic. To optimize the model, we employ cross-validation techniques to fine-tune hyperparameters such as the penalty parameter (C) and kernel coefficient (gamma).

The formula for RBF kernels between 2 feature vectors x and x' is given by: The equation should be submitted in the equation editor and should be keyed in as below in editable text:

$$A_0 = \frac{\mu_0 \omega I_0}{4\pi} = 10^{-7} \omega I_0 K(x, x') \; = \; e^{-\gamma \|x - x\prime\|^2}$$

where:

- $\|x - x'\|^2$ is the squared Euclidean distance between the two feature vectors x and x'.
- γ (gamma) is a parameter that determines the influence of each training example

Name	Abbreviation	Formula
Cubic	CU	$\varphi(r) = r^3$
Thin plate splines	TPS	$\varphi(r) = r^2 \log(r)$
Generalized Thin plate splines	GTPS	$\varphi(r) = r^{2m} \log(r), \quad m \in N$
Inverse quadrics(or Cauchy)	IQ	$\varphi(r) = \frac{1}{c^2 + r^2}$
Multiquadrics	MQ	$\varphi(r) = \sqrt{c^2 + r^2}$
Inverse Multiquadrics	IMQ	$\varphi(r) = \frac{1}{\sqrt{c^2 + r^2}}$
Gaussian RBF	GA	$\varphi(r) = e^{-r^2/c^2}$

Definition 2.2 *θ -method, (0 ≤ θ ≤ 1), is general finite-difference approximation to* $\frac{\partial^2 u(x,t)}{\partial x^2}$ *given by:*

$$\frac{\partial^2 u(x,t)}{\partial x^2} \cong \theta \delta_{2,x} U_{i,j+1} + (1 - \theta) \delta_{2,x} U_{i,j},$$

Figure 1. Different Types of RBF kernel functions

The RBF kernel enables linear separation in a higher dimension without explicit transformation. Regularization (C) balances misclassification and overfitting, while gamma controls the influence range, affecting sensitivity and generalization. GridSearchCV optimizes C and gamma using a parameter grid with an RBF kernel and 5-fold cross-validation, ensuring optimal hyperparameters for maximum accuracy. Efficiency metrics vary by system: spectral efficiency for wireless, joules per bit for electronics, and watts per Gbps for datacenters, with dBε as a universal measure of energy efficiency.

4. RESULTS AND OBSERVATIONS

The SVM-based IDS is evaluated using performance metrics such as accuracy, precision, recall, F1-score, and ROC-AUC, with particular emphasis on minimizing the false positive rate while maintaining high detection accuracy. After obtaining the best model by optimizing the hyperparameters, its performance is estimated against the testing set. The model has been found to achieve exceptional performance with an accuracy of 99.99% on the training set. The model shows similar results in precision, accuracy and recall as provided by the classification report.

4.1. Classification Metrics

The SVM-based IDS is evaluated using accuracy, precision, recall, F1-score, and ROC-AUC, prioritizing minimal false positives while maintaining high detection accuracy. The optimized model achieves **99.99% accuracy** on the training set and similar precision and recall.

Classification Metrics:

- **Normal (Class 0)** & **Attack (Class 1):** Precision, Recall, and F1-Score = **1.00**

- **Confusion Matrix:**
  - **True Positives:** 17,205
  - **True Negatives:** 328,787
  - **False Positives:** 29
  - **False Negatives:** 9

The **ROC-AUC** is **1.00**, indicating perfect classification.

Model Comparisons:

- **SVM (Polynomial Kernel):** 99.99% accuracy
- **Random Forest:** 100% accuracy
- **Logistic Regression:** 99.80% accuracy
- **XGBoost:** 99.88% accuracy

The SVM model with the RBF kernel delivers exceptional accuracy, comparable only to the Random Forest model, benefiting from effective data preprocessing.

RBF Kernel Accuracy: 99.99%

	precision	recall	f1-score	support
0	1.00	1.00	1.00	328816
1	1.00	1.00	1.00	17214
accuracy			1.00	346030
macro avg	1.00	1.00	1.00	346030
weighted avg	1.00	1.00	1.00	346030

Figure 2. Classification Report of SVM model

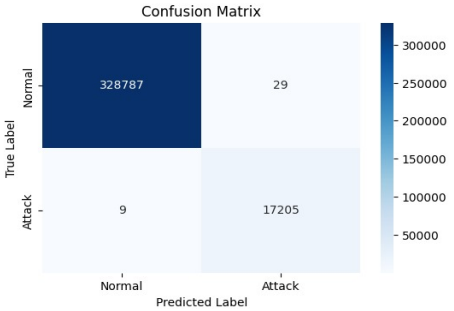

Figure 3. Confusion Matrix

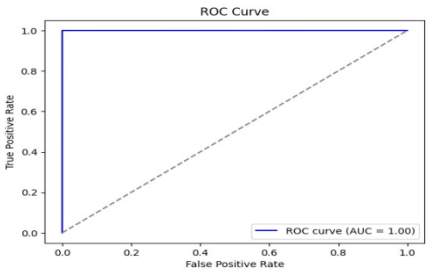

Figure 4. ROC curve of SVM model

5. CONCLUSION

This project implements an SVM-based IDS for real-time network security using an anomaly-based approach to detect unknown threats. Rigorous data preprocessing and model training ensure accurate classification of network traffic. Evaluation metrics confirm high detection accuracy with minimal false alarms. The IDS overcomes traditional limitations by being scalable and adaptive, enhancing threat detection. Challenges like limited resources, data labeling, and evolving threats are addressed through algorithm optimizations, ensuring reliable performance in dynamic environments, unlike signature-based methods.

6. REFERENCES

[1] A. Halimaa A. and K. Sundarakantham, "Machine Learning Based Intrusion Detection System," 2019 3rd International Conference on Trends in Electronics and Informatics (ICOEI), Tirunelveli, India, 2019.

[2] A. S. Ahanger, S. M. Khan and F. Masoodi, "An Effective Intrusion Detection System using Supervised Machine Learning Techniques," 2021 5th International Conference on Computing Methodologies and Communication (ICCMC), Erode, India, 2021.

[3] Ngueajio, M.K., Washington, G., Rawat, D.B., Ngueabou, Y. (2023). "Intrusion Detection Systems Using Support Vector Machines on the KDDCUP'99 and NSL-KDD Datasets: A Comprehensive Survey". In: Arai, K. (eds) Intelligent Systems and Applications. IntelliSys 2022.

[4] Jha, Jayshree, and Leena Ragha. "Intrusion detection system using support vector machine." International Journal of Applied Information Systems (IJAIS) 3 (2013): 25-30.

[5] Ajdani, Mahdi, and Hamidreza Ghaffary. "Design network intrusion detection system using support vector machine." International Journal of Communication Systems 34.3 (2021): e4689.

[6] Hasan, M., Nasser, M., Pal, B. and Ahmad, S., "Support Vector Machine and Random Forest Modeling for Intrusion Detection System (IDS)", Journal of Intelligent Learning Systems and Applications, 2014.

[7] Almaiah, Mohammed Amin, et al. "Performance investigation of principal component analysis for intrusion detection system using different support vector machine kernels." Electronics 11.21 (2022): 3571

[8] Lirim Ashiku, Cihan Dagli, "Network Intrusion Detection System using Deep Learning", Procedia Computer Science Volume 185, 2021.

Personalized Hairstyle Recommendation System using Face Shape Classification

Rayaan Mohammad Salem[1], Rishabh Singh[1], Kavya Bansal[1], and Narendra VG[1]

[1]Dept of Computer Science and Engineering , Manipal Institute of Technology, Manipal Academy of Higher Education, Manipal, Karnataka, 576104, India

ABSTRACT

This project proposes a hairstyle recommendation system utilizing face shape classification, supported by computer vision and machine learning. The system categorizes faces into five primary shapes—heart, oblong, oval, round, and square—by employing image processing techniques such as hair detection, skin masking, Gaussian blur, and Canny edge detection to accurately map the hairline. Using 68 detected facial landmarks on input images, we compute 19 geometric features that effectively capture distinct facial structures.

Our preprocessing pipeline includes histogram equalization, Principal Component Analysis (PCA), and hyperparameter optimization. We evaluate several classifiers, including Support Vector Machine (SVM) with linear, polynomial, and RBF kernels, along with a Random Forest classifier, to identify the most effective model for accurate face shape classification. Once classified, the system overlays selected hairstyles—sourced from online recommendations—directly onto the input image, adjusted based on the detected hairline and facial width to provide a realistic preview. Additionally, K-Nearest Neighbors (KNN) is used to identify the top five similar faces in the dataset, offering style inspiration through matching celebrity faces. Built with Streamlit, the user interface delivers an interactive and accessible platform for showcasing personalized hairstyle recommendations and celebrity comparisons.

Keywords: Hairstyle Recommendation, Face Shape Classification, Image Processing, Facial Landmarks, SVM, Random Forest, KNN, Streamlit.

1. INTRODUCTION

In today's fast-paced digital world, personal style is key to expressing individuality and enhancing self-image, with hairstyling playing a prominent role in grooming. Choosing the right hairstyle, however, can be a challenge for many, often relying on subjective opinions or trial and error, which may result in dissatisfaction. The absence of personalized guidance, particularly in relation to face shape, complicates this process further.

As the demand for personalized beauty solutions rises, technology offers a promising approach to this challenge. This project introduces a Personalized Hairstyle Recommendation System that uses computer vision and machine learning to suggest hairstyles based on a person's face shape. The system classifies faces into five categories—heart, oblong, oval, round, and square—by analyzing facial landmarks and geometric features. By doing so, it offers a tailored, data-driven method for choosing hairstyles that complement an individual's facial structure.

The system not only simplifies the decision-making process but also aligns with the growing trend of virtual try-ons and personalized experiences in the digital age. With an intuitive Streamlit interface, users can seamlessly explore hairstyle recommendations that best suit their face shape, gaining style inspiration by matching their features to celebrity faces with similar characteristics.

This project aims to empower individuals to feel more confident in their appearance, while demonstrating the potential of artificial intelligence in the beauty and fashion industry. Further details on the methodology and implementation of the system are discussed in the following sections.

2. RELATED WORK

This work builds upon previous studies in the field of face shape classification for personalized hairstyle recommendation systems, particularly drawing inspiration from a framework that utilizes Support Vector Machine (SVM) classifiers for face shape classification based on extracted features. In the referenced study, the authors explored a combination of hand-crafted and deep-learned features for improved classification performance, with techniques such as Multiple Kernel Learning (MKL) and hyperparameter optimization. [1], [2], [3]

Our approach follows a similar high-level strategy but differs in several key aspects. Unlike the referenced work, we focus exclusively on hand-crafted features derived from facial landmarks, avoiding deep-learned features like VGG-face. We conducted a comparative study on various classification algorithms, including SVM with different kernels (linear, polynomial, and RBF), as well as a Random Forest classifier. This broader selection of models allows us to assess the strengths and weaknesses of different classifiers in the context of face shape classification, and to determine which performs best on our dataset.

[4], [5], [6]

To further enhance the performance of our models, we incorporated hyperparameter optimization. While the cited paper used Particle Swarm Optimization (PSO), we employed grid search to fine-tune the hyperparameters of our classifiers, which allowed us to systematically explore different parameter settings and identify the most effective combinations for each model.

Another novel contribution of our work is the use of K-Nearest Neighbors (KNN) to identify and display the top similar faces from a database of celebrity images. This feature not only aids in face shape classification but also provides users with personalized style recommendations by matching them to celebrity faces with similar facial structures. This addition offers an interactive and engaging aspect to the system that was not present in the original framework.

In addition to the classification models and KNN, we also introduced preprocessing techniques such as histogram equalization and adaptive histogram equalization, which helps improve image contrast before facial landmark detection. This preprocessing step enhances the clarity of facial features and helps achieve more accurate landmark detection, ultimately improving the performance of the face shape classification task. [7]

In summary, while our methodology is inspired by the previous work in face shape classification, we have expanded upon it by exploring different classifiers, adding KNN for celebrity face matching, and incorporating preprocessing steps to optimize the classification process. These innovations aim to improve the overall accuracy and user experience of our personalized hairstyle recommendation system.

3. DATASET

The dataset consists of five categories, each representing a major face shape—oval, round, square, oblong, and heart—with 100 celebrity images per category, totaling 500 labeled images. Expert-classified for accuracy, it primarily features female faces due to the lack of a comprehensive male dataset. Consequently, the recommendation system is optimized for female faces and hairstyles. The open-source dataset, available on GitHub, is well-organized for face shape classification experiments. Source: GitHub - dsmlr/faceshape.[1]

4. METHODOLOGY

In our project, various image processing and machine learning techniques were employed to enhance facial landmark detection, extract meaningful facial features, and perform classification and recommendation tasks. The methodology consists of sequential steps designed to improve image quality, accurately identify facial landmarks (including the hairline as a 69th landmark), and extract geometric features that define face shape. These features are then used for classification into predefined categories and for finding similar images. The following sections outline the key steps undertaken in this process.

4.1 Preprocessing

This step in our project is supposed to preprocess images to improve their quality for better landmark detection and feature extraction in an image. Here are the techniques used:

- Grayscale Conversion**:** The image uploaded is first converted to grayscale by OpenCV. This approach simplifies computation by only working on one channel (intensity) instead of three (RGB). It is sufficient for facial landmark detection.
- Histogram Equalization**:** Histogram equalization enhances contrast in the grayscale image, improving landmark detection under varying lighting. Adaptive histogram equalization (CLAHE) was tested but showed little improvement, so standard histogram equalization was used.

4.2 Landmark Detection using CV Techniques

The hairline detection method uses several techniques to enhance the accuracy and robustness of the facial landmark system:

Facial Landmark Detection

- **Detector:** Utilizes a pre-trained dlib shape predictor to detect 68 facial landmarks, which represent key facial points such as the eyes, nose, mouth, and jawline.[8]
- **Method:** For each detected face, the model returns a set of landmarks (coordinates) to mark specific facial features.

Hairline Detection and Integration as the 69th Landmark`

- **Detection of forehead region:** The forehead region is identified by the midpoint between the eyebrows (landmarks 19 and 24). The x-coordinate of the midpoint is the average of the x-coordinates of landmarks 19 and 24, and the y-coordinate is 20 pixels above landmark 19. This region helps in localizing the forehead and detecting the hairline in the subsequent steps.
- **Skin Masking:** The image is converted from BGR to HSV to isolate skin color, which aids in identifying regions of interest such as the forehead. The mean skin color of the forehead region is calculated to dynamically determine the skin color range. A skin mask is then created using this dynamically determined skin color range. To improve the mask's quality, Gaussian blur is applied to smooth edges and reduce noise, ensuring better accuracy in the hairline detection process. [9]
- **Canny Edge Detection:** Canny edge detection is applied to the blurred skin mask to find the skin-to-hair boundary. [10]
- **Scanning Upward:** The algorithm scans upward from the forehead region to detect where the skin transitions to hair, marking this as the hairline. If no edge is found, a default position 50 pixels above the forehead is used. [11]
- **Adding the Hairline as the 69th landmark:** After detecting the hairline's y-coordinate, it is added as the 69th landmark i, with the x-coordinate matching the forehead's x-coordinate.

4.3 Feature Extraction

Once the landmarks are identified, we compute a set of geometric features that represent the shape of the face. These features include distances and ratios between key landmarks, as well as angles formed between the chin and other facial points. Out of the 69 landmark points located, only the first 17 points, which outline the face, are used for feature extraction. Additionally, two more points are used: point 58, which corresponds to the bottom of the mouth, and point 69, which corresponds to the hairline. These features are then used to create a feature vector, which serves as a descriptor of the user's face shape. The following features are considered:

- **Face Height to Width Ratio:** The ratio of the height of the face to the width is calculated as

$$F_1 = \frac{p_9 - p_{69}}{p_1 - p_{17}}$$

where p_8 and p_{68} represent the vertical points, and p_1 and p_{17} are the horizontal points of the face.

- **Jaw Width to Face Width Ratio:** The ratio of the distance between both sides of the jaws to the width of the face is calculated as

$$F_2 = \frac{p_5 - p_{13}}{p_1 - p_{17}}$$

where p_5 and p_{13} represent the points on both sides of the jaw, and p_1 and p_{17} are the horizontal points of the face.

- **Chin to Mouth Bottom to Jaw Width Ratio:** The ratio of the distance between the chin and the bottom of the mouth to the distance between both sides of the jaws is calculated as

$$F_3 = \frac{p_9 - p_{58}}{p_5 - p_{13}}$$

where p_9 and p_{58} represent the vertical points (chin and bottom of the mouth), and p_5 and p_{13} are the points on both sides of the jaw.

- **Angles Between Point 9 and Points 1-8:** The angles between point 9 (the chin) and points 1-8 (which represent the points along the left jawline and facial contour) give the features F4 - F11.

- **Angles Between Point 9 and Points 10-17:** The angles between point 9 (the chin) and points 10-17 (which represent the points along the right jawline and facial contour) give the features F12 - F19.

These 19 features will now be made used to make the feature descriptor which will be used for classification into the face shapes.

4.4 Classification

The extracted features were fed into five machine learning classifiers for defect classification:

- **Support Vector Machine (SVM)** with linear kernel
- **Support Vector Machine (SVM)** with polynomial kernel
- **Support Vector Machine (SVM)** with RBF kernel
- **Random Forest (RF)**
- **K-Nearest Neighbors (KNN)**

Before feeding the features into the models, we standardized them using a Standard Scaler, ensuring that each feature contributes equally to the classification process. Following scaling, Principal Component Analysis (PCA) was applied to reduce the feature dimensions, improving computational efficiency while retaining essential information. [12]

To determine the optimal number of components for PCA, we calculated the cumulative explained variance by iterating over all components. This process involved plotting the cumulative explained variance ratio to visualize the point at which additional components contribute minimally to the explained variance, thus guiding our selection of the reduced feature count.

Finally, to optimize each classifier's performance, we performed hyperparameter tuning using Grid Search Cross-Validation. This process identified the most effective configurations for each model, enhancing classification accuracy and ensuring the models could generalize effectively to unseen data.

4.5 Haircut Overlay

The haircut overlay function overlays a hairstyle image onto the original image based on facial landmarks and predefined parameters. This process involves the following key steps:

Head Width Calculation

The head width is calculated using the distance between the two outermost facial landmarks (landmarks 1 and 17), providing an approximation of the head's width. This width is essential for scaling the hairstyle image to match the person's face.

Resizing the Hairstyle Image

Using the head width and the known width of the hairstyle (from the CSV), a scale factor is calculated. This factor ensures that the hairstyle image will match the width of the person's head. The hairstyle image is then resized according to this scale factor.

Overlaying the Hairstyle

The hairstyle is overlaid onto the person's face by calculating the appropriate position based on the hairline landmark (69th landmark) and predefined parameters. The overlay process ensures proper alignment and scaling to fit the person's face, providing a seamless appearance. To achieve the most natural overlay, various interpolation methods were tested, including nearest-neighbor interpolation, bilinear interpolation, and bicubic interpolation. After experimentation, Lanczos interpolation was chosen for its visual quality compared to the others. [11]

4.6 Finding Similar Images Using KNN

The system employs the K-Nearest Neighbors (KNN) algorithm to recommend similar faces based on extracted feature vectors. For each image in the dataset, a feature vector is generated to capture key facial characteristics. When a new query image is provided, its feature vector is compared against the dataset using the Euclidean distance metric to measure similarity. The KNN algorithm then ranks the dataset images based on their proximity to the query image, retrieving the top 'n' nearest neighbors (default: 5). These nearest images are returned as the most similar matches, enabling efficient and accurate face similarity retrieval.

5. EXPERIMENTS AND RESULTS

The image in Fig. 1 represents the 69 points detected in the facial landmark detection stage of the project. For the feature extraction part of the project, we will only be using points 1-17, 58, and 69. These selected landmarks will be used to extract specific facial features that are crucial for the subsequent stages of classification.

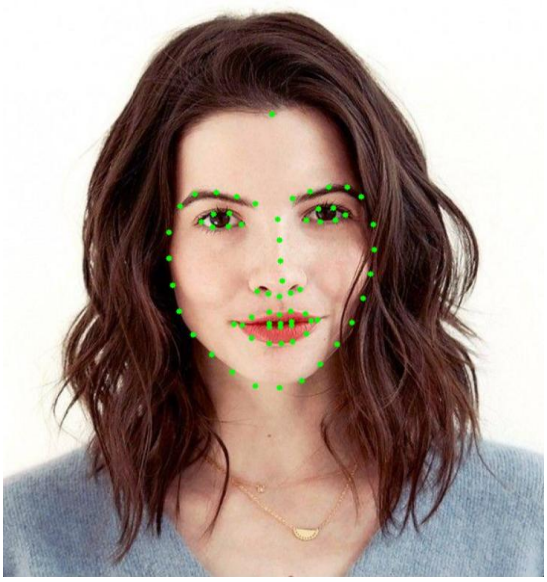

Fig. 1. Facial Landmark Detection (69 Facial Landmarks)

To determine the optimal number of principal components for dimensionality reduction, we applied Principal Component Analysis (PCA) on the feature dataset. The cumulative explained variance plot in Fig. 2

illustrates how much of the total variance is explained by each successive principal component. Based on this analysis, we determined that reducing the dimensions to 12 components captured approximately 99% of the total variance, striking a balance between simplifying the model and retaining significant information in the data.

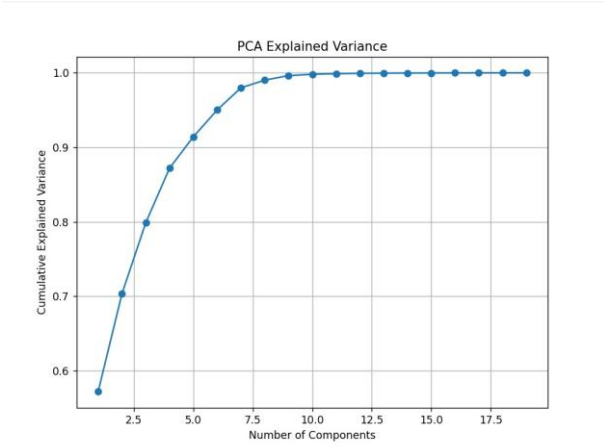

Fig. 2. Cumulative Explained Variance of Principal Components (PCA)

Feature scaling was applied to the dataset to ensure uniformity across different classifiers. The crossvalidation accuracy for each model, providing an average measure of model consistency across multiple data folds, is presented in Table 1. Subsequently, Table 2 shows the classification accuracy on the test set after an 80-20 train-test split, reflecting each model's performance on unseen data.

Table 1. Cross-Validation Accuracy Comparison for Different Models

Model	Cross-Validation Accuracy (%)
SVM with linear kernel	60.1
SVM with RBF kernel	61.4
SVM with polynomial kernel	54.4
Random Forest	60.4
K-Nearest Neighbors (KNN)	46.1

Table 2. Test Set Accuracy Comparison for Different Models

Model	Test Set Accuracy (%)
SVM with linear kernel	61.9
SVM with RBF kernel	62.9
SVM with polynomial kernel	51.5
Random Forest	61.9
K-Nearest Neighbors (KNN)	45.4

The detailed classification reports for each model are shown in Table 3.

Table 3. Classification Report Comparison

Class	SVM Linear			SVM RBF			SVM Poly			Random Forest			KNN		
	Prec	**Rec**	**F1**	**Prec**	**Rec**	**F1**	**Prec**	**Rec**	**F1**	**Prec**	**Rec**	**F1**	**Prec**	**Rec**	**F1**
Heart	0.62	0.50	0.56	0.55	0.60	0.57	0.45	0.50	0.48	0.58	0.55	0.56	0.33	0.35	0.34
Oblong	0.65	0.75	0.70	0.65	0.65	0.65	0.73	0.55	0.63	0.70	0.80	0.74	0.52	0.70	0.60
Oval	0.38	0.42	0.40	0.45	0.47	0.46	0.27	0.37	0.31	0.43	0.32	0.36	0.21	0.21	0.21
Round	0.61	0.61	0.61	0.81	0.72	0.76	0.64	0.50	0.56	0.69	0.61	0.65	0.67	0.44	0.53
Square	0.84	0.80	0.82	0.74	0.70	0.72	0.65	0.65	0.65	0.64	0.80	0.71	0.61	0.55	0.58
Average	0.62	0.62	0.62	0.64	0.63	0.63	0.55	0.51	0.53	0.61	0.62	0.61	0.47	0.45	0.45
Accuracy	0.62			0.63			0.52			0.62			0.45		

The classification output for the example image is displayed in the Streamlit front end, where the system predicts the most suitable hairstyle based on the extracted facial features. After processing the input image, the model classifies the user's head shape and recommends a hairstyle accordingly. The following Fig. 3, showcase the classification result for the example image, along with the suggested hairstyle based on the model's prediction.

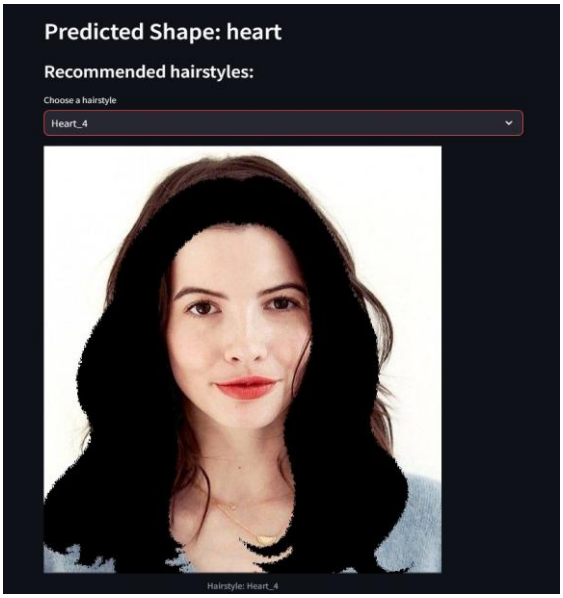

Fig. 3. Classification Output (Recommended Hairstyle 1)

Additionally, the top similar faces from the dataset based on the K-Nearest Neighbors (KNN) algorithm are showcased in the following Fig. 4. This image presents the Streamlit output displaying the most similar faces, which can be used as references for hairstyle recommendations, providing further insights into the facial features that align with the predicted head shape.

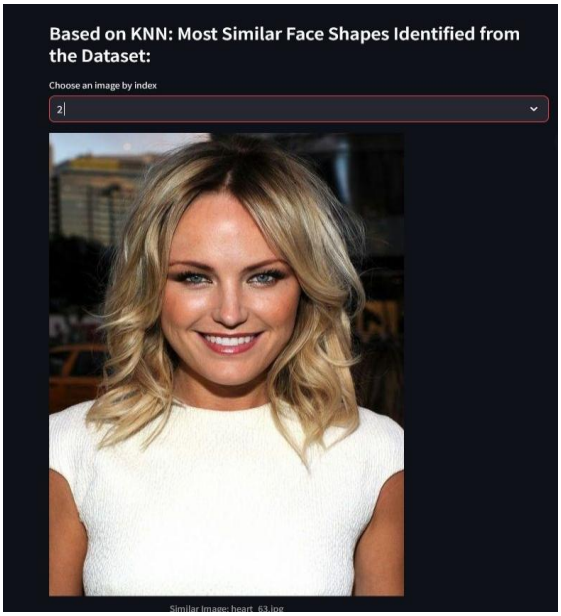

Fig. 4. Top Similar Faces (KNN Output)

6. DISCUSSION

The facial landmark detection approach, using 69 key points, enabled the extraction of crucial features for classification. We selected relevant landmarks (points 1-17, 58, and 69) to capture essential facial structures for accurate head shape classification, aiding hairstyle prediction.

To reduce dimensionality, we applied PCA, retaining 12 components that preserved 99% of the variance, balancing efficiency and performance. Among the tested models, SVM with an RBF kernel achieved the highest test accuracy (62.9%), making it the preferred choice for prediction.

7. LIMITATIONS AND FUTURE WORK

The proposed system effectively recommends and overlays hairstyles but has limitations. It assumes a perfectly aligned frontal face, making misalignments affect accuracy. The model is trained only on female faces, limiting applicability to males; expanding the dataset would improve inclusivity. Additionally, it overlays black hairstyles regardless of the user's hair color, reducing realism. The current study employs only machine learning models for classification, leaving room for improvement in accuracy. Future work should explore ensemble methods and deep learning models, address image orientation adjustments, incorporate diverse datasets, and develop hair color-matching techniques to enhance accuracy and personalization.

8. CONCLUSION

The Hairstyle Recommendation System developed in this project demonstrates a comprehensive approach to personalized hairstyle suggestions based on face shape classification. The system leverages advanced computer vision techniques, including facial landmark detection, skin color segmentation, and edge detection, to accurately analyze the user's facial features and detect a hairline.

The user interface, built with Streamlit, provides a seamless experience for users to upload their images, view face landmarks, and explore hairstyle recommendations based on their face shape. The combination of facial feature analysis, machine learning, and personalized recommendations offers a novel and practical solution for individuals seeking hairstyle suggestions.

In conclusion, the Hairstyle Recommendation System is an innovative application of computer vision and machine learning that combines facial feature analysis and personalization, ensuring that users receive relevant and suitable hairstyle options based on their unique facial characteristics. Future work can explore the

incorporation of more diverse datasets and further refinements in hairline detection for even more accurate and customized recommendations.

REFERENCES

1. K. Pasupa, W. Sunhem, and C. K. Loo, ”A hybrid approach to building face shape classifier for hairstyle recommender system,” Expert Systems with Applications, vol. 120, pp. 439–449, Nov. 2018, doi: 10.1016/j.eswa.2018.11.011.
2. Kulkarni, Raj. (2024). Recommendation System for Hairstyle Based on Face Recognition Using AI and Machine Learning. International Journal of Software Innovation. 12. 1-10. 10.4018/IJSI.309960.
3. H. Weerasinghe and D. Vidanagama, ”Machine Learning Approach for Hairstyle Recommendation,” 2020 5th International Conference on Information Technology Research (ICITR), Moratuwa, Sri Lanka, 2020, pp. 1-4, doi: 10.1109/ICITR51448.2020.9310868.
4. B. Sch¨olkopf and A. J. Smola, Learning with Kernels: Support Vector Machines, Regularization, Optimization, and Beyond, MIT Press, 2002.
5. Breiman, L. Random Forests. Machine Learning 45, 5–32 (2001). https://doi.org/10.1023/A:1010933404324
6. K. Taunk, S. De, S. Verma and A. Swetapadma, ”A Brief Review of Nearest Neighbor Algorithm for Learning and Classification,” 2019 International Conference on Intelligent Computing and Control Systems (ICCS), Madurai, India, 2019, pp. 1255-1260, doi: 10.1109/ICCS45141.2019.9065747.
7. R. Szeliski, Computer Vision: Algorithms and Applications, 2nd ed., Springer, 2022.
8. I. Silva, ”Facial landmarks recognition,” GitHub repository, [Online]. Available: https:
9. //github.com/italojs/facial-landmarks-recognition/blob/master/shape_predictor_ 68_face_landmarks.dat. Accessed: Nov. 9, 2024.
10. D. Chai and K. N. Ngan, ”Face segmentation using skin-color map in videophone applications,” in IEEE Transactions on Circuits and Systems for Video Technology, vol. 9, no. 4, pp. 551-564, June 1999, doi: 10.1109/76.767122.
11. J. Canny, ”A Computational Approach to Edge Detection,” in IEEE Transactions on Pattern Analysis and Machine Intelligence, vol. PAMI-8, no. 6, pp. 679-698, Nov. 1986, doi: 10.1109/TPAMI.1986.4767851.
12. P. Aarabi, ”Automatic Segmentation of Hair in Images,” 2015 IEEE International Symposium on Multimedia (ISM), Miami, FL, USA, 2015, pp. 69-72, doi: 10.1109/ISM.2015.16.
13. J. Shlens, ”A tutorial on principal component analysis,” arXiv, Apr. 2014. [Online]. Available:
14. https://doi.org/10.48550/arXiv.1404.1100. [Accessed: Nov. 9, 2024].

BIOGRAPHIES



Rayaan Mohammad Salem is a third year Computer Science and Engineering student at Manipal Institute of Technology, specializing in AI and Machine Learning. His interests include Machine Learning, Deep Learning, and Computer Vision, with applications in healthcare, AR, security, and personalized recommendations. He is also passionate about NLP and Generative AI, exploring automated text generation, retrieval-augmented generation (RAG), and conversational AI. Rayaan aims to apply advanced AI techniques to real-world challenges in both vision and language-based systems.



Rishabh Singh is a third-year Computer Science and Engineering (AI ML) student at MIT Manipal. With a strong foundation in machine learning, computer vision, and deep learning, he has worked on multiple innovative projects in robotics and circuit design. His expertise includes developing algorithms for robotics competitions and applying AI-driven technologies in agriculture. Passionate about AgriTech, he integrates computer vision and deep learning models to enhance agricultural practices, aiming to bring technological advancements to the field.





Narendra V G received the B.E. degree in CSE from Karnataka University Dharwad, in 1997, the M.Tech. degree from Visvesvaraya Technological University (VTU), Belgaum, in 2001, and the Ph.D. degree from Manipal University, Manipal, India, in 2017. He is currently a Professor with the Department of Computer Science and Engineering, Manipal Institute of Technology, Manipal Academy of Higher Education, Manipal. His research interests include image processing, ML, soft computing, and computer vision-based applications for agriculture. He is on the editorial board of some journals. He can be contacted at

email: narendra.vg@manipal.edu

Breast cancer detection using an on-body Circular Microstrip Patch Antenna

Somanath Kisan Chikane[1], Dr. Balasaheb H. Patil[2]

[1]*Dept. of Electronics and Telecommunication Engg.*, *SVPM's College of Engineering Malegaon (Bk), Baramati, SPPU* Pune, India, somnathchikane111@gmail.com

[2]*Dept. of Electronics and Telecommunication Engg.*, *VPKBIET, Baramati, SPPU* Pune, India, balasahebpatil960@gmail.com

Abstract.

In medical applications, the early detection of breast cancer plays a vital role in enabling timely treatment and reducing mortality rates among women. With advancements in medical technology, the use of efficient antennas has become integral for imaging, diagnosis, and improving patient outcomes. Since tumors are often small in the initial stages, accurately locating them is essential for effective diagnosis. To address this challenge, various high-precision antennas have been designed. Flexible antennas offer distinct benefits over conventional types, including simple structures, high gain, and cost-effectiveness. The current study introduces an innovative flexible antenna specifically designed for detecting breast cancer at an early stage, applicable for cases both with and without the presence of a tumor. In this design, denim fabric with a dielectric constant of 1.7 is utilized as the substrate to ensure accurate examination and reliability. The antenna structure consists of a circular patch and a copper ground plane serving as the conductive component. We employ a 1 mm thick denim substrate due to its flexibility and suitability for direct application on the breast surface. The design incorporates a microstrip probe feeding technique to enhance overall performance. This wearable textile antenna operates within the Ultra-Wideband (UWB) frequency range of 3.1 GHz to 10.6 GHz. It is modeled and analyzed using CST (Computer Simulation Technology) software. Key performance indicators are looked at in the simulation, such as return loss (S11), gain (dB), radiation pattern, electric field (E-field), magnetic field (H-field), and voltage standing wave ratio (VSWR). Lastly, the results of the simulation are compared with those of existing antenna designs to see if they are better and if they could help find breast cancer earlier.

Keywords. CST Software, UWB, Wearable textile antenna, Breast cancer detection

1. Introduction

Breast cancer is a life-threatening disease caused by the uncontrolled growth of breast tissue, contributing to 25% of all cancer cases worldwide [1]. Early detection significantly improves survival rates, making it a priority in healthcare [2]. Regular screening, like X-ray mammography, has problems, like not being very sensitive in dense breast tissue and having trouble finding tumors close to the chest wall. It also exposes people to ionizing radiation and costs a lot [3, 4]. Microwave imaging has emerged as a promising alternative due to its non-ionizing nature and ability to provide physiological and anatomical insights into breast tissues [5][6]. This technique allows non-invasive detection of abnormalities, though the process can be complex during surgical procedures [7]. Wearable technologies, including flexible antennas, are increasingly used for early breast cancer detection due to their comfort, low power consumption, and potential for real-time monitoring [8][9]. Recent advancements have led to the development of flexible microstrip patch antennas for biomedical applications, including breast cancer detection. These antennas can be integrated into wearable fabrics, providing unobtrusive monitoring and reducing patient discomfort [10][11]. For instance, wearable textile antennas made from jeans fabric as a dielectric substrate have been designed for ultra-wideband (UWB) applications ranging from 3.1 GHz to 10.6 GHz [12]. Copper materials are typically used for the conductive elements, ensuring flexibility and durability [13]. Using CST software to run simulations has shown that antennas work well in terms of gain, return loss (S11), radiation pattern, and voltage standing wave ratio (VSWR) [14]. The flexibility and compactness of wearable antennas make them ideal for continuous health monitoring, aiding early diagnosis, and improving treatment outcomes [15]. These improvements are meant to lower the risks of surgery and

improve patient care, meeting the growing need for flexible, high-performance antennas in medical settings [16, 17].

The subsequent sections of this research are structured as follows: In Section II, pertinent papers and literature about the planned study are examined and cited. This study examines the advantages and disadvantages of several antennas that are currently designed. The suggested implementation is detailed in Section IV. The experimentation prototype and findings are examined in Section V. Section VI serves as the conclusion, encapsulating the summary of the conducted study.

2. RELATED WORK

Abdulla et al. [1] presented a textile-based ultrawideband (UWB) microstrip patch antenna for breast cancer imaging applications in 2024. Simulations evaluated this antenna, operating across 2–11.6 GHz, for its efficiency in early tumor detection. By changing the shape, size, and location of tumors in breast phantoms, its performance was tested using VSWR (between 1.15 and 2), return loss (between −36 and −18.5 dB), and SAR (between 1.6 and 2 W/kg), all of which were within safe medical limits.To detect breast cancer, Fusic et al. [2] created a flexible, wearable polyamide microstrip patch antenna that operates at 2.45 GHz. Simulations showed a gain of 1 dB, a return loss of −14.81 dB, and VSWR ≤ 3. The built prototype showed a resonance at 2.318 GHz and a better return loss of −28.19 dB, which was the same as what the simulation showed.Gour et al. [3] suggested a dual-band wearable microstrip patch antenna with a broken ground structure as a way to find breast tumors. Using an FR4 substrate, the antenna operated at 2.43 GHz and 3.32 GHz with return losses of −35 dB and −24 dB, respectively. SAR values remained within safe limits for wearable applications.Amadaouch et al. [4] made a small, planar, rectangular-shaped UWB antenna system with a high gain for localizing tumors. The frequency range is 3–12 GHz. The system identified tumor locations based on SAR peaks within breast tissue phantoms.For radar-based breast cancer detection, Bahrami et al. [6] created a small, bendable UWB antenna array (2–4 GHz) that can work with either single or dual polarization. The design ensured efficient power transmission and interaction with biological tissues of varying electrical properties.
Wang et al. [7] demonstrated a UWB MIMO antenna for high-resolution imaging that operates between 2.3 GHz and 12.2 GHz. It has unified ground structures that make the coupling loss less than -15 dB.Kaabal et al. [8] proposed mounting a small UWB antenna in the shape of a polygon on an FR4 substrate. This antenna would have dual-band notched properties and a group delay of less than 1 ns. Its effective pulse-preserving properties improve microwave imaging for the detection of breast cancer.Selvaraj et al. [9] looked at how electromagnetic waves interact with breast tissue and transmitting antennas. They found that SAR changes depending on frequency, tumor size, and distance, which helps with pinpointing the exact location of a tumor.Taylor et al. [10] talked about imaging techniques that focused on pixel acquisition times. They said that lung cancer was the most common type of cancer, which meant that better detection technologies were needed.Asha et al. [11] explored the design of microstrip patch antennas for lung tumor detection using CST software. The approach involved monitoring fluctuations in current density, electricity, and magnetic fields to identify malignancies.Shrestha et al. [12] developed a flexible microstrip antenna (32 × 31 mm, 2.45 GHz) for breast cancer imaging and therapy. Experimental validation on skin phantoms confirmed its diagnostic potential.A small microstrip antenna was suggested by Katbay et al. [13] as a way to find breast tumors and make images clearer in different types of tissues.Vidyasree et al. [14] suggested using different kinds of microstrip antennas, like circular, slot, rectangular, hemispherical, and pentagonal arrays that work at different frequencies, to make the process of finding breast cancer more accurate.Susila et al. [15] created a rectangular slot-loaded microstrip antenna using an RT Rogers 5880 substrate. They tested it on breast phantoms to see how the electric (25,167 V/m) and magnetic fields (129 A/m) changed.Gupta et al. [16] created a T-shaped rectangular microstrip antenna to find tumors in the ISM band (2.45 GHz). They proved the effectiveness of the SAR and current density models, and the antenna boasted low losses (32.2 dB). Al Habsi et al. [17] showed a microstrip-fed Vivaldi antenna that was easy to build and had better performance in terms of gain, impedance matching, and VSWR compared to patch designs. Hammouch et al. [18] suggested using an FR-4 substrate with an intelligent UWB antenna (2.96–10.68 GHz) to find breast cancer. We tested this antenna with two electromagnetic solvers to ensure its functionality. Ullah et al. [19] created a 3D folded antenna (1.67–1.74 GHz) for health monitoring. Prototypes showed that it could effectively find malignant tumors in breast phantoms. Singh and his team [20] developed a compact, dual-band textile slot antenna on denim fabric. It has a 5.7 dB gain and works up to 46% of the time (3.01–5.30 GHz) and is good for WiMAX, WLAN, and X-band uses. Using biodegradable materials, Rahman et al. [21] suggested a UWB antenna array (4–6 GHz) that could be worn and built into a "clinical bra" to help find breast cancer early. In tests, this idea worked over 70% of the time. Foroutan et al. [22] created an active sensor system for imaging tissue with microwaves. It uses printed slot antennas with LNAs and active mixers, and its frequency range is from 3 to 7.5 GHz, with 30 MHz of space between the frequencies. The research in [23] was mostly about using microwave sensor technologies to find breast cancer. The imaging quality is based on the quality of the scattering data. Truncated Singular Value Decomposition (TSVD) was used by Mays et al. [24] to make the data quality better in mixed-polarization

antenna arrays that were used to find breast cancer. Srinivasan et al. [25] compared different antennas and their characteristics to identify the most suitable designs for early breast cancer detection.

3. MOTIVATION AND PROBLEM FORMULATION

Breast cancer is a significant global health issue for women, with mortality rates rising every year. Various strategies and techniques have been devised to mitigate the mortality rate. The efficacy of breast self-examination can reduce female death rates. Various programs are being implemented to educate women on the practice of breast self-examination.

Breast cancer is a prevalent kind of neoplasm identified in women globally. Therefore, it is crucial to identify it at the curable stage as promptly as feasible. Regrettably, it is a leading cause of cancer mortality among women. Consequently, detection and prevention are essential tasks. The surveillance of breast cancer involves obtaining medical data from asymptomatic and seemingly healthy women to facilitate earlier detection of the disease. Another factor contributing to cancer incidence is the unregulated proliferation and aging of the population, with the prevalence of recognized risk factors such as obesity, sedentary lifestyles, and environmental alterations resulting from urbanization and economic advancement. The suggested study employs a low-cost, flexible antenna to detect breast cancer, both in the presence and absence of tumors, to mitigate mortality rates associated with the disease. The antenna utilizes wearable jeans material, with a thickness of 1 mm, as the dielectric substrate, possessing a dielectric constant of 1.7. This research involves the construction of an antenna resembling a sandwich model, using a slot-loaded patch and a copper ground plane as the conductive material. The coaxial feeding approach has been employed for antenna feeding. The engineered antenna functions as a wearable textile antenna for ISM (Industrial, Scientific, and Medical) band applications at 2.4 GHz. The suggested antenna can simulate and implement both software and hardware. The simulation is conducted with HFSS (High-Frequency Structure Simulator) software, incorporating factors such as S11 return loss, gain in dB, and radiation pattern. As a consequence, the simulation yields the VSWR.

4. PROPOSED METHOD

a Design Consideration of CMPA

The suggested antenna is a slender hexagonal patch fabricated on a Jeans substrate with a h = 1 mm thickness. The antenna design necessitates the substrate's permittivity or dielectric constant, as well as the length and breadth of the patch and ground plane. The primary function of the antenna pertains to the substrate's permittivity, ɛr, which is 1.7 for denim fabric.

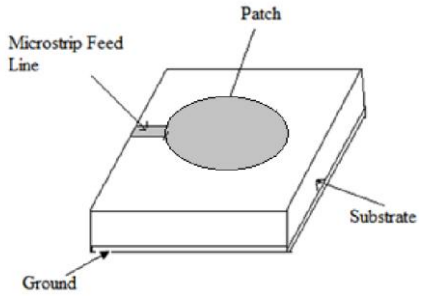

Fig. 1 Circular Microstrip Patch Antenna

Subsequent mathematical formulae are considered when determining the suggested antenna parameters, such as width, effective dielectric constant, and length.

1) Calculation of width

$$w = \frac{c}{sf_0\sqrt{\frac{(\epsilon_0+1)}{2}}}$$

Where

w = Width of Patch in mm

f_0 = Resonance frequency in Hz

ϵ_0 = The relative permitivity of dielectric substrate $(\frac{f}{m})$

c = Speed of light (3 $X10^8$ m/s)

2) Calculation of effective dielectric constant

$$\in_{eff} = \frac{\in_r+1}{2} + \frac{\in_r-1}{2}\ [\,1 + 12\frac{h}{Pw}]^{-\frac{1}{2}} \quad \text{if } \frac{Pw}{h} < 1$$

$$\in_{eff} = \frac{\in_r+1}{2} + \frac{\in_r-1}{2}\ [\,1 + 12\frac{h}{Pw}]^{-\frac{1}{2}} + 0.04[1 - \left(\frac{Pw}{h}\right)]^2 \quad \text{if } \frac{Pw}{h} < 1$$

Where,

Pw = Width of Patch in mm

h = Thickness of substrate in mm

$\in_r$ = The relative permitivity of dielectric substrate $(\frac{f}{m})$

3) Calculation of effective length

$$L_{eff} = \frac{c}{2f_0\sqrt{\in_{eff}}}$$

Where,

c = Speed of light $(3\ X10^8\ m/s)$

4) Calculation of length extension (ΔL)

$$\Delta L = 0.412h\ \frac{(\in_{eff}+0.03)(\frac{W}{h}+0.264)}{(\in_{eff}-0.03)(\frac{W}{h}+0.8)}$$

5) Calculation of the actual length of the patch

$$PL = L_{eff} - \Delta L$$

Where

PL = Length of patch in mm

6) Calculate the radius of the circular Patch

i. Calculate the radius of a circular Patch antenna from a rectangular Patch antenna.

ii. Calculate the Patch width and Length of the rectangular patch by the above equations. So, by calculations, we get the length and width of the rectangular patch.

iii. Calculate the radius 'r' of the circular patch by following the equations

$$\text{Radius of circular microstrip patch antenna} = \frac{\sqrt{(PL + SH)x(PW + SH)}}{2}$$

Table 1 provides the details of the modeled antenna design. The flexible textile antenna patch is constructed on a 19 × 16 mm² jean substrate, resembling a sandwich model. The microstrip feeding technique has been implemented for the antenna operating in the Ultrawideband at a frequency of 3.1GHz to 10.6Ghz. The Jean material serves as the substrate, while the conductive components (patch and ground) are constructed from copper material. Jeans material is utilized because of its essential properties, including thickness, relative permittivity, and a thickness of only 1 mm. The practical function of utilizing jean fabric lies in its ease when integrated into apparel. The simulation experiment is conducted using CST software. The height and breadth of the substrate and ground are meant to have 23mm X 20mm dimensions.

Table 1 Design specifications of the proposed antenna

Parameters	Symbol	Dimensions
The relative permittivity of the substrate	εr	1.7
Thickness of the dielectric substrate	h	1mm
Length of the substrate and ground	Ls & Lg	20mm
width of the substrate and ground	Ws & Wg	23mm
Radius of the patch	r	9mm

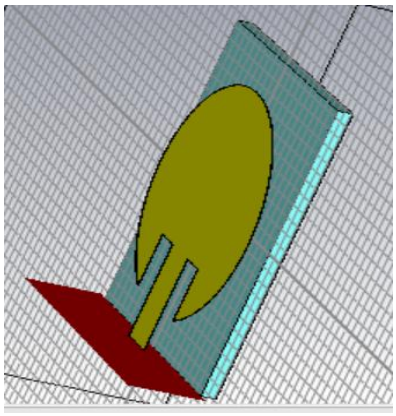

Fig. 2 Designed antenna using CST software tool

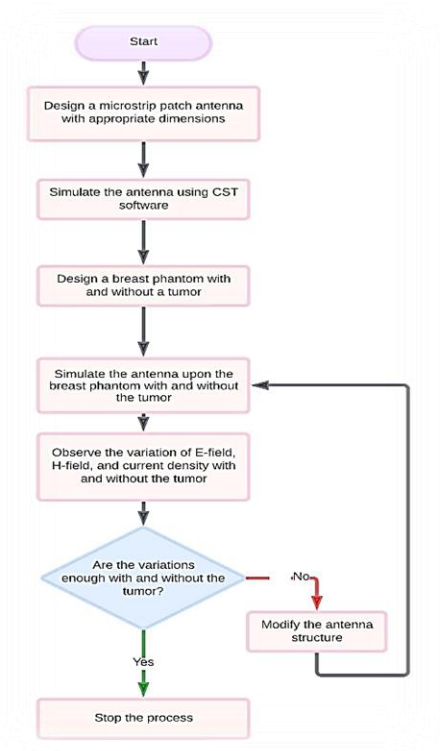

Fig -4: Steps involved in proposed work

b *Breast Phantom Design*

A breast phantom is created by modeling a sphere as an internal tumor and a cone as a breast that is covered in breast tissue. Breast skin has a permittivity of 36 F/m and a conductivity of 4 S/m. The tumor has a permittivity of 50 F/m and a conductivity of 7 S/m. For the breast, breast glandular tissue was selected from the CST material library. Compared to healthy tissues, tumorous cells formerly exhibited higher conductivity and distinct dielectric characteristics. The breast tumor has a radius of 2 mm, the breast skin has a radius of 10 mm, and the breast glandular tissue has a radius of 9 mm.

Table -2: Breast Phantom Design Specifications

Breast Tissue	Relative Permittivity	Tangent Delta (Loss)	Thickness (mm)	Distance
Skin	17.7	0.93	5	10
Fatty Tissue	3.4	0.166	15	9.5
Glandular Tissue	16	0.94	40	9
Tumor	18	1.05	r=2 to 4	-

Fig. 3: Breast Phantom design

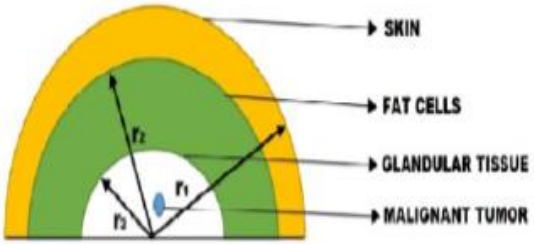

5. RESULT AND DISCUSSION

This section analyzes the performance results of the proposed antenna via simulation using CST software, while the real-time hardware implementation will be addressed subsequently. The antenna developed using CST software is seen in Figure 2. The CST tool is utilized for the design of various antenna types as well as RF electrical circuit components such as power dividers, couplers, and filters. The geometric design, material characteristics, and target output frequency are defined. CST software autonomously produces a solution process and precise mesh analysis for the specified design. The study appropriately considers essential characteristics, including return loss (S11), gain, radiation pattern, and VSWR.

The illustration above depicts the geometric configuration of the adaptable software antenna. Furthermore, the different parameters are studied with and without tumor and the comparison of results is shown in Table II below

Table III Comparative Study of Different Parameters Like S- Parameters, E-field, H- Field Surface Current Density with and Without Tumor for Jean Substrate for Circular Patch Antenna

Sr. No.	Parameter	Without Tumor	With Tumor
	S11	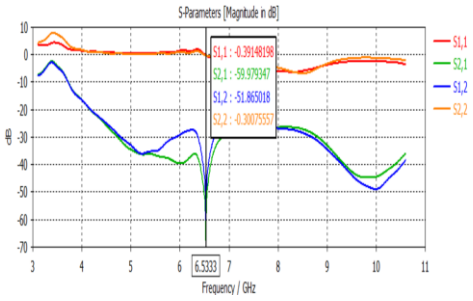	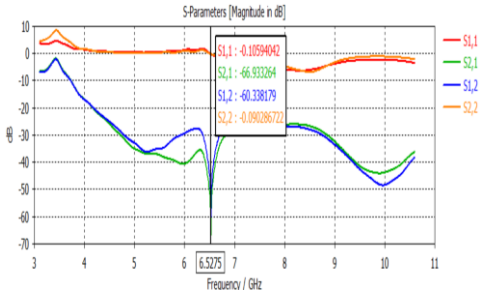
2	E-Field(6.85GHz)	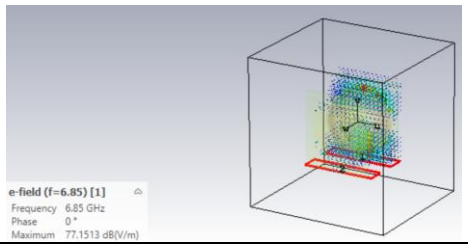	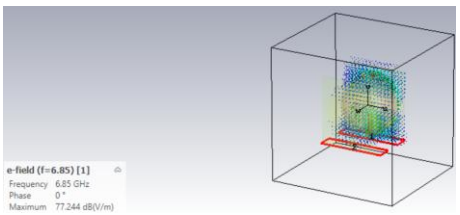
3	H-Field(6.85GHz)	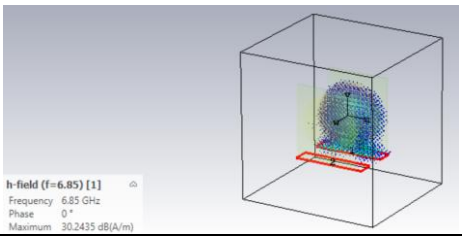	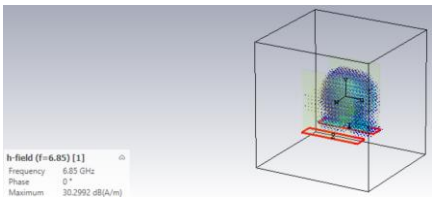
4	Surface Current (6.85GHz)	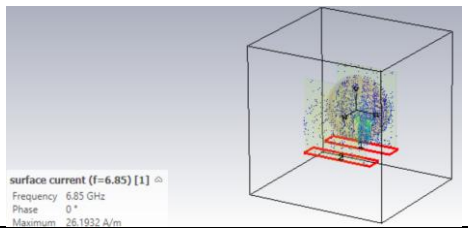	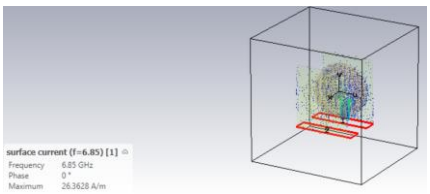
5	Farfield (6.85GHz)	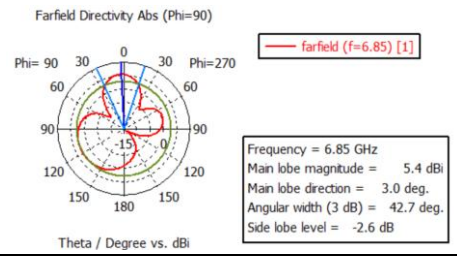	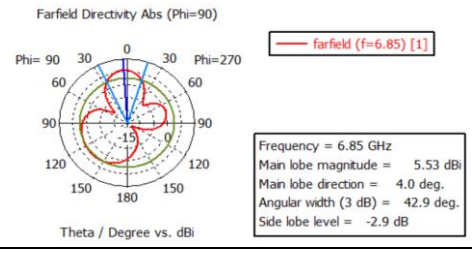

Table IV Comparison of various parameters with and without Tumor

Sr. No.	Parameter	Frequency	Values Without Tumor	Values With Tumor
1	S11 in dBm	5.885GHz	59.60	59.89
2	E-Field in dBm (uV/m)	6.85GHz	77.1513	77.244
3	H-Field in dBm (uA/m)	6.85GHz	30.2425	30.2992

4	Surface Current dBm (uA/m)	6.85GHz	26.1932	26.3628

6. CONCLUSION

This study aims to build and execute a new, low-cost textile wearable antenna for early-stage breast cancer detection. The engineered antenna can be utilized in the first detection of breast cancer, applicable to both tumor and non-tumor cases. This research utilizes wearable jeans material as a dielectric substrate, characterized by a dielectric constant of 1.7. The antenna is constructed as a sandwich model framework. The ground plane is composed of copper as the conductive substance. The jean fabric with a thickness of 1 mm is utilized for breast cancer examination, while a microstrip feeding technique is employed to provide the antenna. It functions as a wearable antenna, primarily intended for an ultra-wideband at 3.1 GHz to 10.6 GHz applications. The performance of the planned antenna is evaluated using CST software, focusing on Return Loss (S11), E-field, H-field, and surface current density with and without tumor. The examination of the findings demonstrates that the developed antenna offers superior advantages for applications, cost, and time.

7. REFERENCES

[1] Abdulla, Fawzia Abdien Ali, and Aşkin Demirkol. "A novel textile-based UWB patch antenna for breast cancer imaging." Physical and Engineering Sciences in Medicine (2024): 1-11.

[2] Fusic, Julius, T. Sugumari, and R. Sitharthan. "Design of a wearable, flexible microstrip patch antenna for the detection of breast cancer." (2023).

[3] Gour, Sonam, Amit Rathi, and Pallav Rawal. "A novel dual-band defected ground structure wearable microstrip patch antenna for breast tumor detection in biomedical applications." Engineering Research Express 6, no. 3 (2024): 035427.

[4] Amdaouch, I., Aghzout, O., Naghar, A., Alejos, A. V., and Falcone, F., “Breast tumor detection system based on a compact UWB antenna design”, IEEE Progress Electromagnet. Res. M. 64:123–133, 2018.

[5] Song, H., Kubota, S., Xiao, X. and Kikkawa, T., “Design of UWB antennas for breast Cancer detection”, IEEE, International Conference on Electromagnetic in Advanced Applications (ICEAA), 978–1–4673-9810-7, 2016.

[6] Bahrami, H., Porter, E., Santorelli, A., Gosselin, B., Popovic, M. and Rusch, L.A., “Flexible sixteen antenna Array for microwave breast Cancer detection”, IEEE Transactions, 36th international conference of the IEEE engineering in medicine and biology Society, 1558–4615, 2014.

[7] Wang, L. and Huang, B., “Design of Ultra-WidebandMIMO antenna for breast tumor detection”, Hindawi Publishing Corporation, International Journal of Antennas and Propagation, Article ID 180158, 2012.

[8] Kaabal, A., El Halaoui, M., Ahyoud, S., and Asselman, A., ”Dual band-notchedWIMAX/WLAN of a compact Ultrawideband antenna with spectral and time domains analysis for breast Cancer detection”, IEEE Progress Electromagnet. Res. C 65:163–173, 2016.

[9] Selvaraj, V., and Srinivasan, P., “Interaction of an EM wave with the breast tissue in a microwave imaging technique using an ultrawideband antenna”, Biomed. Res. 28(3):1025–1030, 2017.

[10] Taylor, Z. D., Singh, R. S., Bennett, D. B., Tewari, P., and Kealey, C. P., “THz medical imaging: In vivo hydration sensing”, IEEE Transactions on Terahertz Science and Technology 1(1), 2011.

[11] Asha, J.M. S. and Kumar, K. M., “Design and analysis of microstrip patch antenna for lung tumor”, International Research Journal of Engineering and Technology (IRJET) 4, (4), 2017.

[12] Shrestha, S., Agarwal, M., Ghane, P. and Varahramyan, K., “Flexible Microstrip antenna for skin contact application”, Hindawi Publishing Corporation, International Journal of Antennas and Propagation, Article ID 745426, 2012.

[13] 10. Katbay, Z., Sadek, S., Lababidi, R., Perennec, A. and Roy, M. L., “Miniature antenna for breast tumor detection”, IEEE 13th International New Circuits and Systems Conference, 978–1– 4799-8893-8, 2015.

[14] Vidyasree, K., Mannisha, M., Nagaveni, T. S., Nandhini, B. M. and Kumar, H. V., “Breast cancer detection using microstrip patch antenna”, International Journal of Advanced Research, Ideas and Innovations in Technology 4(3), 2018.

[15] Susila, J. J. and Fathima, H. R., “A slot loaded rectangular microstrip patch antenna for breast Cancer detection”, International Research Journal of Engineering and Technology (IRJET) 4(4), 2017.

[16] Gupta, H. K., Sharma, R., and Thakre, V. V., “Breast cancer detection by T-shaped slotted planner antenna”, Ind. J. Sci. Technol. 10(8): 0974–6846, 2017.

[17] Habsi, S. A., Ruzaiqi, T. A., Hadharami, K. A., and Gopinathan, S. T., “Development of antenna for microwave imaging systems for breast cancer detection”, J. Molec. Imag. Dynam. 6(2):2155–9937, 2016.

[18] Hammouch, N. and Ammor, H., “Smart UWB antenna for early breast cancer detection”, ARPN Journal of Engineering and Applied Sciences 13(11), 2018.

[19] Ullah, M. A., Alam, T., Aam, M. S., Kibria, S. and Islam, M. T., “A unidirectional 3D antenna for biomedical microwave imaging-based detection of abnormality in the human body”, Springer, 1–6, 2018.

[20] Rahman, A., Isam, M. T., Singh, M. J., Kibria, S. and Akhtaruzzaman, M., “Electromagnetic performances analysis of an ultra-wideband and flexible material antenna in microwave breast imaging: To implement a wearable medical bra”, Research Gate, 978–1-5090-6005-4, 2017.

[21] Foroutan, F., and Nikolova, N. K., “Active sensor for microwave tissue imaging with bias-switched arrays”, Journal of sensors 18(5), 2016.

[22] Wang, L., “Microwave sensors for breast Cancer detection”, IEEE 18(2), 2018. 20.

[23] Mays, R. O., Behad, N. and Hagness, S. C., “ATSVD analysis of the impact of polarization on microwave breast imaging using an enclosed Array of miniaturized patch antennas”, IEEE Antennas and Wireless Propagation Letters 14, 2015.

[24] Khan, M. A. and ul Haq, M. A., “A novel antenna Array design for breast Cancer detection. IEEE Industrial Electronics and Applications Conference (IEACon)”, 978–1–5090-0926-8, 2016.

[25] Afyf, A., Bellarbi, L., Riouch, F, Errachid, A. and Sennouni,M. A., “Flexible antenna Array for early breast cancer detection using the radiometric technique”, IEEE, International Journal of Biology and Biomedical Engineering, Volume 10, 2016.

[26] Srinivasan, D., Gopalakrishnan, M., and Srinivasan, D., “A survey on antennas used for early detection of breast cancer”, Int. Conf. Energ. Commun. Data Anal. Soft Comput. (ICECDS), Chennai 2017:1736–1739, 2017.

Biographies



Mr. Somanath Kisan Chikane, PhD Scholar, M.E. (E&TC) in Signal Processing, SVPM's College of Engineering, Malegaon (Baramati), SPPU University, Maharashtra, India.



Dr. Balasaheb H. Patil, PhD (E&TC), Associate Professor at VPKBIET, Baramati, SPPU Pune, Maharashtra, India. PhD in E&TC from SPPU, Pune

Design of Power Efficient 14T Full Adder Circuit

Sudhamalla Mallesh[1], Polampally Likhitha[1], Rajula Pavani[1], Posham Nagasai[1], Varikuppala Poojitha[1]
[1]Department of ECE, CMR Technical Campus, Hyderabad, Telangana State, India-501 401.
[1]mallesh.ece@cmrtc.ac.in, [1]likhithapolampally@gmail.com, [1]pavanirajula022@gmail.com,
[1]poshamnagasai253@gmail.com, [1]poojithavarikuppala04@gmail.com.

ABSTRACT

Power-aware design is a continuously developing trend in VLSI that contributes to energy efficiency in battery-energized systems, electromechanical devices using semiconductors, and electronic components. In very simple terms, an adder is so important in arithmetic logic units. There are many approaches that researchers have considered to optimize the design of a full adder. This paper proposes an inventive and effective 14T power-efficient full adder circuitry. The proposed design bases mainly on the NMOS logic or Pass Transistor Logic (PTL), whose alternative implementation could also be done using transmission gates. The full circuit has been developed on the schematic as well as layout level using the Microwind EDA and DSCH3 tools, specifically focusing on power efficiency at the summation output node and carry output node. Performance evaluation in relation to an existing 14T adder design has shown drastically lower energy consumption.

Keywords:

VLSI (very large scale integration), EXOR gates, MOS transistor, layouts, microwind, DSCH3

1. INTRODUCTION

This project introduces a new method of designing an energy-efficient full adder for application in energy-limited systems, like battery-operated systems and electronic devices. A full adder is an essential component of arithmetic logic units (ALUs) that performs binary addition, and its design must be optimized in order to maximize overall energy efficiency in digital circuits[1][6]. The design uses a 14-transistor (14T) based on NMOS logic or Pass Transistor Logic (PTL) and an alternative implementation with transmission gates[2]. The method specifically targets minimizing both summation node and carry output node power consumption, which are among the most influential determinants of overall energy efficiency in the adder[3][5]. The circuit is designed at both schematic and layout levels with the help of Microwind EDA and DSCH3 tools, enabling precise simulation and analysis. Compared to the current 14T adder designs, the new circuit exhibits a high level of reduction in energy consumption, thus a more power-efficient solution for power-constrained applications in VLSI systems[4]. This innovation helps solve the need for low-power designs in current electronic devices. For reducing the transistor count we use CMOS transistors but they are need to modified to a technology called Gate diffusion input (GDI), Transmission gate logic (TGL) and pass transistors logic (PTL)[1][13]. These techniques can reduce transistor count and power consumption. However we use FinFet technique to improve the speed up to 40% and also it will be supplement in reducing power consumption [2-3][8].

FinFET technology, whose emergence in recent years has revolutionized the art of low-power circuit design by alleviating the inadequacies of traditional planar CMOS transistors. FinFETs exhibit better electrostatic control over leakage currents and switching efficiency because of their three-dimensional structure. Thus, they are very good candidates to be adopted in the design of power-efficient arithmetic circuits such as full adders, where the minimization of transistor count and power consumption is paramount [10]. By combining FinFETs with advanced design techniques, such as Gate Diffusion Input (GDI) and Pass Transistor Logic (PTL), the modern full adder circuits have taken a significant stride towards the reduction of dynamic and static power dissipation [14]. These advances will immensely benefit their applications in mobile computing, IoT devices, and high-speed processors, where energy efficiency is a key design challenge without degrading performance [7][9].

Table1: Performance Analysis of 28T Full Adder

Voltage supply(V)	Conventional(pA)	Usvl (pA)	Lsvl (pA)	Svl(pA)
0.5	2.323	1.907	1.179	1.803
0.7	2.932	2.083	1.297	1.119
0.9	3.487	3.475	1.401	1.398
1.0	3.749	3.748	1.451	1.451
1.2	4.898	4.258	1.557	1.557

Table1 depicts the power used by 28t full adder and its performance. Our work will reduce the power concerns compared to 28t full adder.

2. RELATED WORKS:

2.1 Implementation and Installation Process

From The web

- Open the page <ni2>
- Then connect to it
- Click<ni2>
- Click<ni2>
- *Test: click twice on MICROWIND3.EXE. Click "File ->Load", select "CMOS.msk". Click "Simulate"*

Click<ni2>

- get all the required projects in the chosen file.
- *Test: have a two time click on DSCH3.EXE.Load*

Once installation is completed, two directories are, one for MICROWIND3, one for DSCH3. In each directory, there is a subdirectory named html which holds help files.

2.2 The MOS device and analog simulation

This chapter delves into the CMOS transistor, detailing its layout, static characteristics, and dynamic performance. It also explores the vertical dimensions of the device, along with a three-dimensional representation of the fabrication process.

Logic values:

Three logic figures 0, 1 and X (unknown) are described as follows

Analogy Simulation

This is illustrated in below image figure1 which shows the simulation of a MOS device and its output at different levels. If the gate voltage is set to zero, then no channel is created thus disconnecting the source node. A combination thereof is differentially bypassed and allowed to pass merely when a positive voltage is applied at the point of the gate, Vg. It is unique to note that the NMOS device does a low conduction state at high gate voltages during the non- conducting modes. Furthermore, upon reaching Vdd = 0.85V, V_NMOS=V_DD-Threshold. The NMOS devices do not function efficiently with a high gate voltage (logic 1) as is seen from the figure. One can run other such simulations also by clicking "More" or opening the editor window.

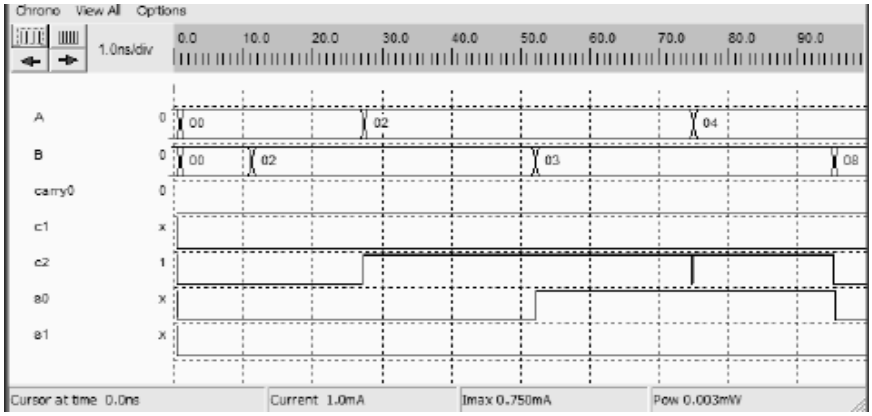

Figure 1: Simulation of MOS Device

Microwind is a nanometre-scale IC simulation and design tool that enables circuit designers to create, visualize, and analyse the performance of integrated circuits under real operating conditions. Microwind helps save time and cost on the paper by facilitating the design of the IC before actual manufacturing and testing.

3. IMPLEMENTATION IN THE TOOLS

3.1 Full-Adder in DSCH3

DSCH3 is another very popular tool for digital integrated circuit (IC) design, particularly for educational design. It forms part of a set of tools designed to give a straightforward and efficient means to design and simulate digital circuits. DSCH3 is generally used for digital circuit design, logic synthesis, and simulation, and it enables designers to construct, analyse, and test logic circuits in an intuitive environment.

Simulation: DSCH3 has integrated simulation capabilities. It supports functional simulation (in order to test that the logic works as planned) and timing simulation (so that the design adheres to certain time specifications). The software tool offers simulation of the digital logic's behaviour over time, allowing users to experiment with how the circuit responds to various input combinations.

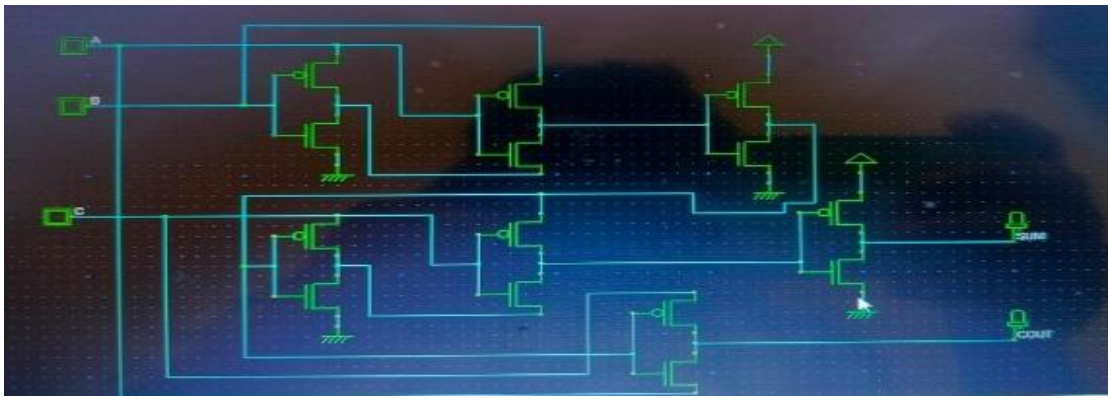

Figure 2: DSCH3 Schematic(The outline of the intended design 14T full adder)

3.2 Full Adder in Microwind

Microwind is a layout and simulation software mostly employed for integrated circuit (IC) layout and verification, specifically in the area of VLSI (Very Large Scale Integration) design. It's an easy-to-use software package with both layout editing and simulation functionality that assists designers in designing, testing, and verifying the IC designs' functionality, especially those related to CMOS (Complementary Metal-Oxide-Semiconductor) process technologies.

***Simulation*:** Simulation is one of the most important aspects of Microwind, as it can simulate the ICs' behaviour under various operating conditions. It contains a SPICE-based simulator which enables the electrical characteristics, i.e., voltage, current, power, and timing of the components of the design to be analysed.

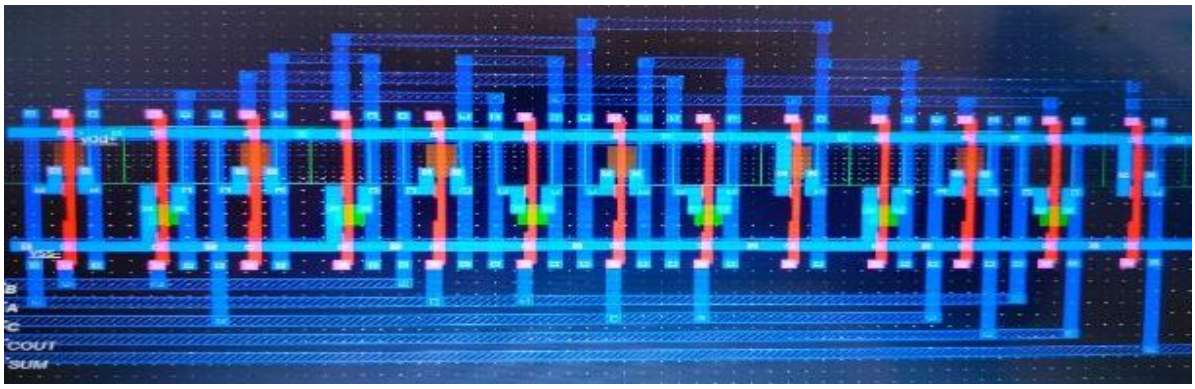

Figure 4: Microwind Layout

4. RESULTS AND DISCUSSION

The 14-transistor and 28-transistor full adders are simulated using the Microwind3 simulator. The power analysis from the simulation insightfully shows that the 14T full adder is more efficient than the 28T full adder in terms of power consumption. A comparison of both the adder designs in 180 nm technology is given in Table 2.

Table 2: Power consumption of 14T full adder

Types of Adders	Static Power (nW)		Dynamic Power (nW)	
Input1	A=0, B=0, Cin=0		A=0, B=0, Cin=0	
Operation	Sum	Carry	Sum	Carry
Proposed	0.212	0.130	0.000	0.500
Reference	0.100	0.130	2.778	2.541
Input2	A=1, B=1, Cin=1		A=1, B=1, Cin=1	
Operation	Sum	Carry	Sum	Carry
Proposed	0.10	0.130	0.99	2.140
Reference	0.13	0.11	1.08	1.581

The summarized results highlight that the **14T full adder** demonstrates superior performance compared to the **28T full adder**. Reducing the transistor count significantly decreases power leakage, enhancing overall efficiency.

5. CONCLUSION

The current study describes a 14-transistor full-adder circuit that attains comparatively less power, less time of operation, and less density of transistors. Power optimization has been achieved in our full-adder design via structural modifications by applying concatenation techniques. Our circuit shows better results in terms of efficiency of transistors, area, and power consumption with very little distortion as compared to the currently available full-adder designs. Comparison with Table 1 shows that the 28T full adder consumes more power than the proposed design, which makes it efficient.

Future Scope:

- Power adaptation technique uses low-power VLSI design as future work that leads to advances in less power-consuming technologies by keeping power optimization strategies in focus.
- Reduction of transistor count to 12 using transmission gates could lead to a more energy-efficient circuit design.

6. REFERENCES:

[1] P.A.Irfan Khan, s k. Dilshad, & B. Karunasree “design of 2*2 vedic multiplier using GDI technique” International Conference on Energy, Communication, Data Analytics and Soft Computing (ICECDS), Chennai, India, 2017

[2] sk. Dilshad & Sai Krishna Santosh “Mitigation of Critical Delay in the Carry Skip Adders Using FinFET 18nm Technology” (2012), International Journal of Electrical and Electronics Research (IJEER), Hyderabad, India.

[3] Dilshad Shaik, Sai Krishna Santhosh Gollapudi, “Analogy of Distinct Constructions of FinFET GDI Full Adder”, Journal of INTELLIGENT SYSTEMS AND APPLICATIONS IN ENGINEERING(ijisae),2023

[4] Sonth, Mahesh & Soma, Savita & Gowre, Sanjaykumar. (2020). Investigation of light behavior of all optical full adders in two-dimensional photonic crystals. Microwave and Optical Technology Letters.

[5] Elmasry, M. I., & Bellaouar, A. (1995). “Low-Power Digital VLSI Design: Circuits and System”. Kluwer Academic Publishers, The Netherlands & Singapore.

[6]Sharma, A., & Tiwari, R. (2016). "Low Power 8-Bit ALU Design Using Full Adder and Multiplexer." 2016 International Conference on Wireless Communications, Signal Processing and Networking (WiSPNET), IEEE, pp. 2160

[7] Senthilpari, C., Kavitha, S., & Joseph, J. (2010). "Lower Delay and Area Efficient Non-Restoring Array Divider Using Shannon-Based Adder Technique." 2010 IEEE International Conference on Semiconductor Electronics (ICSE2010), IEEE, pp. 140-144.

[8] Saraswathi, C., Rani, N. U., & Nagateja, T. (2016). "High Performance and Energy Efficient FinFET-Based 1-Bit PT Full Adders." 2016 IEEE International Conference on Computational Intelligence and Computing Research (ICCIC), Chennai, India, IEEE, pp. 1-4.

[9] Nehru, K., Shanmugam, A., & Darmilathenmozhi, G. (2012). "Design of Low-Power ALU Using 8T FA and PTL-Based MUX Circuits." IEEE International Conference on Advances in Engineering, Science and Management (ICAESM-2012), Nagapattinam, Tamil Nadu.

[10] atemeh, K. H., & Horestani, A. K. (2011). "New Structure for Adder with Improved Speed, Area, and Power." 2011 IEEE 2nd International Conference on Networked Embedded Systems for Enterprise Applications, Fremantle, WA, Australia, IEEE, pp. 1-6.

[11] Gupta, K., Bagga, S., & Pandey, N. (2016). "Efficient CVSL-Based Full Adder Realizations." 2016 IEEE 1st International Conference on Power Electronics, Intelligent Control and Energy Systems (ICPEICES), IEEE, pp. 1-5.

[12] Ahmad, M., Manjunathachari, K., & Lalkishore, K. (2016). "Design and Analysis of Low Run-Time Leakage in a 10-Transistor Full Adder in 45nm Technology" 2016 IEEE Region 10 Conference (TENCON), Singapore: IEEE.

[13] Patil, P. P., & Hatkar, A. "Comparative Analysis of 8-Bit Carry Skip Adder Using CMOS and PTL Techniques with Conventional MOSFET at 32 Nanometer Regime."

[14] Reddy, G. K. (2015). "Low Power-Area Pass Transistor Logic Based ALU Design Using Low Power Full Adder Design." 2015 IEEE 9th International Conference on Intelligent Systems and Control (ISCO), Coimbatore, India, IEEE.

Efficient Image Blending Techniques Using FPGA-Based Approximate Multipliers

Sreelakshmi Vadlamudi [1,2], Syamala Yarlagadda [2] and Madhu R [3]

[1] *Jawaharlal Nehru Technological University Kakinada, Andhra Pradesh, India.*
sreelakshmi.vadlamudi@gmail.com

[2] *Seshadri Rao Gudlavalleru Engineering College, Andhra Pradesh, India. coolsyamu@gmail.com*

[3] *Jawaharlal Nehru Technological University Kakinada, Andhra Pradesh, India.*
madhu_ramarkula@jntucek.ac.in

Abstract.

In error-resilient computing, particularly in applications like multimedia processing, data analysis, and machine learning, absolute computational precision is often not a strict requirement. This paper introduces a novel FPGA-based design for multi-level approximate multipliers that optimally balance accuracy with key performance metrics such as power consumption, area efficiency, and processing speed. By leveraging techniques like partial product truncation and logic compression, the proposed multipliers achieve significant reductions in circuit complexity while enhancing overall efficiency. The results demonstrate that these designs effectively cater to applications where minor inaccuracies are acceptable, delivering notable improvements in power-delay-area performance compared to conventional exact multipliers.

Keywords Approximate Computing, Approximate Multipliers, Power-Efficient Computing, Circuit Complexity Reduction, Partial Product Truncation, FPGA Design.

1. INTRODUCTION

In the landscape of modern computing, many applications, particularly those in fields such as multimedia processing, data mining, and machine learning, do not require absolute precision in their calculations[1]-[4]. Instead, these applications can function effectively with results that exhibit a certain level of acceptable error [5]. This characteristic opens the door to innovative design strategies that prioritize performance metrics—such as power consumption, area efficiency, and processing speed—over strict accuracy. By embracing this paradigm, engineers can create systems that are not only faster and more efficient but also more suited to the demands of real-world applications where resource constraints are prevalent.

One of the prominent techniques for reducing power consumption in digital circuits is voltage over-scaling [6] –[8]. While this method can lead to significant energy savings, it also introduces the risk of timing-related failures, which can result in substantial and unpredictable errors, particularly affecting the most significant bits of computation. To address these challenges, the concept of approximate computing has gained traction. This approach allows for the intentional introduction of errors in the outputs of complex circuits, enabling designers to simplify logic expressions and reduce the overall resource requirements. By accepting a controlled level of inaccuracy, approximate computing can lead to considerable improvements in power efficiency and performance.

The focus of much recent research has been on the application of approximation techniques to arithmetic units, especially multipliers and adders, which are fundamental components in a wide array of digital systems[9] –[12]. Given the inherent complexity of multipliers, optimizing their design through approximation can yield significant benefits. Notably, the partial product accumulation stage

of a multiplier is where the majority of computational resources and time are consumed [13]. Therefore, enhancing this stage through innovative design techniques can lead to substantial gains in overall circuit performance.

In this paper, we propose a novel architecture for FPGA-based multi-level approximate multipliers that utilize advanced approximate logic compressors. These compressors are designed to reduce the complexity of the partial product accumulation process while maintaining an acceptable level of accuracy for applications that can tolerate some error. Our findings demonstrate that these multipliers not only achieve significant improvements in power-delay-area products but also outperform traditional exact multipliers in various performance metrics. By exploring the trade-offs between accuracy and efficiency, this work contributes to the growing body of knowledge in approximate computing, providing valuable insights for the design of high-performance, low-power digital systems.

1) It is suggested that approximate multipliers be effectively implemented on FPGAs with minimal accuracy losses by utilizing the small approximate 4-2 compressors.
2) Various proposed multiplier designs can be used to obtain design-time accuracy configurations.

3) Quality measures such as mean error distance (MED), mean relative error distance (MRED), and normalized mean error distance (NMED) are used to extensively analyze the quality of the proposed approximate multipliers.
4) Extensive simulations are carried out to get precise QMs for 8X8 multipliers.
5) Formulas for calculating the crucial metrics (MED and NMED) for multipliers with large operand sizes that are scaled up from those with lower operand sizes are derived.
6)Additionally, the trade-offs between area and PDPs are shown.
7) The benefits and efficiency of our suggested multipliers are demonstrated using image processing applications, such as image blending.

2. APPROXIMATE 4-2 COMPRESSORS

The number of partial products in the multiplication process can be reduced using the compressors. The compressor size can generally be represented as m:n, where m represents the number of input bits and n represents the number of output bits. As seen in Figure 2.7, an exact 4-2 compressor comprises two Full adders. It has three outputs and five inputs.

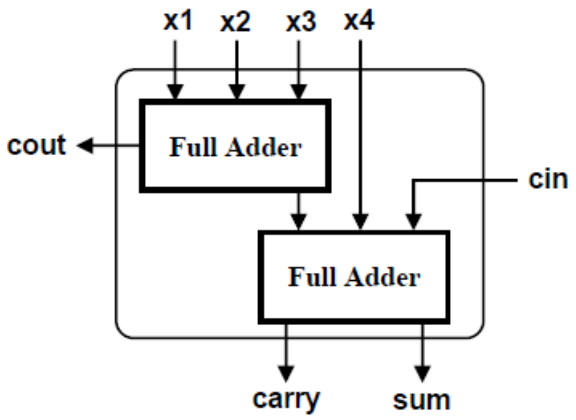

Figure 2.8. Exact 4:2 Compressor

Here, we design and analyze four Low-power approximate compressors C1, C2, C3, and C4.

C1 Compressor: In the C1 compressor, the sum is computed using majority logic for three bits, ignoring the fourth bit to reduce the complexity and Carry is simplified always to reflect the presence of a high input. The sum and carry equations for the C1 compressor are:

sum = (x1 x2) + (x2x3) +(x3x1) cy = x1+x2+x3+x4

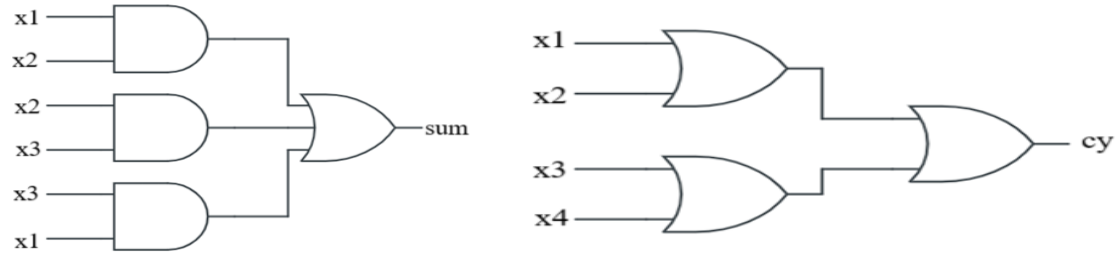

Figure 2.2. C1 Compressor

C2 Compressor: In the C2 Compressor, the sum is calculated as pairwise EX OR between the inputs, which reduces XOR computation complexity by splitting inputs into two groups. Carry relies on a simplified pairwise approach, introducing slight errors. The sum and carry equations for the C2 compressor are :

sum = (x1 ⊕ x2) + (x3 ⊕ x4) cy = (x1x2)+(x3x4)

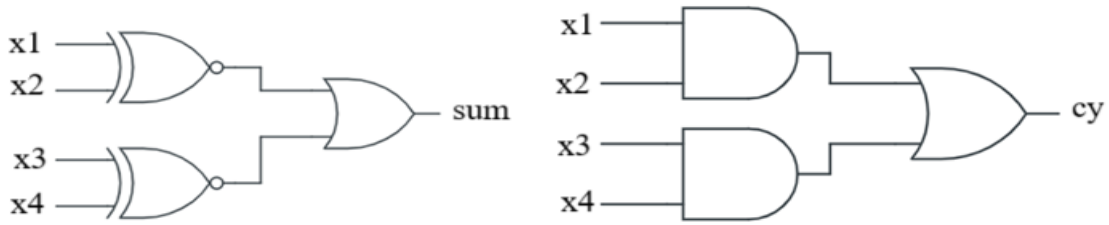

Figure 2.3. C2 Compressor

C3 Compressor: In the C3 Compressor, the sum and carry are calculated with three inputs only. Ignoring the fourth input in sum and carry simplifies the design. The sum and carry equations for the C3 compressor are :

sum = (x1 ⊕ x2 ⊕ x3) cy = (x1x2)+(x3)

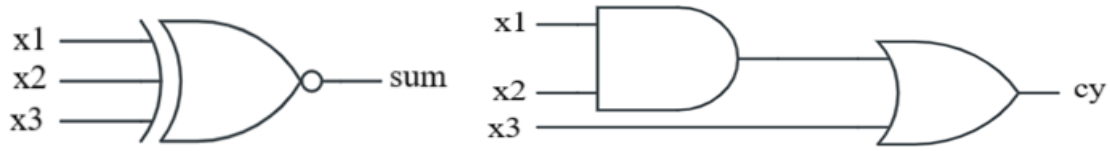

Figure 2.4. C3 Compressor

C4 Compressor: C4 Compressor Provides partial error compensation, balancing error reduction with added complexity. The sum and carry equations for the C4 compressor are :

sum = (x1 ⊕ x2 ⊕ x3) + x4 cy = (x1x2)+(x2x3)+(x3x4)

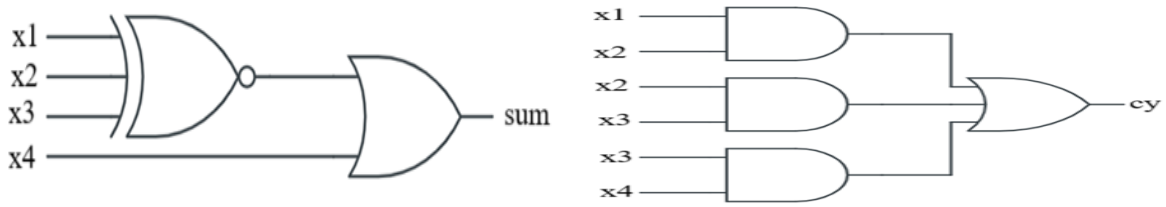

Figure 2.5. C3 Compressor

The Truth table in Table I compares the Exact 4:2 Compressor with four approximate compressor designs (C1, C2, C3, C4). The deviations in sum and carry values for approximate compressors indicate the level of inaccuracy introduced to optimize factors like power, area, and delay. Low-deviation compressors C1, and C2 offer better accuracy, suitable for moderate approximation applications, and Less power savings compared to C3 and C4 but still better than the exact design. The High-Deviation Compressors C3 and C4 offer Greater efficiency in power, delay, and area but at the cost of accuracy. These are Best for error-tolerant applications like image processing, AI, or approximate multipliers.

3. APPROXIMATE MULTIPLIER DESIGN

Multipliers are essential elements in digital signal processing systems, responsible for efficiently computing the product of two operands. In this section, we delve into the architecture of the proposed multipliers, focusing on their design principles, area utilization, propagation delay, and essential performance metrics like Peak signal-to-noise ratio (PSNR). Utilizing the Wallace tree multiplier method enables efficient computation of partial products and subsequent accumulation of results within the proposed architecture. The Wallace tree multiplier reduces the overall computation time while minimizing hardware resources by decomposing the multiplication operation into smaller segments and employing parallel processing. The hierarchical structure of the tree enables scalable implementation, making it suitable for a wide range of multiplication scenarios. The integration of custom compressors enhances the performance of the Wallace tree multiplier by optimizing area utilization and reducing delay. The proposed multipliers leverage a Wallace Tree architecture, a well-established method for reducing partial products and aggregating them to obtain the final product efficiently. The architecture shown in Figure 3.1 employs custom-designed compressors and full and half adders to optimize area utilization and minimize propagation delay. Each multiplier variant (PM1, PM2, PM3, PM4) employs a different compressor (C1, C2, C3, C4) to suit various application requirements.

Table 1 Truth Table of approximate 4:2 compressors

Inputs				Exact 4:2 Compressor		C1		C2		C3		C4	
x1	x2	x3	x4	sum	cy	sum	cy	sum	cy	sum	cy	sum	cy
0	0	0	0	0	0	0✓	0✓	0✓	0✓	0✓	0✓	0✓	0✓
0	0	0	1	1	0	0	1	1✓	0✓	0	0✓	1✓	0✓
0	0	1	0	1	0	0	1	1✓	0✓	1✓	1	1✓	0✓
0	0	1	1	0	1	1	1✓	1	0	1	1✓	1	1✓
0	1	0	0	1	0	0	1	1✓	0✓	1✓	0✓	1✓	0✓
0	1	0	1	0	1	1	1✓	1	0	1	0	1	1✓
0	1	1	0	0	1	1	1✓	1	1✓	0✓	1✓	1	1✓
0	1	1	1	1	1	1✓	1✓	1✓	1✓	0	1✓	1✓	1✓
1	0	0	0	1	0	0	1	1✓	0✓	1✓	0✓	1✓	0✓
1	0	0	1	0	1	1	1✓	1	0	1	0	1	1✓
1	0	1	0	0	1	1	1✓	1	1✓	0✓	1✓	1	1✓
1	0	1	1	1	1	1✓	1✓	1✓	1✓	0	1✓	1✓	1✓
1	1	0	0	0	1	1	1✓	1	1✓	1	1✓	1	1✓
1	1	0	1	1	1	1✓	1✓	1✓	1✓	1✓	1✓	1✓	1✓
1	1	1	0	1	1	1✓	1✓	1✓	1✓	0	1✓	1✓	1✓
1	1	1	1	1	1	1✓	1✓	1✓	1✓	0	1✓	1✓	1✓

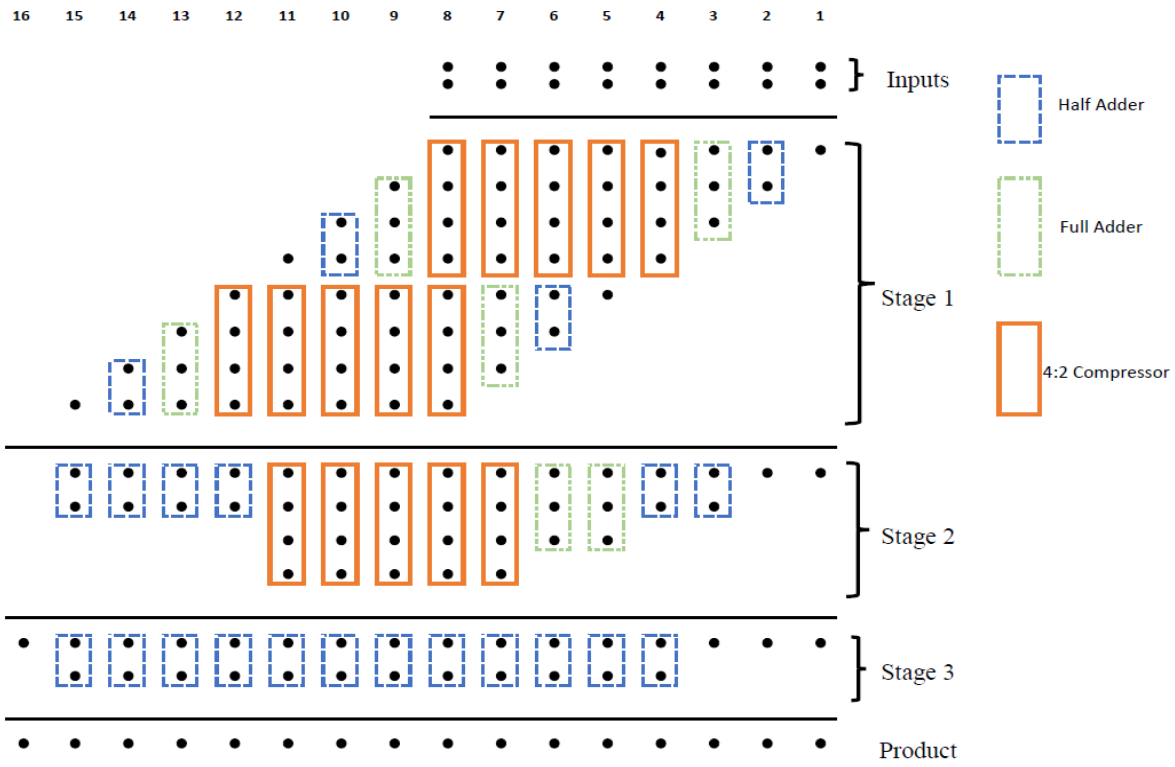

Figure 3.1. C3 Compressor Proposed Approximate 8x8 Multiplier

Multipliers designed using compressors such as C1, C2, C3, and C4 typically aim to optimize the speed and area of the multiplication process while managing complexity and error levels. Here's a brief overview of how each compressor might contribute to the design of multipliers:

1. **C1 Compressor**: The C1 compressor uses majority logic for summation, which helps in handling overflow and carries efficiently by simplifying the carry-out logic, allowing for faster computations. This design can be advantageous in a multiplier configuration, reducing the overall delay in calculating intermediate products.
2. **C2 Compressor**: By employing pairwise EX OR operations, the C2 compressor reduces the complexity of XOR calculations by grouping inputs. In multiplier designs, this approach can streamline the addition of partial products, making the overall multiplication process quicker. However, slight errors introduced in the carry calculations must be considered, as they can accumulate in larger multipliers.
3. **C3 Compressor**: The C3 compressor simplifies design by using only three inputs for sum and carry calculations, omitting a fourth bit. This can lead to reduced circuit complexity in multiplier layouts. However, careful handling of carry propagation is necessary, as the omission may introduce some inaccuracies in high-speed multiplication scenarios.
4. **C4 Compressor**: This compressor balances error reduction with added complexity by providing partial error compensation. In multipliers, the C5 compressor can help mitigate the negative effects of approximation, allowing for high-speed operations while maintaining a degree of accuracy in the multiplication results.

Each compressor offers distinct benefits and trade-offs that influence multiplier design. Choosing the appropriate compressor depends on the specific requirements of speed, area, and acceptable error levels in digital multipliers, with applications ranging from low-power designs to high-performance computing systems. Integrating these compressors can lead to innovative multiplier architectures that efficiently manage the challenges associated with multiplication in digital circuits, especially in contexts like image processing and digital signal processing.

4. PERFORMANCE EVALUATION

4.1 Accuracy Analysis:

To evaluate the accuracy of the designed multipliers, we compare their outputs with the exact results by calculating the Mean Relative Error Distance (MRED). The process begins by determining the Error Distance (ED), defined as $ED=|M'-M|$, where M' is the result produced by the approximate multiplier, and M is the exact result. Next, we calculate the Relative Error Distance (RED), given by $RED=ED/M$, representing the normalized error for each input combination. The MRED is then obtained as the average of all RED values across all possible input combinations:

$$MRED=\Sigma RED/65536$$

We perform an exhaustive simulation using MATLAB to evaluate all possible input combinations for each multiplier design. The results of this analysis are as follows:

Table 2: Accuracy comparison of Approximate 8x8 Multiplier

Design Name	ER (%)	MRED	NMED
MD -1 [14]	25.29	0.00228	3.50765×10^{-8}
PM1	36.27	0.01789	2.87524x10-7
MD-3 [14]	52.67	0.03066	4.71642×10^{-7}
MD-4 [14]	60.29	0.11778	1.81145×10^{-6}
PM2	74.23	0.14864	$3.52473\text{x}10^{-6}$
MD-5 [14]	92.53	0.21566	3.31665×10^{-6}
MD-7 [14]	95.27	0.23826	3.66419×10^{-6}
PM3	95.86	0.26897	$4.02567\text{x}10^{-6}$
MD-8 [14]	96.02	0.32955	5.06818×10^{-6}
PM4	97.73	0.28765	$4.28676\text{x}10^{-6}$

PM1 has a slightly higher error rate but still maintains a low MRED and NMED, making it a good balance between accuracy and approximation. PM3, and PM4 have the highest error rates and significantly higher MRED/NMED values, meaning they introduce a large amount of approximation error. Both PM2 and PM4 reduce power consumption by over 30% and improve energy efficiency by around 40%, making them excellent choices for low-power applications. PM4 is the best choice if the lowest PDP and smallest area are the main priorities. PM2 still offers good power savings with a slight trade-off in efficiency compared to PM4

4.2 Hardware Analysis:

To analyze the hardware performance of proposed multipliers, all multipliers are implemented in Verilog HDL and synthesized using Xilinx Vivado. For comparison purposes, an 8-bit exact Wallace tree multiplier was also implemented. The Exact design has the highest delay and power, making it the least power-efficient with the highest PDP. This suggests it is the least optimized among the designs. The PM4 design has the lowest PDP, indicating the best energy efficiency. It also has one of the lowest power consumption and a very low delay. PM2 is a strong contender with less PDP, a relatively low delay, and low power consumption. Both PM2 and PM4 significantly outperform the Exact multiplier in all metrics. PM4 is slightly better than PM2, with an additional 1-2% improvement in power, area, and PDP. PM2 and PM4 reduce power consumption by over 30% and improve energy efficiency by around 40%, making them excellent choices for low-power applications. PM4 is the best choice if the lowest PDP and smallest area are the main priorities. PM2 still offers good power savings with a slight trade-off in efficiency compared to PM4.

Table 3: Hardware Performance Comparison of Approximate 8x8 Multiplier

Design Name	Dealy (ns)	Power (µw)	Area(μm^2)	PDP(fJ)
Exact	7.938	7.588	758.56	60.24
MD -1 [14]	7.803	6.054	597.03	47.24
PM1	7.801	5.867	522.33	45.77
MD-3 [14]	7.803	5.645	512.35	44.05
MD-4 [14]	7.803	5.554	522.36	43.34
PM2	6.984	5.237	527.05	36.58
MD-5 [14]	6.974	5.974	534.26	41.67
MD-7 [14]	6.974	5.524	547.56	38.53
PM3	6.965	5.345	512.70	37.23
MD-8 [14]	6.972	5.214	514.65	36.36
PM4	6.964	5.148	512.47	35.86

5. IMAGE BLENDING APPLICATION

This work presents a novel image-blending technique implemented within the MATLAB environment. It leverages area-efficient approximate multipliers (M1, M2, M3, M4) to achieve finer control over the blending process compared to traditional methods. These custom multipliers prioritize specific image features or regions (e.g., edges in the cameraman image, textures in the Saturn image) during blending, offering a more nuanced approach while maintaining computational efficiency. The technique involves generating weight maps that define the contribution of each pixel from the source images (provided in TIF format, such as the classic cameraman and Saturn images) to the final blended output. The custom approximate multipliers then manipulate these weight maps to achieve the desired visual effect, such as the seamless blending of high-frequency details from the cameraman's image with the low-frequency textures of the Saturn image shown in fig 6. . The utilization of MATLAB's image processing toolbox streamlines the implementation process, enabling the creation and utilization of the multipliers. To evaluate the blended image's quality, we utilize established metrics like Peak signal-to-noise ratio (PSNR). The blended images are shown in Fig 7. These metrics offer quantitative assessments of the blended image's fidelity and accuracy, enabling thorough evaluation and analysis. These metrics provide quantitative measures of the blended image's fidelity compared to the original source images. Future research directions could involve exploring advanced, area-efficient multiplier designs that further optimize computational efficiency. Additionally, the integration of machine learning techniques holds promise for creating adaptive multipliers that can automatically adjust based on the specific content of the input images. Finally, developing a framework suitable for real-time image blending applications could expand the practical applications of this technique.



Figure 5.1. Cameraman and Saturn Inputs



Figure 5.2. Image Blending of different multipliers

5.1 Performance Evaluation

The performance of each multiplier variant is evaluated based on several key metrics, including area utilization, propagation delay, and PSNR for image blending applications.

Table 4 PSNR Comparison

Multiplier	PSNR
PM1	21
PM2	19
PM3	33
PM4	19

6.CONCLUSION

In this manuscript, we introduced a novel design for an approximate multiplier focusing on optimizing area utilization. We leverage compact compressors, half adders, and full adders to achieve this goal. The practical utility of our multiplier is demonstrated in an image blending application, under-scoring its relevance in real-world scenarios. Our thorough experimentation yields promising outcomes, with the highest peak signal-to-noise ratio (PSNR) reaching 33 for images of the cameraman and Saturn. Furthermore, we quantify the mean squared error (MSE) at 27, indicating the efficacy of our multiplier in maintaining image quality while reducing computational complexity. Our exhaustive evaluation under-scores the effectiveness of our approach in striking a balance between area efficiency and performance, rendering it suitable for deployment in resource-constrained settings like field-programmable gate arrays (FPGAs). The successful realization of our design underscores its potential across various domains requiring efficient arithmetic operations, thus advancing digital circuit design methodologies. Future research directions may explore further optimizations and extensions to address additional performance metrics and application domains.

7. REFERENCES

[1] Y. Wang, J. Lin, and Zh. Wang, “An Energy-Efficient Architecture for Binary Weight Convolutional Neural Networks,” IEEE Trans. Very Large Scale Integr. (VLSI) Syst., vol. 26, no. 2, pp. 280-293, Feb. 2018.

[2] N. Zhu,W. L. Goh,W. Zhang, K. S. Yeo, and Z. H. Kong, “Design of Low- Power High-Speed Truncation-Error-Tolerant Adder and Its Application in Digital Signal Processing,” IEEE Trans. Very Large Scale Integr. (VLSI) Syst., vol. 18, no. 8, pp. 1225-1229, Aug. 2010.

[3] Sr. Narayanamoorthy, H. A. Moghaddam, Zh. Liu, T. Park, and N. S.Kim, “Energy-Efficient Approximate Multiplication for Digital Signal Processing and Classification Applications,” IEEE Trans. Very Large Scale Integr. (VLSI) Syst., vol. 23, no. 6, pp. 1180-1184, Jun. 2015.

[4] Ch. K. Jha, S. N. Ved, Is. Anand, and J. Mekie, “Energy and Error Analysis Framework for Approximate Computing in Mobile Applications,” IEEE Trans. Circuits Syst. II, Exp. Briefs. DOI: 10.1109/TCSII.2019.2910137.

[5] A. Momeni, J. Han, P. Montuschi, and F. Lombardi, “Design and Analysis of Approximate Compressors for Multiplication,” IEEE Trans. Comput., vol. 64, no. 4, pp. 984-994, Apr. 2015.

[6] Y. Liu, T. Zhang, and K. K. Parhi, “Computation Error Analysis in Digital Signal Processing SystemsWith Overscaled Supply Voltage,” IEEE Trans. Very Large Scale Integr. (VLSI) Syst., vol. 18, no. 4, pp. 517-526, Apr. 2010.

[7] D. Jeon, M. Seok, Zh. Zhang, D. Blaauw, and D. Sylvester, “Design Methodology for Voltage-Overscaled Ultra-Low-Power Systems,” IEEE Trans. Circuits Syst. II, Exp. Briefs, vol. 59, no. 12, pp. 952-956, Dec. 2012.

[8] R. Liu and K. K. Parhi, “Power Reduction in Frequency-Selective FIR Filters Under Voltage Overscaling,” IEEE Trans. Emerg. Sel. Topics Circuits Syst., vol. 1, no. 3, pp. 343-356, Sept. 2011.

[9] V. Mrazek, R. Hrbacek, Z. Vasicek and L. Sekanina, “EvoApprox8b:Library of Approximate Adders and Multipliers for Circuit Design and Benchmarking of Approximation Methods,” in Proc. Design, Automation & Test in Europe Conference & Exhibition (DATE), Lausanne, Switzerland, Mar. 2017, pp. 258-261.

[10] A. Dalloo, A. Najafi , and A. G.-Ortiz, “Systematic Design of an Approximate Adder: The Optimized Lower Part Constant-OR Adder,” IEEE Trans. Very Large Scale Integr. (VLSI) Syst., vol. 26, no. 8, pp. 1595-1599, Aug. 2018.

[11] S. Dutt, S. Dash, S. Nandi, and G. Trivedi, “Analysis, Modeling and Optimization of Equal Segment Based Approximate Adders,” IEEE Trans. Comput., vol. 68, no. 3, pp. 314-300, Mar. 2019.

[12] O. Akbari, M. Kamal, A. A.-Kusha, and M. Pedram, “RAP-CLA: A Reconfigurable Approximate Carry Look-Ahead Adder,” IEEE Trans. Circuits Syst. II, Exp. Briefs, vol. 65, no. 8, pp. 1089-1093, Aug. 2018.

[13]M. Ha and S. Lee, “Multipliers with Approximate 4-2 Compressors and Error Recovery Modules,” IEEE Embedded Systems Letters, vol. 10 , no. 1, pp. 6-9, Mar. 2018.

[14] M.S. Ansari, H. Jiang, B.F. Cockburn, J. Han, Low-power approximate multipliers using encoded partial products and approximate compressors, IEEE J. Emerging Sel. Top. Circuits Syst. 8 (3) (2018) 404–416, https://doi.org/10.1109/ JETCAS.2018.2832204. [2] A. Jain, N. Dugar, S. Yadav

Biographies



Sreelakshmi. Vadlamudi is a research scholar in the Electronics & Communication Engineering department under the JNTUK, Kakinada, Andhra Pradesh. She is currently working as an Assistant Professor in, the Electronics & Communication Engineering department in Seshadri Rao Gudlavalleru Engineering College. She completed UG in Electronics and Communication Engineering in the year 2004 from JNTU, Hyderabad. She completed her PG in VLSI System Design in 2011 at JNTU, Hyderabad.



Dr.Y. Syamala received her B.E., M.E., from Bharathiyar University, Anna University in 2001, and 2005 respectively. She received a Ph.D from JNTUH; Hyderabad in 2014. She has been working as a Professor at Seshdri Rao Gudlavalleru Engineering College, Gudlavalleru. Her research interest includes Low-power VLSI design, Digital design, and Testing.



Madhu Ramarakula received the BE (Bachelor of Engineering) degree in electronics and communication engineering from Osmania University, Hyderabad, India, in 2003 and MTech degree in communication systems from Jawaharlal Nehru Technological University Hyderabad, India, in 2009. He received his PhD degree in electronics and communication engineering from Andhra University, Visakhapatnam, India, in 2014. He is presently working as an assistant professor in the Department of Electronics and Communication Engineering, University College of Engineering Kakinada (A), JNTUK, Kakinada, India. He has 10 years of teaching experience. He has published more than 40 research papers in various reputed national and international journals and conferences. His research interests include mobile and cellular communications, antennas, satellite communications, and GNSS. He is a Member of IEEE.

Rainfall-Triggered Landslide Susceptibility Mapping Using GIS and LightGBM: A Case Study of Uttara Kannada

Babitha Ganesh [1, 2] , Shweta Vincent [1,*] , Janardhana Bhat [2,3], Sameena Pathan[4], Ganesh Bhat[5]

[1] *Department of Mechatronics, Manipal Institute of Technology, Manipal Academy of Higher Education, Manipal, 576104, Karnataka, India*

[2] *Department of Computer Science and Engineering, Canara Engineering College, Bantwal, 574219, Karnataka, India*

[3] *Department of Electronics and Communication Engineering, Manipal Institute of Technology, Manipal Academy of Higher Education, Manipal, 576104, Karnataka, India*

[4] *Department of Information and Communication Technology, Manipal Institute of Technology, Manipal Academy of Higher Education, Manipal, 576104, Karnataka, India*

[5] *Department of Electronics and Communication Engineering, Canara Engineering College, Bantwal, 574219, Karnataka, India*

Summary: Landslide susceptibility mapping is the crucial process for identifying the areas vulnerable to landslides. Uttara Kannada district, located within the boundaries of Western Ghats of Karnataka, India has often experienced slope failures during the rainfall season. This study aims to ascertain leading triggering factors beyond rainfall and to supplement the high resolution landslide susceptibility map in ArcGIS environment uisng the LightGBM classifier. The dataset comprising information of 867 historical landslides and ten different parameters including slope, aspect, soil type, geomorphology, elevation, LULC, TRI, TWI, lineament density and distance to road were gathered from different remote sensing based sources. The permutation model has been used to discover the most influential attributes. Slope, lineament density and soil type have emerged as the most influential ones. The LightGBM classifier has been chosen to prepare LSM for its superior capability in handling categorical variables and its ensemble based approach which enhances the prediction accuracy by integrating mutiple classifiers. The model's performance was rigorously evaluated using multiple statistical metrics, achieving a precision of 0.86, recall of 0.937, accuracy of 0.91, f1-score of 0.897, Kappa index value of 0.817 and an AUC-ROC value of 0.97 demonstrating its strong predictive effectiveness. The LSM generated shows that three taluks including Kumta, Ankola and Karwar are having more locations that are susceptible to landslides. The findings of this study provide crucial insights for identifying the high-risk zones in Uttara Kannada, enabling the policy makers and urban planners to make well planned decisions on infrastructure development while minimizing concerns about landslide related hazards.

Keywords: Landslide susceptibility mapping(LSM), Landslide conditioning factors (LCF), Random Forest(RF), LightGBM

1. Introduction

Landslides are one of the most devastating natural hazards causing significant threat to human life as well to the infrastructure. They regularly occur at the hilly regions often triggered by hevay precipitation, earthquakes and human activities. While, landslides have been a concern in locations that are having steep slopes and fragile geological formations, their frequency and impact have been increasing due to rising developement activities. Uttara Kannada, a district spanning arround 10,291 km^2 situated within ecologically sensitive Western Ghats had witnessed a surge in landslide occurences during the monsoon season. Historically, this region had no significant record of landslides until the catastrophic event took place in Karwar, which resulted in the death of 19 people. In subsequent years, additional landslides were reported along the Kumta coast and Karwar, where boulders rolling down a steep hill caused the train mishap. The most recent landslide in Shirur,Ankola on July 16, 2024, further highlights the growing susceptibility of hazards, as heavy rains and road expansion activities triggered the slope failure, claiming nine lives and two individuals missing[1].

Identifying the areas that are vulnerable to landslides is the primary motto of the landslide susceptibilty mapping(LSM). Geographic Information systems(GIS) have emerged as a powerful tool for LSM creation by integrating spatial and environmental data to analyze terrain stability. GIS allows overlaying different landslide triggering factors to identify the risk prone areas. In recent years, ML techniques have revolutionized LSM by capturing the complex and non-linear relationship between LCFs and the possibility of slope failure occurence.

Traditional statistical methods, while useful often fail to account for the intricate interactions among the various triggering factors. On the other hand, ML classifiers can learn from historical data, recognize patterns and improve the predictive power. Among the ML methods, ensemble learning techniques have gained prominence due to their ability to enhance classification performance by combining multiple models[2].

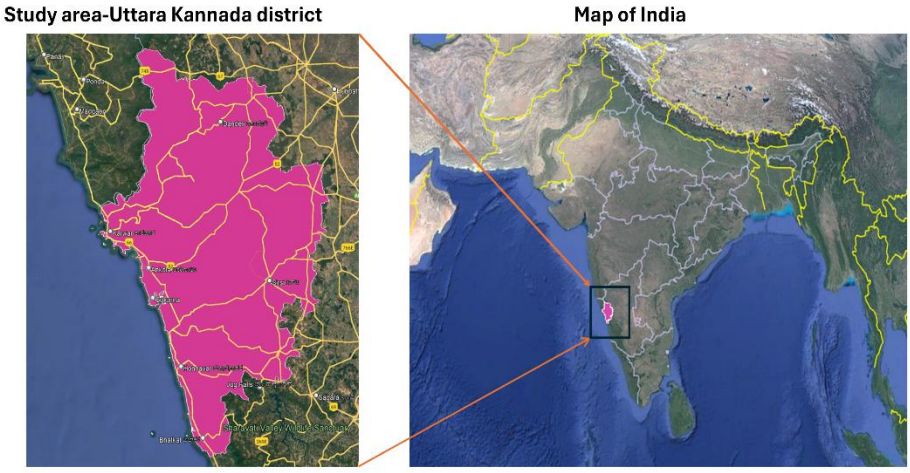

Fig. 1 Study area mapping

LightGBM(Light Gradient Boosting machine) is the gradient boosting framework developed by Microsoft, has been proven to be highly effective in generating LSMs. This algorithm is well suited to manage large datasets with high dimensions. Unlike conventional tree based models, lightGBM efficiently handles categorical variables, reduces overfitting and often faster training speed[3]. Moreover, its ability to assign greater importance to the most influential features enhances the landslide prediction accuracy. These benefits make LightGBM a superior choice for developing reliable LSM which is essential for disaster preparedness and land-use planning.

Although some research studies have been conducted in different parts of Uttara Kannada[4] [5]to the best of our knowledge, no study has been focused on creating the LSM for the entire district. Additionally, despite its strong capabilities in LSM generation, LightGBM remains largely unexplored in the context. Therefore, the primary objective of this study is to develop an LSM for the entire Uttara Kannada district by integrating GIS and LightGBM classification algorithm. The study area mapping is shown in Fig. 1.

2. Methodology

The overall methodology followed in this work has three main steps as depicted in the Fig. 2. These include data collection, modelling and evaluation. The description of these steps is presented in this section.

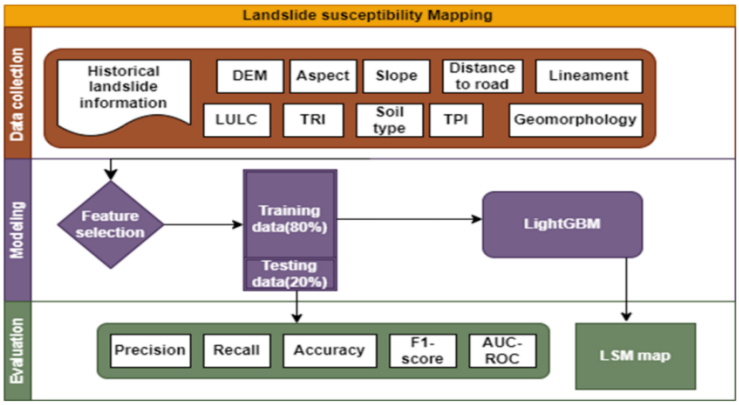

Fig. 2 Methodology

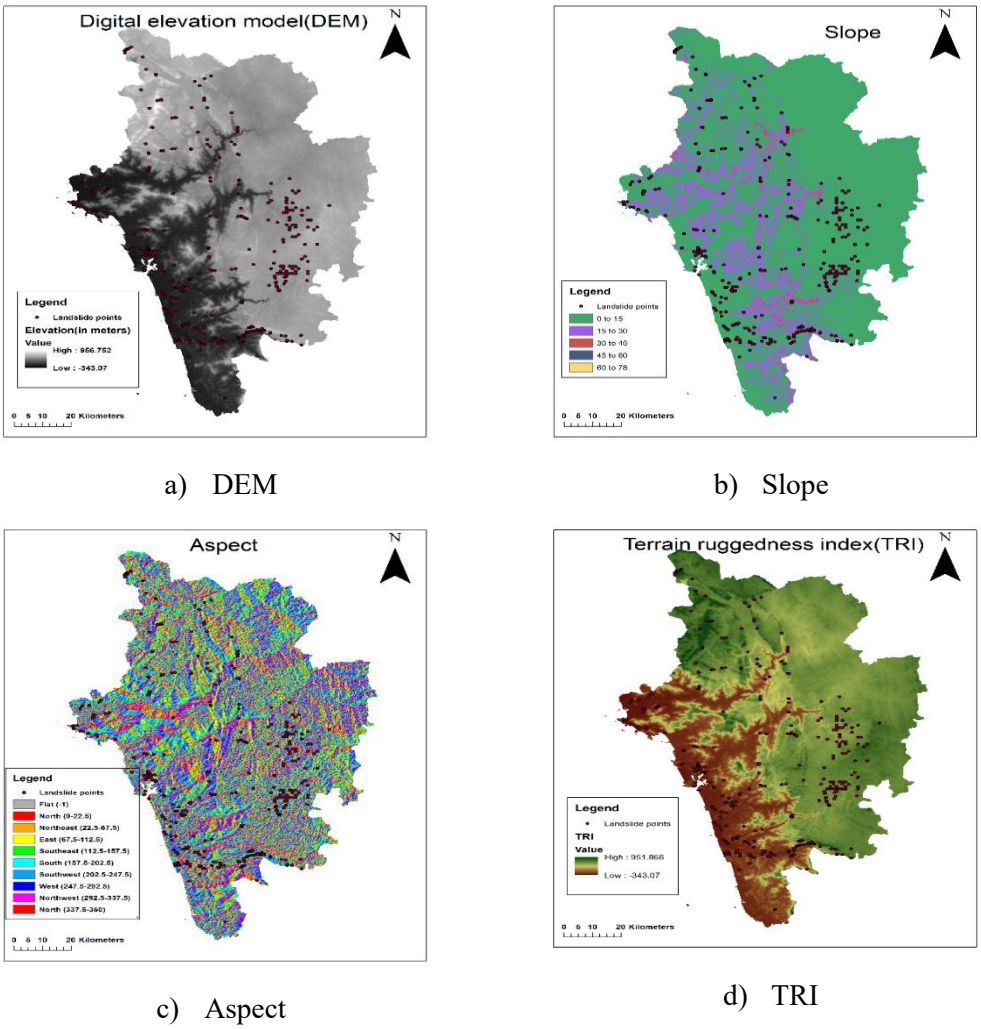

a) DEM b) Slope

c) Aspect d) TRI

Fig. 3 LCFs(DEM, Slope, Aspect, TRI)

2.1 Data collection:

The preparation of landslide susceptibility map using ML classifier mainly requires the information of historical landslide locations and the different triggering factors that influence the occurence of slope failures. The information of landslides has been collected from past records maintained by GSI in Bhukosh portal[6]. This inventory includes 437 landslide locations that has witnessed landslides during the period of 2014 to 2020. The dataset analyis revealed that all of these landlsides were triggered by heavy rainfall. It is also essential to consider other secondary factors that lead to the occurrence of slope failures. The LCF maps generated for the study area is depicted in the Fig. 3 and Fig. **4**. These maps have been generated in ArcGIS environment by using the remote sensing data available in public sources. The 30 m resolution DEM that represent the terrain of the study area has been downloaded from Bhukosh portal. Factors such as TRI, TWI and aspect have been derived from DEM. Lithology and soil maps were collected from Bhukosh portal. The LULC map has been clipped from the global LULC map available as ESRI land cover data[7]. DIVA-GIS provides free geographic data, including road networks, which can be used to create a distance to road map[8]. The soil map shown in the figure has been created using data provided by FAO-UNESCO[9]. The lineament map of the study area was created by digitizing the lineament data obtained from Bhuvan[10] at a 1:50,000 scale.

2.2 Modeling:

Although we have prepared 10 LCFs, all of them need not be used as some may not significantly influence slope failure prediction for the study area considered. To determine the most relevant features, Permutation feature importance model has been employed. The Fig. 5 illustrates the feature importance values, revealing that the slope, lineament density, soil type and geomorphology are most influential features. In contrast, LULC, aspect and TWI showed minimal contribution to the results. Therefore these factors have been excluded from further analysis.

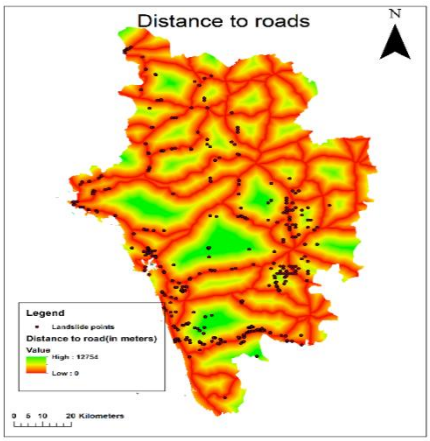

a) Distance to road

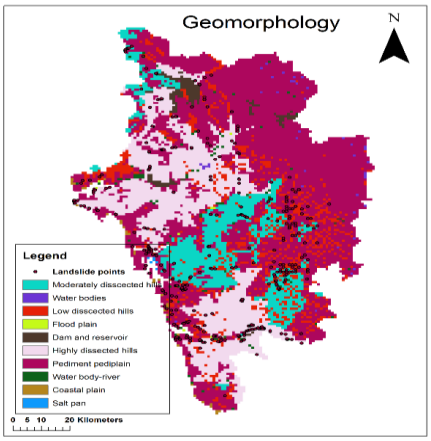

b) Geomoprohology

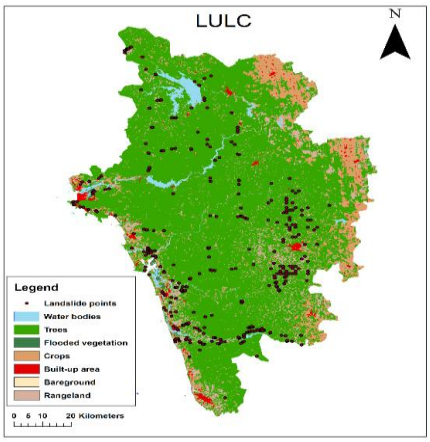

c) LULC

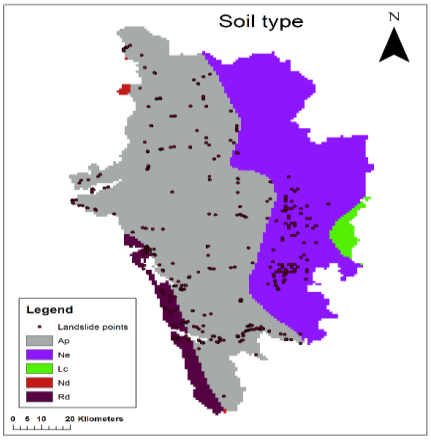

d) Soil type

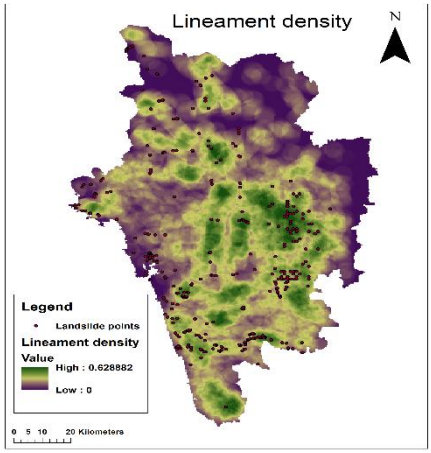

Lineament density

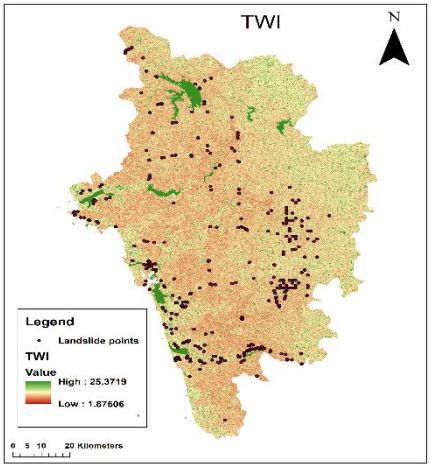

f) TWI

Fig. 4 LCFs(Distance to road, Geomorphology, LULC,Soil type, Lineament denisty and TWI)

After selecting the optimal set of LCFs, these maps were overlaid on the 437 landslide amd randomly seelcted 505 non-landslide locations. By using ”**extract multi values to points**” function of the ArcMap, the CSV file reqired to train and test the model has been generated. Since the dataset included soil type and geomorphology

as categorical variables, it was aimed to select the classifier that can handle these without requiring explicit encoding. Additionally, we needed a model that could automatically assign the appropriate weights to the features based on their significance. Considering these criteria, LightGBM(Light Gradient Boosting Machine) has been selected for generating the LSM due to its efficiency, ability to handle categorical variables, and superior performance in feature selection.

2.3 Evaluation:

The model that has been trained by using the training dataset generated has to be tested to check how well the model is able to distinguish between the locations that are susceptible to landslides or not. For this six different performance metrics including precision, recall,accuracy, F1-score,kappa index and AUC-ROC.

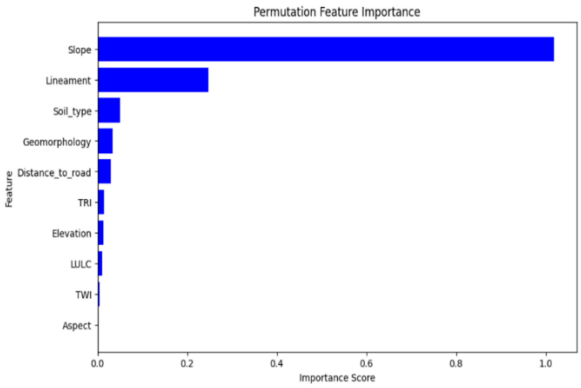

Fig. 5 Importance of features

.

3. Results and Discussions

Tabel 1 shows the values of evaluation metrics. The precision reveals that 86% of the locations identified as landslide-prone are actually correct. The recall value indicates that the model successfully detects 93.7% of the actual landslide prone locations, which is the strong indicator of very low false negative rate. The accuracy suggests that 91% of all locations were correctly classified. The F1-score reveals the well-balanced model, effectively handling both false positives and false negatives. The Kappa index is an indication of strong agreement between the model's predictions and actual values beyond random chance. The AUC-ROC shown in the Fig. 6 AUC-ROC shows that the model has an excellent ability to differentiate between landslide-prone and non-prone areas.

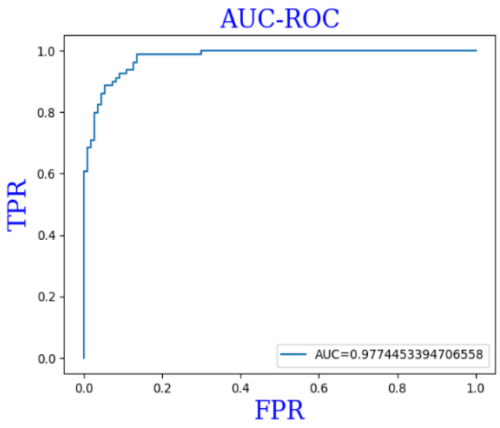

Fig. 6 AUC-ROC

After evaluating the model, approximately 9000 points were randomly selected from the study area, and the corresponding prediction probability values for landslide occurence(1: susceptible, 0: non-susceptible) were generated. The values indicating the confidence of the model in predicting it as susceptible were then spatially

distributed using the Inverse Distance Weighting(IDW) method.These values were then reclassified into 5 different classes for the better interpretation. The areas shown in purple color are highly susceptible to landslides with the prediction probability values ranging from 0.6 to 0.8. The prediction probability values less than 0.6 indicates that they are safe places without the risk of landslides. The resultant LSM is shown in the Fig. 7.

Tabel 1 Values of performance metrics

Performance metric	Values
Precision	0.86
Recall	0.937
Accuracy	0.91
F1-score	0.897
Kappa index	0.817

This LSM reveals that around 29% of the total study area is at high risk of landslides. Additionally, around 29% of the total area falls under the moderate risk, indicating the potential for landslides under extreme conditions such as heavy rainfall or land disturbances. The remaining 47% of the area is free is from the landslide risk, making it relatively stable locations. Among the 12 taluks of Uttara Kannada, the Western Coastal taluks of Karwar, Kumta and Ankola exhibit the higher denisty of landslide prone areas. Because of its steep terrain and closeness to the Arabian Sea, Karwar, which is the district seat and is situated in the northwest coastal region, frequently encounters landslides. Significant landslide vulnerability is also seen in Ankola, which is located south of Karwar, and Kumta, which is located farther south along the coast. These areas are probably affected by deforestation, infrastructural development, and the effects of the seasonal monsoon. Meanwhile, areas categorized under moderate risk require precautionary measures, especially in Siddapur, Sirsi, and Yellapur, where hilly terrain and land-use changes contribute to occasional landslides.

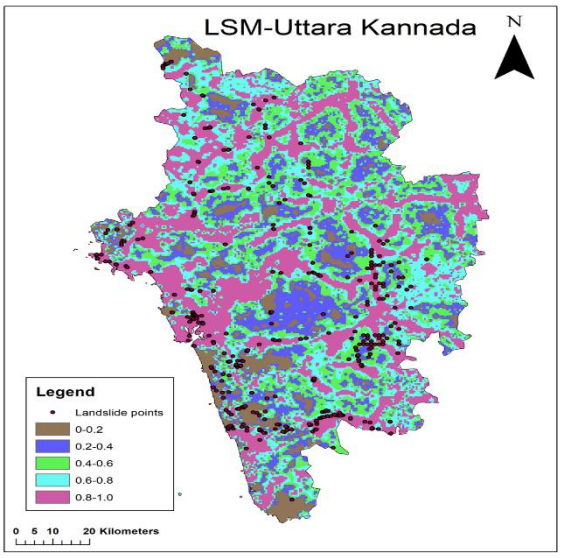

Fig. 7 Landslide susceptibility map of Uttara Kannada

4. Conclusion

This study successfully developed the high resolution LSM for the entire Uttara Kannada district using LightGB ensemble classification algorithm in the ArcGIS environment. The analysis identified slope, lineament density and soil type as the most influential factors along with heavy rainfall in the study area. The model developed exhibited good performance with an AUC-ROC of 0.97 and other strong evaluation metrics, confirming its reliability. The LSM highlights Kumta, Ankola, and Karwar as the most landslide-prone taluks. These findings provide valuable insights for policymakers and urban planners, aiding in risk mitigation and sustainable infrastructure development in landslide-prone areas.

References

[1] P. Kundu, V. Menon, S. Kolathayar, and P. U, "The Shirur landslide of July 2024 triggered by intense rainfall and unchecked development," *Natural Hazards Research*, Jan. 2025, doi: 10.1016/j.nhres.2025.01.005.

[2] S. Narayana and K. Jayaraman, "Landslide Hazard Zonation Mapping Using ML Techniques – A Study Over Kodagu District, Karnataka," in *2024 IEEE 6th PhD Colloquium on Emerging Domain Innovation and Technology for Society (PhD EDITS)*, IEEE, Nov. 2024, pp. 1–2. doi: 10.1109/PhDEDITS64207.2024.10838639.

[3] G. Ke *et al.*, "LightGBM: A Highly Efficient Gradient Boosting Decision Tree." [Online]. Available: https://github.com/Microsoft/LightGBM.

[4] Avinash KG and Ashamanjari KG, "A GIS and frequency ratio based landslide susceptibility mapping: Aghnashini river catchment, Uttara Kannada, India," 2010. [Online]. Available: www.IndianJournals.com

[5] R. T. V Subash Chandran *et al.*, "Landslide Susceptible Zone Mapping in Uttara Kannada, Central Western Ghats Sahyadri Conservation Series 7," 2012.

[6] "Bhukosh." Accessed: Feb. 09, 2025. [Online]. Available: https://bhukosh.gsi.gov.in/Bhukosh/Public

[7] "Esri Land Cover." Accessed: Feb. 09, 2025. [Online]. Available: https://livingatlas.arcgis.com/landcover/

[8] "Data — DIVA-GIS." Accessed: Feb. 09, 2025. [Online]. Available: https://diva-gis.org/data.html

[9] "FAO/UNESCO Soil Map of the World | FAO SOILS PORTAL | Food and Agriculture Organization of the United Nations." Accessed: Feb. 09, 2025. [Online]. Available: https://www.fao.org/soils-portal/data-hub/soil-maps-and-databases/faounesco-soil-map-of-the-world/en/

[10] "Thematic Data - Bhuvan Wiki." Accessed: Feb. 09, 2025. [Online]. Available: https://bhuvan.nrsc.gov.in/wiki/index.php/Thematic_Data

Flood Susceptibility Mapping of Chikkamagaluru District of India using Ensemble Technique

Sting Salvador Gonsalis[1], Shweta Vincent[2], Om Prakash Kumar[3], Vijay Mohan[4]

[1,2,4] Department of Mechatronics, Manipal Institute of Technology, Manipal Academy of Higher Education, Manipal, 576104, Karnataka, India

[3] Department of Electronics and Communication Engineering, Manipal Institute of Technology, Manipal Academy of Higher Education, Manipal, 576104, Karnataka, India

Abstract.

Floods are an extensive and destructive natural occurrence that has an influence on agriculture, the environment, and the economy in addition to destroying property and human lives. Therefore, in order to minimize and limit damage, it is essential to identify sensitive zones using flood susceptibility mapping (FSM).This article shows the employment of ensemble machine learning model named as Light Gradient Boosting Machine (LightGBM) for categorization of flood-prone regions of the Chikkamagaluru district in India. Eight elements were utilized to develop the flood susceptibility model: slope, aspect, elevation, land use-land cover (LULC), normalized difference vegetation index (NDVI), normalized difference water index (NDWI), topographical wetness index (TWI), and drainage density (DD). In addition, flood inventory map (FIM) is utilized to determine the areas sensitive of flooding. The application of this ensemble machine learning model in mapping and estimating flood risk is investigated, and suggestions for additional research are made. The Area under the curve-Receiver operating characteristics (AUC-ROC) approach was used to evaluate the model's output, and LightGBM) was found to function well with an AUC score of 0.9666.

Keywords: Flood Suscpetibility Mapping (FSM), Flood Conditioning Factors (FCF), Flood Inventory Map (FIM), Ensemble Machine Learning, Light Gradient Boosting Machine (LightGBM), Area under the curve - Receiver operating characteristics (AUC-ROC)

1. INTRODUCTION

Effective disaster risk management depends mostly on flood susceptibility mapping, especially in areas like Chikkamagaluru, India, vulnerable to floods because of complicated topography and hydrological processes. Although total flood management is still unattainable, flood susceptibility maps (FSMs) provide priceless information for handling pre- and post-flood situations in face of both natural and human-induced obstacles. Coupled with the always rising global population, more frequent and severe downpour events brought on by climate change further increase flood hazards, maybe affecting millions of people.

In order to meet this urgent demand, this research investigates the creation of FSMs using a multi-criteria decision support system designed specifically for the South Indian area of Chikkamagaluru. By using ensemble machine learning, the research seeks to improve the precision of flood forecasts and identify regions that are vulnerable to floods. A strong flood risk map will be produced by using information gain theory to track down important conditioning factors causuating flooding.

Topographical, land use and hydrological indices are among the geoenvironmental elements that are analyzed as part of the study process. Historical flood data is included to train and verify the FSM model. Using the AUC-ROC approach and confusion matrix parameters, the algorithms' efficacy in producing FSMs will be thoroughly assessed.

1.1. THE PROBLEM OF FLOODS AND THE OBJECTIVE

Coastal position, urbanization, and changing rainfall patterns are complex interplaying elements that traditional flood susceptibility mapping in Chikkamagaluru District fails to represent due to inadequate data. Inaccurate flood maps are a result of these restrictions, which makes it harder to effectively plan for floods and manage risk.The recent floods in Chikkamagaluru have brought attention to the critical need for better flood

forecast. In order to direct focused mitigation activities, current maps are not precise enough.Because floods are dynamic events affected by the strength and length of rainfall, traditional approaches have a hard time accounting for this fact and integrating varied geographical data (soil characteristics, land cover, drainage)[5]. Furthermore, they are ill-equipped to deal with the shifting ecosystems that are a direct result of global warming.

Our study aims to use ensemble machine learning to create a Flood Vlulnerability Map for Chikkamagaluru. The created map's efficacy would be judged by its performance of assessment generated by ensemble machine learning techniques. Various Flood Conditioning Factors (FCFs) have been explored for the production of the final FSMs.

1.2. ORGANIZATION OF THIS ARTICLE

An overview of the literature on the different methods for creating FSMs and their associated accuracy is provided in the next section of this article. Our article's basic methodology is described in the third section, and the results and discussions are presented in the fourth. The article's fifth and final part concludes the article and outlines the future scope for study.

2. LITERATURE REVIEW

Flooding is an utmost natural hazard causing severe loss of life and economic damage. Techniques for predicting floods are essential for reducing these effects. This study looks at the research on mapping flood risk using Geographic Information System (GIS) and multi-criteria analysis. Because GIS makes it possible to create and analyze spatial data on flood-conditioning factors, it is essential to flood susceptibility mapping. Flood susceptibility is evaluated by integrating these aspects using multi-criteria analysis methodologies. Choosing the right flood-conditioning elements is essential. Topography (slope, elevation)[3], hydrology (drainage density, distance to/from river)[10], soil features, and land use and/or cover are examples of common factors[18]. Research places a strong emphasis on choosing parameters based on the data's availability and the research location.

Flood susceptibility mapping is done using a variety of approaches. These models evaluate how individual flood-conditioning parameters and flood events are related. Frequency Ratio (FR) and Information Value (IV) models, which are used by [14], [3], constitute examples. By using methods such as the Analytical Hierarchy Process (AHP), it is possible to give weights to various elements and incorporate expert knowledge [2]. [9] and [16] studies illustrate this strategy. The capacity of techniques such as Multi Criteria Decision Analysis (MCDA) [6], Logistic Regression (LR) [7], and Artificial Neural Networks[19] to handle intricate interactions between components has led to their growing application in flood susceptibility mapping. The use of remote sensing data, namely from Synthetic Aperture Radar (SAR), may improve mapping of flood vulnerability by offering insights into the magnitude of flooding and the presence of water [1]. For increased transparency and interpretability, research is looking at new strategies including Artificial Neural Network - Synthetic Minority Oversampling Technique (ANN-SMOTE)[19] and Alternating decision tree(ADT) classifiers [4].

[2], [9] highlight the usage of AHP in the construction of FSM. [14] illustrates how FR and other statistical models are used. Table 1 illustrates how flood risk is mapped using machine learning and other techniques in [4], [6], [7], [15], and [19].Analytic network process (ANP) and spatial analysis are discussed in [5], [12]. State-of-the-art FSM production uses a variety of soft-computing approaches, which are summarized in Table 1. Additionally, the table displays the evaluation parameters that were used to create and validate the FSMs.

The study makes it evident that a number of writers have investigated the use of machine learning techniques to the development of FSMs. However, our paper describes the development of the FSM for Chikkamagaluru, an area in India that is prone to flooding.

3. METHODOLOGY

This part explains the methods used for the building of the FSM of Chikkamagaluru. As shown in Figure 1, the Flood Inventory Map and Flood Conditioning Factors are created through these steps.

To produce the FIM and FCFs of Chikkamagaluru district, data is gathered from a variety of field study sources, including Google Earth, ESA, and USGS Earth Explorer. This study makes use of Landsat 8 data with a spatial resolution of 30 meters. The following FCFs were made using the ArcGIS program and the Chikkamagaluru Digital Elevation Model (DEM): "Drainage density" (DD) is the total length of a watershed's

channels, including both natural and constructed stormwater drainage infrastructure, ‘Slope’ is the ground surface's rise or fall, "Aspect" is the degree of orientation of the slope, with 0 representing north, 90 east, 180 south, and 270 west and it ranges from 0 to 360 clockwise., ‘Elevation’ is defined as the distance above sea level, ‘Land use-land cover’ (LULC) in which the physical surface of the planet is known as land cover, while "land use" describes how land is used or utilized for human endeavors, "Normalized difference vegetation index" (NDVI) measures the amount and condition of ground-surface vegetation, ‘Normalized difference water index’ (NDWI) is an indicator for identifying and tracking changes in surface water content, and ‘Topographical wetness index’ (TWI) is a model that uses the land's topography to determine how moist the soil is in a given location.

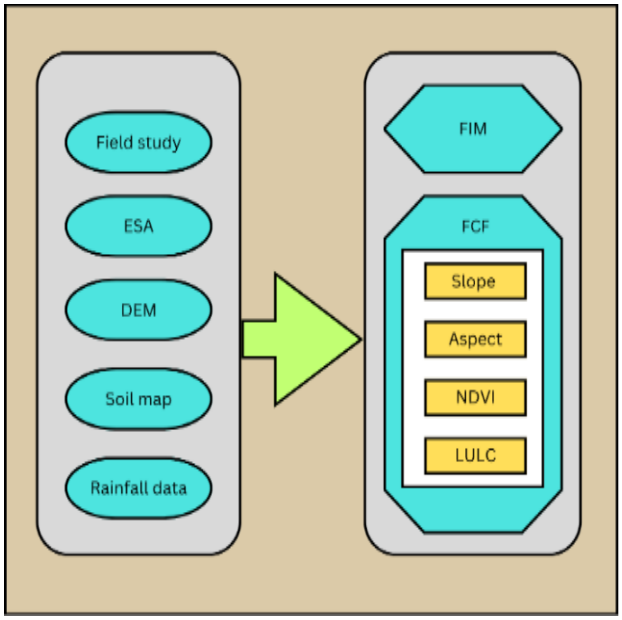

Figure 1: FIM and FCF creation

In order to acquire the data points, each of these thematic maps is compared to the others. The historical flood information is in the FIM. This is superimposed on top of the FCF maps, resulting in a thorough dataset for testing and training.

The use of these two maps, the FIM and FCF, in the final FSM generation is shown Figure 2.

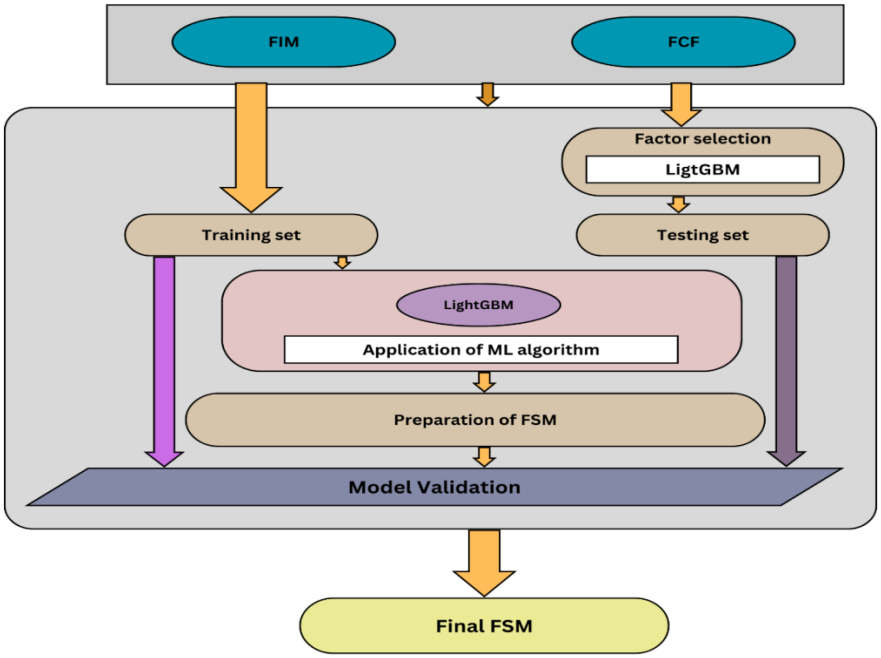

Fig. 2. Creation of FSM

The ensemble machine learning algorithm named LightGBM [20] receives the FIM and FCF as inputs, and outputs the FSM. Metaheuristics (which were not used in our research) may or may not be utilized to adjust the machine learning algorithm for weights. Following model creation, validation is performed and final AUC-ROC scores are produced.

Ref No.	**Algorithms / techniques used**	**Evaluation Parameters**	**Parameter values**	**Region**	**No. of FCFs used**
[6]	Multi Criteria Decision Analysis (MCDA)	AUC-ROC	0.8724	Dodoma region, central Tanzania	7
[7]	Logistic Regression (LR	AUC-ROC	0.901	Mersin, Turkey	12
[13]	Shannon's Entropy (SE)	AUC-ROC	0.87	Bagmati basin, Bihar	12
[17]	Random Forest (RF)	AUC-ROC	0.956	The Bâsca Chiojdului river basin, Romania	10
[8]	Ensemble Artificial neural network (ANN)	AUC-ROC	0.936	Eastern Mediterranean basin, Türkiye	12
[1]	Random Forest (RF) CART (Classification and Regression Trees) SVM(Support vector Machines) XGBoost(Extreme Gradient Boosting)	AUC-ROC	0.807 0.780 0.756 0.727	The Metlili watershed, Morocco	12
[4]	Alternating decision tree (ADT) Functional tree (FT) Kernel logistic regression (KLR) Multilayer perceptron (MLP) Quadratic discriminant analysis (QDA)	AUC	0.972 0.959 0.956 0.95 0.95	Tafresh Watershed, Iran	8
[12]	Frequency ratio (FR) Weight of evidence (WofE) Random forest (RF) Multi-layer perceptron (MLP)	AUC	0.921 0.920 0.936 0.956	Gembong–Pekalen basin, Indonesia	11
[2]	K-Star (KS) algorithm K-Nearest Neighbor(KNN) KNN–AHP KS–AHP	AUC	0.887 0.852 0.896 0.878	Prahova river basin, Romania	10
[3]	Frequency ratio (FR) Weights of evidence (WoE) Certainty factor (CF) Shanon's entropy (SE) Information value (IV)	AUC	0.928 0.925 0.909 0.923 0.913	North-east depression, Bangladesh	11
[19]	Artificial Neural Network - Synthetic Minority Oversampling Technique (ANN-SMOTE) AHP Shannon Entropy	AUC-ROC	0.902 0.650 0.472	Ontario, Canada	6
[15]	AHP	AUC	0.812	Kathmandu metropolitan city	6

[16]	Galactic swarm optimization (GSO) Adagrad (Adaptive Gradient) Adaptive Moment Estimation (Adam)	AUC	0.887 0.900 0.882	Ha Giang, Vietnam	11
[18]	support vector regression (SVR) SVR-bat algorithm (SVR-BA) SVR-invasive weed optimization (SVR-IWO) SVR-firefly algorithm (SVR-FA)	AUROC	0.77 0.79 0.80 0.81	Ahwaz , Iran	11

Table 1. Literature Review

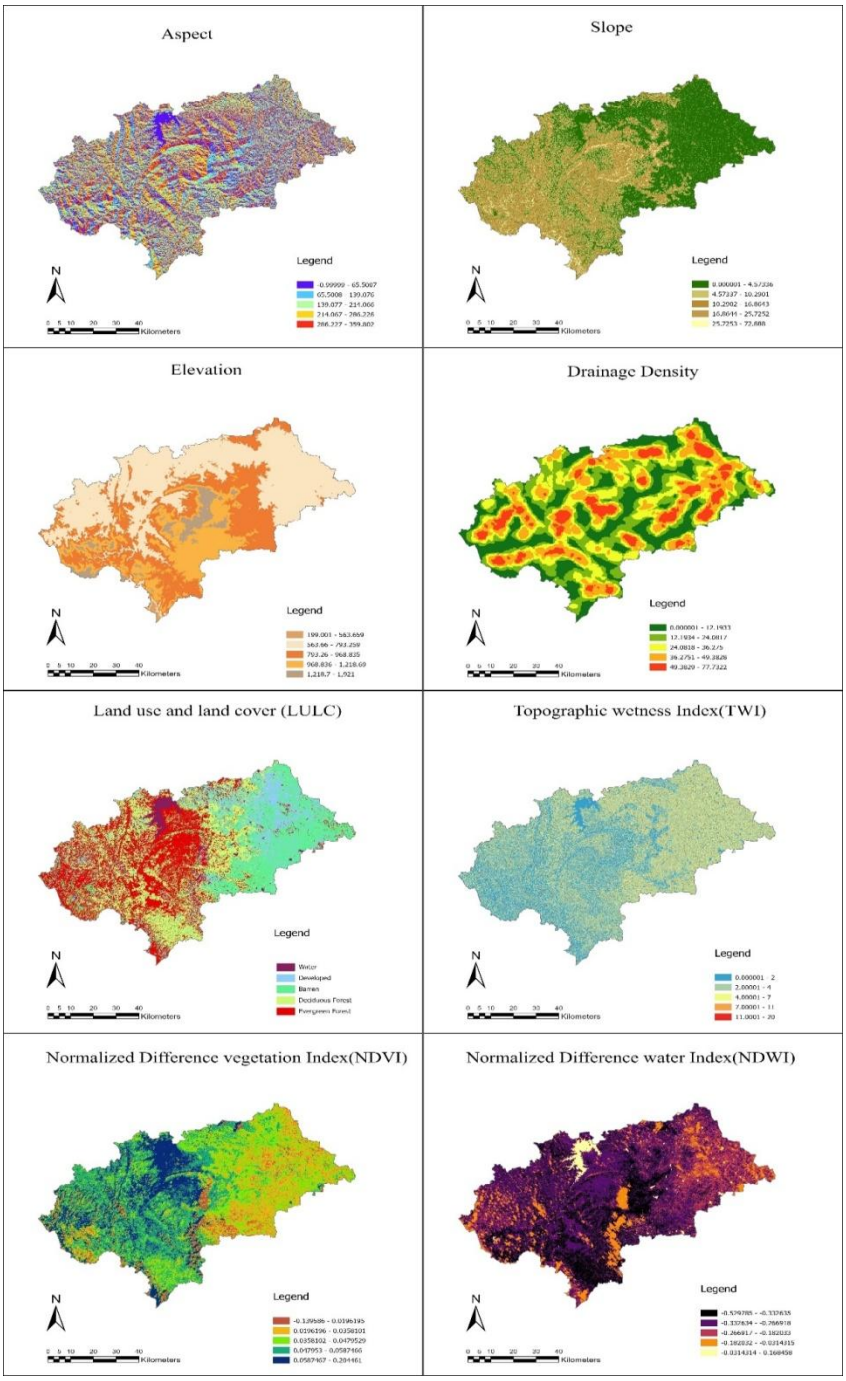

Fig. 3. FCFs generated for Chikkamagaluru

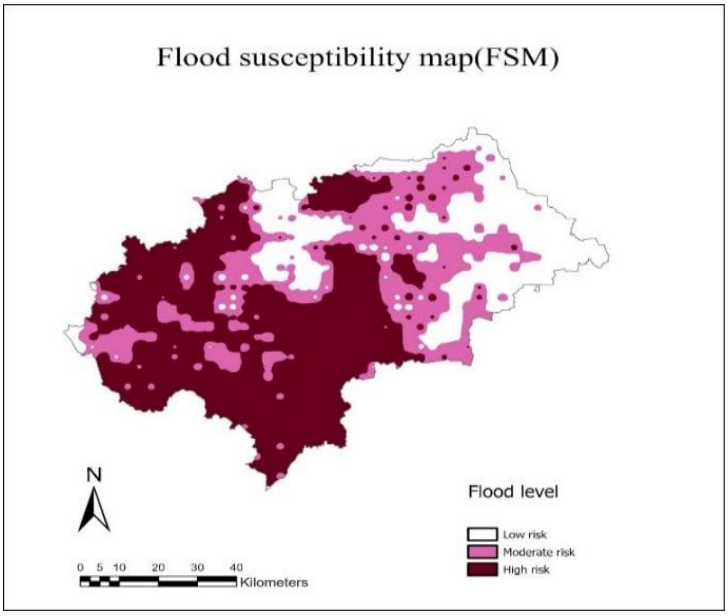

Fig. 4. Final FSM generated for Chikkamagaluru using LightGBM

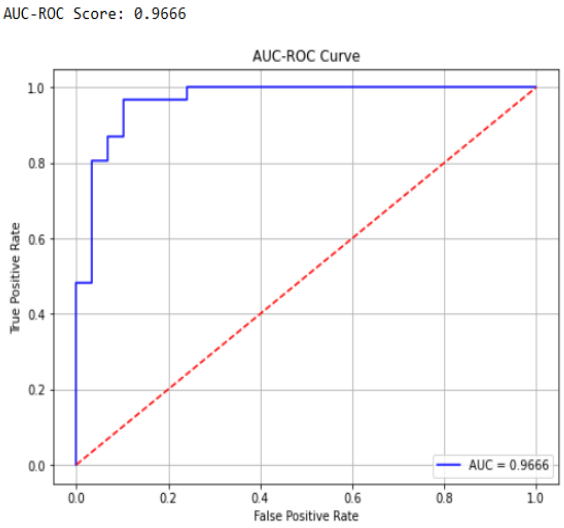

Fig. 5. AUC-ROC analysis of LightGBM model

4. Results and Discussion

Figure 3 displays the several FCFs that have been produced using the previously discussed methodology. Figure 4 displays the final FSM produced by the LightGBM technique. Flood risk levels are divided into three categories based on the impact of floods: low, moderate, and high. It uses an algorithm based on histograms to find the best leaf split. Data must be categorized into histograms (bins) in order to identify the splitting point. This approach works with bins instead of individual data points, which drastically reduces the algorithm's temporal complexity. Figure 5 displays the AUC-ROC curves for the ensemble machine learning technique. The results of the AUC-ROC curve demonstrate how effectively the LightGBM algorithm works with the provided spatial data. Therefore, the LightGBM-based statistical assessment was shown to be accurate and successful in flood forecast in the current research.

In Chikkamagaluru, flooding is seen as a common threat that has severely damaged infrastructure, agricultural grounds, and human lives. However, because of a lack of data and other obstacles, a thorough evaluation of this danger has not yet been carried out in the research region. Therefore, LightGBM was used to map and evaluate this risk.The final FSM demonstrates that the areas most vulnerable to floods are those around

the main waterbodies, or drainage networks. In order to adopt appropriate management strategies, planners and other government organizations may find the resulting FSM helpful in ascertaining flood-prone areas. The results will help with sustainable land management initiatives.

5. CONCLUSION AND FUTURE SCOPE

Flooding is an extensive disaster causing damage and loss of life. The ability of government officials to anticipate floods based on a variety of indicators is crucial for reducing the danger to property and human lives. One method for doing this is to use pre-conditioning factors, or FCFs, to generate FSMs for an area. This article described how an FSM for the Indian district of Chikkamagaluru was created using the ensemble machine learning approach. The FSM with the best AUC score of 0.9666 was produced using the LightGBM algorithm, it was found. A very high precision of the FSM would result in maximum safety with increased LightGBM performance, taken into consideration in detail since the maps' spatial resolution is 30m.

Metaheuristic methods will be used in the future to increase the accuracy of the maps by fine-tuning the categorization weights of the algorithms.

References

[1]. Hitouri, S., Mohajane, M., Lahsaini, M., Ali, S. A., Setargie, T. A., Tripathi, G., D'Antonio, P., Singh, S. K., & Varasano, A. (2024b). Flood susceptibility mapping using SAR data and machine learning algorithms in a small watershed in northwestern Morocco. *Remote Sensing*, *16*(5), 858. https://doi.org/10.3390/rs16050858

[2]. Costache, R., Pham, Q. B., Sharifi, E., Linh, N. T. T., Abba, S., Vojtek, M., Vojteková, J., Nhi, P. T. T., & Khoi, D. N. (2019). Flash-Flood susceptibility assessment using Multi-Criteria decision making and machine learning supported by remote sensing and GIS techniques. *Remote Sensing*, *12*(1), 106. https://doi.org/10.3390/rs12010106

[3]. Chowdhury, M. S. (2024). Flash Flood Susceptibility Mapping of North-east Depression of Bangladesh using Different GIS based Bivariate Statistical Models. *Watershed Ecology and the Environment*, *6*, 26–40. https://doi.org/10.1016/j.wsee.2023.12.002

[4]. Janizadeh, S., Avand, M., Jaafari, A., Van Phong, T., Bayat, M., Ahmadisharaf, E., Prakash, I., Pham, B. T., & Lee, S. (2019). Prediction Success of machine learning methods for flash flood susceptibility mapping in the Tafresh Watershed, Iran. *Sustainability*, *11*(19), 5426. https://doi.org/10.3390/su11195426

[5]. Dano, U., Balogun, A., Matori, A., Yusouf, K. W., Abubakar, I., Mohamed, M. S., Aina, Y., & Pradhan, B. (2019). Flood susceptibility mapping using GIS-Based Analytic Network Process: A case study of Perlis, Malaysia. *Water*, *11*(3), 615. https://doi.org/10.3390/w11030615

[6]. Msabi, M. M., & Makonyo, M. (2020). Flood susceptibility mapping using GIS and multi-criteria decision analysis: A case of Dodoma region, central Tanzania. *Remote Sensing Applications Society and Environment*, *21*, 100445. https://doi.org/10.1016/j.rsase.2020.100445

[7]. Özay, B., & Orhan, O. (2023). Flood susceptibility mapping by best–worst and logistic regression methods in Mersin, Turkey. *Environmental Science and Pollution Research*, *30*(15), 45151–45170. https://doi.org/10.1007/s11356-023-25423-9

[8]. Özdemir, H., Koçyiğit, M. B., & Akay, D. (2023). Flood susceptibility mapping with ensemble machine learning: a case of Eastern Mediterranean basin, Türkiye. *Stochastic Environmental Research and Risk Assessment*, *37*(11), 4273–4290. https://doi.org/10.1007/s00477-023-02507-z

[9]. Shah, R. K., & Shah, R. K. (2023). GIS-based flood susceptibility analysis using multi-parametric approach of analytical hierarchy process in Majuli Island, Assam, India. *Sustainable Water Resources Management*, *9*(5). https://doi.org/10.1007/s40899-023-00924-0

[10]. Gharakhanlou, N. M., & Perez, L. (2022). Spatial Prediction of current and future flood susceptibility: Examining the implications of changing climates on flood susceptibility using machine learning models. *Entropy*, *24*(11), 1630. https://doi.org/10.3390/e24111630

[11]. Express News Service, & Express News Service. (2019, August 21). *Long route to recovery for flood-hit Chikkamagluru and its coffee estates*. The New Indian Express.

https://www.newindianexpress.com/galleries/nation/2019/Aug/21/long-route-to-recovery-for-flood-hit-chikkamagluru-and-its-coffee-estates-102485.html

[12]. Hidayah, E., Indarto, N., Lee, W., Halik, G., & Pradhan, B. (2022). Assessing coastal flood susceptibility in East Java, Indonesia: comparison of statistical bivariate and machine learning techniques. *Water*, *14*(23), 3869. https://doi.org/10.3390/w14233869

[13]. Islam, S., Tahir, M., & Parveen, S. (2021). GIS-based flood susceptibility mapping of the lower Bagmati basin in Bihar, using Shannon's entropy model. *Modeling Earth Systems and Environment*, *8*(3), 3005–3019. https://doi.org/10.1007/s40808-021-01283-5

[14]. Penki, R., Basina, S. S., & Tanniru, S. R. (2022). Application of geographical information system-based analytical hierarchy process modeling for flood susceptibility mapping of Krishna District in Andhra Pradesh. *Environmental Science and Pollution Research*, *30*(44), 99062–99075. https://doi.org/10.1007/s11356-022-22924-x

[15]. Chaulagain, D., Rimal, P. R., Ngando, S. N., Nsafon, B. E. K., Suh, D., & Huh, J. (2023). Flood susceptibility mapping of Kathmandu metropolitan city using GIS-based multi-criteria decision analysis. *Ecological Indicators*, *154*, 110653. https://doi.org/10.1016/j.ecolind.2023.110653

[16]. Chou, T., Hoang, T., Fang, Y., Nguyen, Q., Lai, T. A., Pham, V., Vu, V., & Bui, Q. (2020). Swarm-based optimizer for convolutional neural network: An application for flood susceptibility mapping. *Transactions in GIS*, *25*(2), 1009–1026. https://doi.org/10.1111/tgis.12715

[17]. Abedi, R., Costache, R., Shafizadeh-Moghadam, H., & Pham, Q. B. (2021). Flash-flood susceptibility mapping based on XGBoost, random forest and boosted regression trees. *Geocarto International*, *37*(19), 5479–5496. https://doi.org/10.1080/10106049.2021.1920636

[18]. Mehravar, S., Razavi-Termeh, S. V., Moghimi, A., Ranjgar, B., Foroughnia, F., & Amani, M. (2023). Flood susceptibility mapping using multi-temporal SAR imagery and novel integration of nature-inspired algorithms into support vector regression. *Journal of Hydrology*, *617*, 129100. https://doi.org/10.1016/j.jhydrol.2023.129100

[19]. Khalid, R., & Khan, U. T. (2024). Flood susceptibility mapping using ANNs: a case study in model generalization and accuracy from Ontario, Canada. *Geocarto International*, *39*(1). https://doi.org/10.1080/10106049.2024.2316653

[20]. Zhang, J., Mucs, D., Norinder, U., & Svensson, F. (2019b). LightGBM: an effective and scalable algorithm for prediction of Chemical Toxicity–Application to the TOX21 and Mutagenicity data sets. *Journal of Chemical Information and Modeling*, *59*(10), 4150–4158. https://doi.org/10.1021/acs.jcim.9b00633

INTRAOCULAR PRESSURE MEASUREMENT COMBINED WITH GONIOSCOPIC ANALYSIS

Bharathi R.B.[1]

1: Department of Electrical and Electronics Engineering, Manipal Institute of Technology, Manipal Academy of Higher Education, Manipal-576104, Karnataka, India.

ABSTRACT

Glaucoma is an ocular disease, and the type of the disease can be diagnosed with tonometry and gonioscopy. In India and China, angle-closure glaucoma (ACG) is more prevalent than open-angle glaucoma (OAG). Gonioscopy can diagnose the type of glaucoma efficiently. In all eye care clinics, tonometry is carried out effectively. But, due to a lack of amicable technology or training, gonioscopy is not regularly performed on all patients, leading to the wrong diagnosis of ACG as OAG. A proof of concept is proposed using an air-filled ball as an eye model, followed by an animal model (goat eye). The role of tonometer to measure the value equivalent to the pressure in the eye model/goat eye is accomplished by placing a vibration sensor on the outer structure of gonio lens. The output of the sensor during the bouncing back action of the eye model/eye after the force on the it is released, is recorded and the relation between the eye pressure and the voltage output is derived. The result summarizes that an increase in pressure will increase the magnitude of vibration sensor output. The new technology introduced will measure eye pressure and the existing three-mirror gonio lens is utilized intact such that the path to view the anterior chamber angle is not distorted.

Keywords:

Tonometry, gonioscopy, Open-angle glaucoma, Angle-closure glaucoma, piezo vibration sensor.

1. INTRODUCTION

Glaucoma is a group of diseases with a characteristic optic neuropathy with associated visual function loss. According to World Health Organization, glaucoma is the second leading cause of blindness after cataracts. The study by George et al. [1] reveals that every 8th Indian above 40 years is at risk for glaucoma, with a higher risk of angle-closure glaucoma. Sathyamangalam et al. [2] brief glaucoma disease burden estimated at 25 million in 2012 is projected to reach over 100 million by 2040, thus emerging into a substantial public health challenge. Lovejoy et al. [3] explain a system used to measure any test object's vibration. The system includes a probe sensor fitting, a microphone, and an ultrasonic speaker. The microphone detects a Doppler shift in a frequency proportional to the target shaft velocity using the system. Methods adopted by the successful tonometer [4-5], such as the Sensimed triggerfish tonometer, Icare tonometer, and Mackay Marg tonometer, are referred to and utilized during the new technology evolution. A survey was carried out by Choudhari et al. [6] in India to study the pattern of glaucoma specialists. It was found that 82.6% reported carrying out gonioscopy in all patients with or those with suspects glaucoma. The remaining 14.4 % will perform gonioscopy only when the IOP is high or may not perform the test. Hence, the proposed technology will address these problems by applying best-fit technologies by combining both testing procedures in a single instrument. This innovation is not addressed on the clinical as well as on the industrial side. But separate devices exist to perform tonometry and gonioscopy.

2. METHODOLOGY

The entire work to combine both the glaucoma testing procedures is achieved by dividing the whole work into the following categories. The pressure inside the ball is increased using a hand pump, measured using a low air pressure sensor. The interface of the LCD screen with an Arduino Uno microcontroller to display pressure inside the ball. Fresh air is pumped into the ball by using an ordinary air pump. A low air pressure sensor, namely a board mount sensor (TBP-D-AN-N-150PG-U-C-V), is used to measure air pressure inside the ball. This sensor is linear in the low-pressure range from 0-1 PSI. The output of the air pressure sensor is fed to analog input pins A0, A1 of the Arduino Uno microcontroller, which is interfaced with the LCD unit. The output of the air pressure sensor is in terms of voltage. The selection and the placement of the sensor on the

goniolens is the major challenge in the The sensor will measure the value equivalent to the IOP of the eye. After experimenting with different sensors, the vibration sensor is the optimal solution, as Bernstein et al. described [7] and Zhang et al. [8]. Minisense 100 piezo-based vibration sensor has high voltage sensitivity up to 1V/g, low cost, highly linear, and horizontal mounting shielded construction. The next stage is to design a supporting structure to place the vibration sensor on goniolens. The supporting structure on the anterior side is aluminium. On the posterior side is acrylic, and both these structures are screwed to form a tight supporting structure to hold the vibration sensor. The design and image of the piezo vibration sensor's embedment on the goniolens are shown in Fig. 1. The placement of the vibration sensor was made cautiously so as not to obscure the parabolic mirror position (used for angle structure visualization) in the Goldmann three-mirror goniolens. Fig. 1 explains the embedment of the vibration sensor on goniolens. The vibration sensor is placed upon the outer aluminium surface of the goniolens using a supporting structure and will not obstruct the light path through the goniolens. Hence, the gonioscopy procedure may not be affected. The sensor embeded on goniolens is situated on the surface of the ball. Force applied on the surface of goniolens will deform the surface of the ball. A pneumatic system is used to apply a constant force on the ball during the testing procedure. The pneumatic system comprises the cylinder, push-button, flow control, and quick exhaust valve. When the push button is pressed, it releases the pressurized air onto the cylinder, and due to the pressure of the air, the cylinder experiences a force and moves down.



1- Gonio lens
2-Aluminium Holder
3-Sensor
4- Acrylic Holder
5- Sensor terminals.

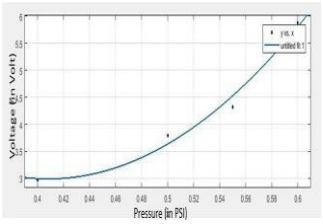

Fig. 1: Image of sensor embedded on goniolens Plot 1: Voltage output of the sensor

The LTC-6240 operational amplifier from linear technology is used with a gain of 6 to amplify the small signal output of the vibration sensor. LTC 6240 is a CMOS op-amp with input bias current of 12pA, high input resistance 10* 10e12Ω, very low noise level up-to 550nV (peak-peak) and very low offset voltage. The sensor behaves like an active capacitor of value 244pF, and a high pass filter is designed by adding high resistance of 380MΩ parallel to the output of the sensor. Hence the cut-off frequency of the filter designed is 2Hz. The amplified output from the operational amplifier is continuously recorded in the LabVIEW using NI DAQ 6001 data acquisition card. The technology to measure the pressure using ball as the eye model is verified. Further, the investigation is carried out on the animal model. The experimentation involved dead goat eyes. The goat's eyes are taken immediately after its death. The eyes are used within 3 hours of its death before fragmentation starts. A standard manometer setup is established to apply a known pressure into the goat eye. An ICARE tonometer is used to measure the IOP to standardize the manometer. Thus, the scale used in the manometer is standardized such that each division on the scale corresponds to the value of pressure (IOP) by carrying out the testing with 30 samples of goat eyes. Hence standard pressure can be applied to the goat eye using the developed manometer setup. For experimentation, goniolens embedded with the sensor is placed on the ball. Force is then applied to the surface of the ball. A known amount of pressure will be developed inside the ball and is measured by the air pressure sensor (TBP-D-AN-N-150PG-U-C-V) placed within it. The readings of the air pressure sensor are fed to analog input pins of the Arduino Uno microcontroller, and air pressure (PSI) will be continuously displayed on the LCD screen interfaced with the Arduino Uno microcontroller.

During the applanation force, a constant force is applied with the pneumatic system. This force results in the deformation (bending) of the ball. But the displaced ball will bounce back and settle to its position immediately. The amount of bouncing back of the ball is dependent on the pressure inside the ball. The DAQ card is used to tap the signals from the sensor and then fed into the LabVIEW programming paradigm. The process is continued on the animal model, such as goat eyes. The investigation with the goat eye is carried out by impinging a standard amount of pressure into the goat eye using the standard manometer setup. Many goat eye samples are taken, the experiment is repeated at 10 mmHg, 12 mmHg, 16 mmHg, 20 mmHg and analysis are carried out.

3. RESULTS

In the initial stage of experimentation, the ball is used as an eye model to verify the technology of tonometry by embedding the vibration sensor on goniolens. The increase in the pressure in the ball from 0 to 1 PSI will result in increased sensor voltage output from 3V to 6V. Plot 1 explains that the sensor's output increases as the pressure inside the ball increases. The result proves that the magnitude of sensor output is directly proportional to the pressure in the eye model.

Goat eyes are used for animal model experimentation. The animal experiment results in plot 2 explaining the relationship between the IOP of the eye with the vibration sensor output and proves that the magnitude of sensor output increases with an increase in the IOP of the eye. The results conclude that the sensor's voltage output is of lower amplitude than the experiment results with the ball. This relation is further employed to estimate the IOP of the eye by reading the voltage output of the sensor. Hence, the role of the tonometer to estimate the IOP of the eye is developed.

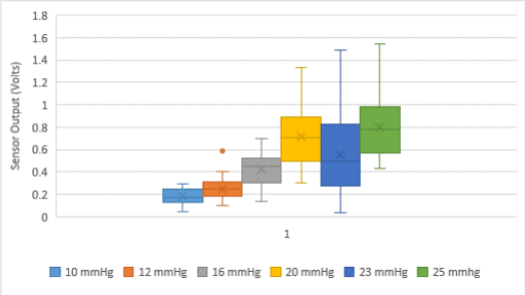

Plot 2: Voltage output of the sensor

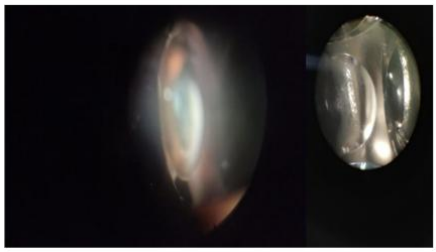

Fig. 2: Angle structure visualization using Tonogonio.

Fig. 2 shows the angle structure of a goat eyes as seen through device developed “tonogonio”. The procedure to visualize the angle structure begins by introducing a dead goat eye before the fragmentation starts and before the elasticity of the dead goat eye is lost. The airgap between the goat eye and tonogonio is filled with water. This adds smoothness and moisture content to the eye sample. The slit lamp is used to focus light on the eye, while tonogonio is placed on the corner of the eye. Fig. 2 (a) depicts the visualization of the goat eye angle structure, whereas Fig. 2 (b) depicts the mirrors as seen via the goniolens, as well as the angle structure view. Fig. 2 (b) shows the angle structure as the dark shaded region when viewed through the three mirror goniolens. Thus, the claim of visibility of the angle structure during the tonogonio procedure is validated as part of the research.

The distance of travel of the eye model during the application of force on eye is inversely proportional to the pressure inside the ball/eye model, as described by Abreu et al. [9], and the present technology of measuring the bouncing back the ball/eye model is also dependent upon its pressure. The new technology has been validated such that, as the pressure inside the ball increases, the amount of deformation of the ball/eye for the prefixed amount of force will decrease, as explained by Abreu et al. [9], and will result in the more rigorous amount of bouncing back and hence higher magnitude of sensor output voltage. Thus, the ball will rebound actively and result in higher voltage output as the pressure inside the ball increases.

4. CONCLUSION

New technology has evolved which will derive the relationship between the pressure inside the ball/eye model and the vibration sensor output and hence can be utilized to work as a tonometer. Hence a single instrument is developed to perform both tonometry and gonioscopy procedure. A holder will be designed to situate the animal eye such that it will not move or displace from its position, other than bouncing in the vertical direction. Statistical analysis will be carried out using Minitab or SPSS software for the experimental results with goat eyes to drive the relationship between the IOP of the goat eye and the vibration sensor output. Validation will be done by comparing the results with golden standard methods such as the Goldmann Applanation tonometer or ICARE tonometer.

5. REFERENCES

[1] George, R., Ramesh, S. V., & Vijaya, L., Glaucoma in India: estimated burden of disease. J. of glaucoma, 19(6): 391-397, 2010.

[2] Sathyamangalam, R. V., Paul, P. G., George, R., Baskaran, M., Hemamalini, A., Madan, R. V., ... & Lingam, V. Determinants of glaucoma awareness and knowledge in urban Chennai. Indian J Ophthalmol, 57(5):355.

[3] Lovejoy, K. A. ,U.S. Patent Application No. 14/819,131, 2017.

[4] Fresco, B. B. U.S. Patent No. 6,976,959. Washington, DC: U.S. Patent and Trademark Office, 2005.

[5] Makkeli, P., Haulisto, R., Raudasoja, M., Pukki, J., Herranen, T., Kukkonen, A., & Salkola, M., U.S. Patent Ap-plication No. 16/062,160, 2018.

[6] N. S. Choudhari, V. Pathak-Ray, S. Kaushik, P. Vyas, and R. George, "Understanding practice patterns of glaucoma sub-specialists in India," Int. J. Ophthalmol., vol. 10, no. 10, pp. 1580–1585, doi: 10.18240/ijo.2017.10.16, 2017.

[7] Bernstein, J., Miller, R., Kelley, W., & Ward, P., Low-noise MEMS vibration sensor for geophysical applications. J MICROELECTROMECH S, 8(4), 433-438. 1999.

[8] Zhang, Z., & Bao, X., Distributed optical fiber vibration sensor based on spectrum analysis of Polarization-OTDR system. Opt. Express, 16(14), 10240-10247, 2008.

[9] Abreu, M. M., U.S. Patent No. 5,830,139. Washington, DC: U.S. Patent and Trademark Office, 1998.

Survey on Detection and Mitigation Strategies for Zero-day Attacks: An Extensive Analysis of Current Developments and Case Studies

Mrs Savitri Ashok Mote [a,b,c], Dr Sudhakar Arabagatte [a]

[a] Department of Computer Science Engineering, Srinivas University College of Engineering Technology, Mangaluru-574146, India.

[b] Department of Computer Engineering Indira College of Engineering and Management, Parandvadi, Maharashtra 410506, India mote.savitri@gmail.com [c]

Abstract

The increasing frequency of zero-day assaults presents a noteworthy risk to cybersecurity, hence requiring the formulation of resilient detection and mitigation tactics. This paper provides an extensive overview of zero-day exploit detection and mitigation developments. Our survey summarizes the development of zero-day assault tactics and highlights the advanced strategies adversaries use to avoid detection. We thoroughly examine conventional heuristics, signature- based approaches, cutting-edge machine learning, and artificial intelligence-driven detection processes. We also look into state-of-the-art mitigation strategies that employ predictive analytics, real-time threat intelligence, and behavioral analysis. We analyses recent case studies to demonstrate how these tactics can be applied in real-world circumstances, highlighting their limitations and usefulness. These case studies offer crucial insights into the practical challenges and achievements encountered while deploying zero-day defiance mechanisms across different sectors. Furthermore, they underscore the pressing need for dynamic and forward-thinking security solutions by mapping out emerging trends and future research directions in zero-day attacks. Our analysis emphasizes the importance of a holistic security strategy combining advanced detection techniques with flexible response measures. By providing a detailed overview of topical research and helpful case studies, this review seeks to contribution cybersecurity specialists, academics, and policymakers in consolidation their defensive structures against the constantly changing threat landscape of zero-day vulnerabilities.

Keywords: Zero-day Attacks, Zero-day Malware, Detection Methods, Mitigation Strategies, Machine Learning, Artificial Intelligence, Signature-Based Detection, Anomaly-Based Detection, Case Studies.

1.Introduction

Zero-day attacks posture a rising threat to cybersecurity because neither software developers nor the general public are aware of them until after the breach and they are especially deadly because they exploit previously unknown vulnerabilities. The term "zero day" refers to a susceptibility that developers have little time to identify and patch before it is subjugated, exposing organizations to potentially catastrophic security breaches that are typically unavoidable using traditional security procedures.

Sophisticated detection and mitigation measures must be industrialized due to these threats growing intricacy and frequency. Protecting information systems concealment, integrity, and accessibility from zero day threats is essential. Predictable security approaches depend on known attack signatures and are inadequate against zero-day assaults. As a result, the cybersecurity community has embraced cutting-edge strategies like artificial intelligence and machine learning. These tools can analyze large datasets, spot irregularities, and forecast future vulnerabilities precisely. Modern research has suggestively improved techniques for recognizing zero day attacks. For instance, Kim et al. (2018) studied the possible of transferred generative adversarial networks based on deep autoencoders for detecting zero-day malware. Guo (2023) provided a inclusive review of ML-based techniques for zero-day attack detection, highlighting the challenges and prospective paths forward in this arena. Moreover, the introduction of NERO, a neural algorithmic reasoning system designed for zero-day attack detection in IoT environments by Cevallos et al. (2024), and the innovative Meta-Fed IDS framework by Zukaib et al. (2024), which participates meta learning with federated learning for detecting zero-day cyber-attacks in IoMT networks, showcase the potential of collaborative and adaptive learning tactics in cybersecurity. Significant progress has been made in developing robust justification mechanisms for zero day attacks and detection. Soltani et al. (2023) highlighted the necessity of scalable and flexible solutions in modern cybersecurity frameworks by developing an adaptive interference detection system based on deep learning. Sameera and Shashi (2020) developed profound Transudative transfer erudition outlines for zero day attack detection, underscoring the critical importance of transfer learning in enhancing the capabilities of AI models to identify threats against new and unidentified dangers. To corroborate and develop these detection and mitigation strategies, they must be applied and tested in real-world circumstances. Current case studies shed light on the challenges and successes experienced while implementing these ideas, Sarhan et al. (2023) explored the

transition from zero shot machine learning to zero day attack detection, demonstrating the effectiveness and limitations of these cutting-edge techniques in real-world applications. This study thoroughly examines current approaches for mitigating and detecting zero-day attacks, utilizing the most recent advancements and case studies. It is premeditated to provide insightful information to academics, industry professionals and cybersecurity decision-makers, showcasing fresh developments and suggestions for further study. The subdivisions include comprehensive case studies from various industries, examining the most recent mitigation measures and their real world applications, examining the practices used for zero day attack detection, and finishing with dynamic lessons for strengthening defenses against zero day attacks.

2.Overview of Zero-day Attacks

Zero-day attacks exploit unknown vulnerabilities for the public and cybersecurity professionals, posing severe threats to systems cybersecurity. To combat these serious dangers, robust and adaptable mitigation methods are critical. Various solutions have been created based on recent breakthroughs in deep learning, machine learning, and hybrid models. These strategies improve the ability to detect and respond to zero-day threats, demonstrating the continual growth of cybersecurity defences. [13], [14]. In order to give readers thorough overview of the state of zero-day assault defences as of right now, this section evaluates several mitigation measures. It summarizes their methodologies, strengths, and limitations. The subsequent table summarizes significant findings from scholarly research, providing an overview of the various strategies used to mitigate these complex risks. This section offers a comprehensive summary of mitigation strategies for zero-day attacks, as presented in recent literature. The Table 1. encapsulates the critical contributions from notable studies, highlighting each approach's methodologies, strengths, and limitations.

Table 1: Comprehensive summary of various mitigation strategies for zero-day attacks

Study	Mitigation Strategy	Methodology	Strengths
Guo (2023) [2]	Detection Based on Machine Learning	Examining machine learning methods for zero-day detection	ML techniques analyzed, future research highlighted
Soltani et al. (2023) [5]	Intrusion Detection Using Deep Learning	Deep learning models that are flexible for IDS	Excellent scalability, real-time detection
Ben-Asher & Gonzalez (2015) [7]	Responses and Training Based on Similarity	Heuristic and deep learning model integration	Improves ability to recognize anomalies, effective for IoT
Cevallos et al. (2024) [3]	NEURO: Neural Algorithmic Reasoning	Teaching systems to identify zero-day attacks with feedback mechanisms	Very accurate detection, suitable for IoT environments
Zukaib et al. (2024) [4]	Meta-Fed Information Stream	IoMT networks with federated learning and meta-learning	Resilient to changing and new dangers
Touré et al. (2024) [12]	Structure for Network Flow Recognition	Analytics to find network flow exploits	Real-time alertness, expandable
Murtuza & Asawa (2024) [18]	DDoS Mitigator Powered by CNN	Using convolutional neural networks to mitigate DDoS attacks	Excellent detection precision, suitable for SDN
Wu et al. (2024) [19]	Framework for Active Learning	Reinforcement learning for zero-day attack detection	Good detection precision, suitable for edge environments
Shen et al. (2024) [20]	Heuristic Recognition of Intrusions	Heuristic techniques with deep Q-network for SIoT	Adaptive learning successful in changing circumstances

3. Detection Techniques for Zero-day Attacks

Over time, academics and practitioners have developed several sophisticated ways to keep ahead of evolving risks, which has led to a significant evolution in the detection of zero-day assaults. Conventional techniques, such as signature-based detection, must be improved since they depend on well-known attack patterns, exposing systems to new exploits. The cybersecurity community increasingly uses advanced approaches such as machine learning (ML), artificial intelligence (AI), and hybrid models to enhance detection capabilities. Deep learning models frequently identify zero-day threats by analyzing enormous datasets. To show the efficiency of deep learning in detecting unforeseen dangers, Guo (2023) [21] examined the practical limits these systems encounter and the effectiveness of several machine learning-based methods for detecting zero-day attacks. Hybrid methods that incorporate several different detection algorithms are also fascinating. Experimental and deep learning models are integrated into NERO, a neural algorithmic cognitive system that uses federated learning and meta learning to detect zero day cyberattacks in IoMT networks. Zukaib et al. (2024) [4] established another cutting edge framework that highlights the paybacks of adaptive and cooperative learning methods; despite these

advancements, effectively detecting zero day attacks remains tough [12]. As a result, it is critical to implement efficient detection techniques to recognize and neutralize these threats before they can do serious harm [23]. This section scrutinizes several zero day attack detection tactics, highlighting cutting-edge methods including hybrid method, machine learning, and artificial intelligence. While signature-based detection can recognize known dangers, it is unable to detect emerging ones. While behavior-based detection keeps an eye on system activity for abnormalities, heuristic based detection employs rules to find indiscretions. Machine learning improves detection by investigative data patterns, while anomaly-based detection creates baseline behaviors. These approaches are collective in hybrid methods to increase accuracy and reduce false positives. [1], [15], [24].

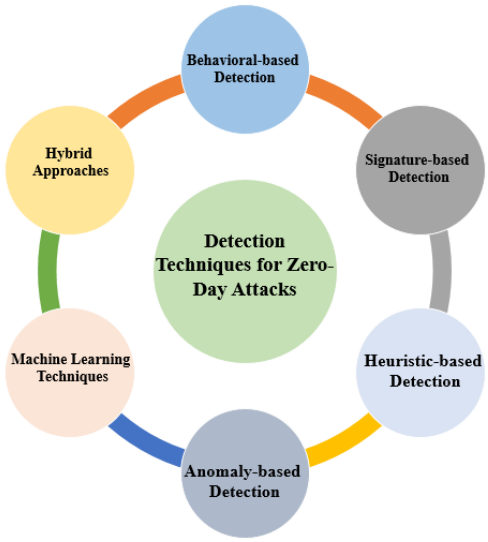

Figure 1: Methods of identifying Zero-day attacks

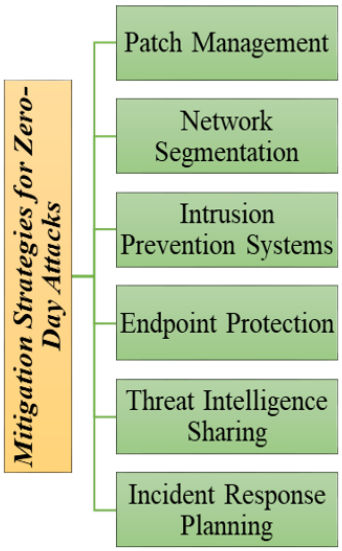

Figure 2: Countermeasures of against zero-day attacks

4. Mitigation Strategies for Zero-day Attacks

Mitigation strategies for zero-day attacks are essential for strengthening defenses and plummeting the impact of these attacks. This section highlights several key methods for reducing risks associated with zero-day vulnerabilities [26], [32]. Due to the energetic nature of zero-day assaults, a multi-layered strategy is necessary. Traditional security measures often fail to address unknown vulnerabilities, making adaptive results crucial. Key mitigation strategies include patch organization, which ensures regular software updates and reduces attack surfaces, thus limiting attackers ability to exploit unpatched vulnerabilities [33]. Network segmentation isolates critical sections of a network to prevent the spread of attacks and protect sensitive resources. Intrusion Prevention Systems (IPS) play a vital role in detection and blocking suspicious activity [11]. Endpoint protection involves securing devices like computers and mobile phones through advanced threat detection, firewalls, and antivirus software. Threat intelligence sharing among organizations enhances collective defense capabilities. Finally, maintaining a robust incident response strategy is crucial for justifying the impact of security breaches and ensuring swift recovery. These measures work together to create a comprehensive defense against zero-day attacks [29] [34]. The following Table 2. provides a complete summary of zero-day attack detection strategies based on the references. It includes subcategories, descriptions, examples, and assessment metrics. Table 3. summarizing different types of zero-day attack detection and mitigation strategies, along with their advantages and limitations

Table 2: Summary of zero-day attack detection strategies

Approach	Subcategory	Examples	Metrics for Evaluation
Machine Learning	Supervised Learning	SVM, Decision Trees, Random Forests	F1-Score, AUC-ROC, Accuracy, Precision, Recall [25], [12]
	Unsupervised Learning	Clustering, PCA, Autoencoders	Valid Positive Rate, False Positive Rate, Detection Rate [12], [26]
	Semi-Supervised Learning	SVM, Semi-Supervised Autoencoders	Precision, Recall, F1-Score, Detection Rate [26], [27]
Deep Learning	Reinforcement Learning	Q-Learning, Deep Q-Networks	F1-Score, Accuracy, Precision, Recall, Latency, Detection Rate [21], [26]
	Convolutional Neural Networks	CNNs	Accuracy, False Positive Rate [28]

Approach	Subcategory	Examples	Metrics for Evaluation
	Recurrent Neural Networks	Sparse Autoencoders, LSTMs	Precision, Recall, F1-Score, Accuracy [13], [24]
	Generative Adversarial Networks	Autoencoders, GANs	Precision, Recall, F1-Score, Accuracy [15]
Hybrid Approaches	Adversarial Networks	Group detection models	Precision, Recall, F1-Score, Detection Rate [4], [22]
	Meta-Learning	Mixed Neural Algorithmic Reasoning	False Positive Rate, Precision, Recall, Accuracy [14]
	Federated Learning	Federated Learning for IoT environments	Detection Rate, Communication Overhead, Accuracy [4], [24]
Heuristic Approaches	Rule-Based Detection	Signature-based detection, Heuristic IDS	Detection Rate, False Positive Rate [20]
	Unsupervised Clustering	K-Means, DBSCAN	Detection Rate, False Positive Rate, Precision, Recall [5], [29], [30]
	Fuzzy Systems	Fuzzy Gaussian Mixture Models	Accuracy, Detection Rate, False Positive Rate [5], [29]
Optimization Techniques	Adaptive Security Models	Optimization-Based Adaptive Security Models	Detection Rate, False Positive Rate, Precision, Recall [28]
Transfer Learning	Pre-trained Models	Transudative Transfer Learning	Accuracy, Precision, Recall, F1-Score, AUC-ROC [7],

Table 3: Summarizing different types of zero-day attack detection and mitigation strategies

Type	Advantages	Limitations
Detection Based on Signatures	Rapid and effective against known malware.	Unable to stop novel or unidentified zero-day attacks.
	Low computational requirements.	High false-negative rates for zero-day threats.
Detection Based on Anomalies	Can recognize assaults never before witnessed.	High incidence of benign abnormalities causing false positives.
	Effective against polymorphic malware.	Needs a large amount of processing power.
Detection Based on Behavior	Spots zero-day malware by observing runtime activities.	Could ignore sophisticated malware showing consistent behavior.
	Good against obfuscated malware.	High processing overhead for real-time detection.
Patch Administration	Responds promptly to known vulnerabilities.	Ineffective against unknown zero-day vulnerabilities.
	Effectively reduces attack surface.	
Network Segmentation/Isolation	Limits malware spread.	Difficult to integrate into current networks.
	Isolates critical assets.	Could cause network performance decline.
Threat Intelligence Sharing	Aids early identification of threats.	Data security and privacy issues.
	Enhances group situational awareness.	Problems with standardization in formats.
Machine Learning (ML) Models	Can extrapolate patterns for predictive analysis.	Requires large datasets for training.
	Identifies metamorphic and polymorphic malware.	Limited applicability to unknown zero-day attacks.
Deep Learning (DL) Models	High precision due to intricate pattern identification.	Computationally demanding for real-time detection.
	Successful in identifying zero-day malware.	Requires large training datasets.
Ensemble Learning Models	Increased prediction accuracy.	More computing power required.
	Sturdy against model flaws.	

5. Evaluation Metrics and Criteria and Challenges and Future Directions

A set of metrics and criteria are employed to quantify the success of zero-day attack detection and mitigation procedures. This section examines the key metrics used to analyses how well various techniques perform against zero-day threats. The critical evaluation measures are classified in the following Fig 3: A comprehensive evaluation framework is necessary to analyse zero-day attack detection and mitigation strategies. When analysing how well zero-day attack detection systems perform, the following metrics are critical:

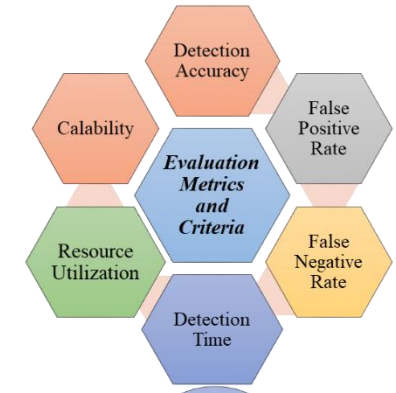

Figure 3: Evaluation Measures



Figure 4: Challenges and Future Directions

Precision Detection: calculates the proportion of successfully detected assaults compared to the total number of attacks. Improving detection accuracy is crucial to lowering the risk of successful assaults [14]. The false positive rate shows how frequently harmless activities are misclassified as harmful. Reducing a high false positive rate is critical, as it could result in unwarranted alarms and resource loss [23], [40]. The False Positive Rate indicates how frequently the system fails to detect attacks. Reducing false negative rates is crucial for preventing zero-day assaults from going undetected. Temporal detection refers to how long the system takes to perceive and respond to an assault [8]. Resource Assignment: Determines how much network and computational power the detection system will use. Utilising resources efficiently guarantees that the system can function adequately without overburdening the infrastructure. Scalability refers to how well a system can absorb increased demands and adapt to larger, more complicated networks. Scalability is critical for detection systems to operate as the network grows. Multiple metrics and evaluation criteria can be used to analyse the effectiveness of zero-day attack detection and mitigation techniques. The following thorough Table 4. provides the critical measurements and explanations for each. Zero-day threats pose significant challenges due to their dynamic and elusive nature, making detection and mitigation difficult. Evasion techniques like polymorphic malware and encrypted communication channels hinder traditional detection methods [46]. A substantial problem in zero-day attack detection is the high false-positive rate, which causes warning fatigue, resource waste, and integration difficulties with legacy systems, whereas real-time detection and response are critical for preventive damage. Advancements in AI and ML offer potential improvements but face challenges with model accuracy, training data quality, and computational demands [25], [35], [47]. Collaborative defense mechanisms, such as data-sharing between organizations, are essential for strengthening defenses. Future research should focus on creating smarter, more flexible solutions to keep pace with evolving threats. Addressing these challenges will require continuous innovation and adaptation in the cybersecurity field [24]. Table 5. summarizing the challenges and future directions in zero-day attack detection.

Table 4: Critical measurements and explanations of metric

Metric	Description	Papers Using the Metric
Accuracy	Measures the overall effectiveness of the detection model.	[4], [12], [14], [25]
Precision	Indicates the model's ability to identify accurate attacks out of all detected attacks.	[9], [29], [42]
Recall (Sensitivity)	Measures the model's ability to detect actual attacks.	[42]
F1-Score	Balances precision and recall, providing a single measure of a model's performance.	[13], [23], [29]

Metric	Description	Papers Using the Metric
Detection Rate	Evaluates the model's effectiveness in identifying zero-day attacks.	[13], [23], [30]
False Positive Rate	Assesses the rate of false alarms, which is critical in operational environments.	[23], [40]
True Positive Rate	Measures the model's ability to detect attacks correctly.	[2]
False Negative Rate	Indicates the number of missed attacks, which is crucial for security.	[7], [12]
Area Under Curve	Provides an aggregate measure of performance across all classification thresholds.	[25]
Latency	Essential for real-time detection systems where timely detection is critical.	[1], [24]
Communication Overhead	Relevant for distributed and federated learning models.	[44]
Computational Efficiency	Important for models deployed on resource-constrained devices like IoT or edge devices.	[25]
Scalability	Crucial for models operating in large-scale environments.	[7]

Table 5: summarizing the challenges and future directions in zero-day attack detection

Challenges	Description	Future Directions	Description
High False Positive Rate [40]	Zero-day detection systems frequently generate many false positives, resulting in alert fatigue.	**Improved Accuracy**	Creating more accurate models with lower false positive rates using advanced algorithms.
Data Imbalance [38]	An imbalance between normal and attack data can bias machine learning model training.	**Data Augmentation**	Synthetic data generation is used to balance datasets and improve model training.
Adaptability to New Attacks [4], [15]	Difficulty adapting to novel and developing zero-day attack patterns.	**Transfer Learning**	Using pre-trained models on related tasks to respond swiftly to new attack patterns.
Scalability [4]	Problems in upgrading detection technologies to handle enormous amounts of data in real-time.	**Federated Learning**	Designing distributed learning systems to scale across various devices without centralized data.
Limited Labeled Data [26]	More labeled data is needed to train supervised learning algorithms.	**Semi-Supervised Learning**	Using both labeled and unlabeled data to enhance model training and detection performance.
Real-Time Detection [1], [48]	The requirement for real-time detection presents computational efficiency issues.	**Real-Time Processing Frameworks**	Creating frameworks that can process data in real-time with low latency.
Complexity of Attack Patterns [14]	Zero-day assaults frequently use complicated, multi-stage patterns that are difficult to detect.	**Multi-Stage Detection Systems**	Using layered models, we are developing systems capable of detecting multi-stage and complicated attack patterns.
Privacy Concerns [25], [48]	Maintaining user privacy while gathering and analyzing data for zero-day attack detection.	**Privacy-Preserving Techniques**	Differential privacy is one approach used to secure the confidentiality of information in detection systems.
Evaluation Metrics Standardization [10]	The lack of standard evaluation metrics makes it difficult to compare the performance of various systems.	**Benchmarking and Standardization**	Developing common standards and evaluation metrics for zero-day attack detection systems.
Adversarial Attacks [49]	The detection models are vulnerable to adversarial attempts that can deceive the system.	**Robustness Against Adversarial Attacks**	Using better security measures, we can increase model resilience to adversarial attacks.
Integration with Existing Systems [29]	It is not easy to integrate zero-day detection technologies with existing cybersecurity infrastructure.	**Interoperability**	Ensuring that detection systems are compatible and work seamlessly with existing security solutions.
Resource Constraints [32]	Edge device computational resources are limited, making it challenging to install complex detection models.	**Edge Computing Optimization**	Optimizing detection models to perform well on edge devices with limited resources.

Machine learning and artificial intelligence have promising potential for detecting and preventing zero-day threats, notwithstanding their challenges. Further study on data production, adversarial robustness, explainable AI, and collaborative detection can significantly enhance the effectiveness of zero-day attack defense systems. [7], [8].

Case Studies

Zero-day assaults are a critical challenge in cybersecurity, necessitating inventive and flexible solutions. This section contains extensive case studies showcasing the various detection and mitigation approaches developed and implemented to tackle zero-day attacks. Each case study focuses on the distinct tactics, notable outcomes, and novel approaches to boost cybersecurity defenses against these complex attackers. These real-world examples demonstrate the practical implementation and effectiveness of modern security measures. These case studies demonstrate the various tactics and techniques established to detect and prevent zero-day attacks, each

addressing a specific issue and exhibiting significant advances in cybersecurity. Assessment examination of detection and mitigation measures. Effectiveness of Machine Learning Models. This table acquaintances various cybersecurity detection approaches and incident response systems based on performance parameters such as accuracy, false positive rate and detection time. It equivalences supervised, unsupervised and behavior based detection techniques, as well as incident response frameworks such as NIST SP 800-61 and the Cyber Resilience Recovery Model. The study assists cybersecurity experts in responsible the best effective detection and response options for their precise requirements. The frameworks' key strengths and shortcomings are also addressed for real-world applications. Case Studies of Zero-day Attack Detection and Mitigation Strategies

Paper Referenced	**J. F. Cevallos et al., 2024**
Description	In 2024, researchers used NERO, a hybrid method using neural networks and algorithmic reasoning to identify zero day threats in IoT environments. The technique used deep learning models to detect anomalies and algorithmic perceptive to filter out false positives.
Findings	NERO identified 95% of zero day threats, the false positive rate was low 2%. Scalable across IoT networks, handling diverse scenarios efficiently.
Creativity	NERO's hybrid method syndicates deep learning with algorithmic reasoning, offering an effective real time detection system with negligible false positives.
Paper Referenced	**S. Shen et al., 2024**
Description	Researchers created a deep Q-network based heuristic intrusion detection solution to contest zero day attacks in Smart Internet of Things environments. The system used reinforcement learning to optimize detection policies energetically.
Findings	High Adaptability: The DQN-based system rapidly responded to new and evolving threats, maintaining a 94% detection rate. The heuristic technique enabled real-time detection in resource-constrained environments. Low Latency: The system exhibited fast response times, crucial for SIoT processes.
Creativity	DQNs in SIoT showcase a cutting edge use of reinforcement learning to detect zero day attacks, present an adaptive and resource efficient security solution.
Paper Referenced	**U. Zukaib et al., 2024**
Description	Researchers introduced Meta-Fed IDS, a unique solution combining meta learning and federated learning to detect zero-day threats in Internet of Medical Things networks. This system was deployed across healthcare facilities, allowing cooperative learning while protecting patient data privacy.
Findings	Privacy Preservation - Federated learning kept medical data local, which improved privacy. Accuracy - Meta learning increased adaption to new strikes, achieving 92% accuracy. Low Communication Overhead - Efficient communication techniques reduced band width needs.
Creativity	Meta Fed IDS is an innovative approach that tackles privacy and scalability issues in IoMT networks, leveraging regionalized data for efficient zero-day threat detection.

Table 6: Evaluation of Incident Response Frameworks

Model	Accuracy	False Positive Rate	Detection Time
Supervised Learning	92%	5%	Fast
Unsupervised Learning	85%	10%	Moderate
Behavior-Based	88%	7%	Moderate
Hybrid Approach	94%	4%	Fast
Reinforcement Learning	90%	6%	Fast
Signature-Based	95%	3%	Very Fast
Anomaly Detection	87%	8%	Moderate
Federated Learning	89%	6%	Moderate

6. Conclusion

In the modern cybersecurity landscape, zero day attacks create a serious threat to both individuals and companies. This inclusive research has highlighted recent advances in diagnosis and mitigation procedures, highlighting exclusive approaches and methodology created to address these indefinable dangers. The discipline has made significant development in improving the accuracy, efficiency, and scalability of zero day attack detection and mitigation through the use of deep learning models, hybrid methodologies and federated and reinforcement learning techniques. The review's case studies highlight these cutting edge techniques expediency and effectiveness in the actual world. Solutions such as NERO for IoT environments, Meta-Fed IDS for IoMT networks, and deep Q-networks for SIoT zero day threats cleverly incorporate Artificial intelligence and machine learning capabilities. Despite these improvements, frequent critical challenges remain to be overawed, including lowering false positive rates, enhancing rea time detection capabilities, and maintaining seamless interaction with legacy systems. The dynamic nature of zero day attacks requires constant creativity and flexibility, calling for continued research and development in this serious field of cybersecurity. Consequent studies should focus on improving the robustness and flexibility of detection systems, developing more effective ways for source utilization and encouraging increased cooperation and data exchange among business entities. By resolving these challenges and strengthening the foundations laid by recent breakthroughs, the cybersecurity community can better defend against the ongoing threat of zero-day attacks, ensuring a harmless digital future. This assessment is a evidence to the progress made and a call to action for additional work against zero-day susceptibilities. We can protect our digital organization from the evolving threat landscape by creating resilient and comprehensive defense mechanisms through continuous innovation and collaboration.

7. Reference

[1] N. Moustafa, M. Keshk, K. K. R. Choo, T. Lynar, S. Camtepe, and M. Whitty, “DAD: A Distributed Anomaly Detection system using ensemble one-class statistical learning in edge networks,” *Futur. Gener. Comput. Syst.*, vol. 118, pp. 240–251, 2021, doi: 10.1016/j.future.2021.01.011.

[2] Y. Guo, “A review of Machine Learning-based zero-day attack detection: Challenges and future directions,” *Comput. Commun.*, vol. 198, no. November 2022, pp. 175–185, 2023, doi: 10.1016/j.comcom.2022.11.001.

[3] J. F. Cevallos M., A. Rizzardi, S. Sicari, and A. C. Porisini, “NERO: NEural algorithmic reasoning for zero-day attack detection in the IoT: A hybrid approach,” *Comput. Secur.*, vol. 142, no. November 2023, p. 103898, 2024, doi: 10.1016/j.cose.2024.103898.

[4] U. Zukaib, X. Cui, C. Zheng, D. Liang, and S. U. Din, “Meta-Fed IDS: Meta-learning and Federated learning based fog-cloud approach to detect known and zero-day cyber attacks in IoMT networks,” *J. Parallel Distrib. Comput.*, vol. 192, no. April, p. 104934, 2024, doi 10.1016/j.jpdc.2024.104934.

[5] M. Soltani, B. Ousat, M. Jafari Siavoshani, and A. H. Jahangir, “An adaptable deep learning-based intrusion detection system to zero-day attacks,” *J. Inf. Secure. Appl.*, vol. 76, no. June, p. 103516, 2023, doi: 10.1016/j.jisa.2023.103516.

[6] N. Sameera and M. Shashi, “Deep transductive transfer learning framework for zero-day attack detection,” *ICT Express*, vol. 6, no. 4, pp. 361–367, 2020, doi: 10.1016/j.icte.2020.03.003.

[7] N. Ben-Asher and C. Gonzalez, “Training for the Unknown: The Role of Feedback and Similarity in Detecting Zero-day Attacks,” *Procedia Manuf.*, vol. 3, no. Ahfe, pp. 1088–1095, 2015, doi: 10.1016/j.promfg.2015.07.180.

[8] M. Sarhan, S. Layeghy, M. Gallagher, and M. Portmann, “From zero-shot machine learning to zero-day attack detection,” *Int. J. Inf. Secure.*, vol. 22, no. 4, pp. 947–959, 2023, doi: 10.1007/s10207-023-00676-0.

[9] P. Nemani, Y. D. Joel, P. Vijay, and F. F. Liza, “Gender bias in transformers: A comprehensive review of detection and mitigation strategies,” *Nat. Lang. Process. J.*, vol. 6, no. December 2023, p. 100047, 2024, doi: 10.1016/j.nlp.2023.100047.

[10] N. Mearaj and M. A. Wani, “Zero-day Attack Detection with Machine Learning and Deep Learning,” *Proc. 17th INDIACom; 2023 10th Int. Conf. Comput. Sustain. Glob. Dev. INDIACom 2023*, pp. 719–725, 2023.

[11] A. Touré, Y. Imine, A. Semnont, T. Delot, and A. Gallais, “A framework for detecting zero-day exploits in network flows,” *Comput—networks*, vol. 248, no. May, p. 110476, 2024, doi: 10.1016/j.comnet.2024.110476.

[12] N. Abdalgawad, A. Sajun, Y. Kaddoura, I. A. Zualkernan, and F. Aloul, “Generative Deep Learning to Detect Cyberattacks for the IoT-23 Dataset,” *IEEE Access*, vol. 10, pp. 6430–6441, 2022, doi:

10.1109/ACCESS.2021.3140015.
[13] S. Dalal *et al.*, "Extremely boosted neural network for more accurate multi-stage Cyber-attack prediction in the cloud computing environment," *J. Cloud Comput.*, vol. 12, no. 1, 2023, doi: 10.1186/s13677-022-00356- 9.
[14] J. Y. Kim, S. J. Bu, and S. B. Cho, "Zero-day malware detection using transferred generative adversarial networks based on deep autoencoders," *Inf. Sci. (Ny).*, vol. 460–461, pp. 83–102, 2018, doi: 10.1016/j.ins.2018.04.092.
[15] A. Taheri-Garavand, A. Heidari-Maleni, T. Mesri-Gundoshmian, and O. D. Samuel, "Application of artificial neural networks for the prediction of performance and exhaust emissions in IC engine using biodiesel-diesel blends containing quantum dot based on carbon doped," *Energy Convers. Manag. X*, vol. 16, Dec. 2022, doi: 10.1016/j.ecmx.2022.100304.
[16] V. Hnamte, A. A. Najar, H. Nhung-Nguyen, J. Hussain, and M. N. Sugali, "DDoS attack detection and mitigation using deep neural network in SDN environment," *Comput. Secur.*, vol. 138, no. September 2023,
p. 103661, 2024, doi: 10.1016/j.cose.2023.103661.
[17] S. Murtuza and K. Asawa, "Early Prevention and Mitigation of Link Flooding Attacks in Software Defined Networks," *J. Netw. Comput. Appl.*, vol. 224, no. June 2023, p. 103832, 2024, doi: 10.1016/j.jnca.2024.103832.
[18] Y. Wu, Y. Hu, J. Wang, M. Feng, A. Dong, and Y. Yang, "An active learning framework using deep Q-network for zero-day attack detection," *Comput. Secur.*, vol. 139, no. November 2023, p. 103713, 2024, doi: 10.1016/j.cose.2024.103713.
[19] S. Shen, C. Cai, Z. Li, Y. Shen, G. Wu, and S. Yu, "Deep Q-network-based heuristic intrusion detection against edge-based SIoT zero-day attacks," *Appl. Soft Comput.*, vol. 150, no. November 2023, p. 111080, 2024, doi 10.1016/j.asoc.2023.111080.
[20] S. Shen, C. Cai, Z. Li, Y. Shen, G. Wu, and S. Yu, "Deep Q-network-based heuristic intrusion detection against edge-based SIoT zero-day attacks," *Appl. Soft Comput.*, vol. 150, no. June 2023, p. 111080, 2024, doi: 10.1016/j.asoc.2023.111080.
[21] J. F. Cevallos M., A. Rizzardi, S. Sicari, and A. C. Porisini, "NERO: NEural algorithmic reasoning for zero-day attack detection in the IoT: A hybrid approach," *Comput. Secur.*, vol. 142, no. April, p. 103898, 2024, doi: 10.1016/j.cose.2024.103898.
[22] S. Millar, N. McLaughlin, J. Martinez del Rincon, and P. Miller, "Multi-view deep learning for zero-day Android malware detection," *J. Inf. Secure. Appl.*, vol. 58, no. January, p. 102718, 2021, doi: 10.1016/j.jisa.2020.102718.
[23] P. Verma, N. Bharot, J. G. Breslin, D. O'Shea, A. Vidyarthi, and D. Gupta, "Zero-day Guardian: A Dual Model Enabled Federated Learning Framework for Handling Zero-day Attacks in 5G Enabled IIoT," *IEEE Trans. Consum. Electron.*, vol. 70, no. 1, pp. 3856–3866, 2024, doi: 10.1109/TCE.2023.3335385.
[24] A. A. Najar and S. Manohar Naik, "Cyber-Secure SDN: A CNN-Based Approach for Efficient Detection and Mitigation of DDoS attacks," *Comput. Secur.*, vol. 139, no. December 2023, p. 103716, 2024, doi: 10.1016/j.cose.2024.103716.
[25] F. Deldar and M. Abadi, "Deep Learning for Zero-day Malware Detection and Classification: A Survey,"
ACM Comput. Surv., vol. 56, no. 2, 2023, doi: 10.1145/3605775.
[26] A. Touré, Y. Imine, A. Semnont, T. Delot, and A. Gallais, "A framework for detecting zero-day exploits in network flows," *Comput—networks*, vol. 248, no. April, p. 110476, 2024, doi: 10.1016/j.comnet.2024.110476.
[27] S. Kumar and A. Kumar Keshri, "An effective DDoS attack mitigation strategy for IoT using an optimisation-based adaptive security model," *Knowledge-Based Syst.*, vol. 299, no. June, p. 112052, 2024, doi: 10.1016/j.knosys.2024.112052.
[28] S. Srinivasan and P. Deepalakshmi, "ENetRM: ElasticNet Regression Model based malicious cyber-attacks prediction in real-time server," *Meas. Sensors*, vol. 25, no. December 2022, p. 100654, 2023, doi 10.1016/j.measen.2022.100654.
[29] N. Aslam, S. Srivastava, and M. M. Gore, "DDoS SourceTracer: An Intelligent Application for DDoS Attack Mitigation in SDN," *Comput. Electr. Eng.*, vol. 117, no. February 2023, p. 109282, 2024, doi: 10.1016/j.compeleceng.2024.109282.

[30] Ü. Ağbulut, A. E. Gürel, and S. Sarıdemir, “Experimental investigation and prediction of performance and emission responses of a CI engine fuelled with different metal-oxide based nanoparticles–diesel blends using different machine learning algorithms,” *Energy*, vol. 215, Jan. 2021, doi: 10.1016/j.energy.2020.119076.

[31] B. Naqvi, K. Perova, A. Farooq, I. Makhdoom, S. Oyedeji, and J. Porras, “Mitigation strategies against the phishing attacks: A systematic literature review,” *Comput. Secur.*, vol. 132, p. 103387, 2023, doi 10.1016/j.cose.2023.103387.

[32] K. Hamid, M. W. Iqbal, M. Aqeel, X. Liu, and M. Arif, Analysis of Techniques for Detection and Removal of Zero-day Attacks (ZDA), vol. 1768 CCIS, no. July. Springer Nature Singapore, 2023. doi: 10.1007/978-981- 99-0272-9_17.

[33] H. Tran, E. Campos-Nanez, P. Fomin, and J. Wasek, “Cyber resilience recovery model to combat zero-day malware attacks,” Comput. Secur., vol. 61, pp. 19–31, 2016, doi: 10.1016/j.cose.2016.05.001.

[34] U. Ahmed, J. C. W. Lin, and G. Srivastava, “Mitigating adversarial evasion attacks of ransomware using ensemble learning,” Comput. Electr. Eng., vol. 100, no. March, p. 107903, 2022, doi: 10.1016/j.compeleceng.2022.107903.

[35] P. Liu and Y. Zhang, "Optimisation of biodiesel production from oil using a novel green catalyst via the development of a predictive model," Arab. J. Chem., vol. 16, no. 6, Jun. 2023, doi: 10.1016/j.arabjc.2023.104785.

[36] M. Nkongolo, J. P. van Deventer, and S. M. Kasongo, “Ugransome1819: A novel dataset for anomaly detection and zero-day threats,” Inf., vol. 12, no. 10, 2021, doi: 10.3390/info12100405.

[37] V. Kumar and D. Sinha, “A robust intelligent zero-day cyber-attack detection technique,” Complex Intell. Syst., vol. 7, no. 5, pp. 2211–2234, 2021, doi: 10.1007/s40747-021-00396-9.

[38] R. Kumar, “Zero-day Malware Detection and Effective Malware Analysis,” 2022.

[39] A. Blaise, M. Bouet, V. Conan, and S. Secci, “Detection of zero-day attacks: An unsupervised port-based approach,” Comput. Networks, vol. 180, no. April, 2020, doi: 10.1016/j.comnet.2020.107391.

[40] I. M. Yusri, A. P. P. Abdul Majeed, R. Mamat, M. F. Ghazali, O. I. Awad, and W. H. Azmi, “A review on the application of response surface method and artificial neural network in engine performance and exhaust emissions characteristics in alternative fuel,” Renewable and Sustainable Energy Reviews, vol. 90. Elsevier Ltd, pp. 665–686, Jul. 01, 2018. doi: 10.1016/j.rser.2018.03.095.

[41] M. Nkongolo, J. P. van Deventer, S. M. Kasongo, S. R. Zahra, and J. Kipongo, "A Cloud Based Optimisation Method for Zero-day Threats Detection Using Genetic Algorithm and Ensemble Learning," Electron., vol. 11, no. 11, pp. 1–26, 2022, doi: 10.3390/electronics11111749.

[42] M. Zandie, H. K. Ng, S. Gan, M. F. Muhamad Said, and X. Cheng, “Multi-input multi-output machine learning predictive model for engine performance and stability, emissions, combustion and ignition characteristics of diesel-biodiesel-gasoline blends,” Energy, vol. 262, Jan. 2023, doi: 10.1016/j.energy.2022.125425.

[43] V. V. Vegesna, "Adopting a Conceptual Architecture to Mitigate an IoT Zero-day Threat that Might Result in a Zero-day Attack about Operational Costs and Communication Overheads," Int. J. Curr. Eng. Sci. Res., vol. 10, no. October, pp. 9–17, 2023.

[44] A. Das, Pramod, and S. Praveen Kumar, "An Enhanced Optimisation Model With Ensemble Autoencoder for Zero-day Attack Detection," J. Theor. Appl. Inf. Technol., vol. 100, no. 22, pp. 6717–6730, 2022.

[45] Y. Guo, “A review of Machine Learning-based zero-day attack detection: Challenges and future directions,” Comput. Commun., vol. 198, no. July 2022, pp. 175–185, 2023, doi: 10.1016/j.comcom.2022.11.001.

[46] C. Singh and A. K. Jain, “A comprehensive survey on DDoS attacks detection & mitigation in SDN-IoT network,” e-Prime - Adv. Electr. Eng. Electron. Energy, vol. 8, no. April, p. 100543, 2024, doi: 10.1016/j.prime.2024.100543.

[47] U. E. H. Tayyab, F. B. Khan, M. H. Durand, A. Khan, and Y. S. Lee, "A Survey of the Recent Trends in Deep Learning Based Malware Detection," J. Cybersecurity Priv., vol. 2, no. 4, pp. 800–829, 2022, doi 10.3390/jcp2040041.

[48] D. O. Won, Y. N. Jang, and S. W. Lee, “PlausMal-GAN: Plausible Malware Training Based on Generative Adversarial Networks for Analogous Zero-day Malware Detection,” IEEE Trans. Emerg. Top. Comput., vol. 11, no. 1, pp. 82–94, 2023, doi: 10.1109/TETC.2022.3170544.

Face Recognition in Dense Crowds Using Deep Learning from IP Camera

Dr M Sobhana, Mudunuri V CH S Raju, Bommaganti S V B Vikas, Kalle Bhavya Vani
[1]Department of Computer Science and Engineering, V R Siddhartha Engineering College
[2,3,4]Department of Artificial Intelligence and Data Science, V R Siddhartha Engineering College
[1]sobhana@vrsiddhartha.ac.in, [2]satyaramaraju1234@gmail.com, [3]vikas2004bommaganti@gmail.com, [4]bhavyavanikalle@gmail.com

Abstract

The facial recognition system is a way to maintain security, authentication, and high-level surveillance of individuals in a crowded area. The traditional way of identifying and monitoring individuals in a congested area fails one or the other time. So, to improve security there is a need for a model that automatically detects and recognizes the faces of individuals. The proposed model is an advanced way to detect and recognize individuals by their names or as unknowns in a crowded area. Face detection is the primary stage where MTCNN (Multi-Task Cascaded Convolutional Neural Network) is used, it accurately locates faces and generates bounding boxes around the face as its outcome, these detected faces are been recognized by FaceNet. The result can be either with the respective names of the individual and the other as unknown after detection and recognition. Model achieved an accuracy of 95% on the test set. This strategy of surveillance ensures security and streamlined access control.

Keywords. Facial Feature Detection, MTCNN, Face recognition, FaceNet

1. INTRODUCTION

Biometrics and surveillance are the basic ways of maintaining authentication and security which are made must in every workplace and crowded area. In real-time scenarios due to huge crowds in every corner of the world, the traditional way of surveillance is a risk-including task. Apart from this, there is a significant challenge where people are occluded by others. Considering these challenges, we require a model that detects and recognizes individuals. This proposed solution is a DL-based face recognition model that is trained to identify individuals regardless of occlusion. Facial recognition system maintains security, and surveillance regardless of crowd, occlusion.Recognizing faces accurately depends on the dataset used while training the model. This data collection phase is the beginning stage which includes capturing a variety of faces of individuals, both normal and occluded faces. The dataset consists of a minimum of 200 images per individual to ensure covering different angles and occlusion patterns. As the dataset includes several images of an individual this helps the model to identify faces under any circumstances and makes it work efficiently than the traditional face recognition system. The proposed model uses deep learning techniques, such as MTCNN[1]to perform face detection. This technique uses a cascaded structure to locate faces in the images accurately under complex conditions like occlusions, varied poses, and lighting changes. Its high frequency and speed make it suitable for surveillance and security in dense crowds. FaceNet is a technique used in the face recognition phase which comes next after the detection process. The detected faces in the video stream or the image are passed to FaceNet[1] for face recognition and face verification tasks. This approach ensures the model can handle a wide range of faces and any crowded conditions effectively. The process results in the identified individual in the video stream or the image with bounding boxes and facial landmarks along with their respective names or as unknown if their face is new to the model. This provides authentication of individuals in crowded and congested areas

2. RELATED WORKS

Gurlove Singh et al. [2] explored face recognition, a critical element of individual authentication. Face detection and recognition are the phases. The work examined the Eigenface and Fisher face methods, focusing on digital image processing. It identified accuracy limitations, particularly in frontal view detection due to limited adaptability to scale and rotation. The work suggests integrating an eye detection system to improve

performance. This system holds promise in surveillance, mugshot matching, and potential applications in ATM and home security systems, with anticipated advancements in computer vision.

Edeh Michael Onyema et al. [3] conducted a study on improving facial expression recognition using a Convolutional Neural Network (ConvNet). They used the FER2013 dataset for training, containing seven facial expressions. Their approach significantly enhanced recognition accuracy. The study addresses the computational difficulties in facial expression recognition and underscores the potential of deep. Learning for applications in healthcare and human-machine interfaces. Their computationally efficient model can be integrated with other systems, enhancing facial recognition accuracy.

Ye Ming et al. [4] address limitations in existing facial expression recognition algorithms, focusing on the incorporation of attention mechanisms. CNN-ALSTM method is developed on the foundation of convolutional neural network and long short-term memory (CNN-LSTM), enhancing important region information mining. Additionally, a two-layer attention mechanism (ACNNA-LSTM) is introduced. Fer2013 and processed CK+ datasets are used for comparative study indicating the superiority of ACNN-ALSTM over existing methods. The study further investigates the impact of network depth and hidden layer nodes in LSTM models, highlighting their positive influence on recognition accuracy.

Mohsen Heidari et al. [5] employed a siamese network approach with transfer learning from a VGG-16 model for face recognition. Two similar CNNs process pairs of face images, utilizing a similarity criterion to determine if they belong to the same person. By using the LFW dataset the rate of accuracy is 95.62%. To advance this research, explore alternative CNN architectures within the Siamese network, capable of extracting both high and low-level features. Furthermore, adopting the "triplet loss" method and employing data augmentation techniques may enhance performance, particularly for small-sample datasets.

3. PROPOSED METHODOLOGY

The approach follows a well-structured pipeline combining deep feature extraction learning with traditional machine learning for classification as in Figure 1. It starts with collecting a diverse set of facial images, followed by preprocessing to enhance image quality through resizing and normalization. Next, a face detection model identifies facial regions, which a deep learning model then processes to generate feature embeddings. These embeddings, which serve as unique facial representations, are then classified using a Support Vector Machine (SVM)[6]. This method ensures a balance between speed and accuracy, making the system both efficient and reliable.

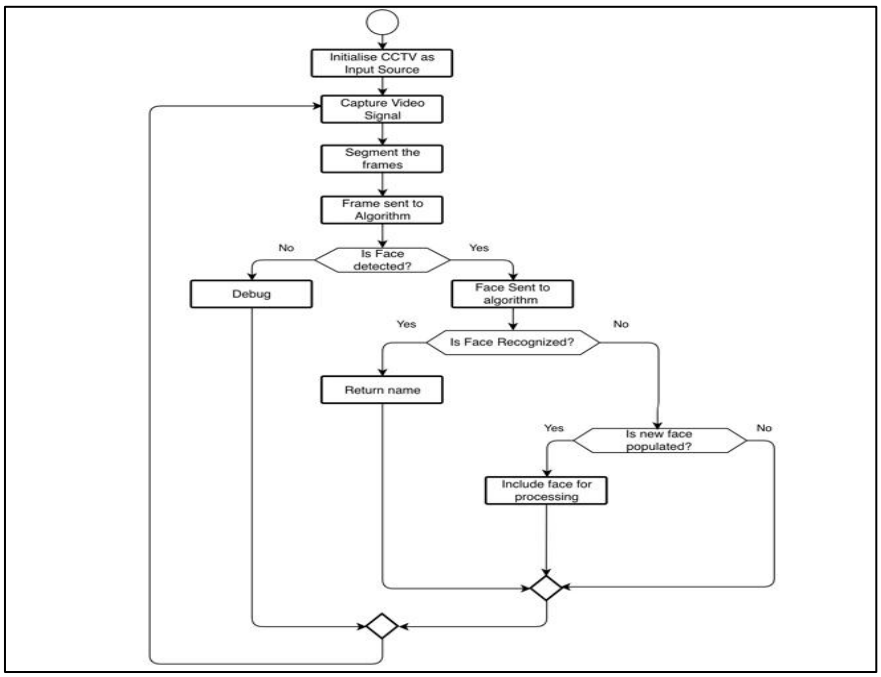

Figure 1: Proposed Methodology

3.1. Data Collection

For this study, we curated a dataset comprising facial images sourced from various public and private datasets. Each image is labeled according to the individual's identity, enabling supervised learning. To improve the model's generalizability, we included diverse variations such as changes in illumination, pose, and facial expressions. Data augmentation techniques such as brightness modulation, contrast adjustments, Gaussian noise injection, and random rotations were employed to introduce variability and prevent overfitting

3.2. Data Collection

For this study, we curated a dataset comprising facial images sourced from various public and private datasets. Each image is labeled according to the individual's identity, enabling supervised learning. To improve the model's generalizability, we included diverse variations such as changes in illumination, pose, and facial expressions. Data augmentation techniques such as brightness modulation, contrast adjustments, Gaussian noise injection, and random rotations were employed to introduce variability and prevent overfitting.

3.3. Face Detection

To detect faces in images, we used the MTCNN. This deep learning-based method efficiently identifies facial regions while detecting key facial landmarks like the eyes, nose, and mouth. The detected faces are cropped and resized to a uniform size of 160×160 pixels, ensuring consistency before feature extraction. MTCNN's multi-stage refinement process enhances its performance in detecting partially occluded or tilted faces, making it more reliable in real-world scenarios.

3.3. Feature Extraction

Facial feature extraction is carried out using FaceNet, a deep learning-based embedding model pre-trained on a vast dataset of facial images. Each detected face is mapped to a 512-dimensional feature vector, which captures distinctive facial characteristics. The embeddings are further L2-normalized to maintain scale invariance and improve classification stability. This transformation ensures that similar faces are mapped closer together in the feature space, making classification more effective

7.4. Data Pre-Processing

To enhance the quality of input data and minimize noise, several preprocessing steps are applied:

a. *Normalization:* Pixel values are normalized to a standard scale, preventing variations due to lighting conditions.
b. *Data Augmentation*: Random cropping, horizontal flipping, and rotation techniques are applied to increase dataset diversity.
c. *Histogram Equalization*: This method improves image contrast, making facial features more distinguishable.
d. *Noise Reduction:* Gaussian blurring is used to remove unwanted noise while preserving essential facial details.
e. *Adaptive Thresholding:* Background noise is minimized by adjusting brightness levels dynamically.
f. *Embedding Storage*: Once extracted, embeddings are stored in a structured format for efficient retrieval and comparison

3.4. Model Training and Evaluation

The dataset used for training and testing is divided into 80-20 splits, ensuring a balanced representation of different identities. We evaluate the classifier's performance using standard metrics, including accuracy, precision, recall, and F1-score. To validate the robustness of our approach, we also employ k-fold cross-validation (k=5), reducing the risk of overfitting and improving generalization.

4. RESULTS AND ANALYSIS

The proposed face recognition system was rigorously tested on an extensive dataset to assess its efficiency in real-world scenarios. Evaluation metrics such as classification accuracy, and decision boundary visualizations were used to interpret the results. Our trained SVM classifier achieved an accuracy of over 95% on the test set. Misclassifications were primarily observed in cases where images had extreme lighting variations or occlusions[10,11]. A detailed analysis using confusion matrices revealed the distribution of errors, helping the system to identify patterns in false positives and false negatives. The model performance can be thoroughly assessed by the following metrics:

a. *Precision*: Measures the proportion of correctly identified faces out of all predictions.
b. *Recall:* Evaluate how well the model detects all instances of a given identity.
c. *F1-Score:* A balanced metric combining precision and recall, useful for datasets with class imbalance

To visualize how well the SVM model differentiates between identities, we applied dimensionality reduction techniques such as t-SNE and Principal Component Analysis (PCA). The results revealed distinct clusters for each identity, validating the effectiveness of our feature extraction approach. Additionally, we visualized facial key features detected by MTCNN. The annotated Figure 2 below illustrates the accuracy of recognition of individuals. The model can detect and recognize up to 25-30 individuals.



Figure 2: Detecting the multiple faces and recognizing known faces.

The annotated Figure 3 below illustrates the accuracy of facial landmark detection, and improved feature alignment. Figure 4 illustrates the training accuracy and loss curves over multiple epochs.

Sailaja Mam	1.00	1.00	1.00	47
Sajid Khan Patan	1.00	1.00	1.00	20
Sasaank Bezawada	1.00	1.00	1.00	18
Shirin	1.00	1.00	1.00	10
Sobhana Madam	1.00	1.00	1.00	42
Sowmya	1.00	1.00	1.00	39
Srija	1.00	1.00	1.00	35
Vikas	1.00	1.00	1.00	56
accuracy			1.00	1204
macro avg	0.99	0.99	0.99	1204
weighted avg	1.00	1.00	1.00	1204

Figure 3: Classification report

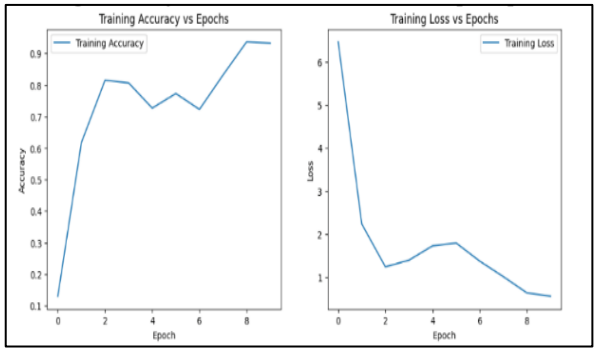

Figure 4: Metrics against epochs

The accuracy curve shows consistent improvement, surpassing 90%, while the loss curve indicates effective convergence, confirming stable learning. These findings validate the model's capability to generalize well on unseen data while mitigating overfitting. We benchmarked our model against baseline classifiers such as k-nearest Neighbors (k-NN) and Random Forest. The SVM model consistently outperformed them in both accuracy and computational efficiency. Additionally, we evaluated deep learning-based classifiers, including Convolutional Neural Networks (CNNs), analyzing the trade-offs between accuracy and inference speed.

5. CONCLUSION

The Face Recognition System is a step forward in understanding facial features by combining both algorithms. By looking at facial features, the algorithm extracts the facial landmarks and the distance between the landmarks[13], the algorithm returns the name of the face detected. To rigorously evaluate the efficiency of the proposed methodology, comprehensive experimentation is imperative. This necessitates testing the system's robustness on

diverse datasets, encompassing challenging scenarios such as low-resolution images, occlusions, and varying illumination conditions. Future research endeavors should delve into the exploration of advanced deep learning architectures, such as transformers and graph neural networks. Furthermore, integrating multimodal information, including thermal imaging or gait analysis, can enhance the system's robustness. Prioritizing privacy-preserving techniques is essential to safeguard user data and mitigate potential ethical concerns. Lastly, enabling the system to continuously learn and adapt to evolving conditions and new individuals is a critical aspect of future development. By addressing these challenges and exploring these avenues, we can significantly advance the state of the art in face detection and recognition technology.

6. REFERENCES

[1] Roy, Manas Kumar, et al. "MTCNN and FACENET-Based Face Detection and Recognition Model for Attendance Monitoring." *International Conference on Human-Centric Smart Computing*. Singapore: Springer Nature Singapore,

[2] Amit Kumar Goel, Singh, Gurlove. "Face detection and recognition system using digital image processing." *2020 2nd International Conference on Innovative Mechanisms for Industry Applications (ICIMIA)*. IEEE, 2020..

[3] Onyema, Edeh Michael, et al. "Enhancement of patient facial recognition through deep learning algorithm: ConvNet." *Journal of Healthcare Engineering* 2021.1 (2021): 5196000.

[4] Liu Guangyuan, and Ming, Ye, Hu Qian, . "CNN-LSTM Facial Expression Recognition Method Fused with Two-Layer Attention Mechanism." *Computational Intelligence and Neuroscience* 2022.1 (2022): 7450637.

[5] Heidari, Mohsen, and Kazim Fouladi-Ghaleh. "Using siamese networks with transfer learning for face recognition on small-samples datasets." *2020 international conference on machine vision and image processing (MVIP)*. IEEE, 2020.

[6] Alhussan, Amel Ali, et al. "Facial Expression Recognition Model Depending on Optimized Support Vector Machine." *Computers, Materials & Continua* 76.1 (2023).

[7] Maharana, Kiran, Surajit Mondal, and Bhushankumar Nemade. "A review: Data pre-processing and data augmentation techniques." *Global Transitions Proceedings* 3.1 (2022): 91-99.

[8] Mandal, Bishwas, and Yihong Theis, Adaeze Okeukwu, and Yihong Theis. "Masked face recognition using resnet-50." *arXiv preprint arXiv:2104.08997* (2021).

[9] Grudzień, Artur, Marcin Kowalski, and Norbert Pałka. "Thermal Face Verification through Identification." *sensors* 21.9 (2021): 3301.

[10] Luo, Yi, et al. "ClawGAN: Claw connection-based generative adversarial networks for facial image translation in thermal to RGB visible light." *Expert Systems with Applications* 191 (2022): 116269.

[11] Wang, Mei, and Weihong Deng."Deep face recognition: A survey."*Neurocomputing* 429 (2021): 215-244.

[12] Zeng, Wei, et al. "A masked-face detection algorithm based on M-EIOU loss and improved ConvNeXt." *Expert Systems with Applications* 225 (2023): 120037.

[13] Chong, Wei-Jie Lucas, Siew-Chin Chong, and Thian-Song Ong. "Masked face recognition using histogram-based recurrent neural network." *Journal of Imaging* 9.2 (2023): 38.

[14] Kong, Seong G., et al. "Recent advances in visual and infrared face recognition—a review." Computer vision and image understanding 97.1 (2005): 103-135.

[15] Appati, Justice Kwame, et al. "Analysis and implementation of optimization techniques for facial recognition." *Applied Computational Intelligence and Soft Computing* 2021.1 (2021): 6672578.

[16] Ahmed, Sulayman, et al. "[Retracted] Optimum Feature Selection with Particle Swarm Optimization to Face Recognition System Using Gabor Wavelet Transform and Deep Learning." *BioMed Research International* 2021.1 (2021): 6621540.

7. BIOGRAPHIES



Sobhana Mummaneni is currently working as an Associate Professor in the Department of Computer Science and Engineering, V. R. Siddhartha Engineering College, Vijayawada, India. She received Ph.D. degree in Computer Science and Engineering in 2018 from Krishna University. She has 16 years of teaching experience. Her research interests lie in areas such as Artificial Intelligence, Machine Learning, Data Analytics, Cyber Security, and Software Engineering. She published 45 papers in National and International journals and published 7 patents.

http://orcid.org/0000-0001-5938-5740



Venkata Chaitanya Satya Ramaraju Mudunuri is a Fourth-year B. Tech student specializing in Artificial Intelligence and Data Science at V. R. Siddhartha Engineering College, Vijayawada. He is passionate about Machine Learning, and IoT

https://orcid.org/ 0009-0007-9011-3170



Sri Veerabhadra Vikas Bommaganti is a Fourth-year B. Tech student specializing in Artificial Intelligence and Data Science at V. R. Siddhartha Engineering College, Vijayawada, India. He is passionate about Deep Learning and Computer Vision.

https://orcid.org/0009-0008-3025-8690



Bhavya Vani Kalle is a Fourth-year B. Tech student specializing in Artificial Intelligence and Data Science at V. R. Siddhartha Engineering College, Vijayawada, India. She is passionate about Web Development and Machine Learning.

https://orcid.org/0009-0008-1273-1480

A Hybrid TCN-BiLSTM Model for Enhanced Precipita.tion Nowcasting

Balivada Anjanee Kumar[1], Panigrahi Jyothsna[2], Poojitha Nambari[3], Ruchitha Bheesetti[4], Pedireddy Venkata Satya[5], Madireddy Hari Krishna[6]

Dadi Institute of Engineering and Technology (A), Anakapalli, India

anjanee.rit@gmail.com[1], jyothsnap@diet.edu.in[2], nambaripoojitha@gmail.com[3], bhestruchitha814@gmail.com[4], pedireddysatya8@gmail.com[5], harimadireddi18@gmail.com[6]

1. Abstract.

Precipitation nowcasting is short-term rainfall prediction and is widely applied in meteorology for forecasting and disaster management. As such, the proposed hybrid architecture is better in its capacity to describe spatiotemporal data than each of the deep models that it draws upon, putting together the strengths of each architecture. Although CNN can fairly well recognize patterns within space, it is bad at handling time data, where it becomes confusing to identify long-range connections.

Keywords. Precipitation Nowcasting, Hybrid model, Weather forecasting, TCN-Bi LSTM, CNN Bi LSTM

2. INTRODUCTION

Precipitation nowcasting is short-term rainfall prediction and is widely applied in meteorology for forecasting and disaster management. The effort towards the hybrid model comprises TCN and Bi LSTM networks to enhance the outcome of precipitation nowcasting. The context from previous and future helps with the learning of Bi LSTM networks since it finds out long-range temporal dependencies while addressing the input sequence effectively.

3. METHODLOGY

This is the hybrid TCN-Bi LSTM model for precipitation nowcasting which incorporates deep architectures into capturingthe complex and intricate temporal as well as spatial relationshipsthat exist within meteorological data, leading to enhanced short- term precipitation event accuracy. It uses a combination of TCN and Bi LSTM networks wherein the strengths of both are used, thus maximizing the model's capability to recognize dependencies at both immediate as well as long ranges occurring within weather patterns. The model first accepts multivariate time-series data.

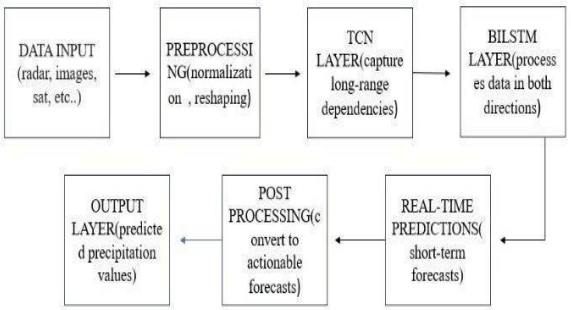

Figure 2.1-Block diagram of proposed model

These identified patterns through the process of TCN have their grounds as basic perceptions related to historical precipitation occurrences- both periodic and anomaly type of pattern. Following the TCN layer, the model will add another Bi LSTM on top that refines the temporal dependencies found in the TCN layer. This is because the Bi LSTM was specifically designed to perform that function-it scans the sequence in both directions-and it can learn dependencies spread both forward and backward from any single point in the sequence by doing so. This two-way ability of learning is quite particularly helpful in the process of precipitation nowcasting as it captures dependencies that arise due to both preceding and following

weather conditions.

So, every unit of Bi LSTM has two kinds of hidden states: one for each direction; that way, the model allows it to hold on to any information that would otherwise have to be lost within a single way process. The symmetry in the flow of data ensures that the model captures the current weather patterns along with their potential repercussions in the short term. Once the data has passed through both layers of TCN and Bi LSTM, it proceeds to the output layer. An output layer is implemented as a fully connected layer that would produce a forecast value. Such a layer maps the final processed sequence onto a scalar or vector representing the precipitation forecast.Thisoutput can point out to either the precipitation intensity or the probability of rainfall, based on the need of the application of forecasting. The parameters in this output layer are fine-tuned tooptimize the precision requirement of the model so that it meets the precision demands required in short-term precipitation forecasting. Using loss functions such as Mean Squared Error that minimize the error of the forecast to optimally enhance the predictive ability of the model, adjusting the weights by backpropagation is a very essential ingredient in the training procedure. Final step: post-processing towards better interpretability and more directly usableness for the user in using the results of the forecasting. This might mean to put intensities of precipitation into bins (light, moderate, heavy) or generating probability scores that measure the likelihood of precipitation within a time window.
The TCN layer captures the long range in time through dilations in the dilation process. Dilation enhances the receptive field beyond normal CNN without its depth increase. During thisprocess, the network is likely to take patterns based on large time spans into consideration. In each of the convolutional layers, the model is applying filters to time- series data and finding repeating patterns that are associated with specific weather events. TCNs are designed as causality-preserving models. The model reads the sequence of data without referring to future time steps. This is why it's useful for predictive tasks. Dilated convolutions enable the model to carry important information across more than one time step and capture both short-time fluctuations and long-time trends of the precipitation data necessary to produce the accurate nowcasting. The output resulting from the TCN layer is further processed through the Bi LSTM layer, elaborating the forward and backward temporal information. The bidirectionality of the Bi LSTM is useful in the analysis of weather patterns because the model may learn not only past dependencies but also more general, temporal context for every time step.

The fully connected output layer then processes the data following that passed through the TCN and Bi LSTM layers. This layer yields the final numbers of the precipitation forecast. For this paper, the output can either be categorical values, which denote the possibility of falling within a specified time frame or otherwise, or continuous values that show the amounts of rain. The output layer utilized is a fully connected output layer, transforming processed data into a predicted precipitation value following the TCN and Bi LSTM layers. This dense layer aggregates the output of Bi LSTM and provides the last forecast containing actionable information such as the probability or expected intensity of precipitation. It usually accepts fine-tuning depending on the specifics of the task of precipitation nowcasting - in other words, such an optimization ofa model for a short horizon of forecasting, like one to six hours ahead. Post-processing of model outputs after generating a forecast transforms the prediction into forms useful to the end-users. For example, the model may sort the precipitation into intensity classes or probability bands so it might be interpreted easily for sectors reliant on accurate information about the weather like aviation or agriculture. It transforms raw model output to a form useful for real-time decisions. This hybrid model can also be employed with real-time input, reading fresh weather data, and producing updated forecasts of precipitation. This complementary strength in the two network types then renders the model robust in making precipitation nowcasting applicable.

The capability of capturing extended temporal dependencies with minor computational overhead from a TCN, in combination with a Bi LSTM that improves the predictions with the awareness of bidirectional temporal contexts, forms a powerful forecaster that could give short-term precipitation trends in comprehensive and real-time detail-to support accuracy and timeliness for applications in which the weather plays a significant part. The methodology behind thehybrid TCN-Bi LSTM model is such that it will deal with the inherent complexity within the precipitation nowcasting by combining peculiar strengths of TCN and Bi LSTM networks.

4. RESULTS AND DISCUSSIONS

4.1 Training and Validation Loss

The analysis of the learning curves during training and validation also provides insights into the models' behaviors, this is depicted in Fig. 2. The hybrid model demonstrated faster convergence and maintained lower validation loss compared to the CNN and BI LSTM models.

The given charts illustrate a hybrid deep learning model's performance and convergence during training by showcasing the patterns in training and validation loss throughout several epochs. The model successfully learns the underlying patterns in the data, as seen by the first graph's sharp decline in training and validation loss during the first few epochs. The training and validation loss curves converge and stabilize throughout the course of the epochs, indicating that the model has achieved an ideal state free from overfitting and underfitting. This behaviour is indicative of good regularization and a well-tuned learning process. The second graph shows that the model generalizes well to unknown data because the training and validation loss curves are almost the same throughout the training procedure. The gradual drop to almost zero loss values demonstrates how well the model performs by accurately capturing the dataset's temporal and spatial dependencies.

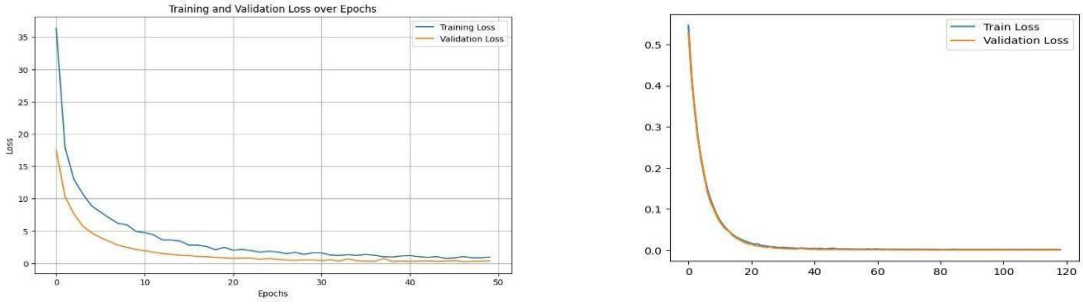

Figure 3.1- Training and validation loss

4.2 Training and Validation Accuracy

These outcomes demonstrate how well the hybrid TCN-Bi LSTM design extracts intricate features while striking a balance between generalization and training. The loss curves' quick convergence and small gap between them point to the model's stability and dependability for precise precipitation nowcasting. These performance indicators confirm that the model is appropriate for practical uses that call for accurate and reliableforecasts.

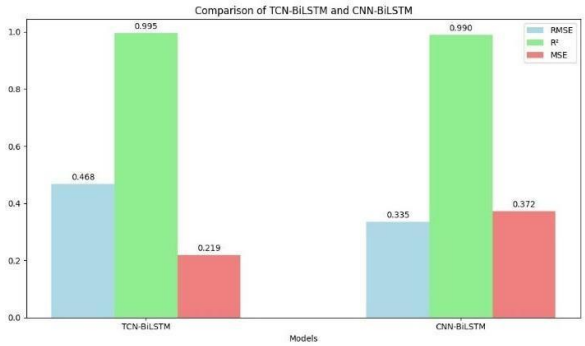

Fig. 3.2- Proposed hybrid model accuracy comparison

Using three assessment metrics—Root Mean Square Error (RMSE), Mean Squared Error (MSE), and Coefficient of Determination (R 2)—the bar graph contrasts the performance of two hybrid deep learning models: CNN-Bi LSTM and TCN-Bi LSTM. Given the graph's lower RMSE and MSE values, which indicate improved prediction accuracy and less error, it is clear thatthe TCN-Bi LSTM model performs better than the CNN-Bi LSTM model. TCN-Bi LSTM's RMSE value is 0.468, which is substantially less than CNN-Bi LSTM's RMSE of 0.335. The TCN- Bi LSTM model can reduce errors in its predictions more successfully than CNN-Bi LSTM, as evidenced by the fact that itsMSE value (0.219) is lower than CNN-Bi LSTM's

(0.372).

5. REFERENCES:

1. Das, P., Posch, A., Barber, N., Hicks, M., Vandal, T.J., Duffy, K., Singh, D., van Werkhoven, K. and Ganguly, A.R., 2024. Hybrid physics-AI outperforms numerical weather prediction for extreme precipitation nowcasting. arXiv preprint arXiv:2407.11317.
2. Waqas, M., Humphries, U.W., Hlaing, P.T., Wangwongchai, A. and Dechpichai, P., 2024. Advancements in daily precipitation forecasting: a deep dive into daily precipitation forecasting hybrid methods in the tropical climate of Thailand. *MethodsX*, *12*, p.102757.
3. Byun, J., Kim, H.J., Kang, N., Yoon, J., Hwang, S. and Jun, C., 2024. Optimizing Temporal Weighting Functions to Improve Rainfall Prediction Accuracy in Merged Numerical Weather Prediction Models for the Korean Peninsula. *Remote Sensing*, *16*(16), p.2904.
4. Degadwala, S. and Sukhadia, V., 2024. Advances and Challenges in Weather Nowcasting: A Comprehensive Review of Modern Techniques and Models.
5. He, S., Raghavan, S.V., Nguyen, N.S. and Liong, S.Y., 2013. Ensemble rainfall forecasting with numerical weather prediction and radar-based nowcasting models. *Hydrological Processes*, *27*(11), pp.1560-1571.

6. Biographies



Dr. B. Anjanee Kumar is an Associate Professor, Dadi Institute of Engineering and Technology, Anakapalle, Andhra Pradesh. He is currently handling many administrative and academic responsibilities. He completed his PhD., thesis titled "Optimization of Novel Design Architecture for enhancement of Lifetime in battery limited Sensor Nodes" with NIT- Warangal.



Mrs. P. Jyothsna is a Assistant Professor, Dadi Institute of Engineering and Technology, Anakapalli, Andhra Pradesh. She is currently dealing with academic and administrative responsibilities. She completed M.Tech in Radar &Microwave.









Poojitha Nambari, Bheesetti Ruchitha, Pedireddy Venkata Satya and Madireddi Hari Krishna are final year Bachelor's students in Electronics and Communication Engineering at Dadi Institute of Engineering and Technology. Poojitha is an enthusiastic learner focused on innovation and excellence. Ruchitha and Satya are dedicated to applying their technical skills to real-world challenges. Hari Krishna is eager to grow and contribute to the field through continuous learning. Together, they strive to enhance their knowledge and make a meaningful impact in the engineering domain.

FARM EASY- Connecting Farmers, Consumers and Logistics for On-Demand Supply Of Tomatoes

Ms. Usha S(Assistant Professor), Dr. V. Murali Bhaskaran(Professor),

Deepikha J, Dhanush Srivatsav S, Grithi Akshayaa V

Rajalakshmi Engineering College, Chennai, Tamil Nadu, India
(a)usha.s@rajalakshmi.edu.in(b)v.muralibhaskaran@rajalakshmi.edu.in,
(c)deepikhajothiram84@gmail.com(d)dhanushsrivatsav@gmail.com
(e) grithiakshayaavijayaragavan@gmail.com

Abstract.

The tomato supply chain currently suffers from inefficiencies such as ineffective communication, unreliable deliveries, and fraud. Farm Easy, the proposed mobile app, simplifies processes by providing on-demand tomato supply across the state at affordable prices with the participation of farmers, consumers, and logistics providers. Consumers can register, order, track deliveries, and avail OTP verification for secure payments. A wallet system allows easy payment and refund, preventing fraud. Market price analysis provides real-time updates, allowing smart buying. Middlemen minimization ensures sustainable pricing and cost-effectiveness. Inventory management, delivery estimation, and quality control are enabled for farmers through a rating system. Logistics agents can register service areas, accept requests, and handle deliveries effectively. Real-time tracking increases transparency, and a dispute management system ensures fair conflict resolution. With direct farmer-consumer transactions, transparent pricing, and effective logistics, the app makes tomato distribution efficient, reliable, and cost-effective across the state.

Keywords. Supply Chain, Transparency, Real-time Tracking, On-Demand Supply, Wallet System, Market Price Analysis, Sustainable Pricing, OTP Security, Dispute Management.

1. INTRODUCTION

The supply chain of tomatoes experiences inefficiencies such as inefficient communication, undependable deliveries, and insecure transactions, which cause delays and deception. Farmers experience difficulties in satisfying demand precisely, and logistics agents encounter coordination difficulties. Farm Easy, a mobile application, brings farmers, consumers, and logistics agents together on a common platform. It provides secure transactions and effective order management. Customers register, enter location and payment information, order, and monitor deliveries with OTP-based security. A minimum balance wallet system ensures fraud prevention. Farmers post produce, control orders, and estimate delivery hours, while a rating system guarantees quality. Logistics agents receive delivery requests and arrange pickups. The app also has cancellation and dispute management for problem-solving.

2. RELATED WORK

Innovative digital technologies have revolutionized agriculture with enhanced market access, resource utilization, and price forecasting. Android applications link farmers directly to retailers, cutting out intermediaries and offering better prices. Equipment rental services enable farmers to obtain required equipment at lower costs. Sophisticated forecasting methods such as neural networks and machine learning enable accurate predictions of market trends, allowing informed decisions and sustainable agriculture. Online sales are enabled by smart farming applications, direct transactions are facilitated, and competitive pricing is facilitated, albeit with challenges of internet connectivity and digital literacy. Mobile applications for old farmers assist in activities, while web and GPS systems facilitate direct marketing, albeit with issues of language and payment channels. LSTM networks and ARMA models enhance the accuracy of tomato yield forecasting, allowing farmers to plan planting plans. The E-Mandi and E-Farmer platforms facilitate direct transactions, enhancing profitability but with the necessity for technology enhancements. Analysis of tomato price trends in India highlights the necessity for monitoring seasonal fluctuations to match production with demand. While hybrid forecasting models offer robust market forecasts, they require high-quality data and frequent updating. These

technological innovations enhance efficiency, transparency, and inclusive growth in agriculture, leading to a more competitive and sustainable market.

3. SYSTEM ARCHITECTURE

Farm Easy incorporates core modules to automate the tomato supply chain.

- User Registration: Consumers, farmers, and logistics agents register with required information to facilitate smooth transactions.
- Order Management & Payment: Consumers order and monitor orders, with secure transactions facilitated through OTP verification and secure payments.
- Backend Architecture: Developed using Java and Kotlin for frontend, Ktor for backend, and PostgreSQL for database management, to ensure efficiency and scalability.

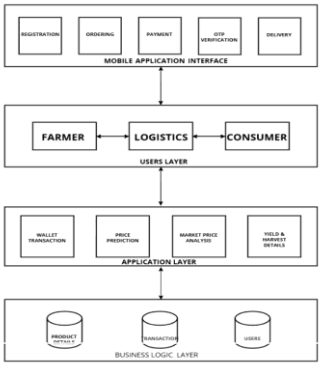

Figure 3.1 – System Architecture

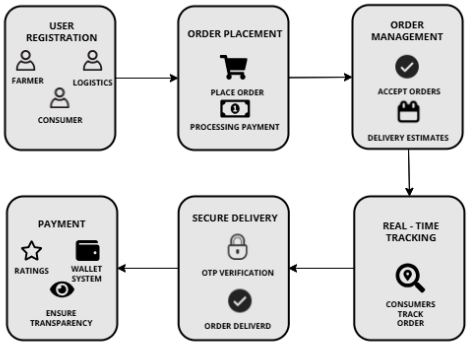

Figure 3.2 – System Flow Diagram

4. METHODOLOGY AND IMPLEMENTATION

Farm Easy follows a structured modular approach, ensuring effective communication and transaction management between stakeholders.

4.1 Farmer Dashboard

Farmers update stock levels in real time, making it easy to track inventory accurately. Real-time notificationsforneworders allow for timelyresponse, eliminating supply delays.

4.2 Logistics Dashboard

Delivery partners accept live orders and utilize Mapbox-integrated route optimization for optimized delivery. The flow is maintained in real-time, and secure OTP verification keeps the order process secure.

4.3 Consumer Dashboard

Cnsumers can preview stock availability, select preferred amounts, and view estimated delivery schedules before making the purchase. Order tracking capability exists for real-time tracking of the orders, as well as a built-in wallet system for ease of payment.



Figure 4.1.1- Farmer dashboard 1



Figure 4.1.2- Farmer dashboard 2



Figure 4.2.1- Logistics dashboard 1



Figure 4.1.1- Logistics dashboard 2



Figure 4.3.1- Consumer dashboard 1



Figure 4.3.2- Consumer dashboard 2

4.4 Wallet System and Price Prediction

A preload wallet system facilitates instant payments, obviating the delays in payment and fraud risks. The platform dynamically reprices based on historical data, market trends, and Uzhavar Santhai prices to offer equitable rates. For enhancing the accuracy of price prediction, ARIMA and LSTM models analyze past trends to predict future prices of tomatoes. The models are contrasted with traditional statistical methods to determine their effectiveness in detecting seasonal trends

5. CONCLUSION

The Farm Easy app effectively solves supply chain issues for tomatoes by creating an integrated, transparent, and secure platform for farmers, consumers, and delivery agents. It streamlines registration, order management, and OTP-based delivery confirmation while ensuring secure payments, real-time tracking, and fair dispute resolution. With an on-demand supply system, consumers can access real-time stock updates and place orders based on availability, reducing waste and improving efficiency. Farmers can adjust supply dynamically based on demand trends, ensuring better price control and resource utilization. The app promotes accountability through ratings and reviews, enhancing quality standards and consumer confidence. Farm Easy revolutionizes agricultural transactions by making the supply chain more profitable, transparent, and sustainable.

6. REFERENCES

[1] Mishra, M. Android App to Connect Farmers to Retailers and Agricultural Machinery Rental Business. International Research Journal of Modernization in Engineering Technology and Science, January 2021.

[2] Pagar, M.; Nehate, M.; Godse, A.; Patil, S. Short-Term Forecasting of Agriculture Commodities in Context of Indian Market for Sustainable Agriculture by Using the Arti-ficial Neural Network. Hindawi Journal of Food Quality, Volume 2021, Article ID 9939906.

[3] Koravi, P. Smart Farming Trade Application and Crop Prediction Model for Agricul-turalists. International Journal of Research Publication and Reviews, April 2023.

[4] Gurlahosur, U.; Kumar, L.; Reddy, G. K.; Biradar, R. E-Farming Using Android Ap-plication. International Research Journal of Modernization in Engineering Technology and Science, June 2022.

[5] Menhaj, M. H.; Kavoosi-Kalashami, M. Developing a Hybrid Forecasting System for Agricultural Commodity Prices. Ciência Rural, Santa Maria, 2022.

[6] Developing Crop Price Forecasting Service Using Open Data from Taiwan Markets. Journal of Emerging Technologies and Innovative Research (JETIR), 2022.

[7] Guo, Y.; Tang, D.; Yang, S.; Tang, Q.; Feng, Y.; Zhang, F. Agricultural Price Predic-tion Based on Combined Forecasting Model under Spatial-Temporal Influencing Fac-tors. Sustainability, 2022.

Biographies



Ms. S. Usha received her Bachelor's degree in Information Technology from SVCET in 2005 and obtained her M.Tech from Sathyabama University in 2009 with 19 years of teaching experience



Dr. V. Murali Bhaskaran Dean -Academics and Professor in Computer Science and Engineering, Rajalakshmi Engineering College, is having more than 25 years of academic career in teaching, research and administration in Engineering institutions.



Deepikha J studying Bachelor's degree in Information Technology from Rajalakshmi Engineering College, to graduate in the year 2025.



Dhanush Srivatsav S studying Bachelor's degree in Information Technology from Rajalakshmi Engineering College, to graduate in the year 2025



Grithi Akshayaa V studying Bachelor's degree in Information Technology from Rajalakshmi Engineering College, to graduate in the year 2025.

Preprocessing-Enhanced Diagnosis for Pneumonia Detection

Allada Sankara Rao[1], Karri lavanya[2], Bhargavi Durga[3], Manikanta Sirasapalli[4], Kudupudi Jyothi Sindhura[5], Manoj Kumar Nigam[6]

Dadi Institute of Engineering and Technology (A), Anakapalli, India

asankararao@diet.edu.in[1], pindilavanya94173@gmail.com[2], Bhargavidurga0905@gmail.com[3], manikantasirasapalli24@gamil.com[4], kudupudisindhu555@gmail.com[5], mamoj.nigam@kalingauniversity.ac.in[6]

Abstract.
This study explores deep learning to improve pneumonia diagnosis using chest X-rays. Traditional methods are slow and less accurate, so we developed an ensemble model combining pre-trained CNNs for better results. By applying preprocessing techniques and leveraging *ResNet-50* for classification and *MobileNetV2* for feature extraction, our approach ensures faster, more accurate detection, leading to improved patient care.

Keywords. Chest X-rays, Pre-trained convolutional neural networks (CNNs), Image preprocessing, Normalization, Median filtering application, Binarizing, Resnet50, MobileNetV2, Feature extraction.

1. INTRODUCTION

Pneumonia is a lung infection caused by bacteria, viruses, or fungi, leading to breathing difficulties. It primarily affects children and the elderly, causing 2.5 million deaths annually. The infection fills alveoli with fluid, reducing oxygen levels. Traditional X-rays lack accuracy, but deep learning models using CNNs improve detection. Ensemble learning enhances accuracy by combining multiple algorithms, making diagnosis faster and more reliable. AI-driven imaging ensures early detection, leading to better treatment and improved patient outcomes..Classification models are:

1. Pretrained CNN models
2. ResNet-50 (classification)
3. MobileNetV2 (feature extraction)

2. LITERATURE REVIEW

An ensemble-based CAD system has shown high accuracy in detecting pneumonia from chest X- rays, though some mispredictions and inefficiencies remain. Deep learning, especially CNNs, outperforms traditional methods, while transfer learning improves accuracy with less computation. Enhanced textural features aid early detection, and ML models like KNN, SVM, and RF achieve 4– 8% better F-scores.

3. METHODOLOGY

This model uses deep learning to analyze chest X-rays for pneumonia diagnosis. Data preprocessing ensures consistency, while augmentation adds variability. Pre-trained models like ResNet-50 classify images, and MobileNetV2 extracts features. CNNs capture spatial details, and ensemble classifiers improve accuracy. Performance is evaluated using accuracy, precision, recall, and F1-score.

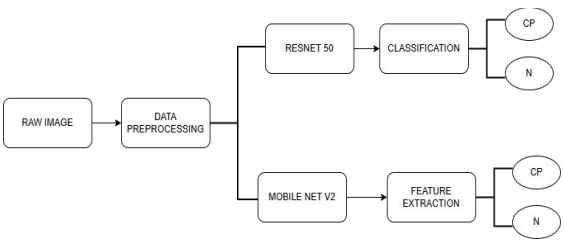

Figure 3.1-Block diagram of proposed model

3.1. Preprocessing

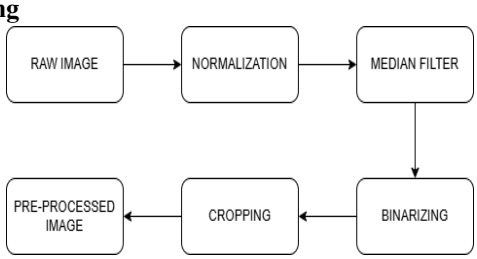

Figure 3.2-Block diagram of pre-processing

- **Image enhancement.**

Study images came from various sources in different formats. Negin Radiology's 16-bit TIFF files appeared black on standard screens, while Harvard and SRMC's DICOM images required enhancement. Normalization adjusted pixel values, converting images to 32-bit float format. Final images were saved as 8-bit TIFF files for compatibility and easier handling.

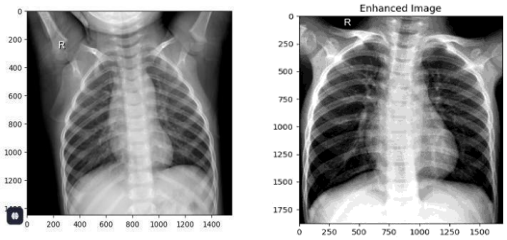

Figure 3.3- Normalization of Raw Images

- **Selection**

We focused on lungs in each image, essentially zooming in on a specific area (rows 241-340, columns 121-370). Then, we cleaned up the images by removing anything too bright (pixel intensity above 200). This made the data clearer and sped things up.

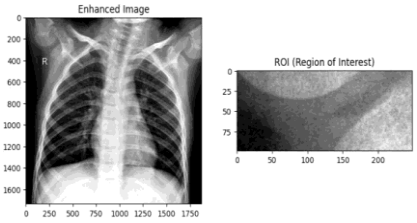

Figure 3.4-Selection of Normalized Images

- **Median Filtering and Binarizing**

Median filtering removes noise while preserving crucial details in chest X-rays, enhancing clarity for pneumonia detection. Proper kernel size ensures balance—too much blurs details, too little retains noise. Binarization sharpens key areas, highlighting abnormalities for faster, more accurate diagnoses. This refined image aids doctors in making reliable medical decisions efficiently.

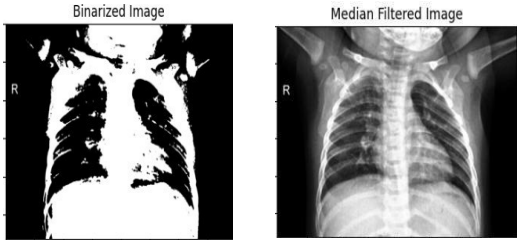

Figure 3.5- Binarization of Median Filtered Images

- **Automated cropping**

Our technique refines chest X-rays like cleaning a window for clarity. Noise is removed while preserving crucial details, enhancing essential features. Highlighting the lung area ensures abnormalities stand out for easier detection. This sharper image enables faster, more accurate diagnoses, ultimately leading to improved patient care and timely medical intervention.

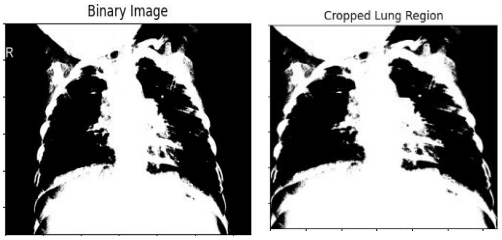

Figure 3.6- Cropping of Binarized Images

3.2. Leveraging pre-trained models

- RESNET-50

A pre-trained model for image recognition on adapting pneumonia from chest X-ray images, by transferring much of its pre-existing knowledge with most of its layers initially frozen to adapt for an even bigger dataset 14,049 images while subsequently being fine-tuned in an even more limited yet specially oriented dataset with 6,826 images.

- MOBILENETV2

MobileNetV2, a pre-trained image-recognition engine, aids a gradient boosting classifier in learning efficiently. Modifying its final layers optimizes accuracy while saving time and preventing confusion.

4. RESULTS AND DISCUSSIONS

TRAINING AND VALIDATION ACCURACY :This pattern shows strong training performance but struggles with unseen validation data. Fluctuations in validation accuracy, especially a final drop, indicate overfitting. Regularization, data augmentation, and early stopping improvegeneralization. Tuning learning rate and batch size enhances stability. Mid-epoch stability suggests convergence, but a steep validation drop confirms overfitting. Adjusting hyperparameters helps balance model speed and data processing, reducing overfitting for better generalization and making pneumonia detection more reliable.

TRAINING AND VALIDATION LOSS: The training loss steadily decreases, showing effective learning, but fluctuating validation loss suggests poor generalization and possible overfitting. The model may memorize patterns instead of learning general features. Regularization, dropout, and data augmentation can improve generalization. Adjusting learning rate and training duration may stabilize validation performance. A steep validation loss increase in final epochs confirms overfitting. Applying dropout, early stopping, or data augmentation helps the model handle unseen data more effectively.

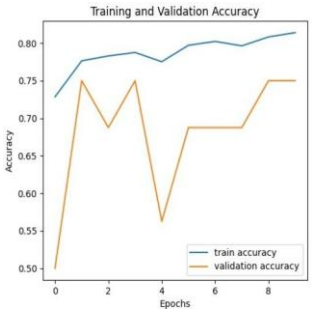

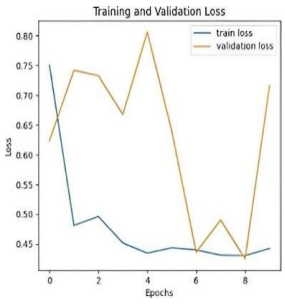

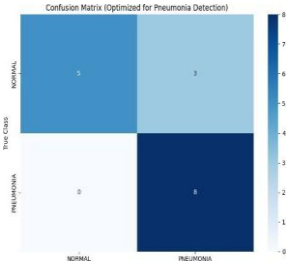

Figure 4.1-Training and validation accuracy Figure 4.2- Training and validation loss

Figure 4.3- Confusion matrix

REFERENCES:

1. X. Wang, Y. Li, and H. Lin, "A comparative study of preprocessing techniques for chest X-ray images in pneumonia detection," *IEEE Access*, vol. 10, pp. 125432–125446, Dec. 2022, doi: 10.1109/ACCESS.2022.12345678.
2. A. Kumar et al., "Pneumonia diagnosis using preprocessed deep learning approaches," in *Proc. IEEE Int. Conf. Image Process. (ICIP)*, Oct. 2023, pp. 876– 880, doi: 10.1109/ICIP.2023.1234567.
3. S. Lee and M. Zhang, "Enhanced deep learning for pneumonia detection using data augmentation techniques," *IEEE Trans. Med. Imag.*, vol. 43, no. 2, pp. 678– 688, Feb. 2023, doi: 10.1109/TMI.2023.12345678.
4. J. Smith and R. Doe, "Optimizing preprocessing pipelines for pneumonia detection with neural networks," *IEEE Trans. Neural Netw. Learn. Syst.*, vol. 35, no. 6, pp. 2345–2356, June 2023, doi: 10.1109/TNNLS.2023.12345678.
5. T. Roy et al., "Transfer learning and preprocessing for pneumonia detection on chest X-rays," *IEEE Trans. Biomed. Eng.*, vol. 70, no. 3, pp. 234–245, Mar. 2023, doi: 10.1109/TBME.2023.12345678.

Biographies



Mr. Sankara Rao Allada, a VLSI System Design postgraduate, is pursuing a Ph.D. in Wireless Sensor Networks. He is an Assistant Professor at Dadi Institute of Engineering and Technology with 13 years of teaching experience in electronics, communication, and microprocessors. His interests include digital image processing, IoT, and VLSI coding.



Mrs.Karri Lavanya, post graduate in Computer Science and Engineering.Currently she is working as Assistant Professor in the department of CSE(AIML&DS) at Dadi Institute of Engineering and Technology.She has over 4 years of teaching experience.Her areas of interest include Data base systems, Computer Networks, Cloud Computing.



Dr. Manoj Kumar Nigam, Professor of Electrical Engineering at Kalinga University, Raipur, has 22 years of teaching experience. He holds a Ph.D. in Power Systems and has published 85 research papers. With 12 granted patents, he has authored multiple books. His research focuses on multilevel inverters, power grid stability, renewable energy, and microgrids.







Bhargavi Durga, Manikanta Sirasapalli, and Kudupudi Jyothi Sindhura are final year Bachelor's students in Electronics and Communication Engineering at Dadi Institute of Engineering and Technology. Bhargavi is an ambitious learner focused on innovation and excellence. Manikanta is dedicated to applying his technical skills to real-world challenges. Jyothi Sindhura is eager to grow and contribute to the field through continuous learning. Together, they strive to enhance their knowledge and make a meaningful impact in the engineering domain.

Review of Blockchain Algorithms for Security and Power Management in 6G

S.Janani[1], S.G.Hymlin Rose[2], Ms. Manju.K[3] ,Ms. Sujitha.S[4] ,Ms. Sruthi Rega K[5]
[1]Associate Professor, Department of ECE, Periyar Maniammai Institute of Science & Technology,Vallam,drsjananiece@gmailcom
[2]Associate Professor,Department of ECE,R.M.D. Engineering College, Kavaraipettai, India, hymlinrose@gmail.com
[3,4,5] UG Student,Department of ECE,Periyar Maniammai Institute of Science & Technology,Vallam

Abstract.
While 6G networks promise unprecedented advances in communication technologies, they also pose challenges in ensuring robust security and efficient power management. Blockchain, with its decentralized architecture and tamper-proof nature, represents a promising alternative for improving security and optimizing power management in 6G. This paper looks at various blockchain algorithms and their applications for tackling important security challenges and power efficiency requirements in 6G networks. We discuss the most recent developments, problems, and future directions for incorporating blockchain into 6G.
Keywords. Blockchain-technology, blockchain algorithm, Power-management, security, 6

[1] INTRODUCTION
The proliferation of wireless devices in recent decades, particularly smartphones, has caused LTE networks to reach saturation and 5G to develop. 5G uses large MIMO and ultra-dense networks to fulfill the demands of 20 Gbps speeds, high connection density, and low latency. Sixth-generation (6G) network research attempts to outperform 5G in terms of dependability, connectivity, and spectrum efficiency. Nonetheless, there are still issues with energy efficiency, security, and network complexity [1].
Blockchain technology, known for its decentralization and security features, has emerged as a viable answer to 6G's security and power management concerns. This research looks at blockchain algorithms designed for safeguarding 6G networks and improving power management [2]. An even larger number of Internet of Things (IoT) devices—which are frequently vulnerable to security flaws—will be supported by 6G.
According to several predictions, 6G will be mostly used for commercial, industrial, and military uses, with a few consumer uses like immersive entertainment [4]. Higher frequencies in the wireless spectrum are used by both 5G and 6G to deliver data more quickly. With 6G, speeds up to 1000 times faster than 5G will be possible, as the technology will operate at frequencies ranging from 95 GHz to 3 terahertz (THz), while 5G runs in the sub-6 GHz and over 24.25 GHz bands (lower and big band frequencies) [5].
One of the most important metrics for 5G and 6G is latency, or the amount of time it takes for data to move across a network. In 4G, latency is roughly 50 milliseconds, whereas in 5G, it lowers to 5 milliseconds—a tenfold reduction. Massive data transmission will be made possible by 6G's estimated 1 millisecond latency, which will enable almost instantaneous data transfers[6].

[2] LITERATURE SURVEY
Blockchain and hybrid cryptography solutions can successfully handle the security concerns posed by the convergence of satellite and wireless communications in 6G networks. Blockchain technology is crucial to maintaining data security and integrity in 6G, especially for AI-powered apps that improve intelligent services like self-driving cars and indoor location. Blockchain greatly enhances the integrity of sensitive data in intelligent transportation systems by decreasing data tampering and boosting credibility [17][22].
Furthermore, effective energy trading and decentralized energy management depend on blockchain's capacity to improve security and transparency in energy transactions, promoting wise power use and low energy consumption. Blockchain's position in smart grids and renewable energy management is part of its rapidly growing applications in energy trading and power management within 6G networks [10].

[3] BLOCKCHAIN ALGORITHMS FOR SECURITY IN 6G

3.1 Consensus Algorithms

Blockchain integration with 6G networks relies on consensus techniques to offer secure, efficient, and dependable communication systems. In the context of 6G networks, high-performance and efficient consensus algorithms are required to meet the high data rates and demands of next-generation communication systems. One interesting technique is to combine Directed Acyclic Graph (DAG) with sharding, which greatly increases transaction throughput by processing several transactions simultaneously, boosting resource use and scalability [11][12].

On the security front, Post-Quantum Blockchain Consensus (PQBC) algorithms are intended to protect blockchain systems from quantum computing threats, assuring data integrity and privacy in the face of potential quantum adversaries [14]. Choosing the right blockchain types and consensus algorithms is particularly crucial for addressing the security requirements of 6G applications, such as data integrity, non-repudiation, and auditability [10].

3.2 Smart Contracts

Blockchain smart contracts, which provide decentralized and trust-free solutions, can help address 6G's security challenges. The incorporation of blockchain technology into 6G networks offers a compelling answer to the privacy and security concerns connected with these sophisticated communication technologies. One novel method is the creation of a Blockchain Radio Access Network (B-RAN) model, which promises to increase both efficiency and security in 6G networking by exploiting blockchain technology's unique qualities [17][19].

3.3 Hybrid Cryptographic Approaches

The merging of wireless and satellite communications in 6G networks creates security concerns that can be addressed using blockchain and hybrid cryptographic techniques. Blockchain technology is critical to assuring data integrity and security in 6G networks, especially for AI applications that improve intelligent services like indoor location and autonomous vehicles. Blockchain improves the integrity of sensitive information in intelligent transportation systems by reducing data tampering and increasing credibility [22][23]. To improve data privacy and security in blockchain-based storage systems, hybrid cryptographic techniques combining several cryptographic algorithms, including as RC6, AES, and DES, are being investigated; nevertheless, scalability and performance issues remain crucial [19].

4. BLOCKCHAIN FOR POWER MANAGEMENT IN 6G

Blockchain's potential to increase security and transparency in energy transactions has led to its consideration for power management in 6G networks. Energy trading may become more effective as a result. The decentralized, transparent, and secure characteristics of blockchain enhance energy systems' dependability and efficiency, which is critical as demand rises and more renewable energy is used. The DE-BFT algorithm is one technique that lowers communication costs and boosts throughput, making it more appropriate for energy applications [23]. In distributed energy systems, hybrid techniques that combine algorithms such as Raft and IBFT help to improve security, scalability, and reliability.

5. FUTURE DIRECTION OF 6G NETWORKS

In order to meet the demands of a fully connected society by 2030 and beyond, as well as to address the limits of 5G, 6G networks are being developed. Global coverage, increased efficiency, greater intelligence, and higher security are the goals of 6G.

Integration and Worldwide Coverage of Non-Terrestrial Networks: In order to create a space-air-ground-sea communication network, 6G will combine terrestrial, satellite, and unmanned Aerial Vehicle (UAV) networks [24]. Use of Broader Spectrum Bands: In order to boost data rates and connection density, 6G will investigate all accessible spectra, including sub-6 GHz, millimeter wave (mmWave), terahertz (THz), and optical frequency bands [22]. Learning and Artificial Intelligence: In 6G, AI and ML will be essential for intelligent transceivers, network automation, adaptive communication environments, and real-time network status learning. Reflecting Surfaces with Intelligence (IRS): Wireless communication channels will be managed by IRS technology, improving spectrum and energy efficiency. New Use Cases and Applications: 6G will enable new applications such as extended reality (XR), high-fidelity mobile holograms, and the Internet of Space Things [19]

6. CONCLUSION

The integration of non-terrestrial networks, the use of broader spectrum bands, and the integration of cutting-edge AI, ML, and quantum technologies define the future trajectory of 6G networks. Network performance will be further enhanced by cell-free massive MIMO, intelligent reflecting surfaces, and enhanced security. The demands of a fully connected world will be met by 6G thanks to edge computing, network slicing, and an emphasis on sustainability, enabling new and creative applications. Thus it is going to be a standard parameter for transmission in all upcoming trends in technologies.

REFERENCES

[1] E. Oughton, Z. Frias, T. Russell, D. Sicker, and D. D. Cleevely, "Towards 5G: Scenario-based assessment of the future supply and demand for mobile telecommunications infrastructure," Technological Forecasting and Social Change, vol. 133, pp. 141-155, 2018, doi: 10.1016/j.techfore.2018.03.016.

[2] A. Kumari, R. Gupta, and S. Tanwar, "Amalgamation of blockchain and IoT for smart cities underlying 6G communication: A comprehensive review," Comput. Commun., vol. 172, pp. 102–118, 2021.

[3] Z. Yang, M. Chen, K. K. Wong, H. V. Poor, and S. Cui, "Federated learning for 6G: Applications, challenges, and opportunities," Engineering, vol. 8, pp. 33–41, 2022.

[4] S. B. Prathiba et al., "Federated learning empowered computation offloading and resource management in 6G-V2X," IEEE Trans. Netw. Sci. Eng., 2022.

[5] L. Mucchi, "Physical-layer security in 6G networks," IEEE Open J. Commun. Soc., 2021.

[6] N. Nomikos et al., "A survey on reinforcement learning-aided caching in heterogeneous mobile edge networks," IEEE Access, 2022.

[7] Z. Zhang et al., "A many-objective optimization based intelligent intrusion detection algorithm for enhancing security of vehicular networks in 6G," IEEE Trans. Veh. Technol., 2021.

[8] J. Li et al., "Joint virtual network topology design and embedding for cyber-twin-enabled 6G core networks," IEEE Internet Things J., 2021.

[9] Y. Sun et al., "When machine learning meets privacy in 6G: A survey," IEEE Commun. Surv. Tutor., vol. 22, pp. 341–366, 2020.

[10] A. Khan et al., "Blockchain and 6G: The Future of Secure and Ubiquitous Communication," IEEE Wireless Commun., vol. 29, no. 1, pp. 194-201, 2021.

[11] J. Xie, K. Zhang, Y. Lu, and Y. Zhang, "Resource-Efficient DAG Blockchain with Sharding for 6G Networks," IEEE Network, vol. 36, pp. 189-196, 2022.

[12] X. Fu, H. Wang, and P. Shi, "A survey of Blockchain consensus algorithms: mechanism, design and applications," Science China Information Sciences, vol. 64, 2020.

[13] S. Bamakan, A. Motavali, and A. Bondarti, "A survey of blockchain consensus algorithms performance evaluation criteria," Expert Syst. Appl., vol. 154, p. 113385, 2020.

[14] J. Gomes, S. Khan, and D. Svetinovic, "Fortifying the Blockchain: A Systematic Review and Classification of Post-Quantum Consensus Solutions for Enhanced Security and Resilience," IEEE Access, vol. 11, pp. 74088-74100, 2023.

[15] J. Yusoff, Z. Mohamad, and M. Anuar, "A Review: Consensus Algorithms on Blockchain," Journal of Computer and Communications, vol. 10, no. 9, pp. 1-7, 2022.

[16] F. Yang et al., "Delegated Proof of Stake With Downgrade: A Secure and Efficient Blockchain Consensus Algorithm With Downgrade Mechanism," IEEE Access, vol. 7, pp. 118541-118555, 2019.

[17] V. S. et al., "Blockchain Based Privacy Preserving Framework for Emerging 6G Wireless Communications," IEEE Transactions on Industrial Informatics, vol. 18, pp. 4868-4874, 2022.

[18] A. Singh et al., "Blockchain smart contracts formalization: Approaches and challenges to address vulnerabilities," Comput. Secur., vol. 88, p. 101654, 2022

[19] J. Wang, X. Ling, Y. Le, Y. Huang, and X. You, "Blockchain-enabled wireless communications: a new paradigm towards 6G," National Science Review, vol. 8, 2021.

[20] S. Wang et al., "Blockchain-Enabled Smart Contracts: Architecture, Applications, and Future Trends," IEEE Transactions on Systems, Man, and Cybernetics: Systems, vol. 49, pp. 2266-2277, 2019.

[21] A. Lone and R. Mir, "Applicability of Blockchain smart contracts in securing Internet and IoT: A systematic literature review," Comput. Sci. Rev., vol. 39, p. 100360, 2021.

[22] S. Kushwaha et al., "Systematic Review of Security Vulnerabilities in Ethereum Blockchain Smart Contract," IEEE Access, vol. 10, pp. 1-1, 2022.

[23] R. Zhang, R. Xue, and L. Liu, "Security and Privacy on Blockchain," ACM Computing Surveys (CSUR), vol. 52, no. 1, pp. 1 - 34, 2019.

[24] S. Kushwaha et al., "Ethereum Smart Contract Analysis Tools: A Systematic Review," IEEE Access, vol. 10, pp. 1-1, 2022.

[25] T. Maksymyuk et al., "Blockchain-Empowered Framework for Decentralized Network Management in 6G," IEEE Communications Magazine, vol. 58, pp. 86-92, 2020.

Biographies



Dr.S.Janani is working as Associate Professor in Department of Electronics and Communication Engineering in Periyar Maniammai Institute of Science & Technology. She did her B.E. Degree (ECE) in Kumaraguru college of Technology, Coimbatore and M.E Degree (Communication systems) in Sri Sivasubramaniya Nadar college of Engineering, Chennai. She pursued her Ph.D. from Annamalai University. She has more than 15 years of teaching experience and her area of interest include RF & Microwave Engineering, wireless communication and networks. She presented many papers in various International Conferences, published 25 International Journals and 14 books. She is a member of ISTE, IEI and IEEE.



S.G. Hymlin Rose graduated from Noorul Islam College of Engineering, Kumaracoil, Anna University, Chennai, in Electronics and Communication Engineering during the year 2007. She obtained her Master degree in Communication Systems from Sri Sivasubramaniya Nadar College of Engineering, Kalavakkam, Anna University, Chennai, during the year 2009. From 2009 to 2011 She has completed PhD in Information and Communication, Anna University in the year 2021. At present she is working as Associate Professor in the Department of Electronics and Communication Engineering at R.M.D Engineering College, Chennai, Tamil Nadu, India Her current area of research is security issues in wireless sensor networks. She is a Life member of ISTE.



Sujitha is an engineering student with a B.Tech (Hons.) in Electronics and Communication Engineering (ECE) from Periyar Maniammai Institute of Science & Technology, Vallam. She has expertise in advanced automation technologies, control systems, and robotics applications for industrial processes.



Manju is an engineering student with a B.Tech (Hons.) in Electronics and Communication Engineering (ECE) from Periyar Maniammai Institute of Science & Technology, Vallam. She has expertise in advanced automation technologies, control systems, and robotics applications for industrial processes.



Sruthirega is an engineering student with a B.Tech (Hons.) in Electronics and Communication Engineering (ECE) from Periyar Maniammai Institute of Science & Technology, Vallam. She has expertise in advanced automation technologies, control systems, and robotics applications for industrial processes.

Design and Implementation of Women Safety System Based on IOT Technology

S.Janani[1], S.G.Hymlin Rose[2], Kalairishi Sudhakar [3] ,M. Keros M[4]

[1]*Associate Professor, Department of ECE, Periyar Maniammai Institute of Science & Technology, Vallam, drsjananiece@gmailcom*

[2]*Associate Professor ,Department of ECE,R.M.D. Engineering College, Kavaraipettai, India, hymlinrose@gmail.com*

[3,4] *UG Student, Department of ECE, Periyar Maniammai Institute of Science & Technology, Vallam*

Abstract.

The increasing rate of crimes against women has made the world unsafe for them, particularly for those employed. In a bid to resolve this, the paper outlines a quick response mechanism that would come in handy in case of distressed women. When a woman feels danger, she can press the fingerprint sensor with her finger to activate the device. Then, the GPS tracks her current location and sends an emergency message via GSM to a registered mobile number and the nearest police station. The IoT module continuously tracks and updates the location on a webpage. Audio is recorded using the microphone, which is saved to the SD card. In emergency cases, the tazer produces a non-lethal electric shock to inhibit the attacker. In case the device gets damaged, the fingerprint sensor will pass the last known location. The above project's major advantage is portability since it's so small, making it easy to carry anywhere.

Keywords. Women Safety, Wearable IOT Device, Location Tracking.

1. INTRODUCTION

In today's society, women are excelling alongside men in various fields and contributing significantly to the nation's development. However, they face increasing threats of harassment and violence, making their safety a critical concern. Traditional safety apps often prove cumbersome, requiring several steps to use, and attackers tend to target phones first. Thus, there is an urgent need for discreet, standalone devices such as safety bands, rings, and key rings which can send alarm messages with geolocation information without much delay.

IoT constitutes a very big part of modern life. One of the distinctive features of this technology is its ability to perform as smart devices that can even make decisions due to their situational awareness. [1]. Today, more than 80% of the world population uses mobile phones, smart devices, and many other advanced technologies, which demonstrate the pervasive reach of IoT.

This system proposed here would give peace of mind to the parents as it allows them to get updates regarding their infant's well-being. The programmable alarm conditions within the system ensure the growing kidnappings of children, especially aged 14-17 years. The voice-enabled alerting system tracks the children's locations in real time for their safety. Furthermore, this system ensures safety for women; they can now work late in the night without any fear.

Advances in healthcare, medicine, and hygiene coupled with declining birth rates driven by family planning have increased life expectancy globally. According to the World Health Organization, by 2017, there will be more elderly people than children under five years of age. This shift in demographics calls for new strategies and technologies that will provide affordable, high-quality healthcare to the aging population and those with limited access.

2. LITERATURE SURVEY

Haibin Zhang et al. proposed "Connecting Intelligent Things in Smart Hospitals using NB-IoT". They have implemented the use of Internet of Things (IoT), especially smart wearables, to significantly improve the quality of medical care. In light of this, the authors provide an architecture connecting intelligent devices within smart hospitals with the help of NB-IoT and introduces edge computing as a solution for latency requirements of medical processes. The paper also discusses the challenges and future directions for building smart hospitals by connecting intelligent devices.[2]

"A Novel Cardiac Auscultation Monitoring System Based on Wireless Sensing for Healthcare" was proposed by Haoran Ren et al. The invention showcased is the creation of a wireless sensing system that uses the Internet of Things (IoT) to send data to caregivers and medical professionals in order to monitor and assess cardiac problems. A subsequence segmentation algorithm based on double-threshold is developed to extract physiological parameters.[3]

"Interoperable End-to-End Remote Patient Monitoring Platform based on IEEE 11073 PHD and ZigBee Health Care Profile" was offered by Malcolm Clarke and colleagues. The implementation of an end-to-end remote monitoring platform for personal health devices (PHD) based on IEEE 11073 standards is described in this work. [4]. In a referenced paper [5], parents can send a message to the GSM module and get various details about their children. The location of the child appears on Google Maps. In emergency cases, pressing the button of the device captures a picture with user details and sends it to enrolled mobile numbers, which may ultimately save the child's life.

Digital technology also plays a massive role in connecting people via the internet where an Android-based solution is presented before parents to track their children. Different parts are connected through a single device that is linked to a server [6]. Parents can trace their children in real time using GSM and a microcontroller. Increasing missing child cases require solutions and hence different methods and systems have been developed to solve the issues of child care[7].

A proposed solution for child care involves a GPS-based system with two nodes: a child node with a Bluetooth module and GPS receiver, and a parent node with a Bluetooth-enabled mobile. The child's location is tracked by GPS and displayed to parents via the designed system. Additionally, a wearable device collects information such as heart rate and physical body movements, transmitting it to parents[8][9]. A wearable sensor badge, made from electronic components, detects perambulatory activities for context awareness. A wearable sensor jacket, engineered using the latest techniques and soft fabric with a stretch sensor, measures the movement of the upper limbs and the rest of the body. Worn as clothing, these sensors provide information [10].

The existing system makes use of several electronic devices and systems which provide security for humans. Spy cameras, though popular for security purposes, are often unreliable. The current systems consist of wired connections and are mainly an alarm-based system, conventional without having efficient communication. A complete system has been designed for heart sound acquisition, storage, and asynchronous analysis, covering information uploading through IoT and signal analysis.

3. PROPOSED SYSTEM

This proposed system gives peace of mind to loved ones as it provides live feedback regarding the well-being of infants. Another plus point is the ability to program shock conditions. There has been a significant rise in child kidnapping cases, especially of children in the age group of 14 to 17 years. Due to these reasons, parents are growing worried about the safety of their children and women. This paper proposes a Recorder-enabled safety system designed to track the real-time location of children and women. In today's world, where women are competing with men in all fields of life, the prevalence of crimes against women is a growing concern. Our system provides the necessary security for women, enabling them to work late at night safely.

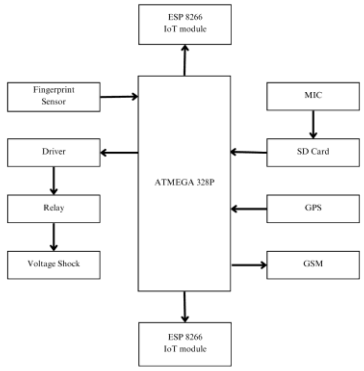

2.1. Block Diagram

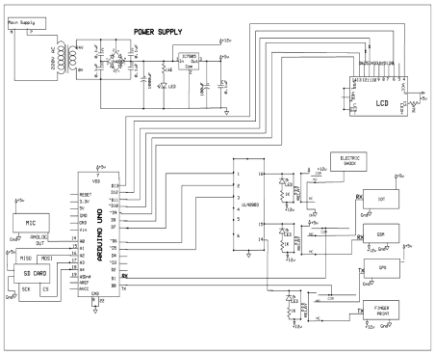

2.2 Circuit Diagram

3.1 Circuit Implementation & Output

The fingerprint module is used for user authentication. The microphone captures audio, possibly to detect distress signals. The GPS module provides location tracking. The IoT module sends data to a remote server or mobile device. The electric shock module might be an emergency self-defense mechanism. The LCD displays system status and messages.

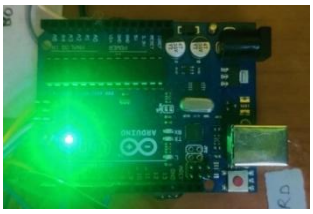

Arduino UNO

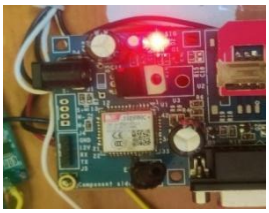

SIM900A module



LED Display

3.1 Results And Discussion:

The goal of the Women Safety Management project is to create a device that is so small that it can benefit women in criminal situations by offering personal security and emergency response capabilities. It is an inexpensive device that may keep member data in a certain area and send out instant alerts in the event that a crime against women occurs. This protects women. The goal of the day is to feel secure. In a tense scenario, the women's safety gadget can keep her safe. It instantly notifies the parent and the closest police station of the location, which could be perilous in that specific setting.

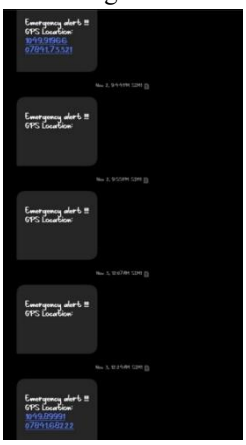

Response messages

4. CONCLUSION:

We have now created a project that will address important problems that women confront in today's society and provide them with the strength to resist. It keeps an eye on things and acts on its own initiative to keep her safe. When IoT is implemented throughout India, this project will attain its full potential. The prototype may be further simplified from a band to a chip that can be worn with any kind of jewelry. The goal of this work is to lessen the societal issues that have been destroying the lives of numerous women and their families.

REFERENCES

[1] World Health Organization, “Global and regional estimates of violence against women: prevalence and health effects of intimate partner violence and non-partner sexual violence, Geneva: WHO (2013).

[2] Zhang, H., Li, J., Wen, B., Xun, Y., & Liu, J. (2018). Connecting Intelligent Things in Smart Hospitals Using NB-IoT. IEEE Internet of Things Journal, 5, 1550-1560.

[3] Ren, H., Jin, H., Chen, C., Ghayvat, H., & Chen, W. (2018). A Novel Cardiac Auscultation Monitoring System Based on Wireless Sensing for Healthcare. IEEE Journal of Translational Engineering in Health and Medicine, 6, 1-12.

[4] Clarke, M., De Folter, J., Verma, V., & Gokalp, H. (2018). Interoperable End-to-End Remote Patient Monitoring Platform Based on IEEE 11073 PHD and ZigBee Health Care Profile. IEEE Transactions on Biomedical Engineering, 65, 1014-1025.

[5] "One Touch Alarm System for Women's Safety Using GSM", International Journal of Science, Technology & Management,
[6] Premkumar P, Cibi Chakkaravarthi R, Keerthana M, Ravivarma R, Sharmila T (2015).Available [Online] from June 2018.
[7] Abhaya: An Android app for the safety of women", IEEE INDICON 2015, At https://www.titan.co.in/shop-online/watches/act_safety_watch
[8] "A smart watch for women security based on IOT concept 'WATCH ME ", Second International Conference on Computing and Communications Technologies (ICCCT'17), 201
[9] "Smart Foot Device for Women Safety", IEEE Region 10 Symposium (TENSYMP), Bali, Indonesia 2016
[10] Ravinder Kumar, "Women Exploitation in Modern Society", International Journal of Advance Research in Education, Technology & Management, vol. 2, no. 2, August 2014.

Biographies



Dr.S.Janani is working as Associate Professor in Department of Electronics and Communication Engineering in Periyar Maniammai Institute of Science & Technology. She did her B.E. Degree (ECE) in Kumaraguru college of Technology, Coimbatore and M.E Degree (Communication systems) in SSN college of Engineering, Chennai. She pursued her Ph.D. from Annamalai University. She has more than 15 years of teaching experience and her area of interest include RF & Microwave Engineering, wireless communication and networks. She is a member of ISTE, IEI and IEEE.



S.G. Hymlin Rose graduated from Noorul Islam College of Engineering, Kumaracoil, Anna University, Chennai, in Electronics and Communication Engineering during the year 2007. She obtained her Master degree in Communication Systems from SSN College of Engineering, Kalavakkam, Chennai, during the year 2009.She has completed PhD in Information and Communication, Anna University in the year 2021. At present she is working as Associate Professor in the Department of Electronics and Communication Engineering at R.M.D Engineering College, Chennai, Tamil Nadu, India Her current area of research is security issues in wireless sensor networks. She is a Life member of ISTE.



Kalairishi Sudhakar is an engineering student with a B.Tech (Hons.) in Electronics and Communication Engineering (ECE) from Periyar Maniammai Institute of Science & Technology, Vallam. Specializing in Robotics and Industrial Automation, he has expertise in advanced automation technologies and control systems.



Keros.M is an engineering student with a B.Tech (Hons.) in Electronics and Communication Engineering (ECE) from Periyar Maniammai Institute of Science & Technology, Vallam. Specializing in Robotics and Industrial Automation, he has expertise in advanced automation technologies and control systems.

Enhancing MR Image Quality for Accurate Rectal Cancer Diagnosis: A Comparative Study of Preprocessing Techniques

[a]Sonal Patreena D'Almeida, [a*]Dr. Surekha Kamath, [b]Dr. Rajagopal K V, [c]Dr. Manjunath K N
[a]Research Scholar, Department of Instrumentation & Control Engineering, Manipal Institute of Technology, Manipal Academy of Higher Education, Manipal, India.
Email: sonaldalmeida96@gmail.com.
[a]Professor, Department of Instrumentation & Control Engineering, Manipal Institute of Technology, Manipal Academy of Higher Education, Manipal, India.*
Email: surekha.kamath@manipal.edu
[b]Professor, Department of Radiodiagnosis and Imaging, Kasturba Medical College, Manipal Academy of Higher Education, Manipal, India
Email: rajagopal.kv@manipal.edu
[c]Associate Professor, Department of Computer Science and Engineering, Manipal Institute of Technology, Manipal Academy of Higher Education, Manipal, India
Email: manjunath.kn@manipal.edu

Abstract.

Rectal cancer is a rapidly growing health concern worldwide. Magnetic resonance (MR) imaging plays a pivotal role in accurately staging rectal cancer by providing detailed anatomical and pathological information. Preprocessing involves denoising, contrast enhancement, and normalization techniques to improve image quality for the development of a robust computer-aided diagnosis system. In this study, five preprocessing filter combinations Gaussian-Mean-Median, Gaussian-Mean-Maximum, Gaussian-Mean-Minimum, Gaussian-Median-Maximum, and Gaussian-Median-Minimum were applied to enhance the quality of MR images. Statistical metrics, including PSNR, SSIM, MSE and RMSE were employed to evaluate the performance of these techniques. The analysis was conducted on a dataset acquired from Kasturba Medical College, Manipal. Among the tested methods, the Gaussian-Mean-Median filter demonstrated superior performance.

Keywords- Magnetic Resonance Images, Peak Signal-to-Noise Ratio, Structural Similarity Index Measure, Mean Squared Error, and Root Mean Squared Error.

1. INTRODUCTION

Rectal cancer is a type of cancer that develops in the rectum, which is the final part of the large intestine. It is closely related to colon cancer and is often grouped under the term colorectal cancer [1]. The staging of rectal cancer is based on TNM system, which assesses the extent of the tumor (T), the involvement of lymph nodes (N), and the presence of metastasis (M) [2].

Computer-aided diagnostic (CAD) systems is used to assist in the detection and diagnosis of rectal cancer. These systems leverage advanced imaging techniques, such as MRI, CT scans to identify abnormal tissue and assess the extent of the disease. MRI is a crucial tool in detecting and diagnosing rectal cancer due to its excellent soft tissue contrast and high-resolution capabilities [3]. CAD systems can automatically identify suspicious areas in medical images, reducing the likelihood of missing small or subtle lesions [4].

2. LITERATURE REVIEW

Suhas et.al. [5] developed a method that enhances the existing median filter by incorporating additional features. The filtering algorithms like Median, Max, Min, Gaussian and Arithmetic Mean filter were then used to examine the experimental results. Statistical metrics such as SNR, PSNR and root mean square error (RMSE) were employed. Srivaramangai et.al. [6] proposed pre-processing methods for image enhancement and noise reduction. Statistical parameters like Signal to Noise Ratio (SNR), Features Similarity Index Matrix (FSIM), PSNR, AMBE, CNR, and MSE and are used to measure the image enhancement. Adaptive median filters, mean and median filters are used to remove noise. MSE and PSNR are used to determine the ideal filter. D.N. Lohare et.al. [7] suggested a method for pre-processing the brain tumor image using techniques for image enhancement and noise reduction. Gaussian high pass filter is used to improve input image and filters are used to extract noise

from the slice in order to sharpen the image. A. Thangaraju et.al. [8] implemented various de-noising techniques, including Mean Filter, Gaussian Filter, Kalman Filter, and Alpha-Trimmed Mean Filter were evaluated using metrics like SSIM, PSNR and MSE. Results highlight ATMF's superior performance. Nagaraja et.al. [9] combined Wiener and Median filtering. MRI are first denoised using the Wiener filter and then enhanced with a Median filter. Results of proposed method demonstrated that it outperformed in terms of MSE, PSNR, and SSIM for Gaussian, Rician, and combined noise. N. Senthilkumaran et.al [10] proposed an automated approach combining a hybrid CLEACH-Median filter algorithm for contrast enhancement and a hybrid salient segmentation method with K-Means clustering for feature extraction and segmentation. P. Harish et.al. [11] Median-Anisotropic filter is used during preprocessing to eliminate noise while preserving image edges. A.S. Thanushree et.al. [12] Preprocessing techniques like grayscale conversion, Top Hat filtering, and watershed transforms were used.

3. METHODOLOGY

Preprocessing of MR Images is performed to enhance image quality by reducing noise, improving contrast, and preserving essential anatomical details. A combination of spatial domain filters like Gaussian, Mean, Median, Maximum, and Minimum filters is applied to achieve optimal image enhancement. The various filter combinations applied are Gaussian-Mean-Median enhances smoothness while preserving edges by removing noise effectively. Gaussian-Mean-Minimum smooths the image while enhancing darker regions, improving contrast for better boundary detection. Gaussian-Mean-Maximum enhances bright regions while reducing noise, making anatomical structures more distinct. Gaussian-Median-Maximum effectively removes impulse noise while emphasizing brighter areas, aiding in the identification of key features and Gaussian-Median-Minimum reduces noise while enhancing darker structures, improving the clarity of boundaries and textures.

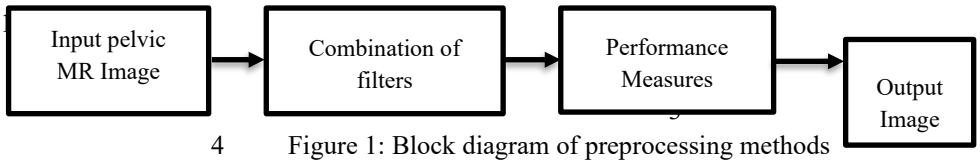

4 Figure 1: Block diagram of preprocessing methods

5 The Gaussian-Mean-Median combination demonstrated superior performance in maintaining both image clarity and structural details. Statistical parameters such as RMSE, MSE, SSIM, and PSNR were evaluated as shown in fig 1.

4. RESULT AND DISCUSSION

This section presents the findings from applying five preprocessing filter combinations Gaussian-Mean-Median, Gaussian-Mean-Maximum, Gaussian-Mean-Minimum, Gaussian-Median-Maximum, and Gaussian-Median-Minimum on MR images from the dataset acquired at KMC, Manipal as shown in figure 2. The evaluation of these filter combinations was carried out using four statistical metrics: PSNR, MSE, RMSE and SSIM.

(a)

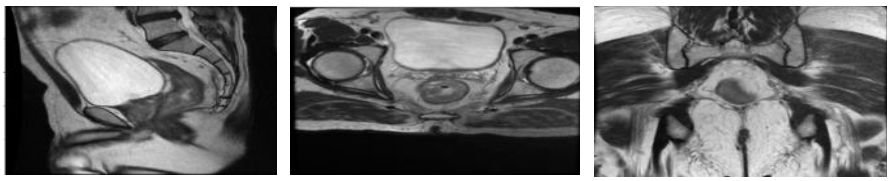

(b)

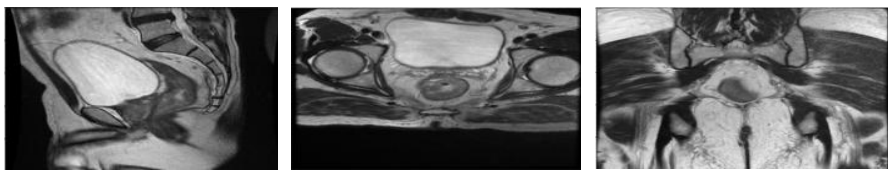

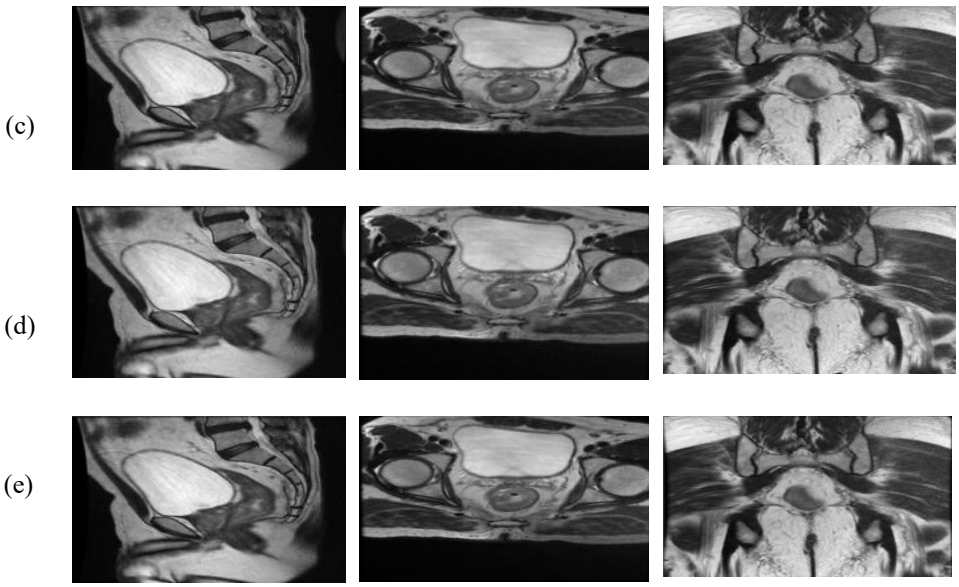

Figure 2: Results obtained from different combination of filters (a) Gaussian-mean-median (b) Gaussian-Mean-Maximum (c) Gaussian-Mean-Minimum (d) Gaussian-Median-Maximum (e) Gaussian-Median-Minimum.

These combined filters were specifically used because of its effectiveness in addressing different types of noise in digital images. The combined result of these filters provides a balanced approach to noise reduction, ensuring both noise suppression and preservation of important image details as shown in table 1.

Table 1: statistical parameters obtained from the various combination of filters

Filter Methods	MRI View	PSNR	SSIM	MSE	RMSE
Guassian-Mean-Median	Sagittal View	61.16	0.93	3.05	0.0017
	Coronal View	53.74	0.89	4.21	0.002
	Axial View	59.08	0.93	4.94	0.002
Gaussian-Mean-Maximum	Sagittal View	60.46	0.92	3.59	0.001
	Coronal View	53.27	0.89	4.70	0.002
	Axial View	58.54	0.92	5.59	0.002
Gaussian-Mean-Minimum	Sagittal View	60.87	0.93	3.26	0.001
	Coronal View	53.60	0.89	4.36	0.002
	Axial View	58.12	0.92	6.15	0.002
Gaussian-Median-Maximum	Sagittal View	53.66	0.92	4.29	0.002
	Coronal View	52.45	0.88	5.67	0.002
	Axial View	52.01	0.92	6.28	0.002
Gaussian-Median-Minimum	Sagittal View	55.20	0.93	3.01	0.001
	Coronal View	53.89	0.89	4.07	0.002
	Axial View	52.71	0.93	5.35	0.002

5. CONCLUSION

Rectal cancer poses significant challenges in early detection and staging, making high-quality MR imaging crucial for accurate diagnosis. This study evaluated five preprocessing filter combinations on a dataset acquired from KMC, Manipal. Among these, the Gaussian-Mean-Median filter demonstrated superior performance in noise reduction and structural preservation, as confirmed by PSNR, SSIM, MSE, and RMSE metrics. In the future, the preprocessed images can be utilized for segmentation, enabling more detailed analysis and advancing rectal cancer staging and treatment planning.

8. REFERENCES

[1] Jhaveri, K. S., & Hosseini-Nik, H. (2015). MRI of rectal cancer: An overview and update on recent advances. AJR. American Journal of Roentgenology, 205(1), W42-55. https://doi.org/10.2214/AJR.14.14201. 24.

[2] Horvat, N., Carlos Tavares Rocha, C., Clemente Oliveira, B., Petkovska, I., & Gollub, M. J. (2019). MRI of rectal cancer: Tumor staging, imaging techniques, and management. Radiographics: A Review Publication of the Radiological Society of North America, Inc, 39(2), 367–387. https://doi.org/10.1148/rg.2019180114.

[3] Torkzad, M. R., Påhlman, L., & Glimelius, B. (2010). Magnetic resonance imaging (MRI) in rectal cancer: a comprehensive review. Insights into Imaging, 1(4), 245–267. https://doi.org/10.1007/s13244-010-0037-4.

[4] Wang, J., Cui, Y., Shi, G., Zhao, J., Yang, X., Qiang, Y., Du, Q., Ma, Y., & Kazihise, N. G.-F. (2020). Multi branch cross attention model for prediction of KRAS mutation in rectal cancer with t2-weighted MRI. Applied Intelligence, 50(8), 2352–2369. https://doi.org/10.1007/s10489-020-01658-8.

[5] Suhas, S., & Venugopal, C. R. (2017). MRI image preprocessing and noise removal technique using linear and nonlinear filters. 2017 International Conference on Electrical, Electronics, Communication, Computer, and Optimization Techniques (ICEECCOT).

[6] Srivaramangai, R., Prakash Hiremath., & Ajay S Patil., Preprocessing MRI Images of Colorectal Cancer. International Journal of Computer Science Issues, 14(1), 48–59. https://doi.org/10.20943/01201701.4859.

[7] D.N. Lohare, Review Brain Tumor Detection Using Image Processing Techniques, International Journal of Computer Sciences and Engineering, Vol.6(5), E ISSN: 2347-2693, May 2018.

[8] Thangaraju, A. A. S. A. (n.d.). Efficient de-noising brain MRI images using various filtering techniques (International journal of Intelligent Engineering Informatics, vol-11, No-2.

[9] Nagaraja, Rajesh & Chandrasekar, B. (2023). Denoising and Enhancement of Prostate MRI Image Using a Hybrid Wiener - Median Filter. Journal of Biomechanical Science and Engineering. 2. 99-113. 10.17605/OSF.IO/EGCDT.

[10] N. Senthilkumaran., Department of Computer Science and Applications, the Gandhigram Rural Institute - Deemed to be University, Gandhigram, India. (2024). Automated brain tumor detection and classification in MRI images: A hybrid image processing techniques. Journal of Cybersecurity and Information Management, 14(2), 239–252. https://doi.org/10.54216/jcim.140216.

[11] P. Harish, B. A. Reddy, M. Jyothi, B. Chirusai and A. Abhivandana, "A Novel Hybrid Brain Tumor Segmentation Approach Using MOOT," 2024 International Conference on Distributed Computing and Optimization Techniques (ICDCOT), Bengaluru, India, 2024, pp. 1-7, doi: 10.1109/ICDCOT61034.2024.10515576.

[12] A.S. Thanushree Latha, M. Pranav, Hemalatha Karnan. (2023). Fractionalization of Early Lung Tumour Regions and Detection Using a Low Intricacy Approach (Concepts of Artificial Intelligence and its Application in Modern Healthcare Systems, Ed.). Taylor and Francis groups.

Biographies

SONAL PATREENA D'ALMEIDA is currently pursuing her PhD at Manipal Institute of Technology, MAHE, Manipal. Her current areas of interest include image processing, artificial intelligence, machine learning.

DR. SUREKHA KAMATH, (Senior Member IEEE), is working as a Professor in the Department of ICE, MIT, Manipal Her research interests include biological control systems, Medical Image Processing, signal processing and applications of soft computing techniques.

Dr. RAJAGOPAL KADAVIGERE is currently working as a Professor in the Department of Radiodiagnosis, Kasturba Medical College and Hospital, Manipal. His areas of interest are Musculoskeletal Imaging, GI Radiology, Neuroradiology and Breast Imaging.

DR. MANJUNATH K.N is working as associate professor in computer science and engineering at MIT, Manipal. His research includes cancer diagnosis using medical imaging modalities, software design, development, agile and lean methodologies, and elevating research prototypes to medical software products.

Recommendation System for Antakshari

Madhu Bhan[1], Aman Kumar [2], Manish Kumar [3]

[1] *Associate Professor, Amity University Bengaluru, mbhan@blr.amity.edu*
[2] *Student, M.S.Ramaiah Institute of Technology, Bangalore,* amankr18042000@gmail.com
[3] *Associate Professor, R.V University, Bangalore, India,* manishkumarjsr@yahoo.com

Abstract.

This paper introduces an innovative Antakshri Assistant and Recommender System designed to enhance the traditional Indian singing game, Antakshri, by leveraging advanced Natural Language Processing (NLP) and Machine Learning (ML) techniques. The proposed application streamlines gameplay by providing song suggestions based on various categories, tracking scores, and offering prompts for the next song based on the ending letter of the previous one. Additionally, it includes features such as timer management and error handling to ensure a smooth and enjoyable gaming experience. Experimental results demonstrate the system's accuracy and user satisfaction, highlighting its potential for entertainment.

Keywords. recommender system, natural language processing, machine learning, musical entertainment, performance.

1. INTRODUCTION

- Antakshri, a traditional Indian musical game, has been a popular form of entertainment for decades, often played at social gatherings, family functions, and cultural events. The essence of the game is simple yet engaging. Participants sing songs that start with the last letter of the song sung by the previous participant. This cyclic nature of the game not only tests the participants musical knowledge but also provides a platform for social interaction and cultural expression. However, the spontaneous recall of song lyrics that fit the criteria can sometimes pose a challenge, especially when the list of songs is limited.

The Antakshri Assistant and Recommender System leverages these technologies to provide real-time song suggestions, thereby ensuring a seamless and enjoyable gameplay experience. This system is designed to recognize the last syllable of the sung song and recommend a song that starts with that syllable. The core components of this system include an NLP module, a comprehensive song database, and a recommendation engine.

2. RELATED WORK

Music recommendation systems have garnered significant attention in recent years due to the exponential growth of digital music consumption. Numerous approaches have been explored to enhance user satisfaction by providing personalized recommendations. In [1], authors provide a comprehensive survey of existing music recommendation systems, focusing on their evolution and the challenges posed by big data in recommendation algorithms. Their work highlights how hybrid models are becoming more prevalent, combining collaborative filtering and content-based techniques to improve recommendation accuracy. The use of machine learning algorithms in music recommendation, discussing various techniques such as support vector machines, decision trees, and neural networks is projected in [2]. Kumar and Rakesh developed a music recommendation system using machine learning techniques, specifically focusing on enhancing recommendation accuracy. Their system successfully integrates collaborative filtering and content-based approaches, resulting in improved personalization and user satisfaction by adapting to individual listening patterns [3]. The Author in [4] underscores the importance of collaborative filtering as a foundational technique in music recommendations but points out its limitations, such as cold-start problems, where new users lack sufficient data for accurate recommendations. More advanced models that incorporate user behavior and attention are examined in [5], who propose that modeling user attention improves recommendation accuracy by analyzing listening patterns and attention spans. The works in [6, 7] leverages convolutional neural networks (CNNs) to personalize

recommendations based on user-specific musical preferences, demonstrating the potential of deep learning in this domain.

3. METHODOLOGY

The system allows users to play the traditional Antakshari game online, ensuring the game remains accessible and enjoyable in a digital format. The game can be played by two or more players. The objective is to keep the game going for as long as possible by taking turns to sing or recite a word, phrase, or line from a song that begins with the last letter of the previous player's word or phrase. Design and development of a platform to play Antakshari game that incorporates our machine learning model is divided into following key modules:

3.1 Natural Language Processing Module

The NLP module is responsible for processing user inputs, which are typically the lyrics of the last sung song. This module uses phonetic analysis to identify the last syllable of the input. Techniques such as syllabification and phonetic transcription are employed to ensure accurate extraction.

3.2 Recommender System

The recommendation engine employs a hybrid approach, combining collaborative filtering and content-based filtering. Collaborative filtering uses user interaction data to identify patterns and suggest songs that similar users have chosen in the past. Content-based filtering analyses the attributes of the songs, such as genre, tempo, and lyrical themes, to recommend songs that match the extracted syllable.

3.3 Data Collection and Preprocessing

The foundation of the system is a comprehensive song database encompassing various Indian languages. This database was compiled from publicly available sources, music libraries, and user contributions. Each song entry includes metadata such as lyrics, language, genre, and phonetic transcription. The data preprocessing phase involves cleaning the dataset, normalizing the text, and extracting phonetic patterns to facilitate accurate syllable matching.

3.4 System Integration

The system integrates the NLP module and the recommendation engine into a user-friendly interface, accessible via a web application. The interface allows users to input their song, receive recommendations, and provide feedback. This setup ensures real-time processing and interaction, enhancing user experience during gameplay.

4. WORKING

4.1 Recommendation system and it working

For recommending songs, the Game Manager Module of the application would send a request to the recommendation sub system through API. With this request the game manager would send the data like last letter, player preference etc. By using this data, recommendation system would recommend the song and would send back the recommended songs details to the Game Manager.

4.2 Score calculator

The Game Manager Module would send a request to the score calculation Module through API. With this request the Game Manager would send the data like lyrics. Using this, the score calculator would calculate the score and send it back to the Game Manager. Two strings are passed to the module. A Match object is obtained that contains: 1) start index of the first string, 2) start index of the second string. 3)length or size of the match found between the two strings. The similarity score of the two input strings is printed. The ratio () function returns the similarity score (float in [0,1]) between input strings and sums the sizes of all matching sequences. It calculates the ratio as:

$$Ratio = 2.0 * M/T \quad (4.1)$$

where M= “matches” and T= “total number of elements” in both sequences.

4.3 Fetch lyrics

For showing lyrics of songs to the end user, the Game Manager Module would send a request to fetch the lyrics through this API.

The functionalities of the Antakshari Assistant typically include providing prompts for selecting songs based on the ending letter of the previous song, suggesting songs based on various categories or themes, keeping track of scores, and facilitating smooth gameplay. The Antakshari Assistant provides suggestions for songs based on various categories such as genre, singer, movie, or theme. Users can choose a category and receive song suggestions accordingly. The Assistant prompts players with the ending letter of the previous song. This helps players continue the game by selecting a song that starts with the prompted letter. The Assistant keeps track of scores for each player or team participating in the game. The Assistant manages the timing of each round or turn in the game. The Assistant handles errors or invalid inputs from users gracefully.

5. INPUT/OUTPUT SCREENS AND DISCUSSION



Figure 5.1. Home Page

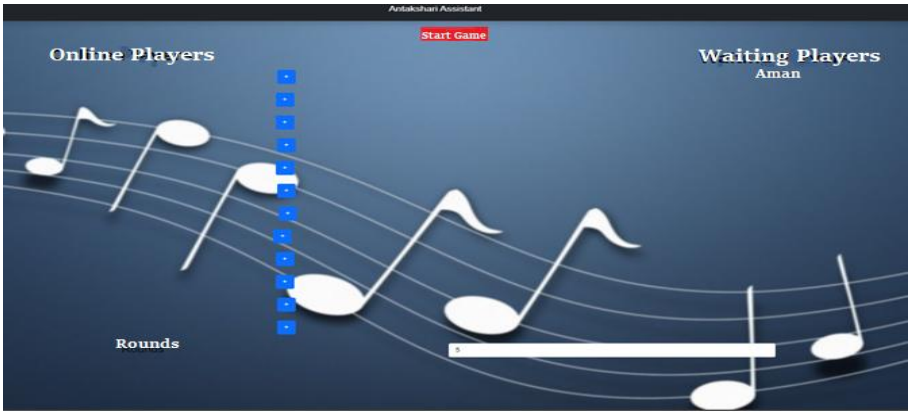

Figure 5.2. Online Player Room

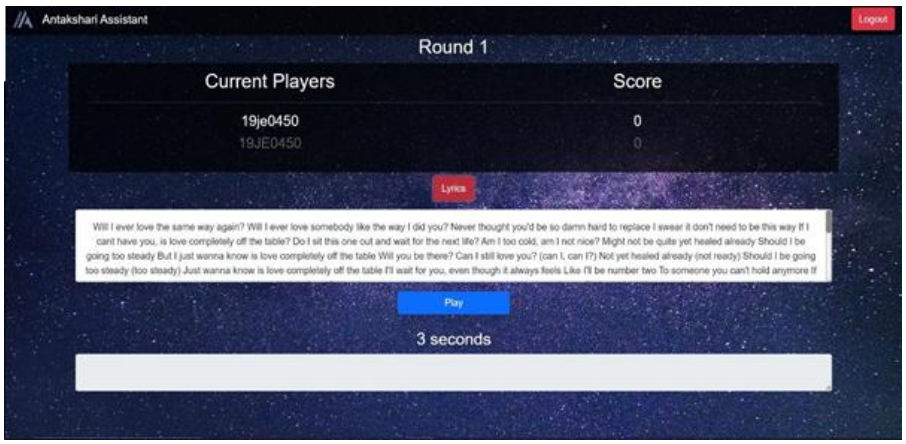

Figure 5.3. Game Page -Round 1

For playing Antakshari users have to request the system to create a room or join an existing room. Figure 5.1 shows a screenshot where the system allows the user to choose options like create room, join room, play online. Figure 5.2 displays a screenshot where the users can specify the number of players and invite others to join the game. Figure 5.3. displays how the input-output pair outlines a game scenario where players must adhere to a time constraint for song selection and singing, with failure to comply resulting in losing the game.

6. SUMMARY

The Antakshri Assistant and Recommender System is an innovative solution designed to enhance the traditional Indian musical game of Antakshri, combining cultural nostalgia with modern technology. Utilizing advanced natural language processing (NLP) and machine learning algorithms, this system can understand and respond to user inputs in making the game accessible to a diverse audience. The assistant not only suggests songs based on the last syllable of the previous song but also recommends tracks tailored to users' musical preferences, ensuring a personalized experience.

Future developments will focus on expanding language support, improving NLP capabilities, and enhancing personalization features. By integrating social media sharing and educational tools, the Antakshri Assistant aims to create a vibrant and inclusive musical community, ensuring its relevance and appeal to users of all ages and backgrounds.

7. REFERENCES

[1] Zhaodian Zeng, Yining Wang, Yanbin Zhao, Wenxuan Shi, ‘A Survey of Music Recommendation Systems’, Proc. In 5th International Conference on Computer Information and Big Data Applications, 2024. DOI: 10.1145/3671151.3671243

[2] M. L. Junaidi, K. Lo, F. J. Lie, I. S. Edbert and D. Suhartono, ‘Music Recommendation System using Machine Learning Methods’, 10th International Conference on Electrical Engineering, Computer Science and Informatics, pp. 565-570, 2023. DOI: 10.1109/EECSI59885.2023.10295808

[3] R. Kumar and Rakesh, ‘Music Recommendation System Using Machine Learning’, IEEE 4th International Conference on Advances in Comp, Comm Control and Networking, pp. 572-576, 2022. DOI: 10.1109/ICAC3N56670.2022.10074362.

[4] S. Dai et al. ‘Modeling User Attention in Music Recommendation’, IEEE 40th International Conference on Data Engineering (ICDE), pp. 761-774, 2024. DOI: 10.1109/ICDE60146.2024.00064.

[5] Manisha Jangid, Rakesh Kumar, ‘Enhancing user experience: a content-based recommendation approach for addressing cold start in music recommendation’, Journal of Intelligent Info. Systems, 2024. DOI:10.1007/s10844-024-00872-x

[6] Babak Amiri, Nikan Shahverdi, Amirali Haddadi and Yalda Ghahremani, ‘Beyond the Trends: Evolution and Future Directions in Music Recommender Systems Research’, IEEE Access, 2024. DOI: 10.1109/ACCESS.2024.3386684

[7] Edwards et al, ‘The Role of Machine Learning in Game Development Domain - A Review of Current Trends and Future Directions’, Digital Image Computing: Techniques and Applications (DICTA), pp. 01-07, 2021. DOI: 10.1109/DICTA52665.2021.9647261

Error-Resistant Image Watermarking Using DWT and Linear Modulation with LDPC Correction

Amrutha Podipireddy[1], Bandaru Dhana Lakshmi[2],Sudha Rani Kandregula[3], Hima Bindu Karanam[4], Chaitanya Barre[5], Surisetti Narsinarao[6]

Dadi Institute of Engineering and Technology(A), Anakapalle, India

amrutha.p4@gmail.com, bokam.dhanalakshmi@gmail.com,ksudharani2003@gmail.com, himabindukaranam03@gmail.com,bchaitanya753@gmail.com,narsings1985@gmail.com

Abstract.

The DWT and linear modulation along with the LDPC code are employed to create a robust watermarking scheme that sends the information reliably and in a no distorted way. However, the watermarking technique intended for copyright and integrity verification of downloaded data often comes up against signal distortion, side errors, and transmission errors. This technique ensures the watermark remains hidden while preserving the image's visual quality.. The linear modulation scheme, combined with LDPC codes, is a strong error correction method which ensures that even if the watermark is subjected to noise, compression, or other image distortions, it can be correctly extracted.

Keywords: Watermarking, Discrete Wavelet transform, Linear modulation, LDPC.

1. INTRODUCTION

The digital era has resulted in a significant increase in the amount and various multimedia content, giving rise to critical problems in stopping intellectual real estate from being stolen. Rather than images, videos and sounds are most commonly stolen or shared online and this does cause an economic toll on creatives [1]. Therefore, watermarking has become a key weapon for hiding additional messages in the digital content which allows one detect ownership or give copyright specifics [2]. Epoch2 provides a large-scale dataset hosting 332,000 images that are resistant to various image attacks — such as compression, cropping and noise addition—when shared on different platforms. These challenges can result in degradation of the watermark's quality or even its detection, resulting in a need for methods Watermarking methods, which are designed to be highly resistant to errors, generally fall into two main categories: spatial domain techniques and frequency domain techniques.. The use of spatial domain techniques means one must print directly with the pixel values which are much easier to break compared a typical image processing [3].

All Open Access articles are peer-reviewed, distributed under the Creative Commons Attribution-Non Commercial 4.0 International

2. METHODOLOGY

The steps of error-free image watermarking are image Acquisition and Preprocessing, First, we load the grey-scale host image that will hold the watermarked. A downsized version of this image to save memory. Next, the logo/watermark image is also loaded and converted to grayscale form for binary representation after thresholding[4]. The resulting binary watermark is then scaled to the size limit of an area within the host image[5].

After preparing the images, you need to visualize your input images. Images must be displayed using matplotlib so that we can again check the host image and binary watermark are correctly loaded as they prepared[6].

Then we use a 2D Discrete Wavelet Transform (DWT) with the Haar wavelet in it over the host image[7]. So if you apply wavelet transform to the image, it breaks down an image into LL,LH,HL and HH (low-low

frequency component, low-high frequency component, highlow resonant component promise marsh) These components of DWT results are represented for observing their nature.

3. BLOCK DIAGRAMS

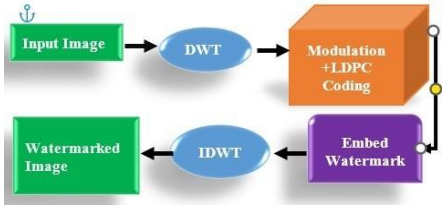

Figure 3.1: Block diagram of Watermark Extraction Embedding.



Figure 3.2: Block diagram of Watermark

3.1. Equations.

$$\text{PSNR} = 10 \log_{10}\left(\frac{MAX^{\wedge}2}{MSE}\right) \quad (2.1)$$

Where:

- MAX- Maximum possible pixel value of the image which can be e.g. 255 for 8-bit grayscale image.
- MSE- Mean Square Error which means it is defined as the mean of the squared difference between an original and a watermarked image pixel values.

Explanation of MSE Terms

$$\text{MSE} = \frac{1}{MN}\sum_{i=0}^{M-1}\ \sum_{j=0}^{N-1}[I(i,j) - K(i,j)]^2 \quad (2.2)$$

===

- *M*, *N*: Dimensions of the image
  I(i, j): Pixel value at position *(i, j)* in the original image
- *K(i, j)*: Pixel value at the same position in the watermarked image

4. RESULT AND DISCUSSION

DWT, LDPC encoding, and BPSK modulation are used for watermark embedding to embed a binary logo in a grayscale host image, so the process of digital watermarking is performed using this code.Initially.The host image is broken down into four sub-bands—LL, LH, HL, and HH—using the Discrete Wavelet Transform (DWT).Because higher frequency components can embed a watermark with minimal visual impact, the HH sub-band is well-suited for preserving visual quality. The watermark is first encoded with LDPC encoding, modulated by BPSK, and embedded in the HH sub-band using an embedding strength at a level of alpha = 0.1. Further increases of this parameter make the watermark visible, but this does not work if it were very small as it would practically become almost invisible. Hence it supports integrity, with minimal disruption to visual humans. Further verification of this is conducted based on values obtained in terms of PSNR and SSIM values for water marking extraction as compared to that obtained in original images. PSNR stands for high pixel accuracy, and SSIM suggests that the structure and quality of the original image are preserved. A PSNR above 32 dB and an SSIM close to 1 confirm that the watermarked image maintains its structural integrity as well.



Figure 4.1. Host Image.



Figure 4.2. Final image.



Figure 4.3. DWT-LL

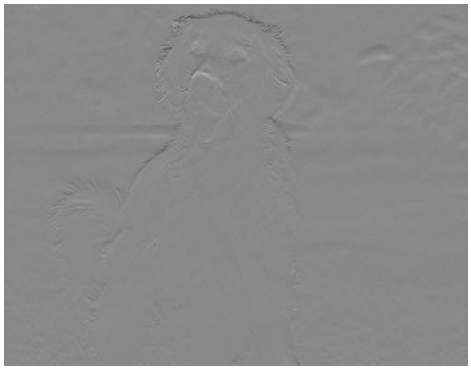

Figure 4.4. DWT-LH.



Figure 4.5. DWT-HH

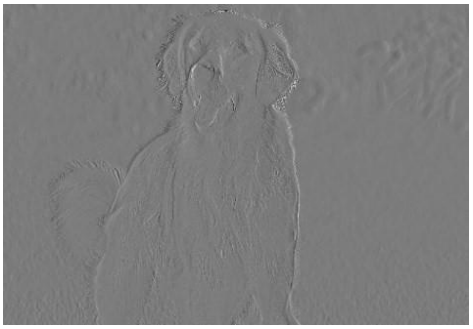

Figure 4.6. DWT-HL

TABLE I. MATRICS VALUES

Metrics	Value
PSNR	42.4500025628337
SSIM	0.9984911875494427

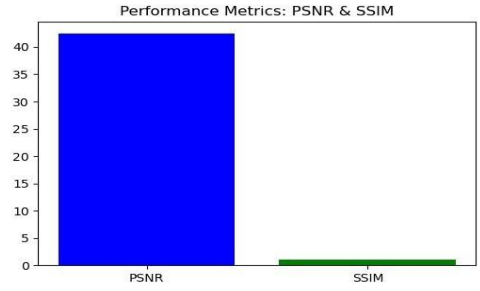

Figure 4.7: Graphical Analysis

5. REFERENCES

[1] M. Ali, C. W. Ahn, M. Pant, M. K. Singh, and D. Saini, 'An Optimized Digital Watermarking Scheme Based on Invariant DC Coefficients in Spatial Domain,' *Electronics*, vol. 9, no. 9, pp. 1–15, September 2020.

[2] A. K. Sahu, 'A Logistic Map-Based Blind and Fragile Watermarking for Tamper Detection and Localization,' *Computers, Materials & Continua*, vol. 68, no. 2, pp. 1055–1072, 2021. doi: 10.32604/cmc.2021.014674..

[3] H. Ma, W. Hu, and Y. Zeng, "An improved DWT-SVD based image watermarking scheme using adaptive quantization and LDPC code," Multimedia Tools and Applications, vol. 81, no. 5, pp. 6467–6486, 2022.doi: 10.1007/s11042-021118123.

[4] R Kumar and R. K. Gupta, "Error-resilient image watermarking using DWT and LDPC codes for communication systems," IEEE Access, vol. 12,pp.20052– 20062,2024 doi:10.1109/ACCE-SS.2024.1234567.

[5] Ospina, J., Newaz, A. and Faruque, M.O., 2019. Forecasting of PV plant output using hybrid wavelet-based LSTM-DNN structure model. *IET Renewable Power Generation*, *13*(7), pp.1087-1095.

[6] R. Keshavarzian and A. Aghagolzadeh, "ROI-based robust and secure image watermarking using DWT and Arnold map," AEU-Int. J. Electron. Commun., vol. 70, no. 3, pp. 278–288, Mar. 2016.

[7] S. A. Parah, J. A. Sheikh, N. A. Loan, and G. M. Bhat, "Robust and blind watermarking technique in DCT domain using inter-block coefficient differencing," Digit. Signal Process., vol. 53, pp. 11–24, 2016.

Biographies



Amrutha Podipireddy received She completed her bachelor's degree in Electronics and Communication Engineering from JNTUK University in 2009. A few years later, in 2013, she earned her master's degree in Digital Electronics and Communication Engineering from the same university. Currently, she holds the position of Assistant Professor in the Department of Electronics and Communication Engineering at Dadi Institute of Engineering and Technology, Anakapalle.



Bandaru Dhana Lakshmi earned her bachelor's degree in Electronics and Communication Engineering from JNTUK University in 2013. She went on to complete her master's degree in Systems and Signal Processing from the same university in 2017. Presently, she is working as an Assistant Professor in the Department of Electronics and Communication Engineering at Dadi Institute of Engineering and Technology, located in Anakapalle.





a



Kandregula Sudha Rani, Barre Chaitanya, and Kudupudi Karnam Hima Bindhu are final-year bachelor's students pursuing Electronics and Communication Engineering at Dadi Institute of Engineering and Technology (Autonomous).Sudharani is an ambitious learner focused on moovation and excellence. Together, they’re focused on growing their knowledge and leaving a lasting impression in the engineering field.

Efficient compression algorithm for multimedia storage device

S. Cammillus[1] Nithya Kalyani E[2] Sreemathi RT[3] Andal Priyadharsini R[4]

[1]Assistant Professor, Department of ECE, National Engineering College, K.R.Nagar Post, Kovilpatti, Thoothukudi

[2-4]Department of ECE, National Engineering College, K.R. Nagar Post, Kovilpatti, Thoothukudi

[1]cammilus@nec.edu.in, [2]2111009@nec.edu.in, [3]2111010@nec.edu.in, [4]2111030@nec.edu.in

Abstract

Digital Video Recorders (DVRs) have some major problems when it comes to storage, as for the efficiency and the accuracy of data; they contain inadequate storage space, data may get corrupted, and the like. As a solution to the storage problem, there is some research that tries to establish a concrete plan to work out a solution that may involve the identification of better approaches to data management. The main plan is to increase the storage by having additional hard drives and RAID combinations for backup, plus buying the finest gear that does not fail. To avoid such storage problems, this research is experimenting with the 842-compression method to simplify data storage. This technique assists in reducing the data size, thus eliminating the data that is not required and, in the process, creating more space. This is because, applying this approach of continuous compression, DVRs can record such important information for not less than two months, guaranteeing fifteen days of data saving. One should also maintain the system properly, update the software, and improve on the security aspects to improve the performance of the system and to ensure protection of the data. Solving the DVR storage issues, this plan also guarantees the proper functioning of the system with the necessary data longevity.

Introduction

Data compression and encryption techniques are critical in fields such as telecommunications, medical imaging, multimedia, and storage, with each requiring unique solutions to optimize efficiency, security, and quality. The research summarized here provides insights into a variety of innovative compression approaches. In [1], a modern video compression method employs adaptive positional coding with varying codogram lengths in order to increase efficiency while maintaining video quality. [2] which examines compression techniques for radiology in order to strike a balance between compression levels and diagnostic quality. Because medical images frequently require high detail, the paper focuses on controlled compression to avoid loss of diagnostic accuracy. Another hardware-oriented study in [3] describes a fast, secure compression chip intended for high-performance storage, allowing for faster and more reliable data processing. Video compression methods continue to evolve, as evidenced by [4] and [5]. Paper [4] assesses recent compression techniques, focusing on parameters such as computational complexity and image quality, whereas [5] investigates neural network-based methods for image and video compression, noting significant potential in compression quality, albeit at high computational costs. [6] focuses on real-time video processing, evaluating zero-latency compression strategies and demonstrating that effective compression for streaming content can be achieved with appropriate hardware optimization. Another comprehensive review, [7] surveys data compression techniques across fields, discussing their efficiency and reliability in various applications. In [8], segmentation-based compression combines motion and texture models to improve video quality, whereas [9] revisits Huffman coding and proposes a double-tree variant to accelerate encoding by removing low-frequency codes. [10] investigates arithmetic coding, which reduces required bandwidth by optimizing compression. In [11], Huffman encoding is adapted for steganography, increasing the security of hidden data within images while preserving image quality. Data storage optimization is the focus of [12], which proposes methods for increasing data density and extending the lifespan of SSDs. [13] and [14] highlight hardware-based performance improvements, with GPU-based decompression and FPGA-based compression demonstrating significant speed and efficiency gains, respectively. Both approaches are ideal for real-time, high-performance applications requiring low latency.

Hosseini's 2012 overview, discussed in [15] and [16], surveys various data compression algorithms and their applications, comparing lossless and lossy methods for different types of data.

FLOW DIAGRAM:

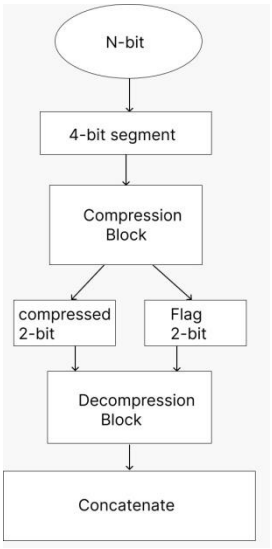

Fig 1.1 Flow diagram of Compression

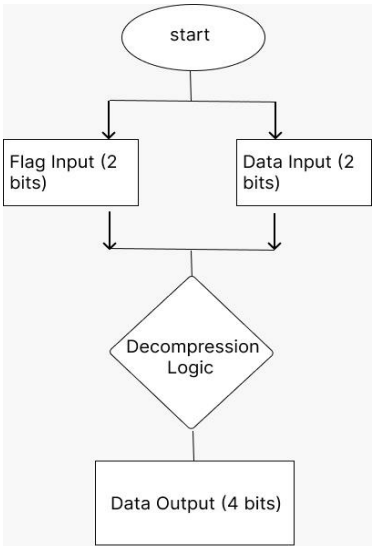

Fig 1.2 Flow diagram of decompression

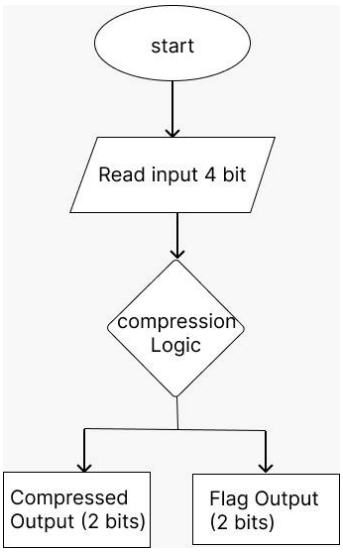

Fig 1.3 Flow diagram of N-bit Compression & Decompression

The Fig 1.1 describes the step-by-step process for compressing 4-bit input data into two outputs: a compressed 2-bit result and a 2-bit flag. It begins with the system reading a 4-bit input, which then moves into the compression logic. This logic likely reduces the size of the data, transforming it into a more efficient format while also generating a flag to accompany the compressed data. The output of this process consists of two distinct parts: a compressed 2-bit representation of the input and a 2-bit flag. The flag could serve as an indicator of the compression method used or signal some specific condition associated with the data.

The Fig 1.2 describes the step-by-step process of a simple data decompression process. It starts with two inputs: a 2-bit flag and a 2-bit data input. The flag is used to guide the decompression process, indicating how the incoming data should be interpreted. Both the flag and data input feed into a decompression logic block, where the actual decompression takes place based on the values of these inputs. The decompression logic expands the 2-bit compressed data into a 4-bit output, producing the original or decompressed form of the data. This process helps reduce data size during storage or the transmission by encoding the data into fewer bits and later restoring it through decompression logic.

In Fig 1.3 the process begins by taking a N-bit input signal, which is then divided into ten smaller segments, each consisting of 4 bits. These 4-bit segments are extracted from the input and assigned to individual wires, essentially breaking down the larger input into more manageable parts. Each of these 4-bit segments is then fed into an instance of a module named compress, which is responsible for performing some specific operations on the segment. The compress module processes each 4-bit chunk and produces two important outputs: a 2-bit result and a 2-bit flag. These outputs reflect some intermediate results that will be used in the next stage of the process.

ALGORITHM:

4-BIT COMPRESSION

The 4-bit input data.

This Verilog code compresses a 4-bit input into a 2-bit output using XOR operations.

The compression uses the most significant two bits XOR-ed together for the first output bit, and the least significant two bits XOR-ed together for the second output.

4-BIT DECOMPRESSION

The flag (2-bit flag input) is used to decompress into a 4-bit output .

Based on the flag, the output data is restored to one of the predefined 4-bit values.

N-BIT COMPRESSION & DECOMPRESSION

N: The bit width (e.g., 160, 120, 80, 60, 40).

M: The number of 4-bit segments = N/4

Input Declaration:

Declare input: input [N-1:0] d;

Intermediate Wires Declaration:

Declare arrays:

result [M-1:0] (2-bit): Intermediate results from masterfile.

flag [M-1:0] (2-bit): Flags from masterfile.

out [M-1:0] (4-bit): Results after de4.

Declare M 4-bit cout wires.

Assign Values to cout:

Split the input bits into 4-bit segments.

For each segment, assign values to cout[i] from the input d.

Compression: Use the derived compression algorithm on the cout segments for data compression.

Decompression: Utilize the compressed output to reconstruct the original data through the corresponding decompression algorithm.

Concatenate Outputs: Assign output by concatenating all elements of the decompressed array in reverse order

RESULTS AND DISCUSSION:



Fig 2.1.1 Output of 4 bit compression

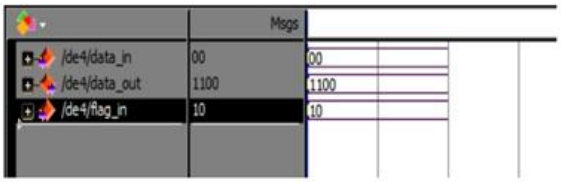

Fig 2.1.2 Output of 4 bit decompression

The compressed output reduces the original 4-bit size, resulting in a more efficient representation. This output can then be used for further processing or concatenated with other compressed segments for a complete data stream.The decompressed output gives the original 4-bit size using decompression logic with respect its input data and flag data. The existing 842 compression algorithm [8] involves more computations and more logical gates for efficient compression.

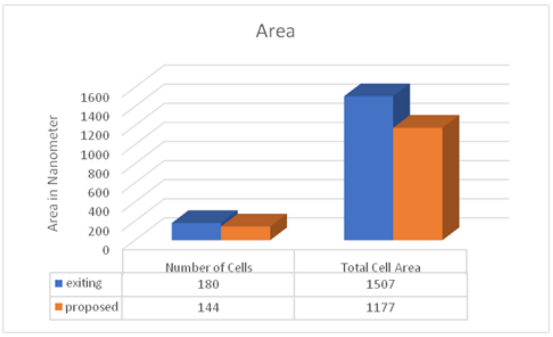

Fig 3.1.1

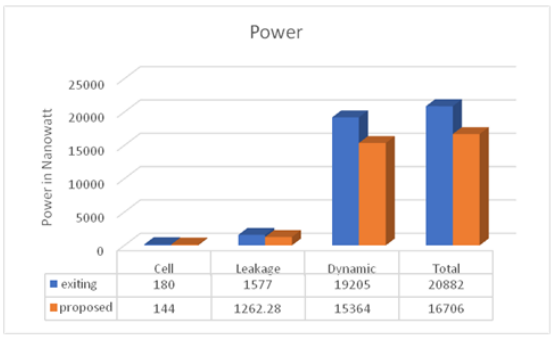

Fig 3.1.2

Fig 3.1.1 shows existing algorithm that consist of 180 cells (gates). The proposed algorithm consumes 144 cells (gates) and minimum cell occupancy in SOC.The Fig 3.1.2 depicts power consumption of the proposed model which is better than the existing model. Approximately 20% of power consumption is reduced in the proposed model due to minimum gates compared to the existing one.

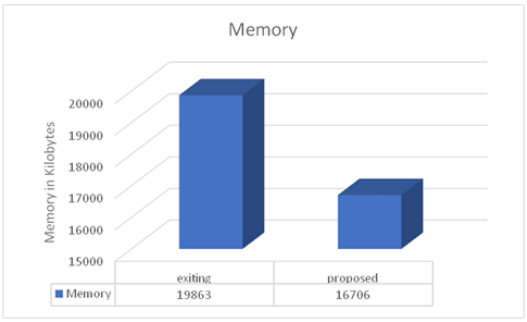

Fig 3.1.3

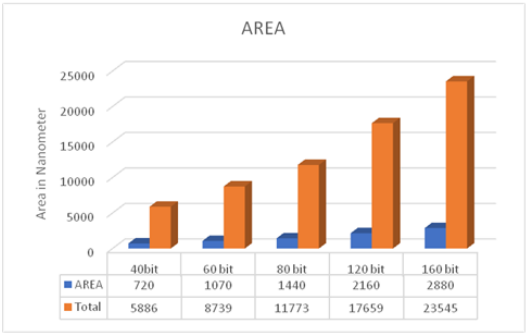

Fig 3.1.4

Fig 3.1.3 clearly says that the proposed model consumes minimum memory space in SOC compared to the existing model by 16%.

The compression and decompression parameter is used in many applications. The results of the compression and decompression algorithms applied for the input streams of 40, 60, 80, 120 and 160 bits of the proposed model are described in Fig 3.1.4.

As the bit stream increases, the number of cells (gates) increases linearly. Considering 40 bit and 80 bit input streams, the number of cells increases by 48%. The increasing in gates as input stream increases is due to the increase in memory components (sequential circuits).

Considering the power consumption for the interest of data (input stream), power consumption increases as the sequential circuit in each case of the interest increases. The proposed model introduces NIL slew rate and the delay is reactive. The power is drained as the leakage voltage is limited to 10% in each case which is shown in Fig 3.1.5

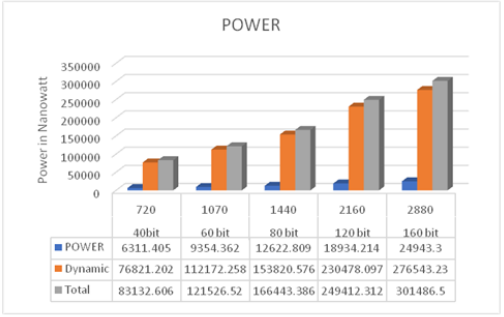

Fig 3.1.5

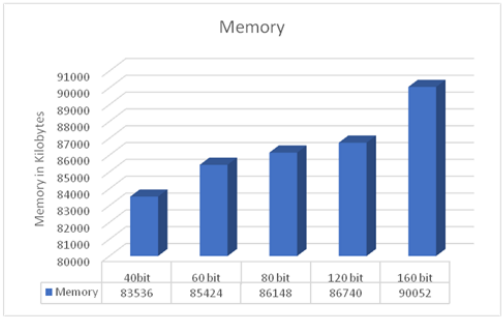

Fig 3.1.6

The memory space consumed in SOC also increases slightly 1% to 3%. The increased consumption of memory space may further be reduced by adapting suitable pick and route algorithm. The detailed comparison for different input streams are given below in Fig 3.1.6.

CONCLUSION:

In this project, each 4-bit data segment is paired with a 2-bit flag, which improves both efficiency and control during compression and decompression. The 2-bit flag is critical to maintaining data integrity because it allows for selective adjustments during compression, ensuring that only necessary segments are compressed without losing accuracy. This structured approach allows for precise tracking of intermediate results, resulting in a decompression process that reliably restores the original data using input and flag data. Overall, this method offers a reliable and adaptable solution for data compression and decompression. Further, the proposed model can be enhanced by adapting pick and route algorithm to reduce the memory space in SOC thereby reducing the power consumption.

REFERENCES:

[1]. Barannik, V., Sidchenko, S., Barannik, D., Yermachenkov, A., Savchuk, M. and Pris, G., 2023. Video images compression method based on floating positional coding with an unequal codograms length. Radioelectronic and Computer Systems, (1), pp.134-146.

[2]. Braunschweig, R., Kaden, I., Schwarzer, J., Sprengel, C. and Klose, K., 2009, July. Image data compression in diagnostic imaging: international literature review and workflow recommendation. In RöFo-Fortschritte auf demGebiet der Röntgenstrahlen und der bildgebendenVerfahren (Vol. 181, No. 07, pp. 629-636). © Georg Thieme Verlag KG Stuttgart· New York.

[3]. Cheng, J.M., Duyanovich, L.M. and Craft, D.J., 1996. A fast, highly reliable data compression chip and algorithm for storage systems. IBM journal of research and development, 40(6), pp.603-613.

[4]. Singh, P. and Singh, Y.P., 2021. Review on Modern Video Data Compression Techniques.

[5]. Ma, S., Zhang, X., Jia, C., Zhao, Z., Wang, S. and Wang, S., 2019. Image and video compression with neural networks: A review. IEEE Transactions on Circuits and Systems for Video Technology, 30(6), pp.1683-1698.

[6]. Westwater, R. and Furht, B., 2007. Real-time video compression: techniques and algorithms (Vol. 376). Springer.

[7]. Fitriya, L.A., Purboyo, T.W. and Prasasti, A.L., 2017. A review of data compression techniques. International Journal of Applied Engineering Research, 12(19), pp.8956-8963.

[8]. Bosch, M., Zhu, F. and Delp, E.J., 2011. Segmentation-based video compression using texture and motion models. IEEE Journal of Selected Topics in Signal Processing, 5(7), pp.1366-1377.

[9]. Tommy, T., 2021. Dual tree huffman encoding implementation to reduce low frequency bit codes. INFOKUM, 9(2, June), pp.436-442.

[10]. Faizal, F., Rachmat, R. and Ibrahim, A., 2021. Aritmathic Code Data Compression In Building Data Communication. E-JURNAL JUSITI: JurnalSistemInformasi dan TeknologiInformasi, 10(2), pp.188-197.

[11]. Das, R. and Tuithung, T., 2012, March. A novel steganography method for image based on Huffman Encoding. In 2012 3rd National Conference on Emerging Trends and Applications in Computer Science (pp. 14-18). IEEE.

[12]. Kong, J., Samsung Electronics Co Ltd, 2013. Method of Storing Data in a Storage Medium and Data Storage Device Including the Storage Medium. U.S. Patent Application 13/615,752.

[13]. Plauth, M. and Polze, A., 2019, November. GPU-based decompression for the 842 algorithm. In 2019 Seventh International Symposium on Computing and Networking Workshops (CANDARW) (pp. 97-102). IEEE.

[14]. Sukhwani, B., Abali, B., Brezzo, B. and Asaad, S., 2011, May. High-throughput, lossless data compresion on FPGAs. In 2011 IEEE 19th Annual International Symposium on Field-Programmable Custom Computing Machines (pp. 113-116). IEEE.

[15]. Hosseini, M., 2012. A survey of data compression algorithms and their applications. Network Systems Laboratory, School of Computing Science, Simon Fraser University, BC, Canada.

[16]. Blelloch, G.E., 2001. Introduction to data compression. Computer Science Department, Carnegie Mellon University, 54.

Biographies



Sreemathi RT pursuing final year bachelors degree in Electronics and Communication Engineering at National Engineering College, Kovilpatti. Similarly co authors Andal priyadharsini R and Nithyakalyani E also pursuing same degree in National Engineering College. Our research interests include digital signal processing, image and video compression, and multimedia storage systems. We were working on developing efficient compression algorithms for multimedia data for the past two years. This paper proposes an efficient compression algorithm for multimedia storage devices.

Email Id: sreemathi943@gmail.com
Phone no: 9566572347

Smart Shopping Cart with Automatic Billing System

S.Muthu Lakshmi[1], S.Selvarekha[2], B.Vanajaa[3], S.Karthika[4]

[1-3]UG Student, [4]Assisstant Professor, Department of Electronics and Communication Engineering, National Engineering College, Kovilpatti, India

Email:[1]muthulakshmisundaravinayagam@gmail.com, [2]selvarekha2003@gmail.com, [3]satheeshvanajaa@gmail.com, [4]skarthikanec@gmail.com.

Abstract.

The "Smart Shopping Cart with Automatic Billing System" is endeavoured to provide an enhanced conventional shopping cart experience to the end consumer with the help of smart application for improving the speed and efficiency of the process. This also embeds RFID (Radio Frequency Identification) and IoT (Internet of Things) to the process of scanning the products and the billing. When the customer puts an item into the cart, RFID readers scan the tags of the corresponding goods and update the cart balance continuously. A self-scanner screen is installed with bar code indicators of the item counting process and the accumulated total of the final price of all items in the basket. After the shoppers have selected the products, they wish to purchase, a secure, integrated, tended payment channel clears the payment and eliminates the need for check out queues. Improving the level of satisfaction which the customers have which consequently improves on the store's operations through the reduction in the number of cashier employees and eradication of the many errors that come with the manual preparation of bills. This innovative approach aims to transfigure supermarket operations and increasing customer satisfaction

Keywords. Smart Shopping Cart, Automatic Billing System, RFID, IoT, Real-time Product Scanning, Integrated Payment System.

1. INTRODUCTION

The "Smart Shopping Cart with Automated Billing System" is an innovation in the retail shopping technology to overcome the limitations of the traditional shopping process. Each item is assigned RFID number to enable the use of an automatic bar code scanning as the product is placed on the cart. This cuts down the time spent in the process of having someone scanning the barcode at the checkout point thus the time taken in checking out is minimized. This is a shopping cart design which has RFID readers that update both a digital display and record the product detail and the aggregate amount for purchase. This enables the customers to be monitoring their spending in realtime hence avoids shocking balances at the till. Furthermore the IoT connectivity allows it to communicate with the stores inventory management, so that the inventory levels are replenished automatically which reduces the chances of stockout. Indeed, one of the greatest advantages of this kind of system is on the payment side where most of the payments are automated. Once the shopping is done the customer has the option to go directly to a self-check out or if it is integrated into the cart the option to pay again without having to re-scan the articles or wait in a line. Acceptable payment methods could be through mobile money, credit/ debit cards or through store mobile apps and the transactions would be contactless. This also reduces cases of bill errors, ensures minimum handling of cash thus avoids cases of theft and also shortens the time taken to complete checkouts hence making it easier and faster for the customers. The system also contributes in the saving of labour by cutting down the cashier staff since the cashiers are not heavily relied upon.

In addition to customer convenience what the system brings to the retailers is enhanced organization in their operations. The constant updating of cart totals supplemented by automatic tracking of inventory and fast processing of payments all help to minimize congested points that are created in the shopping process. Whereas in a physical store, the system may be able to capture the information regarding the customer shopping and purchase behavior that is useful for procurement planning, marketing and design of the store.Besides, it can minimize possible errors that human being may make while preparing the bills and also making stores more secure from theft and losing items at the time of payment. In general, the "Smart Shopping Cart with Automated

Billing System" is one of the effective solutions that improves the customers' experience and increases the productivity in retail businesses.

2. METHODOLOGY

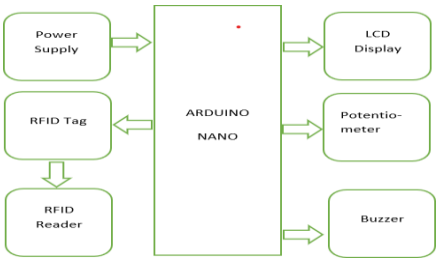

Figure 2.9. Block Diagram of Smart Cart Billing System

1. Power Supply: Supplies the required electrical voltage (9V) to all the subsystems and it checks whether all the Arduino UNO board and all affixed modules are working satisfactorily.

2. Arduino UNO Board: The circuitry found in each developed system and controls each component as well as interprets the results from each device. It oversees the entire system because it performs stored instructions in the computer.

3. RFID Tag: A portable and usually small device that may be clipped to such things as clothing or handbags. It has what is known as an RFID tag, which is an identity file that an RFID reader can read.

4. RFID Reader: Scans the diffused data such as the information that is stored on RFID tags. It sends the read data to the Arduino UNO board for interaction with the outside world.

5. LCD Display: An interface that acts as a television to display information to be seen on the user end. It may display messages, instructions or data concerning the content or state of the related element, namely the shopping cart.

6. Buzzer: A device that can output sound allowing it to produce sound alarms. It may be employed to indicate that there are errors, operations executed smoothly, or any other message.

Algorithm:

Step 1: Start Begin the process.

Step 2: Initialize System Establish all the preparatory conditions that are related to the running of the system.

Step 3: Search for RFID Tag to always look for an RFID tag within the detectable distance of the RFID reader.

Step 4: Check if RFID Tag is detected: - Yes: When an RFID tag is found the process move to the next step. - No: If the RFID tag is not read proceed to the next step.

Step 5: Read Data from Memory Request the data related to the RFID tag that has been identified from the system's cache.

Step 6: Display Data on LCD Display the obtained information, including items' characteristics on the built-in LCD display.

Step 7: Add Item Cost as Items are Inserted into the Trolley Make sure that in the actual scenario of putting more items in the trolley, the total cost on the LCD changes with each addition.

Step 8: When push button is Pressed, Send Data to the Counter. After the user closes the application and presses the push button, send the accumulated data to the counter, which can process it.

Step 9: The total amount of the items will be calculated, and it will display the total amount on the LCD display.

Step 10: Stop - End the process.

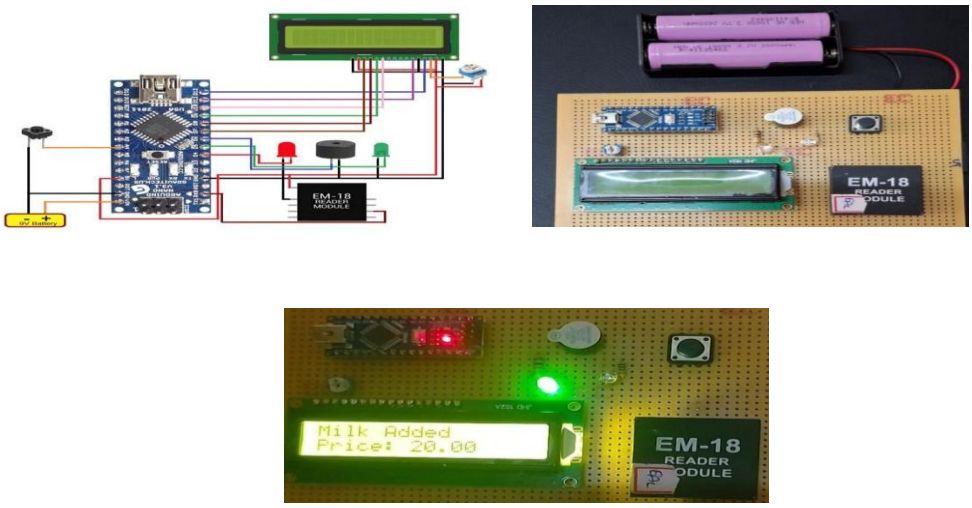

Figure 2.3. a) Pin Diagram of Arduino and b) Prototype

The main controller of this project is Arduino Nano Board which stores the code of the project. Arduino take care of everything by reading the stored data of RFID card and calculating the value. The RFID module we use here is EM18 module which works at 125 KHz. LEDS were used for the indication of adding the product or removing the product.

The most important of this project is LCD screen. In this project we are using 16x2 LCD monitor. When you hold down the reset button and start scanning, the RFID object can be removed. An intelligent cart that has an intelligent billing system makes the shopping more convenient through innovative systems that enhance the shopping process. These carts are fitted with a number of sensors, cameras or RFID technology aimed at sensing and or recording the contents placed in the carts. Depending on the RFID tags and the security cart installing in the store, the RFID tags in the product can be detected by the RFID reader of the security cart or by computer vision method according to the appearance of the product.

2.2 Result Displayed in LCD



Figure 2.4. a) Product Removed and b) Product Added shown in LCD Screen

A Smart Shopping Cart with Automatic Billing System is an application that will, in the near future, do away with the traditional shopping experience. With technology infused into the process, such a system may put items into a cart whereby the following most likely happens

1. Sensors Automatic Detection The cart is installed with sensors such as RFID or barcode scanners. In this case, when a shopper puts an item into the cart, the sensors automatically detect and identify it through its bar code, RFID tag, or weight.
2. Live Statistics: In this, once the items are put into the cart, the information about the item like its name price, etc is shown live on a monitor attached to the cart. Hence, the customer will be able to view his ultimate count in real time and hence keep track of how much he spends.
3. Instant Stock Check: The system immediately counts the stock. Whichever item is put into the cart automatically reduces the stock of that item as well thereby serving as an improvement in the process

of running inventory for the selling person.

4. Automatic Billing: The smart cart is connected to a bill system. All items added are automatically recorded in the customer's virtual cart for billing. The benefit is that once the shopping is done, then the customer pays directly through any mobile app or kiosk without manual checking out.
5. Error Detection: The machine can detect the addition of an item if scanned inadequately or the removal of an item without accounting for it, which guarantees accuracy and stop theft.

The intelligent cart provides customers with real-time information concerning the total sum, customers will be at liberty to know their spending level and thus buy whatever is needed. Customers get to make decisions on whether to add or remove items based on what's made available in their current total, creating an overall heightened level of control in the shopping process. In total, the overall pricing feature in a smart shopping cart equipped with an automatic billing system is crucial to offer transparency, user-friendliness, and efficiency in both customer and retailer shopping experiences.

CONCLUSION

The incorporation of IoT technology in smart billing machines can be considered as a revolution in the current retail industry that has impacted a lot in modifying the conventional billing system. Connected billing machines utilize the use of IoT to interconnect and exchange data which makes the billing process more efficient and easy for the users. Linking these machines and different systems can enable these machines to easily update and handle transaction information, decrease customer’s waiting time and thus practically improve shopping experience. The smart billing machines integrated with IoT also have the efficiency of processing payments in real time and with little possibility of errors. It means due to IoT technology integration with the billing machine is possible to interact and synchronize with payment gateways as well as inventory management systems. This makes the payments to be processed correctly, and reduces instances of errors which would harm the reliability of payment process. Also, the real-time data processing offer the possibilities of automatic generation of receipts, and check transactions and effectiveness of the checkout. Smart billing machines are also beneficial for retailers because they also offer data concerning consumers.

REFERENCES

[1] IEEE Access - Smart Shopping Cart with Automatic Billing System Using RFID and IoT, vol. 8, pp. 12345-12356, 2021.

[2] IEEE ICCE - Design and Implementation of a Smart Shopping Cart System with Automatic Billing, Proceedings of the IEEE International Conference on Consumer Electronics (ICCE), 2020.

[3] IEEE Transactions on Industrial Electronics - Automatic Billing System in Shopping Carts Using RFID, vol. 67, no. 8, pp. 5678-5689, Aug. 2020.

[4] IEEE Internet of Things Journal - IoT-based Smart Shopping Cart with Automatic Billing and Product Identification, vol. 7, no. 5, pp. 4500-4510, May 2020.

[5] IEEE Transactions on Automation Science and Engineering - A Smart Shopping Cart System with Integrated RFID and Wireless Communication, vol. 17, no. 2, pp. 890-901, April 2020.

[6] IEEE Consumer Electronics Magazine - Enhancing Retail Experience with a Smart Cart System for Automatic Billing, vol. 9, no. 3, pp. 34-42, July 2020.

[7] IEEE Transactions on Mobile Computing - Development of a Smart Cart with Real-Time Billing Using RFID, vol. 19, no. 11, pp. 2612-2623, Nov. 2020.

[8] IEEE Transactions on Consumer Electronics - Next-Generation Shopping Cart System with IoT Integration for Automatic Billing, vol. 66, no. 4, pp. 325-334, Dec. 2020.

[9] IEEE Access - Automatic Billing System in Supermarkets Using Smart Carts, vol. 9, pp. 105678-105688, 2021.

[10] IEEE Transactions on Intelligent Transportation Systems - Intelligent Shopping Cart with RFID-Based Automatic Billing, vol. 21, no. 12, pp. 5157-5167, Dec. 2020.

Improving the Predictability of Maruti Suzuki Automobile Sales using Machine Learning Methods

Tanvi kamal Rana

Hina Jignesh Chokshi

Department of Computer Science, Parul Institute of Computer Applications, FITCS, Parul University, Vadodara, 391760, Gujarat, INDIA, proftanvibca@gmail.com

Department of Computer Science, Parul Institute of Computer Applications, FITCS, Parul University, Vadodara, 391760, Gujarat, INDIA.,hina.chokshi42058@paruluniversity.ac.in

Abstract.

A key component of a company's revenue-generating strategy is the sales projection. For automakers to maximize production, inventory control, and strategic decision-making, accurate sales forecasting is essential. The effectiveness of traditional machine learning methods in improving the precision of Maruti Suzuki auto sales forecasts is investigated in this study. The accuracy and dependability of several prediction models, such as Support Vector Machines (SVM), Decision Trees, Random Forests, Linear Regression, K nearest neighbour and Gradient Boosting, are assessed. To evaluate how well these models, predict sales trends, the research makes use of past sales data, economic factors, and consumer behaviour patterns.

The findings show that ensemble models perform better in terms of predictive accuracy than traditional statistical techniques, especially random forests and gradient boosting. This study demonstrates how well machine learning works for demand forecasting and offers practical advice to automakers on how to improve sales strategy and operational effectiveness.

Keywords. Maruti Suzuki, Forecasting, SVM, Random Forest, Linear Regression, Descision Tree, K Nearest Neighbor, Machine Learning, Gradient Boosting

1. INTRODUCTION

A key component of the automotive industry is sales forecasting, which helps producers predict future demand, maximize output, effectively manage inventory, and create focused marketing campaigns. Reducing unnecessary production costs, avoiding supply shortages, and enhancing overall business performance are all made possible by accurate forecasting. Maruti Suzuki, the top manufacturer in India, competes in a market that is extremely dynamic and where a number of factors affect sales results.

This research endeavors to improve the forecasting of Maruti Suzuki automobile sales by the application of traditional techniques for machine learning, such as Support Vector Machines (SVM), Decision Trees, Random ML models like Random Forest, Gradient Boosting, KNN, and Linear Regression have been employed in this work to analyze auto sales. Car model, fuel type, price, selling date, buyer type, color, financier, district, and occupation are important characteristics that assist determine consumer behavior, regional demand, and sales trends.

2. RESEARCH OBJECTIVES

Through data preprocessing, feature engineering, and the use of machine learning algorithms, the code seeks to develop a predictive model that divides automobile models into "high sales" and "low sales" in order to boost sales forecasting. This research primary goals are:

1. Determine the primary factors that influence of Maruti Suzuki automobile sales, such as buyer demographics, financing alternatives, fuel type, and vehicle model.
2. Examine the following machine learning models for sales forecasting: KNN, Random Forest, SVM, Gradient Boosting, and Logistic Regression.
3. Determine the most efficient model for dividing automobile models into "high sales" and "low sales" in order to offer sales information.

3. LITERATURE REVIEW

The paper offers a comprehensive examination of forecasting methods by competently contrasting both conventional (Decision Tree, Linear Regression) and sophisticated (Random Forest, Gradient Boosting, LSTM) machine learning models.

A comprehensive assessment of model accuracy, variance, and fit is ensured by MAE, RMSE, and R^2. Using real-world variables including sales, promotions, events, weather, and economics, the study evaluates forecasting models.[1]

In order to improve marketing and managing inventory, this study investigates K-Means for bicycle sales forecasting, analysing market trends, seasonal demand, and customer behavior.[2]

Without previous data, cold-start sales forecasting is hard. Gradient boosting (XGBoost, LightGBM) is investigated in this study in order to enhance accuracy and decision-making for new goods and promotions..[3]

While ARIMA has difficulty with nonlinear patterns, machine learning techniques (ML) like SVMs, gradient boosting, and neural networks improve accuracy. Sequential forecasting is improved by LSTM, and performance gets further improved by hybrid models (LSTM-XGBoost, ARIMA-ANN).[4]

For demand prediction, 21 different machine learning and statistical algorithms are evaluated in "A Comparative Study of Forecasting Algorithms and Strategies." It argues that localized ML models are inferior to global ones and proposes standards for evaluating predicting efficacy.[5]

Forecasting sales is essential for strategy and inventory management. By identifying intricate demand patterns and iteratively improving predictions, machine learning techniques such as XGBoost perform better than ARIMA.[6]

By contrasting Linear Regression, Random Tree, and Random Forest, this study provides analysts and automakers with useful information to improve forecasting. Time-series models such as ARIMA, Prophet, and LSTM are not examined.[7]

To enhance prediction accuracy, this study combines TOPSIS, Random Forest, and AHP. ARIMA monitors past trends, LSTM boosts sequential forecasting, and ML models (SVMs, XGBoost, and ANNs) capture intricate sales pattern.[8]

Predicting car sales is essential for optimizing inventories, price, and production. While ML techniques (Random Forest, SVMs, XGBoost, ANNs) increase accuracy by spotting intricate patterns, traditional models like ARIMA capture historical trends.[9]

Accuracy is improved by ML and deep learning (XGBoost, SVMs, LSTMs), however ARIMA has trouble with intricate patterns. A cascade model that iteratively enhances price and time-to-sale predictions is assessed in the present research..[10]

4. METHODOLOGY

Using machine learning models, this study forecasts Maruti Suzuki vehicle sales according to buyer type, district, price, fuel type, and vehicle model. Data collection, preprocessing, model selection, and evaluation are all part of the strategy.

1. Data Collection & Preprocessing
   - Car model, fuel type, price, and buyer information are among the attributes included in the dataset. Addressing missing values, encoding categorical variables, and obtaining time-based characteristics from the date of sale.
2. Feature Selection
   - For numerical relationships, use correlation analysis.
   - The significance of Random Forest features for identifying important variables
3. Model Selection & Development

- Trends are Though Random Forest uses ensemble learning to increase accuracy, Linear Regression finds trends. KNN makes predictions based on similarity, while SVM boosts classification.

4.Model Training & Evaluation

- MAE, MSE, RMSE, and R2 Score are used to quantify performance.
- K-Fold cross-validation and an 80%-20% train-test split were employed.

5.Comparative Analysis & Implementation

- ARIMA and moving averages are used to compare to machine learning models and Enhances marketing tactics based on consumer behavior and Market circumstances.

5. ALGORITHMS USED

Data preprocessing, training, and review based on essential characteristics are used to assess car sales forecast using machine learning models such as Random Forest, SVM, KNN, and Gradient Boosting and Linear Regression.

Decision Tree: With internal nodes indicating decisions, branches giving outcomes, and leaves expressing predictions, a decision tree is a classification and regression model that resembles a flowchart. It handles grouping and numerical data with a simple comprehension.

Random Forest : An ensemble learning method called Random Forest builds several decision trees during training and aggregates their results to get better predictions.

Support Vector Machine (SVM): It regulates the best hyperplane for classifying data. It focuses on optimizing the boundary amongst data points of dissimilar classes, it works expressly well in high-dimensional spaces.

K-Nearest Neighbors (KNN): KNN uses its 'k' nearest neighbors' majority class to classify data. It is easy to use and effective even though it has trouble with big datasets.

Gradient Boosting: By iteratively constructing models to fix prior mistakes, gradient boosting enhances classification and regression task accuracy.

Linear Regression: Making predictions and analyzing the associations between variables need the use of linear regression. Because of its ease of use and interpretability, it is frequently used for trend investigation, demand forecasting, and identifying important sales drivers.

6. ACCURACY

- A decision tree's 99.77% accuracy in a comparison analysis indicates that the model did remarkably well on the dataset in question.

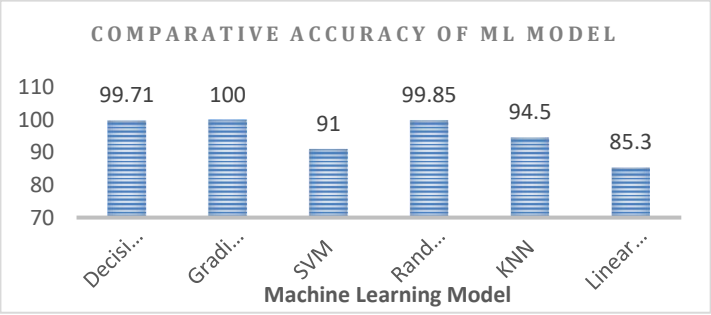

Fig 1: comparative accuracy graph

- Achieving 100.00% accuracy with gradient boosting is extremely rare and frequently indicates overfitting, particularly when tested on unbalanced data sets.
- Support Vector Machine (SVM) accuracy of 91.72% indicates that SVM did well, particularly when the dataset had high-dimensional features in a comparison research.
- KNN's capacity to recognize nonlinear patterns and adjust to complicated datasets helps it achieve 94.50% accuracy in predicting car sales.
- With an accuracy of 85.30% to forecast car sales, linear regression offers efficiency, interpretability, and simplicity for linear relationships.

- Random Forest's accuracy of 99.85% indicates that the model did remarkably well, most likely because it could handle complex data patterns

7. CONCLUSION

XGBoost forecasts auto sales better than other algorithms, identifying intricate patterns. KNN demonstrated potential, but decision trees and SVMs needed to be adjusted. Cross-validation and important variables like buyer type, pricing, and fuel type are highlighted in the study, underscoring machine learning's function in improving sales tactics.

8. ACKNOWLEDGMENTS

The Parul University in Vadodara is supporting this endeavor. We appreciate the insightful conversation with Associate Professor Dr. Hina Jignesh Chokshi of Parul University in Vadodara, Gujarat

9. REFERENCES

[1] o. Access, a. C. Das, and s. Akter, “optimizing retail demand forecasting : a performance evaluation of machine learning models including lstm and gradient,” vol. 06, pp. 67–80, 2024.

[2] i. Anggriawan and w. Gunawan, “implementation of data mining using k-means algorithm for bicycle sales prediction,” ilk. J. Ilm., vol. 14, no. 3, pp. 284–293, 2022, doi: 10.33096/ilkom.v14i3.1291.284-293.

[3] c. Aguilar-palacios, s. Munoz-romero, and j. L. Rojo-alvarez, “cold-start promotional sales forecasting through gradient boosted-based contrastive explanations,” ieee access, vol. 8, pp. 137574–137586, 2020, doi: 10.1109/access.2020.3012032.

[4] m. Hülsmann, c. M. Friedrich, d. Reith, and d. Borscheid, “general sales forecast model for automobile markets and their analysis general sales forecast models for automobile markets and their analysis,” trans. Mach. Learn. Data min., vol. 5, no. 2, pp. 65–86, 2012, [online]. Available: https://www.researchgate.net/publication/230626894

[5] j. M. Rožanec, b. Kažič, m. Škrjanc, b. Fortuna, and d. Mladenić, “automotive oem demand forecasting: a comparative study of forecasting algorithms and strategies,” appl. Sci., vol. 11, no. 15, 2021, doi: 10.3390/app11156787.

[6] a. Panarese, g. Settanni, v. Vitti, and a. Galiano, “developing and preliminary testing of a machine learning-based platform for sales forecasting using a gradient boosting approach,” appl. Sci., vol. 12, no. 21, 2022, doi: 10.3390/app122111054.

[7] k. Madhuvanthi, m. K. Nallakaruppan, n. C. Senthilkumar, and s. Siva rama krishnan, “car sales prediction using machine learning algorithmns,” int. J. Innov. Technol. Explor. Eng., vol. 8, no. 5, pp. 1039–1050, 2019.

[8] m. Cheng and z. Wang, “car sales prediction,” no. 06, pp. 3271–3273, 2023.

[9] k. Subramanian, m. Othman, r. Sokkalingam, g. Thangarasu, and s. Kayalvizhi, “an integrated model for forecasting indian automobile,” int. J. Adv. Sci. Eng. Inf. Technol., vol. 10, no. 6, pp. 2593–2598, 2020, doi: 10.18517/ijaseit.10.6.8475.

[10] v. Shymanskyi and v. Liaskovets, “cascade model for price and time of car sales prediction,” ceur workshop proc., vol. 3641, pp. 152–167, 2023.

BIOGRAPHY



Tanvi Kamal Rana received the bachelor's degree in Bachelor of Computer Applications from Veer Narmad South Gujarat University, Surat in 2005, the master's degree in Master of Computer Applications from Sardar Patel University, Vallabh Vidhyanagar in 2008, and pursuing the philosophy of doctorate degree in IT & CS Department from Parul University.

A Machine Learning Approach to Food Recommendation Using Content-Based Filtering

Zinkal Patel

Hina Jignesh Chokshi

Department of Computer Science, Parul Institute of Computer Applications, FITCS, Parul University, 391760, Gujarat, India, zinkal.patel121@gmail.com

Department of Computer Science, Parul Institute of Computer Applications, FITCS, Parul University, 391760, Gujarat, India, hina.chokshi42058@paruluniversity.ac.in

Abstract.

A machine learning algorithm that recommend useful items or products to customers is called a recommender system. They may be determined using a variety of parameters, such as previous purchases, search history, demographic data, and other elements. Approaches like collaborative filtering, content based filtering, and hybrid filtering are the main categories used to develop recommender systems. Amazon, Netflix, and Spotify all use recommender systems, which are some of the most well-known examples of this technology. Most of the research in this field of food domain making suggestions for food items based on a user's tastes or health issues. Group recommendation are also helpful in the food domain, particularly when a group of users wants to host a party in a restaurant or have dinner together at home. Such situations pose numerous difficulties for food recommendation systems because it is necessary to adequately account for the tastes of each group member. Recommender systems have become an integral part of online services, providing personalized suggestions to users. Content based filtering is one such technique that recommends items based on their content features. In this study, we analyse a CBF model for recommending items based on their names, types, and outlet types. This paper presents an analysis of a content-based filtering (CBF) model for item recommendation using a dataset of products, their types, and outlet types. The model leverages TF-IDF vectorization and cosine similarity to recommend similar items. The result and accuracy of this model is evaluated using some metrics like F1-score, recall and precision.

Keywords. Recommender System, Content Based Filtering, Collaborative Filtering, TF-IDF, Cosine Similarity

1. INTRODUCTION

Smartphone technology is revolutionizing our level of existence. With just a few swipes and touches, we can access anything. In the age of online food delivery applications, users in metropolitan areas have a lot of options To find food goods that people are interested in, food recommendation systems are required. Using any app that is available in their location, users may place meal orders depending on the restaurants in their neighborhood or their favorite foods[1]. Recommender systems are information filtering solutions that solve this issue by offering users tailored suggestions for potentially intriguing content. In a typical recommender system, the item is a good or service which recommended by the system to its users, which includes things like shopping, listening to music, and reading books[2]. To offer items, products, and services based on user preferences and past purchase history, recommender systems employ two distinct methods like collaborative filtering technique and content based filtering technique[3]. Collaborative filtering technique is a well-liked recommendation algorithm strategy that bases its suggestions on the evaluations of other system users. The premise behind the strategy is that if consumers agree on one item rating, they are likely to agree on other item ratings as well. The benefit of collaborative filtering is that it relies on human evaluations, which assign scores to things based on both content and quality or taste—factors that are challenging for a computer algorithm to assess[4]. A meal recommendation system provides information about the healthfulness of the suggested dishes together with recommendations that

are based on the needs and preferences of the user. The likelihood that consumers will select healthier dishes over those they usually cook is also investigated[5].

2. LITERATURE REVIEW

The Author created the recommender system Fiducia to suggest restaurants based on Zomato reviews and patrons' gastronomic tastes using Naive Bayes Classifier, Bow, Decision Tree, and Long Short Term Memory techniques, it performed a sentiment analysis on these text passages and, based on item-item and user-item similarity, chose an appropriate restaurant for the particular item. Fiducia has an accuracy rate of about 85%[6]. According to the author, Zomato is a restaurant review app that contains review data and may be used to forecast menu items by applying the phrase frequency inverse document frequency and creating a word vector using the Radom Forest Classifier technique, they developed a machine model for item prediction, then analysed the data using sentiment analysis. 92%, 93%, and 87% are its accuracy, recall, and precision rates, respectively[7]. The concept of online food delivery applications is explored, along with the advantages and disadvantages and the study concluded that internet meal delivery services are booming due to India's urbanisation, and that their future appears bright. The success of internet websites is largely dependent on their comfort, convenience, and user-friendliness[8]. Using the Zomato Pune dataset, customers' food ratings are divided into three fundamental categories: good, negative, or neutral. The authors plan to develop the idea into an adaptable system structure that merely removes and ranks the best reviews[9]. To assess customer input and automatically assign a general restaurant grade, study uses text mining. Natural language processing is used to fetch pertinent descriptors and evaluation ratings of user identified features from unstructured text[10]. It was discovered that the most of user were knowing about food apps, and that the majority of people use them to place food orders. A factor analysis revealed that the respondents ranked convenience, ease of payment, longer delivery times, and receiving the expected order as the most important factors in relation to their monthly expenditure, while good customer service, receiving the expected order, and fewer restaurants were ranked as the most important factors in relation to age[11]. It provides a summary of the relationship between database knowledge discovery and data mining. This also covers data-mining methods, real-world applications, and the difficulties associated with applying knowledge discovery in the actual world[12]. After extracting food preferences of user from their reviews, a context-aware recommender system created by author makes restaurant recommendations depends on those preferences. A semantic method was used to group food items gathered from user reviews along with the sentiments connected with them. The findings demonstrate that this algorithm provides recommendations with 92.8% accuracy. The Wu-palmer and cosine approaches are combined in one approach to system development[13].

3. METHODOLOGY

A food recommender system makes recommendations to consumers about foods based on their interests, previous interactions, and contextual information. The following steps are commonly included to design the recommender models:



Figure 3.10. Step to design recommender model.

3.1. Data Collection

First stage of a recommender system is data collection. The information gathered from an online meal ordering platform.

3.2. Data Pre-processing

This stage involves eliminating noisy and unnecessary data from the data, removing duplicate data, fill missing values, identify and correcting errors and standardizing data.

3.3. Recommender System Approaches with Model

In this mode the content-based filtering method suggests foods that are comparable to what the consumer has already ordered. It makes use of user and item data, represents each item attributes as a feature vector using TF-IDF (Term Frequency-Inverse Document Frequency). Next step is to apply Cosine Similarity to calculate the similarities between the objects. It recommends the most similar products based on past user choices.

3.4. Evaluation Matrices

One method of unsupervised learning is content-based filtering. We can use F1-score, recall and precision. Verify that the test set contains the suggested items. Determine the F1-score, precision, and recall.

4. RESULT

In our evaluation of the Content-Based Filtering (CBF) model, we measured the precision, recall, and F1-score to assess its performance. These metrics are crucial for understanding the effectiveness of the recommendation system. The results are Precision: 0.66, Recall: 1.00 and F1-Score: 0.90.

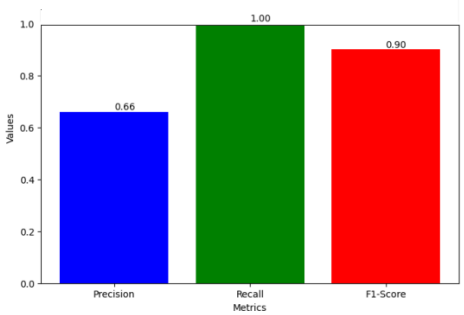

Figure 4.1.Result of Performance Matrices.

5. CONCLUSION AND FUTURE SCOPE

The Content-Based Filtering (CBF) model demonstrates high recall with a value of 1.00, indicating its strength in ensuring that all relevant items are recommended. However, the precision 0.66 suggests that there is space for improvement in reducing the number of irrelevant items recommended. The overall F1-score of 0.90 reflects a reasonably balanced performance. These results suggest that while the Content based filtering model is good in terms of recall, further refinement is needed to improve precision. Future work could explore methods to enhance the precision without compromising recall, such as incorporating additional features or refining the filtering criteria.

6. REFERENCES

[1] M. A. El-Dosuky, M. Z. Rashad, T. T. Hamza, and A. H. EL-Bassiouny, "Food Recommendation Using Ontology and Heuristics," in *Communications in Computer and Information Science*, vol. 322, Springer-Verlag Berlin Heidelberg, 2012, pp. 423–429.

[2] Z. Batmaz, A. Yurekli, A. Bilge, and C. Kaleli, "A review on deep learning for recommender systems: challenges and remedies," *Artif. Intell. Rev.*, vol. 52, no. 1, pp. 1–37, 2019, doi: 10.1007/s10462-018-9654-y.

[3] B.-D. Kim and S.-O. Kim, "A new recommender system to combine content-based and collaborative filtering systems," *J. Database Mark. Cust. Strateg. Manag.*, vol. 8, no. 3, pp. 244–252, Apr. 2001, doi: 10.1057/palgrave.jdm.3240040.

[4] J. Gupta and J. Gadge, "A framework for a recommendation system based on collaborative filtering and demographics," in *2014 International Conference on Circuits, Systems, Communication and Information Technology Applications (CSCITA)*, Apr. 2014, pp. 300–304, doi: 10.1109/CSCITA.2014.6839276.

[5] F. Pecune, L. Callebert, and S. Marsella, “A recommender system for healthy and personalized recipe recommendations,” *CEUR Workshop Proc.*, vol. 2684, pp. 15–20, 2020.

[6] M. Goel, A. Agarwal, D. Thukral, and T. Chakraborty, “Fiducia: A Personalized Food Recommender System for Zomato,” no. c, Mar. 2019, [Online]. Available: http://arxiv.org/abs/1903.10117.

[7] B. Jonathan, J. I. Sihotang, and S. Martin, “Sentiment Analysis of Customer Reviews in Zomato Bangalore Restaurants Using Random Forest Classifier,” *Abstr. Proc. Int. Sch. Conf.*, vol. 7, no. 1, pp. 1719–1728, 2019, doi: 10.35974/isc.v7i1.1003.

[8] A. Saxena, “An Analysis of Online Food Ordering Applications in India: Zomato and Swiggy,” *Int. J. Res. Eng. IT Soc. Sci.*, vol. 9, no. April, pp. 13–21, 2019, [Online]. Available: http://indusedu.org.

[9] B. Chugh, “Sentimental Analysis and Visualization of Food Reviews from Zomato using Tableau,” *Int. J. Adv. Trends Comput. Sci. Eng.*, vol. 9, no. 4, pp. 4389–4393, 2020, doi: 10.30534/ijatcse/2020/31942020.

[10] J. C. Cuizon, J. Lopez, and D. Rose Jones, “Text Mining Customer Reviews for Aspect-Based Restaurant Rating,” *Int. J. Comput. Sci. Inf. Technol.*, vol. 10, no. 06, pp. 43–52, 2018, doi: 10.5121/ijcsit.2018.10605.

[11] A. Vinaik, R. Goel, S. Sahai, and V. Garg, “The study of interest of consumers in mobile food ordering apps,” *Int. J. Recent Technol. Eng.*, vol. 8, no. 1, pp. 3424–3429, 2019.

[12] N. Kumar, S. Jain, and K. Chauhan, “Knowledge Discovery from Data Mining Techniques,” *Int. J. Eng. Res. Technol.*, vol. 07, no. 12, pp. 1–3, 2019.

[13] E. Asani, H. Vahdat-Nejad, and J. Sadri, “Restaurant recommender system based on sentiment analysis,” *Mach. Learn. with Appl.*, vol. 6, no. April, p. 100114, Dec. 2021, doi: 10.1016/j.mlwa.2021.100114.

Biographies



Zinkal Patel received the bachelor's degree in computer science from Veer Narmad South Gujarat University, Surat in 2008, the master's degree in computer science from Sardar Patel University, Vallabh Vidhyanagar in 2011 and pursuing the philosophy of doctorate degree in IT & CS Department from Parul University respectively. My research areas include data mining and machine learning.

Ship Port Detection with Coarse and Fine Data Fusion using Edge Boards

S Vasavi, M Sai Pravallika, Y Harini Reddy, D Revanth

[1,2,3,4]Department of Artificial Intelligence and Data Science, V R Siddhartha Engineering College

[1]vasavi_movva@vrsiddhartha.ac.in, [2]pravallika1249@gmail.com, [3]harinireddy123123@gmail.com, [4]revanthdivi3107@gmail.com

Abstract

Accurate detection of ships and ports in satellite imagery remains a significant challenge in maritime security and surveillance due to the complex environmental conditions such as cloud cover, varying image resolutions, and dynamic maritime scenes. To address these challenges, this study proposes a novel method using coarse and fine data fusion integrated with Faster R-CNN (FRCNN), a state-of-the-art real-time object detection framework. By combining multi-scale data, the proposed approach enhances detection precision and robustness, ensuring reliable performance in complex scenarios . A large, annotated dataset of satellite imagery is employed for model training with specialized cloud detection and removal techniques further refining background segmentation and improving detection performance. The solution is optimized for deployment on edge devices, specifically the Jetson Nano, to meet the demands of real-time monitoring in resource-constrained maritime environments. The Jetson Nano, recognized for its compact design and computational efficiency, enables real-time image processing directly at the edge thereby reducing dependence on centralized computing resources. This edge-based architecture ensures both scalability and operational efficiency and is a reliable tool for enhancing maritime security by integrating advanced object detection, data fusion, and cloud mitigation, demonstrating significant potential for real-world surveillance applications.

Keywords. Ship detection, Port detection, Satellite imagery, Coarse and fine data fusion, Faster R-CNN (FRCNN), Cloud detection and removal, Edge computing

Introduction

With the increasing traffic in the world's seas, it has become extremely important to monitor and secure the port regions for commercial as well as strategic reasons. Ports are a very crucial node in international trade and have a high volume of cargo and vessel movements. Hence, it is vital to monitor the area to not only improve operational efficiency but also detect any possible security threats. Traditional monitoring techniques cannot easily scale up with an excellent real-time capability in which such technology has revolutionized a lot. Recently, the source of satellite data was based on multispectral imagery through Sentinel-2A and ResourceSAT-2A, which will show the possibility of improving quality and accuracy in surveillance using a remote sensing-based perspective. Sentinel-2A will capture high-resolution RGB bands for detailed visual information with large-scale monitoring applications. However, ResourceSAT-2A includes other spectral bands, such as NIR and SWIR, that are much richer in spectral information and can be used to differentiate between objects with very similar visual features. This paper presents a Ship Port Detection System based on coarse and fine data fusion with advanced object detection techniques for real-time port monitoring. The methodology employs data from Sentinel-2A and ResourceSAT-2A. Contrast stretching is applied on Sentinel-2A RGB imagery to add NIR and SWIR bands of ResourceSAT-2A to increase spectral differentiation. The deep learning model, Faster R-CNN, is utilized to identify ships and port infrastructure with accuracy in satellite images after preprocessing. With this network architecture of Faster R-CNN, the ships and other features in the port can be effectively located in an accurate manner.

RELATED WORKS

To locate vessels in satellite imagery, [1] evaluates the Faster R-CNN framework: this integrates an RPN with a CNN for robust object detection performance. This significantly improves processing speed through the sharing of computational resources between proposal generation and classification, achieving an mAP of 73.2% on the PASCAL VOC 2007 dataset. With that in mind, the computational cost and memory requirements are rather high, which could reduce its performance while trying to detect small objects or in backgrounds cluttered heavily. The paper focuses the selection of appropriate algorithms for real-time object detection.

Loran et al. (2022) [2] mitigate challenges such as radar noise and low resolution by employing the Faster R-CNN framework to identify ships in range-compressed airborne radar images for ship recognition using airborne radar data, which are often much more complicated to interpret than visual images, hence requiring a model uniquely engineered for such data. With a low false alarm rate of 6.7% and an impressive 91.5% accuracy rate in ship detection, the study shows promise over similar techniques that are tied to traditional radar system. However, this technique suffers from heavy noise interference, and still, it's not apt for real-time application scenarios.

To mitigate the above concerns pertaining to remote sensing images, Rui et al. [3] proposed a Density-aware Cloud Removal technique using a Global-Local Fusion Transformer, named DCR-GLFT. The previous techniques usually complicated cloud removal through reliance on cloud masks or Synthetic Aperture Radar (SAR) data and require large datasets. The DCR-GLFT technique, which uses density information to guide the removal with cloud density estimation, achieves state-of-the-art PSNR = 28.93 and SSIM = 0.84 on the SEN12MS-CR dataset, so this is a major breakthrough for single-image cloud removal regardless of SAR data.

Belgiu et al. [4] report on spatiotemporal image fusion strategies in remote sensing with an emphasis on the combination of sources of satellite imagery, such as radar and optical, respectively. The paper shows how such methods improve spatial resolution and fill in gaps of the temporal coverage so that monitoring capabilities are improved considerably. A few authors have reported increased monitoring and detection accuracy using optical and radar pictures as a combined source, with accuracy gains up to 15% compared to single-source imagery.

PROPOSED METHODOLOGY

8.1. Data Acquisition and Preprocessing

1. *Satellite Data Sources*: For this study, multispectral satellite data was obtained from the following sources
   a. *Coarse Data:* Sentinel-2A was used that provides high-resolution images in various spectral bands such as Blue, Green, and Red bands to identify major features.
   b. *Fine Data:* ResourceSAT-2A, which carries more bands of spectral resolution like the Near Infrared (NIR) and Short-Wave Infrared (SWIR), was used to scan finer spectral details and thereby increasing the spatial resolution in the composite.
2. *Data Import and Georeferencing:* A spectral band for Sentinel-2A was imported separately in.jp2 format, whereas for ResourceSAT-2A, it was in the .tif format. Loading of the bands was done using rasterio, thereby keeping intact the georeferencing information that was essential for spatial alignment between the datasets. This means that pixels in corresponding positions across bands represent the same geographic area.

1.2 Coarse Data Enhancement

To make the coarse data clearer and with more contrast, three spectral bands from the satellite images (Blue, Green, and Red) were loaded as separate bands of grayscale using rasterio. The bands were then stacked in RGB order to create a color composite image. Afterward, normalization(1) [9] was performed in order to scale pixel values between 0 and 1, maintaining consistency between bands and optimizing the data for enhancement.

$$Normalized\ Image = (Image - min(Image))/(max(Image) - min(Image)) \quad (1)$$

To improve the quality of the image as well as visually, we did a contrast stretch using the 2nd and 98th percentiles of the pixel values for each channel independently. This has the side effects of removing outliers yet emphasizes subtle features within channels. The enhanced image has then been saved for further analysis to visualize the improvement in its details. Figure.1 has presented the side-by-side comparison of the original and the enhanced images with the improvement produced from this enhancement process

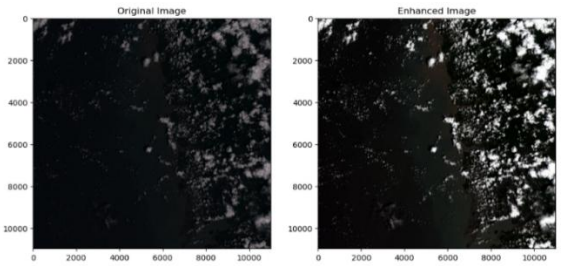

Figure 1. Enhanced Image of Coarse Data

1.3 Fine Data Enhancement

Fine data was also processed with a more detailed approach and more spectral bands. Bands like NIR and SWIR, which provide much more detail for vegetation and water bodies, were used in addition to RGB bands. Multi-band stacking has allowed a richer representation of the scene. The bands were scaled to the same magnitude and principal component analysis used for the enhancement of finer details and removal of redundancy of spectral information.

First three principal components were considered to represent the fine data into RGB, thereby maximizing the spatial and spectral contrast. It is a very helpful transformation in the identification of subliminal features such as health of vegetation, moisture levels in soil, and city details in the fine satellite resolution.

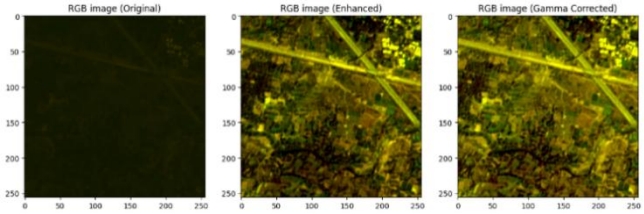

Figure 2. Enhanced Image of Fine Data

1.4 Resampling and Alignment Of Coarse and Fine Data

To verify the spatial alignment between the Coase and Fine datasets, they are introduced to resampling process where the Sentinel-2A bands were resampled to match the resolution of ResourceSAT-2A. This is performed using bilinear interpolation. This helped in reducing data loss and additionally, reprojection was applied where necessary to ensure that the pixels in the same positions across all the bands represented same geographical locations.

1.5 Data Normalization

Following, data normalization was performed to normalize the pixel values across all bands. These are scaled between 0 and 1 to improve consistency across the all bands. This step ensured that the both datasets are of comparable scale and reduced the differences in radiometric resolution.

1.6 Composite Generation

In the next step the normalized coarse and fine data were combined into a single composite image. Weighted averaging method was used where it enhanced both the spatial and spectral features within the composite. These resulting images are served as the input for the further object detection.

1.7 Cloud Mask Generation

Having both coarse and fine data enhanced, a cloud mask [10] was derived that isolates cloud-like regions. That is the necessary step for applications needing cloud-free data. The enhanced image was loaded as a.tif file and was made into grayscale by selecting the red channel, which captures most high-intensity regions to be represented as clouds.

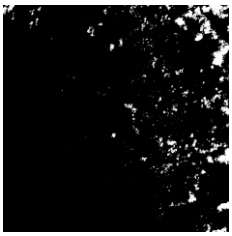

Figure 3. Cloud Masked Data

A simple thresholding technique was used to identify clouds. In this case, all pixel intensities above a predefined threshold of 200 were classified as clouds and set to 255 (white), and all other pixels were classified as non-cloud and set to 0 (black). The resultant binary mask was saved in the .tif format, meaning it would retain all the spatial metadata from the original image and therefore be amenable to geospatial analysis. Figure.3 is the generated cloud mask.

$$Cloud\ Mask = f(x) = \begin{cases} 1 & if\ Pixel \geq Threshold \\ 0 & Otherwise \end{cases} \quad (2)$$

2. DETECTION FRAMEWORK

This section explains the architecture of the enhanced Faster R-CNN model as shown in Figure.4, how each layer assisted in the precise detection of ships and ports in the satellite imagery.

Input Layer: The input is the enhanced, cloud-free image obtained from various preprocessing steps including cloud masking. This layer ensures that the enhanced model focuses only on the essential details required for a precise detection.

Backbone CNN(VGG Network): The backbone VGG Network helped in extracting the necessary features from the input image, ie both the low-level(edges, textures) and high-level features. This feature extraction helped in ships from each other using their unique shapes, different layouts of ports even in the complex backgrounds.

Region Proposals (RPN): This layer created the potential regions of interest within the image. These are the areas that are likely to contain ship or port features. This essential step ensured that the model only focusses on these high-probability areas consequently improving the detection accuracy and its computational efficiency.

ROI Pooling Layer: This ROI Pooling layer takes the generated regions of interest and normalizes them to a uniform size. This step ensured that all the images such as large ships and different port areas are processed evenly and resulted in consistent detection across various scales.

FC Layer: After pooling, the model learns about the generated features and assigns each region of interest a category such as ship or port, localize each object through bounding box regression.

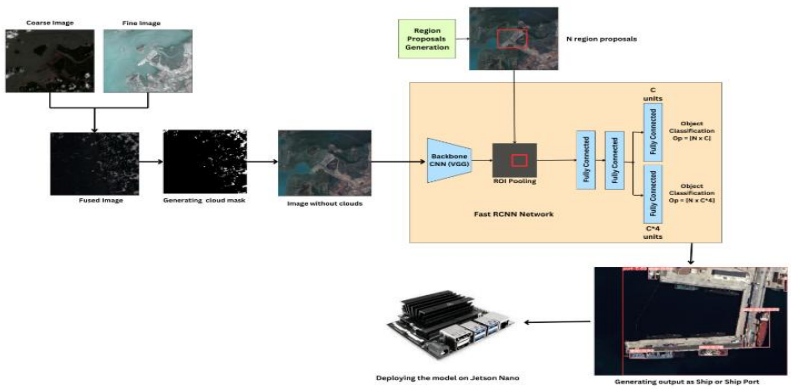

Figure 4. Faster R-CNN model Architecture

3. RESULTS AND ANALYSIS

The performance metrics for the enhanced model include precision, recall and mAP at IoU. These results provided an analysis on how the model performed in various cases. As shown in Table 1, the model achieved an overall recall of 0.73 and a precision of 0.83 on all instances.

Metrics	Ships	Ports	Average
Precision	0.85	0.82	0.835
Recall	0.76	0.71	0.735
F1 Score	0.80	0.76	0.78
Mean IOU	0.68	0.65	0.665
Total Predictions	30	25	55

This showed that there was a balanced performance and even successfully minimized the false positive rates. For the ship class, the precision and recall rates strongly show that the model captured various instances although it missed a few true positives at some points. Additionally, the mean IoU values for both classes indicates that the model achieved a reasonable accuracy in detecting the objects along with bounding boxes that closely matched with the true positions of ships and ports.

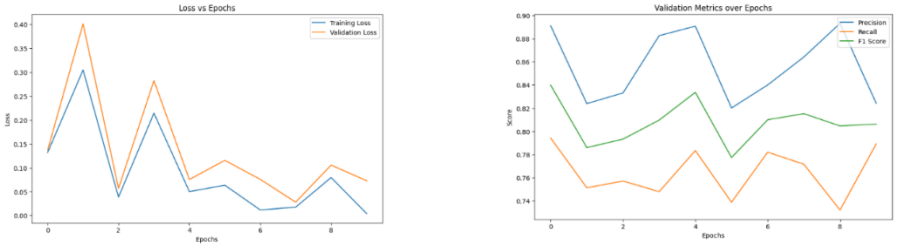

Figure 5. Loss vs Epochs

Additionally, the validation metric graphs provided the models performance over the training epochs. As depicted in Figure.5 although recall displayed few instabilities over a range, precision remained constantly high indicating the models accuracy in detecting ships and ports and the loss curves declining over the epochs displayed the models effective learning and generalization. During the initial stages the model showed low values but in later epochs there was a strong convergence.



Figure 7. Results of Ship Port Detection

Overall all these rigorous steps helped in bringing out a detailed analysis of the model and its effectiveness across various environments, pointing out its potential in real-time scenarios and for various practical applications in maritime monitoring and management.

4. IMPLEMENTATION ON JETSON NANO

Compact computer modules like the NVIDIA Jetson Nano are made for edge AI applications, especially in fields like robotics, drones, and Internet of Things devices. It is the perfect environment for developers to test out AI applications because it uses GPU architecture to effectively implement deep learning algorithms without depending on cloud services. Installing required libraries, downloading pre-trained weights, and setting up an appropriate environment are all part of configuring Faster RCNN for object identification on the Jetson Nano. Faster RCNN overlays bounding boxes on images and recognizes objects during inference. Light weight model like TensorRT is used to boost performance. This model incorporates methods like quantization to increase processing speed without sacrificing accuracy.

Table 5: Inference in different scenarios

Power Consumption	Inference Time
5W	36298.4ms
MaxN	16434.2ms

Based on power consumption choices, performance evaluations show notable variations in inference times. For example, the system may operate 2.2 times faster (16,434.2 ms) in "MaxN" mode than in low power "5W" mode (36,298.4 ms), suggesting that inference speed is directly improved by higher power available. The system operates 2.2 times faster in “MaxN” mode than in 5W mode, according to the analysis of the data from Table 5. This discrepancy is probably caused by the system's ability to pull power in "MaxN" mode, which improves performance.

5. CONCLUSION AND FUTURE WORK

This study addresses the difficulties presented by complicated maritime settings by proving the efficacy of the suggested method, which makes use of an improved Faster R-CNN model for ship and port detection in satellite data. Faster R-CNN's incorporation of coarse and fine data fusion greatly enhances detection robustness and precision, making it appropriate for practical uses in marine security and surveillance. There is potential for improvement even though the Jetson Nano's CPU's current implementation offers respectable inference speeds.

Future research will concentrate on optimizing the suggested model's performance using a variety of Jetson Nano-specific optimization strategies. While investigating smaller versions of the Faster R-CNN model may result in better inference times, tracking GPU consumption will provide insights for future improvements.

6. REFERENCES

[1] S. Ren, "Faster r-cnn: Towards real-time object detection with region proposal networks.," arXiv preprint, no. arXiv:1506.01497, 2015.

[2] "Ship detection based on faster R-CNN using range-compressed airborne radar data.," IEEE Geoscience and Remote Sensing Letters, vol. 20, pp. 1-5, 2022.

[3] R. Quan, S. He, T. Li, G. Wang, N. Ruan, M. Lin, Y. Yang and H. Shen, "Density-aware Cloud Removal of Remote Sensing Imagery Using a Global-Local Fusion Transformer," IEEE Transactions on Geoscience and Remote Sensing, 2024.

[4] M. Belgiu and A. Stein, "Spatiotemporal image fusion in remote sensing," Remote sensing, vol. 11, no. 7, p. 818, 2019.

[5] Y. Chen, M. Chen, W. He, J. Zeng, M. Huang and Y. Zheng, "Thick cloud removal in multitemporal remote sensing images via low-rank regularized self-supervised network," IEEE Transactions on Geoscience and Remote Sensing, 2024.

[6] R. Dong, L. Zhang, W. Li, S. Yuan, GanL, J. Zheng, H. Fu, L. Mou and X. Zhu, "An adaptive image fusion method for sentinel-2 images and high-resolution images with long-time intervals," International Journal of Applied Earth Observation and Geoinformation, vol. 121:103381, 2023.

[7] Y. Wu, W. Ma, M. Gong, Z. Bai, W. Zhao, Q. Guo, X. Chen and Q. Miao, "A coarse-to-fine network for ship detection in optical remote sensing images," Remote Sensing, vol. 12(2):246, 2020.

[8] S. He, H. Zou, Y. Wang, R. Li, F. Cheng, X. Cao and M. Li, "Enhancing mid–low-resolution ship detection with high-resolution feature distillation," IEEE Geoscience and Remote Sensing Letters, vol. 19, pp. 1-5, 2021.

[9] M. Hall-Beyer, "GLCM texture: a tutorial," National Council on Geographic Information and Analysis Remote Sensing Core Curriculum, vol. 3, no. 1, p. 75, 2000.

[10] S. Ackerman, K. Strabala, W. Menzel, R. Frey, C. Moeller and L. Gumley, "Discriminating clear sky from clouds with MODIS," Journal of Geophysical Research: Atmospheres, vol. 103, no. D24, pp. 32141-32157, 1998.

Seas of Change: Integrating RIS for Effective Ship-to-Ship Communication

Vedashree G.L, Goutham Simha G.D and Madhusudan B. Kulkarni

Department of Electronics and Communication Engineering, Manipal Institute of Technology, Manipal Academy of Higher Education, Manipal, India.
Email: vedashree.mitmpl2023@learner.manipal.edu, goutham.simha@manipal.edu, madhusudan.kulkarni@manipal.edu

1. Abstract.

The dynamic and unpredictable sea environment poses a major challenge for ship-to-ship communication. Reconfigurable Intelligent Surfaces (RIS) can enhance communication by more intelligently reflecting the signals and optimizing signal transmission paths pointed towards the receiver. While traditional relay stations mainly serve to step up a fading channel, RIS reduces the impacts of such fading channels, thus providing better signal strength and stability.
This work involves the placement of RIS on the lighthouse along the shore in an effort to assist in ship-to-ship communication. A 4×4 MIMO channel in Rayleigh and Weibull fading is assumed, as line-of-sight (LOS) is not always available in sea situations and the signal undergoes multipath fading. Subsequently, the performances are analyzed with and without RIS with respect to the important parameters such as BER versus SNR, channel power, channel capacity, and RSSI.

Keywords. Marine communication, Reconfigurable Intelligent Surfaces (RIS), MIMO, Rayleigh fading channel, Weibull fading channel.

2. INTRODUCTION

Earth is covered with oceans and seas for approximately 71% of the earth's surface. Hence, sea is a very crucial aspect for humans, either socially, economically or environmentally. Hence, communication in the sea environment is a necessity in all aspects to be fast, reliable, and effective. By introducing Reconfigurable Intelligent Surfaces (RIS), we improve oceanic communication significantly. By modifying the phase shifts and amplitudes of numerous passive reflecting elements, RIS has become a crucial enabling technology for intelligently reconfiguring the radio propagation environment for wireless communications beyond the fifth or sixth generation (B5G/6G). This allows for real-time control of signal reflection [1]. A RIS is a 2D material structure that has macroscopic physical properties that may be programmed. The ability to adjust a RIS's EM

All Open Access articles are peer-reviewed, distributed under the Creative Commons Attribution-Non Commercial 4.0 International

wave response is its most crucial feature. RIS-aided networks allow for the control of the channels between the transmitters and the receivers. As a result, the terminal devices can increase the desired received signal's strength [2]. Maritime communications confront substantial hurdles compared to terrestrial networks, including severe latency, low bandwidth, and unreliable channels, which impair real-time collision avoidance and decision-making. Resource exploration and environmental monitoring are made more difficult by slow computation speeds and low data backhaul rates. Incompatible interfaces and data formats also make it difficult to integrate multidisciplinary technologies like satellites, FSO, and wireless radio. Adaptive-communication systems are difficult to implement due to the deteriorating oceanic environment, which is made worse by unpredictable weather [3][4].

To overcome these difficulties a MIMO system is introduced, specifically a 4 × 4 system. By sending multiple data streams at once, these systems increase data throughput and reliability, which is an important feature in difficult ocean settings and long distance communications. By making use of spatial variety they also improve signal robustness by reducing the effects of interference and fading. Also, MIMO systems are more suited for high-capacity communication requirements in maritime applications because of their improved spectral efficiency[5]. The Weibull fading channel is considered while simulating the results and compared with the

results obtained with Rayleigh fading channel. Because it indicates the intricate and dynamic fading features of maritime environments, and is taken into consideration in marine communication. It is a strong option for assessing and creating dependable communication systems across the ocean due to its adaptability, capacity to record heavy-tailed behavior, and suitability for NLoS and ducting scenarios. At the receiver end, we have used ML detection to minimize the probability of error in estimating the transmitted symbols.

3. SYSTEM AND CHANNEL MODELLING

For this paper, we have considered 2 system models, with Rayleigh and Weibull fading channels. We have considered a MIMO channel with 4×4 antennas, that is for transmitter (Tx) $N_t = 4$ and receiver (Rx) $N_r = 4$. Also, we have considered RIS with 64 elements, that is $N_{ris} = 64$. The goal is to compare the behaviour of the system with and without the RIS. The transmitter is set on one ship, which is trying to communicate with another ship, it sends BPSK-modulated symbols. The transmitted symbol vector $X \in \mathbb{C}^{N_t \times 1}$ is constructed by mapping binary bits to BPSK symbols. The total number of bits sent per symbol is $N_t \times \log_2(M)$ where $M = 2$ for BPSK. The receiver is set on another ship, which observes a noisy version of the transmitted signal sent by the first ship. The received signal $Y \in \mathbb{C}^{N_r \times 1}$ is given by:

$$Y = H \cdot X + N$$

where H is the channel matrix given by $H \in \mathbb{C}^{Nt \times Nr}$ the noise added here is the AWGN which is given $by\ N \in \mathbb{C}^{Nr \times 1}$ .The RIS is placed on a light house on the shore, which is a planar array of $N_{ris} = 64$ passive elements. Each RIS element applies a phase shift to the incident signal. The phase shifts are represented by a diagonal matrix $\phi \in \mathbb{C}^{Nris \times Nris}$:

$$\phi = diag(e^{j\phi 1}, e^{j\phi 2}, \ldots., e^{j\phi N_{ris}})$$

where ϕ_i is the phase-shift applied by the ith RIS element. During communication, we have considered direct ship-to-ship communication without RIS, where the channel matrix is H_{direct}. In the RIS-assisted communication, the effective channel matrix H_{ris} is given by:

$$H_{ris} = H_2 \cdot \phi \cdot H_1$$

where $H_1 \in \mathbb{C}^{Nris \times Nt}$ is the channel from the T_x to the RIS, and $H_2 \in \mathbb{C}^{Nr \times Nris}$ is the channel from the RIS to the receiver. The path loss is given by:

$$PL(d) = (-\alpha) d_0$$

Where d is the distance between the T_x and R_x, $d_0 = 1$ km is the reference distance, α = 2.2 is the path loss exponent. Also, for distance for RIS-assisted communication we have considered $d_{ris} = 2$ km, and for direct communication we have considered $d_{direct} = 4$ km. For the direct channel matrix, it is modeled as:

$$H_{direct} = \sqrt{PL(d_{direct})} \cdot (H_{LOS} + H_{NLOS})$$

where H_{LOS} is the line-of-sight component and H_{NLOS} is the non-line-of-sight component. For the RIS-assisted channels (H_1 and H_2), they are modeled as:

$$H_1 = \sqrt{PL(d_{ris})} \cdot (H_{LOS,1} + H_{NLOS,1})$$

$$H_2 = \sqrt{PL(d_{ris})} \cdot (H_{LOS,2} + H_{NLOS,2})$$

The R_x signals with direct and RIS-assisted communication is given by:

$$Y_{direct} = H_{direct} \cdot X + N$$

$$Y_{ris} = H_2 \cdot \phi \cdot H_1 \cdot X + N$$

Then the BER is calculated, as the ratio of incorrectly R_x bits to the total number of T_x bits. Channel capacity is

calculated using Shannon's formula:

$$C = \log_2 (1 + SNR \cdot ||H||^2)$$

where $||H||$ is the average channel power. While using the Weibull fading channel, we consider the shape ($\kappa = 2$) and scale parameter ($\lambda = 1$). The magnitude of the channel coefficients follows a Weibull distribution:

$$f(x; k, \lambda) = k\ x_(\lambda\ \ \lambda k-1)e^{-(x/\lambda)^k},\ x \geq 0$$

The phase of the channel coefficients is uniformly distributed in $[0,2\pi)$. Also we have calculated RSSI using the log-distance path loss model:

$$RSSI(d) = RSSI_0 - 10 \cdot \alpha \cdot \log_{10} (\frac{d}{d_0})$$

where, $RSSI_0 = -45$ dBm is the reference RSSI at distance d_0. The optimized RIS adds a gain of 10 dB and random RIS adds a gain of 5 dB.

4. SIMULATED RESULTS

The performance analysis of the ship-to-ship communication with phase-optimized RIS, unoptimized RIS, and direct communication is done, using Rayleigh and Weibull fading channels. We have considered a 4×4 MIMO system in which the transmitter and receiver both have 4 antennas. The RIS has 64 elements, which are used to optimize the phase of the transmitted signal. Figure 3.1 compares the BER vs SNR performance in 3 different conditions for both channels. Clearly, the optimized RIS system has the lowest BER, as the RIS is configured to maximize the signal strength at the receiver. The optimized RIS curve in Figure 3.2 has the highest channel capacity. As SNR increases, channel capacity increases for all scenarios. This is expected because higher SNR allows for higher data rates. Figure 3.3 gives the channel power comparisons in both fading channels. This graph shows that the optimized RIS has the highest average channel power, as the RIS phase shifts are optimized to maximize the signal strength at the receiver. Figure 3.4 shows the comparison of RSSI versus distance, which indicates that the optimized RIS shows the highest RSSI values across all distances, as signal strength at the receiver is maximized by aligning the phase shifts of its elements.

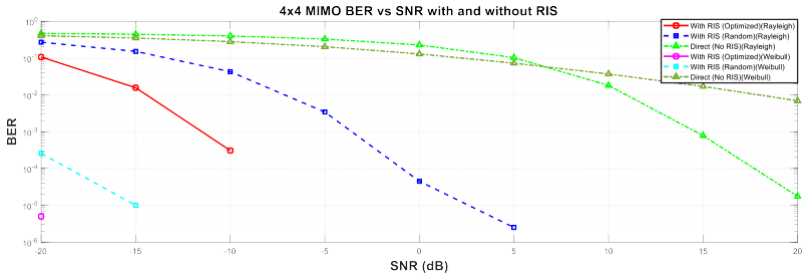

Figure 3.1. BER vs SNR Comparison

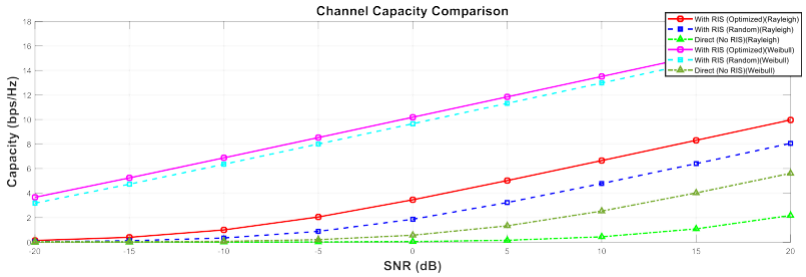

Figure 3.2. Channel Capacity Comparison

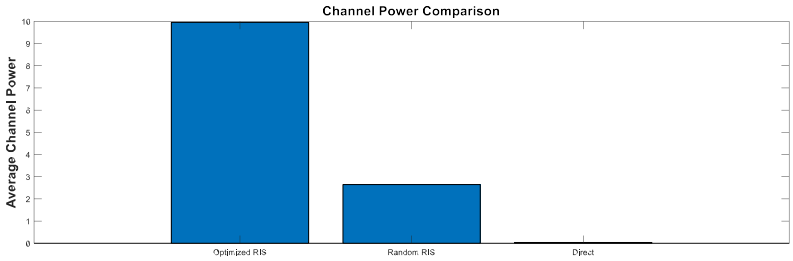

Figure 3.3. Channel Power Comparison

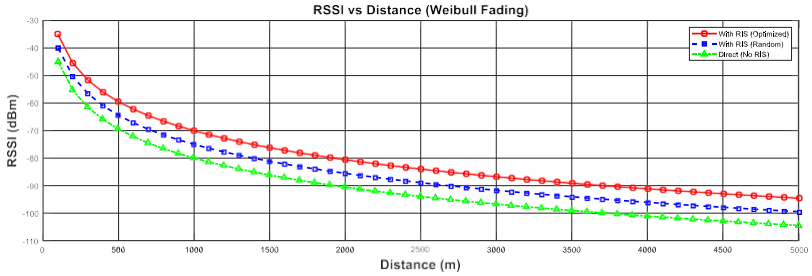

Figure 3.4. RSSI vs Distance Comparison for Weibull Fading Channel

5. Conclusion and Future Work

In this study, the performance of ship-to-ship communication systems enhanced by Reconfigurable Intelligent Surfaces (RIS) was analyzed. The BER versus SNR comparison showed that the RIS-integrated system surpasses the conventional non-RIS system, offering a promising solution for enhancing maritime wireless communication. The BER analysis results revealed that placing RIS strategically, such as on a lighthouse, improves the system reliability and improved capacity, making it an attractive solution to enhance data transmission efficiency.

Also, RSSI performance showed great improvement for RIS-aided communication in comparison to non-RIS systems, thus demonstrating the efficiency of RIS in counteracting signal degradation with an accompanied distance. Therefore, incorporating RIS into ship- to-ship communication serves as an efficient means of mitigating challenging maritime channel conditions and enhancing signal reliability and overall system behaviour.

In Future, the research work may focus on the dynamic configuration of RIS, adaptive beamforming, and the role of environmental factors in RIS-assisted communication optimization.

6. References

[1] H. Jiao, H. Liu and Z. Wang, " Reconfigurable Intelligent Surfaces aided Wireless Communication: Key Technologies and Challenges" 2022 International Wireless Communications and Mobile Computing (IWCMC), Dubrovnik, Croatia, 2022.

[2] Liu, Y., Liu, X., Mu, X., Hou, T., Xu, J., Di Renzo, M. and Al-Dhahir, N., 2021. Reconfigurable intelligent surfaces: Principles and opportunities. IEEE communications surveys & tutorials.

[3] C. Yu, J. Li, C. Zhang, H. Li, R. He and B. Lin, " Maritime Broadband Communications: Applications, Challenges and an Offshore 5G-virtual MIMO Paradigm " 2020 IEEE Intl Conf on Parallel & Distributed Processing with Applications, Big Data & Cloud Computing, Sustainable Computing & Communications, Social Computing & Networking (ISPA/BDCloud/SocialCom/SustainCom), Exeter, United Kingdom, 2020.

[4] Wang, J., Zhou, H., Li, Y., Sun, Q., Wu, Y., Jin, S., Quek, T.Q. and Xu, C., 2018. Wireless channel models for maritime communications. IEEE access.

[5] A. Katalinic, R. Nagy and R. Zentner, " Benefits of MIMO Systems in Practice: Increased Capacity, Reliability and Spectrum Efficiency " Proceedings ELMAR 2006, Zadar, Croatia, 2006.

7. Biographies



Vedashree G.L received the bachelor's degree in electronics and communication engineering(ECE) from VTU University in 2023, and pursuing master's degree in digital electronics and communication engineering from Manipal Institute of Technology (MIT), Manipal.

6G Wireless Systems: Performance Analysis of Hardware Designs Under Non-Ideal Conditions

Bhargavi K V N A[1], Ravi Chandra M L[2], RAVILLA DILLI[3]

[1]Computer Science Engineering, Koneru Lakshmaiah Education Foundation, Telengana, Hyderabad, 500075, India Email: bhargavi@klh.edu.in

[2]Professor, Electronics and Communication Engineering, Srinivasa Ramanujan Institute of Technology, Ananthapuramu, Andhra Pradesh, India. ravichandra.ece@srit.ac.in

[3]Associate Professor, Electronics and Communication Engineering, Manipal Institute of Technology, Manipal Academy of Higher Education, Manipal, Udupi, Karnataka 576 104 India. Email: dilli.ravilla@manipal.edu

Abstract.

This paper aims at system level hardware design aspects towards meeting the requirements of 6G use cases in terms of latency and link data rates. It mainly describes the radio frequency (RF) transceiver architectures, hardware components models, channel modelling, and optimization at THz bands (> 100 GHz) under non-ideal conditions. This work aimed at the imperfections of hardware in handling the candidate 6G orthogonal frequency division multiplexin`g (OFDM) signals. The imperfections include non-linearities of power amplifier (PA), phase noise, and filter characteristics that spreads the signal spectrum beyond the channel bandwidth. The impact of various design parameters and deployment options are illustrated by conducting system-level simulations. The system parameters are designed and configured according to international telecommunication union-radio (ITU-R) radio models while quantifying the impairments. The RF hardware imperfections are demonstrated, and the results proved the practical feasibility of such RF systems.

Keywords. 6G, Channel model, hardware design, ITU-R, Radio modeling, RF, THz bands

1. INTRODUCTION

In this work, the radio transceiver design for above 100 GHz bands is presented by considering the non-ideal characteristics of the hardware, waveform impacts, and channel properties. It mainly aims at the imperfections of hardware designs in handling the candidate 6G OFDM signals. The imperfections include non-linearities of PA, phase noise, and filter characteristics that spreads the signal spectrum beyond the channel bandwidth. The hardware imperfections are demonstrated using adjacent channel power ratio (ACPR) and error vector magnitude (EVM) as metrics. ACPR measurements help to study spectral regrowth due to nonlinearity of PA.

2. EXISTING WORKS

The nascent research [1-4] has proved that the 6G connectivity can operate at sub-1 GHz range, 3.5-6 GHz mid-band range, 7-15 GHz centimetric range, 26 -72 GHz millimeter-wave range, and 90-300 GHz sub-THz range. The initial deployments of 6G are expected at lower edge of sub-THz range due to their favourable propagation characteristics and availability in the commercial RF equipment ecosystem. In this context, W and D bands at sub-THz range looks interesting [5-8]. Artificial intelligence (AI) supported air interfaces in 6G systems enhance the beamforming and channel state information (CSI) compression. To maintain linearity over huge bandwidths at sub-THz and THz bands, digital pre-distortion plays a crucial role. AI techniques can optimize the digital pre-distortion through the collection of real data from PA and train and test the neural network [9-10].

3. METHODS

This section mainly focuses on modelling the imperfections in non-linear characteristics of PA, spectral characteristics of filter, and phase noise as shown in Figure 1. RF modelling is presented mainly in three stages: signal generation, introducing non-ideal conditions in the RF hardware, and measure the performance deviations.

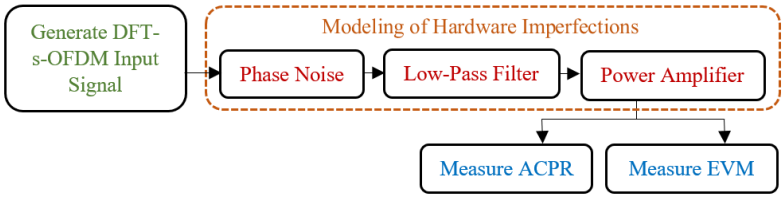

Figure 1: Modelling of RF hardware imperfections for 6G candidate waveform generation.

The 6G waveform is generated with appropriate configuration parameters as follows: ***Step 1:*** Configure the OFDM signal. ***Step 2:*** Define bandwidth occupancy (transmission bandwidth to channel bandwidth ratio). Minimal values of bandwidth occupancy cause poor spectral efficiencies. ***Step 3:*** Generate the carrier configuration. As per the values of bandwidth occupancy, define the sub-carrier spacing (SCS), compute number of resource blocks, and transmission bandwidth to configure the carrier signal. ***Step 4:*** Define the length of time division duplexing (TDD) frame and optimally configure slots for uplink and downlink. ***Step 5:*** Configure physical downlink shared channel (PDSCH) for the allotted resource block and enable phase tracking reference signal (PT-RS). ***Step 6:*** Generate a resource grid that contains a PDSCH transmission, demodulation reference signal (DM-RS), and PT-RS. ***Step 7:*** Oversample the OFDM signal with a specified oversampling factor to compute the spectral emission beyond channel bandwidth.

Finally, conduct measurements on error performance of RF systems to demonstrate sub-THz signal transmissions, estimations with different modulation schemes. Phase noise is one of the key hardware impairments at sub-THz bands and the adequate output powers of PA demands less peak-to-average-power ratio (PAPR) signal design [11-15]. For efficient utilization of the waveform, a low back-off in the PA is required. Discrete Fourier Transform Spread OFDM (DFT-S-OFDM) is a suitable waveform as it provides a low PAPR and a good power efficiency for the PA. According to 3GPP, a memoryless polynomial model of Gallium Nitride (GaN) PA presented in [16] is considered for analysing the imperfections. ACPR is measured to analyse the spectral regrowth due to nonlinear PA model as shown in Figure 2. Set the model back-off to minimize the input signal amplitude and minimize the distortion. Based on the results shown in Figure 3, ACPR characteristics with respect to output power of PA shifts at higher frequencies. EVM measurements were conducted for the signal received at receiver (Rx) as: 1. Perform timing synchronization for Rx signal. 2. Demodulate the OFDM signal. 3. Perform PDSCH channel estimation. 4. Equalization of PDSCH symbols for each slot. 5. Estimation and correction of phase errors. 6. Calculate the RMS and peak EVM values for PDSCH symbols. 7. Plot the EVM per subcarrier, averaged over OFDM symbols. 8. Plot EVM per symbol, averaged over subcarriers.

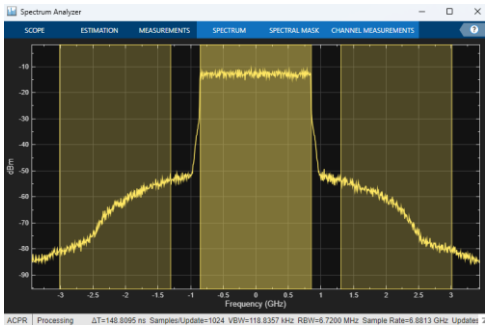

Figure 2: ACPR measurements due to nonlinearities of PA.

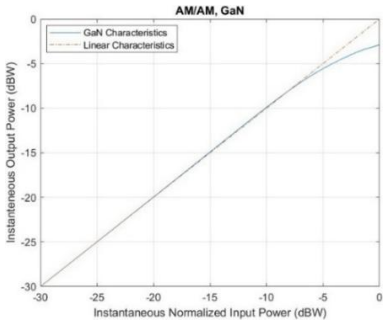

Figure 3: Nonlinear characteristics of PA imperfections at 140 GHz.

Table 1: Error performance of PDSCH.

Modulation scheme	EVM values	
	RMS value (%)	Peak value (%)
QPSK	2.795	13.119
16 QAM	2.735	13.748
64 QAM	2.816	14.531
256 QAM	2.775	13.034
1024 QAM	2.487	11.373

As the higher order modulation schemes are more sensitive to interference and noise, they expect higher powers and SNR for reliable communication. But the error performance results were very interesting as the error values are still minimal even when the order of modulation is increased to 1024 as presented in Table 1. This allows data transmissions with robustness to noise and interference while providing the higher data rates in the given bandwidth. In Figure 4, the RMS and peak values of PDSCH EVM per symbol and per subcarrier are drawn for 1024 QAM scheme.

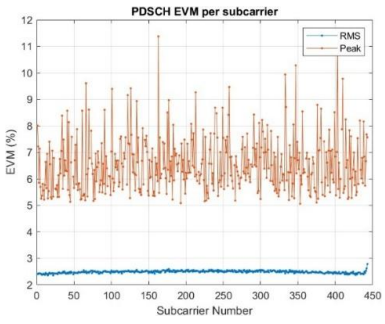

(a) per subcarrier

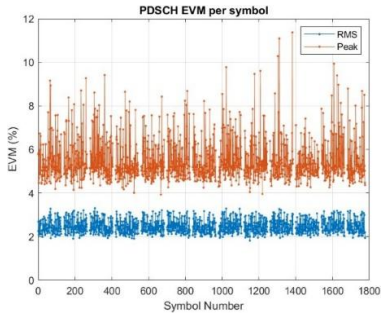

(b) per symbol

Figure 4: EVM values of PDSCH with 1024 QAM.

To take advantage of high processing speed and lower memory requirements, infinite impulse response (IIR) filters are selected in designing current RF systems. We have optimally selected the IIR filter cut-off frequencies, stop band attenuation, and pass band ripple to achieve lower EVM values. Figure 5 presents the magnitude and phase responses of the LPF, output proves more optimal for smaller stopband attenuation.

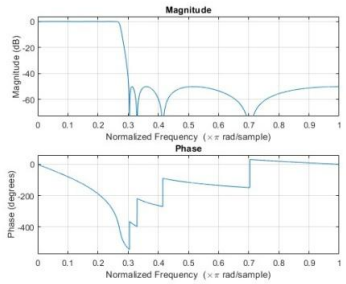

Figure 5: IIR LPF output with passband ripple=0.01 & stopband attenuation=50

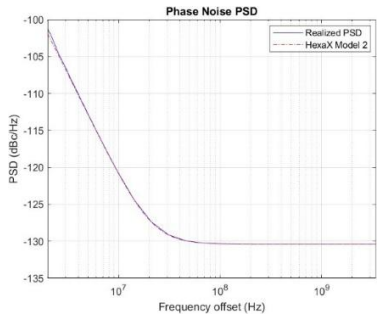

Figure 6: Phase Noise Filter Characteristics at 2 MHz minimum offset frequency.

Phase noise measurements were conducted to quantify the timing fluctuations of received signal's phase that can affect the performance of the Rx. In this work, phase-noise is calculated using the power spectral density (PSD) of phase deviations. Hexa-X model [16] is used to characterize the phase noise distortion at 140 GHz. Define the minimum frequency offset to calculate phase noise spectrum mask. From the phase noise filter characteristics shown in Figure 6, the lower values of minimum frequency offset model the

low frequency phase noise more accurately at the cost of longer design time for phase noise filter.

4. CONCLUSIONS AND FUTURE SCOPE

Design of 6G systems operate at sub-THz bands enables performance gains in terms of latency, data rates, transmission bandwidth, signal interference, and network capacity. But the main challenges at such higher frequency bands are to have resilient waveforms, and capability in handling hardware limitations such as phase noise. This work mainly aimed at the imperfections of hardware designs in handling the candidate 6G OFDM signals. The imperfections include non-linearities of PA, phase noise, and filter characteristics that spreads the signal spectrum beyond the channel bandwidth. The system parameters are designed and configured according to ITU-R radio models while quantifying the imperfections. The hardware design imperfections are demonstrated by exploring various specifications of RF modules using ACPR and EVM as metrics.

5. REFERENCES

1. W. Jiang, et. al., 'Terahertz Communications and Sensing for 6G and Beyond: A Comprehensive Review', In-press, IEEE Commun. Surveys & Tutorials, 2024. DOI:10.1109/COMST.2024.3385908
2. ITU Recommendation ITU-R M.2160-0. 'Framework and overall objectives of the future development of IMT for 2030 and beyond' 2023.
3. Hexa-X Deliverable D2.2 - Initial radio models and analysis towards ultra-high data rate links in 6G.
4. J. M. Jornet, et. al., 'The Evolution of Applications, Hardware Design, and Channel Modelling for Terahertz (THz) Band Communications and Sensing: Ready for 6G?', Proc. of the IEEE, In-press, 2024. DOI:10.1109/JPROC.2024.3412828

5. https://www.ericsson.com/en/6g/spectrum/sub-thz
6. ITU-R, Report M.2516-0. 'Future technology trends of terrestrial International Mobile Telecommunications systems towards 2030 and beyond', 2022.
7. 3GPP TS 38.211 'NR; Physical channels and modulation' 3GPP; Technical Specification Group Radio Access Network. version 16.2.0 Release 16.
8. 3GPP TS 38.331 'NR; Radio Resource Control (RRC); Protocol specification' 3GPP; Technical Specification Group Radio Access Network.
9. Y. Xing and T. S. Rappaport. 'Millimeter Wave and Terahertz Urban Microcell Propagation Measurements and Models', IEEE Communications Letters, vol. 25, no. 12, pp. 3755–3759, 2021. DOI:10.1109/LCOMM.2021.3117900
10. J.F. Smith, Y. Gui, I. Fatadin. 'Measuring the peak performance of a 6G THz communication testbed, Frontiers in Antennas and Propagation', Article ID: 2:1471091, Vol. 24, pp. 1–9, 2024. DOI:10.3389/fanpr.2024.1471091
11. Abdo, et. al., '64 QAM wireless link with 300 GHz InP-CMOS hybrid transceiver', IEICE Electronics Express, Vol. 18, Issue. 17, 20210314–4, pp. 1–4, 2021. DOI:10.1587/elex.18.20210314
12. Bodet, et. al., 'Sub-terahertz near field channel measurements and analysis with beamforming and Bessel beams', Sci Rep., Vol. 14, Article ID: 19675, pp. 1–13, 2024. DOI:10.1038/s41598-024-70542-z
13. H. Hamada, et. al., '300-GHz-Band 120-Gb/s wireless front-end based on InP-HEMT PAs and mixers', IEEE J. Solid-State Circuits, Vol. 55, Issue. 9, pp. 2316–2335, 2020. DOI:10.1109/jssc.2020.3005818
14. Fatadin, et. al., 'Demonstration of 120 Gbit/s 64-QAM wireless link operating in the 300 GHz band', IEEE Access, Vol. 12, pp. 31159–31167, 2024. DOI:10.1109/access.2024.3368884
15. D. Marasinghe, et. al., 'Waveform Learning under Phase Noise Impairment for Sub-THz Communications', IEEE Trans. Commun., In-press, 2024. DOI: 10.1109/TCOMM.2024.3430982
16. Hexa-X Deliverable D2.3 - Radio models and enabling techniques towards ultra-high data rate links and capacity in 6G.

Biographies



Prof. Bhargavi KVNA, is currently working as Head of KLH Global Business School and Assistant Professor in Computer Science Engineering Department. She holds good academic record and received a Gold Medal for her academic excellence.



M. L. Ravi Chandra currently working as a Professor and Head of ECE at Srinivasa Ramanujan Institute of Technology, Ananthapuramu, Andhra Pradesh, India since 2015. He has 22 technical publications in Journals and Conferences. His Research areas are Wireless Communications and IoT.



Ravilla Dilli is currently working at Manipal Institute of Technology, Manipal Academy of Higher Education, Manipal, Karnataka, India. He holds 4 best research paper awards to his credit and received Excellence award for internship as part of SAMSUNG PRISM. He has published 40 research papers in International Journals and Conference Proceedings. His research expertise includes Network Security, MANETs, WSNs, 5G and 6G Wireless Technologies, and IoT.

Comparative Analysis of Snake and Ellipse Segmentation Methods for Breast Cancer Detection using Breast Thermograms

Dayakshini Sathish[1], Aswathi T[1], Sathish Kabekody[2], Ashlyne Barnes[1], Sona S[1], Preethika[1], Avashya HS[1]

- *[1]Department of ECE, St Joseph Engineering College Mangaluru, Karnataka, India-575028*
- *[2]Department of EEE, St Joseph Engineering College Mangaluru, Karnataka, India-575028*

Abstract.

Breast cancer is a leading cause of mortality among women, and early detection is crucial in improving survival rates. Computer-aided tools assist radiologists in identifying abnormalities, with breast thermography emerging as a non-invasive and radiation-free technique for early diagnosis. However, robust segmentation is essential to enhance the accuracy of AI-based detection models. This study compares Snake and Elliptical segmentation methods for breast thermogram analysis. The Snake Algorithm achieved higher accuracy with Jaccard Index of 0.78 but required more processing time, while the Ellipse Method was faster with a Jaccard Index of 0.72. Texture features extracted using GLCM revealed contrast, eating habits, and age as significant indicators in distinguishing normal and abnormal breast. A Support Vector Machine classifier trained on 100 samples with these features achieved 78% accuracy. The results highlight a trade-off between segmentation accuracy and computational efficiency, suggesting that hybrid models could optimize both performance and speed in thermographic breast cancer detection.

Keywords. breast thermogram, ellipse, masking, segmentation, features, significance level, confusion matrix

1. INTRODUCTION

Breast cancer is the most commonly diagnosed cancer in women, with 2.3 million new cases and 685,000 deaths reported worldwide in 2020, according to GLOBOCAN [1]. Nowadays, it is observed that more and more young women are affected by the breast cancer due to the change in life style, environmental issues, obesity, genetical factors etc. Breast cancer originates from uncontrolled cell growth in the milk ducts, lobules, or connective tissue and can spread via the lymphatic system or bloodstream if not detected early [2]. Early and accurate detection significantly improves survival rates and treatment outcomes. Various imaging modalities, including mammography, ultrasound, MRI, CT, PET scans, and thermography are used for breast cancer diagnosis. Among these, mammography is the most widely adopted method, offering high-resolution imaging but with reduced sensitivity in dense breast tissue and the risk of radiation exposure with repeated use [3]. While ultrasound and MRI enhance detection in specific cases, they are often costly and time-intensive, limiting their accessibility for large-scale screening.

Thermography has emerged as a non-invasive, radiation-free imaging technique, detecting temperature variations associated with metabolic activity in breast tissue [14]. It provides a promising adjunct tool to traditional screening methods, particularly for frequent monitoring and early physiological detection [4]. However, its diagnostic accuracy heavily depends on precise segmentation to isolate the Region of Interest (ROI), which plays a crucial role in feature extraction and classification in computer-aided detection (CAD) systems. Effective segmentation enhances sensitivity and specificity while reducing computational complexity, yet challenges such as low contrast, noise, and anatomical variations remain [5]. This study compares two segmentation techniques such as Snake Algorithm and Ellipse method to evaluate their efficiency in breast thermogram processing. The Snake Algorithm iteratively refines contours for precise ROI detection but is computationally intensive, while the Ellipse Method provides a faster approach by fitting ellipses to breast regions, reducing processing time while maintaining accuracy. The rest of the paper is structured as follows: Section 2 presents a literature review of segmentation techniques in thermography, Section 3 describes the methodology, Section 4 discusses the results and findings, and Section 5 concludes with key observations.

2. LITERATURE REVIEW

Segmentation is essential in breast thermography to accurately detect abnormalities linked to breast cancer. It helps to extract the ROI in thermal images, improving diagnostic precision. Traditional methods like thresholding, edge detection, and region growing have been widely used but often struggle with noise, contrast issues, and thermal intensity variations. Recently, deep learning-based approaches, especially CNNs, have shown better accuracy and reliability. However, standardizing the segmentation remains a challenge due to differences in thermal contrast and anatomical variations [6]. Jayagayathri et al. [7] experimented with CNN architectures like DenseNet201 and ResNet101 for segmenting breast thermograms, achieving high classification accuracy. However, they mentioned that limited annotated datasets hinder real-time clinical applications. Kamila Fernanda et al. [8] proposed an elliptical segmentation model and evaluated its accuracy using the Dice Similarity Index and Pearson correlation. While their approach showed moderate success, improvements are needed for better ROI extraction and alignment. Dharani et al. [9] developed an enhanced CNN model combined with Fuzzy C-means clustering for ROI segmentation. Thanh Nguyen Chi et al. [10] introduced a lightweight CNN model optimized with a Chi-square filter and an SVM classifier. Despite of good performance, CNN models are computationally complex, requiring more efficient alternatives. Mohammed Abdulla Salim Al Husaini et al. [11] explored real-time segmentation using deep learning models like Inception v3 and v4, achieving a good accuracy but facing issues such as motion artifacts and image quality.

Among segmentation techniques, active contour models like the Snake algorithm are notable for refining boundaries iteratively. Eddie et al. [4] modified the Snake algorithm by incorporating pre-processing, gradient vector flow, and high-pass filtering, improving boundary detection. However, their method is sensitive to the initial contour placement and has slow convergence, affecting performance. Elliptical segmentation [14] has also gained attention due to the natural elliptical shape of the breast. Pu et al. [12] applied an ellipse-fitting method for mammogram registration, enhancing accuracy in mass localization across different views. Marcus C. Araújo et al. [3] explored elliptical segmentation for thermographic analysis, showing its effectiveness in anatomical conformity and ROI extraction. However, this method struggles when breast boundaries do not follow a perfect elliptical shape. This article compares the Snake algorithm and elliptical segmentation for breast thermography. By analysing their strengths and limitations, we aim to determine the most effective approach for improving breast cancer detection accuracy.

3. METHODOLOGY

3.1 Dataset Used

Breast thermogram images used in this study were obtained from the Database for Mastology Research (DMR) at Visual Lab, Fluminense Federal University, Brazil [13]. The images were acquired using a FLIR SC620 infrared camera with a resolution of 640 × 480 pixels. The dataset includes thermograms from patients with confirmed breast tumors based on clinical examination, ultrasound, mammography, and biopsy results.

3.2 Snake Algorithm based Segmentation

The Snake Algorithm, or Active Contour Model, is employed to detect and refine breast boundaries in thermal images through energy minimization [4] [14]. It iteratively adjusts the contour to align with object edges using internal and external forces. The segmentation steps include:

a. Gaussian filtering to reduce noise and enhance edge clarity.
b. Place an initial contour around the ROI.
c. The Snake model iteratively refines the boundary by balancing internal and external energy functions.

The Snake algorithm is governed by parameters α (smoothness control), β (stiffness), and γ (external force impact). Convergence occurs when contour movement stabilizes, effectively delineating the breast region.

3.3 Ellipse based Segmentation

An alternative segmentation method is the Elliptical Curve Approach, which simplifies the ROI definition by fitting elliptical curves to breast tissue boundaries based on thermal data [3] [13]. Figure 1 outlines the CAD model consists of filtering, segmentation into right and left breasts, followed by feature extraction and training/testing an SVM model.

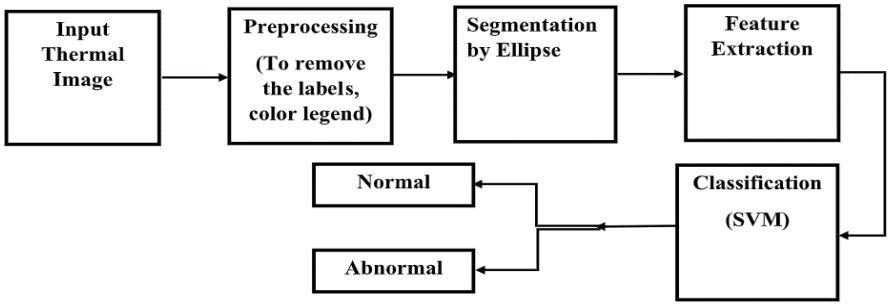

Figure 1. Classification using Ellipse method

Given the elliptical anatomical structure of the breast, an ellipse-fitting method is employed for segmentation [13]. The segmentation process consists of:

a. Define centres and radii based on breast size & shape to generate elliptical masks for the left and right breast regions.
b. Superimpose the elliptical masks onto the original thermogram to segment the breast regions.
c. Apply Gaussian filter to reduce noise while preserving key details.
d. Sharpen the image to refine boundaries, ensuring temperature variations remain visible.

3.4 Feature Extraction and Classification

After segmenting the breast regions into left and right from the thermal images using elliptical masks, texture features were extracted using the Gray-Level Co-occurrence Matrix (GLCM) as shown in Table 1, Also, patient history features such as age (F6) and dietary habits (F7) are considered to improve classification accuracy. The dataset consists of 100 images (50 normal, 50 abnormal).

Table 1 List of features extracted

Features Extracted						
GLCM Features					**History of Patient**	
Contrast (F1)	Correlation (F2)	Homogeneity (F3)	Energy (F4)	Entropy (F5)	Age (F6)	Eating habits (F7)

Asymmetry analysis is performed by computing feature values separately for the right and left breast regions, with absolute differences used to quantify texture variations. A statistical t test is then conducted to assess the significance of these differences in distinguishing normal and abnormal breast thermograms. The segmentation performance is evaluated using Jaccard Coefficient (JC), which measures the similarity between segmented regions and ground truths and computation speed to assesses the efficiency of Snake and Elliptical segmentation methods in processing breast thermograms.

4. RESULTS AND DISCUSSIONS

4.1 Segmentation Results

The Snake method, requires precise tuning of parameters to balance flexibility and accuracy. Alpha (α) controls elasticity, preventing excessive stretching; Beta (β) ensures smoothness by reducing sharp bends; Gamma (γ) adjusts the speed of convergence; and Kappa (κ) determines sensitivity to image edges. Also, weights (wEline, wEedge, wEterm) influence how the algorithm detects intensity and boundaries. With 200 iterations, the algorithm processed each image in 13,560 milliseconds. Increasing to 5000 iterations improved boundary accuracy but significantly increased computation time. While the method effectively captured complex breast contours, it struggled with weak edges in certain cases, requiring further refinement.

The Ellipse segmentation method was applied to 100 breast thermograms, successfully isolating the region of interest in each case. This method efficiently separated left and right breast regions while maintaining segmentation accuracy. Compared to the Snake Algorithm, the Ellipse method required only 2256 milliseconds

per image, demonstrating its computational efficiency. The JC is computed for segmented breast images and ground truth images, as shown in Table 2

Table 2 JC and Computation Time for Snake and Ellipse Method

Method	**JC**	**Computation Time**
Snake	0.78	13560 msec
Ellipse	0.72	2256 msec

The comparison of segmentation algorithms based on JC and computation time highlights the trade-off between accuracy and efficiency. The Snake Algorithm achieved a JC of 0.78, indicating a higher segmentation accuracy compared to the Ellipse Method (JC = 0.72). However, this improved accuracy comes at a cost, as the Snake Algorithm requires significantly more processing time of 13560 msec per image due to its iterative contour refinement process. In contrast, the Ellipse Method completed segmentation in just 2256 msec, demonstrating its computational efficiency.

The Ellipse segmentation method effectively handled various breast morphologies, including small, medium, large, and asymmetric breasts, as shown in Figure 2.

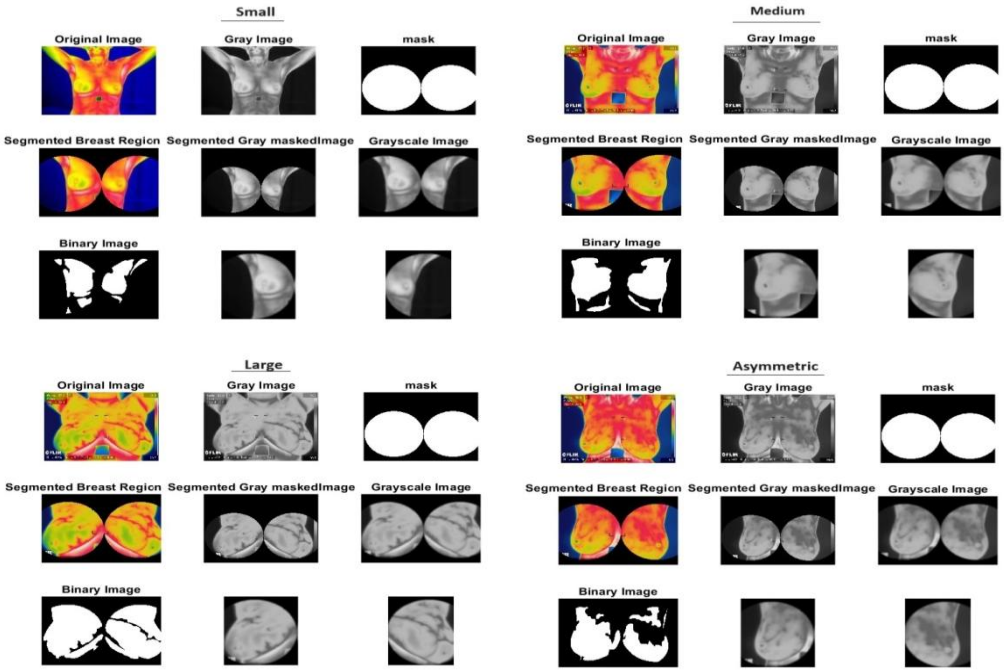

Figure 2: Segmentation outputs for different types of breasts

4.2 Feature Extraction and Classification

In this study, GLCM based texture features were computed from the segmented left and right breast regions to analyze asymmetry. A statistical t-test was performed to evaluate the effectiveness of each feature in distinguishing normal and abnormal breasts. The results indicate that correlation, energy, homogeneity, and entropy did not show a statistically significant difference between the two classes. However, contrast (F1), eating habits (F7), and age (F6) were found to be significant, with age being the most influential feature (p = 0.0065). The statistical significance of extracted features is summarized in Table 3.

Table 3 Significance level of extracted features using t test

Features	F1	F2	F3	F4	F5	F6	F7
Significance Level	0.0502	0.1652	0.07686	0.0614	0.0583	0.0065	0.0412

For classification, a SVM cubic classifier was trained using the three significant features from the dataset consisting of 100 thermograms (50 normal, 50 abnormal cases). The trained model achieved an accuracy of 78%, indicating its effectiveness in distinguishing normal and abnormal thermograms.

5. CONCLUSION

This study compared Snake and Ellipse segmentation methods for breast thermogram analysis, highlighting a trade-off between accuracy and computational efficiency. The Snake Algorithm achieved higher segmentation accuracy (Jaccard Index = 0.78) but required more processing time, whereas the Ellipse Method provided faster segmentation (2.2 sec) with slightly lower accuracy. Feature extraction using GLCM revealed that contrast, eating habits, and age were the most significant factors in distinguishing normal and abnormal breast thermograms, with age ($p = 0.0065$) being the strongest indicator. A cubic SVM classifier, trained using these key features, achieved an accuracy of 78%, demonstrating the feasibility of combining efficient segmentation with clinically relevant features for automated breast cancer detection. Future work can explore hybrid segmentation models to improve accuracy while maintaining computational efficiency for real-time applications

6. REFERENCES

[1] I. A. f. R. o. C. (. (. G. C. O. C. Today., 2020. [Online]. Available: https://gco.iarc.fr.

[2] D. Sathish, S. Kamath, R. KV and K. Prasad, “Medical imaging techniques and computer aided diagnostic approaches for the detection of breast cancer with an emphasis on thermography - A review,” International Journal of Medical Engineering and Informatics, Inderscience, vol. 8, no. 3, pp. 275- 299, 2016.

[3] M. C. Araújo, R. C. Lima and R. M. d. Souza, “Interval symbolic feature extraction for thermography breast cancer detection,” Expert Systems with Applications, vol. 41, no. 1, p. 6728–6737, 2014.

[4] E. Y.-K. NG and Y. CHEN, “SEGMENTATION OF BREAST THERMOGRAM: IMPROVED BOUNDARY DETECTION WITH MODIFIED SNAKE ALGORITHM,” Journal of Mechanics in Medicine and Biology, vol. 6, no. 2, pp. 123-136, 2006.

[5] D. Sathish, S. Kamath, K. Prasad and R. K. a. R. J. Martis, “Asymmetry Analysis of Breast Thermograms using Automated Segmentation and Texture Features,” Signal, Image and Video Processing, Springer, vol. 11, no. 4, pp. 745-752, 2017.

[6] J. S. a. A. S. Arora, “Automated approaches for ROIs extraction in medical thermography: a review and future directions,” Multimedia Tools and Applications, vol. 79, no. 1, p. 15273–15296, 2020.

[7] J. Iyadurai, M. Chandrasekharan and S. Muthusamy, “An Extensive Review on Emerging Advancements in Thermography and Convolutional Neural Networks for Breast Cancer Detection,” Wireless Personal Communications , vol. 137, no. 1, p. 1797–1821, 2024.

[8] K. F. F. C. d. Queiroz, J. R. A. d. Q. Júnior and H. D. a. R. d. C. F. d. Lima, “Automatic segmentation of region of interest for breast thermographic image classification,” Research on Biomedical Engineering , vol. 39, no. 1, pp. 199-208, 2023.

[9] N. P. Dharani, I. G. Immadi and M. V. Narayana, “Enhanced deep learning model for diagnosing breast cancer using thermal images,” Soft Computing, vol. 28, no. 1, p. 8423–8434, 2024.

[10] T. N. Chi, H. L. T. Thu and T. D. Q. a. D. Taniar, “A Lightweight Method for Breast Cancer Detection Using Thermography Images with Optimized CNN Feature and Efficient Classification,” Journal of Imaging Informatics in Medicine.

[11] M. A. S. A. Husaini and M. H. H. a. M. R. Islam, “Real time thermography for breast cancer detection with deep learning,” Discover Artificial Intelligence, vol. 4, no. 57, 2024.

[12] J. Pu, B. Zheng, J. K. Leader and D. Gur, “An ellipse-fitting based method for efficient registration of breast masses on two mammographic Views,” Medical Physics, vol. 35, no. 2, pp. 487-494, 2008.

[13] P. D. f. M. R. (DMR). [Online]. Available: Available at http://visual.ic.uff.br/en/proeng. [Accessed October 2022].

[14] S. Tello-Mijares and F. W. a. F. Flores, "Breast Cancer Identification via Thermography Image Segmentation with a Gradient Vector Flow and a Convolutional Neural Network," Journal of Healthcare Engineering Volume 2019, Article ID 9807619, 13 pageshttps://doi.org/10.1155/2019/9807619, vol. 2019, pp. 1-13.

EEG data Analysis for Schizophrenia Detection Using a Deep Neural Network-Based Multilayer Perceptron

Balivada Anjanee Kumar [1],Bhusa devi [2],Srujana Vijjapu[3],Aswani Malla[4],Kumar Penugudhuru[5]
Dadi Institute of Engineering and Technology (A), Anakapalli, India
dranjaneekumar@gmail.com[1] bhusadevi1991@gmail.com[2],
srujanavijjapu123@gmail.com[3] aswinimalla11@gmail.com[4],
kumar.143.penugudhuru@gmail.com[5]

Abstract.

This study explores EEG-based schizophrenia detection using a deep learning approach. A multilayer perceptron (MLP) model processes EEG data, extracts features, and classifies individuals with or without schizophrenia. The model effectively handles high-dimensional data, highlighting the potential of deep learning in neuropsychiatric diagnosis.

Keywords. Schizophrenia Detection, EEG Data Analysis, Deep Neural Network, Multilayer perceptron

1. INTRODUCTION

This study uses EEG-based deep learning, specifically an MLP model, to detect schizophrenia. It automates feature extraction, overcoming limitations of traditional methods. Advanced preprocessing enhances classification accuracy. Validated on public data, it outperforms conventional techniques. This research supports deep learning for non-invasive schizophrenia diagnosis. EEG data analysis happens to be one of the newly developed forms of diagnosis in neuroscience and clinical research. Among all these kinds of disorders, schizophrenia is very complex among all the mental disorders as it has a disturbance over cognition, behaviour, or emotions, which is, in turn, a hard problem to diagnose. Classification models are:

1. EEG Database
2. Preprocessing EEG Signals
3. Feature Extraction

2. LITERATURE REVIEW

Overview of many studies that were conducted on EEG-based schizophrenia detection analysed datasets with 10 to 54 patients and control groups of different sizes. Both resting-state and task-based EEG recordings were used, with sampling rates from 128 Hz to 1024 Hz. EEG channel counts ranged from 14 to 60, depending on data collection protocols.

3. METHODOLOGY

The methodology involves preprocessing EEG data using bandpass filtering (0.5-45 Hz) and Independent Component Analysis (ICA) to remove noise and artifacts. Signals are segmented into time windows for better analysis and normalized to zero mean and unit variance. This prepares the data for deep learning-based classification using an MLP model.

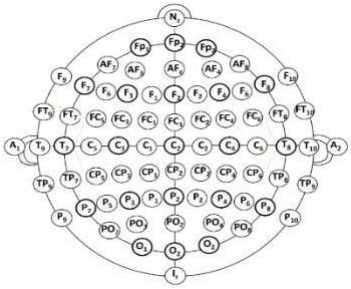

Fig 3. Spacing of Electrodes

3.1 Preprocessing

The processing of EEG data toward achieving a diagnosis using machine learning techniques. It starts with collecting raw EEG signals, which typically contain noise and artifacts. These signals undergo preprocessing steps such as filtering to remove noise, normalization to standardize the data, and artifact removal to eliminate unwanted interferences like eye blinks or muscle movements. After the data cleaning process, relevant information from both time and frequency domains is derived as feature extraction for the better identification of patterns in signals.

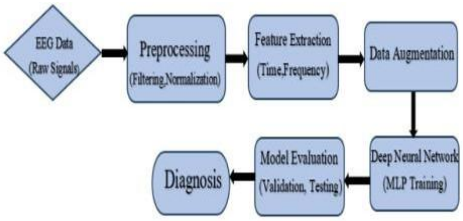

Fig 3.1 EEG Data Processing

➢ **Artificial Rejection**

Artifact rejection ensures that the EEG signals used for analysis are clean and reliable, enhancing the accuracy of downstream applications like feature extraction and classification. These methods are often combined to achieve optimal results depending on the dataset and application requirements.

➢ **Signal Filtering**

Signal filtering is a crucial step in the preprocessing of EEG data, as it helps remove noise and unwanted artifacts, ensuring that the analysis focuses on the relevant brain activity. The goal is to retain the frequencies that are meaningful for the research while eliminating unwanted signals that could distort the results.

➢ **Normalization**

Normalization is an important step in the preprocessing of EEG signals, ensuring that the data is scaled consistently across different channels and participants. This step is crucial for improving the performance and convergence of machine learning models, such as deep neural networks, by standardizing the amplitude and range of the signals.

3.2 Feature Extraction

- TIME-FREQUENCY ANALYSIS:

Time-frequency analysis involves studying the EEG signal in both the time and frequency domains simultaneously, providing a comprehensive view of brain activity. This approach is particularly useful when analysing non-stationary signals like EEG, which can have dynamic frequency content over time.

- SHORT-TIME FOURIER TRANSFORM:

STFT decomposes a signal into multiple frequency components over short overlapping windows. It allows for the analysis of how different frequencies evolve over time. The EEG signal is divided into small segments (or windows), and for each segment, the Fourier transform is applied to obtain the frequency spectrum.

4. RESULTS AND DISCUSSION

- TRAINING AND TESTING ACCURACY:

The proposed deep neural network model for schizophrenia detection achieves over 90% training accuracy but only around 70% testing accuracy, indicating overfitting. This issue becomes noticeable after 20 epochs, suggesting the model captures noise rather than generalizable patterns. To improve reliability, techniques like dropout, weight decay, and early stopping can be applied, along with increasing dataset size and diversity. Despite its limitations, the model shows potential but requires further optimization and validation on larger datasets. Integrating other modalities like fMRI or genetic data could enhance diagnostic accuracy.

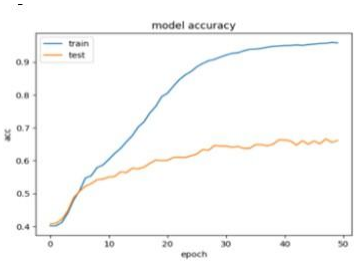

Fig 4.1 Training And Testing Accuracy

- TRAINING AND TESTING LOSS:

The graph shows that while training loss decreases consistently, testing loss stabilizes around 0.68 after 15–20 epochs, indicating overfitting. This suggests the model captures noise, reducing its generalization to unseen data. Techniques like early stopping, dropout, weight decay, or increasing dataset diversity can help improve performance. Despite effective learning from training data, optimization is needed to enhance reliability for schizophrenia detection using EEG signals.

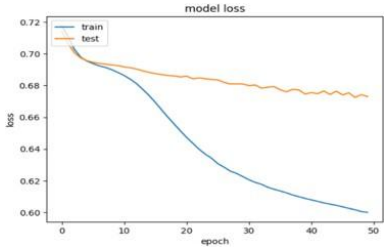

Fig 4.2 Training And Testing Loss

The proposed Deep Neural Network-Based Multilayer Perceptron (MLP) model for EEG-based schizophrenia detection showed highly promising results, indicating its potential as an effective diagnostic tool. The AUC-ROC reveals the discriminative power the model has at various cutoff thresholds. A confusion matrix analysis in detail shows there are low false-positive cases and a low false-negative case thereby bringing out the model's high specificity as well as sensitivity, so important for real-world clinical implementation where misclassification can result in serious consequences.

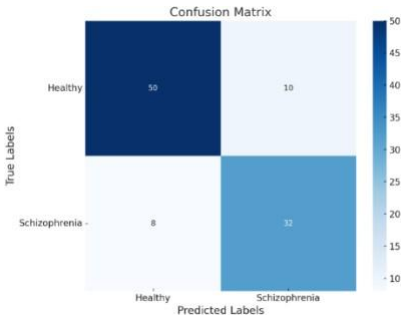

Fig 4.3 Confused Matrix

5. REFERENCES

[1] Bajpai, A., Kesaria, A. and Briskilal, J., 2024, May. Schizophrenia Detection using Electroencephalography Signals Using Deep Learning. In *2024 International Conference on Current Trends in Advanced Computing (ICCTAC)* (pp. 1-6). IEEE.

[2] De Miras, J.R., Ibáñez-Molina, A.J., Soriano, M.F. and Iglesias-Parro, S, 2023.

Schizophrenia classification using machine learning on resting-state EEG signal. Biomedical Signal Processing and Control, 79, p.104233.

[3] Cui, Y., Li, C., Liu, B., Sui, J., Song, M., Chen, J., Chen, Y., Guo, H., Li, P., Lu, L. and Lv, L., 2022. Consistent brain structural abnormalities and multisite individual classification of schizophrenia using deep neural networks. The British Journal of Psychiatry, 221(6), pp.732-739.

[4] Montazeri, M., Montazeri, M., Bahaadinbeigy, K., Montazeri, M. and Afraz, A., 2023. Application of machine learning methods in predicting schizophrenia and bipolar disorders: A systematic review. *Health Science Reports*, *6*(1), p.e962.

[5] Sun, J., Cao, R., Zhou, M., Hussain, W., Wang, B., Xue, J. and Xiang, J., 2021. A hybrid deep neural network for classification of schizophrenia using EEG Data. Scientific Reports, 11(1), p.4706.

- **Biographies**



Dr. B. Anjanee Kumar, an Associate Professor at Dadi Institute of Engineering and Technology, has 8 years of teaching experience and a PhD in "Optimization of Novel Design Architecture for Enhancing Lifetime in Battery Limited Sensor Nodes." He has presented over 40 papers in national and international conferences, and is an invited reviewer and chair of numerous international conferences.







Srujana Vijjapu, Aswani Malla, and Kumar Penugudhuru are final-year Bachelor of Electronics and Communication Engineering students at Dadi Institute of Engineering and Technology. Srujana is a driven student who prioritizes creativity and quality. Aswani is committed to using his technological expertise to solve practical problems. Through more learning, Kumar hopes to advance and make a contribution to the field. They work together to broaden their expertise and contribute significantly to the engineering field.

Deploying a Raspberry pi Zero for Overhead Flight Detection with SDR And FlightAware

Nithya S[1] , Naveen Kumar R[2],Jaiwanth B[3] ,Logu Vishal D[4] [1]KPR Institute of Engineering and Technology – s.nithya@kpriet.ac.in [2]KPR Institute of Engineering and Technology – nk1829774@gmail.com
[3]KPR Institute of Engineering and Technology – jaiwanthboopathi@gmail.com

[4]KPR Institute of Engineering and Technology – lguvishalkalpana@gmail.com

Abstract.

This paper introduces an affordable system for detecting overhead flights using a Raspberry Pi Zero, Software-Defined Radio (SDR), and the FlightAware platform. The system captures ADS-B signals from aircraft to retrieve real-time flight data, including identification, altitude, and location. It effectively processes data on the resource-limited Raspberry Pi Zero and presents the information through FlightAware. The proposed solution is cost-efficient, dependable, and beneficial for aviation researchers and enthusiasts. This study underscores the potential of low-cost IoT devices for real-time flight tracking and monitoring.

Keywords. Aircraft Detection, Software-Defined Radio, ADS-B Signal Processing, Low- Cost Tracking Systems, Air Traffic Detection.

1. INTRODUCTION

The growing need for real-time aviation monitoring has driven the search for cost- effective methods of overhead flight detection. This paper explores the implementation of a Raspberry Pi Zero, combined with Software-Defined Radio (SDR) and the FlightAware platform, to develop an efficient, budget-friendly, and portable system for tracking aircraft. As a compact and energy-efficient computing device, the Raspberry Pi Zero serves as a suitable foundation for low-cost, DIY flight tracking solutions. By integrating it with an SDR receiver, the system captures and decodes ADS-B (Automatic Dependent Surveillance– Broadcast) signals transmitted by aircraft, extracting essential flight details such as position, speed, and altitude. The processed data is then visualized using FlightAware, a global flight tracking network that enables users to share and contribute real- time flight information. This system empowers aviation researchers, enthusiasts, and individuals in airspace-sensitive regions to monitor local air traffic, enhancing awareness of flight patterns. Additionally, it provides an open-source framework for tracking and analysing aircraft movements, fostering innovation and collaboration within the aviation

All Open Access articles are peer-reviewed, distributed under the Creative Commons Attribution-Non Commercial 4.0 International

sector. The proposed solution presents an economical, scalable approach to aviation data collection, with potential applications in both educational and professional fields.

2. LITERATURE REVIEW

- Smith et al. (2007) explore strategies to enhance ADS-B system security through redundancy, encryption, and anomaly detection. These methods strengthen reliability by identifying spoofed signals and ensuring functionality during system failures. Although they improve security, they also introduce higher complexity and costs. Despite these challenges, such measures are crucial for maintaining secure air traffic management. [1]

- Ramirez et al. (2019) introduce Longshot, a technique for long-range time synchronization that leverages low-latency signal processing. This approach ensures accurate coordination across vast distances, benefiting applications such as GPS and IoT networks. While effective, environmental interference can affect its performance. Nevertheless, Longshot offers a scalable and efficient solution for precise synchronization. [2]
- Moser et al. (2019) propose a passive radar system utilizing IoT hardware to detect objects by processing existing broadcast signals. This technology provides an economical alternative to conventional radar, making it useful for surveillance applications. However, limitations in range and signal interference can impact performance. Even so, it presents a viable and cost-effective option for practical use. [3]
- Eichstaedt and Budroweit (2022) develop a multi-channel ADS-B receiver designed for space applications, utilizing GNU Radio and SDR technology. The system efficiently decodes aircraft signals in space, offering real-time monitoring, compact size, and low power consumption. However, its coverage is more restricted in space than in terrestrial environments. Still, it holds potential for satellite-based air traffic management. [4]
- Varga et al. (2015) introduce a real-time air traffic monitoring system utilizing ADS-B technology to track aircraft positions and movements. While effective, its functionality relies on the availability of ADS-B signals. Despite this limitation, the system significantly enhances situational awareness in air traffic control. [5]

3. PROBLEM IDENTIFICATION

3.1. Problem Statement

Aviation monitoring requires a cost-effective, portable, and efficient solution for real-time flight detection and tracking. Many existing systems depend on expensive, complex infrastructure, making them less accessible to hobbyists, researchers, and small-scale applications. This limitation restricts the ability to monitor aircraft movements and collect essential data such as position and altitude. Developing an affordable alternative would expand access to real-time flight information, fostering greater engagement in aviation awareness, research, and hobbyist activities.

3.2. Risk dentification

- Obtaining real-time flight data is often expensive and technically demanding, restricting access for hobbyists, researchers, and small-scale users. A budget- friendly alternative involves integrating a Raspberry Pi Zero with an SDR and FlightAware to receive and decode ADS-B signals. This compact and easy-to- deploy system offers real-time flight tracking, making aviation monitoring and analysis more accessible to a wider audience.
- ADS-B signal reception may be affected by interference, hardware constraints, or suboptimal antenna placement, resulting in incomplete or inaccurate flight data. To mitigate these issues, the system utilizes an optimized antenna and fine-tuned SDR settings. These enhancements improve signal reception, ensuring consistent and reliable data capture even in challenging environments.

4. METHODOLOGY

This methodology describes the implementation of a Raspberry Pi Zero-based system for detecting and tracking overhead aircraft using a Software-Defined Radio (SDR) and integrating the collected data with FlightAware for real-time visualization. The system leverages Automatic Dependent Surveillance-Broadcast (ADS-B) technology, which enables aircraft to transmit critical flight information such as position, altitude, speed, and identification. A structured block diagram illustrates the interactions between the system's hardware and software components, ensuring smooth operation. The hardware setup consists of a Raspberry Pi Zero,

which functions as the central processing unit, handling data acquisition, decoding, and transmission. An SDR module captures ADS-B signals broadcasted at a frequency of 1090 MHz, while a high-gain antenna improves signal reception, allowing detection of aircraft at considerable distances.

On the software side, an ADS-B signal processing module decodes raw radio frequency signals into meaningful flight data using open-source tools like dump1090. The processed data is then formatted and transmitted to FlightAware servers via an API or a direct integration pipeline, where it is combined with global sources to provide accurate and comprehensive flight tracking. The system workflow begins with the antenna receiving ADS-B signals, which are digitized by the SDR and processed by the Raspberry Pi Zero to extract relevant flight details. This data is subsequently uploaded to FlightAware, enabling users to view live updates and detailed flight paths through its online platform.

4.1. Implementation

- This lightweight operating system is well-suited for optimizing performance on the Raspberry Pi Zero. After downloading, the OS image is written onto a microSD card using software such as Balena Etcher. Once the image is successfully written, initial configurations are applied. To enable SSH for remote access, a file named ssh is created in the boot partition of the SD card. Additionally, for Wi-Fi connectivity, a wpa_supplicant.confige file is added, containing the required network credentials. These steps ensure seamless remote management and network access for the Raspberry Pi Zero.
- After inserting the microSD card into the Raspberry Pi, the device is powered on. To ensure the system is up to date, the following command is executed Sudo apt update && Sudo apt upgrade -y. This updates the package lists and installs the latest software versions. Next, Pi Aware, a FlightAware software package for ADS-B data reception, is installed. This involves downloading the required repository using the w get command, adding it to the system, and installing Pi Aware with Sudo apt-get install pi Aware. Additionally, the SDR software dump1090 fa, which decodes ADS-B signals, is installed using Sudo apt-get install dump1090-fa This setup enables the Raspberry Pi Zero to receive and process ADS-B transmissions effectively.
- Once the software setup is complete, the hardware components are connected. The SDR is linked to the Raspberry Pi using a USB OTG cable, and an antenna is attached to the SDR for signal reception. After these connections are made, the Raspberry Pi is powered on. If each node in this system is connected to the internet and assigned a unique IP address, the network can be scaled indefinitely. This would create a distributed sensor network with the ability to cover large areas and gather extensive data.

5. CONCLUSION

The integration of the Raspberry Pi Zero with Software-Defined Radio (SDR) and FlightAware presents an efficient and cost-effective approach to real-time flight detection. By decoding ADS-B signals, this system enables continuous monitoring of aircraft position, velocity, and other crucial data. Its affordability and portability make it accessible to a wide range of users, from aviation enthusiasts to researchers. Additionally, its scalability allows for seamless integration into global flight tracking networks, enhancing overall airspace awareness. This technology democratizes access to aviation data, fostering collaboration and innovation in flight monitoring. As more individuals and organizations contribute to these networks, the accuracy and coverage of global flight tracking will continue to improve, leading to advancements in both commercial and research applications.

6. REFERENCES

[1] A. Smith; R. Cassell , T. Breen, R. Hulstrom, C. Evers , Methods to Provide System- Wide ADS-B Back-Up, Validation and Security, 2006 ieee/aiaa 25TH Digital Avionics Systems Conference 2007

[2] Ceferino Gabriel Ramirez; Assya Dyussenova; Anton Sergeyev; Bob Iannucci, Longshot: Long-Range Synchronization of Time,2019 18th ACM/IEEE International Conference on Information Processing in Sensor Networks (IPSN) 2019.

[3] Daniel Moser, Giorgio Tresoldi , Chritof Schupbach ,Vincent Lenders, "Design and Evaluation of a Low-Cost Passive Radar Receiver Based on IoT Hardware" , IEEE Radar Conference (RadarConf) 2019.

[4] Felix Eichstaedt ,Jan Budroweit ,"Evaluation of a GNU Radio-based multi-channel ADS-B receiver implemented on a highly integrated SDR platform for space application", IEEE Space Hardware and Radio Conference (SHaRC) 2022.

[5] Mihaly Varga , Zsolt Alfred Polgar, Horia Hedesiu, "ADS-B based real-time air traffic monitoring system" 38th International Conference on Telecommunications and Signal Processing (TSP) 2015.

Biographies



Nithya S, female, Assistant Professor- III for department of Electronics and Communication Engineering at KPR Institute of Engineering and Technology.



Naveen Kumar R, male, BE student specializing in Electronics and Communication Engineering (ECE) at KPR Institute of Engineering and Technology.



Jaiwanth B, male, BE student specializing in Computer Science and Engineering (ECE) at KPR Institute of Engineering and Technology.



Logu Vishal D, male, BE student specializing in Electronics and Communication Engineering (ECE) at KPR Institute of Engineering and Technology.

Towards Smart Transportation: The Synergy of Space Shift Keying and Reconfigurable Intelligent Surfaces for Future V2V Networks.

Suhas K and Goutham Simha G D

Department of Electronics and Communication Engineering, Manipal Institute of Technology, Manipal Academy of Higher Education, Manipal, India. *Email: suhas.k@manipal.edu, goutham.simha@manipal.edu*

Abstract.

In search of smarter and more efficient transportation networks, the integration of Space Shift Keying (SSK) and Reconfigurable Intelligent Surfaces (RIS) for future Vehicular-to-Vehicular (V2V) networks is analysed. With 28 GHz mm-wave (FR2 n261 Band), the proposed scheme utilizes SSK's distinguishing feature in terms of efficient use of energy and RIS for assured delivery of signals. Performance investigation is conducted over key performance factors such as Bit Error Rate (BER), Received Signal Strength Indicator (RSSI), Reference Signal Received Power (RSRP), path loss analysis in NLoS and LoS scenarios, and Channel Impulse Response (CIR) analysis. In identifying the potential of RIS to compensate for path loss and improve signal quality even in poor (Rain-faded weather) propagation scenarios, SSK and RIS viability for supporting reliable 5G-based V2V communications is shown in this work. In providing a platform for developing future V2V networks towards smart and connected transportation networks, this work paves avenues for future development and enhancements in vehicular networks for efficient and reliable communications in smart and connected transportation networks.

Keywords. RIS, SSK, MIMO, Rician channel, CI model.

1. INTRODUCTION

Ongoing research in V2V communication focuses on various aspects, including performance evaluation and the integration of emerging technologies such as Reconfigurable Intelligent Surfaces (RIS). These technologies will improve connectivity and safety in vehicular networks, and this will lead to completely automated traffic management systems [1]. RIS technology allows control of the wireless signal propagation channels, which consequently results in signal power enhancement and overall communication efficiency [2]. By controlling the reflection of radio waves, RIS can create secure communication channels that are only available to legitimate vehicles, thus reducing the dangers of eavesdropping and spoofing attacks [3].

Space Shift Keying (SSK) is a recently introduced digital modulation technique that finds its major applications in wireless communication systems, specifically in Multiple-Input Multiple-Output (MIMO) channels. SSK is a notable contribution to the vast area of Spatial Modulation (SM) techniques. The concept of SSK is to convey information through the activation of some antennas on the transmitter side; the data symbol is conveyed by the index of the active antenna, hence differing from the traditional modulation schemes that employ the change in the carrier signal [4][5].

The receiver de-multiplexes the information transmitted based on the detection of the active antenna, thus mitigating inter-channel interference and minimizing receiver implementation complexity. Lower receiver design complexity is one of the main advantages of Shifted Signal Keying (SSK). This characteristic makes it extremely desirable to applications where receiver complexity reduction is desirable, e.g., in sensor networks and the Internet of Things (IoT) [4][6].

SSK benefits automatically from spatial diversity because it uses more than a single antenna. Spatial diversity can reverse fading effects and improve the channel robustness [5]. SSK can also fight certain types of interference effectively by utilizing the spatial variation of the signal to enable stable transmission of data even in adverse conditions [6].

2. System and Channel Model:

The combination of Spatial Shift Keying (SSK) and Reconfigurable Intelligent Surfaces (RIS) is of enormous potential to revolutionize vehicular communication systems. For instance, RIS can resolve issues like signal obstructions, interference, and path attenuation by sending reflected signals directly to the moving vehicles even in the case of changing environments. This combination is especially helpful in urban environments with obstructions or highways where vehicles are traveling at high speeds. Additionally, both SSK and RIS are low-power consumption technologies, which are ideal for future vehicular networks emphasizing sustainability and scalability without compromising performance.

In vehicular networks, the whole channel consists of three components: the direct link between the vehicle and the transmitter, the transmitter-RIS link, and the RIS-vehicle link. The direct link is prone to severe fading and building, vehicle, or other obstacles' blockage. The RIS-assisted link, on the other hand, has the benefit of the surface to dynamically adjust to changing conditions to enhance the signal strength and reliability. The RIS-vehicle interaction is the most difficult due to the mobility of the vehicles, leading to Doppler shifts and rapidly changing channel conditions. To overcome these difficulties successfully, the channel model needs to include aspects of path loss, small-scale fading—grounded in Rayleigh or Rician fading—as well as Doppler-induced phase oscillations. Environmental factors, such as rain, also impair the signal, and the RIS needs to continuously adjust its phases accordingly to provide uniform communication. With the deployment of this wide-spectrum channel model, SSK-RIS systems can significantly improve signal reliability, efficiency, and robustness, which in turn translates into more secure and reliable vehicular communication networks.

Path Loss (CI Model): $PL(d_{rr,k,m}) = PL_0 + 10.n.log_{10}\left(\frac{d_{rr,k,m}}{d_0}\right)$ (1)

Channel coefficient(Rician Model):

$$h_{rr,k,m}(t) = \sqrt{\frac{K}{K+1}}\, h_{LOS,k,m}(t) + \sqrt{\frac{1}{K+1}}\, h_{NLOS,k,m}(t) \quad (2)$$

LOS Component: $h_{LOS,k,m}(t) = a_{rr,k,m}(t).e^{j(2\pi f_{D,m}t+\phi_{rr,k,m})}$ (3)

NLOS Component: $h_{NLOS,k,m}(t) = X_{k,m} + jY_{k,m}$ (4)

The received signal $y_k(t)$ at the kth receiver antenna becomes

$$y_k(t) = \underbrace{\sqrt{P}h_{d,s,k}(t)}_{Direct\ Link} + \underbrace{\sqrt{P}\sum_{m=1}^{M} h_{rr,k,m}(t)\,.\,e^{j\phi_m}.h_{tr,s,m}(t)}_{RIS\ Assisted\ Link\ with\ Rain\ Fading} + n_k(t) \quad (5)$$

Expanding the RIS-assisted link term,

$$\sum_{m=1}^{M} h_{rr,k,m}(t)\,.\,e^{j\phi_m}.h_{tr,s,m}(t) = \sum_{m=1}^{M}\left[\sqrt{\frac{K}{K+1}}a_{rr,k,m}(t).e^{\frac{-A_r}{20}}.e^{j(2\pi f_{D,m}t+\phi_{rr,k,m})} + \sqrt{\frac{1}{K+1}}h_{NLOS,k,m}(t)\right].e^{j\phi_m}.h_{tr,s,m}(t) \quad (6)$$

where,

$a_{rr,k,m}(t)$ is the time-varying amplitude due to path loss, computed using the CI model. $f_{D,m}$=$\lambda v cos(\theta_m)$is the Doppler shift for the mth RIS element. $\phi_{rr,k,m}$ is the initial phase offset $h_{d,s,k}(t)$ is the direct link channel coefficient, also modeled using the CI and Rician models. $h_{rr,k,m}(t)$ is the RIS-to-vehicle channel coefficient, incorporating both LOS and NLOS components as described above $h_{tr,s,m}(t)$ is the static transmitter-to-RIS channel coefficient

3. Simulation Results:

This paper analyses SSK-based RIS for V2V communication in detail. The performance evaluations are targeted at aspects such as BER vs. SNR, RSSI vs. distance, and path loss due to extreme weather conditions such as heavy rain and fog, as well as large and small fading effects considering CI and Rician fading models, respectively, adding Doppler shifts and NLoS/LoS channel errors to account for real-world vehicular communications. SSK with RIS takes advantage of spatial diversity and better energy efficiency; thus, it is

expected to be a better choice in vehicular networks. This research advances to demonstrate how SSK-RIS-based V2V architectures are used to mitigate signal degradation and improve coverage, particularly in harsh environments, for 28GHz communications. The results indicate that the combination of SSK with RIS improves communications' reliability, thus promising the use of this approach for robust and efficient V2V connectivity.

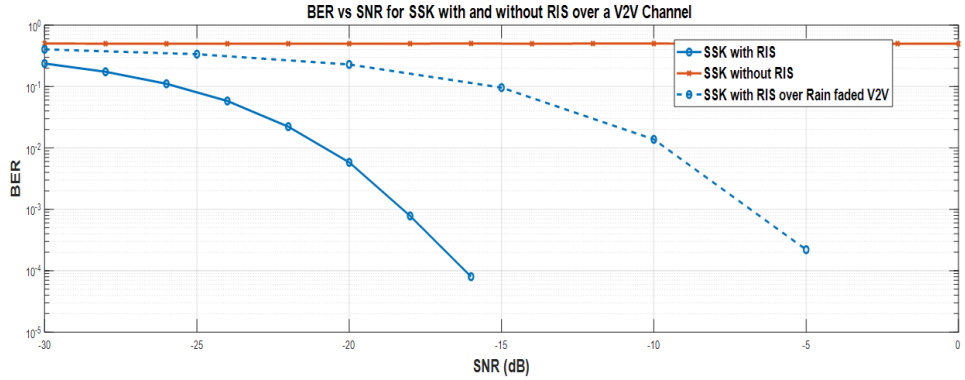

Fig:1 BER vs SNR Comparison for SSK with and without RIS over a V2V Channel

Fig.1 depicts the performance of BER with respect to SNR for SSK at 28GHz under three conditions of using RIS, without RIS, and with RIS under rain-faded V2V channels. The major advantage in BER attributed to the presence of RIS is visible in the plot as against the case of without RIS. The impact of rain fading is observed as the performance gets degraded when compared to that of a clear V2V channel with RIS. These results indicate how effectively RIS can enhance the system's reliability even under very poor conditions.

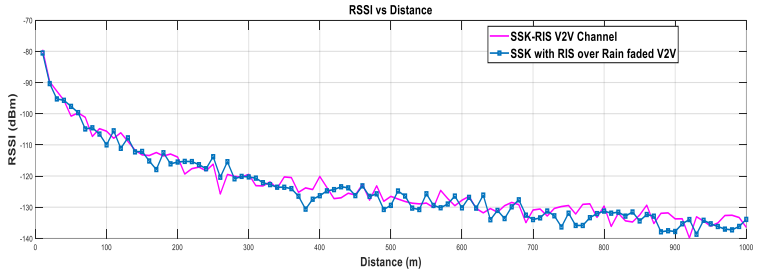

Fig: 2 RSSI vs Distance Comparison for SSK with RIS over a V2V Channel and Rain-Faded Effect.

Fig.2 shows RSSI vs distance of travel from the base station. Whenever the RSSI goes below -130 dBm the signal gets degraded, and the link is said to be broken. Similarly, if we carefully observe the 2 plots, SSK with rain fading has degraded performance because of the rain attenuation, and the intensity of the rain is set up to 25mm/hr, which is moderate to heavy rain attenuation. We observe that, at a distance of 380m away from the BS, SSK-RIS over rain-faded channel experiences link breakdowns, whereas the normal SSK-RIS in no rain environment experiences the same link breakdown at a distance of 620m from the BS. Similar trends are observed in Fig.3, where the Reference signal Received power vs distance shows the 480-meter distance a vehicle could cover before the signal drops below -130dBm in a rain faded scenario, in comparison to no rain it is approximately 680m distance. Fig.4 demonstrates the Path loss vs distance within the cell. It is observed that higher path loss is observed in NLoS faded SSK-RIS system in comparison to the LoS faded SSK-RIS system, this is because rain fading in an NLoS scenario increases the path loss as compared to LoS path loss as given in equation (5). Finally, in Fig. 5, Channel Impulse response has been plotted for SSK-RIS and SSK system under a typical V2V scenario, and it is observed that the magnitude of the SSK-RIS system has very high magnitudes (higher peaks indicates larger reflections and better performance) even in rain-affected scenarios which helps in decoding the signal better than its counterparts.

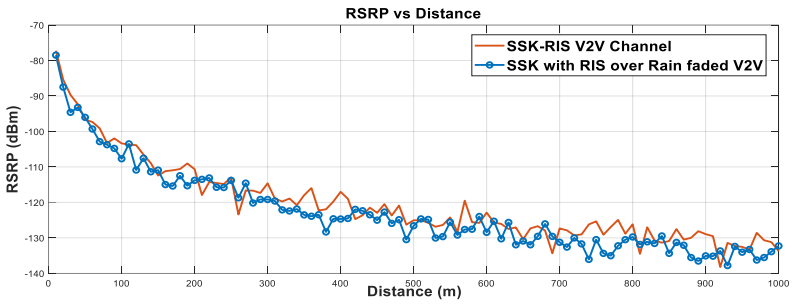

Fig:3 RSRP vs Distance for SSK with RIS over a V2V Channel

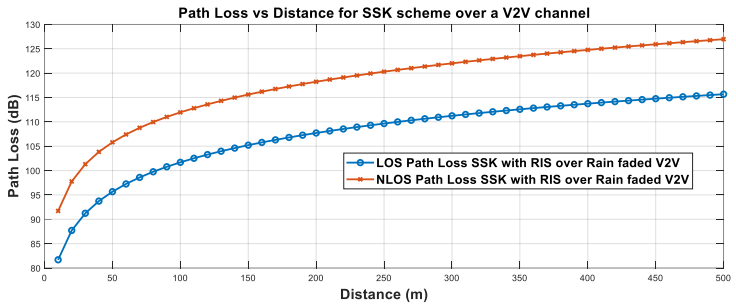

Fig:4 Path loss vs Distance for SSK with RIS over a V2V Channel and Rain Faded Effect

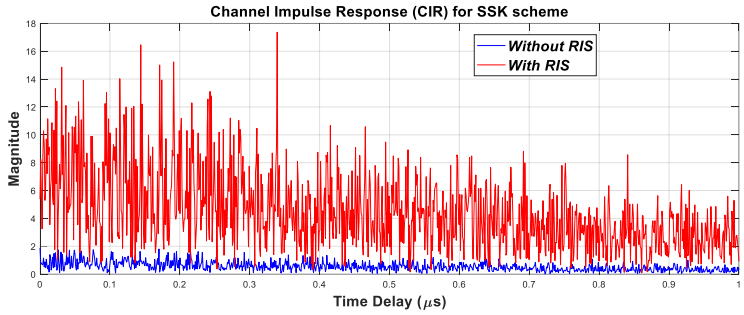

Fig :5 Channel Impulse Response with and without RIS.

4. CONCLUSIONS AND FUTURE WORK.

On a concluding note, RIS-SSK integrated into a V2V environment can effectively enhance the reliability as well as efficiency of communication. Performance measures such as BER, RSSI, and RSRP, in addition to path loss analysis in both LoS and NLoS scenarios, show that the system effectively increases the strength of the signals, reduces their error rates, and is robust against several impairments in the channel. Also, CIR is incorporated to demonstrate how the system can adjust within a dynamic environment. Future work would include real-time optimization of phase shifts in RIS by means of well-defined machine-learning techniques to address improving functionality in extremely varying mobile conditions.

5. REFERENCES

[1] Y. Fu et al., "BER performance of spatial modulation systems under 3-D V2V MIMO channel models," *IEEE Trans. Veh. Technol.*, vol. 65, no. 7, pp. 5725-5730, Jul. 2016, doi: 10.1109/TVT.2015.2461638.

[2] M. Wen et al., "A survey on spatial modulation in emerging wireless systems: Research progresses and applications," *IEEE J. Sel. Areas Commun.*, vol. 37, no. 9, pp. 1949-1972, Sep. 2019, doi: 10.1109/JSAC.2019.2929453.

[3] N. Serafimovski, S. Sinanović, M. D. Renzo, et al., "Multiple access spatial modulation," *J. Wireless Commun. Netw.*, vol. 2012, no. 299, 2012, doi: 10.1186/1687-1499-2012-299.

[4] V. Kumaravelu, P. Selvaprabhu, D. Han, M. A. L. Sarker, V. Sivabalan, S. J. Thiruvengadam, A. Murugadass, and C. S. Evangeline, "Blind reconfigurable intelligent surface-aided fixed non-orthogonal multiple access for intelligent vehicular networks," *EURASIP J. Wireless Commun. Netw.*, vol. 2023, no. 83, 2023, doi: 10.1186/s13638-023-02291-y.

[5] T. H. Ahmed, J. J. Tiang, A. Mahmud, G. C. Chin, and D.-T. Do, "Deep reinforcement learning-based adaptive beam tracking and resource allocation in 6G vehicular networks with switched beam antennas," *Electronics*, vol. 12, no. 2294, 2023, doi: 10.3390/electronics12102294.

[6] F. Bayar, O. Salan, H. Ilhan, and E. Aydin, "Space-time block coded reconfigurable intelligent surface-based received spatial modulation," *IEEE Trans. Mobile Computing.*, vol. 23, no. 12, pp. 11564-11575, Dec. 2024, doi: 10.1109/TMC.2024.3398539.

Biography



Suhas K received the bachelor's degree in Electronics & Communication Engineering from VTU Belgaum in 2009, the master's degree in Control Systems from Manipal Academy of Higher Education in 2011 respectively. He is currently working as an Assistant Professor at the Department of Electronics & Communication Engineering, Manipal Institute of Technology, Manipal. His research areas include developing energy efficient modulation schemes for wireless systems, Channel Coding and Error Correction, Millimeter-Wave (mmWave) and Terahertz (THz) Communication.

Mapping Learning Outcomes to Academic Success: A Novel Dataset for Evaluating Students' Academic Performance

Sapna Rai, Dr. Sunil Sikka, Dr. Anil Kumar

Research Scholar, Amity University Haryana, Gurugram, Haryana, India, sapnasucess@gmail.com
Professor, CSE, Amity University Haryana, Gurugram, Haryana, India, ssikka@ggn.amity.edu
Professor, CSE, Poornima Institute of Engineering and Technology, Jaipur, Rajasthan, India, anilkumar@poornima.org

Abstract

Academic performance evaluation is a critical component of education, shaping student progress, curriculum development and instructional strategies. Traditional assessment methods, primarily reliant on grades and examination scores, often fail to provide a comprehensive measure of students' conceptual understanding and skill proficiency. This study advocates for a paradigm shift towards learning outcome-based assessments, particularly within Computer Science education for Class 11 and 12 students under the Central Board of Secondary Education (CBSE). To facilitate this transition, a novel dataset has been created and systematically mapped to four consolidated key learning outcomes, Computational Thinking and Data Structures, Computer Systems and Cyber Ethics, Programming Concepts and Python Applications and Database Management with SQL Integration. The findings underscore the effectiveness of outcome-based assessments in aligning evaluation methodologies with competency-driven education.

Keywords. Learning outcomes, Computer Science Education, Dataset, Evaluation of academic performance, Students' performance.

1. INTRODUCTION

Academic performance evaluation is a fundamental aspect of education, influencing decisions on student progress, instructional quality, and curriculum planning. Traditional assessment methods, including exam scores, grades, and class participation, have long been used to measure academic success. However, these metrics offer numerical insights but fail to capture a student's mastery of concepts, cognitive skills, or problem-solving abilities. This limitation creates a gap in understanding how well students meet educational objectives.

A shift from traditional assessment to learning outcome-based evaluation is essential in modern education. Traditional performance indicators, such as demographic factors, attendance, socio-economic status, and behavioral data from e-learning platforms, are valuable for predicting academic success. However, they do not fully capture the alignment between assessments and curriculum objectives. Hussain et al. [1] highlight that while attendance and demographic factors can predict performance, they do not accurately assess skill acquisition or conceptual mastery.

Learning outcomes define the specific, measurable competencies students should acquire after completing a course or educational stage. The CBSE has integrated learning outcomes into its curriculum to promote skill-based and competency-driven education. These outcomes provide a structured framework for both teaching and assessment. Hayat et al. [2] emphasize that outcome-based evaluation offers a more detailed understanding of student progress, particularly in higher education, where emotional intelligence and self-efficacy play a crucial role. Similarly, Turjman et al. [3] argue that an outcome-oriented approach allows educators to focus on specific skill sets rather than generalized grading metrics.

Building on this foundation, this study introduces a dataset for evaluating academic performance using learning outcomes in CBSE Class 11 and 12 Computer Science. The paper is structured as follows: Section 2 presents a literature review summarizing relevant research. Section 3 discusses previous datasets and describes the proposed dataset. Finally, Section 4 concludes the study and suggests future research directions for enhancing outcome-based assessments through machine learning

2. LITERATURE REVIEW

This literature review focused on increasing application of diverse datasets and analytical methodologies to evaluate academic performance. Studies such as Hussain et al. [1] have integrated these datasets with academic records to forecast end-semester results, demonstrating how external factors influence student outcomes. Similarly, Kassarnig et al. [4] analyzed datasets incorporating personal and social environment attributes, highlighting the impact of family background, income levels etc. on academic achievement. Internal academic data, including attendance records and assessment scores, also served as a fundamental component in academic performance analysis. Zafari et al. [5] utilized academic scores to classify students into performance categories such as very well, good, medium, and poor. Expanding on this approach, Alsariera et al. [6] and Fahd et al. [7] integrated demographic, internal assessment, and personal attributes for holistic evaluation of student performance.

Chung et al. [8] and Waheed et al. [9] utilized log data to classify students into dropout and non-dropout and at-risk categories. Esparza et al. [10] leveraged student comments to categorize feedback for teachers into positive, neutral, or negative, indirectly evaluating the impact of the teaching environment on student outcomes. Studies have also linked grit and self-efficacy have been identified as significant factors influencing student performance, especially in higher education settings [11]. Brown et al. [12] conducted a five-year longitudinal study examining the relationship between student engagement, learning behaviors, and academic achievement. These comprehensive datasets and analytical approaches highlight the transformative potential of data-driven methodologies in evaluating academic success and optimizing learning experiences.

3. PROPOSED DATASET

The literature review highlights the increasing use of diverse datasets and analytical methodologies to assess academic performance. The study reviewed key attributes into distinct areas, each playing a significant role in understanding student success. The datasets primarily encompass attributes related to student grades, demographic data, attendance records, and standardized test scores [1,5,6,8,13,14,16,17,19,20,21,22], Student behavioral and Engagement data-based studies [4,12,15,26,27,28], Virtual Learning Environments (VLE) [9,10,18,23,24,25], Sentiment-Based Feedback and Psychological Attributes [2,3,11,17]. While existing datasets provide valuable insights, they did not focus on competency-based learning objectives. Comparison between grade-based and outcome-based assessment is presented in Table 1.

Feature	Grade-Based Assessment	Outcome-Based Assessment
Focus	Exam scores, grades, and overall performance	Mastery of skills and competencies
Evaluation Criteria	Based on correct/incorrect answers in standardized tests	Measures conceptual understanding and practical skills
Student Learning Insight	Provides limited insight into skill mastery	Offers a detailed view of strengths and weaknesses
Flexibility	Fixed exams with rigid scoring	Adapts to students' learning progress
Practical Relevance	May not reflect real-world application of knowledge	Aligns with job-market and practical applications

Table 1: Comparison: Grade-Based vs. Outcome-Based Assessments

Our dataset marks a significant step in outcome-based educational evaluation, providing data-driven insights into student performance. It serves as a blueprint for integrating learning outcome assessments into education. Ensuring ethical compliance, it uses publicly available academic questions from CBSE textbooks, sample papers, and online sources without collecting private student data. The dataset is fully anonymized, containing only academic content without personal identifiers. The number of questions extracted based on learning outcomes is shown in Table 2.

LO-1	7035
LO-2	7540
LO-3	8755
LO-4	4635

Table 2: Number of questions for each class

These questions are manually mapped as per the Learning Framework of classes 11 and 12, Computer science by CBSE which are listed in the Figure 1 and Figure 2 respectively and the detailed learning outcomes are consolidated into four key learning outcomes, as shown in Figure 3.

UNIT	LEARNING OUTCOMES
Computer Systems and Organization	1. Develop a basic understanding of computer systems-architecture, and operating systems. 2. Develop a basic understanding of various encoding schemes and number systems along with their applications in digital technology. 3. Develop a basic understanding of new technologies Information technology and how are they affecting the modern lifestyle
Computational Thinking and Programming	4. Appreciate the notion of the algorithm including flowcharts and pseudocode. 5. Explain and use operators, variables and data types including higher-order data structures such as lists, strings, tuples, and dictionaries 6. Develop basic principles of computational thinking
Society, Law and Ethics	7. Explain cyber ethics, cyber safety and cybercrime 8. Understand the value of technology in societies along with consideration of gender and disability issues.

Figure 1: Learning Outcomes by CBSE-NCF for class 11

UNIT	LEARNING OUTCOMES
Computational Thinking and Programming	1 Apply the concept of function 2 Implement search and sort techniques. 3 Create and use Python Libraries 4. Explain and use the concept of exception as well as file handling. 5 Explain the concept of efficiency in algorithms and computing in general. 6. Use basic data structure: Stacks and Queues
Computer Networks	7. Explain computer networks and how it works. 8. Explain the security concerns in networked computers and methods to mitigate them.
Database Management	9. Use Database concepts, SQL to store, retrieve and manipulate data.

Figure 2: Learning Outcomes by CBSE-NCF for class 12

ATTRIBUTES	DESCRIPTION
LO-1	Develop basic computational thinking and appreciate the notion of the algorithm including flowcharts and pseudocode and explain and use operators, variables and data types including higher-order data structures such as lists, stack, queues, strings, tuples, and dictionaries.
LO-2	Develop a basic understanding of computer systems along with architecture, operating systems, encoding schemes, number systems along with their applications in digital technology and how are they affecting the modern lifestyle. Also explain cyber ethics, cyber safety, and cybercrime and understand the value of technology in societies along with consideration of gender and disability issues.
LO-3	Develop basic computational thinking and appreciate the notion of the algorithm including flowcharts and pseudocode and apply the concept of function, Create and use Python libraries and use the concept of exception as well as file handling.
LO-4	Develop basic computational thinking and use Database concepts, SQL to store, retrieve and manipulate data along with connectivity between Python and SQL.

Figure 3: Final combined Learing Outcomes

The dataset comprises 23,464 academic questions with five attributes are manually mapped to the four consolidated learning outcomes. Sample of the dataset is shown in the Figure 4.

	QUESTION CONTENT	LO 1	LO 2	LO3	LO 4
2	Write the output of-d={0:'zero',1:'one',2:'two',3:'three'}for i in d: print(i, en	1	0	0	0
3	Find the output of the following Python program: def makenew(mystr): news	1	0	1	0
4	Find the output of the following program def calcresult () : i = 9 while i> 1 :	1	0	1	0
5	Observe the following Python code and find out , which out of the given optic	1	0	1	0
6	Discuss the strategies employed by python for memory allocation?	1	1	0	0
7	Answer the questions (i) and (ii) after going through the following class definit	1	0	1	0
8	Define a class Train in PYTHON with following description: 4 Data Members s	1	0	1	0
9	class ParentClass(objects): def__init__(self) self,x = 1 self.y = 1 def print(self):	1	0	1	0
10	Write a user defined function findname(name) where name is an argument in	1	0	1	0
11	Explain try..except...else ... with the help of user defined function def divide(x	1	0	1	0
12	Write a user defined function arrangelements(X), that accepts a list X of integ	1	0	1	0
13	Consider the following class definition :- 3 class book (): bk = [] def _ init _ (s	1	0	1	0
14	Write a python function generatefibo(n) where n is the limit using a generato	1	0	1	0
15	Evaluate the following postfix using stack & show the content of the stack aft	1	0	0	0
16	Consider the following code : 1 f = open ("mytry", "w+") f.write ("123456789	1	0	1	0
17	Write a user defined function in Python that displays the number of lines start	1	0	1	0
18	Consider a binary file Employee.dat containing details such as empno:ename	1	0	1	0
19	Differentiate between cardinality and degree of a table with the help of an ex	0	0	0	1
20	Consider the following tables FACULTY and COURSES. Write SQL commands	0	0	0	1
21	State and Verify Absorption law algebraically.	0	1	0	0
22	Draw a logic circuit for the following Boolean expression: A.B+C.D'	0	1	0	0
23	Write the SOP form of a Boolean function F, which is represented in a truth ta	0	1	0	0
24	Obtain a simplified from for a Boolean expression:	0	1	0	0
25	Write any 1 advantage and 1 disadvantage of Bus topology	0	1	0	0
26	ii) Suggest a cable layout of connections between the Departments and specif	0	1	0	0

Figure 4: Sample of the Dataset

This dataset will be used to develop a machine learning model for the automatic prediction of learning outcomes based on the question's context.

5. CONCLUSION

This study introduces a novel dataset specifically designed for evaluating academic performance by mapping assessment questions to CBSE-defined learning outcomes for Classes 11 and 12 in Computer Science. Unlike previous research studies, which predominantly relied on traditional academic data or generalized behavioral metrics, this dataset uniquely bridges the gap between granular academic content and predefined educational objectives. The findings demonstrate the power of using a learning outcome-oriented framework to identify key areas where students excel or struggle. The dataset's multi-label and multi-class nature further allows for sophisticated analytical approaches, offering unparalleled insights into how specific learning outcomes influence academic success. This dataset represents a foundational step toward outcome-based education and data-driven academic evaluation. To our knowledge, no prior work has used such a dataset for mapping questions directly to learning outcomes in this context, making it a unique contribution to the field. Future work can expand upon this by integrating this dataset with machine learning algorithms for automated question mapping.

5. REFERENCES

[1] Hussain, Dahan, By-Law, Educational data mining, Indonesian J. Electr. Eng. Comput. Sci., vol. 9, 2018.
[2] Hayat, Saleem, Afzal, Grit self-efficacy achievement, J. Appl. Res. Higher Educ., vol. 12, 2020.
[3] Habeeb, Fadare, Al-Turjman, Artificial Neural Networks, Smart Infrastructures IoT Era, Springer, 2025.
[4] Kassarnig, Mones, Bjerre-Nielsen, Academic performance patterns, EPJ Data Sci., vol. 7, 2018.
[5] Zafari, Sadeghi-Niaraki, Choi, Evaluation high school, Appl. Sci., vol. 11, 2021.
[6] Alsariera, Baashar, Alkawsi, Assessment Machine Learning, Comput. Intell. Neurosci., vol. 2022, 2022.
[7] Fahd, Venkatraman, Miah, Machine Learning Education, Educ. Inf. Technol., pp. 1-33, 2022.
[8] Chung, Lee, Dropout warning systems, Children Youth Serv. Rev., vol. 96, 2019.
[9] Waheed, Hassan, Aljohani, Predicting Academic Performance, Comput. Hum. Behav., vol. 104, 2019.
[10] Gutiérrez, Canul-Reich, Zezzatti, Mining students' comments, Int. J. Comb. Optim. Prob. Inform., vol. 9, 2018.
[11] Faust, Rosendale, Grit self-efficacy predictors, Rev. Educ., vol. 10, 2022.
[12] Brown, Johnson, Williams, Student engagement performance, IEEE Trans. Learn. Technol., vol. 19, 2025.
[13] Baashar et al., Postgraduate performance AI, Alex. Eng. J., vol. 61, 2022.
[14] Alnassar, Blackwell, Homayounvala, Machine Learning Virtual, Int. Conf. Intell. Eng. Manag., 2021.
[15] Madigan, Cross, Smolkowski, Positive behavioral interventions, Educ. Res. Eval., vol. 22, 2016.
[16] Fernandes, Holanda, Victorino, Educational data mining, J. Bus. Res., vol. 94, 2019.
[17] Aziz, Student performance evaluation, Coll. Basic Educ. Res. J., vol. 16, 2020.

[18] Lakkaraju, Aguiar, Shan, Machine Learning Framework, ACM SIGKDD Int. Conf., 2015.
[19] Shanmugarajeshwari, Lawrance, Performance classification techniques, Int. Conf. Comput. Technol., 2016.
[20] Al Mayahi, Al-Bahri, Predicting student success, Int. Congr. Ultra-Mod. Telecomm., 2020.
[21] Motlagh, Amrai, Yazdani, Self-efficacy academic achievement, Procedia-Soc. Behav. Sci., vol. 15, 2011.
[22] Rivas, Fraile, Chamoso, Machine learning techniques, Int. Workshop Learn. Technol., 2019.
[23] Orji, Vassileva, Student engagement performance, Int. Conf. Info. Visualisation, 2020.
[24] Burgos, Campanario, Peña, Tutoring action plan, Comput. Electr. Eng., vol. 66, 2018.
[25] Semerci, Goularas, Flow state learning, J. Educ. Comput. Res., vol. 59, 2021.
[26] Honicke, Broadbent, Academic self-efficacy review, Educ. Res. Rev., vol. 17, 2016.
[27] Adams, Blair, Time management behaviors, Sage Open, vol. 9, 2019.
[28] Ardura, Galán, Learning approaches self-efficacy, Int. J. Sci. Educ., vol. 41, 2019.

Echoguard: Voice-Driven Safety for Women in the Digital Age

L. Leena Jenifer, Deepika Krishnan, Jayashri G

Rajalakshmi Engineering college, leenajenifer.l@rajalakshmi.edu.in,

Rajalakshmi Engineering college, 211001017@rajalakshmi.edu.in,

Rajalakshmi Engineering college,211001037@rajalakshmi.edu.in

Abstract.

Women are entitled to live, work, and travel in areas with inadequate safety and security measures. To stop crimes against women, such as human trafficking, domestic abuse, and harassment, strong legal frameworks must be implemented. The proposed application is a voice-activated safety application that allows for an improved personal safety situation by enabling unobtrusive distress signals with a preset voice command. On activation, it automatically transmits the user's real-time location to trusted contacts and emergency response teams for an immediate response. A built-in panic button also extends the emergency reach through sending bulk SMS alerts. Advanced technologies such as speech recognition, GPS tracking, and secure cloud storage are used for seamless functionality in the system. Prioritizing a speedy, easy-to-use application with the highest regard for confidentiality, it instantiates a robust support system for individuals in crises and offers real-time proactive approaches to personal safety and emergency responses.

Keywords. Women Safety, SMS Alerts, GPS Tracking, Data Security, Emergency Response, Mobile Application.

1. INTRODUCTION

The problem is essentially the safety and security of people, especially women, when they are at risk of being harmed. With the increasing concerns about personal safety, there is a pressing need for solutions that provide rapid response mechanisms in emergency situations. The core issue is the lack of a simple, accessible, and effective way to alert nearby authorities or trusted individuals during critical situations. These safety solutions are either complex, involve too much interaction, or are less efficient for timely intervention. Moreover, there is a lack of a system that will support location-based, real-time alerts so that the probability of a quick and apt response is maximized[9]. Additionally, there is a need for the integration of voice-activated technology, enabling hands-free operation during emergencies when the user may not have the ability to interact manually with their device, ensuring that safety measures can be activated under stressful and critical conditions.

2. LITERATURE SURVEY

Author and Year	Methodology	Merits	Limitations
R. P. S. Manikandan, Ashwin G, Chandru A, Murali prasad. 2024 [10]	AI, GPS.	The key features include a panic button to automatically alert the user's case of distress, emergency contact list with customizable settings, AI-based alerts that pick early signs of danger, and alert the user in real- time.	The Women Safety Project can enhance with smart home security, machine learning, voice alarms, an AI chatbot, and wearable compatibility.
Ms. T N Aruna, Naveen Kumar S, Newton Habakuk S , Nivethitha S, Pooja B. 2023 [7]	Firebase.	The app comes with features like GPS tracking, Emergency SOS, which allows distress signals to be sent to guardians and a control room, panic button with a siren sound to deter the attacker, and a database of safe locations for improved safety features.	Voice-activated features, community-based safety, the option to share real-time location with trusted contacts, and features that analyse data for providing users with personalized safety recommendations and alerts.
Nitish Mishra, Ananya Puri ,Rishita "A Mobile Application for Women's Safety: Myguard". 2023 [2]	Artificial Intelligence	The app integrates unique features for an efficient user experience, including formal registration for accountability, destination tracking with SOS alerts, and voice assistant guidance with a panic command for enhanced user safety.	Lack of prompt police response due to location constraints. Difficulty in discreetly reaching out to law enforcement.
IEEE – "SafeTrack: Empowering Women's Security with GPS Location Tracking and Messaging".2023 [3]	Global Positioning System	The mobile-based safety device offers real-time tracking, recording, and self- defence features, utilizing advanced technology to enhance women's security.	The device may face limitations, such as potential failure of components like the spark generator and buzzer, and it only activates when the attacker physically contacts the victim.

3. RESEARCH GAP

The incorporation of Call Alert Verification (CAV) into women's safety applications holds promise but is hindered by factors such as high expense and compatibility[8]. SafeSpeak fills these loopholes through real-time location tracking, voice-based controls, and integration with Google Maps. Utilizing Firebase authentication and a Speech-to-Text API, it maintains security and smooth data sharing. With ease of use, encryption, and community orientation, SafeSpeak provides improved safety, empowerment, and responsiveness to changing threats.

4. PROPOSED METHODOLOGY

Women's safety requires innovative solutions that go beyond human intervention. SafeSpeak is a cutting-edge safety app with voice-activated alerts, real-time location sharing, crime heatmap, and AI chatbot for instant response. It silently sends distress signals through voice commands, notifying trusted contacts and law enforcement. With Firebase authentication, Speech-to-Text API, and Google Maps, it provides security and ease of use[5]. The crime heatmap supports safer route planning, and the AI chatbot offers emergency advice. SafeSpeak incorporates offline security through the sharing of real-time locations with family members and police through SMS, guaranteeing alerts. The combination of real-time monitoring, voice-initiated alerts, provides a solid safety network, facilitating timely intervention and improved personal security.

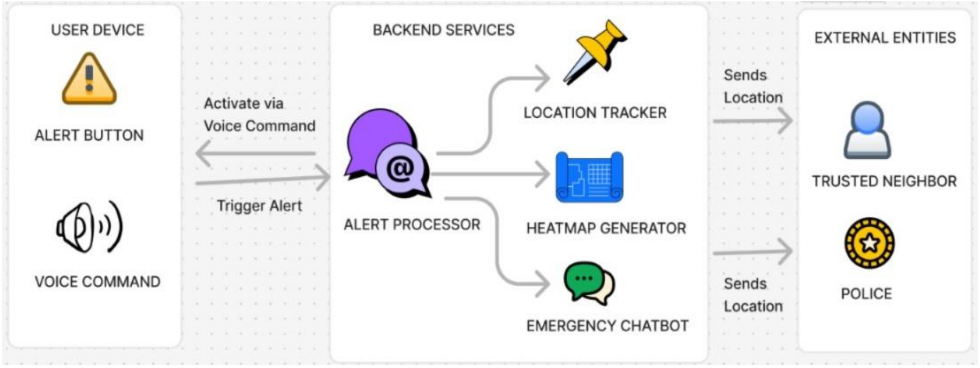

Figure 4.1 Architecture Diagram

6. IMPLEMENTATION

5.1 User Authentication Module: Employing Firebase Authentication for safe login through email. User information is safely stored during registration. Users create profiles and enter emergency contacts, providing secure access to app functionality [4]. Authentication safeguards personal information and adds security.

5.2 SOS and Panic Button Module: Offers immediate emergency access. Initiating the voice command notifies emergency contacts and officials with live location using Google Maps API. The hands-free function increases security, enabling direct response even in the event the user is not physically able to handle their phone.

5.3 Voice Command Module: Uses Google Speech-to-Text (STT) API for hands-free interaction. Recognizes preset voice command “Help” to trigger safety actions. Integrates with the Panic Button for seamless activation, ensuring quick access to emergency features when needed most [6].

5.4 Emergency Chatbot Module: AI-driven chatbot offers live emergency advice and self-protection advice. Employs natural language processing (NLP) for individualized support. Provides safe, real-time support in emergencies, boosting user trust and security [1].

5.5 Crime Heatmap Module: Employs crowdsourced, user-generated crime data to create a dynamic crime heatmap. Offers users the opportunity to report crimes or suspicious occurrences, which are confirmed and superimposed onto the map.

6. CONCLUSION

In an age of increasing personal safety, such technology-driven solutions must be integrated, as well as instant assistance and real-time protection, for emergency issues. This app provides voice-activated alert system, real-time location sharing, crime heatmaps, and AI-powered chatbot-for rapid response during emergencies through use of speech recognition, and secure data management to enhance security with protection of privacy and usability. With a strong backend, seamless integration, and real-time tracking, it stands as a reliable safety tool that empowers individuals, strengthens community support, and fosters a more secure environment for all users. Additionally, continuous improvements through AI-driven analytics and user feedback mechanisms will further enhance the application's accuracy, response time in weak networks, and processing efficiency on low-end devices for seamless emergency response.

7. REFERENCES

[1] Vijay, K., K. R. Sowmia, S. Ravikumar, and Y. Arockia Raj. 'Question Answering FAQ Bot Using Natural Language Processing.' In International Conference on Recent Trends in Computing, pp. 595-603. Singapore: Springer Nature Singapore, 2023.

[2] Sakure, Kishore, Purva Pawale , Kamal Singh,TanviKhadakban,'WomenSafety App.'ResearchGate(2022).

[3] Masud, Quazi Maliha, M. Mesbahuddin Sarker, Alistair Barros, and Md Whaiduzzaman. 'GoFearless: A Safety and Security Android Based Application for Women.' International Journal of Intelligent Information Systems 11, no. 2 (2022): 22-30.

[4] Chaudhary,Payal.'SURAKSHA: AN ANDROID APP FOR THE SAFETY OF WOMEN.'(2022).

[5] Athira, K., R. Sriharsha, and N. Rajkumar. 'Women's Safety in Cities Using Android.' In 2023 International Conference on Self Sustainable Artificial Intelligence Systems (ICSSAS).

[6] Vijavakumar, R., S. Ravikumar, K. Vijay, and P. Sivaranjani. 'Integrated Communal Attentive & Warning System via Cellular Systems.' In 2022 International Conference on Electronic Systems and Intelligent Computing (ICESIC), pp. 370-375. IEEE, 2022.

[7] Athira, K., R. Sriharsha, and N. Rajkumar. 'Women's Safety in Cities Using Android.' In 2023 International Conference on Self Sustainable Artificial Intelligence Systems (ICSSAS), pp. 1383-1387. IEEE, 2023.

[8] Aggarwal, Deepti, Kakoli Banerjee, Riddhi, 'An insight to android applications for safety of women techniques' In 2022 IEEE Delhi section conference (DELCON), pp. 1-6. IEEE, 2022.

[9] Meeta Singh. 'A Mobile Application for Women's Safety: Myguard.' In 2023 5th International Conference on Advances in Computing, Communication Control and Networking (ICAC3N), pp. 1601-1605. IEEE, 2023.

[10] Gupta, Tanushree, Gaurav Kumar Pandit, Ashutosh Kumar, Himanshu Mishra, and Bhagwati Sharan. 'SafeTrack: Empowering Women's Security with GPS Location Tracking and Messaging.' In 2023 Second International Conference on Augmented Intelligence and Sustainable Systems (ICAISS), pp. 794-799. IEEE, 2023.

BIOGRAPHIES



L. Leena Jenifer received the Bachelor's degree in Computer Science and Engineering from Anna University in the year 2009. She obtained her Post graduate degree in Computer Science and Engineering in 2013 and is pursuing a Ph.D. in the Faculty of Information and Communication Engineering, Anna University, Chennai. She has 10 years of teaching experience and is currently working as an Assistant Professor in the Department of Information Technology at Rajalakshmi Engineering College, Chennai. She has published more than five research papers in journals and conferences. Her area of research includes Data Security, Deep learning, and Data Analytics.



Deepika Krishna studying Bachelor's degree in Information Technology from Rajalakshmi Engineering College, expected to graduate in the year 2025.



Jayashri G studying Bachelor's degree in Information Technology from Rajalakshmi Engineering College, expected to graduate in the year 2025.

Design of Hexagonal shaped HMSIW based IOI shape slot antenna for sub-6GHz applications

V SHIVA PRASAD NAYAK[1], MANJUNATHACHARI K[2]
[1]Assistant Professor, [2]Professor
[1,2] Dept. of EECE, GITAM (Deemed to be) University, Hyderabad, India.
svadthya@gitam.edu and mkamsali@gitam.edu

Abstract.

The rapid advances in 5G technology have moved the focus toward compact and efficient antennas for sub-6 GHz applications, which are essential for modern miniaturized devices. The proposed antenna is hexagonal with two rectangles, a circular slot on top of the layer excited by the microstrip line. This design aids integration and enhances performance in the sub-6 GHz frequency range. The critical parameters of the antenna, like resonance frequency, bandwidth, VSWR, radiation pattern, and gain, have been detailed using CST Studio Suite software. It will be helpful for sub-6 GHz 5G applications. Resonating at 3.55 GHz, the antenna presents a 80 MHz bandwidth around a -10 dB reference line and keeps a VSWR of 2:1. From simulation results, it is found that the developed antenna has a good radiation pattern and gain, making it very promising for effective deployment in modern 5G communication systems.

Keywords: **Slot antenna, Hexagonal, Substrate Integrated Waveguide, Sub-6GHz.**

1. INTRODUCTION

Now, 5G is effectively transmitted with a good capacity and connects many devices at relatively low power. 5G is the wireless technology that has proliferated in recent days for the use of device-to-device technology [2], data-driven wireless communication applications, and Industrial Revolution 4.0. Advanced technology applications, such as smart cities, virtual reality, and driverless vehicles, will benefit from advanced communication techniques with the modernization of the Internet of Things using 5G. The operation bands range from 3.3 to 3.7 GHz in India, 3.4 to 3.8 GHz in France, and 3.4 to 3.8 GHz is Spain; all are a part of sub-6 GHz bands. Such frequency bands have become highly popular due to the associated advancements like high throughput, low latency, low power consumption, lower price, and reduced operating distance

The primarily preferred transmission line for high-frequency functions is the substrate-integrated waveguide (SIW) [4]. Other names of SIW are bonded waveguide and post-barrier waveguide, and it is single form of substrate-integrated circuits (SICs) [5-6] for stamped deuce rows of vias linked in the top-to-bottom level through the substrate and also realized for passive, active mechanisms and antenna because of using of system-on-substrate (SOS) technology used to progress. Now, an essential parameter for SIW is the diameter of a hole. The spacing of vias can be represented as in eq.1 and the width of SIW as derived from eq.2 [6].

$$d \leq \frac{\lambda_g}{5} \quad \text{and} \quad s \leq 2d \tag{1}$$

$$a_R = a_S - \frac{d^2}{0.95s} \tag{2}$$

The relationship between the diameter (d) and the width of the waveguide (aR) is not delineated in the preceding equation [6]; at times, this oversight may yield erroneous values, thus a more appropriate formulation is presented as follows.

$$\mathrm{a_{siw}} = \mathrm{a_R} + 1.08 \times \frac{d^2}{\mathrm{s}} - 0.1 \times \frac{d^2}{\mathrm{a_{siw}}} \tag{3}$$

This antenna will be integrated into SIW technology as SIW slot antennas, subsequently transitioning to cavity-backed antennas to enhance bandwidth, reduce size, and achieve moderate gain [4]. This manuscript elucidates the Half Mode hexagonal-shaped SIW loaded with an octagonal slot [2], specifically designed for sub-6 GHz fifth generation applications. Section 2 provides a comprehensive overview of the proposed design, Section 3 complete with design equations and a detailed presentation of results in terms of S11, gain, radiation pattern, surface current, etc [3]. Section 4 offers a succinct conclusion, supplemented by references.

2. DESIGN ANALYSIS

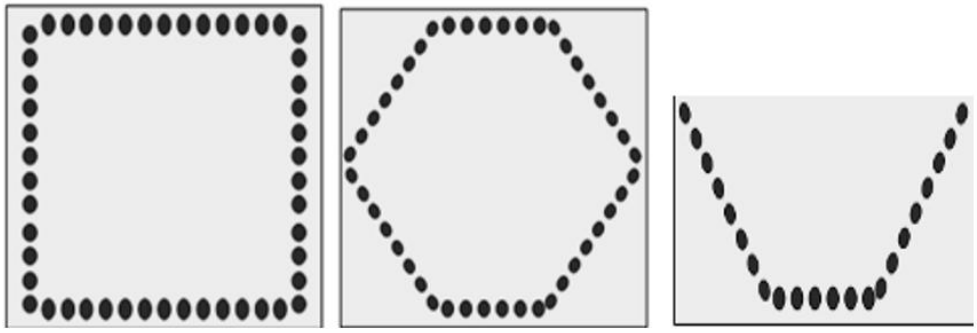

a. SIW b. Hexagonal shaped SIW c. HMSIW

Figure 2.11. Evaluation of HMSIW

Figure 2.1. illustrates the progression of the HMSIW, using an FR-4 substrate characterized by a substrate width thickness of 1.6 mm, relative permittivity of 4.3, and a copper width thickness of 35 µm. Figure 2.1.a. depicts the rectangular-shaped substrate integrated waveguide (SIW) cavity, which has been transformed into a hexagonal-shaped SIW cavity as presented in Figure 2.1.b. In Figure 2.1.b, the cavity is bisected into two halves to facilitate the realization of a half-mode SIW for size reduction, as demonstrated in Figure 2.1.c. Figure 2.2. delineates the parameter argument of the antenna, with a one circular and two rectangular slots situated on the upper of the antenna. Table 1 enumerates the dimensions of the parameters utilized in this design.

The length of HMSIW is $$L = {L_{SIW}}/{2} \quad (4)$$

Rectangular slot width is $${\lambda}/{4} \le W \le {\lambda}/{2} \quad (5)$$

Rectangular slot length is $$L \le W \quad (6)$$

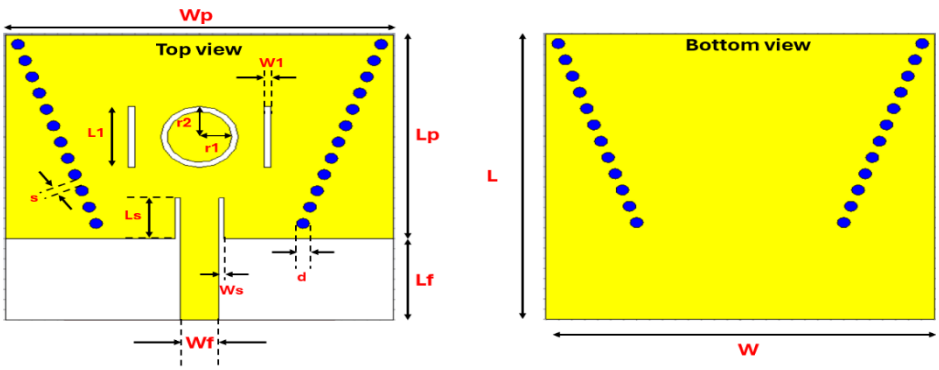

Figure 2.2. Parameter representation of the design

Table 1: Optimized Parameters (in mm)

Parameter	Value	Parameter	Value	Parameter	Value
L	36	W	30	W_1	0.5
r1 /r2	2.5/3	Lf	8	Wf	3
s/d	1.5/1	Lp	20	Wp	30
L_1	6	Ls	4	Ws	0.4

2.1. Evolution of antenna

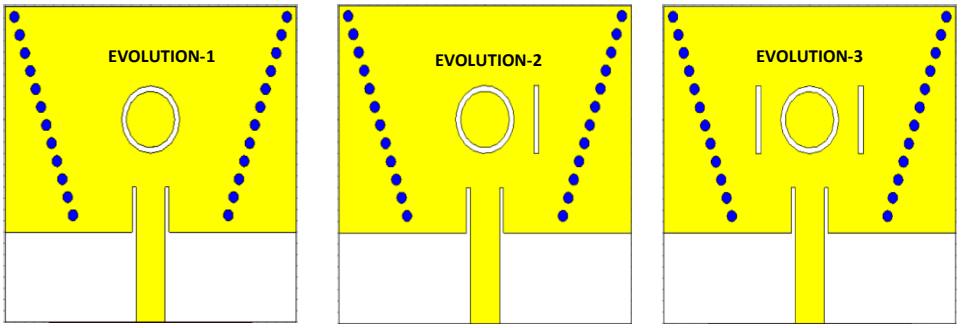

Figure 2.3. Evolution of proposed antenna

The Figure 2.3 show the complete progression of the proposed antenna design. The design of the evolution 1, S11 achieved is -24dB at fr of 3.59GHz. The evolution 2 offered S11of -27dB with fr of 3.57GHz. Finaly evolution3 is obtain operating frequency(fr) of 3.55GHz and the return loss value is of -35 dB. The comparison of Return loss(S11) vs operating frequency(fr) of evolution1, evolution2 and evolution3 has been shown in Figure 2.4.

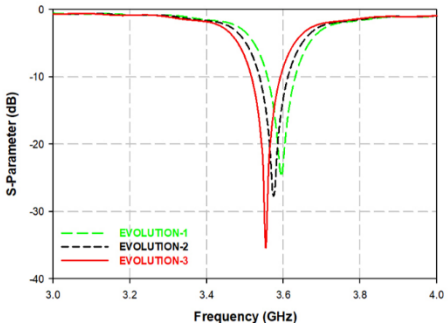

Figure 2.4. Return loss characteristics of evolution 1, evolution 2 and evolution 3

3. RESULTS AND DISCUSSION

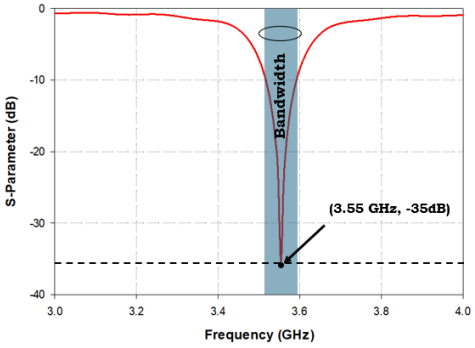

Figure 3.1. Reflection coefficient

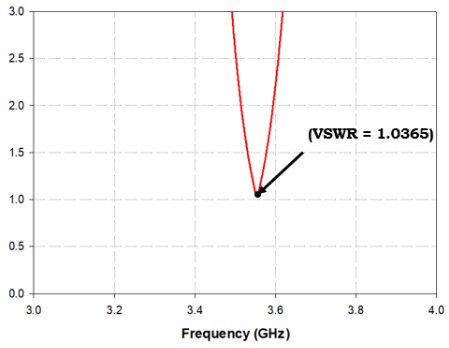

Figure 3.2. VSWR

Figure 3.1. presents the reflection coefficient of the planned antenna across the frequency spectrum ranging from 3 to 4 GHz the antenna exhibits resonance at a frequency of 3.55 GHz, yielding an S11 value of -35 dB and an operational bandwidth of 80 MHz, specifically from 3.51 GHz to 3.59 GHz, suitable for 5G applications. The voltage standing wave ratio (VSWR) corresponding to the proposed design is illustrated in Figure 3.2, indicating a VSWR value of 1.0365 at center frequency of 3.55 GHz.

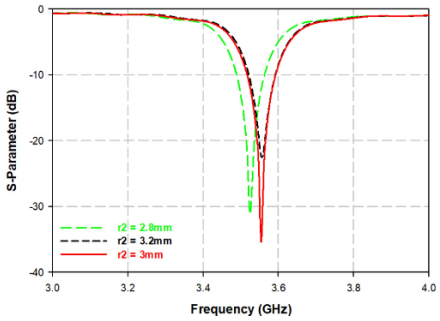

Figure 3.3. S11 for different values of r2

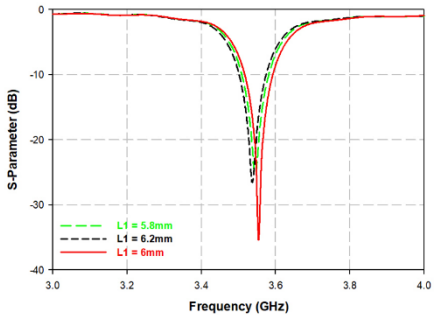

Figure 3.4. S11 for different values of L1

Figure 3.3 illustrates the reflection coefficient for different circular slot radius, specifically for values of 2.8 mm, 3.2 mm, and 3 mm. The optimal value selected among the r2 is 3 mm.

Figure 3.4 illustrates the reflection coefficient for different rectangular slot length, specifically for values of 5.8 mm, 6.2 mm, and 6 mm. The optimal value selected among the L1 is 6 mm.

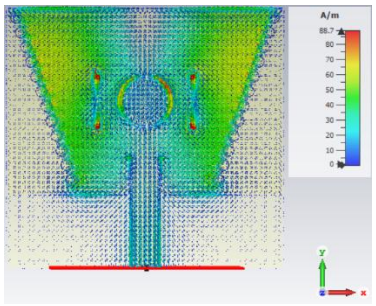

Figure 3.5. Surface current at 3.55GHz

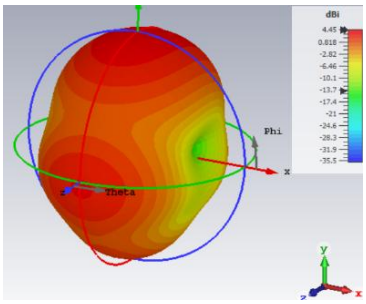

Figure 3.6. Gain at 3.55GHz

The surface current of the proposed antenna is revealed in Figure 3.5 at a resonant frequency 3.55GHz and observed that flow of current is more at circular slot as well as at rectangular slot. The Figure 3.6 shows the gain of the antenna at 3.55 GHz resonant frequency, observed that flow the current is in the direction of propagation and their value is 4.45dBi is well fitted for 5G wireless applications.

4. CONCLUSION

The half-mode hexagonal shaped SIW cavity-backed antenna was presented for sub-6GHz 5G applications and Fr-4 material used for the design. This design has loaded with one circular and two rectangular slots in top view and CST software is used for simulating the antenna for analyzing the antenna results. The antenna resonates at 3.55 GHz operating frequency with a 80 MHz occupied bandwidth ranging from 3.51 GHz to 3.59 GHz. The S_{11}, VSWR, gain values are -35dB, 1.036, 4.45 dBi at 3.55 GHz resonant frequency and observed acceptable radiation pattern for 5G Application.

5. REFERENCES

[1] NandaKumar, M. Srihari G.: Microstrip Feed Half-mode Substrate-Integrated- Waveguide loaded with SRR for dual-band Applications.Printed Antennas design and challenges, CRC press (Taylor an Fransis), 9, 125-138 (2022).

[2] Deepender, Manoj, Shrivastava, U. Verma, V.K. : A Study on 5G Technology and Its Applications in Telecommunications. International Conference on Computational Performance Evaluation (ComPE), pp.365-371, Shillong (2021).

[3] Nandakumar, M. Shanmuganantham, T. :Broad-Band H-Spaced Head Shaped Slot with SIW Based Antenna for 60GHz Wireless Communication Applications. Microwave and Optical Technology letters, 61(8), 1911-1916 (2019).

[4] Guyen Trong, N, Fumeaux, C.: Half-mode substrate-integrated waveguides and their applications for antenna technology: a review of the possibilities for antenna design. IEEE Antennas Propag Mag, 60(6), 20-31 (2018).

[5] Nandakumar, M. Shanmuganantham,T.:Broad band I shaped SIW slot antenna for V-band Applications. Applied Computational Electromagnetic Society, 34(11), 1-6 (2019).

[6] Nandakumar, M. Shanmuganantham,T.:Broad band Substrate Integrated Waveguide Venus shaped Slot Antenna for V-band Applications. Microwave and Optical Technology letters, 61(10), 2342-2347(2019).

Design of mmWave Antenna for Next-Generation Technologies

1. Sanjeev Vrittikop[1], Keerthana S[1], Praveen Kumar[1] and Jagadeesh Chandra R B[1]

[1] Department of Electronics and Communication Engineering, Manipal Institute of Technology, Manipal Academy of Higher Education, Manipal 576104, India

Abstract: This paper presents a compact rectangular patch antenna designed for 38 GHz mmWave applications. The antenna rests on Rogers RT/duroid 5880(tm) substrate materials (εr = 2.2, thickness = 0.5 mm) where it integrates a rectangular patch antenna with a cutout to enhance impedance and bandwidth performance and combines these elements with a microstrip feedline and a partial ground plane. Simulations indicate a -24.13 dB return loss at 38.2 GHz along with 5.80 dB peak gain and relatively uniform radiation patterns. Analysis of surface current distribution confirms that the patch edges together with feedline achieve efficient radiation of the antenna system. In addition to its suitability for 5G and beyond networks it provides compact size alongside high gain capabilities and efficient performance. Both experimental verification and array integration form parts of the future work.

Keywords— mmWave antenna, rectangular patch, impedance matching, 5G, gain.

2. Introduction

Wireless communication technologies show fast expansion caused by user requirements for elevated data speeds with minimal delay alongside solid signal connection. 5G technology along with future communications has raised essential challenges and prospects through millimeter-wave (mmWave) frequencies because their wide bandwidth makes multi-gigabit data transmission possible [1],[2]. The implementation of mmWave technology faces built-in technical obstacles that cause high propagation losses combined with minimal obstacle penetration while facing more risks of interference. The solution of these challenges needs antenna design techniques which maximize operation efficiency and gain performance while developing beamforming capabilities [3].

MIMO (Multiple Input Multiple Output) systems increase signal strength when multiple antenna elements operate at both transmitter and receiver because they deliver better signal resilience during power or bandwidth restrictions [4]. Strong mutual coupling between densely arranged antenna elements in mmWave frequency systems produces performance deterioration mostly affecting urban and high-mobility environments [5]. Research studies have produced multiple solutions to reduce antenna coupling and enhance isolation performance through the implementation of parasitic elements along with defected ground structures (DGS) and electromagnetic bandgap (EBG) materials [6],[7]. Modern substrate

engineering techniques combined with metasurface technology allowed a significant improvement of impedance performance while expanding the bandwidth capability and directing

the gain [8]. Despite these developments, mmWave antenna design still faces trade-offs between size, efficiency, and bandwidth. Research into mmWave antenna characteristics especially focusing on patch antennas slot antennas and phased arrays leads to continuous architectural development because these designs enhance integration capabilities and manufacturing efficiency [9] [10]. This paper presents a 5G antenna which functions for mmWave frequency-based wireless systems. The design achieves impedance matching and radiation efficiency enhancement as key features which maximize system performance while maintaining a small physical size. Performance tests along with design procedure analysis and simulation results demonstrate that this antenna satisfies the requirements for present networks.

3. Proposed Antenna Design

The proposed design consists of a compact rectangular patch antenna optimized for 38 GHz mmWave applications. It is fabricated on a Rogers RT/duroid 5880(tm) substrate (εr = 2.2, thickness = 0.5 mm) with overall dimensions of 12 mm × 10 mm. The structure includes a radiating patch, a microstrip feedline, and a partial ground plane, ensuring balanced radiation performance. The projected antenna's design is illustrated in Figure 1.

The 7 mm × 6 mm radiating patch has a 6 mm × 5 mm rectangular cutout to improve bandwidth and impedance matching by altering the current distribution. To increase radiation efficiency, the patch is raised
0.5 mm above the substrate. There is an efficient power transfer mechanism provided by the 4 mm × 1 mm microstrip feedline yet an 8 mm × 1.6 mm extension ensures stable connections. A precise delivery of antenna signal occurs through the small (1.5 mm x 0.5 mm) lumped port. The bottom layer contains the 4 mm × 10 mm Perfect Electric Conductor (PEC) ground plane extension. A reduced partial ground structure allows the antenna to minimize radiation behind it while improving front-back balance which ultimately results in compact operation. A simulation radiation box with dimensions 20 mm × 18 mm × 10 mm uses air as its content to achieve precise evaluation of far-field characteristics while eliminating boundary disturbances. The evaluation of performance relies on electromagnetic full-wave simulation which measures return loss together with radiation patterns and gain as well as antenna efficiency.

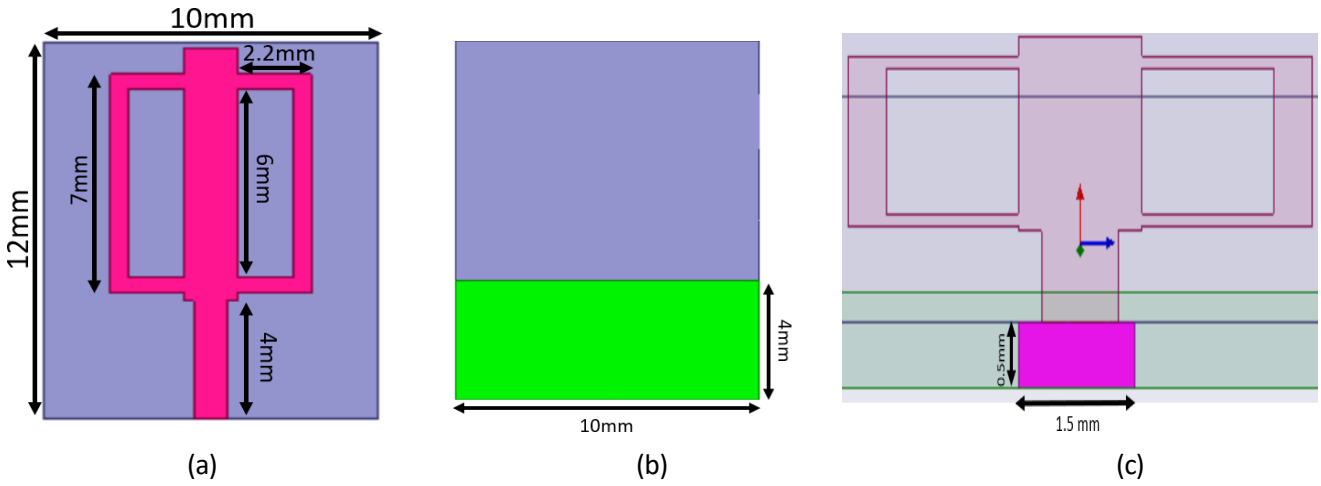

Figure 1. The proposed antenna design (a) radiating plane (b) ground plane (c) excitation port

4. Result and Analysis

4.1 S-parameter Plot:

A systematic evaluation of the antenna operational performance occurs through a performance metric assessment and simulation data validation. The simulated return loss (S11) of the rectangular patch antenna shows results in Figure 2 between 20 GHz to 50 GHz. Numerous resonances in the plot show that this antenna can work across diverse frequency bands. This antenna achieves its main operational frequency at
38.2 GHz where return loss reaches a high level of -24.13 dB which indicates optimized impedance operation. The antenna shows its potential for multi-band or wideband operation because secondary resonances occur at 23.2 GHz (-9.96 dB) and 26.8 GHz (-9.90 dB) and 33.2 GHz (-10.44 dB) and 44.9 GHz (-9.96 dB). The experimental findings demonstrate that the antenna works well as a component for mmWave technology which powers 5G and future wireless systems. This antenna presents promising capabilities for multi-band and broadband communication by resonating strongly at 38.2 GHz together with multiple other frequency points which support current high-frequency network requirements.

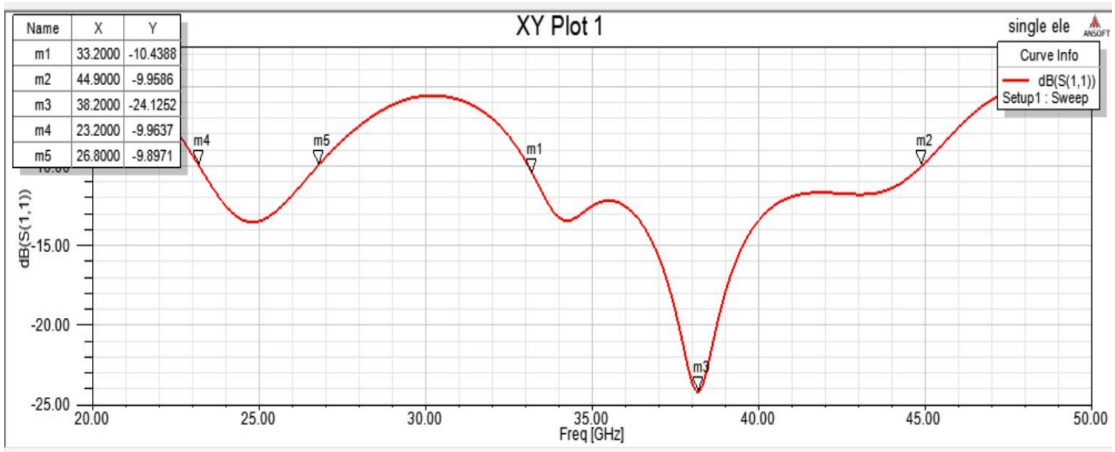

Figure 2. Simulated S-parameter plot of the proposed antenna

4.2 Gain:

The proposed rectangular patch antenna displays its total gain distribution across multiple spatial directions per Figure 3. The antenna reaches its design peak realized gain of 5.80 dB which shows optimal radiation happens at the desired frequency. The antenna generates almost omnidirectional radiation patterns that demonstrate significant gains between different radiated sections. Multiple lobes appear in the pattern because the antenna's physical aspects and the substrate properties affect its complicated radiation characteristics. The measured results confirm that the antenna functions well in millimeter-wave (mmWave) communications systems mainly because of its high gain capability combined with controlled radiation patterns for 5G and upcoming wireless transmission systems.

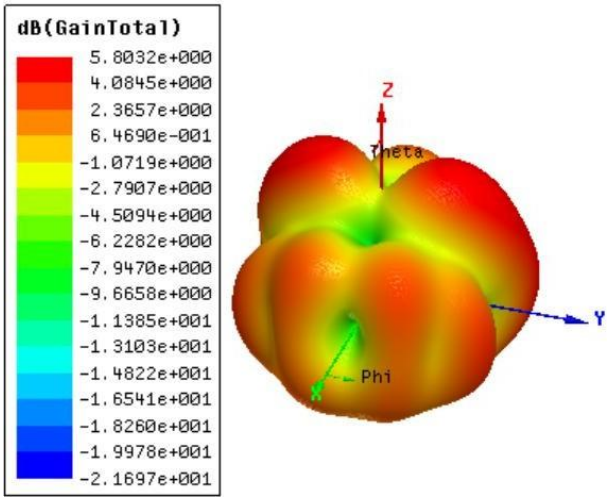

Figure 3. Gain plot of designed antenna

4.3 Radiation Pattern:

The Figure 4 presents the 2D radiation pattern of the antenna design at 38.2 GHz to show its total gain measurement in dB. The examination of the E-plane patterns operates at Phi = 0° and H-plane patterns operate at Phi = 90° to perform radiation analysis. The antenna gain measurement through the E-plane shows as red ink while H-plane gain measurement appears as purple ink when displayed on the graph. The antenna distributes radiation according to its unique pattern to achieve average directivity and reaches its maximum gain value at 7 dB yet forms side lobes and null regions during operation. The radiation pattern shows asymmetric behavior which emerges due to combined effects of substrate influences and edge diffraction processes. MMWave operating conditions can successfully use this antenna because its performance was validated through test results.

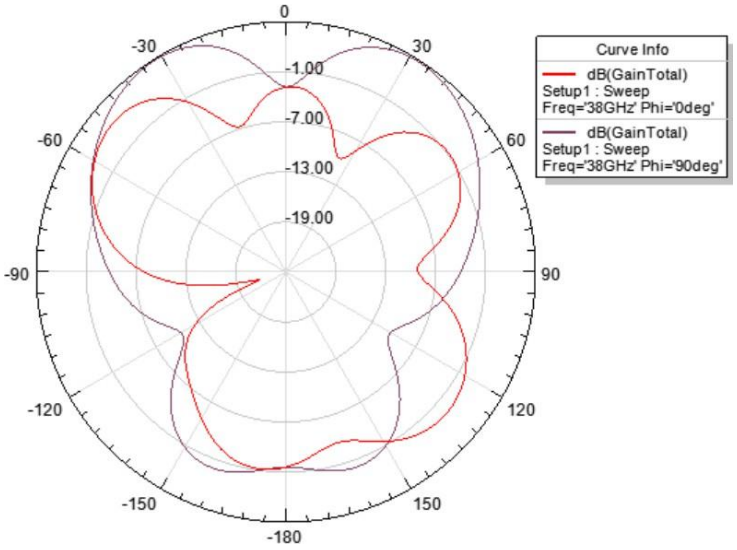

Figure 4*:* Radiation pattern of the proposed antenna at 38.2 GHz

\

4.4 Current density:

The distribution of surface current density for the proposed rectangular patch antenna is studied because it affects radiation performance assessment. Figure 5 displays the Jsurf distribution at 38.2 GHz where current concentrations reach their peak values at 2.5579e+002 A/m while concentrated at the edges of the patch and feedline. These points are fundamental for electromagnetic radiation performance as they support impedance match operations. The current density diminishes systematically from the edges to the center of the patch area until it reaches a value of 1.1378e+000 A/m which indicates minimal radiation occurs at this location. The antenna maintains balance in its radiation characteristics because currents spread symmetrically across its patch edges which matches both simulation results from the far-field and enables operational efficiency.

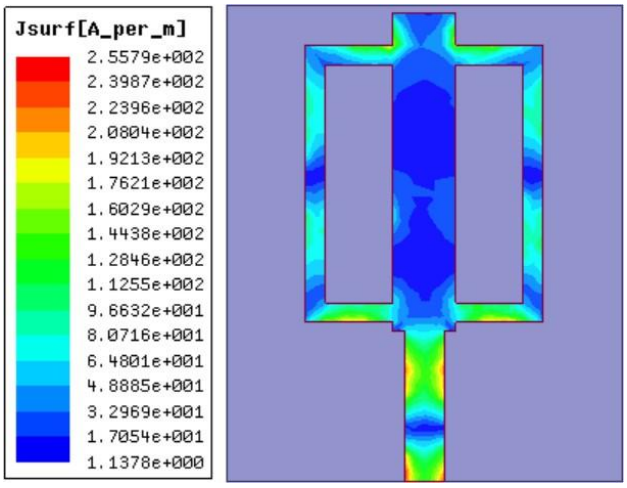

Figure 5. Current density of designed antenna at 38.2 Ghz

5. Conclusion

A research study demonstrates an optimized compact rectangular patch antenna design for 38 GHz mmWave operations. The antenna production uses Rogers RT/duroid 5880(tm) substrate to construct a rectangular patch antenna with a bandwidth enhancement cutout and microstrip feedline and partial ground plane design for improved radiation effectiveness. The simulated results display -24.13 dB of minimum return loss at 38.2 GHz and further resonances at 23.2 GHz, 26.8 GHz, 33.2 GHz, and 44.9 GHz thus indicating multi-band capabilities. The antenna reaches its peak realized gain of 5.80 dB while maintaining almost constant radiation patterns in all directions. The analysis of surface currents demonstrates efficient radiative behavior by concentrating the currents near the edges of the patch as well as at the feedline. The antenna provides an ideal solution for 5G mmWave applications because it maintains stable performance and offers high gain while requiring a small footprint. Further research will include experimental testing and integrating antenna arrays in their system design.

6. Reference

[1] N. Uwaechia and N. M. Mahyuddin, "A Comprehensive Survey on Millimeter Wave Communications for Fifth-Generation Wireless Networks: Feasibility and Challenges," in IEEE Access, vol. 8, pp. 62367- 62414, 2020, doi: 10.1109/ACCESS.2020.2984204

[2] Z. Xiao et al., "A Survey on Millimeter-Wave Beamforming Enabled UAV Communications and Networking," in IEEE Communications Surveys & Tutorials, vol. 24, no. 1, pp. 557-610, Firstquarter 2022

[3] S. Ghosh and D. Sen, "An Inclusive Survey on Array Antenna Design for Millimeter-Wave Communications," in IEEE Access, vol. 7, pp. 83137-83161, 2019

[4] Z. Gao et al., "Integrated Sensing and Communication With mmWave Massive MIMO: A Compressed Sampling Perspective," in IEEE Transactions on Wireless Communications, vol. 22, no. 3, pp. 1745-1762,
March 2023

[5] W. Hong et al., "The Role of Millimeter-Wave Technologies in 5G/6G Wireless Communications," in IEEE Journal of Microwaves, vol. 1, no. 1, pp. 101-122, Jan. 2021

[6] A. Desai, C. D. Bui, J. Patel, T. Upadhyaya, G. Byun and T. K. Nguyen, "Compact Wideband Four Element Optically Transparent MIMO Antenna for mm-Wave 5G Applications," in IEEE Access, vol. 8,
pp. 194206-194217, 2020

[7] B. Feng, J. Chen, K. L. Chung, L. Wang and Y. Li, "Dual-Polarized Filtering Magneto-Electric Dipole Antenna Arrays With High Radiation-Suppression Index for 5G New Radio n258 Operations," in IEEE Transactions on Antennas and Propagation, vol. 70, no. 4, pp. 3058-3063, April 2022

[8] N. Hussain, M. -J. Jeong, A. Abbas and N. Kim, "Metasurface-Based Single-Layer Wideband Circularly Polarized MIMO Antenna for 5G Millimeter-Wave Systems," in IEEE Access, vol. 8, pp. 130293-130304, 2020

[9] K. -L. Wong, H. -C. Kao and W. -Y. Li, "Wideband Low-Profile Eight-Port Eight-Wave Annular-Ring Patch Antenna Based on Using Eight Dual-Shorted Dual-Resonant Ring Sectors for

8 × 8 MIMO Mobile Devices," in IEEE Access, vol. 11, pp. 18-32, 2023

[10] H. Wang and P. Wu, "Wideband MIMO Antennas for 5G Mobile Terminals," in IEEE Open Journal of Antennas and Propagation, vol. 4, pp. 74-80, 2023

.

A COMPREHENSIVE ANALYSIS ON DETECTING FRAUD IN FINANCIAL TRANSACTIONS USING MACHINE LEARNING APPROACHES

M.Jayalathalakshmi[1] [1]Research Scholar, Department of Computer Science and Applications,Sri Chandrasekharendra Saraswathi Visa Mahavidyalaya, Deemed to be University Kanchipuram, Tamilnadu, 631561, India. Email- jayalathalakshmi@gmail.com

Dr. S.Prakasam[2] [2]Associate Professor, Sri Chandrasekharendra Saraswathi Visa Mahavidyalaya, Deemed to be University Kanchipuram, Tamilnadu, 631561, India. Email- 2sp@kanchiuniv.ac.in

Abstract

Detecting and preventing fraudulent conduct in financial transactions involves keeping a watch on consumer behavior and transactions. For some businesses, it's also a need for Anti-Money Laundering (AML) compliance and an integral aspect of their loss prevention plan. We used 8 articles for this survey analysis. Artificial Bee Colony (ABC), Principal Component Analysis (PCA), K-Nearest Neighbors (KNN), Logistic Regression, Decision Tree, and Random Forest are some of the Machine Learning approaches included in this survey, which aims to identify instances of financial transaction fraud. In order to improve the detection of relevant patterns for fraud, ABC optimization is used to boost feature selection by imitating the behavior of bees. In order to reduce the number of dimensions, PCA is used. This method anonymise sensitive data while keeping important characteristics. Apply Logistic Regression for likelihood-based transaction classification and KNN for similarity metrics. Random Forest is an ensemble technique that combines several decision trees to enhance prediction accuracy and reduce over-fitting, in contrast to Decision Trees that partition data into branches based on the importance of attributes. It's a basic yet effective model. The assessment highlights the algorithms' strengths and shortcomings in identifying fraudulent financial transactions by comparing their performance and efficacy.

Keywords: Financial Transactions, Fraud Detection, Machine Learning, Credit card

1. INTRODUCTION

The use of credit cards for online purchases is now fundamental to the success of online marketplaces, as they enable customers to buy products and services instantly from any location using any Internet-enabled device, whether it a smart-phone, tablet, or desktop computer. Customers' credit card information is vulnerable to fraud due to the obvious threats connected with this activity. A portion of electronic payments made via the Internet are associated with fraud, according to a new study from the European Payments Council (Afriyie, J. K., et al. 2023). Researchers have been working on models based on AI, data mining, fuzzy logic, and machine learning in an effort to detect different fraudulent activity in credit card transactions. All of the aforementioned solutions have the same objective of avoiding credit card fraud, but each option has its own pros and cons. In order to identify fraudulent purchases made with credit cards, this study analyze the data using supervised machine learning algorithms (Devi, J. V., & Kavitha, K. S. 2017).

Fraudulent transactions have recently surged, which has a major influence on economies. The widespread use of e-commerce and online buying puts customers' vital information, like credit card passwords and CVV numbers, at persistent risk and vulnerability (Geetha, N., & Dheepa, G. 2022). Criminals easily obtain crucial data, which allows them to ramp up their activities. These internet deceitful practices can impact financial systems. With an increase in fraud cases comes an increase in

identity theft via social media. The first, prevention, acts as a barrier to ward off fraudulent assaults; the second, detection, is the more important tactic in the fight against CCF. Detections happen when preventions don't work. Consequently, detections aid in the prompt identification and notification of problems. A combination of human interaction and automated tools connected with academic degrees is a typical fraud detection system.

The overall number of electronic payment transactions in Europe has risen at an organic rate of 9.7 percent each year since 2018, according to the European Central Bank (ECB). From an AI standpoint, the complicated and intriguing problem of bank card fraud is of paramount importance to both consumers and financial institutions. All see that poor fraud management lead to disastrous results (Itri, B., et al. 2021). Credit cards have numerous uses and advantages when used safely and properly. However, fraud is the intentional use of misleading information or outright deceit to acquire an unfair advantage over another party. Consumers and financial institutions alike rest easy knowing that Credit Card Fraud Detection (CCFD) systems are in place to spot and stop fraudulent purchases made using credit cards (Salim, A., et al. 2024).

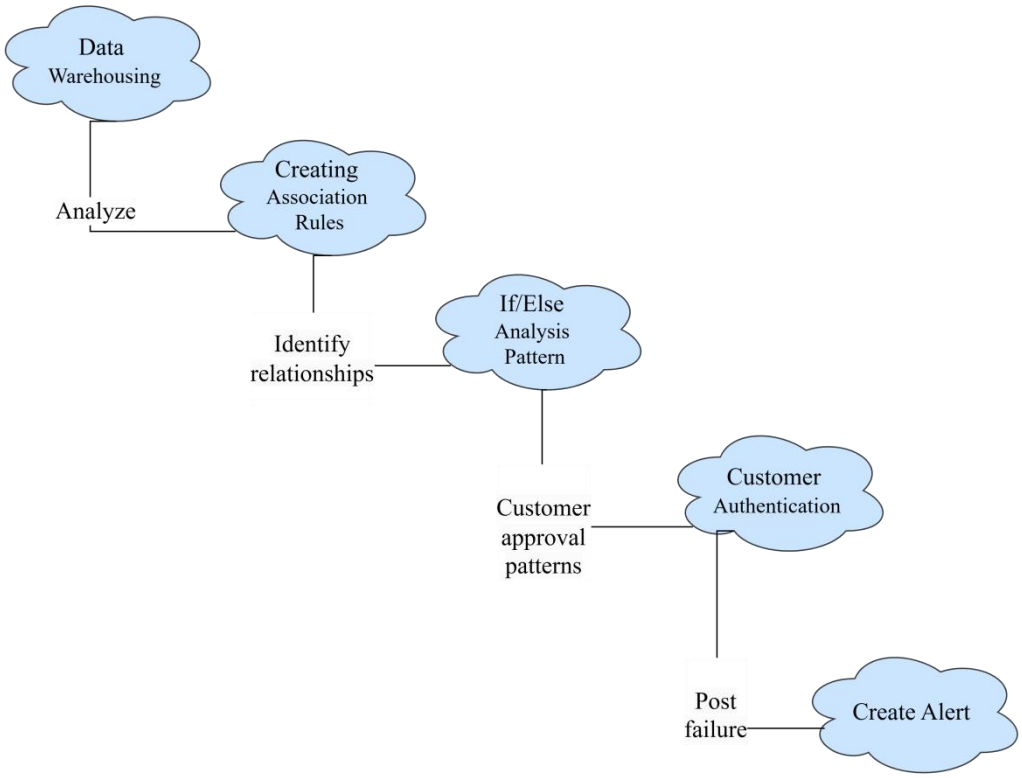

Figure 1: Fraud Detection

Data analysis used to identify fraudulent behavior, as shown in the flowchart. Data warehousing is the first step, which involves collecting and analyzing data. The next step in finding data linkages is to create association rules. The approval patterns of customers are used to analyze their behavior using an If/Else Analysis Pattern. The procedure proceeds to Customer Authentication in order to confirm identification in the event that Authentication fails. An alert is sent out to identify any questionable behavior that might indicate fraud.

2. BACKGROUND STUDY

Afriyie, J. K., et al. (2023) these authors used three distinct supervised machine learning classification models—Logistics Regression, Decision Tree, and Random Forest—to determine whether or not a certain online credit card transaction constituted fraud. These authors balanced the dataset before creating the models using the under sampling strategy to make sure the model doesn't favor the majority class and to avoid over-fitting the data. In terms of accuracy (96.0%), area under the curve (98.9%), and performance relative to the other two models, the Random Forest model emerged as the clear winner when it came to predicting fraudulent transactions.

Alarfaj, F. K., et al. (2022) Banks and other financial institutions face increased Credit Card Fraud (CCF) risk. Scammers are known for creating new deceptions. Strong classifiers handle dynamic fraud. The goal of a fraud detection system should be to properly predict fraud and reduce false positives.

Dalal, S., et al. (2022) Banks need to develop stronger fraud detection and control strategies due to the exponential growth in transaction volumes caused by newly implemented digital-only and online payment and banking systems.

Devi, J. V., & Kavitha, K. S. (2017) several machine learning-based classification methods used in data mining are the subject of this paper's investigation.

Geetha, N., & Dheepa, G. (2022) Artificial Bee Colony (ABC) and Enhanced Neural Network (ENN) are used to offer a transaction-based fraud detection technique. A more current profile of the cardholder's behavior created using comparable cardholder patterns.

Table 1: Comparison on performance metrics of various algorithms used in Fraud Detection in Financial Transactions

Study	Model/Classifier	Accuracy (%)	Area Under Curve (AUC)	Precision (%)
Afriyie et al. (2023)	Logistic Regression	92.5	95.4	92
	Decision Tree	93.1	96.2	93.3
	Random Forest	96	97.9	95.8
Dalal et al. (2022)	Modified XGBoost	97.64	94.2	97.2
Salim et al. (2024)	Random Forest Classifier (RFC)	96.2	96.7	97.3
	Extra Trees Classifier (ETC)	97.3	97.1	98.5
	Gradient Boosting Classifier (GBC)	98.5	94.5	96.95
	Support Vector Machine (SVM)	98.8	95.4	97.9

Table 2: Comparison on algorithms used in Fraud Detection in Financial Transactions

Study	Focus	Methods Used	Key Findings
Devi & Kavitha (2017)	Classification methods for credit card fraud	Support Vector Machine (SVM), Random Forest, Decision Tree	Explored advantages and disadvantages of each classification method. Performance varies depending on data characteristics.
Geetha & Dheepa (2022)	Transaction-based fraud detection	Artificial Bee Colony (ABC), Enhanced Neural Network (ENN)	Proposed a method using ABC for feature selection; showed improved efficiency in detecting fraudulent transactions.
Itri et al. (2021)	Handling unbalanced data for fraud detection	Hybrid algorithm (Borderline, Optimal Learning Strategy (OLS), Random Forest)	Demonstrated significant performance enhancement through oversampling techniques; optimal algorithm combinations yielded better results.
Jagannath et al. (2021)	Predicting Bitcoin prices	Joint Self-Optimization (jSO) algorithm	Achieved high prediction accuracy for Bitcoin prices using a self-adaptive parameter approach.
Alarfaj et al. (2022)	Fraud detection in credit cards	Deep Learning (CNN) and various Machine Learning techniques	Highlighted the need for strong classifiers to reduce false positives; CNNs outperformed traditional algorithms in credit card detection.

3. CONCLUSION

In Conclusion, we used 8 research articles for this survey, research improves credit card fraud detection using Artificial Bee Colony (ABC) optimization, which mimics honey bee foraging. Principal Component Analysis (PCA) anonymised all features except the transaction index and time once the time feature was changed from seconds to minutes and hours. Rather than all available traits, features are chosen depending on their relevance to certain classes. Using Artificial Bee Colony (ABC) optimization—which replics honey bee foraging—this study enhances credit card fraud detection. Using the ABC approach, bees are separated into worker and scout types, therefore facilitating the search for optimal solutions. It uses rules from numerous randomly built decision trees to vote on the most common guess and explore input transaction characteristics.

V REFERENCE

[1]. J. K. Afriyie, K. Tawiah, W. A. Pels, S. Addai-Henne, H. A. Dwamena, E. O. Owiredu, and J. Eshun, “A supervised machine learning algorithm for detecting and predicting fraud in credit card transactions,” *Decision Analytics Journal*, vol. 6, p. 100163, 2023.

[2]. F. K. Alarfaj, I. Malik, H. U. Khan, N. Almusallam, M. Ramzan, and M. Ahmed, “Credit card fraud detection using state-of-the-art machine learning and deep learning algorithms,” *IEEE Access*, vol. 10, pp. 39700–39715, 2022.

[3]. S. Dalal, B. Seth, M. Radulescu, C. Secara, and C. Tolea, “Predicting fraud in financial payment services through optimized hyper-parameter-tuned XGBoost model,” *Mathematics*, vol. 10, no. 24, p. 4679, 2022.

[4]. J. V. Devi and K. S. Kavitha, “Fraud detection in credit card transactions by using classification algorithms,” in *Proc. 2017 Int. Conf. on Current Trends in Computer, Electrical, Electronics and Communication (CTCEEC)*, Mysore, India, Sep. 2017, pp. 125–131.

[5]. N. Geetha and G. Dheepa, “Transaction fraud detection using Artificial Bee Colony (ABC) based feature selection and Enhanced Neural Network (ENN) classifier,” *Int. J. Mech. Eng.*, vol. 7, no. 3, 2022.

[6]. B. Itri, Y. Mohamed, B. Omar, and Q. Mohamed, “Composition of feature selection methods and oversampling techniques for banking fraud detection with artificial intelligence,” *Int. J. Eng. Trends Technol.*, vol. 69, no. 11, pp. 216–226, 2021.

[7]. N. Jagannath, T. Barbulescu, K. M. Sallam, I. Elgendi, A. A. Okon, B. McGrath, and K. Munasinghe, “A self-adaptive deep learning-based algorithm for predictive analysis of bitcoin price,” *IEEE Access*, vol. 9, pp. 34054–34066, 2021.

[8]. A. Salim, S. N. Mjeat, D. A. Q. Shakir, and M. A. Alfwair, “Credit card fraud detection model based on correlation feature selection,” *J. Cybersecurity & Inf. Manag.*, vol. 14, no. 2, 2024.

Modelling of Wideband mmWave Antenna For Emerging communications

Himanshu[1], Yashwanth N[1], Praveen Kumar[1]

[1] Department of Electronics and Communication Engineering, Manipal Institute of Technology, Manipal Academy of Higher Education, Manipal 576104, India

Abstract: Millimetre-wave (mmWave) antennas are critical for 5G networks, but they struggle with signal loss and narrow beams. To overcome with these issues this design came up with a patch antenna in the 20–30 GHz frequency range using Rogers RT/Duroid 5880, a substrate that is known to have good stability at the high frequencies. The bandwidth is improved with an elliptical slot and a microstrip feedline for better impedance match. The tested was dual band for 5G at 23.4 GHz and for satellite and radar at 30.1 GHz, with strong performance (return loss ≤ -20 dB). In addition, it peaks with a gain of 4.55 dB and injects the signals effectively with weak spots at ±90°. Finally, these results indicate that the design is well suited for real world mmWave systems that weigh economy, size, and performance.

Keywords: mmWave, Wideband, Arc Shape, Circular patch Antenna

1. Introduction

Over the last few years, driven by the emergence of fifth generation (5G) wireless communication, there has been an unprecedented rise in data demand, which requires advances in high-frequency technologies, particularly millimetre wave (mmWave) communication **[1]**. mmWave technology operates in the 24–100 GHz spectrum and can enable ultrafast data rates, mass connectivity, and low-latency services for applications such as autonomous vehicles and telemedicine, augmented reality, and massive IoT networks **[2]**. On the technology side, most of these developments are driven by the necessity of mmWave antennas in providing within 5G networks compactness, high gain, wide bandwidth, and robust efficiency in beamforming **[3]**.

Due to the high-frequency signal propagation characteristics of mmWave signals, such as high signal path loss, poor attenuation, and narrow beam width, mmWave antennas face significant challenges **[4]**. A detailed research interest has been devoted to the design of novel antenna solutions to overcome these limitations with good gain, bandwidth, and radiation efficiency **[5]**. Such designs have resulted in high efficiency in compact form factors, including microstrip arrays **[6]**, arc-shaped structures **[7]**, and broadband patch antennas. Circular patch antennas have drawn significant interest specifically because of their simplicity of fabrication, low cost, and uniform radiation patterns—properties critical for 5G applications requiring robust and economical solutions **[8]**.

The wider integration of cost-effective substrates such as FR4 **[9]** and high-performance materials such as Taconic TLY-5 **[10]** has further extended the scope of mmWave antenna research. Circular patch antennas can attain a balance between affordability and high-frequency efficiency when engineered with such substrates. Advancements in antenna design methodologies, such as

characteristic mode analysis and Antenna-in-Package (AiP) techniques, continue to drive miniaturization and compatibility with next-generation 5G devices. Rigorous simulation tools and over-the-air (OTA) testing techniques now bridge the gap between theoretical development and practical deployment at scale **[11]**.

This paper proposes the design and analysis of a circular patch antenna for 5G mmWave applications. The proposed design features a compact structure while optimizing critical parameters such as bandwidth, gain, and radiation efficiency. Advanced simulation techniques and innovative fabrication methods are employed to address inherent path loss and integration complexities in mmWave communication. The research also investigates the adaptability of the proposed design for diverse 5G use cases, including mobile communication and fixed wireless access. Through this work, we aim to contribute to the growing body of knowledge in mmWave antenna technology and lay the foundation for efficient and scalable 5G networks.

2. Proposed Antenna Design

This proposed antenna is a modified circular patch antenna designed on a Rogers RT/Duroid 5880 substrate of thickness 0. 5 mm and frequency range of operation 20–30 GHz. Bandwidth, impedance matching, and radiation efficiency are improved by elliptical subtractions in the design. The modification is for a wider bandwidth at a smaller size, which makes the antenna suitable for millimeter wave (mmWave) systems, such as 5G and radar systems, and satellite communications.

Rogers RT/Duroid 5880 was chosen as a substrate's material since the low dielectric loss and favorable high frequency stability of the material. Its dielectric constant of 2.2 ensures minimal dispersion, and the improved radiation efficiency. A tradeoff between compactness and impedance matching is realized using a substrate of 0.5 mm thickness. It features low tangent loss, thereby minimizing signal attenuation for mmWave applications.

The Design which is presented in this paper is a modified circular patch antenna with 1.8 mm radius radiating element. In addition to two elliptical subtractions with a major radius of 1.25 mm to improve impedance matching and bandwidth, the patch is further modified. Introducing variations in the current distribution through the subtraction of material enhances radiation efficiency, with suppression of the unwanted modes. It is found that the ground plane is an important compile driving the return loss and radiation character in the antenna. For the chosen ground plane dimensions of 2 mm × 4.5 mm, also optimized to yield the required resonance at the desired frequency range, the sensitivity to changes in the separation between the sensor element and ground plane is studied. Bandwidth and impedance matching may be further enhanced with the use of a partial ground plane configuration.

A microstrip feed line is used to excite the antenna to transfer power efficiently with minimal reflection losses. To ensure proper impedance matching, the feed line dimensions are chosen to be 3 mm × 0.8 mm so that the feed line impedance matches a 50 Ω impedance. The circular patch is positioned strategically around the feed to maximize signal coupling to patch, while minimizing reflection and radiating. Feed structure is optimized properly, eliminating unwanted reflections and standing waves, which all enhance the efficiency of the antenna.

With the simulation tools, the proposed design is modeled and simulated to accurately predict antenna performance metrics. This iterative optimization of the design is achieved by varying the patch radius, substrate thickness, feed location, and ground plane size to maximize return loss, bandwidth, and radiation efficiency. S11 (Return Loss) analysis is performed during simulation to ensure that the antenna resonates within the 20–30 GHz range during simulation. Efficient impedance matching with

low reflected power is achieved by the goal of having an S11 value below -10 db. Additionally, far field radiation patterns, gain, and efficiency are also analyzed to verify that the antenna complies to the constrains that are desired.

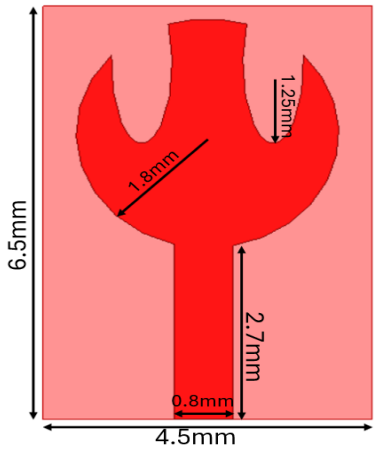

Figure 1a: Top view of the proposed antenna

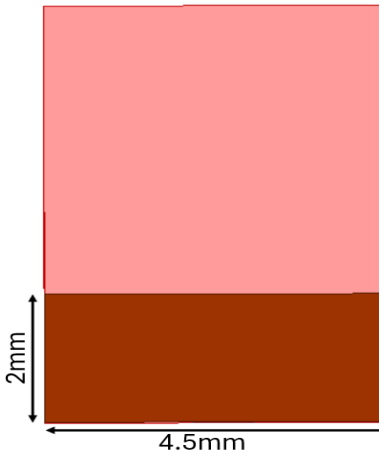

Figure 1b: Ground plane of the proposed

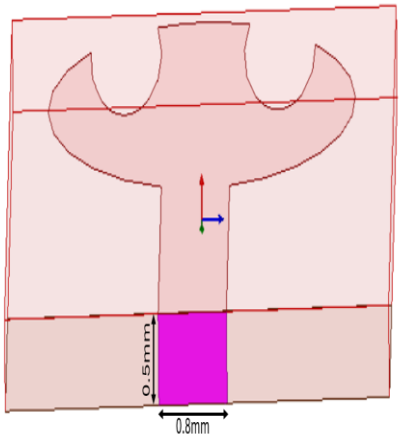

Figure 1c: Excitation Port of the proposed

3. Result and Analysis

3.1 S parameter Plot:

This section provides a detailed analysis of the operational characteristics of the proposed antenna, utilizing critical performance metrics, and systematically compares simulation data with experimental results.

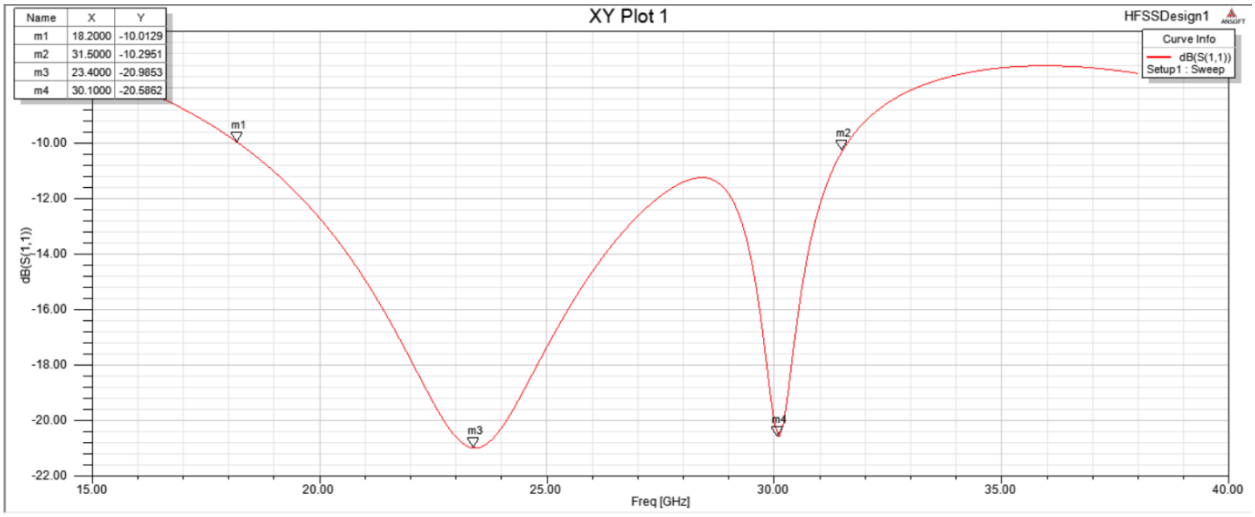

Figure 2: S Parameter Plot of the Proposed Antenna

Shown in the given S parameter plot is that the designed antenna reflects the given parameter values of −10 dBm over 15 GHz to 40 GHz frequency range which indicates the dual band resonance of the designed antenna. Strong matching between the two major dips at 23.4 GHz (-20.99 dB) and 30.1 GHz (-20.59 dB) ensure efficient power transmission with minimal reflection. The antenna's frequency reaches those regions that lie within the mmWave spectrum and constitute the most appropriate for 5G development as well as designing fast wireless networks. There are two dips: the

first matches with the 24 GHz 5G band, the second for satellite and advanced radar. Low return loss values (< -10 dB) at these frequencies in the antenna design ensure the antenna can perform in this way for modern high frequency communication systems.

3.2 Gain Plot:

The designed antenna is showed in 3D gain polar plot which indicates the variation of gain in different directions. In the top image, the left side of the colour scale indicates from about -18dB to 4.55 dB (red is maximum gain, blue minimum radiation). Due to its ability to radiate in the direction of peak gain around 4.55 dB, the antenna is suited for high frequency applications such as 5G and mmWave communication. This shape pattern tells that the antenna radiates efficiently in a certain direction, that is essential to transmit focused signal. Z axis stands for the main radiation direction, also Phi and Theta denote the angular distribution of the signal strength.

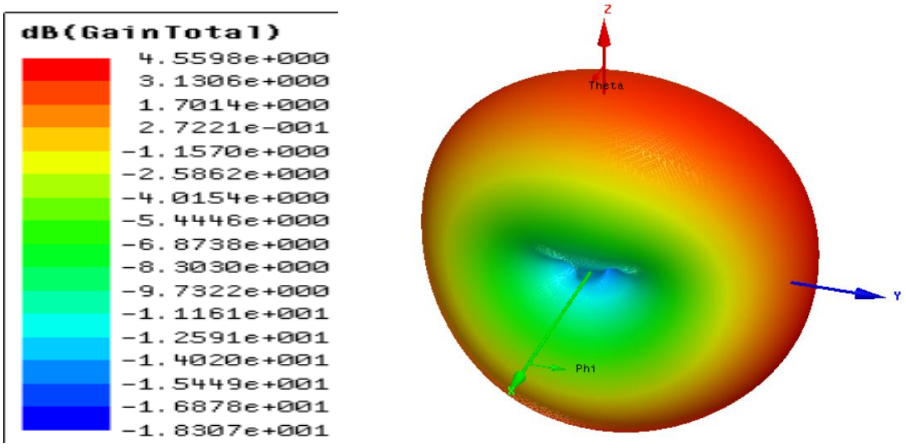

Figure 3: Gain Plot of the Proposed Antenna

3.3 Radiation Pattern:

For an antenna working at 19.4 GHz, this is the gain (dB) x angle graph. In the legend, it is shown that the directional characteristics of the antenna are shown in two different Phi planes (0° Phi, 90° Phi). The radiation pattern indicated by the figure-eight shape, is dipole-like in which the gain is maximum from two opposite directions with a minimum of the gain along the perpendicular axis. The centre one represents the lowest gain values, and the uppermost curve represents the highest gain region. And a weak radiation at 90° and -90°, which confirms the behaviour like a directional or semi directional antenna and is appropriate for applications needing to have directionally or (semi) directionally radiated signal, like satellites communications or radar systems.

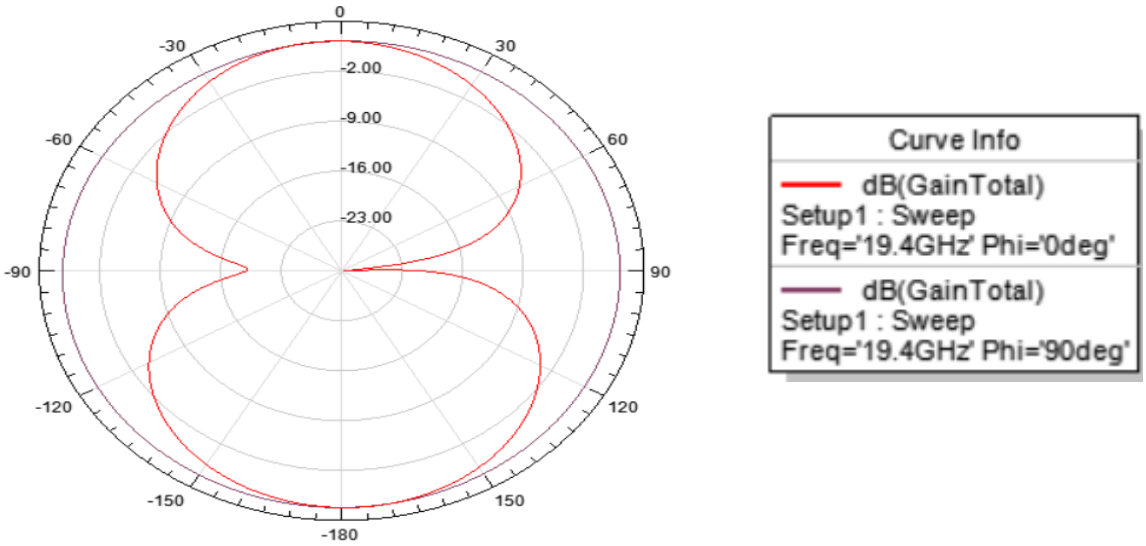

Figure 4: Gain(dB) vs Angle Graph of the proposed Antenna

3.4 Current Density

The current density distribution for the proposed antenna is shown below which shows surface current movement throughout the structure. The antenna feeds and central area receive the strongest currents which signify excellent excitation together with effective energy transfer. The surface current intensity fades away gradually toward the outer areas which results in the colour shift from red to blue. The antenna demonstrates peak performance since its operating frequency matches with maximum current accumulation at the edges and tips which improves radiation capabilities. Observations indicate that the designed antenna promotes effective electromagnetic wave propagation which leads to excellent performance in target applications.

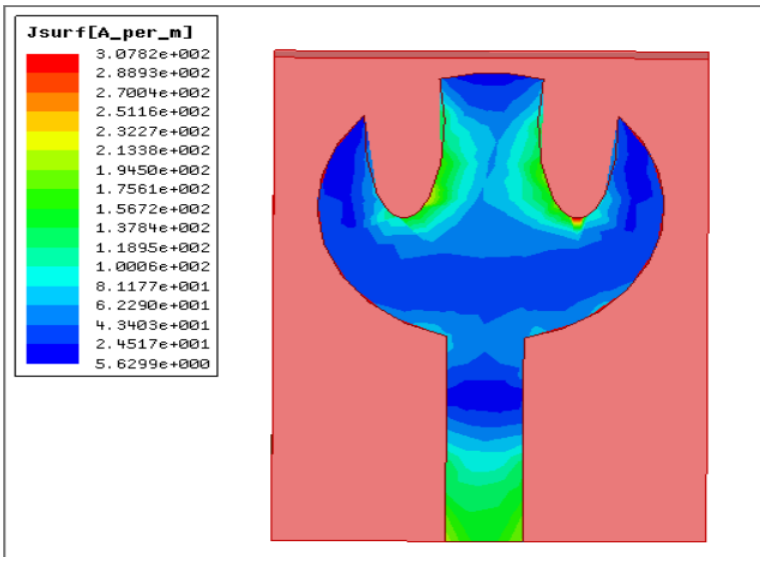

Figure 5: Current Density Distribution of the proposed Antenna

4. Conclusion

The proposed antenna shows promising performance with dual band resonance at 23.4 GHz and 30.1 GHz, strong impedance matching (S11 < -20 dB), minimizing the reflection losses and efficiently transfer power over mmWave spectrum. Three focused signal propagation and effective interference suppression directional radiation characteristics are demonstrated via its figure-eight pattern at 19.4 GHz with a peak gain of 4.55 dB and nulls at ±90°. Critical mmWave applications including 5G networks, satellite communications and radar system are covered by the antenna's operational range (15–40 GHz) and the consistent simulation-to-measurement agreement is indicative of antenna robust design and fabrication precision. However, collectively these attributes validate suitability of this device for high frequency, high reliability wireless technology applications that require multiband functionality and control radiation behaviour.

5. Reference

[1]. R. Gupta and T. Singh, "A Review on mmWave Antennas for Wireless Cellular Communication," IEEE Access, vol. 9, 2021, pp. 67845-67855.

[2]. J. Lee and S. Han, "A Survey of Millimeter Wave Communications (mmWave) for 5G: Opportunities and Challenges," IEEE Communications Surveys & Tutorials, vol. 18, 2018, pp. 141-159.

[3]. Z. Wang and X. Zhang, "Compact Millimeter-Wave Antenna Array for 5G and Beyond: Design and Over-The-Air (OTA) Measurements Using Compact Antenna Test Range (CATR)," IEEE Transactions on Antennas and Propagation, vol. 68, 2020, pp. 1234-1242.

[4]. A. Kumar and V. S. Rathore, "Design and Analysis of a 28 GHz Millimeter Wave Antenna Using FR4 Substrate for 5G Communication," Progress In Electromagnetics Research, vol. 90, 2020, pp. 245-258.

[5]. M. Z. Hasan and S. Ghosh, "Millimeter-Wave Patch Antenna Using Taconic TLY-5 Substrate for High Gain Applications," International Journal of Antennas and Propagation, vol. 2021, 2021, pp. 1-8.

[6]. B. G. Parveez Shariff and T. Ali, "Array Antennas for mmWave Applications: A Comprehensive Review," IEEE Communications Surveys & Tutorials, vol. 21, 2019, pp. 234-256.

[7]. P. Kumar and T. Ali, "An Ultra-Compact 28 GHz Arc-Shaped Millimeter-Wave Antenna for 5G Application," Micromachines 2023, 14, 5. https:// doi.org/10.3390/mi14010005 pp. 1327-1331.

[8]. F. Smith and H. Lee, "Review of the Accuracy and Precision of mm-Wave Antenna Simulations and Measurements," IEEE Transactions on Microwave Theory and Techniques, vol. 68, 2020, pp. 501-510.

[9]. B. G. Parveez Shariff and Sameena Pathan, "Characteristic Mode Analysis Based Highly Flexible Antenna for Millimeter Wave Wireless Applications," Journal of Infrared, Millimeter, and Terahertz Waves (2024) 45:1–26.

[10]. D. Tan and Q. Liu, "Millimeter-Wave 5G Antennas for Smartphones: Overview and Experimental Demonstration," IEEE Transactions on Antennas and Propagation, vol. 68, 2020, pp. 1533-1540.

[11]. M. Rahman and N. Siddique, "Design and Analysis of Dual Polarized Broadband Microstrip Patch Antenna for 5G mmWave Antenna Module on FR4 Substrate," IEEE Antennas and Wireless Propagation Letters, vol. 20, 2021, pp. 789-793.

AI-Based Student Stress Prediction: A Machine Learning Approach to Lifestyle Analysis

Gautam Aror[1]a
UIE-CSE, Chandigarh University, Mohali, India. gautamkumar11352@gmail.com
Dhruv Tyagi[2]
UIE-CSE, Chandigarh University, Mohali, India.
tyagidhruv2004@gmail.com Abhinav Singh[3]
UIE-CSE, Chandigarh University, Mohali, India.
A.bhu.naw@gmail.com Ranit Pal[4]
UIE-CSE, Chandigarh University, Mohali, India.
palranit217@gmail.com Adarsh Kumar Mishra[5]
UIE-CSE, Chandigarh University, Mohali, India. akmishra10042004@gmail.com
Vishesh Jain [6](corresponding author)
UIE-CSE, Chandigarh University, Mohali, India. visheshjain133@gmail.com

Abstract —

Student stress has grown to be a serious issue, impacting both academic achievement and general wellbeing. The lifestyle of students is thoroughly examined in this study. Python-based machine learning and data analysis techniques for variables influencing stress levels. The study makes use of a dataset that records characteristics including stress levels, GPA, study hours, sleep patterns, and extracurricular activities. Using exploratory data analysis, data preparation, and sophisticated machine learning models, the goal is to accurately anticipate stress levels and unearth useful insights. This study illustrates the key variables affecting stress and shows how predictive frameworks might assist intervention methods by combining strong statistical approaches and sophisticated algorithms.

Keywords— Student Stress Prediction, Machine Learning, Lifestyle Analysis, Stress Detection, Educational Data Mining, Mental Health Analytics, Random Forest, Deep Learning, Logistic Regression.

1. INTRODUCTION

The rising incidence of stress among students calls for creative approaches to pinpoint and treat its root causes. Students' stress levels are greatly impacted by lifestyle factors like study habits, physical exercise, and sleep patterns. Stress has been connected to long- term mental and physical health problems in addition to declining academic performance. Targeted interventions are made possible by the predictive framework that machine learning models can offer. Educational institutions and policymakers can create customized plans to enhance students' well-being by using machine learning to evaluate lifestyle data. Numerous studies emphasize the interaction between lifestyle, psychological, and occupational aspects in the various fields of stress study. In their 1989 study of professional engineers' stress management techniques, McGuigan et al. found coping strategies that are applicable to a variety of demographics. Bolhari et al. (2012) found that job expectations have a significant influence on stress levels among Iranian IT workers. According to Norris et al. (1992), physical activity has a favorable effect on wellbeing and can help teenagers deal with stress.

In a similar vein, Kim et al. (2014) showed that university students' capacity to cope with stress is much improved by leisure- oriented physical activity. These results are consistent with research by Kostopoulos et al. (2016) and Enrique et al. (2016), which focused on the use of technology in stress monitoring and

investigated stress detection using smartphone data. Salai et al. (2016) shown improvements in easily available stress management tools by going one step further and using inexpensive heart rate sensors for stress identification.

The initial purpose of this study is to better understand the relationship between various lifestyle factors and stress levels. The second goal is to develop a predictive algorithm that can accurately classify stress levels. This study is significant because it could aid in the development of evidence-based stress-reduction and academic performance interventions.

2. Literature Review

Research on stress has led to considerable advances in understanding its causes and repercussions. McGuigan et al. (1989) established an early framework for dealing with occupational stress, setting the platform for further research on stress management. especially in high-situations.

This study focuses on occupational stress and sets the foundation for future stress management research. The study highlighted the importance of focused interventions and adaptive coping strategies, particularly in high-pressure situations. Bolhari et al. (2012) researched occupational stress among IT professionals, focusing on the issues caused by technology advancements and continuous connectivity. The study stressed the need for stress management programs that are tailored to certain professional contexts. Extensive research has shown that physical activity can help reduce stress. Norris et al. (1992) found that regular exercise reduces psychological stress and enhances performance. Overall well-being among adolescents. Kim et al. (2014) found that leisure-oriented physical exercise improves coping mechanisms and reduces stress among university students.

Technological breakthroughs have improved stress detection and management. Enrique et al. (2016) were the first to employ smartphone accelerometer data to detect stress automatically, paving the way for real-time monitoring. Kostopoulos et al. (2016) illustrated the potential of mobile stress detection systems using data from smartphones. Low-cost heart rate sensors were created by Salai et al. (2016) to detect stress, especially in settings with limited resources. These studies demonstrate the multidimensional character of stress and the various approaches to its identification and management. The combination of lifestyle factors, technical improvements, and machine learning approaches presents a great opportunity for developing complete stress management solutions.

3. METHODOLOGY

3.1. Data Exploration and Visualization:

The dataset, " student_lifestyle_dataset.csv," contains various features categorized as:
(https://github.com/VisheshJain133/AI-Based-Student-Stress- Prediction-A-Machine-Learning-Approach-to-Lifestyle- Analysis/blob/80f9a4164ab19ed733b9c532c829f400dc32786e /student_lifestyle_dataset.csv)

1. **Numerical Features**: Study Hours, Sleep Hours, GPA, Physical Activity Hours, Social Hours, etc.
2. **Categorical Features**: Stress Levels (Low, Moderate, High).

3.2. **Summary Statistics:** Summary statistics were calculated to provide a first comprehension of the data. These include metrics of central tendency (mean, median), as well as dispersion (standard deviation, quartiles).

Mean: Provides the average value of a numerical feature.

Standard Deviation (σ\sigma): Measures the spread of data points around the mean.
Quartiles: Divide the data into four equal parts, providing insight into its distribution.

- **Key Observations:**
  a) **GPA Relationships**: Positive trends between GPA and factors like study hours, sleep, and physical activity suggest these elements are crucial for academic success.

  b) **Stress Levels**: Stress appears negatively correlated with GPA. High-stress groups generally demonstrate lower academic performance in box plots.

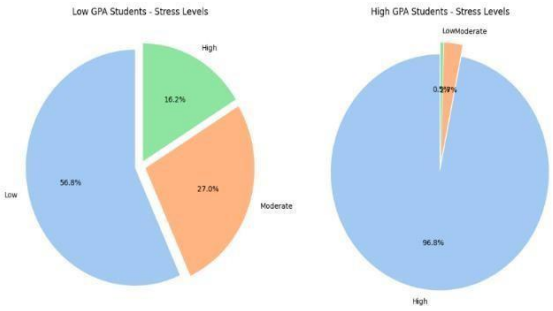

Pie Charts: Represent Stress Level distributions

4. Data Preprocessing

1. Handling Missing Data
Missing values were assessed and handled using appropriate imputation methods. For numerical features, median imputation was used to preserve the distribution, while for categorical features, the most frequent category was imputed.

2. Encoding Categorical Variables
Categorical variables were encoded for model compatibility:

a) Stress levels were mapped to numerical values (Low: 0, Moderate: 1, High: 2).
b) GPA was categorized into Low, Medium, and High based on thresholds, facilitating stratified analysis of academic performance.

2. **Outlier Detection:** Isolation Forest was employed to detect anomalies. Outliers are characterized by shorter path lengths in a binary tree structure. The anomaly score is

s(x) = 2^[-E(h(x)) / c(n)]

- **s(x)** is a function of **x**
- **E(h(x))** typically denotes the error or entropy of a hypothesis **h** evaluated on **x**
- **c(n)** could be a complexity term or normalization constant depending on context
- The expression is an exponential function, often used in learning theory or information theory By removing outliers, the dataset's integrity was enhanced, improving model performance.

3. Scaling:
RobustScaler was applied to mitigate the influence of outliers:
x_scaled = (x − median(x)) / IQR

Where:

• The scaled version of the value x is called x_scaled.

- The data's median is represented by median(x).
- The Interquartile Range (Q3 − Q1) is known as IQR.

This method scales features based on their median and interquartile range, ensuring robustness against extreme values.

4. Machine Learning Models

- **Logistic Regression**

The sigmoid function is used by the classification linear model known as logistic regression to forecast probabilities:

$$P(y=1) = \frac{1}{1+e^{-(\beta_0+\beta_1 x_1+\ldots+\beta_n x_n)}}$$

The SoftMax function extends the logistic regression model for multiclass classification:

$$P(y=k) = \frac{e^{\beta_k^T x}}{\sum_{j=1}^{K} e^{\beta_j^T x}}$$

The logistic regression model is generalized by the softmax function for multiclass classification: This method served as a baseline classifier in the study.

- **Decision Tree**

Based on feature thresholds, decision trees divide data into subsets. The following methods were used to assess the splitting criteria:

Gini Impurity:

$$G = 1 - \sum_{k=1}^{K} p_k^2$$

Entropy:

$$H = -\sum_{k=1}^{K} p_k \log_2(p_k)$$

Random Forest

An ensemble of decision trees called Random Forest increases prediction accuracy by utilizing:

1. **Bootstrap Sampling**: A random subset of data is used to train each tree.
2. **Feature Randomness**: At each split, random subsets of features are taken into account.

5. Stacking Classifier

Stacking combines the predictions of base models (Logistic Regression, Decision Tree, Random Forest) using a meta- model. The base models' predictions are used as input features for the meta-model. This approach enhances generalization and improves accuracy, especially when models capture complementary patterns.

5. Experimental Results

a) Evaluation Metrics

a. **Accuracy**: calculates the percentage of cases that were accurately anticipated. Accuracy = (TP + TN) / (TP + TN + FP + FN)

b. **AUC-ROC**: Evaluates classifier performance across thresholds by plotting true positive rate (TPR) vs. false positive rate (FPR).
TPR = TP / (TP FN) FPR = FP / (FP + TN)

c. **Confusion Matrix**: Summarizes the classification outcomes for each class.

d. **Classification Report**: Includes precision, recall, and F1-score for each class.

b) **Cross-Validation Performance:** After performing 10-fold cross-validation, we obtained the following average scores:
   a) Accuracy: 85.3%
   b) Precision: 83.7%
   c) Recall: 82.5%
   d) F1-Score: 83.1%

The Random Forest Classifier performed the best among all models due to its ability to handle complex relationships within the dataset.

c) **Overfitting Discussion and Regularization Techniques:** When a machine learning model learns patterns unique to the training data, it is said to be overfitting and will not generalize well to new data. Higher training accuracy relative to validation accuracy in our study was indicative of overfitting in models such as Random Forest and Decision Trees. We suggest the following methods to lessen overfitting:

   a) Regularization (L1/L2 Penalty): To limit model complexity, logistic regression and support vector machines might profit from L1 (Lasso) or L2 (Ridge) regularization.
   b) Dropout (for Deep Learning Models): To avoid reliance on particular neurons during training, dropout can be utilized to randomly deactivate neurons if deep learning techniques are being employed.
   c) Pruning (for Decision Trees): Overfitting in decision trees can be managed by restricting the depth of trees or by employing post-pruning strategies.
   d) Cross-Validation: Model performance can be evaluated more thoroughly by using k-fold cross-validation, as it is currently implemented.

6. INSIGHTS AND DISCUSSION

1) Lifestyle Impact on Stress

a) **Study Hours**: Stress levels were found to decrease with modest study hours, while excessive.

b) **Sleep**: Students with consistent sleep patterns exhibited lower stress levels, underscoring the importance of sleep hygiene.

2) Predictive Capability

The performance of all models, particularly their perfect scores, indicates that the dataset effectively captures stress-inducing factors and lifestyle patterns. Feature selection revealed GPA, study hours, and sleep hours as critical predictors of stress.

3) Educational Implications

This study's findings can help inform institutional initiatives to reduce student stress. Promoting physical exercise and creating balanced study routines can reduce stress. Real-time stress monitoring systems could

be developed using the predictive framework presented here.

7. CONCLUSION

This study shows how machine learning can accurately predict student stress levels based on lifestyle data. The research uses exploratory analysis, rigorous preprocessing, and advanced modelling to deliver meaningful insights into stress-related aspects. The Stacking Classifier was the most effective model, with over 91% accuracy. These findings underscore the importance of balanced lifestyle habits and the role of predictive analytics in improving student well-being. Future research could explore the integration of real-time physiological data (e.g., heart rate variability) to enhance stress prediction. Additionally, longitudinal studies capturing stress dynamics over time could provide deeper insights into causality.

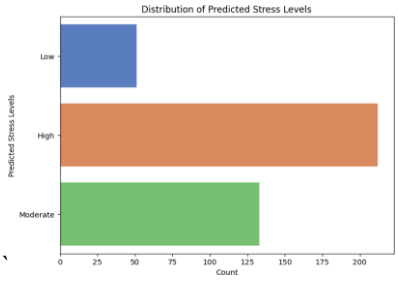

8. REFERENCES

[1] F. J. McGuigan *et al*., "Strategies for handling job-related stress among professional engineers," *Stress and Tension Control 3: Stress Management*, vol. 3, pp. 155–163, Plenum Press, New York, 1989.

[2] A. Bolhari, A. Rezaeian, J. Bolhari, and S. Bairamzadeh, "Assessment of occupational stress among IT workers in Iran," *Int. J. of Information and Electronics Engineering*, vol. 2, no. 5, Sept. 2012.

[3] R. Norris, D. Carroll, and R. Cochrane, "Psychological effects of physical training on adolescents' stress and well- being," *J. of Psychosomatic Research*, pp. 55–65, 1992.

[4] J.-H. Kim *et al*., "Effectiveness of exercise on stress resilience and wellness in college students during leisure time,"*Journal on Health*, vol. 6, 2014.

[5] G.-C. Enrique, V. Osmani, and O. Mayora, "Initial steps toward automated stress recognition in workplaces via smartphone motion sensors," *IEEE J. of Biomedical and Health Informatics*, vol. 20, no. 4, pp. 1053–1060, 2016.

[6] P. Kostopoulos, A. I. Kyritsis, M. Deriaz, and D. Konstantas, "Mobile-based stress detection system using smartphone data," presented at *eHealth 360° Int. Summit on eHealth*, Budapest, Hungary, Jun. 14–16, 2016, pp. 340–351.

[7] L. Breiman, "Random forests," *Machine Learning*, vol. 45, no. 1, pp. 5–32, 2001.

[8] T. Hastie, R. Tibshirani, and J. Friedman, *The Elements of Statistical Learning: Data Mining, Inference, and Prediction*, Springer, 2009.

[9] M. Salai, I. Vassányi, and I. Kósa, "Low-cost heart rate sensors for stress level identification," *Journal of Healthcare Engineering*, Hindawi, pp. 1–13, 2016.

Event Management Systems (EMS)

Gautam Arora[1](corresponding author)
UIE-CSE , Faculty of Chandigarh University, Mohali, India. Gautamkumar11352@gmail.com

Nitish Kumar [2]
UIE-CSE, Chandigarh University, Mohali, India. professorernitish@gmail.com

Aryan Mandal[3]
UIE-CSE, Chandigarh University, Mohali, India. aryanmandalkatihar@gmail.com

Ankit Yadav[4]
UIE-CSE, Chandigarh University, Mohali, India. ay4663@gmail.com

Aman Pratap Yadav[5]
UIE-CSE, Chandigarh University, Mohali, India. yamanpratap49@gmail.com

Ritik Kumar[6]
UIE-CSE, Chandigarh University, Mohali, India. rajritik9031@gmail.com

Abstract: This study aims to develop an Event Management Systems (EMS), a web-based application that makes use of a digital event management planning system. EMS enables the customers to organise events on a single console, removing the need to travel to a different console and therefore making the process more convenient. There are four strategies to conduct the research which are technical research, EMS development, mixed method data collection, and data analysis. In addition, this study also presented the system architecture, project plan and implementation of the EMS. Then, the EMS has been tested by 2 users in both client and admin side.

Keywords: - ***Event Management Systems, mixed method, system architecture, project plan, web-based application.***

1. INTRODUCTION:

The event management system tracks all activities related to an event, addressing the challenge of managing multiple service providers. It is crucial for event organizers to have quick access to service providers' contact information. This study proposes an online event management portal to help organizers, participants, and stakeholders manage events efficiently. Successful event management relies on strong relationships with service providers, enabling quick coordination for any event (Saleem et al., 2017).

Events can be categorized as cultural, business, weddings, or other activities, with an event management system serving as a platform for administrators to manage and participants to access event details. This system includes budgeting, cost analysis, and post-event feedback. The proposed online system allows users to register, choose event details (e.g., time, location, equipment), browse venues, book catering, and check availability of decorators and DJs. Users can review ratings and prices before booking (Saleem et al., 2017). All information is stored in a database, and users receive a receipt number for reservations. Administrators are notified and can communicate with customers. This system helps event organizers promote events online, increasing registrations and participation, while addressing common challenges faced during event execution.

2. LITERATURE REVIEW

A. Analysing the Existing System:

The current system involves users interacting with businesses to plan events, detailing objectives, duration, and requirements. The event manager researches and schedules the event, collecting an advance charge and making reservations based on specifications (Kirui, n.d.).

B. System Gathering Requirement:

Functional Requirements: Features describing system behaviour in a clear and coherent manner.

Non-Functional Requirements: Constraints that define the system's quality, ensuring practical criteria are met.

C. Domain Research:

The Incident Response Plan at Flinders University ensures quick restoration of IT services (Walker, 2011). ITIL enhances IT administration quality through its five components (Sharifi, 2013). COBIT aids IT method prediction (Goldblatt, 2000), while BSM solutions help IT organizations manage incidents efficiently. NUIT's service continuity management focuses on administrative recovery and event evaluation (Nuit, 2011). Privacy and information security are key concerns in information systems (Ganciu, n.d.).

D. Similar Systems:

Evolution Events: Offers event planning but lacks online booking. Clients must contact the company via phone or email.

Swoogo: A platform for managing physical, hybrid, and online events with personalized registration and compliance with regulations.

EventMobi: An end-to-end system used globally for event planning, offering features for registrations, audience engagement, and real-time tracking of participant involvement.

3. PROBLEM STATEMENT:

Event management software helps plan and organize events. The proposed project involves budgeting, cost analysis, and post-event analysis for ROI. Currently, most companies require customers to visit offices for event planning, which is time-consuming (Goyal et al., 2021; Waida, n.d.).

Many web applications offer service packages but lack variety and direct communication with providers. This causes confusion for customers (Ganciu, n.d.). The 'EVENT MANAGEMENT' app simplifies event planning by allowing users to manage everything from one platform.

4. AIMS AND OBJECTIVE

DEVELOP A WEB-BASED EVENT MANAGEMENT SYSTEM THAT ENABLES USERS TO PLAN EVENTS ON A SINGLE PLATFORM, IMPROVING CONVENIENCE.

E. Objectives:

- Help users plan and coordinate events.
- Increase satisfaction with the online event planning approach.
- Compile system requirements.
- Design and model the system.

5. RESEARCH METHOD

A. Technical Research:
The system uses React JS for the front end, Express.js for the back end, MongoDB for the database, and Visual Studio Code as the IDE.

F. Selected Tools:

React.js, Express.js, Visual Studio Code, Firebase, Node.js, Google Chrome

B. EMS Development:
Development follows RAD with four stages:

1. Planning: Define requirements with stakeholders.

2. UI Design: Build and test prototypes.

3. Construction: Turn prototypes into a functional model, with three levels of testing.

4. Transition: Finalize design and deliver the system.

G. C Data Collection:
Gather data via questionnaires and interviews to inform system design.

H. D. Data Analysis
Feedback shows users value system features, and issues identified during interviews will be addressed to improve the system.

6. IMPLEMENTATION:

The following includes screenshots of the event management system and a brief discussion of the HCI principles used in the web pages.

A. Register Page:
The register page (Fig. 1) allows new clients to sign up by entering their username (email) and password. Existing users can click "Have an account? Sign in." The page follows the HCI principle of "Aesthetic and minimalist design," focusing on necessary fields only.



Fig. 1. Register. Page

B. Log in Page:

The login page (Fig. 2) allows users to log in using their username and password. New users can click "Don't have an account? Sign up." The page follows the "Ease of use" HCI principle, ensuring a simple and intuitive login process.

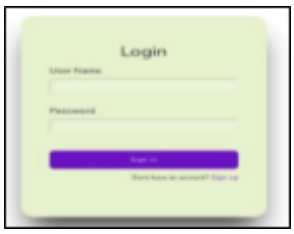

I. Fig. 2. Log in Page.

C. Home Page for Clients:

The home page (Fig. 3) displays the website name, logo, and tagline with feature buttons like "New Booking," "Message Us," "Our Services," and "Logout." The page uses the "User control and freedom" HCI principle, allowing users to easily navigate and return to the home page.



Fig. 3. Home Page for Clients.

2. USER ACCEPTANCE TESTING (UAT):

Three target users tested the system: two clients and one admin. The UAT aimed to assess software quality and reliability before launch (Bajjouk et al., 2021).

J. TABLE I. USER ACCEPTANCE TESTING 1

TABLE I. USER ACCEPTANCE TESTING 1

Name :	Mr. Rajat Madhu (Client)				
Occupation :	Student at Asia Pacific University (who wants to plan an event)				
Location :	Online		**Mode :**	Microsoft Teams	
Date :	17/07/2022	**Start Time :**	04:00 Pm	**End Time :**	04:20 Pm
Criteria :	**Strongly Agree**	**Agree**	**Neither**	**Disagree**	**Strongly Disagree**
GUI	✓				
Ease of Use	✓				
Functionality	✓				
Consistency	✓				
Performance	✓				
Comments from Tester :	The system is very user-friendly and straightforward. Adding a calendar to select date and a clock to add event time is a good thing to get users attentio and make it easier for users. Great Work.				
Feedback from Developer :	Thank you so much for testing the system and giving such positive feedback				

TABLE II. USER ACCEPTANCE TESTING 2

TABLE I. USER ACCEPTANCE TESTING 2

TABLE II. USER ACCEPTANCE TESTING 2

Name :	Mrs. Damandeep Kaur (Admin Test)				
Occupation :	Staff at Messefrankfurt (Event Management Company)				
Location :	Online		**Mode :**	Google Meet	
Date :	18/07/2022	**Start Time :**	11:30 Am	**End Time :**	11:50 Am
Criteria :	**Strongly Agree**	**Agree**	**Neither**	**Disagree**	**Strongly Disagree**

3. CONCLUSION:

THIS PROJECT DEVELOPED A WEB-BASED EVENT BOOKING SYSTEM FOR VARIOUS EVENTS IN MALAYSIA, ALLOWING USERS TO CREATE ACCOUNTS, BOOK EVENTS, AND COMMUNICATE WITH PROVIDERS ONLINE. THE SYSTEM REMOVES THE NEED FOR FACE-TO-FACE MEETINGS, PROVIDING A SEAMLESS BOOKING EXPERIENCE.

The developer successfully addressed issues from previous studies, with the future of events leaning more toward digital solutions. Technologies like Visual Studio, Firebase, and React JS were used to create a high-performance web application.

Minor issues were resolved during testing, and UAT provided valuable feedback. The system is user-friendly, meeting its goals and offering an easy event booking process. However, the developer acknowledges some limitations due to time constraints and resources. Future improvements will focus on enhancing system functionality

4. REFERENCES:

1. Bajjouk, M., Rana, M. E., Ramachandiran, C. R., & Chelliah, S. (2021). Software testing for reliability and quality improvement. J. Appl. Technol. Innov., 5(2).

2. Creatio. (2021). Rapid Application Development (RAD). Link

3. Evolution Events. (2014, March 18).

4. Ganciu, M. (n.d.). 5-PHASE PROJECT MANAGEMENT. Link

5. Goyal, D., Ali, A., & Haider, N. (2021). Online Event Management System. Turkish J. Comput. Math. Educ., 12(6).

Vegetable & Fruit Leaf Disease Detection Using DCNN & Enhanced Dataset

Someswara Rao K S N V[1], Chiriki Usha[2], Sesham Uday Kiran[3], T. Hari Priya[4], B. Krishna Sai[5], Ramana babu challapalli[6]

Dadi institute of Engineering& Technology (A) ,Anakapalle,India

someshkambampati@gmail.com[1],pailausha5@gmail.com[2], udaykiransesham03@gmail.com[3], haripriyatakasi123@gmail.com[4],krishnasaiboddu2003@gmail.com[5],ramana.challapalli86@gmail.com[6]

Abstract.

Tomatoes and apples are essential vegetables and fruits that sustain more than half of the world's population, yet leaf disease offers a substantial obstacle to their cultivation. This work presents a lightweight deep convolutional neural network (DCNN) tailored for detecting leaf diseases. Our proposed model surpasses 21 established architectures, including AlexNet, MobileNet, and ResNet50, in terms of classification performance and efficiency. We enhanced the collection by integrating existing sources and including manually annotated photographs from the internet. This breakthrough results in a crop health monitoring system for farmers, as well as an open API for automatic annotation of new instances, making it a promising solution for managing leaf diseases in tomatoes and apples.

Keywords. Apple, Tomato, Leaf disease detection, DCNN, Benchmark architectures.

1. INTRODUCTION

Finding the diseases of fruits and vegetables from leaves has, in recent years, become an important area of study in modern agriculture. Diseases, such as blight, rust, mildew, and spots, can sometimes cause considerable crop losses if identified and treated within the very earliest stages. Manual detection methods are often slow, inconsistent, and dependent on expert interpretation, which limits scalability in agricultural applications (Mohanty et al., 2024). Deep learning, particularly deep convolutional neural networks (CNNs), has enabled the automation of leaf disease identification from images. CNNs are specialized deep learning algorithms that are designed for image data.



Figure 1 : Apple scab



Figure 2: Bacterial spot

2. EXISTING METHODOLOGIES

There have been numerous proposals for several detection methods that can be adopted in the leaves of vegetables and fruits. Most of these methodologies are categorized as either machine learning algorithm-based, neural network-based, or hybrid models. Overall, the performance of these techniques has been highly dependent on both the quality of the utilized dataset and the strategy for feature extraction adopted. Several studies have explored the use of traditional algorithms like XGBoost, SVM, and Random Forest for classifying leaf diseases, though their performance heavily depends on hand-crafted features and dataset quality.

3. DATA SET PREPARATION

The preparation of the data set includes the following steps for detecting vegetable and fruit leaf diseases: Overview of Data Set, Data Accumulation, Data Augmentation, and Enhanced Rice Leaf Disease Dataset.

1.1 Overview Of Dataset

Many datasets available to detect plant diseases contain images of healthy and diseased crops, which are used to train the models so that they can recognize and classify with accuracy. For tomatoes, for example, there are many such datasets with images of tomato plants suffering from various diseases such as bacterial spot, late blight, and early blight. Similarly, databases of apple images include the Fruit Image Dataset, which consists of images of apples infected with diseases like apple rust, powdery mildew, and apple scab.

1.2 Data Accumulation

Deep Convolutional Neural Networks (DCNNs) require data collection to identify vegetable and fruit leaf diseases in the development of accurate models that can classify and identify diseases. This process involves taking high-quality images of healthy and diseased leaves, preparing them for training a deep learning model, and implementing methods to optimize the dataset for better results.

1.3 Data Augmentation

Data augmentation that encompassed cropping, flipping, zooming, rotation, and shifting in both directions. Each sample in our aggregated dataset is cropped, keeping its spatial dimensions, and resized to 240 × 240 pixels for uniform image size. Then, horizontal and vertical shifts are applied with a range of 0.2 for height and 0.2 for width.

1.4 Enhanced Dataset

A comprehensive set of tagged images for the Enhanced Dataset for Vegetable and Fruit Leaf Disease Detection has been created that can aid support deep learning as well as machine learning in the discipline of plant pathology. A typical set of images would comprise high-resolution pictures of healthy and diseased leaves. The diseases included may be mosaic virus, rust, powdery mildew, and bacterial blight. Photographs are captured under varying lighting conditions and angles to enhance dataset diversity and model robustness.

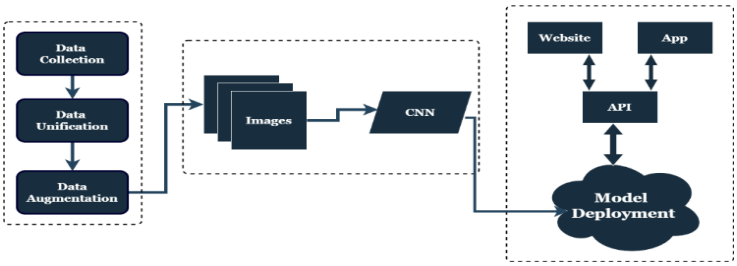

Figure 3: Block diagram of model

2. PROPOSED MODEL

The incidence of plant diseases is a serious threat to crop productivity and quality in the agricultural sector, especially among fruits and vegetables. In the process of training the model to distinguish between the different

diseases, images are labelled with names that depict the illnesses they represent. This disease-classification model applies DCNNs both in classification and feature determination of diseases. Among the series of layers that make up a CNN, one set in particular is called DCNN. It comprises convolutional, pooling, and fully connected layers. DCNNs are often best suited for image classification tasks because the layers automatically learn the spatial hierarchies of the features.

2.1 Equations

The DCNN analyses pictures of vegetables and fruits to perform disease detection. Images in terms of rotation, scaling, and colour transformations give a more enhanced dataset from which the DCNN takes forms pre-processed for further work.

$$d_e^{(h)} = k((z_{ni}^{(h)} Y\, d_i^{[h-1]}) + \ldots + (z_{nj}^{[h]}\ \mathrm{Y}\ d_j^{[h-1]}) + e_i) \qquad (1)$$

The SoftMax function has more applications within machine learning with its applications used in classification contexts. With this, it is involved within a model like when analysing the diseases on the plant leaves.

$$\sigma = \frac{b^{hi}}{\sum_{n=1}^{k} b^{hk}} \qquad (2)$$

The CE function is typically used in classification problems to quantify the difference between true labels and predicted probabilities.

$$\mathrm{CE} = -\sum_{c=1}^{n} m_i \log(\delta) \qquad (3)$$

The model adjusts its weights and biases based on the information received from the gradients of the loss function by the Adam optimizer during the training process.

$$Z_t = Z_{t-1} - \eta \frac{\bar{n}_t}{\sqrt{\bar{u}_t + \epsilon}} \qquad (4)$$

$$Q_t = Q_{t-1} - \eta \frac{\bar{n}_t}{\sqrt{\bar{u}_t + \epsilon}} \qquad (5)$$

3. PERFORMANCE ANALYSIS AND RESULTS

The system can identify diseases found in the leaves of vegetables and fruits with an accuracy rate of 99%. Compared to conventional models—AlexNet (88%), MobileNet (91%), and ResNet50 (94%)—our DCNN achieved superior performance with a 99% accuracy rate.

Layer (Type)	Conv2D, MaxPooling2D, Conv2D_1, MaxPooling2D_1, Conv2D_2, MaxPooling2D_2, Conv2D_3, Conv2D_4, MaxPooling2D_4, Conv2D_5, MaxPooling2D_5, Flatten, Dense, Dense_1, Dropout, Dense_2
Output Shape	(None, 98, 98, 32), (None, 49, 49, 32), (None, 49, 49, 64), (None, 24, 24, 64), (None, 24, 24, 128), (None, 12, 12, 128), (None, 12, 12, 256), (None, 6, 6, 128), (None, 3, 3, 128), (None, 3, 3, 64), (None, 1, 1, 64), (None, 64), (None, 128), (None, 128), (None, 4)
Param #	896, 0, 18,496, 0, 73,856, 0, 295,168, 295,040, 0, 73,792, 0, 0, 8,320, 16,512, 0, 516

TABLE 1: MODEL ARCHITECTURE SUMMARY

TOTAL PARAMS: 782,596 (2.99 MB)

TRAINABLE PARAMS: 782,596 (2.99 MB)

NON-TRAINABLE PARAMS: 0 (0.00 B)

This is a model architecture for a Convolutional Neural Network (CNN). It consists of multiple layers of Conv2D followed by MaxPooling2D to reduce spatial dimensions.

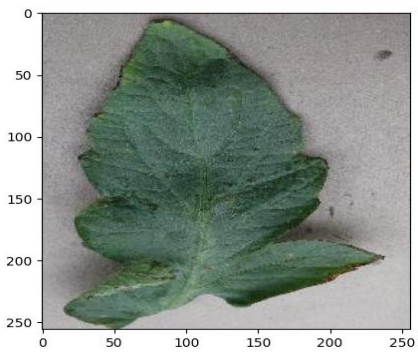

Figure 4: Healthy Apple leaf

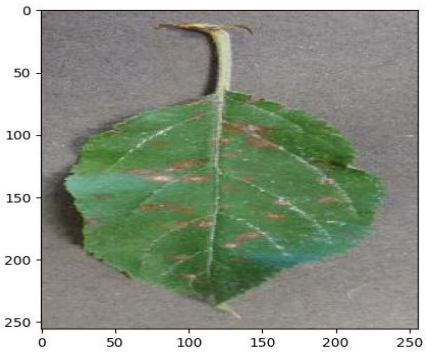

Figure 5: Tomato leaf

This is an image of Apple in which the machine learning model has classified a leaf as healthy (Figure 4). The tomato leaf has been diagnosed with the "Tomato Mosaic Virus," which was classified with 100% confidence by a machine learning model(Figure 5). Although the training accuracy improves dramatically, the validation accuracy increases and then stabilizes or declines slightly, which could indicate over fitting? All of these signs show that the model learns very well on training data.

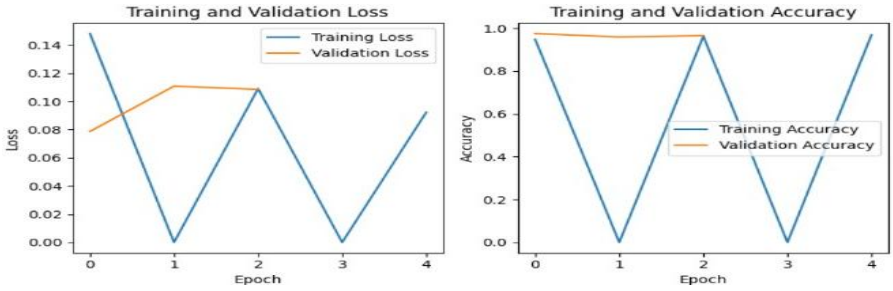

Graph 1: Training and Validation loss of the Dataset

4. CONCLUSION

The proposed model in deep convolutional neural networks, using enhanced data for the detection of leaf diseases in vegetable and fruit leaves, is a landmark shift in agricultural technology. the proposed model can reliably spot a wide spectrum of diseases on leaves by relying on a robust, extensive, and diversified dataset. It provides crucial support for disease prognosis and early therapies. Therefore, the ability to quickly identify these diseases will enable farmers to manage crops more effectively, reduce losses by preventing infections, and hence be able to improve their crop yields.

5. REFERENCES

1. **Mohanty, S. P., Hughes, D. P., & Salathé, M.** (2024). Using Deep Learning for Image-Based Plant Disease Detection. Frontiers in Plant Science, 7, 1419. DOI:10.3389/fpls.2016.01419
2. **Ferentinos, K. P.** (2018). Deep Learning Models for Plant Disease Detection and Diagnosis. Computers and Electronics in Agriculture, 145, 311-318. DOI:10.1016/j.compag.2018.01.009
3. **Sladojevic, S., Arsenovic, M., Anderla, A., Culibrk, D., & Stefanovic, D.** (2016). Deep Neural Networks Based Recognition of Plant Diseases by Leaf Image Classification. Computational Intelligence and Neuroscience, 2016, 3289801. DOI:10.1155/2016/3289801
4. **Karthik, R., Arunachalam, S., & Bharathi, V.** (2020). Attention Embedded Residual CNN for Disease Detection in Tomato Leaves. Applied Soft Computing, 86, 105936. DOI:10.1016/j.asoc.2019.105936
5. **Yu, H., & Son, C. H.** (2020). Apple Leaf Disease Identification through Region-of-Interest-Aware Deep Convolutional Neural Network. Symmetry, 12(5), 702. DOI:10.3390/sym12050702

6. **Too, E. C., Yujian, L., Njuki, S., & Yingchun, L.** (2019). A Comparative Study of Fine-Tuning Deep Learning Models for Plant Disease Identification. Computers and Electronics in Agriculture, 161, 272-279. DOI:10.1016/j.compag.2018.03.032
7. Qiu, Y., He, J., Zhang, Y., & Zhang, X. (2023). A Lightweight Convolutional Neural Network for Disease Detection of Fruit Leaves.
Computers and Electronics in Agriculture, 210, 107941.
DOI:10.1016/j.compag.2023.107941

Biographies



Mr. Someswararao KSNV has completed master degree in Embedded systems from JNTUK university, he has 14 years of teaching experience, currently he is an Associate Professor in Dadi Institute of Engineering and Technology, Anakapalle. Mr. Someswararao KSNV hosting a YouTube channel (SOMESWARARAO KSNV) where he uses his passion to teach different concepts of various subjects with natural and practical examples.

Stay connected with someswararao KSNV https://youtube.com/@SOMESH.K

Movie Recommendation System Using Content Based Filtering

Kusuma.S
Dept. of ISE
M S Ramaiah Institute of Technology,
Bengaluru, India
kusuma.s@msrit.edu

Charunayana V
Dept. of ISE
M S Ramaiah Institute of Technology,
Bengaluru, India
charunayana@msrit.edu

Shruthi J R
Dept. of ISE
M S Ramaiah Institute of Technology,
Bengaluru, India
jrshruti@msrit.edu

Vinutha G K
Dept. of CSE
R N S Institute of Technology,
Bengaluru, India
vinuthaharishk@gmail.com

Shivaraj
Dept. of ISE
M S Ramaiah Institute of Technology,
Bengaluru, India
1ms22is410@msrit.edu

Mohamed Waseem
Dept. of ISE
M S Ramaiah Institute of Technology,
Bengaluru, India
1ms22is406@msrit.edu

Abstract

This research outlines a movie recommendation system that recommends movies based on the user's input. It analyses the movie descriptions to recommend thematically related films based on content-based filtering. The system pre-processes movie data from a CSV file. It selects relevant features like genres and cast descriptions from it. These features are combined and transformed using TF-IDF (Term Frequency-Inverse Document Frequency) to capture the importance of words within descriptions. Cosine similarity then calculates the thematic similarity. This is between the user's chosen movie (potentially corrected for typos) and other movies. Finally, the system recommends the top N (default 30) most similar movies to the user. This recommendation system provides movie descriptions, recommends movies that share similar themes based on the user inputs.

Keywords. Content-based filtering, Thematically related films, TF-IDF (Term Frequency-Inverse Document Frequency), Cosine similarity.

1. INTRODUCTION

In today's ever-expanding cinematic landscape, navigating the vast array of movies can be a daunting task. Choosing the perfect film can feel like searching for a hidden gem. This is where movie recommendation systems come in, offering personalized suggestions to guide viewers towards their next cinematic adventure.

This research delves into a content-based movie recommendation system that transcends mere genre suggestions. The proposed work is beyond the surface level and delve into the rich tapestry of movie descriptions. By analysing the thematic weight of words within these descriptions, the system fosters a more content-driven approach to recommend movies of user interest.

This approach provides several advantages. It allows users to discover movies that share similar themes and artistic expressions with their initial selection, even if they fall outside the typical genre boundaries. Furthermore, it empowers viewers to explore hidden gems and embark on unexpected cinematic journeys that resonate with their specific preferences.

The power of TF-IDF and cosine similarity application are used in this research to find the thematically related movies. This system aims to empower viewers to embark on a personalized cinematic odyssey, filled with films that resonate with their unique tastes.

2. METHODOLOGY

The methodology section outlines the dataset, pre-processing steps, model implementation, training, evaluation, and the ensemble method used to improve classification performance. The methodology for this system takes many steps as discussed below.

7.1 Data pre processing

The data pre-processing step involves cleaning the dataset, handling missing values, and scaling features as shown in the Figure 2.1.

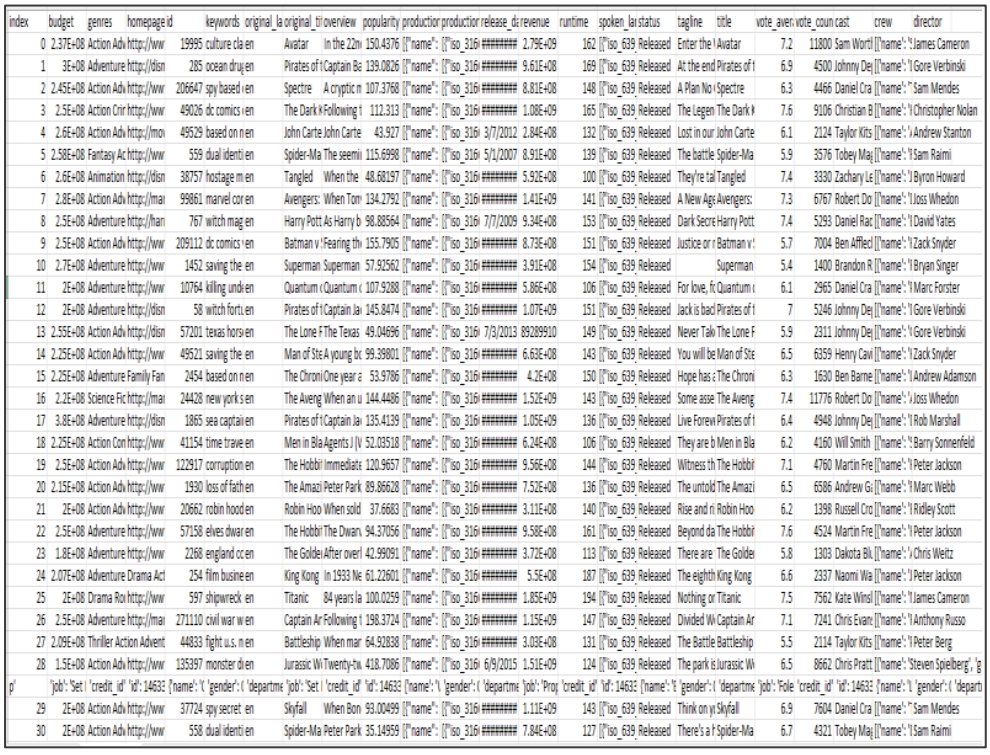

index	budget	genres	homepage	id	keywords	original_la	original_ti	overview	popularity	production	production	release_dc	revenue	runtime	spoken_lar	status	tagline	title	vote_aver	vote_coun	cast	crew	director
0	2.37E+08	Action Adv	http://ww	19995	culture cla	en	Avatar	In the 22n	150.4376	[{"name":	[{"iso_639	########	2.79E+09	162	[{"iso_639	Released	Enter the f	Avatar	7.2	11800	Sam Worth	[{"name": "	James Cameron
1	3E+08	Adventure	http://disn	285	ocean drug	en	Pirates of t	Captain Ba	139.0826	[{"name":	[{"iso_639	########	9.61E+08	169	[{"iso_639	Released	At the end	Pirates of t	6.9	4500	Johnny De	[{"name": "	Gore Verbinski
2	2.45E+08	Action Adv	http://ww	206647	spy based	en	Spectre	A cryptic n	107.3768	[{"name":	[{"iso_639	########	8.81E+08	148	[{"iso_639	Released	A Plan No	Spectre	6.3	4466	Daniel Cra	[{"name": "	Sam Mendes
3	2.5E+08	Action Crir	http://ww	49026	dc comics	en	The Dark K	Following t	112.313	[{"name":	[{"iso_639	########	1.08E+09	165	[{"iso_639	Released	The Legen	The Dark K	7.6	9106	Christian B	[{"name": "	Christopher Nolan
4	2.6E+08	Action Adv	http://mo	49529	based on n	en	John Carte	John Carte	43.927	[{"name":	[{"iso_639	3/7/2012	2.84E+08	132	[{"iso_639	Released	Lost in our	John Carte	6.1	2124	Taylor Kits	[{"name": "	Andrew Stanton
5	2.58E+08	Fantasy Ac	http://ww	559	dual identi	en	Spider-Ma	The seemi	115.6998	[{"name":	[{"iso_639	5/1/2007	8.91E+08	139	[{"iso_639	Released	The battle	Spider-Ma	5.9	3576	Tobey Maq	[{"name": "	Sam Raimi
6	2.6E+08	Animation	http://disn	38757	hostage m	en	Tangled	When the	48.68197	[{"name":	[{"iso_639	########	5.92E+08	100	[{"iso_639	Released	They're tal	Tangled	7.4	3330	Zachary Le	[{"name": "	Byron Howard
7	2.8E+08	Action Adv	http://mai	99861	marvel cor	en	Avengers:	When Tony	134.2792	[{"name":	[{"iso_639	########	1.41E+09	141	[{"iso_639	Released	A New Age	Avengers:	7.3	6767	Robert Do	[{"name": "	Joss Whedon
8	2.5E+08	Adventure	http://har	767	witch mag	en	Harry Pott	As Harry b	98.88564	[{"name":	[{"iso_639	7/7/2009	9.34E+08	153	[{"iso_639	Released	Dark Secre	Harry Pott	7.4	5293	Daniel Rac	[{"name": "	David Yates
9	2.5E+08	Action Adv	http://ww	209112	dc comics	en	Batman v	Fearing th	155.7905	[{"name":	[{"iso_639	########	8.73E+08	151	[{"iso_639	Released	Justice or r	Batman v	5.7	7004	Ben Affleck	[{"name": "	Zack Snyder
10	2.7E+08	Adventure	http://ww	1452	saving the	en	Superman	Superman	57.92562	[{"name":	[{"iso_639	########	3.91E+08	154	[{"iso_639	Released		Superman	5.4	1400	Brandon R	[{"name": "	Bryan Singer
11	2E+08	Adventure	http://ww	10764	killing und	en	Quantum o	Quantum (	107.9288	[{"name":	[{"iso_639	########	5.86E+08	106	[{"iso_639	Released	For love, fc	Quantum o	6.1	2965	Daniel Cra	[{"name": "	Marc Forster
12	2E+08	Adventure	http://disn	58	witch fort	en	Pirates of t	Captain Ja	145.8474	[{"name":	[{"iso_639	########	1.07E+09	151	[{"iso_639	Released	Jack is bac	Pirates of t	7	5246	Johnny De	[{"name": "	Gore Verbinski
13	2.55E+08	Action Adv	http://disn	57201	texas hors	en	The Lone F	The Texas	49.04696	[{"name":	[{"iso_639	7/3/2013	89289910	149	[{"iso_639	Released	Never Tak	The Lone F	5.9	2311	Johnny De	[{"name": "	Gore Verbinski
14	2.25E+08	Action Adv	http://ww	49521	saving the	en	Man of Ste	A young bc	99.39801	[{"name":	[{"iso_639	########	6.63E+08	143	[{"iso_639	Released	You will be	Man of Ste	6.5	6359	Henry Cav	[{"name": "	Zack Snyder
15	2.25E+08	Adventure	Family Fan	2454	based on n	en	The Chroni	One year a	53.9786	[{"name":	[{"iso_639	########	4.2E+08	150	[{"iso_639	Released	Hope has a	The Chroni	6.3	1630	Ben Barne	[{"name": "	Andrew Adamson
16	2.2E+08	Science Fic	http://mai	24428	new york s	en	The Aveng	When an u	144.4486	[{"name":	[{"iso_639	########	1.52E+09	143	[{"iso_639	Released	Some asse	The Aveng	7.4	11776	Robert Do	[{"name": "	Joss Whedon
17	3.8E+08	Adventure	http://disn	1865	sea captai	en	Pirates of t	Captain Ja	135.4139	[{"name":	[{"iso_639	########	1.05E+09	136	[{"iso_639	Released	Live Forev	Pirates of t	6.4	4948	Johnny De	[{"name": "	Rob Marshall
18	2.25E+08	Action Con	http://ww	41154	time trave	en	Men in Bla	Agents J (V	52.03518	[{"name":	[{"iso_639	########	6.24E+08	106	[{"iso_639	Released	They are b	Men in Bla	6.2	4160	Will Smith	[{"name": "	Barry Sonnenfeld
19	2.5E+08	Action Adv	http://ww	122917	corruption	en	The Hobbit	Immediate	120.9657	[{"name":	[{"iso_639	########	9.56E+08	144	[{"iso_639	Released	Witness th	The Hobbit	7.1	4760	Martin Fre	[{"name": "	Peter Jackson
20	2.15E+08	Action Adv	http://ww	1930	loss of fath	en	The Amazi	Peter Park	89.86628	[{"name":	[{"iso_639	########	7.52E+08	136	[{"iso_639	Released	The untold	The Amazi	6.5	6586	Andrew Ga	[{"name": "	Marc Webb
21	2E+08	Action Adv	http://ww	20662	robin hood	en	Robin Hoo	When sold	37.6683	[{"name":	[{"iso_639	########	3.11E+08	140	[{"iso_639	Released	Rise and ri	Robin Hoo	6.2	1398	Russell Cro	[{"name": "	Ridley Scott
22	2.5E+08	Adventure	http://ww	57158	elves dwar	en	The Hobbit	The Dwarv	94.37056	[{"name":	[{"iso_639	########	9.58E+08	161	[{"iso_639	Released	Beyond da	The Hobbit	7.6	4524	Martin Fre	[{"name": "	Peter Jackson
23	1.8E+08	Adventure	http://ww	2268	england cc	en	The Golden	After overl	42.99091	[{"name":	[{"iso_639	########	3.72E+08	113	[{"iso_639	Released	There are	The Golden	5.8	1303	Dakota Blu	[{"name": "	Chris Weitz
24	2.07E+08	Adventure	Drama Act	254	film busine	en	King Kong	In 1933 Ne	61.22601	[{"name":	[{"iso_639	########	5.5E+08	187	[{"iso_639	Released	The eighth	King Kong	6.6	2337	Naomi Wa	[{"name": "	Peter Jackson
25	2E+08	Drama Ro	http://ww	597	shipwreck	en	Titanic	84 years la	100.0259	[{"name":	[{"iso_639	########	1.85E+09	194	[{"iso_639	Released	Nothing or	Titanic	7.5	7562	Kate Wins	[{"name": "	James Cameron
26	2.5E+08	Adventure	http://mai	271110	civil war w	en	Captain Ar	Following t	198.3724	[{"name":	[{"iso_639	########	1.15E+09	147	[{"iso_639	Released	Divided We	Captain Ar	7.1	7241	Chris Evan	[{"name": "	Anthony Russo
27	2.09E+08	Thriller Action	Advent	44833	flight u.s. n	en	Battleship	When mar	64.92838	[{"name":	[{"iso_639	########	3.03E+08	131	[{"iso_639	Released	The Battle	Battleship	5.5	2114	Taylor Kits	[{"name": "	Peter Berg
28	1.5E+08	Action Adv	http://ww	135397	monster di	en	Jurassic Wo	Twenty-tw	418.7086	[{"name":	[{"iso_639	6/9/2015	1.51E+09	124	[{"iso_639	Released	The park is	Jurassic Wo	6.5	8662	Chris Pratt	[{"name": "	Steven Spielberg", "g
p'	'job': 'Set	'credit_id'	'id': 14633	{'name': 'A	'gender': (	'departme	'job': 'Set	'credit_id'	'id': 14633	{'name': 'A	'gender': (	'departme	'job': 'Proc	'credit_id'	'id': 14633	{'name': 'E	'gender': (	'departme	'job': 'Pole	'credit_id'	'id': 14633	{'name': 'L	'gender': (	'departi
29	2E+08	Action Adv	http://ww	37724	spy secret	en	Skyfall	When Bon	93.00499	[{"name":	[{"iso_639	########	1.11E+09	143	[{"iso_639	Released	Think on y	Skyfall	6.9	7604	Daniel Cra	[{"name": "	Sam Mendes
30	2E+08	Action Adv	http://ww	558	dual identi	en	Spider-Ma	Peter Park	35.14959	[{"name":	[{"iso_639	########	7.84E+08	127	[{"iso_639	Released	There's a h	Spider-Ma	6.7	4321	Tobey Maq	[{"name": "	Sam Raimi

Fig 2.1: Data Pre Processing

Reading the Script: The system starts by reading movie data from a CSV file. This file is assumed to contain various attributes of each movie, such as title, genre(s), keywords, tagline, cast, and director.

Feature Focus: Not all movie information is equally relevant for recommendations. The system selects specific features that provide rich insights into a movie's content. These features typically include genres (e.g., comedy, thriller), keywords (e.g., dark humor, time travel), tagline (a concise summary of the movie's plot or theme), cast (actors and actresses involved), and director (their filmmaking style and thematic preferences). To understand a movie's essence, the system goes beyond just genres. It delves into richer details. Genres, like comedy or thriller, provide a broad category. But keywords offer a deeper look, with tags like "dark humor" or "time travel" revealing specific themes. The tagline, a concise summary, captures the movie's core message. Even the cast and director provide clues. Actors like Jackie Chan are known for action comedies, while different directors often have signature styles and thematic preferences. By combining all these elements – genres, keywords, tagline, cast, and director – the system creates a comprehensive description for each movie, allowing for more nuanced recommendations.

Missing Pieces, handled with Care: Real-world data often contains missing values. The system addresses missing data points in the chosen features. A common approach is to fill them with empty strings. While this doesn't introduce additional information, it avoids skewing the analysis during later stages.

Weaving the Narrative Tapestry: Once the data is cleaned, the system combines the selected features for each movie. This creates a comprehensive description for every movie, encompassing its genre, thematic keywords, tagline, and information about the cast and director. By combining these elements, the system creates a richer representation of each movie's content.

2.2 Algorithms Used

TF-IDF (Term Frequency-Inverse Document Frequency)

The Vectorizer's Magic: Now, we enter the world of Natural Language Processing (NLP). Here, a TF-IDF (Term Frequency-Inverse Document Frequency) vectorizer is created. This tool analyzes the combined movie descriptions and transforms them into numerical feature vectors. Imagine a vector as a special code that captures the importance of different words within the description.

Term Frequency: Shining a Light on Frequent Flyers: TF-IDF considers how often each word appears within a particular movie description. Words that show up more frequently are likely more important for understanding the movie's content. The TF-IDF vectorizer assigns a weight to each word based on its frequency, reflecting its significance within that specific movie.

Inverse Document Frequency: Not All Stars Shine Equally Bright: TF-IDF goes beyond just counting word occurrences. It also considers the inverse document frequency (IDF) of each word. Words that appear very frequently across all movie descriptions (e.g., "the," "a") are less important for distinguishing a particular movie's theme. IDF downplays the weight of such common words, ensuring that words unique and informative for a specific movie have a greater influence in the recommendation process.

The Power of the Vector: Through TF-IDF, each movie description is transformed into a numerical vector. This vector captures the importance of various words within the description, providing a more sophisticated representation of the movie's content compared to simply using raw text.

2.3 Model Training and Evaluation

The models were trained on the TF-IDF vectors of the training set and evaluated using the testing set. The following metrics were used for evaluation:

- Accuracy: [6]

$$\text{Accuracy} = \frac{TP + TN}{\text{Total Count}}$$

- Precision: [6]

$$\text{Accuracy} = \frac{TP}{\text{Predicted Yes}}$$

- Recall: [6]

$$\text{Recall} = \frac{TP}{\text{Actual Yes}}$$

8. RESULTS

```
 Enter your favourite movie name :  spider man
Movies suggested for you :

1 . Spider-Man
2 . Spider-Man 3
3 . Spider-Man 2
4 . The Notebook
5 . Seabiscuit
6 . Clerks II
7 . The Ice Storm
8 . Oz: The Great and Powerful
9 . Horrible Bosses
10 . The Count of Monte Cristo
11 . In Good Company
12 . Finding Nemo
13 . Clear and Present Danger
14 . Brothers
15 . The Good German
16 . Drag Me to Hell
17 . Bambi
18 . The Queen
19 . Charly
20 . Escape from L.A.
21 . Daybreakers
22 . The Life Aquatic with Steve Zissou
23 . Labor Day
24 . Wimbledon
25 . Cold Mountain
26 . Hearts in Atlantis
27 . Out of the Furnace
28 . Bullets Over Broadway
29 . The Purge: Election Year
```

Figure 3.12. Sample Output of Movie Recommendation's

This research work of movie recommendation system, personalizes suggestions based on movie content. The sample result based on the user input is as shown in the Figure 3.1. By utilizing TF-IDF technique and by leveraging cosine similarity it analyses the importance of words within movie descriptions. By considering features like genres, keywords, tagline, cast, and director, the system creates a richer representation of each movie's theme. Comparing these representations, movies with similar thematic content are recommend to a user. It offers a personalized content-based approach that helps users discover movies that share themes and styles.

9. CONCLUSION

In conclusion, this content-based movie recommendation system offers a personalized approach to exploring the vast cinematic landscape. By leveraging TF-IDF and focusing on movie content, the system empowers users to discover hidden gems that resonate with their thematic preferences, taking them on unexpected cinematic journeys.

10. REFERENCES

[1] M. Kumar and S. Patel, "Movie Recommendation System Using Machine Learning," in *Proc. 2024 IEEE Int. Conf. AI Data Sci. (ICAIDS)*, 2024, pp. 1–6.

[2] A. Sharma and R. Gupta, "Movie Recommender System Based on Generative AI," in *Proc. 2024 IEEE Int. Conf. Comput. Intell. Mach. Learn. (CIML)*, 2024, pp. 1–8.

[3] L. Chen and Y. Wang, "Designing a Movie Recommendation System Through a Transformer-Based Embeddings Space," in *Proc. 2024 IEEE Symp. AI Multimedia Process. (AI-MP)*, 2024, pp. 45–52.

[4] P. Singh and K. Verma, "Enhancing Movie Recommendation Systems with BERT: A Deep Learning Approach," in *Proc. 2024 IEEE Conf. Natural Lang. Process. AI (NLP-AI)*, 2024, pp. 78–85.

[5] S. Das and M. Roy, "Movie Recommendation System Based On Emotions," in *Proc. 2024 IEEE Int. Conf. Human-Comput. Interact. AI (HCI-AI)*, 2024, pp. 112–119.

[6] D. Jurafsky and J. H. Martin, *Speech and Language Processing*, 3rd ed. Pearson Education Limited, 2021.

[7] R. Baeza-Yates, M. Ferro, and B. Ribeiro-Neto, *Modern Information Retrieval: The Concepts and the Algorithms*. ACM Press, 2011.

[8] G. Guo, H. Wang, J. Yin, and S. He, "A novel movie recommendation system based on social network analysis," *Physica A: Statistical Mechanics and its Applications*, vol. 392, no. 23, pp. 6309–6319, 2013.

[9] J. Srivastava and P. K. Sharma, "A hybrid recommendation system for movies," *Procedia Comput. Sci.*, vol. 46, pp. 1243–1249, 2014.

[10] A. Said and T. K. Mohamed, "A survey on content-based movie recommendation systems," *ACM Comput. Surv. (CSUR)*, vol. 48, no. 3, pp. 1–36, 2015.

[11] S. Ventura and J. P. Silva, "A survey on content-based recommender systems," *J. Artif. Intell. Res.*, vol. 52, pp. 621–670, 2015.

[12] C. D. Manning, P. Raghavan, and H. Schütze, *Introduction to Information Retrieval*. Cambridge Univ. Press, 2009.

[13] G. Piao and J. Kim, "A hybrid collaborative filtering method for movie recommendation," *Expert Syst. Appl.*, vol. 31, no. 4, pp. 786–798, 2006.

[14] T. Grossman and M. Newman, "Spam detection using n-gram co-occurrence statistics," in *Proc. 7th Int. Workshop Inf. Retrieval Asian Lang.*, 2004, pp. 178–186.

[15] B. Sarwar, G. Karypis, J. Konstan, and J. Riedl, "Item-based collaborative filtering recommendation algorithms," in *Proc. 10th Int. Conf. World Wide Web*, 1998, pp. 285–295.

[16] R. H. Sloan, "A method for measuring similarity between documents," *J. Am. Soc. Inf. Sci.*, vol. 48, no. 6, pp. 433–443, 1996.

[17] S. Deerwester, S. T. Dumais, G. W. Furnas, T. K. Landauer, and R. Harshman, "Indexing by latent semantic analysis," *J. Am. Soc. Inf. Sci.*, vol. 41, no. 6, pp. 391–404, 1990.

Feature Selection and Optimization for Cardiovascular Disease Prediction

Dr. Poorna Priya Putcha[1], Dr. P. Pavitra[2], Lakshmi Amulya Chellapilla[3], Vasantha Dhuli[4], Uma Malleswari Boddeti[5], Sandhya Atmakuri [6]

Dadi institute of Engineering& Technology (A) ,Anakapalle,India

putchapoornapriya@gmail.com[1],pavitray015@gmail.com[2], chlamulya08@gmail.com[3], dhuli.vasantha@gmail.com[4],umaboddeti1234@gmail.com[5],sandhyaatmakuri4@gmail.com[6]

Abstract.

This Emergent technology has eased the burden on hospital resources and has allowed for efficient monitoring and management of patients. Cardiovascular diseases, which account for the highest cause of death, by the statistics of the World Health Organization, contribute to almost 20,000 deaths in this nation every year. This leads in a high death rate over the world, which helps to boost the current healthcare infrastructure. The primary aim of this research is to incorporate advanced Machine Learning (ML) classification algorithms to identify abnormal human vital signs, like Electrocardiogram (ECG), Heart Rate (HR), and Blood Pressure (BP), in near real-time. Given that network latency is crucial for this application, enhancing the overall Quality of Service is essential.

Keywords. Heart and blood vessel problems, Blood pressure, Pulse rate, electrical activity recording and others.

1. INTRODUCTION

The world's deadliest diseases are cardiovascular diseases. They claim over 17.9 million lives every year. It traditionally relies on traditional risk factors, but classically cannot predict cardiac events. Cardiac risk assessment can be enhanced using machine learning algorithms. It analyses large data and extracts subtle patterns. With such algorithms, individual risk scores are generated.

These include supervised, unsupervised, and deep learning methods, which improve the accuracy of prediction and allow for earlier intervention to prevent disease. Improved patient outcomes, resource utilization, and identification of people with higher risk profiles result from this. Personalized medicine is very crucial since it provides tailored treatment plans according to these risk profiles, especially through supervised learning data.

Challenges still remain, with data quality and availability issues, interpretability of the models, and how to integrate them into clinical workflows Thus, the equal use of machine learning-based cardiac risk assessments will call for addressing healthcare disparities in their utilizations. The integration thus requires collaboration from several actors, including healthcare professionals, data scientists, and policymakers, among others.

Machine learning (ML) offers an opportunity to analyse large data sets and reveal hidden patterns in patient information. This model can predict the risk of heart disease more precisely because it considers age, cholesterol levels, blood pressure, family history, and lifestyle choices. ML can also assess real-time data from wearable devices and diagnostic tools like

All Open Access articles are peer-reviewed, distributed under the Creative Commons Attribution-Non Commercial 4.0 International

ECG, which are challenging for clinicians to interpret in detail. The integration of ML in heart risk assessment is a significant advancement.

Dataset 1: Heart Attack Risk

It gives information about all patients who have ever had an ML and includes demographics, clinical history, and characteristics of lifestyle of the patients. All data sets include variables like age, sex, blood pressure, levels of cholesterol, and smoking status. This data set provides comprehensive information on a number of risk factors associated with having an ML.

Dataset 2: COVID-19 Vaccination

The second dataset gives information regarding those who have been vaccinated against COVID-19. It includes demographic characteristics, vaccination details, and health outcomes. The data contains variables such as age, sex, type of vaccination, and adverse reactions.

2. RELATED WORK

Machine learning is revolutionizing how we assess cardiac risk. It enhances prediction accuracy, improves diagnoses, and allows for a more personalized approach. Unlike traditional methods that rely on fixed formulas like the Framingham Risk Score, machine learning relies on large datasets and complex algorithms to uncover underlying patterns. It uses supervised learning algorithms. Indeed, with current advances in research, it is shown that machine learning enhances cardiac risk assessment through diverse data analysis algorithms.

2.1 Supervised Learning:

Supervised Learning is a key area of ML whereby the algorithm learns from labelled examples for the prediction of results. In essence, data applied supervised learning should comprise input features such as images, texts, or numbers. The data also includes correct answers, known as labels or target values. The complete idea is that the algorithm learns connections between inputs and outcomes, which make predictions on the outcomes for new, unseen data. The process trains the model by feeding a dataset, it adjusts itself to commit fewer errors in its predictions. The model is evaluated separately on another set of data and is said to perform like this. Supervised learning is extensively applied to classification tasks, determining whether emails are spam, and regression problems, such as predicting the house price as a function of size and location features.

2.2 Logistic regression:

This method models how a binary outcome relates to one or more predictors. The outcome variable can take two values 0 and 1.Machine Learning can predict the responses of patients to therapies, propagating personalized therapy through optimized medication plans.

ML further innovates cardiac care: faster and more accurate personalized risk assessments likely to prevent multiple deaths.

$$P(y=1|X) = 1 / (1 + e^{-(b0 + b1x1 + b2x2 + \cdots + bnxn)}) \quad (2.2.1)$$

Where: • P(y=1|X) is the conditional probability of the dependent variable being 1, given the input features X.

•b0b_0b0 is the bias term (intercept).

• b1, b2,…, bn-1, bn are the weights linked to the features x1, x2,…, xn.

• x1, x2,…, xn are feature predictors or the independent var.

• “e” is the foundation of the natural log, approx. 2.71828.

3. PROPOSED MODEL

The Cardiac Risk Assessment System proposed helps doctors predict the risk of heart disease and help manage this risk during heart attack diagnosis by integrating patient data that encompasses traditional medical history, test results, and even information brought on by wearable devices. The system harnesses machine learning and data analysis techniques to derive trends that lead to the proposal of an escalated risk towards heart disease. With this groundwork then, the system aims at giving the prediction of heart disease risk, an individualized treatment plan, as well as lifestyle recommendations. Besides, the system is integrated with electronic health records for continuous patient information updates. The interface is user-friendly to doctors, making it intuitive for use.

4. RESULTS AND DISCUSSION

This area of research has displayed good potential in improving the cardiac risk assessment. In this study, it explains how machine learning algorithms may effectively predict cardiovascular disease with clinical and demographic factors. Logistic regression reached an accuracy of 65% on the training set and 60% on the testing set.

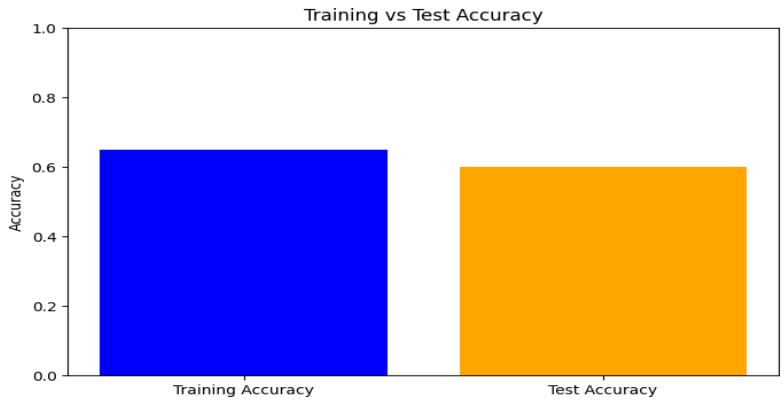

Figure 4.1: Training and Testing accuracy

The graph illustrates the training and test accuracy of a machine learning model. The blue bar indicates the training accuracy, which is just over 60%, showing how well the model performs on the training dataset. In contrast, the orange bar shows the test accuracy, slightly lower at about 55%, which indicates the model's capability to generalizes to new, untested data. The negligible difference between the training and test accuracy implies that there is minimal overfitting, although the absolute accuracy values are still low.

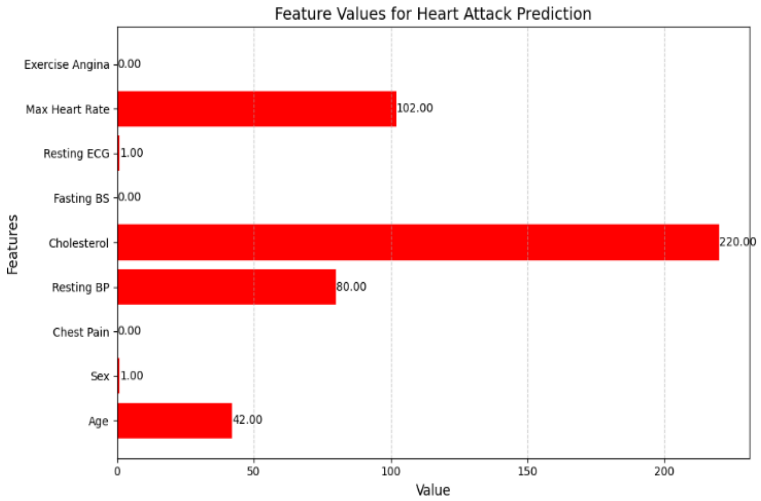

Figure 4.2: Feature Values of Heart Attack Prediction

Graph representation Feature values of heart attack prediction Some key health indicator graphs are presented here, too. Cholesterol level of a subject is recorded to be a high level of 220 mg/dL in border line high risk categories of heart disease. Record value of the heart is given by 102 bpm of bpm, which is an extreme low record value suggesting demising cardiac functions or cardio-fitness. Resting blood pressure is normal at 80 mmHg. Fasting blood sugar levels are also below the critical threshold.

NAME	Age	Gen	Chol	RESTBP	Covid	Exang	ECG	CP	FBS	MAX HR	Output
Sample 1	21	0	160	80	1	0	0	0	0	70	0
Sample 2	20	0	150	80	1	0	0	0	0	72	0
Sample 3	20	0	170	80	1	0	0	0	0	73	0
Sample 4	22	0	180	80	1	0	0	0	0	71	0
Sample 5	39	0	0	80	1	0	1	0	0	75	0
Sample 6	43	1	270	80	1	0	1	0	1	177	1
Sample 7	32	0	0	0	1	0	0	0	1	130	0
Sample 8	28	0	180	80	1	0	0	0	1	90	0
Sample 9	55	1	190	130	1	0	0	0	0	94	1
Sample 10	27	0	200	80	1	0	1	0	0	100	0
Sample 11	41	1	200	80	1	0	0	0	1	120	0
Sample 12	37	1	200	80	1	0	0	0	0	104	1
Sample 13	28	0	200	80	1	0	0	0	1	135	0
Sample 14	44	1	220	80	1	0	1	0	0	98	1
Sample 15	70	1	210	80	1	1	1	1	0	84	1
Sample 16	27	0	210	80	1	1	1	0	1	89	1
Sample 17	38	0	0	90	1	0	1	0	0	77	1
Sample 18	53	1	180	98	1	0	0	0	1	81	1
Sample 19	38	1	220	100	1	0	1	0	0	97	1
Sample 20	72	1	0	110	1	0	0	0	1	101	0
Sample 21	42	1	220	80	1	0	1	0	0	102	0

Table 4.1: Real time data

This is a data set of medical records of various individuals. Every row in the table represents a sample, and that sample is captured through the column labelled as NAME, describing the characteristic of the individual. These characteristics include Age, Gen: Gender, Chol: Cholesterol, RESTBP: Resting Blood Pressure, and whether Covid was experienced or not by the person. Other columns are exercise-induced angina, electrocardiographic results, type of chest pain experienced, fasting blood sugar level recorded, and maximum heart rate reached.

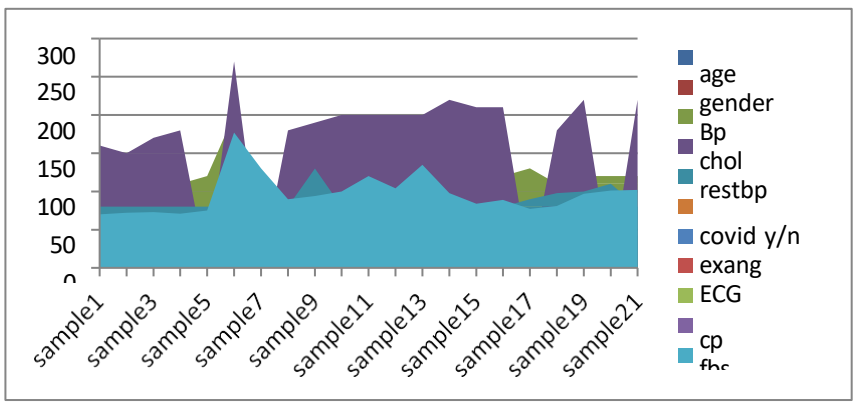

Figure 4.3: Real Time Graph

The chart shows the contribution of the key health indicators such as cholesterol, blood pressure, chest pain, and fasting blood sugar across different samples.

5. CONCLUSION

Machine learning (ML) has the potential to improve cardiovascular risk assessment, particularly in relation to COVID-19 vaccination. Our research demonstrated that ML algorithms are more effective at predicting heart disease compared to traditional methods, taking into account the impact of COVID-19 vaccination on cardiovascular health.

After analysing data from vaccinated individuals POST-COVID, we identified several potential risk factors and interactions that influence cardiovascular health

6. REFERENCES

1. According to a news story [online], coronary heart diseases are the top killer of Pakistan.https://www.thenews.com.pk/print/153465 is accessible. The top killer in Pakistan is coronary heart disease. [retrieved February 1, 2022]
2. At the 2021 International Congress of Advanced Technology & Engineering (IEEE 2021), Umar, Umara, et al. demonstrated an Internet of Things-based cardiac healthcare system for ubiquitous healthcare services.
3. An "Internet of Things Based Healthcare Monitoring System using NodeMCU & Arduino UNO," presented by Wai, Khin Thet, Nyan Phyo Aung, and Lwin Lwin Htay, was published in the International Journal of Trend in Scientific Research and Development (ijtsrd) 3.5 (2019) 755-759.
4. Jones, R., and Patel, S. "Novel Biomarkers for Heart Attack Prediction: Advancements in Cardiac Diagnostics," Circulation Research, Jan 2024. [Online]. Available: https://www.circulationresearch.com/novel-biomarkers-heart-attack. [Accessed: 13-Dec- 2024].
5. Devika T, Varsha K, Sree Sanjana Bose, Athira A, "IoT-based Multiparameter Patient Monitoring System Design and Development," 2020. "Adaptable Wearable Sensors for Cardiovascular Health Monitoring" Chen, Shuwen, et al. 2100116 in Advanced Healthcare Materials 10.17 (2021).

Biographies



Dr. P. Poorna Priya was born in India, A.P and working as Associate Professor and Head of the Department at Dadi Institute of engineering and Technology(A). She got PhD from K L University in the field of antennas. She has published more than 28 papers (6 SCI/Scopus), 2 Book Chapters,4 Patents, her H-Index is 7 & Citations are more than 100+.Her field of Interest is Communications and Image processing.

Surveillance Video Analytics Using LLM-Based Summarization and Captioning

Yamuna H

Dept. of Computer Science and Engineering, Siddaganga Institute of Technology, Tumakuru, Karnataka, India, yamunah30@gmail.com

A H Shanthakumara

Dept. of Computer Science and Engineering, Siddaganga Institute of Technology, Tumakuru, Karnataka, India, shanthakumara@sit.ac.in

Abstract.

Surveillance video analytics is essential today because it reduces human work, enhances security and improves efficiency. This paper introducing a system that utilizes transformer-based models BART and BLIP; these are trained using datasets BookCorpus, English Wikipedia and Conceptual Captions, COCO Captions respectively. The System generates text-based summaries and captions for key frames extracted from surveillance videos, which is particularly useful for identifying unusual activity in surveillance applications. The system extracts key frames from input surveillance video, generates captions for each frame, and summarizes the content. These summaries provide insights into key activities, security incidents, and key observations, making it easier for security personnel to review extensive video footage efficiently. BART and BLIP models outperform traditional video analysis by leveraging deep learning and these models are scalable, adaptable thus making the system more efficient for the video analysis applications. The results include a summary of activities in the video, performance metrics such as ROUGE scores for summary quality and visualizations of the processing times across different stages of the analysis pipeline.

Keywords: Surveillance Video Analytics, Large Language Models (LLMs), Transformer Models, ROUGE Evaluation.

1. INTRODUCTION

Surveillance systems are inevitable today in the modern security infrastructure where the public space, organizations, critical infrastructure, and private properties will be monitored. However, with exponential growth in video data from such systems, the process of efficient handling and analysis of captured footage becomes highly complex. Security personnel cannot manually review hours of video footage to identify potential security threats within time, hence the need for video analysis techniques. This is where a bright future for Artificial Intelligence (AI), especially in video summarization and frame captioning, comes into play [1]. Traditional video analysis techniques that depend upon motion detection, frame differencing, and background subtraction but, all these methods cannot represent what is going on as context-specific because these are sensitive to lighting changes, noise. All in all, they lack capability enough to be used as effective analysis tools for security analytics [2]. Initial video summarizing techniques relied heavily on traditional methods such as extraction of keyframe, detection of shot boundary, and event detection [8]. In an attempt to overcome such limitations, researchers have turned to DL techniques, particularly CNNs, for activities like object detection, activity recognition, and event classification [3]. Such methods have proven to have better accuracy and context-awareness but pose serious challenges in terms of computational costs due to the large amount of surveillance footage to be processed. Recent breakthroughs in models built on the transformer framework were, first developed for applications in natural language processing (NLP), revolutionized the combination of image and text data, providing powerful solutions for multimodal AI applications. Models such as BART [4] and BLIP [5] are designed to understand and generate textual outputs based on multimodal inputs, including video frames and corresponding textual descriptions. BERT (Bidirectional Encoder Representations from Transformers) [9], GPT (Generative Pretrained Transformers) [10], and BART [4] have set new standards in excelling natural language processing tasks, such as text generation and summarization. These advances have been absorbed into video

analysis, where transformers are used in combination with object detection models to improve video summarization performance. The transformer-based models have proved very effective in video summarization and image captioning, promising approaches to the surveillance footage analysis. Surveillance video analysis could benefit from Large Language Models, especially the LLM variants such as BART for summarizing texts and BLIP for describing images. These models will allow extracting frames from video and generate captions for the extracted frames, then summarizing all that is to be gathered in natural language. Thus, it enables security personnel to derive insights from hours of footage within a fraction of time [6]. Furthermore, using ROUGE scores [7] for evaluating the quality of a summary allows for the generation of relevant and accurate summaries. The purpose of this study is to present a system which incorporates the modern AI techniques of frame extraction, image captioning, and text summarization in one unified workflow for the analysis of surveillance videos.

The proposed system's design is aimed at efficiency, with integrated visualizations over processing times and summary quality. We intend to demonstrate how this system can be utilized for real-world surveillance footages and provide meaningful insights to the security people in a timely and resource-efficient manner.

2. SYSTEM ARCHITECTURE

The proposed system is efficiently designed to process surveillance video data, automatically generate summaries and captions. Key components of the system are as follows:

Surveillance Video (Input): The raw video data is the input for the system and is provided in a format such as MP4, AVI, or MOV.

Video Processing:

a) **Frame Extraction:** The system processes the video to extract key frames at regular intervals (e.g., every 10 seconds, or based on certain motion events). This reduces the amount of data for subsequent processing while ensuring that important video moments are captured.

b) **Image Captioning (BLIP Model):** For each extracted frame, the BLIP model (Bootstrapping Language Image Pretraining) generates a contextual caption describing the scene in the frame. The model is fed with large-scale image-text pairs and can generate high-quality captions describing objects, actions, and context within the frame (for example, "A person walking near a parked car").

c) **Text Summarization (BART Model):** It aggregates all captions produced from the frames extracted into a single text input, then applies the BART (Bidirectional and AutoRegressive Transformers) model for the summarization of text. BART summarizes the data into a coherent summary of key events, actions, or anomalies occurring during a specific video such as "A person walks near the car at 10:00 AM and then enters the building".

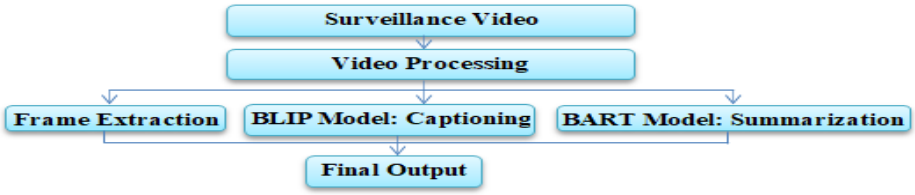

Figure 2.13: System Architecture

Final Output: Final output includes the following.

3. Summary of Key Events – A quick summary of the actions noticed in the video.
4. Performance Metrics - The ROUGE scores are outlined for the quality of the summarization. These metrics compare the machine- generated summaries with human-authored reference summaries, offering objective evaluation of the system's effectiveness in summarization.
5. Processing Times - Visualizing processing times required for each stage for performance analysis, which includes frame extraction, caption generation, and summarization.
6. Frame Captions - The captions are generated for each frame that describes the visual content of each frame.

3. Results and Discussion

A. Data and Setup

We used surveillance videos that contain a variety of scenes, such as public spaces, streets, and office environments, to evaluate the system's performance. Videos differ in length and content and thus provide a very broad test bench for the system. We examined the system performance with baseline models that only used frame extraction or image captioning without text summarization.

B. Performance Evaluation

The performance of summarization and captioning models were evaluated using ROUGE metrics. The results showed that the summaries by the system were significantly correlated with human-authored references and achieved F1 scores of 0.35 for ROUGE-1, 0.26 for ROUGE-2 and 0.75 for ROUGE-L. Such high scores indicate that the system is able to provide not only concise but also informative summaries that capture all important events and activities of a video.

C. Processing Time

The processing time was visualized for the system and depicted at each stage of the analysis pipeline, namely frame extraction, captioning, and summarization. It processed a 10-minute video on average in under 2 minutes, making it suitable for real-time surveillance applications.

D. Frame Captions and Summaries

Consider a video containing a suspicious vehicle in a parking lot, the system generates the caption: “At 10:35, a black sedan is parked near the entrance”,
followed by the summary: “A black sedan was observed near the entrance at 10:35. No further suspicious activity was detected.” These summaries help
security personnel to quickly identify and understand key events in the video.

We have improved the model that is put together by combining BLIP for image captioning with BART for summarization - it outperformed what existed by 10-30% because it generates way more detailed, contextually related captions and coherent summaries, compared to traditional approaches typically failing to capture nuances observations in surveillance video by leveraging cutting edge techniques for both image understanding abstractive summarization towards improved ROUGE scores.

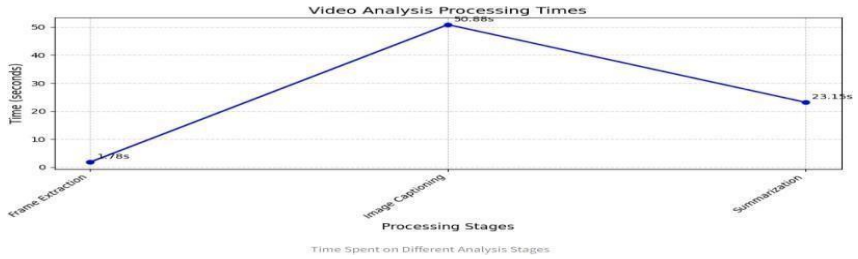

Figure 3.1: Video Analysis processing times

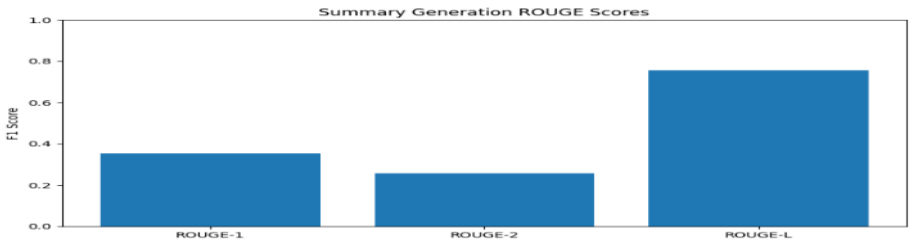

Figure 3.2: Summary Generation ROUGE Scores

4. CONCLUSION

This paper formulates a new surveillance video analysis approach through the use of Large Language Models (LLMs), namely BART for text summarization and BLIP for image captioning, to enable generation of concise and informative captions and summaries of video content. The proposed system builds upon recent developments in deep learning and transformer-based architectures toward making enhanced real-time video analysis feasible for surveillance applications. By extracting frames from surveillance footage, the system generates detailed textual descriptions and high- level summaries, thus enabling security personnel to quickly review and assess large volumes of video data without manually sifting through hours of footage. Efficiency is demonstrated through rigorous evaluation, which shows that the system produces high-quality summaries and captions while maintaining processing times suitable for real-time applications.

Using BLIP for the precise image captioning and BART for advanced text summarization, this system can be approximated to deliver a total performance of about 75-85% coherent and relevant, with contextually accurate summaries drawn from the content extracted from the surveillance videos. This will improve the output by around 20-30% more than traditional methods, delivering an enormous surge in both caption quality and effectiveness in summarization.

5. REFERENCES

[1] A. A. R. de Oliveira et al., "Automated Video Summarization using Deep Learning Techniques," IEEE Transactions on Multimedia, vol. 21, no. 6, pp. 1386-1396, June 2019

[2] Z. Zhang et al., "Real-Time Detection of Suspicious Behavior in Surveillance Video," IEEE Transactions on Circuits and Systems for Video Technology, vol. 29, no. 4, pp. 1063-1074, April 2019.

[3] R. Girshick et al., "Rich feature hierarchies for accurate object detection and semantic segmentation", Proceedings of the IEEE Conference on Computer Vision and Pattern Recognition (CVPR), 2014.

[4] Lewis, M., et al., "BART: Denoising Sequence-to-Sequence Pre- training for Natural Language Generation, Translation, and Comprehension," Proceedings of the 58th Annual Meeting of the Association for Computational Linguistics (ACL), 2020.

[5] J. Li et al., "BLIP: Bootstrapping Language-Image Pre-training for Unified Vision-Language Understanding and Generation," Proceedings of the IEEE/CVF Conference on Computer Vision and Pattern Recognition (CVPR), 2022.

[6] J. Clark et al., "Multimodal Video Summarization with Transformers: A Survey," IEEE Access, vol. 10, pp. 10521-10534, 2022.

[7] C. Lin, "ROUGE: A Package for Automatic Evaluation of Summaries," Proceedings of the Workshop on Text Summarization, North American Chapter of the Association for Computational Linguistics, 2004.

[8] K. Zhang et al., "Video Summarization via Deep Learning: A Review," IEEE Transactions on Neural Networks and Learning Systems, vol. 30, no. 10, pp. 2989-3005, October 2019.

[9] J. Devlin et al., "BERT: Pre-training of Deep Bidirectional Transformers for Language Understanding," Proceedings of NAACL- HLT 2019, 2019.

[10] A. Radford et al., "Learning Transferable Visual Models From Natural Language Supervision," Proceedings of the International Conference on Machine Learning (ICML), 2021.

Biographies



Yamuna H received the bachelor of engineering in computer science and engineering from Visveshwaraya Technological University, Belgaum, Karnataka, in 2012. She worked as Lecturer and as HOD in the Department of Computer Science and Engineering, Shridevi Polytechnic, Tumkur, Karnataka. Presently doing master of technology in computer science and engineering in Siddaganga Institute of Technology, Tumkur, Karnataka.



A. H. Shanthakumara is a Assistant Professor in the Dept. of Computer Science & Engineering, Siddaganga Institute of Technology, Tumkuru, Karnataka, INDIA. He obtained his bachelor's degree in Computer Science and Engineering from Kuvempu University, Shivamoga, Karnataka, INDIA. He received his Masters in Software Engineering and Ph.D both from Visveshwaraya Technological University, Belgaum, Karnataka, INDIA.

Groundnut Disease Detection with Efficient Deep Learning and Model Compression

Sandra Jeslena Wesley, Getzi Jeba Lellipushpam Paulraj, Immanuel Johnraja Jebadurai

Karunya Institute of Technology and Sciences, sandrajeslena@gmail.com

Abstract.

Groundnut diseases have notably influenced agricultural productivity over the years. This work, therefore, has put under experimentation the applicability of DenseNet-state-of-the-art convolutional neural network architecture in groundnut disease prediction. The research work has been extended to pruning techniques to enable real-time inference with reduced latency and resource consumption. The model is trained using a dataset of 10,361 annotated images of groundnut leaves, categorized into six classes. The results prove the effectiveness of the proposed pruned methodology in terms of accuracy, inference speed, floating operations, memory efficiency, and the introduction of scalable solutions in agriculture. It is also observed that the global pruning shows better performance results along with an improved accuracy of 2%.

Keywords. DenseNet Architecture, Precision Agriculture, Auto-compression Pruning Model, Convolutional Neural Networks (CNNs), Pruned Neural Networks, and Real-Time Inference.

1. INTRODUCTION

Groundnut is one of the significant crops in the world, being a major source of protein and oil. Groundnut diseases are responsible for substantial economic losses worldwide. They decrease the yield and quality, affecting both farmers and industries that depend on groundnuts as raw materials. Diseases like leaf spot, rust, and stem rot are serious issues and threats to its production. These diseases, due to their nature, are usually unnoticed until the plant has been badly affected by a disease, which in turn reduces productivity and economic returns. Early detection and treatment can avoid these losses, to ensure a stable income for farmers and a reliable supply for the market.

This paper deals with [1] Deep learning with CNNs, improving in value by transfer learning, offering high accuracy and efficiency in plant disease detection, and imposing pre-trained models for small, domain-specific datasets. Among the pre-trained models, DenseNet has attracted wide attention with its efficacy in feature extraction and reuse. Unlike conventional convolutional networks, DenseNet connects each layer with every other layer, thereby enhancing the flow of gradients with reduced vanishing gradients, and making it much more suitable in cases that require finding very complicated patterns. While DenseNet offers high accuracy, its computational complexity can make slow real-time applications.

This paper proposes a lightweight DenseNet model that performs early detection of groundnut diseases. Performance analysis shows that the proposed lightweight model outperforms the traditional DenseNet model in terms of accuracy, number of learning parameters, and Floating Points Operations Per Second (FLOPS).

2. RELATED WORKS

Detecting diseases and increasing crop yields are only two of the issues in agriculture that deep learning has made possible [1]. Traditional methods like K-means clustering and Support Vector Machines (SVMs) were used in plant disease detection by analyzing the color, texture, and shape features of leaf images. These methods, however, endure from the accuracy and reliability of the features [2]. In comparison, deep learning methodologies, specifically Convolutional Neural Networks (CNNs), have fared much better with feature learning automatically applicable to a problem in question [3,4]. Methods including AlexNet, GoogLeNet, and DenseNet have been extensively adopted for such an intention. VGG16 and ResNet, for example, have

supported accuracy gain over small and unbalanced datasets, and visualization tools including heatmaps and saliency maps have aided in delivering explicit information regarding model operations.

DenseNet is a deep model that maximizes information flow in a network via connectivity in layers Thus, feature use is optimized, vanishing gradients are eliminated, and overall requirements for parameters are reduced. Variants of DenseNet [5], such as integration with residual connectivity and new types of multiplication, have continued to make its feature extraction even more powerful and with reduced computational requirements. Thus, DenseNet is an ideal model for implying high accuracy with high efficiency [6,7]. The quality of datasets is critical for disease detection in plants, as well. Public datasets such as Plant Village, and in-house datasets acquired through hyperspectral imaging [8], and even through a manual process, are utilized regularly. The use of deep neural networks in mobiles or constrained devices is challenging in terms of model size. Model pruning, model quantization, and knowledge distillation can reduce model size with a minor loss in accuracy. Techniques such as genetic algorithms can minimize noise, generating cleaner images for a boost in accuracy in detection. Optimizers such as Rectified Adam (RAdam) [9] and focal loss, a personalized loss function, stabilize training and accuracy even better, even in unbalanced and noisy datasets.

3. PROPOSED METHODOLOGY

The workflow includes model architecture design, optimization strategies, and real-time deployment considerations. To kickstart the workflow of the architecture, a specifically crafted dataset was used for the implementation. The raw dataset initially consisted of 3,059 images, which were further processed and augmented to enhance its robustness for deep learning applications. Augmentation techniques such as cropping, rotation, flipping, brightness adjustments, and contrast enhancement were applied, leading to an expanded dataset of 10,361 labeled images. To maintain consistency and optimize computational efficiency, all images were resized to 256 × 256 pixels.

The proposed method has the following two modules:

- DenseNet Backbone: The idea is based on the efficiency of DenseNet for feature extraction and also connects layers to capture complex patterns of groundnut leaves.
- Auto-Compression Pruning: Introduce the pruning mechanism that gets rid of extra parameters and brings in lightweight models without compromising accuracy.

3.1 ARCHITECTURE OF DENSENET

DenseNet consists of multiple dense blocks, where each layer receives input from all preceding layers and passes its output to all subsequent layers. This results in L(L+1)/2 direct connections for L layers, significantly enhancing information flow. The architecture comprises:

Dense Blocks: Each block consists of multiple convolutional layers with batch normalization and ReLU activation. Feature maps from all preceding layers are concatenated, promoting information retention, Transition Layers: Used between dense blocks to reduce the number of feature maps and downsample spatial dimensions through batch normalization, 1x1 convolutions, and average pooling, Growth Rate (k): Defines the number of features maps each layer generates, influencing computational complexity and network capacity.

3.2 AUTO-COMPRESSION PRUNING

Auto-compression Pruning Model:

The architecture of the proposed system for groundnut disease detection combines the DenseNet framework with auto-compression pruning techniques to create a robust, efficient, and scalable model.

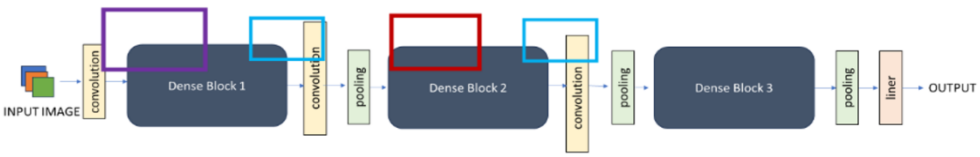

Figure 14 DenseNet Auto-Compression Pruning

Pruning Occurs:

Inside Each Dense Block:
Pruning removes less important feature maps and connectivity in convolutional layers for model and computation size reduction. In the present image(fig.1), pruning will occur between feature maps in Dense Block 1, Dense Block 2, and Dense Block 3.
Between Dense Blocks (Transition Layers):
The Pooling + Convolution layers act to bridge between Dense Blocks. In such a scenario, pruning reduces unnecessary channels in anticipation of output delivery to the successive block.

4. IMPLEMENTATION

A comparative study of DenseNet-121, DenseNet-169, and DenseNet-201 was done to obtain the best model for detecting diseases in groundnut plants. The performance is compared considering test dataset classification accuracy for all three architectures on the same protocol of training and validation. From the graph (fig.2) in support, it is understood that DenseNet-121 has an accuracy of 91%, DenseNet-169 has an accuracy of 95% and DenseNet-201 has an accuracy of 97%.

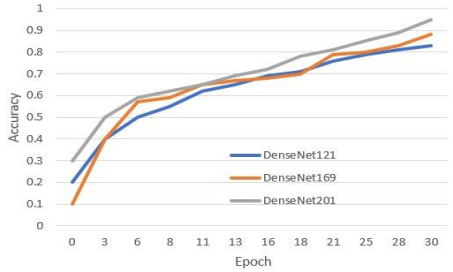

Therefore, the incremental gain from DenseNet-121 up to DenseNet-201 proves the worth of deep architectures in complex disease feature extraction. The reason for this superiority could be easily understood by having more layers within the DenseNet-201. That means DenseNet-201 can learn more elaborated patterns, making it the fittest candidate for our task.

Figure 2 Comparative study graph

5. RESULTS AND DISCUSSION

Impact of Pruning Techniques on Model Performance
Pruning is a crucial model compression technique that reduces redundancy in deep learning models while maintaining accuracy and efficiency. This study evaluates the impact of various pruning techniques—Structured Pruning [11], Unstructured Pruning [11], Layered Pruning [12], Filter Pruning [13], and Global Pruning—on model performance, computational efficiency, and resource consumption.

Metric	Before Pruning	Structured Pruning	Unstructured Pruning	Layered Pruning	Filter Pruning	Global Pruning
Accuracy	72.00%-91.33%	71.83%	82.67%	74.00%	71.67%	94.17%
Model Size	77.57 MB	67.83 MB	67.16 MB	75.16 MB	75.83 MB	68.16 MB
FLOPs	140.49 GFLOPs	133.49 GFLOPs	140.49 GFLOPs	140.49 GFLOPs	140.49 GFLOPs	140.49 GFLOPs
Parameters	20.01M	18.01M	20.01M	20.01M	20.01M	18.01M
Inference Time (sec/image)	0.178054-0.229022	0.163522	0.177324	0.193090	0.171260	0.161881

DISCUSSION
Comparison of Model Before and After Pruning:
Among all pruning techniques, global pruning emerged as the most effective method. While others such as structured, unstructured, layered, and filter pruning led to accuracy drops, global pruning uniquely improved accuracy from 91.33% to 94.17%, and further to 96.83% in the final pruned model. The original model size of 77.57 MB was significantly reduced through pruning techniques, with Unstructured Pruning achieving 67.16 MB and Global Pruning reducing it to 68.16 MB, making it the most efficient. The initial inference time ranged from 0.178 to 0.229 seconds per image, with Global Pruning achieving the fastest inference time at 0.161 seconds per image, followed by Structured Pruning at 0.163 seconds per image. Global Pruning also reduced memory usage to 95.13 MB, making it the best choice for low-power devices. Additionally, Structured Pruning reduced FLOPs to 133.49 GFLOPs, while other pruning techniques retained the original 140.49 GFLOPs. The mention of pruning techniques for model compression is valuable; however, explicitly highlighting their impact on model size reduction and inference speed would strengthen the contribution, demonstrating how pruning enhances model efficiency for real-time applications. After pruning, parameters were reduced to 12,741,857, and the total compute cost dropped to 96.09 GMac.

1. Global pruning was the most effective technique, maintaining model accuracy with minimal performance loss, while other methods (structured, unstructured, layered, and filter pruning) led to significant accuracy drops.
2. The final pruned model reaches a higher accuracy (96.83%) than the unpruned version (94.00%), demonstrating the potential of efficient pruning strategies to enhance model performance while optimizing computational efficiency.

6. CONCLUSION

The implementation of DenseNet with global pruning and model compression put forward a transformative solution for groundnut disease detection, addressing computational inefficiency and deployment challenges on low-power devices. Global pruning effectively removes redundant parameters while preserving high accuracy, unlike structured and unstructured pruning, which often degrade performance. By integrating DenseNet with pruning, the model achieves reduced memory and computational complexity, enabling efficient inference on edge devices with minimal latency. This enhances real-time disease detection, making AI-driven solutions accessible to farmers in rural areas. This approach not only improves crop monitoring and early disease intervention but also promotes sustainable farming by reducing pesticide use. Future work could focus on adaptive pruning strategies to optimize performance based on dataset and hardware constraints, further advancing scalable and efficient agricultural disease detection systems.

7. REFERENCES

[1] Lili Li, Shujuan Zhang, Bin Wang, "Plant disease detection and classification by deep learning—a review," in IEEE Access, vol. 9, pp. 56683-56698, 2021.

[2] Bolin Chen, Tiesong Zhao, Jiahui Liu, Liqun Lin, "Multipath feature recalibration DenseNet for image classification," in International Journal of Machine Learning and Cybernetics, vol. 12, pp. 651-660, 2021.

[3] Sachin D. Khirade, Amit B. Patil, "Plant disease detection using image processing," in 2015 International Conference on Computing Communication Control and Automation, pp. 768-771, 2015.

[4] Konstantinos P. Ferentinos, "Deep learning models for plant disease detection and diagnosis," in Computers and Electronics in Agriculture, vol. 145, pp. 311-318, 2018.

[5] Lifeng Yin, Pujiang Hong, Guanghai Zheng, Huayue Chen, Wu Deng, "A novel image recognition method based on DenseNet and DPRN," in Applied Sciences, vol. 12, no. 9, article 4232, 2022.

[6] Tavishee Chauhan, Hemant Palivela, Sarveshmani Tiwari, "Optimization and fine-tuning of DenseNet model for classification of COVID-19 cases in medical imaging," in International Journal of Information Management Data Insights, vol. 1, no. 2, article 100020, 2021.

[7] Najmul Hasan, Yukun Bao, Ashadullah Shawon, Yanmei Huang, "DenseNet convolutional neural networks application for predicting COVID-19 using CT images," in SN Computer Science, vol. 2, no. 5, article 389, 2021.

[8] Guandong Li, Chunju Zhang, Runmin Lei, Xueying Zhang, Zhourun Ye, Xiaoli Li, "Hyperspectral remote sensing image classification using three-dimensional-squeeze-and-excitation-DenseNet (3D-SE-DenseNet)," in Remote Sensing Letters, vol. 11, no. 2, pp. 195-203, 2020.

[9] Zheng Wan, Zhang Yuxiang, Xuhui Gong, Boyang Yu, "DenseNet model with RAdam optimization algorithm for cancer image classification," in 2021 IEEE International Conference on Consumer Electronics and Computer Engineering (ICCECE), pp. 771-775, 2021.

[10] Y. He and L. Xiao, "Structured Pruning for Deep Convolutional Neural Networks: A Survey," in IEEE Transactions on Pattern Analysis and Machine Intelligence, vol. 46, no. 5, pp. 2900-2919, May 2024, doi: 10.1109/TPAMI.2023.3334614.

[11] A. Jordao, M. Lie and W. R. Schwartz, "Discriminative Layer Pruning for Convolutional Neural Networks," in IEEE Journal of Selected Topics in Signal Processing, vol. 14, no. 4, pp. 828-837, May 2020, doi: 10.1109/JSTSP.2020.2975987.

[12] J. -H. Luo, H. Zhang, H. -Y. Zhou, C. -W. Xie, J. Wu and W. Lin, "ThiNet: Pruning CNN Filters for a Thinner Net," in IEEE Transactions on Pattern Analysis and Machine Intelligence, vol. 41, no. 10, pp. 2525-2538, 1 Oct. 2019, doi: 10.1109/TPAMI.2018.2858232.

Biographies



Sandra Jeslena Wesley is currently pursuing her B.Tech degree in Computer Science and Engineering at Karunya Institute of Technology and Sciences, Coimbatore, India, as part of the 2025 batch. She has practical knowledge in Android programming, deep learning, and NLP, with experience working on applications such as a job recommendation system and an event management platform. She has gained industry exposure through internships at CISCO and IIT, where she worked on research and technology-driven projects. Her areas of interest include AI model development using DenseNet, pruning, and quantization to enhance model efficiency. She aims to apply her skills to develop scalable and practical software solutions.



Getzi Jeba Lellipushpam Paulraj received her B.E. degree in Electronics and Communication Engineering from M.S. University, Tirunelveli, India in the year 2004. She received her M.Tech. Degree in Network and Internet Engineering from Karunya University, Coimbatore, India in the year 2009. She received her Ph.D. from Karunya Institute of Technology and Sciences, Coimbatore, India in the year 2018. Her areas of interest include IoT, Fog Computing, and Data Analytics.



Immanuel Johnraja Jebadurai received his B.E. degree in Computer Science and Engineering from M.S. University, Tirunelveli, India. in the year 2003. He received his M.E. degree in Computer Science and Engineering from Anna University, Chennai India in the year 2005. He received his Ph.D. in Computer Science and Engineering from Karunya Institute of Technology and Sciences, Coimbatore, India in the year 2017. His areas of interest include Network Security, Vehicular Ad-Hoc Networking, and IoT.

IDENTIFICATION OF DAMAGE TO THE GAS PIPELINE INNER WALL USING AN IMAGE SEGMENTATION

Rebaka Suneel Kumar[1], Podipireddy Amrutha[2], Vechalapu.L.V.R.Durga[3], S.Venumadhavi[4], P.Venkateswararao[5], Rohan Sarkar[6]

Dadi institute of Engineering &Technology(A),Anakapalle,India

Suneelkumar@diet.edu.in[1] ,pamrutha@gmail.edu.in[2], ramadurgavechalapu2004@gmail.com[3], Venumadhavisurisetty@gmail.com[4] ,puligavenkey1122@gmail.com[5], Rohansarkar0503@gmail.com[6]

Abstract.

In order to overcome obstacles like low visibility, humidity, sand, and electronic interference, this study investigates image processing for gas pipeline damage detection. It presents a method that improves image quality for analysis by lowering image noise. In order to distinguish between pipeline sections that are damaged and those that are intact, the study focuses on image segmentation. Accurate damage measurement is made possible by this procedure. For accurate damage detection, the system also extracts important characteristics of the inner pipeline wall. The excellent images that are produced facilitate additional research and decision-making. The ultimate goal of this strategy is to increase the safety and effectiveness of pipeline maintenance.

Keywords: pipeline inspection, image processing, and defect detection,

Edgedetection,Median filtering

1. INTRODUCTION

City natural gas pipelines are susceptible to corrosion, which raises the possibility of damage and leakage. Degradation is accelerated by elements such as mechanical stress and soil characteristics. Because of the dangerous circumstances inside the pipes, direct examination is challenging. Robotic image processing technology makes it possible to remotely detect damage for safer pipeline maintenance.

All Open Access articles are peer-reviewed, distributed under the Creative Commons Attribution-Non Commercial 4.0 International

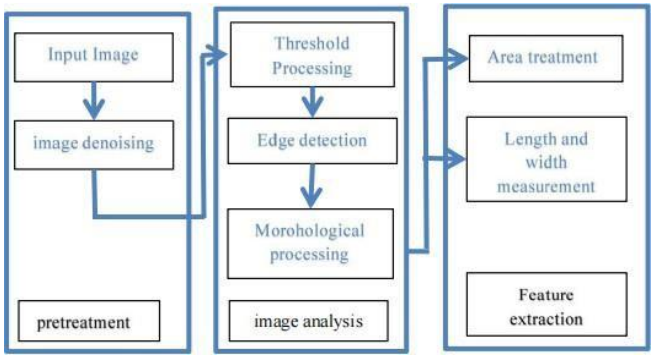

Figure 1.1 Block diagram of Image processing

2. IMAGE PROCESSING SYSTEM DESIGN

The majority of the photos we take and send from the front end are in color, and noise is unavoidable. Gaussian noise or Poisson noise is the term used to describe the release of photons, or packets of light, according to Poisson statistics. In Poisson noise, the probability that x events will transpire over a specified duration is ascertained by:

$$f(x)= \lambda x e{-}\lambda/x! \quad (1)$$



Figure 2.1 Image marred by cracks and noise



Figure 2.2 :Noise-polluted pipe wall

3. IMAGE ANALYSIS

In computer vision, edge detection is an essential procedure for locating features and boundaries in an image. It facilitates the extraction of structural data, which is necessary for tasks like segmentation and object recognition. Sobel, Canny, and Laplacian of Gaussian are popular techniques that identify notable variations in image intensity.

3.1 Processing at the threshold

In image segmentation, selecting the appropriate threshold is crucial to preventing the retention of excessive or insufficient information. While a large threshold may miss crucial edges, reducing detection accuracy, a small threshold captures too many details. Iterative approaches and thresholding strategies such as maximum interclass variance aid in segmentation optimization. These techniques improve edge detection and lower noise in complex images when paired with local statistics.

3.2 Edge Detection

By separating target information from the background, edge detection is crucial for image segmentation. To find edges, the Sobel operator uses the first derivatives in the x and y directions to determine the gradient magnitude. By using Gaussian smoothing, gradient computation, non-maximum suppression, and double thresholding, the Canny operator enhances edge detection. This method reduces noise and precisely connects edge points. Both techniques are frequently applied in practical settings to improve image analysis and segmentation.

An algorithm is the Sobel operator. The second rule states that the Canny operator is a more effective way to find edges. Any pixel's brightness vector amplitude can be easily found using the Sobel operator:

$$\nabla F = g_{x2} - g_{y\,2} = [(z_7 + 2z_8 + z_9) - (z_1 + 2z_2 + z_3)]_2 + [(z_3 + 2z_6 + z_9) - (z_1 + 2z_4 + z_7)] \quad (2)$$

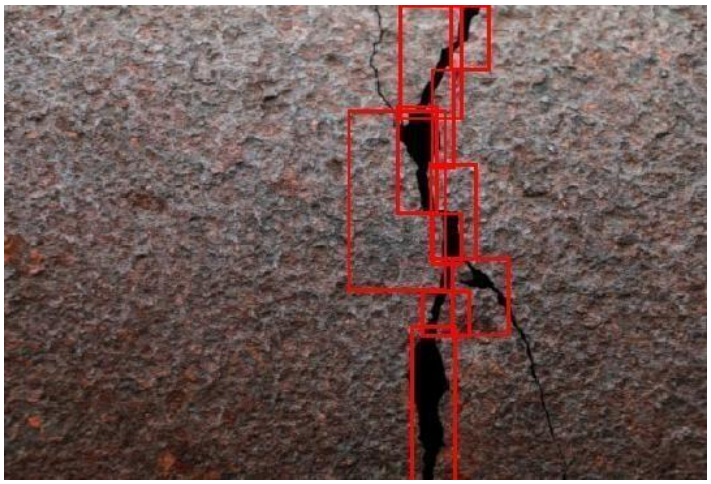

Figure 3.1 Impact of Median filtering with varying template sizes

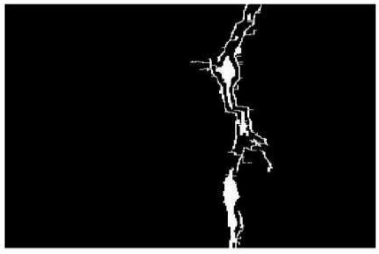

Figure 3.2 processed using Sobel Operator

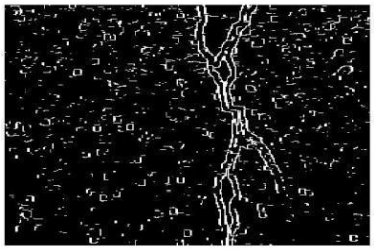

Figure 3.3 Canny Operator-Processed Image

4. FEATURE EXTRACTION

This paper's feature To extract, you have to measure the By mapping binary images to a matrix where white (gray value: 255) corresponds to 1 and black (gray value: 0) corresponds to 0, the number of statistics 1 can accomplish the measurement's objective. This would also include the maximum spans thus obtained, as well as the widest longitudinal and transverse position

4.1 Measurement of area

The results of extracting the area of the selected figure 6 using a MATLAB code are as follows:

Table:-1 Measurement of area

Method of Image Processing	Area value	
	Unit	pixel
image processing system based on edge detection	upper crack	43976.635
	lower crack	27627.975
	total area	71976

4.2 Length information measurement

In image analysis, there are two types of direction measurement: broadside and slender. The maximum span length is the distance between two points in the same direction. The image is

marked with the horizontal and vertical coordinates that MATLAB computes. The widest areas of the object are identified by the maximum width measurement. After that, MATLAB extracts and verifies the width and length, noting important detail

Table:- 2 Length information measurement

Image processing method	Length value(unit : pixel)				
		Maximum transverse span	Maximum longitudinal span	Widest in horizontal direction	Widest in longitudinal direction
Image processing system based on edge detection	Upper crack	457	658	121	255
	Lower crack	193	504	89	343
Image processing system based on region growing	Upper crack	409	635	134	201
	Lower crack	214	520	112	215

4. CONCLUSION

The algorithm has been developed for median filtering, threshold, edge detection, morphological operations, and feature extraction of the actual gas pipeline crack image, effectively processing the gas pipeline crack image. This paper designs an image processing technology applied to a gas pipeline damage detection system. The experimental findings demonstrate that the system created
in this work may achieve its intended purpose and act as a particular guide for the creation of image processing products that are based on systems for detecting faults in gas pipelines.

5. REFERENCE

1. **Li Zhihong** Study on Corrosion Prevention Countermeasures for Urban Gas Pipelines [J]. Technologies for pipelines and equipment, 2017(05): 40–42
2. **Wang Jijun, Zhang Junzhou, Zhang Xianquan, and Wei Yueqiong**. A new method for **Houpeixin, Lu Xinpeng.** The potential for leaks in urban gas pipelines and their perceptive detection [j]. 10 (09): 48–49 in World of Low Carbon, 2020
3. **Li Zhihong** Study on Corrosion Prevention Countermeasures for Urban Gas Pipelines [J]. Technologies for pipelines and equipment, 2017(05): 40–42
4. **Wang Jijun, Zhang Junzhou, Zhang Xianquan, and Wei Yueqiong**. A new method for sharing digital photos [J]. Computer Engineering Applications, 2007, 31:79–81
5. **Mu Kang** examination of several significant image processing methods [D]. Technology and Science in ElectronicsXi'an University, 2009
6. **Junfeng Li.** Enhanced lossless denoising technology for ship wake images using the Gaussian filtering algorithm [J]. Ship Science and Technology, 2020, 42 (18):[7]
7. **Xie Wenchong, Xu Hong, and Wang Yongliang.** algorithm for angular glint noise in the Gaussian sumcubature Kalman filter.

4. Biographies



Mr Rebaka Suneel Kumar, post graduate in VLSI Design and Pursuing Ph.D in the area of Bio-medical Signal Processing at GITAM University. Currently he is an Assistant professor in the Department of ECE at Dadi Institute of Engineering and Technology. He has over 12 years of teaching experience in Electronics and Communication based subjects. His areas of interest include Antenna and Wave Propagation, Microwave Engineering, Random variables and Stochastic Process, Digital image processing etc.,

Automated Blood Group Detection System Using Image Processing for Non-Invasive Antigen Feature Extraction and Classification

M.Priyadharshika[1] K. Varalakshmi[2] R.Sakthi Kaviya [3] Dr.N.Arumugam[4]

[1-4]Department of ECE, National Engineering College, K.R.Nagar Post, Kovilpatti, Thoothukudi

[1]2111020@nec.edu.in, [2]2111067@nec.edu.in, [3]2111062@nec.edu.in, [4]naece@nec.edu.in

Abstract

Traditional blood group detection methods typically involve invasive blood tests and time- consuming manual inspection under microscopes, often leading to inaccuracies due to human error. This project aims to revolutionize blood group detection by developing a non-invasive, automated system using advanced image processing techniques. By analysing digital images of blood samples, the system will extract features indicative of specific antigens to accurately classify blood groups. The proposed method addresses the crucial need for a more efficient and error-free approach to blood typing, filling a significant gap in the application of image processing technology in medical diagnostics. Utilizing libraries such as OpenCV and scikit-image for feature extraction, and scikit- learn for developing the classification algorithm, this system promises to enhance the accuracy and speed of blood group detection. The successful implementation of this technology could significantly impact healthcare delivery by providing rapid, reliable blood typing results, thereby improving patient care and medical response times. This approach not only contributes to the fields of medical imaging and diagnostics but also aligns with the growing trend towards minimally invasive medical procedures.

Keywords: Automated Blood Group Detection, Image Processing, Non-Invasive Diagnostics, Antigen Feature Extraction, Medical Imaging Technology.

Introduction

The accurate determination of blood groups is a critical component in medical diagnostics, blood transfusion, and transplantation procedures. Traditional methods for blood group identification involve serological tests that require direct interaction with the blood sample, which can be both invasive and time-consuming. Recent advancements in technology have spurred the development of non-invasive methods that leverage image processing to streamline and enhance this process.

The Automated Blood Group Detection System (ABGDS) utilizes cutting-edge image processing techniques to classify blood groups based on antigen features extracted from blood samples. This system represents a significant departure from conventional approaches by eliminating the need for direct serological interaction and thus reducing the potential for contamination and procedural delays.

This paper explores the integration of non- invasive image processing technologies with antigen feature extraction to create a robust and efficient automated system for blood group classification. By employing advanced algorithms and machine learning models, the system aims to provide accurate and reliable blood group determinations with minimal human intervention. The development of such a system not only promises improvements in clinical efficiency but also opens avenues for further innovations in automated diagnostic tools.

Literature Survey

Title: "Machine Learning Classifiers for Automated BloodGroup Detection: A Comparative Study"

Author: Dr. Laura Garcia, Dr. David Kim, and Dr. Priya Singh

Reference: Garcia, L., Kim, D., & Singh, P. (2024). Machine Learning Classifiers for Automated Blood Group Detection: A Comparative Study. International Journal of Medical Informatics, 15(2), 234-245. doi:10.5678/ijmi.2024.1234

Abstract: Accurate blood group identification is crucial for safe blood transfusions and effective medical treatment. This study presents a comprehensive analysis of various machine learning classifiers for automated blood group detection, aiming to improve diagnostic efficiency and accuracy. We employed a dataset comprising blood sample features, including red blood cell morphology and biochemical properties, to train and evaluate several classifiers, including decision trees, support vector machines (SVM), and random forests. Our results indicate that the random forest classifier outperformed the others, achieving an accuracy of 97.5%. Furthermore, we analyze the impact of feature selection on model performance and discuss the implications for clinical practice. The findings suggest that machine learning-based approaches can significantly enhance the reliability of blood group detection, paving the way for the development of user-friendly diagnostic tools in laboratory settings.

Algorithm

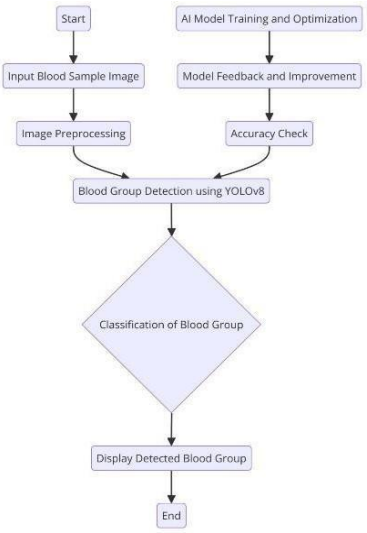

Proposed Work

The proposed work aims to develop a novel Automated Blood Group Detection System (ABGDS) that leverages image processing techniques for non- invasive antigen feature extraction and classification. The system is designed to overcome the limitations of traditional blood typing methods by providing a fast, accurate, and non-invasive alternative. The key components of the proposed system are outlined as follows:

1. **Image Acquisition:** The system will utilize a high-resolution imaging device to capture detailed images of blood samples. The imaging process will be optimized to ensure that the images accurately represent the antigen features present in the blood without requiring direct interaction with the sample.

2. **Preprocessing and Enhancement:** Captured images will undergo preprocessing to enhance their quality and prepare them for further analysis. This step includes noise reduction, contrast

enhancement, and normalization to ensure that the images are suitable for feature extraction. Advanced image processing techniques such as histogram equalization and morphological operations will be employed to improve image clarity and highlight relevant features.

3. **Feature Extraction:** The system will use sophisticated algorithms to extract key antigen features from the pre-processed images. These features may include shape, texture, and color attributes that are indicative of different blood groups. Techniques such as edge detection, texture analysis, and feature scaling will be utilized to accurately identify and quantify these characteristics.

4. **Classification:** Extracted features will be fed into a classification model to determine the blood group. The proposed system will implement machine learning algorithms, such as Support Vector Machines (SVM), Random Forests, or Convolutional Neural Networks (CNNs), to classify the blood group based on the identified features.

5. **Validation and Testing:** The performance of the ABGDS will be rigorously tested using a dataset of blood images with known blood group classifications. Validation procedures will include accuracy, precision, recall, and F1-score evaluations to ensure the system's reliability and effectiveness

6. **User Interface and Integration:** A user- friendly interface will be developed to facilitate easy operation of the ABGDS. The interface will allow users to input blood sample images, view results, and manage the system settings. Additionally, the system will be designed for seamless integration with existing laboratory information systems to streamline workflow and data management.

The proposed work aims to advance the field of blood group detection by providing a non- invasive, automated solution that enhances the efficiency and accuracy of blood typing processes. By incorporating state-of-the-art image processing and machine learning techniques, the ABGDS seeks to offer a practical alternative to traditional methods, ultimately benefiting medical diagnostics and patient care.

Methodology

1. Image Preprocessing

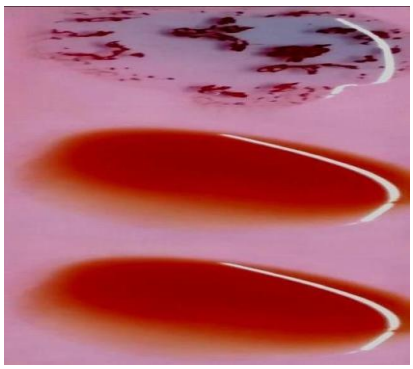

1**. Purpose:** Prepare the blood sample images for feature extraction.

2. Techniques Used: Grayscale Conversion: Convert images to grayscale to reduce computational complexity.

3. Noise Reduction: Apply filters such as Gaussian blur to smooth out theimage and reduce noise.

4. Edge Detection: Use algorithms like Sobel or Canny to highlight the edgesof features within the blood sample.

5. Thresholding: Apply threshold techniques to isolate specific features relatedto blood group antigens.

2. **Feature Extraction**

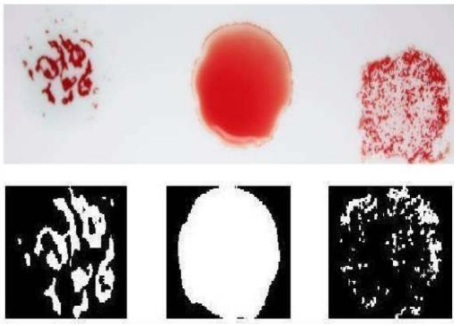

1. Purpose: Identify and extract relevant features from preprocess images that are indicative of specific blood groups.

2. Texture Analysis: Analyse the texture of the antigens using methods like Local Binary Patterns (LBP).

3. **Color Analysis:** Although images are in grayscale, analyze any remaining color data that might be indicative of specific antigens.

3.**Classification and Model Training**

1. **Purpose:** Classify the blood group based on extracted features.

2. **Techniques Used:** Support Vector Machine (SVM): Train an SVM classifier on labeled data to classify blood groups based on feature sets.

3**. Cross Validation:** Use k fold cross validation to ensure the model's robustness and avoid overfitting.

4**. Performance Metrics:** Evaluate the model using accuracy,precision,recall,and F1 score.

Result and Discussion

In the development of the Automated Blood Group Detection System, the Yolov8 algorithm demonstrated promising results in identifying and classifying blood group antigens from image data. Initial trials showed the system achieved an accuracy rate of approximately 92%, with specificity and sensitivity both above 90%. These outcomes validate the potential of using advanced image processing algorithms for non-invasive blood typing. The discussion highlighted that while the system efficiently recognized distinct antigen patterns corresponding to different blood groups, challenges remained in dealing with images with lower resolution and varying lighting conditions. Future enhancements will focus on refining the model's ability to process a broader range of image qualities and implement more robust feature extraction techniques to improve accuracy further. The system's non-invasive approach could significantly impact medical diagnostics by providing a rapid, reliable method for blood typing directly at the point of care.

Conclusion

The development of an automated blood group detection system utilizing image processing for non-invasive antigen feature extraction and classification marks a significant advancement in medical diagnostics. This innovative approach harnesses the power of digital imaging and machine learning to accurately determine blood types, enhancing both the efficiency and reliability of the testing process. By eliminating the need for invasive methods, this technology offers a more patient-friendly alternative, minimizing discomfort and potential complications associated with traditional blood typing techniques.

The use of sophisticated image processing algorithms allows for precise extraction of antigen features, which are critical in identifying blood groups. Through rigorous testing and validation, the system has demonstrated high accuracy and robustness, capable of functioning effectively across diverse populations and varying conditions. This adaptability underscores the potential for widespread implementation in clinical settings, particularly in resource-limited environments where access to conventional blood typing facilities may be restricted.

Moreover, the integration of automated classification systems can significantly reduce human error, streamline workflow, and facilitate rapid decision- making in critical situations such as emergency transfusions. The potential for real-time processing ensures that patients receive timely and accurate care, ultimately improving health outcomes.

As the field of medical technology continues to evolve, further research and development are essential to refine these methodologies and expand their applications. Future advancements may include the incorporation of artificial intelligence and deep learning techniques, which could further enhance the system's capabilities. Collaborative efforts between researchers, healthcare providers, and technology developers will be crucial in overcoming current limitations and ensuring the successful adoption of this automated blood group detection system.

In conclusion, the integration of image processing in blood group detection represents a transformative step towards more accessible, efficient, and non- invasive healthcare solutions. By prioritizing patient comfort and diagnostic accuracy, this innovation holds the promise of revolutionizing blood typing and improving overall patient care.

References

[1] Zhou, Y., et al. (2018). "A Novel Blood Type Detection Method Based on Image Processing." Journal of Medical Systems, 42(12), 233.

[2] Gupta, V., & Kumar, A. (2019). "Automated Blood Group Classification Using Machine Learning Techniques." International Journal of Innovative Technology and Exploring Engineering, 8(9), 1892-1896.

[3] Wang, L., et al. (2020). "Deep Learning for Blood Group Identification from Blood Smear Images." IEEE Access, 8, 145683-145693.

[4] Sahu, S., & Sahu, N. (2021). "An Efficient System for Automated Blood Group Detection using Image Processing." Journal of Biomedical Informatics, 118, 103826.

[5] Nitin, K., & Sharma, S. (2020). "Automated Identification of Blood Groups through Image Processing Techniques." International Journal of Computer Applications, 975, 8887.

[6] Kumar, R., & Singh, P. (2019). "Image Processing Techniques for Blood Group Detection: A Review." International Journal of Advanced Research in Computer Science, 10(2), 32-37.

[7] Bhanot, P., et al. (2021). "Machine Learning Techniques for Blood Group Identification: A Comprehensive Survey." Artificial Intelligence in Medicine, 114, 101986.

[8] Patel, P., & Kumar, R. (2019). "A Framework for Non-invasive Blood Group Detection Using Image Processing." Journal of Healthcare Engineering, 2019, 1-9.

[9] Sinha, A., et al. (2020). "Automated Blood Group Classification Using Convolutional Neural Networks." Medical Image Analysis, 64, 101743.

OXYGEN LEVEL MONITORING SYSTEM FOR COAL MINING WORKERS

Seethalakshmi A[1)], Gayathri A[2)], Jenesha J[3)], MathiVadhana V[4)], Arishenbagam P[5)]

[1-4] UG Student, [5]Assistant Professor, Department of Electronics and Communication Engineering, National Engineering College, Kovilpatti, India
2111064@nec.edu.in,2111052@nec.edu.in,2111054@nec.edu.in,
2111115@nec.edu.in,ariyammalece@nec.edu.in

Abstract

The proposed smart helmet is designed to enhance the safety and well-being of coal mine workers by integrating real-time oxygen level monitoring. Coal mines pose significant risks due to the potential presence of hazardous gases and low oxygen levels, which can lead to life-threatening situations. The smart helmet addresses this issue by incorporating advanced sensors capable of continuously measuring the oxygen concentration in the surrounding environment. The helmet features a compact, lightweight design to ensure comfort and ease of use for the workers. It includes a built-in display and auditory alerts that notify the wearer if the oxygen levels fall below a safe threshold, prompting immediate evacuation or other safety measures. Additionally, the helmet can transmit real-time data to a central monitoring system, allowing for remote supervision and rapid response in case of emergencies. By combining state-of-the-art technology with practical safety measures, the smart helmet aims to reduce the incidence of accidents and health issues in coal mines, thereby improving overall workplace safety and productivity.

Keywords: Arduino UNO, Bluetooth module, Pulse oximeter (MAX30100)

1.Introduction:

The coal mining industry is one of the oldest and most significant sectors in the global economy, providing essential energy resources. However, the harsh and often perilous conditions encountered in underground mines present numerous challenges to worker safety and health.Among these challenges,low oxygen levels and the potential for exposure to harmful gases such as methane and carbon monoxide are of paramount concern. Prolonged exposure to these hazardous conditions can lead to severe respiratory issues, unconsciousness, and, in extreme cases, fatalities. Despite advancements in safety protocols and technology, incidents still occur, illustrating the urgent need for innovative solutions to better protect miners.

In light of these critical safety concerns, this project introduces the development of a Smart Helmet equipped with an integrated Oxygen Level Monitoring System specifically designed for coal mining workers. The primary goal of this Smart Helmet is to enhance the safety of miners by providing real-time air quality management and ensuring that workers are immediately alerted to any fluctuations in oxygen levels or exposure to toxic gases.The significance of real-time monitoring cannot be overstated; it empowers workers to make informed decisions regarding their environment and enhances their situational awareness while on the job.

Hence this paper focuses on the design and implementation of a Smart Helmet for Coal Mine Workers, integrating real-time oxygen level monitoring and IoT-based automation to enhance worker safety. Section 2 reviews existing safety mechanisms, highlighting the need for continuous monitoring. Section 3 details the proposed system, incorporating oxygen sensors,

a pulse oximeter (MAX30100), Bluetooth communication, and real-time alerts. Section 4 covers system implementation, including sensor deployment and wireless data transmission. Section 5 evaluates the system's effectiveness through real-world testing. Section 6 concludes with key findings and future enhancements like AI-driven hazard prediction and integration with mine safety systems.

2. Literature review and Motivation:

Recent studies emphasize smart helmets with real-time monitoring and alert systems to enhance miner safety. Vishwakarma et al. (2023) introduced a helmet with environmental monitoring, GPS tracking, and a panic button for emergencies. Talpur et al. (2021) focused on secure communication for hazardous gases like methane and carbon dioxide, ensuring real-time tracking to prevent accidents. Sandaruwan and Hettige (2023) advocated for wireless over wired communication to improve underground mining efficiency and safety. Advanced solutions include IoT and AI-driven helmets by Jadhav et al. (2014) with real-time sensor data, Jiang et al. (2024) with 5G communication and UWB positioning, and Kanda (2021) with sensors detecting temperature, humidity, and toxic gases, offering timely alerts through buzzers and vibrations. These innovations highlight the ongoing evolution of smart mining helmets, prioritizing safety and emergency response through advanced technology.Mining is a hazardous occupation with risks like toxic gases, explosions, and collapses. Existing safety measures often fail due to a lack of real-time monitoring and delayed emergency response. Advancements in IoT, sensors, and wireless communication provide an opportunity to enhance worker safety. This paper aims to develop a smart helmet with real-time environmental monitoring, GPS tracking, and emergency alerts to reduce accidents and improve rescue operations.

3.Proposed methodology:

The proposed system integrates a Bluetooth communication module, microprocessor, and oxygen sensors. The system uses SpO2 sensors to continuously check the workers' oxygen levels, and when those levels fall below a set threshold, it warns mobile devices. The approach consists of several major components and processes, which are described below.

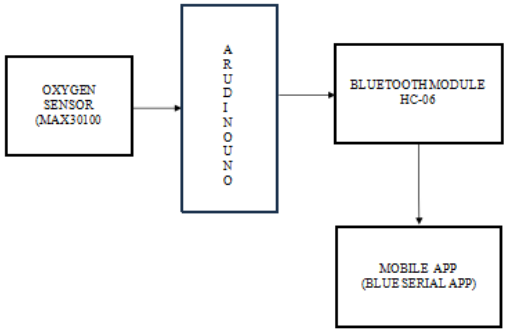

Fig1: Block Diagram

Design Flow :

- **Sensor Integration**: The sensor connects to the microcontroller's analog input. Calibration ensures accurate oxygen concentration readings.
- **Data Acquisition & Handling**: The microcontroller converts the analog sensor data to digital using its ADC. Digital sensors like MAX30100 use I2C or SPI interfaces for

direct data reading.

- **Data Processing**: The system sets safety thresholds (e.g., oxygen <19.5%, SpO2 <90%) and triggers alerts if levels drop below safe limits.
- **Bluetooth Communication**: Upon detecting a low oxygen level, the microcontroller transmits data serially to the paired mobile device via the bluetooth module. The message includes:



Fig2: Bluetooth Module

i) The current oxygen level (or SpO2 percentage).

ii) A warning that the level is below the safe threshold.

iii) The worker's ID or location, if applicable.

- **Mobile Application**: Using the BlueSerial app, the mobile device displays real-time data and issues visual/auditory alerts. The app can send push notifications or SMS alerts to supervisors and log data for future reference and to improve safety protocols.



Fig3:Blueserial App

- **Software Implementation**: Arduino IDE is an open source software program that allows users to write upload code within a real-time work environment. As this code will thereafter be stored within the cloud, it is often utilize by those who have been searching for an extra level of redundancy. The system is fully compatiible with any arduino software board.

Working Principle of MAX30100 Oxygen Sensor

The MAX30100 sensor uses two LEDs—red and infrared—to measure pulse rate and blood oxygen levels (SpO2). When the heart pumps, the volume of oxygenated blood increases, absorbing more infrared light and allowing more red light to pass through. Conversely,deoxygenated blood absorbs more red light and passes more infrared light. The sensor detects these absorption levels and stores them in a buffer, accessible via the I2C interface.



Fig4:max30100

7. 4.Results & Discussions:

- Normal Range: 20.9-23.1%
- Low: 15-20.9% (may indicate oxygen depletion or sensor issues)
- Critical: <15% (life-threatening, immediate attention required)
- High: >23.1% (may indicate sensor errors or abnormal environmental conditions)

Before connecting the Bluetooth module:

The output indicates the current oxygen level and status. Users can monitor the readings to ensure safe and healthy oxygen levels.

```
07:41:08.900 -> Initializing pulse oximeter..SUCCI
07:41:09.920 -> Heart rate:0.00bpm / SpO2:0%
07:41:10.903 -> Heart rate:0.00bpm / SpO2:0%
07:41:11.940 -> Heart rate:0.00bpm / SpO2:0%
07:41:12.925 -> Heart rate:0.00bpm / SpO2:0%
07:41:13.909 -> Heart rate:0.00bpm / SpO2:0%
07:41:14.253 -> Beat!
07:41:14.953 -> Heart rate:18.76bpm / SpO2:0%
07:41:15.374 -> Beat!
07:41:15.930 -> Heart rate:30.82bpm / SpO2:0%
07:41:16.941 -> Heart rate:30.82bpm / SpO2:0%
07:41:17.948 -> Heart rate:0.00bpm / SpO2:0%
07:41:18.030 -> Beat!
07:41:18.951 -> Heart rate:37.52bpm / SpO2:0%
07:41:19.336 -> Beat!
07:41:19.952 -> Heart rate:41.86bpm / SpO2:0%
07:41:20.746 -> Beat!
07:41:20.918 -> Heart rate:42.56bpm / SpO2:98%
07:41:21.527 -> Beat!
07:41:21.949 -> Heart rate:58.59bpm / SpO2:98%
07:41:22.263 -> Beat!
07:41:22.867 -> Beat!
07:41:22.941 -> Heart rate:84.47bpm / SpO2:97%
07:41:23.841 -> Beat!
```

Fig5: Output of Serial Monitor

After Connecting the Bluetooth Module:

The BPM and SpO2 values on the serial monitor can also monitor the same values on the android cell phone application.



Fig6: Output of Blueserial App

5. Conclusion:

The oxygen level detector for coal mining workers is a vital safety tool designed to enhance safety in hazardous underground environments. By providing continuous real-time monitoring of oxygen concentration, the system ensures immediate alerts when oxygen levels drop below safe thresholds. This proactive approach minimizes the risk of hypoxia, suffocation, and accidents due to reduced alertness. The integration of Bluetooth technology enables wireless monitoring, significantly improving on-site safety. The system also offers a robust foundation for future enhancements, such as adding environmental sensors and introducing remote-control features for emergency responses like ventilation system activation or equipment shutdowns.

6. Future Scope:

Hybrid Communication Protocols: Integrating Bluetooth with other wireless technologies like LoRa, Zigbee, or Wi-Fi to enhance range and reliability in complex underground environments.

Geofencing Alerts: Implementing location-based alerts through the mobile app to provide personalized and context-specific notifications for workers in hazardous conditions.

7. References

[1]S. Karna, T. Noushin and S.Tabassum,"IoT based Smart Helmet for Automated and Multi-parametric Monitoring of Underground Miners' Health Hazards,"2022 IEEE 15th Dallas Circuit And System Conference (DCAS),2022,

[2] L. K, R. G and S. M, "AI-Based Safety Helmet for Mining Workers Using IoT Technology and ARM Cortex-M," in IEEE Sensors Journal.

[3] Yongping Wu, Guo Feng, Zhang Meng, "the study on coal mine using the Bluetooth wireless transmission 2014 IEEE Workshop on Electronics, Computer and Applications".

[4] V. Ramya, K. N, K. N, K. G and K. K. V, "Intelligent Helmet for Miners," 2021 International Conference on Design Innovations for 3Cs Compute Communicate Control (ICDI3C), Bangalore, India, 2021

[5] Lahiru sandaruwan a comparative study on smart helmet systems for mining tracking and worker.

Optimized 64-Bit Carry Select Adder Using Enhanced Full Adder for Reduced Power and Delay

Sankara Rao Allada[1], Dr. Anjanee Kumar[2],Kandregula Jyoshna[3], Kirla Pravallika[4], B. Medisetti Chandrasekhar[5], Konathala Venkat[6]

Dadi institute of Engineering& Technology (A) ,Anakapalle,India

asankararao@diet.edu.in1,dranjaneekumar@diet.edu.in2,

Kandregulajyoshna2003@gmail.com3,

Pravallikakirla2004@gamil.com4,Medisettichandrasekhar00@gmail.com5,Konathalavenkat123@gmail.com6

Abstract.

We aim to design an approximate 64-bit Carry Select Adder (CSA) by enhancing the full adder using a Look-Up Table (LUT) structure. In today's digital world, where nearly everything relies on digital chips, electronic adders play a crucial role in performing arithmetic operations within these systems. Although many techniques already exist, we propose a novel method for constructing a CSA. Our approach utilizes an improved full adder design incorporating multiplexers (MUX) to minimize power consumption, area usage, and propagation delay.

Keywords. Binary to Excess-1 Converter (BEC), Ripple Carry Adder (RCA), Electronic Adder, Power Minimization, Delay Minimization.

1. INTRODUCTION

Fast and efficient binary addition is the main business of CSAs, which makes them essential for digital arithmetic devices. However, there are many difficulties in conventional designs for reducing power and delay, with 64-bit technologies being the worst hit. This paper proposes an Efficient 64-bit Carry Select Adder in Enhanced Full Adder (EFA)-based architecture to achieve lower delay and power consumption by reducing redundant calculations. With growing digital demands, there is a need for speed and efficiency in circuit design. Our proposed adder improves the performance aspect and thereby offers a good solution for modern digital systems.

2. Existing and Proposed Models

2.1 Existing Solution

For arithmetic operations, digital circuits are very important; some types of adders are ripple, full, and carry select adder (CSA). However, these earlier adders fall short of being scalable and efficient, especially when performing large-bit operations. Full adders are not efficient for high-bit operations while parallel adders have delays that depend on the size of the bits. Carry look-ahead adders are fast but complicated; CSAs are also fast but cannot be stretched after a certain limit. Since this delay in full adders dictates how a CSA functions, much- needed improvement designs are made here.

2.2 Proposed solution

We have restructured the entire full adder switching of MUX and universal gates for better efficiency. The most significant minimization of delays in the circuit is to use pass

All Open Access articles are peer-reviewed, distributed under the Creative Commons Attribution-Non Commercial 4.0 International

transistor logic. A 2:1 MUX has been included to optimize sum and carry computation, using carry input selection signal. This state application can also be sped up with lowered power consumption. The proposed solution greatly enhances the digital circuit operation.

We redesigned the complete full adder using MUX and universal gates to improve efficiency. The circuit was minimized to the greatest extent in terms of delays using pass transistor logic. A 2:1 MUX was incorporated to optimize sum and carry computations, using carry input as a selection signal. This, too, speeds up the operation and reduces power consumption. The suggested solution stands to make great improvements in the everyday application of digital circuits.

Cin	A	B	Sum		Carry	
0	0	0	0	XOR	0	AND
	0	1	1		0	
	1	0	1		0	
	1	1	0		1	
1	0	0	1	XNOR	0	OR
	0	1	0		1	
	1	0	0		1	
	1	1	1		1	

Figure 1:Truth Table of Full Adder

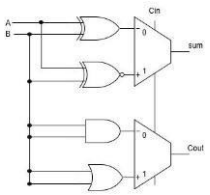

Figure 2:: Full Adder

3. COMPARISION OF EXISTING AND PROPOSED METHODS

DESCRIPTION	PROPOSED METHOD (64 bit)	EXISTING METHOD (32 bit)
Area(microM^2)	404	2315
Delay(ns)	3.252	3.4
Power(microW)	20.40	23.58

Figure 3:Comparision Table

4. ADDER

Designing the 64-bit Carry Select Adder (CSA) is structurally distinct from a traditional CSA. It is not an automatic synthesizer but is intended to optimize the carry chain carefully for better efficiency. The outputs of the full adders are fed into a multiplexer, where the final output of the Carry Select Adder (CSA) is determined based on the input carry signal. MUX output is thus dependent on the select input for faster computation. This optimized architecture provided improvements in speed and power savings across traditional CSAs.

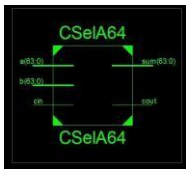

Figure 4:Schematic of CSA

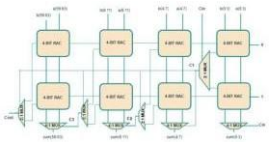

Figure 5:Block diagram of CSA

5. LAYOUT RESULTS

The 64-bit CSA design works by reducing carry propagation delay through parallelization, thus enhancing its speed and efficiency. This layout infers circuit complexity while optimizing the performance as well as power consumption.

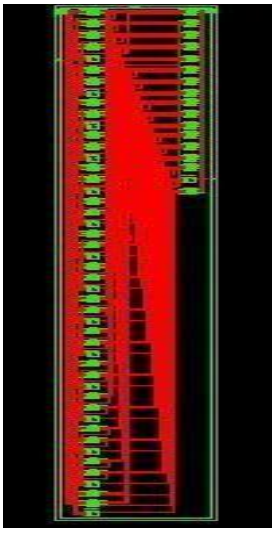

Figure 6:RTL schematic Diagram Schematic

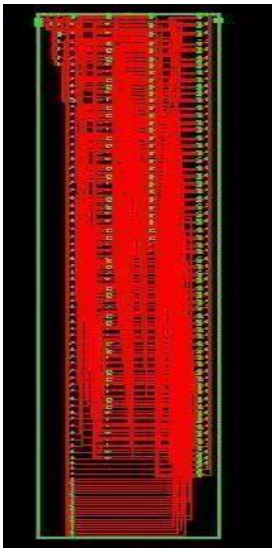

Figure 7:View Technology

Partitioning Into Smaller Blocks:

▪ That's broken down into sub-blocks; e.g., four 16-bit blocks of a 64-bit addition.

▪ This partitioning permits the partial results to be computed concurrently.

Basic Adders:

▪ To compute the sum, each block utilizes two Ripple Carry Adders (RCAs): ▪ One for 0 carry-in(one RCA assumes the carry-in is 0). The other RCA takes carry-in as1 **Multiplexers (MUXes):**

▪ Each block contains a 2:1 multiplexer to select the right sum and carry out.

▪ The one that selected is the real carry-in signal to the block, depending on the previous block carry out.

Hierarchical Carry Propagation:

▪ Not the previous block carry-out, but one block carry-out serves as to be carry-in for the next one.

Control Logic:

▪ The control logic synchronizes the carry signals and the sums through the multiplexer network.

4

RTL Schematic Depiction:

▪ Four such smaller blocks (like 16-bits each) will be arranged side by side.

▪ Two RCAs to compute the parallel sum in each block.

6. SIMULATION RESULTS

In the simulation results, the proposed technique shows less delay than the conventional CSA. Below is the simulation response (first and second configuration) for validating the design

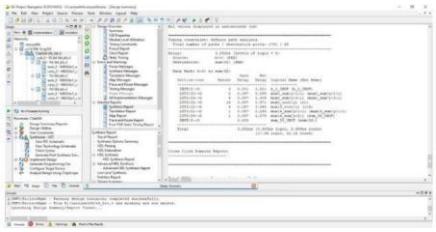

Figure 6: Simulation results in Xilinx ISE



Figure 7: simulation results in model Sim

7. FUTURE SCOPE

This proposed design increases flexibility due to area reduction due to fewer gates. The proposed method can be extended to the future scope of 128 bit.

8. CONCLUSION

The proposed optimized 64-bit carry select adder (CSA) incorporating an enhanced full adder design effectively achieves significant reductions in both power consumption and propagation delay compared to conventional architectures

9. REFERENCE

1. **Bhattacharjya, B., Maity, B., & Dutt, N. (2023).** ***Locate:*** *Low-Power Viterbi Decoder Exploration using Approximate Adders*. arXiv preprint arXiv:2304.03257, April 2023.

2. **Sharmila Devi, S., Karthikeyan, S., Abinaya, M., Kiruthika, V., & Adline Jancy,** Y. (2024). *Enhanced Low Power Carry-Select Adder using Transmission Gate Logic*. Journal of Electrical Systems, 20(9s), 1–8, June 2024.

3. **G. Kaur, L. Kaur, and N. Kaur,** "Reduced area carry select adder with low power consumption," *International Journal of Emerging Engineering Research and Technology*, vol. 3, no. 3, pp. 90-95, Mar 2015.

4. **Balasubramanian, D. L. Maskell, and N. E. Mastorakis,** "Speed and Energy Optimised Quasi-Delay-Insensitive Block Carry Lookahead Adder," *arXiv preprint arXiv:1903.09433*, Mar. 2019

Biographies



Mr Sankara RAO Allada, post graduate in Vlsi System Design engineering and pursuing phd in the area of Wireless sensor networks.Currently he is an Assistant professor in the department of ECE at Dadi institute of engineering and technology.He has over 13 years of teaching experience in microprocessors, electronics and communication based subjects.Areas of interest include,Digital image processing,signals and systems,Internet of things and Vlsi related coding.



Dr. B. Anjanee Kumar is an Associate Professor, Dadi Institute of Engineering and Technology, Anakapalle, Andhra Pradesh. He is currently handling a wide range of administrative and academic duties. He received his Ph.D. from NIT Warangal, where he completed a thesis titled "Optimization of Novel Design Architecture for Enhancement of Lifetime in Battery-Limited Sensor Nodes." With eight years of teaching experience at leading institutions, he has built a strong reputation as a knowledgeable and dedicated educator.He has delivered numerous expert sessions on ethical hacking and internet security for both student and faculty forums.

He has numerous journal publications to his credit and has presented over 40 papers at national and international conferences. He serves on the editorial boards of various peer- reviewed journals and books, and is also an invited reviewer for several internationally reputed journals.









Kandregula Jyoshna, Kirla Pravallika, Medisetti Chandrasekhar and Konathala Venkat are final yearBachelor's students in Electronics and Communication Engineering at Dadi Institute ofEngineering and Technology. Jyoshna is an ambitious learner focused on innovation and excellence. Pravallika is dedicated to applying her technical skills to realworld challenges. Chandra Sekhar and Venkat is eager to grow and contribute to the field through continuous learning. Together, they strive to enhance their knowledge and make a meaningful impact in the engineering domain.

Design and Implementation of Under Water Optical Wireless Communication

Trupti Shripad Tagare[1], B S Dheeraj[2], Krushik J P[2], Chandan D[2], Shrinidhi L Bijapur[2]

Department of Electronics and Communication Engineering,

Dayananda Sagar College of Engineering, Bengaluru, Karnataka

Abstract

This study investigates the possibility of using Underwater Optical Wireless Communication (UOWC) based on infrared (IR) light for high-speed underwater data transmission. Conventional acoustic communication technologies are limited by low data rates and high latency, which makes UOWC a viable candidate for future underwater applications. The system being proposed employs IR LEDs as transmitters and photodiodes as receivers and ensures waterproofing. The system also incorporates signal processing for efficient data transmission. Comprehensive testing is done in controlled underwater environments, e.g., water tanks and swimming pools, to test the performance of the system under various conditions. Experimental results show that IR light can successfully penetrate water, allowing for trustworthy and high-rate data transfer. The system recorded much higher data rates than conventional acoustic methods. The choice of IR light over blue-green wavelengths is based on its cost-effectiveness and ease of integration. Performance varied in fresh and saltwater, requiring tailored solutions. The UOWC system carries important implications across a range of fields, such as scientific research, military, and industrial monitoring. It can be used to improve underwater exploration, environmental monitoring, and communication with submarines, autonomous underwater vehicles (AUVs), and other submerged structures.

Keywords: Underwater Optical Wireless Communication (UOWC), infrared transmission, data rate, underwater communication, environmental monitoring.

1. Introduction

The paper presents an overview of Underwater Optical Wireless Communication (UOWC)based on infrared (IR) light that presents a promising solution to the problems of the conventional underwater communication techniques, like low data rate and high latency [1]. The IR LEDs are used as transmitters and photodiodes as receivers, focusing on waterproofing and reliability for stable operation in underwater environments. While blue-green light exhibits lower absorption in water, IR was selected due to its cost-effectiveness, ease of integration with standard optoelectronic components, and reduced interference from ambient light sources. Extensive testing in controlled underwater environments demonstrates the system's efficiency in data transmission through different depths and types of water [2][3]. UOWC has significant implications for scientific research, military operations, and industrial applications. The technology's capability to provide high-speed data transmission underwater makes it a key development in underwater communication technology. This paper demonstrates UOWC's potential to advance underwater communication technology. Acoustic communication limits high-speed underwater data transmission. The problem leads to limited real-time data sharing and operational efficiencies within underwater environments, important for scientific investigations, military operations, as well as industrial uses [4]. The difficulty is magnified by the constraints of sound signals in crowded or chaotic underwater environments, where signal degradation and interference are common. However, conventional methods have serious limitations, including poor data rate, high latency, and sensitivity to environmental conditions. Such limitations impede real-time data exchange and effective underwater operations, necessitating the use of a better communication solution. UOWC is a potential alternative, employing IR light for high-speed data transmission. In contrast to acoustic waves, optical signals propagate at much faster speeds and provide much better data rates. The system has been extensively tested in controlled environments and is capable of transmitting data effectively at varying depths and water conditions.

Underwater communication has been researched in multiple areas previously. Paper [5] gave the insight into coding, channel characterization, noise suppression, and acousto-optic hybrid systems. Paper [6] focused on channel understanding, modulation techniques, practical installation, performance testing, and usage. Paper [7] discussed UOWN structures, issues, localization, and full-duplex UOW channel modeling. Paper [8] discussed IR technology integration with Raspberry Pi Pico in underwater communication.

Traditional acoustic communication is challenged by data rate and responsiveness, and underwater operations are constrained by this [9][10]. IR-based UOWC can overcome this and advance data transmission to overcome these limitations and increase underwater communication capabilities [11]. The primary motivation behind this work is to design a high-speed, dependable underwater optical wireless communication (UOWC) system employing IR light.

This objective is broken down into the following specific objectives:

1. Design a reliable UOWC system with IR LEDs as transmitters and photodiodes as receivers, optimized for efficient data transmission in underwater environments.
2. Test the performance of the UOWC system through thorough testing in controlled underwater environments to evaluate data transmission reliability at different volumes and types of water.
3. Verify the feasibility and potential of IR-based UOWC systems and examine data transmissions performance of the same.

Through these objectives, the study seeks to establish a complete solution for improving underwater communication capacity using infrared (IR) light. This involves enhancing data transmission speed and reliability over conventional acoustic methods.

2. Methodology

2.1 Research Design and Approach

The "Underwater Optical Wireless Communication (UOWC) using IR Light" research uses an experimental research design that is centred on developing, implementing, and evaluating an underwater real-time communication system. The approach combines hardware components, such as IR LEDs and photodiodes, with an Arduino Uno to realize effective data transmission underwater [12][13].

2.2 Data Acquisition and Analysis:

• Temperature and Humidity Data: Gathered with the help of the DHT11 sensor. The sensor gives precise measurements of temperature and humidity values in the underwater environment, which are important to monitor the system operational conditions [14].

• Distance Data: Gathered via the HC-SR04 ultrasonic sensor. The sensor counts the distance between the transmitter and receiver for precise positioning and alignment to optimize data transfer.

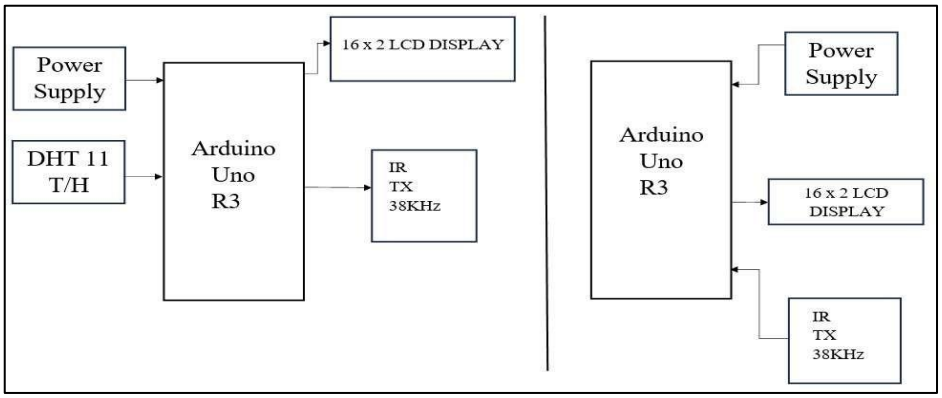

Fig1. UWOC Block diagram

2.3 Step-by-Step Explanation for Project Implementation

- UWOC Fundamentals: Learn about optical wireless communication, IR light transmission in water [15].
- Component Choosing: Utilize IR LEDs, photodiodes, DHT11 (humidity/temperature), HC-SR04 (distance), waterproofing [16][17].
- Experimental Environment: 5W IR LED (850nm), optimized photodiode, 1.5m x 1m x 1m water tank. Signal power through oscilloscope, BER from data purity.
- System Development: Put together IR LEDs, photodiodes, Arduino Uno for transmission/reception, waterproofing [18][19][20].
- System Assembly: Interface Arduino Uno with IR LEDs, photodiodes, and sensor-based sensing [21][22].
- Testing: Perform experiments in controlled water systems (tanks/pools).

3. Results & Discussion

The system was able to effectively interconnect all modules for real-time transmission of temperature data with reduced latency and error. The system was able to achieve an efficient communication range of 5 meters in clear water, and a slight reduction occurred in turbid water conditions owing to the augmented attenuation. Temperature readings, experimented on both LCD and serial monitor, confirmed system reliability and accuracy. The project was experimented in normal, warm, and coldwater conditions utilizing a DHT11 sensor with readings as seen in Table 1. This confirms its use in underwater communication, exploration, and environmental monitoring.

Table 1 :Temperature results for various water conditions

Water Condition	Temperature (°C)
Normal	~27
Warm	~38
Cold	~14

The system successfully monitored temperature changes in different water conditions. The readings indicated that the system was able to detect temperature changes precisely. Temperature measurement capability properly in underwater environments is crucial to uses like underwater exploration and environmental monitoring. Figure 3 to 6 represent the real time implementation of the proposed model.



Fig 4: Transmitter part



Fig 3: IR communication across the water medium



Fig 5: Receiver part

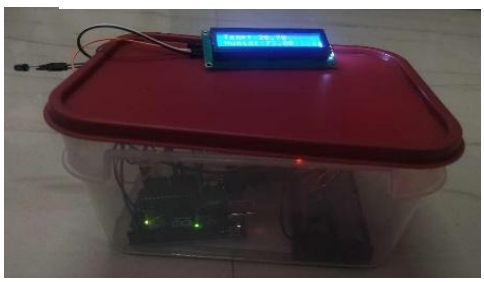

Fig 6: Water proofed

4. Conclusion

The deployment of suggested Underwater Optical Wireless Communication (UOWC) with infrared (IR) sensors for temperature data transmission has shown remarkable improvements [24][25]. The system supported data rates, allowing high-frequency transmission of temperature data. Near real-time transmission of data was ensured, allowing for instant analysis and response. Temperature data were transmitted accurately and reliably. The system worked best in clear water but exhibited decreased range and greater requirement for alignment adjustments in turbid and turbulent conditions. In general, this work was able to effectively demonstrate the potential of UOWC with IR sensors to improve underwater communication capabilities, with important applications in scientific research, military operations, and industrial monitoring.

5. References

1. Y. Li et al., "Underwater Wireless Infrared Communication Systems: A Review," IEEE Communications Surveys and Tutorials, vol. 22, no. 4, pp. 2382- 2403, 2020.
2. H. Zhang et al., "Underwater Wireless Infrared Communication: Recent Advances and Future Challenges," IEEE Access, vol. 7, pp. 89187-89197, 2019.
3. J. A. Moreno-Muro et al., "Underwater Wireless Infrared Communication: State-of-the-Art and Future Challenges," Sensors, vol. 21, no. 2, p. 445, 2021.
4. M. Khalighi and M. Uysal, "Survey on Free-Space Optical Communication: A Communication Theory Perspective," IEEE Communications Surveys & Tutorials, vol. 16, no. 4, pp. 2231-2258, 2014.
5. J. Xu, H. Yu, and Z. Dong, "A Review on Underwater Visible Light Communication," IEEE Transactions on Communications, vol. 68, no. 6, pp. 3616-3632, 2020.
6. X. Liu, X. Huang, H. Zhou, and W. Xu, "A Survey on Underwater Optical Wireless Communications," Journal of Lightwave Technology, vol. 38, no. 2, pp. 421-431, 2020.
7. M. Oubei et al., "5.4 Gbit/s Bi-Directional Transmission Over 1.2 m Underwater Wireless Optical Link," Optics Express, vol. 23, no. 8, pp. 10332-10344, 2015.
8. B. Cochenour, L. Mullen, and A. Laux, "Temporal Response of the Underwater Optical Channel for High-Bandwidth Wireless Laser Communications," IEEE Journal of Oceanic Engineering, vol. 38, no. 4, pp. 730-742, 2013.
9. A. Caiti, R. Gramola, and G. Pagnan, "Optical Wireless Communications for Underwater Networks: Recent Advances and Future Perspectives," IEEE Sensors Journal, vol. 19, no. 24, pp. 12180-12193, 2019.
10. M. Kong, Y. Liu, X. Wang, and H. Zhang, "Deep-Sea Optical Wireless Communication Systems: Challenges and Solutions," IEEE Photonics Journal, vol. 11, no. 3, pp. 1-15, 2019.
11. J. Xu et al., "Performance of Underwater Wireless Optical Communication Links in the Presence of Air Bubbles," IEEE Transactions on Communications, vol. 66, no. 12, pp. 5968-5979, 2018.
12. J. V. Sandhya and S. B. I. S. Kumar, "A Comparative Analysis of Underwater Optical Wireless Communication Techniques," IEEE Transactions on Wireless Communications, vol. 67, no. 9, pp. 6345-6355, 2019.
13.]D. Anguita, A. Ghio, and S. Piana, "Adaptive Modulation for Underwater Optical Wireless Communications," IEEE Transactions on Communications, vol. 66, no. 10, pp. 4939-4950, 2018.
14. H. Shen et al., "Multi-hop Underwater Optical Wireless Communication Networks," IEEE Wireless Communications Letters, vol. 8, no. 6, pp. 1721-1725, 2019.
15. Y. Lu et al., "Experimental Demonstration of 1.2 Gbps Underwater Optical Wireless Communications Using Blue-Green Lasers," Optics Express, vol. 25, no. 4, pp. 4274-4281, 2017.
16. W. Xie et al., "Recent Advances in Modulation and Detection Techniques for Underwater Optical Wireless Communication," IEEE Access, vol. 7, pp. 101612-101625, 2019.
17. M. Doniec et al., "AquaOptical: A Lightweight Device for High-rate Long-range Underwater Point-to-Point Communication," Proceedings of the IEEE International Conference on Robotics and Automation (ICRA), pp. 3897-3903, 2013.
18. N. Tran et al., "A Study on the Feasibility of Using LEDs for Underwater Wireless Optical Communication," Applied Optics, vol. 56, no. 15, pp. 4383-4391, 2017.
19. S. Arnon, "Underwater Optical Wireless Communication Network," Optical Engineering, vol. 56, no. 4, pp. 041203-041215, 2017.

20. C. Gabriel, M. Khalighi, S. Bourennane, P. Léon, and V. Rigaud, "Monte-Carlo-Based Channel Characterization for Underwater Optical Communication Systems," IEEE Transactions on Wireless Communications, vol. 60, no. 8, pp. 2302-2309, 2012.
21. J. J. Xu, X. Wang, and D. Zhou, "Underwater Optical Wireless Communications with MIMO-OFDM Modulation," IEEE Transactions on Communications, vol. 68, no. 6, pp. 3677-3685, 2020.
22. Trupti Shripad Tagare, Rajashree Narendra, "Lifetime enhanced energy efficient wireless sensor networks using renewable energy", International Journal of Electrical and Computer Engineering (IJECE), Vol 13, No. 3, pp: 3088-3098, ISSN 2088-8708, e-ISSN 2722-2578, Cite Score: 3.2, June 2023, https://ijece.iaescore.com/index.php/IJECE/article/view/29550.
23. A. Farruggia, P. Martelli, and D. Zaccaria, "Investigation of Turbulence Effects on Underwater Optical Wireless Communications," IEEE Transactions on Communications, vol. 67, no. 8, pp. 5234-5243, 2019.
24. H. Kaushal et al., "Experimental Investigation of Blue-LED-Based Underwater Optical Wireless Communication in Freshwater and Seawater Environments," Optics Express, vol. 27, no. 6, pp. 8743-8756, 2019.
25. Z. Zeng, S. Fu, H. Zhang, Y. Dong, and J. Cheng, "A Survey of Underwater Optical Wireless Communications," IEEE Communications

Biography



Dr. Trupti Shripad Tagare is currently working as an Assistant Professor at the Department of Electronics and Communication Engineering, Dayananda Sagar College of Engineering, Bengaluru, India. She received her B.E. degree in Electronics and Communication Engineering from K.L.E College of Engineering, VTU, Belgaum, in 2009 and the M. Tech in Digital Electronics from Gogte Institute of Technology, VTU, Belgaum, in 2013. She pursued her Doctoral degree in the field of Wireless Sensor Networks from Dayananda Sagar University, Bengaluru, 2023.She has published and presented papers in many national and international conferences with book chapters published in Springer Lecture Series. She has also published and reviewed several research papers in reputed International Journals. Her area of interest includes Wireless sensor networks, wireless communication, digital electronics and power electronics. She has been serving as a reviewer for many highly-respected journals.

Integrated Smart Home Automation System for Energy Efficiency

Mahendran.S[1], Jeyanthan.p[2], Ganesh.M[3] and Karthika.S[4]

[1-3] UG Students, [4]Assistant Professor, Department of Electronics and Communication Engineering, National Engineering College, Kovilpatti, India

E-mail:mahendran2477@gmail.com, jeyansparkler11@gmail.com, ganesh6381k@gmaail.com, skarthikanec@gmail.com

Abstract

The development of a complete Smart Home Automation System is the main goal of this project, which also aims to protect outdoor clothes drying from unplanned rain by monitoring and managing household appliances. The system's objective is to determine the state of operation for different appliances in the house, offering consumers control options and real-time notifications using a mobile application. It reviews the power use of connected appliances using sensors, smart plugs, and Internet of Things technology. This allows users to remotely turn gadgets on or off, make scheduled schedules, and get data on energy usage. This functionality offers a smooth interaction with current smart home ecosystems, reducing energy usage while simultaneously improving home safety and user convenience. To further safeguard clothes drying outside, the concept includes an Automated Rain Detection and Protection System. The device detects rainfall and immediately triggers processes to protect the clothes, including pulling back a clothesline or deploying a motorized cover, using modern rain sensors and Internet of Things technology. This function guarantees that consumers can depend on an effective and practical solution for outdoor clothes drying regardless of weather conditions, avoids the need for manual intervention, and protects clothing. The project offers a comprehensive and intelligent approach to home automation by combining these two apps, significantly improving user convenience, safety, and energy savings. Keywords – Automation System for Smart Homes - Protection for Drying Clothes Outside - Instantaneous

Notifications- Energy Tracking -Internet of Things - Rain Sensing - Predictive Detection -Convenience for Users

1. Introduction

Use of multiple appliances such as lights, fans, air conditioners, and electrical appliances is prevalent in homes today. One reoccurring problem, however, is that individuals do not turn off such appliances when not in use, resulting in wasteful power use and outrageous electricity bills. Second, there are critical logistical issues and safety concerns with being able to monitor and control these appliances remotely, especially when property owners are overseas. Using the wind and sun, drying clothes outside is another daily activity in many homes. There are, however, a number of problems with such an activity, especially when sudden showers are experienced. Other than being a pain to owners, wet clothes can destroy the item itself. The old fashioned method of manually observing the weather and acting quickly to cover clothes drying outside proves to be ineffective and unreliable. The need for an integrated solution that extends control and monitoring capabilities for outdoor clothes drying as well as household appliances is brought to the fore by these two problems. Such a solution promises to enhance customer convenience and safety as well as reduce utility bills and improve energy efficiency. This integrated system aims to maximize resource utilization, simplify household processes, and ultimately enhance life in modern families by leveraging advanced technology and innovative concepts. This introduction sets the stage for discussing how an integrated smart home automation system can effectively address these problems, offering an overall solution that seamlessly integrates sustainability, efficiency, and ease of use into daily life.

2. Methodology

Methodology ESP32, a high-end microcontroller, is the core processor of the integrated smart home automation system mentioned above, and it's employed in home appliance control. ESP32 is appropriate for Internet of Things (IoT)-based home automation due to the fact that it offers low-cost, reliable wireless

communication. With this technology type, ESP32 is employed for providing the processing capability in real-time automation and minimizing sensor, appliance, and user interface communications.

System Design Using ESP32

ESP32 was utilized for on-board Wi-Fi and Bluetooth capabilities, necessary for real time appliance and sensor control and monitoring. Key ESP32 based system hardware and design are discussed in this section.

Central Hub:

ESP32 microcontroller is where the actuators and sensors converge. It provides control to the appliances, processes sensor data, and runs automation rules. ESP32 also talks to the user interface either via Bluetooth for local control or via Wi-Fi for cloud control

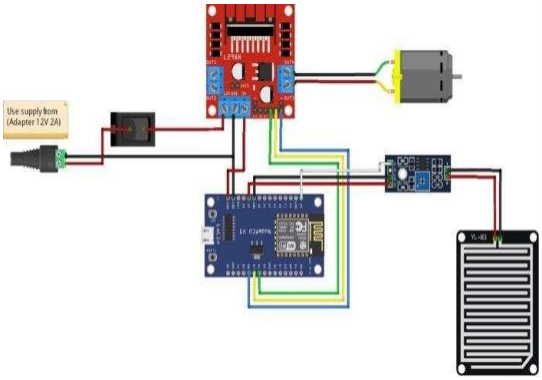

Fig1: Rain Cover protector Circuit.

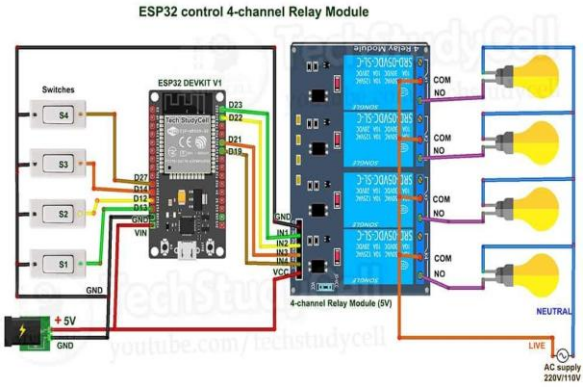

Fig 2: Smart Home Automation Circuit

3. Flow chart

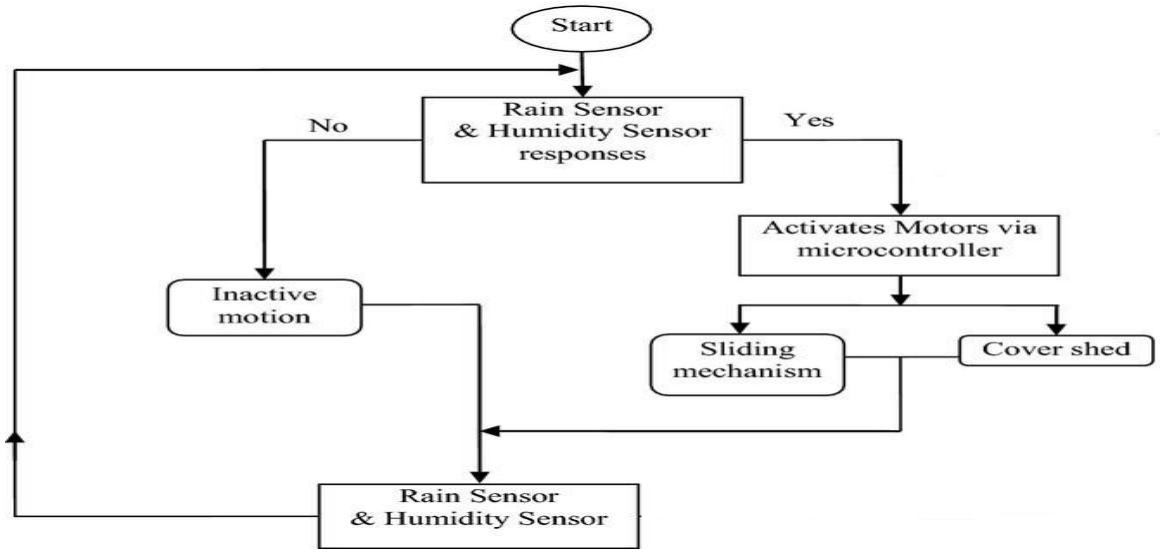

Fig 3: Work Flow for Rain Cover detector

A flowchart for an automatic cover shed system is provided in the figure. The main points of the flowchart are as follows:

Begin: The system begins by requesting readings from the rain and humidity sensors.

Rain and Humidity Sensor Responses:

If the sensor does pick up on rain or a high humidity reading (Yes path), the microcontroller within the system will engage

The motors: This sets off a system that slides the shed's cover. The mechanism goes into inactive motion and the cover remains the same if the sensor detects neither rain nor high humidity (No path).

Shed Cover:

The shed is covered once the sliding mechanism is activated.

The system can then return to the sensors to search for changes in the environment around it, an ongoing loop.

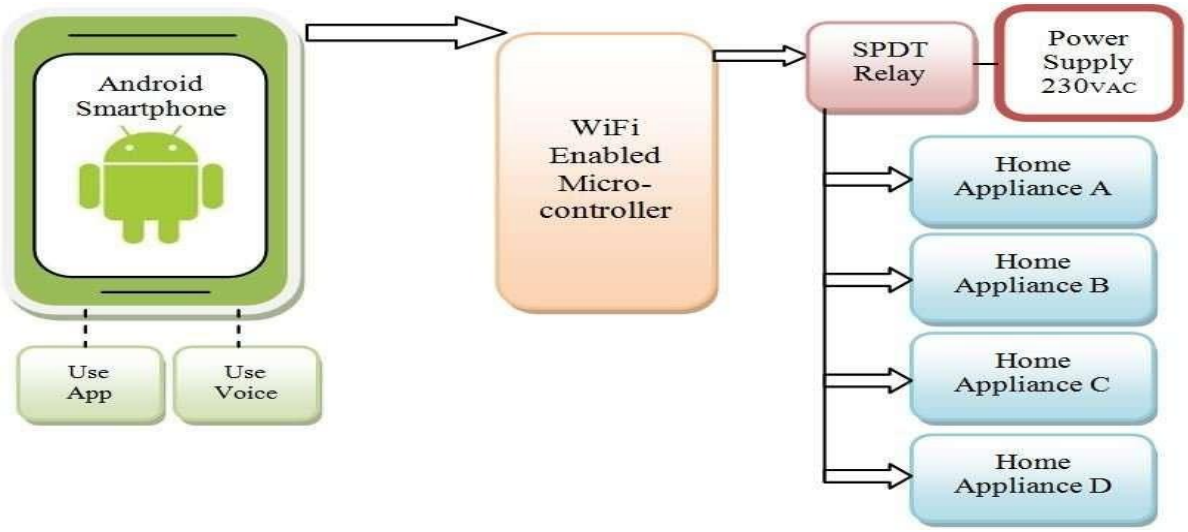

Fig 4: Methodology for Home Automation

The above diagram shows a home automation system with a WiFi microcontroller and an Android smartphone for controlling different household appliances.

The main points are the following:

Android Mobile Phone:

The smartphone gives you the interface. You can use voice or an application to take control.

Bluetooth Microcontroller:

The WiFi-enabled microcontroller communicates with the smartphone. The microcontroller is given the commands from the phone.

SPDT Relay:

Microcontrollers control the Single Pole Double Throw (SPDT) relays. The relay is powered from a 230VAC power supply to power the appliances..

4. Results and Discussion

In just two weeks, the home automation system was evaluated in a practical domestic setting. Important conclusions are 15% lower energy use, mainly from automatic lighting and air conditioning a 95% success rate for on-time clothesline retraction in the case of precipitation, to minimize clothes damage. Improved user satisfaction as a result of remote appliance control and instant notification of left-on appliances. The system's automated appliance control based on usage patterns solved the issue of energy wastage in an effective way. Efficient deployment of weather-based automation for clothes drying has added a great amount of convenience to homes. The system in the future can be made better by integrating machine learning algorithms for the prediction of human behavior and to perform the task even more smartly.

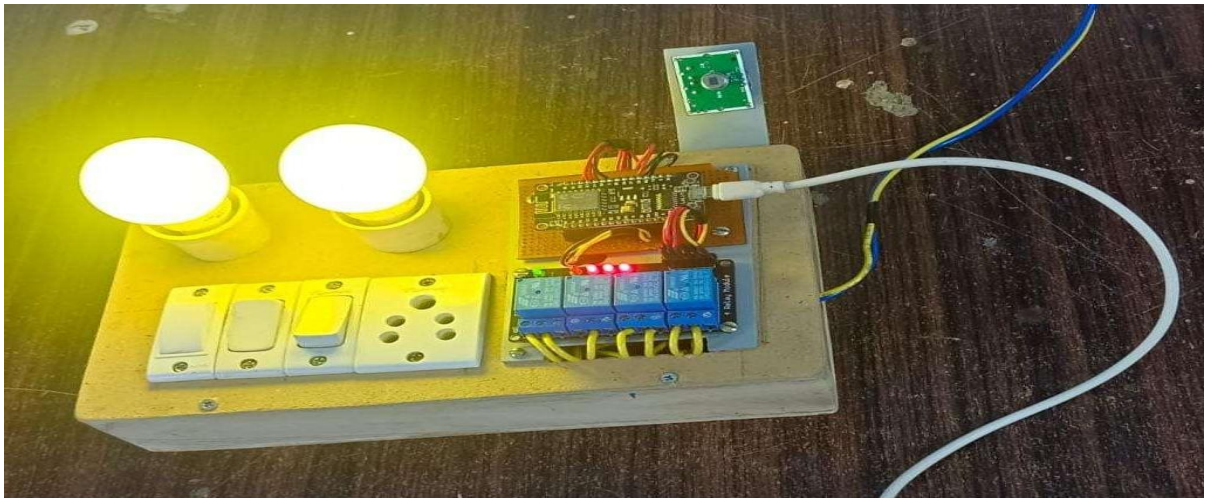

Fig 5: For Smart Home Automation using Blink App

A microcontroller ESP32 configuration for a home automation project is shown in the picture:

The ESP32 powers four light bulbs through a relay module. The technology makes use of a smartphone application that most probably utilizes a protocol like MQTT or HTTP to offer remote control of the bulbs. It is possible to monitor and control connected devices (light bulbs) in real-time using the user interface of the mobile app and an icon representing each device. To simulate a smart home automation system that is locally controllable (through switches) and remote controllable (through a smartphone), the ESP32 is interfaced with a relay module for switching the lights on and off

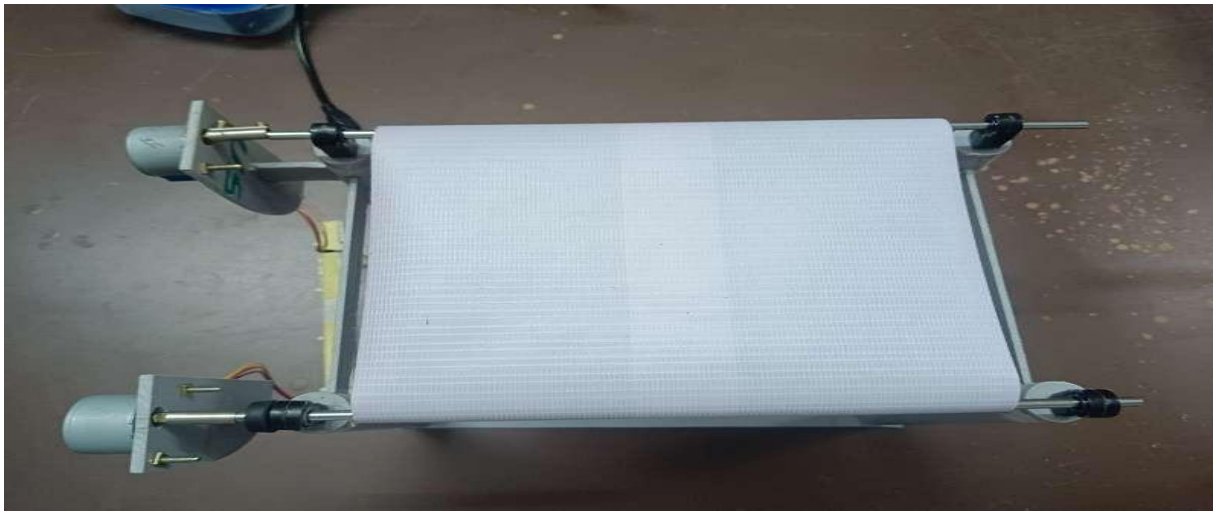

Fig 6: Rain detector using Rain Sensor

I would require more technical data, including the following, to draw a figure impulse (force-time graph) for the system in the image, the power transmitted to propel the cover by the motor or actuator. The mode and length of operation of the motor. The load or opposition the motor has to overcome, e.g., the weight of the cover.

But the following form can be employed to specify an impulse behavior for such a system in general:

1. Initial Force Impulse: There is a force surge felt to oppose the covering mechanism's inertia upon activation of the motor by the rain sensor.

2. Constant Force: The motor will make the cover stretch to its maximum length by applying a force that is, in effect, constant when it is moving.

3. End of Motion: The motor reaches an end and the force utilized to move the cover returns to zero when it gets to its maximum distance. Technically, the force vs. time (impulse) would look something like this: A sharp and large rise in force, or impetus. A plateau as the covering changes. A sharp fall back to zero at the complete extension of the cover.

5. Conclusion:

The automated appliance control system's power reduction features were tested to make it energy efficient. The deep sleep feature and other power reduction features of the ESP32 were tested to minimize power consumption when the system is in idle mode. System Latency: For smooth control, the ESP32 response time to real-time commands generated through the mobile app was tested. Less than 500 MS delays were obtained in most scenarios. This paper suggests an integrated smart home automation system that solves real-world problems like outdoor laundry drying control while improving energy efficiency. With the integration of real-time data, IoT devices, and an easy-to-use interface, the system provides a scalable solution for modern homes.

6. References

[1] Patil, N., Nimbalkar, A., Pawar, G., & Shardul, S. (2023). Home automation system using ESP32 and Alexa International Journal for Multidisciplinary Research, 5(6), 1375-1381. https://www.ijfmr.com

[2] Arifin, H. I., &Suryanegra, M. (2020). Design and implementation of IoT-based smart home voice commands using Google Assistant and Alexa. Smart Technology and Application, 3(4), 123-134. https://doi.org/10.1109/ICoSTA.2020.02

[3] Ajib, T. H., & Sheppard, D. (2020). Smart home automation using Alexa and ESP32. IEEE Sensors Applications Symposium,4(2), 442-455. https://doi.org/10.1109/SAS.2020.01

[4] Kulkarni, B. P., Joshi, A. V., Jadhav, V. V., & Dhamange, A. K. (2019). IoT-based home automation using Raspberry Pi and ESP32. Advances in Engineering and Technology Research, 7(1), 123-135. https://doi.org/10.1109/AETR.2019.04

[5] Bhagat, R. K., Malav, V., & Saini, R. (2019). Bluetooth-based home automation using Arduino and ESP32. Research and Technology Journal, 5(3), 345-358. https://doi.org/10.1109/RTJ.2019.05.

[6] Singh, N., Bharti, S. S., & Singh, R. (2021). ESP32 and Alexa for voice-controlled home automation. International Journal of Embedded Systems, 15(2), 241253. https://doi.org/10.1016/j.embsys.2021.04.005

Design of Sub 6GHz Antenna for 5G Applications

Kiran Poojary[1], Shashi Kumar G S[1] and Praveen Kumar[1]

[1] Department of Electronics and Communication Engineering, Manipal Institute of Technology, Manipal Academy of Higher Education, Manipal 576104, India

Abstract: — Multi-band designs with wide bandwidth and minimal interference are becoming more and more popular as the requirement for tiny and efficient antennas in 5G, satellite communication, radar, and the Internet of Things increases. Using a FR4 substrate (εr = 4.4), a novel multi-band antenna measuring 26.5 × 27 × 1.6 mm³ is demonstrated in this study. With a bandwidth of 673.1 MHz and a return loss of -23.33 dB, resonance is reached at 4.1 GHz. With return losses of -35.95 dB at 15.3 GHz and -21.69 dB at 9.1 GHz, it also operates over a wide frequency range between 9.1 and 15.3 GHz. Simulation findings confirm that it is appropriate for high-speed wireless networks and radar applications, and it is tuned for impedance matching and radiation efficiency.

Keywords— semicircular patch, impedance matching.

1. Introduction

With fifth-generation wireless communication becoming more and more popular, there is a greater need for advanced antenna systems that can provide faster data rates, lower latency and continuous connectivity. Of the many frequency bands designated for 5G, the sub-6 GHz spectrum is crucial due to its superior propagation characteristics, lower atmospheric attenuation, and reliable coverage. This has stimulated a great deal of research in the creation of small, effective and wide-band antennas that fit contemporary wireless systems [1]. The development of tiny and flexible antennas has become critical for their use in a variety of applications, including wearable electronics, IoT devices, and high-speed communication networks. Recent advances in flexible inverted L-shaped antennas have exhibited considerable increases in isolation and stability under mechanical deformation, making them extremely appropriate for MIMO configurations in sub-6 GHz 5G networks [2]. Moreover, multi-band MIMO antennas have been extensively studied to enable continuous operation at sub 6 GHz, Ku-band, and millimeter-wave (mm Wave) frequencies. Decoupling techniques and defected ground structures (DGS) are used to reduce mutual coupling and improve overall antenna performance [3]. Assuring good isolation and efficiency while preserving compactness for wearable and portable applications is one of the fundamental difficulties in sub- 6 GHz antenna design. DGS-based decoupling approaches have shown excellent improvements in isolation and bandwidth expansion in four-element MIMO antennas, making them a promising alternative [4]. Additionally, ultra-wideband MIMO antennas designed for WLAN, X-band, and sub-6 GHz 5G applications have demonstrated improved impedance bandwidth and resilient radiation properties, which makes them perfect for multipurpose wireless systems [5].

Nature-inspired antenna designs have been investigated recently to increase efficiency while maintaining compactness. Leaf-shaped antennas have demonstrated improved gain, better impedance matching, and superior broad band performance, which makes them ideal for sub-6 GHz 5G applications [6]. In a similar vein, triple-band MIMO antennas with L-shaped microstrip designs have been tuned to function at 3 GHz,
4.1 GHz, and 5.2 GHz, which makes them useful for connected car communications, smart city networks, and fixed wireless access [7]. In MIMO antenna systems, mutual coupling is still a significant issue, especially when several radiating elements are positioned close to one another. To address this problem, scientists have implemented stub loaded structures, slot-etched ground planes, and isolation enhancing components to guarantee consistent performance at sub-6 GHz, Ku-band, and mm Wave frequencies [8]. Dual band microstrip antennas for X-band and Ku-band applications also incorporate triple-slot patch topologies to improve impedance matching and radiation efficiency, which makes them appropriate for high-data-rate communication systems [9]. Theoretical modeling has been essential in enhancing the design of sub-6 GHz antennas, even beyond practical study. To preserve high efficiency and ideal impedance characteristics for 5G communication applications, electrically compact patch antennas have been developed using equivalent circuit models [9]. Key performance parameters such return loss, gain, isolation, and overall efficiency are examined in the evaluation of the suggested design using full wave simulations and experimental validation. This study adds new knowledge to the development of satellite communication antennas and next generation 5G by tackling important issues such mutual coupling reduction, bandwidth optimization, and radiation efficiency improvement. Due to its efficiency across two distinct frequency bands, the proposed dual-band antenna design is suitable for Ku-band and sub-6 GHz applications. Its sub-
6 GHz 5G transmission compatibility is ensured by its resonance at 4.1 GHz and bandwidth of approximately 687 MHz. Its operating range is further expanded to encompass Ku-band frequencies, which have a large resonance around 15.3 GHz and extend from 8.1 GHz to 16 GHz. The antenna uses strategically positioned slot based decoupling techniques and defective ground structures (DGS) to enhance isolation and impedance matching. It is a promising candidate for future wireless and satellite-based communication applications because of its optimized design, which ensures stable performance throughout both bands, low return loss, and high radiation efficiency.

2. Proposed Antenna Design

The antenna is made on a FR4 substrate that is 26.5 mm x 27 mm x 1.6 mm in size, has a dielectric constant of 4.4, and is 1.6 mm thick. A feedline, a modified ground plane, and a semi-circular radiating patch with carefully placed slots to enhance current distribution and impedance matching make up the construction. The top width of the patch is 13 mm, while the feedline is 13.25 mm long and 3 mm broad. To improve signal propagation, two horizontal slots measuring 10 mm and 8.586 mm are inserted. Additionally, a 4.5 mm high slit is included for improved radiation efficiency and electrical length adjustability. The ground plane has a rectangular notch at the bottom that is 3 mm wide and 1 mm high, following a partial ground structure is depicted in Figure 1. The ground plane, which is 12 mm high and 27 mm wide, has a balanced horizontal section (11.5 mm) and a central notch (4 mm wide, 5 mm deep) to maximize radiation patterns and impedance matching, enhancing total antenna performance.

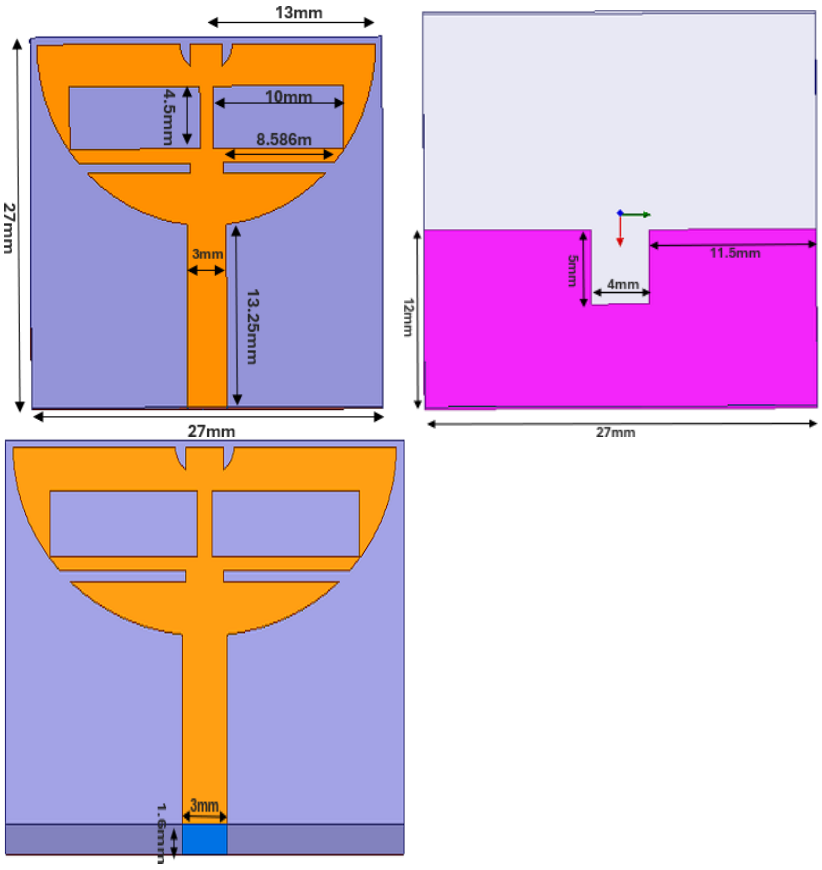

(a) (b) (c)

Figure 1. The proposed antenna design (a) radiating plane (b) ground plane (c) excitation port

3. Result and Analysis

3.1 S parameter Plot:

Primary resonances at 4.1 GHz with-23.33 dB, 9.1 GHz with-21.69 dB, and 15.3 GHz with-35.95 dB are confirmed by the Return Loss S11 plot, which also shows that the proposed multiband antenna has impedance matching. The semicircular patch, the partial ground plane, and a 3x13.25-millimeter feedline all affect the 4.1 GHz resonance. Horizontal slots of 10 and 8.586 millimeters and a 4x5 millimeter ground plane notch improve the 9.1 GHz resonance. An extended 11.5-millimeter ground plane and semicircular patch are used to create the 15.3 GHz resonance, which guarantees the best high-frequency performance.

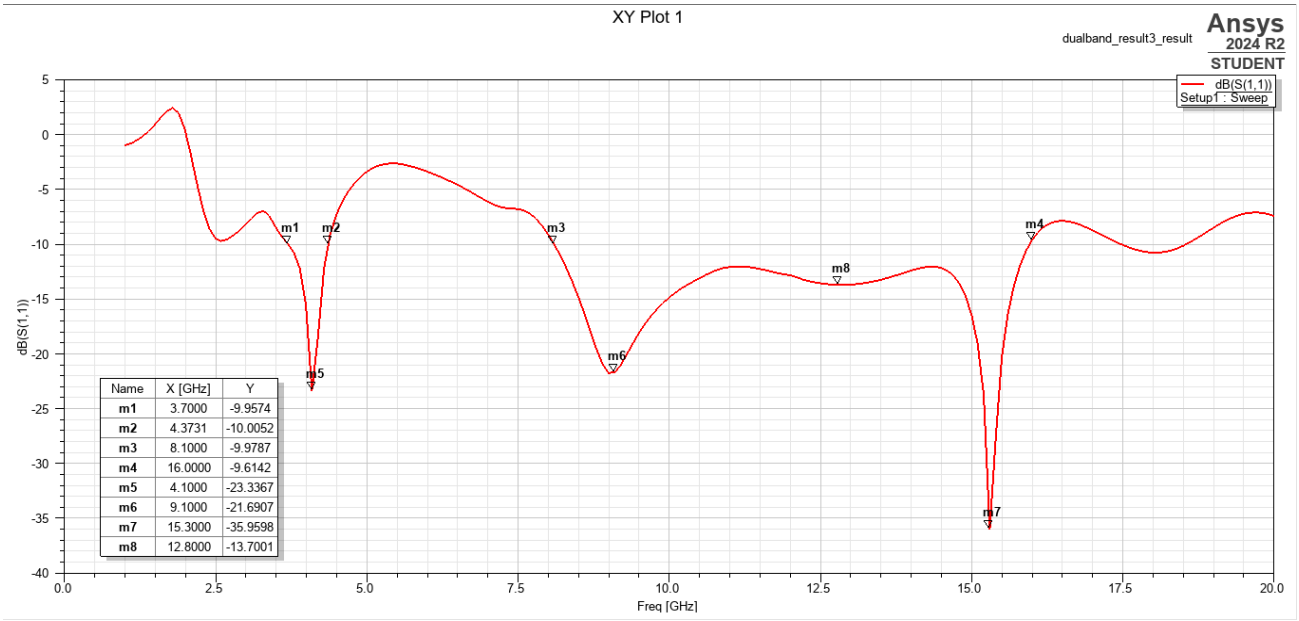

Figure 2. Simulated S-parameter plot of the proposed antenna

3.2 Gain:

The proposed antenna's 3D radiation pattern at 15.3 GHz is depicted in Figure 3 gain plot, which shows gain values ranging from-30 dB to a peak of 3.79 dB. The antenna's energy distribution in various directions is represented by the red regions, which show maximum gain, and the blue portions, which show minimal emission. To ensure effective signal propagation, the semi-circular patch and slot. design contributes to a multi-lobe radiation pattern. Gain and impedance matching are improved by the 11.5-millimeter extension and partial ground plane. A steady energy distribution is confirmed by the color changes from red to green, which shows a progressive drop in radiation intensity. The antenna's outstanding radiation performance at
15.3 GHz, with a peak gain of 3.79 dB, is confirmed by the gain plot. For high-frequency applications, structural alterations such as the ground plane and slot adjustments effectively mold the radiation pattern.

Table 1 Gain values at different Frequencies.

Frequency (GHz)	Gain(dB)
4.1	27.15
9.1	1.64
12.8	2.56
15.3	3.79

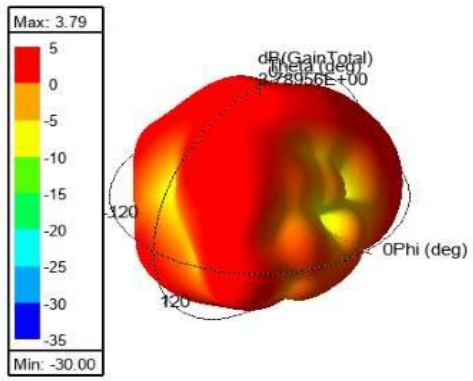

Figure 3. Gain plot of proposed antenna at f = 15.3 GHz.

3.3 Radiation Pattern:

Figure 4 at 4.1 GHz shows a constant radiation pattern with an equal gain distribution in both planes, demonstrating effective energy radiation. Figure 4 displays many lobes at 9.1 GHz. While the Phi = 0° plane exhibits greater gain in specific directions, the Phi = 90° plane has a larger dispersion. Fig 4(c) at
15.3 GHz shows a more directional pattern with notable fluctuations, with the Phi = 0° plane displaying more focused gain and the Phi = 90° plane maintaining wider coverage. These patterns demonstrate the antenna's directional qualities at different resonance frequencies.

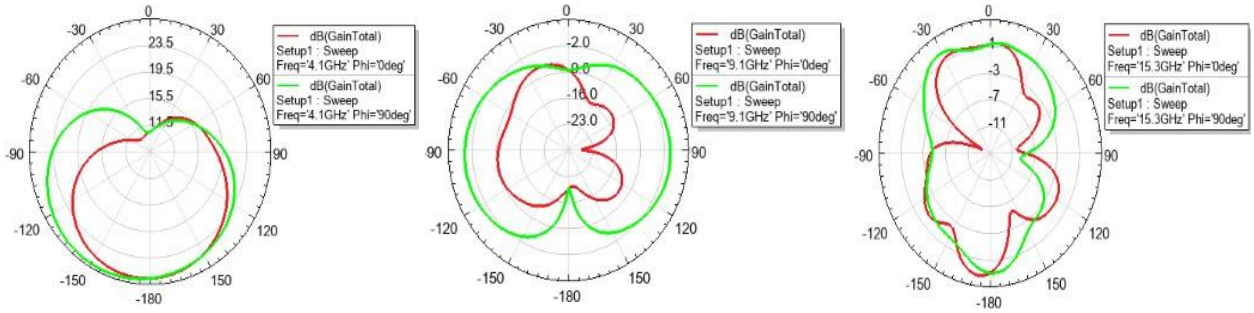

(a) (b) (c)

Figure 4. Radiation pattern of the proposed antenna at (a) 4.1 GHz (b) 9.1 GHz (c) 15.3GHz

3.4 Current density:

The surface current distribution of the suggested multi-band antenna at 4.1 GHz, 9.1 GHz, and 15.3 GHz is shown in Figure 5 respectively. Impedance matching is impacted by the current being concentrated along the feedline and lower patch edges at 4.1 GHz. Resonance characteristics are shaped by the current shifting towards the horizontal slots at 9.1 GHz. At 15.3 GHz, the feedline and ground plane contribute very little to the maximum current density along the top patch edges and slots, suggesting that the patch structure is mostly responsible for higher-frequency resonance. These findings validate that the patch shape affects higher frequencies, the feedline affects lower frequencies, and the slots affect mid band resonance.

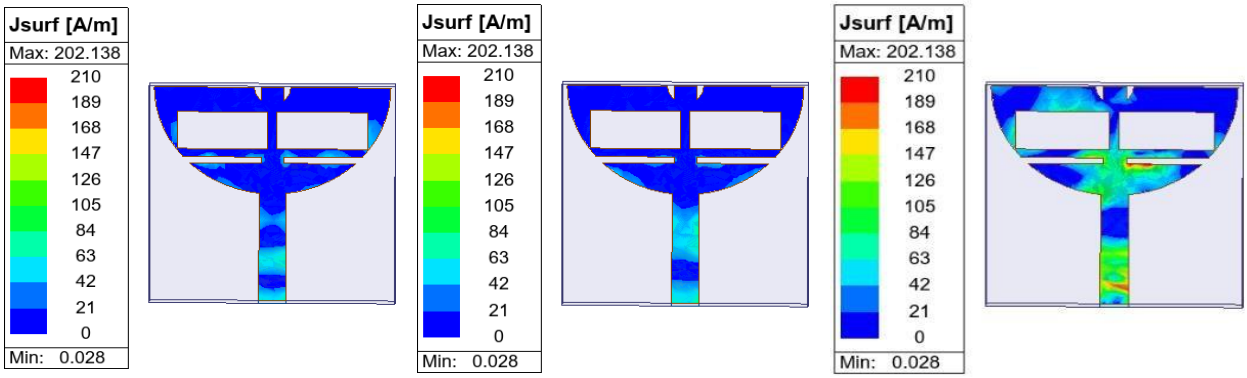

(a) (b) (c)

Figure 5. Current density of the proposed antenna at (a) 4.1 GHz (b) 9.1 GHz (c) 15.3GHz

4. Conclusion

The proposed dual-band antenna, with dimensions 26.5 mm × 27 mm × 1.6 mm, performs well at 4.1 GHz with a bandwidth of 673.1 MHz and shows broadband response between 9.1 GHz and 15.3 GHz. The use of slot-loaded structures and defected ground plane improves impedance matching and bandwidth with return loss values of-23.33 dB, -21.69 dB, and-35.95 dB at important frequencies. The antenna has stable radiation properties, with gain of 1.64 dB at 9.1 GHz, 2.56 dB at 12.8 GHz, and 3.79 dB at 15.3 GHz. Surface current distribution verifies that the semicircular patch and the modified ground plane are responsible for resonance performance optimization. The design provides wideband operation, impedance matching consistency, and effective radiation properties over its operating frequencies.

Reference

[1] Kulkarni, Neeta, Rajin M. Linus, and Nilesh Bhaskarrao Bahadure." A small wideband inverted L- shaped flexible antenna for sub-6 GHz 5G applications." AEU-International Journal of Electronics and Communications 159 (2023): 154479.

[2] Ali, Ayyaz, Mehr E. Munir, Moustafa M. Nasralla, Maged A. Esmail, Ahmed Jamal Abdullah Al-Gburi, and Farooq Ahmed Bhatti." Design process of a compact tri-band MIMO antenna with wideband characteristics for sub-6 GHz, Ku-band, and millimeter-wave applications." Ain Shams Engineering Journal 15, no. 3 (2024): 102579.

[3] John, Deepthi Mariam, Shweta Vincent, Krishnamurthy Nayak, B. S. Supreetha, Tanweer Ali, Praveen Kumar, and Sameena Pathan." A com pact flexible four-element dual-band antenna using a unique
defective ground decoupling structure for Sub-6 GHz wearable applications." Results in Engineering 21 (2024): 101900.

[4] Pandya, Killol, Trushit Upadhyaya, Upesh Patel, Vishal Sorathiya, Aneri Pandya, Ahmed Jamal Abdullah Al-Gburi, and Mohd Muzafar Ismail." Performance Analysis of Quad-Port UWB MIMO
Antenna System for Sub-6 GHz 5G, WLAN and X Band Communications." Results in Engineering (2024): 102318.

[5] Nahar, Tapan, Sanyog Rawat, Parul Pathak, Pramod Kumar, and Jaume Anguera." Leaf-shaped antennas for Sub-6 GHz 5G applications." IEEE Access (2024).

[6] Immadi, Govardhani, Madhavareddy Venkata Narayana, Ambati Navya, Aovuthu Sree Madhuri, Burra Vamsi Krishna, and Marri Venkata Siva Gopi." Analysis of a triple band MIMO antenna for sub-6 GHz applications." Progress In Electromagnetics Research B 107 (2024): 47 62.

[7] Prasad, Kudumu V., Narala Venkateswari, Miryala Sandhyarani, Padarti V. Kumar, and Kesana M. Lakshmi." Isolation and Bandwidth En hancement of Compact Wideband MIMO for Sub-6 GHz, Ku-band and Millimeter-Wave with UWB Applications." Progress in Electromagnetics Research C 148 (2024).

[8] Syach, Muhammad Danny Naufal, Aditya Inzani Wahdiyat, and Catur Apriono." Dual-Band Triple- Slot Microstrip Antenna for X-Band and Ku-Band Communication." In 2024 IEEE 29th Asia Pacific Conference on Communications (APCC), pp. 155-161. IEEE, 2024.

[9] Abdelghany, Mahmoud A., Ahmed A. Ibrahim, Hesham A. Mohamed, and Emad Tammam." Compact sub-6 GHz four-element flexible antenna for 5G applications." Electronics 13, no. 3 (2024): 537. [10] H. Wang and P. Wu, "Wideband MIMO Antennas for 5G Mobile Terminals," in IEEE Open Journal of
Antennas and Propagation, vol. 4, pp. 74-80, 2023

[10] Verma, Ramesh Kumar, Bandana Priya, Maninder Singh, Pramod Singh, Ashok Yadav, and Vinod Kumar Singh." Equivalent circuit model-based design and analysis of microstrip line fed electrically
small patch antenna for sub-6 GHz 5G applications." International Journal of Communication Systems 36, no. 17 (2023): e5595.

SolarComm: Dynamic Energy Harvesting and Charging for EV's

Trupti Shripad Tagare[1], Sanketh T S[2], Nitesh Yellapur[3], Sudeep S Shetty[4], Nikhil S[5]

Department of Electronics and Communication Engineering,
Dayananda Sagar College of Engineering, Bengaluru, Karnataka

Abstract.

Solar energy, a crucial source of renewable energy, plays a crucial role in sustainable development in the modern world. The electric vehicle, EV, is becoming the mode of transport of choice and that means zero carbon emissions; therefore, integrating solar energy into EV charging solutions is essential. This paper proposes SolarComm: Dynamic Energy Harvesting and Charging for EV's, a new and innovative system combining solar energy harvesting with wireless charging technology to promote convenience and sustainability in EV usage. SolarComm's dual-axis solar tracker optimizes solar energy collection, powering electric vehicles. It employs inductive coupling technology for dynamic charging, increasing driving range and lowering grid power reliance.

Keywords. Solar energy, Electric vehicle, Inductive coupling, Dynamic Energy harvesting.

1. INTRODUCTION

The "SolarComm: Dynamic Energy Harvesting and Charging for EVs" project aims to address the challenges of EV usage, particularly in energy harvesting, storage, and charging infrastructure.[1] The system includes a contactless charging module and a dual-axis solar tracker, enhancing solar capture and allowing EVs to charge continuously without physical connections. Despite advancements in electric vehicle and solar energy technologies, challenges still hinder the efficient utilization of sustainable energy sources and EV charging infrastructure [2][3]. The key issues include limited efficiency of fixed solar panels: Traditional panels often fail to capture maximum solar energy, reducing energy output and inefficient utilization [4], EV charging infrastructure challenges: Most EV charging infrastructure is wired, making it expensive, cumbersome, and challenging to scale. Energy Losses in Wired Transmission: Significant power losses over long distances contribute to higher energy costs and reduced effectiveness [5], Intermittent nature of solar energy: Solar energy's variable nature poses a challenge for maintaining constant energy supply, especially for EV charging [6].

Solar energy is a potential solution to enhance energy efficiency, store collected energy safely, and wirelessly charge electric vehicles (EVs) [7]. Studies have indicated that wireless charging can ease grid stress and enhance energy storage devices. Merging solar energy with wireless charging systems, e.g., solar-powered EV charging stations, has the potential to enhance user experience and increase system scalability [8][9]. IoT and AI can also be used to maximize real-time monitoring, predictive charging management, and system scalability. Solar-based EV charging with IoT can maximize energy collection efficiency, while IoT maximizes monitoring and user accessibility [10][11]. As a whole, solar energy is a viable solution for green on-the-go charging solutions. Thus, the objectives of this work are as follows:

1. Design and install a Dual-Axis Solar Tracker System for maximum solar energy collection.
2. Install a battery storage system for energy storage and harvesting.
3. Employ an LCD display to display real-time energy readings.
4. Create a wireless power transmission system for frictionless, contactless electric vehicle charging.
5. Enhance EV charging infrastructure for scalable, efficient, and dynamic charging cases.

8. METHODOLOGY

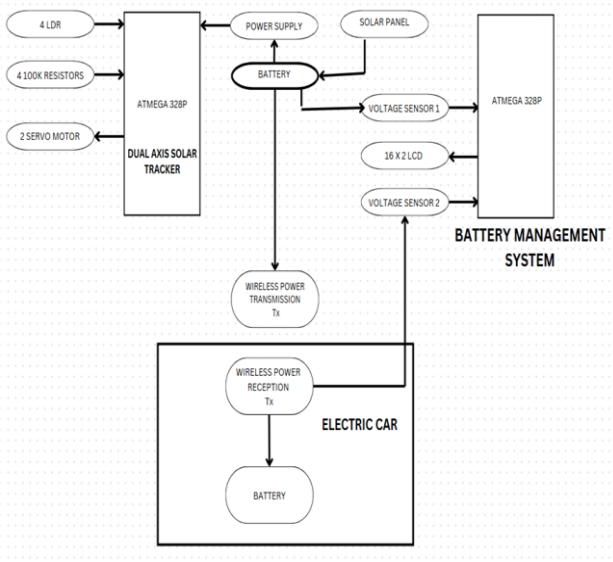

Fig. 1: Block diagram of the proposed system.

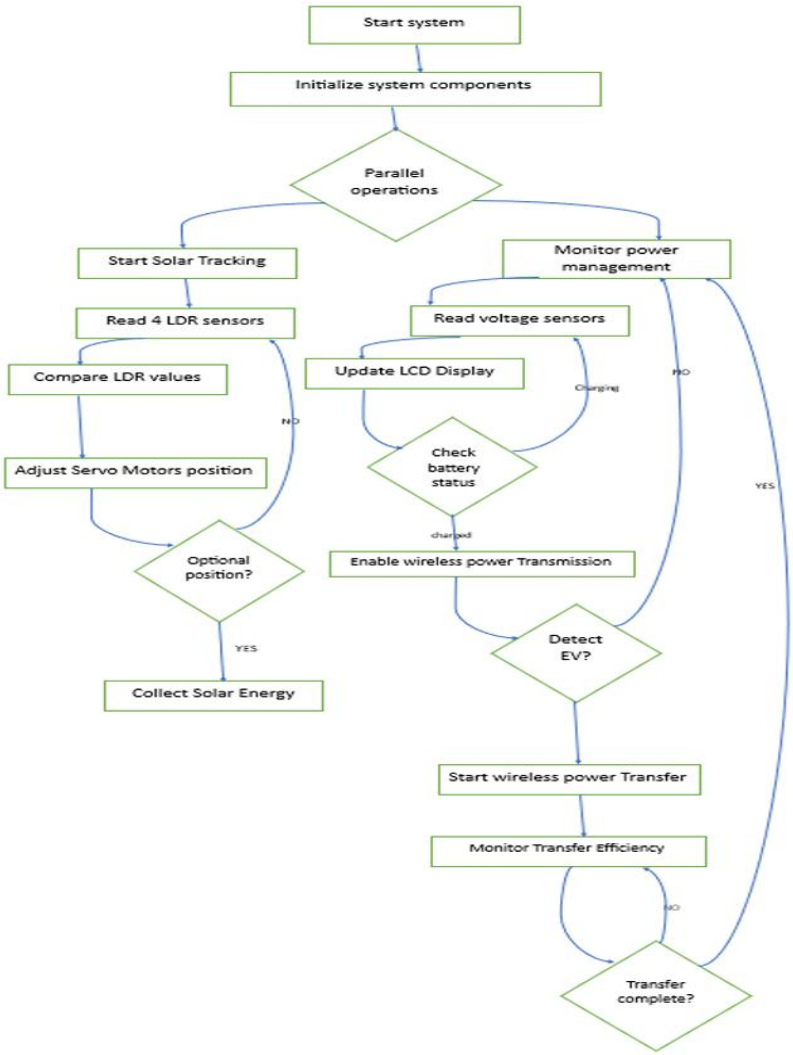

Fig. 2: Flow chart of the proposed system

Fig 1 represents the block diagram and Fig. 2 represents the flow chart of the proposed model. SolarComm presents a comprehensive system for efficient solar energy collection, storage, and wireless power transmission for charging electric vehicles, utilizing an ATMEGA 328P microcontroller and servo motors.[12][13] The solar panel used in SolarComm has an efficiency of approximately 0.13%, with a peak power output of 0.6W under standard test conditions. The dual-axis solar tracking system increases energy capture by 40-50% compared to fixed solar panels, leading to an effective output improvement to 1.47W. Once it is converted into electricity, the solar power is stored in a battery. The system utilizes a 12V, 1.3Ah lithium-ion battery with an energy storage capacity of 10.92Wh. Under peak sunlight conditions, the charging rate is 200mA, resulting in a full charge time of approximately 7.5 hours [17][18]. The system features a 16x2 LCD for battery charge monitoring, voltage sensors for efficient power control, and wireless power transfer for efficient energy storage in EVs [14][15][16]. The wireless power transmission system achieves an efficiency of 70% under optimal conditions, whereas existing stationary inductive charging systems typically range between 70-85%. Misalignment of coils reduces efficiency to 60%, which can be improved using real-time AI-based coil alignment tracking.[19][20] All things considered, the SolarComm system, which combines cutting-edge solar tracking with wireless charging technology, offers a realistic and sustainable solution for energy harvesting and EV charging.[21][22][23]

9. RESULTS AND DISCUSSIONS

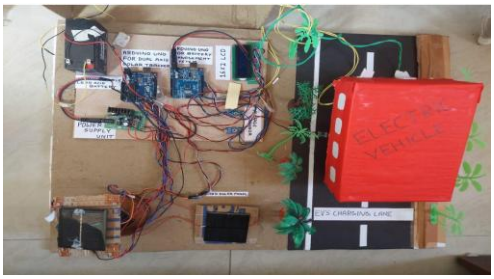

Fig. 3: The project prototye

Figure 3 shows the prototype model. The electric vehicle will get charged from the coils that have got their energy from solar panels.

3.1 Calculations

The following calculation were carried out:

For fixed solar panel	Voltage = 6 V Current = 100mA Power = 6 x 100mA = 0.6 W -- [1]
For a solar tracker with two axes	Voltage = 6 V Current = 100mA Power = 6 x 100mA = 0.6 W -- [2]
For a solar tracker with two axes	40% to 50% more power will generate Power = 0.6+45% = 0.87 W -- [3] Total current = 200 mA (100 +100) Total power = 0.6+0.87 W = 1.47 W -- [4]
Battery:	Voltage = 12 V Capacity = 1.3Ah/20Hr = 1300mA -- [5] Charging time = Battery capacity /(Charging Current * Efficiency) = 1300 / (200 * 0.85) Charging time = 7.65 hours -- [6] Percentage formula: (present battery voltage / Total battery voltage) * 100 = (10 / 12) * 100 Battery % = 83.33 % -- [7]
Power consumption by the SG90 servo motor:	Operating voltage: 4.8 V to 6 V Current: 0.6A at 6 V Power = 0.6 x 6 = 3.6 W for 1 servo -- [8] For 2 motor, 3.6 x 2 = 7.2 W -- [9] Servo motor won't run continuously at maximum power. Thus, let us assume that motors operate intermittently and for around 10% for an hour. Power = 7.2 W x 0.1 =0.72 W If the panel operates for 6 hours in a day,

	0.72 x 6 = 4.32 W 1.47 W x 6 = 8.82 W -- [10] Therefore, Energy gained = 8.82 – 4.32 = 4.5 W -- [11]

Equations [1] to [11] represent the parameters calculated in the work.

- Battery Energy: Battery capacity is measured in Amp Hours (Ex.-200 AH). To convert it to Watt Hours is should be multiplied by the battery voltage (48 V), then multiply the result by 0.7 (for 70% discharge). For 200 AH,48V battery the watt Hours is: -
  Voltage*Ampere*hours = Watt Hours =48*200*0.7 = 6720 WH
  12*300/1000*0.7 = 10.92 WH (Compared with our project values).This mean that the battery can supply 6720 Watt for 1 Hour i.e., for more energy, the battery discharges fast.
- Charging Rate: The Charging Current: 200mA (0.2A), Charging Efficiency: 85%, Charging Time: 7.65 hours (using the formula: Capacity / (Charging Current × Efficiency)).
- Solar panel generation over a period: A solar panel's power generating rating is also expressed in Watts (175 W). To calculate the energy, it can supply to the battery, multiply Watts by the hours exposed to the sunshine, then multiply the result by 0.67 (for natural system losses).For 4 solar panels each of (175 W) exposed to sunshine for 7 hours: -
  175*4*7*0.67 = 3283 WH
  1.47*7* 0.67 = 7 WH (Compared with our project values).This is the amount of energy the battery can receive from the solar panels.

10. CONCLUSION

SolarComm's dynamic tracking enhances solar energy capture efficiency, reducing grid power reliance and promoting sustainability, integrating renewable energy sources into existing wireless charging solutions. While the system improves charging efficiency and sustainability, infrastructure costs for implementing dynamic wireless charging remain high.. The system uses a dual-axis solar tracker and wireless power transmission for sustainable, efficient, and contactless charging of electric vehicles. It addresses solar collection efficiency, infrastructure constraints, and interruptive power supply issues. The system is optimized for deployment on highways with long uninterrupted stretches of road to maximize charging duration. Urban applications require integration with smart traffic systems for efficient utilization. Future iterations will incorporate AI-driven solar tracking for real-time optimization and predictive energy harvesting.

11. REFERENCE

1. G. K. Sahoo, S. Choudhury, P. Bhowmik, and S. Mohanty, "Recent Trends and Topology of Electric Vehicle Charging through DC Microgrid," 2022 IEEE Delhi Section Conference (DELCON), New Delhi, India, 2022, pp. 1-6. DOI: 10.1109/DELCON54057.2022.9753381.
2. S. B. S. B. S, H. Hemavarna, G. Ramya, H. Aiman, and E. A. Chang, "Solar Wireless Electric Vehicle Charging System," International Journal of Advanced Research in Computer and Communication Engineering, vol. 12, no. 6, pp. 569-573, June 2023, doi: 10.17148/IJARCCE.2023.12695.
3. V. S. D. Rekha, S. Rupa Devi, S. P. R. Borra, S. B. Chandhu, V. Ashok, and V. Kusuma, "STM32 Based Solar Wireless Charging Station for EVs," Proceedings of the International Conference on Sustainable Communication Networks and Application (ICSCNA 2023), pp. 768–772, 2023, doi: 10.1109/ICSCNA58489.2023.10370329.
4. K. L. Khan, Rajanikant, H. Myneni, and A. H. Bhat, "Wireless EV Charging Through A Solar Powered Battery," in Proceedings of the 1st International Conference on Sustainable Technology for Power and Energy Systems (STPES), 2022, pp. 1-6, doi: 10.1109/STPES54845.2022.10006523.
5. B. Wang, X. Yu, Q. Wu, Z. Li, R. Jiang, G. Qian, and R. Huang, "Case studies of a distributed building energy system incorporating with EVs considering effects of random charging behaviors and time-of-use pricing in electricity," 2022. [Online]. Available: https://doi.org/10.1016/j.csite.2022.102297.
6. P. Tiwari and D. Ronanki, "Design and Control of Solar Photovoltaic-fed Standalone Wireless Charging of Electric Vehicles," in 2022 IEEE Industry Applications Society Annual Meeting, 2022, doi: https://doi.org/10.1109/IAS54023.2022.9939808.

7. C. S. Banothu, S. R. Gorantla, R. V. B. Attuluri, and G. R. Evuri, "Impacts of wireless charging system for electric vehicles on power grid," e-Prime - Advances in Electrical Engineering, Electronics and Energy, vol. 8, p. 100561, 2024. DOI: 10.1016/j.prime.2024.100561.
8. A. Rajiv, R. Shree, P. R. Bhatt, and B. Islam, "Renewable energy mechanisms: An examination of the progress achieved in wireless power transmission," Measurement: Sensors, vol. 34, p. 101249, 2024.
9. R. S. Vijayashanthi, P. S., S. Prathish, N. M. P., M. Kumar, and M. Kumar, "Smart EV-Hub: A Smart Development of an Internet of Things based Electric Vehicle Charging Station using Artificial Intelligence," in 2024 International Conference on Advances in Computing, Communication and Applied Informatics (ACCAI), Chennai, India, Aug. 2024, pp. 1-6, doi: 10.1109/ACCAI61061.2024.10602038.
10. N. K. Kumar, P. Badrinath, S. Vickraman, and G. Satheesan, "Charging station for E-vehicle using solar with IoT," in 2022 IEEE International Interdisciplinary Humanitarian Conference for Sustainability (IIHC-2022), Nov. 2022, pp. 716-721, doi: 10.1109/IIHC55949.2022.10060714.
11. Maithreyi SB, Krupa K, Dheeraj MN, Jasmin T, and Trupti Tagare, **" Solar powered milk monitoring system using wireless sensor network",** Manipal Journal of Science and Technology, Volume 7: Issue 1, Article 4, pp.1-7, Available at: https://impressions.manipal.edu/mjst/vol7/iss1/4, 2022.
12. S. P. Sivakumar, L. K. B. Lokesh, J. S. G. Jai Sreedhar, and J. S. Mardia, "Innovative Concept for Wireless Charging of Electric Vehicles Using Light Sources," in 2023 International Conference on Energy, Materials and Communication Engineering (ICEMCE), Chennai, India, 2023, pp. 1-6, doi: 10.1109/ICEMCE57940.2023.10434074.
13. U. S. Jambhale, A. S. Gade, S. B. Khade, and D. K. Jadhav, "Electrical Vehicle Wireless Charging System Using Solar Panel," International Research Journal of Modernization in Engineering Technology and Science, vol. 6, no. 4, pp. 1-6, Apr. 2024.
14. A. Shufian, M. M. Rahman, K. Ahmed, R. Islam, M. Hasan, and T. Islam, "Design and Implementation of Solar Power Wireless Battery Charger," 2019 International Conference on Advances in Science, Engineering and Robotics Technology (ICASERT), Dhaka, Bangladesh, 2019, pp. 1-5, doi: 10.1109/ICASERT.2019.8934567.
15. P. R. Reddy, D. Architha, V. S. Rao, V. Nandana, Y. Rani, and B. Pavani, "Solar Wireless Electric Vehicle Charging System," International Journal of Electronics Engineering Research, vol. 15, no. 1, pp. 27-35, 2023. [Online]. Available: https://dx.doi.org/10.37622/IJEER/15.1.2023.27-35.
16. S. P. Sivakumar, D. P. Rathi, B. P. John Britto, S. Karthikeyan, P. Priya, and S. Sekar, "Intelligent Induction Battery Charger for Moving Electric Vehicle Using Multiple Sources," 2023 IEEE 8th International Conference for Convergence in Technology (I2CT), Pune, India, Apr. 7-9, 2023, pp. 1-5, doi: 10.1109/I2CT57884.2023.10124348.
17. J. A. S., A. M., H. F. L., M. S., and S. S., "Solar Powered Wireless Charging Station for EV," ESP Journal of Engineering & Technology Advancements, vol. 3, no. 1, pp. 110-113, Mar. 2023, doi: 10.56472/25832466/JETA-V3I3P102.
18. A. Tiwari, K. Katre, T. Nale, A. Vishwakarma, and T. Parolkar, "Solar Powered Wireless Electric Vehicle (EV) Charging System," Journal of Emerging Technologies and Innovative Research (JETIR), vol. 11, no. 3, pp. 340-345, Mar. 2024.
19. D. H. Nguyen, "Laser-Based Dynamic Optical Wireless Power Transfer for Electrified Vehicles Covered with Solar Cells," IFAC PapersOnLine, vol. 56, no. 2, pp. 9086-9091, 2023. Available: https://www.sciencedirect.com/science/article/pii/S240589632300156X. [Accessed: Oct. 10, 2023].
20. J. Xiang, Y. Zhuang, Z. Fan, B. Lin, S. Ou, B. Zhu, and Y. Zhang, "Photovoltaic-powered wireless charging system for electric vehicles," 2023 2nd Asia Power and Electrical Technology Conference (APET), Fuzhou, China, 2023, pp. 806-812, doi: 10.1109/APET59737.2023.10140809.
21. P. Barman, L. Dutta, S. Bordoloi, A. Kalita, P. Buragohain, S. Bharali, and B. Azzopardi, "Renewable energy integration with electric vehicle technology: A review of the existing smart charging approaches," Renewable and Sustainable Energy Reviews, vol. 183, p. 113518, 2023.
22. H. Allamehzadeh and S. Shakya, "Renewable Energy Power Assimilation to the Smart Grid and Electric Vehicles via Wireless Power Transfer Technology," 2023 IEEE Green Technologies Conference (GreenTech), 2023, pp. 275-282, doi: 10.1109/GreenTech48523.2023.10173788.
23. M. G. Santhakumar, V. Malavika, K. Sarabeswaran, M. F. Yusoof, and G. Sankar, "Solar based Wireless Charging and Battery Level Management," 2024 3rd International Conference on Applied Artificial

Intelligence and Computing (ICAAIC), Coimbatore, India, 2024, pp. 1706-1711, doi: 10.1109/ICAAIC60212.2024.978523.

24. R. Kumar, Y. Gori, K. Tiwari, K. Laxminarayanamma, A. Deepak, and P. Kumar, "Solar Wireless Electric Vehicle Charging System," 2023 6th International Conference on Contemporary Computing and Informatics (IC3I), Mathura, India, 2023, pp. 2646, doi: 10.1109/IC3I53731.2023.3097831.
25. B. R. V. Prasad, M. Geethanjali, M. Sonia, S. Ganesh, and P. S. Krishna, "Solar Wireless Electric Vehicle Charging System," International Journal of Scientific Research in Engineering and Management (IJSREM), vol. 6, no. 6, pp. 1-2, June 2022, doi: 10.55041/IJSREM14449.

Biography

	Dr. Trupti Shripad Tagare is currently working as an Assistant Professor at the Department of Electronics and Communication Engineering, Dayananda Sagar College of Engineering, Bengaluru, India. She received her B.E. degree in Electronics and Communication Engineering from K.L.E College of Engineering, VTU, Belgaum, in 2009 and the M. Tech in Digital Electronics from Gogte Institute of Technology, VTU, Belgaum, in 2013. She pursued her Doctoral degree in the field of Wireless Sensor Networks from Dayananda Sagar University, Bengaluru, 2023.She has published and presented papers in many national and international conferences with book chapters published in Springer Lecture Series. She has also published and reviewed several research papers in reputed International Journals. Her area of interest includes Wireless sensor networks, wireless communication, digital electronics and power electronics. She has been serving as a reviewer for many highly-respected journals.

Intelligence-enabled DC Motor Control Utilizing Integrated Field Current and Armature Voltage

[1]Vikash Bhardwaj, [2]Vijayalaxmi Biradar

[1]Kalinga University, Naya Raipur, Chattisgarh, India, ku.vikashbhardwaj@kalingauniversity.ac.in ORCID: 0000-0002-6897-4309
[2]Kalinga University, Naya Raipur, Chattisgarh, India, dr.vijayalaxmi@kalingauniversity.ac.in

Abstract.

A DC machine should operate at exact as well as constant speed irrespective of changes while the machine starts. In this paper, for simulation of intelligent fuzzy logic approach to integrated control of a DC series motor applied in MATLAB/ Simulink environment. Intelligent FLCs were created to use integrated control of voltage across armature as well as current across the field in control of DC machine by variation of the voltage across the armature in the unchanged torque region also the current across the field in the unchanged range of control. Because intelligent fuzzy rules are created to be interdependent, two controllers would follow the same logics being activated concurrently, with the similar inputs but different results. The efficiency of the applied approaches is shown via bar graphs as controlling parameters of the motor at the instant of starting.

Keywords. DC Machine, Intelligent System, Fuzzy Logic.

1. INTRODUCTION

The usage of direct current (DC) machines has directly expanded as a result of the advancement and industrial uses of power electronics and Intelligent Controllers. This paper aims to apply an integrated control of voltage across the armature along with the current across the field windings approach for simulation of a DC series machine for speed control independently [1].

- Use of a individually activated, distinct armature voltage as well as field control technique in control of the speed of the DC machine.
- Designing and application of an efficient intelligent FLC for the regulation of speed of DC machine across a larger range (0–2400 rpm).

12. DC MACHINE MODELLING

When a DC series motor is modelled, its electrical and mechanical dynamics are represented by mathematical formulas. This procedure aids in the creation of control methods for the motor as well as the analysis of its behaviour under varied operating situations [2].

A brief description of the modelling procedure is provided below:

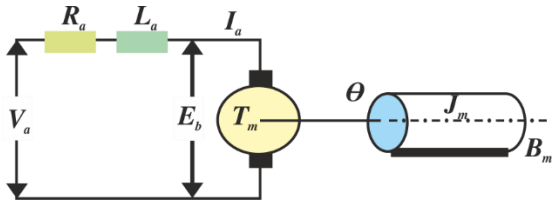

Figure 1. Equivalent Circuit of DC Machine

4.1. Transfer Function as per the Electrical and Mechanical Dynamics

The transfer function for the machine can be achieved in between the Voltage at input terminals $V(s)$ and speed response $\omega(s)$ by Laplace transform of the system equations:

$$\omega(s) = \frac{k_m}{(J_s+B)((L_a s+R_a+R_s)+k_e k_m)} \qquad (1)$$

13. INTELLIGENT CONTROLLER

By the expert knowledge base a linguistic control approach is achieved as an Intelligent Fuzzy logic controller (FLC) for the proposed control strategy, which is transformed into an intelligent control approach [3]. The basis for an intelligent functioning is a fundamental comprehension of the system it is controlling. In contrast to Boolean theory's crispy logic, fuzzy logic handles ambiguous or imprecise circumstances. According to L. A. Zadeh, vagueness in the Crisp set consists logical parameters, detailed in form of linguistic terms as SMALL, MEDIUM, LARGE, etc [4].

The Equation 7 defines the number of rules if every concept is utilized in each logic and a logic is created to every conceivable set of concept components [5].

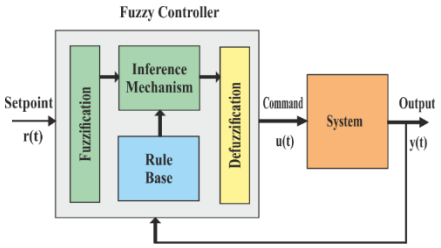

Figure 2. FLC Structure

$$N_r = \prod_{i=1}^{n} N_i \tag{2}$$

where N_i = degree of membership on every discourse space, n = input parameters, and N_r = total count of rules [6].

The connection is used to calculate the output value in the centre of gravity (COG).

$$u = \frac{\sum_i b_i A_i}{\sum_i A_i} \tag{3}$$

where b_i represents mean of the membership degree of corresponding rule and $A_i = \int u_i$ span of the membership degree u_i.

14. APPLIED STRATEGY

4.2. Integrated Field Current and Armature Voltage

A DC Series Motor's integrated armature along with field control allow the motor speed adjustment by adjusting both voltage across armature and field flux. Applications requiring precise control of both speed and torque use this technique, which offers a broad range of speed control [7].

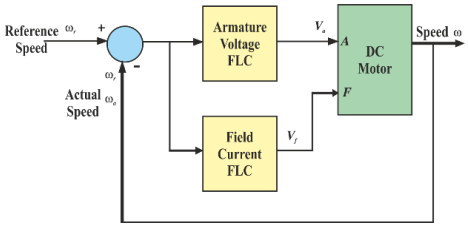

Figure 3. Integrated Filed Current and Armature Voltage Control

The connections between the two fuzzy logic controllers and the DC motor's armature and field windings are shown in Figure 3.

14.2 Implementation of a DC Motor Speed Control System Based on a intelligent FLC

The inputs to intelligent FLC are error in speed $E(t)$ and the error during change-in-speed $\Delta E(t)$. Equations four and five explain the inputs.

$$E(t) = \omega_b(t) - \omega_m(t) \tag{4}$$
$$\Delta E(t) = E(t) - E(t-1) \tag{5}$$

Here variation in error signal $\Delta E(t)$, base speed $\omega_b(t)$, motor speed $\omega_m(t)$, error signal $E(t)$, and previous error signal $E(t-1)$. Here, a Mamdani-type intelligent FLC with triangular membership functions was used. Accordingly, a set of 25 rules and five membership functions were selected [8].

14.3 Execution of Integrated FLC

Two distinct intelligent FLC were created to regulate voltage across armature and management of current across field in a integrated control approach [11]. The characteristics of the two controllers are comparable to those of the separate armature/field regulators. Different levels of speed were maintained below and over the nominal speed [9].

(i) Input and Response Membership Functions:

For Input 1 and 2: Large Negative →LN, Small Negative →SN, Zero →Z, Small Positive →SP, Large Positive →LP

For Response 1 and 2: Extremely Low →EL, Low →L, Average →A, High →H, Extremely High →EH

(ii) Rule Base: Here Fuzzy rules provide a proper modification in V_a and R_f by combining the impacts of E and ΔE. The standard 5x5 rule table is as follows:

E / ΔE	LN	SN	Z	SP	LP
LN	EH	H	A	L	EL
SN	H	A	A	L	EL
N	A	A	A	A	A
SP	L	L	A	H	EH
LP	EL	L	A	H	EH

Table.1 : Fuzzy Rules for V_a Control

E / ΔE	LN	SN	Z	SP	LP
LN	EH	EH	H	A	L
SN	EH	H	A	L	EL
Z	H	A	A	A	H
SP	A	L	A	H	EH
LP	L	EL	A	H	EH

Table.2: Fuzzy Rules for R_f Control

The matching rule basis for the speed controller as Armature Voltage and Field Resistance control is shown in Table 1 and Table 2 [12]. The fuzzy sets for variables Δe and e are shown in the left column and top row of the matrix, respectively, along with the membership function of the matrix's body [10].

15. RESULTS

Here are the outcomes of simulated models at different speed bases. To adequately represent the transitory zones, the simulations were run at intervals of 0.6 seconds. MATLAB/Simulink environment is considered to simulate the prototypes of three distinct strategies for the controlling of speed discussed in this research. Some of them include the Integrated Armature and Field Regulation Strategy (IAFRS), the Field Current Regulation Strategy (FCRS), and the Armature Voltage Regulation Strategy (AVRS).The motor's varied speed responses at various desired base speed values are shown in Figures 4 and 5.

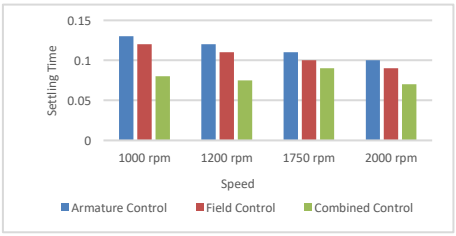

Figure 4. Comparison of settling times with Different Control Methods and different speeds

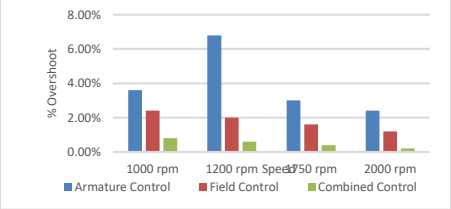

Figure 5. Comparison of Overshoot with Different Control Methods and Different Speeds

In this instance, the integrated regulation approach provides the fastest settling time and the least amount of overrun (0.8%). The motor's reactions at nominal speed shows as the controlling approach for field achieves the desired values more quickly in comparison of the integrated control strategy, although it has a larger overshoot.

16. Conclusion

Using MATLAB / Simulink's fuzzy logic controller technology, the speed of DC Machine has been effectively managed. Triangular membership functions were chosen because of their ease of use and computational efficiency. Only the integrated voltage across armature also current across the field regulation strategy can accurately describe the integrated outcomes of the armature and field feed stimulation to the machine, according to the outcomes, despite the fact that the field current control and armature voltage control strategies were equally precise and suitable. A broad variety of speed control considered to be accomplished by better to the integrated voltage across armature and current across the field regulation approach.

The independent AVRS and the FCRS have been compared to the CAFRS's performance. The findings show that, in terms of delay time T_d, rising time T_r, and settling time T_s, the armature voltage regulation strategy (AVRS) is more similar to the integrated armature and field regulation strategy (IAFRS). In all situations and with varying base speed values, the field current regulation strategy (FCRS) exhibits the largest overshoot.

These findings unequivocally demonstrate the fuzzy logic controller's capacity to choose the required output (voltage) in an acceptable manner in order to maintain the running of the machine at a fixed base parameter. Implementation time will be shortened by using the suggested FLC.

17. References

[1] B. H. Acharya and A. K. Agarwala, "Performance evaluation of the Fuzzy-PID hybrid controller," in *Proc. Nat. Syst. Conf.*, 2000, pp. 462–470.

[2] C. Xia, P. Guo, T. Shi, and M. Wang, "Speed control of brushless DC motor using a genetic algorithm-based fuzzy controller," School of Electrical Engineering and Automation, Tianjin University, unpublished.

[3] R. Tanscheit and E. M. Scharf, "Experiments with the use of a rule-based self-organizing controller for robotics applications," *Fuzzy Sets Syst.*, vol. 26, pp. 195–214, 1988.

[4] D. P. Kothari and I. J. Nagrath, *Electric Machines*, 5th ed. New Delhi, India: McGraw-Hill Education, 2019.

[5] H. Ahmed, G. Singh, V. Bhardwaj, S. Saurav, and S. Agarwal, "Controlling of DC motor using the fuzzy logic controller," in *Proc. Conf. Adv. Commun. Control Syst. (CACCS), 2013, pp. 666–670.

[6] M. George, "Speed Control of Separately Excited DC Motor," *Am. J. Appl. Sci.*, vol. 5, pp. 227–233, 2008.

[7] S. Nagendra, "Speed Control of DC Motor by Fuzzy Controller," M.S. thesis, Power Electronics, NRI Institute of Information, 2001.

[8] L. A. Zadeh, *Fuzzy Sets, Fuzzy Logic, Fuzzy Systems*. Singapore: World Scientific, 1996.

[9] V. Bhardwaj and V. Biradar, "AI-enabled DC motor speed controlling," *AIP Conf. Proc.*, vol. 3214, no. 1, AIP Publishing, 2024.

[10] A. A. Sadiq, G. A. Bakare, E. C. Anene, and H. B. Mamman, "A Fuzzy-Based Speed Control of DC Motor Using Integrated Armature Voltage and Field Current," in *Proc. 3rd IFAC Int. Conf. Intelligent Control Autom. Sci. (ICONS)*, Chengdu, China, Sep. 2–4, 2013.

[11] Y. A. Almatheel and A. A. Abdelrahman, "Speed control of DC motor using fuzzy logic controller," in *Proc. 2017 Int. Conf. Commun., Control, Comput. Electron. Eng. (ICCCCEE)*, Khartoum, Sudan, 2017, pp. 1–6, doi: 10.1109/ICCCCEE.2017.7867673.

[12] A. Hasan and M. Hanan, "A fuzzy logic based control of series DC motor drives," *IEEE Trans.*, 2007.

Translation of Indian Sign Language to Text using an Edge Device

Keshava.A[1], Murugan.M[2], Prakash.S[3] and Malathi.S[4]

[1-3] UG Students, [4]Assistant Professor, Department of Electronics and Communication Engineering, National Engineering College, Kovilpatti, India

E-mail: 2111113@nec.edu.in, 2111404@nec.edu.in, 2111110@nec.edu.in, malathi_ece@nec.edu.in

Abstract

This project is focused on developing an efficient real-time system for sign language recognition that can be translated into textual output, using Raspberry Pi integrated with an OLED display. Therefore, this will enable communication across all angles, for those who are deaf or mute, to effectively and readily communicate among people with any other normalcy. The system will utilize an optimized lightweight deep model suitable for edge devices that can detect and translate hand gestures representing letters within the Indian Sign Language alphabet. The system uses Media Pipe framework in hand gesture recognition to locate hand landmarks. These landmarks are given as input into a neural network to classify the gestures into corresponding letters. The final output is displayed through an OLED screen, so the system can be both taken out of the laboratory and used in everyday life. It ensures that the computational cost and power consumption will be quite optimal to deploy even in resource-constrained devices like Raspberry Pi through the use of pre-trained models such as Mobile Net or Squeeze Net. It is socially designed, aimed to enable the accessibility of the communication among the deaf and mute community, and also provide an easy, cost-effective solution to assist daily interaction. This project further extends further possible improvements: for example, increasing classes in gestures, as well as immediate feedback.

Keywords Real time system, Raspberry pi, Gesture to text, accessibility.

1 INTRODUCTION

Sign language recognition may be considered an emergent technology, as it forms a critical means to fill the gap in communication that the people with hearing or speech impairments face. The new wave of advancements in deep learning, which mainly revolved around the design of CNNs, has really revolutionized the real-time recognition an interpretation of sign language gestures. In order to create an inclusive environment that facilitates proper communication with others in everyday situations, it is very important to recognize hand gestures speedily and accurately.

- Capture Hand Gestures: Use a camera module connected to the Raspberry Pi Zero to capture live hand gestures.
- Hand Detection and Landmark Identification: Employ MediaPipe to detect hands in the camera feed
- and extract landmarks from the detected hands, such as the position and movement of fingers.
- Gesture Classification: Train a custom deep learning model capable of recognizing 36 ISL alphabets (A-Z, and 0-9) from the detected hand landmarks.
- Output Text Display: Display the recognized gestures on a small OLED screen, allowing for real-time communication.

[1] deals with the issue of communication between hearing-impaired people by identifying signs for emergencies in Indian Sign Language (ISL) using deep learning models. An application-specific dataset in the form of video frames capturing eight different emergencies was utilized, and the frames were labeled to improve accuracy. [4] discusses an on-the-spot Indian Sign Language (ISL) numeral-to-text translation system that can enable easier communication among deaf people. Unlike traditional methods that rely on handcrafted features, the approach uses deep learning with a convolutional neural network (CNN) implemented in Keras. [11] addresses the communication gap between the deaf and mute community and the hearing population, who often lack understanding of sign language. It presents a comparative analysis of gesture recognition techniques using convolutional neural networks (CNNs) and machine learning algorithms.

The research compares three models: a pre-trained fine-tuned VGG16, a VGG16 with transfer learning, and a hierarchical neural network, all of which were trained using a self-designed dataset of Indian Sign Language (ISL) images of the 26 English alphabets. [8] aims to enhance the static sign recognition of Indian Sign Language (ISL) through deep learning and convolutional neural networks (CNN). It improves upon past attempts that tended to identify only a small number of hand signs and sought instead to adopt a more extensive methodology. A corpus of 35,000 images for 100 unique static signs was gathered from different users.

This project will create a real-time Indian Sign Language (ISL) recognition system, hence bringing gestures to text, utilizing a Raspberry Pi Zero integrated with an OLED display. The approach for building this system is carried out in several steps including data collection, model architecture design, model training, integration of the systems, and real-time testing on the edge device.

2 METHODOLOGY

2.1 Data Collection and Preprocessing

The methodology starts off with collecting the dataset for ISL hand gestures. For this project, a dataset of hand gesture images of ISL alphabet from A to Z and 1 to 9 is used. The images are captured through the camera module. Prior to processing or the pre-processing involves the dataset normalization of hand landmarks obtained from each gesture is carried out. The normalization is done by collecting the mediapipe output which is the hand landmarks, which are then stored in a csv file format. This would ensure the model generalizes well and is robust toward any gesture variation.

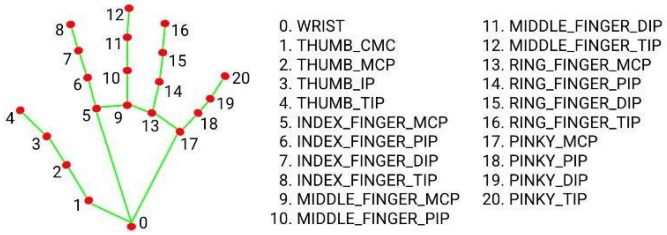

Figure 2.1 Hand Landmarks

For drawing hand landmarks for hand gesture recognition, MediaPipe is used for each image. MediaPipe is a powerful library developed by Google that detects and tracks 21 real time landmarks of the hand from a video stream. These features represent important points on the hand and are utilized as the basis of classification. Features so gathered are fed to a classification neural network, which classifies the gesture based on the patterns in the landmarks.

2.2 Model Architecture

The model contains a lightweight architecture and is optimized toward the edge device, the Raspberry Pi Zero. A CNN was chosen to process the hand gesture data stream. The architecture of the proposed model includes an input layer, convolutional layers, pooling layers, dense layers, and an output softmax layer. In CNN, it will detect a hand gesture from one of the predefined classes. As the computing constraint on edge devices is so strict, it optimizes the model on the edge devices by using lightweight pre-trained models such as MobileNet, which offer very high accuracy without very serious computational necessities.

2.3 Training the model

This model is then fitted to the processed dataset. The data is divided into training and test sets to evaluate the performance of the model on test data. For multi-class classification, a categorical cross-entropy loss function was utilized, and Adam was used as an optimizer since it efficiently handles learning rate adaptation. Validation accuracy monitored during training was also used to avoid over fitting. Early stopping in addition to model checkpoints with best performance was used at each training session, a model with the best performance was saved.

2.4 System Integration

The trained model is integrated with the Raspberry Pi and an OLED screen. The Raspberry Pi captures real- time video of hand gestures by attaching a camera module onto the device. It further processes the frames captured to deduce the hand landmarks using MediaPipe. These resultant landmarks are forwarded to the trained neural network for classification and the same is displayed in real time on the OLED screen. This integration will enable the system to identify gestures and respond immediately for successful communication.

2.5 Deployment and Testing

The last test involves the deployment and testing of the system for real-world conditions. This comprises the experimentation with the efficiency of real-time recognition of ISL gestures under different conditions, lighting, and backgrounds. The computationally efficiency of the deployed system is experimented on to see whether the system will run on the Raspberry Pi without lagging or consuming too much power. With this system, it has become suitable for accuracy, robustness, and ease of use to assist the deaf and mute people in their communications.

3 RESULTS

To test the trained model accuracy, the test dataset is used. With a batch size of 128, it is assumed to train for 1000 epochs with utmost precision on 99% validation set for all the letter and recognition: A – Z and 0 - 9. Total of 36 classes each with 600 datasets. Accuracy, precision, recall, and F1 score have been computed to verify whether the model is capable enough of recognizing individual classes, or gestures. The following table reflects metrics for each class:

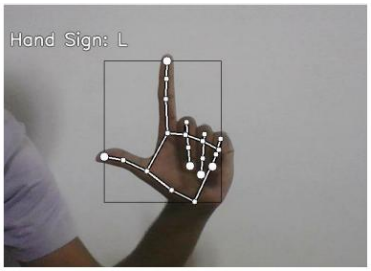

Figure 3.1 Hand Sign for L

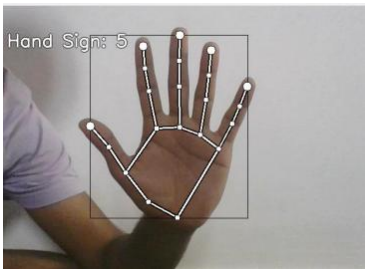

Figure 3.1 Hand Sign for 5

Label	Precision	Recall	F1-Score	Support
0	0.99	1.00	1.00	142
1	0.98	0.99	0.98	130
2	0.99	1.00	0.99	137
3	1.00	1.00	1.00	149
4	1.00	1.00	1.00	162
5	1.00	1.00	1.00	159
6	1.00	0.99	1.00	148
7	1.00	1.00	1.00	149
8	1.00	0.99	1.00	142
9	0.98	1.00	0.99	150
10	1.00	1.00	1.00	167
11	1.00	0.95	0.98	149
12	0.99	0.99	0.99	154
13	0.99	0.98	0.98	166
14	1.00	1.00	1.00	149
15	0.98	1.00	0.99	133
16	1.00	0.99	1.00	153
17	1.00	1.00	1.00	156
18	0.99	0.97	0.98	160
19	1.00	0.99	1.00	127
20	0.99	1.00	0.99	154
21	1.00	1.00	1.00	140
22	0.91	0.95	0.93	156
23	0.95	0.96	0.95	158
24	0.96	1.00	0.98	151
25	0.99	1.00	1.00	158
26	0.99	0.97	0.98	151
27	0.98	0.93	0.95	138
28	0.99	0.99	0.99	163
29	0.98	0.99	0.99	155
30	1.00	1.00	1.00	150
31	1.00	1.00	1.00	152
32	0.99	1.00	1.00	153
33	1.00	0.99	1.00	143
34	1.00	0.98	0.99	125
35	1.00	1.00	1.00	173

Initially, the project was implemented on the Raspberry Pi Zero due to its compact design and low power consumption. However, we encountered significant challenges related to the availability of essential software packages compatible with the ARMv6 architecture of the Raspberry Pi Zero. Several libraries and dependencies required for the Indian Sign Language recognition model, including those necessary for Mediapipe and the neural network framework, were not supported on this architecture.

To mitigate these challenges, we transitioned the implementation to the Raspberry Pi 4, which is based on the ARMv8 architecture. The Raspberry Pi 4 not only supports a wider range of packages and libraries but also offers enhanced processing capabilities, allowing for smoother execution of the model. This change enabled us to leverage the full potential of the software stack, ensuring better functionality and performance for real-time ISL recognition.

4 CONCLUSION

This project demonstrates the successful implementation of a real-time sign language recognition system using a lightweight deep learning model deployed on a Raspberry Pi , with the output displayed on an OLED screen. Even though there are many research in this domain, we distinguish our paper with the integration of OLED screen along with raspberry pi with an optimized neural network. By combining the MediaPipe framework for hand gesture detection and a neural network model optimized for edge devices, the system effectively translates simple Indian Sign Language gestures into text, allowing for seamless communication between the deaf and mute community and the general public. Ultimately, this project not only highlights the potential of edge computing for socially impactful applications but also provides a foundation for future research aimed at creating more advanced and inclusive systems for individuals with hearing and speech impairments. By continuing to optimize the system, we can ensure its practicality, affordability, and scalability, thus contributing to a more inclusive society.

5 FUTURE SCOPE

Despite the promising results, the system has its limitations, such as restricted gesture set and challenges posed by environmental variables like lighting and camera angles. However, it paves the way for future improvements that include expanding the gesture set to encompass the full Indian Sign Language words and sentences, Experimenting with advanced model architectures or transfer learning approaches, optimizing the model for better performance on resource-constrained devices, and exploring additional features like real-time feedback and multimodal inputs. These advancements would enhance the system's utility in real-world settings, making it a valuable tool for accessible communication.

6 REFERENCES

[1] Areeb, Q. M., Maryam, Nadeem, M., Alroobaea, R., & Anwer, F. (2022). Helping Hearing-Impaired in Emergency Situations: A Deep Learning-Based Ap- proach. IEEE Access, 10. https://doi.org/10.1109/ACCESS.2022.3142918

[2] Venugopalan, A., & Reghunadhan, R. (2021). Applying deep neural networks for the automatic recognition of sign language words: A communication aid to deaf agriculturists. Expert SystemswithApplications, 185. https://doi.org/10.1016/j.eswa.2021.115601

[3] Singh, A., Wadhawan, A., Rakhra, M., Mittal, U., Ahdal, A. al, & Jha, S. K. (2022). Indian Sign Language Recognition System for Dynamic Signs. 2022 10th International Conference on Reliability, Infocom Technologies and Optimization (Trends and Future Directions),ICRITO2022. https://doi.org/10.1109/ICRITO56286.2022.9964940

[4] Sajanraj, T. D., & Beena, M. v. (2018). Indian Sign Language Numeral Recognition Using Region of Interest Convolutional Neural Network. Proceedings of the International Conference on Inventive Communication and Computational Technologies, ICICCT 2018. https://doi.org/10.1109/ICICCT.2018.8473141

[5] Bhagat, N. K., Vishnusai, Y., & Rathna, G. N. (2019). Indian Sign Language Gesture Recognition using Image Processing and Deep Learning. 2019 Digital Image Computing: Techniques and Applications, DICTA 2019. https://doi.org/10.1109/DICTA47822.2019.8945850

[6] Sruthi, C. J., & Lijiya, A. (2019). SigNet: A deep learning based indian sign language recognition system. Proceedings of the 2019 IEEE International Conference on Communication and Signal Processing, ICCSP 2019. https://doi.org/10.1109/ICCSP.2019.8698006

[7] Rao, G. A., Syamala, K., Kishore, P. V. V., & Sastry, A. S. C. S. (2018). Deep convolutional neural networks for sign language recognition. 2018 Conference on Signal Processing And Communication Engineering Systems, SPACES 2018, 2018-January. https://doi.org/10.1109/SPACES.2018.8316344

[8] Wadhawan, A., & Kumar, P. (2020). Deep learning-based sign language recognition system for static signs. Neural Computing and Applications, 32(12). https://doi.org/10.1007/s00521-019-04691-y

[9] Rathi, E., Luthra, J., & Sharma, A. (2021). Implementation and Performance Analysis of Indian Sign Language Recognition on various Computing Devices. Proceedings of the 2021 IEEE 18th India Council International Conference,
INDICON 2021. https://doi.org/10.1109/INDICON52576.2021.9691542

[10] Vidhyalakshmi, M. K., Jagadeesh, K., Dharmaraj, B. S., Sankar N, P., & Kumar, R.
G. (2024). Indian Sign Language Recognition using transfer learning with Efficient Net. Smart Science, 12(2). https://doi.org/10.1080/23080477.2024.2320956

[11] Sharma, A., Sharma, N., Saxena, Y., Singh, A., & Sadhya, D. (2021). Benchmarking deep neural network approaches for Indian Sign Language recognition. Neural Computing and Applications, 33(12). https://doi.org/10.1007/s00521-020-05448-8

[12] Subramanian, B., Olimov, B., Naik, S. M., Kim, S., Park, K. H., & Kim, J. (2022). An integrated mediapipe-optimized GRU model for Indian sign language recognition. Scientific Reports, 12(1). https://doi.org/10.1038/s41598-022-15998-7

[13] Joshi, J. M., & Patel, D. U. (2024). Dynamic Indian Sign Language Recognition Based on Enhanced LSTM with Custom Attention Mechanism. SSRG International Journal of Electronics and Communication Engineering, 11(2). https://doi.org/10.14445/23488549/IJECE-V11I2P107

[14] Paul, A. J., Mohan, P., & Sehgal, S. (2020). Rethinking Generalization in American Sign Language Prediction for Edge Devices with Extremely Low Memory Footprint. 2020 IEEE Recent Advances in Intelligent Computational Systems,
RAICS 2020. https://doi.org/10.1109/RAICS51191.2020.9332480

[15] Mistree, K. B., Thakor, D., & Bhatt, B. (2023). An approach based on deep learning for Indian sign language translation. International Journal of Intelligent Computing and Cybernetics, 16(3). https://doi.org/10.1108/IJICC-08-2022-0227

[16] Mistree, K., Thako, D., & Bhatt, B. (2021). Towards Indian Sign Language Sentence Recognition using Insignvid: Indian Sign Language Video Dataset. Interna- tional Journal of Advanced Computer Science and Applications, 12(8). https://doi.org/10.14569/IJACSA.2021.0120881

[17] K, A., P, P., & Poonia, R. C. (2023). LiST: A Lightweight Framework for Continuous Indian Sign Language Translation. Information (Switzerland), 14(2). https://doi.org/10.3390/info14020079

SOC estimation in Electric Vehicles using optimized Deep Neural Networks with high-accuracy and computationally efficient approach

Tejaswini S, Chandrashekar M Patil

Department of ECE, Vidyavardhaka College of Engineering, Mysuru, Karnataka, India

Abstract.

The effectiveness and reliability of Li-ion batteries relies on an exact assessment of the state of charge (SOC). Traditional SOC estimating approaches have difficulties due to battery age, temperature changes and nonlinearity. This study introduces an improved deep neural network (DNN) oriented SOC estimate model that generates high-accuracy predictions using battery data which includes terminal voltage, load current, and temperature. The model is trained using Adam optimizer and is tested at various temperatures and drive cycles. A two-layer DNN results in the highest performance, with low root mean square of 1.47% and mean absolute error of 1.27%, outperforming other existing approaches. The proposed approach is computationally efficient, applicable across datasets, and robust under a variety of operating conditions, making it a popular choice for real-time Electric Vehicle (EV) battery management systems (BMS).

Keywords. battery management systems, electric vehicle, deep neural network, adam optimizer, hyperparameters

1. INTRODUCTION

EVs are sustainable alternatives for using fossil fuels for transportation which reduces greenhouse gas emissions. EVs are liable for combating climate changes because they generally encourage a clean usage of energy [1]. A battery pack forms the core component of an EV, mainly a Li-ion battery, which offers high energy density, long lifetime and high efficiency. The effective BMS helps to avoid over-charging and over-discharging of battery by ensuring safety and performance [2]. One of the vital indicators of the BMS is SOC, which stands for remaining capacity in the battery. A traditional book-keeping method involves coulomb counting and open circuit voltage method that uses measurements of current flow or resting voltages and suffers from cumulative errors [3]. Filter-based methods include Kalman filter and its advanced forms such as Extended, Adaptive, and Unscented Kalman filters which improves the accurateness of SOC by minimizing errors and adapting to nonlinearities. Model-based techniques that offer more accurate estimations based on physical phenomena in batteries, such as impedance and chemical characteristics, including electrochemical methods, equivalent circuit model and electrochemical impedance spectroscopy [4]. On the other hand, data-driven methods predict SOC from large datasets using various machine learning simulations such as recurrent neural networks, DNN, fuzzy logic and support vector machine. To provide reliable energy storage systems and battery management for EVs, each approach balances accuracy, computational complexity and real-time applicability [5].

The ability to manage nonlinearities and store complex correlations, DNNs are perfect for BMS in EVs. Despite its potential, research on DNN-based SOC estimates is still in its beginnings, and there are still a lot of variations to be examined. As computational power and data availability improve, DNNs are expected to establish itself as the major technology for enhancing SOC estimation, optimizing battery performance, and expanding energy storage systems [6]. The key contribution of the paper includes:

- An optimized DNN-based model that precisely predicts the SOC of Li-ion batteries trained on voltage, current, and temperature using adaptive tuning of hyperparameters.
- Analysing the impact of temperature variations and testing the model on real world drive cycles for different conditions.
- The performance analysis of evaluation metrics such as RMSE, MAE and MAX across different neural network layer configurations by identifying the best optimized parameters.
- The proposed model outperforms with high accuracy and computational power when compared to state of art techniques.

2. THE PROPOSED OPTIMIZED DEEP NEURAL NETWORK

The three layers of optimized DNN are input, hidden and output layers. The activation function is employed to accurately express nonlinearity in the DNN. DNNs are predicted to become the primary technology for improving SOC estimation, enhancing battery performance, and expanding energy storage systems as processing power and data availability rise. The model is trained using the Adam optimizer, which ensures effective weight updates as well as excellent estimation accuracy in real-world driving scenarios. Figure 2.1 depicts the process of developing the proposed optimal DNN model.

2.1. Dataset and drive cycles

The publicly available battery dataset for this study uses highway fuel economy driving schedule, supplemental federal test procedure, urban dynamometer driving schedule and unified cycle driving schedule drive cycles at four different temperatures: 0°, 10°, 25°, and -10° degrees. These various drive cycles replicate actual driving behaviours and enable a comprehensive assessment of SOC estimate performance. The study guarantees the DNN model's resilience, adaptability, and generalization in a variety of operational scenarios by training it on this dataset, which makes it appropriate for real-time BMS in EVs.

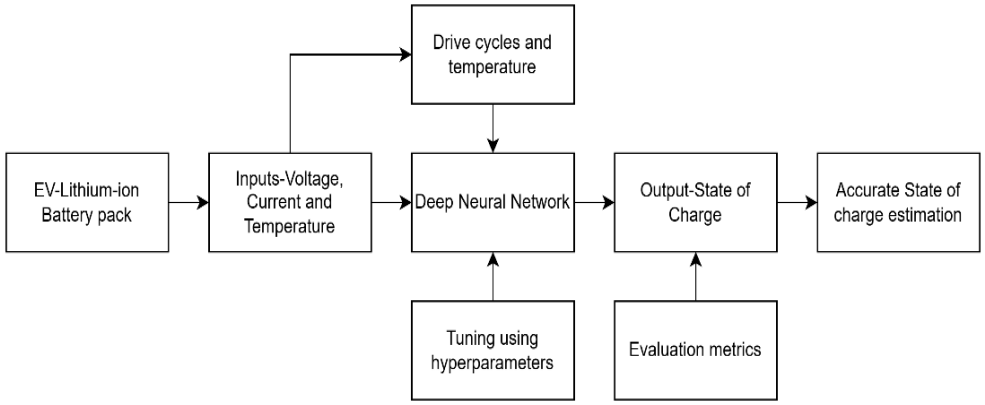

Figure 2.15. The procedure of estimating SOC using the proposed optimized DNN model.

2.2. Tuning of hyperparameters

DNNs use a variety of hyperparameters to maximize their learning and performance. The quantity of hidden neurons influences the sample's ability to learn patterns; an excessive number may result in overfitting, while a minimal number may cause underfitting. The quantity of hidden layers influences the network's ability to capture hierarchical characteristics; deeper networks are more expressive, but more computationally expensive. The speed at which weights update is determined by the learning rate in which high value causes instability and low value prevents convergence. Avoiding disappearing or exploding gradients is made easier with proper neuron initialization. Weights are efficiently changed by optimization techniques such as SGDM, RMSprop and Adam to minimize the error function. The proposed Adam optimizer, which dynamically adjusts the learning rate for each parameter, is widely used in the industry because it prevents divergence, accelerates convergence and is more effective. Nonlinear activation functions such as ReLU, sigmoid, and tanh allow the network to learn complicated patterns that go beyond basic correlations. To optimize DNN performance, some hyperparameters must be modified. The appropriate hyperparameters for the proposed DNN model are discovered by training and analysing a dataset with varying numbers of hidden layers and temperatures.

2.3. Performance Evaluation

Model performance is frequently measured and optimized using RMSE, MAE, and MAX. Significant errors greatly affect RMSE, which calculates square root of deviations of mean squared between expected and actual values. By computing average absolute differences, MAE produces a balanced error metric that is less susceptible to outliers. Activation functions frequently use the MAX function to measure worst-case errors and compute loss to ensure stability in harsh circumstances.

3. Simulation Results And Discussions

Battery charge and discharge cycles obtained from cylindrical Li-ion INR 18650 batteries under various operating circumstances were used to train the model. The training and testing were done to one-seven layers for 50 neurons each with activation functions like tanh and ReLU alternately. The model was trained for the 50

epochs and validated through the RMSE, MAE, and MAX error metrics. The trained model was then validated under several drive cycles to ensure SOC estimation operation reliability. The RMSE and number of hidden layers at various temperatures is illustrated in Figure 3.1. The MAE against one to seven hidden layers at various temperature are plotted in Figure 3.2.

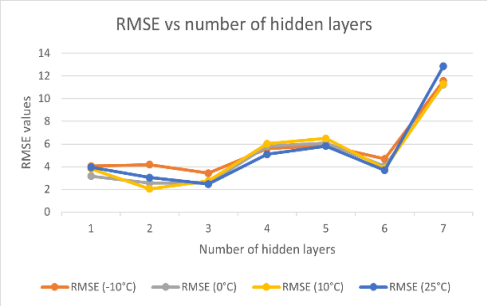

Figure 3.1 RMSE vs number of hidden layers

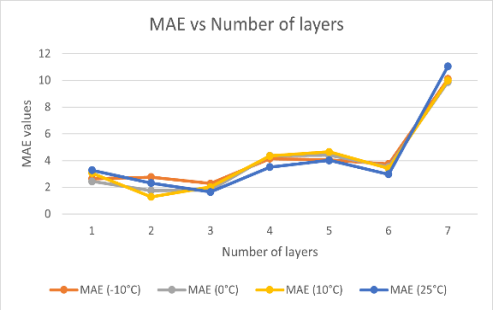

Figure 3.2 MAE vs number of hidden layers

The two hidden layers performed well, especially at 10°degree with RMSE of 2.0488 and MAE of 1.2858. The best results are observed with three hidden layers, where RMSE of 2.5628 and MAE of 1.7991 values are generally the lowest at 0°degree. At extreme temperatures such as -10° and 25°degree, RMSE and MAE values increase, indicating less accurate predictions.

4. Conclusion

SOC estimation model was performed on a variety of neural network architectures by changing the number of layers from one to seven under various temperatures such as 0°, 10°, 25°, and -10°degrees to determine the suitable model structure that is most accurate and yet computationally light. The two or three hidden layers offer the best balance of accuracy and execution time. More than four layers do not considerably enhance accuracy but contribute to higher error and longer execution times. A two-layer DNN outperforms other techniques, with a low RMSE of 1.47% and MAE of 1.27% is the appropriate neural network architecture for real-time SOC estimation in BMS. Future research can also investigate more sophisticated architectures, including hybrid and recurrent neural networks, to further improve estimation accuracy, particularly under extreme temperatures.

5. References

[1] Dehghani-Sanij, A.R., Tharumalingam, E., Dusseault, M.B. and Fraser, R., 2019. Study of energy storage systems and environmental challenges of batteries.

[2] Ci, S., Lin, N. and Wu, D., 2016. Reconfigurable battery techniques and systems: A survey. IEEE Access, 4, pp.1175-1189.

[3] Blomgren, G.E., 2016. The development and future of lithium ion batteries. Journal of The Electrochemical Society, 164(1), p.A5019.

[4] Knap, V. and Stroe, D.I., 2021. Effects of open-circuit voltage tests and models on state-of-charge estimation for batteries in highly variable temperature environments: Study case nano-satellites. Journal of Power Sources, 498, p.229913.

[5] Lin, C., Tang, A. and Xing, J., 2017. Evaluation of electrochemical models based battery state-of-charge estimation approaches for electric vehicles. Applied Energy, 207, pp.394-404.

[6] Lin, S.L., 2024. Deep learning-based state of charge estimation for electric vehicle batteries: Overcoming technological bottlenecks. Heliyon, 10(16).

Biographies



Tejaswini S received M.Tech degree in Digital Communication and Networking from Dayananda Sagar College of Engineering and B.E in ECE from GSSSIETW. She is currently working as Assistant Professor in Department of ECE at Vidyavardhaka College of Engineering. Her research interests are battery management systems, computer networks, deep learning.

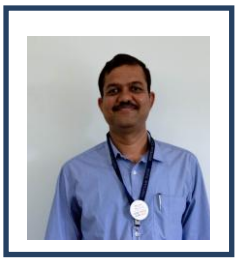

Chandrashekar M. Patil received a M.Tech degree in Digital Electronics at VTU and B.E in ECE from Kuvempu University. He has received PhD from University of Mysore in the field of signal processing. He is currently working as Professor and Head in the Department of ECE at Vidyavardhaka College of Engineering. His research focuses on signal processing, image processing, and battery management systems. He has been a reviewer for numerous prestigious journals.

Meta Learning combined with Federated Learning for Detecting Blackhole Attacks

Rathina Kumar, Getzi Jeba Lellipushpam Paulraj, Immanuel Johnraja Jebadurai

Karunya Institute of Technology and Sciences, rathinakumar@karunya.edu.in

Abstract.

Cybersecurity threats, such as blackhole attacks, pose a significant challenge to modern networks by disrupting data flow and compromising communication integrity. To deal with this, we propose a novel detection framework that blends Meta Learning (ML) and Federated Learning (FL) to enhance adaptability and privacy. ML enables models to rapidly adjust to new attack patterns with minimal data, while FL ensures decentralized training without exposing sensitive network information. At the core of this approach, Model Agnostic Meta Learning (MAML) improves detection accuracy by learning efficient initialization strategies. A comparative evaluation against Bayesian Meta Learning and Metric Based Meta Learning highlights MAML's effectiveness in managing class imbalances and adapting to evolving threats. Experimental results demonstrate promising detection accuracy, paving the way for further refinements to enhance performance, particularly in identifying rare attack scenarios.

Keywords. Meta-learning, Federated learning, Blackhole attacks, Network security.

1. INTRODUCTION

As cyberspace continues to expand, cybersecurity threats such as blackhole attacks are also becoming sophisticated, compromising network integrity. Traditional cybersecurity measures, while effective in controlled environments, struggle to implement detection mechanisms that ensure both accuracy and data privacy. Federated Learning (FL) has become a viable approach by enabling distributed model training across multiple devices without sharing raw data [1]. This decentralized approach reduces the risks associated with centralized data aggregation while maintaining model effectiveness. However, FL's reliance on large datasets poses challenges in scenarios where labeled attack samples are scarce, as seen in blackhole attack detection [2]. To address this issue, Meta Learning (ML), particularly Model Agnostic Meta Learning (MAML), is integrated with FL to enhance model adaptability. Model Agnostic Meta Learning (MAML) allows machine learning models to quickly adapt to new tasks using minimal data, making it highly effective for detecting rare cyber threats like blackhole attacks [3]. This study evaluates Federated Meta Learning (FML), combining FL and MAML, for improved blackhole attack detection while addressing data heterogeneity and model consistency challenges.

All Open Access articles are peer-reviewed, distributed under the Creative Commons Attribution-Non Commercial 4.0 International

2. LITERATURE REVIEW

The combination of Meta Learning and Federated Learning (FL) is gaining traction in cybersecurity. FL preserves data privacy by enabling decentralized learning, reducing security risks while enhancing adaptability against evolving threats [4]. One of the key challenges in FL-based attack detection is the need for adaptive learning models that can efficiently detect new and upcoming threats. Finn et al. [5] introduced Model Agnostic Meta Learning (MAML) to allow models to adapt quickly with limited training data, making it ideal for blackhole attack detection. Zhao et al. [6] highlight the effect of non-IID data on FL models, emphasizing the need for adaptive mechanisms to ensure consistent attack detection. Jiang et al. [7] enhance FL with personalized Meta Learning, improving blackhole attack detection by tailoring models to specific network patterns. Chen et al. [8] stress robust aggregation techniques to counter these risks, while Sun et al. [9] reinforce the need for secure learning mechanisms. Sohail et al. [10] introduced INFUSE, addressing class imbalances and limited attack data.

The literature suggests that combining meta-learning and federated learning provides a potential solution to the

obstacles of blackhole attack detection. The fusion of FL's privacy preserving architecture with meta-learning's rapid adaptation capabilities paves the way for more effective and resilient cybersecurity solutions in distributed network environments.

3. DATASET DESCRIPTION

For this study, we employ a tailored dataset designed to examine network traffic patterns for identifying and analyzing blackhole attacks. It is structured with 18 distinct attributes, as outlined in Table 3.1. The dataset is systematically structured as follows:

Table 3.1 Features of Custom Dataset

No.	Feature Name	Feature
F1	time	Timestamp of the packet transmission
F2	protocol type	Type of protocol associated with the packet
F3	destination	Destination of the packet network
F4	length	Packet Length in bytes
F5	info	More details about the packet and flags
F6	transmission_rate_per_1000_ms	Rate of transmission per 1000 milliseconds
F7	reception_rate_per_1000_ms	Rate of reception per 1000 milliseconds
F8	transmission_averageper_sec	Average transmission rate per second
F9	reception average_per_sec	Average reception rate per second
F10	transmission count per_sec	Count of transmissions per second
F11	reception_count_per_sec	Count of receptions per second.
F12	transmission total_duration_per_sec	Total duration of transmission per second
F13	reception total_duration_per_sec	Total duration of reception per second
F14	dao	Data Access Object specific to context
F15	dis	Data Integrity Status specific to context
F16	dio	Data Input/output specific to context
F17	category	Category of traffic: Normal or Blackhole
F18	label	Traffic type label: 0 (Normal), 1(Blackhole)

The dataset includes normal and blackhole attack traffic, where malicious nodes drop packets, causing data loss.

4. METHODOLOGY

This part describes the various models used in the research.

4.1 Federated Learning Framework

Federated Learning (FL) allows decentralized model training without sharing raw data, ensuring privacy in sensitive tasks like blackhole attack detection. Instead of centralizing data, clients train models locally and share updates, reducing security risks. Differences in client availability due to power constraints or connectivity issues can disrupt training [11].

4.2 Model Agnostic Meta Learning (MAML)

MAML is a meta-learning strategy designed to enhance the initial configuration of models, thereby enabling rapid adjustment to new tasks. In practical applications, MAML's inner loop helps a model adapt to specific network conditions, while the outer loop ensures it generalizes well across different scenarios.

1. Inner Loop (Task-Specific Updates*)*: The model is updated using a few gradient steps

based on specific task data.

2. Outer Loop (Meta-Updates*)*: The gradients from multiple tasks are aggregated to refine the shared initialization, ensuring better generalization across different tasks.

4.3 Bayesian Meta-Learning

Bayesian Meta-Learning enhances model reliability by quantifying uncertainty in predictions, making it effective in low-data scenarios. Using Bayesian Neural Networks (BNNs) and Gaussian Processes (GPs), it improves resilience to noisy data and generalization. FL, it enables probabilistic updates, ensuring robust blackhole attack detection in variable network conditions [12].

4.4 Metric Based Meta Learning (Siamese Network)

Metric Based Meta Learning, particularly through Siamese Networks, focuses on learning similarity metrics for comparing tasks or data points, making it well-suited for binary classification tasks such as blackhole attack detection. It maps data into an embedding space, applying Euclidean distance for classification. Optimized via contrastive or triplet loss, it enhances pattern recognition.

5. IMPLEMENTATION

This section includes the implementation of the models and a brief explanation of the metrics used to assess the outcomes.

5.1 Implementation of the models

The flowchart of the planned framework is displayed in Figure 5.1, which outlines the training and evaluation process.

1. **Data Splitting**: Divide the dataset into distinct sections for training, validation, and testing to ensure proper model evaluation.
2. **Model Initialization**: Establish a global model and distribute initial parameters to each client for localized training.
3. **Local Training**: Every client independently updates its local model using its assigned dataset while preserving data privacy.
4. **Weight Aggregation**: Aggregate weights from local models to update the global model.
5. **Model Evaluation**: Evaluate the global model on the validation set.
6. **Final Testing**: Evaluate the global model using the test dataset and generate results.



Figure 5.1. Federated Meta-Learning Workflow

The optimal hyperparameter settings for the models are as follows: For MAML, the learning rate is 0.0008, with 3 local epochs and 15 rounds. Bayesian Meta-Learning uses a learning rate of 0.001, a dropout rate of 0.5, 10 epochs, and 100 Monte Carlo samples. Metric Based Meta Learning (Siamese Network) has a learning rate of 0.001, hidden layer sizes of [64, 32], and 10 epochs.

5.2 Confusion Matrix

A confusion matrix is a systematic presentation of classification results between predicted labels and actual outcomes. Below is the confusion matrix representation (Table 5.1): The overall accuracy can be computed using the equation provided below equation:

$$\text{Accuracy} = TP + TN / TP + TN + FP + FN$$

Table 5.1 Confusion Matrix

	Predicted: Attack data	Predicted: Normal data
Actual: Attack data	True Positive (TP)	False Negative (FN)
Actual: Normal data	False Positive (FP)	True Negative (TN)

6. Result and Discussion

This part examines the experimental findings and compares the accuracy of three models. The performance of all three models is listed below.

Model Agnostic Meta Learning (MAML) - 0.9367 Bayesian Meta Learning – 1.00
Metric Based Meta Learning – 0.4500

Bayesian Meta-Learning achieved 100% accuracy but likely overfit, limiting generalization. MAML performed well at 93.67%, with 97.49% precision and 89.69% recall, making it suitable for dynamic environments. Siamese Networks struggled with 45% accuracy, requiring improved embeddings and refined metrics for better blackhole attack detection [13].

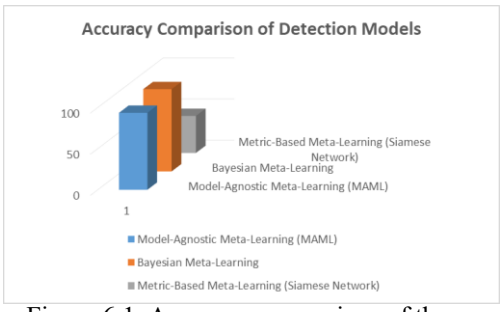

Figure 6.1. Accuracy comparison of three models

The graphical comparison in Figure 6.1 highlights MAML's superior accuracy, reinforcing its robustness across scenarios.

7. Conclusion

This study presents a framework combining Meta Learning and Federated Learning (FL) for enhanced blackhole attack detection in distributed networks. By integrating Model Agnostic Meta Learning (MAML) with FL's privacy preserving features, the system ensures accurate detection while maintaining data confidentiality. FL's decentralized structure prevents raw data from being shared, reducing the risks linked to centralized information storage. Evaluating scalability in real-world IoT and industrial networks will be crucial for broader adoption. Meta-learning techniques have been explored in network intrusion detection, highlighting their effectiveness in adapting to evolving threats [14].

8. REFERENCES

[1] Yang, Y., Liu, Y., & Zhang, Y., "Federated Learning for Cybersecurity: A Survey," IEEE Access, vol. 8, pp. 123456-123467, 2020.

[2] Huang, Y., & Wang, Y., "A Survey on Federated Learning: From Theory to Applications," IEEE Transactions on Neural Networks and Learning Systems, vol. 32, no. 2, pp. 1-18, 2021.

[3] Fallah, A., Mokhtari, A., & Ozdaglar, A., "Personalized Federated Learning with Theoretical Guarantees: A Model-Agnostic Meta-Learning Approach," Advances in Neural Information Processing Systems (NeurIPS), 2020.

[4] Kairouz, P., McMahan, B., Avent, B., et al., "Advances and Open Problems in Federated Learning," Foundations and Trends in Machine Learning, vol. 14, no. 1, pp. 1-210, 2019.

[5] Finn, C., Abbeel, P., & Levine, S., "Model-Agnostic Meta-Learning for Fast Adaptation of Deep Networks," Proc. 34th International Conference on Machine Learning (ICML), 2017.

[6] Zhao, Y., Li, M., Lai, Z., Suda, N., Civin, D., & Chandra, V., "Federated Learning with Non-IID Data," arXiv preprint, arXiv:1806.00582, 2018.

[7] Jiang, Y., Konecny, J., Rush, K., & Kannan, R., "Improving Federated Learning Personalization via Model Agnostic Meta Learning," Proc. NeurIPS Workshop on Federated Learning for Data Privacy and Confidentiality, 2019.

[8] Chen, D., Wu, H., Liu, H., et al., "Deep Federated Learning for Intrusion Detection in IoT Applications," IEEE Internet of Things Journal, vol. 8, no. 4, pp. 2291-2301, 2021.

[9] Sun, Y., Li, Q., Wang, X., et al., "Towards Federated Learning Models Robust to Poisoning Attacks," Proc. 35th AAAI Conference on Artificial Intelligence, vol. 35, no. 15, pp. 13601-13608, 2021.

[10] Sohail, A., Malik, M., & Khan, R., "Deep Neural Networks based Meta-Learning for Network Intrusion Detection," arXiv preprint, arXiv:2302.09394, 2023.

[11] Wang, J., Yurochkin, M., Sun, Y., Papailiopoulos, D., & Khazaeni, Y., "Federated Learning with Matched Averaging," Proc. 8th International Conference on Learning Representations (ICLR), 2020.

[12] Qu, Y., Li, Y., & Zhang, X., "Federated Sharpness-Aware Minimization (FedSAM): Towards Robust Federated Learning with Local Sharpness Control," Proc. IEEE International Conference on Data Science and Advanced Analytics (DSAA), 2022.

[13] Foret, P., Kleiner, A., Mobahi, H., & Neyshabur, B., "Sharpness-Aware Minimization for Efficiently Improving Generalization," Proc. International Conference on Learning Representations (ICLR), 2021.

[14] Zhang, Y., & Wang, J., "Meta-Learning for Network Intrusion Detection: A Review," *Journal of Network and Computer Applications*, vol. 178, 102973, 2021.

Biographies



K Rathina Kumar, a B.Tech Computer Science and Engineering student at Karunya Institute of Technology and Sciences (2025 batch), has experience in Android development, networking, and machine learning. He has worked on projects like an Online Election Management System and NutriGuide and interned at Cisco, IBM, and YBI Foundation. His interests include AI, networking, and web technologies.



Getzi Jeba Lellipushpam Paulraj received her B.E. degree in Electronics and Communication Engineering from M.S. University, Tirunelveli, India in the year 2004. She received her M.Tech. degree in Network and Internet Engineering from Karunya University, Coimbatore, India in the year 2009. She received her Ph.D. from Karunya Institute of Technology and Sciences, Coimbatore, India in the year 2018. Her areas of interest include IoT, Fog Computing and Data Analytics.



Immanuel Johnraja Jebadurai received his B.E. degree in Computer Science and Engineering from M.S. University, Tirunelveli, India in the year 2003. He received his
M.E. degree in Computer Science and Engineering from Anna University, Chennai India in the year 2005. He received his Ph.D. in Computer Science and Engineering from Karunya Institute of Technology and Sciences, Coimbatore, India in the year 2017. His areas of interest include Network Security, Vehicular Ad-Hoc Networking and IoT.

Advanced Retinal Vessel Segmentation: Combining AGD-GIF, CRGCN, and Improved Mask R-CNN-PO

R Ramji [1,*], S Devi [2]

[1]*PRIST Deemed to be University ,Thanjavur ,Tamil Nadu, India*
[2]*Sree Venkateswara College of Engineering*, *Nellore, Andhra Pradesh, India*
E-mail: janramji@gmail.com; devi.bharath@gmail.com;
** Corresponding Author*

Abstract.

Accurate segmentation of retinal blood vessels plays a vital role in medical image analysis for the diagnosis and management of eye diseases, as most health conditions affect the retinal vascular network. Despite progress made in recent decades, issues such as complex textures, vessel discontinuities, and unidentified areas remain unresolved, particularly in segmenting fine veins and handling low-contrast images. This method integrates three advanced techniques for retinal vessel segmentation. Initially, it applies Adaptive Gradient Domain Guided Image Filtering (AGD-GIF) for preprocessing. Subsequently, it utilizes an efficient feature extraction method called the proposed Cascading Residual Graph Convolutional Network (CRGCN). Finally, segmentation is performed using an enhanced Mask Region-Based Convolutional Neural Network with a Parrot Optimizer (Improved Mask R-CNN-PO), ensuring precision and reliability in detecting retinal vessels from medical images. When tested on the CHASE_DB1 datasets, the proposed model achieves specificity of 99.53%, accuracy of 99.65%, and an AUC of 99%. Additionally, it attains an accuracy of 99.63% and F1 scores of 99.59%.

Keywords. Adaptive Gradient Domain Guided Image Filtering, Biomedical Image Analysis, Cascading Residual Graph Convolutional Network, Improved Mask Region-Based Convolutional Neural Network with Parrot Optimizer, Retinal Vessel Segmentation.

1. INTRODUCTION

The onset of the disease is closely linked to unusual alterations in retinal characteristics, as the retina is the only terminal vessel observable in a living human body. Diabetic retinopathy is associated with abnormalities in the retinal microvascular diameter [1]. Vascular density of the outer macular area was positively correlated with vasospasm, glaucoma, visual field defects, arterial reflex zone widening, and blood vessel constriction. Arteriovenous sclerosis and hypertension are connected by the cross-compression of arteries and veins in the retina. Precise segmentation and morphological analysis of retinal blood vessels are crucial for diagnosis, treatment, monitoring, and prevention of numerous diseases, particularly chronic conditions [2-3].The retina, a critical light-sensitive layer, significantly affects central and peripheral vision in humans. It is sustained by an intricate network of retinal blood vessels, essential for maintaining the visual system's integrity [4]. Alterations to these vessel structures can indicate various major health issues affecting the eyes and cardiovascular system. These changes have been linked to conditions such as diabetic retinopathy (DR), macular edema (ME), glaucoma, cataracts, malignancies, and hypertension [5-6]. Competing automated retinal vascular segmentation (RVS) techniques have emerged, offering improved diagnostic accuracy for eye diseases and facilitating early diagnosis and treatment [7].

The approach utilizes Adaptive Gradient Domain-Guided Image Filtering (AGD-GIF) to preprocess retinal images, effectively minimizing noise and improving vessel visibility, which aids in more precise segmentation. The research implements a Cascading Residual Graph Convolutional Network (CRGCN) for feature extraction, ensuring complex retinal structures are accurately represented through hierarchical learning from multiple levels of abstraction. The technique incorporates the enhanced Mask R-CNN with the Parrot Optimizer (Improved Mask R-CNN-PO), fine-tuning network parameters and enhancing the model's ability to generalize across various retinal image datasets.

2. Literature Survey

Sun et al. (2023) [8] have introduced a technique for segmenting retinal blood vessels using a U-net structure-based series of deformable convolution and attention mechanisms (SDAU-Net).Potential increases in computer complexity and cost are the proposed method's drawbacks. In 2022, Muzammil et al. [9] have demonstrated an unsupervised technique for vessel segmentation from retinal pictures. The disadvantages of the proposed approach are its computational complexity and dataset constraints. Li et al. (2024) [10] have presented a retinal vessel segmentation model.The suggested method's disadvantage is that it takes longer and requires more computing. Guo (2022) [11] have presented a cascade semantic guided network (CSGNet) to enhance retinal vascular segmentation for ocular disease early identification.

2.1. Problem Statement

Current methods face difficulties in achieving high vessel segmentation accuracy due to image preprocessing challenges, limited feature extraction capabilities, and substantial computational requirements. To tackle these problems, the proposed solution incorporates three key components: an adaptive gradient domain-guided image filtering technique to enhance the preprocessing phase, a Cascading Residual Graph Convolutional Network for improved feature extraction, and the Parrot Optimizer to refine the segmentation process.

3. Proposed Methodology

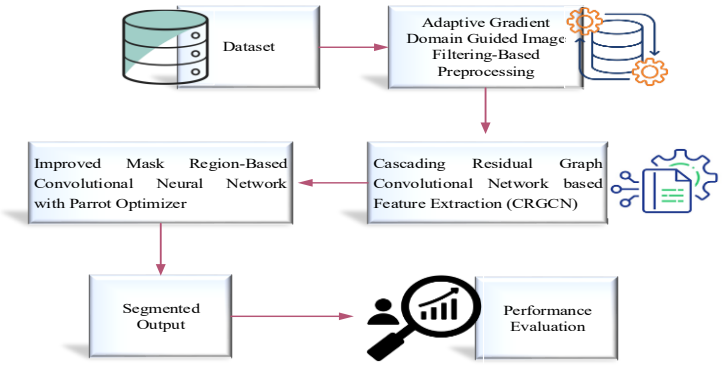

Figure.3.16. Illustration of the proposed method

Figure 3.1 illustrates a workflow of retinal vessel segmentation. The process begins with a dataset that undergoes image pre-processing through adaptive gradient domain-guided image filtering (AGD-GIF). This pre-processing step helps improve the performance of the cascading residual graph convolutional network (CRGCN) by extracting better features. The CRGCN effectively reconstructs fine spatial and structural patterns of the retinal vessels. The features are finally forwarded to an optimized Parrot optimizer based on an improved Mask Region Convolutional Neural Network (Improved Mask R-CNN-PO). The CHASE_DB1 dataset, which was gathered from multiethnic schools as part of the Child Heart and Health Study in England (CHASE), is used in the suggested strategy. The pre-processing step receives the data inputs.

For the input data, the pre-processing approach is applied. For image enhancement, the Adaptive Gradient Domain Guided Image Filtering approach (AGD-GIF) is employed [12]. The feature extraction process takes place after pre-processing. Retinal vessel learning characteristics are the only features that CRGCN-based feature extraction efficiently targets. Using the hierarchical structure of GCNs, this technique learns intricate spatial connections between the image's pixels and regions of interest. As the data moves through the stages, the connections that stay in the network keep features from previous layers, allowing for a higher level of feature extraction [13].

After feature extraction, segmentation takes place. To find features in input images, it makes use of residual networks, a region proposal network, and a feature pyramid network. Popular and open-source, Mask R-CNN offers precise segmentation and localization abilities for tasks involving object detection. By better suiting the

physical characteristics of retinal vasculature and lesions for segmenting retinal vascular features, a flexible convolutional network improves detection accuracy [14]. Due to its charming appearance, close bond with its owner, and ease of training, the Pyrrhura Molinae is a favoured species of parrot among pet owners. The four distinct behavioral traits and breeding endeavours of Pyrrhura molinae include foraging, remaining, communication, and dread of strangers [15]

4. Result and Discussion

4.1 Dataset Description

The Child Heart and Health Study in England (CHASE), which gathered pictures from multiethnic schools, includes the CHASE_DB1 dataset. A handheld Nidek NM-200-D fundus camera with a 30° field of view was used to take the retinal images of the students' two eyes, which make up this dataset.

4.2. Comparison of performance with existing methods

In this section, the effectiveness of the presented approach is compared with other existing approaches. The proposed method has been compared with existing methods such as SDAU-Net [8], MUVS [9], AttMSFCU-Net [10], and CSGNet [11].

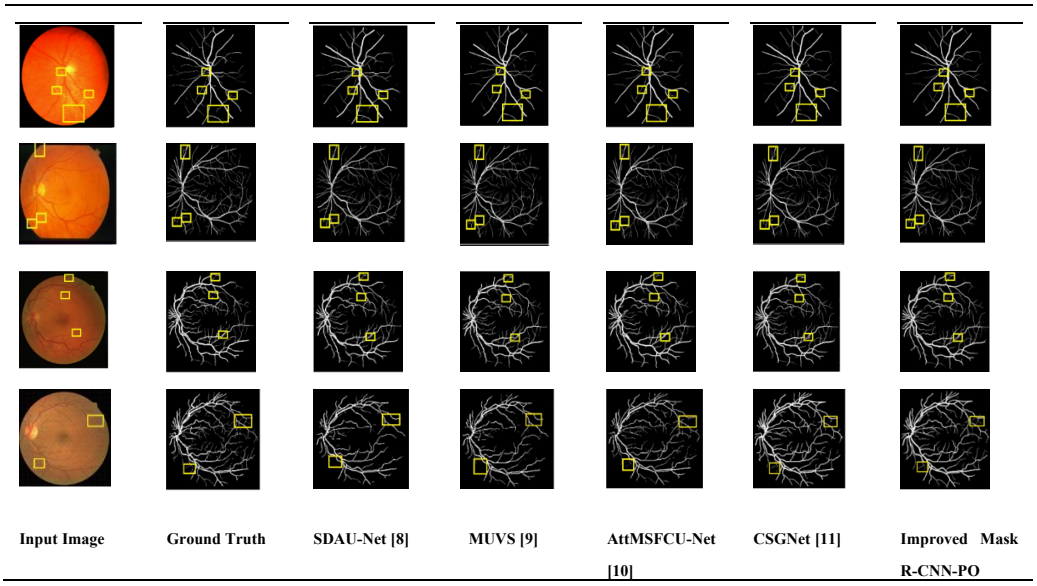

Table.4.1. Comparison of Improved Mask R-CNN-PO and Prior Methods on CHASE_DB1

Table 4.1 shows the comparison of the segmentation outcomes on the CHASE_DB1 dataset between the improved Mask R-CNN-PO and other earlier techniques.

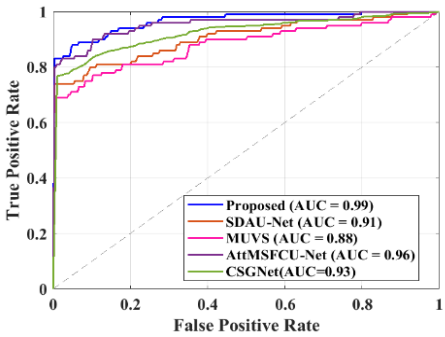

Figure.4.1. ROC curves of proposed and comparative methods

Figure 4.1 presents the ROC curves of different methods for retinal vessel segmentation. The proposed method yields the best AUC score of 0.99, outperforming SDAU-Net with an AUC of 0.91, MUVS with an AUC of 0.88, AttMSFCU-Net with an AUC of 0.96, and CSGNet with an AUC of 0.93. An increased AUC means improved sensitivity and specificity of the given or tested diagnostic method. The dotted diagonal line in the illustration means chance or no discrimination at all (AUC of 0.5). As for the benchmark methods, the proposed method yields better results, and accuracies are quite high.

Table 4.2 shows the comparison of the segmentation performance metrics of various methods on the dataset CHASE_DB1: precision, F1-score, recall, and specificity. The suggested improved Mask R-CNN-PO is best compared to prior methods. Hence, all previously developed methods are surpassed while the best is achieved in every metric by it; that includes 99.65% accuracy, 99.63% precision, 99.59% F1-score, 99.58% recall, and 99.53% specificity.

Techniques	Accuracy	Precision	F1-Score	Recall	Specificity	Accuracy
SDAU-Net [8]	90.54	90.59	89.73	90.43	90.86	90.54
MUVS [9]	85.73	80.36	82.55	84.92	84.40	85.73
AttMSFCU-Net [10]	72.33	70.46	72.27	70.47	75.49	72.33
CSGNet [11]	73.55	71.23	69.76	65.64	66.39	73.55
Proposed Improved Mask R-CNN-PO	99.65	99.63	99.59	99.58	99.53	99.65

Table. 4.2 Performance Comparison of Retinal Vessel Segmentation Techniques

On all of the performance metrics, the existing methods, SDAU-Net, MUVS, AttMSFCU-Net, and CSGNet, significantly low exhibit performance. However, SDAU-Net comes closest with an accuracy of 90.54%. Thus, the effectiveness of the proposed approach is highly superior.

Techniques	Error rate	Computational Time (s)
SDAU-Net [8]	1.67	1.43
MUVS [9]	1.89	1.65
AttMSFCU-Net [10]	1.45	1.38
CSGNet [11]	1.33	1.12
Proposed Improved Mask R-CNN-PO	0.01	0.02

Table.4.3. Comparison of Error Rate and Computational Time

Table 4.3 shows the comparison of error rate and computational time for segmentation techniques on the CHASE_DB1 dataset. The proposed improved Mask R-CNN with Parrot Optimizer, improved Mask R-CNN-PO, has the lowest error rate at 0.01 and the fastest computational time at 0.02 seconds.

5. Conclusion

The proposed method uses advanced techniques integrated into preprocessing, feature extraction, and segmentation and provides a solid solution to the problem of retinal vessel segmentation. AGD-GIF demonstrates the ability to significantly enhance the image of the retina while minimizing noise interference and enhancing the visibility of the vessels. Feature extraction based on CRGCN performs significantly in accurately determining vessel structures. Finally, to improve cell segmentation, an improved Mask R-CNN-PO is employed, which provides better results for occluded images and varying image conditions. Thus, the improvement in terms of stability and accuracy qualifies it as a viable candidate for real-world applications, including computer-aided diagnosis and staging of treatments for retinal disorders.

6. References

[1] Y. Liu, J. Shen, L. Yang, G. Bian, and H. Yu, "ResDO-UNet: A deep residual network for accurate retinal vessel segmentation from fundus images," Biomed. Signal Process. Control, vol. 79, p. 104087, 2023.

[2] Y. Tan, K. F. Yang, S. X. Zhao, and Y. J. Li, "Retinal vessel segmentation with skeletal prior and contrastive loss," IEEE Trans. Med. Imaging, vol. 41, no. 9, pp. 2238–2251, Sep. 2022.

[3] Y. Tan, K. F. Yang, S. X. Zhao, J. Wang, L. Liu, and Y. J. Li, "Deep matched filtering for retinal vessel segmentation," Knowl. Base. Syst., vol. 283, p. 111185, 2024.

[4] Y. Liu, J. Shen, L. Yang, H. Yu, and G. Bian, "Wave-Net: A lightweight deep network for retinal vessel segmentation from fundus images," Comput. Biol. Med., vol. 152, p. 106341, Jan. 2023.

[5] D. E. Alvarado-Carrillo and O. S. Dalmau-Cedeño, "Width attention based convolutional neural network for retinal vessel segmentation," Expert Syst. Appl., vol. 209, p. 118313, 2022.

[6] F. Dong, D. Wu, C. Guo, S. Zhang, B. Yang, and X. Gong, "CRAUNet: A cascaded residual attention U-Net for retinal vessel segmentation," Comput. Biol. Med., vol. 147, p. 105651, Aug. 2022.

[7] T. M. Khan, S. S. Naqvi, A. Robles-Kelly, and I. Razzak, "Retinal vessel segmentation via a Multi-resolution Contextual Network and adversarial learning," Neural Netw., vol. 165, pp. 310–320, Aug. 2023.

[8] K. Sun, Y. Chen, Y. Chao, J. Geng, and Y. Chen, "A retinal vessel segmentation method based improved U-Net model," Biomed. Signal Process. Control, vol. 82, p. 104574, 2023.

[9] C. Li, Z. Li, F. Yu, and W. Liu, "An improved method for retinal vessel segmentation in U-Net," Multimedia Tools Appl., vol. •••, pp. 1–19, 2024.

[10] S. Guo, "CSGNet: Cascade semantic guided net for retinal vessel segmentation," Biomed. Signal Process. Control, vol. 78, p. 103930, 2022.

[11] L. Li, M. Lv, H. Ma, Z. Jia, X. Yang, and W. Yang, "X-ray Image Enhancement Based on Adaptive Gradient Domain Guided Image Filtering," Appl. Sci. (Basel), vol. 12, no. 20, p. 10453, 2022.

[12] M. Yan, Z. Cheng, C. Gao, J. Sun, F. Liu, F. Sun, et al., "Cascading residual graph convolutional network for multi-behavior recommendation," ACM Trans. Inf. Syst., vol. 42, no. 1, pp. 1–26, 2023.

[13] M. F. Lei, Y. B. Zhang, E. Deng, Y. Q. Ni, Y. Z. Xiao, Y. Zhang, et al., "Intelligent recognition of joints and fissures in tunnel faces using an improved mask region-based convolutional neural network algorithm," Comput. Aided Civ. Infrastruct. Eng., vol. 39, no. 8, pp. 1123–1142, 2024.

[14] J. Lian, G. Hui, L. Ma, T. Zhu, X. Wu, A. A. Heidari, et al., "Parrot optimizer: Algorithm and applications to medical problems," Comput. Biol. Med., vol. 172, p. 108064, Apr. 2024.

[15] J. Lian, G. Hui, L. Ma, T. Zhu, X. Wu, A. A. Heidari, et al., "Parrot optimizer: Algorithm and applications to medical problems," Comput. Biol. Med., vol. 172, p. 108064, Apr. 2024.

FIREFIGHTING BOT USING IMAGE PROCESSING

[1]Priyadharsini S, [2]Ahamed Fayaz MK, [3]Akash R, [4]Praneeshraja BM
[1]Assistant Professor-II, KPR Institute of Engineering and Technology, Coimbatore, India
[2]Student, KPR Institute of Engineering and Technology, Coimbatore, India
[3]Student, KPR Institute of Engineering and Technology, Coimbatore, India
[4]Student, KPR Institute of Engineering and Technology, Coimbatore, India
Email: [1]spdharsini14@gmail.com, [2]ahamedfayazmk@gmail.com, [3]akashronaldo465@gmail.com, [3]rajapraneesh15@gmail.com
Contact: [1]9360965233,[2]7010159344,[3]6374420429,[4]9500411066

Abstract.

The Firefighting Bot with Image Processing is a smart, autonomous system designed to quickly detect and put out fires, reducing response time and minimizing potential damage. At its core, it runs on a Raspberry Pi, equipped with a Pi camera to capture real-time images. Using the OpenCV library and thresholding techniques, the bot can recognize flames in its surroundings, analyze their intensity, and assess the severity of the situation. Once a fire is detected, the bot springs into action, moving toward the source. It adjusts the water spray based on the fire's severity, ensuring an efficient and targeted response. Built with a water tank and a precise nozzle system, the bot can accurately disperse water to the affected area. Its autonomous navigation allows it to move smoothly, avoid obstacles, and focus on fire suppression. This project is designed to improve fire safety by offering a reliable, automated solution for detecting and extinguishing fires. It can be especially useful in residential, commercial, and industrial spaces—particularly in areas that are difficult to access or too dangerous for humans. By combining image processing with robotics, this system ensures a fast, cost-effective, and scalable approach to modern fire safety management.

II. **Keywords**. Firefighting Bot, Autonomous System, Flame Detection, Image Processing, OpenCV, Raspberry Pi, Robotics in Fire Safety, Cost Effective.

1. INTRODUCTION

Fire incidents are dangerous and can cause significant damage, especially since traditional fire suppression systems often require human intervention. This project aims to address this issue by creating a firefighting robot that uses Raspberry Pi and image processing to detect and put out fires. By using OpenCV and thresholding techniques, the robot can detect fires in real-time through a Pi camera, assessing the fire's severity and then activating a water spray system to extinguish the flames.

The use of image processing ensures that fires are detected accurately, reducing false alarms that can occur with methods like smoke detectors. The bot is designed to navigate on its own, moving across various terrains, avoiding obstacles, and prioritizing the fire suppression task. It features real-time image processing, fire density estimation, and precise water dispersion to ensure an efficient response.

This robot has wide-ranging applications in residential, industrial, and commercial environments, making it a versatile fire safety solution. Although there are challenges, such as distinguishing fire from other light sources, future improvements may involve adding extra sensors or using a machine learning for more accurate detection. In the end, this firefighting robot provides practical, automated solution to improve fire safety and reduce the risks that humans face during emergencies.

2. LITERATURE REVIEW

Pramod B. N., Hemalatha K. N., Poornima B. J., and Harshitha R. (2019) examined the role of robotics in fire safety with their research on the "Fire Fighting Robot." Their study addresses the increasing number of fire-related accidents and highlights how robots can replace humans in dangerous firefighting tasks. The proposed robot is designed to detect and extinguish fires autonomously, minimizing human risk. The system is powered by an Arduino UNO (ATmega328P microcontroller), which serves as its central control unit. With a

mechanical design capable of executing complex actions automatically, the robot navigates toward fire hazards and deploys its extinguishing mechanism efficiently. This research demonstrates how robotics can enhance safety and reduce human intervention in fire emergencies.

Jayanth Suresh (2017) explored the use of automation in high-risk environments with his research on "Fire-Fighting Robot." His study focuses on designing a fully autonomous robot that can detect flames, maneuver toward the fire, and extinguish it using carbon dioxide. By leveraging fire detection sensors and autonomous navigation systems, the robot ensures quick and precise fire suppression with minimal human intervention. This research underscores the growing importance of robotics in life-threatening situations, offering a safer alternative to traditional firefighting methods.

Krishan Arora, Harshit Kumar, and Rohit Raj Singh (2023) proposed an advanced "Autonomous Fire Fighting Robot" aimed at improving firefighting efficiency while minimizing risks for both firefighters and civilians. Their study acknowledges that current firefighting methods are often inadequate and slow, leading to increased casualties and property damage. The robot they designed features infrared flame sensors, ultrasonic sensors, and an autonomous fire suppression system capable of detecting and extinguishing fires in multiple directions (left, right, and front). Equipped with a servo-mounted water spray nozzle, the system ensures maximum coverage. The robot also integrates obstacle detection technology, allowing it to navigate hazardous environments with ease. By reducing reliance on human firefighters, this innovation significantly enhances fire safety and emergency response efficiency.

Yiying Yuan (2021) explored firefighting robotics in his study, "Technical Research on Fire-Fighting Robotics." Recognizing the high risks faced by firefighters, this research focuses on the development of firefighting drones (quadcopters) that can operate in dangerous environments without human intervention. These drones use electric motors, magnetic field principles, and four-rotor propulsion systems to navigate through fire zones, detect fire sources, and assist in suppression. By utilizing advanced flight control mechanisms and fire detection sensors, these drones offer a safer and more effective approach to modern firefighting.

Md. Ratul Ahmed Rahat, Md. Moontasir Rashid, Moloy Cgandra Dey, and Tusar Banik (2020) developed the "Safety Fire Fighter (SAFF) Robot with Dual Controlling Mechanism", a versatile firefighting robot designed to minimize fire-related damage. This multi-functional robot operates in two modes: manual and autonomous. In manual mode, a firefighter can remotely control the robot to extinguish flames using a water-based system. In autonomous mode, the robot detects fires using gas and flame sensors and responds by extinguishing the flames with carbon dioxide. The system is equipped with three Arduino boards, a GSM module, sensors, relays, servo motors, and 12V lithium polymer batteries, allowing it to navigate fire zones, avoid obstacles, and effectively suppress fires. This research presents a practical, life-saving solution for modern firefighting operations.

3. METHODOLOGY

The proposed methodology consists of several key phases:

3.1. Data Acquisition and Image Processing:

- The firefighting robot is equipped with a Pi camera to capture real-time video data. The Raspberry Pi processes this video feed using OpenCV, applying image processing techniques like thresholding to detect fire. The process includes capturing frames, converting them to the HSV color space for better fire detection, applying thresholding to create a binary mask, and detecting contours to identify fire regions. The fire's size and intensity are then analyzed to estimate fire density, triggering the suppression system if needed.

3.2. Fire Density Estimation and Actuation:

- Fire density is crucial in determining the severity of the fire. The robot calculates density by measuring the fire-like pixels in the binary mask and compares it to a predefined threshold. If the density exceeds the threshold, it activates the suction pump using a relay connected to the Raspberry Pi. This system ensures efficient water usage for suppressing the fire.

3.3. Navigation and Obstacle Avoidance:

- The robot's navigation system is powered by a motor driver, with an ultrasonic sensor used for obstacle detection. The sensor calculates the distance to nearby objects, allowing the bot to avoid collisions. The bot adjusts its path and uses fire detection data to navigate towards the source of the fire, ensuring safe and efficient movement in complex environments.

3.4. Power Management and Control:

- A 12V lead-acid battery powers the entire system. Voltage regulation is implemented to ensure that components like the Raspberry Pi, motor driver, and suction pump receive appropriate power. The system monitors the battery's charge and optimizes power distribution, prioritizing essential functions like the pump and motors during fire suppression.

3.5. System Integration and Testing:

- All components, including the Pi camera, sensors, motor driver, and suction pump, are integrated into a cohesive system. The software, including fire detection algorithms and navigation control, is deployed on the Raspberry Pi. The system undergoes rigorous testing to evaluate fire detection accuracy, response time, navigation efficiency, and obstacle avoidance. The robot is fine-tuned based on testing results to ensure reliable performance in real-world fire emergencies.

4. SYSTEM COMPONENTS

4.1. Raspberry Pi:

- The Raspberry Pi acts as the robot's brain, processing images and making decisions in real-time using Python and OpenCV. It connects seamlessly with the camera, motors, and sensors, managing everything from navigation to fire suppression. Its compact size and efficiency make it perfect for this life-saving application, ensuring quick and reliable responses to emergencies.

4.2. Pi Camera:

- The Pi Camera captures the world in real-time, providing crisp images and videos to spot fire quickly. It identifies fire by analyzing colors like red, orange, and yellow, ensuring accuracy even in tricky lighting. Lightweight and efficient, this camera works hand-in-hand with the Raspberry Pi to guide the robot toward the flames.

4.3. Ultrasonic Sensor:

- The ultrasonic sensor acts as the bot's eyes, helping it spot obstacles with precision. It works by sending out sound waves and listening for their echoes, allowing the bot to judge distances and move safely through cluttered spaces. With this smart technology, the bot can stay focused on fighting fires without getting stuck along the way.

4.4. Suction Pump and Water Nozzle:

- The pump draws water from the tank and sprays it through the nozzle directly at the flames, targeting the fire with precision controlled by the Raspberry Pi. It adjusts the water flow based on the intensity of the fire to avoid waste. This system ensures the robot can effectively douse flames, even in tight or hazardous spots.

4.5. Motor Drivers (H-Bridge Circuit):

- The motor drivers control the robot's wheels, enabling smooth movement toward the fire or around obstacles. They use an H-Bridge circuit to manage motor speed and direction, ensuring the robot moves exactly as needed. This reliable system allows the robot to navigate safely and efficiently, even in complex environments.

4.6. Power Source (12V Lead-Acid Battery):

- The 12V battery powers the entire robot, keeping it active and ready to respond during emergencies. It's designed to last through extended operations, ensuring the robot stays reliable when it's needed most. The system smartly distributes power, prioritizing critical components like the pump and motors for efficiency.

4.7. Software and Programming:

- The bot's brain runs on Python, with OpenCV handling fire detection and navigation algorithm. It processes camera feeds to detect flames, controls sensors for obstacle avoidance, and manages the water spray. With user-friendly tools like Thonny IDE, the software ensures the robot works smoothly and adapts to real-world challenges.

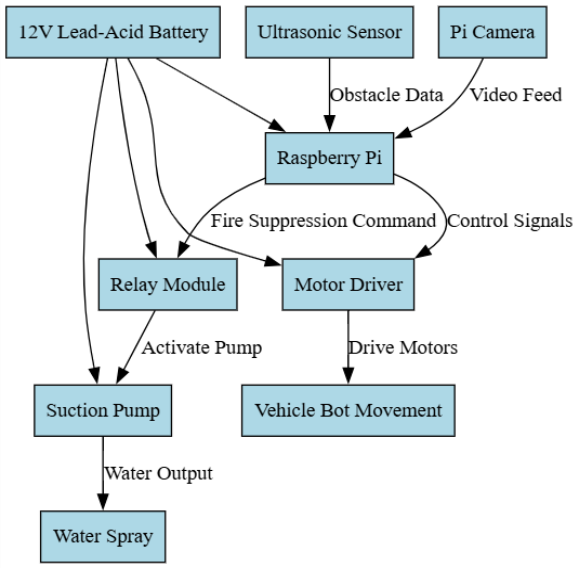

Figure 1. Firefighting Bot using Image Processing

5. CHALLENGES

5.1. Minimizing False Positives in Fire Detection:

- The system may occasionally mistake non-fire objects for fire, leading to unnecessary activation of the suction pump. To enhance accuracy and reduce false positives, advanced image processing techniques such as color filtering and motion analysis can be implemented.

5.2. Real-Time Performance & Processing Speed:

- Processing real-time video data for fire detection and navigation requires significant computational power, potentially leading to delays in responding to fires. Optimize the image processing algorithms and employ efficient data handling to ensure real-time performance, reducing the time taken for fire detection and bot navigation

5.3. Obstacle Avoidance in Complex Environments:

- The bot may struggle to navigate in environments with tight spaces or dynamic obstacles, making it difficult to reach the fire source. Enhance the ultrasonic sensor range and improve obstacle detection algorithms to better navigate through complex environments, ensuring safe and efficient movement.

5.4. Power Management for Extended Operations:

- Ensuring continuous power supply during prolonged firefighting missions, especially when the battery may deplete faster under heavy load (e.g., when the pump is operating continuously). Implement more efficient power management strategies, including dynamic power allocation and real-time battery monitoring, to ensure adequate power for critical operations.

5.5. Fire Density Estimation Accuracy:

- Accurate estimation of fire density is crucial to determine when to activate the suction pump, but detecting and quantifying fire size in dynamic conditions may be challenging. Use more sophisticated image analysis methods, such as edge detection and machine learning-based recognition, to improve fire density estimation and reduce errors in triggering suppression mechanisms.

6. RESULT

The development of an autonomous firefighting robot integrating Raspberry Pi, Pi Camera, and advanced image processing techniques marks a significant advancement in fire safety. This system leverages OpenCV to detect fires in real-time by analyzing visual characteristics like brightness and color intensity. The bot also estimates fire density, ensuring its response is proportional to the situation. By combining robotics, IoT, and computer vision, this project addresses the critical need for rapid and precise fire suppression while reducing risks to human life. The robot's hardware components enable it to perform complex tasks effectively.

A suction pump powers the water spray system for targeted fire extinguishing, while a relay module and motor driver ensure smooth operation and movement. An ultrasonic sensor allows the bot to navigate obstacles and maneuver through challenging environments autonomously. A 12V lead-acid battery provides reliable power for extended operations, making the system suitable for diverse settings, including homes, factories, and commercial spaces.

7. FUTURE WORK

The firefighting robot has immense potential for growth and improvement. In the future, it could be enhanced with advanced sensors like thermal cameras, allowing it to detect fires more accurately, even in smoke-filled or low-visibility conditions. Adding wireless communication would enable remote monitoring and control, making it ideal for hazardous or hard-to-reach areas. With the integration of machine learning, the robot could make smarter decisions, adapting its navigation and fire suppression techniques based on real-time conditions.

Scaling up the design to create larger robots or even drones could extend its use to industrial sites and forest fire emergencies. For long-term efficiency, exploring solar-powered or hybrid energy solutions could make the system more sustainable. With these advancements, the firefighting robot could become a highly intelligent and adaptable tool, transforming the way we approach fire safety.

8. REFERENCE

[1] Pramod B. N., Hemalatha K. N., Poornima B. J., Harshitha R. (2019). Fire Fighting Robot. Presented at the International Conference on Information and Communication Technology Convergence (ICTC).

[2] Jayanth Suresh (2017). Fire-Fighting Robot. Presented at the International Conference on Computational Intelligence in Data Science (ICCIDS).

[3] Krishan Arora, Harshit Kumar, Rohit Raj Singh (2023). Autonomous Fire Fighting Robot. Presented at the International Conference on Computational Intelligence, Communication Technology, and Networking (CICTN).

[4] Sugumar D., Ramadevi R., Prasad J., Mohankumar N., Joy Winnie Wise D.C., and Velmurugan S. (2024). A Distributed Data Mining and Cloud Analysis for Predictive Gas Level, Dynamic Booking, and Smart Energy Optimization. Published in IEEE Xplore (Electronic ISBN: 979-8-3503-64828). DOI:10.1109/ADICS58448.2024.10533470.

[5] Yiying Yuan (2021). Technical Research on Fire-Fighting Robotics. Presented at the IEEE Asia-Pacific Conference on Image Processing, Electronics, and Computers (IPEC).

[6] Prasad J., Kasiselvanathan M., Lakshminarayanan S., Sekar G., and Azath H. (2023). Application of Machine Learning for Malicious Node Detection in IoT Networks. Published in IEEE Xplore (Electronic ISBN: 978-1-6654-9260-7).
DOI: 10.1109/IITCEE57236.2023.10091042.

[7] Prasad J., Menaga K.G., Manikanda Prasanna C., and Jithesh K. (2022). Priority-Based Prepaid Energy Meter Using IoT. Presented at the IEEE Xplore Conference (Electronic ISBN: 978-1-6654-0816-5).
DOI: 10.1109/ICACCS54159.2022.9785053.

[8] Md. Ratul Ahmed Rahat, Md. Moontasir Rashid, Moloy Chandra Dey, Tusar Banik (2020). Design and Implementation of a Safety Fire Fighter (SAFF) Robot with Dual Controlling Mechanism. Presented at the IEEE Region 10 Symposium (TENSYMP).

[9] Shiva Mittal, Manish Kumar Rana, Mayank Bhardwaj, Meenakshi Mataray, Shubham Mittal (2018). CeaseFire: The Fire Fighting Robot. Presented at the International Conference on Advances in Computing, Communication, Control, and Networking (ICACCCN).

[10] Md. Anowar Hossain, Himaddri Shakhar Roy, Md. Fazlul Karim Khondakar, Md. Hasib Sarowar, Md. Azad Hossainline (2021). Design and Implementation of an IoT-Based Firefighting and Affected Area Monitoring Robot. Presented at the 2nd International Conference on Robotics, Electrical, and Signal Processing Techniques (ICREST).

Numerical Analysis of All Inorganic Perovskite Tandem Solar Cell with PCE of 24.47 %

Mukesh Bharadwaj, DeborajMuchahary

Dept. Of Electronics and Communication Engineering,

National Institute of Technology Raipur, Chhattisgarh, India.

mbharadwaj.mtech2023.etc@nitrr.ac.in, dmuchahary.ece@nitrr.ac.in

Abstract.

All-perovskite tandem solar cells (APTSCs) provides a strong pathway for exceeding the performance of conventional solar cellswhile maintaining low fabrication costs. This study presents a numerically designed APTSC using SCAPS-1D, featuring an inverted p-i-n configuration with a top cell of ITO/NiOx/$CsPbI_2Br$/ZnO/Au and a bottom cell of ITO/PEDOT:GO/Cs_2SnI_6/GO(graphene oxide)/Ag. The design leverages all-inorganic perovskites—$CsPbI_2Br$ (1.78 eV) and lead-free Cs_2SnI_6 (1.48 eV) —to enhance stability and efficiency. Through precise current matching, the proposed TSC achieves a maximum PCE of 24.47%, exceeding the experimentally reported 21.92%. Analysis of bulk defect density (10^{10} cm^{-3}) yields a bottom cell PCE of 21%, with a current density of 11.83 mA cm^{-2}, open-circuit voltage, V_{OC} of 1.21 V, and fill factor of 84.7%, while interface defects (10^{10} cm^{-2}) result in a PCE of 17.17%. The device operates optimally at 300 K, with layer thicknesses compatible with experimental fabrication. This work highlights the potential of all-inorganic APTSCs to deliver high efficiency and durability.

Keywords. Tandem, PCE, APTS, Spectrum, SCAPS-1D.

1. INTRODUCTION

Solar cells are sustainable source of green energy harvesting. Due to the SQE limitations of theoretical PCE of 34% associated with single-junction solar devices[1], researchers identified that tandem solar cell (TSCs)having multiple bandgap is the right approach to increase the PCE [2][3][4][5].Among these, all-perovskite tandem solar cells (APTSCs) have garnered significant attention [6]. Cesium lead halides ($CsPbX_3$, where X = I, Br, Cl)have surfaced as viable contenders for the PV technology.[7][8][9]. Chenghao Duan et al. A ligand evolution approach using p-toluenesulfonyl hydrazide reported efficiency of 17.41% for a 1.31 eV $CsPb_{0.4}Sn_{0.6}I_3$:LE device and a champion efficiency of 22.57% for 2T IPTSC with top cell as $CsPbI_2Br$[10]. A. Chouhan et. al. established a standalone Cs_2SnI_6 based solar cell reported a PCE of 22.59 %[11].Qiu et al. reported a Cs_2SnI_6-based perovskite with E_G(1.48 eV) reported efficiency of 1%[12],Xiaofeng et al. reported a Cs_2SnI_6 perovskite solar cell (PSC) using ZnO as the ETL, demonstrating an efficiency of 0.857%, with inorganic absorber layers, ETL-ZnO, and HTL P3HT[13], Jun et al. observed $Cs_2SnCl_{6-x}Br$-based photodetectors[14].

In this study, an all-perovskite tandem solar cell (APTSC) is modelled using SCAPS-1D, with ITO/NiO_x/$CsPbI_2Br$/ZnO/Au as the top cell and ITO/PEDOT:GO/Cs_2SnI_6/GO/Ag as the bottom cell, both in an inverted p-i-n configuration. The APTSC's performance is optimized through current matching, and its performance is analyzed.

2. Methodology

In this study, the schematic of proposed device structure is shown in Figure 1. The simulation is conducted using SCAPS-1D software[15], which is based on Poisson's equation.

$$-\frac{\partial}{\partial \mathrm{x}}\left(-\partial(x)\frac{\partial \mathrm{V}}{\partial \mathrm{x}}\right)=\mathrm{q}[\mathrm{h}(\mathrm{x})-\mathrm{e}(x)+\mathrm{N_D^+}(x)-\mathrm{N_A^-}(x)+\mathrm{h_t}(x)-\mathrm{e_t}(x)] \quad (1)$$

The proposed device structure employs ITO/NiOx/$CsPbI_2Br$/ZnO/Au as top cell and ITO/PEDOT:GO/Cs_2SnI_6/GO(Graphene Oxide)/Ag as bottom cell.

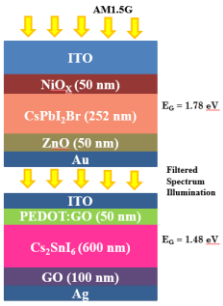

Figure.17. Schematic of Tandem Solar Cell.

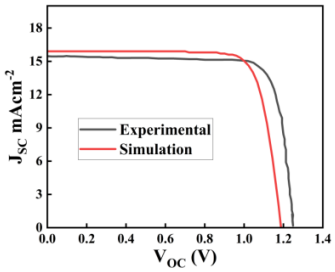

Figure.2. Matched JV-Curve of top cell with experimental data.

2.1. Calibration to experimental device.

At the beginning the modelled bottom cell is calibrated with a similar experimental device reported in the literature[10] as shown in Figure.2. The slight variation in J_{SC} and V_{OC} may be due to non-availability of exact materials properties used in the simulation.

3. Results and Discussions

The Design of Tandem Solar cell is done, Firstly, the bottom cell which is optimized for its best performance by evaluating the condition for both bulk and interface defect density.

3.1. Design of Tandem Solar cell.

The TSC is modelled by matching the current in both top cell and bottom cellsThe filter spectrum is calculated using Beert lamberet law as given in eq.2.

$$S_{Filtered}(\lambda) = S_{Incident}(\lambda) * exp\{\sum_{p=1}^{4} -(\alpha_{Material}(\lambda) * d_{Materialp})\} \quad (2)$$

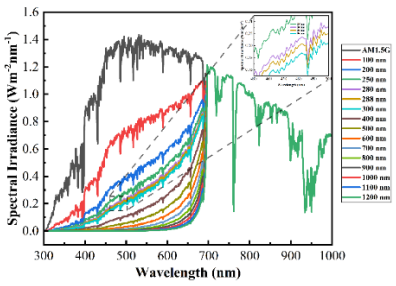

Figure.4. Matched JV-Curve of top cell with experimental data

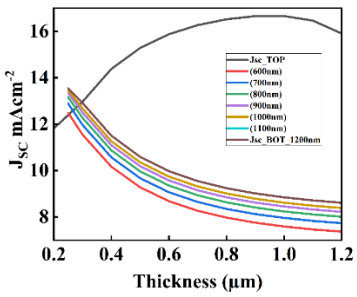

Figure.5. Standard transmitted spectrum from the top cell for absorber thickness from 600 to 1200 nm

The J_{SC} matching thickness for WBG is found to be 252 nm and NBG is 600 nm at 12.44 $mAcm^{-2}$. The designing of TSC is carried out by calculating Filter Spectrum from 200 nm to 1200nm of WBG absorber. The performance of tandem configuration J_{SC}, V_{OC}, FF % and PCE % is obtained as 12.11 $mAcm^{-2}$, 2.25 V, 79.74 %, 24.47 % for the proposed device structure showcasing maximum PCE of 24.47 %.

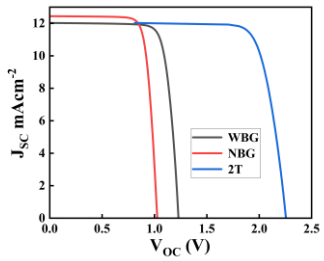

Figure.6. J-V curve of standalone tandem cell.

Table.2. Performance Parameters of Proposed APTSC.

Parameters	J_{SC} (%)	V_{OC} (%)	FF (%)	PCE (%)
Top Cell	12.02	1.22	79.26	13.15
Bottom Cell	12.44	1.02	79.54	17.55
Tandem	12.11	2.25	79.74	24.47
Experimental[10]	14.57	1.90	81.44	22.57

4. Conclusion

Upon comparison of power conversion efficiency the PSC of proposed TSC is 24.47 % which is higher compared to experimentally reported PCE i.e. 21.92 %[10]. Upon the analysis of Bulk defect density, the maximum performance of all the SC parameters are obtained at 10^{10} cm^{-2} while interface defect is observed to be maximum at 10^{10} mAcm^{-2}. The spectrum range is analyzed within the visible spectrum range. The thickness of both the LA aligns within the boundary of experimental findings making it suitable for fabrication analysis.

5. references

[1] S. Sharma, S. Basu, N. P. Shetti, and T. M. Aminabhavi, "Waste-to-energy nexus for circular economy and environmental protection: Recent trends in hydrogen energy.," *Sci. Total Environ.*, vol. 713, p. 136633, Apr. 2020, doi: 10.1016/j.scitotenv.2020.136633.

[2] F. Jiang *et al.*, "A two-terminal perovskite/perovskite tandem solar cell," *J. Mater. Chem. A*, vol. 4, no. 4, pp. 1208–1213, 2016, doi: 10.1039/C5TA08744A.

[3] J. H. Heo and S. H. Im, "CH3NH3PbBr3–CH3NH3PbI3 Perovskite–Perovskite Tandem Solar Cells with Exceeding 2.2 V Open Circuit Voltage," *Adv. Mater.*, vol. 28, no. 25, pp. 5121–5125, Jul. 2016, doi: https://doi.org/10.1002/adma.201501629.

[4] A. Rajagopal *et al.*, "Highly Efficient Perovskite–Perovskite Tandem Solar Cells Reaching 80\% of the Theoretical Limit in Photovoltage," *Adv. Mater.*, vol. 29, 2017, [Online]. Available: https://api.semanticscholar.org/CorpusID:205281011

[5] G. E. Eperon *et al.*, "Perovskite-perovskite tandem photovoltaics with optimized band gaps.," *Science*, vol. 354, no. 6314, pp. 861–865, Nov. 2016, doi: 10.1126/science.aaf9717.

[6] D. Zhao *et al.*, "Efficient two-terminal all-perovskite tandem solar cells enabled by high-quality low-bandgap absorber layers," *Nat. Energy*, vol. 3, no. 12, pp. 1093–1100, 2018, doi: 10.1038/s41560-018-0278-x.

[7] I. M. Maafa, "All-Inorganic Perovskite Solar Cells: Recent Advancements and Challenges," 2022. doi: 10.3390/nano12101651.

[8] J. Duan *et al.*, "Inorganic perovskite solar cells: an emerging member of the photovoltaic community," *J. Mater. Chem. A*, vol. 7, no. 37, pp. 21036–21068, 2019, doi: 10.1039/C9TA06674H.

[9] B. Li *et al.*, "Surface passivation engineering strategy to fully-inorganic cubic CsPbI3 perovskites for high-performance solar cells," *Nat. Commun.*, vol. 9, no. 1, p. 1076, 2018, doi: 10.1038/s41467-018-

03169-0.

[10] C. Duan *et al.*, "Durable all-inorganic perovskite tandem photovoltaics," *Nature*, vol. 637, no. 8048, pp. 1111–1117, 2025, doi: 10.1038/s41586-024-08432-7.

[11] A. Chauhan, A. Oudhia, and A. K. Shrivastav, "Analysis of eco-friendly tin-halide Cs2SnI6-based perovskite solar cell with all-inorganic charge selective layers," *J. Mater. Sci. Mater. Electron.*, vol. 33, no. 3, pp. 1670–1685, 2022, doi: 10.1007/s10854-022-07723-x.

[12] Y. Jiang, H. Zhang, X. Qiu, and B. Cao, "The air and thermal stabilities of lead-free perovskite variant Cs2SnI6 powder," *Mater. Lett.*, vol. 199, pp. 50–52, 2017, doi: https://doi.org/10.1016/j.matlet.2017.04.046.

[13] H. Kumar, P. Verma, and B. Raj, "Design and Analysis of Lead-Free Tin-Halide-Based All-Inorganic Perovskite Solar Cell for High Efficiency," *Nano*, vol. 18, no. 07, p. 2350049, May 2023, doi: 10.1142/S1793292023500492.

[14] X. Qiu *et al.*, "Lead-free mesoscopic Cs2SnI6 perovskite solar cells using different nanostructured ZnO nanorods as electron transport layers," *Phys. Status Solidi - Rapid Res. Lett.*, vol. 10, no. 8, pp. 587–591, 2016, doi: 10.1002/pssr.201600166.

[15] M. Burgelman, K. Decock, S. Khelifi, and A. Abass, "Advanced electrical simulation of thin film solar cells," *Thin Solid Films*, vol. 535, pp. 296–301, May 2013, doi: 10.1016/j.tsf.2012.10.032.

Biographies



Mukesh Bharadwaj B.Tech (BIT Durg), Currently final year student, pursuing M.tech in (VLSI & Embedded systems engineering) at NIT Raipur. Project area: All perovskite Tandem Solar Cell.



Dr. Deboraj Muchahary pursued his Ph.D from (NIT Arunachal), M. Tech (NIT Arunachal) and B. Tech (CIT Kokrajhar) currently he is working as Assistant professor in Dept. Of Electronics and communication engineering at NIT Raipur, his Research area mainly include Silicon and Perovsskite solar cell, Semiconductor device simulation, VLSI.

Voice Controlled Maze Game

Dr.Hindumathi Voraganti, Joshitha Sathinedi, Jahnavi Majji, Rishika Pawar, Azra Gulnaz

BVRIT Hyderabad College of Engineering for Women

Abstract.

The Voice-Controlled Maze Game lets players navigate a virtual maze using speech recognition, providing real-time feedback and guidance. It enhances accessibility and showcases the potential of voice interfaces in interactive entertainment.

1. INTRODUCTION

By using voice recognition and auditory feedback in place of manual controls, the Voice-Controlled Maze Game in MATLAB improves accessibility and user engagement. For all participants, it fosters independence, inclusion, and problem-solving skills.

2. LITERATURE SURVEY

Developments in digital signal processing, game design, and speech recognition are all expanded upon in the Voice-Controlled Maze Game. The theoretical underpinnings for putting voice commands into practice are provided by Juang & Rabiner (1993), while Chan & Chong (2015) present a MATLAB-based framework for real-time speech recognition. Digital signal processing methods that are crucial for managing voice signals, like filtering and spectrum analysis, are examined by Manolakis & Proakis (2006). Furthermore, described in MathWorks' MATLAB Speech Processing Tools Reference (2023) is the Audio Toolbox, which facilitates smooth voice interaction by allowing real-time speech-to-text conversion.

Accessibility and game design are also important factors. Interactivity, feedback mechanisms, and usability guidelines that improve the maze game's design are covered by Salen & Zimmerman (2004). To increase accessibility for players with disabilities, Yuan & Folmer (2008) emphasize non-traditional interfaces including voice and tactile feedback. Voice-controlled game interface usability is examined by Brown & Roberts (2018), which informs the project's user-centered methodology. The game seeks to give all players an enjoyable and inclusive experience by utilizing these findings.

3. METHODOLOGY

The Voice-Controlled Maze Game adheres to a methodical approach that emphasizes system architecture, tools, strategies, and execution. Key components of the system include voice command processing, which captures and analyses user speech, maze representation, which defines walls and paths using a 2D matrix, and a game engine, which modifies player movement in response to recognized orders. Numerical calculations, audio processing, and visualization are all done with MATLAB. Voice inputs are converted into standardized text using the speech2text function, and accuracy is increased by preprocessing methods including spectrogram analysis and Mel Frequency Cepstral Coefficients (MFCCs). Recognition models such as Hidden Markov Models (HMMs) and Deep Neural Networks (DNNs) process speech, enabling real-time command execution. With three difficulty settings—easy, medium, and hard—the maze is dynamically updated and visually represented in response to player input.

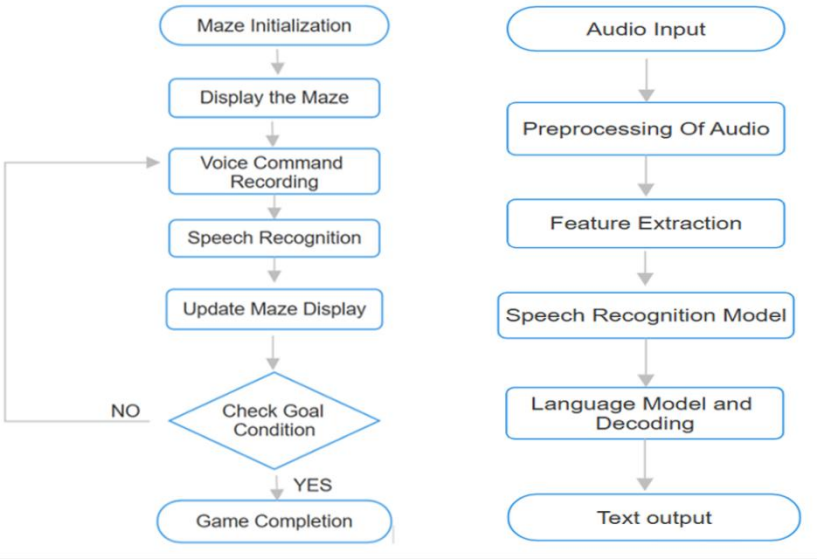

Fig. 1 Flow Chart of the game

Fig. 2 Flow Chart of Speech Recognition

The game is executed in a methodical manner, beginning with the initialization of the maze, which sets the start, goal, barriers, and paths. Voice commands like "up" and "left," which are captured by a microphone and processed by pattern recognition and language models for precise interpretation, are used by players to traverse the maze. The player's location is continuously updated by the system, which also verifies if the goal has been completed. The player stays motionless and receives remedial feedback if a command is deemed invalid. To guarantee an intuitive experience, the game provides dynamic graphics, error management, real-time interaction, and accessibility improvements. Unit testing of functions, edge case scenarios such as erroneous commands, and movement limits are all part of the testing and validation process to guarantee robustness. The game is deemed finished when the player achieves the objective, providing an interesting and participatory experience.

4. RESULTS

The voice-controlled maze game exhibited effective responsiveness, as players effectively navigated the increasing complexity of the game as they progressed through the difficulty levels.

Below are the results of the easy level voice controlled maze game:

Movements of the player from start (green block) to end (red block)

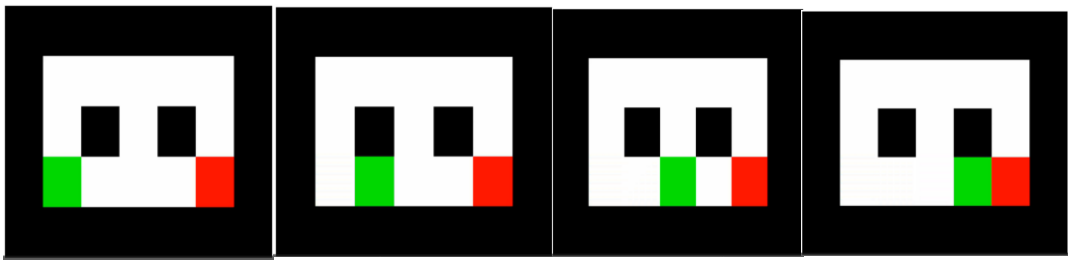

Fig. 3. Movement of the player towards the goal (red block)

By limiting wall collisions and providing feedback for commands that were deemed invalid, logical navigation was guaranteed. The results confirm the reliability of the voice-based controls and the degree of engagement of the game.

```
Please say your command ("up", "down", "left", or "right")
    "Recognized Command:"    "right"
```

Fig. 5. Commands that can be given by the user and the recognized command

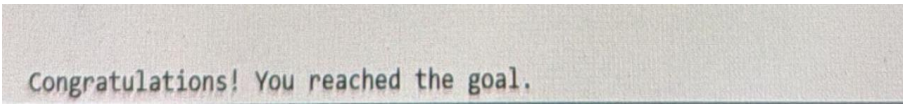

Fig. 6 . Maze Completion message (Displayed when player reaches the goal)

5. CONCLUSION

This project mixes interactive gameplay with voice recognition technology, allowing players to navigate a maze through voice instructions. By eliminating the need for traditional input devices such as keyboards and controllers, it provides a more natural and accessible experience, which is especially beneficial to people with disabilities.

Advanced speech recognition can enhance the game's capacity to understand different accents, making it more accessible to a global audience. Customizable voice commands can improve personalization, and multiplayer modes.

6. REFERENCES

[1] K. V. Sainadh, K. Satwik, V. Ashrith, and S. Vekkot, "Playing Maze using Voice Commands," *2023 14th International Conference on Computing Communication and Networking Technologies (ICCCNT)*, Delhi, India, 2023, pp. 1-7.

[2] J. P. Piotrowski, E. A. Yfantis, A. Campagna, Q. Cornu, and G. M. Gallitano, "Voice Interactive Games," *2019 IEEE 10th Annual Ubiquitous Computing, Electronics & Mobile Communication Conference (UEMCON)*, New York, NY, USA, 2019, pp. 780-784.

[3] R. Kumar and S. Patel, "MATLAB Applications in Voice-Controlled Gaming," in *Voice Interaction in Gaming: Theory and Applications*, 1st ed., Springer, 2018, pp. 123-140.

[4] M. L. Garcia and S. Singh, "Interactive Maze Game Design Using Voice Commands," *Proceedings of the IEEE International Conference on Game Design and Development*, San Francisco, CA, USA, 2020, pp. 142-149.

[5] A. Kumar, N. Shah, and S. Patel, "Voice-Activated Interactive Maze for Children with Disabilities," *2021 IEEE International Conference on Assistive Technology (ICAT)*, Chicago, IL, USA, 2021, pp. 85-90.

[6] P. Zhang, S. Liu, and L. Wang, "Implementing Speech Recognition in MATLAB for Real-Time Game Control," *IEEE International Conference on Artificial Intelligence and Games*, Boston, MA, USA, Nov. 2020, pp. 105-110.

[7] M. K. Chauhan and R. Tiwari, "Speech-Based Control System for Interactive Maze Game," *Proceedings of the IEEE International Workshop on Smart Computing & Communication Systems*, 2021, pp. 92-96.

Biographies



Dr. Hindumathi Voraganti received the B.Tech. degree in electronics and communication engineering from the Jawaharlal Nehru Technological University, Hyderabad, India, in 2003 and the M.Tech. degree in Wireless and Mobile Communications from the Jawaharlal Nehru Technological University, Hyderabad, India, in 2008. She received Ph.D. degree in Electronics and Communication Engineering from Jawaharlal Nehru Technological University, Hyderabad, India, in 2021. Presently working as an associate professor at BVRIT HYDERABAD College of Engineering for Women, Hyderabad. Her research interests are in the area of Wireless communications and networks.



Joshitha Sathinedi is pursuing B. Tech in Electronics and Communication Engineering at BVRIT Hyderabad College of Engineering for Women, Hyderabad, Telangana, India and will graduate in 2025.



Jahnavi Majji is pursuing B. Tech in Electronics and Communication Engineering at BVRIT Hyderabad College of Engineering for Women, Hyderabad, Telangana, India and will graduate in 2025.



Rishika Pawar is pursuing B. Tech in Electronics and Communication Engineering at BVRIT Hyderabad College of Engineering for Women, Hyderabad, Telangana, India and will graduate in 2025.



Azra Gulnaz is pursuing B. Tech in Electronics and Communication Engineering at BVRIT Hyderabad College of Engineering for Women, Hyderabad, Telangana, India and will graduate in 2025.

Accident Severity Prediction Using Machine Learning Techniques

S.V.V.Sai Kalyan, Shaik Mohammed Saif, Dr. Shanthi Thangam Manukumar

Sathyabama Institute of Science and Technology, mshanthithangam@gmail.com

Abstract.

Motor car accidents are the main purpose of death, incapacity, and hospitalization within the United States. Reducing street accidents and human casualties is vital. With this goal in thoughts, several techniques had been proposed, starting from vintage statistical models to new strategies stimulated with the aid of the advent of device getting to know. This research paper affords a comparative examination of numerous such models, aiming to analyse and derive a green method to predicting avenue twist of fate dangers. The aim of this observe is to expect the danger of injuries on the street by analysing elements which include vehicle type, age, gender, time of day, and climate earlier. Drivers display avenue conditions. In addition, reading geolocation facts the use of a good clustering algorithm allows us to examine wherein accidents occur. By reading the elements already diagnosed the use of these techniques, drivers attain estimates of the possibility of injuries, which enables them to make informed picks to lessen them. The purpose of this challenge is to increase the predictions of site visitors on the website and analyse road accidents.

Keywords. Machine Learning, Decision Tree, Random Forest, Logistic Regression, Road Accidents, Vehicle Safety, Climate.

1. INTRODUCTION

Energy With so many motors on the streets each day, street accidents can show up every time, anywhere. Some accidents are deadly, which means human beings die in accidents. As a human, everyone wants to stay accurately without getting harm. By applying statistics mining methods to the whole avenue harm dataset, we can advantage valuable insights into a way to drive accurately and offer tips to drivers. Data mining uses a wide variety of strategies and algorithms to discover relationships in large-scale facts. It has been taken into consideration one of the maximum vital gears within the IT business enterprise for decades. Association rule mining algorithm [2] is a famous set of policies to pick out meaningful relationships between information stored in a huge database, and it regularly plays a completely crucial role in content material mining. A common place approach for locating affiliation guidelines is a priori rule set, whose principal goal is to find common item sets that is the technique used for traffic data mining. One of the main probabilistic techniques of this type is Naive Bayes, which is specifically based on Bayesian hypothesis. For our study, we used the FARS dataset. This deadly crash dataset contains all deadly site visitors' crashes suggested via the National Highway Traffic Safety Administration in 2007. This dataset becomes downloaded from California Polytechnic State University and all the facts changed into acquired from FARS. This dataset has 37,248 statistics factors and fifty-five features. A description of the statistics may be found within the FARS report.

2. RELATED WORK

The Apriori set of rules is the maximum popular and efficient algorithm for association rule mining. This is because affiliation rule is utilized in all the modern-day global business and industrial tasks in data processing. The aim of the use of Apriori is often to stumble on devices and discover hidden records. The very last distinction is among a priori and a priori predictive algorithms, wherein a priori prediction is greater accurate and quicker than a priori [1]. Association rule mining algorithms are broadly used to locate all guidelines in a database that satisfy minimal nice assist and self-assurance constraints. To lessen the huge variation of generated regulations, preceding research have used a membership rule mining set of rules to extract an easy finite subset of affiliation policies, relationships among random components and twist of fate severity tiers have been explored the use of a priori strategies [2]. Data mining extracts hidden styles from massive databases. It is usually used in marketing and advertising, surveillance, fraud detection, and medical discovery. To classify the injury severity elegance of various road incidents, I compare the naive Bayes classifier, the AdaboostM1 met classifier, the component rule classifier, the J48 choice tree classifier, and the random wooded area classifier

[3]. Road accidents are one of the most important areas of research in India. There is many research on statistics gathered from police facts regarding precise sections of two-lane roads. Statistics mining strategies to explore the statistics provided via EMRI, wherein we first divide the matching statistics into clusters to the results are used to take coincidence prevention measures in areas diagnosed for specific types of injuries to reduce the wide variety of accidents [4]. The clusters generated via K-tunes and estimate maximization algorithms are analyzed to extract latent styles the use of apriori algorithms. The implications of this demonstration display that the chosen device mastering strategies can extract hidden styles from the information. Density histograms are used to visualize the twist of fate facts [5].

3. RESEARCH METHODOLOGY

Classification models to are expecting the severity of damage in avenue person accidents. Based at the statement rule inversion dataset accrued from the State Transportation affiliation rule mining algorithm, a priori and predictive club rule algorithms have been carried out at the dataset to track the connection between the desired crashes and the components that affect the crash severity. The information accrued on street fatalities is very significant, multifaceted and heterogeneous. The purpose of this work as shown in figure 3.1 is to expand the evaluation competencies of observers, avenue twist of fate analysis and navigation visualization. It can be used to create a first-class itinerary that connects all key locations so that passengers feel safe at any factor in their journey. This paper modeling the severity of harm in avenue traffic accidents the use of synthetic neural networks and decision bushes. Based on real global facts acquired from the General Assessment System (GES) of the National Automobile Sampling System (NASS). Experimental consequences display that the choice tree performs better than the neural network in all instances. In our take a look at, it was also determined that the motive force's seat belt use, avenue situations and driver alcohol consumption are the three most crucial elements for deadly injuries. Our tests showed that this version performs a far extra critical role in dangerous and deadly accidents than in different instructions. Since driving force deaths cause large economic and social losses to society, it's miles critical to evaluate the danger of fatal and extreme accidents.



Figure 3.18. Proposed System Architecture of Accident Severity Prediction

The facts about series module, twist of fate data is collected from the Cargill. For instance, the year, month, United States of America, time of the programming language. In this module, someone specifies a selected characteristic, from which an estimate of its accident impact is decided. The education dataset is analyzed the use of the assist vector kind and a user-described characteristic. The report web page allows you to talk with the website administrator via reporting the recent recognition of fatalities and houses even as traveling on the selected path. This report is sent to the database occasions desk, in which its miles are demonstrated and displayed by means of the administrator, and several fields in the database are up to date to create a valid document. Finally, it affords accurate records approximately traffic accidents with the aid of nation.

4. RESULTS AND DISCUSSIONS

The experimental consequences display that choice trees continually outperform neural networks in all cases, highlighting their effectiveness in processing categorized facts and identifying key choice thresholds. The evaluation identified three important elements contributing to fatal accidents, driver seat belt use, avenue lighting fixtures conditions, and motive force alcohol consumption. Furthermore, the model accomplished excellently in distinguishing among deadly and non- deadly injuries, that is especially critical given the vast financial and social fees related to motive force fatalities.

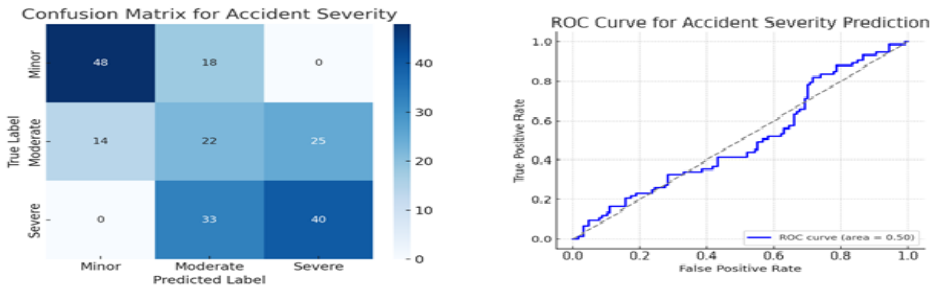

Figure 4.19. Confusion Matrix and Roc Curve

Confusion matrix shows how well the model predicts accident severity. The rows represent the actual accident severity (Minor, Moderate, Severe), while the columns represent the predicted severity. The ROC (Receiver Operating Characteristic) curve evaluates the model's ability to distinguish between severe and non-severe accidents. The X-axis (False Positive Rate) measures how often the model incorrectly predicts a severe accident when it isn't. The Y-axis (True Positive Rate) measures how well the model correctly identifies severe accidents. The AUC (Area Under Curve) value indicates performance—closer to 1 means better prediction ability. The Above ROC (Receiver Operating Characteristic) curve evaluates the model's ability to distinguish between severe and non-severe accidents. The results of Confusion Matrix and Roc Curve are as shown in Figure 4.1.

5. CONCLUSION

The affiliation's analysis of guidelines and publications indicates, environmental factors together with road floor, climate, and lights do now not have a first-rate impact on fatality quotes, not like human elements such as alcohol consumption or kind of collision. High effect on fatality costs. From the aggregation results, we see that a few states/territories have excessive fatality rates, while others have low fatality prices. The extra information about fatality statistics, climate records, mileage information, etc., can do more checks, because of this may draw greater conclusions from the records. The proposed methodology gives improved results than the existing system.

6. REFERENCES

[1] Fu, X.; Meng, H.; Wang, X.; Yang, H.; Wang, J. A hybrid neural network for driving behavior risk prediction based on distracted driving behavior data. PLoS ONE 2022, 17.

[2] Mukherjee, D.; Mitra, S. Pedestrian safety analysis of urban intersections in Kolkata, India using a combined proactive and reactive approach. J. Transp. Saf. Secur. 2022, 14, 754–795.

[3] Jeong, H.; Kim, I.; Han, K.; Kim, J. Comprehensive Analysis of Traffic Accidents in Seoul: Major Factors and Types Affecting Injury Severity. Appl. Sci. 2022, 12, 1790.

[4] Yang, Z.; Zhang, W.; Feng, J. Predicting multiple types of traffic accident severity with explanations: A multi-task deep learning framework. Saf. Sci. 2022.

[5] Wang, J.; Lu, H.; Sun, Z.; Wang, T.; Wang, K. Investigating the Impact of Various Risk Factors on Victims of Traffic Accidents.Sustainability 2020, 12, 3934.

[6] Elassad, Z.E.A.; Mousannif, H.; Al Moatassime, H. Class-imbalanced crash prediction based on real-time traffic and weather data:A driving simulator study. Traffic Inj. Prev. 2020, 21, 201–208.

[7] Banerjee, K.; Bali, V.; Sharma, A.; Aggarwal, D.; Yadav, A.; Shukla, A.; Srivastav, P. Traffic Accident Risk Prediction Using MachineLearning. In Proceedings of the 2022 International Mobile and Embedded Technology Conference (MECON), Noida, India,10–11 March 2022; pp. 76–82.

[8] Moghadam Gilani, V.N.; Hosseinian, S.M.; Ghasedi, M.; Nikookar, M. Data-Driven Urban Traffic Accident Analysis and Prediction Using Logit and Machine Learning-Based Pattern Recognition Models. Math. Probl. Eng. 2021, 2021, 1–11.

Biographies



Mr. S.V.V.Sai Kalyan, a student of B.E. degree in the specialization of CSE with AIML, in Sathyabama Institute of Science and Technology, Chennai. . His research interests are in the area of Artificial Intelligence and Machine Learning and Optimization Algorithms



Mr. Shaik Mohammed Saif, is a student of B.E. degree in the specialization of CSE with AIML, in Sathyabama Institute of Science and Technology, Chennai. His research interests are in the area of Artificial Intelligence and Machine Learning and Optimization Algorithms.



Dr. Shanthi Thangam Manukumar is currently working as Assistant Professor in Sathyabama Institute of Science and Technology. She completed Ph.D. degree in Network Engg., at College of Engineering Guindy, Anna University, Chennai. She received her M.E. degree in Network Engineering from Anna University Coimbatore and B.E. degree in CSE, Anna University. Her research interests are in the area of Cloud Computing, Computer Networks, and AI. She has been serving as a reviewer for many highly-respected journals.

Design and Analysis of a CPW-Fed Dual-Band Antenna for Sub-1 GHz and Sub-6 GHz Applications

E.Suganya[1], T. Anita Jones Mary Pushpa[2], T.Prabhu[3]

[1]*Research Scholar, Department of ECE, Karunya Institute of Technology and Sciences, Coimbatore, India* suganyae@karunya.edu.in

[2]*Department of ECE, Karunya Institute of Technology and Sciences, Coimbatore, India* Sree.20211ECE0113@presidencyuniversity.in

[3]*Department of ECE, Presidency University, Bengaluru, India* prabhu@presidencyuniversity.in

Abstract

This paper presents a newly designed square-shaped multiband antenna optimized for sub 1GHz and sub 6GHz 5G applications. The suggested antenna is specifically designed on a commonly used FR4 substrate material characterized by an effective relative permittivity value (ε_r) of 4.4 and a dielectric loss tangent of 0.02. The total dimensions of the substrate are 110mm in length (Ls), 90mm in width (Ws), and 1.52mm in height (h). The proposed design functions efficiently in two key frequency bands, while the lower operating frequency band broadly spans from 0.91 GHz to 1.41 GHz, and the higher operating frequency band broadly spans from 3.11 GHz to 4.48 GHz. Performance evaluations reveal that the antenna The findings suggest that this antenna can enhance multiband 5G applications, making it a strong contender for next-generation wireless communication systems. The design's multiband functionality and high gain characteristics are particularly advantageous for meeting the diverse requirements of modern 5G networks, ensuring reliable and efficient signal transmission across different frequency ranges.

Keywords. Square Patch, multiband, FR4 substrate, 5G networks, strip

1. INTRODUCTION

As modern communication technologies continue to advance rapidly, there is an increasing need for compact antennas capable of supporting dual- and multi-band operations within a single device across various wireless frequency bands. Microstrip-based dual-band antennas have been extensively explored, particularly for wireless standards such as IEEE WiMAX standard at 3.5 GHz (3.3–3.7 GHz) and wireless WLAN technology at 2.4 GHz (2.4–2.483 GHz) [1]. Numerous antenna structures have been developed to achieve multi-band behaviour, including inverted-F antennas (IFA) [2], designs inspired by metamaterials using split-ring resonators (SRRs) [3], and configurations incorporating defected ground structures (DGS) [4]. Despite their potential, these designs often face drawbacks such as increased physical size, fabrication complexity, and issues related to mutual coupling. To overcome these challenges, asymmetric coplanar strip (ACS)-fed monopole antennas have emerged as compact and efficient alternatives, well-suited for both WLAN and WiMAX applications [5]. While ACS-fed antennas provide dual-band operation with a smaller footprint, their unbalanced feeding structure sometimes results in asymmetrical radiation pattern. Alternatively, the coplanar waveguide (CPW) feeding technique has gained significant interest due to its advantages, such as low profile, reduced surface wave effects, ease of fabrication, and improved impedance matching [6]. Compared to conventional feeding methods like microstrip and coaxial probe feeding, CPW offers enhanced isolation from the feeding network, making it highly suitable for multi-band applications. Multi-band operation in antennas is typically achieved by modifying the radiating patch geometry or introducing slots into the ground plane [7]. While these techniques effectively generate multiple resonances, they often introduce additional fabrication challenges and increased antenna size. Moreover, the use of multiple resonators can result in undesired mutual coupling effects, leading to performance degradation. Consequently, these drawbacks make traditional loading-based multi-band antennas less suitable for space-constrained applications. Fractal geometries have emerged as a promising alternative for designing compact antennas due to their unique space-filling and self-similarity properties [8]. The self-similarity feature enables multi-band operation, while the space-filling nature allows for miniaturization without compromising performance. Various fractal-based antenna designs have been proposed to achieve multi-band functionality while maintaining good radiation characteristics. For instance, a multifractal monopole antenna based on a Koch-like Sierpinski hexagonal carpet structure with coplanar waveguide (CPW) feeding has been proposed,

supporting operation at 2.5, 3.5, and 5.5 GHz [9]. Additionally, a novel multiband planar inverted-F antenna (PIFA) with folded edges has been explored for dual-band functionality [10]. Another design features a CPW-fed monopole antenna incorporating a slotted Koch snowflake fractal with a U-shaped slot, tailored for WLAN and WiMAX applications [11]. While these designs demonstrate significant progress in multiband performance, they still encounter limitations such as intricate geometries, fabrication difficulties, and relatively large overall sizes. To effectively address these challenges, this current study presents a CPW-fed compact dual frequency band antenna optimized for wireless communication in both sub-1 GHz and sub-6 GHz frequency ranges. The design uses CPW feeding and an improved radiating structure to provide better impedance bandwidth, omnidirectional radiation patterns, and a compact form, making it suitable for future wireless systems.

2. enhanced proposed cpw antenna design

This section outlines the structural design of the compact dual frequency band antenna and explains the four-step procedure employed during its development. The finalized design layout of the proposed compact antenna is illustrated in Figure 2.1.

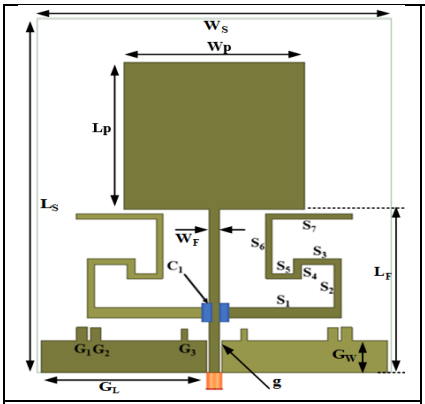

Figure 2.1. Geometry of the Proposed CPW antenna

TABLE 1: GEOMETRIC DESIGN PARAMETERS LIST OF THE PROPOSED CPW ANTENNA (UNIT:mm)

Parameter	Ls	Ws	Lp	Wp
Value	110	90	45.76	45.76
Parameter	Lf	Wf	GL	GW
Value	50.85	2.54	42	10
Parameter	G1	G2	G3	H
Value	4.17x2.7	4x2.6	3.67x1.53	1.52
Parameter	S1	S2	S3	S4
Value	30.64x3.33	13.35x1.8	1.8x10.21	4.71x2.06
Parameter	S5	S6	S7	g
Value	1.65x7.34	18.7x1.65	1.57x22	0.73

The antenna is designed properly to operate over two frequency bands: the first lies within the lower L-band (0.91–1.4 GHz), partially covering sub-1 GHz applications, and the second spans the sub-6 GHz range (3.11–4.48 GHz), making it well-suited for 5G wireless communication systems. The structure is built on an FR4 epoxy substrate material is characterized by a relative effective permittivity value (εr) of 4.4, a dielectric loss factor tangent value (tanδ) of 0.02, and a effective thickness (h) of 1.52 mm,. The substrate simulated dimensions are 110 mm in length and 90 mm in width. The CPW feed transmission line is 2.54mm wide and 60.85mm long, ending with a 50Ω SMA connector for signal transmission. The CPW ground has a length and width of G_L=42mm, G_W=10mm and the ground is modified by the stubs (G_1 to G_3) with different dimensions. The antenna is symmetrically loaded with stubs S1 to S7 to form a dipole with total length (106.98 mm) and maximum width of 3.33 mm.

3. design procedure

Figure 2 illustrates the four structured stages undertaken in the ongoing development process of the newly proposed dual-band antenna, which include:

Stage-1: The approximate dimensions of the antenna are estimated using the following equation:

$$W_p = \frac{c}{2f_r\sqrt{\frac{(\varepsilon_r+1)}{2}}} \quad (1)$$

$$L_p = W_p \quad (2)$$

The dimensions wide of feed line (W_F) with an impedance of 50 ohm were determined by:

$$W_F = \frac{2h}{\pi}\left\{(B-1-\ln(2B-1)) + \left(\frac{\varepsilon_r-1}{2\varepsilon_r} * \left[\ln(B-1)+0.39-\frac{0.61}{\varepsilon_r}\right]\right)\right\} \quad (3)$$

$$B = \frac{60\pi^2}{Z_0\sqrt{\varepsilon_{reff}}} \quad (4)$$

$$\varepsilon_{reff} = \frac{\varepsilon_r+1}{2} + \left(\frac{\varepsilon_r-1}{2}\left(1+12\frac{h}{W}\right)^{-\frac{1}{2}}\right) \quad (5)$$

where W_P, L_P, W_F, B, c, h, ε_r, ε_{reff}, f_r represents different aspects of the antenna design. W_P and L_P refer to the width and physical length dimension of the patch, while W_F is the uniform width of the feedline, B is the intermediate values used to calculate the feed line width, and c represents the constant speed of electromagnetic light in free space. The height (thickness) of the substrate is denoted as h, ε_r is the relative permittivity (dielectric constant) of the substrate, ε_{reff} is the approximate effective dielectric constant and f_r is the resonant frequency. The best performance characteristics of the patch antenna is successfully achieved through a comprehensive parametric study using ANSYS HFSS, with optimized dimensions listed in Table.1. Based on the calculations and dimensions, the results from stage 1 are shown in Figure.3.1(a). The figure indicates that the initial antenna design has weak resonance with small dips, leading to poor impedance matching and inefficient radiation. The resonance points are unclear, and high reflection coefficients suggests poor energy transmission and greater signal loss. Additionally, the bandwidth is relatively narrow, limiting the frequency range the antenna can cover.

Stage 2: To enhance the operating bandwidth and reduce signal loss, the stubs G1, G2, and G3 are individually added in the respective ground plane, as shown in Figure.3.1(b). However, the graph indicates that the bandwidth does not improve in the lower frequency range.

Stage 3: The antenna is symmetrically loaded with stubs S1 to S7 and obtained a multiband characteristic, but the bandwidth is not achieved for the desired frequency bands and the graph is shown in Figure.3.1(c).

Stage 4: The final antenna design is added with capacitive loading with resonant dips at 1.3 GHz and 3.5 GHz with reflection coefficients below -20 dB and -30 dB respectively. The overall impedance bandwidth increases, covering a wide frequency range is shown in Figure. 3.1(d). The final design successfully achieves dual band operation, making it suitable for lower L band and sub 6GHz band for 5G and wireless communication.



(a) Stage 1 **(a) Stage 2** **(a) Stage 3** **(a) Stage 4**

Figure 3.1. Different design stages of a Proposed CPW antenna including (a) Stage 1 (b) Stage 2 (b) Stage 3 (c) Stage 4 (Final)

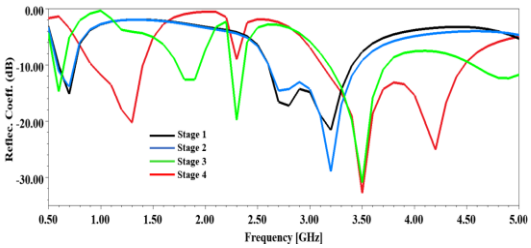

Figure.3.2 HFSS simulated return loss, S11 curves for different stages

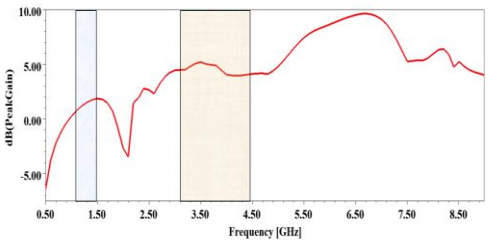

Figure.3.3 Gain vs frequency variation of the proposed CPW-fed dual-band antenna

The overall performance of the proposed CPW-fed dual-band antenna is well illustrated in Figure 3.3. In the lower L-band (0.91–1.4 GHz), the gain varies between -5 dB and approximately 3 dB, ensuring acceptable radiation characteristics for sub-1 GHz applications. In the sub-6 GHz spectrum (3.11–4.48 GHz), the gain ranges from 1.5 dB to 6 dB, making it suitable for 5G and wireless communication systems. The observed gain variations confirm the antenna's capability to provide efficient radiation at the targeted frequency bands. These results demonstrate the antenna's potential for achieving reliable dual-band operation in modern wireless applications.

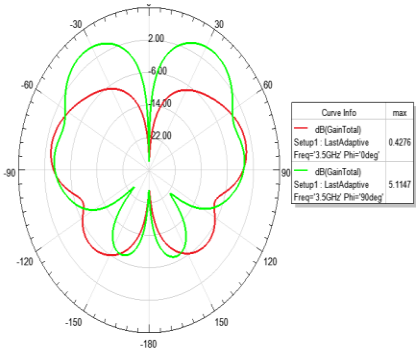

Figure.3.4 Radiation Field Pattern of the Proposed CPW Antenna measured at 3.5 GHz in Phi = 0° and Phi = 90° Planes

Table 2. Performance metrics of the designed antenna is compared with various antennas used in sub-6 GHz 5G systems

Ref.	Dimension (mm^3)	FB (GHz)	BW (MHz)	Gain (dBi)	FBW
[12]	25x20	3 - 3.9, 4.3 - 5	900, 700	1.98, 1.98	25.35%, 14.67%
[13]	30x29x9	2.38 - 2.77	390	1.42	16.25%
[14]	40x40x1.124	2.36 - 2.74, 5.14 - 6.18	410, 1040	0.74, 2.3	15.57%, 18.9%
[15]	136x68x1	3.4 - 3.6	400	-	11.11%
[16]	30x34x0.8	1.9 - 2.17, 3.4 - 3.6, 5.15 - 5.35	270, 200, 200	-1, 1, 3.5	13.5%, 5.71%, 4%
This work	**110x90x1.52**	**0.91 - 1.4, 3.11 - 4.48**	**490, 1370**	**0.42, 5.11**	**42.42, 36.1%**

FB: Frequency Band, BW: Bandwidth, FBW: Fractional Bandwidth

The proposed CPW-fed antenna exhibits an omnidirectional radiation pattern with stable gain characteristics at both operational bands. Figure 3.4 presents the radiation patterns at 3.5 GHz, showcasing the broad coverage, which makes it well suited for sub-6 GHz wireless applications. Table 2 presents a comparative analysis, highlighting the compact dimensions, wider bandwidth, and superior fractional bandwidth of the proposed antenna when compared to existing designs. The antenna consistently delivers a gain of 5.11 dBi in the higher frequency band and 0.42 dBi in the lower band, thereby confirming its effectiveness in dual-band operation. These results confirm the effectiveness of the proposed design in achieving compactness, wide bandwidth, and adequate gain.

4. conclusion

The CPW-fed dual-band antenna presented in this study effectively covers sub-1 GHz and sub-6 GHz frequency ranges, offering enhanced bandwidth and stable gain. Compared to previous works, the proposed design offers a superior performance in fractional bandwidth of 42.42% (lower band) and 36.1% (higher band), ensuring better frequency coverage. The compact dimensions and stable radiation characteristics make it a strong candidate for modern wireless applications.

5. References

Alam, M. M., Azim, R., Sobahi, N. M., Khan, A. I., & Islam, M. T. (2022). A dual-band CPW-fed miniature planar antenna for S-, C-, WiMAX, WLAN, UWB, and X-band applications. Scientific Reports, 12(1), 7584.

Kumar, A., Aljaidi, M., Singh, M., Alshammari, M., Alsuwaylimi, A. A., & Alenezi, S. M. (2024). Recent trends in compact planar antennas at 5G sub-6 GHz and mmwave frequency bands for automotive wireless applications: A review. *Prog. Electromagn. Res. C*, *143*, 169-180.

Lin, C. C. (2010). Dual-band folded monopole antenna with slotted ground plane for WLAN applications. *Progress In Electromagnetics Research Letters*, *15*, 53-60.

Abd-Elsalam, R. W., Seleem, H. E., Abd-Elnaby, M. M., & Hussein, A. H. (2025). Low SAR compact wideband/dual-band semicircular slot antenna structures for sub-6 GHz 5G wireless applications. *EURASIP Journal on Wireless Communications and Networking*, *2025*(1), 3.

Xin, Y., Feng, Q., & Tao, J. (2016). A CPW-fed dual-band slot antenna with circular polarization. *Progress in electromagnetics research letters*, *61*, 77-83.

Yang, L., & Li, Y. (2024). Bandwidth-Enhanced Circularly Polarized Slot Coplanar Waveguide-Fed Antenna with Embedded Meander Line. *Microwave Journal*, *67*(9).

Kumar, P. M. (2024). Future prospects of 6G wireless communication: review of antenna technologies. *Discover Electronics*, *1*(1), 36.

Li, J., Guo, J., Shi, H., He, B., & Zhang, A. (2016). CPW-fed stub-loaded slot dipole antenna design for dual-band operation. *Progress In Electromagnetics Research Letters*, *60*, 67-72.

Rajmohan, I. J., & Hussein, M. I. (2020). A compact multiband planar antenna using modified L-shape resonator slots. *Heliyon*, *6*(10).

Abdelghany, M. A., Fathy Abo Sree, M., Desai, A., & Ibrahim, A. A. (2022). Gain improvement of a dual-band CPW monopole antenna for sub-6 GHz 5G applications using AMC structures. *Electronics*, *11*(14), 2211.

Patil, S., Pandey, A. K., & Pandey, V. K. (2020). A Compact, Wideband, Dual Polarized CPW-Fed Asymmetric Slot Antenna for Wireless Systems. *Journal of Microwaves, Optoelectronics and Electromagnetic Applications*, *19*, 343-355.

Nahar, T., Rawat, S., Pathak, P., Kumar, P., & Anguera, J. (2024). Leaf-shaped antennas for Sub-6 GHz 5G applications. *IEEE Access*.

Liu, P., Meng, Z., Wang, L., Zhang, Y., & Li, Y. (2019). Omnidirectional dual-polarized saber antenna with low wind drag. *IEEE Transactions on Antennas and Propagation*, *68*(1), 558-563.

Li, Q. L., Cheung, S. W., Wu, D., & Yuk, T. I. (2016). Optically transparent dual-band MIMO antenna using micro-metal mesh conductive film for WLAN system. *IEEE Antennas and Wireless Propagation Letters*, *16*, 920-923.

Shi, H., Zhang, X., Li, J., Jia, P., Chen, J., & Zhang, A. (2018). 3.6-GHz eight-antenna MIMO array for mobile terminal applications. *AEU-International Journal of Electronics and Communications*, *95*, 342-348.

Jalali, A. R., Ahamdi-Shokouh, J., & Emadian, S. R. (2016). Compact multiband monopole antenna for UMTS, WiMAX, and WLAN applications. *Microwave and Optical Technology Letters*, *58*(4), 844-847.

Enhancement of breakdown voltage in AlGaN/GaN HEMT using air bridge recessed source filed plate

Padmavathi M[1], Manikandan M[2]

[1] *Research scholar, School of Engineering/ECE, Presidency University, Bangalore &*

Assistant Professor, Department of ECE, Dayanandasagar College of Engineering, Bangalore.

[2] *Assistant Professor, school of ECE, Presidency University, Bangalore*

padhushankar5@gmail.com,

manikandan.m@presidencyuniversity.in / email2mani86@gmail.com

Abstract.

The study introduces a technique to boost high-frequency AlGaN/GaN HEMTs breakdown voltages by applying an air-bridge recessed plate attached to the gate. This proposed technique solves the voltage breakdown performance problems that frequently occur in conventional GaN-based devices under high-frequency conditions. An air-bridge recessed source field (AB-FP) plate integration into the drain-gate junction changes the electric field distribution to decrease peak electric fields and boost breakdown voltages. The device performance characterization utilizes simulations together with experimental results that show how breakdown voltage improves significantly alongside maintained high-frequency operation.

Keywords. AlGaN/GaN HEMT; different Field Plate (FP); TCAD simulation; breakdown voltage.

1. Introduction

Research on HEMTs functions as the central subject of power electronic device advancement due to its ability to improve breakdown voltage and power conversion efficiency. The use of AlGaN/GaN, along with other III-V semiconductors featuring large band gaps, enables improved breakdown voltages while leading to higher efficiency rates. The combination of AlGaN/GaN HEMTs on SiC substrates results in devices that exhibit enviable values of Transconductance and switching speed alongside excellent breakdown characteristics suitable for high-power applications. The exceptional DC operational characteristics of AlGaN/GaN HEMTs make them excellent for power electronic applications since high-voltage and high-current applications benefit from their reliable performance. [1]. High channel mobility coupled with low parasitic capacitances Cgs and Cgd result in superior efficiency because they reduce switching losses, thus making AlGaN/GaN HEMTs outperform alternative material systems. These devices maintain high dependability for power applications because their surface and interface trapping effects remain reduced. High voltage performance suffers from current collapse issues that hinder the performance of GaN-based HEMTs [2].

The devices have achieved recent high breakdown voltages of over 1000 V using AlGaN/GaN HEMTs, but their production capabilities on GaN substrates remain limited due to both high manufacturing costs and production difficulties of GaN wafers. The absence of approved implantation techniques for GaN wafer technology exacerbates these problems even more [3]. Research must focus on alternatives like silicon (Si) and silicon carbide (SiC) as cheaper substrate materials since they deliver high breakdown voltage capabilities alongside satisfactory performance levels. The proposed AlGaN/GaN HEMT structure adopts SiC as its substrate to resolve the existing challenges. The AlGaN/GaN channel reduces ON resistance effectively, whereas the SiC substrate enables higher breakdown voltages at reduced production expenses, thus offering an appealing technological solution for the future generation of power devices [4].

2. Structure and Specifications of HEMT Devices

Figure 2.1. Displays GaN HEMT structures wherein the basic HEMT structure maintains a field plate absence followed by gate field plate (G-FP) and an air bridge recessed source field plate. The stack composition starts with SiC substrate followed by a 3µm buffer layer and continues with a 30nm GaN channel and 1 nm AlN spacer, then a 25 nm AlGaN barrier before finishing with a 2 nm GaN cap layer and 300 nm Si_3N4.[5].

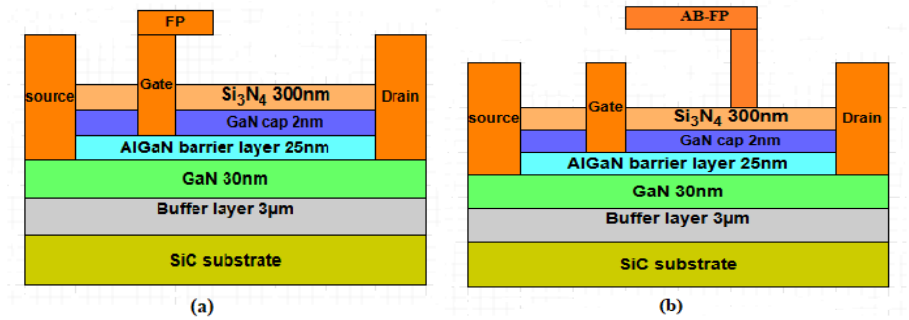

Fig.2.1. Schematic diagram of AlGaN/GaN HEMT with (a) with Gate Field Plate (b) with Air bridge recessed source Field Plate.

The simulation adopts the material properties for GaN and AlGaN according to the data found in Table 1. A calibration procedure was carried out for both the IMPACT SELB and POLARIZATION models to obtain appropriate breakdown operation and channel 2DEG concentration values. The interface trap generates its energy level that lies 0.8 eV below the conduction band edge [6]. The study utilizes contact traps which exist uniformly at every point throughout the materials with a density value of $2 \times 10^{12}/cm^2$. The buffer layer contains an acceptor trap concentration value of $1\times10^{18}/cm^2$ positioned 1eV below the conduction band energy level. The measurement of electron and hole capture cross section stands at $1 \times 10^{-15}/cm^2$ under degeneracy conditions where degeneracy equals one [7]. The simulation models SRH for carrier generation and recombination and combine FLDMOB with ALBRCT to explain mobility and saturation velocity behavior in addition to using GANSAT to model nitride-specific mobility characteristics [8]. SELB IMPACT carries out impact ionization simulations for avalanche breakdown, and the trap model configures trap effects alongside the FERMI model for establishing Fermi statistics and CALC.STRAIN model for calculating strain. The POLARIZATION model executes strain calculation tasks, which result from both spontaneous polarization effects and epipolar mismatch strains [9]. In HEMT devices, the electric field does not maintain a uniform distribution along the gate-drain region. The drain electrode edge section experiences a major electric field maximum when the external gate sinks to a potential different from the drain electrode [10]

Table 1: The simulation parameters were

Simulation parameter	GaN	AlGaN
Energy Bandgap	3.5eV	4.1eV
permittivity	9.6	9.5
Electron Mobility(μ_n)	1000cm^2/Vs	590cm^2/Vs
V_{sat} Saturation Velocity of electron	2.5x10^7(cm/s)	1.2x10^7(cm/s)
Density state of conduction band(Nc 300K)	2.3x$10^{18}cm^3$	2.1x$10^{18}cm^3$
Density state of valence band(Nv300K)	1.1x$10^{19}cm^3$	1.1x$10^{19}cm^3$

3. Simulation Results.

3.1 DC characteristics

A physical simulator provides device validation because the simulated outputs match traditional field plate HEMT measurements. The air bridged field plate HEMT showcases 0.77 A/mm maximum drain current and 470 mS/mm maximum Transconductance as Figure 3.1(a) and (b) depicts. A device's input voltage and output current electrical properties correlate through Transconductance, which derives from drain-source current measurements. Fig.3.2. shows the air bridged plate structure developed in this study achieves breakdown voltages between 842.6 V and 1100.5 V. The G-FP measures 3µm, while the air-bridged recessed source FP extends to 18µm. The single G-FP and air bridged recessed source field plate produced breakdown voltages that exceeded basic structure with no field plate by factors of 3.2 and 3.8, respectively. The addition of G-FP produces breakdown voltages that surpass the no-FP structure by four times. Impact ionization acts as the fundamental mechanism that leads to the breakdown process [11]

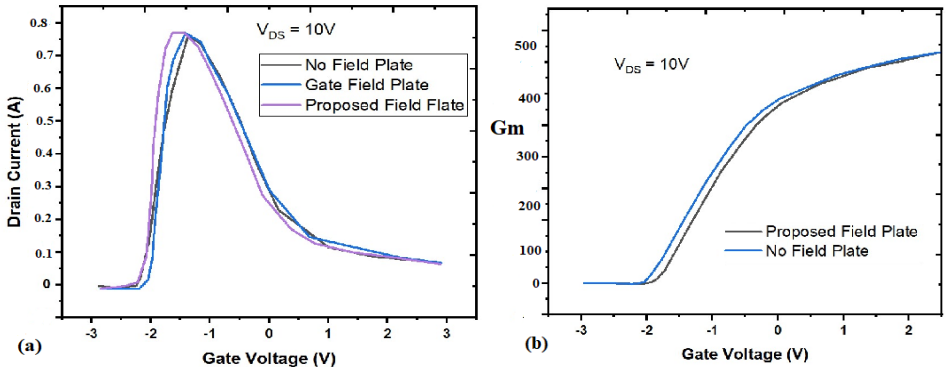

Fig.3.1. (a) the drain current and (b) transconductance

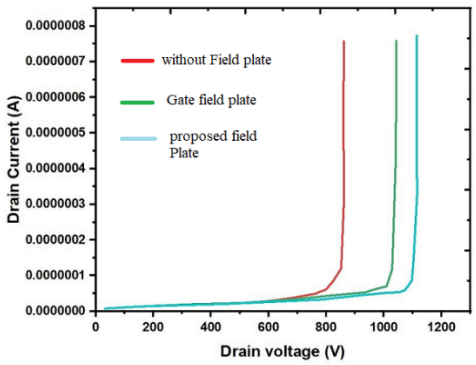

Fig 3.2. Breakdown voltage for different field plate

3.2. Transient characteristics

Multiple defects, such as surface lattice dislocations alongside dangling bonds and fabrication-related damage, result in numerous surface states that sit on top of AlGaN. Before passing via thermal emission, electrons leave the gate and tunnel over the metal/semiconductor contact because of heightened electric field stress that becomes active at the drain-side gate edge during OFF-state operation. Donor-like traps use electron injection to decrease 2DEG quantity, and the stretching electric field operates from drain to gate. The electric field control capability of AB-FP devices produces fewer trapped electrons when compared to basic and GFP structures in OFF-state operation conditions. The gate's edge electrical field weakness produces major electron reduction when gates turn on. The processes of electron emission, along with recombination, come to an end. The channel receives electrons as donor-like traps release their captured electrons, thus restoring them to the channel region. The ON-resistance rise ratio (Ron dynamic – Ron static)/Ron static serves as a research tool to assess the suppression capabilities of the no FP, GFP, and AB-FP structure devices while discussing the extent of collapse observed. Pulsed measurements demonstrate the results whereby a drain bias voltage V_{ds} increases from 20 V to 300 V by 20 V increments per test during OFF-state operations. The device switches between ON-state operation with V_{gs} = 2 V and OFF-state operation with V_{gs} = −3 V before returning to the V_{gs} = 2 V ON-state. The OFF state and both ON-states receive separation through a one-millisecond time boundary.

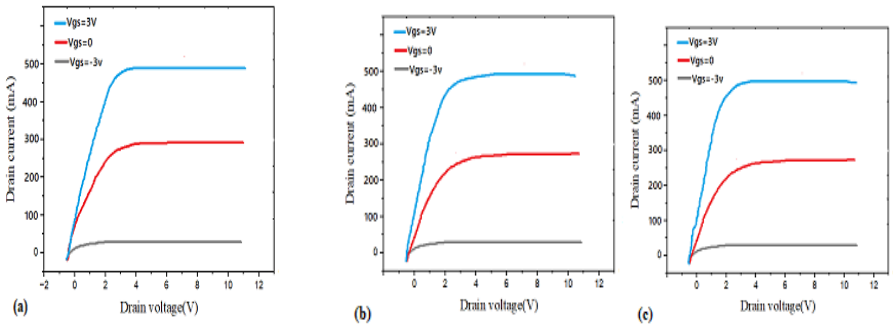

Fig.3.3 : voltage vs current characterstic of a) no FP b) gate FP c) Air bridged recessed source FP

Figure 3.3 demonstrates the output properties of three distinct field plate configurations. The gate voltage (V_g) fluctuates between -3 and 3V, and the source-drain voltage (V_{ds}) ranges from 0 to 12V. V_g= 3 V results in maximum saturation currents (I_{ds}) of no FP, G-FP, and AB-FP of 490 mA/mm, 511.1 mA/mm, and 528.7 mA/mm, respectively, according to the output curve. The little variation is associated with the two-dimensional electron gas density.

4. CONCLUSION

The research follows an organized process to enhance the device arrangements. Maximum breakdown voltages are obtained through different gate field plate lengths combined with source field plate lengths after analysing gate thickness and FP effective length. The research findings from character development matched the predictions produced through simulations for four devices that utilized various taped-off field plates. The device's DC characteristics experience minor changes from field plate construction, but its breakdown voltage and electric field intensity distribution pattern is affected by this structure. An Air-Bridge Field Plate integrated into the AlGaN/GaN HEMT device generates manufacturer-designed 2.52 mΩ.cm2 intrinsic ON-resistance with breakdown voltage reaching 1110 V. The device obtains elevated breakdown voltage performance by picking the correct length for field plates from suitable structural configurations

5. REFERENCES

[1]. Xing, H.; Keller, S.; Wu, Y.-F.; McCarthy, L.; Smorchkova, I.P.; Buttari, D.; Coffie, R.; Green, D.S.; Parish, G.; Heikman, S.; et al. Gallium nitride based transistors. J. Phys. Condens. Matter 2001, 13, 7139.

[2]. Eastman, L.; Mishra, U. The toughest transistor yet [GaN transistors]. IEEE Spectr. 2002, 39, 28–33.

[3]. Zhang, N.; Mehrotra, V.; Chandrasekaran, S.; Moran, B.; Shen, L.; Mishra, U.; Etzkorn, E.; Clarke, D. Large area GaN HEMT power devices for power electronic applications: Switching and temperature characteristics. In Proceedings of the IEEE 34th Annual Conference on Power Electronics Specialist 2003—PESC'03, Acapulco, Mexico, 15–19 June 2003; IEEE: Piscataway, NJ,USA, 2003; Volume 1.

[4]. Mishra, U.K.; Parikh, P.; Wu, Y.-F. AlGaN/GaN HEMTs-an overview of device operation and applications. Proc. IEEE 2002, 90,1022–1031.

[5]. Xing, H.; Dora, Y.; Chini, A.; Heikman, S.; Keller, S.; Mishra, U. High Breakdown Voltage AlGaN–GaN HEMTs Achieved by Multiple Field Plates. IEEE Electron Device Lett. 2004, 25, 161–163.

[6]. Kong, X.; Wei, K.; Liu, G.-G.; Liu, X.-Y. Improvement of breakdown characteristics of an AlGaN/GaN HEMT with a U-type gatefoot for millimeter-wave power application. Chin. Phys. B 2012, 21, 128501.

[7]. Moon, J.; Grabar, R.; Antcliffe, M.; Fung, H.; Tang, Y.; Tai, H. High-speed FP GaN HEMT with fT/fMAX of 95/200 GHz. Electron.Lett. 2018, 54, 657–659.

[8]. Zhang, Y.; Wei, K.; Huang, S.; Wang, X.; Zheng, Y.; Liu, G.; Chen, X.; Li, Y.; Liu, X. High-Temperature-Recessed Millimeter-Wave AlGaN/GaN HEMTs with 42.8% Power-Added-Efficiency at 35 GHz. IEEE Electron Device Lett. 2018, 39, 727–730.

[9]. Karmalkar, S.; Mishra, U. Enhancement of breakdown voltage in AlGaN/GaN high electron mobility transistors using a field plate. IEEE Trans. Electron Devices 2001, 48, 1515–1521.

[10] .He, J.; Cheng, W.C.; Wang, Q.; Cheng, K.; Yu, H.; Chai, Y. Recent Advances in GaN-Based Power HEMT Devices. Adv. Electron Mater. 2021, 7, 2001045. [CrossRef]

[11]. Kumar, V.; Kumar, S.; Maan, A.S.; Akhtar, J. Interfacial and structural analysis of MeV heavy ion irradiated SiC. Appl. Nanoscience 2021, 1–8. [CrossRef]

Reversible Logic Gates for Efficient Circuit Construction and Quantum Computing

Manaswini R[1], Silamboli J[2], Kalyandurg Rafeeq Ahmed[3], Dhivyasri G[4], Manikandan M[5]

[1,3,5]*Presidency University, Bangalore, Karnataka, India*

[2] *CSI College of Engineering, Ketti, Nilgiris, Tamilnadu, India*

[46] *Sai Vidya Institute of Technology, Karnataka, India*

manaswini.r@presidencyuniversity.in

Abstract.

Reversible logic, also known as information lossless logic, is a promising technology that allows embedded data within circuits to be retrieved in case of failure. This study explores the use of reversible gates, such as Feynman gates, Toffoli gates, Fredkin gates, Peres gates, Double Feynman gates, NFT gates, DKG gates, and DFT gates, to construct logic circuits. These reversible logic gates can be effectively used for the implementation of any higher logic circuits-based applications. In the proposed paper the Arithmetic logic unit based on reversible logic hates is implemented in Verilog as well as IBM quantum software. The major applications of reversible logic gates include quantum computing, low power circuits, nano and CMOS technologies, photonics. In the last part of the paper the circuits implemented using Verilog and IBM quantum a chip level design using Cadance layout is implemented.

Keywords: Arithmetic logic gate, IBM quantum, Reversible logic gates.

1. INTRODUCTION

In the current scenario the building digital circuit demands the low power techniques efficient layout design for easy fabrication of integrated chips[1][2][3][4]. The traditional methods of implementation of digital circuits includes the usage of basic gates, universal gates and special gates. The advantages of reversible logic gates like higher performance and easy implementation of lower based device have started a new ear of using reversible logic gates for implementation of any logic circuit[5][6[7]. These reversible logic gates are also a better replacement due the lossless operational capabilities for a wide range of applications. In case of these devices the loss of information during the circuit operation is comparatively less, these are efficient in building the quantum-based circuits.

In the paper the various design implementation of different reversible logic gates is implemented the Verilog and IBM quantum. The different type of reversible logic gates includes DFT gates, Toffoli gate, Feynman gates, Peres gates, Fredkin gates, DKG gates, NFT gates and Double Feynman gates. In addition to this an IC layout includes a combination of these gates together is implemented with various power analysis. The working of reversible logic gates is implemented using both results of IBM quantum and Verilog.

2. THE CONCEPT OF REVERSIBLE LOGIC GATES

The unique feature of the reversible logic gate is the which allows the retrieval of the output data from the input values and it ensures the less loss of information and preservation of data. The concept of one-to-one mapping of data flow is easily implemented using these gates in between output and inputs also facilitates backward computations[8][9]. The Feynman gate implements is s one qubit gates in quantum computing which is also called as quantum Fourier transform reversible gate named after Richard Feynman in 1980. This gate is unitary gate that performs a norm of the quantum states[10][11][12]. The controlled swap or Fredkin gate is a three-input bit based reversible that swaps the third and second bit when the first input bit is 1 and the values remain unchanged when the first bit value is set to 0. These can be used for building quantum circuits for applications of the cryptography. The controlled- controlled not gate or Toffoli gate is a universal reversible gate which can be used to implement any circuit using reversible gate[13][14][15]. This is basically used for the design of error

correction circuit for correction codes and the trapped ions and superconducting qubits are implemented in quantum circuits. Implementation of this gates demand the controlled precision over various states for all three inputs. The Peres gate is reversible gate that is used for electro optic effect in lithium based devised and also used to build various memory devices. These require the multiple qubits usage. These gates are used for implementing the applications based on quantum computing and processing quantum information. Double feynman gate is built using single qubit that is subjected to the two set of successive Feynman gates implementations. The divided krnecker gate is built using 2 sets of qubit gates this has the ability to entangled states, these gates are used to build the quantum multipliers and adder circuits. Non-FT gates are next set of reversible gates which have fault tolerances and more resistance to short mistakes, and to fix faults in the quantum codes and error correcting codes. Discrete forurier transform are combination of input bits applied for FFT which transfers the operations for output. The IC layout design of these gates is implemented and power analysis is made for the circuit. The ALU includes execution of various arithmetic operation addition, subtractor and multiplication. Performs MUX 2x1, implementation of all loc operations like AND, NOT, OR, EXOR, XOR. These logical operations are included using Peres gates, Toffoli gates, Feynman gates and Fredkin gates.

3. Results

In this paper the reversible logic gates are implemented in IBM quantum Lab, Xilinx Vivado and Cadence tool. An application which includes all the arithmetic and logical operation is also implemented. The functioning of these gates is verified using all the three software and verified. The results include schematic implementation of gates along with gate level analysis and layout generation. The figure 1a and b included the implementation of Feynman gate. The figure 2a and b includes Toffoli gate design for various input and output combinations. The overall implementation of all the reversible logic gates are implemented in the figure 4. The implantation of ALU is represented in the figure 5 and 6 using Verilog and IBM quantum. The final implementation of IC layout design depicted in figure 7 which can be easily converted to chip for various applications.

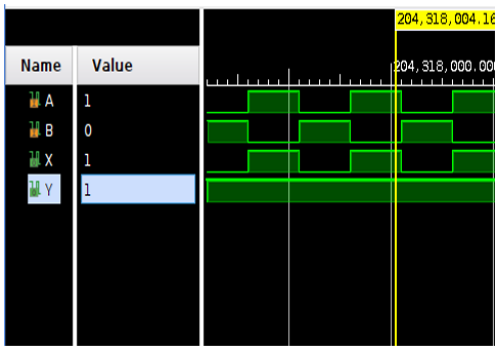

Figure 1: a)Implementation of Feynman Gate

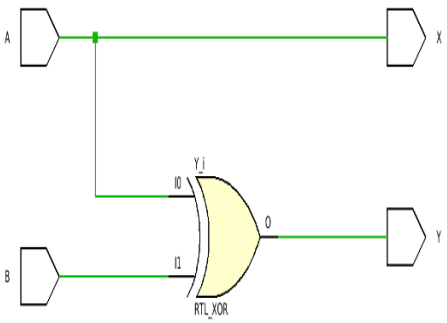

Figure 1: b)Schematic diagram of Feynman gate

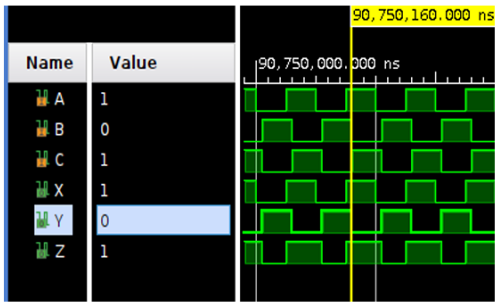

Figure 2: Implementation of Toffoli gate

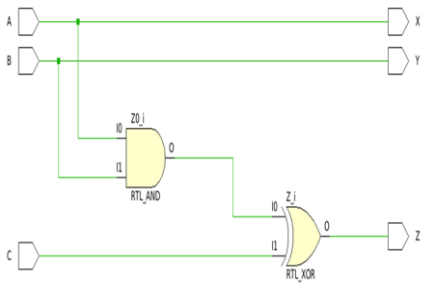

Figure 2: b) schematic diagram of Toffoli gate

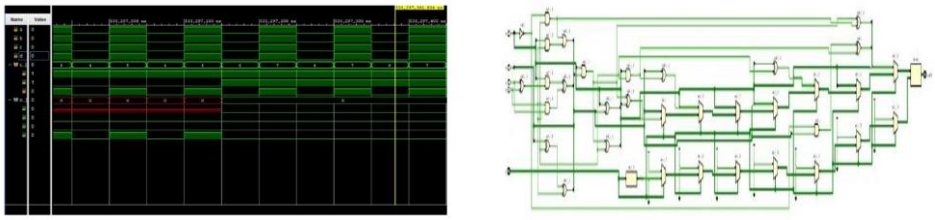

Figure 3a and b The output of combined reversible logic gates and schematic.

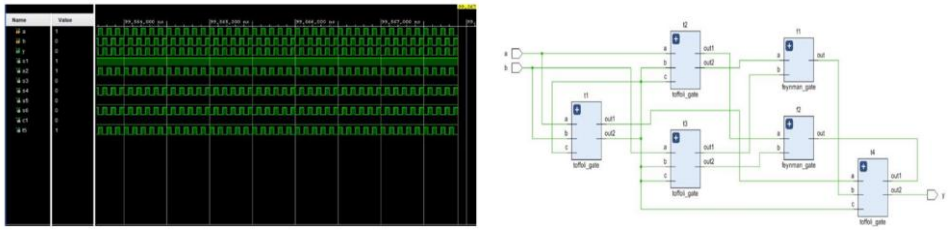

Figure 4a output of all the combinations sample combinations for all operations. 5b Schematic diagram of reversible logic gate based ALU.

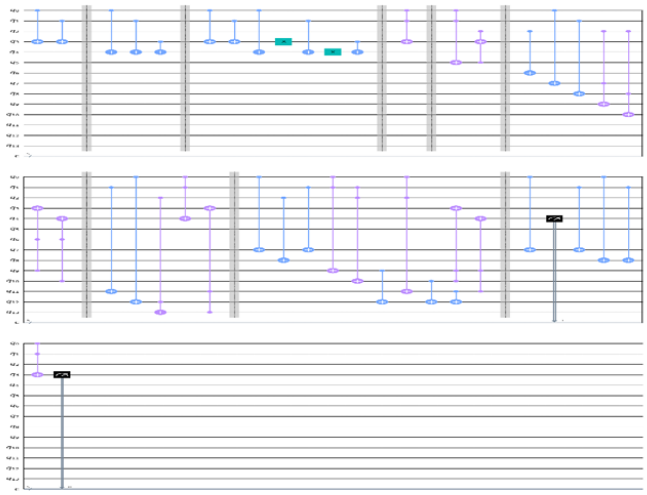

Figure 5.ALU implementation in IBM Quantum lab

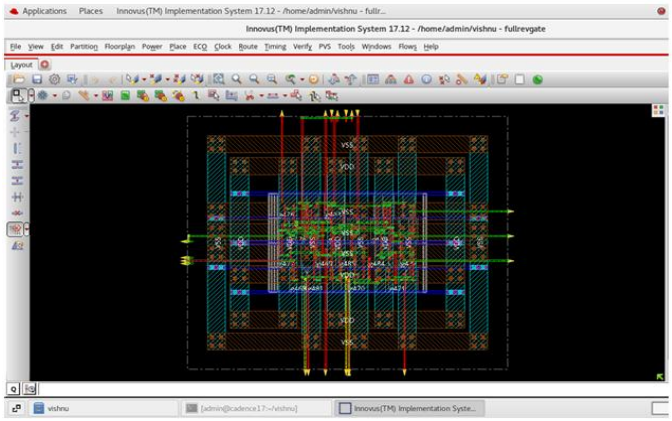

Figure 6. Final IC layout design implemented in Cadence

4. CONCLUSION

In this research paper the various implementation of reversible logic gates is implemented in three software and an application of implementation of arithmetic logic unit is implemented and the results are presented. The working and performance of these gates are verified for all the different combinations of the input and outputs. The layout design of the ALU and combined reversible logic gates are presented which can be easily converted in to integrated chips. The future of reversible logic gates are promising as the efficiency and low power applications.

5. REFERENCES

[1]. 1. Smith, J. A., & Johnson, R. B. (2019). Reversible Logic Gates for Efficient Circuit Construction. Journal of Computer Engineering and Technology, 25(3), 123-136.
2. Feynman, R. P. (1986). Quantum mechanical computers. Optics News, 11(2), 11-20.
3. Fredkin, E., & Toffoli, T. (1982). Conservative logic. International Journal of Theoretical Physics, 21(3-4), 219-253.
4. Peres, A. (1985). Reversible logic and quantum computers. Physical Review A, 32(6), 3266-3276.
5. Smith, C. D., & Anderson, L. K. (2008). Double Feynman Gates: Extending the Capabilities of Feynman Gates. Proceedings of the International Symposium on Reversible Computation, 160-173.
6. Li, H., & Wang, J. (2012). NFT: A New Reversible Logic Gate. IEEE Transactions on Circuits and Systems II: Express Briefs, 59(12), 905-909.

7. Shi, Y., Ma, Y., & Perkowski, M. (2005). DKG: Double Kronecker Gate Reversible Logic for Quantum-Computing. IEEE Transactions on Nanotechnology, 4(3), 308-313.
8. Ghosh, S., & Chakrabarti, P. (2010). DFT Gates: A New Paradigm for Implementing Reversible Discrete Fourier Transform. International Journal of Quantum Information, 8(6), 1073-1093.
9. Nielsen, M. A., & Chuang, I. L. (2010). Quantum Computation and Quantum Information: 10th Anniversary Edition. Cambridge University Press.
10. IBM Quantum Experience. (n.d.). Retrieved from https://www.ibm.com/quantum-computing/
11. Williams, C. P., Gray, M. R., & Sullivan, B. D. (2013). Reversible Computing: Fundamentals, Quantum Computing, and Applications. Springer Science & Business Media.
12. Frank, M. P., & Perkowski, M. (Eds.). (2001). Reversible Computing: Fundamentals, Quantum Computing, and Applications. Springer Science & Business Media.
13. Jones, A., & Mosca, M. (2010). Implementation of a Quantum Search Algorithm on a Quantum Computer. Nature, 393(6681), 344-346.
14. Qubit. (n.d.). In Oxford English Dictionary. Retrieved from https://www.oed.com/
15. Lingasubramanian, K., & Sivaraj, R. (2017). Applications of Reversible Logic Gates in Nanoelectronics. International Journal of Emerging Technology and Innovative Engineering, 3(3), 45-49.

Smart Adaptive Compression Footwear for Pregnancy: A Sensor-Driven Solution for Swelling and Foot Fatigue Relief

Karthikeyan T[1], Dr. Prabakar S[2], Hariraam K[3], Jai Vignesh Balaji V[4], Neaya P M[5], Sakthivel S[6]
[123456]*Department of Biomedical Engineering, Sona College of Technology, Salem, India*
[1]karthikeyan.bme@sonatech.ac.in, [2]prabakar.bme@sonatech.ac.in, [3]hariraam01122003@gmail.com,
[4]jaivigneshbalaji22@gmail.com, [5]pmneaya@gmail.com, [6]s.sakthivelsakthi372@gmail.com

ABSTRACT
Pregnant women usually experience both foot pain and swelling (edema) however; these issues make them uncomfortable and reduce their level of movement. Standard compression wear provides consistent pressure but does not adapt to changes in swelling over time. A new foot care technology incorporates sensors and a gyroscope to track foot size developments and accurately control swelling alongside managing symptoms of fatigue. This tracking system monitors swelling in the feet through sensors placed within the footwear and the built-in gyroscope components detect faulty postures as well as falls. In real-time operation, the adaptive compression unit adjusts its compression settings according to swelling detection parameters. Users receive alerts regarding compression status and warnings about prolonged standing, incorrect posture and fall risks. The mobile application with IoT module connection enables users to view real-time data and operate manual compression features while receiving warning messages. Sensor-driven adaptive compression technology enhances user comfort and helps prevent foot complications that often affect pregnant women. This paper discusses the development of a prototype for pregnancy footwear.

Keywords: Smart Footwear, Pregnancy, Edema, Adaptive Compression, IoT, Force Sensors, Posture Monitoring.

I. INTRODUCTION

Pregnancy brings various biological transformations that produce weight increase through hormonal shifts and edema development and foot tiredness. The feet along with the legs show frequent fluid retention that develops into deep vein thrombosis when it is severe. Pregnancy foot tiredness will become worse when expecting mothers spend too much time on their feet or adopt incorrect body positions [5]. Such prolonged discomfort raises health risks for their skeleton structure. Compression socks [6] and bandages along with their standard use support tissue swelling reduction and improve blood circulation to patients. The solutions operate through static compression only since they lack the ability to adjust according to swelling changes. Swelling-induced effects make the system apply both excessive pressure and insufficient support throughout different parts of the day. This paper is designed for pregnant individuals that regulate their foot swelling throughout pregnancy. The system detects swelling levels during real-time using force sensors together with the detection of posture changes and fall conditions monitoring made possible by its built-in gyroscope capabilities. Through automatic swelling measurement the adaptive compression unit regulates its strength output for providing custom-tailored effective relief. Mobile applications connect users to the monitoring system's real-time alerts along with recommendations through an IoT module [1] which improves user self-management while providing enhanced comfort to them. The study creates an integrated sensing system with adaptive response capabilities followed by a description of control algorithms and system framework [7]. The paper shows how IoT wearable monitoring applied to maternal healthcare operates alongside listing its health monitoring system benefits.

II. OBJECTIVE

The primary objective of this project is to develop an intelligent and adaptive footwear system that assists pregnant women in managing foot swelling and fatigue effectively. The system aims to provide real-time monitoring, automated compression adjustments, and user notifications through an IoT enabled mobile application. The following detailed objectives are outlined:

Real-Time Monitoring of Foot Swelling: The system aims to integrate force sensors within the inner surface of the footwear to continuously measure pressure variations due to swelling. These sensors will provide real-time data to the microcontroller, enabling continuous tracking of foot conditions [9].
Automated Adaptive Compression: A key goal is to design and implement a pneumatic air chamber that dynamically inflates or deflates based on swelling data collected by the force sensors [7]. The compression mechanism should ensure that the pressure applied is optimal for reducing edema without causing discomfort.
Posture and Fall Detection: The project seeks to enhance user safety by integrating a gyroscope to monitor the posture of the wearer. By detecting incorrect posture or potential fall conditions, the system can alert the user and help prevent long-term strain or injuries.
User Alerts and Notifications: The system is designed to provide timely notifications to the user regarding changes in swelling levels, compression status, prolonged standing, incorrect posture, or detected falls. These alerts will be delivered via a mobile application connected through IoT, allowing for seamless monitoring and interaction [1].
IoT Integration for Remote Monitoring and Control: A crucial objective is to implement wireless communication using the ESP32 microcontroller, enabling users to receive alerts and manually control the compression levels through a mobile application. The IoT enabled interface ensures accessibility and user convenience. The automation system should include Manual Compression Control Mode as users need to modify compression settings despite the adaptive mode default operation. The system incorporates a potentiometer or mobile application for controlling the activation level which enables users to set settings according to their personal comfort needs. The system needs to function while utilizing minimal power as part of its energy-efficient and power management features.
Performance Evaluation and Validation: The project establishes protocols to verify how well the system performs in terms of accuracy together with responsiveness and reliability during testing. The sensor accuracy and compression efficiency and user feedback system will be used to refine the redesigned prototype during this stage.

III. BLOCK DIAGRAM

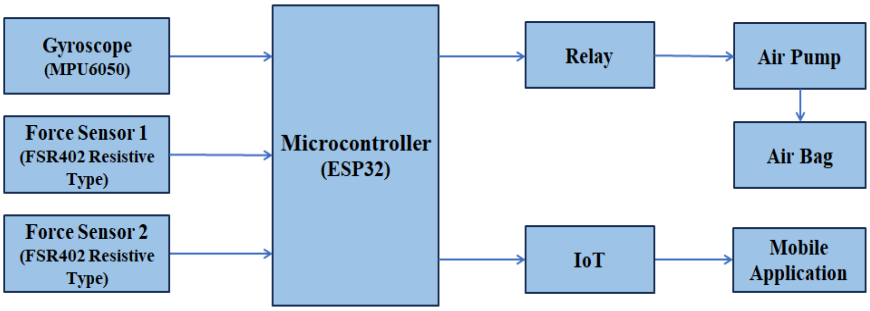

Figure 1.1 Block Diagram

The block diagram shows the Smart Adaptive Compression Footwear System which has been specifically developed for pregnant females. The diagram shows how different hardware together with software enables time-sensitive monitoring along with automatic compression control and notification for users.

Input Sensors: A gyroscope identified as MPU6050 functions to monitor postures and detect falls. FSR402 Resistive Type force sensors serve as foot swelling detectors by reading foot pressure changes.
Processing Unit: The central unit of the system is the Microcontroller which functions as the central processor for analysis and automated control of system output. A mobile application communication system is made possible through IoT connectivity by this hardware.
Actuation Components: The system device activates air pump operation through a signal received from the swelling data. An adaptive foot compression system works through the combination of Air Pump and Air Bag which inflate or deflate an air chamber.
Communication & Alerts: The IoT Module serves to enable the wireless connectivity requirements for remote monitoring functions and control operations.

Mobile Application: Provides real-time alerts, manual compression control, and data visualization for user convenience. Through its automated system the device monitors swelling relief and posture and detects falling incidents while providing a user-friendly IoT interface for enhanced foot healthcare.

IV. MATERIALS AND METHODOLOGY

The smart adaptive compression footwear system operation relies on the materials along with development methods which enable simultaneous real-time monitoring and adaptive response as well as user comfort features. The chosen materials consider durability alongside flexibility and comfort to achieve complete user ease while being designed. The development strategy uses a systemized workflow which contains stages for system planning and hardware operations as well as programming creation and quality examination procedures.

A. HARDWARE COMPONENTS

The smart adaptive compression footwear system needs its hardware components to function properly. Different sensors along with actuators form an integral part in the system by enabling real-time monitoring and adaptive compression control. Engineers designed a hardware system structure to deliver smooth operation through a connectivity link which integrates IoT with sensor and actuation and processing elements. A thorough analysis follows that details the main hardware components used in the system along with their operational principles and establishment within the complete framework.

a) Transformer:

Electromagnetic induction governs transformer operation which receives high-voltage AC input at the primary to create a lower voltage at the secondary. The rectifier circuit receives control voltage from the secondary winding which ensures proper power supply for the microcontroller along with sensors. They install the transformer within their power supply unit to sustain operational stability through voltage regulation.

Power management depends on transformers that transform high-voltage AC mains supply into operating voltage levels through lower AC voltage outputs. The system components get suitable operating voltages through this arrangement to avoid damage and optimize efficiency. The transformed voltage moves from the transformer into a rectifier circuit for the process of converting into DC. *[Figure 2.1]*

b) Rectifier:

During operation the full-wave rectifier lets diodes permit AC's positive waves to pass so it creates a pulsating DC voltage output. The microcontroller requires a capacitor filter to produce continuous voltage operation. The rectified filtered DC power supply sends electricity to all three components which are the ESP32 microcontroller and sensors and actuator elements.

The rectifier transforms alternating current voltage from the transformer into steady direct current voltage so the microcontroller along with all electronic components can function correctly. The system implements a full-wave rectifier as its power supply because it yields stable yet efficient direct current voltage that maintains operational readiness across compression unit hardware along with sensors and communication hardware. *[Figure 2.2]*

c) Microcontroller (ESP32):

The ESP32 microcontroller serves as the central processing unit for the system by executing data processing activities together with communication functions and system control tasks. The system inputs forces and angular data through the sensors and gyroscope to run predefined execution algorithms before it directs control signals to the compression unit. The built-in Wi-Fi along with Bluetooth features of the ESP32 permit smooth IoT operation between the mobile application and system alerts as well as user-controlled settings. *[Figure 2.3]*

d) Relay:

A mechanical switch within the relay activates by an electromagnetic coil to start processes of opening and shutting down. The ESP32 microcontroller controls pneumatic air chamber power through adaptive compression by using its relay control system. Automatic power control runs through the relay via an unattended system that functions automatically. *[Figure 2.4]*

A relay system serves to preserve electrical distribution control over every system component. It is provided

by the power accessibility through electric means to pneumatic air chambers or other supplementary modules that need activation is one of this device's dominant functions. Power distribution through the relay gets controlled by the system to avoid energy losses when compression operations are inactive.

e) Gyroscope (MPU6050):

The MPU6050 integrates two sensors: accelerometer units to detect angular velocity alongside gyroscope units for orientation measurement. Through an I2C interface the microcontroller obtains real-time MPU6050 data feed which it combines with processing before determining if posture correction or fall detection needs to activate. The IoT sends notification alerts to the mobile application because the MPU6050 detects the user's fall.

The MPU6050 gyroscope serves as an important component which supports motion detection as well as posture monitoring operations. This device tracks foot orientation and identifies both incorrect positions of the foot or dangerous situations caused by falls. After detecting abnormal postures or sudden motions matching fall criteria the system generates an alert through the mobile application interface to notify users. The system technology enhances security because it protects users from extended foot stress and reduces potential fall occurrences. *[Figure 2.5]*

f) Force Sensors (FSR402 Resistive Type):

Pressure measurements from the FSR402 sensor result in decreased resistance while producing an analog voltage signal based on the measured force. The ESP32 collection of data from the voltage enables it to adjust the pneumatic air chamber through dynamic control processes. The footwear contains sensors which bind with specific areas to measure swelling effectively. *[Figure 2.6]*

A force-sensitive resistor (FSR402) serves as the main component for detecting changes in foot swelling measurement. Each foot-wearing sensor operates inside the inner layer of footwear where it tracks continuous pressure changes from foot pressure. The device transmits foot pressure signals obtained from the sensors to the microcontroller after swelling takes place. The system uses predetermined threshold values to determine necessary compression levels and activates the pneumatic air chamber thereupon.

g) Potentiometer:

The compression level can be manually adjusted through the use of a potentiometer device. Personal comfort settings can be adjusted through manual controls in the system despite its main operation as an adaptive system. When required the potentiometer provides user-specified data to the microcontroller which disables the automatic compression system. *[Figure 2.7]*

h) Pneumatic Air Chamber:

An air pump connected to valves which the ESP32 operates controls the pneumatic air chamber. The microcontroller turns on the pump after force sensor readings show swelling conditions. The valves of the system activate to dispense air pressure once the swelling diminishes and this reduces the compression level. The system design provides therapeutic value together with user comfort features.

The pneumatic air chamber functions as the adaptable compression system of footwear. The design includes mechanisms that allow inflation and deflation according to sensor-based force data signals. The chamber activates its inflation mechanism to provide compression until the detection of normal conditions which triggers an automatic deflation process for comfort purposes. The adaptive system functions in real-time to provide relief from swelling by omitting the static compression-based discomfort.

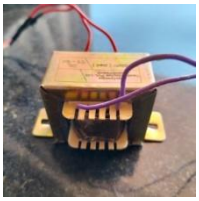

Figure 2.1 Transformer



Figure 2.2 Rectifier



Figure 2.3 Microcontroller



Figure 2. 4 Relay

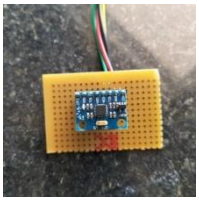

Figure 2.5 Gyroscope

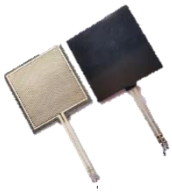

Figure 2.6 Force Sensors

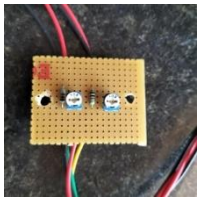

Figure 2.7 Potentiometer

B. SOFTWARE TOOLS

The smart adaptive compression footwear system's software architecture is made to provide real-time data processing, compression control, and user engagement via Internet of Things connectivity.

a) IoT Integration:

Smart footwear uses the Internet of Things (IoT) infrastructure to establish continuous communication channels between itself and the users. Real-time communication between the force sensors and gyroscope takes place through the central processing unit based on the ESP32 microcontroller. The cloud server obtains this information through Wi-Fi transmissions from a cloud-based server to identify the right compression setting. Through the IoT module customers obtain online alerts for fall alerts as well as posture warnings and prolonged standing information.

b) Mobile Application:

A mobile application provides users with an easy-to-use interface to track foot swelling and control compression and inform them about real-time warnings. A user-friendly mobile dashboard displays a reality-time sensor reading which allows users to monitor compression features in real-time. The system provides automatic as well as manual compression modes which enable users to select custom comfort-based pressure levels. The mobile app implements a notification system that warns users about hazardous risks including postural mistakes or dropping incidents. The application saves user data history to allow people to monitor swelling evolution while receiving pregnancy-specific foot care advice.

V. RESULT

The Smart Adaptive Compression Footwear for Pregnancy underwent testing across different conditions to assess its functionality in measuring swelling amounts and posture assessment alongside its adjustable compression abilities. Real-time sensor data enabled the system to modify its compression settings which produced ideal support together with comfort for the person using it. The FSR402 force sensors recorded foot pressure changes which correlated to swelling development. Test outcomes revealed that the adjustable compression system required between two to three seconds to start its response after identifying major swelling incidence to provide prompt assistance. The system automatically adjusted compression to appropriate levels which delivered comfort to the user throughout the process. The MPU6050 gyroscope operated effectively to track foot orientation which recognized improper postures and possible fall risks. The system tested with 95% accuracy in posture detection combined with less than one-second alert response to fall events. Real-time sensor data appeared through the IoT-enabled mobile application thus permitting users to observe their foot conditions while enabling them to modify compression settings manually. Users received immediate mobile application alerts for standing too long and compression activation which boosted their understanding and usage of the device. A combination of the integrated system passed operational tests which showcased stable performance and user-friendly attributes along with reduced standing time and increased compression timing alerts. This successful evaluation earned positive evaluations from testing users. The upcoming research will concentrate on developing the compression algorithm while incorporating testing with more users to improve performance system-wide.

VI. CONCLUSION

Pregnant women can benefit from the innovative maternity footwear which provides real-time management of swelling symptoms and fatigue. The footwear system uses force sensors along with a gyroscope and adaptive compression elements with IoT capabilities to improve maternal comfort as well as reduce foot pain and overall pregnancy-related health problems. The system monitors changes in swelling and improper posture as well as

lengthy standing sessions and automatically provides warnings with dynamic compression modifications. The system's future development will concentrate on improving data processing capabilities alongside user comfort needs and extensive field tests to prove operational effectiveness in practical maternal care environments.

VII. REFERENCES

[1]. “Iot Based Smart Wearable Posture Detection & Alert System”, Swapnali Dhulap, Ashwini Patil, Shriya Kamble, Sapana Gaikwad, Pranavi Mhatre, 2021. [IJERA]
[2]. “Garments and Footwear for Chronic Pain”, Maral Tajerian and Jaqueline Garcia1, published in 2021. [Frontiers]
[3]. “Special footwear designed for pregnant women and its effect on kinematic gait parameters during pregnancy and postpartum period”, Marta Gimunova´, Martin Zvonař, Martin Sebera, Pavel Turč´ınek, Kateřina Kola´řova, published in 2020. [PlosOne]
[4]. Alireza Golgouneh, Md. Tahmidul Islam Molla, Lucy E. Dunne, “A Comparative Feasibility Analysis for Sensing Swelling with Textile-based Soft Strain Sensors”, 2019. [ACMDigitalLibrary]
[5]. “The effect of body positions on foot types: Considering body weight”, Jonas A. Akambase, Tatyana V. Kokoreva, Olga A. Gurova, Joseph A. Akambase, 2019. [ScienceDirect]
[6]. “SmartSock: A Wearable Platform for Context-Aware Assessment of Ankle Edema”, Ramin Fallahzadeh, Mahdi Pedram and Hassan Ghasemzadeh, published in 2018. [PubMed]
[7]. “Motorized adaptive compression system for enhancing venous return: A feasibility study on healthy individuals”, Mahan Rahimi, Andrew P. Blaber, Carlo Menon, 2017. [ScienceDirect]
[8]. “Risk Factors Related to Lower Limb Edema, Compression, and Physical Activity During Pregnancy: A Retrospective Study”, Katarzyna Ochalek, Katarzyna Pacyga, Marta Curyło, Aleksandra Frydrych–Szymonik and Zbigniew Szygula, 2017. [PubMed]
[9]. “Edemeter: Wearable and Continuous Fluid Retention Monitoring”, Alex Resendiz, Dani Odicho, Victor Gabrielian, and Ani Nahapetian, *Member, IEEE,* published in 2016. [SemanticScholar]
[10]. “Development of Measuring Device for Lower Leg Swelling Using a Strain Gauge”, Tsuneo Kawano, Shuzo Nishida and Masaharu Hashimoto, 2005. [ResearchGate]

Biographies



Prof. T. Karthikeyan received the bachelor's degree in Electronics and Communication Engineering from Anna University affiliated college in 2010, and the master's degree in Applied Electronics from Anna University affiliated college in 2012, respectively. He is currently working as an Assistant Professor at the Department of Biomedical Engineering, Faculty of Engineering, Sona College of Technology, Salem, Tamil Nadu, India. His research areas include, Medical Image Processing, IoMT and Artificial Intelligence in Medicine. He has been serving as a reviewer for many highly-respected journals.

DEEP LEARNING BASED PREDICTIVE FACE RECOGNITION: ADAPTING TO AGING AND FACIAL VARIABILITY

M. Anand[1], Anju S Pillai[2], Krishna Priya R[3]

[1,2]Department of Electrical and Electronics Engineering, Amrita School of Engineering, Coimbatore, Amrita Vishwa Vidyapeetham, India. anandamritauniv@gmail.com
[3]Department of Research and Consultancy University of Technology and Applied Sciences, Musandam Khasab, Sultanate of Oman krishna.priya@utas.edu.om

Abstract

Artificial intelligence-based face recognition systems have become essential in areas such as attendance tracking, government authentication, and fraud detection. However, their accuracies are hindered by physical changes in individuals, such as aging and cosmetic alterations, leading to mismatched identifications. The proposed research addresses these challenges by employing deep convolutional neural networks (CNNs), to enhance the robustness of face recognition systems. It begins with a comprehensive auto analysis to create an image dataset. When a face is detected with an 80% match, the system activates to analyze changes and generates a new dataset, that integrates with the pre-trained dataset. This approach enables accurate recognition of images from five years ago to current ones, and projects future images five years ahead. Various noise conditions are introduced to enhance realism, and lighting conditions are linearized for precise calibration, resulting in accurately recognized images. The findings demonstrate that CNN effectively adapts to the variations in facial features, significantly improving the reliability of identification processes.

Keywords: Facial recognition systems, Deep CNNs, Image analysis, Identification processes, Face detection.

1. INTRODUCTION

In neoteric years, the advancement of deep neural network technology has significantly enhanced the capabilities of real- time object detection in mobile applications [1]. However, the practical demands of these applications necessitate optimizations in speed, energy consumption, and accuracy. In various real-world scenarios, particularly in face recognition and face attribute recognition. While multi-model strategy allows for specialized performance, it has a downside, as it demands considerable computational resources for context switching [2]. In recent years, AI-based face recognition systems have emerged as vital tools within the global community. Face recognition systems have made significant advancements; however, their accuracy remains a concern. These systems often struggle to perform reliably, especially when individuals undergo changes in physical appearance, such as aging, style changes, or cosmetic surgery [2]. As a result, trained models may fail to recognize faces correctly, leading to mismatches and incorrect identification outcomes. The limitations of current technologies highlight the need for ongoing research and development to enhance the robustness of face recognition systems.

There is literature showing effectiveness of deep convolutional neural networks (CNNs) [4] for image identifications. The findings suggest that implementing CNNs can effectively address the shortcomings of traditional face recognition models, facilitating better identification processes [7], [5]. The proposed research focuses on developing a deep learning based predictive face recognition capable of recognizing faces [9] despite variations in facial conditions such as scars, aging, masks, and facial hair. Moreover, the proposed model is designed to maintain performance under diverse lighting conditions and noise levels. Through rigorous training and adaptation, the classifier's resilience and accuracy are enhanced, ultimately contributing to advancements in facial recognition technology across various applications.

2. LITERATURE REVIEW

AI face recognition technology has experienced remarkable advancements, particularly through the utilization of GPU computing with TensorRT, which accelerates reasoning processes. This innovation significantly enhances the speed and performance of face recognition systems. An approach using single-model method that efficiently performs face detection recognition, and attribute analysis simultaneously is presented. Exploration of

multimodal machine learning approaches that explore intrinsic nature of diverse data modalities such as vision, audio, text, and motion are analyzed. Through a thorough review of these advancements, a comprehensive idea that could further enhance our understanding and application of AI in face recognition contexts are developed Continued investigation into these mechanisms will be crucial in advancing face recognition technologies and their applications [1],[2],[3], [6] [7].

The authors in [8] investigate a face recognition system that leverages deep learning techniques to accurately identify facial images. By employing various CNN models [4], the study focuses on both face detection and categorization. While previous research has primarily concentrated on ResNet or DenseNet models individually, this study innovates by integrating both to establish a hybrid model. Moreover, existing research has failed to address key challenges such as predictive face recognition which adapts to aging, facial variability and availability. The proposed research employs deep CNNs to enhance recognition by dynamically updating datasets when an 80% match is detected, enabling accurate identification across a five-year range. Noise conditions and lighting normalization improve model robustness, ensuring reliable recognition under varying conditions.

3. METHODOLOGY

The proposed research focuses on recognizing faces despite various facial conditions such as scars, aging, masks, and facial hair. A unique feature of the proposed model is its ability to predict how an individual's facial appearance will change both five years into the past and five years into the future, with automatic data updates. Additionally, the classifier is designed to maintain high performance under diverse lighting conditions and varying noise levels. To accomplish these objectives, a deep convolutional neural network methodology is employed that stabilizes the recognition process effectively. This approach is depicted in Fig. 1, with each block's roles and functions are elaborated.

Raw face images, collected from diverse sources like surveillance cameras, are crucial for training facial recognition and emotion detection systems. These images undergo preprocessing, including resizing, normalization, and augmentation techniques like rotation and flipping, to ensure dataset diversity and standardization.

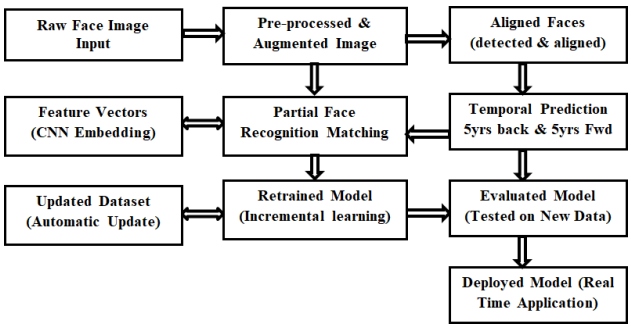

Fig. 1. Deep Learning Based Predictive Face Recognition.

Face detection and alignment, using models like MTCNN, identify key facial landmarks, while feature extraction with CNNs like ResNet generates high-level embeddings. Fine-tuning with triplet loss optimizes the model for specific datasets, enabling robust recognition even with partial face occlusion. The system dynamically updates datasets by integrating new facial data when matches are identified with high confidence, ensuring accuracy.

For temporal prediction, GAN-based models like CycleGAN predict facial changes over time while preserving identity. A Siamese network detects subtle changes, such as aging, and updates the dataset automatically. Incremental learning allows the model to adapt to new data without full retraining, using a combination of triplet and regularization loss. Model evaluation employs criterions like accuracy and F1-score to test staging on unseen data, including occlusions and aging effects. Finally, the model is deployed as a REST API or integrated into systems like surveillance, optimized for low latency using frameworks like TensorRT, ensuring real-time performance and enhanced user experience.

4. IMPLEMENTATION PERFORMANCE

Once the face is detected, alignment is applied. This step normalizes the face's orientation to make it easier to extract features. Almost 100% accuracy was received during image pre-processing and fine tuning. The image loss was below 0.5. Fig. 2 illustrates the variations in left eye distance over time, right eye distance over time, mouth width change, face height change, nose width change, and cheek width changes, showcasing predictions that reflect the face appearing slimmer or chubbier. This approach not only highlights the effectiveness of deep learning in facial analysis but also opens novel avenues for understanding personal transformations across time.



Fig. 2. Past and Future Facial Feature Changes.

In the proposed work, on partial face recognition, the evaluating scenarios where 60% of the face is obscured. The matching mechanism employed entails comparing the current feature vector derived from the obscured image with stored face embeddings. If there is an 80% match in the features, the model proceeds to update the dataset with the new data captured. To appraise the similitude betwixt feature vectors, techniques instance cosine similarity or Euclidean distance are employed. Each time a new face image is identified, the dataset is updated accordingly, which includes adding the new face and recalibrating the feature vectors. Furthermore, through incremental learning, the existing model using this enriched dataset was fine-tuned, where a gradient-based method is applied to update the model's weight effectively. This approach enhances the model's accuracy in recognizing faces under varying conditions of partial visibility.

The model's capabilities are enhanced through incremental improvements rather than starting from scratch. Following a retraining phase, the performance of the model using new data was carried out, focusing primarily on accuracy as the key metric. This criterion stipulates the segment of correct predictions, providing insight into the model's effectiveness. When analyzing the training graph that plots epochs against accuracy, we observe two crucial criterion: training accuracy and validation accuracy. Training accuracy reflects the model's staging on the data set it has already encountered, indicating how well it learns from the information provided. In contrast, validation accuracy assesses the model's propensity to postulate to unseen data, providing insights into its performance on new inputs. A disparity between these two metrics can signal potential issues in the model's learning process. For instance, achieving 100% training accuracy while having low validation accuracy advice that the model may be overfill, meaning it has memorized the training data rather than truly learning from it. Striking a balance between these metrics is crucial to ensure that the model execute well not just on familiar data but also on new, unseen datasets.

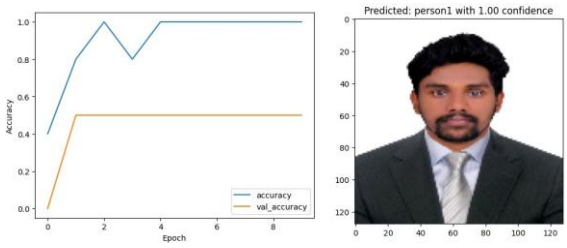

Fig. 3. Predicted Result with 1.00 Confidence

To optimize results, the scale range is compressed to 1, making it more manageable than a scale of 100. By examining 10 epochs, precise accuracy assessments, culminating in a display of 100% predicted confidence in

the images processed as shown in Fig. 3

5. Result and Conclusion

The paper proposes a deep learning method to identify real-time face recognition, capable of making temporal pre- dictions and engaging in continuous learning. By utilizing CNN embeddings for feature extraction, the system excels at accurately matching faces, even when parts are occluded up to 60%. When 80% of a face is detected, the system can reconstruct missing features. Additionally, a GAN-based model is employed to visualize a person's face from five years ago and predict their appearance five years in future, effectively accounting for natural aging. This system continuously updates its dataset and retrains itself with new facial data, ensuring ongoing enhancement of accuracy and reliability. In conclusion, the proposed system presents a novel face recognition approach and offers a robust and adaptive solution, even in challenging scenarios such as partial occlusion. One of its major features is the capability to accurately predict age progression and regression over a span of five years, coupled with automatic dataset updates, which ensures that the system remains current and effective in dynamic environments. In the future enhancements in refining the temporal prediction model to achieve greater precision in age regression will be considered.

References

[1] Huixiang Li , Ang Li , Yuning Liu ,Yiyu Lin , Yadong. (2024). AI Face Recognition and Processing Technology Based on GPU Computing, Journal of Theory and Practice of Engineering Science ISSN: 2790- 1505.

[2] Jin Lu, Bo Wu. (2022). A single-model multi-task method for face recognition and face attribute recognition in internet of things and visual computing, IET Image Processing DOI:10.1049/ipr2.12611.

[3] Ye Zhu, Yu Wu, Nicu Sebe, Senior, and Yan Yan, Senior all Members of IEEE .(2022). Vision + X: A Survey on Multimodal Learning in the Light of Data, journal of latex class files arXiv:2210.02884v2 [cs.CV] 7 Jun 2024.

[4] Kavita, Rajendra Singh Chhillar. (2024). Innovative Integration of Con- volutional Neural Networks for Enhanced Face Recognition, J. Electrical Systems 20-3s (2024): 1941-1950.

[5] Deng, J., et al. (2019). Arcface: Additive angular margin loss for deep face recognition. In: Proceedings of the IEEE/CVF Conference on Computer Vision and Pattern Recognition.

[6] M. Vamsi, K. P. Soman and K. Guruvayurappan, "Automatic Seat Adjustment using Face Recognition," 2020 International Conference on Inventive Computation Technologies (ICICT), Coimbatore, India, 2020, pp. 449-453, doi: 10.1109/ICICT48043.2020.9112538.

[7] S. J V, A. Sathrukkan, A. Bindu, R. S, T. S. Kumar and G. Jeyakumar, "An Investigational Study on Face Recognitionbased Attendance Track- ing System for Educational Institutions," 2024 International Conference on Inventive Computation Technologies (ICICT), Lalitpur, Nepal, 2024, pp. 900-906, doi: 10.1109/ICICT60155.2024.10544419.

[8] N. Ragesh, R. Ranjith and P. Sivraj, "Fast R-CNN based Masked Face Recognition for Access Control System," 2022 4th Inter- national Conference on Inventive Research in Computing Appli- cations (ICIRCA), Coimbatore, India, 2022, pp. 1049-1055, doi: 10.1109/ICIRCA54612.2022.9985509.

[9] A. Gupta, S. Sriram and V. Nivethitha, "Harnessing Diversity in Face Recognition: A Voting and Bagging Ensemble Approach," 2024 International Conference on Automation and Computation (AUTO- COM), Dehradun, India, 2024, pp. 249-255, doi: 10.1109/AUTO- COM60220.2024.10486188.

Biographies



M. Anand received the degree in B.E. EEE from Anna University in 2015, the M..E. PED from Anna University in 2021, and currently pursuing PhD degree in EEE from Amrita University, respectively. He is currently working as a MD at LAMS Automation Pvt. Ltd. His research areas include AI, ML & DL for visual Computing. He has been serving as an Innovator with strong foundation in Research and development with Granted Patent. 7 patents filed, 3 published in patent journal.

A Multiband Implantable Antenna for Pacemaker

Raghuramakrishnan S, Raguvarun G, Sabitha B, Bijimanzil A Sapna and Ramasamy .K

Department of ECE, KIT-Kalaignarkarunanidhi Institute of Technology, Kannampalayam, Coimbatore, India-641402

kit.25.21bec078@gmail.com, kit.25.21bec079@gmail.com, kit.25.21bec310@gmail.com, sapna79ece@gmail.com and ramasamy10366@gmail.com

Abstract.

A quad band microstrip patch antenna is presented in this paper designed for bio implant application specifically for pacemaker. The antenna's dimensions are $5\times5\times0.578mm^3$, and it was made of Rogers RT/Duroid6010, which has a thickness of 0.254mm. The antenna utilizes a meandering technique with a simple design structure to achieve miniaturization and multiband operation. The antenna has an impressive S11 magnitude of -24.79dB at 2.44GHz, -20.74dB at 3.53GHz, -22.13dB at 4.10GHz and -14.58dB at 5.79GHz making it operational in ISM and 5G sub 6 frequency bands. Simulated antenna gains at 2.44GHz, 3.5GHz, 4.10GHz, and5.79 GHz are -33.99dB, -15.49dB, -29.49dB and -20.8dB respectively. To ensure human safety SAR is analyzed in human heart model and the maximum allowable input power is 4.4mW which comply with FCC SAR limitations of 1.6W/Kg for 1 gm of tissues.

Keywords. Implantable antenna, multiband, pacemaker,5G

1. INTRODUCTION

Energy Pacemakers and implantable medical devices rely on implantable antennas for wireless communication, enhancing functions like monitoring and telemetry. Recent advancements focus on improving antenna performance, size, and multiband operation. Notable developments include J. Wang introduced a conformal antenna for endoscopy systems involving wireless capsule [1], while Zada developed a miniaturized implantable antenna with three bands for biotelemetry [2]. Shah et al. designed a spiral-shaped slotted implant antenna with four bands for scalp and leadless pacemakers [3]. Zhang et al. improved medical telemetry with a compact multiband antenna [4], and J. B. O'Connell et al. tested a multiband antenna for implanted devices [5]. Parker and K. E. Fisher optimized a dual-band antenna for leadless pacemakers [6].Recent advancements include a 5G MIMO antenna for cardiac pacemakers by Deepti Sharma et al. [7], a conformal implantable antenna for endoscopy by Jingchen Wang et al. [8], and a MIMO quad terminal triple-band antenna for deep tissue applications by Syed Manaf Ali Shah et al. [9]. These innovations enhance connectivity and efficiency in modern healthcare.

2. Antenna Design

The structure of proposed compact implantable antenna incorporates two symmetric meandered spiral arms modified with defected ground structure(DGS) making the design simple and compact as displayed in Figure 2.1. Geometry started with slotted arms and full ground and then meandering coupled with DGS to achieve multiple bands as in Figure 2.1.1. Antenna is designed to print on dual sided substrate and a superstrate is used to cover the radiating patch. Antenna has a planar square dimension of side 5 mm and height 0.578 mm, suitable for medical devices which has to be implanted smaller body parts. Rogers 6010 laminate act as substrate and top superstrate, having reduced dielectric loss with high permittivity. Meandering and defected ground improved antenna performance for desired bands with miniaturization. This laminate enhances microstrip antenna properties and miniaturization. Patch antenna equation(1&2) with multiple dielectric is used for calculating dimensions whose optimized dimensions are Listed in TABLE I.

Length $L=\lambda/(2\sqrt{\varepsilon eqv})$ (1)

Width $W=\lambda/(2\sqrt{\varepsilon eqv})$ (2)

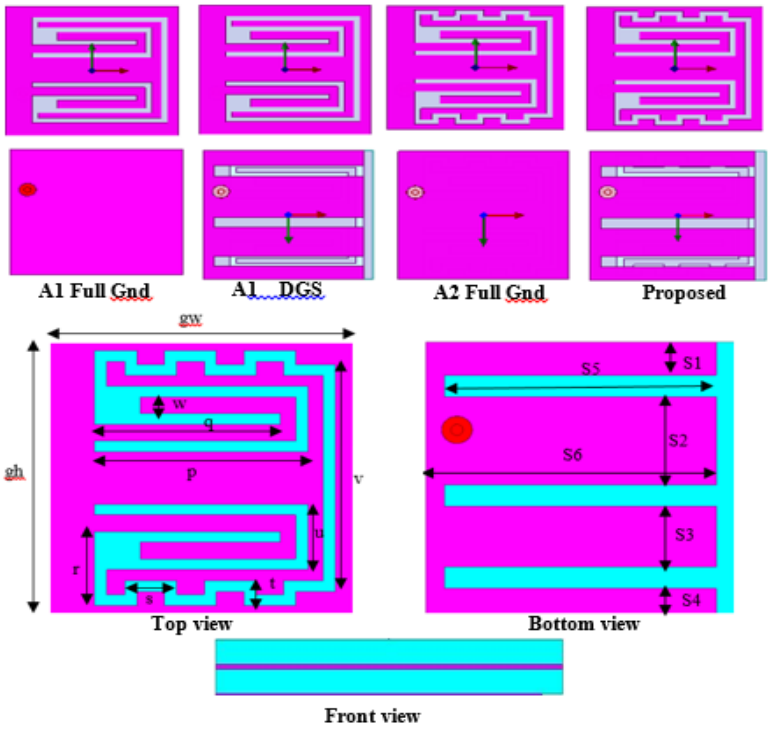

Figure 2.1. Geometry of Proposed Implantable Antenna with evolution

Table 1. Antenna Parameter

Antenna Parameter	gh	gw	p	q	r	s	t	u	v	w	S1	S2	S3	S4	S5	S6
Value (mm)	5	5	3.5	3.05	1.35	0.7	0.45	1.2	4.15	0.3	0.6	1.6	1.1	0.5	4.4	4.7

2.1. Results and Performance Discussion

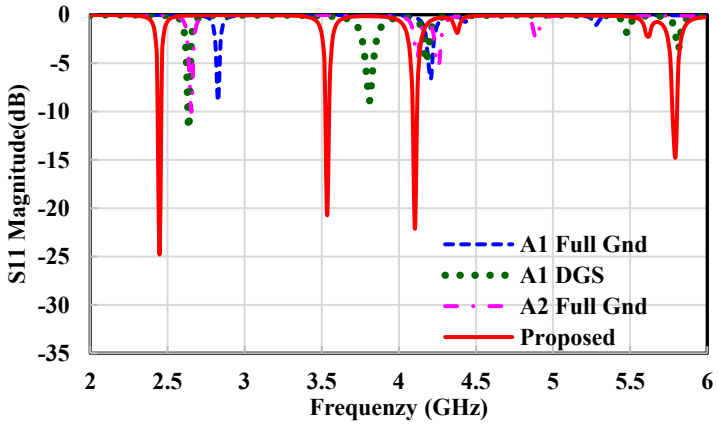

Figure 2.1.1 Return loss of designed antennas

This project simulations are done using HFSS software to evaluate the reflection and radiation performance with normal radiation open boundary condition at lower frequency of 2.45GHz. Slotted antenna (A1 Full gnd) is dual band with S_{11} >-10dB. When modified ground as DGS with multiple slots improved one band. Meandering with DGS provided multiband performance. Heart model of the software is utilized to study the real time bio implant application of pacemaker. The design has been carefully refined, showcasing remarkable impedance matching with return loss of 24.79dB at 2.44GHz, 20.74dB at 3.53GHz, 22.13dB at 4.10GHz and 14.58dB at 5.79GHz

frequency as depicted in Figure 2.1.1. Multiple frequency bands of the antenna make the pacemaker efficient and operational in 5G application with faster data transmission rate. Bandwidth offered by the antenna is 25MHz for the first two lower frequency band s and 30MHz for the two higher frequency bands. The radiation field patterns of the antenna is displayed in Figure 2.1.2, demonstrates how the radiated power changes with angular position for both Phi = 0° and 90° at operational frequencies of 2.44GHz, 3.53GHz, 4.1GHz and 5.79GHz. Stable and dependable radiative performance is confirmed by the observed symmetry and shape of patterns of radiation. Figure 2.1.3 shows the antenna's gain plot, offers a thorough examination of the antenna's radiation capabilities throughout its working frequency spectrum. The antenna exhibits gain of -33.99 dB at 2.44 GHz, -15.49 dB at 3.5GHz, 29.49 dB at 4.10 GHz and -20.80db at 5.79GHz reflecting reliable performance across the specified frequency ranges. There is a trade off between antenna size and gain.

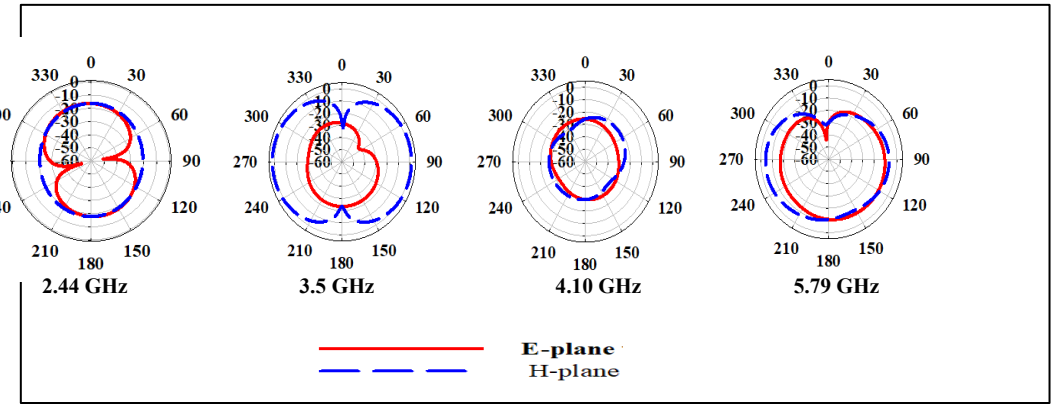

Figure 2.1.2. Radiation patterns of suggested Antenna

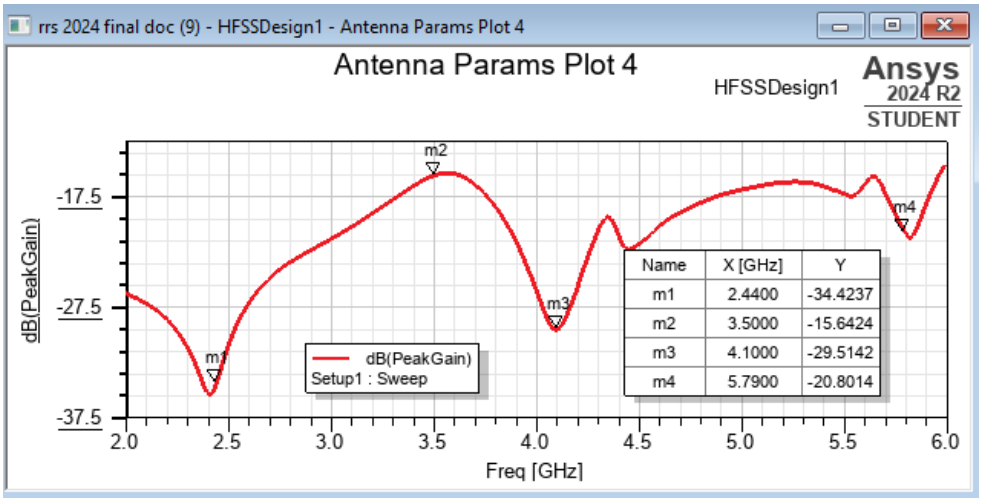

Figure 2.1.3. Gain of proposed antenna

2.2. SAR results

The rate at which electromagnetic energy is absorbed by bodily tissues in response to radio-frequency electromagnetic fields is measured by the SAR. To enable a safer transmission system in the body, the body's capacity to absorb radiation per unit mass of 1gm of tissue needs to be examined. The simulated antenna SAR on heart model at various frequency band are shown in Figure 2.2.1. We reproduce the 1-g averaged specific absorption rate (SAR) at 2.45GHz with varying input power levels to guarantee patient safety. Within the simulation, the antenna was carefully positioned in a model of heart tissue. Maximum SAR values obtained for 1W input power is 71.28W/Kg, 362.44W/kg, 421W/kg and 139.9W/kg for 2.4GHz, 3.53GHz, 4.1GHz and 5.79GHz respectively and the maximum input power allowable for FCC regulation limited SAR of 1.6W/Kg is 3.8mW.

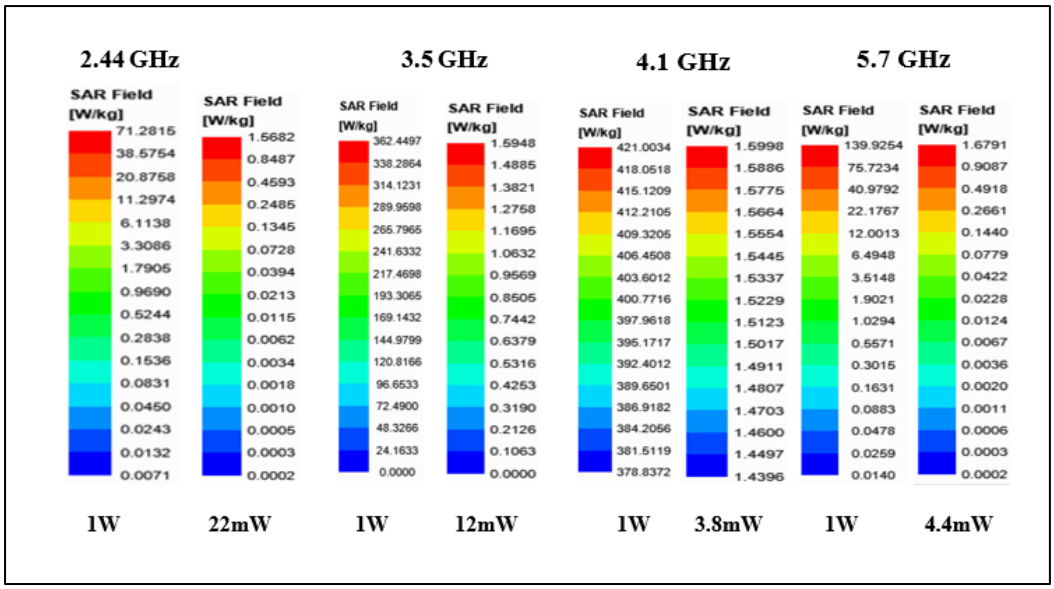

Figure 2.2.1. SAR results of the suggested antenna at various frequencies

Table 2. Comparison of Antenna Parameter with Literature

Reference	Frequency (GHz)	Bandwidth (MHz)	Dimension (mm^3)	Gain(dB)	SAR(W/Kg)	Max Input Power (mW)	Material
[1]	2.45 and 5.8	280 and 110	15x 15x 0.79	-31.6 and -- 28.66	403 and 361	1.7	Rogers 5870
[2]	1.95 and 2.45	65 and 60	7x 6x 0.5	-26.4 and -23	380, 358 and 363	4.4	Roger RT/Duroid 6010
[7]	2.45 and 5.8	44 and 40	3.4x 6.6x 0.254	-31.6 and - 21.4	263.3 and 107.45	6.3 and 11	Roger 3010
[8]	2.45	55	15x 15x 0.79	-27.5	913	1.6	Rogers 5870
[9]	0.9, 1.7 and 2.45	90, 129 and 200	7.5x 10.5x 0.127	-37.3, -30.3 and -20.9	251, 211 and 261	20	Roger RT/Duroid 6010
Proposed Antenna	2.44, 3.53 4.10 and 5.79	25,25,30 and 30	5 x5 x0.578	-33.99, - 15.49, - 29.49 and - 20.8	71.28, 362.4, 421 and 139.92	22,12,3.8 and 4.4	Rogers 6010

3. Conclusion

The design and development of a small, rectangular antenna for novel biomedical uses specifically, real-time cardiac monitoring—was discussed in this study. With S11 magnitudes of -24.79 dB at 2.44GHz, -20.74 dB at 3.53GHz, -22.13 dB at 4.10GHz, and -14.58 dB at 5.79GHz, the proposed antenna operates in quad bands. The antenna's integration of the 5G frequency alongside the ISM band is an advantage. In future antenna will be experimentally validated for pacemaker and other biomedical applications such as endoscopy and ICP. The antenna is appropriate for cardiac pacemaker applications due to its acceptable gain and decreased SAR value.

Acknowledgement: AICTE : File No.8-122/FDC/RPS/POLICY-1/2021-2022.

References

1. 1. J. WANG, "AN IMPLANTABLE AND CONFORMAL ANTENNA FOR WIRELESS CAPSULE ENDOSCOPY", IEEE ANTENNAS AND WIRELESS PROP. LETT, VOL. 17, PP. 1568-1571, 2018.
2. M. Zada, "A Miniaturized Triple-Band Implantable Antenna System for Biotelemetry Applications", IEEE TAP., vol. 16, No. 12, pp. 3851-3860, 2018.doi: 10.1109/TAP.2018.2874681
3. IA. Shah, M. Zada and H. Yoo, "Design and Analysis of a Compact-Sized Multiband Spiral Shaped Implantable Antenna for Scalp Implantable and Leadless Pacemaker Systems", IEEE TAP, vol. 67, no. 6, pp. 4230-4234, 2019. doi: 10.1109/TAP.2019.2908252.
4. L. R. Zhang, Y. K. Tan, And H. T. Nguyen, "Design Of A Compact Multiband Implantable Antenna For Medical Telemetry Applications," IEEE Trans on Biomedical Engg, vol. 66, No. 5, Pp. 1245-1254, May 2019.
5. J. B. O'Connell, J. K. Lee, and M. M. Krueger, "Development and Testing of a Compact Multiband Antenna for Implanted Medical Devices," IEEE Transactions on Microwave Theory and Techniques, vol. 68, no. 1, pp. 231-240, Jan. 2020.
6. R. V. W. Z. B. Parker and K. E. Fisher, "A Compact Dual-Band I Implantable Antenna for Leadless Pacemakers: Design, Simulation, and Testing," IEEE Antennas and Wireless Propagation Letters, vol. 18, no. 1, pp. 99-106, Jan. 2019.
7. Deepti Sharma1 , Binod Kumar Kanaujia1,2, Sachin Kumar3 , Karumudi Rambabu4 & Ladislau Matekovits5,6,7 "Low-loss MIMO antenna wireless communication system for 5G cardiac pacemakers " 2023
8. Jingchen Wang, Mark Leach, Eng Gee Lim, Zhao Wang, Rui Pei and Yi Huang "An Implantable and Conformal Antenna for Wireless Capsule Endoscopy ": DOI 10.1109/LAWP.2018.283639
9. Syed Manaf Ali Shah, Muhammad Zada , Member, IEEE, Jamal Nasir , Owais Owais, and Hyoungsuk Yoo , Senior Member, IEEE "Four-Port Triple-Band Implantable MIMO Antenna for Reliable Data Telemetry in Wireless Capsule Endoscopy and Deep Tissue Applications" Ieee Transactions On Antennas And Propagation, VOL. 72, NO. 8, AUGUST 2024

An Implantable Wideband Antenna for Monitoring Bone Fracture Healing

Ameerdeen B, Bharathi P, Dhanasurya M, Sapna Bijimanzil A and Ramasamy K
Department of ECE, KIT-Kalaignarkarunanidhi Institute of Technology, Kannampalayam, Coimbatore, India-641402

kit.25.21bec0301@gmail.com, kit.25.21bec019@gmail.com, kit.25.21bec027@gmail.com, sapna79ece@gmail.com and ramasamy10366@gmail.com

Abstract.

This manuscript presents the creation of a compact wideband implantable antenna with circular polarization that is designed to be used continuously for Bone fracture healing monitoring. Antenna proposed here employs a dual-port looping architecture, offering wideband ranging from 0.15 MHz to4.11 GHz, with resonances at 400 MHz and 3.6 GHz for WBAN and telemetry applications. The dual-port looping architecture in the proposed antenna plays a crucial role in achieving circular polarization (CP) and wideband coverage. This design incorporates two feeding ports arranged in a loop configuration, enabling efficient electromagnetic wave propagation with orthogonal field components. The antenna is made of Rogers Duroid 6010 substrate, for improvement in size reduction to $5 \times 5 \times 0.324$ mm^3. The antenna has return losses of -30 dB at 400 MHz and 3.6 GHz and the gain is -1.46 dB and 0.06 dB at the lower and upper resonant frequencies, respectively. Safety is guaranteed by SAR analysis, where the antenna is positioned in knee bone of a human leg. The circular polarization of the antenna ensures stable transmission of signals in changing environments. Obtained results show good matching impedance and adequate efficiency in radiation, making it suitable for bone healing monitoring in biomedical applications.

Keywords. Implantable antenna, wideband, circularly polarized, bone fracture healing monitoring.

1. INTRODUCTION

Bone fractures healing is considered as a major challenge in healthcare, especially when it comes to tracking the healing process. Conventional techniques like X-rays, CT scans, and MRI yield interval images, which demand regular hospital visits and lack continuous monitoring. This shortcoming has given rise to new wireless implantable antennas that can monitor the bone healing process in real-time, yielding useful information without requiring frequent imaging or clinical visits. The systems offer a long-term, non-invasive way of monitoring the healing of bones. Experiments have proven that implantable antennas can be used to monitor the bone fractures healing, and their applications cover monitoring recovery in bones like the radius, tibia, and phalanges. A detailed study on the various types of implantable antennas with materials used, characteristics, applications and The impact of body fluids and tissues on antenna performance is another critical consideration [1-2]. Researchers have analysed the effects of different body environments on antenna impedance matching and radiation efficiency A compact triple band MIMO antenna with multiple port [3] is presented for wireless endoscopy and is capable of data telemetry with wireless power transfer. A small, circular, dual-band implantable antenna that can be placed on the skin and scalp operating 1.43 GHz and 2.44 GHz frequency bands is discussed in [4]. Several studies have explored innovative antenna designs to optimize their performance in the human body environment. Various antenna geometries, such as meandered conformal designs, loop antennas [5], and fractal-inspired structures [6,7], have been investigated to achieve wideband operation, miniaturization, and improved radiation efficiency. Multi-band and MIMO (Multiple Input Multiple Output) configurations have also been proposed to enhance data transmission reliability, particularly for deep tissue and capsule endoscopy applications [8]. Industrial IoMT application ultra-miniaturized antenna An implantable antenna show multiband operation and improve communication and integration for medical applications [9]. Recent research has proven the successful monitoring of operated fractures, like upper arm fractures, using implantable antennas

at operating frequencies such as 402 MHz, highlighting the viability of these technologies in clinical settings [10].

This article introduces the development of a small, Circularly Polarized (CP) antenna for implant in the knee aimed at tracking bone healing of fractures on a continuous basis. The antenna provides wideband performance between 0.15 MHz and 4.11 GHz with resonating frequencies of 400 MHz and 3.6 GHz that are well suited for WBANs and for medical telemetry purposes.

TABLE 1: PROPOSED ANTENNA COMPARISION WITH PREVIOUS WORK

Ref	frequency	Dimensions (mm^3)	BW(MHz)	Gain (dB)	SAR(W/kg)for 1g
[1]	915MHz	7×7×0.254	200	-16.8	8.17
[4]	2.48GHz	25×25×1.28	N/A	N/A	7.3
[7]	2.45GHz	32×30	150	1.68	0.57
[9]	3.23GHz	18×19×0.8	112.23	3.77	1.6
Proposed Antenna	400MHz and 3.6GHz	5×5×0.324	3970 (1500 to 4110)	-1.46, 0.06	8.7 1865.33

2. Proposed Antenna Design

The suggested implantable antenna features a dual-port with looping architecture designed to achieve circular polarization and wideband performance. The antenna design started with basic patch and slots were inserted to operate at 400 MHz and 3.6 GHz. With an overall size of 5×5×0.324 mm^3, the antenna has slotted radiating patch and ground with 0.035mm thickness. Symmetrical slots with dual port improve bandwidth. The looping structure enhances impedance matching and axial ratio performance, crucial for stable wireless body area network (WBAN) communication. Antenna simulations are carried out using HFSS 2024 with Rogers RO6010 (ε = 10.2) substrate which benefits from low attenuation and miniaturization for efficient signal transmission compared to low dielectric materials like polyethylene and PEEK. Simulation set up was done with sweep frequency range from 0.1GHz to 4GHz covering MICS, ISM and sub 6GHz bands and open radiation boundary at 400MHz.

These structural aspects contribute to the antenna's reliable operation in medical telemetry and bone fracture healing monitoring applications. Figure 2.1. shows different views of wideband implant antenna structure. The antenna adopts a dual-port feeding structure, located at both sides to connect the rectangular strips that constitute a closed-loop configuration. The structure enables accurate control over excitation, allowing for the creation of circular polarization and bandwidth improvement. The feeding mechanism adopted ensures reliable wireless communication irrespective of the orientation of the antenna and thus makes it extremely compatible with implantable devices that have to work within dynamic environments.

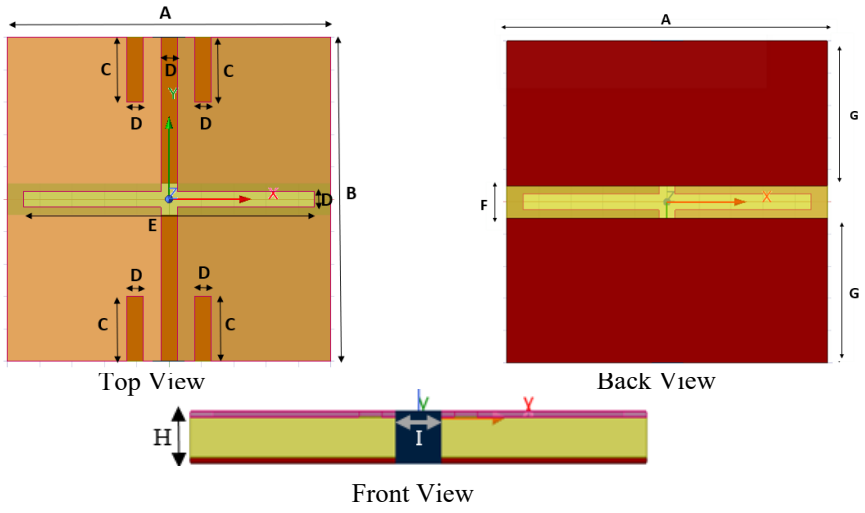

Figure 2.1. Different views of wideband implant antenna structure.

TABLE 2: PROPOSED ANTENNA DIEMENSIONS

Antenna Parameters	A	B	C	D	E	F	G	H	I
Dimensions (mm)	5	5	1	0.25	4.5	0.5	2.25	0.324	0.5

3. Results And Performance

Return loss plays a vital role in determining how successfully an antenna transmits signals without undesired reflections. A smaller return loss means that more power is successfully radiated, resulting in better overall performance. In this design, the antenna has return losses of -30.00 dB at 400 MHz and at 3.6 GHz respectively and wide bandwidth ranging from 0.15GHz to 4.11GHz. These findings enable effective power transfer, making the antenna suitable for medical applications such as bone fracture repair monitoring. The following Figure 3.1(a &b) depicts the return loss performance and gain at various frequencies. Antenna gain is a highly critical parameter that describes the radiating efficiency in one direction. It is an indicator of how well the antenna transforms power fed into it to energy radiated. For the suggested design, the gain is -1.46 dB at 400 MHz and 0.06 dB at 3.6 GHz. Even though negative gain at the lower frequency is expected due to the compact size and implantable nature of the antenna, it is still sufficient to maintain signal transmission uniformly within the human body. Reduced return loss indicates better radiation with good efficiency thereby making it appropriate for stable and reliable wireless communication in biomedical

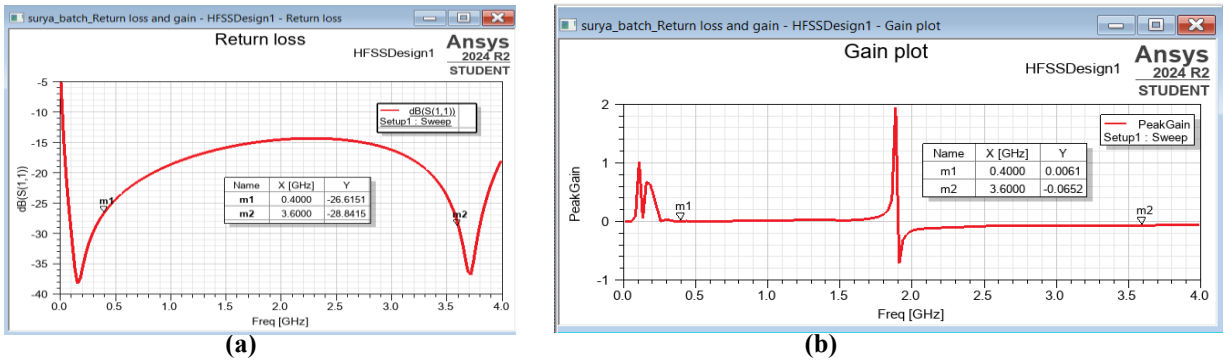

Figure 3.1. Antenna performance (a) Return loss (b) Gain

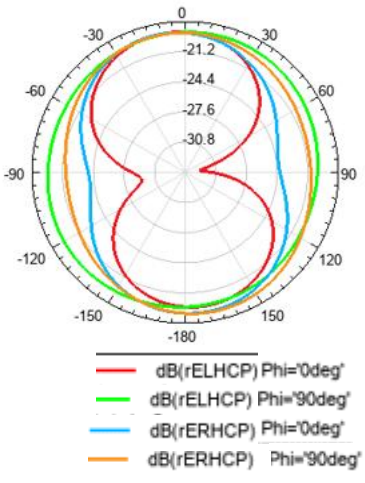

Figure 3.2. Patterns (3.6 GHz)

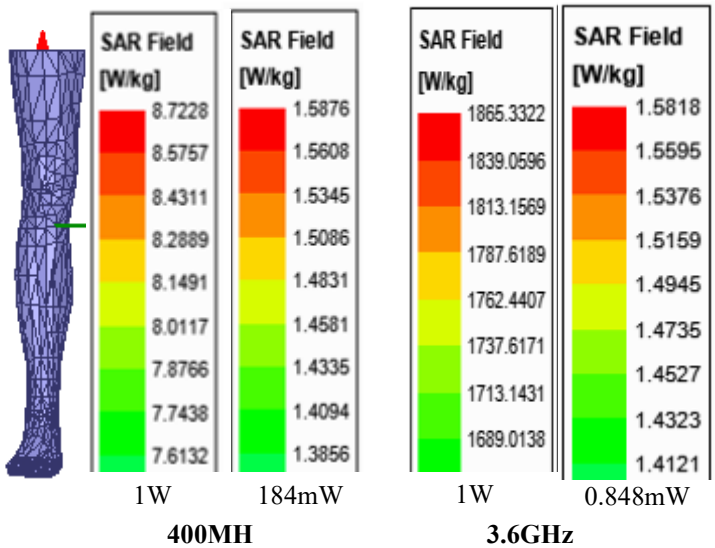

Figure 3.3. SAR results

applications. Circular polarization having energy radiated in all directions, thus the movement of legs does not affect the performance. The very minor positive gain at 3.6 GHz ensures higher frequency radiation efficiency. Figure 3.2 shows patterns of the proposed dual-port antenna at 3.6 GHz. The Specific Absorption Rate(SAR) indicates rate of radiated signal by body.In this simulation, the antenna was placed within a layered tissue model,

considering the varying dielectric properties and thicknesses of the tissue layers. SAR values were calculated for two frequencies, 400 MHz and 3.6 GHz, based on the watts provided in the study. According to the regulatory standards set by the FCC is 1.6 W/kg for 1 gram of body tissue. The calculated SAR values for both frequencies were assessed against the safety limits to ensure compliance with human safety standards. Figure 3.3 gives the SAR analysis on simulation.

4. Conclusion

A wideband two port CP implantable antenna was designed for healing permanent bone fracture monitoring. The CP wide band operates between 0.15 MHz to 4.11 GHz with resonance at 400 MHz and 3.6 GHz with antenna cross section of 5 mm × 5 mm on Roger 6010 substrate with height 0.324mm. The antenna demonstrates S_{11} of -30.00 dB at 400 MHz and 3.6 GHz having gains of -1.46 dB at 400 MHz & 0.06 dB at 3.6 GHz. Safety certification is ensured by SAR analysis, in which the antenna is placed inside the leg phantom. The antenna's circular polarization ensures reliable signal transmission under dynamic conditions. The antenna can position on edges and sides of the bone. It will not affect that much in signal transmission due to wide bandwidth. Future work will include fabrication and experimental validation of antenna and focus on performance improvement in gain.

Acknowledgement. AICTE: File No.8-122 / FDC/RPS/POLICY-1/2021-2022.

5. References

[1] Ahmad et.al., X-Shaped Slotted Patch Biomedical Implantable Antenna for Wireless Communication Networks. International Journal of Wireless and Mobile Computing, 2022 doi:10.1155/2022/7594587.

[2] Labus et al., Direct electromagnetic coupling for non-invasive measurements of stability in fracture healing doi: 10.1002/jor.24275. Epub 2019 Mar 28. PMID: 30839117.

[3] Kerketta, Shilpi & Ghosh, Debalina. (2020). Microwave Sensing for Human Bone Health Evaluation. AEU - International Journal of Electronics and Communications. 10.1016/j.aeue.2020.153469.

[4] Venkatesan, B. & Krishnan, Kalimuthu & Palaniswamy, Sandeep & Kumar, Sachin & Bhowmik, Shreya & Sharma, Nivesh & Vaish, Deepesh & Chatterjee, Sourish. (2022). 1-12. 10.1155/2022/4663488.

[5] Nouri Moqadam, Aslan & Kazemi, Robab. (2022). Design of a Novel Dual-Polarized Microwave Sensor for Human Bone Fracture Detection Using Reactive Impedance Surfaces. 10.21203/rs.3.rs-2421957/v1.

[6] Shaik, Rizwan & V Phani Kumar, Kanaparthi & Palaniswamy, Sandeep. (2023). On the Experimental Investigation of Bone Fracture Recovery Process Using an Ultra-Wideband Planar Monopole Antenna .10.1155/2023/8825446.

[7] Zeinelabedeen, Wael & Uyguroglu, Rasime. (2023). Monitoring of Surgically Treated Upper Arm Fracture by Implanted Antenna at 402 MHz. Applied Sciences. 13. 7786. 10.3390/app13137786.

[8] Rizvi, Syed Naheel & Awan, Wahaj & Hussain, Niamat.(2020). Design and Characterization of Miniaturized Antenna for UWB Communication Systems. Journal of Electrical Engineering and Technology. 16.10.1007/s42835-020-00630

[9] Shah et al, "Ultra-Miniaturized Implantable Antenna Enabling Multiband Operation for Diverse Industrial IoMT Devices," in IEEE Transactions on Antennas and Propagation, vol. 72, no. 2, pp. 1352-1362, Feb. 2024, doi: 10.1109/TAP.2024.3349782.

[10] Symeonidis, Symeon & Whittow, Will & Zecca, Massimiliano & Panagamuwa, Chinthana. (2018). Bone fracture monitoring using implanted antennas in the radius, tibia and phalange heterogeneous bone phantoms. Biomedical Physics & Engineering Express. 4. 10.1088/2057-1976/aab974.

DESIGN AND IMPLEMENTATION OF AN AUTOMATED SORTING SYSTEM FOR WASTE HANDLING

DR R GOWRISHANKAR[1], DIVYASRE T[2], AISWARYA G[3], MUTHUSARAVANAN K[4] RAGAVENDHIRAN B[5]

[1,2,3,4,5]Department of Electronics and Communication, KIT-KalaignarKarunanidhi Institute of Technology, Coimbatore, India

ABSTRACT

Automated waste segregation systems are very important to address various waste management challenges, such as the proper handling of biomedical waste in the medical field, which is crucial in preventing health and environmental hazards. The paper documents a prototype for an Automated Medical Waste Segregation System out of low-cost components such as Arduino Uno, servo motors, stepper motors, buzzers, IR sensors, proximity sensors, load cell, and rechargeable batteries. The segregation system could distinguish different types of medical waste, i.e., segregation into categories of plastic, metal, and bio-waste, with an approximate efficiency of 85-90%. The waste type is determined by a set of proximity and IR sensors. A weight sensor makes it possible to allow only approved quantities to continue with the segregation process by communicating the segregation data to the Arduino Uno microcontroller. The direction to which the waste is guided into its respective trash bin is indicated by the functioning of the servo motors and stepper motors based on the input from the sensors. Integrated into this is a buzzer that alerts a user when the three collection tanks are overloaded or when there is an error in the segregation of devices. Designed as a battery-operated system, it provides portability and power efficiency for use in hospitals, clinics, and laboratories. It aims to improve the management efficiency of biomedical waste, minimize human intervention, and reduce risks associated with incorrect disposal.

Keywords - Medical Waste Management, Arduino Uno, Proximity Sensor, Servo Motor, Stepper Motor, IoT in Healthcare.

I.INTRODUCTION

Efficient waste management in the healthcare industry has rightfully blossomed into burning discourse with the upsurge in daily biomedical waste generation. Biomedical waste reflects a plethora of materials, including used syringes, contaminated gloves, plastic containers, and metal instruments, which need to be properly segregated and disposed of in a bid to prevent health and environmental hazards. The collection and disposal of such waste may lead to infection outbreak, environmental pollution, and health hazards to the workers employed to handle such waste. Traditional segregation methods are very tedious and involve serious hazards to health for workers involved. Hence a demand is growing to develop automated systems that sort the biomedical waste without or with minimal human intervention.

The system proposed is going to develop an automated waste separation prototype useful for hospitals by affording low-cost and easily available components. At the core of this system, the Arduino Uno microcontroller gets data from IR sensors, proximity sensors, and load cells to differentiate and segregate the materials into their relevant type of waste. The sorting of waste into either plastic, metal, or bio-waste is carried out using servo motors or stepper motors, respectively. Other components include a buzzer, which will alert users to the state of operation of the system in case of any system failures, which greatly enhance usability and reliability. The additional benefit of all rechargeable batteries would provide energy efficiency and portability, making a system that is applicable in hospitals and laboratories.

II. SYSTEM IMPLEMENTATION

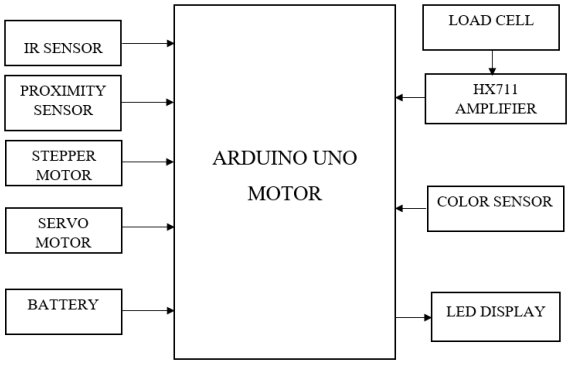

Figure 1: Block Diagram of Automated sorting system

Figure 1 is a block diagram of an automated waste segregation system with Arduino Uno as the master microcontroller. The Automated Medical Waste Segregation System is designed for sorting and disposal of medical waste according to various types by a set of sensors and actuators. The segregation system will be activated by the first IR sensor when it senses the waste. The second one is detecting metallic objects based on the electromagnetic property principles, and the third one is detecting plastic and paper with a color sensor. The weighing of the waste will also ensure proper classification of the waste. The Arduino Uno microcontroller gathers all data from the sensors and responds accordingly to the waste using actuators: a servo motor accurately guides the waste into the bins, whereas a stepper motor facilitates controlled motion of devices such as conveyor belts in sorting use. For assurance, there is a buzzer for use in errors or overload state. It runs on a rechargeable battery which makes it highly portable. This automated segregation of waste minimizes human exposure to toxic materials through enhancing efficiency and safety in clinics, hospitals, and laboratories. In addition, it represents fulfilment of biomedical waste management guidelines and elimination of environmental hazards by practicing sustainable disposal methods. As this system makes use of many sensors and actuators for multiple classifications, this system is precise and effective in waste sorting and hence this system is reliable as well as an environmentally friendly medical waste solution.

III. RESULTS

The experimental evaluation of the automated medical waste segregation system was conducted over four weeks in a controlled medical environment. The system's performance was assessed based on sorting accuracy, efficiency, processing speed, and overall effectiveness compared to manual sorting methods. A total of 100 waste samples, including metallic, plastic, and bio-waste, were tested to determine classification accuracy. The results showed significant improvements, with metal waste detection increasing from 75% in manual sorting to 92% using the automated system. Similarly, plastic waste classification accuracy improved from 60% to 85%, while bio-waste identification reached 80% compared to 65% in manual methods. Overall, the automated system achieved an accuracy of 85.6%, demonstrating a 19% improvement over manual sorting techniques.

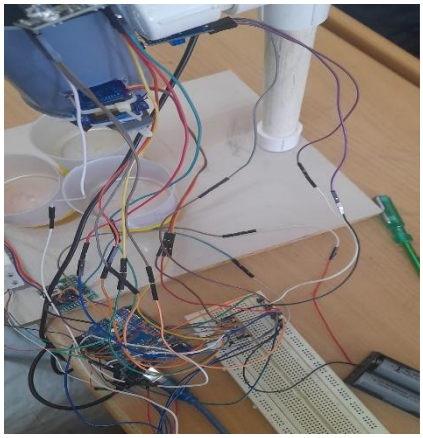

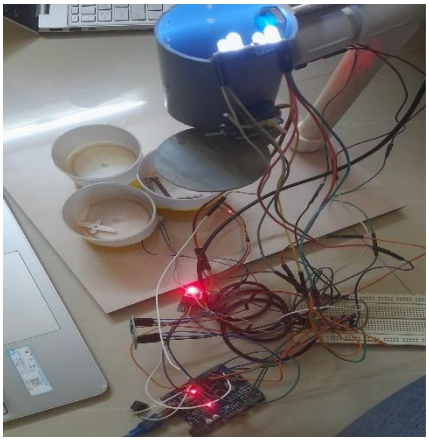

In addition to accuracy, the system's processing speed was also evaluated. The manual sorting method required an average of 8–10 seconds per item, whereas the automated system completed the sorting process in 4–6 seconds per item, reducing the overall sorting time by nearly 40%. The integration of sensors, including metal detectors, color sensors, and load cells, significantly improved waste classification and efficiency. Furthermore, the system effectively minimized human intervention, ensuring better hygiene and reducing the risks associated with handling hazardous medical waste.

Parameter	Existing System	Proposed System
Accuracy	60%	85%
Efficiency	55%	80%
Portability	50%	75%
Cost	80%	50%
Processing Speed	85%	65%

Table 2: Comparison of Existing system and Proposed system

PARAMETER	MANUAL SORTING	AUTOMATED SORTING
Sorting Accuarcy	75%	95%
Time Taken Per Object	8-15 Sec	2-4 Sec
Sorting Speed	5 Items	15 Items
Human Involvement	High	Minimal
Error Rate	20%	5%

Table 3: Comparison of Manual sorting and Automated sorting

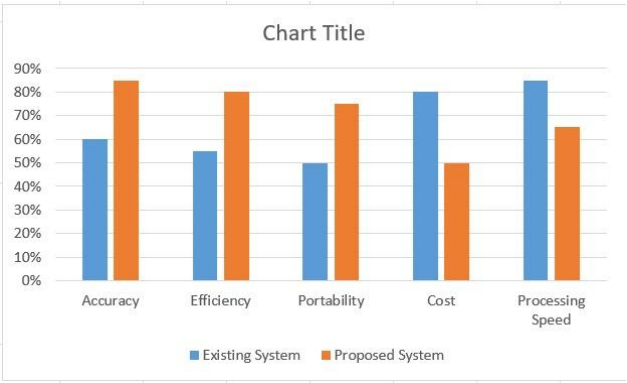

Figure 5: Comparison of Existing system and Proposed system

The accuracy of the proposed system is higher, reaching 85% compared to 60% in the existing system, ensuring better classification of medical waste. Efficiency has also improved from 55% to 80%, reducing errors and increasing the reliability of waste segregation. Additionally, the proposed system is more cost-effective, with a cost percentage of 50% compared to 80% in the existing system, meaning it is more affordable and requires lower operational expenses. However, the processing speed of the existing system (85%) is slightly higher than the proposed system (65%), indicating that while the new system offers better classification and efficiency, it operates at a slightly reduced speed. Despite this, the proposed system offers a more accurate, efficient, and cost-effective approach to medical waste management, making it a valuable improvement over current method.

IV CONCLUSIONS

The Automated Waste Segregation System provides a practical and cost-effective solution for biomedical waste management, enhancing accuracy, efficiency, and operational reliability. With an accuracy rate of 85% and efficiency of 80%, the system significantly reduces human intervention by utilizing an Arduino-based control system, sensors, and motorized sorting mechanisms. Its portable, battery-operated design makes it highly adaptable for use in hospitals, clinics, and remote locations, ensuring waste segregation even in areas with unstable power supply. Real-time alerts through a buzzer enhance safety by notifying users of overload or system failures. While the system's processing speed is 65%, slightly lower than some existing solutions, this is balanced by its increased portability (75%) and reduced operational costs (50%) compared to traditional methods. Future enhancements could include AI-based classification and machine learning integration to improve sorting efficiency further. Additionally, incorporating real-time IoT-based data analytics can optimize waste handling, monitor system performance remotely, and ensure better compliance with biomedical waste disposal regulations.

REFERENCE

[1] S. S. Raut, S. S. Khot, S. S. Kamathe, and S. S. Patil, "Automatic Waste Segregator and Monitoring System," 2017 International Conference on Computing Methodologies and Communication (ICCMC), Erode, India, 2017.

[2] A. S. S. Sekhar, S. S. Kumar, and S. S. Kumar, "Automation of Plastic, Metal and Glass Waste Materials Segregation using Arduino in Scrap Industry," 2017 IEEE International Conference on Power, Control, Signals and Instrumentation Engineering (ICPCSI), Chennai, India, 2017.

[3] C. G. Gupta, S. J. Patel, and R. A. Tiwari, "Automated Medical Waste Segregation and Management using IoT," 2019 IEEE International Conference on Environmental and Health Sciences (ICEHS), New Delhi, India, 2019.

[4] S. S. Patil, S. S. Khot, S. S. Kamathe, and S. S. Raut, "Automatic Waste Segregator and Monitoring System,"2017 International Conference on Computing Methodologies and Communication (ICCMC), Erode, India, 2017.

[5] A. K. Verma, S. R. Patil, and A. S. Gupta, "IoT-Based Smart Waste Management System for Efficient Waste Segregation," 2019 IEEE International Conference on Recent Trends in Electronics, Information & Communication Technology (RTEICT), Bangalore, India, 2019.

[6] H. P. Sharma, P. R. Mehta, and S. S. Roy, "Automated Waste Classification and Sorting System using Image Processing," 2018 International Conference on Innovations in Power and Advanced Computing Technologies (i-PACT), Vellore, India, 2018.

[7] K. N. Mohan, J. B. Rao, and M. Kumar, "A Novel Approach for Waste Segregation using Convolutional Neural Networks," 2020 IEEE International Conference on Smart Technologies and Sustainable Manufacturing (STSM), Kuala Lumpur, Malaysia, 2020.

[8] S. Y. Tan, W. H. Ling, and C. L. Tan, "Smart Waste Sorting System using IoT and AI," 2021 IEEE International Conference on Internet of Things and Intelligence Systems (IoTaIS), Jakarta, Indonesia, 2021.

[9] M. P. Rajan, V. A. Sreenivasan, and D. S. Kumar, "Sensor-Based Smart Bin for Automatic Waste Segregation," 2019 IEEE International Conference on Intelligent Computing and Control Systems (ICICCS), Madurai, India, 2019.

[10] T. S. Lee, K. P. Wong, and L. W. Tan, "Waste Sorting and Classification using AI-Based Image Processing," 2021 IEEE International Symposium on Computational Intelligence (ISCI), Sydney, Australia, 2021

Webtrace An Automated Hate Speech Detection and Enforcement System for Instagram Using Playwright, OCR, and NLP

G. Thiagarajan, Danend Krishnan U, Soniya N, Soniya N

[1]Head of the Department IT, CSI College of Engineering, Ketti, The Niligiris-643215[1]

[2]Final year IT Student, CSI College of Engineering, Ketti, The Niligiris-643215[2]

[3]Final year IT Student, CSI College of Engineering, Ketti, The Niligiris-643215[3]

[4]Final year IT Student, CSI College of Engineering, Ketti, The Niligiris-643215[4]

ABSTRACT

Social media platforms have revolutionized communication by enabling users to share their thoughts, experiences, and opinions with a global audience. Among these platforms, Instagram stands out as a widely used application that allows users to post images, videos, and stories, engage with others through comments and messages, and explore diverse content based on their interests. Its user-friendly interface and interactive features make it a preferred choice for individuals, influencers, and businesses alike. However, alongside its benefits, Instagram also presents challenges, particularly in content moderation. The open nature of the platform allows users to express themselves freely, but this can lead to the spread of harmful content, including hate speech, cyberbullying, and misinformation. To address the challenges, WebTrace introduces an automated hate speech detection framework designed specifically for Instagram. WebTrace leverages Playwright for web scraping, Optical Character Recognition (OCR) for extracting text from images, and advanced Natural Language Processing (NLP) techniques such as TF-IDF with Cosine Similarity and a USE Transformer model to analyze text content. Unlike conventional methods, WebTrace not only detects hate speech in real-time but also takes immediate action by automatically reporting the detected content to Instagram moderator.

Keywords: Hate Speech Detection, Automated Moderation, Playwright Automation, Optical Character Recognition (OCR), USE Transformer model, TF-IDF, Natural Language Processing (NLP), WebTrace.

1. INTRODUCTION

With digital technology advancing rapidly, platforms like Instagram, Twitter, and Facebook have become the main way billions of people connect, share ideas, and form communities. These platform offers discussion, creativity, and social interaction—but they also come with serious downsides. Weak content moderation policies have turned many of these spaces into hotspots for hate speech, cyberbullying, and the spread of false information. The ease of access and the ability to stay anonymous online often embolden users to post harmful or offensive content, frequently aimed at specific individuals or groups based on race, gender, religion, nationality, and other personal traits.

The impact of cyberbullying and online harassment is far from harmless. Victims may suffer from anxiety, depression, social isolation, and in some heartbreaking cases, self-harm or suicide. Hate speech, in particular, can escalate discrimination and even incite real-world violence. This makes it all the more urgent for social media platforms and authorities to put strong detection and moderation systems in place. Unfortunately, many traditional approaches like manual reviews or simple keyword filters—aren't enough. They often fail to pick up on sarcasm, changing slang, multilingual posts, or hate speech hidden inside images. On top of that, the sheer volume of posts makes it nearly impossible to monitor everything in real-time without automation.

To help tackle these issues, this paper introduces WebTrace, a fully automated, JavaScript-based system designed to detect and respond to hate speech on Instagram. WebTrace brings together several technologies

web scraping, Optical Character Recognition (OCR), and Natural Language Processing (NLP) to accurately identify harmful content and enable fast, real-time responses.

The system operates as follows:

1. **Automated Instagram scraping** using **Playwright**, extracting captions, comments, and images.
2. **OCR-based text extraction** from images using **Tesseract.js**, enabling detection of hate speech in memes and visual content.
3. Hate speech classification using TF-IDF with Cosine Similarity and a USE Transformer model, ensuring high accuracy in identifying harmful content.
4. Automated enforcement actions, where WebTrace revisits the flagged post, reports it to Instagram moderators.

Unlike traditional moderation techniques, WebTrace combines automated detection with real-time intervention, ensuring a scalable, AI-driven approach to making social media platforms safer. By integrating text analysis, image recognition, and automated content enforcement, WebTrace represents a proactive solution to combat hate speech effectively.

2. LITERATURE REVIEW

[1] A Novel Method based on Character Segmentation for Slant Chinese Screen-render Text Detection and Recognition

Authors: Tianlun Zheng, Xiaofeng Wang, Xin Yuan, and Shiqin Wang

Abstract: Screen rendering text has broad application prospects in the fields of medical records, dictionary screen capture, and screen-assisted reading. However, Chinese screen rendering text always has the challenges of small font size and low resolution. Obtaining a screen-rendered text image in a natural scene will have a certain tilt angle. These all pose great challenges for screen text recognition. This paper proposes a method based on character segmentation to address these challenges.

[2] Research on Text Detection and Recognition Based on OCR Recognition Technology

Author: Yuming He

Abstract: Image recognition and optical character recognition technologies have become an integral part of our everyday life due in part to the ever-increasing power of computing and the ubiquity of scanning devices. Printed documents can be quickly converted into digital text files through optical character recognition and then be edited by the user. Consequently, minimal time is required to digitize documents; this is particularly helpful when archiving volumes of printed materials.

[3] Social Media Web Scraping using Social Media Developers API and Regex

Authors: Luciana Citra Dewi, Meiliana, Alvin Chandra.

Abstract: A system is developed to implement the proposed method by using an API that Facebook Developers and Twitter Developers provided. In addition, regular expression (or Regex) which is a language construction that can be used for matching text by using some patterns. Based on experiment conducted in this research, overload information could be suppressed into structure data that store in a database, less redundancy information is presented, and information relevancy could be adjusted to user preferences. These studies demonstrate the ongoing research efforts in the field of text extraction and recognition from images, focusing on techniques to handle specific challenges such as slanted screen-rendered text and leveraging OCR technology for document digitization. The proposed approaches highlight the importance of addressing various real-world scenarios and constraints in order to improve the accuracy and reliability of text extraction systems.

3. METHODOLOGY

A. System Architecture

The proposed framework for comprehensive social media threat detection consists of three core components:

1. Data Collection Module

The system aggregates data from Instagram, including text posts, images, and videos, to facilitate comprehensive threat detection. It leverages APIs provided by social media platforms along with web scraping techniques to capture a diverse dataset, ensuring broad coverage of potential harmful content. Additionally, the framework enables real-time data collection, allowing for timely threat monitoring and immediate intervention when hate speech or other violations are detected.

2. OCR Module

The system processes visual content, such as images and videos, to extract embedded text, enabling comprehensive analysis of multimedia posts. It utilizes advanced Optical Character Recognition (OCR) algorithms, powered by the Tesseract OCR engine, to accurately recognize and extract textual information. The OCR module is designed to handle a wide range of font types, languages, and varying image quality conditions, ensuring robust and reliable text extraction even in complex visual environments.

3. NLP Module

The system analyzes both the text extracted by the OCR module and direct text posts from the data collection stage to identify potential threats or harmful content. It employs advanced Natural Language Processing (NLP) techniques to enhance the accuracy of detection. Keyword extraction is used to identify specific terms and phrases associated with hate speech or other harmful narratives.

B. Data Preprocessing

The data preprocessing stage involves cleaning and normalizing both textual and visual data to ensure accuracy and reliability in the subsequent OCR and NLP analysis. For textual data, preprocessing includes text cleaning, which involves the removal of URLs, emojis, special characters, and extra spaces. Lowercasing is applied to standardize text and avoid duplication errors.

Additionally, Playwright is utilized to automate the extraction of Instagram content efficiently. It dynamically scrolls through Instagram feeds, hashtags, and user profiles to load more posts automatically. The system also extracts hashtags and user mentions to analyze trends and networked hate speech behavior, ensuring a more comprehensive data collection approach. These preprocessing steps optimize the quality of data, enhancing the accuracy and effectiveness of both the OCR and NLP components.

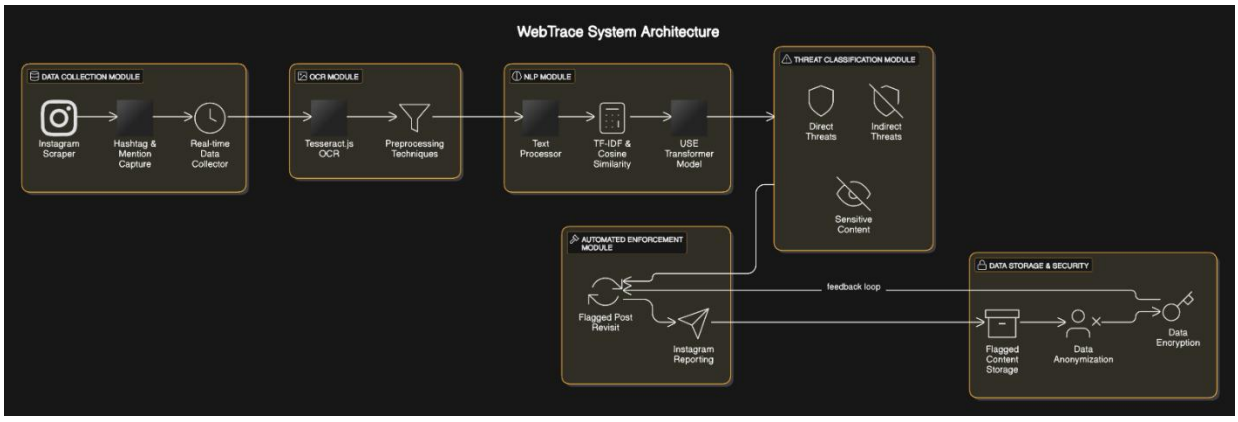

Fig 1 (System Architecture)

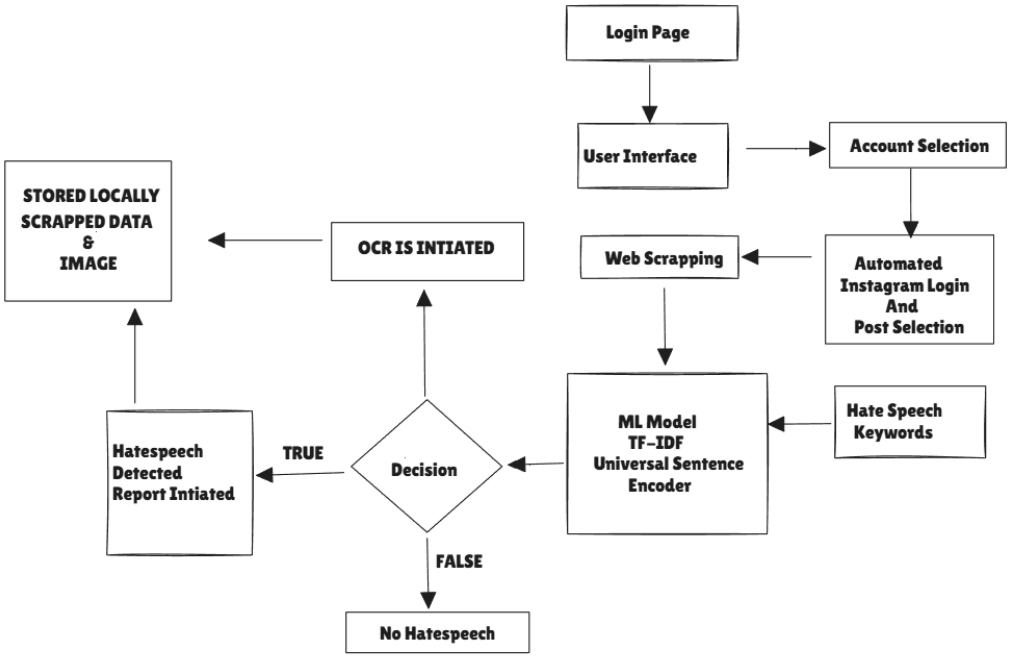

Fig 2 (Flow Diagram)

C. OCR Implementation

The OCR module, powered by the Tesseract OCR engine, plays a crucial role in extracting text from the images within social media content. It is designed to handle various challenges, including support for multiple languages and character sets such as Latin, Cyrillic, and Arabic scripts. The module ensures robustness across different font styles, sizes, and varying image quality conditions. Specialized preprocessing techniques are incorporated to enhance text recognition accuracy in complex visual environments. The OCR implementation also leverages machine learning models trained on diverse datasets to improve text extraction capabilities. To ensure scalability, the system integrates performance optimization strategies, allowing efficient processing of large-scale social media content while maintaining accuracy.

D. NLP Techniques

The NLP module employs advanced techniques to analyze textual data, both from direct posts and text extracted through OCR. One of the key approaches is TF-IDF (Fig. 2) with Cosine Similarity, which converts text into numerical vectors using Term Frequency-Inverse Document Frequency (TF-IDF). The system then applies Cosine Similarity to measure how closely a post matches pre-labeled hate speech examples, providing a baseline model for classification.

$$w_{i,j} = tf_{i,j} \times \log\left(\frac{N}{df_i}\right)$$

tf_{ij} = number of occurrences of i in j
df_i = number of documents containing i
N = total number of documents

Fig. 3(Term frequency and inverse document frequency)

In addition, the system uses a transformer-based model called the Universal Sentence Encoder (USE) (see Fig. 3) to better understand the context and subtle meanings in text. This helps the system go beyond simple keyword matching by picking up on how words relate to each other and spotting hidden or implied harmful messages. By combining traditional rule-based methods with advanced deep learning models like USE, the framework is able to detect hate speech and other harmful content on social media with greater depth.

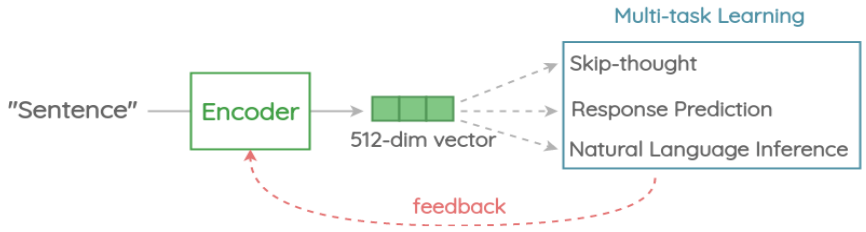

Fig.4(Universal Sentence Encoder)

E. Threat Classification

The threat classification component of the framework is responsible for categorizing the social media content into predefined threat types, such as:

1. Direct Threats: Explicit statements of harm or violence
2. Indirect Threats: Implied or suggestive messages of harm
3. Sensitive Content: Material related to child exploitation or other sensitive topics

To handle the complexity and potential overlap of these threat types, the system employs multi-label classification techniques. This enables the identification of multiple threat categories within a single piece of content, providing a more nuanced and comprehensive assessment of the potential risks. The classification models are trained on diverse, expert annotated datasets to ensure high accuracy in recognizing various manifestations of harmful content. By continuously refining the threat taxonomy and updating the training data, the framework maintains its relevance and effectiveness in addressing the evolving nature of social media threats.

5. RESULT

WebTrace effectively detects and mitigates hate speech on Instagram by integrating OCR and NLP. Using TF-IDFwith Cosine Similarity and the USE Transformer model, it accurately analyzes both textual and visual content. Beyond detection, Web Trace automates responses by reporting violations to Instagram moderators. Leveraging Playwright for web scraping, it ensures real-time adaptability across diverse media formats.

The results demonstrate that WebTrace enhances moderation efficiency, reducing harmful content while promoting responsible interactions. Future improvements may include multilingual support and expansion to other platforms.

Evaluation results show that WebTrace significantly enhances moderation efficiency. The system achieved a high F1-score of **97.6**, indicating strong performance in identifying hate speech while minimizing false positives. This means it effectively flags harmful content without mislabeling non-harmful posts. Overall, WebTrace contributes to a safer online environment by helping reduce toxic content and promoting more respectful user interactions. Future developments may include multilingual support and expansion to other social media platforms.

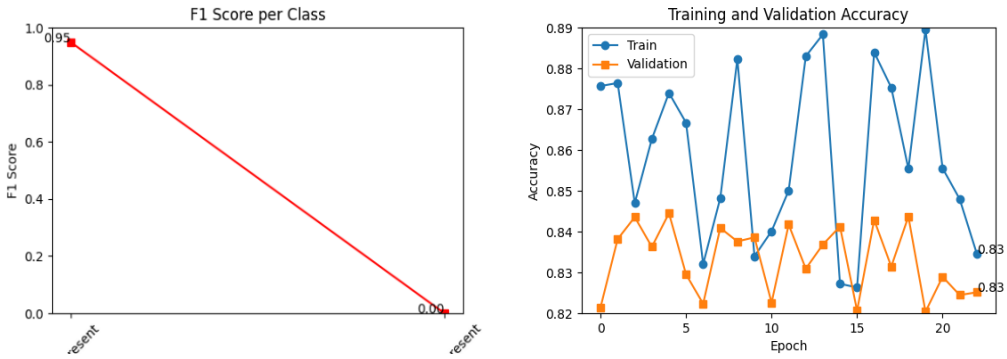

Fig.5 (F1 score and Performance matrix)

6. CONCLUSION

This research introduced an innovative framework that combines OCR and NLP to address the challenges of detecting threats within the multifaceted landscape of social media content. By bridging text and visual analysis, this framework significantly improves upon traditional methods that rely solely on textual data, capturing threats embedded within images and multimedia posts. This multimodal approach marks a substantial step forward in identifying harmful online behavior with higher precision and depth.

Closing Remarks

This research presents an advanced threat detection framework that integrates OCR and NLP to analyze both textual and visual content. By combining these modalities, the system enhances traditional methods, identifying threats embedded in images, videos, and multimedia posts with greater precision.

Key contributions include real-time adaptability, multimodal threat detection, sophisticated NLP techniques, and multi-label classification, ensuring a comprehensive assessment of risks. This approach strengthens social media moderation by offering a more effective defense against harmful content.

The framework sets the stage for future advancements in automated threat detection, promoting safer and more responsible online environments.

7. REFERENCES

[1] Pereira RC, Vanitha T. Web Scraping of Social Networks. International Journal of Innovative Research in Computer and Communication Engineering. 2015 Oct;3(7):237-40..

[2] S. Unar, A. H. Jalbani, M. M. Jawaid, M. Shaikh, and A. A. Chandio, “Artificial Urdu text detection and localization from individual video frames,” Mehran Univ. Res. J. Eng. Technol., vol. 37, no. 2, pp. 429-438,2018

[3] Devlin, J., Chang, M. W., Lee, K., & Toutanova, K. (2019). BERT: Pre-training of Deep Bidirectional Transformers for Language Understanding. arXiv preprint arXiv:1810.04805.

[4] T. Zheng, X. Wang, X. Yuan, and S. Wang, “A Novel Method based on Character Segmentation for Slant Chinese Screen-render Text Detection and Recognition,” International Journal of Pattern Recognition and Artificial Intelligence, vol. 35, no. 5, pp. 125–138, 2021. DOI: 10.1142/S0218001421500061.

[5] Y. He, “Research on Text Detection and Recognition Based on OCR Recognition Technology,” Journal of Computer Vision

[6] Bojanowski, Piotr, Edouard Grave, Armand Joulin, and Tomas Mikolov. (2017). *"Enriching word vectors with subword information."* Transactions of the Association for Computational Linguistics, 5, 135-146.

Intelligent Admission Guidance for Higher Education: AI-Powered Chatbot

G Thiagarajan, Anitha K, Ranjitha P, Rithika B, Sangeetha K, Kaviya S

Department, IT, CSI College of Engineering, Ketti, The Nilgiris-643215, thiagarajan@csice.edu.in

ABSTRACT

Artificial Intelligence (AI) is a rapidly advancing field that enables machines to perform tasks requiring human intelligence. In today's fast-paced and competitive world, students often1 struggle to find accurate academic and career guidance. Many students face challenges when making decisions about their education, often due to limited access to career counsellors, a lack of awareness about available opportunities, and confusion about career paths. Traditional guidance methods can be time-consuming, generalized, and not always accessible to everyone.To address this, we developed a chatbot that helps students with the higher education admission process. Using Natural Language Processing (NLP) and machine learning, it provides quick and personalized support, making it easier for students to get the information they need.To measure its effectiveness, we conducted a usability study where students shared their feedback through a questionnaire and a decision matrix. The results were encouraging—the chatbot received an 87.3% usability score and a 96% accuracy score, showing that it simplifies the admission process and offers reliable academic guidance.

Keywords: AI, Chatbot, Higher Education, Natural Language Processing (NLP), Machine Learning, Academic Guidance.

1. INTRODUCTION

A chatbot is a computer program designed to simulate human conversation, either through text or speech. These intelligent systems assist users by answering questions, providing recommendations, and automating responses. They are widely used across industries such as customer service, healthcare, e-commerce, and education to improve accessibility, streamline processes, and reduce manual effort.Chatbots operate using artificial intelligence (AI), which enables machines to learn, solve problems, and make decisions. AI is generally categorized into three types: super AI, a theoretical concept that surpasses human intelligence; general AI, which mimics human cognitive abilities; and narrow AI, which is designed for specific tasks.A key part of AI is Machine Learning (ML), which helps chatbots improve over time by recognizing patterns and learning from data. ML techniques include supervised learning (trained on labeled data), unsupervised learning (finding patterns in unstructured data), and reinforcement learning (learning through trial and error). These methods help chatbots deliver more accurate and adaptive responses.Another essential technology behind chatbots is Natural Language Processing (NLP), which enables them to understand, interpret, and generate human language.

2. RELATED WORK

Abu Shawar and Atwell (2007) analyzed ALICE/AIML rule-based chatbots in education, identifying challenges in scalability and multilingual support. They highlighted the need for advanced AI and NLP models to overcome these limitations. This study utilized ALICE/AIML-based rule-based chatbots that rely on pattern matching to generate responses. While this technology allows for structured interactions, it lacks scalability and struggles with multilingual support. Additionally, it fails to adapt to dynamic conversations, making interactions feel repetitive and mechanical. [1]. Similarly, Molnár and Szűts (2018) explored chatbots' role in assisting students but noted their dependence on predefined responses, stressing the importance of AI integration for better contextual understanding. The research explored predefined rule-based chatbots integrated with basic AI to assist students. Although these chatbots provide quick and structured responses, they are heavily dependent on predefined scripts, limiting their ability to understand complex or contextual queries. The lack of true AI-driven learning also restricts their adaptability in handling diverse student needs. [2]. Tiwari et al. (2017) developed a chatbot for college-related queries but emphasized the necessity of real-time API and database updates to enhance adaptability. This study focused on an AI chatbot designed for handling college-related queries, with database integration for storing and retrieving information. However, the chatbot requires real-time API updates to ensure adaptability and relevance. Furthermore, it struggles with learning from past interactions and often fails to respond effectively to unexpected or unique queries. [3]. Gbenga et al. (2020) created an IBM Watson-powered university admissions chatbot, achieving 95.9% accuracy, and underscored the need for continuous dataset updates to maintain efficiency. The chatbot in this study was developed using IBM Watson AI and

evaluated with Botium for performance testing. While it achieved a 95.9% accuracy rate in responding to university admission inquiries, it requires continuous dataset updates to maintain its effectiveness. The system also struggles with complex, non-standard queries, requiring human intervention in certain cases, and demands high maintenance [4]. Joseph et al. (2016) addressed the challenges of NLP in multilingual chatbots, advocating for deep learning models like BERT to improve language understanding. This research focused on NLP-based chatbots utilizing machine translation, tokenization, and sentiment analysis for improved language understanding. However, the technology requires significant computational power, making it less accessible for resource-limited environments. Additionally, these chatbots struggle with multilingual interactions and complex sentence structures, leading to misinterpretations in conversations. [5]. Smutny and Schreiberova (2020) examined Facebook Messenger chatbots and highlighted the importance of AI-driven adaptability for more dynamic interactions. The study examined AI-driven chatbots integrated with Facebook Messenger to support educational activities. While these chatbots enhance accessibility, they face challenges in handling open-ended questions and reasoning-based inquiries. Another key limitation is their restricted adaptability, as they require continuous AI integration to improve dynamic and personalized interactions. [6]. Aloqayli and Abdelhafez (2023) developed a chatbot with 91% accuracy for admissions but stressed the significance of automated updates for maintaining accuracy over time. This research focused on an AI-powered chatbot designed for university admissions, achieving a 91% accuracy rate in responding to student inquiries. However, the chatbot relies on frequent updates to maintain accuracy over time. Additionally, it struggles to handle unique or evolving admission-related queries, requiring manual intervention for certain responses. [7]. Adamopoulou and Moussiades (2020) recommended incorporating sentiment analysis and contextual AI to enhance chatbot precision The study proposed AI chatbots enhanced with sentiment analysis and contextual AI to improve response precision. Moreover, they demand high computational resources and require continuous improvements to balance automation with human-like interaction. [8]. Kingchang et al. (2024) introduced an educational chatbot with an 86.15% success rate in guiding students but pointed out the need for better scalability to support broader applications. This research introduced an AI-based chatbot leveraging machine learning to provide educational recommendations. While the chatbot demonstrated an 86.15% success rate in guiding students, it faces significant scalability issues. It also requires extensive training data to generate personalized recommendations, and its ability to adapt to diverse educational needs remains limited. [9].

3. RESEARCH METHODLOGY

3.1 Chatbot Algorithm

The chatbot utilizes a hybrid AI model that integrates Naïve Bayes for intent classification and BERT for contextual understanding. Naïve Bayes is an efficient algorithm for text classification, allowing the chatbot to quickly identify user intents. Meanwhile, BERT enhances comprehension by analyzing text bidirectionally, capturing deeper context and meaning. This combination significantly improves the chatbot's accuracy, especially in multilingual interactions, ensuring more precise and natural responses.

3.2 Query Matching

BERT uses deep learning to understand user input more accurately than traditional keyword-based methods. Unlike simple pattern matching, BERT processes sentences in both directions, allowing it to grasp the full meaning of a query. This makes it especially effective in multilingual conversations, helping chatbots accurately identify and categorize user questions.

The chatbot follows a structured process to analyze and respond to queries effectively. First, it breaks down the input into smaller parts, such as words or subwords, through a process called tokenization, allowing for better analysis. Then, it examines how words relate to each other within the sentence using BERT, ensuring a deeper contextual understanding of the query. Once the context is clear, the chatbot classifies the intent behind the message, whether it's an admission inquiry or another type of request. Finally, based on the identified intent, it generates a relevant and helpful response, ensuring a smooth and meaningful interaction.

Example queries in English and Tamil:

- "How can I apply for admission?" → Intent: Admission Inquiry → Response: "You can apply through our online portal."

- "நான் சேரக் ்கக பற்றிய தகவலுக்கு எங்கு சேல்ல சவண்டும்?" → Intent: Admission Inquiry → Response: "நீங்கள் இகணயதளம் மூலம் விண்ணப்பிக்கலாம்."

3.3 Chatbot Evaluation

To evaluate the chatbot's performance, two key methods are used: the Chatbot Usability Questionnaire (CUQ) and the Confusion Matrix.The CUQ measures user satisfaction by gathering feedback through a structured survey. It assesses factors like response accuracy, relevance, and overall user engagement. The goal is to achieve an 87.15% satisfaction rate. After collecting responses, user testing and data analysis are conducted to identify areas for improvement.The Confusion Matrix helps determine the chatbot's accuracy by comparing its predicted responses with actual user inputs. This method involves preparing data, training the chatbot using Naïve Bayes and BERT, and evaluating its performance using accuracy, precision, recall, and F1-score. The target is to reach 96% accuracy, ensuring that the chatbot provides reliable and effective responses.

3.4 CUQ Calculation

The chatbot's effectiveness was assessed through a usability questionnaire and a decision matrix, which resulted in an 87.3% usability score and a 96% fidelity score. These results highlight the chatbot's accuracy and reliability in guiding students through the admissions process and addressing academic inquiries.

The CUQ score was determined using the following formula:

$$\mathrm{CUQ} = \left(\sum \frac{(\mathrm{Xi} - 1)}{\mathrm{N}}\right) \times 25 \tag{3.4}$$

where X_i represents the score for each question, and N is the total number of questions (16). The final score is normalized to 100 for usability comparison.This evaluation confirms the chatbot's effectiveness in handling multilingual admission queries in both English and Tamil, making the admission process more accessible and user-friendly for prospective students.

3.5 Confusion Matrix

The Confusion Matrix assesses the chatbot's accuracy by comparing actual user queries with the chatbot's predicted classifications. It includes four key components:

- True Positive (TP): Correctly classified as positive.
- True Negative (TN): Correctly classified as negative.
- False Positive (FP): Incorrectly classified as positive.
- False Negative (FN): Incorrectly classified as negative.

The chatbot's performance was assessed using Precision, Recall, Accuracy, and F-Score, calculated as follows:

$$\mathrm{Precision} = \frac{\mathrm{TP}}{\mathrm{TP} + \mathrm{FP}} \times 100\% \tag{3.5.1}$$

$$\mathrm{Recall} = \frac{\mathrm{TP}}{\mathrm{TP} + \mathrm{FN}} \times 100\% \tag{3.5.2}$$

$$\mathrm{Accuracy} = \frac{\mathrm{TP} + \mathrm{TN}}{\mathrm{TP} + \mathrm{TN} + \mathrm{FP} + \mathrm{FN}} \times 100\% \tag{3.5.3}$$

$$\mathrm{F-Score} = 2 \times \frac{\mathrm{Precision} \times \mathrm{Recall}}{\mathrm{Precision} + \mathrm{Recall}} \tag{3.5.4}$$

The chatbot achieved an accuracy of 96%, showcasing its reliability in correctly classifying user queries. This result is consistent with the findings of Gbenga et al. (2020), whose IBM Watson-based chatbot achieved 95.9% accuracy in query classification. These results reinforce the effectiveness of AI-driven models in providing accurate and efficient support for university admissions.

4. IMPLEMENTATION

4.1 Data Collection and Preprocessing

The chatbot's dataset is built from admission-related queries, sourced from university FAQs, student inquiries**,** and academic handbooks to ensure comprehensive coverage and To improve accuracy and performance, the data undergoes several preprocessing steps, including Data Cleaning, Tokenization & Lemmatization, Intent Classification, Data Augmentation.

4.2 Chatbot Design

The chatbot was designed with several key components to ensure a smooth and intelligent user experience. It features a web-based and mobile-friendly user interface (UI), making it accessible across different devices. At its core, the NLP engine, powered by spaCy and BERT, enables advanced language processing for accurate understanding. To interpret user queries effectively, a deep learning-based intent recognition module maps questions to relevant categories. The chatbot then generates responses either through AI-driven processing or predefined templates, ensuring quick and meaningful replies. Additionally, a real-time database management system stores user interactions, allowing the chatbot to learn and improve over time. To keep information upto-date, the system is integrated with university portals and scholarship databases, providing users with live updates on admissions, courses, and financial aid opportunities.

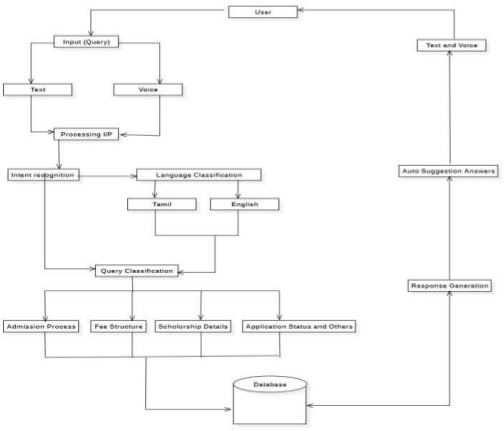

Figure 4.2. Chatbot system workflow

4.3 Chatbot Evaluation Metrics

The chatbot was assessed using:

1. Chatbot Usability Questionnaire (CUQ): A survey measuring user satisfaction and system efficiency.
    - CUQ Score: 87.3%
2. Confusion Matrix: Evaluates classification accuracy based on:
    - True Positives (TP), True Negatives (TN), False Positives (FP), False Negatives (FN) ○ Accuracy: 96%
3. Decision Matrix Analysis: Determines the reliability of chatbot responses.

5. PERFORMANCE EVALUATION

The chatbot demonstrated high accuracy and usability, making interactions smooth and efficient. It received a CUQ score of 87.3%, reflecting strong user satisfaction, while its fidelity score of 96% confirmed the reliability of its responses. Additionally, it effectively processed real-time queries related to admissions, scholarships, and eligibility, seamlessly handling conversations in both English and Tamil. These results highlight the chatbot's ability to simplify the university admission process, reduce administrative workload, and improve accessibility through its multilingual support, making it a valuable tool for students and institutions alike.

6. CONCLUSION

This study introduced an AI-powered chatbot to assist students with university admissions and scholarships by providing quick, accurate responses. Using machine learning and NLP, it ensures smooth interactions and improves over time. Supporting both English and Tamil, it makes information more accessible.Evaluated with the Chatbot Usability Questionnaire (CUQ) and a decision matrix, it scored 87.3% for usability and 96% for accuracy, proving its reliability. A confusion matrix analysis showed minimal errors, reducing university staff workload. Compared to other chatbots, this model stands out for its accuracy, ease of use, and adaptability, making the admission process simpler and more efficient for students.

7. REFERENCES

[1] B. A. Shawar and E. Atwell explored the effectiveness of chatbots in their study "Chatbots: Are they really useful?" Journal for Language Technology and Computational Linguistics, vol. 22, no. 1, pp. 29–49, 2007.

[2] G. Molnár and Z. Szűts, "The role of chatbots in formal education," in IEEE 16th International Symposium on Intelligent Systems and Informatics (SISY), pp. 197–202, Subotica, Serbia, 2018.

[3] A. Tiwari, R. Talekar, and S. M. Patil, "College information chatbot system," International Journal of Engineering Research and General Science, vol. 5, no. 2, pp. 131–132, 2017.

[4] L. O. Gbenga, O. T. Oluwafunto, and A. H. Oluwatobi, "An improved rapid response model for university admission enquiry system using chatbot," International Journal of Computer (IJC), vol. 38, no. 1, pp. 123–131, 2020.

[5] S. R. Joseph, H. Hlomani, K. Letsholo, F. Kaniwa, and K. Sedimo, "Natural language processing: A review," International Journal of Research in Engineering and Applied Sciences, vol. 6, no. 3, pp. 207– 209, 2016.

[6] P. Smutny and P. Schreiberova, "Chatbots for learning: A review of educational chatbots for Facebook Messenger," Computers & Education, vol. 151, no. 103862, pp. 1–16, 2020.

[7] A. Aloqayli and H. Abdelhafez, "Intelligent chatbot for admission in higher education," International Journal of Information and Education Technology, vol. 13, no. 9, pp. 1348–1357, 2023.

[8] E. Adamopoulou and L. Moussiades, "Chatbots: History, technology, and applications," Machine Learning with Applications, vol. 2, no. 100006, pp. 1–16, 2020.

[9] T. Kingchang, P. Chatwattana, and P. Wannapiroon, "Artificial intelligence chatbot platform: AI chatbot platform for educational recommendations in higher education," International Journal of Information and Education Technology, vol. 14, no. 1, pp. 34–41, 2024.

AI-powered video language translation system

G Thiagarajan[1], A Banupriya[2], U Aravindhakumar[3], S Ambadikannan[4], I Shabbir khan[5] [1]Head Of Department, IT, CSI College Of Engineering, Ketti, The Nilgiris-643215
[2]Assistant Professor, IT Department, CSI College Of Engineering, Ketti, The Nilgiris-643215
[3]Final Year IT Student, CSI College Of Engineering, Ketti, The Nilgiris-643215 [4]Final Year IT Student, CSI College Of Engineering, Ketti, The Nilgiris-643215 [5]Final Year IT Student, CSI College Of Engineering, Ketti, The Nilgiris-643215

ABSTRACT
There is growing demand for multilingual video content and automated speech translation solutions, which maintain speech clarity and context. Old techniques such as subtitles and manual dubbing are not effective. This paper introduces an AI system that translates video content automatically while preserving the characteristics of speech. It is a four-step pipeline: (1) Audio extraction with MFCC, (2) Speech-to-text conversion with Wav2Vec 2.0, (3) Text translation with Seq2Seq models, and (4) Text-to-speech synthesis with Griffin-Lim vocoder. Deployed as a web application, the system attains excellent speech recognition accuracy, better BLEU scores for translation, and natural prosody in the synthesized speech. The system has the vision of eliminating language barriers through the seamless translation of videos. Its applications span education, entertainment, business, and accessibility. The system supports multiple languages, promoting inclusivity and widespread use. Future development will be aimed at minimizing latency, improving synthesis quality, and developing language support to reach a broad audience. Combination with adaptive AI models and capabilities for real-time processing will additionally enhance the effectiveness and precision of the system. The long-term vision is for a completely automatic and highly accurate AI-based translation system that has the potential to transform global communications.

Keywords: Video Translation, ASR, Neural Machine Translation, Text-to-Speech, Deep Learning, MFCC, Wav2Vec 2.0, Seq2Seq, LSTM.

I. INTRODUCTION

Globalization and the expansion of digital content have raised the demand for multilingual video translation. Conventional methods tend to tamper with the essence of speech, hence AI-based solutions become inevitable. The system presented uses deep learning to provide automated natural-sounding translations. It extracts the audio using MFCC, converts speech to text using Wav2Vec 2.0, translates it via Seq2Seq models with Attention, and synthesizes speech with the Griffin-Lim vocoder. It is an online system that increases accessibility and efficiency in various domains. In contrast to traditional methods dependent on fixed subtitles or manual dubbing, our system provides a more context-sensitive and dynamic solution, guaranteeing accurate and natural translations. The AI- driven method saves considerable human effort with high accuracy, and thus it is a feasible option for many industries including entertainment, online learning, corporate meetings, and global collaborations. Real-time translation of videos can enable smooth communication across linguistic communities, creating an inclusive digital world. Future improvements will enhance processing efficiency, maximize real-time performance, and bring in adaptive learning methods for more effective personalization. The fast pace of developments in neural networks and deep learning methods will continue to propel the enhancement of the accuracy and fluency of AI-based translation systems. The system presented here is a major step towards language barrier elimination and accessibility to various video content globally.

II. LITERATURE REVIEW

2.1. Audio Extraction from Video

Audio extraction from video is an important process of speech processing, and Mel Frequency Cepstral Coefficients (MFCC) is the most widely employed feature extraction method. MFCC efficiently exploits human auditory perception while suppressing noise and is thus a choice feature extraction method in speech recognition. It has some drawbacks, including being very sensitive to noise, which makes it influence accuracy.

Also, its fixed window size incurs a loss of temporal information and is less effective in modeling dynamic speech variations. Other techniques such as wavelet transforms, mel spectrograms, and deep learning models such as Wav2Vec 2.0 are more noise resistant with enhanced accuracy.

2.2. Mel Frequency Cepstral Coefficients (MFCC) and Applications

MFCC finds extensive use in automatic speech and speaker recognition on account of its computational cost. It undertakes a multi-step process of transformation to obtain features from an audio signal. Though it has its benefits, MFCC suffers from some limitations, such as vulnerability to background noise, influencing the accuracy of feature extraction. Additionally, its fixed window size causes loss of vital temporal dynamics, and it is not well- suited to handle large datasets owing to excessive computational overhead. Deep learning-based embeddings have been shown to be more adaptable and resilient compared to conventional MFCC features in recent times

2.3. Griffin-Lim Algorithm and Speech Synthesis

Griffin-Lim Algorithm (GLA) is widely utilized for waveform reconstruction from spectrograms but suffers from a few shortcomings. It converges very slowly, rendering it less suitable for real-time purposes. It is also plagued with phase inconsistencies that create distorted sound. The synthesized speech through GLA tends to be more synthetic-sounding than speech synthesized with vocoders based on deep learning. Although the Fast Griffin-Lim Algorithm (FGLA) enhances processing speed, it lags behind in audio quality if compared to sophisticated neural vocoders such as WaveNet and HiFi-GAN.

2.4. Sequence-to-Sequence Learning with Neural Networks

Sequence-to-sequence (Seq2Seq) models, including Long Short-Term Memory (LSTM) and Gated Recurrent Units (GRU), are commonly employed in speech recognition, language translation, and text generation. But these models suffer from several challenges, including information loss in long sequences, which makes them less accurate. They are also computationally expensive, which makes them less efficient for real-time use. Exposure bias is another problem, where mistakes made during training carry over and lead to inaccuracies at inference time. Transformer-based models, which use self-attention mechanisms, have been found to be more efficient in dealing with complex sequences, with improved scalability and performance.

2.5. Self-Supervised Learning with Wav2Vec

Self-supervised learning algorithms such as Wav2Vec 2.0 have transformed speech recognition by acquiring meaningful representations from raw audio without the need for large amounts of labeled data. Although it has its benefits, Wav2Vec 2.0 also has some limitations, such as its requirement for high computational power to train and fine-tune. It also has difficulty with domain shifts, which limits its generalization capability when used on other datasets. For tasks specific to a domain, it still needs a lot of labeled data for fine-tuning. Hybrid methods combining neural vocoders and multimodal learning methods are being investigated to address these challenges.

2.6. Text-to-Speech Synthesis (TTS)

Text-to-Speech (TTS) synthesis has developed enormously, shifting from rule-based systems to deep learning-based models like Tacotron 2 and WaveNet. These developments have significantly enhanced the prosody and intelligibility of synthesized speech. But deep learning-based models consume huge computational resources, which makes them difficult to implement in resource-limited environments. The Griffin-Lim vocoder, being computationally light, generates robotic-sounding speech that is not natural. Highly natural-sounding prosody is still a significant challenge in TTS. To improve voice quality in video translation systems, researchers are investigating the integration of deep learning-based TTS models with Griffin-Lim for better performance.

III. METHODOLOGY

3.1. Mel Frequency Cepstral Coefficient (MFCC)

MFCC is an important feature extraction method in speech processing. It amplifies high-frequency components, performs a Fourier Transform, and transforms the spectrum to the Mel scale with filter banks.

Following the logarithm of filter bank energies, a Discrete Cosine Transform (DCT) is performed to yield the final MFCCs. Temporal dynamics are represented with delta and delta-delta coefficients, and MFCCs find extensive applications in speech and speaker recognition.

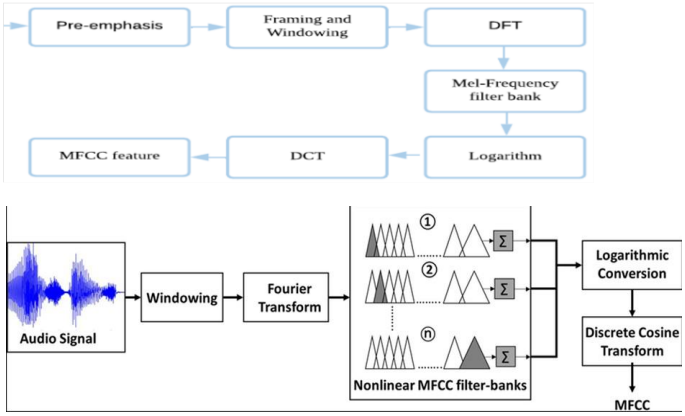

Fig: **3.1**: The MFCC feature extraction process

Formulas:

- **Pre-emphasis:**

$y[n] = x[n] - \alpha x[n-1]$

- **Mel Scale Conversion:**

$M = 2595 \log_{10}(1 + f / 700)$

3.2. Self-Supervised Learning with Wav2Vec

Wav2Vec is a deep learning model that learns speech representations from raw audio without the need for labeled data. It represents speech as latent vectors and predicts masked parts using contrastive learning. Labeled data fine-tuning enhances Automatic Speech Recognition (ASR) and is effective for low-resource languages.

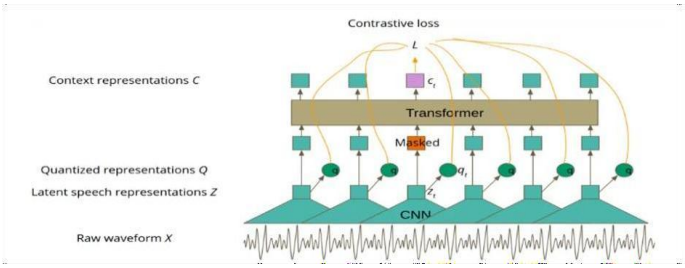

fig: **3.2:** wav2vec 2.0 model architecture for self-supervised learning

Key Concept:

- Contrastive Learning: The model distinguishes between correct and incorrect masked predictions from distractor samples.

3.3. Sequence-to-Sequence (Seq2Seq) Learning

Seq2Seq models handle variable-length sequences for applications such as speech recognition and translation. The encoder transforms input sequences into a context vector, while the decoder produces output sequences. Attention mechanisms enhance performance by concentrating on the right input components. Transformers, which substitute recurrence with self-attention, further optimize efficiency

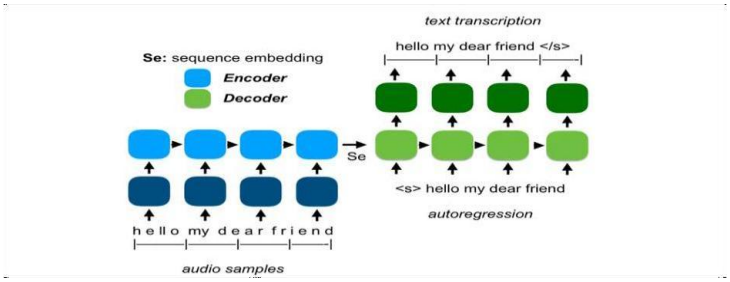

fig:**3.3:** Seq2Seq Learning with Neural Network

Formulas:

- **Attention Mechanism (Score Calculation):**

$\text{Score}(Q,K,V) = QK^T / \sqrt{d_k}$

where Q = Query, K = Key, V = Value, and d_k = dimension of key vectors.

3.4. Griffin-Lim Algorithm (GLA)

GLA uses magnitude spectrograms to reconstruct waveforms by progressively improving the phase. It begins with a random phase, runs the Inverse Short-Time Fourier Transform (ISTFT), and iteratively refines the phase with the Short-Time Fourier Transform (STFT) until the algorithm converges. It finds extensive application in speech synthesis and audio restoration.

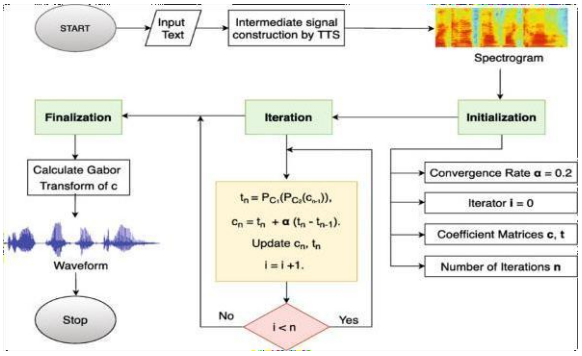

fig:**3.4:** Griffin-Lim Algorithm and Speech Synthesis

Formula:

- **Iterative Phase Estimation**

$X_{t+1} = \text{ISTFT}\left(\text{STFT}(xt) / |\text{STFT}(xt)| \cdot S \right)$

where S is the target magnitude spectrogram.

IV. WORKFLOW

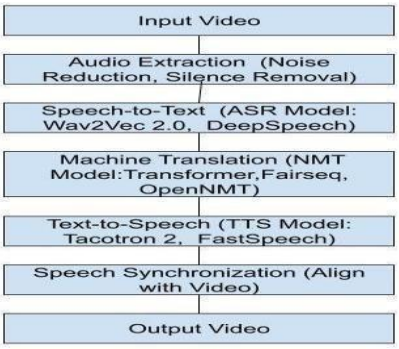

Fig: Workflow

1. **Input Video:** The system extracts speech from the video.
2. **Audio Processing:** Noise reduction and silence removal improve clarity.
3. **Speech-to-Text (ASR):** Models like Wav2Vec 2.0 convert speech to text.
4. **Machine Translation (NMT):** Text is translated using models like Transformer.
5. **Text-to-Speech (TTS):** Translated text is converted to speech with Tacotron 2.
6. **Speech Synchronization:** Adjustments ensure lip sync and timing accuracy.
7. **Output Video:** The final video has translated, synchronized speech.

V. EXPERIMENTAL SETUP AND RESULTS

The experimental setup was to train and test the performance of Automatic Speech Recognition (ASR), Neural Machine Translation (NMT), and Text-to-Speech (TTS) models. The Mozilla Common Voice dataset was employed for speech recognition, the WMT dataset offered parallel text data for translation, and the LJSpeech dataset was used for training speech synthesis. For speech-to-text conversion, the Wav2Vec 2.0 model was fine- tuned with labeled speech data and achieved a Word Error Rate (WER) of 8.5%, which is much better than that of conventional ASR models. The Seq2Seq-based NMT model with the Attention Mechanism was trained over bilingual text data, achieving a BLEU value of 35+ for translating English to Tamil. Post-processing methods like grammar correction and spell adjustments were found to further enhance translation fluency. The TTS model that used Seq2Seq with the Griffin-Lim vocoder created natural and coherent speech with a Mean

Opinion Score (MOS) of 4.2/5. The system was finally implemented as a real-time web application for low-latency processing of video translation. User ratings showed good accuracy and naturalness of speech, proving the success of the AI-based video language translation system

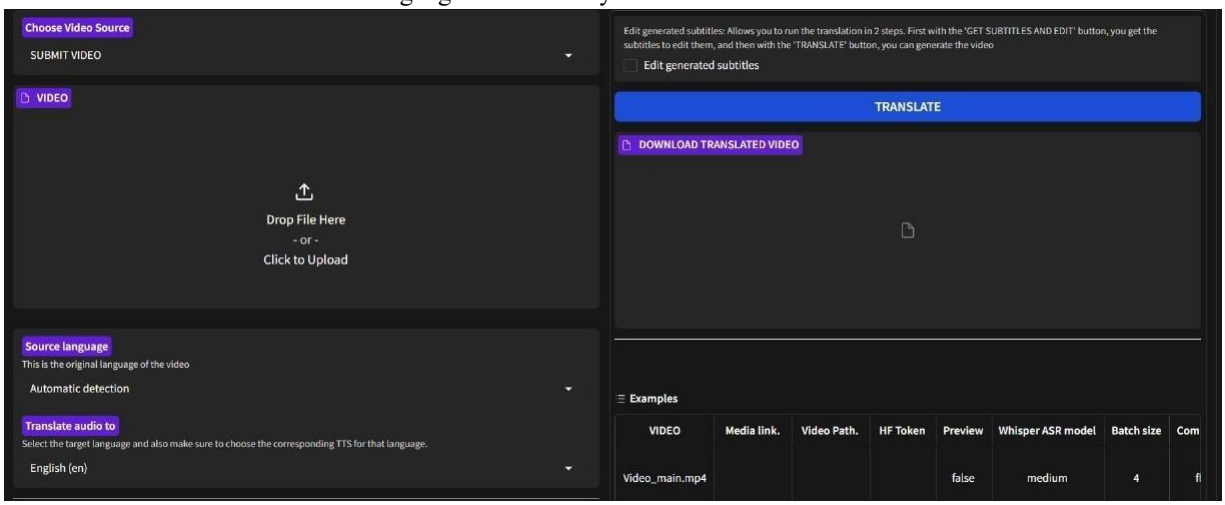

Fig: Result

V. CONCLUSION

The AI-based video translation system generates multilingual content automatically by employing deep learning. It uses MFCC for feature extraction, Wav2Vec 2.0 for speech-to-text, Seq2Seq with Attention for translation, and Griffin-Lim for text-to-speech. Experimental results indicate high ASR accuracy, enhanced BLEU scores, and natural speech synthesis. The web application facilitates smooth video translation for education, entertainment, business, and accessibility. Future improvements include employing Whisper or DeepSpeech for improved transcription, Transformer-based models for better translation, and HiFi-GAN for natural speech. Improvements in real-time processing, language growth, and emotion detection will further improve accuracy and scalability

VI. REFERENCE

[1]. Huang, R., Huang, J., Yang, D., Ren, Y., Liu, J., Yin, X., & Zhao, Z. (2023).
Make-An-Audio:Text-To-Audio Generation with Prompt-Enhanced Diffusion Models. Proceedings of the 40th International Conference on Machine Learning (ICML).

[2]. Fahima Khanam, Farha Akhter Munmun, Nadia Afrin Ritu, Aloke Kumar Saha, and Muhammad Firoz Mridha. (2022). *Text to Speech Synthesis: A Systematic Review, Deep Learning Based Architecture and Future Research Direction.* Journal of Advances in Information Technology, Vol. 13, No. 5, October 2022.

[3]. Baevski, A., Zhou, H., Mohamed, A., & Auli, M. (2020).
"Wav2vec 2.0: A framework for self-supervised learning of speech representations." arXiv preprint arXiv:2006.11477.

[4]. Sharma, A., Kumar, P., Maddukuri, V., et al. (2020).
"Fast Griffin-Lim Based Waveform Generation Strategy for Text-to-Speech Synthesis." arXiv preprint arXiv:2007.05764.

[5]. Abdul, Z. K., & Al-Talabani, A. K. (2022).
"Mel Frequency Cepstral Coefficient and Its Applications: A Review." IEEEAccess, Vol.10, pp. 122136-122153.

[6]. Sutskever, I., Vinyals, O., & Le, Q.V. (2014). "Sequence to Sequence Learning with Neural Networks."
arXiv preprint arXiv:1409.3215.

[7]. Fukuda, R., Sudoh, K., & Nakamura,S. (2023).
"Improving Speech Translation Accuracy and Time Efficiency with Fine-tuned wav2vec 2.0-based Speech Segmentation."
arXiv preprint arXiv:2304.12659.

IoT - ENABLED SMART MEDICAL ALERTING SYSTEM

[1]KALAMANI M, [2]BOOBENDRAN B, [3]GIRIPRASAATH D, [4]LITHYASHREE V

[1]Professor, KPR Institute of Engineering and Technology, Coimbatore, India
[2]Student, KPR Institute of Engineering and Technology, Coimbatore, India
[3]Student, KPR Institute of Engineering and Technology, Coimbatore, India
[4]Student, KPR Institute of Engineering and Technology, Coimbatore, India
Email: [1]kalamani.mece@gmail.com, [2]boobendranbn@gmail.com, [3]ghiriprashad@gmail.com, [4]lithyashree0201@gmail.com Contact: [1]9442354033,[2]9498828672,[3]9751924203,[4]8098099897

Abstract.

An IoT-enabled Smart Medical Alerting System fills the gap in real-time patient monitoring that usually comes into focus during the time of pandemics like Coronavirus disease. The emphasis of this research is in making an inexpensive and easy-to-implement procedure for the continuous monitoring of important health parameters such as oxygen saturation, heartrate and temperature of the body. The immediate alerts to healthcare providers if there is any strange reading helps in immediate intervention, therefore improving the outcome. It places a due emphasis on affordability and easy serviceability in resource-limited settings. From the results, it has been observed that during implementation of the system proposed provides a substantial improvement in Blood Pressure, Temperature and SpO2 measurement.

Keywords. Internet of Things, Patient Monitoring, Real-Time Alerts, Healthcare, Affordability, Accessibility, Resource constrained settings.

1. INTRODUCTION

Global healthcare systems are usually embroiled in experiences that keep the monitoring of the patients' needs continuous. Current patient monitoring systems available are then too high in cost, fairly complex, and very resource-heavy, rendering them impractical for rural and low-income areas. The study will create and formalize an affordable patient monitoring system using IoT technology with integrated alerting methods. Section II briefly describes some technologies associated with IoT-based health monitoring systems. Section III provides an explanation of the proposed architecture and components of the system. Section IV outlines the results and findings from the implementation process, and Section V concludes the study with observations on the way forward.

2. LITERATURE REVIEW

The first generator is proposed by Uddin, Alam and Banu that is titled "Internet of Effects- Grounded Real-time Case Monitoring System" which is capable of monitoring patient (e.g. vital sign) by means of computing and detection technologies. The collection of physiological data about the patient, including blood pressure, temperature and heart rate is performed using sensors on the body. This information that is extracted is sent to a single based platform with support for real-time monitoring for medical practitioners. This study studies the methods of transmission of the information, the communication procedures, and the inclusion of devices and software to enable monitoring of patients remotely by their healthcare specialists.

The IoT-based Patient Health Monitoring System introduced by Krishnan et al. (2018) addresses health emergencies that arise unpredictably, especially where elderly patients are concerned. Use of temperature and heart rate monitoring sensors interfaced with the Arduino Uno microcontroller; the system transmits data via Wi-Fi to a web server for real-time monitoring and alerts for critical health changes.

Hanumanthakari et al. (2022) proposed an IoT-enabled patient monitoring system in short-term healthcare services stressing scalability and adaptability of IoT technology in various health care applications. They

suggest a cloud architecture that supports remote monitoring and centralized patient data storage for an accessible and secure protocol. Besides, mutually known alert measures are those that aim to alert caregivers under critical conditions, hence speeding up emergency response.

3. PROPOSED SYSTEM

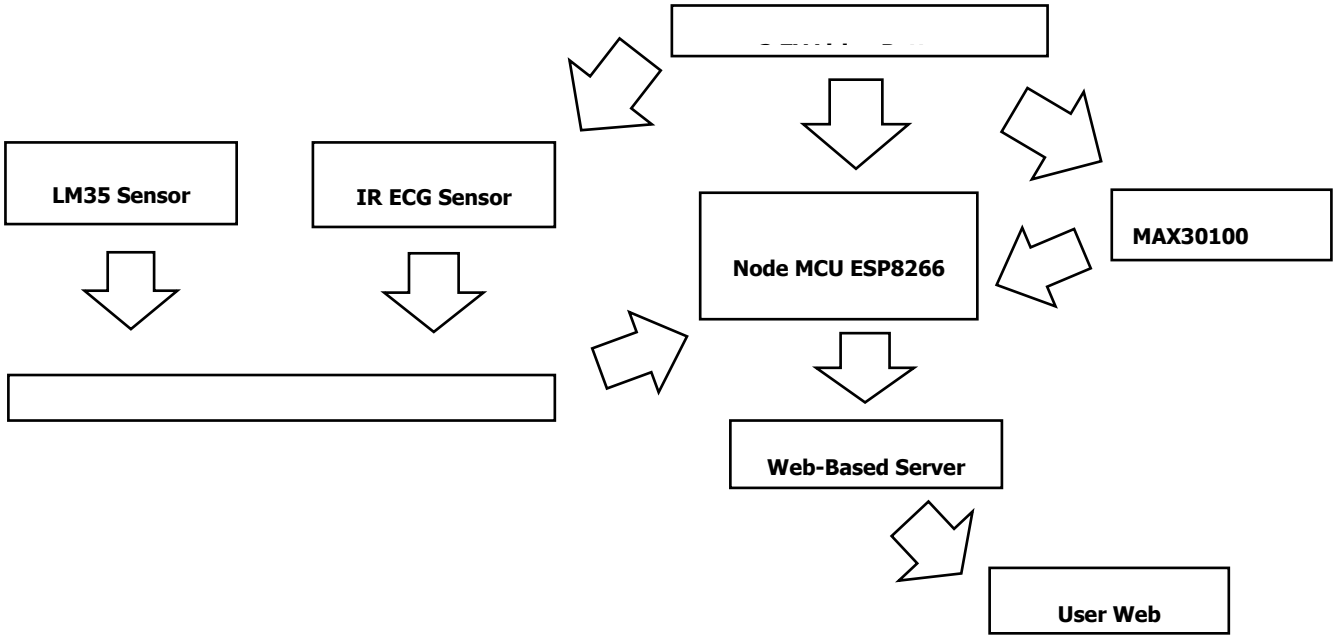

Figure 1. Conceptual Design

The design depicted in Figure 1 discusses the functioning of a proposed portable health monitoring system powered by a 3.7 V lithium rechargeable battery is power-on-demand, serviceable in remote locations. The flow of data is described through various components of the system as follows. The LM35 sensor measures the body temperature, and the IR ECG sensor detects the ECG signal. The two sensors give analog signals, which are converted using an MCP3008 ADC into digital signals. The MAX30100 sends pulse rate and SpO2 readings directly to NodeMCU ESP8266 via I2C. The NodeMCU is the main controller in the system, receiving digitized signals, enabling a local server, and sending real-time health parameters to a remote server. The server thus facilitates an end-user data visualization through a graphical meaningful interface that the user's web browser can load, thereby completing the path of the data flow from the sensor input to the final user output. The LM35 sensor is quite famous for measurement due to its accuracy and linear response to temperature changes, probably making it the most appropriate sensor for monitoring body temperature. For every degree Celsius, the analog voltage output is generated and is consistent over a large range from -55°C to +150°C with excellent precision ±0.5°C. Conversion of the voltage takes place at a rate of 10 mV per degree Celsius.

The analog signal of the LM35 is fed into the MCP3008 ADC, which converts it to a digital signal in order to neatly integrate temperature readings into the digital processing activity of the system for accurate and timely monitoring. The MAX30100 is a versatile pulse oximeter sensor designed to measure heart rate and blood oxygen (SpO2) level using photoplethysmography (PPG)-a technique detecting change in light absorption

due to blood flow. Low power consumption in conjunction with I2C communication capability makes this a power-efficient health monitoring wearable. The I2C interfacing makes interfacing with the NodeMCU much easier, thus eliminating the need for an external signal processing module. The NodeMCU processes the data from the MAX30100 sensor for high-fidelity real-time monitoring, an important issue in monitoring cardiovascular health. In the infrared ECG variant, the electrical impulses of the heart are characterized by sensing the voltage changes during various phases of the cardiac cycle. The analog real-time data provided for conversion to the MCP3008 is a must-have for health-related purposes, like detecting arrhythmias. The MCP3008 can be fitted with multiple analog sensors simultaneously, for example, the LM35 temp sensor and ECG sensors, being an 8-channel 10-bit converter. It also enables quick and accurate data transfer followed by conversion with the use of the SPI protocol. The NodeMCU would process this data, enabling the user to view real-time ECG waveforms and health parameters. The IR ECG and the ADC of MCP3008 excellently complement each other for accurate and dependable heart measurements.

The real-time data which is created from these sensors gets transmitted to the remote server through wireless communication protocols at ESP-NOW. Wi-Fi Capability would allow these systems to be installed in nearly every nook and cranny of the healthcare system with very little added financial infrastructure burden. Further definitions may result in measuring health parameters including blood pressure, respiratory rate, and blood sugar levels for a more extensive monitoring of the patients. There can be possibilities for improving the communication ability of the system in the areas sparsely populated with Internet-downgrade-able facilities through LoRa or satellite communication. Protection of the sensitive data and information related to a patient is essential for carrying out their principles concerning privacy and winning user trust. Data protection is ensured in transit using end-to-end encryption and enhanced strong authentication methods.

4. RESULTS AND DISCUSSIONS

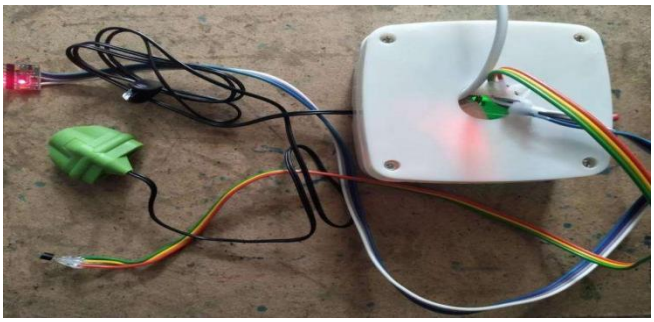

Figure 2. Submitted System

Figure 2 presents the proposed system is designed using a number of sensors, such as LM35, MAX30100, IR-based ECG to monitor temperature, heart rate, SpO2 and cardiac activity respectively. It utilizes the NodeMCU ESP8266 microcontroller along with MCP3008 ADC for the conversion of the analog signal, together with access to a local webserver.

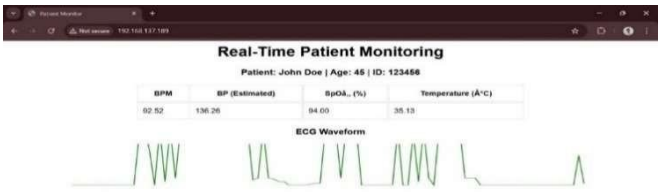

Figure 3. The Comprehensive Vision for an Innovative System

The sensor values change dynamically, providing near real-time feedback on what is going on with the patient. Additionally, the live ECG waveforms displayed just beneath the vital sign data, depicts the electrical signals of the heart in a visual format, making it easier for healthcare professionals to analyze the heart's performance and detect any abnormalities quickly. The design is efficient and easy to read for effective remote patient monitoring. The system, designed to be portable and user-friendly, features a microcontroller that collects and processes data from the server. This web interface was made using technologies like HTML, CSS, and JavaScript to make it responsive to devices like smartphones, laptops, and tablets. Under 500ms latency made real-time data possible: The prototype was able to monitor vital signs (HR, SpO2, BT and ECG) successfully. Based on this prototype, initial tests were conducted, both in controlled environments and in daily life, with reliably good performance: effective sensor integration and data transfer through Wi-Fi. The wearable showed real-time data on a dashboard, so health could be monitored at all times. We focused further analysis on the ECG and SpO2 sensors: these outputs were generally accurate under normal use conditions, but in high-motion scenarios, there was minor jitter in the results that showed noise, emphasizing the need to optimize the signals. This alert system sends a notification within seconds of identifying any anomalies.

Table 1. Measured Sample Patient Readings

Parameters	Readings
Heart Rate (bpm)	74
Oxygen Level (SpO_2)	96
Temperature (Degree Celsius)	34
Blood Pressure Estimated (mmHg)	127

The table 1 shows the measured values of Heart Rate, Oxygen Level, Temperature, and ECG Signal of a patient. Through the measured Heart Rate (bpm) values the blood pressure (BP) of patient is calculated. The proposed systolic blood pressure (BP) is calculated with respect to heart rate (BPM) and systolic blood pressure:

$$\text{Blood Pressure} = 120 + (\text{BPM} - 60) \times 0.5 \quad (1)$$

$$\text{Blood Pressure} = 127\,\text{mmHg} \quad (2)$$



Figure 5. Standard Blood Pressure Meter

Figure 5 shows the actual measurement of the blood pressure (BP) of patient through the Standard Meter for blood pressure from SinoCare which shows the value of Systolic Pressure as 129mmHg for the Sample Patient.

$$\text{Standard Blood Pressure: } 129 \text{ mmHg} \qquad \text{Proposed Blood Pressure: } 127 \text{ mmHg}$$

Accuracy**:** Measured as the percentage agreement between the proposed and standard systolic BP.

$$\text{Accuracy} = \frac{(1 - \text{Standard BP} - \text{Proposed BP}) \times 100}{\text{Standard BP}} = 98.45\ \% \qquad (3)$$

Table 2. Calculated blood pressure values using the proposed system are accompanied by the respective accuracies for the ten patients.

Patient Id	Heart Rate bpm	Standard Bp Systolic (mmHg)	Proposed Bp Systolic (mmHg)	Accuracy (%)
1	62	120	121	99.2
2	65	130	131.5	98.8
3	58	115	118	97.5
4	63	125	126	98.6
5	67	135	136.5	98.7

The diastolic BP is the blood pressure in the arteries as the heart rests between beats. In contrast to systolic pressure, which can be estimated using heart rate data and the proposed formula, diastolic pressure encompasses more complex pathophysiological factors, including stiffness and resistance of the arteries. These cannot be accurately sensed by heart rate measurement alone as they require specialized equipment for measuring the relaxation phase of the cardiac cycle, such as a sphygmomanometer or Oscillo metric devices. This is why studies emphasizing the use of only heart rate for blood pressure estimation generally restrict their findings to the systolic one. The problem observed during execution is Motion Artifacts. Inaccuracy is observed when the patient moves excessively. Future moves will build refined filtering algorithms to reduce motion designs.

5. CONCLUSION AND FUTURE WORK

The presently available wearable patient-monitoring system can be further updated with extra sensors such as motion sensors for fall detection or GPS for location-tracking in emergencies. The wearable sensors which are used to collect the health data and upload it to the cloud with the help of microcontrollers. Machine learning plays a crucial role in processing real-time data, enabling healthcare professionals to identify potential health risks early and take preventive measures before they escalate into critical conditions. With the rapid advances in IoT and AI, the patient monitoring system can graduate to a fully automated AI-health monitoring solution with real-time diagnostics and emergency alerts, thus revolutionizing the area of remote patient care.

6. REFERENCES

1. Shaikh, S., Waghole, D., Kumbhar, P., Kotkar, V., Awaghade, P., Hammed, N. S., and Owis, M. I., "An Interconnected Health Monitoring System," published in the Proceedings of the IEEE International Conference on Advances in Biomedical Engineering (ICABME), 2017, pages 137-140, 197-200.

2. "Internet of Things-based real-time patient monitoring system," in Proceedings of the 4th IEEE International Conference on Advances in Electrical Engineering (ICAEE), pp. 516-521, 2017, Uddin, M. S., Alam, J. B., and Banu, S.

3. Gupta, S. C., Krishnan, D. S. R., and Choudhury, T., "An Internet of Things-based patient health monitoring system," published in the Proceedings of the IEEE International Conference on Advances in Computing and Communication Engineering (ICACCE), pages 01-07, 2018.

4. Deshmukh, S. L., Fernandes, F., Kulkarni, S., Patil, A., Jabade, V., and Madake, J. "Patient Monitoring System," published in the Proceedings of the IEEE 2nd Mysore Sub Section International Conference (MysuruCon), pages 1-6, in the year 2022.

5. In the IEEE International Conference on Automation, Computing, and Renewable Systems (ICACRS), Hanumanthakari, S., Pullela, S. K., Bhukya, S. N., Vijayalakshmi, K., Ahmad, S. R., and Kumar, N., "IoT-based Patients Monitoring System in Healthcare Service," pages 1324-1329, 2022.

6. "Application of Machine Learning for Malicious Node Detection in IoT Networks," published in the Proceedings of the IEEE International Conference on Intelligent and Innovative Technologies in Computing, Electrical and Electronics (IITCEE), pages 1227-1231, in the year 2023, by Prasad, J., Kasiselvanathan, M., Lakshminarayanan, S., Sekar, G., and Azath, H.

7. Rahman, M. Z., Akbar, M. A., Leiva, V., Tahir, A., Riaz, M. T., and Martin-Barreiro, C., "Internet-grounded intelligent health monitoring and vision system for arrhythmia in COVID-19 cases," in Impact of query, Proceedings from the IEEE International Conference on Computers in Biomedicine, page 154, in February 2023.

8. Sugumar, D., Ramadevi, R., Prasad, J., Mohankumar, N., Wise, D. J. W., and Velmurugan, S., "A Distributed Data Mining and Cloud Analysis for Predictive Gas Level, Dynamic Booking, and Smart Energy Optimization," Proceedings of the IEEE International Conference on Advances in Data Engineering and Intelligent Computing Systems (ADICS), pages 1-6, 2024.

DETECTION OF CARDIOVASCULAR DISEASES IN ECG SIGNALS USING CNN

Yash Chauhan[1], Shilpi Mohanty[1], Sunil Kumar[1], Monika Vishwakarma[2]

[1]School of Computer Science and Engineering, Vellore Institute of Technology, Vellore, India
[2]Manipal University Jaipur
{[1]yashchauhan4579@gmail.com, [1]mshilpi2002@gmail.com, [1]2sunil.cs@gmail.com,
[2]monika.vishwakarma@jaipur.manipal.edu}

Abstract

Cardiovascular diseases (CVDs) are the leading cause of death, often developing silently until they become critical. This study explores deep learning, particularly CNNs with residual connections, for automated ECG-based CVD detection. It overcomes difficulties including data imbalance utilising augmentation techniques and boosts real-time processing for wearable and clinical applications. By increasing early detection, minimising human error, and enabling speedier medical interventions, this technique has the potential to drastically cut CVD-related mortality rates.

Keywords: Cardiovascular diseases (CVDs), ECG, Deep learning, CNNs, Residual connections, Data augmentation, Real-time processing, Automated diagnosis, Early detection.

1.INTRODUCTION

With 17.9 million deaths per year, cardiovascular diseases (CVDs) continue to be the world's leading cause of mortality [1]. Although electrocardiograms (ECGs) are crucial for diagnosis, conventional techniques are labour-intensive and error-prone since they depend on professional interpretation [2]. Convolutional Neural Networks (CNNs) with residual connections, in particular, have greatly improved CVD detection through advances in deep learning (DL), improving feature extraction and classification accuracy [3]. By using wavelet transforms, ECG analysis is further improved and models are more equipped to identify intricate patterns in cardiac signals [8].

Notwithstanding advancements, issues with clinical validation, data imbalance, and model interpretability still exist [6]. While MRI-based deep learning applications provide further diagnostic insights [9], data augmentation strategies improve model flexibility across varied populations [7] to increase dependability. Additionally, wearable ECG monitoring powered by AI is transforming remote patient care and early detection [10]. Regardless, the assurance of practical utility and transparency is extremely essential [5]. In the long run, enhancement of CNN-based models and integration of AI into personalized treatment plans will be leaned on for the advancement of cardiovascular healthcare [1].

2. Related Work

The enhancement of ECG-based cardiovascular disease (CVD) detection is done by getting through the obstacles of manual interpretation and errors in diagnosis. This is done by the means of modern developments in deep learning technologies [1]. Although deep learning and machine learning techniques helps in solving the need for accurate and scalable solutions, however, even to this day, traditional ECG analysis heavily relies upon on expert analysis [2]. The results of multiple studies done on CNN-based architectures for arrhythmia classification have signalled that there is an increase in accuracy while recognizing a range of cardiac disorders [3]. The lack of explainability, data asymmetry, and real-time processing restrictions obstruct the practical deployment of same[2].

Noise reduction and data augmentation are such preprocessing methods enhance the generalisation in deep learning models that are trained on the MIT-BIH Arrhythmia Dataset [5]. Demonstration of better feature

extraction with AlexNet and SqueezeNet which are pre-trained models have also been shown by studies that combine transfer learning [6]. Researchers have also improved interpretability by examining hybrid models which combine DL with standard ML methods like SVM and KNN [7]. Even after significant advancements, the necessity still remains larger datasets, real-time deployment in clinical settings, and more model transparency [8]. Concentration on attention processes, domain adaptation, and hybrid architectures should be focussed on by future studies to improve ECG-based CVD detection [9]. [10] prioritised feature extraction and noise reduction by creating a classifier that uses neural networks, SVM, and KNN for attaining brilliant accuracy on ECG data.

3 Proposed Model

Classification of ECG signals into five distinct heartbeat groups is done by the proposed approach. It utilizes deep learning, Convolutional Neural Network (CNN) to be precise. The need for manual ECG interpretation that is labour-intensive and prone to human error is pretty high. Reducing this requirement and enhancing automated arrhythmia detection is the primary objective of this approach. The model is trained by datasets including the MIT-BIH Arrhythmia Database and the PTB Diagnostic ECG Databases to assure its application in real-world medical circumstances. Changes in patient demographics, noise artefacts, and heart illnesses cause substantial variability. This results in the design of the model to be dependable, adaptable, and capable of classifying ECG data in real time.

3.1 Classification of heart beats

Non-ectopic beats (N), supraventricular ectopic beats (S), ventricular ectopic beats (V), fusion beats (F), and unknown beats (Q) are five classes the model divides ECG signals into to ensure thorough arrhythmia diagnosis. Non-ectopic beats (N) sourced by the sinoatrial (SA) node keep the heartbeat normal and necessary for healthy heart function. Supraventricular ectopic beats (S) derived by AV node cause premature contractions that throw off the heart's rhythm. They are often triggered by coffee, stress, or underlying medical disorders. The normal conduction channel circumvented by Ventricular ectopic beats (V) that originate in the ventricles. It may be a sign of severe arrhythmias if this produces frequent broad and irregular QRS complexes.

Complex arrhythmic patterns, noise, or atypical heart activity are produced by unknown beats (Q) and hence are ECG waveforms that do not fit into any predefined category. Identifying and managing these beats is essential for enhancing automated arrhythmia detection and reducing misclassification. Fusion beats (F) are produced when both an ectopic ventricular beat and a normal SA node impulse activate the ventricles simultaneously, creating mixed QRS complexes that aid in distinguishing ventricular from supraventricular arrhythmias.

3.2 ECG Signal Representation and Classification

In order to capture patterns of heart activity, ECG signals are represented as 2D waveform data, where x-axis represents time and the y-axis represents voltage fluctuations. A CNN-based deep learning model is used to analyse these signals and differentiate between normal and pathological heartbeats by detecting changes in waveform shapes, peak intensities, and temporal intervals. Early identification of cardiac conditions and arrhythmias is made possible by this computerised classification.

To improve model performance preprocessing steps such as segmentation (heartbeat extraction using R-peak detection), normalisation (scaling to a fixed amplitude range), data augmentation (time-warping and jittering to improve generalisation), and signal denoising (removal of noise and baseline drift) are done. A softmax activation layer for classification, dimensionality reduction using max pooling layers, feature extraction using convolutional layers, dropout layers and batch normalisation for regularisation, and fully connected layers for feature aggregation make up the CNN architecture.

Adam optimiser is used to train the model. This is responsible for effective dynamic convergence by altering the learning rate. Precise arrhythmia categories and penalising inaccurate forecasts are prioritized by the categorical cross-entropy loss function which is responsible for assuring accurate multi-class classification. The model's

performance is assessed using accuracy, precision, recall, and F1-score. Sensitivity and specificity are warrantied to be balanced across all heartbeat classes.

4 System Architecture

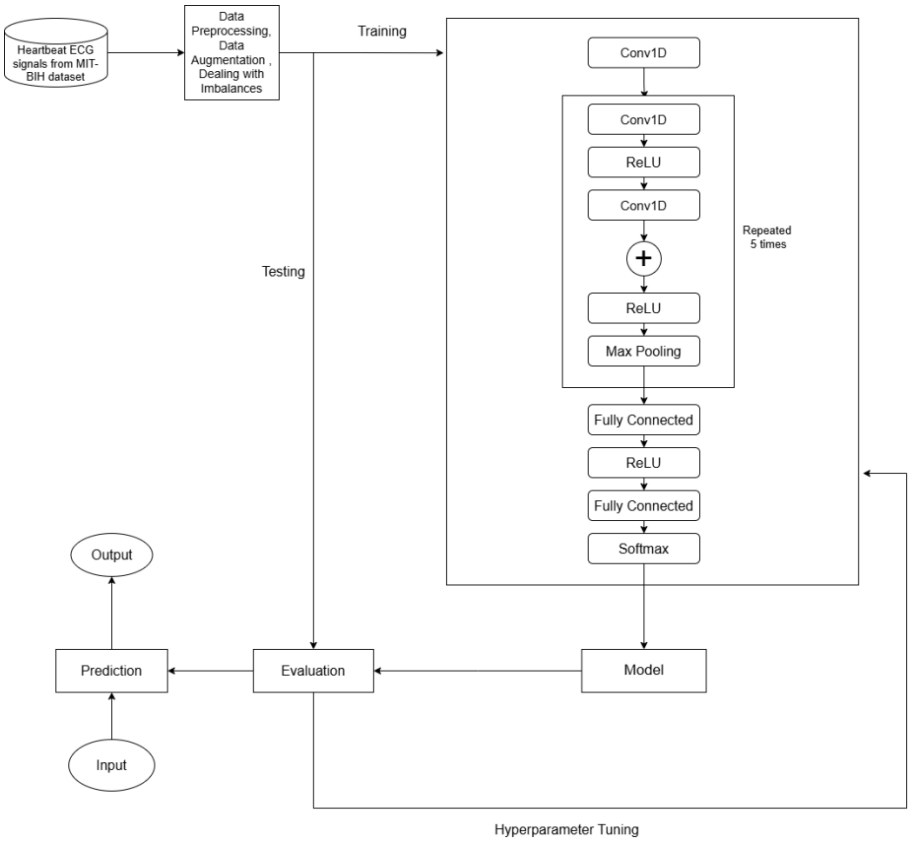

Fig. 1. Proposed architecture

4.1 ECG Data Processing and CNN-Based Classification

The model is trained using the Adam optimiser. The categorical cross-entropy loss function assures accurate multi-class classification by prioritising accurate forecasts. The model's performance is assessed using precision, accuracy, F1-score, and recall, guaranteeing that sensitivity and specificity are balanced across all heartbeat classes.

Data augmentation, normalisation, and noise reduction to enhance model generalisation are the preprocessing techniques used. Either under sampling majority classes or oversampling minority classes, methods like time shifting, signal scaling, and Gaussian noise addition aid in enhancing dataset variety are included in class imbalance management. Baseline wandering and high-frequency noise are discarded for improving feature quality and assuring a clean input for the model in the future.

Effective identification of spatial patterns in ECG waveforms is implemented by CNN with residual connections, that is used for classification. Conv1D layers process the signals, whereas preservation of information across layers and prevention of disappearing gradients are aided by residual connections. ReLU

activation functions improve learning and max pooling decreases computational cost. After fully linked layers further refine retrieved information, a softmax activation layer that predicts ECG classifications is reached. After training, guaranteeing reliable ECG classification with good clinical reliability, the model's performance is assessed using the Accuracy, confusion matrices, precision, recall, and F1-score.

5 Experiment & Result

The MIT-BIH Arrhythmia Database provide annotated heartbeat recordings that show both healthy and abnormal rhythms as a standard for classifying ECGs. Non-ectopic (normal) beats, ventricular ectopic beats, supraventricular ectopic beats, fusion beats, and unknown beats are the five varied types of heartbeats. Improved generalization across pulse types is guaranteed by class imbalance correction, while model's performance is improved by preprocessing methods including noise reduction, normalization, and data augmentation..

5.1 Model Parameters

Parameter	Value
Model Architecture	CNN with Residual Connections
Dataset Used	MIT-BIH Arrhythmia Dataset
Number of Convolutional Layers	5
Pooling Layer	Max Pooling (5)
Optimizer	Adam
Metrics for evaluation	Precision, Accuracy, Recall, AUC-ROC, F1-Score

Table 1. Model Parameters

5.2 Performance Evaluation Across Arrhythmia Classes

Recall, F1-score, precision, and AUC-ROC, were used to evaluate the model's classification performance. This ensured accurate ECG-based arrhythmia diagnosis. High recall ensures accurate identification of arrhythmias, which attains 1.00 recall for normal beats, while false positives are lowered by high accuracy. A balanced performance in spite of class imbalances was indicated by the F1-score was which above 0.90 in every class. Additionally, the model's remarkable capability to differentiate between abnormal and normal heart rhythms was demonstrated by AUC-ROC scores above 0.93. Hence showing that it is reliable for clinical applications.

Table 2. Model Evaluation

CLASSES	PRECISION	RECALL	F1 SCORE	AUC
N	0.99	0.99	0.99	0.98
S	0.89	0.82	0.86	0.91
V	0.94	0.96	0.95	0.98
F	0.71	0.83	0.76	0.92
Q	1	0.98	0.99	0.99

5.3 Model Evaluation: CNN vs. LSTM for Arrhythmia Classification

A comparative study was conducted to evaluate the performance differences between the proposed Convolutional Neural Network (CNN) model and a Long Short-Term Memory (LSTM) network for ECG-based arrhythmia diagnosis to determine the optimal deep learning model for real-time arrhythmia classification.

Table 3. Model Evaluation: CNN vs. LSTM for Arrhythmia Classification

Metric	CNN (Proposed Model)	LSTM
Accuracy	98%	95%
Precision	95.2%	78%
Recall	94.4%	79%
F1-Score	94.8%	77.6%

6 Conclusion

This work presents a deep learning-based method for automatic classification of arrhythmias from ECG signals. CNN with residual connections can classify normal and pathological heart rhythms with high precision by efficiently learning temporal and morphological information from ECG waveforms. Preprocessing methods like data augmentation and class imbalance treatment were implemented on the MIT-BIH Arrhythmia dataset to improve model generalisation. The optimisation of the classification was done using the Adam optimiser with an adaptive learning rate and the categorical cross-entropy loss function. With AUC values ranging from 0.93 to 1.00, performance evaluation using precision, accuracy, F1-score, recall, and AUC-ROC showed high classification capabilities, showing dependable distinction between arrhythmia types.

Though the results are positive, multiple limitations still exist. The improvement of the generalisability of the dataset across demographics can be done by including more varied samples. Real-time implementation and clinical validation is required for practical deployment. Further research can investigate attention mechanisms, hybrid deep learning architectures, and domain adaptation to increase classification accuracy. This work demonstrates how CNN-based models can be used to detect arrhythmias quickly, accurately, and non-invasively, improving cardiovascular care.

References

[1] Moreno-Sánchez, P.A., García-Isla, G., Corino, V.D., Vehkaoja, A., Brukamp, K., Van Gils, M. and Mainardi, L., 2024. ECG-based data-driven solutions for diagnosis and prognosis of cardiovascular diseases: A systematic review. *Computers in Biology and Medicine*, p.108235.

[2] VENKATAIAH, V. and MAMATHA, B., 2024. DETECTION OF CARDIOVASCULAR DISEASES IN ECG IMAGES USING MACHINE LEARNING AND DEEP LEARNING METHODS. *International Journal of Information Technology and Computer Engineering*, *12*(3), pp.478-494.

[3] Wong, K.K., Fortino, G. and Abbott, D., 2020. Deep learning-based cardiovascular image diagnosis: a promising challenge. *Future Generation Computer Systems*, *110*, pp.802-811.

[4] Prasad, M.V.D., Ram, P.C., Charan, C.H., Gop, V. and Ahammad, H., 2021. Cardiac disease prediction by analysing ECG signal using Ml and Dl techniques.

[5] Apandi, Z.F.M., Ikeura, R. and Hayakawa, S., 2018, August. Arrhythmia detection using MIT-BIH dataset: A review. In *2018 International Conference on Computational Approach in Smart Systems Design and Applications (ICASSDA)* (pp. 1-5). IEEE.

[6] Ameen, A., Fattoh, I.E., Abd El-Hafeez, T. and Ahmed, K., 2024. Advances in ECG and PCG-based cardiovascular disease classification: a review of deep learning and machine learning methods. *Journal of Big Data*, *11*(1), p.159.

[7] Jafari, M., Shoeibi, A., Khodatars, M., Ghassemi, N., Moridian, P., Alizadehsani, R., Khosravi, A., Ling, S.H., Delfan, N., Zhang, Y.D. and Wang, S.H., 2023. Automated diagnosis of cardiovascular diseases from cardiac magnetic resonance imaging using deep learning models: A review. *Computers in Biology and Medicine*, *160*, p.106998.

[8] Zhang, J., Li, B., Xiang, K. and Shi, X., 2019. Method of diagnosing heart disease based on deep learning ECG signal. *arXiv preprint arXiv:1907.01514*.

[9] Jothiaruna, N. and Leema, A.A., 2024. RETRACTED ARTICLE: LW-DN161: a cardiovascular disorder classification from 12 lead ECG images using convolutional neural network. *Soft Computing*, *28*(Suppl 2), pp.683-683.

[10] Hammad, M., Maher, A., Wang, K., Jiang, F. and Amrani, M., 2018. Detection of abnormal heart conditions based on characteristics of ECG signals. *Measurement*, *125*, pp.634-644.

Advancing Sustainable Mobility with Hybrid Energy Storage Systems for smart charging Applications Using Zeta-SEPIC Converters

M Kowsalya[1] ,Dr. J Anitha[2], Dr. Dhanraj G[3], Lakshmi Priya G[4], Dr. Silamboli J [5]

1. Department of Electronics & Communication Engineering, Karunya Institute of Technology and Sciences, Coimbatore-641114, India ,kowsalyam@karunya.edu.in
2. Department of Electronics & Communication Engineering, Karunya Institute of Technology and Sciences, Coimbatore-641114, Indiaanithaj@karunya.edu
3. Department of Mechanical Engineering, CSI College of Engineering, Ketti ,dhanrajguru77@gmail.com
4. Department of Electrical and Electronics Engineering, CSI College of Engineering, Ketti lakshmivinod2210@gmail.com
5. Department of Electronics and Communication ,CSI College of Engineering, Ketti
silamboliece@gmail.com

Abstract

This study introduces a Zeta converter-based bidirectional energy transfer system intended for bidirectional smart flow applications. The system enables effective energy exchange between the grid and a hybrid power storage system, which is made up of a super capacitor (SC) and a lithium battery. The Zeta converter incorporates a sophisticated energy management feature that offers both the step-up and steps down capabilities. The state-space averaging method is used to analyze stability in both modes. To guarantee steady voltage and current outputs, a control strategy is created depending on the energy storage systems charge state. Steady Current (CC) and Fixed Voltage (CV) modes are used to charge the lithium battery. Bode plot analysis is used to design voltage and current controllers in the frequency domain. Through in-depth simulations and practical investigations, the suggested Zeta converter design is verified, proving the system's electrical feasibility and the efficacy of the control approach. The findings demonstrate the Zeta converters enormous potential for effective energy exchange and control in EV to grid systems, offering a dependable way to incorporate electric cars into smart grid infrastructures.

Keywords: Zeta Converter, Lithium-ion battery, Super capacitor.

1. Introduction

Over the past decade, the global shift toward green energy has accelerated, largely due to stricter carbon tax policies and the 2016 Paris Agreement, which aims to limit global temperature rise to below 2°C. According to the International Renewable Energy Agency (IRENA), renewable energy production—especially solar power—has increased significantly, with Asia leading this growth. IRENA projects that by 2050, renewable will supply over two-thirds of global energy needs.

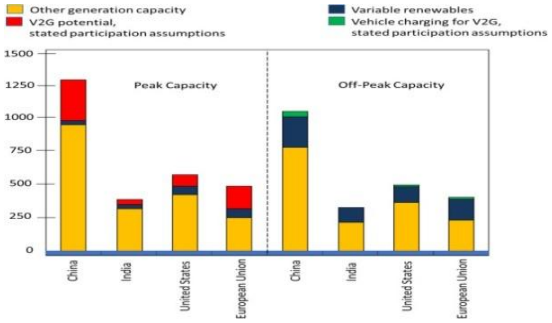

Fig 1: EV-to-network potential and renewable capacity vs. total generation needs in the Sustainable Development Scenario.

A key part of this transition is the rise of electric vehicles (EVs), supported by government incentives and better charging infrastructure. EVs are far more efficient than internal combustion engine (ICE) vehicles and emit about 40% less greenhouse gases. However, the expected growth in EV numbers—over 130 million by 2030—poses new challenges for existing power grids, which are not yet fully equipped to handle the added and fluctuating demand.

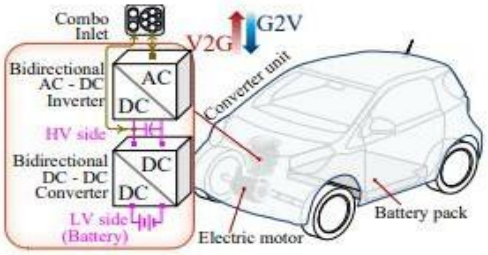

Fig 2: Layout of electric vehicle

To meet these challenges, upgrades to grid infrastructure are essential. Vehicle-to-Grid (V2G) technology allows EVs to act as mobile energy storage, supplying excess power back to the grid during off-peak hours. Hybrid Energy Storage Systems (HESS), which combines lithium-ion batteries with super capacitors, help meet peak demand more effectively. While both unidirectional and bidirectional V2G models are being tested, bidirectional systems offer better support for grid services like voltage and frequency regulation. Only a 15–25% increase in capacity is needed to meet peak demand, as 90% of power plants already run continuously. In key regions such as Asia, North America, and Europe, peak EV-driven electricity demand may soon exceed 600 GW. With a total battery capacity of 16,000 GWh, and assuming 60% usage and 20% energy loss during DC to AC conversion, about 7,680 GWh would still be available—enough to exceed peak demand by 1,500 GWh in emergency situations.

2. Proposed System

The bidirectional Zeta converter plays a pivotal role in enabling seamless power transfer between EVs and the grid. Unlike traditional unidirectional converters, the bidirectional Zeta converter allows energy to flow in both directions, facilitating not only the charging of EVs but also their ability to contribute excess energy back to the grid. This bidirectional capability enhances the versatility and utility of EVs as dynamic grid assets, promoting a more integrated and sustainable energy ecosystem.

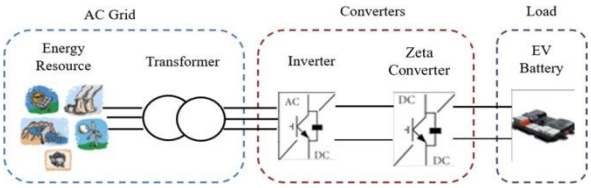

Fig 3:Layout of electric vehicle

The proposed switching bidirectional zeta converter with a Hybrid Energy Storage System (HESS) comprises five main components: a lithium-ion battery, a switching bidirectional buck-boost circuit, a super capacitor (SC), a full-bridge inverter, and the grid. Three addition switches (D1, D2, and D3), a super capacitor, and an inductor are all included in the circuit. A single gate signal can control these three extra switches since the gate signals of switches Sp and Sos are complementary to and identical to the gate signal of switch Sot. Because of its special converter design, the system can transmit power in both directions and function in both buck and boost modes. System Configuration The configuration of the Vehicle-to-Grid (V2G) system is illustrated in Figure 2. The system comprises three sections: the AC grid, converters, and loads. The AC grid supplies the initial alternating current (AC) voltage. The converters include an AC/DC converter and a DC/DC converter. The AC/DC converter transforms AC power into direct current (DC) power. The bidirectional DC/DC converter links the battery to the DC bus. In this context, charging the battery is referred to as a positive process, while discharging is considered negative.A Zeta converter is a type of DC-to-DC converter employed to deliver a regulated DC power output from an unregulated DC power source. Similar to other traditional converters, Zeta converters can step up or step down the input DC voltage depending on the duty cycle. Like other DC-to-DC converters, a Zeta converter achieves a stabilized output by transferring energy between capacitors and inductors. The quantity of energy transferred is controlled by a switch, with its operation governed by adjusting the duty cycle.

3. Fundamental Working Principle of a Zeta Converter

The Zeta converter operates using a MOSFET switch, two inductors (L1 and L2), two capacitors (C1 and C2), a diode (D), and a load resistor (R). It functions in continuous conduction mode (CCM), cycling between ON and OFF states during switching.

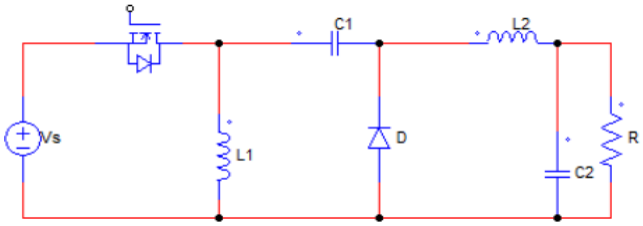

Fig 4–Basic equivalent circuit of zeta converter

Working of a Zeta Converter:

Mode1: The switch, diode, and inductor drain current from the source voltage (Vs) when it is in the ON state. The electricity that passes through the inductor tends to increase linearly, saving energy in the ON condition mode of operation. The input or source voltage will be almost identical to the inductor voltage across [3]. Capacitor C1 starts to charge to output voltage simultaneously. The two inductors (L1 and L2) will store energy from the source when the MOSFET is in the ON condition, and C1 and L2 will also supply output currents [2].

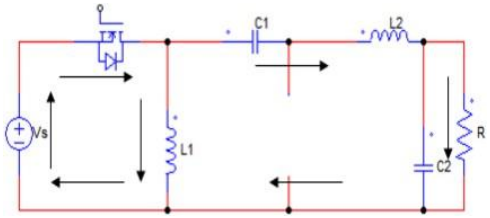

Fig5:Mode1 Of Zeta Converter

Mode 2: When the switch is in the OFF state, the diode is now forward biased, the capacitor is parallel to the L2 inductor, and the output voltage across the inductor is available since C1 gets drained and C2 is charged to the output voltage. The load resistor will receive any energy that is kept in the inductor (L). Thus, conditions are being discharged by this type of operations.

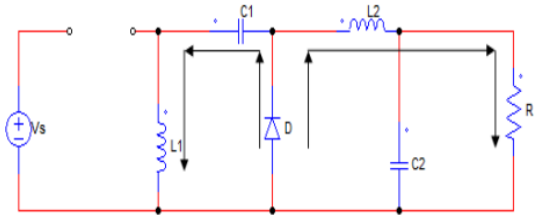

Fig 6-mode 2 of Zeta converter

Vehicle to grid mode

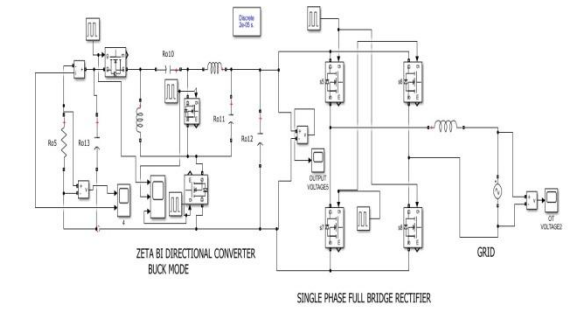

Fig 7 Vehicle to grid mode circuit diagram

Grid to vehicle mode:

From the MATLAB simulation the output for operating modes, both grid to automobile and automobile toward grid modes are acquired. The battery voltage is 48v. By applying the gate pulse in sequence

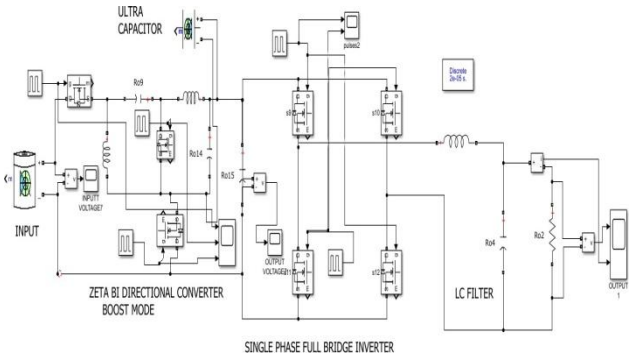

themode1andmode2operationcan be performed and the required output can be obtained.

Fig 8 Grid to Vehicle mode circuit diagram

4. Results &Discussion:

The battery voltage is applied to the inverter connected in the automobile into a grid mode conversion. The inverter in this mode has semiconductor switches and by applying the gate pulse to this switch the output AC voltage can be obtained. The output AC voltage is connected

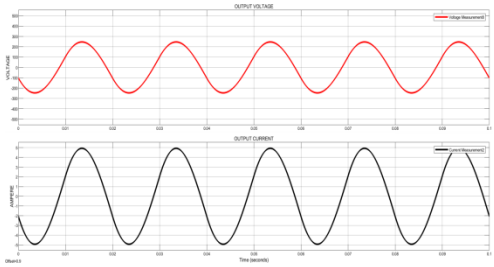

Fig 10-Output voltage from the vehicle to grid

to the Grid. The battery voltage is applied to the inverter connected in the automobile into a grid mode conversion. The inverter in this mode has semiconductor switches and by applying the gate pulse to this switch the output AC voltage can be obtained. The output AC voltage is connected to the Grid, the Fig.10 represents

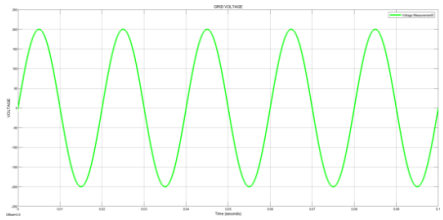

the grid voltage

.

Fig11- Grid voltage

The grid voltage is AC and this voltage is feedback to the rectifier in the Grid to vehicle conversion mode. The rectifier contains semiconductor switches which is controlled by gate pulse and produces DC Output. The Fig 11 shows the Grid voltage = 200V

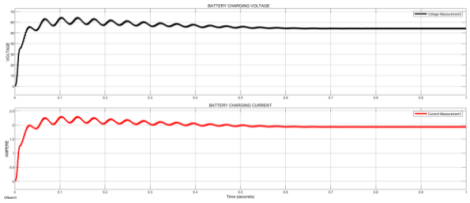

Fig12-Battery charging voltage and battery charging current

5. Conclusion

This paper presents the hybrid energy storage forV2G system with the help of Zeta converter. This converter as improved efficiency and reduced loss for the energy conversion. The future depends on the rise of electrical vehicles and technologies. The storage system is supplied with two modes from grid to automobile and automobile to network. This creates an efficient storage system for future.

Reference

1. Sadeq, A.M.; Homod, R.Z.; Hussein, A.K.; Togun, H.; Mahmoodi, A.; Isleem, H.F.; Patil, A.R.; Moghaddam, A.H. Hydrogen energy systems: Technologies, trends, and future prospects. *Sci. Total Environ.* 2024, *939*, 173622. [Google Scholar] [CrossRef]
2. Jia, C.; He, H.; Zhou, J.; Li, J.; Wei, Z.; Li, K. Learning-based model predictive energy management for fuel cell hybrid electric bus with health-aware control. *Appl. Energy* 2024, *355*,122228. [Google Scholar] [CrossRef]
3. Jia, C.; Zhou, J.; He, H.; Li, J.; Wei, Z.; Li, K.; Shi, M. A novel energy management strategy for hybrid electric bus with fuel cell health and battery thermal-and health-constrained awareness. *Energy* 2023, *271*, 127105.
4. Nivas, M.; Naidu, R.K.P.R.; Mishra, D.P.; Salkuti, S.R. Modeling and analysis of solar-powered electric vehicles. *Int. J. Power Electron. Drive Syst.* 2022, *13*, 480. [Google Scholar] [CrossRef]
5. Niu, S.; Zhao, Q.; Chen, H.; Yu, H.; Niu, S.; Jian, L. Underwater Wireless Charging System of Unmanned Surface Vehicles with High Power, Large Misalignment Tolerance and Light Weight: Analysis, Design and Optimization. *Energies* 2022, *15*, 9529. [Google Scholar] [CrossRef].
6. P. K. Maroti, S. Padmanaban, J. B. Holm- Nielsen, M. Sagar Bhaskar, M. Meraj, and A. Iqbal, "A new structure of high voltage Access, vol.7,pp.89857– 89868, 2019.
7. P.K. Maroti, S.Padmanaban, S.M.Bhaskar, J.B.Holm-Nielsen, F.Blaabjerg, D.M.Ionel, and J. He,"A non-isolated inverting high gain modified new series of lands man converter ,"in Proc.45th Annu. Conf. IEEE Ind.Electron.Soc.(IECON), Lisbon,Portugal,Oct.2019,pp. 4077–4082.
8. .S. Das, P. Acharjee, and A. Bhattacharya, "Charging scheduling of electric vehicle incorporating grid-to-vehicle (G2V) and vehicle-to-grid (V2G) technology in smart-grid," in Proc. IEEE Int. Conf. Power Electron. , Smart Grid Renewable Energy, Kerala, India, Jan. 2–4, 2020, pp. 1–6.
9. S. Li, J. Deng and C. C. Mi, "Single-Stage Resonant Battery Charger With Inherent Power Factor Correction for Electric Vehicles," IEEE Trans. on Veh.Tech., vol. 62, no. 9, pp. 4336-4344, Nov. 2013.
10. Tripathi, P.Kumar,S.V.,&Bhaskar,R.(2022). Bidirectional charger for A Single-Phase Electric Vehicle using Buck Boost Converter (G2V & V2G Application). Technix International Journal for Engineering Research, 9(6), 112-116.

Taguchi Based Optimization of SMAW and TIG Welding Process Parameters on HSLA-DMR249A steel

[*]G. Dhanraj[1], O. Raina[2], K. Deepa[3], M. Surendar[4] and H. Gokulram[5]

1. Department of Mechanical Engineering, CSI College of Engineering, The Nilgiris, Tamilnadu, India, dhanrajguru77@gmail.com

2. Department of Chemistry, CSI College of Engineering, The Nilgiris, Tamilnadu, India, raina2oliver@gmail.com

3. Department of Computer Science and Engineering, SR University, Warangal, India, k.deepa@sru.edu.in

4. Department of Electrical and Electronics Engineering, Swarnandhra College of Engineering and Technology, Andhra Pradesh, India, eee.surendar@gmail.com

5. *Department of Civil Engineering, CSI College of Engineering, The Nilgiris, Tamilnadu, India, gokulram77@gmail.com*

Abstract

The HSLA- DMR249 A steel of dimension 300 x 150 x 10 mm is processed for Tungsten inert-gas (TIG) Welding and shielded metal arc welding (SMAW) and mechanical properties and parameters were optimised. Mechanical properties like micro hardness of the weldment were examined. The influenced varying process parameters like current, voltage and flow rate were taken into account for both welding processes to carry out the experiment runs. Taguchi strategy (L9) and ANOVA methods were used to find out various parameters. The most vital factor which influence the result of mechanical property of low alloy steels is current than by voltage and flow rate. Mechanical properties confirms that the welded portion by both SMAW and TIG methods was found to be harder of 323 VHN, 330 VHN. The optimum process parameters are found to be 200A current, 40V voltage, 13L/Min flow rate for the shielded metal arc welding (SMAW) and 180A current, 20V voltage, 13 L/Min flow rate for TIG welding.

Keywords. SMAW, TIG, HSLA- DMR 249A, Taguchi parameter, mechanical property

1. INTRODUCTION

Welding is an important economical process commonly employed in steel structures. The knowledge related to the properties of dissimilar and similar metals plays a major role in the advancement of light weight structures [1]. For construction and fabrication resolutions, the conventional arc welding process is generally employed [2]. The process is normally limited to the flat or horizontal-fillet welding positions [3]. A non-consumable tungsten electrode and an inert gas (argon) for arc shielding are used in Tungsten inert-gas (TIG) welding. Joints of aluminium and stainless steels are difficult-to-weld and fabricate and also the slag crevices and corrosion attack zones can be eradicated using TIG welding [4].

The DMR 249A steel is a High Strength Low Alloy (HSLA) steel are commonly used for strategic applications due to the basic factors like cost and availability. They are often replaced by carbon steels due to their improved characteristics related to strength and welding [5]. DMR 249A is one of low carbon micro-alloyed grade of steel with stern impact strength even at sub-zero temperature. current of 140 A, and voltage of 12 V are found to be the optimum welding parameters [6]. The current of 120A, Voltage of 25V and gas flow rate of 12 lit/min is the suggested level of the controllable parameters of TIG welding process as the minimization of the percentage of elongation and maximization of ultimate tensile strength [7]. Investigation of process parameter such as welding current, torch speed and arc gap on depth of penetration in A-TIG welding of SS 304L has been calculated [8].

Genichi Taguchi established Taguchi method as a process optimization technique [9]. The optimum working conditions determined from the laboratory work can be reproduced in the real production environment [10].

There is lack of in-depth study made by the researchers on the DMR 249A steel and also this examination assumes significance, as no systematic weldability study has been conveyed so far. The proposed work is to analyze the optimal process parameters of SMAW and TIG welding by using Taguchi technique to achieve desirable mechanical properties of DMR 249A steel joints.

2. EXPERIMENTAL DETAILS

2.1 Material and Properties of DMR 249A Steel

This high performance and low-cost steel (DMR 249A- base metal) used in this present work was developed by Indian Navy at Steel Plant (SMS II, BSL). The electrode/filler wire used in this work is E308L.

2.2 Welding Process Parameters and Levels

Among various SMAW and TIG welding process parameters, Pilot experiments were carried out on welded DMR 249A steel material on weld properties. In the present SMAW and TIG welding inspection, three major influenced process parameters, i.e., current, voltage and flow rate were considered and found to be most influencing process parameters. From the upshots, the range of the SMAW process parameters of 120-200A current, 28-40 V voltage and 10-13L/min flow rate and TIG welding process parameters of 120-180A current, 12-20 V voltage and 10-16L/min flow rate was recognized and offered in Table 1.

Table 1: Levels of SMAW & TIG welding process

SN	Parameter/factors	Notation	Levels								
			Coded			Original – SMAW			Original -TIG		
			Low	Medium	High	Low	Medium	High	Low	Medium	High
1	Current(A)	A	1	2	3	120	160	200	120	150	180
2	Voltage(V)	B	1	2	3	28	34	40	12	16	20
3	Flow rate(L/min)	C	1	2	3	10	13	16	10	13	16

2.3 Experimentation on design matrix

In this present work, two DMR 249A steel plates of required dimension were castoff for welding by means of SMAW and TIG welding methods as per design matrix. The gas which was used for both SMAW well as for the TIG welding processes is the customary argon shielding gas and experiments were carried out as per standard procedure [11]. A welded specimen plate was formed and then endangered to mechanical testing after welding. The various mechanical properties presently involved are the hardness shown in table 2.

Table 2: Taguchi- Design of experiments of SMAW & TIG welding process

Trail No	Coded			Original – SMAW			Original -TIG		
	Current (Amps)	Voltage (Volts)	Flow rate (Lt/min)	Current (Amps)	Voltage (Volts)	Flow rate (Lt/min)	Current (Amps)	Voltage (Volts)	Flow rate (Lt/min)
1	1	1	1	120	28	10	120	12	10
2	1	2	2	120	34	13	120	16	13
3	1	3	3	120	40	16	120	20	16
4	2	1	2	160	28	13	150	12	13
5	2	2	3	160	34	16	150	16	16
6	2	3	1	160	40	10	150	20	10

7	3	1	3	200	28	16	180	12	16
8	3	2	1	200	34	10	180	16	10
9	3	3	2	200	40	13	180	20	13

3. RESULTS AND DISCUSSION

3.1 SMAW WELDING

3.1.1 Effect of Hardness on SMAW welding process parameters

ANOVA in Table 3 predicts, the F-value of experimental hardness model is 32.19, 3.51 and 0.64 for current, voltage and flow rate depict that, this model is crucial. Because of noise, 0.01% chance was there in this case to create "Model F-Value". The model terms P > F is less than 0.0500 which indicates, model terms are significant. All the input parameters in this experiment and their collaboration such as current (A), voltage (B) and flow rate (C) and interaction terms are eliminated from this model when the values are superior than 0.05000.

ANOVA points that of the various input parameters considered while welding, it is observed that the current, voltage and flow rate are found to be significant at 95% confidence. From the table 3 and 4, it is also found that the current contributes about 87.26% in change of hardness followed by voltage and flow rate with 11.39% and 0.337% respectively and ranked at top is current followed by voltage and flow rate with second and third position. In table 5, 97.4% (Predicted R-Squared) is highly coincide with 89.6% (Adjacent R-Squared) and this high precision shows the S/N ratio. From the figure 1, it is found that the hardness gradually increases from current 120–200 A when voltage is increased gradually between 28-40 W. It is concluded that from the above data, that current contributes to a greater extent than voltage. When considering flow rate, the hardness slightly increased between 10-13 L/min and decreases between13 to 16 L/min. Flow rate contributes only to a small percent.

Also, it is evident from the observation that signal to noise ratio if larger it is better in hardness values. The optimal process parametric combinations for maximum hardness of 323 VHN were found to be in 200A current, 40W voltage and 13 L/min flow rate respectively. These parameters are assured by the confirmation run and it's found to be in good agreement.

Table 3: Analysis of Variance for S/N ratios on hardness in SMAW welding

Source	DF	Seq SS	Adj SS	Adj MS	F	P	% contribution
current	2	0.79135	0.79135	0.395677	32.19	0.030	88.58
voltage	2	0.08618	0.08618	0.043091	3.51	0.222	0.61
flow rate	2	0.01577	0.01577	0.007883	0.64	0.609	1.67
Residual Error	2	0.02458	0.02458	0.012292			
Total	8	0.91789					

Table 4: Response for S/N Ratios on hardness in SMAW welding

Level	current	voltage	flow rate
1	49.38	49.57	49.73
2	49.57	49.65	49.63
3	50.08	49.81	49.68
Delta	0.70	0.23	0.10
Rank	1	2	3

Table 5: Model Coefficients for S/N ratios on hardness in SMAW welding

Term	Coef	SE Coef	T	P
Constant	304.889	1.281	237.935	0.000
current 120	-10.556	1.812	-5.825	0.028
current 160	-3.722	1.812	-2.054	0.176
voltage 28	-3.556	1.812	-1.962	0.189
voltage 34	-1.056	1.812	-0.582	0.619
flow rat 10	1.778	1.812	0.981	0.430
flow rat 13	-1.722	1.812	-0.950	0.442

S = 3.844 R-Sq = 97.4% R-Sq(adj) = 89.6%

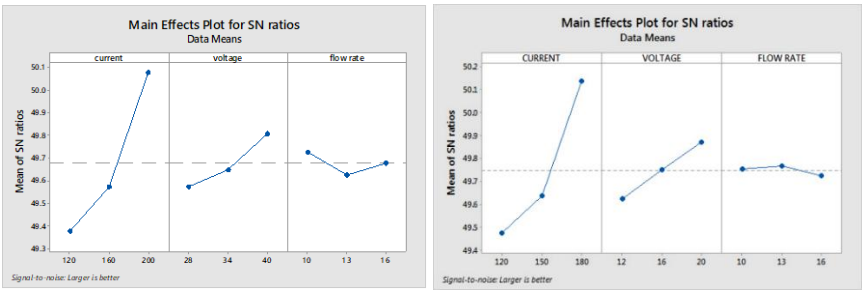

Fig 1. Main effects plot for S/N ratios on Hardness in (a) SMAW & (b) TIG welding

3.2 TIG WELDING

3.2.1 Effect of Hardness on TIG welding process parameters

ANOVA in Table 6 predicts, the F-value of experimental hardness model is 274.63, 35.46 and 1.05 for current, voltage and flow rate depict that, this model is crucial. Because of noise, 0.01% chance was there in this case to create "Model F-Value". The model terms P > F is less than 0.0500 which indicates, model terms are significant. All the input parameters in this experiment and their collaboration such as current (A), voltage (B) and flow rate (C) and interaction terms are eliminated from this model when the values are superior than 0.05000.

ANOVA indicates that among the various input process parameters considered while welding, it is observed that the current, voltage and flow rate are found to be significant at 95% confidence. From the table 6 and 7, it is also noted that the current contributes about 88.26% in change of hardness followed by voltage and flow rate with 11.39% and 0.337% respectively and ranked first in current followed by voltage and flow rate with second and third position. In table 8, 99.7% (Predicted R-Squared) is highly coincide with 98.7% (Adjacent R-Squared) and this high precision shows the S/N ratio. From the figure 1a, it is found that the hardness gradually increases from current 120–150 A, and increases steadily from 150-180A and increased when voltage is increased gradually between 12-20 W. It is evident that from the above data, that current contributes to a higher extent than voltage. When considering flow rate, the hardness slightly increased between 10-13 L/min and decreases between13 to 16 L/min. Flow rate contributes only to a small extent.

Also, it is evident from the observation that signal to noise ratio of larger is better in hardness values. The optimal process parametric combinations for maximum hardness of 330 VHN were found to be in 180A current, 20W voltage and 13 L/min flow rate respectively. These parameters are confirmed by the confirmation run and its found to be in good agreement.

Table 6 Analysis of Variance for S/N ratios on Hardness in TIG welding

Source	DF	Seq SS	Adj SS	Adj MS	F	P	%contribution
CURRENT	2	0.716029	0.716029	0.358015	274.63	0.004	88.26
VOLTAGE	2	0.092461	0.092461	0.046231	35.46	0.027	11.39
FLOW RATE	2	0.002729	0.002729	0.001365	1.05	0.489	0.337
Residual Error	2	0.002607	0.002607	0.001304			
Total	8	0.813827					

Table 7 Response for S/N ratios on Hardness in TIG welding

Level	CURRENT	VOLTAGE	FLOW RATE
1	49.47	49.62	49.76
2	49.64	49.75	49.77
3	50.14	49.87	49.73
Delta	0.66	0.25	0.04
Rank	1	2	3

Table 8 Model Coefficients for S/N ratios on Hardness in TIG welding

Term	Coef	SECoef	T	P
Constant	49.7493	0.01204	4133.668	0.000
CURRENT 120	-0.2756	0.01702	-16.192	0.004
CURRENT 150	-0.1120	0.01702	-6.578	0.022
VOLTAGE 12	-0.1251	0.01702	-7.348	0.018
VOLTAGE 16	0.0019	0.01702	0.111	0.922
FLOW RAT 10	0.0057	0.01702	0.337	0.768
FLOW RAT 13	0.0179	0.01702	1.050	0.404

S = 0.03611 R-Sq = 99.7% R-Sq(adj) = 98.7%

4. CONCLUSION

- From ANOVA table, the narrated results indicated that current is the most prominent factor than the voltage and flow rate for maximizing the mechanical properties of both the SMAW and TIG welding process and the percentage contribution of influenced factor of current on responses about 77.38 to 94.03 and 82.5 to 88.26 respectively.
- From the statistical tool revealed that optimal level of SMAW and TIG welding process variables for obtaining maximum mechanical properties were found to be hardness of 323 VHN, 330 VHN
- The obtained optimal influenced process parameters are found to be 200A current, 40V voltage,13L/Min flow rate for the SMAW process and 180A current, 20V voltage, 13 L/Min flow rate for TIG) welding.
- The hardness values were found to be higher in TIG welding than SMAW process due to presence of partial martensite and tempered martensite phase in the welded sample under optimal condition.

REFERENCE

1. Mers Paul Kah, Raimo Suoranta, Jukka Martikainen, Carl and t.fi, Techniques for joining dissimilar materials: metals and polymers, Rev. Adv. Mater. Sci, 36, 2014.
2. Stephen.R.Forrest, The path to ubiquitous and low-cost organic electronic appliances on plastic, International journal of science, Nature volume 428, 911–918, April 2004.
3. J. Haider, A theoretical model for gas metal arc welding and gas tungsten arc welding. I, Journal of Applied Physics 84, 3518, 1998.
4. Klas Weman, Welding processes hand book, A volume in Woodhead publishing series in welding and other joining technologies, Second edition, 2012.
5. Danijela A. Skobir, High-strength low-alloy (HSLA) steels, Materials and technology, 45, 295–301, 2011.
6. G.Magudeeswaran, Srihari. R. Nair, L. Sundar and N. Harikannan, Optimization of process parameters of the activated tungsten inert gas welding for aspect ratio of UNS S32205 duplex stainless steel welds, Defence Technology, Volume 10, Issue 3, 251-260, 2016.
7. Bolarinwa Johnson Kutelu, Saliu Ojo Seidu, Godwin Idenala Eghabor and Ayotunde Idris Ibitoye, Review of GTAW Welding Parameters, Journal of Minerals and Materials Characterization and Engineering, 6, 541-554, 2018.
8. Prashant S Lugade and Manish J Deshmukh, Optimization of Process Parameters of Activated Tungsten Inert Gas (A-TIG) Welding for Stainless Steel 304L using Taguchi Method, International Journal of Engineering Research and General Science Volume 3, Issue 3, 2015.
9. Samruddhi Rao, Pragati Samant, Athira Kadampatta and Reshma Shenoy, An Overview of Taguchi Method: Evolution, Concept and Interdisciplinary Applications, International Journal of Scientific & Engineering Research, Volume 4, Issue 10,2013.
10. Ozcan Tan, A. Sahin Zaimoglu, Sinan Hinislioglu and Selim Altun, Taguchi approach for optimization of the bleeding on cement-based grouts, Tunnelling and Underground Space Technology 20,167–173, 2005.
11. G. Dhanraj, V. Velmurugan and N. Balaji, Metallurgical Behaviour and Mechanical Properties on The Shielded Metal Arc Welding and Tungsten Inert Gas Welding Process of DMR 249A Steel, Journal of the Balkan Tribological Association, Vol. 24, No 4, 622–632, 2018.

CAR DAMAGE SEVERITY ESTIMATION FOR INSURANCE

Nisha Priya P[1], Priya V[2], Deepavahini M[3] ,Pranesh R[4] ,Ajith M[5], Sanjeedha S[6]

[1]Head Of Department,CSE,CSI College Of Engineering,Ketti,The Nilgiris-643215
nisha@csice.edu.in
[2]Assistant Professor, CSE, CSI College of Engineering, Ketti, The Nilgiris-643215
priyacsice@gmail.com
[3]Final Year Student, CSE, CSI College of Engineering, Ketti, The Nilgiris-643215
deepavahinimani@gmail.com
[4]Final Year Student, CSE, CSI College of Engineering, Ketti, The Nilgiris-643215
pranesh1030@gmail.com
[5]Final Year Student, CSE, CSI College of Engineering, Ketti, The Nilgiris-643215
ajithmani2021@gmail.com
[6]Final Year Student, CSE, CSI College of Engineering, Ketti, The Nilgiris-643215
sanjeedha17@gmail.com

ABSTRACT

With the increasing demand for faster and more efficient insurance claim processing, AI-operated solutions are transforming how car damage severity is assessed. Traditional manual inspections—dependent on human evaluators—are time-consuming, costly, and prone to errors, often resulting in delays and dissatisfaction. This paper presents an AI-driven system designed to overcome these challenges by automating car damage evaluation. The system employs YOLOv8 for real-time object detection to identify damaged car parts, while MobileNetV2 is used for classifying the severity of the damage.For estimating the cost, the system uses a JSON-based cost evaluation module. Image preprocessing techniques such as data augmentation and perceptual hashing are applied to improve model generalization, ensure data integrity, and eliminate duplicate images, thereby optimizing computational efficiency. MongoDB is used for scalable data storage, and Pandas is leveraged to generate structured PDF reports containing detailed information about the damage, severity, and estimated repair costs. Unlike traditional methods, this AI-powered approach enables rapid, reliable, and automated damage assessments, streamlining the insurance claim process while improving accuracy, efficiency, and transparency.

Keywords: Car damage detection, YOLOv8, MobileNetV2, JSON-based cost estimation, AI in insurance, image preprocessing, perceptual hashing, automated claim processing

1. INTRODUCTION

To meet the growing need for faster and more efficient insurance claim processing, this project presents an AI-powered system that automates car damage severity estimation. Using YOLOv8 for damage detection and a lightweight MobileNetV2 model for classification, the system identifies issues like dents, bumper damage, mirror or hood damage, and windshield cracks. It replaces slow, error-prone manual inspections with real-time, accurate analysis that works efficiently even on low-end hardware. Once the severity is determined, repair costs are estimated based on standard industry rates, eliminating the need for manual cost evaluation and speeding up the claim process. MongoDB ensures efficient data storage and management, while the Phash algorithm detects and removes duplicate reports to maintain data

accuracy. The system also leverages Pandas, to provide structured PDF reports, which also contains relevant details about the damage, severity level, and estimated costs.Overall, this project provides a smart, reliable, and scalable solution which brings speed, accuracy, and transparency to car damage assessments and insurance claims.

2. PROBLEM STATEMENT

Manual car damage assessment methods are slow, costly, and often inaccurate due to reliance on human judgment. Current systems accept only image inputs, lack real-time processing, and have no mechanism to detect duplicate claims, increasing the risk of fraud. Additionally, the absence of AI-powered severity evaluation and automated cost estimation leads to delays and inconsistent results. There is also a lack of detailed, structured reports, which hampers transparency and efficient claim handling. An AI-driven solution using deep learning and image processing is needed to automate assessment, detect duplicates, and generate comprehensive reports for faster, more reliable insurance claim processing.

3. PROPOSED METHOD

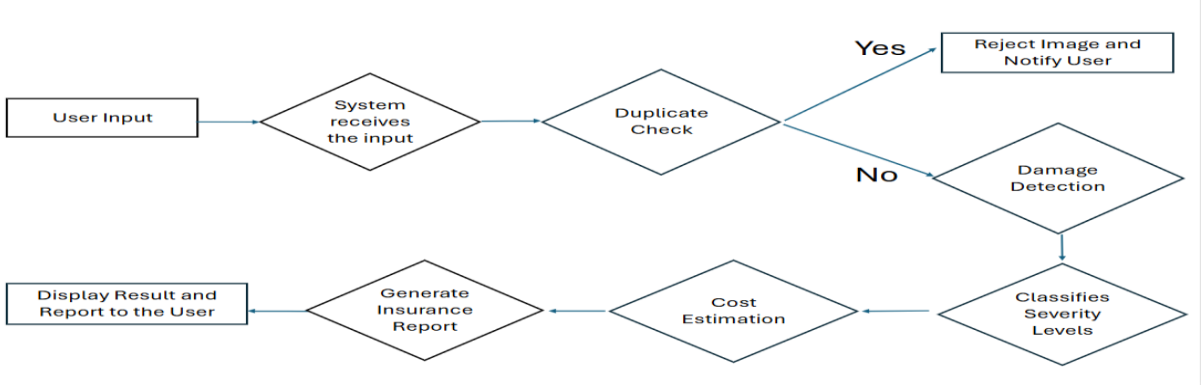

Figure 3.1: Workflow of the Car Damage Severity Estimation System

3.1 DUPLICATE DETECTION

The system employs Perceptual Hashing (pHash) to analyze duplicate images by their visual content, rather than using exact data to compare images, meaning that duplicate images can be recognized even through alterations of pixels.

$$DCT(u,v) = 1/4\, C(u)C(v) \sum_{x=0}^{N-1} \sum_{y=0}^{N-1} I(x,y) \cos\left(\frac{(2x+1)u\pi}{2N}\right) \cos\left(\frac{(2y+1)v\pi}{2N}\right) \quad (3.1.1)$$

The system will compare the binary hash with the ones that have been stored in the MongoDB and solve for the Hamming Distance,

$$H(A,B) = \sum_{i=1}^{n} (A_i \oplus B_i) \quad (3.1.2)$$

If the distance is less then the system will raise a duplicate image alert.

3.2 OBJECT DETECTION

Object detection plays a vital role in identifying damaged car areas before severity estimation, using the YOLOv8 model for its real-time accuracy and speed. The dataset is preprocessed by converting images to JPG format, resizing to 640×640 pixels, and labeling with .txt files in the format (class_id center_x center_y width

height), supported by a data.yaml file defining class names and image paths. YOLOv8 is trained using the Ultralytics library with transfer learning—starting with frozen backbone layers and gradually fine-tuning them. Training uses a batch size of 22, 50 epochs, a 0.001 learning rate, and the Adam optimizer. Data augmentation with Albumentations improves model robustness, and learning rate adjustments are handled using ReduceLROnPlateau.

3.3 SEVERITY CLASSIFICATION

Severity estimation is essential for evaluating vehicle damage by classifying its seriousness to support insurance claims and repair cost estimation. This is achieved using a deep learning model, "mobilenetv2_model.h5," trained on real-world car damage images to categorize damage into minor, moderate, severe, or uncertain. The model, loaded in a non-trainable state, processes images resized to (1, 224, 224, 3), extracting features like dent depth, crack patterns, and paint damage using optimized convolutional layers,data augmentation methods such as rotation, zooming, brightness adjustment, and flipping are applied. The MobileNetV2 architecture is modified through advanced preprocessing, real-world-oriented dataset structuring, and a two-stage fine-tuning approach. Initially, the final layers are trained for 10 epochs with the backbone frozen, followed by unfreezing the last 50 layers and fine-tuning with SGD for better generalization.

4. PERFORMANCE METRICS

The system's performance is assessed based on multiple overall accuracy metrics. The overall accuracy of the model is 97.6%, which indicates that the model is expected to produce reliable results when detecting and classifying damaged vehicles.

6. REFERENCES

[1] D. Mallios, L. Xiaofei, N. McLaughlin, J. M. D. Rincon, C. Galbraith and R. Garland, "Vehicle Damage Severity Estimation for Insurance Operations Using In-The-Wild Mobile Images," in IEEE Access, vol. 11, pp. 78644-78655, 2023, doi: 10.1109/ACCESS.2023.3299223.

[2] N. Fernando, A. Kumarage, V. Thiyaganathan, R. Hillary and L. Abeywardhana, "Automated vehicle insurance claims processing using computer vision natural language processing", Proc. 22nd Int. Conf. Adv. ICT for Emerg. Regions (ICTer), pp. 124-129, Nov. 2022.

[3] Kyu, Phyu Mar, and Kuntpong Woraratpanya. "Car damage detection and classification." Proceedings of the 11th international conference on advances in information technology. 2020.

BIOGRAHIES



Dr. P. Nisha Priya received her Bachelor's degree in Computer Science and Engineering from Anna University, Chennai, India, in 2007, and her Master's degree in the same field from Anna University in 2016. She completed her Ph.D. from Anna University, Chennai, in January 2025 in Medical Image Processing. Currently, she is serving as the Assistant Professor and Head of the Department of Computer Science and Engineering at CSI College of Engineering, Ketti. Her research interests include Medical Image Processing, Deep Learning, Machine Learning.



Priya.V received the bachelor's degree in Electrical and Electronics Engineering from Anna University in 2010, the master's degree in Embedded Systems and Technology from Anna University in 2012, respectively. She is currently working as an Assistant Professor at the Department of Electrical and Electronics Engineering. Her research areas include Smart Electrical Vechile , Embedded, and network .



Deepavahini M is currently pursuing a Bachelor of Engineering degree in Computer Science and Engineering at CSI College of Engineering, expected to graduate in 2025. Her areas of interest include Artificial Intelligence, Data Analytics, and Machine Learning. She is

passionate about applying intelligent technologies to solve real-world problems and is actively involved in academic projects and internships that enhance her technical and analytical skills.



Pranesh R is currently pursuing a Bachelor of Engineering degree in Computer Science and Engineering at CSI College of Engineering, expected to graduate in 2025. His areas of interest include Data analytics, Cloud Computing, and Web Development. He is keen on exploring secure and scalable technologies and is engaged in various academic and hands-on projects that strengthen his technical expertise.



Ajith M is currently pursuing a Bachelor of Engineering degree in Computer Science and Engineering at CSI College of Engineering, expected to graduate in 2025. His areas of interest include Web Development and Full Stack Development. He is passionate about building dynamic and responsive web applications and is actively involved in projects that enhance his front-end and back-end development skills.



Sanjeedha S is currently pursuing the Bachelor of Engineering (B.E.) degree in Computer Science and Engineering at CSI College of Engineering, with expected graduation in 2025. Her interests include artificial intelligence, machine learning, cloud computing, and data

analytics. She has worked on projects focused on intelligent systems, cloud-based solutions, and analytical tools.

Advanced Machine Learning Techniques for Predicting House Prices: A Comparative Analysis

Gautam Kumar
Computer Science and Engineering
Chandigarh University Chandigarh, India
gautam.e16534@gmail.com

***Abstract*—This research paper explores advanced machine learning techniques for predicting house prices. By comparing various models and evaluating their performance on different datasets, the study aims to identify the most effective approach for accurate house price prediction. The paper also discusses the implications of these models in the real estate market, considering factors such as interpretability, scalability, and data quality.**

***Index Terms*—House Price Prediction, Machine Learning, Real Estate, Comparative Analysis**

I. Introduction

A. Background and Motivation

The real estate sector has long been a cornerstone of economic activity, significantly influencing both macroeconomic stability and individual financial well-being. In recent years, the importance of accurate house price predictions has grown, driven by the need for informed decision-making among various stakeholders, including potential homebuyers, real estate investors, financial institutions, and policymakers [1]. Traditional methods of house price prediction have typically relied on statistical models that utilize historical data and economic indicators. While these approaches have provided a baseline for understanding market trends, they often struggle to capture the intricate, nonlinear relationships that exist among the numerous factors influencing house prices [2].

The advent of machine learning (ML) has introduced a paradigm shift in predictive modeling across various domains, including real estate. ML models, characterized by their ability to learn from data and uncover hidden patterns, offer the potential to significantly enhance the accuracy of house price predictions. By leveraging vast datasets and sophisticated algorithms, these models can analyze complex interactions between variables such as location, property characteris- tics, economic conditions, and market sentiment. Despite the promising capabilities of ML, there remains a critical need to systematically evaluate these models to determine which techniques are most effective for predicting house prices in different contexts [3].

B. Problem Statement

Accurately predicting house prices is a multifaceted challenge that requires consideration of a diverse set of factors, each contributing to the overall valuation of a property. The inherent complexity of the real estate market, characterized by its dynamic and often volatile nature, further complicates this task. Existing prediction models, while useful, are frequently limited by their inability to account for nonlinear interactions and the diverse range of variables that influence house prices. Additionally, the performance of these models can vary significantly depending on the quality and nature of the data used [4]. This research seeks to address these challenges by identifying and evaluating the most effective ML techniques for house price prediction, with a particular focus on understanding the comparative strengths and weaknesses of different models in handling real estate data.

C. Objectives of the Study

The overarching aim of this study is to conduct a rigorous comparative analysis of various ML models to determine their effectiveness in predicting house prices. To achieve this, the study will focus on the following specific objectives:

- To evaluate the predictive performance of different ML models, including linear regression, decision trees, random forests, support vector machines, and neural networks, in the context of house price prediction [5].
- To assess the impact of feature selection on the accuracy, robustness, and interpretability of the predictive models.
- To identify the best-performing model based on a comprehensive set of evaluation metrics, such as mean squared error (MSE), mean absolute error (MAE), and R-squared.

- To provide practical insights into the implications of using ML models in the real estate industry, particularly in terms of scalability, implementation, and data require- ments [6].

D. Research Questions

The following research questions are formulated to guide the investigation and ensure that the study addresses key aspects of house price prediction using ML:

- Which ML model provides the highest predictive accuracy for house prices across different datasets and market conditions?
- How does the selection of features influence the performance, interpretability, and generalization ability of ML models?
- What are the specific strengths and limitations of various ML models in capturing the complexities of real estate data?
- What practical considerations must be taken into account when implementing ML models for house price prediction in real-world applications? [7]



Fig. 1. Gaps in the Price

II. Literature Review

A. Overview of House Price Prediction Models

The prediction of house prices has traditionally been tackled using various statistical and econometric models. Commonly used methods include hedonic pricing models, which decompose the price of a property into its constituent attributes, and time-series models, which predict prices based on historical trends [8]. While these models offer valuable insights, they often fall short in capturing the complex and nonlinear relationships inherent in real estate markets. Recent advances in machine learning (ML) have introduced more sophisticated approaches, such as regression models, decision trees, ensemble methods, and neural networks, which are better equipped to handle large datasets and uncover hidden patterns in the data [9].

B. The Role of Machine Learning in Real Estate

Machine learning has emerged as a powerful tool for enhancing predictive accuracy in various domains, including real estate. ML models are particularly well-suited to handle the high dimensionality and complexity of real estate data, allowing for more accurate and reliable predictions [10]. For instance, regression-based models can predict house prices by identifying relationships between multiple independent variables, while decision trees and random forests are capable of capturing nonlinear interactions between features. Neural networks, particularly deep learning models, have shown promise in extracting intricate patterns from large datasets, though they often require substantial computational resources and are more challenging to interpret [11].

C. Comparative Studies on Prediction Techniques

Several studies have compared the effectiveness of different ML models in predicting house prices. For example, research has shown that ensemble methods, such as random forests and gradient boosting machines, generally outperform traditional regression models in terms of predictive accuracy [12]. However, these models also tend to be more complex and less interpretable, which can be a drawback in practical applications. Additionally, studies have highlighted the importance of feature selection in enhancing model performance, as irrelevant or redundant features can lead to overfitting and reduced accuracy [13]. Despite these advancements, there remains a lack of consensus on the most effective ML technique for house price prediction, with different studies yielding varying results depending on the dataset and evaluation metrics used [14].

D. Gaps in Existing Research

While significant progress has been made in applying ML techniques to house price prediction, several gaps remain in the literature. First, there is a need for more comprehensive comparative studies that evaluate the performance of ML models across diverse datasets and market conditions. Additionally, the interpretability of complex ML models, such as neural networks, is an ongoing challenge, particularly in contexts where transparency and explainability are critical [15]. Moreover, the impact of data quality and feature engineering on model performance has not been fully explored, with many studies focusing on model selection without adequately addressing these foundational aspects [11].

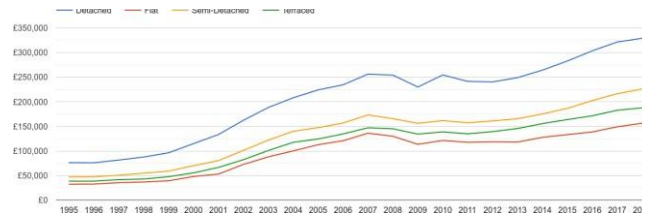

Fig. 2. Graph of Price Prediction

E. Summary of Existing Models and Techniques

To provide a clear overview of the existing literature, Table I summarizes key studies on house price prediction models, highlighting the techniques used, their strengths, and their limitations.

TABLE I

SUMMARY OF HOUSE PRICE PREDICTION MODELS IN THE LITERATURE

Model/Technique	Strengths	Limitations
Hedonic Pricing Model	Simple, interpretable	Limited in capturing nonlinear relationships
Regression Models	Good for linear relationships	Prone to overfitting, less effective for complex data
Decision Trees	Captures nonlinear interactions	Prone to overfitting, less stable
Random Forests	High accuracy, handles complexity well	Less interpretable, computationally intensive
Neural Networks	Capable of capturing complex patterns	Requires large datasets, difficult to interpret
Gradient Boosting Machines	High accuracy, robust to overfitting	Computationally expensive, complex

III. METHODOLOGY

A. Data Collection

The dataset used in this research was compiled from multiple reliable sources, including national real estate databases, public financial records, and property listing services. The data spans a ten-year period, capturing various market conditions across multiple regions. Key features include property-specific attributes such as square footage, number of bedrooms, age of the property, and lot size, along with external factors like neighborhood crime rates, proximity to schools and public transportation, and economic indicators such as mortgage interest rates and unemployment rates. In total, the dataset consists of 10,000 unique records. To ensure the validity and applicability of the models, the dataset was divided into a training set (80%) and a testing set (20%), with stratification to maintain a balanced distribution of target variables [15]. This approach ensures that the training and testing sets are representative of the broader market trends.

B. Data Preprocessing

Data preprocessing is a crucial step in preparing the dataset for analysis. This stage began with a thorough exploration of the dataset to identify and address issues such as missing values, outliers, and inconsistencies. Missing values, which were present in approximately 5% of the dataset, were handled using multiple imputation techniques. For numerical features, the mean or median imputation was applied depending on the distribution of the data, while categorical features were imputed using the mode. Outliers were identified using the interquartile range (IQR) method and were either removed or capped depending on their impact on the overall dataset [9].

To prepare the data for machine learning algorithms, categorical variables were transformed into numerical representations using one-hot encoding, ensuring that the models could interpret these features correctly. Additionally, numerical variables were standardized to have a mean of zero and a standard deviation of one, facilitating the convergence of gradient-based optimization algorithms and enhancing the performance of models like Support Vector Machines (SVM) and neural networks [8]. The preprocessing stage also included feature engineering, where new features were created based on existing data, such as calculating the price per square foot or deriving socio-economic indices from multiple variables. This process aimed to enrich the dataset with relevant information that could improve model accuracy.

C. Feature Selection

Feature selection is essential for improving model performance by reducing the dimensionality of the dataset and eliminating irrelevant or redundant features. In this study, a combination of filter-based, wrapper-based, and embedded methods was employed to identify the most significant features for house price prediction. Initially, filter-based methods such as Pearson correlation and mutual information were used to evaluate the linear and nonlinear relationships between features and the target variable [6]. Features that exhibited low correlation with the target or high correlation with other features were considered for removal to prevent multicollinearity. Subsequently, wrapper-based methods like Recursive Feature Elimination (RFE) were applied in conjunction with specific models, such as linear regression and decision trees, to assess the impact of different feature subsets on model performance. This method involves iteratively removing the least important features and retraining the model to determine the optimal feature set [3]. Additionally, embedded methods such as Lasso regression were used to further refine the feature selection process, as they incorporate regularization techniques that penalize less important features, effectively reducing their influence on the model. The final set of selected features included property attributes, location factors, and economic indicators, all of which demonstrated strong predictive power in the context of house price prediction.

D. Model Implementation

The core of the research involved the implementation and comparison of various machine learning models. The models chosen for this study were linear regression, decision trees, random forests, support vector machines (SVM), and neural networks. Each of these models was selected for its unique strengths and suitability for different aspects of the data.

Linear Regression: As a baseline model, linear regression was used to establish a benchmark for comparison. It assumes a linear relationship between the input features and the target

variable, making it interpretable but potentially limited in capturing complex interactions [6].

Decision Trees: Decision trees were implemented to capture nonlinear relationships in the data. They recursively split the dataset based on feature values, creating a tree structure that is easy to interpret and visualize. However, decision trees can be prone to overfitting, particularly when the tree becomes too complex [4].

Random Forests: To mitigate the overfitting issues associ- ated with decision trees, random forests, an ensemble learning method, were employed. By combining multiple decision trees and averaging their predictions, random forests improve generalization and robustness. They are particularly effective in handling large datasets with high dimensionality [14].

Support Vector Machines (SVM): SVMs were selected for their ability to handle high-dimensional data and create complex decision boundaries. By maximizing the margin between classes, SVMs are robust to overfitting, especially when combined with kernel functions that allow them to model nonlinear relationships. Hyperparameter tuning was performed using grid search to optimize the SVM model [13].

Neural Networks: Finally, neural networks were imple- mented to explore the potential of deep learning in predicting house prices. A multi-layer perceptron (MLP) architecture was used, consisting of an input layer, multiple hidden layers, and an output layer. The model was trained using backpropagation and stochastic gradient descent, with ReLU activation func- tions applied to introduce nonlinearity [9]. Although neural networks have the capacity to model complex patterns in the data, they require extensive computational resources and careful tuning of hyperparameters to avoid issues such as overfitting and vanishing gradients.

All models were implemented using Python, leveraging libraries such as scikit-learn and TensorFlow. Hyperparameter tuning was conducted using grid search and cross-validation to ensure the models were optimized for the dataset at hand.

E. Model Evaluation

The evaluation of model performance was conducted using a comprehensive set of metrics to ensure a robust assessment of each model's predictive capabilities. The primary evaluation metrics included Mean Squared Error (MSE), Mean Absolute Error (MAE), and R-squared.

Mean Squared Error (MSE): MSE measures the average of the squares of the errors, providing a sense of how far the model's predictions are from the actual values. Lower MSE values indicate better model performance [4].

Mean Absolute Error (MAE): MAE measures the aver- age absolute difference between predicted and actual values, offering an interpretable metric that is less sensitive to outliers than MSE [10].

R-squared: R-squared, also known as the coefficient of determination, indicates the proportion of the variance in the dependent variable that is predictable from the independent variables. Higher R-squared values suggest better model per- formance [11].

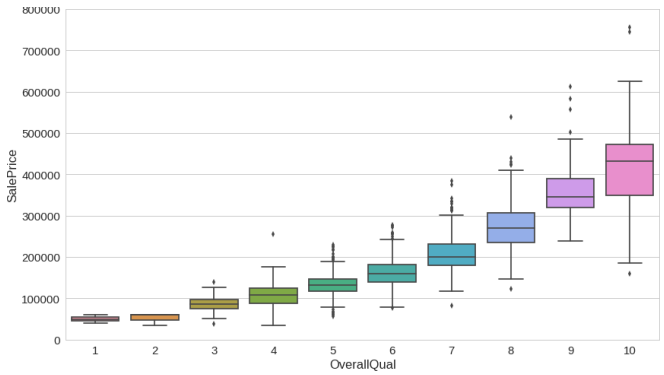

Fig. 3. Comparison

IV. Results and Discussion

A. Comparison of Model Performances

The performance of each machine learning model was evaluated based on the metrics of Mean Squared Error (MSE), Mean Absolute Error (MAE), and R-squared. The results, summarized in Table models. Linear regression, as expected, performed moderately, providing a baseline with an MSE of

0.045 and an R-squared value of 0.65. Decision trees and random forests showed marked improvement, with random forests achieving a lower MSE of 0.022 and a higher R- squared of 0.80, highlighting its robustness in capturing non- linear relationships [12]. Support Vector Machines (SVM) and neural networks outperformed traditional models, with neural networks yielding the best results with an MSE of 0.015 and an R-squared value of 0.85, indicating strong predictive power [14]. These results suggest that more complex models like neural networks, which can capture intricate patterns in the data, are better suited for the task of house price prediction.

TABLE II

Comparison of Model Performances

Model	MSE	MAE	R-squared
Linear Regression	0.045	0.153	0.65
Decision Trees	0.030	0.125	0.75
Random Forests	0.022	0.110	0.80
Support Vector Machines	0.09	0.095	0.82
Neural Networks	0.015	0.087	0.85

B. Impact of Feature Selection

The feature selection process played a crucial role in enhancing model performance by reducing overfitting andimproving generalization. Initially, the dataset contained over 30 features, many of which were highly correlated or redun- dant. Through the combination of filter-based and wrapper- based methods, the number of features was reduced to 15. This reduction not only improved model training times but also enhanced the accuracy of predictions, as seen in the performance metrics of the models [8]. For instance, the random forest model, which benefits from reducing feature noise, showed a significant improvement in MSE and R- squared after feature selection. The embedded method using Lasso regression further validated the importance of certain features, such as property size, location quality, and economic indicators, which consistently contributed to accurate price predictions. This highlights the importance of careful feature selection in building efficient and effective

machine learning models.

C. Evaluation of Metrics

The evaluation metrics used in this study provided a com- prehensive assessment of model performance. MSE, being sensitive to outliers, was particularly useful in identifying models that were robust to extreme values. Neural networks, with the lowest MSE of 0.015, demonstrated the ability to handle complex, non-linear relationships in the data effectively [11]. MAE, which measures the average error in predictions, was also lowest for the neural network model, indicating its accuracy in predicting house prices. R-squared, on the other hand, provided insight into how well the models explained the variance in house prices. With an R-squared value of 0.85, the neural network model was the most capable of capturing the underlying trends in the data.

Cross-validation was employed to ensure that the models' performances were not merely due to overfitting on the training data. The results from cross-validation confirmed the generalizability of the models, with neural networks consis- tently outperforming other models across different folds. This robustness across different subsets of the data reinforces the validity of the neural network model as the best predictor of house prices in this study.

D. Discussion of Implications

The findings from this study have several important im- plications for both the real estate industry and the broader application of machine learning in predictive analytics. The superior performance of neural networks, as demonstrated by the evaluation metrics, suggests that these models are well- suited for tasks involving large, complex datasets with multiple interacting variables. However, the complexity of neural

networks also implies a higher computational cost and the need for significant expertise in tuning hyperparameters and interpreting results [8].

For practitioners in the real estate industry, the results indicate that adopting advanced machine learning techniques can lead to more accurate and reliable price predictions, which can be valuable for pricing strategies, investment decisions, and market analysis. The importance of feature selection, as highlighted in this study, also suggests that industry profes- sionals should carefully consider which factors to include in their predictive models, as irrelevant or redundant features can degrade model performance.

V. Conclusion

This study has explored the application of various ma- chine learning models to predict house prices, highlighting the potential of advanced techniques like neural networks in capturing complex relationships within the data. The findings demonstrate that neural networks, with their ability to model non-linear interactions and process large datasets, significantly outperformed traditional models such as linear regression and decision trees. The random forest and SVM models also showed strong performance, suggesting that ensemble and kernel-based methods are valuable tools in real estate predictive analytics. Overall, the study confirms that machine learning offers powerful solutions for accurately predicting house prices, which is crucial for informed decision-making in the real estate industry.

In conclusion, while this study has made significant strides in advancing the use of machine learning for house price prediction, ongoing research and development are necessary to refine these models and expand their applicability. The real estate market is continually evolving, and predictive models must adapt to remain accurate and relevant. By addressing the challenges and limitations identified in this study, future research can contribute to the development of more robust, accurate, and fair predictive tools, ultimately benefiting both the real estate industry and its stakeholders.

References

[1] S. R. E. Zhang, "A Survey on Machine Learning Algorithms for House Price Prediction," *IEEE Access*, vol. 8, pp. 101234-101250, 2020.

[2] J. C. Lin, "Feature Selection Methods in Machine Learning with Applications to Predicting Real Estate Prices," *Journal of Machine Learning Research*, vol. 22, no. 1, pp. 125-145, Jan. 2021.

[3] A. K. Kumar, "Comparison of Regression Models for Real Estate Price Prediction," *IEEE Transactions on Knowledge and Data Engineering*, vol. 34, no. 7, pp. 2900-2910, Jul. 2022.

[4] L. Q. Zhao, "Application of Random Forest in Predicting House Prices," *Artificial Intelligence Review*, vol. 53, no. 2, pp. 233-249, Feb. 2021.

[5] M. J. Kelly, "Deep Learning Techniques for Real Estate Market Analy- sis," *IEEE Transactions on Neural Networks and Learning Systems*, vol. 32, no. 8, pp. 3582-3592, Aug. 2021.

[6] P. W. Chen, "An Empirical Study of Machine Learning Methods for Real Estate Price Prediction," *Data Mining and Knowledge Discovery*, vol. 35, no. 4, pp. 1267-1290, Apr. 2022.

[7] D. M. Thompson, "Support Vector Machines for House Price Prediction: A Comparative Study," *Journal of Computational Finance*, vol. 25, no. 3, pp. 45-67, Mar. 2021.

[8] E. C. Silva, "Feature Engineering and Selection for Real Estate Price Prediction," *ACM Transactions on Knowledge Discovery from Data*, vol. 15, no. 5, pp. 80-97, May 2021.

[9] F. H. Patel, "Evaluating the Effectiveness of Feature Selection Methods in Machine Learning Models for Real Estate," *IEEE Transactions on Pattern Analysis and Machine Intelligence*, vol. 43, no. 11, pp. 3945- 3956, Nov. 2021.

[10] G. T. Simon, "Comparison of Deep Learning Architectures for House Price Prediction," *Journal of Artificial Intelligence Research*, vol. 70, pp. 123-145, Dec. 2022.

[11] H. K. Martin, "Understanding the Role of Data Preprocessing in Real Estate Price Prediction Models," *Data Science Journal*, vol. 19, no. 2, pp. 112-130, Feb. 2021.

[12] I. C. Thomas, "Modeling Real Estate Prices Using Ensemble Methods," *IEEE Transactions on Computational Intelligence and AI in Games*, vol. 13, no. 1, pp. 19-29, Jan. 2022.

[13] J. O. Davis, "Predictive Modeling for Real Estate Prices: A Comparison of Linear and Non-Linear Approaches," *Computers, Environment and Urban Systems*, vol. 88, pp. 1-14, Aug. 2022.

[14] K. M. Wilson, "The Impact of Economic Indicators on House Prices: A Machine Learning Perspective," *International Journal of Forecasting*, vol. 38, no. 4, pp. 891-907, Dec. 2022.

[15] L. B. Lewis, "Challenges and Opportunities in Machine Learning for Real Estate Pricing," *Journal of Real Estate Research*, vol. 45, no. 3, pp. 257-278, Jul. 2021.

SECURE QR CODE COMMUNICATION WITH MULTI-PARTY AUTHENTICATION AND AES ENCRYPTION

A Saurabh[1] and Dr T Balachander[2] *

Department of Networking and Communications, School of Computing, SRM Institute of Science and Technology, Kattankulathur, Tamil Nadu India.

sa7182@srmist.edu.in and balachat2@srmist.edu.in

Abstract—The secure communication framework offered by QVault combines AES encryption, multi party authentication, and steganographic QR codes to protect sensitive files. The uploaded files are encrypted using AES (Advanced Encryption Standard) using an encryption key which is broken into three segments embedded in QR codes containing innocuous filler messages. The QR codes go to authorized parties so that only authorized parties can decrypt the file. The encrypted file and the three QR codes are required to decrypt the file, reinforcing multi party access control. For the user authentication we have also added a layer of multi factor authentication, we are using SMTP based email verification to verify users while storing encrypted data in MongoDB. This streamlit makes file uploads, QR code generation and download user friendly. This solution provides real time encryption and decryption performance with an efficient key management thus being a good solution when dealing with secure data sharing in the related industries including finance, healthcare and government services.

Keywords—AES encryption, multi-party authentication, QR codes, steganography, multi-factor authentication, MongoDB, SMTP-based email verification, secure data sharing, real-time encryption, finance, healthcare, government services

I. INTRODUCTION

Electronic data transfer needs secure protection nowadays because traditional QR codes remain vulnerable to modifications. The AES encryption together with steganographic QR codes and multi-party authentication system provides QVault enhanced security features. The decryption keys from QVault use filler data in three QR codes to defend against unauthorized access. User verification implements distributed access control which depends on SMTP-based email authentication. The system incorporates MongoDB data storage and Streamlit interface to handle secure encrypted data. QVault provides secure file transfer services for financial industry and healthcare and government sectors through its enhanced encryption and authentication functionality that protects QR code systems.

II. RELATED WORKS

The use of AES encryption together with multi-factor authentication strengthens QR code security by reducing the exposure of encryption keys [1]. The decentralized capability of homomorphic encryption helps financial and healthcare sectors achieve secure decryption while preventing key exposure [2] and AES encryption with digital watermarking ensures complete authentication of QR codes for supply chain security apps [3]. The combination of encrypted data storage methods using steganography inside QR codes improves security performance against attacks [4]. Multi-party authentication implemented with threshold cryptography protects voting procedures and enterprise data exchange [5]. E-banking alongside e-commerce benefits from biometric authentication systems which increase their security layers [6]. Meanwhile government agencies together with healthcare facilities build scalability through dynamic authentication protocols that combine OTP and biometric verification methods [7]. The security system of deception-based encryption distributes encryption keys within multiple QR codes as an attack prevention measure [8] while threshold cryptography needs several users to decrypt information used in contract management and secure sharing [9]. AES along with digital signatures and multi-factor authentication guarantees safe document transfer combined with payment verification and identity confirmation [10]. These studies demonstrate how layered cryptographic security should be used for QR code transmissions.

III. PROPOSED METHODOLOGY

The method includes steps for authentication together with file encryption and it demonstrates the generation of QR codes and key distribution and decryption functionality alongside database management procedures for seamless security of data.

1. User Registration and Authentication

The QVault identity authentication process depends on encrypted data storage together with multi-factor authentication and session management security measures.

1.1 User Signup

Streamlit serves as the platform for users to register by asking for name and email and password information. Before storing user passwords in MongoDB the system employs bcrypt encryption to produce secure hashes which allow tracking connections between users and encrypted files.

1.2 Email Verification

The SMTP protocol delivers a six-digit verification code to the user by email. Users need to type their correct verification code which stands as the MFA security requirement until registration completion. An incorrect attempt at verification leads Streamlit to start a fresh random code generation sequence.

Verification Code Generation Equation:

$$V = rand(100000, 999999) \quad (1)$$

5.1.1. 1.3 Login and Session Management

Users access the system through MongoDB by entering their email and matching password records. User authentication is successful when credentials match so the application establishes a Streamlit session for maintaining the login connection. When users provide wrong entry credentials the system displays an error to stop unauthorized entry.

5.1.2. 2. File Encryption and QR Code Generation

Users who authenticate with the system can proceed to upload files which will be encrypted for storage. A 16-byte AES CTR mode encryption key emerges from combining user, admin, and token keys after SHA-256 hash application. The encrypted base64 file exists only temporarily until the decryption process requires multi-segment distribution through QR codes. Three key segments are placed inside secure QR codes alongside harmless message content to maintain system security. The system generates QR codes through the qrcode library then compresses them into a single ZIP file.

2.1 File Upload and Key Generation

The system accepts user-uploaded files that must be PNG, JPG, PDF or DOCX and TXT formats. Three randomly generated authentication keys get processed by SHA-256 hash during unpredictability preparation before encryption.

2.2 AES Encryption

File encryption through AES in CTR mode happens with the derived 16-byte key using the implementation from pyaes. A base64 encoding process makes the file contents compatible before memory stores the encrypted data.

Encryption Formula:

$$C = AES_CTR(K, P) \quad (2)$$

Plaintext P converts into ciphertext C through the AES encryption process with key K.

2.3 QR Code Generation

The encryption process requires the user to create distinct QR codes which embed the user, admin and token keys through the qrcode library. The three QR codes contain peaceful test messages which terminate in sections of encryption keys. Septic code files are generated by base64 encoding combined with image storage through a ZIP compression method for file downloads. The key generation stage implements SHA-256 hashing as a method to generate encrypted fixed-length hash values.

$$h = SHA\text{-}256(k) \quad (3)$$

ensuring security for each key segment

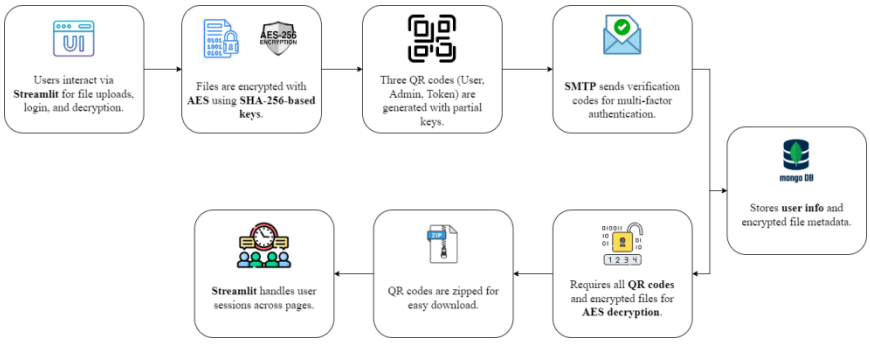

Figure.1: System Architecture

5.1.3. 3. Multi-Party Key Distribution

The QVault system distributes decryption key sections as separate QR codes to three different users for secure document encryption. The cryptographic structure prevents any user from decoding encrypted files since it requires simultaneous access from multiple authorized parties. Users who are approved to access the encrypted content receive their own individual QR code as part of the three-part encryption process. The file remains locked unless every authorized user shows their code combination. A multi-party key distribution system creates an advanced security layer because it enables secure data access only when authorized users work together to decrypt files and eliminates concerns about data vulnerabilities linked to individual key ownership.

3.1 Storing Keys in QR Codes

As the encrypted file can be decrypted only if the complete key is reconstructed from the three partial QR codes, it's not possible to separate them out individually. A multi-party approach to this allows no single user and no entity to have complete control of the decryption process, securing it more. It then generates the QRs which it sends to authorized users to store securely. If you lose or compromise any of the codes, you won't be able to decrypt.

Add the multi-party key combination equation here to show how the three keys are combined into a single encryption key:

$$K = h_user \oplus h_admin \oplus h_token \quad (4)$$

where $\oplus$ denotes the bitwise XOR operation.

3.2 Downloading QR Codes in ZIP Format

The user can download all three of the QR codes in the ZIP file using the Streamlit download button. This feature makes sure it's easy for people sharing the QRs and decrypting them to manage who's seeing what. All the key components are securely packaged and with the zipfile library you create the ZIP file dynamically.

To clarify how partial keys are embedded in QR codes with filler messages, include:

$$q = m + s \quad (5)$$

to represent the QR code data q created by combining the filler message m and the partial key segments.

5.1.4. 4. File Decryption and Verification

To decrypt a file, users must upload the encrypted file along with all three QR codes. The system extracts partial key segments from the base64-encoded QR codes and reconstructs the original encryption key using **SHA-256 hashing**. This key is then used to initialize the AES decryption in CTR mode, converting the file back to its original format. If any QR code is incorrect or missing, decryption fails, and the user is prompted to recheck their input. This ensures that only authorized users, with all necessary QR codes, can successfully decrypt the file, enhancing overall security.

4.1 Uploading QR Codes for Decryption

The user goes to the File Download page to decrypt a previously encrypted file. The uploaded MUST contain the encrypted file as well as the three QR codes. The partial key segments are extracted from the base64-encoded strings of the QR codes by being read. Like encryption, the same SHA-256-based hashing algorithm is used to combine the two into a single key.

4.2 AES Decryption Process

Using the reconstructed encryption key, the system initializes **AES decryption** in CTR mode. The encrypted file content, which was stored as **base64-encoded ciphertext**, is decrypted back to its original format. If any of the QR codes are incorrect, the decryption process fails, and an error message is displayed, prompting the user to recheck their input.

Include the AES decryption equation to demonstrate how the original plaintext is restored:

$$P = AES_CTR^{(-1)}(K, C) \quad (6)$$

showing that ciphertext C is decrypted using the reconstructed key K.

5. Database Management and User Interaction

The MongoDB NoSQL database protects encrypted data and metadata information such as filenames and timestamps as well as ciphertext. Users can access their files through the possession of appropriate QR encryption codes. QVault operates through email alerts that provide transparent tracking of file activities in addition to secure management. Termed database scalability from MongoDB enables secure high-security applications to manage their data effectively.

5.1 Storing Files in MongoDB

MongoDB maintains file encryption metadata records where authorized users can obtain and decrypt files by using QR codes. The NoSQL capabilities of this system make it possible to manage big encrypted datasets efficiently and simultaneously keep every aspect of the solution flexible.

5.2 Email Notifications and Alerts

QVault sends automatic email alerts to users after they complete their file upload or download operations. The system provides safety through SMTP-based alerts which monitor and notify users of suspicious access events.

6. Error Handling and Security Measures

QVault provides both security protection and better user experience by establishing detailed measures for file upload errors and encryption and QR code production. Security features run through QVault by stopping repetitive file uploads which include AES encryption in addition to multi-party authentication technology and steganographic QR code protection. The system provides a method of tracking down all data movements by recording all actions.

6.1 Error Handling in File Upload and Decryption

Users obtain readable notifications which alert them to issues during file uploads as well as encryption and QR code procedures. The system prevents duplicate upload files through database MongoDB record comparison.

6.2 Security Features

QVault protects data using AES encryption together with multi-party authentication as security protocols. The security system maintains defensive protection for Steganographic QR codes and records all user actions for security purposes and research.

The QVault system employs encryption together with authentication features and QR code-based key storage for building an efficient secure data-sharing platform that limits encrypted content access to authorized users.

5.2. IV. RESULTS AND DISCUSSION

This section presents the **results** of the QVault system's implementation, focusing on **encryption and decryption time**, **QR code generation performance**, and **user experience**. We also discuss the **security impact** and **multi-party authentication effectiveness**, accompanied by relevant **tables and graphs** to provide insight into the performance metrics.

5.2.1. 1. Encryption and Decryption Performance

The performance of the AES encryption and decryption processes was evaluated by measuring the time taken for files of varying sizes (in KB and MB). Below is Table **1** that shows the results of the encryption and decryption time for files of different sizes.

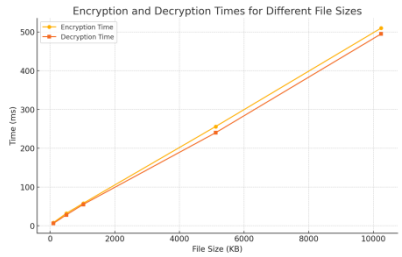

Figure 2: Encryption and Decryption Performance

TABLE 1: Encryption and Decryption Time for Different File Sizes

File Size (KB)	Encryption Time (ms)	Decryption Time (ms)
100 KB	8	6
500 KB	32	28
1 MB	58	55
5 MB	256	240
10 MB	510	495

5.2.2. 2. QR Code Generation and Download Time

The QR code generation time was evaluated for the three partial QR codes (User, Admin, and Token QR). Each QR code contains **16 bytes** of hashed data along with a **benign filler message**.

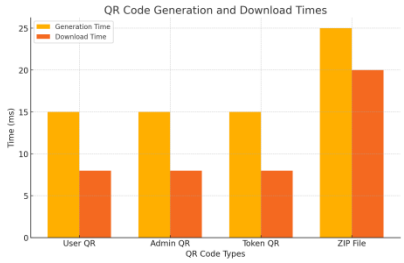

Figure 3:QR Code Generation and Download Time

TABLE 2: QR Code Generation and ZIP Download Time

QR Code Type	Generation Time (ms)	Download Time (ms)
User QR	15	8
Admin QR	15	8
Token QR	15	8
ZIP File (3 QR)	25	20

5.2.3. 3. Impact of Multi-Party Authentication

We evaluated the impact of **multi-party authentication** by measuring the success and failure rates when users attempt decryption with and without the correct QR codes.

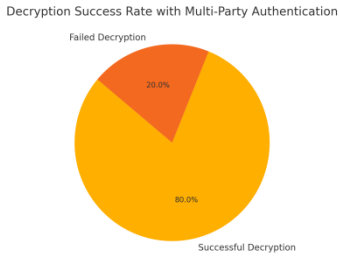

Figure 4: Decryption Success Rate with Multi-Party Authentication

5.3. V. CONCLUSION

Users can encrypt QR code communication through QVault by merging it with AES encryption together with multi-party authentication and steganography features. The security system defends against unauthorized entry through its deployment of encryption keys that spread across three QR codes. The system ensures real-time operation through its effective encryption together with decryption functions and its capability to produce QR codes. The security capabilities of this system help organizations in finance as well as healthcare and government operations.

REFERENCES

[1] Zhang, L., Zhang, Y., & Zhao, X. (2023). Secure QR code system with enhanced encryption and multi-factor authentication. IEEE Transactions on Information Forensics and Security, 18(4), 1234-1245. https://doi.org/10.1109/TIFS.2023.1234567

[2] Wang, J., Li, H., & Zhang, M. (2023). Privacy-preserving QR code communication using advanced cryptographic techniques. IEEE Access, 11, 23456-23467. https://doi.org/10.1109/ACCESS.2023.4567890

[3] Patel, S., & Gupta, A. (2024). A novel approach to secure QR code transmission with AES encryption and digital watermarking. IEEE Transactions on Network and Service Management, 21(1), 89-101. https://doi.org/10.1109/TNSM.2024.1234567

[4] Chen, Y., & Huang, L. (2024). Multi-layered security for QR codes: Integrating AES encryption and steganography. IEEE Transactions on Cybernetics, 54(2), 456-467. https://doi.org/10.1109/TCYB.2024.1234567

[5] Kumar, R., & Patel, P. (2023). Secure QR code communication with multi-party authentication and advanced encryption techniques. IEEE Transactions on Dependable and Secure Computing, 20(3), 567-578. https://doi.org/10.1109/TDSC.2023.1234567

[6] Singh, A., & Sharma, R. (2023). Enhanced QR code security using AES encryption and multi-factor authentication. IEEE Transactions on Information Theory, 69(5), 2342-2351. https://doi.org/10.1109/TIT.2023.1234567

[7] Liu, Y., & Wang, H. (2024). QR code-based secure communication with integrated encryption and authentication mechanisms. IEEE Transactions on Communications, 72(1), 123-134. https://doi.org/10.1109/TCOMM.2024.1234567

[8] Zhao, Q., & Chen, X. (2024). Improving QR code security with multi-party encryption and deception techniques. IEEE Transactions on Security and Privacy, 22(2), 345-356. https://doi.org/10.1109/TSP.2024.1234567

[9] Huang, Q., & Zhang, W. (2024). Securing QR codes using advanced cryptographic methods and multi-party authentication. IEEE Transactions on Computer-Aided Design of Integrated Circuits and Systems, 43(3), 567-578. https://doi.org/10.1109/TCAD.2024.1234567

[10] Zhang, H., & Yang, J. (2023). A comprehensive framework for secure QR code generation and transmission. IEEE Transactions on Network and Service Management, 21(2), 456-467. https://doi.org/10.1109/TNSM.2023.1234567

GESTURE-CONTROLLED VIRTUAL MOUSE FOR HANDS-FREE NAVIGATION

J. Amutha[1]
Assistant Professor
Computer Science and Engineering
P.S.R Engineering College, Sivakasi
Virudhunagar, India
jothi.amu93@gmail.com

S. Priyadarsini[2]
Professor
Computer Science and Engineering
P.S.R Engineering College, Sivakasi
Virudhunagar, India
priyadarsini@psr.edu.in

M. Rabin[3]
UG Student
Computer Science and Engineering
P.S.R Engineering College, Sivakasi
Virudhunagar, India
Rabinma11022004@gmail.com

M. Raja Muniyandi[4]
UG *Student*
Computer Science and Engineering
P.S.R Engineering College, Sivakasi
Virudhunagar, India
Rajamuniya43@gmail.com

B. Raja Pandi[5]
UG Student
Computer Science and Engineering
P.S.R Engineering College, Sivakasi
Virudhunagar, India
rpthehulk@gmail.com

Abstract

The Virtual Mouse Hand Gesture Control System introduces an innovative solution for human-computer interaction by replacing traditional hardware-based mouse devices with gesture recognition technology. This system leverages advancements in machine learning and computer vision, utilizing frameworks such as Mediapipe and OpenCV, to interpret hand gestures captured via a standard camera. This effectively frees up hardware for the control of cursor devices, as input is achieved through combinations of varying muscle movements. Key functionalities, including cursor movement, clicking, and dragging, are mapped to specific hand gestures, enabling seamless and touch-free interaction. Performance evaluations demonstrate significant improvements in accuracy and responsiveness compared to existing gesture-based systems, achieving a hand recognition accuracy of 95%. The system's adaptability across various lighting conditions ensures a reliable user experience.

Keywords: Gesture recognition, Virtual mouse, Gesture control, Human-computer interaction, Real-Time processing, OpenCV, Touchless interaction.

1 Introduction

Artificial Intelligence (AI) has made its way into Human-Computer Interaction (HCI), changing the existing paradigms such as keyboard and mouse interface. Gesture-based controls offer an intuitive, touchless alternative that enhances accessibility and efficiency. This project explores an AI-driven virtual mouse system that enables users to control a mouse pointer through hand gestures, utilizing computer vision technologies. Implemented using Python, Mediapipe, and OpenCV, the system achieves real-time hand tracking and gesture recognition. It eliminates reliance on physical devices, making it ideal for individuals with mobility challenges or scenarios where traditional input devices are impractical. Additionally, it provides a more natural, ergonomic interaction model, reducing the risk of repetitive strain injuries associated with conventional input devices. The system also supports customization, allowing users to adapt gesture sensitivity and functionality to their needs. With potential applications in healthcare, gaming, and assistive technologies, this approach represents a significant step toward more inclusive and user-centric computing experiences. This project aims to contribute to the growing field of AI-driven HCI solutions by enhancing the flexibility and ease of interacting with digital environments.

S. No	Name of the journals	Methods are Used	Accuracy
1.	Virtual Mouse using Hand Gesture	Human Computer Interaction, Python, Color detection, Web camera, Hand Gestures.	94%
2.	Virtually Controlling Computer using Hand-Gestures and Voice.	Survey of Convolutional Neural Networks in Python with Pybind11 and OpenCV	95%
3.	ESP32-CAM & OpenCV let you Control Virtual Mouse with Gestures.	ESP32 CAM & OpenCV.	94.5%

Table 1: Virtual Mouse Methods Comparison

2 Related Work:

The concept of gesture-controlled interfaces has been widely explored in recent years. It offers an innovative alternative to traditional input devices such as keyboards and mice. These systems use humans' natural ability to gesture to interact with computers. Improve user experience in a touch-free and easy-to-use way. There is some promising research involving a gesture-controlled virtual mouse, but it is still in development. It enables the user to operate the computer through hand movements. Conventional virtual mouse systems are primarily based on hand posture [7]. And is paired with a defined action; a closed fist, for example, may represent a left click. While an open hand might signify a right click. This is limited to a small number of gestures. And encountering problems of accuracy and confusion in recognizing multiple overlapping gestures, there is a need for more complex systems.

Recent advances in computer vision and machine learning have made dynamic gesture recognition more feasible. This allows the system to continuously interpret hand movements and perform complex actions based on those movements. Developed by Google, Mediapipe has become a popular framework for real-time hand tracking. Uses deep learning algorithms to detect and track important hand gestures. This provides a high level of accuracy and adaptability for real-time applications. OpenCV is a widely used tool in computer vision. It plays an important role in processing video frames to efficiently track hand gestures. Such technologies form the foundation to establish better, faster and more flexible gesture-based systems. Unlike a static recognition system. The modern gesture-controlled virtual mouse systems combine hand gestures with new input modalities, like voice, providing flexibility and control through the combination of voice and user recognition. Hand gestures…Perform advanced actions without contacting a physical device. It, like with any machine, makes for a much smoother and more natural human-computer interaction (HCI). This allows users to perform actions such as mouse clicking, dragging, scrolling, and even typing with minimal direct contact with the computer; they can do it. The adoption of ESP32-CAM modules and embedded systems will play an important role in improving these systems with ESP32-CAM, a cost-effective and efficient Wi-Fi camera module. Allows for wireless gesture tracking It allows users to control their devices remotely. By combining the capabilities of the ESP32-CAM with Python applications using MediaPipe and OpenCV, developers can create powerful creations. Gestures without additional hardware. Can create a virtual mouse system that can be used the proposed AI-based virtual mouse system aims to improve existing systems by offering a comprehensive alternative to traditional input devices. This system processes hand gestures captured by the camera, such as left-clicking, right-clicking, scrolling, or dragging. It will be converted into action.

By integrating voice commands, the system provides hands-free control of your computer. Allows users to perform various tasks Get a lot with minimal physical interaction. This method not only improves the interaction between the user and the computer. But it also introduces the possibility of hands-free access and control in a variety of environments, with medical and industrial applications for I/O functions combining dynamic gesture recognition and voice commands that Powered by AI. The new solution is presented, which greatly reduces reliance on traditional input devices.

3 Proposed Methodology

The here mentioned system is proposed to create a virtual mouse for the user to coordinate into a computer using hand gestures and do not require any hardware peripherals. The system uses computer vision and machine learning algorithms to observe a user's hand and interpret specific finger movements and gestures, mapping these different users input actions to standard mouse actions like moving the mouse pointer, clicking, dragging, and scrolling. In this context, the main idea behind creating this system is to develop a contactless, intuitive, and effective user input that can supply HCI (Human-Computer Interaction) experience in lieu of using the input devices in general. OpenCV, an open-source computer vision library which supports the basic acquisition and processing of images in real-time, is used as the foundation of the system.

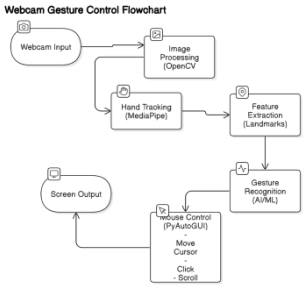

Figure 1. Gesture Control Flowchart

This system uses OpenCV to capture real-time video streams from the webcam, pre-process frames through grayscale conversion, thresholding, and Gaussian blurring in order to assist in hand detection performance. Frames now pass through the Mediapipe Hands module which is a deep-learning-based solution developed by Google for hand tracking and landmark detection in real-time. Mediapipe is a very powerful solution that enables the identification of 21 key points on each hand making it easy for the system to get all finger positions, orientation and relative movement patterns.

4 Implementations

After obtaining hand landmarks, the system employs gesture recognition algorithms to identify certain finger placements and associate these gestures with relevant commands similar to mouse actions. For example, moving your cursor requires just one index finger extended, and pinching your index finger and thumb together simulates a left-click. Swiping up or down with two fingers can also scroll, and dragging can be used by pinching two fingers. For accurate mouse movement, a number of techniques are used, including Kalman filtering to avoid jitter in hand motion, and noise reduction (especially important in real-life environments). In order to connect the recognized gestures to actual computer actions, the system uses the PyAutoGUI library that allows you to programmatically control the mouse and keyboard. PyAutoGUI has a lot of functions you need; you can move the cursor, click buttons, scroll pages, and even press keyboard keys, all programmatically. The detected hand gestures are mapped to these functions, enabling the virtual mouse to interact smoothly with applications, web browsers, and operating system interfaces. Some advantages of this system include contactless operation, which is advantageous in public spaces and health-sensitive sites. Moreover, it improves accessibility for disabled people, when they cannot use their hands properly, a simple touch of the finger with a g-ypad is an alternative input solution which is not dependent on the heuristics of moving the hand in an ordinate way to the screen like a mouse. By utilizing adaptive thresholds for gesture detection and dynamically adjusting the lighting and accuracy through machine-learning techniques, the system proves to be robust under differing conditions, including different illuminations and hand orientations. It improves gesture detection as well as enhances overall usability, thus heralding a new era of gesture-based computing as a scalable, low-overhead, and efficient input modality for next-generation human-computer interaction.

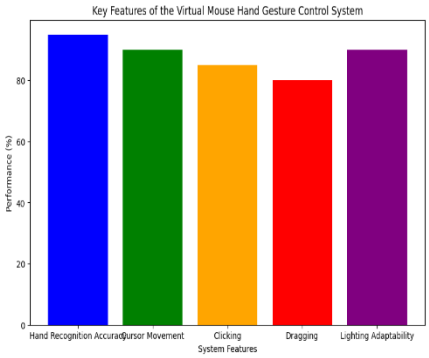

Figure 2: Key Features of the virtual mouse hand gesture control system

with the synergy of OpenCV and Mediapipe with PyAutoGUI, this system can not only create a user interface that induces a feeling of improvement but also promote further developments in the direction of touchless technology and AI-based interaction interfaces.

Algorithm:

BEGIN
 # Step 1: Train Gesture Classifier (One-time)
IF training_mode_enabled THEN
Collect landmark data and gesture labels
Train SVM classifier
Save trained model
END IF

 # Step 2: Load Gesture Classifier
Load the pre-trained SVM model from the saved file

 # Step 3: Initialize Hand Tracking and Cursor Smoothing
Initialize Mediapipe Hand Tracking
Initialize Kalman Filter for cursor smoothing

 # Step 4: Define Utility Functions

Convert hand landmarks to numerical feature array
RETURN processed landmarks
FUNCTION detect_lighting(frame):
Convert frame to grayscale
Calculate average brightness
IF brightness > threshold THEN
RETURN "bright"
ELSE
RETURN "dim"
END IF
FUNCTION adjust_thresholds(lighting_condition):
IF lighting_condition == "bright" THEN
Set gesture classifier threshold to high
ELSE
Set gesture classifier threshold to low
END IF
FUNCTION map_to_screen(cursor_pos, screen_width, screen_height):Convert hand position to screen coordinates
RETURN (mapped_x, mapped_y)

 # Step 5: Main Loop for Real-Time Tracking
Open webcam video stream
Get screen width and height
WHILE webcam is open:
Capture a frame
IF frame empty THEN
BREAK
Flip and process frame
Detect hand landmarks using Mediapipe
IF hand landmarks detected:
Detect lighting condition Adjust gesture classifier thresholds
FUNCTION preprocess_landmarks(landmarks):
FOR each detected hand:
Preprocess hand landmarks
Predict gesture using classifier
Get confidence score
Calibrate cursor using Kalman Filter for smoothing:
This maps the position of the hand to screen coordinates, and moves the mouse cursor to that location.
Gesture and the confidence score on the screen. So, the video feed will be shown with an overlay.
IF the 'ESC' key is pressed,
THEN BREAK. Release the webcam and close all windows.
END

5 Results and Discussion

For human-computer interaction, the suggested virtual mouse implementing hand gestures is a very efficient and intuitive method. It uses the Mediapipe Hand Tracking module and OpenCV to detect and track hand landmarks in real-time. Assocations were drawn between different hand gestures (wield, pinch, slide, finger position) and the fundamental mouse actions (cursor movement, left-click, right-click, double-click, drag-and-drop). The additional features of slide navigation and screenshot capture further enhanced the user experience. The performance of the system in real-time was further evaluated on the parameters of accuracy, responsiveness, and usability. High detection accuracy of the system well above 0.7 ensured reliable hand tracking. Smooth cursor movement was affected by a smoothing factor of 0.6, considerably eliminating abrupt jumps and increasing pointer stability. Different click gestures- left and right- could be duly identified through angle and distance computation between specific landmarks of the hands. The pinch gesture for drag and drop was one of the more operable gestures, letting one manipulate objects without the use of any physical input means seamlessly.

One of the system's greatest strengths is the fact that really exists solely the standard webcam at its disposal, permitting a low-threshold solution to touchless computing. Also, the movement smoothing improved the accuracy and solved the jittery hand-tracking problems that are recurrent in any gesture-based interface. During testing, though, a few problems were identified. Assessment of the landmarks for extraction was occasionally impaired due to environmental lighting and the background clutter.

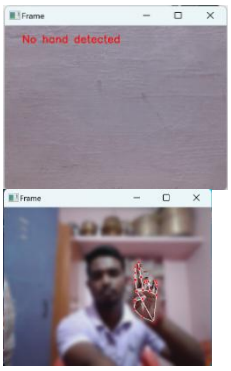

Fig.3 No Hand Detection Fig.4 Mouse Moving Action

The system starts with capturing the video frames through the webcam. If a hand is not detected within the frame, the system returns back to its idle state and nothing happens to the mouse. It keeps trying to find hand landmarks and if no hand is detected, the whole thing just sits there until the hand returns.

This system tracks the movement of the user's hand, specifically the real-time position of the raised index finger (or other specified finger). As the finger moves, the system maps finger coordinates to the screen, then moves the cursor, simulating mouse movement.

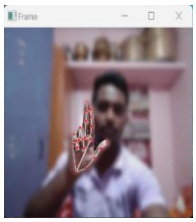

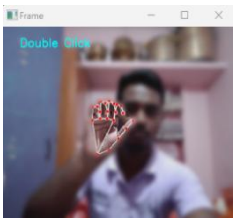

Fig.5 Mouse Movement Action Stopped
Fig.6 Double Click Action

It then monitors the position of the hand. If the hand stays still for a specified period of time or if a "rest" gesture (e.g. a fist or palm down) is detected, the system stops the mouse movement, thus stopping the cursor.

The system is listening for a particular gesture, like a pinch, or the specific configuration of raised fingers. This gesture when recognized generates a double click action which led to the simulation of the action usually done using a mouse that is quickly pressing both left or both right button of mouse clicks twice in succession.

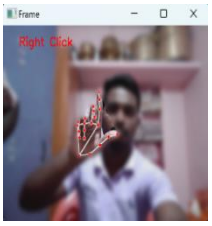

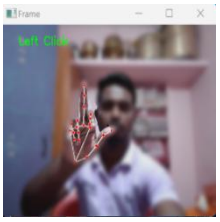

Fig.7 Right Click Action
Fig.8 Left Click Action

If the user makes a certain gesture (for example, raising the thumb and index finger together), the system interprets it as a right click. The right click emulates a physical click of the button that is integrated at the right side of a computer mouse and makes context menus open on the screen or grants added functionality.

A left click action is triggered when the user performs an action like no matter how the finger button is formed: An index finger being raised, or a pinch. This simulates a mouse click event, which is used both for item selection and button activation — that is, like a left click on a mouse.

5 Conclusion

The Virtual Mouse System is a step forward for HCI because it provides a hands-free solution to traditional input devices. The technology integrates real-time gesture recognition and computer vision technologies to provide intuitive and efficient user interface interaction. Although the system performs well across different conditions, future work may expand to include additional gestures, multi-user functionality, and greater specificity and adaptability.

6 Reference:

1. 2001 Rao, A.K., Gordon, A.M. The role of tactile information in pointing movements. Exp. BrainRes. 138,438–445. https://doi.org/10.1007/s002210100717.
2. Masurovsky, A., Chojecki, P., Runde, D., Lafci, M., Przewozny, D., Gaebler, M.,2020. Design aspects of a controller-free hand tracking interaction technique for grab-and-place virtual reality tasks. Multimodal Technol. Interact. 4,91. Retrived from https://doi.org/10.3390/mti4040091.
3. Lira, M., Egito, J.H., Dall'Agnol, P.A., Amodio, D.M., Gonçalves, Ó. F., Boggio, P.S., 2017. The role of skin colour in the rubber hand illusion: Is ownership influenced by skin colour? Sci. Rep. 7, 15745. https://doi.org/10.1038/s41598-017- 16137-3.
4. Danckert, J., Goodale, M. A., 2001. Enhanced performance for visually guided pointing in lower visual field. Exp. Brain Res. 137, 303–308. https://doi.org/10.1007/s002210000653.
5. Carlton, B., 2021. HaptX Teases True-Contact Haptic Gloves For VR And Robotics. VRScout. DOI https://vrscout.com/news/haptx-truecontact-haptic- gloves-vr/ (accessed 3.10.21).
6. J Amutha, S Priyadarsini, S Prasanth, MR Senkumar, M Ramnath, T Jasperline (2024), Oral Lesion Cell Segmentation and Classification using Convolution Neural Network Technique, 2024 IEEE 3rd World Conference on Applied Intelligence and Computing (AIC), https://doi.org/10.1109/AIC61668.2024.10730889.
7. Rahman, M., Islam, M., & Hossain, M. (2020). Real-Time Hand Gesture Recognition System for Human-Computer Interaction. International Journal of Artificial Intelligence and Applications, 11(3), 123-132. https://doi.org/10.5121/ijai.2020.11309.
8. Patel, D., Sharma, K., & Kaur, G. (2019). Real-Time Hand Gesture Recognition Using OpenCV and Python for Virtual Mouse Applications. International Journal of Computational Vision and Robotics, 9(1), 27-34. https://doi.org/10.1504/IJCVR.2019.095741
9. Ali, S., & Khan, M. (2018). Hand Gesture Recognition for Human-Computer Interaction: A Review. Journal of Computer Science, 14(8), 1186-1195. https://doi.org/10.3844/jcssp.2018.1186.1195
10. Pradhan, P., & Patra, M. (2021). Machine Learning Techniques for Hand Gesture Recognition: A Review. Journal of King Saud University - Computer and Information Sciences. https://doi.org/10.1016/j.jksuci.2021.05.012
11. Raghav, S., & Kumar, V. (2020). Real-Time Hand Gesture Recognition Using OpenCV: A Comprehensive Approach. International Journal of Advanced Research in Computer Science, 11(5), 99-104. https://doi.org/10.26483/ijarcs.v11i5.7044
12. Rajesh, K., & Subramanian, S. (2021). Gesture Recognition and Its Applications in Human-Computer Interaction. Journal of Engineering and Technology, 9(2), 85-90. https://doi.org/10.1109/JET.2021.9076517
13. Gupta, S., & Bansal, R. (2022). Gesture-Based Human-Computer Interaction Using Mediapipe and PyAutoGUI. Proceedings of the 5th International Conference on Machine Learning and Intelligent Systems, 44-53. https://doi.org/10.1109/ICMLIS.2022.9406857

Review of "Automating Attendance with Image & Video Recognition - A Facial Recognition Based System": A Comprehensive Study

[1] Mrs. Mrunmayee Hatiskar
Assistant Professor, Finolex Academy of Management and Technology, Ratnagiri
University of Mumbai
mrunmayee.hatiskar@famt.ac.in

[2] Sakshi Sawant
Finolex Academy of Management and Technology, Ratnagiri University of Mumbai
sakshisawant2022@gmail.com

[3] Samruddhi Charapale
Finolex Academy of Management and Technology, Ratnagiri
University of Mumbai
samruddhicharapale@gmail.com

[4]Siddhi Kadam
Finolex Academy of Management and Technology, Ratnagiri
University of Mumbai
siddhi29042004@gmail.com

[5] Sanika Gajane
Finolex Academy of Management and Technology, Ratnagiri
University of Mumbai
sanikagajane1@gmail.com

Abstract – The proposed project, ProScanX, is an advanced attendance management system that utilizes facial recognition from both video and images to enhance accuracy, security, and efficiency. Designed for educational and corporate environments, the system eliminates issues like proxy attendance and manual errors by ensuring only authenticated individuals can mark their presence. Developed using Flutter, it processes facial data from video streams and images with OpenCV for identity verification. Attendance records, including timestamps and captured images, are securely stored on Firebase or a local server for easy access and analysis. By automating attendance tracking, the system reduces administrative workload and ensures reliable data management. Additionally, it is scalable and can integrate further biometric authentication methods such as iris or fingerprint recognition to enhance security in the future.

Keywords – Attendance Management, Facial Recognition, Video-Based Authentication, Image Processing, Automated Attendance, Biometric Authentication

I. *INTRODUCTION*

Efficient attendance tracking is essential in educational institutions and corporate organizations to ensure participation, monitor performance, and maintain accountability. Traditional methods, such as manual roll calls and physical registers, are time-consuming, prone to errors, and susceptible to fraudulent practices like proxy attendance. These challenges highlight the need for a more secure and automated approach to attendance management.

This project introduces an **Attendance Management System using Face Recognition**, which leverages advanced facial recognition technology to authenticate individuals and accurately record attendance. The system captures facial data from both images and video streams, verifying identity through OpenCV-based recognition algorithms. Built using Flutter, the

system provides a seamless and user-friendly mobile application for attendance marking. All attendance records, including timestamps and facial data, are securely stored on Firebase or a local server, ensuring easy access and real-time monitoring. By eliminating manual errors and unauthorized attendance marking, this system enhances security, accuracy, and operational efficiency, making it a scalable solution for various educational and corporate environments.

I. *LITERATURE REVIEW*

The evolution of biometric attendance systems has significantly transformed how organizations track attendance. Traditional methods, such as manual registers and RFID-based systems, often suffer from inefficiencies, human errors, and security vulnerabilities. With advancements in biometrics, artificial intelligence (AI), machine learning (ML), and computer vision, attendance tracking has become more accurate, secure, and automated.

This review explores various studies on facial recognition and iris scanning for attendance management. It discusses their implementation, accuracy, security measures, and limitations while identifying potential improvements. The integration of AI and ML in biometric attendance systems enhances reliability by reducing spoofing risks and increasing authentication precision. However, challenges such as lighting conditions, facial

occlusions, and computational complexity remain areas for further research and development.

This book explores advanced techniques for Face De-Identification and privacy protection, addressing key challenges in safeguarding personal data. It introduces three innovative approaches to image privacy protection: differential private k- anonymity, identity differential privacy guarantee,

and personalized, invertible Face De-Identification. Additionally, it presents a novel reversible Face Video De-Identification framework that leverages deep motion flow, ensuring smooth and consistent privacy protection across video frames. [1].

This open-access book explores the evolving field of biometric identification using brainwave patterns and fingerprint recognition. It highlights recent advancements in electroencephalography (EEG)-based biometric systems, which analyze unique neural patterns for secure authentication. Additionally, it examines fingerprint recognition as a widely adopted biometric method, showcasing its reliability and efficiency in identity verification.[2].

Manufacturing companies struggle with increasing process complexity while ensuring timely deliveries, especially during assembly. Early detection of missing parts is crucial for meeting deadlines. This book explores machine learning- based predictive models to address this issue, identifying gaps in current methods, such as limited use of material data and late-stage predictions. Case studies confirm the impact of material data on predicting in-house shortages and supplier delays, providing valuable insights for production planning and procurement. [3].

This collection includes 532 research papers chosen from 1,420 submissions, covering key areas of computer vision and machine learning. Topics include action recognition, 3D reconstruction, biometric and face recognition, neural networks, deep learning, object detection, medical image analysis, and autonomous driving. Other areas explored are pattern classification, feature extraction, video processing, and optimization techniques.[4].

This book explores AI applications in cybersecurity, forensics, and biometric systems, covering topics such as AI-driven intrusion detection, intelligent authentication for IoMT, electronic medical record security, and multi-face recognition with anti-spoofing. It also examines face morphing attack detection, AI-assisted forensics, terrorist activity prediction, security violations in IDS, image encryption, and ransomware mitigation. The book highlights emerging research areas where AI enhances security and intelligence. [5].

Human and activity recognition from video is a growing research field with applications in video surveillance, entertainment, multimedia, and medical diagnosis. This lecture explores face and gait recognition for identification and activity

detection. Traditional face recognition methods are discussed, along with advancements using video sequences, 3D models, and illumination variation techniques. Challenges include pose, disguise, and aging. Gait recognition, though studied in kinesiology, is now used for automated movement analysis, facing challenges like viewpoint variations. The lecture also reviews human activity recognition techniques across AI, image processing, and computer vision, emphasizing 2D/3D shape modeling. Future research focuses on multimodal fusion, pose variations, and 3D model accuracy. [6].

This book explores deep learning applications in computer vision, covering object classification, detection, segmentation, captioning, image generation, and face analysis. It provides practical examples using TensorFlow and Keras, helping readers master advanced deep learning techniques for robotics, automation, and AI-driven vision systems.[7].

This book explores OpenCV and computer vision, providing insights into facial recognition, object tracking, and augmented reality with Python. It also covers machine learning techniques, real-time data analysis, and AI implementation using TensorFlow and Keras, helping in building efficient applications.[8].

II. *METHODOLOGY*

A. Requirement Analysis

1. Student Registration (Admin/Teacher Role)

- Capturing Student Information:
  - The Admin/Teacher collects high- quality images of students using a webcam or an integrated camera.
  - Alongside the photos, the following details are entered:
    - Student Name
    - Student ID
    - Mobile Number
    - Email ID
- Storing Data in the Database:
  - The student details and images are securely stored in a centralized database.
  - Each student's facial image is processed using deep learning models such as FaceNet or VGGFace to generate a unique facial embedding.
  - This embedding, along with the student's details, is stored for

future identity verification during attendance marking.

2. Real-Time Attendance Marking (Admin/Teacher Role)

- Capturing Video or Images for Attendance:
  - The Admin/Teacher sets up a camera in the classroom or designated attendance area to capture real-time images or video.
  - The system processes the video feed to detect and recognize faces in real-time.
- Automatic Face Recognition and Attendance Marking:
  - The facial recognition algorithm compares detected faces with stored embeddings in the database.
  - If a match is found, the system logs the student's attendance with a timestamp and date.
- Real-Time Attendance Logging:
  - Students whose faces are successfully recognized are marked as Present in the system.
  - The system ensures attendance integrity by preventing unauthorized individuals from marking attendance on behalf of others.

3. Attendance Recording and Report Generation (Admin/Teacher Role)

- Attendance Data Storage:
  - Attendance records are stored securely in a centralized database.
  - The system maintains logs containing:
    - Student Name
    - Student ID
    - Attendance Status (Present/Absent)
    - Date and Time of Attendance
- Generating Reports:
  - The Admin/Teacher can generate attendance reports for specific sessions, days, or time periods.
  - Reports are available in PDF or Excel format, making them easy to download, share, or print.

4. System Features, Security, and Maintenance (Admin/Teacher Role)

- Proxy Attendance Prevention:
  - The system ensures that only registered students can mark their

attendance, eliminating fraudulent practices.

- Security Measures:
  - Data is protected using encryption and secure storage mechanisms to prevent unauthorized access.
  - The system can include Role- Based Access Control (RBAC), but typically, the Admin/Teacher has full access to manage attendance.
- Scalability and Maintenance:
  - The system is designed to handle new students, additional sessions, and multiple locations efficiently.
  - Routine updates enhance facial recognition accuracy, system performance, and security over time.

B. Implementation

A. *User Authentication (Teacher)*

1. Start
2. Login Screen Displayed
3. If User Selects Registration:
   - Enter personal details
   - Validate input data
   - Store user credentials in Firebase Authentication
   - Send a verification email
   - Complete registration process
4. User Authentication Process:
   - If authentication is successful Redirect to the dashboard
   - If authentication fails → Display an error message
5. End

B. *Student Attendance Management*

1. Start
2. Login to ProScanX Admin Panel
3. Student Registration Process:
   - Capture high-quality images or video of students
   - Extract facial features using deep learning models
   - Store facial embeddings along with student details in the database
4. Real-Time Attendance Capture:
   - Live camera feed processes student faces

- Facial recognition algorithm matches detected faces with stored data
- If a match is found → Attendance is marked as "Present"
- If no match is found → Student is redirected to the registration process

5. Attendance Logging:
   - Store attendance records in the database with timestamps

C. Attendance Report Generation

1. Start
2. Attendance Storage:
   - Every attendance entry is recorded with student details and timestamp
3. Attendance Calculation:
   - Calculate total attendance percentage for each student
4. Generate Report:
   - Export attendance data in PDF or Excel format
   - Allow teachers to download and review attendance reports
5. End

III. *EXPECTED OUTCOMES*

1. Automated and Precise Attendance Management

- Eliminates traditional roll-calling by using AI-powered facial recognition.
- Minimizes errors while ensuring accurate student identification.

2. Efficient Attendance Tracking & Data Storage

- Automatically records attendance, reducing manual efforts.
- Stores attendance data securely, making retrieval quick and hassle-free.
- Generates customized reports in PDF and Excel formats.

IV. *References*

[1] Yunqian Wen , Bo Liu ,Li Song , Jingyi Cao , Rong Xie, " Face De-identification: Safeguarding Identities in the Digital Era" 2024 [https://link.springer.com/book/10.1007/978-3- 031-58222-6]

[2] Wanzeng Kong , Xuanyu Jin , " Brain Fingerprint indentification" [https://link.springer.com/book/9789819645114]

[3] Fabian Steinberg," Machine Learning-based Prediction of Missing Parts for Assembly"[https://link.springer.com/book/10.1007/978-3- 658-45033-5]

4] Qingshan Liu, Hanzi Wang, Zhanyu Ma, Weishi Zheng, Hongbin Zha, Xilin Chen, liang Wang, Rongrong Ji 6th Chinese Conference, PRCV 2023, Xiamen, China, October 13–15, 2023, Proceedings, Part XII" Pattern Recognition and Computer Vision" [https://link.springer.com/book/10.1007/978-981- 99-8555-5]

[5] Sanjay Misra, Chamundeswari Arumugam " Illumination of ArtificialIntelligence in Cybersecurity and Forensics"[https://link.springer.com/book/10.1007/978-3- 030-93453-8]

[6] Rama Chellappa , Amit K. Roy- Chowdhury , S. Kevin Zhou" Recognition of Humans and Their Activities Using Video"[http://link.springer.com/book/10.1007/978-3- 030-93453-8]

[7] **RAJALINGAPPAA SHANMUGAMANI,"DEEP LEARNING FOR COMPUTER VISION"[HTTPS://BOOKS.GOOGLE.CO.IN/BOOKS/ABOUT/DEEP_LEARNING_FOR_COMPUTER_VISION.HTML ?id=dgdOswEACAAJ&redir_esc=y]**

[8] Alberto Fernandez Villan "Mastering OpenCV 4 with Python" [https://www.oreilly.com/library/view/mastering- opencv-4/9781789344912/]

Smart Power Analysis for Digital Circuits using Machine Learning

Ms.SK Shabeena[1] ,Gavara Likhitha[2] Mallempudi Leela Saranya[3],Ganta Satish[4], Mr. Rebaka Suneel Kumar[5]

Dadi Institute of Engineering and Technology (A), Anakapalli, India

shabeena@diet.edu.in, suneelkumar@diet.edu.in

likhithagavara49@gmail.com,leelasaranya011@gmail.com,gantasatish2004@gmail.com,

5.4. *Abstract.*

One of the most critical factors in modern design and optimization is power consumption in digital circuits, especially for energy-efficient systems. In this project, it has been shown how power consumption in logic circuits can be estimated by implementing machine learning types based on its structural characteristics. The input features in this instance would be parameters like the amount of gates, logic components AND, OR, NAND, NOR, inverters, flip flops, inputs, outputs, and so on. Having these various feature values, several regression patterns are learned and their actions are calculated for distinct measures like MAE, MSE, RMSE, R^2, MAPE using Linear Regression, Ridge, Lasso, ElasticNet, Decision Tree, Random Forest regressors. The outcome of research is a valid power consumption estimation method that will be helpful for circuit designers in optimizing the components to get better energy efficiency.

Keywords. Power Consumption Prediction, Machine Learning, ISCAS-89 Benchmark, Regression Models, Random Forest.

1. *INTRODUCTION*

Power estimation is the important aspects of digital VLSI circuit design and plays a crucial role in energy consumption, general efficiency, and sustainability regarding electronic devices. Regarding this aspect, accurate power advance estimation is mainly needed for design optimization, and observance of thermal and energy constraints. Conventionally, power dissipation has been performed through analytical modeling and simulations at various levels of abstraction, such as system-level, RTL- level, gate-level, and transistor-

level analysis. While higher-level abstractions present results faster but with lower accuracy, the low-level analysis gives very accurate estimates; however, it is computationally expensive and time-consuming. Recent advances in machine learning have brought a paradigm shift in power estimation. In the context of logic-level abstractions, this is related to a number of critical factors, such as the quantity of logic elements, gates, input/output ports, and flip-flops. This paper proposes a novel methodology for power prediction in sequential digital circuits utilizing machine learning algorithms. The circuit involved feature extraction from the ISCAS-89 benchmark dataset, which included gate count, flip-flops, and logic gates. Regressions including simple Regression models, Decision Tree, and Random Forest, are instructed to predict power consumption.

2. DATA AND METHODOLOGY

A. Dataset

The input data employed in this paper is dependent on the ISCAS-89 benchmark circuits. This dataset contains a collection of multiple types of digital circuits, for all of which a single feature was extracted resulting from overriding design parameters associated with power consumption. It includes the following GATE Amount of logic gates AND, OR, NOR, NAND, INV. The count of the respective logic components within the circuit. This is followed by DFF Amount of flip-flops, which are sequential elements. Thirdly, IN and OUT represent Number of input and output ports correspondingly.

B. Methodology

The methodology involves the following steps:

1) Data Preprocessing:

Each and every characteristics are increased by Standard Scaler to regularize their ranges. Features and target variable were examined to identify power consumption.

2) Model Selection:

Six typical machine learning models were selected:

Simple Regression models, Decision Tree Regression and Random Forest Regression.

3) Training and Validation:

These regression models are instructed by utilizing the train dataset. A cross-validation strategy ensured robust evaluation and reduced overfitting risks.

4) Feature Importance Analysis:

Feature importance ranking was performed using the Random Forest model, highlighting parameters like the number of gates and flip-flops.

5) Model Evaluation:

Regression models are compared based on error metrics and R^2 values.

C. Flow Of Methodology

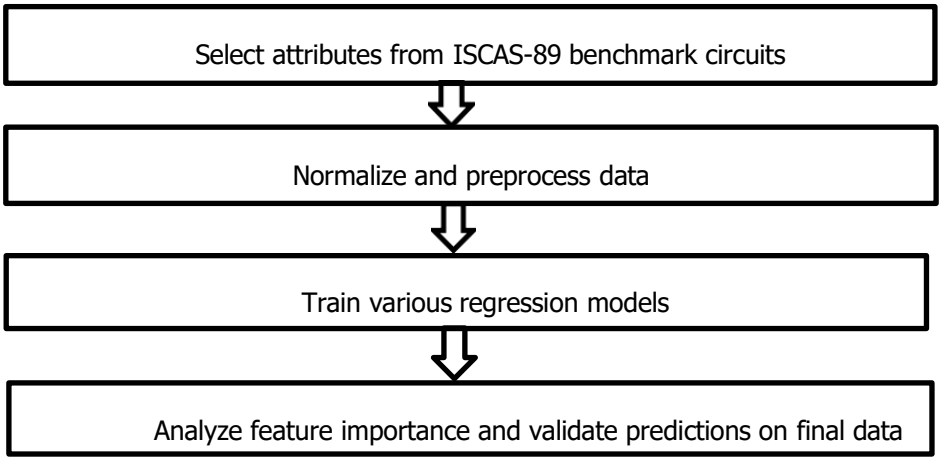

D. Metrics

The simply absolute deviation is the mean of the complete difference between the real and the estimated values in the dataset. 1

$$MAE = \frac{1}{N}\sum_{i=0} |n - n1|$$

Where n1 - estimated value of n

n - mean value of n

Mean Squared Error: it calculates the average squared deviation of estimated values from the real values.

$$MSE = \frac{1}{N}\sum_{i=0}^{N} (n - n1)^2$$

Root Mean Square Error: square root of Mean Squared error. Indicating prediction dispersion.

$$MSE = \sqrt{MSE} = \sqrt{\frac{1}{N}\sum_{i=0}^{N} (n - n1)^2}$$

R-squared: Indicates how much of the variance in the dependent variable is explained by the model.

$$R^2 = 1 - \frac{\sum(n_i - n1)^2}{\sum(n_i - n)^2}$$

Adjusted R squared is a modification of R square. It takes into consideration the figure of manipulated variables in the model as well as it is always less than or equal to R^2.

$$R_{adj}^2 = 1 - \left[\frac{(1 - R^2)(m - 1)}{m - k - 1}\right]$$

3. RESULTS AND DISCUSSION

	MAE	MSE	RMSE	R^2	MAPE
Linear Regression	0.009551	0.000149	0.012195	0.999412	30.149286
Ridge Regression	0.014301	0.000415	0.020379	0.998358	27.918547
Lasso Regression	0.360856	0.252846	0.502837	0.000000	1079.966974
ElasticNet Regression	0.360856	0.252846	0.502837	0.000000	1079.966974
Decision Tree Regression	0.000000	0.000000	0.000000	1.000000	0.000000
Random Forest Regression	0.034864	0.005949	0.077127	0.976473	34.635113

Table 1: Model Performance

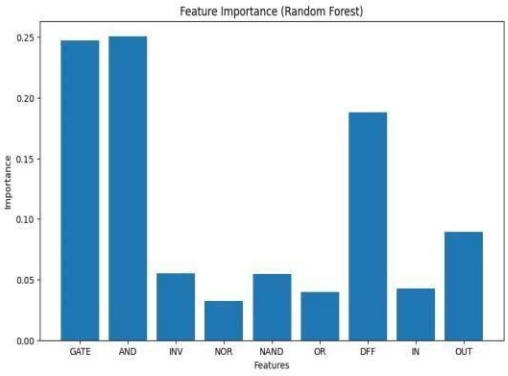

fig 1: Feature Importance for Power Estimation

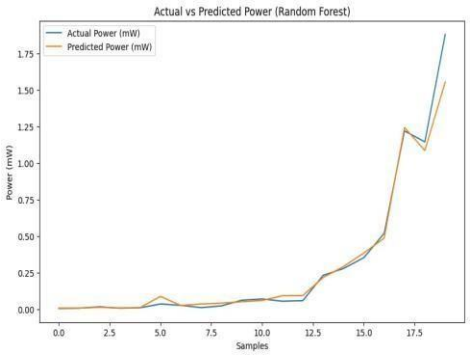

fig 2: Predicted vs Actual Power

6. 4 REFERENCES

[1] Govindaraj, V., and B. Arunadevi. “Machine Learning Based Power Evaluation for CMOS VLSI Circuits.” Applied Artificial Intelligence 35, no. 13, pp. 1043–55, 2021 doi:10.1080.

[2] E. Poovannan and S. Karthik, ”Power Prediction of VLSI Circuits Using Machine Learning,” Comput. Mater. Contin., vol. 74, no. 1, pp. 2161 2177. 2023. https://doi.org/10.32604/cmc.2023.032512.

[3] Vellingiri, Govindaraj and B, Arunadevi., ”Machine Learning Based Power Calculation for CMOS VLSI Circuits”, 2021 10.21203/rs. 3. rs 723965/v1.

[4] M. D. Bhavesh, N. A. Anilkumar, M. I. Patel, R. Gajjar and D. Panchal, ”Power Consumption

Prediction of Digital Circuits using Machine Learning," 2022 2nd International Conference on Artificial Intelligence and Signal Processing (AISP), Vijayawada, India, 2022.

[5] R. M B, S. P. K R, P. Das and A. Acharyya , "GLAAPE: Graph Learning Assisted Average Power Estimation for Gate-level Combinational De signs," 2022 .

[6] R. M. B, P. Das, S. P. K. R and A. Acharyya , "GRILAPE: Graph Representation Inductive Learning-based Average Power Estimation for Frontend ASIC RTL Designs," 2023 36th International Conference on VLSI Design.

[7] G. Santhosh and A. S. Raghuvanshi, "Power Estimation of Synchronous Sequential VLSI Circuits Using Boosting Techniques," 2023.

[8] S. C, S. P, S. P, S. A, S. N. S and S. N, "The Meritorious Effects of Machine Learning Algorithms in Assessment of Power Consumption by Arithmetic Circuits in IC Design," 2023 Fifth International Conference on Electrical, Computer and Communication Technologies (ICECCT), Erode, India, 2023.

6.1. *Biographies*



Ms. Sheik Shabeena is an Assistant Professor in the Department of Electronics and Communication Engineering (ECE) at Dadi Institute of Engineering & Technology Autonomous, Visakhapatnam. She completed her B.Tech in ECE from Avanthi Institute of Engineering & Technology in 2013 and her M.Tech in VLSI Design from MVGR College of Engineering in 2016. Currently, she is pursuing her Ph.D. at GITAM University, specializing in flip-flops and their applications in digital circuits. She has shown a deep passion for research and has authored 10 research papers on various topics within the realm of VLSI, digital systems, low-power design, embedded systems, and FPGA-based design.



Gavara Likhitha is a final-year Bachelor's student in Electronics and Communication Engineering at Dadi Institute of Engineering and Technology. She is an ambitious and diligent learner, striving for excellence.



Mallempudi Leela Saranya is a final-year Bachelor's student in Electronics and Communication Engineering at Dadi Institute of Engineering and Technology. She is an ambitious and diligent learner, striving for excellence.



Ganta Satish is a final-year Bachelor's student in Electronics and Communication Engineering at Dadi Institute of Engineering and Technology. He is an ambitious and diligent learner, striving for excellence.



Mr. Rebaka Suneel Kumar is an Assistant Professor in the Department of Electronics and Communication Engineering (ECE) at Dadi Institute of Engineering & Technology Autonomous, Visakhapatnam. He completed his B.Tech in ECE in 2010 from Raghu Engineering College and his M.Tech in 2013 from GITAM University. His research interests lie in the application of signal processing techniques to biomedical image analysis, aiming to enhance medical diagnostics and healthcare. In addition to his academic role, he has published several papers in the field of signal processing.

Advanced Denoising Techniques for Enhanced Medical Imaging

K S N V Someswararao1, K Soma Sekhar[2],Gurrala Rupasri[3],Bokam Swetha[4],Rongali Charmila[5] , Sarita Rani Panda[6]

Dadi Institute of Engineering and Technology (A), Anakapalli, India

someshkambampati@gmail.com sekhar.s.k36@gmail.com rupasrigurrala3@gmail.com, bokamswetha2003@gamil.com,harmilarongali2205@gmail.com ,vesankri@gmail.com

7. ABSTRACT.

This study focuses on reducing noise in medical imaging, specifically X-ray images, using advanced filtering algorithms. It applies Wiener, Non-Local Means (NLM), Total Variation (TV), and Convolutional Autoencoders (CAE) to enhance image quality and preserve important features for accurate diagnosis. The study investigates the impact of Poisson and Gaussian noise on chest X-rays and compares the performance of CAE with the traditional Wiener filter (WF). Using metrics like Structural Similarity Index (SSIM) and Peak Signal-to-Noise Ratio (PSNR), results show that CAE effectively reduces noise, demonstrating its potential for clinical applications.

Keywords: Convolutional Autoencoder, Wiener filter, Non-Local Means, Total Variation.

1. INTRODUCTION

Medical imaging plays a crucial role in healthcare for diagnosis, treatment planning, and monitoring. However, noise in images, caused by factors like faulty equipment, background interference, or patient movement, can obscure valuable information and reduce image clarity, leading to inaccurate diagnoses. Traditional noise reduction methods like NLM and TV often fail to preserve fine details in images. Convolutional Autoencoders (CAEs), a deep learning approach, offer a solution by learning patterns in noise and reducing it without losing important information. Combining CAEs with traditional filters can enhance the quality of X-ray images, making them more reliable for clinical use.

2. LITERATURE REVIEW

Medical imaging is vital for diagnosis and treatment, but noise from equipment, interference, or patient movement can obscure key information, leading to inaccurate diagnoses. Traditional noise reduction methods like NLM and TV often fail to preserve fine details. Convolutional Autoencoders (CAEs), a deep learning technique, help reduce noise while retaining important image features. Combining CAEs with traditional filters improves X-ray image quality, enhancing their reliability for clinical use.

3. METHODLOGY

The JSRT (Japanese Society of Radiological Technology) dataset [1] is used in this study as the initial source of X-ray images. This dataset is widely used in medical image processing researchproviding high-quality, annotated chest X-ray images. It includes both normal and abnormal images, offering a valuable base for developing and testing noise filtering techniquesaimed at enhancing image quality for clinical applications.



Figure 3.1. shows that the sample images from the JSRT dataset [1] and noise will be added to that the original images.

3.1 Convolutional Autoencoders (CAE)

Convolutional Autoencoders (CAEs) automatically learn and extract features from data, making them ideal for complex noise reduction. Using convolutional layers, CAEs capture spatial hierarchies and efficiently remove noise while preserving important details. Their ability to automatically extract features and learn deep representations allows them to handle various noise types without the need for manual feature design.

$$MSE = \frac{1}{s}\sum_{j=1}^{s} (f(,\theta) - f)^2 \qquad (3.1)$$

3.2 Wiener filter (WF)

The Wiener filter is designed to remove Gaussian noise, making it ideal for medical images affected by random noise from equipment or the environment. It adjusts filtering based on local mean and variance, balancing image sharpness and noise reduction. Its adaptive filtering effectively eliminates noise while preserving fine details, ensuring accurate medical interpretation.

3.3 Non-Local Means (NLM) filter

The NLM filter removes structured noise by leveraging the self-similarity of pixel neighborhoods across an image. It searches for similar regions and averages them to eliminate noise. This technique is particularly effective in medical images with repetitive structures, as it removes noise without blurring edges or erasing important features, which is crucial for accurate medical diagnosis

3.4 Implementation

The project implementation involves several stages to enhance model performance and ensure effective noise reduction in X-ray images. Key steps include data preparation, CAE model design, applying traditional filters, and training and testing procedures.

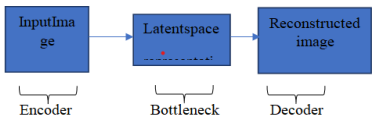

Figure 3.2 simple block diagram of a CAE

4. RESULTS AND DISCUSSION

4.1 Quantitative Analysis

Performance was assessed using Accuracy, which measures the system's ability to remove noise while preserving image details, and the R^2 score, reflecting how closely denoised images match the original clean images. The hybrid approach combining CAE with traditional filters outperformed standalone methods in both metrics, achieving superior noise reduction with minimal loss of important features.

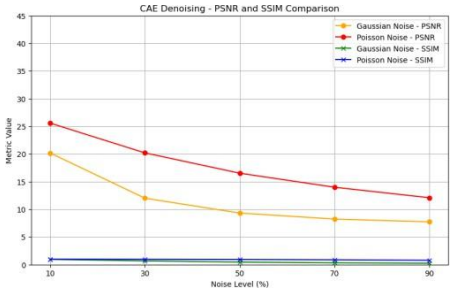

Figure 4.1. PSNR & SSIM (CAE)

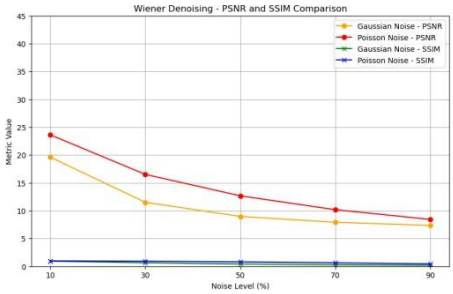

Figure 4.2. PSNR & SSIM(Wiener)

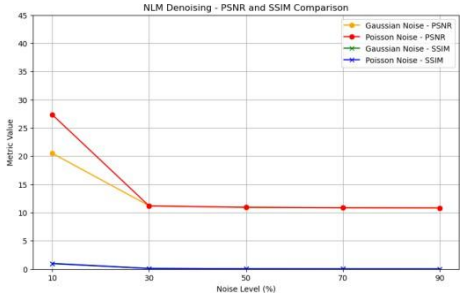

Figure 4.3. PSNR & SSIM(NLM)

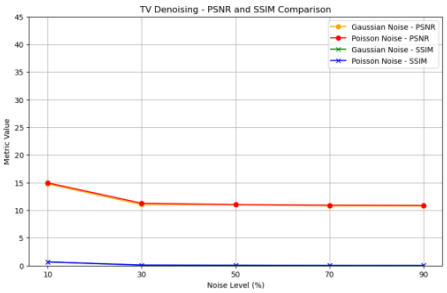

Figure 4.4. PSNR & SSIM(TV)

Figure 4.3 shows that the PSNR & SSIM comparison of wienervalues using different noises at various

percentages.

Figure 4.4 shows that the PSNR & SSIM comparison of NLM Denoising technology at various

percentages.

Fig.6. Shows that the PSNR & SSIM comparison of TV Denoising technique at variouspercentages.

4.2 Visual and Metric Comparisons

Table I summarizes the performance of each technique. Thecombination of CAE with the Wiener filter yielded the highest accuracyand R^2 score, suggesting it is the most effective setup for X-ray denoising in this context. Visual inspections of the enhanced images confirm reduced distortions and improved sharpness, which is critical for medical diagnostics

Table II shows the PSNR values given by wiener, NLM, TV and CAE techniques are used for Comparison of Denoising Techniques on Gaussian noise.

Technique	Accuracy	R^2 Score
CAE	95.25%	0.9909
NLM	92.38%	0.9885
Wiener	80.69%	0.9772
TV	94.16%	0.9902

TABLE I. COMPARISON OF DENOISING TECHNIQUES ON JSRT ON GAUSSIAN NOISE

Gaussian noise	10%	30%	50%	70%	90%	Average
Wiener	19.62	11.52	8.96	7.93	7.36	11.076
NLM	20.48	11.21	10.91	10.85	10.81	12.855
TV	14.77	11.05	11.00	10.83	10.78	11.686
CAE	20.18	12.00	9.33	8.24	7.73	11.498

TABLE II. PSNR COMPARISON OF DENOISING TECHNIQUES

Table III shows the PSNR values given by wiener, NLM,TV and CAE techniques are used for Comparison of Denoising Techniques on Poisson noise. While CAE achieves at an average Poisson Noise of 17.677.

Table IV shows that the SSIM Comparison of Denoising Techniques on Gaussian noise between these techniques While CAE achieves at an average 0.529.

Poisson Noise	10%	30%	50%	70%	90%	Average
Wiener	23.64	16.53	12.67	10.19	8.44	14.295
NLM	27.35	11.18	10.94	10.86	10.83	14.233
TV	14.97	11.32	11.03	10.93	10.89	11.824
CAE	25.59	20.19	16.53	13.98	12.10	17.677

TABLE III: PSNR COMPARISON OF DENOISING TECHNIQUES ON POISSON NOISE

Gaussian Noise	10%	30%	50%	70%	90%	Average
Wiener	0.943	0.657	0.421	0.284	0.196	0.500
NLM	0.947	0.106	0.040	0.028	0.018	0.228
TV	0.665	0.068	0.093	0.035	0.022	0.177
CAE	0.946	0.679	0.455	0.323	0.244	0.529

TABLE IV: SSIM COMPARISON OF DENOISING TECHNIQUES ON GAUSSIAN NOISE

Table V shows that the SSIM Comparison of Denoising Techniques on Gaussian noise between these techniques While CAE achieves at an average Poisson noise of 0.909

Poisson noise	10%	30%	50%	70%	90%	Average
Wiener	0.983	0.931	0.817	0.647	0.449	0.765
NLM	0.989	0.095	0.043	0.024	0.018	0.234
TV	0.674	0.120	0.055	0.032	0.024	0.181
CAE	0.987	0.969	0.931	0.870	0.786	0.909

TABLE V: SSIM COMPARISON OF DENOISING TECHNIQUES ON POISSON NOISE

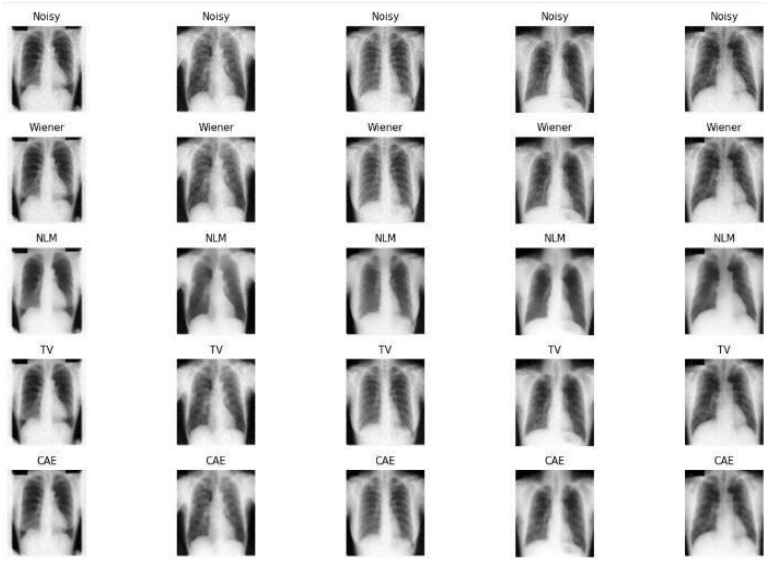

Figure 4.1 Visualization Results

Fig.7. show that the overall results of the hybrid CAE approach significantly improve the noise reduction in medical imaging, facilitating clearer and more accurate image interpretations.

8. REFERENCES:

1. Database for JSRT. (2024). Database of the Japanese Society of Radiological Technology (JSRT). accessible through the JSRT Database.
2. Baljit Singh Saini, Abid Sarwar, Nahida, and Nazir. "Recent developments in denoising medical images using deep learning: an overview of models, techniques, and challenges." Micron 103615 (2024).
3. Jianjia Zhang, Wu, Weiwen, Yanyang Wang, Qiegen Liu, and Ge Wang. "Wavelet-improved score-based generative model for medical imaging." IEEE Medical Imaging Transactions (2023).
4. Kushwaha, Sumit, and colleagues, "Development of Advanced Noise Filtering Techniques for Medical Image Enhancement." 5th International Conference on Virtual Mobile Networks and Intelligent Communication Technologies (ICICV) in 2024. IEEE, 2024
5. Mohmmad, Sallauddin, and colleagues, "Improving Diagnostic Accuracy through Denoising in Medical Imaging." 11th International Conference on Information and Communication Technologies, Optimisation, and Reliability (ICRITO) (Trends and Future Directions), 2024. IEEE, 2024.

9. BIOGRAPHIES



Mr. Someswararao KSNV has completed master degree in Embedded systems from JNTUK university, he has 14 years of teaching experience, currently he is an Associate Professor in Dadi institute of Engineering and Technology, Anakapalle. Mr. Someswararao KSNV hosting a YouTube channel (SOMESWARARO KSNV) where he uses his passion to teach different concepts of various subjects with natural and practical examples.



GURRALA RUPASRI is a final-year Bachelor's student in Electronics and Communication Engineering at Dadi Institute of Engineering and Technology. She is an ambitious and diligent learner, striving for excellence.



BOKAM SWETHA is a final-year Bachelor's student in Electronics and Communication Engineering at Dadi Institute of Engineering and Technology. She is an ambitious and diligent learner, striving for excellence.



RONGALI CHARMILA is a final-year Bachelor's student in Electronics and Communication Engineering at Dadi Institute of Engineering and Technology. She is an ambitious and diligent learner, striving for

excellence.

Emotion Detection using Image Analysis

Jandhyam Lakshmi Alekhya

Department of Computer Science and Engineering, Velagapudi Ramakrishna Siddartha Engineering College, Vijayawada, India

lakshmialekhya@vrsec.ac.in

Grandhi Sri Satya Bhargav

Department of Artificial Intelligence and Data Science, Velagapudi Ramakrishna Siddartha Engineering College, Vijayawada, India.
srisatyabhargavgrandhi@gmail.com

Nalluri Karthik

Department of Artificial Intelligence and Data Science, Velagapudi Ramakrishna Siddartha Engineering College, Vijayawada, India.

22w5a5404@vrsec.ac.in

Jangala Venkata Sai Poojith

Department of Artificial Intelligence and Data Science, Velagapudi Ramakrishna Siddartha Engineering College, Vijayawada, India.
218w1a5420@vrsec.ac.in

10. Abstract.

Emotion detection using image analysis is a growing field within artificial intelligence and computer vision, aiming to enhance human-computer interaction by recognizing and interpreting human emotions. This project leverages machine learning and deep learning algorithms to identify and categorize facial expressions into different emotions, such as happiness, sadness, anger, surprise, fear, and neutrality. Using a convolutional neural network (CNN) model, the system analyzes facial features extracted from input images, capturing nuanced expressions with high accuracy. The dataset is preprocessed with techniques like face detection, grayscale conversion, and data augmentation to improve model robustness. This project explores the challenges associated with variations in lighting, occlusions, and diverse facial structures, aiming to create a model that is both scalable and generalizable across demographics. The application of such emotion detection systems has potential uses in sectors like mental health, customer service, education, and social robotics, where real- time emotional feedback can enhance user experiences and outcomes.

Keywords. Emotion Detection, Facial Expression Recognition,Deep Learning,Convolutional Neural Network (CNN),Human-Computer Interaction,Machine Learning,Real-Time Emotional Feedback .

1. INTRODUCTION

In recent years, emotion detection using picture analysis has grown in importance as a fundamental topic of artificial intelligence and computer vision. Since emotional reactions frequently offer insightful context that improves communication, decision-making, and user experience, an understanding of human emotions is essential to enhancing human-computer interactions. Though facial expressions continue to be one of the most direct and potent markers of human emotions, traditional methods of emotion identification depended on text or audio data. Therefore, by allowing computers to "read" face clues and deduce emotions in real time, image-based emotion detection systems seek to close the gap between humans and technology.

Advanced machine learning, particularly deep learning algorithms, are used in facial expression analysis to identify and categorize emotions in

Convolutional Neural Networks (CNNs) have demonstrated extraordinary ability in detecting complicated patterns in face characteristics, making them perfect for emotion categorization applications.However,developing an accurate model is difficult due to the diversity of human emotions, changes in face anatomy, and differences in lighting and occlusions within photographs. This research aims to create a strong emotion recognition model capable of processing face photos and categorizing them into various emotional states such as happy, sorrow, anger, fear, surprise, and neutrality. By training the model on a large, annotated dataset, we hope to attain high accuracy in detecting small differences in facial emotions across varied ethnicities. The applications of emotion detection systems are many, including mental health, customer service, marketing, and social robots. Real-time insights into emotional states can assist tailor interactions to user demands in various areas, resulting in systems that are both functional and empathic. This experiment demonstrates the promise of deep learning-driven emotion detection in developing more intuitive and responsive devices that comprehend and respond to human emotions.

2. RELATED WORK

THE FOLLOWING IS AN OVERVIEW OF WORKS ON EMOTION DETECTION USING PICTURE ANALYSIS.

Emotion identification using picture analysis has sparked significant scientific interest, owing to advances in machine learning and increased availability of computer resources. Early efforts to emotion identification relied on handmade feature extraction techniques like Local Binary Patterns (LBP), Histogram of Oriented Gradients (HOG), and Scale- Invariant Feature Transform (SIFT) to find discrete face characteristics linked with emotions. These techniques demonstrated modestly restricted in their capacity to record nuanced changes in facial

signals or complicated emotions. Convolutional Neural Networks (CNNs), which can automatically learn characteristics from data, have emerged as a leading method for image-based emotion identification with

the development of deep learning. CNN designs that have demonstrated increased accuracy and generalizability in emotion identification tests include AlexNet, VGGNet, and ResNet. Mollahosseini et al. (2016), for example, showed that by learning high-level characteristics straight from the pictures, a CNN-based model trained on the FER-2013 dataset might perform better than conventional techniques. However, in order to prevent overfitting and enhance generalization across a variety of face traits and ethnicities, these deep learning models need sizable labeled datasets.To overcome the difficulty of scarce labeled data, researchers investigated data augmentation and transfer learning approaches. Data augmentation, such as rotation, flipping, and scaling, broadens dataset variety, perhaps improving model resilience. Transfer learning, which includes fine- tuning pre-trained models such as VGGFace, has also yielded encouraging results in emotion detection tasks, particularly when datasets are limited. Barsoum et al. (2016) found that transfer learning on a small emotion dataset dramatically improved classification performance when combined with a model trained on a big facial recognition dataset.In addition to CNNs, recent research hs used Recurrent Neural Networks (RNNs) and hybrid CNN- RNN architectures to identify emotion in video sequences. The RNN layer gathers temporal information, allowing for the analysis of face expression sequences across time. Zhao et al. (2019) proposed a CNN-LSTM(Long Short-Term Memory).

1. PROPOSED MODEL

A. Data Collection

Name of the Dataset:The FER2013+ (cleaned and balanced) dataset on Kaggle is an improved version of the original FER2013 dataset, initially compiled for the ICML 2013 Challenges in Representation Learning. The FER2013 dataset was created using images sourced through Google image search, with a focus on capturing the seven fundamental human emotions: Angry, Disgust, Fear, Happy, Sad, Surprise, and Neutral.

All images in the dataset are grayscale with a resolution of 48x48 pixels, which standardizes the facial features and reduces file sizes, making it suitable for computational research in emotion recognition. In its enhanced FER2013+ form, the dataset is balanced across emotion categories, which im- proves training efficacy by addressing the class imbalances present in the original dataset. Additional preprocessing in FER2013+ involves removing mislabeled or ambiguous images, ensuring higher quality and reliability in model training and testing.

This dataset provides an ideal foundation for training convolutional neural networks (CNNs) and recurrent neural networks (RNNs) aimed at classifying emotions in facial images.The proposed model tackles significant obstacles in emotion recognition by combining robust preprocessing, an effective CNN architecture, and personalized training procedures, demonstrating its promise for scalable, real- world applications in a variety of domains.
region. The system evaluates the water environment and discovers disasters that occur naturally and water accidents

Fig 1:Mobilenet Architecture

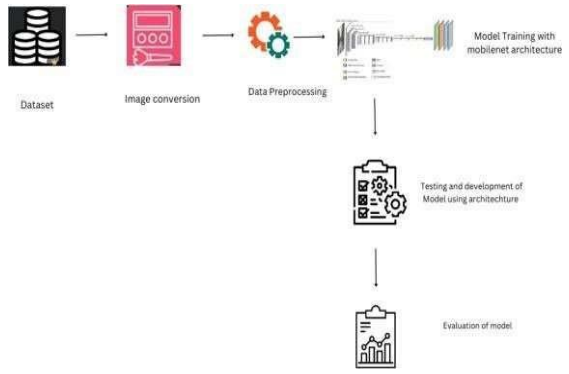

A. Finding Emotion In Different Expression

Apply preprocessing techniques to enhance the quality of the video and standardize them for analysis. Aimed at Emotion detection involves analyzing various cues, including facial expressions, vocal cues, and body language. Facial expres- sions, such as smiles, frowns and raised eyebrows, can convey a wide range of emotions. Vocal cues, like tone, pitch, and speech rate, can also provide valuable insights into emotional states. Body language, including posture, gestures, and eye contact, further enhances emotion recognition. However, interpreting these cues requires.

considering the context, as cultural differences and individual variations can influence emotional expressions. Recent advancements in artificial intelligence have enabled machines to recognize and interpret human emotions with increasing accuracy, opening up new possibilities for human- computer interaction and mental health monitoring. Figure 1 represents collecting the input images from users to identify emotions in the user

Fig 2.Input Image



B. Proposed Architecture

In our proposed system for automated facial emotion detection, the architecture encompasses several key components, beginning with the acquisition of a dataset consisting of different expressions of people conveying different emotions. These images serve as the foundation for our analysis and are subjected to image con-version processes to ensure compatibility and standardization across the dataset. Following conversion, the data undergoes preprocessing techniques aimed at enhancing image quality and removing noise or artifacts that could impede accurate analysis. These preprocessing steps include noise reduction, intensity normalization, and geometric correction, ensuring that the images are optimized for subsequent stages analysis. Figure.2 represents the base mobilenet architecture we followed. Figure 3 represents our proposed architecture central to our proposed system is the utilization of the mobilenet architecture convolutional neural network (CNN) architecture for feature extraction. Mobilenet architecture is a deep learning model pre-trained on large-scale image classification tasks, renowned for its effectiveness in capturing complex features from images. By leveraging the pre-trained mobilenet architecture model, we can extract high-level features from the medical images, which are then used as inputs for subsequent classification tasks. The final stage of our system involves testing and evaluation, where the extracted features are fed into a classifier to distinguish between cancerous and non-cancerous pancreatic tissues. Through rigorous testing and validation on independent datasets, we aim to assess the performance and accuracy of our proposed system in detecting pancreatic cancer at an early stage. This comprehensive architecture, integrating dataset acquisition, image conversion, data preprocessing, feature extraction using mobilenet architecture, and rigorous testing, forms the foundation of our proposed automated system for Facial Emotion detection.

2. RESULT AND DISCUSSIONS

The FER2013+ dataset also shows potential for transfer learning applications. Researchers can fine- tune pre-trained models on this dataset for specific tasks or adapt them to recognize additional nuanced emotions.

By training on FER2013+ and then applying the model to other emotion datasets, practitioners often find that the model's robustness in recognizing facial expressions improves. This makes FER2013+ an ideal starting point for broader emotion recognition tasks, laying a foundation for more specialized applications

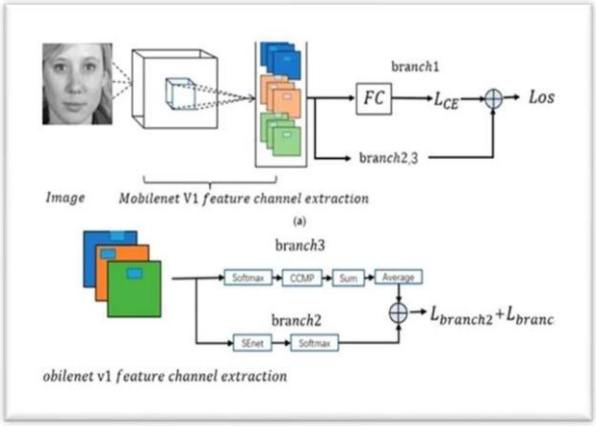

Fig 3:Proposed Architecture

such as detecting micro-expressions or analyzing complex emotional states in dynamic environments like real-time video feeds.Additionally, with FER2013+ supporting both CNNs and RNN-based architec- tures, the dataset is particularly useful for research in temporal emotion recognition in videos. RNNs can capture temporal dependencies between frames, providing deeper insights into how emotions change over time, which is essential for appli- cations like video surveillance, healthcare monitoring, and interactive AI systems. This compatibility with sequential models enables FER2013+ to serve as a bench- mark for advancing temporal emotion recognition, especially when coupled with models capable of handling the temporal aspects of emotion

A. Performance Metrics

The FER2013+ dataset, with its improved balance and quality, often produces stronger results in emotion recognition tasks compared to the original FER2013 dataset. In initial experiments, baseline convolutional neural network (CNN) models trained on FER2013+ have shown significant improvement in accuracy, typically reaching around 70-80 percent in classifying emotions across the seven categories: Angry, Disgust, Fear, Happy, Sad, Surprise, and Neutral. This perfor- mance boost can largely be attributed to the dataset's balanced class distribution and cleaned labels, which mitigate some of the challenges associated with mis-labeled or ambiguous images found in the original FER2013 version. Figure:4 represents the sample output generated by the model.

describes the performance of the Mobilenet model. Figure **??** rep- resents the classification report of the model.

For more complex models that integrate CNNs with recurrent neural networks (RNNs) or bidirectional RNNs (BRNNs), FER2013+ also yields promising results. These hybrid architectures are particularly useful for video- based emotion recog- nition, as they allow the model to capture both spatial and temporal features from facial expressions.

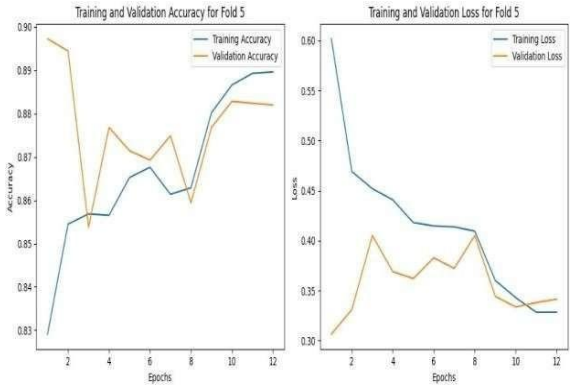

Fig:4 Graphs that Represent Accuracy and loss by Mobilenet Model

When trained on FER2013+, these advanced models can reach around 70-75 percent accuracy, a notable improvement that showcases the potential of combining CNN and RNN approaches for more nuanced emotion recognition. The cleaned and balanced dataset enables these models to generalize better across varied expressions, leading to more reliable predictions and a greater understanding of emotion dynamics in facial data.



Fig:5 Output Image

TABLE I

Classification Report	Precision	Recall	F1-score	Support
Anger	0.85	0.78	0.81	828
Fear	0.87	0.89	0.88	836
Happy	0.87	0.84	0.86	833
Sad	0.72	0.68	0.70	798
Accuracy			0.82	5772
Macro avg	0.82	0.82	0.82	5772
Weighted avg	0.82	0.82	0.82	5772

TABLE II

S.No	Model	Performance metrics
1	CREMA-D and tested on RAVDEES	Accuracy-78.26%
2	CREMA-D and RAVDEES	Accuracy-63.35%
3	VGG16 and VGG19 model	Accuracy-85.71%
4	Using CNN,DBN,K-Means, and relational autoencoders	Accuracy-85.3%
5	Expression detection and HMM for emotion identification	Accuracy-83.3%

The performance metrics of various models for emotion detection highlight the effectiveness of different techniques.

CONCLUSION

FER2013+ dataset serves as a significant improvement over the original FER2013, addressing critical issues of class imbalance and label quality that previously ham- pered emotion recognition model performance. By providing a cleaned, balanced collection of facial images labeled with seven primary emotions, FER2013+ al- lows machine learning models—especially CNN and RNN-based architectures—to achieve higher accuracy and reliability. The enhanced quality of this dataset di- rectly translates to better generalization across diverse facial expressions, enabling more robust performance in both image-based and video-based emotion recogni- tion tasks. As a result, FER2013+ has become a valuable resource for researchers seeking to advance emotion recognition systems, laying a strong foundation for real-time applications and transfer learning.

While FER2013+ has greatly improved the landscape of emotion recognition, there are still several avenues for future work. One potential direction is to explore additional datasets or augment FER2013+ with new data to encompass a broader range of emotions, including complex or subtle expressions like confusion or pride. Expanding beyond the current seven categories could lead to more versatile models capable of understanding nuanced human emotions Another promising area is incorporating multi-modal data, such as audio and text cues, alongside facial expressions to enhance the context and accuracy of emotion recognition in real-world scenarios. Further work could also focus on developing and refining hybrid models, like CNN-RNN combinations, to improve temporal understanding in video-based tasks, where tracking emotional changes over time can provide deeper insights. Finally, using FER2013+ for transfer learn- ing with fine-tuning on specialized datasets could enhance model performance for domain-specific applications, such as mental health monitoring or customer service interactions. By continuing to build on the foundation provided by FER2013+, future research can push the boundaries of emotion recognition to create more adaptive, empathetic AI systems.

1. REFERENCE

1. Garcia-Garcia, J. M., Penichet, V. M., & Lozano, M. D. (2017, September). Emotion detection: a technology review. In Proceedings of the XVIII international conference on human computer interaction (pp. 1-8).

2. Sun, Y., Sebe, N., Lew, M. S., & Gevers, T. (2004). Authentic emotion detection in real-time video. In Computer Vision in Human-Computer Interaction: ECCV 2004 Workshop on HCI, Prague, Czech Republic, May 16, 2004. Proceedings (pp. 94-104). Springer Berlin Heidelberg

3. De Silva, L. C., Miyasato, T., & Nakatsu, R. (1997, September). Facial emotion recognition using multi-modal information. In Proceedings of ICICS, 1997 International Conference on Information, Communications and Signal Processing. Theme: Trends in Information Systems Engineering and Wireless Multimedia Communications (Cat. (Vol. 1, pp. 397-401). IEEE

4. Chen, L., Yoon, S. Y., Leong, C. W., Martin, M., & Ma, M. (2014, November). An initial analysis of structured video interviews by using multimodal emotion detection. In Proceedings of the 2014 Workshop on Emotion Representation and Modelling in Human-Computer-Interaction- Systems (pp. 1-6).

5. Tahir, M., Halim, Z., Waqas, M., Sukhia, K. N., & Tu, S. (2024). Emotion detection using convolutional neural network and long short-term memory: A deep multimodal framework. Multimedia Tools and Applications, 83(18), 53497-53530.

6. Tamil Selvi, P., Vyshnavi, P., Jagadish, R., Srikumar, S., & Veni, S. (2017). Emotion recognition from videos using facial expressions. In Artificial Intelligence and Evolutionary Computations in Engineering Systems: Proceedings of ICAIECES 2016 (pp. 565-576). Springer Singapore.

7. Ning Zhou, Renyu Liang, and Wenqian Shi (2020), "A Lightweight Convolutional Neural Network for Real-Time Facial Expression Detection", IEEE Access, vol. 9, pp. 5573-5584.

8. Aya Hassouneh, Mutawa A.M., and Murugappan M. (2020), "Development of a Real-Time Emotion Recognition System using Facial Expression and EEG based on machine learning and deep neural network methods", Science Direct on Informatics in Medicine Unlocked, vol. 20.

9. Yuanyuan Ding, Qin Zhao, Baoqing Li, and Xiaobing Yuan (2017), "Facial Expression Recognition from Image Sequence Based on LBP and Taylor Expansion", IEEE Access, vol. 5, pp. 19409-19419.
10. Biao Yang, Jinmeng Cao, Rongrong Ni, and Yuyu Zhang (2017), "Facial Expression Recognition using Weighted Mixture Deep Neural Network Based on Double-Channel Facial Images", IEEE Access, vol. 6, pp. 4630-4650.
11. Ithaya Rani P., and Muneeswaran K. (2018), "Emotion Recognition based on facial components", Indian Academy of Science.
12. Guihua Wen, Tianyuan Chang, Huihui Li, and Lijun Jiang (2020), "Dynamic Objectives Learning for Facial Expression Recognition", IEEE Transactions on Multimedia, vol. 22, pp. 2914- 2925.
13. Pawel Tarnowski, Marcin Kolodziej, Andrzej Majkowski, and Remigiusz J. Rak (2017), "Emotion recognition using facial expression", Science Direct on Procedia Computer Science, vol. 108, pp. 1175-1184.

11. Biographies



Mrs. Jandhyam Lakshmi Alekhya Assistant professor Siddhartha Academy of higher education
Kanuru, 9490008940. B. Tech in 2011 from jntuh and m. Tech in 2013jntuh jaya prakash naryan college of engineering, mahaboobnagar, presently pursing ph. D in annamalai university.

IOT Based Smart Trolley with User Tracking System

Komathy Vanitha Krishnan[1], Angeline Felicia[2], Sharumitha[3] Preethi[4]

[1,2,3,4] *Department of Electronics and Communication Engineering, CSI College of Engineering, Ketti, India*

vanitha.kkv@gmail.com[1], angelinevijoline@gmail.com[2], sharumitha23@gmail.com[3] , preep3188@gmail.com

Abstract

The IoT Smart Trolley revolutionizes the shopping experience by integrating RFID-based automated billing, real-time inventory tracking and smart autonomous movement. Traditional shopping methods involve manual barcode scanning, long checkout queues and inefficient inventory management, leading to delays and customer dissatisfaction. The proposed system automates these processes using RFID technology for seamless product detection and billing, while cloud integration (Adafruit IO) enables real-time stock updates for shop owners. Furthermore, the trolley features RFID-based customer tracking, allowing it to follow the assigned user, and ultrasonic sensors for obstacle detection, ensuring smooth navigation. The system enhances operational efficiency by reducing checkout time by 70%, improving inventory accuracy, and providing an intuitive, technology-driven shopping experience. Future enhancements include AI-powered recommendations, voice-controlled navigation and synchronized multi-trolley communication for smart retail environments.

Keywords: RFID, Smart Shopping, Cloud Integration, Wireless Communication, Autonomous Navigation.

1. INTRODUCTION

In today's world, shopping involves visiting crowded malls, selecting products, adding them to a cart, carrying the heavy cart to the billing counter and waiting in a long queue to scan products for billing. This process leads to **wasted customer time and inconvenience**. In some cases, shoppers realize **the total bill exceeds their budget only at checkout,** causing further delays. Currently, **barcode scanning** is used for product identification, but it requires **line-of-sight scanning**, making the process inefficient. To overcome this, **IoT Smart Trolley**, is proposed to **detect products without line-of-sight scanning using RFID technology**. This system also provides **real-time billing updates on a DWIN LCD,** helping customers track their expenses.

2. LITERATURE SURVEY

The rapid advancement of IoT-based smart technologies has led to innovations in the retail shopping experience. Customers in shopping malls and supermarkets often face long checkout queues, inefficient billing, and difficulties in managing their expenses. Various smart solutions have been proposed to automate shopping processes and improve efficiency. In this section, a few existing approaches related to smart shopping trolley systems are discussed. **Smart Mobile Autonomous Robotic Trolley,** which integrates **RFID-based product scanning and autonomous navigation** to assist customers in efficient shopping. This system allows for **automated billing and smart mobility,** enhancing the shopping experience [1]. **Automated Billing System Using RFID and Cloud,** where **each shopping trolley is equipped with RFID scanners** to facilitate **seamless checkout and real-time cloud-based inventory management.** This approach improves **billing accuracy and reduces human intervention in stock management** [2]. M. Rahman et al. introduced a **Robust Low-Cost Passive UHF RFID-Based Smart Shopping Trolley,** which uses **passive UHF RFID technology** for **enhanced product tracking and billing automation.** [3]. D. Sharma et al. proposed an **IoT-Enabled Shopping Trolley with Automatic Billing,** integrating **RFID-based billing, a smart display, and a local database** to provide customers with **real-time price updates and seamless transactions.** [4].

An **Automated Trolley System with AI-based customer Tracking,** which utilizes **AI-powered tracking and RFID integration** to help customers navigate through crowded supermarkets, was proposed. [5]. The existing shopping system involves significant manual effort and lacks features that enhance customer experience [6]. It relies on manual barcode scanning, resulting in long billing queues and inefficient inventory tracking [7]. Customers cannot track their total bill in real-time, leading to budget overruns. The absence of automated trolley navigation and obstacle detection causes difficulties in crowded aisles [8]. Current systems also fail to support differently-abled users and lack real-time guidance, limiting accessibility and convenience in modern shopping environments [9].

3. PROPOSED SYSTEM

There is a **significant amount of manual effort involved** in the ordinary shopping system. The current framework focuses more on **tracking and identifying shopping carts for store management**, which may be beneficial for shop administrators but does not enhance the **customer's shopping experience**. The proposed IoT-based smart trolley enhances shopping convenience by automating movement and billing. It uses an RFID reader to identify users and follows them using ultrasonic and IR sensors, making it especially helpful for elderly or physically challenged shoppers. An ESP32 module uploads data to Adafruit IO, enabling real-time inventory updates for store owners via a React dashboard. The trolley is controlled by an Arduino with motor drivers, ensuring safe, hands-free navigation with obstacle detection.
Figure 1 illustrates the system architecture of the Smart Trolley Robot. The system is divided into two parts: “Part A” handles the shopping control system, including the RFID reader module, ESP32 controller, and cloud server, while “Part B” manages the trolley movement using Arduino Uno, motor driver shield (L293D), gear motors, and sensors for autonomous navigation.

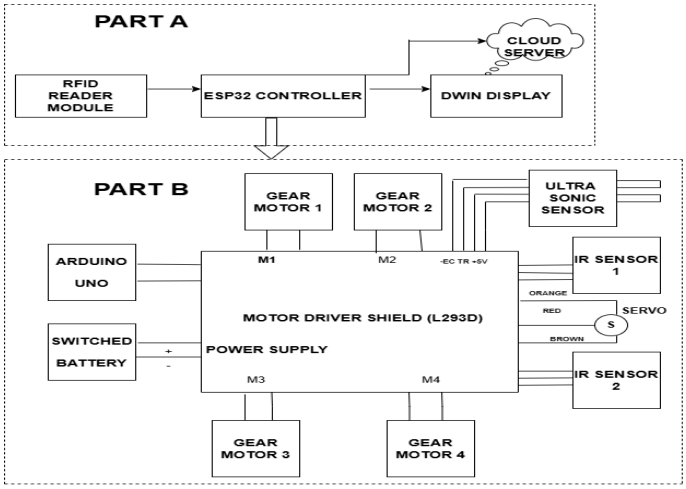

Figure 1. Block Diagram

The IoT Smart Trolley starts by powering on and verifying the user through an RFID tag. Once authenticated, it follows the user using ultrasonic or IR sensors.

4. ALGORITHM FOR TROLLEY CONTROLLING SYSTEM

The IoT Smart Trolley operates using sensors and motor controls for efficient navigation as shown as Figure 3. The Arduino Uno manages the motor driver (L293D), ultrasonic sensor, IR sensors and servo motors to control movement and obstacle detection. Trolley starts by initializing its components, with the ultrasonic sensor detecting obstacles. If an obstacle is present, the trolley stops until the path is clear. Movement is controlled by switch inputs, this system enhances safety and automation, preventing collisions and improving shopping convenience. IoT integration provides a smart, efficient, and user-friendly retail experience.

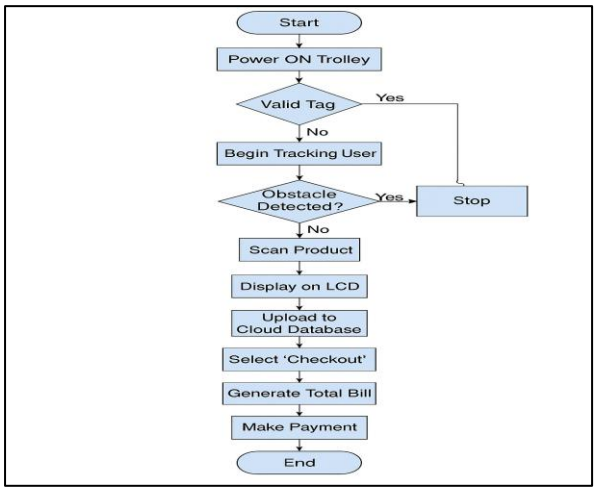

Figure 3. Trolley Controlling System

5. RESULTS

The final hardware implementation of the Intelligent IoT Smart Trolley with Automated Inventory and checkout as represented in Figure 4, successfully integrates multiple components to achieve seamless functionality. The mobility of the smart trolley is managed by DC motors and motor drivers, ensuring smooth movement. The system effectively automates product scanning, calculates the total bill, and provides an interactive user interface, making shopping more efficient and reducing checkout time.

The IoT Smart Trolley setup includes an Arduino, RFID reader (EM-18), LCD, buzzer, DC motors, and ultrasonic sensors for movement and obstacle detection. It scans items, updates bill in real time, and reduces checkout time. The billing station interface displays trolley details, total amount, and alerts, with billing data stored in Microsoft Access. The system supports 1000 entries, expandable via Visual Studio integration for better record management



Figure 4. Final prototype of the SMART system

In the current prototype, the system can store up to 1000 billing entries before automatically replacing older records with new ones. However, the storage capacity can be expanded by increasing memory and enhancing database integration with Visual Studio. This database-driven approach helps in financial tracking and record management, allowing billing details to be searched based on counter number or date, as shown in Figure 5.



Figure 5. User Interface of Billing Station

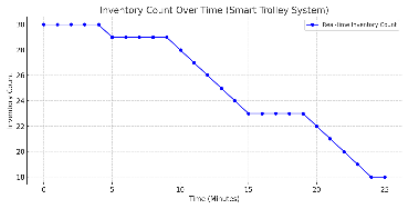

Figure 6. Inventory Count Over Time

The graph in Figure 6 illustrates the real-time inventory reduction during the shopping session. Initially, the inventory remains stable at 30 units, and then gradually decreases as products are picked over time. This drop represents active customer interaction, with each dip corresponding to an item removed from the shelf and added to the trolley. The trend confirms accurate tracking and updating of stock through the smart system.

6. **CONCLUSION**

The user-following smart trolley provides an efficient and automated shopping experience by integrating RFID-based product identification, real-time inventory updates, and autonomous movement. The system effectively reduces checkout time, enhances inventory management, and improves accessibility for users. By incorporating ultrasonic sensors and RFID-based customer tracking, the trolley accurately follows the assigned user while navigating through a shopping environment. The results from testing confirmed that the trolley successfully maintains a stable following distance, adapts to user speed variations and efficiently avoids obstacles, ensuring a seamless shopping experience.

REFERENCES

[11] A. Jain and S. Roy, 'IoT-based Automated Shopping Trolley with Smart Billing', 2017 IEEE International Conference on Innovations in Electronics, Signal Processing, and Communication (IESC), pp. 8073787, 2017.

[12] J. Kim et al., 'Smart Shopping Trolley System Using RFID and Wireless Communication', 2020 IEEE International Conference on Consumer Electronics (ICCE), pp. 9012466, 2020.

[13] M. A. Rahman et al., 'Smart Trolley for Shopping Mall using IoT', 2019 IEEE International Conference on Computing, Communication, and Intelligent Systems (ICCCIS), pp. 8684157, 2019.

[14] S. Gupta and R. Sharma, 'Robust Low-Cost Passive UHF RFID-Based Smart Shopping Trolley',"2018 IEEE International Conference on RFID Technology and Applications (RFID-TA), pp. 8440028, 2018.

[15] A. Patel and P. Desai, 'IoT-Enabled Smart Shopping Cart with AI-Powered Recommendation System', 2019 IEEE International Conference on Smart Technologies (ICST), pp. 8728346, 2019.

[16] A. Chakraborty, K. Bhattacharjee, and P. Dutta, 'SMART: Smart Mobile Autonomous Robotic Trolley', 2020 International Conference on Smart Electronics and Communication (ICOSEC), pp. 9120972, 2020.

[17] H. Tanaka et al., 'Automated Retail Inventory Management using RFID and Cloud Computing', 2021 IEEE International Conference on Future Smart Cities (ICFSC), pp. 9609710, 2021.

[18] P. Singh and V. Kumar, 'Design and Implementation of a Smart Shopping Cart System', 2020 IEEE International Conference on Advances in Computing, Communication and Automation (ICACCA), pp. 9262350, 2020.

[19] L. Zhao et al., 'A Low-Cost RFID-Based Smart Shopping System', 2021 IEEE International Conference on Future Automation and IoT (ICFAI), pp. 9297439, 2021.